

VOL. 6

POLYMER

*The Chemistry, Physics and Technology of
High Polymers*

Editorial Board

C. H. BAMFORD, PH.D., SC.D., F.R.S.

Campbell Brown Professor of Industrial Chemistry, University of Liverpool

C. E. H. BAWN, C.B.E., F.R.S.

*Grant Brunner Professor of Inorganic and Physical Chemistry,
University of Liverpool*

GEOFFREY GEE, C.B.E., F.R.S.

Sir Samuel Hall Professor of Chemistry, University of Manchester

ROWLAND HILL, PH.D.

Director of Research, I.C.I. Fibres Division, Harrogate

BUTTERWORTHS
LONDON

Kinetic Measurements on the Cobalt-60 Gamma-initiated Polymerization of Isobutene in the Presence of Zinc Oxide

F. L. DALTON

A dilatometric study has been made of the rate of radiolytic polymerization of isobutene in the presence of zinc oxide, samples being stirred during irradiation. Above a minimum stirring speed, polymerization rate is not dependent on stirring rate. The dependence of polymerization rate on amount of additive used, radiation intensity, and temperature, are presented. Molecular weight data for the polymer samples obtained are given, and an hypothesis of the reaction mechanism is offered.

SEVERAL early papers on the polymerization of isobutene by means of ionizing radiation have suggested that the reaction is cationic¹⁻⁷, and that the rate can be increased by a wide range of solid additives^{2, 3, 5, 7}. This effect of additives was initially ascribed to a rise in the *G* value for chain initiation. Our own earlier work⁸ has shown that if extreme care is taken in the preparation of samples much higher rates than those reported previously could be obtained, and we tentatively concluded that the additives suppressed the termination step and led to transfer controlled molecular weights as well as affecting chain initiation. All work so far published on these systems has been preliminary in character and has not aimed at obtaining a series of reproducible measurements from which kinetic deductions might properly be made. The aim of this paper is to present a number of such measurements using zinc oxide as an additive. It was hoped that this study would lead to a full understanding of the system, but although some deductions can be made a complete quantitative description of the reaction is not yet possible.

EXPERIMENTAL

Both isobutene and zinc oxide were obtained and purified as described previously⁸. The vacuum system, source and dilatometer design were also unchanged except for the following two modifications. First, to enable stirring to be carried out by the method described below, three glass beads 3-4 mm in diameter were placed in the dilatometer bulb, and secondly, the lens and mirror system used to follow the change in meniscus level during the run was replaced by a closed circuit television assembly (Beulah Electronics Ltd, New Cross, London, England). The molecular weights of polymers produced were measured viscometrically, and again details have been given previously⁸. It should be noted, however, that many of the molecular weights reported in this work are above the upper limit of 1 260 000 for which the viscosity/molecular weight relation used has been verified.

The technique used for the measurement of polymerization rates was modified from that described earlier so that the dilatometer contents could be thoroughly mixed during irradiation. The filled dilatometer was gripped by a clamp mounted on the axis of a laboratory flask-shaker. Oscillation of the dilatometer with the shaker caused three glass beads in the dilatometer bulb to give a milling action and this stirred the bulb contents thoroughly. A scale was attached to the stem of the dilatometer and was observed along the plane in which movement took place. This enabled the scale and meniscus to be read accurately while the dilatometer was in violent motion. A diagram of the assembly is shown in *Figure 1*. An alternative stirrer in which the end of the dilatometer stem was gripped in the chuck of an oscillating motor was used for some experiments.

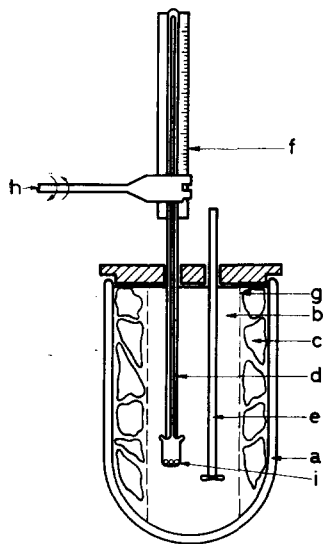


Figure 1—Diagram of experimental assembly. (a) Dewar vessel; (b) trichloroethylene; (c) solid carbon dioxide; (d) dilatometer; (e) stirrer; (f) scale; (g) wire gauze cylinder; (h) arm of laboratory shaker; (i) glass beads

Measurements made at temperatures other than -78°C necessitated placing a copper cooling coil, through which coolant from a cryostat could be passed, in the region of our bath normally occupied by solid carbon dioxide.

RESULTS

Preliminary experiments were carried out using zinc oxide of 17.4 and $0.17\text{ m}^2/\text{g}$ surface area to investigate the variation of polymerization rate with stirrer speed. Using the stirring technique outlined above and shown in *Figure 1*, it was found that if the contents of the dilatometer appeared thoroughly mixed on inspection (using a transparent Dewar vessel) the polymerization rate obtained was not changed by further increasing the speed of the stirrer. The alternative stirrer described above gave identical rates with similar samples. Furthermore, when 50 per cent of $17.4\text{ m}^2/\text{g}$ zinc oxide was used, giving a bulb filled with powder, the rate of polymerization obtained with and without stirring was the same. It is clear that the

POLYMERIZATION OF ISOBUTENE

reaction does not depend critically on stirring: it is only necessary for the zinc oxide to be distributed uniformly throughout the dilatometer bulb. Since the viscosity of the liquid phase increased during polymerization it was essential to ensure that uniform mixing was maintained throughout a run. Failure to observe this requirement led to rates which fell with increasing conversion over the first four to five per cent (roughly to the solubility limit of polyisobutene in its monomer), and then remained as a constant, but too low, value instead of the linear rate plots normally obtained. In the stirred system, conversion versus time plots remained linear at low concentrations of additive, in direct contrast to the behaviour of unstirred systems reported earlier⁸. All rate data reported in this communication have been obtained from linear conversion versus time plots obtained at a stirring rate above the critical level with one exception, described below. Runs were continued to about ten per cent conversion in all cases. Our equipment does not allow us to follow post irradiation effects for the first minute after the radiation source is removed; subsequently no post irradiation reaction could be detected.

In order to investigate the dependence of rate on the relative amounts of isobutene and zinc oxide present, four series of experiments were carried out at nominal intensities* of 5 775 and 390 rad/h using 17.4 and 0.17 m²/g zinc oxide. With the higher surface area material, the zinc oxide concentration was varied from 5 to 50 per cent by weight; the latter amount represents the largest quantity of zinc oxide of this surface area which can be packed conveniently into a dilatometer bulb. With the lower surface area of zinc oxide the concentration was varied from 10 to 70 per cent by

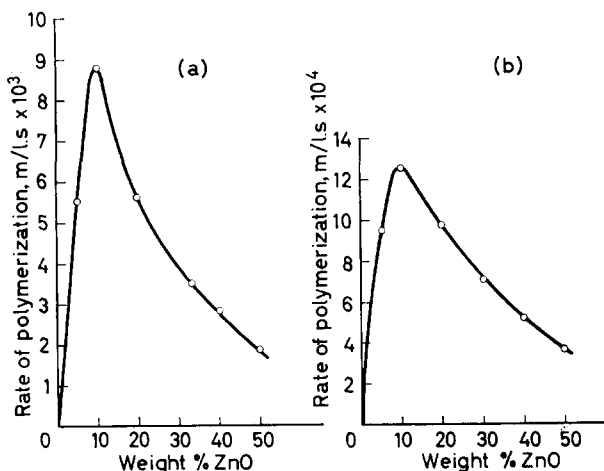


Figure 2—Rate of polymerization as a function of zinc oxide concentration for 17.4 m²/g zinc oxide. (a) Nominal intensity 5 775 rad/h; (b) nominal intensity 390 rad/h

*By nominal intensity is meant the intensity measured by the Fricke dosimeter ($G_{\text{Fe}^{3+}} = 15.5$) when a sample was placed in the position of the dilatometer bulb: the bath contained a liquid whose electron fraction at room temperature was equal to that of trichlorethylene at -78°C .

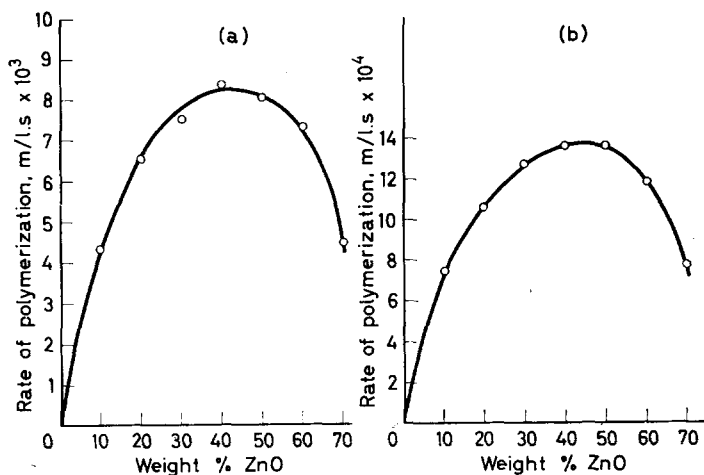


Figure 3—Rate of polymerization as a function of zinc oxide concentration for 0.17 m²/g zinc oxide. (a) Nominal intensity 5775 rad/h; (b) nominal intensity 390 rad/h

weight. The temperature was -78°C in all cases, and the data obtained are given in *Table 1*, while plots of rate of conversion versus zinc oxide concentration are shown in *Figures 2* and *3*. The conversion versus time plot obtained with 50 per cent of 17.4 m²/g zinc oxide at the higher intensity was not linear; it showed a slight but definite upward curvature. An arbitrary choice of the average rate between two and seven per cent conversion has been used in *Table 1* and *Figure 2*, but since the curvature is very slight, any other choice of rate would not affect the general pattern of our results. It can be seen that the plots exhibit a maximum, the position of which is not dependent on intensity, but which is markedly altered by changing the surface area of the zinc oxide.

It is possible from the points at each weight fraction of 17.4 m²/g zinc oxide and 0.17 m²/g zinc oxide to calculate an intensity exponent, and the results of such calculations are given in *Table 2*. As a measurement was made at 33½ per cent zinc oxide instead of 30 per cent in the series at high intensity and high surface area, an interpolation was necessary to obtain the rate at 30 per cent additive in this case. Reference to *Figure 2(a)* will show that this involves no significant error. It can be seen from *Table 2* that the intensity exponent does not appear to vary widely as the amount of zinc oxide is increased or to depend on the surface area of the additive. The mean value for the higher surface area material is 0.65, for the lower, 0.66.

Table 1 shows the molecular weights obtained from the above experiments by viscometric measurements. It can be seen that the values have a rather wide spread but display no significant trend. This spread was found

POLYMERIZATION OF ISOBUTENE

Table 1

Surface area of ZnO m ² /g	Wt % ZnO	Nominal intensity rad/h	Actual intensity (absorption by i-C ₄ H ₈ +ZnO) rad/h	Intensity if significant absorption by ZnO only rad/h	Rate of polymerization m.l. ⁻¹ .sec ⁻¹ × 10 ³	Viscosity average mol. wt × 10 ⁻⁴	G _(-monomer) based on total energy absorbed × 10 ⁻⁴
17.4	5	5 775	6 000	243	5.53	2.23	4.32
17.4	10	5 775	5 941	486	8.79	3.96	6.82
17.4	20	5 775	5 820	972	5.62	3.58	3.93
17.4	33.3	5 775	5 660	1 620	3.47	—	2.15
17.4	40	5 775	5 580	1 944	2.80	3.48	1.61
17.4	50	5 775	5 460	2 430	1.83	2.42	0.931
17.4	5	390	405	16.4	0.945	2.30	11.0
17.4	10	390	401	32.8	1.26	2.40	14.1
17.4	20	390	393	65.6	0.989	4.43	10.2
17.4	30	390	384	98.4	0.704	3.25	6.82
17.4	40	390	376	131	0.517	2.47	4.41
17.4	50	390	369	164	0.364	2.47	2.74
0.2	10	5 775	5 941	486	4.32	1.98	3.28
0.2	20	5 775	5 820	972	6.52	2.86	4.57
0.2	30	5 775	5 700	1 458	7.51	2.02	4.81
0.2	40	5 775	5 580	1 944	8.37	3.34	4.81
0.2	50	5 775	5 460	2 430	8.02	2.79	4.09
0.2	60	5 775	5 340	2 916	7.30	2.24	3.21
0.2	70	5 775	5 220	3 402	4.47	1.86	1.64
0.2	10	390	401	32.8	0.746	3.26	8.40
0.2	20	390	393	65.6	1.06	3.42	10.9
0.2	30	390	384	98.4	1.27	2.66	12.0
0.2	40	390	376	131	1.36	2.33	11.6
0.2	50	390	369	164	1.36	3.30	10.3
0.2	60	390	360	197	1.18	3.08	7.72
0.2	70	390	352	230	0.770	3.17	4.18

to be due to the extreme ease with which high molecular weight polyisobutene can be degraded in solution by cavitation. Purification had been achieved by extracting the reaction products with carbon tetrachloride and precipitating into a tenfold excess of stirred methanol. It was found that even gentle shaking of the reaction products with carbon tetrachloride to dissolve out the polymer led to some degradation if the molecular weight

Table 2

Surface area of ZnO m ² /g	Wt % ZnO	Intensity exponent	Surface area of ZnO m ² /g	Wt % ZnO	Intensity exponent
17.4	5	0.66	0.2	10	0.65
17.4	10	0.73	0.2	20	0.67
17.4	20	0.66	0.2	30	0.66
17.4	30	0.63	0.2	40	0.67
17.4	40	0.63	0.2	50	0.66
17.4	50	0.60	0.2	60	0.67
			0.2	70	0.67

was initially above about 1–2 000 000, although stirring during the polymerization had no observable effect upon the molecular weight. In view of the sensitivity of the molecular weight of recovered polymer to shearing forces (see below), it is surprising that the molecular weight of the polymer as well as the rate of polymerization was unaffected by changes in stirrer speed. However, no indication of a variation of molecular weight with stirring speed was detected and this would suggest that the ready degradation of recovered polymer in solution by shear is due either to oxidative processes or to its greater extension in homogeneous solution. It appears that any form of cavitation of the solution causes degradation, and it is imperative to avoid this if meaningful molecular weights are to be obtained. In all subsequent experiments shaking was avoided during extraction, and consistent molecular weights were obtained, though extreme care was essential. Recently, results of a study on the sensitivity of high molecular weight polyisobutene to mechanical shearing in solution have been reported⁹, and bear out the somewhat limited observations on the phenomena which we have made. In the light of this knowledge the molecular weights of *Table 1* must be regarded as minimum values.

Experiments were next carried out to determine the dependence on temperature of both the rate of polymerization and the molecular weight of the polymer produced, using 40 per cent zinc oxide of 0.17 m²/g surface area. Rate experiments were carried out between 0° and –78°C, while molecular weight determinations were made over the range 0° to –120°C. The rate measurements were stopped at higher temperatures owing to lack of precision on the cooling bath below –80°C, which made accurate dilatometry impracticable. The data obtained are shown in *Table 3*, while *Figures 4(a)* and *4(b)* show plots of log rate versus reciprocal temperature and log viscometric molecular weight versus reciprocal temperature respectively. The bracketed values of molecular weight in *Table 3* are values obtained if no special care is taken during a determination, and give some idea of the significance of accidental degradation. From *Figure 4(a)* the overall activation energy of the reaction is –0.01 kcal, that is, within

Table 3

Temperature °K	Rate of polymerization m.l. ⁻¹ sec ⁻¹ × 10 ³	Viscosity-average molecular weight × 10 ⁻⁵
273	1.38	1
248.5	1.37	2.70
233	1.39	7.94
212.3	—	24.0
195	1.36	64.7 (23.3)
173	—	>72.0 (44.5)
159	—	Not measurable (46.9)

experimental error, zero. In *Figure 4(b)* a minimum value of molecular weight is shown at a temperature of –100°C, and no values for lower temperatures are given. This is because at the very high molecular weights produced the polymer is degraded merely by passing down the capillary of

POLYMERIZATION OF ISOBUTENE

the viscometer. For the -100°C polymer, therefore, solutions were used only once and not diluted *in situ*, as is usual. Even so, some degradation occurred during measurement, and at still lower temperatures the greatly

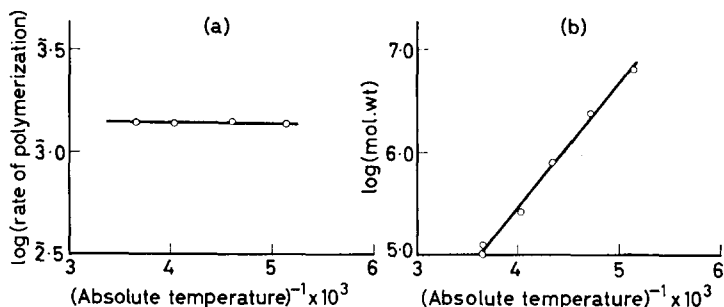
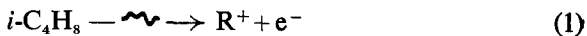


Figure 4—(a) Log polymerization rate versus reciprocal temperature; (b) Log viscometric molecular weight versus reciprocal temperature

increased molecular weight made even a rough estimate impossible. The deviation from linearity of the plot of Figure 4(b) shown by the last point is therefore of doubtful kinetic significance and it is justifiable to obtain an ‘activation energy of molecular weight’ from the slope of the line through the other points: this procedure gives a value of -5.7 kcal. It should be noted that no significant variation of molecular weight with conversion was found between two and twelve per cent conversion.

DISCUSSION

There has been in the past a considerable amount of speculation as to the mechanism of the additive effect in isobutene polymerization. The earliest suggestion was that electrons formed by the action of high energy radiation on the liquid isobutene according to the reaction



could be trapped at sites on the zinc oxide, thus leading to an increased G value for initiation. Assuming no transfer reactions occurred, it was calculated that a rise in $G_{\text{initiation}}$ from 0.1 to a maximum of 2.8 would account for the observed effects². In our own earlier work⁸ it was shown that this view could not be a complete explanation, since calculations of $G_{\text{initiation}}$ by this method gave values as high as 274. We suggested therefore that chain transfer was important in this system and that the termination rate might well be depressed. We also pointed out the possibility of initiation in an absorbed layer of isobutene in the surface of the zinc oxide, a process which we have come to consider increasingly important in view of the work of Barry and Klier^{10, 11}, and Kohn¹², and our own later results. Semenov¹³ has tentatively proposed that pre-orientation of monomer molecules on the surface of the solid leads to an almost instantaneous

polymerization of many molecules in the displacement time of carbon atoms by an energy chain process.

Before considering in detail possible mechanisms to account for results obtained in this study, let us consider some more general points of relevance. It has been generally assumed that solid additives increase the rate of the cationic polymerization of isobutene which occurs in their absence. However, recent work has shown that this 'homogeneous' reaction is not a simple homogeneous process but a more complex one¹⁴, involving the surface of the reaction vessel to a considerable extent. It will be wise, therefore, to consider the polymerization in the presence of additives as a complete problem in itself, rather than as a modification of a well understood process. It has been shown that a wide range of solids can act as additives. We ourselves¹⁵ have obtained high rates using glass powder, aerosil, zinc oxide, nickel oxide, cobalt oxide, magnesium oxide, chromium oxide, graphite, sodium chloride and powdered gold, and further compounds have been found effective in other studies^{2,5}. This makes it difficult to accept theories which involve a specific orientation of isobutene molecules with respect to each other at the solid surface since it is unlikely that the range of different solids known to be effective would all give similar alignment to isobutene molecules. We have previously shown that the very high temperature-independent rates obtainable with isobutene in the presence of zinc oxide cannot be obtained with other monomers which are subject to cationic polymerization¹⁶, although small increases of rate were not excluded. A recent paper¹⁷ has suggested that the rate of styrene polymerization at low temperatures can be increased by factors as high as ten in the presence of aerosil, but there is no evidence of any solid-monomer combination showing behaviour parallel to that of isobutene. The gamma-induced polymerization in the presence of additives also shows several features exhibited by the more conventional reaction initiated by chemical means. In particular, the work of Kennedy, Thomas and their colleagues¹⁸⁻²⁵ using aluminium chloride as initiator has shown that rate is independent of temperature at least down to -80°C , and that molecular weight is markedly dependent on temperature. Kennedy and Thomas also note²³ that the log molecular weight versus reciprocal temperature plot falls from a linear relation as temperature is lowered and attach a kinetic significance to this result. Although we observed this effect at about the same degree of polymerization, we doubt if it has a significance in our case for the reasons given above.

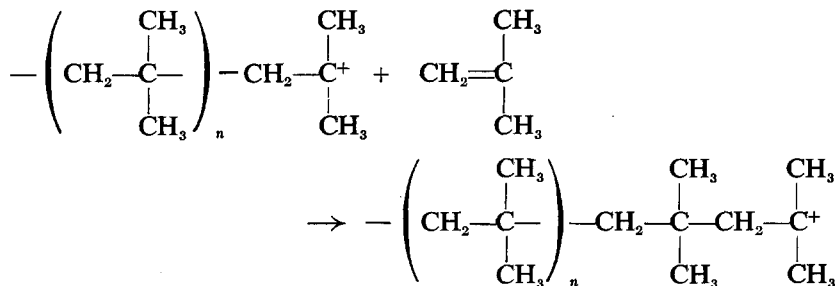
Considering the initiation process there are two main possibilities. First, ions may be formed in the liquid phase by reaction 1 and the electron absorbed on to the zinc oxide by reaction with a positive site on the surface. It is essential to postulate that such sites are formed by radiation and are transient, since it has been shown that the polymerization of isobutene with aluminium chloride is not affected by zinc oxide¹⁹, and also that pre-irradiation of the zinc oxide does not alter the rate of the radiation-initiated polymerization. The second possibility is that positive holes and electrons are formed in the zinc oxide by irradiation, and that the positive holes, migrating to the surface of the zinc oxide, react with isobutene

POLYMERIZATION OF ISOBUTENE

molecules absorbed on the surface to give (isobutene)⁺ ions which initiate the polymerization. The existence of such ions has been postulated by Barry and Klier¹¹ to explain their results on the conductivity changes on irradiation in zinc oxide having absorbed hydrogen or isobutene in the surface. Also Kohn¹² has observed the formation of positive ions from hydrocarbons absorbed on the surface of silica gel on irradiation. This second possibility allows a tentative explanation of the observed facts. It has been shown by Fowler²⁶ that the conductivity (\propto the number of electrons) produced in an irradiated solid is proportional to (intensity) ^{Δ} where Δ can vary between 0.5 and 1 for different solids. This would suggest that the number of positive holes and therefore the rate of initiation should be proportional to I^Δ , and hence differing intensity exponents should occur if different additives are used. Such an explanation of the 0.66 dependence on intensity found for zinc oxide predicts that the exponent would not change with additive/monomer ratio or surface to volume ratio of the additive (the observed behaviour), while any explanation based on competing termination processes meets difficulties in this respect. The observation that the use of both nickel oxide and powdered glass as additives gives intensity exponents of about one¹⁵, can also be fitted into this picture. It is possible to see why isobutene is unique in giving such high rates compared with other cationic monomers. The absorbed (isobutene)⁺ ion will remain absorbed until sufficient propagation reactions have occurred to enable the absorption energy of the initial ion, now an uncharged terminal unit, to be compensated by the random thermal energy of the growing chain; and if an electron moving through the zinc oxide neutralizes the growing (but short) chain before desorption, then the formation of high molecular weight chains will be inhibited. It has been stated²⁷ that isobutene has a much higher rate constant for propagation than other cationic monomers and, if this is so, then it is clear that an additive effect such as we envisage occurring readily with isobutene would with other monomers be greatly reduced or even completely eliminated.

A possible test of the basis of the above hypothesis, i.e. that the important ionization is that produced in a solid, is the irradiation of a zinc oxide-isobutene mixture with 2 357 Å ultra-violet (u.v.) light, which is not capable of ionizing isobutene but which can produce positive holes and electrons in zinc oxide. If ionic polymerization occurs, then a mechanism depending on energy absorption in the solid is confirmed, while an absence of polymerization would suggest that the liquid phase ionization is essential. Such an experiment was carried out, and it was found that there was initially a polymerization which rapidly stopped at conversions around 0.1 per cent. This result is somewhat equivocal, but we suggest that the production of charges exclusively in the surface layers of the additive by u.v. light leads to many rapid neutralization steps prior to desorption of growing cations, resulting in a surface coating of the zinc oxide particles and their deactivation.

Having left the surface of a zinc oxide particle as a relatively short-chain cation, the polymerizing chain will undergo a large number of propagation steps of the type



and some features of this phase of the reaction will now be discussed. In contrast to the conventional ionic polymerization, the growing cation does not have a gegenion intimately associated with it, and this may lead to differences in k_p . Polyisobutene is soluble in its monomer only to about four per cent concentration, so that at an early stage in the reaction precipitation of the polymer will occur. In studies on free radical polymerization in precipitating systems, for example the homopolymerization of acrylonitrile or the polymerization of styrene in methanol solution, it has been found that precipitation leads to an extremely complex kinetic situation. However, as overall rate is not affected by the onset of precipitation in our system, and addition of hydrocarbon solvent to both the aluminium chloride¹⁹ and the radiation-initiated²⁸ polymerization leads to no marked change in the reaction at the solvent concentration at which precipitation is eliminated, we presume that there is little or no effect on the kinetics. This means that, owing to the swollen nature of the polymer coil, monomer can still get to the cationic site without additional restriction. We consider that the molecular weight of the polymer is transfer controlled because of the ludicrously high $G_{\text{initiation}}$ values obtained on the contrary assumption by dividing $G_{(-\text{monomer})}$ by degree of polymerization, and the fact that, while molecular weight is temperature-dependent, the overall polymerization rate is not. Also, work with conventional initiators has led to the conclusion that transfer control occurs generally. Such a transfer reaction would allow the active cation to be terminated by the neutralization process discussed below rather than leaving long-lived 'buried' cations which would cause a marked polymerization after the cessation of irradiation. As mentioned in the results section, no long-lived after-effect could be observed. An additional cause of the lack of effect of precipitation on the kinetics may be that the high propagation rate leads to a molecule undergoing effective physical termination (transfer) before it has time to precipitate. The rate constant for transfer may well be different from that prevailing in the conventionally initiated polymerization because of the presence of a neighbouring gegenion in this latter case. The actual reaction of transfer is probably proton expulsion or proton transfer to monomer. It is unlikely to involve reaction with ion pairs formed directly by radiation in the liquid phase, since such a reaction would be expected to be temperature-independent.

The nature of the termination step in conventional ionic polymerization of isobutene is at present far from clear, and it is not possible to utilize

POLYMERIZATION OF ISOBUTENE

the data available to assist in understanding the radiation-initiated reaction. However, since we have already argued against reaction with negative ions formed in the liquid phase (which is an unusual form of chain transfer rather than a true termination) and there is no obvious mechanism by which electrons can be discharged from the solid phase into the liquid phase, the most likely suggestion is that charge neutralization occurs when a growing chain arrives at a zinc oxide particle. Since a very long-chain molecule moves relatively slowly through the medium, it may be that on arrival at a zinc oxide particle the growing ion remains at the surface long enough to undergo neutralization by an electron in the zinc oxide irrespective of the electron concentration: alternatively, if the long-chain cation stays at the surface only briefly, this concentration may be important. In either case, high molecular weight polymers are built up because of the large number of propagation steps which can occur while the cation diffuses from one zinc oxide particle to another.

A general scheme such as that suggested above, in which initiation and termination both occur at the surface of zinc oxide particles, and initiation is due to energy absorption within a particle, suggests that as the concentration of zinc oxide tends to zero, the $G_{(-\text{monomer})}$ value based on energy absorbed in the zinc oxide only should become increasingly large. Owing to the different numbers of particles per unit volume when equal weight fractions of zinc oxides of differing specific surface area are used, each surface area of zinc oxide should have a unique curve. Also, since rate of

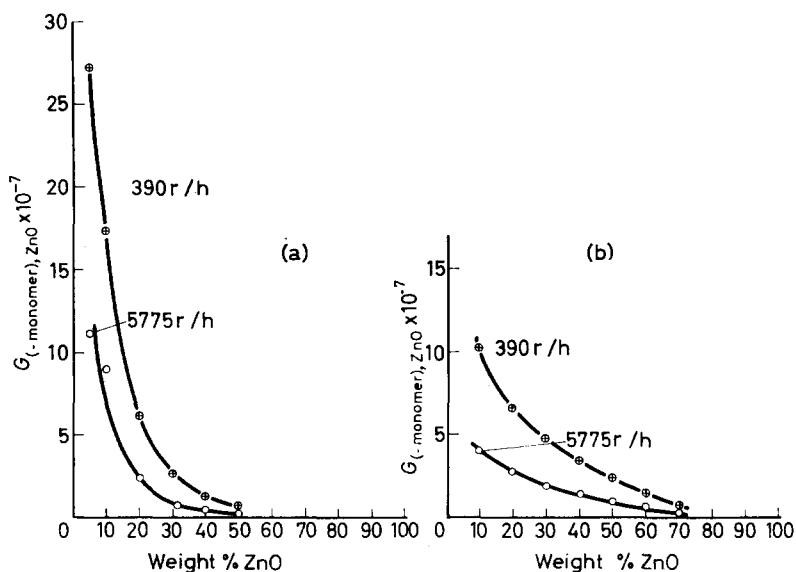


Figure 5—(a) $G_{(-\text{monomer})}$ based on energy absorbed in zinc oxide as a function of zinc oxide concentration, using $17.4 \text{ m}^2/\text{g ZnO}$; (b) $G_{(-\text{monomer})}$ based on energy absorbed in zinc oxide as a function of zinc oxide, using $0.17 \text{ m}^2/\text{g ZnO}$

initiation is proportional to (intensity)^{0.66}, the curves will shift with changing intensity. The relevant data of *Table 1* have been used to calculate $G_{(-\text{monomer})}$ values based on energy absorption of zinc oxide, and these are plotted as a function of composition in *Figure 5* for each surface area and intensity studied. The curves fall steadily with increasing zinc oxide concentration as predicted: with the high surface area material enormous G values are observed. The consistently lower values for low surface area material would be expected on the assumption that zinc oxide powder consists of spherical particles of small radius for high surface areas and larger radius for low surface areas.

The maximum in the rate versus composition curves shown in *Figure 2* can be thought of as due to an increasing rate of initiation, owing to increasing zinc oxide concentration, being outweighed by a more rapidly increasing rate of termination as the zinc oxide particles become increasingly close together. The position of the maximum will depend on the surface area of the zinc oxide, since from the above discussion it influences both the rate of initiation and the rate of termination, and these effects do not balance. The drop in monomer concentration with increasing zinc oxide concentration cannot explain the maximum, as it changes relatively little (from 12.45 mole/l. to 9.70 mole/l.) between 0.05 and 0.70 weight fraction zinc oxide, owing to the high density of the oxide.

The value of approximately zero for the overall activation energy of the reaction is also explicable. It is generally accepted for radiolytic reactions that the energy of activation of the initial process is zero, that is, in this case the rate of formation of positive holes and electrons is independent of temperature. Subsequent ion-molecule and ion recombination reactions in the solid should be independent of temperature, though the desorption of the isobutene cation from the surface may depend to some extent on temperature. If this dependence is sufficiently small compared with the exponential dependence customarily encountered, the overall activation energy will be given by $E_p - fE_t$, where E_p is the activation energy of the propagation reaction, E_t the activation energy of the termination reaction, and f is a factor between 0.5 and 1 whose value depends on the precise nature of the termination reaction. Since termination is a charge recombination process, no exponential temperature dependence is to be expected, although small changes due to the change in mobility of growing chains may be expected. The propagation step is an ion-molecule reaction of a type which has been shown theoretically²⁹ to require no appreciable activation energy, and practical studies support this result; hence $E_p - fE_t$ would be expected to be approximately zero, any small value being due to the non-exponential effects mentioned above, and possibly to E_p differing slightly from zero.

The fact that oxygen inhibits the radiolytic polymerization but does not affect the aluminium chloride initiated reaction is presumably due to the absorption of oxygen on to the surface of the zinc oxide, where it will exist as O^- , $O^{\cdot-}$ or O_2^- : these entities would capture positive holes which reach the surface of the additive and prevent initiation. It is probably the removal of small traces of absorbed oxygen from the additive surface by

POLYMERIZATION OF ISOBUTENE

heating at 400°C *in vacuo* before use which has enabled us to obtain higher rates of polymerization than have been reported elsewhere.

Although only qualitative in nature, the mechanism outlined above seems able to explain all our observations on the polymerization of isobutene in the presence of zinc oxide. Further work is in progress which it is hoped will clarify and increase our understanding of this radiolytic polymerization.

NOTE ADDED IN PROOF

Since the preparation of this paper a significant study, by David, Provoost and Verduyn, of some features of the radiation-initiated polymerization of isobutene has been published (*J. Polym. Sci. C*, **1964**, No. 4, 1135).

The author wishes to thank Miss J. Bartlett for skilful technical assistance throughout this work.

*Radiation Branch, Isotope Research Division,
Wantage Research Laboratory (A.E.R.E.),
Wantage, Berks*

(Received March 1964)

REFERENCES

- 1 DAVISON, W. H. T., PINNER, S. H. and WORRALL, R. *Chem. & Ind.* **1957**, No. 38, 1274
- 2 WORRALL, R. and CHARLESBY, A. *Internat. J. appl. Radiation and Isotopes*, 1958, **6**, 8
- 3 DAVISON, W. H. T., PINNER, S. H. and WORRALL, R. *Proc. Roy. Soc. A*, 1959, **252**, 187
- 4 COLLINSON, E., DANTON, F. S. and GILLIS, H. A. *J. phys. Chem.* 1959, **63**, 909
- 5 WORRALL, R. and PINNER, S. H. *J. Polym. Sci.* 1959, **34**, 229
- 6 CHARLESBY, A., PINNER, S. H. and WORRALL, R. *Proc. Roy. Soc. A*, 1960, **259**, 386
- 7 DAVID, C., PROVOOST, F. and VERDUYN, G. *Polymer, Lond.* 1963, **4**, 391
- 8 DALTON, F. L., GLAWITSCH, G. and ROBERTS, R. *Polymer, Lond.* 1961, **2**, 419
- 9 MERRILL, E. W., MICKLEY, H. S. and RAM, A. *J. Polym. Sci.* 1962, **62**, 5109
- 10 BARRY, T. I. and KLIER, K. *Faraday Society Discussion*, Paris, 1960
- 11 BARRY, T. I. and KLIER, K. *Coll. Czech. chem. Commun.* 1962, **27**, 1320
- 12 KOHN, H. W. *J. phys. Chem.* 1962, **66**, 1017 and 1185
- 13 SEMENOV, N. N. *J. Polym. Sci.* 1961, **55**, 563
- 14 BARTLETT, J. A. and DALTON, F. L. To be published
- 15 DALTON, F. L. and HAYAKAWA, K. Unpublished results
- 16 DALTON, F. L. and HAYAKAWA, K. *Polymer, Lond.* 1963, **4**, 285
- 17 CHARLESBY, A. and MORRIS, J. *Proc. Roy. Soc. A*, 1963, **273**, 387
- 18 KENNEDY, J. P. and THOMAS, R. M. *J. Polym. Sci.* 1960, **45**, 227
- 19 KENNEDY, J. P. and THOMAS, R. M. *J. Polym. Sci.* 1960, **46**, 233
- 20 KENNEDY, J. P. and THOMAS, R. M. *J. Polym. Sci.* 1960, **46**, 481
- 21 KENNEDY, J. P. and THOMAS, R. M. *J. Polym. Sci.* 1961, **49**, 189
- 22 KENNEDY, J. P. and THOMAS, R. M. *J. Polym. Sci.* 1961, **55**, 311
- 23 KENNEDY, J. P. and THOMAS, R. M. *Advances in Chemistry series No. 34*, 1962, 111
- 24 KENNEDY, J. P., KIRSHENBAUM, I., THOMAS, R. M. and MURRAY, D. C. *J. Polym. Sci. A.*, **1963**, No. 1, 331
- 25 KIRSHENBAUM, I., KENNEDY, J. P. and THOMAS, R. M. *J. Polym. Sci. A*, **1963**, No. 1, 789
- 26 FOWLER, J. F. *Proc. Roy. Soc. A*, 1956, **236**, 464
- 27 PENFOLD, J. and PLESCH, P. H. *Proc. chem. Soc.* August 1961, 311
- 28 DALTON, F. L. To be published
- 29 EVANS, A. G. and POLYANI, M. *J. chem. Soc.* **1947**, 252

The Effect of Oxidation on Spherulite Size in Polyethylene Films

H. A. LANCELEY*

Well resolved and thus readily identifiable spherulites appear in crystallized polyethylene films only after the polymer has been heated to temperatures 100° to 200°C in excess of the crystal melting point. Infra-red examination of samples of a low pressure polyethylene heated in air and in vacuo reveals that oxidation is also necessary before these morphological changes occur. It is suggested that temporary crosslinks between oxygen containing groups in neighbouring chains is responsible for the change in spherulite density observed.

THERE have been many reports over the past decade of the formation of spherulitic structures in a variety of crystallizable polymers, including polyethylene, when a thin film of the polymer, usually confined between microscope cover slips, is first melted and is then crystallized on a hot stage maintained at a temperature lower than the thermodynamic crystal melting point, T_m . It has been widely accepted that the growth of spherulitic structures is characteristic of the manner in which high polymers crystallize from the melt and, indeed, optical microscope evidence for the mechanisms of nucleation and growth of spherulites obtained in this way has been utilized in attempts to account for the crystallization behaviour of polymers in bulk.

Recently, however, it has been suggested¹, and the present work confirms, that well resolved and readily identifiable spherulites do not as a rule appear in polyethylene films unless these be subjected previously to extremely high temperatures or when other rather special crystallization conditions apply. Thus, the birefringent structures observed by means of the polarizing microscope, in polyethylene heated to temperatures only slightly in excess of T_m , present an overall grainy appearance whatever the degree of supercooling, which, if due to the presence of spherulites, indicates that these must have dimensions considerably less than the 10^{-2} to 10^{-1} cm normally associated with such structures. By contrast, pre-heating of the polymer in air to temperatures 100° to 200°C above T_m for short periods of time enables the large, readily identifiable spherulites so often described to be produced at some lower temperature, and, during subsequent melting and re-crystallization, the polyethylene conforms to the, by now, well established pattern of behaviour.

However, experience shows that, even after conditioning polyethylene in this way, large spherulites grow only in isolated regions and almost invariably either at the edges of the film where the sample is exposed to the atmosphere or in areas where pockets of air have become trapped between polymer and glass covering slip. The indications are, therefore, that spherulite growth on this scale (diameter of 10^{-2} to 10^{-1} cm) is not representative of the original material, but that it occurs only where the polyethylene is chemically or physically modified.

Oxidation is known to give rise to structural changes in polyethylene in the solid state², but, so far as can be ascertained from the literature, the

*Present address: Shell Chemical Co. Ltd, Carrington Plastics Laboratory, Urmston, Manchester.

effect of oxidation of the molten polymer on subsequent crystallization behaviour has not been studied.

Since spherulite size is believed to be an important factor influencing the mechanical properties of crystalline polymer films³ and, as processing of polyethylene in air at elevated temperatures is a standard industrial practice, it is evidently desirable that the factors determining spherulite size in these circumstances be investigated.

EXPERIMENTAL

A low pressure polyethylene, Marlex 50, was used in all experiments. The physical properties of this polymer, measured by the methods described below, are listed in *Table 1*.

Table 1. Comparison of melting temperature, density and weight average molecular weight for Marlex 50 polyethylene samples

<i>Material</i>	T_m (°C)	g/cm^3	\bar{M}_w
Original Marlex 50	134	0.961	79 000
Marlex 50 pre-heated in air	129	0.961	63 000
Marlex 50 pre-heated in air and recovered from tetralin	132	—	63 000
Marlex 50 pre-heated <i>in vacuo</i>	134–135	—	—

It was necessary first of all to establish conditions under which Marlex 50 crystallizes to form readily identifiable large spherulites. Heating the polymer to 145°C in the form of a thin film between glass cover slips on a microscope hot stage and crystallizing, either isothermally at different degrees of supercooling or simply by cutting off the power supply and allowing the stage to cool, invariably produced the result shown in *Figure 1*. After removing the upper cover slip and heating to 240°C in air for two minutes, each of these methods of cooling gave rise to the formation of large spherulites, cf. *Figure 2*. In order to perform the experiment in the absence of air a vacuum desiccator was employed. The confined space precluded the use of a second hot plate, which would have enabled the crystallization to be carried out under isothermal conditions, and a technique was therefore devised whereby a chosen temperature cycle, indicated by a calibrated copper-constantan thermocouple placed in contact with the polymer sample, could be followed accurately in successive experiments.

Samples of polyethylene, about 0.2 mm in thickness, were supported on glass cover slips, or in certain cases on thin rocksalt plates, which in turn were mounted in shallow depressions drilled in a thin brass disc. As shown in *Figure 3*, the disc could be placed either on the electrically heated hot plate, A, or on the surrounding thermally insulated platform, B, by means of a cranked glass guiding rod sealed to the rim of a standard B.34 cone, which was rotated in a matching socket in the desiccator lid. A simple fractionating head allowed electrical leads to be taken out through a close-fitting rubber bung and at the same time the system was attached through a tap in the other arm to a high vacuum line. The hot plate was maintained

THE EFFECT OF OXIDATION ON SPHERULITE SIZE

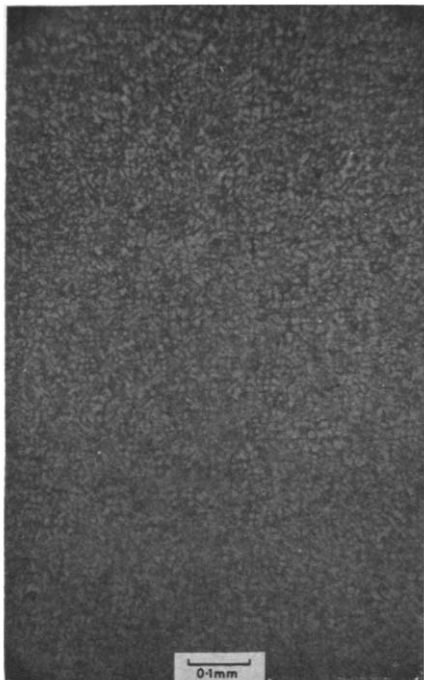


Figure 1—Marlex 50 sample heated between cover slips to 145°C, and cooled according to curve plotted in *Figure 4*

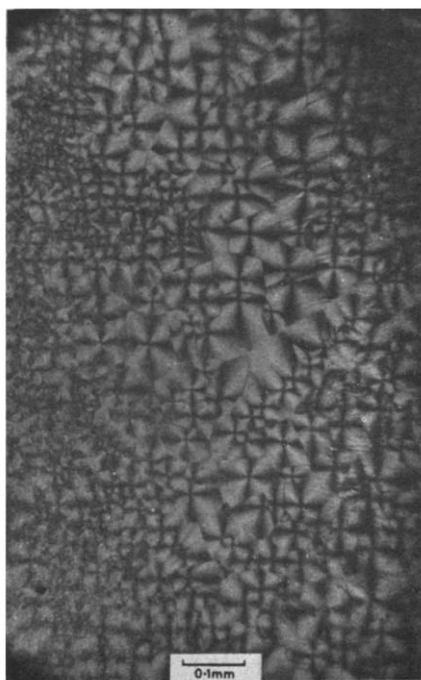
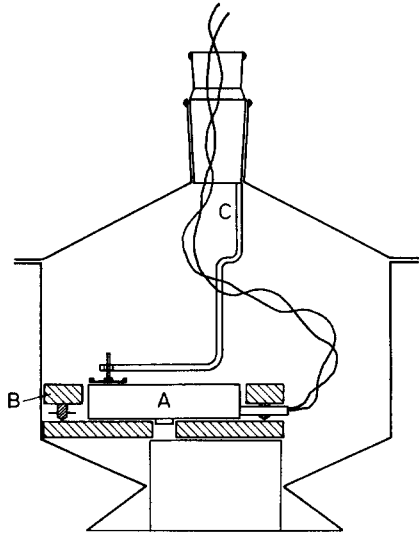


Figure 2—Marlex 50 sample heated to 238°C in air, and cooled according to curve plotted in *Figure 4*

at 290°C by manual adjustment of a rheostat and samples were rapidly transferred to the hot plate for a period of two minutes before returning them to their original position on the insulated surround. The experiment was repeated several times on samples heated in air and under high vacuum.

Figure 3—Vacuum desiccator showing hot plate, A, thermally insulated platform, B, and sample transfer device



In Figure 4 is plotted the temperature cycle followed by each polyethylene sample, the different symbols used referring to successive operations and revealing the accuracy with which the cycle was reproduced. Some experi-

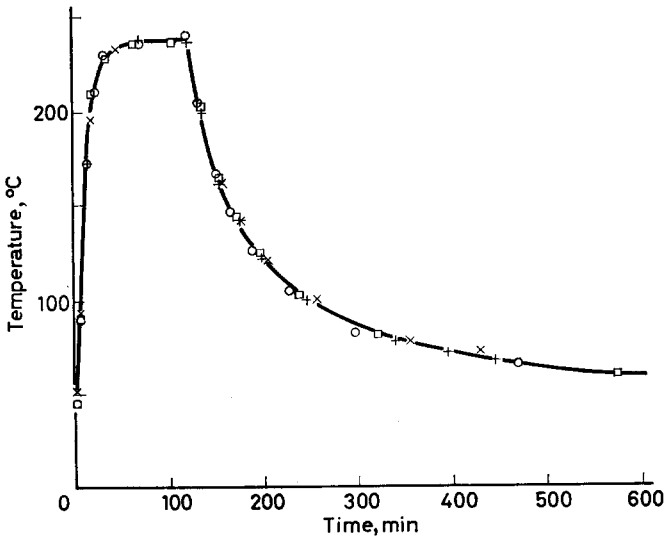


Figure 4—Temperature cycle: symbols refer to four different series of measurements

ments were performed on thin rocksalt plates, which also allowed infra-red spectra to be obtained. The same maximum temperature of 238°C was attained, but, because of the greater thickness of the rocksalt plate compared with a glass cover slip, cooling was rather more rapid than that recorded. However, results were identical for samples supported on the two different media.

All samples were examined under the polarizing microscope between crossed polars before and after heat treatment, photographs being taken of the birefringent structures appearing. Other physical properties were measured as follows.

Infra-red analysis was carried out by means of a Unicam S.P. 200 double beam recording spectrophotometer, using a rocksalt prism.

Melting temperatures were determined by observing the disappearance of birefringence from the films when heated on a microscope hot stage at a constant rate of 0.1°C per minute. Films not subjected to the high temperature cycle were previously melted at 145°C and were then allowed to crystallize under the same conditions by cooling along the curve already described for the cycled samples.

The density of the original polymer was determined directly by weighing, whilst heat treated samples were transferred to an alcohol-water density gradient column which was calibrated using chips of high and low pressure polyethylene of known density.

Molecular weights were calculated from the measured solution viscosities in tetralin at 120°C using Duch and Küchler's equation

$$[\eta] = 2.36 \times 10^{-4} \bar{M}_w^{0.78}$$

where $[\eta]$ is the intrinsic viscosity and \bar{M}_w is the weight average molecular weight. In order to obtain sufficient heat treated polyethylene for these measurements ten to twelve samples were subjected to the high temperature cycle in air and subsequently combined. Solutions were made up separately and passed through a heated, sintered glass filter (Porosity 4) directly into the viscometer, which was maintained at 120°C in a thermostatically controlled bath. No insoluble fraction was observed.

RESULTS AND DISCUSSION

The spherulitic structure resulting from the controlled heat treatment of polyethylene in the presence of air is shown in *Figure 2*. Under high vacuum the same heat treatment of identical original samples produced no detectable change in the structure—*Figure 5* (cf. *Figure 1*). Other properties of the heat treated polyethylene are included in *Table 1* and may be compared with those for the original material.

That there was no measurable change in density suggests that the degree of crystallinity remains essentially unaltered after exposure of the polyethylene to air at high temperatures. However, the density would also depend upon the oxygen uptake and on any loss of material as volatile oxidation products.

Infra-red analysis revealed marked differences between the two samples. Thus, whereas spectra for polyethylene heated *in vacuo* matched those of

the original material almost exactly, heating in air gave rise to new absorption peaks in the region $1\,650$ to $1\,800\text{ cm}^{-1}$, at $3\,460\text{ cm}^{-1}$ and at $1\,180\text{ cm}^{-1}$. In addition there was an overall increase in absorption between 800 cm^{-1} and $1\,400\text{ cm}^{-1}$. In many respects the absorption curves for the

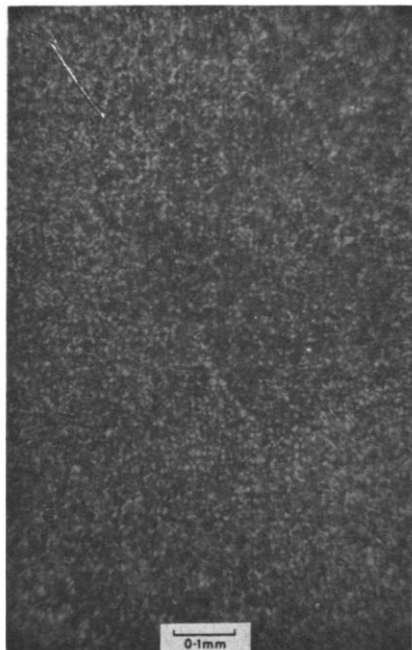


Figure 5—Marlex 50 sample heated to 238°C under high vacuum and cooled according to curve plotted in *Figure 4*

heat treated samples resemble published spectra for heat oxidized high pressure polyethylene. Thus, the multiple peak between $1\,650\text{ cm}^{-1}$ and $1\,800\text{ cm}^{-1}$ approximates to that obtained by Rugg, Smith and Bacon⁵ using a high resolution instrument, the greatest absorption at $1\,709\text{ cm}^{-1}$ and $1\,723\text{ cm}^{-1}$ being identified respectively with carboxylic acid carbonyl groups and with carbonyl groups within the polyethylene chain. At somewhat higher frequencies distinct shoulders provide evidence for aldehyde groups and possibly ester groups, but these are present in much lower concentrations. The peak appearing at $1\,180\text{ cm}^{-1}$ is also associated with carboxyl groups and has been attributed previously⁶ to the C—O vibration. The broader less intense absorption occurring at $3\,460\text{ cm}^{-1}$, corresponds to the O—H stretching vibration. Contributions to this bond are made by hydroperoxide, hydroxide and carboxyl groups. Its appearance at this frequency rather than at the $3\,600\text{ cm}^{-1}$ normally assigned to free hydroxyl groups shows that hydrogen bonding occurs. The overall increase in absorption between 800 cm^{-1} and $1\,400\text{ cm}^{-1}$ has also been noted previously⁶ as a result of oxidation of high pressure polyethylene, the effect being attributed in part to optical scattering by the solid film. From an evaluation of the double bond and methyl group content of Marlex 50, Smith⁷ deduced that the polymer consists predominantly of the mono-olefin

$\text{CH}_3(\text{CH}_2)_n\text{CH}=\text{CH}_2$, there being very few branches. It is now widely accepted⁸ that thermal oxidation of polyethylene proceeds via an auto-catalytic free radical mechanism involving the formation of intermediate hydroperoxides, which subsequently decompose to give the observed oxygen containing products. In Marlex 50, as a result of this kind of mechanism, carbonyl groups would appear preferentially at positions adjacent to the terminal double bonds, but ultimately at random points within the polymer chains. Carboxyl groups, on the other hand, can only occur in terminal positions and, in order to account for the carboxyl content observed in oxidized films, it seems likely that some chain scission has taken place. The solution viscosity measurements confirm that this is so, the intrinsic viscosities of the original polyethylene and that heated in air being 1.56 and 1.30, corresponding to weight average molecular weights of 79 000 and 63 000 respectively.

There is no *a priori* reason for supposing that a reduction of molecular weight of this order, or the introduction of oxygen containing groups, can in themselves be the cause of such a marked physical change in the polymer. However, carboxyl and ketonic carbonyl groups and hydroperoxides are known to be capable of strong polar interaction (producing hydrogen bonds for example) and it is now postulated that temporary crosslinks between neighbouring chains, formed as a result of such interaction between suitably disposed oxygen containing groups, can give rise to a network structure within the melt. The constraints imposed on molecular chains making up such a network could be manifested in two ways: (1) as a decrease in the mobility of chain segments, and (2), since the crosslinking units will not possess the same structure as the rest of the chain, as a lowering of T_m , thus effectively reducing the degree of supercooling. Both of these effects would contribute to a lowering of the spherulite nucleation density⁹.

Table 1 shows that a lowering of T_m does take place as a result of the oxidation of polyethylene in the melt and calculations based on the melting points of normal paraffins¹⁰ indicate that the observed decrease in the average molecular weight is insufficient to account for this difference of five degrees. Richards^{10b} has pointed out that T_m is depressed most by the inclusion of low molecular weight materials, which may be produced if scission took place near the chain ends. However, his experiments on the effect of the addition of degraded high pressure polyethylene (mol. wt 650) on the melting point of the original high molecular weight material (mol. wt 14 000) show that to produce a depression of five degrees more than 50 per cent by weight must be added, thus greatly reducing the average molecular weight. In Richards's experiments the degree of crystallinity was markedly reduced also, a change which was not experienced in the present work.

The formation of permanent crosslinks in Marlex 50 resulting from the effect of ionizing radiation on the molten polymer¹¹ leads to a decrease in the equilibrium value of the melting temperature. Undoubtedly, few permanent crosslinks exist in the thermally oxidized polyethylene, for no appreciable gel fraction was isolated, but oxygen containing groups are present in high enough concentrations to allow sufficient temporary crosslinks to be formed.

Whilst the lowering of T_m may be explained satisfactorily in the above way the observed change in nucleation density must depend upon other factors also, since, in isothermal crystallization experiments on the original Marlex 50, spherulite size was not greatly dependent upon the degree of supercooling. However, if molecules are attached to neighbouring molecules at random points along their length, relative movement must be limited and, for a given degree of supercooling, the number of locations at which nucleation can now proceed must necessarily be reduced.

This explanation implicitly assumes that, in polyethylene cooled from the melt, nucleation occurs sporadically as distinct from the alternative of growth from pre-determined centres. Much recent work on the crystallization of polymers suggests that the latter frequently appears to occur, though there are indications¹² that predetermined nucleation is a limiting case where sporadic processes have ceased in a time which is small compared with the time for complete crystallization.

Sharples and co-workers¹ suggest that, in thin films, adhesion to the supporting medium, which contracts at a lower rate with fall in temperature, produces a biaxial strain, thus giving rise to a reduction in the nucleation rate, as shown recently by Palmer¹³.

This does not apply in the present case since oxidized films removed from the cover slip and floated on silicone oil during subsequent melting and crystallization runs still produce the type of spherulitic structure shown in *Figure 2*. Nor is it possible by this means to account for the unchanged structure shown here to result from thermal treatment of polyethylene in the absence of air. As has been described already¹, however, once the heat treated polyethylene has been in solution the structure reverts to the original unresolvable state. Present samples recovered from tetralin solution and freed from solvent have been found to behave in this way. Infra-red examination shows that the oxygen containing groups are still present and in the same concentration. It is suggested that temporary crosslinks, formed during the high temperature cycle and dependent upon simultaneous oxidation of neighbouring chains, have been broken and the molecules dispersed. On recovering the polymer from solution these groups are no longer in a position to interact and nucleation can proceed as in the unoxidized material. It is of interest to note in this connection that the melting point of the oxidized polyethylene recovered from tetralin was found to be 132°C compared with the value 129°C before the polymer was dissolved. That the position and orientation of the oxygen containing groups is important is also underlined by the observation¹⁴ that oxidation of polyethylene in bulk, by passing oxygen through the molten polymer, does not produce a significant decrease in the spherulite nucleation density.

*AMF British Research Laboratory,
Blounts Court, Sonning Common,
Reading, Berks.*

(Received March 1964)

REFERENCES

- ¹ BANKS, W., HAY, J. N., SHARPLES, A. and THOMSON, G. *Nature, Lond.* 1962, **194**, 542

THE EFFECT OF OXIDATION ON SPHERULITE SIZE

- BANKS, W., HAY, J. N., SHARPLES, A. and THOMSON, G. *Polymer, Lond.* 1964, **5**, 163
- ² WINSLOW, F. H., ALOISIO, C. J., HAWKINS, W. L., MATREYEK, W. and MATSUOKA, S. *Chem. & Ind.* 1963, 533
- ³ OHLBERG, S. M., ROTH, J. and RAFF, R. A. V. *J. appl. Polym. Sci.* 1959, **1**, 114
- ⁴ DUCH, E. and KÜCHLER, L. *Z. Elektrochem.* 1956, **60**, 220
- ⁵ RUGG, F. M., SMITH, J. J. and BACON, R. C. *J. Polym. Sci.* 1954, **13**, 535
- ⁶ THOMPSON, H. W. and TORKINGTON, P. *Proc. Roy. Soc. A*, 1945, **184**, 3
- CROSS, L. H., RICHARDS, R. B. and WILLIS, H. A. *Disc. Faraday Soc.* 1950, **9**, 235
- ⁷ SMITH, D. C. *Industr. Engng Chem. (Industr.)*, 1956, **48**, 1161
- ⁸ GRASSIE, N. *The Chemistry of High Polymer Degradation Processes*. Butterworths: London, 1956
- ⁹ MANDELKERN, L. *Chem. Rev.* 1956, **56**, 952
- ^{10a} GARNER, W. E., VAN BIBBER, K. and KING, A. M. *J. chem. Soc.* 1931, 1533
- ^{10b} RICHARDS, R. B. *Trans. Faraday Soc.* 1945, **41**, 127
- ¹¹ PRICE, F. P. *J. phys. Chem.* 1960, **64**, 169
- ¹² SHARPLES, A. *Polymer, Lond.* 1962, **3**, 250
- ¹³ PALMER, R. P. *Trans. Plastics Inst.* In press
- ¹⁴ SHARPLES, A. Private communication

Molecular Weight Dependence of Isothermal Long Period Growth of Polyethylene Single Crystals

A. PETERLIN

The long period growth L of polyethylene single crystals during annealing requires an increase in length of all straight sections of every single macromolecule between the fold planes. The material needed has to be transported from the free ends toward the centre of the macromolecule. In order to explain the temperature dependence of long period growth rate, the transport has to proceed by collective jumps of all monomers of one straight chain section between the fold containing surfaces. The number of such jumps needed for a given thickness increase in unidirectional motion or random diffusion is proportional to $(M/L)^2$ and $(M/L)^3$ respectively. The growth rate hence turns out to be strongly dependent on molecular weight M . In the most probable case of random diffusion the L versus $\log t$ curves are shifted by $3 \log M$ to higher times.

The growth rate extremely rapidly increases when the extended chain length is only two, three or even four times larger than the long period L . The transformation of the folded into extended chain crystal in such a case is achieved in a time which roughly equals the time needed for isothermal single crystal growth to $L_{\text{ext.}}/4$. This time, of course, is shorter the lower the molecular weight and the higher the temperature. Such a mechanism may eventually explain the formation of extended chain crystals observed in fractionated samples of low molecular weight isothermally crystallized from melt close to 130°C and in whole Marlex samples crystallized from melt under high pressure at 230°C .

THE experimentally established¹⁻⁶ long period growth of polyethylene single crystals during annealing at constant temperature and especially its dependence on the logarithm of annealing time^{5,6} can be written as⁷

$$L = L^* [1 + 2.303B \log(t + C)] \quad (1)$$

L^* the ordinate intercept of the asymptote ($C=0$) at $t=1$ (see Figure 1'), $C = \exp [(L_0/L^* - 1)/B]$ with L_0 crystal thickness at $t=0$, $2.303L^*B$ slope of the asymptote in the plot of L over $\log t$. A theoretical explanation was suggested by considering the surface nucleation⁵ and the mechanism of mass transport⁷ to the fold planes from the free ends of the macromolecules. The latter may either proceed by successive individual jumps of a single dislocation or by collective jumps of all the monomer units of one straight section of the macromolecule between the fold containing surfaces. It was shown in a previous paper⁷ that collective jumps lead to a temperature dependence of L^*B in agreement with experimental data so that only this case will be treated in that which follows.

Some experiments with fractionated polyethylene by Takayanagi⁸ show a substantial dependence of crystal thickness growth on molecular weight. The smaller M the larger seems to be L^*B . Such a dependence can be

derived from our model by more detailed consideration of the transport mechanism, particularly of the number of jumps necessary for a thickness increase by $d_0 = 2.53 \text{ \AA}$, the length of a monomer unit. This number depends strongly on molecular weight of the sample. With short molecules the transport ways from the ends through the centre of the molecule are relatively short so that the growth rate is larger than with long molecules.

ACTIVATION ENERGY OF CRYSTAL THICKENING

The free energy increase for formation on the fold containing surface of a nucleus of lateral dimension x (quadratic cross section) which is by d_0 thicker than the original crystal reads⁵

$$\Delta F = 4xd_0\sigma - 2x^2d_0\sigma_e/L \quad (2)$$

where σ and σ_e are surface energy density at lateral and fold surface respectively, and L is the long period. For a circular cross section one would have π instead of 4 in the first and $\pi/2$ instead of 2 in the second term. The uncertainty due to the special choice of cross section is actually negligible.

The maximum of free energy increase $\Delta F^* = 2d_0L\sigma^2/\sigma_e$ determines the lateral dimensions $x = x^* = \sigma L/\sigma_e$ of the critical nucleus. It just represents the activation energy for surface nucleation by which the crystal increases its thickness. If the nucleation process is the slowest step in long period growth, the thickening rate turns out to be

$$dL/dt = A \exp(-\Delta F^*/kT) = A \exp(-b'L) \quad (3)$$

By comparison with equation (1) one obtains

$$A = L^*B \exp(1/B)$$

$$b' = 2d_0\sigma^2/\sigma_e kT = 1/L^*B$$

$$dL/d \log t = 2.303L^*B = 1.601\sigma_e kT/d_0\sigma^2 \quad (4)$$

With $\sigma_e = 49$, $\sigma = 12.2 \text{ erg/cm}^2$ and $d_0 = 2.52 \text{ \AA}$ suggested by Hoffman and Weeks⁹, one obtains for the slope of L versus $\log t$ curves $2.303L^*B = 0.208T \text{ [\AA]}$, i.e. 83.6 \AA at 130°C . The nearly twice as large σ_e value postulated recently by Mandelkern *et al.*¹⁰, Frank and Tosi¹¹ and by Wunderlich¹² yields $0.4T$, i.e. 160 \AA at 130°C . The slopes according to equation (4) have the correct order of magnitude although they are markedly larger than the observed values, but completely fail to show the experimentally established strong temperature dependence of L^*B which between 100° and 130° increases by a factor of more than ten (*Figure 1*).

An additional increase in temperature dependence of L^*B is produced by the mass transport mechanism from the free ends of the macromolecule to the fold planes. If one assumes that, in order to transport a monomer unit into the latter, the whole straight section of the chain between the fold planes jumps as an entity by d_0 , the activation energy for such a collective jump is LE_m/d_0 (where E_m denotes the energy barrier between consecutive equilibrium positions of the monomer and L/d_0 is the number of monomers in the section). The growth rate hence, besides, the above mentioned activation energy for nucleation, also contains the activation energy for mass transport and reads

LONG PERIOD GROWTH OF POLYETHYLENE SINGLE CRYSTALS

$$\frac{dL}{dt} = A \exp(-LE_m/d_0kT - 2d_0L\sigma^2/\sigma_e kT) = A \exp(-bL)$$

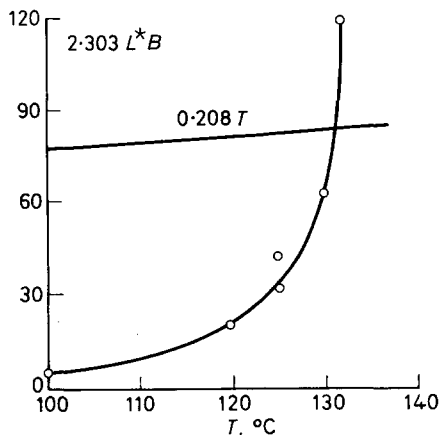
$$b = (E_m/d_0 + 2d_0\sigma^2/\sigma_e)/kT \quad (5)$$

yielding the slope

$$L^*B = 1/b = kT/(E_m/d_0 + 2d_0\sigma^2/\sigma_e) \quad (6)$$

This expression differs from equation (4) by the barrier energy term E_m/d_0 which not only reduces the too high values of equation (4) but also provides, by its temperature dependence, an explanation for the experimental data as shown in *Figure 1*. The rapid increase of L^*B when approaching the

Figure 1—Long period growth rate coefficient $2.303L^*B = dL/d \log t$ from equation (1) as a function of temperature according to Fischer and Schmidt⁶. The broken line $0.208T$ is calculated from equation (4) with Hoffman and Weeks's data⁹ for $\sigma_e/\sigma^2 = 0.33$



melting point is a consequence of the rapid decrease of E_m in good agreement with different estimates of the lattice force field as a function of temperature¹³. With increasing unit cell expansion, the energy barriers separating the equilibrium positions of monomers rapidly decrease and nearly vanish at the melting point. The activation energy E_m derived from experimental values L^*B agree fairly well with data calculated from unit cell expansion⁷.

Equations (3) and (5) differ in the value of the coefficients b' and b but are identical as far as the dependence on L and t is concerned. By introducing homogeneous coordinates $\lambda = b'L$ or bL respectively and $\tau = At$ both can be written as

$$d\lambda/d\tau = e^{-\lambda} \quad (7)$$

with the general solution

$$e^\lambda = \tau + \tau_0 \quad (8)$$

By putting the integration constant $\tau_0 = 0$ one obtains the asymptotic solution $\exp(\lambda) = \tau$ or $\lambda = 2.303 \log \tau$ plotted in *Figure 3*.

DETAILED TRANSPORT MECHANISM

The coefficient A in equation (5) contains all other factors which, besides the activation energy, affect the mass transport. Among them the most important are the frequency ν of longitudinal oscillation of the straight segment and the number of jumps needed for the transport of monomer units from the free ends to the fold planes. The frequency ν given by the

restoring force f and the mass M_0 of the monomer as $\nu = (f/M_0)^{1/2}/2\pi$ turns out to be independent of the length L of the straight section and of the degree of polymerization $P = M/M_0$. It therefore does not affect the growth rate as far as its dependence on L and M is concerned. The number of jumps needed for an increase of long period by d_0 , however, is smaller the shorter the chain and the longer the straight sections. A chain of length Pd_0 has $n = Pd_0/L$ straight sections (Figure 2). In order to increase the thickness by d_0 , one has to transport n monomers from the free ends into internal straight sections between the fold planes, $n/2$ from each side.

If the transport is *unidirectional*, i.e. every jump is in the right direction so that it transports monomers from the free ends to the internal folds, and if, for sake of simplicity, one assumes that the thickness increase is achieved by adding one monomer to each fold so that the crystal grows in thickness by $d_0/2$ at each fold containing surface, the extreme sections have to jump $(n-1)/2$ times each (n odd), the next section $(n-3)/2$ times and so on through the central section which does not have to jump at all. If n is

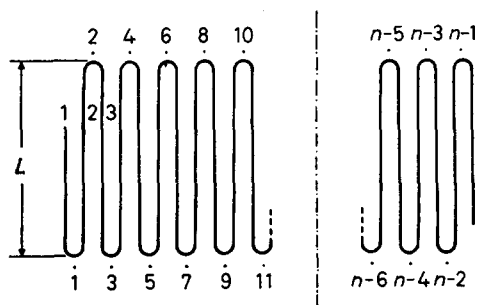


Figure 2—Polyethylene macromolecule in folded chain crystal with $n = Pd_0/L$ straight sections and $n-1$ folds. In order to increase the thickness by d_0 (length of monomer), one has to add one monomer at every fold, i.e. altogether $n/2$ or $n/2-1$ monomers have to be transported from each end of the macromolecule

even, one has to start on one side with $n/2$ and on the other side with $(n/2-1)$ jumps and then decrease the number by one at every subsequent section. Altogether one needs $(n-1)(n+1)/8 \sim n^2/8 = (Pd_0/L)^2/8$ jumps from each end of the macromolecule. The growth rate hence reads

$$dL/dt = 8\nu (L/Pd_0)^2 e^{-bL} = d'L^2 e^{-bL}$$

$$d' = 8\nu/P^2 d_0^2 \tag{9}$$

or in homogeneous coordinates $\lambda = bL$, $\tau = d't/b = t\tau^*$

$$d\lambda/d\tau = \lambda^2 e^{-\lambda} \tag{10}$$

The solution turns out to be

$$\overline{Ei}(\lambda) - e^\lambda/\lambda = \tau + \tau_0$$

$$\overline{Ei}(\lambda) = \int_0^\lambda (e^x/x) dx \tag{11}$$

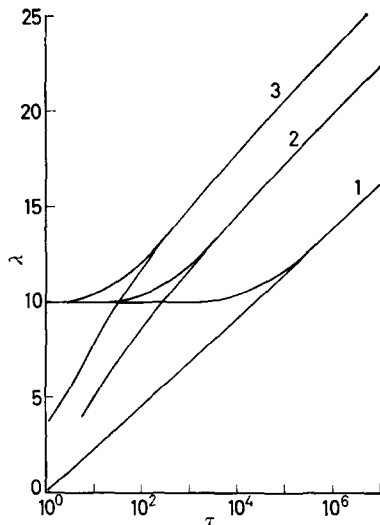
0.3725

The integration constant $\tau_0 = C\tau^*$ is given by the long period value L_0 at $\tau = t = 0$. The constant 0.3725 corresponds to the function tabulated by

Jahnke and Emde¹⁴. The asymptotic solution according to equation (11), plotted in *Figure 3* as a function of $\log \tau$, is situated above the values $\lambda = 2.303 \log \tau$ of the asymptotic solution of equation (7). This is a consequence of the factor λ^2 in equation (10).

However, since there is no force pulling the monomers and the straight sections in the right direction, unidirectional motion is rather unlikely. One has to assume that the whole transport proceeds by *random diffusion*. In

Figure 3—Reduced long period λ (asymptotic solution, $C=0$) as a function of $\log \tau$ according to equation (7) [1], equation (11) [2] and equation (15) [3]. The growth of initial length λ_0 with time is also shown. From λ_0 one obtains the integration constant τ_0 . The ratio τ_0/τ^* determines how rapidly the crystal grows.



such a case the number of jumps for transporting one monomer from the end of the macromolecule to any fold is equal to half the square of unidirectional jumps needed for the same transport. Consequently, the total number of jumps from one end of the macromolecule for increasing the thickness by d_0 turns out to be

$$(n-1)n(n+1)/24 \sim n^3/48 = (Pd_0/L)^3/48 \quad (12)$$

The rate of thickness growth reads

$$\begin{aligned} dL/dt &= 48\nu (L/Pd_0)^3 \exp(-bL) = aL^3 \exp(-bL) \\ a &= 48\nu/P^3d_0^3 \end{aligned} \quad (13)$$

or in homogeneous coordinates $\lambda = bL$, $\tau = at/b^2$

$$d\lambda/d\tau = \lambda^3 e^{-\lambda} \quad (14)$$

with the solution (*Figure 3*)

$$f(\lambda) = \frac{1}{2} [\overline{Ei}(\lambda) - e^\lambda/\lambda - e^\lambda/\lambda^2] = \tau + \tau_0 \quad (15)$$

The corresponding plot of the asymptotic solution as a function of $\log \tau$ (*Figure 3*) is situated above that from equations (7) or (11).

A comparison of the three curves shows only slight changes in slope due to the factors λ^2 and λ^3 . With the exception of the area at rather small τ

between 1 and 10^2 where the curves 1 and 2 increase more rapidly, the slope is roughly 2.303 yielding $2.303/b$ for the L versus $\log t$ plot. The details of the transport mechanism (unidirectional flow or random diffusion) only influence the constant a which shifts the log time scale against that of $\log \tau$ but in practice do not influence the slope. This result also applies when the mass transport is performed by individual jumps of Reneker's type dislocations. For unidirectional motion one obtains $d\lambda/d\tau = \lambda \exp(-\lambda)$ and for random diffusion $\lambda^2 \exp(-\lambda)$ with $\lambda = b'L$ [see equation (3)]. In a λ versus $\log \tau$ plot the corresponding solutions $\tau = \overline{Ei}(\lambda)$ and $\overline{Ei}(\lambda) - \exp(\lambda)/\lambda$ have slopes practically identical with $\exp(\lambda)$, i.e. $2.303/b'$. Therefore, also with mass transport by individual jumps of dislocations the detailed consideration of the number of jumps needed for long period growth does not markedly change the much too small temperature dependence of the growth rate⁷.

In order to obtain the time dependence of long period for a crystal with initial thickness λ_0 at $\tau=0$ one has to determine the integration constant $\tau_0 = f(\lambda_0)$, i.e. the abscissa of the intercept of the asymptote with the horizontal line through the ordinate λ_0 . The complete solution λ as a function of $(\tau + \tau_0)$ starts as a horizontal line with the ordinate intercept λ_0 . With approaching $\tau = \tau_0$ it gradually bends into the asymptote as shown in *Figure 3*. The transition is rather sharp so that the deviation from the horizontal part or from the asymptote is below one per cent when $\log \tau$ differs from $\log \tau_0$ by ± 1 . The curves in *Figure 3* explain very well the extremely rapid growth of long period when λ_0 is smaller than λ^* , the asymptotic reduced crystal thickness at $t=1$, i.e. at $\tau^* = a/b^2$ (random diffusion) or a'/b (unidirectional transport) respectively. In such a case the constant $C = b^2\tau_0/a$ or $b\tau_0/a'$ respectively is smaller than the time unit (for instance, 1 min) and the crystal grows from λ_0 to λ^* in a time smaller than the unit. If, however, the crystal has an initial thickness $\lambda_0 > \lambda^*$ the constant C is large, the growth is drastically reduced and may be even unnoticeable during normal observation time. The value τ_0 , or still better τ_0/τ^* , determines the time scale for long period growth during isothermal annealing of crystals with initial length λ_0 .

The curves in homogeneous coordinates λ, τ may be adapted easily to specific experimental data, i.e. to the intercept L^* and the slope $2.303L^*B$ at the intercept ($t=1$) by considering the following relationship

$$\begin{aligned} d\lambda/d \ln \tau &= \tau / (d\tau/d\lambda) = \tau \lambda^3 / e^\lambda \\ \lambda^* / (d\lambda/d \ln \tau)^* &= L^* / (dL/d \ln t)^* = L^* / L^* B = 1/B \\ &= \exp \lambda^* / \tau^* \lambda^{*2} \\ B &= (dL/d \log t)^* / 2.303 L^* \\ \tau^* &= B e^{\lambda^*} / \lambda^{*2} \end{aligned} \tag{16}$$

The last equation can be solved graphically by plotting, in addition to the curve λ as a function of $\log \tau$, the curve $\tau = B \exp \lambda / \lambda^2$ (*Figure 4*). The intersection yields λ^* and τ^* corresponding to L^* and $t=1$ respectively, and hence $b = \lambda^* / L^*$ and $a = \tau^* b^2$.

LONG PERIOD GROWTH OF POLYETHYLENE SINGLE CRYSTALS

From the data of Fischer and Schmidt one obtains $L^* = 240 \text{ \AA}$ and $2.303L^*B = 62 \text{ \AA}$ for $T_a = 130^\circ\text{C}$ yielding $1/2.303B = 3.84$ and $\log \tau = \lambda/2.303 - 2 \log \lambda - 0.947$. The latter curve is nearly parallel to $\tau = f(\lambda)$ so that graphically the intersection cannot be determined with high

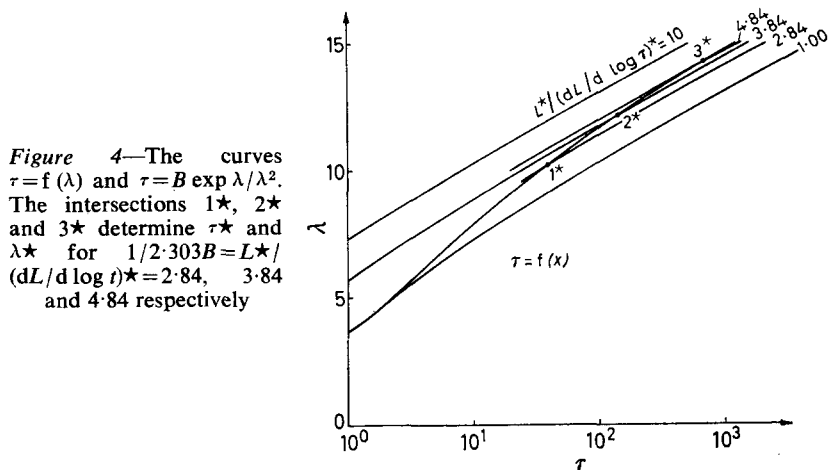


Figure 4—The curves $\tau = f(\lambda)$ and $\tau = B \exp \lambda/\lambda^2$. The intersections 1^* , 2^* and 3^* determine τ^* and λ^* for $1/2.303B = L^*/(dL/d \log t)^* = 2.84, 3.84$ and 4.84 respectively

precision. One obtains $\lambda^* = 12.36$ and $\tau^* = 2.24$ yielding $b = 0.0515 \text{ \AA}^{-1}$ and $a = 2.24 \text{ min}^{-1}$. In Figure 4 two additional curves with $1/2.303B = 2.84$ and 4.84 are plotted, leading to $\lambda^* = 10.16$ and 14.55 , $\tau^* = 1.60$ and 2.95 respectively. The higher B the more the $\tau = B \exp \lambda/\lambda^2$ curve is shifted to the right, leading to a smaller λ^* and τ^* and consequently to a smaller b and a .

The molecular weight dependence of long period growth is contained in the factor a . According to equation (13), it is inversely proportional to the third power of molecular weight

$$a_M = a_0 (M_0/M)^3 \tag{17}$$

where a_0 corresponds to M_0 . The same applies to the homogeneous coordinate

$$\tau_M = \tau_0 (M_0/M)^3 \tag{18}$$

The λ curve consequently is shifted horizontally by $3 \log (M/M_0)$ in the λ versus $\log \tau$ plot (Figure 5). The curve in the centre corresponds to annealing of Marlex 50 at 130°C , the left and the right one to a polyethylene sample with ten times smaller and larger molecular weight respectively. With any initial long period L_0 of polyethylene crystals one obtains a family of curves [equation (15)] corresponding to different molecular weights. The smaller P or M the sooner the horizontal section bends in the asymptote, the shorter the times for significant increase of long period. At any given time the crystal thickness, due to isothermal annealing, is markedly greater for low than for high molecular weight samples. The resulting change in long period growth rate is spectacular. Single crystals with 200 \AA initial length grow to 300 \AA thickness in 10^{-2} , 10 and 10^4 minutes, 400 \AA in 0.4 , 4×10^2 and 4×10^3 minutes, respectively. However,

one must not forget that some modifications of our final results [equation (15)] are necessary as soon as the extended chain length Pd_0 is not a great many times larger than L . This correction has first to be applied to the left curve in *Figure 5* with the smallest molecular weight.

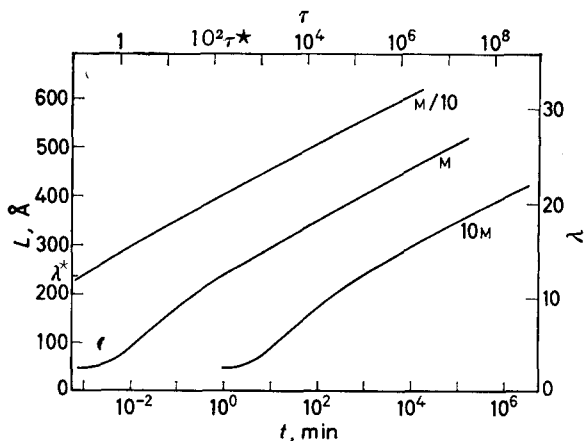


Figure 5—Horizontal shift of asymptotic λ versus $\log \tau$ curves with degree of polymerization of polyethylene. The central curve corresponds to annealing at 130°C of Marlex 50 single crystals ($\tau^* = 2.24$, $\lambda^* = 12.36$)

With mass transport by individual jumps of Reneker type dislocations the molecular weight dependence is similar to that in equations (17) and (18) with the second instead of third power in (M_0/M) . Consequently the time scale in λ versus $\log \tau$ curves is shifted horizontally by $2 \log M$, the molecular weight dependence is a little smaller than in the above treated case of collective jumps.

Because annealing also takes place during isothermal crystallization¹⁵, the long period in the solidified sample will be larger for low than for high molecular weight polyethylene. The effect is more conspicuous the higher the chain mobility, i.e. the closer the crystallization temperature to the melting point. At lower temperatures the growth rate soon becomes so small that the increase of long period during isothermal crystallization is not very important.

LONG PERIOD GROWTH AT SMALL Pd_0/L

The above considerations are a rather good approximation for large values of $n = Pd_0/L$ but they fail at small n because one has replaced the correct expression for the number of necessary jumps by the one term with the highest power of n [equation (12)]. Moreover, one completely neglected the fact that as a rule the sections containing the free ends of the folded macromolecule are shorter than L and consequently, due to a smaller activation energy, can jump much faster than a full length section. As a consequence, with low n , e.g. 2, 3 or even 4, the long period growth during isothermal annealing is markedly accelerated as compared with our data

for large n . In this case, only the sections containing the free ends of the macromolecule have to jump in order to increase the long period. The first jump at the most requires an activation energy $E_m L/d_0$, the next one $E_m(L/d_0 - 1)$ and so on. The long period growth proceeds faster and faster like an avalanche until such a crystal transforms into an extended chain crystal.

Let us assume that at the beginning one has $Pd_0 = 4L_0$, i.e. four straight sections are parts of a single macromolecule. For the sake of simplicity, the number of monomers in the three folds will be neglected. The length L' of the section containing the free end of the macromolecule is connected with the long period L by

$$L' + L = 2L_0 \quad (19)$$

The growth rate of crystal thickness turns out to be

$$\begin{aligned} dL/dt &= (\nu d_0/2) \exp [-(L'E_m/d_0 + \Delta F^*)/kT] = a'' e^{-b''L} \\ a'' &= (\nu d_0/2) \exp (-2L_0 E_m/d_0 kT) \\ b'' &= (E_m/d_0 - 2d_0 \sigma^2/\sigma_e)/kT \end{aligned} \quad (20)$$

with the solution

$$\begin{aligned} e^{-\lambda} &= \tau_0 - \tau \\ \lambda &= b''L & \lambda_0 &= b''L_0 \\ \tau &= a''b''t & \tau_0 &= e^{-\lambda_0} \end{aligned} \quad (21)$$

The crystal redoubles its thickness ($\lambda_2 = 2\lambda_0$) in $\tau_2 = \tau_0(1 - \tau_0)$, i.e. in time t_2 where

$$\begin{aligned} t_2 &= \exp(-b''L_0) [1 - \exp(-b''L_0)] / a''b'' \\ &= \exp(bL_0) \times [1 - \exp(-b''L_0)] 2kT / \nu d_0 (E_m/d_0 - 2d_0^2 \sigma^2/\sigma_e) \end{aligned} \quad (22)$$

The main contribution is that of the first factor. If, in the brackets, one neglects the negative term, t_2 roughly equals the time needed for crystal thickness to grow to L_0 from any initial value lower than L_0 . This may be a very short time. A similar consideration can be applied to the last step by which the thickness increases from $2L_0$ to $4L_0$ and the folded chain crystal transforms into an extended chain crystal.

Such a transformation may occur preferentially with low molecular weight samples where the extended chain length Pd_0 is not a great many times larger than L . In the case studied by Anderson¹⁶, samples with M below 12 000, i.e. Pd_0 below 1 100 Å, yielded extended chain crystals when slowly crystallized at nearly 130°C. At such a temperature L_0 is between 200 and 300 Å, and one has exactly the case of avalanche-like long period growth. At a lower crystallization temperature, however, the starting long period and, to a still higher degree, the mobility are so much smaller that folded chain crystals may persist and remain nearly unchanged during crystallization. This applies particularly when crystallization occurs during rapid cooling or quenching. Of course, the lowest temperature at which, during isothermal crystallization, the initially folded chain crystals are

transformed into extended chain crystals depends on the molecular weight of the sample. It decreases with decreasing M . On the other side, with larger M one had to go so close to the melting point in order to obtain a sufficiently large long period $L \sim Pd_0/4$ that such an experiment is very likely to be extremely difficult to perform.

Extended chain crystals obtained with unfractionated polyethylene at high temperature (230°C) and high pressure¹⁷ may very likely be explained in a similar way. Due to the high pressure the free energy difference between the crystal and the melt is reduced, the length L_n of the minimum stable nucleus increased. If now this length becomes close to one quarter of the extended chain length of polyethylene molecules in the sample, the avalanche-like long period growth rapidly transforms the folded into extended chain crystals. The non-uniform length of these crystals is most likely due to the local fluctuation of average molecular weight.

The author gratefully acknowledges the financial support of this work by the Camille and Henry Dreyfus Foundation.

*Camille Dreyfus Laboratory,
Research Triangle Institute,
P.O. Box 490, Durham, N.C.*

(Received April 1964)

REFERENCES

- ¹ KELLER, A. and O'CONNOR, A. *Disc. Faraday Soc.* 1958, **25**, 114
- ² RÅNBY, B. G. and BRUMBERGER, H. *Polymer, Lond.* 1960, **1**, 399
- ³ STATTON, W. O. and GEIL, P. H. *J. appl. Polym. Sci.* 1960, **3**, 357
- ⁴ STATTON, W. O. *J. appl. Phys.* 1961, **32**, 2332
- ⁵ HIRAI, N., YAMASHITA, Y., MATSUHATA, T. and TAMURA, Y. *Rep. Res. Lab. Surface Sci., Okayama U.* 1961, **2**, 1
- ⁶ FISCHER, E. W. and SCHMIDT, G. *Angew. Chem.* 1962, **74**, 551
- ⁷ PETERLIN, A. *Polymer Letters*, 1963, **1**, 279
- ⁸ TAKAYANAGI, M. *Rep. Progr. Polymer Phys. Japan*, 1964, **7**, 77
- ⁹ HOFFMAN, J. D. and WEEKS, J. J. *J. chem. Phys.* 1962, **37**, 1723
- ¹⁰ MANDELKERN, L., POSNER, A. S., DORIO, A. F. and ROBERTS, D. E. *J. appl. Phys.* 1961, **32**, 1509
- ¹¹ FRANK, F. C. and TOSI, M. *Proc. Roy. Soc. A.* 1961, **263**, 323
- ¹² WUNDERLICH, B. *J. Polym. Sci. A*, 1963, **1**, 1245
- ¹³ PETERLIN, A., FISCHER, E. W. and REINHOLD, CHR. *J. Polym. Sci.* 1962, **62**, 559
PETERLIN, A., FISCHER, E. W. and REINHOLD, CHR. *J. chem. Phys.* 1962, **37**, 1403
- ¹⁴ JAHNKE, E. and EMDE, F. *Tables of Functions.* Dover: New York, 1945
- ¹⁵ WEEKS, J. J. *J. Res. Nat. Bur. Stand. A*, 1963, **67**, 441
PETERLIN, A. *J. appl. Phys.* 1964, **35**, 75
- ¹⁶ ANDERSON, F. R. Paper BB4 in *Electron Microscopy*, edited by S. S. Breese, Jr. Academic Press: New York, 1962
ANDERSON, F. R. *J. appl. Phys.* 1964, **35**, 64
- ¹⁷ GEIL, P. H., ANDERSON, F. R., WUNDERLICH, B. and ARAKAWA, T. *J. Polym. Sci. A*, 1964, **2**, 3707

The Upturn Effect in the Non-Newtonian Viscosity of Polymer Solutions

Mrs S. P. BUROW, A. PETERLIN and D. T. TURNER

Previously consideration of the hydrodynamic consequences of the separation of the segments of a macromolecule in laminar flow has led to the prediction that a very long polymer molecule in an extremely viscous solvent should have a limiting viscosity number which increases with the gradient G or, more precisely, with the parameter $\beta = M[\eta]_0 \eta_0 G / NkT$ which is defined below. Experiments in Cannon-Fenske and Single-Pass capillary viscometers reveal such upturns of viscosity in solutions of polymethylmethacrylate in Aroclor and polyisobutene in polybutene oligomers which, as predicted, are very sensitive to molecular weight (1 to 7×10^6) and solvent viscosity ($\eta_0 = 1$ to 100 poise). A satisfactory comparison with theory is presented using values of $[\eta] = \eta_{sp}/c$, extrapolated to $c=0$, for solutions of polymethylmethacrylate in Aroclor in the concentration range 0.125 to 2.0×10^{-3} g/cm³.

IT HAS been predicted theoretically¹ that the ratio of the limiting viscosity numbers at shear stresses τ and zero, $[\eta]/[\eta]_0$, may increase with increase of $\beta = M[\eta]_0 \eta_0 G / NkT$: where M denotes the number average molecular weight; η_0 is the viscosity of solvent; G is the velocity gradient; N is Avogadro's number; k is Boltzmann's constant; and T is absolute temperature. The increase is a consequence of the separation of the segments of a macromolecule in laminar flow, and may be explained by reference to *Figure 1* which suggests the rotation and periodic ellipsoidal expansion of a macromolecule at a velocity gradient G . This behaviour brings into play two opposing contributions to $[\eta]$ due to the changing hydrodynamic interactions of the segments. There is a negative contribution arising from the opposing movement of segments in opposite quadrants and a positive one

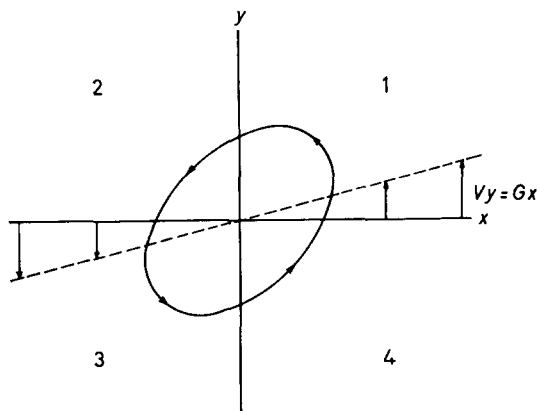


Figure 1—Distortion of a flexible macromolecule as it rotates in laminar flow. V_y is the velocity along the y axis

from the cooperative movement of segments in the same quadrant. These contributions modify the value of Λ , the mean hydrodynamic resistance

coefficient of a segment, to be used in equation (1) in a way which has been related to average molecular expansion and introduces a dependence on shear stress. Let Z be the number of statistically independent links in the macromolecule and R the radius of gyration; then

$$[\eta] = (NZR^2/6M) \Delta \quad (1)$$

Segment separations actually occur periodically as, during each rotation, the macromolecule is twice extended (in quadrants 1 and 3) and twice compressed (in quadrants 2 and 4). The extent of segment separation depends on the inherent flexibility of the macromolecule and on the frequency of application and magnitude of the shear stress. The time of application of the shear stress is inversely proportional to the angular frequency, $G/2$. Therefore, the upturn effect should be favoured by using an extremely viscous solvent which results in the application to the macromolecules of a very high shear stress, τ , at low gradients ($\tau = \eta_0 G$). Moreover, the upturn effect is expected to be more pronounced the longer the macromolecule (cf. *Figure 11*, with Z as parameter).

The bulk of experimental work on polymer solutions has been with solvents of viscosity *ca.* 10^{-2} P and shows that, under such conditions, $[\eta]$ only decreases with increasing G . There have been a few investigations^{2,3} with more viscous solvents ($\eta_0 \sim 1$ to 10^2 P) which revealed upturns in viscosity, but it is uncertain whether such data can be adduced to support the theory described above. A direct test of the theory with solutions of polystyrene ($M_w = 4.7$ and 10.6×10^6) did not reveal⁴ any upturn in $[\eta]/[\eta]_0$. Subsequently, upturns in viscosity were observed with the following solutions⁵⁻⁷: polystyrene and polymethylmethacrylate (PMMA) in Aroclor, and polyisobutene in polybutene oligomers. It was suggested that such behaviour may be rather general for solutions of very long macromolecules in extremely viscous solvents. With PMMA in Aroclor, values of $[\eta]$ were obtained which provided evidence that the upturn effect is intramolecular in origin but were defined by approximately co-linear values of η_{sp}/c for only three concentrations, a fourth being either erratic or inconsistent⁷. The present paper reports more precise data and offers an experimental check of the theoretical predictions of *Figure 11*.

EXPERIMENTAL

Materials

Polymethylmethacrylates (PMMA: $M_w = 1.1$ and 4.2×10^6) were prepared by Dr A. Schindler, by bulk polymerization of the purified monomer to < 10 per cent conversion with azobisisobutyronitrile at 50° and 60°C; the polymer was purified by precipitation. Donated samples of polyisobutene (PIB) had the following viscosity average molecular weights (toluene at 25°): Dr J. Rehner, Jr (Esso Research), 6.3×10^6 ; Dr W. Philippoff (Esso Research), 3.6×10^6 , Vistanex, 1.3×10^6 . Samples of Aroclor (a chlorinated diphenyl) were donated by the Monsanto Chemical Co. and polybutene oligomers by the Amoco Chemical Corpn.

Preparation of solutions

Polymer (0.2g) was dissolved in a mobile solvent (25 cm³: PMMA in chloroform; PIB in petroleum ether, b.pt 40° to 60°C) containing 0.1 per

NON-NEWTONIAN VISCOSITY OF POLYMER SOLUTIONS

cent *tert.* butyl catechol as antioxidant. This solution was thoroughly mixed with the viscous solvent (100 cm³) and the volatile solvent then pumped off *in vacuo* at 50° with occasional gentle stirring. After about two weeks, when no further evolution of solvent was apparent, the above treatment was prolonged for a further week and the solution then assumed to be free of the volatile solvent. Solutions prepared in this way were diluted with the viscous solvent to provide concentrations in the range 2.0 to 0.125 × 10⁻³ g/cm³ which were used in experiments to obtain values of $[\eta]$.

In one experiment solutions of each concentration of PMMA were made up separately (results in *Figure 6*). The solutions were pumped *in vacuo* in pairs and the rate of removal of solvent found to be much slower than in the previous experiments with single solutions. After five weeks the excess weight with reference to the (Aroclor + polymer) was reduced to 0.3 to 0.5 per cent for all the solutions and the similarly treated Aroclor. No further loss of weight occurred after one week of further pumping and it was concluded that, substantially, all the chloroform had been removed.

Previous work indicates that polymer degradation occurs readily on shearing viscous solutions of long macromolecules^{2,3,5,8}. The present solutions were also found to be very sensitive in this respect and, therefore, stirring of cold solutions was avoided as far as practicable. For the same reason, the solutions were not strained through porous sinters as is otherwise the preferred practice with solutions prior to polymer characterization.

Viscometry

Mr J. P. Knudsen (Chemstrand Research Center) kindly undertook the accurate measurement of some of the capillary radii in viscometers which were used to calibrate others by comparison of flow times of Aroclor and NBS standards. The viscometers are specified in *Table 1*. The numbers 8 and 3 following viscometer initial letter designation refer to the approximate radius of the capillary in cm × 10²; subsequently, it is sometimes convenient to refer to these values as 'wide' and 'narrow' capillaries, respectively.

Table 1. Specification of viscometers

<i>Character</i>	<i>Cannon-Fenske (U-tube)</i>			<i>Single-Pass</i>
	<i>CF8A</i>	<i>CF8B</i>	<i>CF3</i>	<i>SP8</i>
<i>R</i> (cm)	0.0805	0.0816	0.027	0.08
<i>L</i> (cm)	7.7	7.7	7.5	8.5
Efflux volume (cm ³)	1.517	1.586	1.5	variable
Filling volume (cm ³)	10	10	10	variable

Liquids were forced through capillaries under air pressures of up to 100 cm of mercury, measured with a mercury manometer, which virtually were kept constant during runs by a manostat of large volume. Viscometers were immersed in baths kept at constant temperature accurate to ±0.015°. In the *Cannon-Fenske* viscometer the time (*t*) to fill the efflux volume (*v*) was observed against a rising meniscus. To allow for displacement of

liquid levels in the viscometer during a run, a back pressure of 1.17 cm of mercury was subtracted from the manometer readings to give the driving pressure (P). The liquid was pressed back gently with a rubber air bulb and 15 minutes allowed for the viscous liquid to drain from the walls before making a further run. In the *Single-Pass* viscometer the sheared liquid is rejected after a single pass through the capillary into a horizontal side arm, in which v/t may be estimated by following the travel of the meniscus. From time to time this method was checked by expulsion of the liquid into a small fixed volume. In both these efflux measurement techniques pressure corrections due to changing liquid levels during a run were negligible and so the driving pressure was read directly from the manometer.

Analysis of results

In a capillary tube the shear stress varies from zero along the axis to a maximum value, $\tau_{\max.} = RP/2L$, at the wall. The viscosity and gradient at the wall may be calculated for a non-Newtonian liquid from the following equations due to Claesson and Lohmander⁹:

$$\eta = \pi R^4 P t / 2 V L [3 + F(P)]$$

$$G = V [3 + F(P)] / \pi R^3 t$$

$$F(P) = -d \ln t / d \ln P$$

Experimental plots of $F(P)$ in preliminary experiments gave straight lines of slope not more than 1.2. Because of the smallness of the corrections involved, $F(P)$ has been taken as unity throughout this work and Poiseuille's equation used without modification to calculate a measure of viscosity which will be termed the 'apparent' viscosity.

In preliminary experiments with Aroclor 1248 the kinetic energy correction was found to be less than one per cent even for the highest values of P and, therefore, was neglected in all subsequent work.

RESULTS AND DISCUSSION

Polymer degradation

Figure 2 shows in detail how the apparent viscosity, η^* , of a $1.0 \times 10^{-3} \text{g/cm}^3$ solution of PMMA changes over a whole range of driving pressures, up to 40 cm of mercury, in successive runs irrespective of whether P is increased or decreased. In run 5 readings were continued up to a higher pressure, 80 cm of mercury, and this is partly responsible for the more drastic drop of η^* in run 6. However, it should also be noted that this effect is exaggerated because run 5 is unusual in giving higher values of η^* than run 4. This general behaviour together with occasional reversals similar to that observed in runs 4 and 5, has been observed in other PMMA solutions covering the concentration range of 0.25 to $2.0 \times 10^{-3} \text{g/cm}^3$. Runs 1 and 5 of the lowest concentration are also conveniently shown in the figure. In addition, similar but less extensive results have been reported previously for a solution of polyisobutene in a polybutene oligomer⁶. The viscosity of the solutions does not change even after standing for several days and therefore it seems certain that irreversible changes occur during shearing which are probably due to polymer degradation. It would be desirable to check this point in more conventional solvents but, unfor-

tunately, attempts to recover the polymer quantitatively from Aroclor have not been successful.

There have been many reports of polymer degradation in solvents of viscosity of the order 10^{-1} to 10^{-2} P at high velocity gradients of the order 10^4 to 10^5 sec^{-1} . The consensus of opinion in such cases is that degradation is caused by the interaction of macromolecules and in one case; for PIB in a mixture of mineral oil and kerosine, it has been reported that this opinion

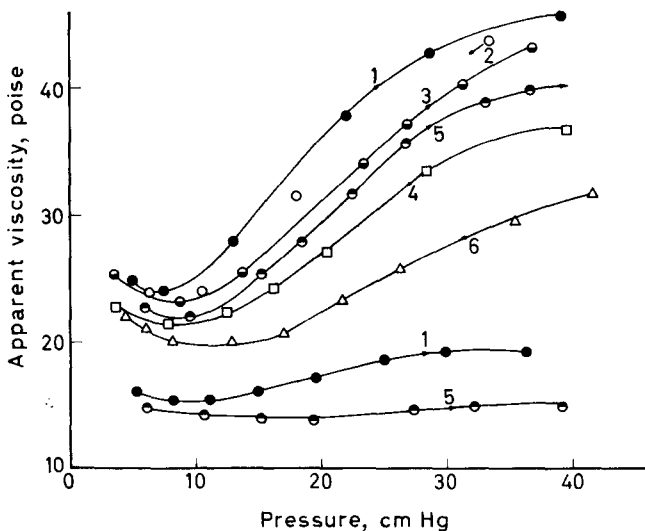


Figure 2—Effect of repeated shearing of a PMMA solution in a CF8 viscometer. Temperature 15°C. Arrowheads indicate whether successive measurements were made at increasing (→) or decreasing pressures

is borne out by extrapolation of data to infinite dilution¹⁰. The present findings are of interest in that degradation occurs at very low gradients of $< 10^2 \text{ sec}^{-1}$ and, following on from the viewpoint that the upturn is intramolecular in origin, it is tempting to suspect that this is also likely to be true of the closely related degradation reaction. The direct degradation of polymers by shearing forces exerted on single molecules by the solvent, $\tau_{\text{max.}} \sim 4 \times 10^5 \text{ dyne/cm}^2$ for $P=40 \text{ cm}$ of mercury, would be of particular interest because there appears to be more hope of theoretical treatment, as shown for example by the work of Frenkel¹¹, than in the intermolecular case. So far, however, experiments designed to decide whether the degradation observed in these experiments is inter- or intra-molecular have proved inconclusive.

One point which is clear about polymer degradation in the present solutions is that it can have an enormous influence on the upturn effect. This was encountered in an extreme form in an experiment to compare wide and narrow capillaries, CF8 and CF3 viscometers, as shown by Figure 3 in which η^* is plotted against $\tau_{\text{max.}}$, instead of P . The wide capillary gives the usual upturn but little or no such effect is observed with the

narrow one. The reason for this behaviour is clarified by a further experiment with a fresh charge of unshered solution in the narrow capillary viscometer. A first measurement gave a value for η^* comparable (although lower) to the value obtained with the wide capillary. The solution, instead of being forced back with an air bulb as in the convenient standard pro-

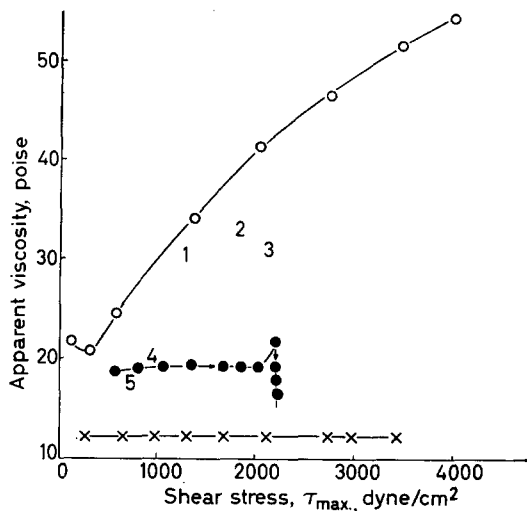


Figure 3—Comparison of CF8 and CF3 viscometers. PMMA in Aroclor 1248; 1×10^{-3} g/cm³; temperature = 15°C. ○ Solution in CF8 viscometer; ● Solution in CF3 viscometer; 1–5 Solution in CF3 viscometer, free-fall drainage; × Solvent in CF8 and CF3

cedure, was allowed to drain through the capillary overnight before each further run. Viscosity values consistent with an upturn are also suggested by the results for runs 1 to 3 but there is additionally an indication of a progressive degradation which is most evident in runs 4 and 5.

Other factors which may affect viscosity

Apart from polymer degradation, there are at least two other factors which may influence the viscosity of the solutions studied here. The first of these relates to the observation that the more concentrated ones appear to be visco-elastic. Davies⁸ has observed, previously that a 2 per cent solution of PMMA ($M = 0.25 \times 10^6$) in a low viscosity solvent (η_0 of the order 10^{-2} P) is visco-elastic. Further, when forced through an Ubbelohde viscometer it gives an upturn which occurs at gradients $\geq 5 \times 10^2$ sec⁻¹, the value apparently depending on the ratio of R/L for the capillary. Theoretically, it seems obscure why visco-elasticity should lead to an upturn but the fact that it is observed in both sets of experiments coupled with the fact that Davies phenomenologically related results are unexplained should be noted.

A second very unusual factor which might be suspected of influencing the viscosity of these solutions is suggested by experimental observations which, so far, have been limited to a 1.0×10^{-3} g/cm³ solution of PMMA. Shearing at constant gradient has been found to result in time-dependent changes of viscosity, streaming birefringence and extinction angle¹². For example, when the solution is sheared at 18 sec⁻¹ in a cone-and-plate viscometer, the viscosity gradually increases towards a maximum value in

about three minutes and then decreases again in a comparable time to something near its initial value. If the solution is stationary for 15 minutes or more, depending on the temperature, the cycle may be repeated. This effect is not yet clear even on a phenomenological basis but, in view of the long relaxation times and of the fact that it does not occur at lower concentration, it would appear to be intermolecular in origin.

The time-dependent viscosity effect raises two questions in connection with the present work. First, does any viscosity build-up occur during successive runs in a Cannon-Fenske viscometer? Direct comparison of a solution in CF8 and SP8 viscometers suggests that this is unimportant under the present experimental conditions (*Figure 4*). Secondly, is an effect of this kind of importance during the time the molecules are sheared in the capillary tube? On the average, a molecule traverses the capillary tube in $\pi R^2 L t / V$ sec and, from the representative results in *Figure 3* (o), this takes

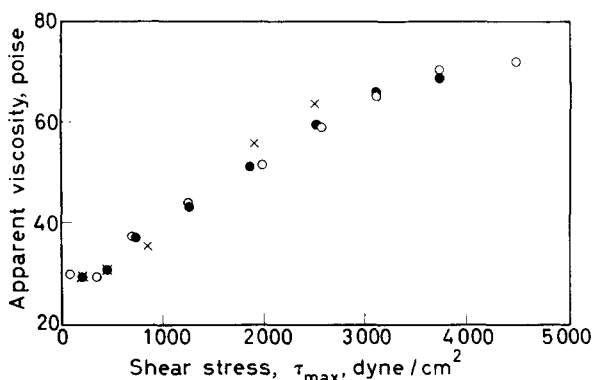


Figure 4—Comparison of CF8 and SP8 viscometers. PMMA in Aroclor 1248; 2×10^{-3} g/cm³; temperature = 15°C. × CF8 data, P increasing in succeeding runs; ● SP8 data (side arm efflux); ○ SP8 data (efflux bulb)

about 14 sec at the upturn ($t \sim 135$ sec). At the present stage of knowledge, the consequences of this fairly prolonged shearing cannot be assessed.

Extrapolation of viscosity data to infinite dilution

It is difficult to assess in detail the effects mentioned in the preceding section but since they are all intermolecular in origin it should be possible to eliminate their viscosity contribution by extrapolation to infinite dilution. Attention has been concentrated on solutions of PMMA ($M_w \sim 4.2 \times 10^6$) in Aroclor 1248. In an experiment at 15° with a CF8 viscometer linear plots of η_{sp}/c versus c were obtained for the concentrations 0.25, 0.5 and 1.0×10^{-3} g/cm³ but 2.0×10^{-3} g/cm³ gave low values. *Figure 5* shows results derived from a similar experiment at 10° using viscometers CF8A and CF8B. The latter viscometer contained solvent which was run with each solution in turn in the other viscometer under a common driving pressure. It will be seen that the solvent is Newtonian and gives similar results in each of the four runs. The solutions occasionally give erratic results which at one concentration, 0.5×10^{-3} g/cm³, do not provide satisfactory definition of an η^* versus P curve. These data also define a co-

linear relationship for η_{sp}/c versus c with three of the concentrations but this time the $0.5 \times 10^{-3} \text{ g/cm}^3$ values are generally low.

It is believed that the Cannon-Fenske viscometer gives erratic results because polymer degradation is generally largely confined to the same volume of liquid (about 1.5 out of 10 cm^3 which passes to and fro through

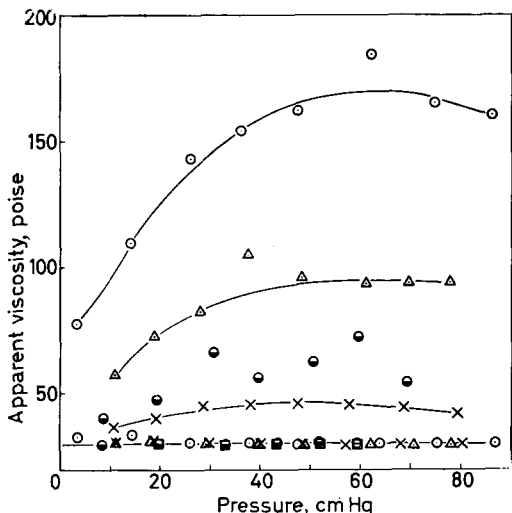


Figure 5—Viscosity data for various concentrations of a PMMA solution in a CF8 viscometer. Aroclor 1248; $T=10^\circ\text{C}$. \circ $2 \times 10^{-3} \text{ g/cm}^3$; \triangle $1 \times 10^{-3} \text{ g/cm}^3$; \bullet $0.5 \times 10^{-3} \text{ g/cm}^3$; \times $0.25 \times 10^{-3} \text{ g/cm}^3$; $\circ \triangle \times$ Solvent, bottom curve only

the capillary. Occasionally, however, the pressing back technique causes more extensive mixing and a higher viscosity is measured in the succeeding run. This belief is based on experiments in which the efflux portion of the Aroclor (1.5 cm^3) was marked with a dyestuff and the colour boundary observed during experiments similar to those used to obtain the data in Figure 5.

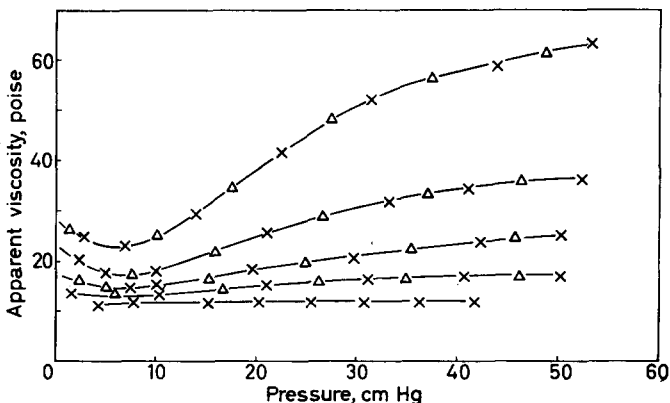


Figure 6—Viscosity data for various concentrations of a PMMA solution in an SP8 viscometer. Aroclor 1248; $T=15^\circ\text{C}$. Concentrations are, from top to bottom, 1.0 , 0.5 , 0.25 , 0.125 and $0 \times 10^{-3} \text{ g/cm}^3$. \times Increasing pressures; \triangle Decreasing pressures

NON-NEWTONIAN VISCOSITY OF POLYMER SOLUTIONS

Consistent results, reproducible for a given solution, were obtained in a first attempt with an SP8 viscometer at 15°C (*Figure 6*). These gave four approximately co-linear values of η_{sp}/c versus c for various values of P , as shown in *Figure 7*. The rather low slopes of these lines imply that intermolecular contributions to the viscosity are relatively small in the concen-

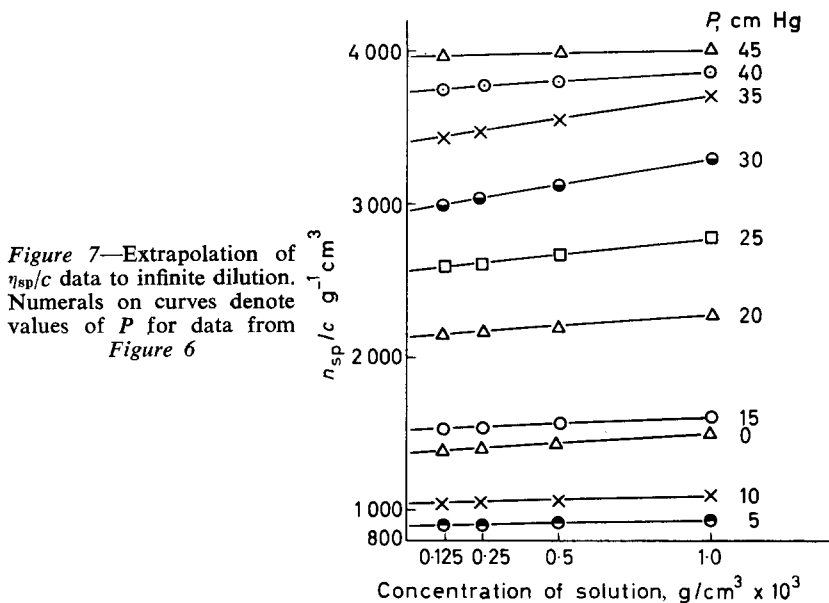


Figure 7—Extrapolation of η_{sp}/c data to infinite dilution. Numerals on curves denote values of P for data from *Figure 6*

tration range 0.125 to $1.0 \times 10^{-3} \text{ g}/\text{cm}^3$ and show, conclusively, that the limiting viscosity number itself increases with driving pressure in the range $P = 15$ to 45 cm of mercury.

Comparison of experiment with theory

The sensitivity of the upturn effect on the molecular weight of the polymer is shown in *Figure 8* for polyisobutenes of varying molecular weight in a Newtonian polybutene solvent. Little or no upturn is detected under these experimental conditions for the polymer of $M_v = 1.3 \times 10^6$ but the effect is pronounced for 3.6×10^6 and much more so for 6.3×10^6 . Fewer data are available for PMMA but, consistently, no upturn was detected in the sample of $M \sim 10^6$ under conditions where it was obvious with the similar polymer of higher molecular weight. It is also consistent with a sensitive dependence on molecular weight that, as a result of polymer degradation, the right hand part of the curves in *Figure 2* drop so sharply. In other experiments, not reported here, it was found that by prolonged shearing the upturn may be depressed to such an extent that the solution behaves like one made up from a polymer of $M \sim 10^6$.

The influence of solvent viscosity was studied by taking advantage of the marked dependence of the viscosity of Aroclor on temperature (cf. *Figure 9*). At 40° flow times were too rapid to cover an extensive range of driving pressures but at 25°, where this was practicable, only a small

upturn occurred. In further runs on the same solution the temperature was lowered and at 7° the upturn is enormous. Runs at still lower temperatures

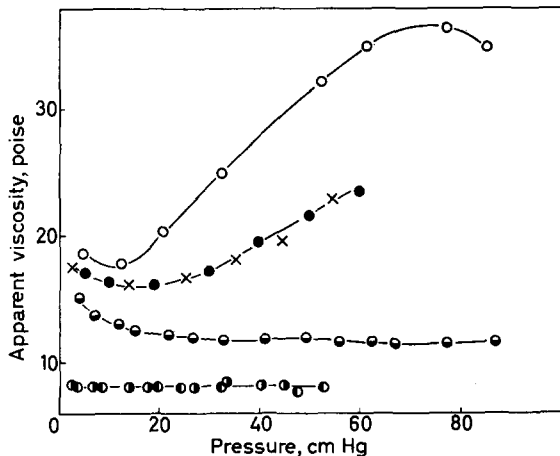


Figure 8—Influence of molecular weight of polymer on upturn effect. Polyisobutenes in a polybutene solvent (L50); 2×10^{-3} g/cm³; $T = 7^\circ\text{C}$; CF8 viscometer.
 ○ $M_v 6.3 \times 10^6$; ●, × $M_v 3.6 \times 10^6$; ● $M_v 1.3 \times 10^6$
 ● ● Solvent

were avoided because of inconveniently long flow times. It would be desirable to complement this work with a study of the influence of viscosity in a range of chemically similar solvents at constant temperature. Attempts

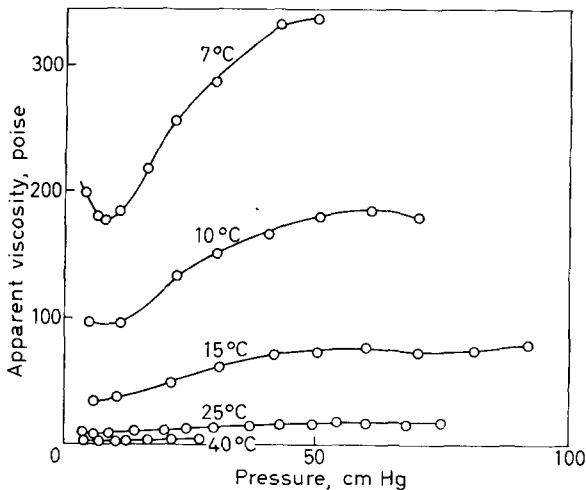


Figure 9—Influence of solvent viscosity on upturn effect. PMMA in Aroclor 1248 (2×10^{-3} g/cm³); CF8 viscometer

made in this direction with a range of polybutene oligomers were thwarted because of limited solubility of PIB in the more viscous members.

The fact that polymer molecular weight and solvent viscosity influence

NON-NEWTONIAN VISCOSITY OF POLYMER SOLUTIONS

the upturn in the way anticipated, of course, only substantiates the theory in a broad sense. A more critical test of the theory is possible by comparison of the $[\eta]/[\eta]_0$ versus β curves in *Figure 11* with the experimental values for PMMA. In order to proceed with this comparison the following equations will be used: $\eta_0 G = \tau_{\max.} = RP/2L$; $M_n = M_w/1.7 = 2.5 \times 10^6$ (cf. ref. 13 for justification of choice of denominator). Only a rough estimate of $[\eta]_0$ is possible on the basis of an admittedly ill-defined extrapolation of the data in *Figure 6* to $P=0$. This gives a value of $1400 \text{ g}^{-1} \text{ cm}^3$ (*Figure 7*) which seems sensible for a polymer of such high molecular weight as may be judged by an arbitrary choice of the reasonable values of $K=10^{-2}$ and $\alpha=0.8$ for substitution in the Mark-Houwink equation, $[\eta]$ in $\text{g}^{-1} \text{ cm}^3 = KM^\alpha$, which gives a value of $1300 \text{ g}^{-1} \text{ cm}^3$. Experimental values of $[\eta]/[\eta]_0$ versus

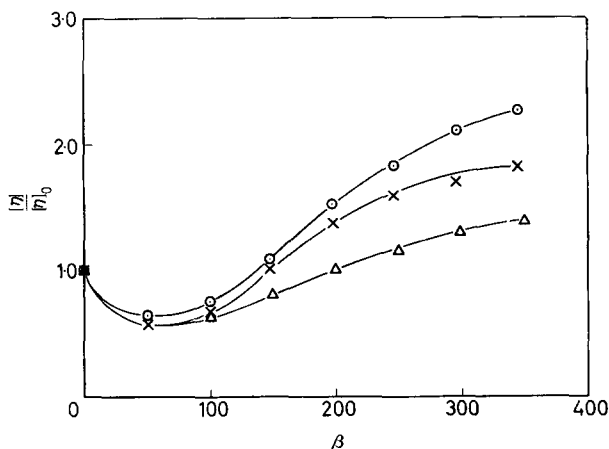


Figure 10—Experimentally determined dependence of upturn of $[\eta]/[\eta]_0$ on β . \circ SP8; 15°C. \times CF8; 15°C. \triangle CF8; 10°C

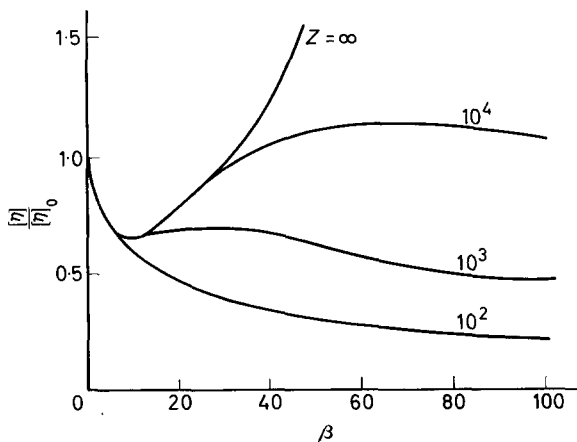


Figure 11—Theoretically predicted dependence of upturn on β

β are plotted in *Figure 10*. Most reliance is placed on results obtained with the Single-Pass viscometer and the lower values of $[\eta]/[\eta]_0$ for the Cannon-Fenske data are tentatively attributed to polymer degradation.

Comparison of *Figures 10* and *11* shows that the experimentally observed upturn is higher than that predicted theoretically for a polymer with $Z=0.5 \times 10^4$. Another difference is that the experimental results suggest that the theoretical values of β are too small by something less than one order of magnitude. A shift of this type is to be expected because the dumbbell model used in theoretical treatments strongly exaggerates coil deformation in laminar flow¹⁴. The above differences are, therefore, not surprising and should not detract from the good general agreement between *Figures 10* and *11*.

Finally, looking at the problem in perspective, it is claimed that a reasonable case has been made to show that PMMA solutions show an upturn effect similar to that predicted by theory. There are indications that PMMA solutions have very unusual unexplained rheological properties and the main evidence adduced relates to viscosity data extrapolated to infinite dilution which is interpreted as being due to the properties of single macromolecules. With polystyrene solutions, there is a conflict of evidence. Wolff was unable to detect any upturn and other data⁶, while hinting rather strongly of such an effect with reference to η^* alone, has yet to be demonstrated on extrapolation to infinite dilution. An experimental decision concerning these differences is clearly very important.

The authors gratefully acknowledge financial support by the Camille and Henry Dreyfus Foundation. Professor G. Meyerhoff is thanked for initiating preliminary experiments in this programme during a summer leave of absence from Mainz University. Dr R. Buchdahl and Dr M. L. Williams of the Chemstrand Research Center are thanked for the loan of a Képès cone-and-plate viscometer, which was used to check some of the data reported above.

*Camille Dreyfus Laboratory,
Research Triangle Institute,
Durham, N.C., U.S.A.*

(Received May 1964)

REFERENCES

- ¹ PETERLIN, A. *J. Polym. Sci.* 1952, **8**, 621; *J. chem. Phys.* 1960, **33**, 1799; *Makromol. Chem.* 1961, **44-46**, 338; *Kolloidzshr.* 1962, **182**, 110; 'Symposium on Non-Newtonian Viscosity', *ASTM Publ. No. 299*, 1962, p 115; 'Non-Newtonian intrinsic viscosity of polymer solutions', presented at Fourth International Congress of Rheology at Brown University, 1963
- ² SCHNURMANN, R. *Proc. First Internat. Rheol. Congr.* (Scheveningen, 1949) Part II, p 142
- ³ SELBY, T. W. and HUNSTAD, N. A. 'Symposium on Non-Newtonian Viscosity', *ASTM Publ. No. 299*, 1962, p 98
- ⁴ WOLFF, C. *J. Chim. phys.* 1962, **59**, 413
- ⁵ PETERLIN, A. and TURNER, D. T. *Nature, Lond.* 1963, **197**, 488
- ⁶ BUROW, MRS S. P., PETERLIN, A. and TURNER, D. T. *Polymer Letters*, 1964, **2B**, 67

NON-NEWTONIAN VISCOSITY OF POLYMER SOLUTIONS

- ⁷ PETERLIN, A. and TURNER, D. T. *J. chem. Phys.* 1963, **38**, 2315
- ⁸ DAVIES, C. N. *Proc. First Internat. Rheol. Congr.* (Scheveningen, 1949) Part II, p 152
- ⁹ CLAESSON, S. and LOHMANDER, H. *Makromol. Chem.* 1961, **34-36**, 461
- ¹⁰ RODRIGUEZ, F. and WINDING, C. C. *Industr. Engng Chem. (Industr.)*, 1959, **51**, 1281
- ¹¹ FRENKEL, J. *Acta phys.-chim. U.S.S.R.* 1944, **19**, 50
- ¹² PETERLIN, A., PHILIPPOFF, W. and TURNER, D. T. To be published
- ¹³ AYREY, G. and MOORE, C. G. *J. Polym. Sci.* 1959, **36**, 41
- ¹⁴ PETERLIN, A. *J. chem. Phys.* 1963, **39**, 224

Thermal Degradation of an Aromatic Polypyromellitimide in Air and Vacuum II—The Effect of Impurities and the Nature of Degradation Products

S. D. BRUCK

The effect of impurities on the thermal degradation of poly-[N,N'-(p,p'-oxydiphenylene) pyromellitimide] (du Pont's 'H'-film) is discussed. Purification of the polymer in dimethylformamide decreases the rates of degradation both in air and in vacuum, but only slightly reduces the activation energies. Infra-red and mass spectrometric data suggest the participation of polypyromellitic acid (polyamide acid) impurity in the degradation process by thermal cleavage of its carboxyl and hydrolytic scission of its amide groups. As far as the vacuum pyrolysis of the main polyimide chains is concerned, the activation energy of 74 kcal/mole, bond dissociation energies, and elemental analysis of the residue remaining after pyrolysis suggest that the primary scission occurs at the imide bonds, most likely followed by a secondary cleavage resulting in the elimination of CO groups.

IN PREVIOUS publications^{1,2} the rates and activation energies for the thermal degradation of unpurified and unfractionated poly-[N,N'-(p,p'-oxydiphenylene) pyromellitimide] (du Pont's 'H'-film) were discussed.

The object of the present investigation was (a) to obtain the rates and activation energies of the thermal degradation of a *purified* sample of this polyimide and to compare the results with those previously obtained on the unpurified material, (b) to analyse some of the volatile degradation products by mass spectrometry and infra-red (i.r.) spectrophotometry, and (c) from the available experimental evidence suggest a possible mechanism for the thermal degradation of the polymer and its impurities.

EXPERIMENTAL DETAILS

(a) *Thermogravimetry*

Thermogravimetric studies were conducted with a Cahn RG electrobalance by a method already discussed¹. One mil (0.001 in.) thick industrial samples of 'H'-film, poly-[N,N'-(p,p'-oxydiphenylene) pyromellitimide], were used, as obtained from E. I. du Pont de Nemours and Company, Incorporated.

(b) *Purification of 'H'-film*

In view of the severe degradation of the polymer in boiling dimethylformamide, the purification was carried out at room temperature. Approximately 150 mg of 'H'-film was soaked in 50 ml of dimethylformamide for 72 hours, followed by soaking in 50 ml of distilled water for 24 hours, and finally soaking in 50 ml of ethyl alcohol for 24 hours. The polymer was dried at 120°C for 12 hours in a vacuum oven, and stored in a desiccator.

(c) *Infra-red absorption measurements*

The direct absorption spectrum of the undegraded, one-mil thick film in the region of 2.4 to 3.5 microns was obtained on a Beckman DK-2A spectrophotometer. The other i.r. spectra were obtained by a potassium bromide pelleting technique on a Beckman IR-7 spectrophotometer. The pellets were dried at 120°C in vacuum for 24 hours and stored in a vacuum desiccator prior to use.

DISCUSSION OF RESULTS

(1) *Rates and activation energies*

During the previously reported heat degradation studies on unpurified 'H'-film^{1,2}, a pale yellow material appeared in the combustion tube at a place immediately next to the hot zone. This material formed at an early stage of the pyrolysis experiments in vacuum, in the temperature range of 200°C to 250°C, was partially soluble in dimethylformamide, and constituted approximately two to three per cent of the original samples. In an attempt to remove or diminish this material, the 'H'-film samples were extracted at room temperature with dimethylformamide, and thermogravimetric experiments were then conducted on this purified film. The nature of the pale yellow degradation product can best be discussed later, following the presentation of the results on the thermogravimetric experiments.

Figure 1 shows the percentage volatilization of the purified 'H'-film in air as a function of time between 442°C and 485°C. As indicated, essentially total volatilization takes place at 485°C in approximately five hours of heating, whereas at 442°C only about 20 per cent weight loss occurs during a similar period. Zero time in Figure 1 (and on appropriate subsequent figures) signifies the time at which thermal equilibrium had been attained.

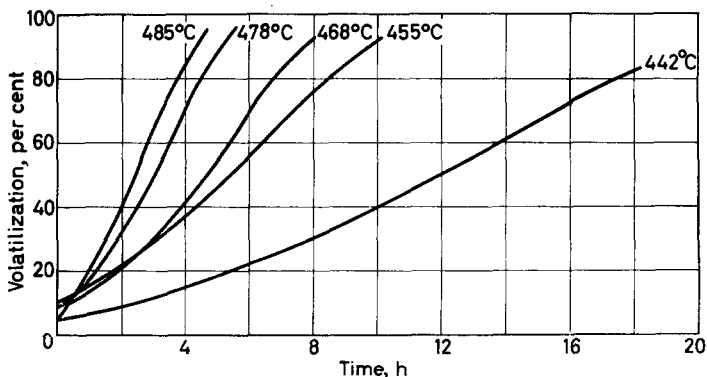


Figure 1—Thermal degradation of purified 'H'-film in air

The small weight losses at zero time that are evident in Figure 1 arise from some unavoidable volatilization during the pre-equilibrium heating-up period.

From the thermal degradation curves the corresponding rates were calculated with an electronic computer, as shown in Figure 2. The data indicate the appearance of distinct maxima between approximately 45 and 55 per

THERMAL DEGRADATION OF AN AROMATIC POLYPYROMELLITIMIDE II

cent volatilization. The thermal degradation of the purified material proceeds at rates that are lower by approximately 40 per cent in comparison with the rates of the unpurified product¹. Although the rates are lower, the rate curves are essentially similar in both cases.

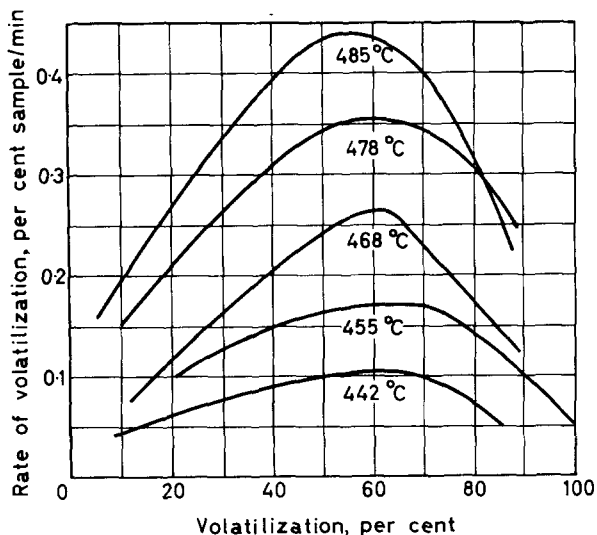


Figure 2—Rates of thermal degradation of purified 'H'-film in air

Figure 3 illustrates the thermal degradation of purified 'H'-film in vacuum between 585°C and 632°C. After the initial fairly rapid degradation the curves approach the limiting value of approximately 40 per cent which is 10 to 15 per cent below the value observed for the unpurified material¹.

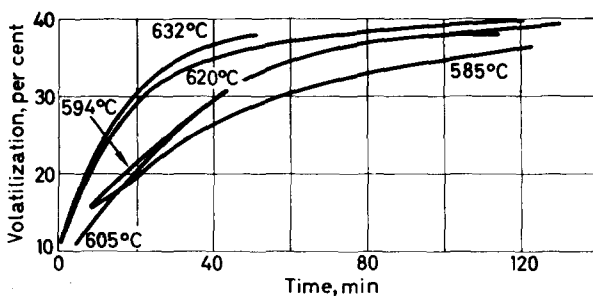


Figure 3—Thermal degradation of purified 'H'-film in vacuum

Figure 4 shows the corresponding rates of degradation. The extrapolated initial rates are slower by a factor of approximately four in comparison with those of the unpurified material¹.

The activation energies for the thermal degradation in air and vacuum of the purified 'H'-film were calculated from the well-known Arrhenius

relationship ($k = Se^{-E/RT}$, where k is the rate constant, E is the activation energy in kcal/mole, R is the gas constant, T is the absolute temperature and S is a frequency factor), by plotting either the maximum rates (for degradation in air), or the extrapolated 'apparent initial' rates (for

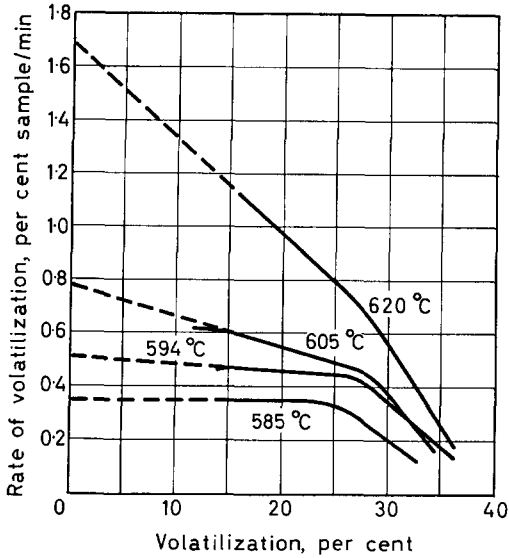


Figure 4—Rates of thermal degradation of purified 'H'-film in vacuum

degradation in vacuum) against the reciprocal of the absolute temperatures. Figure 5 illustrates the Arrhenius plots for the thermal degradation in air of both purified and unpurified 'H'-film [data for the latter are reproduced

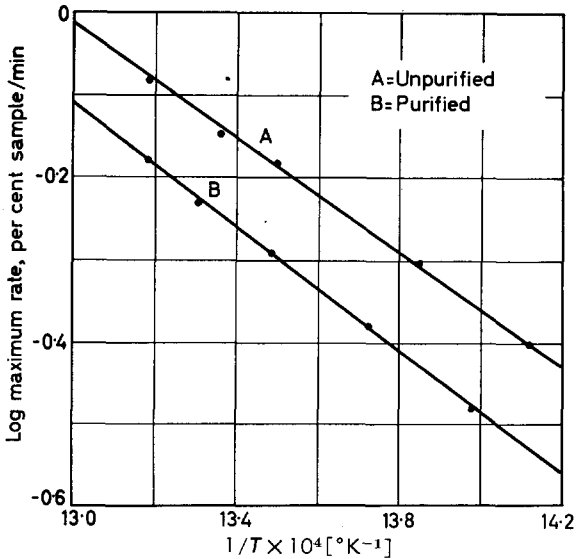


Figure 5—Arrhenius plots for the thermal degradation of unpurified and purified 'H'-film in air

THERMAL DEGRADATION OF AN AROMATIC POLYPYROMELLITIMIDE II

from the previous publication¹]. From the slopes, the calculated activation energy was found to be 33 and 31 kcal/mole for the thermal degradation in air of the purified and unpurified polymers, respectively.

The Arrhenius plots for the thermal degradation in vacuum are illustrated in *Figure 6*. The calculated activation energy for the vacuum pyrolysis is 74 and 73 kcal/mole for the purified and unpurified material, respectively.

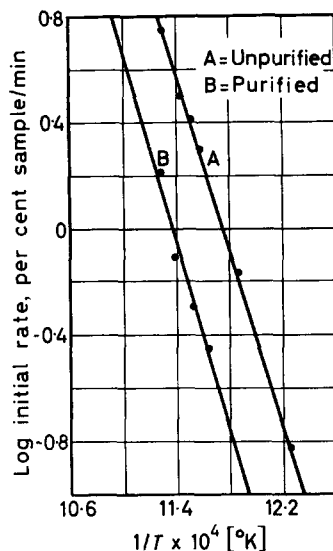


Figure 6—Arrhenius plots for the thermal degradation of unpurified and purified 'H'-film in vacuum

(2) *The nature of the degradation products*

In discussing the nature of the degradation products of 'H'-film it is desirable to differentiate between those that arise from impurities and those that originate from the degradation of the main polyimide chains. While it is not as yet possible to identify clearly the origin of each component, the following discussion will attempt to illuminate the problem.

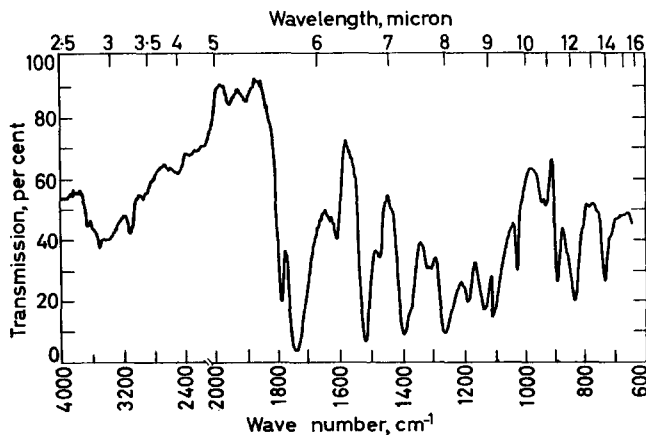


Figure 7—Infra-red absorption spectrum of unpurified 'H'-film (KBr pellet, Beckman IR-7)

The i.r. spectra of undegraded and unpurified 'H'-film are shown in *Figures 7 and 8*. The significant bands for the purposes of this discussion are the imide bands at 1780 cm^{-1} and 720 cm^{-1} , the aromatic $=\text{C}-\text{H}$ stretching band at 3080 cm^{-1} , and the $-\text{NH}$ stretching band at 3380 cm^{-1} .

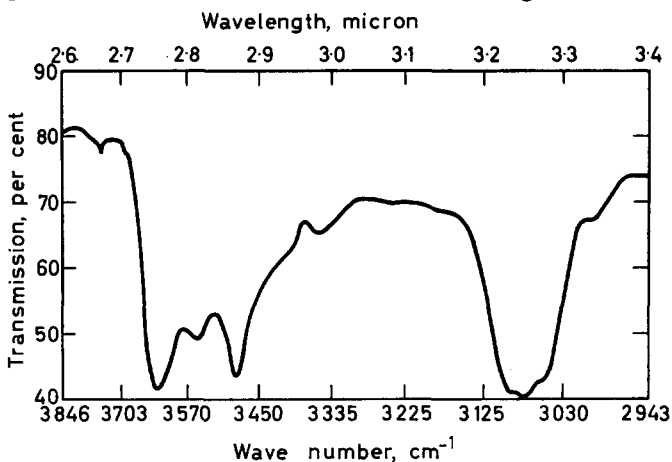
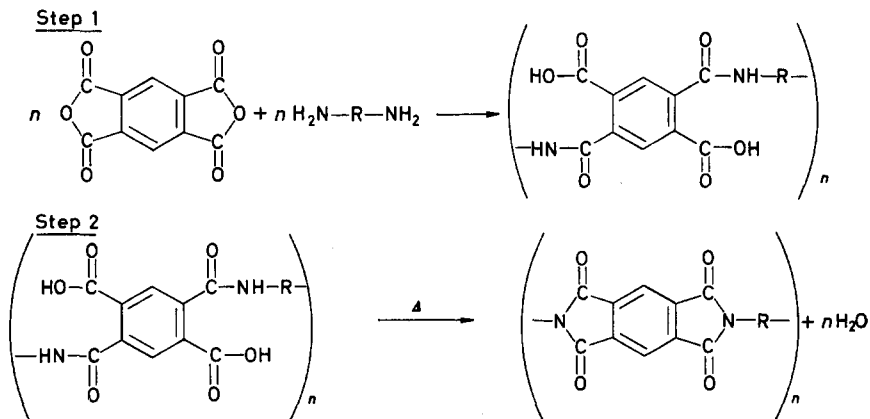


Figure 8—Infra-red absorption spectrum of unpurified 'H'-film between 2.6 and 3.4μ (0.001 in. thick film, Beckman DK-2A)

This last band would not be present in a pure polyimide. The bands between 3450 cm^{-1} and 3650 cm^{-1} may arise from $-\text{OH}(\text{H}_2\text{O})$ and/or $-\text{NH}$ groups.

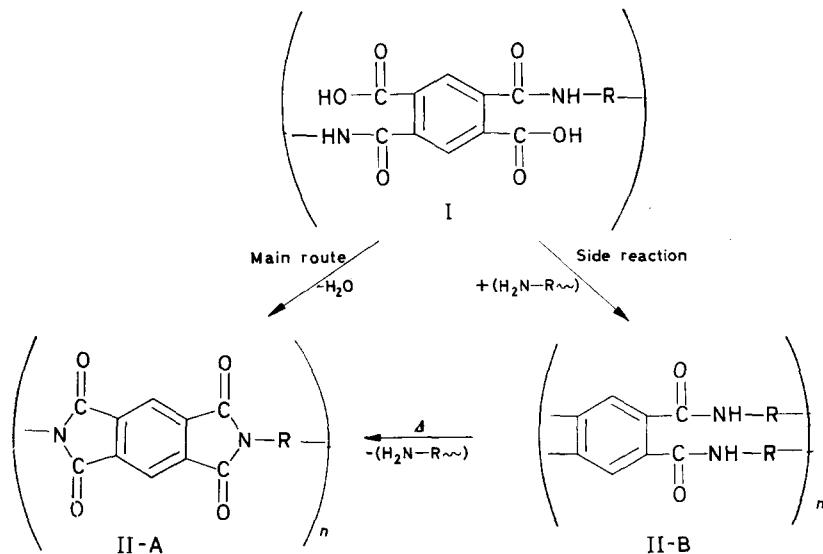
To account for the $-\text{NH}$ stretching band at 3360 cm^{-1} an examination of the synthetic process is necessary²⁻⁴. In the first step, pyromellitic dianhydride reacts with bis(4-aminophenyl) ether to form the intermediate polypyromellitic acid (also called polyamic acid) which is soluble in dimethylformamide and dimethylacetamide. This is followed by a second step in which the polypyromellitic acid is heated (while in solution) to undergo an intramolecular cyclodehydration (imidization) reaction yielding the insoluble polyimide.

The two-step reaction scheme may be written as follows:

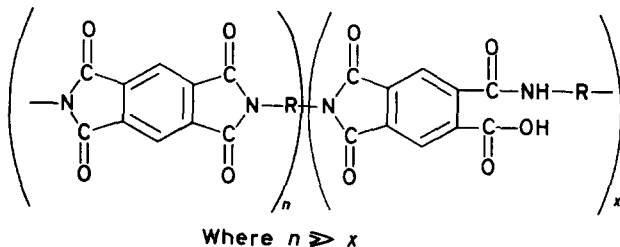


THERMAL DEGRADATION OF AN AROMATIC POLYPYROMELLITIMIDE II

It has been proposed⁵, however, that the imidization reaction (step 2) may occur in at least two ways, according to the following :



It is possible that the intramolecular cyclodehydration reaction is incomplete giving rise to *some* polymer chains of randomly alternating units of (II-A), (I), and (II-B), rather than being composed of only polyimide units (II-A). However, the presence of (II-B) is less probable than that of (I) because in the former case branching and crosslinking would be expected and also because of steric factors. Hence in order to account for the presence of —NH groups it is suggested that the unpurified sample of 'H'-film probably contains small amounts of uncyclized polyamic acid units (I), either as a mixture or perhaps in the form of a copolymer. Such a copolymer may be written as follows :



The —NH groups of (I) would then be responsible for the absorption peak at 3 360 cm⁻¹.

The bands between 3 450 cm⁻¹ and 3 650 cm⁻¹ may be due to amino-impurities, especially since aromatic amines are known to absorb in this region, and/or to —OH(H₂O) groups.

Examination of the i.r. spectrum of the pale yellow degradation product,

shown in *Figure 9*, adds further weight to this argument. As seen, a strong band appears at 3400 cm^{-1} and a smaller one at 1680 cm^{-1} , in addition to the imide absorption peaks (1780 cm^{-1} and 720 cm^{-1}). The band at 3400 cm^{-1} represents the $-\text{NH}$ stretching mode, whereas the band at

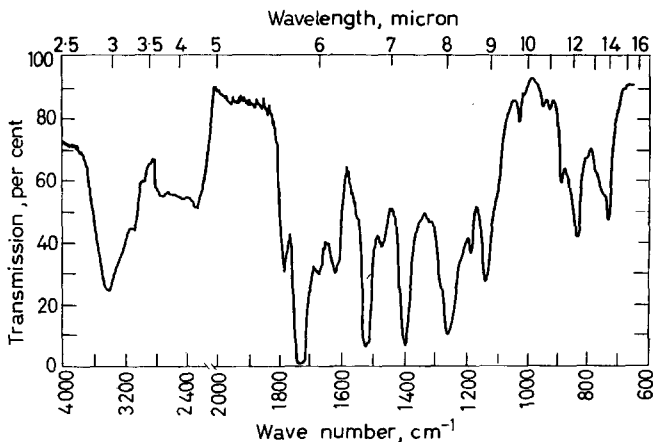


Figure 9—Infra-red absorption spectrum of yellow degradation product (KBr pellet, Beckman IR-7)

1680 cm^{-1} is probably due to carbonyl groups of amide units. These latter features of the i.r. spectrum are similar to those of polyamic acid³.

In this connection, it is interesting to note that it is apparently possible to facilitate the complete conversion of the polyamic acid intermediate into the polyimide if special conditions are used. In a recent paper³ it was shown that a 0.1 mil (0.0001 in.) thick polyamic acid film, dried at 80°C for two hours, subsequently heated to 300°C over a period of 45 minutes and held at 300°C for an additional one hour, was apparently completely converted to the polyimide, as evidenced by the disappearance of the NH band at 3400 cm^{-1} and by the appearance of the imide band at 1780 cm^{-1} and 720 cm^{-1} . However, this sample might have been prepared under more stringent conditions than are employed in the plant production of 'H'-film, which could account for the presence of small amounts of polyamic acid in the commercial samples used in the present work.

Table 1. Mass spectrometric analysis of the gaseous degradation products of 'H'-film at liquid nitrogen temperature (Vacuum pyrolysis, 600°C , 4h, 10^{-3} mm of mercury)

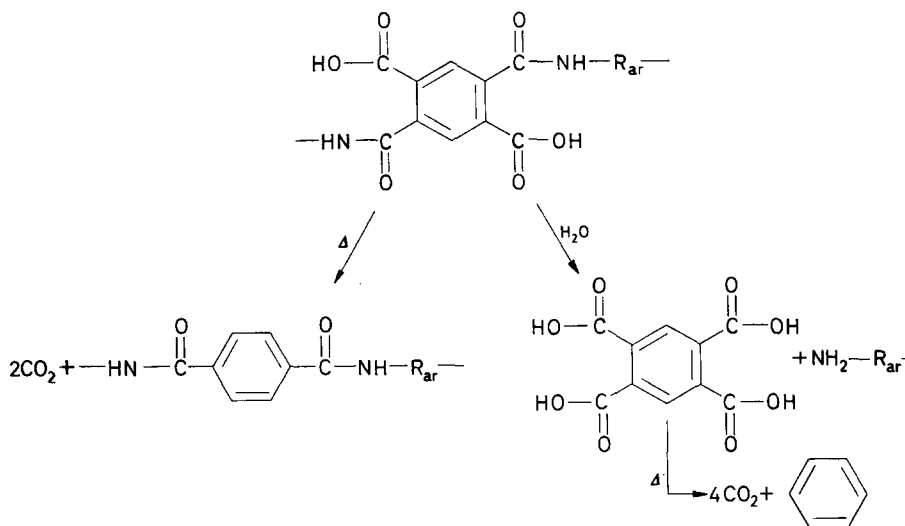
Component	A	B
	Unpurified H-film mole %	Purified H-film mole %
Carbon dioxide	38.0	25.4
Water	53.0	72.6
Ammonia	2.1	None
Hydrogen cyanide	5.6	None
Hydrocarbons	0.8	1.0
Aniline	0.05	0.05
Benzene	0.6	0.4
Phenol	0.04	0.2
Benzonitrile	0.06	0.1

THERMAL DEGRADATION OF AN AROMATIC POLYPYROMELLITIMIDE II

Further evidence as to the nature of the pale yellow material arises from the mass spectrometric analysis of the volatile degradation products collected at liquid nitrogen temperature. *Table 1* summarizes the results of the thermal degradation of both unpurified and purified polymer in vacuum (600°C, 4 hours). With the unpurified polymer (column A), the volatile degradation products showed carbon dioxide and water as the major constituents, some ammonia, hydrogen cyanide, and lesser amounts of olefins, benzene, phenol and benzonitrile. Purification of the polymer in dimethylformamide decreased the production of carbon dioxide, and eliminated ammonia and hydrogen cyanide from the gaseous degradation products (column B).

It should be noted that the mass spectrometric data do not include decomposition products such as carbon monoxide and hydrogen since these will condense below the temperature of liquid nitrogen. However, it is expected that the pyrolysis of the polyimide chains would give rise to large quantities of carbon monoxide, as will be discussed later. Consequently, it appears that the products collected at -196°C reflect primarily the degradation of impurities, such as uncyclized *polyamic acid* units, rather than the main degradation of the *polyimide* chains.

Such polyamic acid units are expected to decarboxylate at elevated temperatures and undergo free radical as well as hydrolytic scissions. The hydrolytic scission and the thermal decarboxylation steps may be written as follows:



The hydrolytic scission of polyamic acid could arise from catalytic amounts of absorbed water molecules held by hydrogen bonding. It has been shown by several investigators that the *complete* removal of all water from polyamides is extremely difficult, if not impossible, below the melting point of the polymer. The works of Straus and Wall^{6,7} on the pyrolysis of polyamides indicate the production of large quantities of carbon dioxide even in well-dried samples. *Table 2* shows the results of the mass spectrometric analysis

of the volatile degradation products (collected at liquid nitrogen temperature) of Nylon-6 during pyrolysis in vacuum, as compiled from the data of Straus and Wall⁷. As seen, the major degradation products are carbon dioxide and

Table 2. Mass spectrometric analysis of the volatile degradation products of Nylon-6 (polycaprolactam) collected at liquid nitrogen temperature during pyrolysis in vacuum

Component	Nylon-6(mol. wt 60000)	Nylon-6(mol. wt 30000)
	Mole %	Mole %
Carbon dioxide	59.4	55.8
Water	35.6	35.4
Saturated aliphatic hydrocarbons	1.0	0.5
Unsaturated aliphatic hydrocarbons	3.7	2.4
Aromatic compounds	0.3	5.9
<i>Total</i>	100.0%	100.0%
Fraction of pyrolysed polymer:	10%	5%

water. If, however, only a thermal free-radical mechanism were operative, carbon dioxide would not be expected in appreciable amounts in the degradation products. The production of large quantities of carbon dioxide in the vacuum pyrolysis of polyamides was also observed by other investigators⁸.

With 'H'-film, the small quantity of polyamic acid impurity could thus undergo hydrolytic scission (in addition to thermal cleavage of its free carboxyl groups), resulting in the production of carbon dioxide. Table 1 indicates that with the unpurified 'H'-film 38 mole per cent carbon dioxide was produced during vacuum pyrolysis. The decreased production of 24.5 mole per cent dioxide with the purified 'H'-film suggests the partial removal of the polyamic acid impurity from the polymer. The overall results are thus in conformity with the data of other investigators on the thermal degradation of polyamides. Once hydrolytic scission occurs, the amine-containing part of the ruptured chain could further degrade to produce the nitrogenous fractions observed by mass spectrometry. It is significant that the formation of nitrogenous products was limited to the pyrolysis of the unpurified polymer, suggesting that they may originate from species *other than the imide groups*, in accordance with the above scheme.

The presence of water in the degradation products of 'H'-film may be due to absorbed moisture that could not be removed under normal drying conditions (120°C, 12 h, 10⁻² mm of mercury) and may arise also from the further imidization (cyclodehydration) of some of those unreacted polyamic acid units which do not suffer decarboxylation and hydrolytic scission during the extended thermal exposure.

Thus, the small quantity of polyamic acid present as an impurity in 'H'-film could undergo at least four types of reactions: (1) decarboxylation, (2) hydrolytic scission, (3) thermal free-radical degradation, and (4) further imidization. Reactions (1) and (2) will yield carbon dioxide, whereas reaction (4) produces water. It is quite possible that all four of these proceed to some extent simultaneously during pyrolysis.

THERMAL DEGRADATION OF AN AROMATIC POLYPYROMELLITIMIDE II

As far as the main thermal degradation of the polyimide chains is concerned an exact mechanism cannot be written at this time. However, some evidence for the main degradation path may be gained from the elemental analyses of the undegraded 'H'-film and of the residue remaining after pyrolysis in vacuum (600°C, 4 h, 10⁻³ mm of mercury). The results which are summarized in *Table 3* indicate that the degraded material contains almost the same percentage of nitrogen as the undegraded material. It appears that heat degradation in vacuum results in the loss of carbon

Table 3. Elemental micro analyses of undegraded 'H'-film and of residue remaining after pyrolysis in vacuum (600°C, 4 h, 10⁻³ mm of mercury)

Element	'H'-film (unpurified)		Residue	
	Found (%)	Theoretical* (%)	Found (%)	Theoretical† (%)
Oxygen	67.5	69.1	81.0	80.0
Nitrogen	2.8	2.6	2.7	3.6
Hydrogen	7.9	7.3	8.3	10.3
Carbon	21.0	20.6	4.2	5.5

*Based on 100 per cent poly-[N,N'-(p,p'-oxydiphenylene pyromellitimide)].

†Assuming the loss of four CO groups per repeat unit.

monoxide (condensable below liquid nitrogen temperature) from the imide groups, and the simultaneous recombination and retention of the imido-nitrogen atoms with the formation of a condensed product. The presence of carbon monoxide in the degradation products is also confirmed by the mass spectrometric analysis of the volatile materials formed during the vacuum pyrolysis of 'H'-film in a closed system. The data, summarized in *Table 4*, indicate that the major degradation products are carbon monoxide and carbon dioxide. Assuming that the carbon monoxide originates from the imide groups and that the carbon dioxide arises from the thermal decarboxylation and hydrolytic scission (catalysed by absorbed moisture) of

Table 4. Mass spectrometric analysis of the gaseous degradation products of unpurified 'H'-film during vacuum pyrolysis in a closed system (610°C, 4 h, 10⁻⁵ mm of mercury)

Component	Mole %	Weight %	Weight, mg
Hydrogen	9.0	0.64	0.021
Methane	1.1	0.63	0.021
Ammonia	1.2	0.73	0.024
Water	7.6	4.90	0.162
Hydrogen cyanide	1.3	1.26	0.042
Carbon monoxide	60.5	60.73	2.004
Carbon dioxide	19.0	29.97	0.989
Benzene	0.3	0.84	0.028
Phenol	0.02	0.07	0.002
Benzonitrile	0.06	0.22	0.007

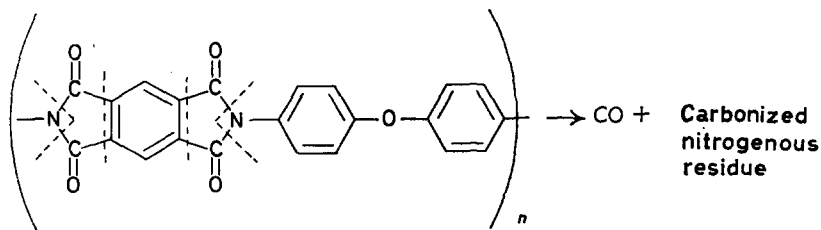
Total volatile products = 3.300 mg

Weight of sample before pyrolysis = 9.9 mg.
 Weight of non-volatile degradation products = 0.3 mg.
 Weight of residue = 6.3 mg.
 Total weight loss of sample = 33.3 per cent.

the *polyamic acid* groups, it appears that the polymer consists of approximately 78 per cent polyimide—and 22 per cent uncyclized polyamic acid units.

In summary therefore, the thermal degradation of unpurified industrial samples of 'H'-film in vacuum involves both polyamide and polyimide units through at least the following major paths:

- (1) *Hydrolytic* scission of the amide groups of polyamic acid impurity present in the polymer;
- (2) Thermal decarboxylation of residual polyamic acid impurity;
- (3) Thermal free radical degradation of the *amide* groups of polyamic acid impurity by homolytic scission, initiated at the C—N bond beta to the carbonyl as proposed by several workers for polyamides^{7,8};
- (4) Thermal free radical degradation of the *imide* units of the polymer with the elimination of carbon monoxide (as the major component) and the formation of a carbonized nitrogenous residue:



Since the molecular weight of the repeat unit of the above poly-[*N,N'*-(*p,p'*-oxydiphenylene) pyromellitimide] is 382, the loss of four CO groups per repeat unit would represent approximately 30 per cent weight loss based on a 100 per cent pure polyimide. This is in fairly good agreement with the thermogravimetric results (~ 40 per cent weight loss) in vacuum, especially when considering the additional volatilization arising from the degradation of polyamic acid impurities. The approximate dissociation energies of the chemical bonds present in the polymer indicate that the *imide* bond is the weakest. Hence the activation energy of 74 kcal/mole for the vacuum pyrolysis suggests that the *primary* scission of the chain occurs at this linkage, most likely followed by a secondary cleavage resulting in elimination of CO groups.

It is obvious that routes (1), (2) and (3) would not be applicable to *pure* polyimide samples in which either complete imidization could be affected or from which the small quantities of uncyclized polyamic acid could be removed (for example by controlled pyrolysis in vacuum in the temperature range of 250°C to 350°C). The elimination of polyamic acid impurities could be important to certain aero-space applications in which surfaces of electronic components might become contaminated by impurities escaping under space conditions.

THERMAL DEGRADATION OF AN AROMATIC POLYPYROMELLITIMIDE II

This work was supported by the Bureau of Naval Weapons, Department of the U.S. Navy, under Contract NOW62-0606-c. The infra-red analyses were carried out with the assistance of Mr R. E. Ruckman of the Applied Physics Laboratory, The Johns Hopkins University. The mass spectrometric analyses were done by Mr William Dorko of the National Bureau of Standards. The author thanks Dr Leo A. Wall of the National Bureau of Standards for permission to reproduce some of his data on Nylons.

*Applied Physics Laboratory,
The Johns Hopkins University,
8621 Georgia Avenue, Silver Spring,
Maryland, U.S.A.*

(Received May 1964)

REFERENCES

- ¹ BRUCK, S. D. *Polymer, Lond.* 1964, **5**, 435
- ² BRUCK, S. D. *Polymer Preprints*, p 148, 147th National Meeting, American Chemical Society, Philadelphia, Pennsylvania, 5 to 10 April 1964
- ³ SROOG, C. E., ABRAMO, S. V., BERR, C. E., EDWARDS, W. M., ENDREY, A. L. and OLIVIER, K. L. *Polymer Preprints*, p 132, 147th National Meeting, American Chemical Society, Philadelphia, Pennsylvania, 5 to 10 April 1964
- ⁴ AMBORSKI, L. E. *Industr. Engng Chem., Prod. Res. and Devel.* 1963, **2**, 189
- ⁵ WRASIDLO, W., HERGENROTHER, P. M. and LEVINE, H. H. *Polymer Preprints*, p 141, 147th National Meeting, American Chemical Society, Philadelphia, Pennsylvania, 5 to 10 April 1964
- ⁶ STRAUS, S. and WALL, L. A. *J. Res. Nat. Bur. Stand.* 1959, **63A**, 269
- ⁷ STRAUS, S. and WALL, L. A. *J. Res. Nat. Bur. Stand.* 1958, **60**, 39
- ⁸ ACHHAMMER, B. G., REINHART, F. W. and KLINE, G. M. *J. Res. Nat. Bur. Stand.* 1951, **46**, 391

On Free Radical Polymerizations With Rapidly Decaying Initiators

C. H. BAMFORD

Molecular weight distributions resulting from vinyl polymerizations in which the initiator concentration decays in a first-order or a second-order manner have been calculated, using a steady state treatment. It is assumed that the monomer concentration is constant, that the mean chain-length is long and that primary termination and retardation are unimportant. An expression for the intrinsic viscosity of the total polymer as a function of time is derived, and a method is outlined for obtaining the final number average and degree of polymerization from the measured value of $[\eta]$. A related method for determining $k_p k_t^{-1/2}$ is also described. The general case in which the stationary state treatment is inapplicable is considered and expressions for the radical concentration, the conversion and the number-average are obtained for first-order decay of the initiator.

WE HAVE recently investigated some vinyl polymerizations in which the initiators have a relatively short half-life (30 min or less) under the conditions of the experiments¹. To obtain a sufficient weight of polymer for characterization in such circumstances it often happens that the period of reaction must extend to at least one half-life of the initiator, with the result that the molecular weight distribution departs significantly from the instantaneous form (e.g. the 'most probable' distribution) even when the monomer concentration is held constant. Since we wished to determine the number-average molecular weights viscometrically a knowledge of the distributions was required. This case does not seem to have been considered explicitly in the literature, so that it was necessary to derive expressions for the distributions. Further, calculation of the intrinsic viscosities from the distributions showed that degrees of polymerization may be simply deduced from measurements of $[\eta]$ with the aid of a correction factor (F), the value of which does not depend on whether termination occurs by combination or disproportionation.

A related problem is the estimation of the ratio $k_p k_t^{-1/2}$ (k_p , k_t are the propagation and termination coefficients for the monomer, respectively) using a rapidly decaying initiator. When the rate of initiation is constant the ratio is usually evaluated from simultaneous measurements of the rates and degrees of polymerization. As will appear subsequently, a procedure involving a second factor (V) may be devised for obtaining the information from analogous measurements when the rate of initiation decays during the reaction.

In this paper we outline the calculations of the molecular weight distributions and the functions F , V for systems in which the initiator decays in a first-order, and a simple second-order, manner. The former case is probably more common in practice. Although no new principles are

involved in these calculations we thought it worthwhile placing the results on record since this type of problem is likely to arise frequently in work on new initiators. For this purpose we use the stationary-state treatment and thus assume (a) that the life of the mean kinetic chain is short compared to the half-life of the initiator. Other assumptions are that (b) the monomer concentration is constant, (c) the mean chain-length is long, and (d) primary termination and retardation are unimportant. Finally, we include a consideration of the general case (for first-order initiator decomposition) which does not involve the assumption of a stationary state.

FIRST-ORDER DECAY OF INITIATOR

Termination by disproportionation

Negligible chain transfer—Let C , \mathcal{I} represent the initiator concentration and rate of initiation at time t , respectively. If k_1 is the velocity coefficient for the decomposition of the initiator, and n the number of initiating radicals (assumed constant) arising from decomposition of one molecule of initiator, we have

$$\mathcal{I} = nk_1 C = nk_1 C_0 e^{-k_1 t} \quad (1)$$

Thus

$$\begin{aligned} d\mathcal{I}/dt &= nk_1 dC/dt = -nk_1^2 C_0 e^{-k_1 t} \\ &= nk_1^2 C = -k_1 \mathcal{I} \end{aligned} \quad (2)$$

If $[M]$ is the monomer concentration and

$$k_p [M] k_t^{-1/2} = a \quad (3)$$

we have

$$-d[M]/dt = a \mathcal{I}^{1/2} \quad (4)$$

or, by equation (2),

$$d[M]/d\mathcal{I} = a/k_1 \mathcal{I}^{1/2} \quad (5)$$

Further, the concentration $d[P_r]$ of chains of length r arising during the polymerization of $-d[M]$ moles of monomer is given by²

$$d[P_r] = -(d[M]/\bar{r}^2) e^{-r/\bar{r}} \quad (6)$$

Here \bar{r} is the mean (instantaneous) chain length, assumed to be large, and is expressed as a function of \mathcal{I} by equation (7).

$$\bar{r} = a \mathcal{I}^{-1/2} \quad (7)$$

To calculate the required distribution we eliminate $[M]$, \bar{r} from equation (6) using (5) and (7), and integrate between the limits of \mathcal{I} , thus obtaining

$$\begin{aligned} [P_r] &= -\frac{1}{ak_1} \int_{\mathcal{I}_0}^{\mathcal{I}_1} \mathcal{I}^{1/2} \exp(-r\mathcal{I}^{1/2}/a) d\mathcal{I} \\ &= \frac{2a^2}{r^3 k_1} \left\{ \exp(-r\mathcal{I}_1^{1/2}/a) \left(\frac{r^2 \mathcal{I}_1}{a^2} + \frac{2r \mathcal{I}_1^{1/2}}{a} + 2 \right) \right. \\ &\quad \left. - \exp(-r\mathcal{I}_0^{1/2}/a) \left(\frac{r^2 \mathcal{I}_0}{a^2} + \frac{2r \mathcal{I}_0^{1/2}}{a} + 2 \right) \right\} \end{aligned} \quad (8)$$

Chain transfer included—Equations (1) to (6) are still valid, but (7) must be replaced by

$$\bar{r} = \frac{k_p [\text{M}]}{k_f [\text{S}] + (\mathcal{J} k_t)^{\ddagger}} = \frac{a}{k_f k_t^{-\ddagger} [\text{S}] + \mathcal{J}^{\ddagger}} \quad (9)$$

where k_f is the rate constant for transfer to the compound S (assumed present in constant concentration), and the term $k_f [\text{S}]$ is understood to include all transfer processes. It is now convenient to replace \mathcal{J} by a new variable \mathcal{J}^{\ddagger} defined by

$$\mathcal{J}^{\ddagger} = k_f k_t^{-\ddagger} [\text{S}] + \mathcal{J}^{\ddagger} \quad (10)$$

so that

$$d\mathcal{J} / \mathcal{J}^{\ddagger} = d\mathcal{J} / \mathcal{J}^{\ddagger} \quad (11)$$

and

$$\bar{r} = a \mathcal{J}^{-\ddagger}$$

From equations (5), (6) and (11) it follows that the required distribution is given by

$$[\text{P}_r] = -\frac{1}{ak_1} \int_{\mathcal{J}_0}^{\mathcal{J}_1} \mathcal{J}^{\ddagger} \exp(-r \mathcal{J}^{\ddagger} / a) d\mathcal{J} \quad (12)$$

and hence by (8) in which the \mathcal{J} s are replaced by the corresponding \mathcal{J} s.

Moments—From equation (8) the moments of the distribution may be shown to have the values in equations (13)

$$\left. \begin{aligned} \sum_r [\text{P}_r] &= (\mathcal{J}_0 - \mathcal{J}_1) / k_1 \\ \sum_r r [\text{P}_r] &= (2a / k_1) (\mathcal{J}_0^{\ddagger} - \mathcal{J}_1^{\ddagger}) \\ \sum_r r^2 [\text{P}_r] &= (2a^2 / k_1) \ln (\mathcal{J}_0 / \mathcal{J}_1) \end{aligned} \right\} \quad (13)$$

Hence we have for the final number and weight averages, \bar{r}_{nf} and \bar{r}_{wf} , respectively:

$$\left. \begin{aligned} \bar{r}_{nf} &= 2a / (\mathcal{J}_0^{\ddagger} + \mathcal{J}_1^{\ddagger}) \\ \bar{r}_{wf} &= a \ln (\mathcal{J}_0 / \mathcal{J}_1) / (\mathcal{J}_0^{\ddagger} - \mathcal{J}_1^{\ddagger}) \end{aligned} \right\} \quad (14)$$

The expression for the final number average may be calculated directly. For, from equation (5), the total number of moles of monomer polymerized is easily seen to be $2a(\mathcal{J}_0^{\ddagger} - \mathcal{J}_1^{\ddagger}) / k_1$, and the total number of chains started is $n(C_0 - C_1)$ or $(\mathcal{J}_0 - \mathcal{J}_1) / k_1$. The ratio of these two numbers gives \bar{r}_{nf} at once.

If transfer is significant the relations (13) and (14) hold with the \mathcal{J} s replaced by the corresponding \mathcal{J} s. Note that the expressions (8), (13), (14) and the corresponding and related expressions in later sections depend on the validity of the stationary state approximation and that they cannot be used when this does not hold, e.g. for $\mathcal{J}_1 = 0$.

Termination by combination

Negligible chain transfer—Equations (1) to (5) are valid, but (6) and (7) must be replaced² by (15) and (16):

$$d [P_r] = -(4d [M]/\bar{r}^3) r e^{-2r/\bar{r}} \quad (15)$$

$$\bar{r} = 2a \mathcal{J}^{-1/2} \quad (16)$$

By following the procedure already outlined we obtain for the distribution the expression (17).

$$[P_r] = \frac{a^2}{r^3 k_1} \left\{ \exp(-r \mathcal{J}_1^{1/2}/a) \left(\frac{r^3}{a^3} \mathcal{J}_1^{3/2} + \frac{3r^2}{a^2} \mathcal{J}_1 + \frac{6r}{a} \mathcal{J}_1^{1/2} + 6 \right) \right. \\ \left. - \exp(-r \mathcal{J}_0^{1/2}/a) \left(\frac{r^3}{a^3} \mathcal{J}_0^{3/2} + \frac{3r^2}{a^2} \mathcal{J}_0 + \frac{6r}{a} \mathcal{J}_0^{1/2} + 6 \right) \right\} \quad (17)$$

Moments—From expression (17) we may derive the following moments:

$$\left. \begin{aligned} \sum_r [P_r] &= (\mathcal{J}_0 - \mathcal{J}_1)/2k_1 \\ \sum_r r [P_r] &= (2a/k_1) (\mathcal{J}_0^{1/2} - \mathcal{J}_1^{1/2}) \\ \sum_r r^2 [P_r] &= (3a^2/k_1) \ln(\mathcal{J}_0/\mathcal{J}_1) \end{aligned} \right\} \quad (18)$$

and hence the final number and weight averages:

$$\left. \begin{aligned} \bar{r}_n &= 4a/(\mathcal{J}_0^{1/2} + \mathcal{J}_1^{1/2}) \\ \bar{r}_w &= 1.5a \ln(\mathcal{J}_0/\mathcal{J}_1)/(\mathcal{J}_0^{1/2} - \mathcal{J}_1^{1/2}) \end{aligned} \right\} \quad (19)$$

Combination and chain transfer—This case is more complicated than those we have considered hitherto since two molecular weight distributions of different types exist in the polymer, and the relative proportions of these is a function of the rate of chain starting.

The final molecular weight distribution is shown in equation (20)

$$[P_r] = \frac{a^2}{r^3 k_1} \left\{ \exp(-r \mathcal{J}_1^{1/2}/a) \left(\frac{r^3}{a^3} \mathcal{J}_1^{3/2} + \frac{3r^2}{a^2} \mathcal{J}_1 + \frac{6r}{a} \mathcal{J}_1^{1/2} + 6 \right) \right. \\ \left. - \exp(-r \mathcal{J}_0^{1/2}/a) \left(\frac{r^3}{a^3} \mathcal{J}_0^{3/2} + \frac{3r^2}{a^2} \mathcal{J}_0 + \frac{6r}{a} \mathcal{J}_0^{1/2} + 6 \right) \right. \\ \left. - \frac{r^2}{a^3} \frac{k_2 [S]}{k_1^{1/2}} (\mathcal{J}_1 \exp[-r \mathcal{J}_1^{1/2}/a] - \mathcal{J}_0 \exp[-r \mathcal{J}_0^{1/2}/a]) \right\} \quad (20)$$

where the \mathcal{J} s are defined by equation (10). The moments are given in expressions (21).

$$\left. \begin{aligned} \sum_r [\mathbf{P}_r] &= \frac{\mathcal{J}_0 - \mathcal{J}_1}{2k_1} + \frac{k_t[\mathbf{S}]}{k_1 k_t^\dagger} (\mathcal{J}_0^\dagger - \mathcal{J}_1^\dagger) \\ \sum_r r [\mathbf{P}_r] &= \frac{2a}{k_1} (\mathcal{J}_0^\dagger - \mathcal{J}_1^\dagger) = \frac{2a}{k_1} (\mathcal{J}_0^\dagger - \mathcal{J}_1^\dagger) \\ \sum_r r^2 [\mathbf{P}_r] &= \frac{6a^2}{k_1} \left\{ \frac{1}{2} \ln \frac{\mathcal{J}_0}{\mathcal{J}_1} - \frac{k_t[\mathbf{S}]}{3k_t^\dagger} \cdot \frac{\mathcal{J}_0^\dagger - \mathcal{J}_1^\dagger}{\mathcal{J}_0^\dagger \mathcal{J}_1^\dagger} \right\} \end{aligned} \right\} \quad (21)$$

Intrinsic viscosities

If the intrinsic viscosity of a homogeneous polymer of degree of polymerization r is given by an equation of the Mark-Houwink type—

$$[\eta] = K (M_0 r)^\alpha \quad (22)$$

M_0 being the molecular weight of the monomer and K, α constants, it is well-known² that for a non-homogeneous polymer of the same kind

$$\eta = K M_0^\alpha \sum_r r^{1+\alpha} [\mathbf{P}_r]$$

where η is the 'ideal' viscosity, i.e. $c[\eta]$, c being the base-molar concentration. The sum may be evaluated from the distribution equations (8), (17) and (20) by integration. From (8) we obtain

$$[\eta] = K \Gamma(2 + \alpha) M_0^\alpha \bar{r}_{nf}^\alpha \frac{1 - z^{1-\alpha}}{(1-\alpha)(1-z)} \left(\frac{1+z}{2} \right)^\alpha \quad (23)$$

where

$$z = (\mathcal{J}_1 / \mathcal{J}_0)^\dagger = (C_1 / C_0)^\dagger \quad (24)$$

Now $K \Gamma(2 + \alpha)$ is the K value K_a holding for a most probable molecular weight distribution²; it follows from equation (23) that \bar{r}_{nf} may be evaluated from the intrinsic viscosity/molecular weight relation applicable to the most probable distribution provided the intrinsic viscosity used is that observed multiplied by a factor $F_1(z, \alpha)$ given by

$$F_1(z, \alpha) = \frac{(1-\alpha)(1-z)}{1-z^{1-\alpha}} \left(\frac{2}{1+z} \right)^\alpha \quad (25)$$

That is

$$[\eta] F_1(z, \alpha) = K_a (M_0 \bar{r}_{nf})^\alpha \quad (26)$$

As $z \rightarrow 1$, $F_1(z, \alpha) \rightarrow 1$ as would be expected, while $F(0, \alpha) = 2^\alpha (1-\alpha)$. For $z < 1$, $F_1(z, \alpha) < 1$. Plots of $F_1(z, \alpha)$ against z are given in Figure 1 for two typical values of α ; these curves can be used (with interpolation if necessary) in computing final number-average degrees of polymerization by the procedure described above if α lies in the range covered.

If transfer is significant equations (23) and (25) still hold, but z must be defined in terms of \mathcal{J} , i.e. $z = (\mathcal{J}_1 / \mathcal{J}_0)^\dagger$. Obviously in cases of excessive transfer $\mathcal{J}_1 = \mathcal{J}_0$, so that $z = 1$; the distribution under these conditions does not deviate from the most probable.

For termination by combination, we obtain from (17) by a similar procedure

$$[\eta] = K \frac{\Gamma(3 + \alpha)}{2^{1+\alpha}} M_0^\alpha \bar{r}_{nf}^\alpha \frac{1 - z^{1-\alpha}}{(1-\alpha)(1-z)} \left(\frac{1+z}{2} \right)^\alpha \quad (27)$$

Since² the K value for polymers having a 'combination' distribution $K_c = K\Gamma(3 + \alpha)/2^{1+\alpha}$, it follows that the factor $F_1(z, \alpha)$ is again given by

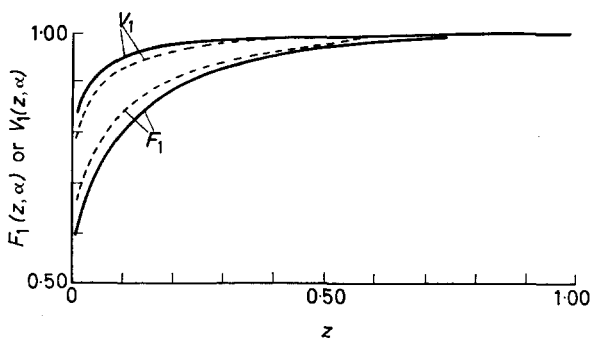


Figure 1— $F_1(z, \alpha)$ and $V_1(z, \alpha)$ as functions of z (first-order decay of initiator). Full curves: $\alpha=0.76$; broken curves: $\alpha=0.66$

equation (25). Thus the number-average may be obtained from the intrinsic viscosity corrected by the factor $F_1(z, \alpha)$ by using the Mark-Houwink equation in which K has the value appropriate for a combination polymer prepared at a constant rate of initiation. In other words, equation (26) applies, with K_d replaced by K_c .

For simultaneous combination and transfer we obtain from (20)

$$[\eta] = \frac{K\Gamma(3 + \alpha)}{2^{1+\alpha}} M_0^{\alpha} \bar{r}_{nf}^{\alpha} \frac{\{(1+z)/2 + \phi_0\}^{\alpha}}{1-z} \times \left(\frac{1+z^{1-\alpha}}{1-\alpha} + \frac{\phi_0(1-z^{-\alpha})}{2+\alpha} \right) \quad (28)$$

where

$$\phi_0 = \frac{k_f[S]}{(k_t \mathcal{J}_0)^{\frac{1}{2}}} = \frac{k_f[S]}{k_f[S] + (k_t \mathcal{J}_0)^{\frac{1}{2}}} \quad (29)$$

The relation thus involves an addition variable ϕ_0 which depends on the relative importance of transfer and combination. If $\phi_0=0$, equation (28) can be reduced to equation (27), while if $\phi_0=1$, corresponding to excessive transfer, equation (28) is equivalent to equation (23) as would be expected, since the distribution then assumes the 'most probable' form. Clearly equation (28) is a much less useful relation in practice than equation (23) since its application requires a knowledge of ϕ_0 .

Calculation of $k_p k_t^{-\frac{1}{2}}$

We consider first the case of termination by disproportionation. The ratio $k_p k_t^{-\frac{1}{2}} (=a/[M])$ is readily calculated when the rate of initiation is constant from the well-known relation

$$-\bar{r} \, d[M]/dt \equiv \bar{r}\omega = a^2 \quad (30)$$

which holds in the absence of transfer. When the initiator decays rapidly we measure a mean rate $\bar{\omega}_t$ which from equation (13) is seen to be

$$\begin{aligned}\bar{\omega}_t &= \Delta M/t = (1/t) \sum_r r [P_r] \\ &= (2a/k_1 t) (\mathcal{G}_0^\ddagger - \mathcal{G}_1^\ddagger)\end{aligned}\quad (31)$$

hence from equation (14) we obtain for the product

$$\bar{r}_{\eta} \bar{\omega}_t = \frac{4a^2}{k_1 t} \cdot \frac{\mathcal{G}_0^\ddagger - \mathcal{G}_1^\ddagger}{\mathcal{G}_0^\ddagger + \mathcal{G}_1^\ddagger} = a^2 \left\{ -\frac{2}{\ln z} \cdot \frac{1-z}{1+z} \right\} \quad (32)$$

The term in braces is less than unity for $z < 1$, so that the values of $k_p k_t^{-1}$ calculated from the product of the mean rate and the final number-average are lower than the true values.

It follows from the section 'Intrinsic viscosities' that if the number-average is calculated from $[\eta]$ without use of the factor $F_1(z, \alpha)$, the value obtained \bar{r}_η is higher than \bar{r}_{η} . Thus it is of interest to examine the magnitude of the product $\bar{r}_\eta \bar{\omega}_t$. We see from equation (26) that

$$\bar{r}_\eta^z = \bar{r}_{\eta}^z / F_1(z, \alpha) \quad (33)$$

hence from equation (32)

$$\frac{\bar{r}_\eta \bar{\omega}_t}{a^2} = -\frac{1}{\ln z} \left\{ \frac{1-z^{1-\alpha}}{(1-z)(1-z)^{1-\alpha}} \right\}^{1/\alpha} \equiv V_1(z, \alpha) \quad (34)$$

Graphs of the function $V_1(z, \alpha)$ are shown in *Figure 1* for $\alpha=0.76$ and $\alpha=0.66$. For $z > 0.1$ ($z=0.1$ corresponds to 99 per cent consumption of initiator), V_1 differs from unity by less than 7.5 per cent. Thus a reasonably accurate value of a may often be obtained simply from the product of the *uncorrected* viscometric degree of polymerization and the mean rate of polymerization. Values of $V_1(z, \alpha)$ obtained from equation (34), or from the curves in *Figure 1* by interpolation, may be used to calculate accurate values of a in the general case.

When termination is by combination, we have, for a constant rate of initiation in the absence of transfer

$$\bar{r}_\omega = 2a^2 \quad (35)$$

From equations (19) and (31) we derive

$$\bar{r}_{\eta} \bar{\omega}_t = 2a^2 \left\{ -\frac{2}{\ln z} \cdot \frac{1-z}{1+z} \right\} \quad (36)$$

an expression which stands in exactly the same relation to equation (35) as equation (32) does to equation (30). Since equation (33) is valid, the relation corresponding to equation (34) must be

$$\bar{r}_\eta \bar{\omega}_t / 2a^2 = V_1(z, \alpha) \quad (37)$$

and may be used in determining a from $\bar{\omega}_t$ and \bar{r}_η .

SECOND-ORDER DECAY OF INITIATOR

The relevant equations in this case are

$$-dC/dt = k_2 C^2 \quad (38)$$

$$\mathcal{J} = -n dC/dt = nk_2 C^2 \quad (39)$$

The calculation of $[P_r]$, the moments of the distribution and the function $F_2(z, \alpha)$ may be carried out as indicated earlier, and we give the results without details.

Termination by disproportionation

Equations (40) to (42) summarize the main results for insignificant transfer.

$$[P_r] = \frac{an^\dagger}{r^2 k_2^\dagger} \left\{ \exp(-r\mathcal{J}_1^\dagger/a) \left(\frac{r}{a} \mathcal{J}_1^\dagger + 1 \right) - \exp(-r\mathcal{J}_0^\dagger/a) \left(\frac{r}{a} \mathcal{J}_0^\dagger + 1 \right) \right\} \quad (40)$$

$$\left. \begin{aligned} \sum_r [P_r] &= \frac{n^\dagger}{k_2^\dagger} (\mathcal{J}_0^\dagger - \mathcal{J}_1^\dagger) \\ \sum_r r [P_r] &= \frac{an^\dagger}{2k_2^\dagger} \ln \frac{\mathcal{J}_0}{\mathcal{J}_1} \\ \sum_r r^2 [P_r] &= \frac{2a^2 n^\dagger}{k_2^\dagger} \left(\frac{1}{\mathcal{J}_1^\dagger} - \frac{1}{\mathcal{J}_0^\dagger} \right) \end{aligned} \right\} \quad (41)$$

$$\left. \begin{aligned} \bar{r}_{nf} &= \frac{a}{2} \cdot \frac{\ln(\mathcal{J}_0/\mathcal{J}_1)}{\mathcal{J}_0^\dagger - \mathcal{J}_1^\dagger} \\ \bar{r}_{wf} &= \frac{4a}{\ln(\mathcal{J}_0/\mathcal{J}_1)} \left(\frac{1}{\mathcal{J}_1^\dagger} - \frac{1}{\mathcal{J}_0^\dagger} \right) \end{aligned} \right\} \quad (42)$$

Termination by combination

Equations (43) to (45) hold for this case if transfer is negligible.

$$[P_r] = \frac{an^\dagger}{2r^2 k_2^\dagger} \left\{ \exp(-r\mathcal{J}_1^\dagger/a) \left(\frac{r^2}{a^2} \mathcal{J}_1 + \frac{2r}{a} \mathcal{J}_1^\dagger + 2 \right) - \exp(-r\mathcal{J}_0^\dagger/a) \left(\frac{r^2}{a^2} \mathcal{J}_0 + \frac{2r}{a} \mathcal{J}_0^\dagger + 2 \right) \right\} \quad (43)$$

$$\left. \begin{aligned} \sum_r [P_r] &= \frac{n^\dagger}{2k_2^\dagger} (\mathcal{J}_0^\dagger - \mathcal{J}_1^\dagger) \\ \sum_r r [P_r] &= \frac{an^\dagger}{2k_2^\dagger} \ln \frac{\mathcal{J}_0}{\mathcal{J}_1} \\ \sum_r r^2 [P_r] &= \frac{3a^2 n^\dagger}{k_2^\dagger} \left(\frac{1}{\mathcal{J}_1^\dagger} - \frac{1}{\mathcal{J}_0^\dagger} \right) \end{aligned} \right\} \quad (44)$$

$$\left. \begin{aligned} \bar{r}_{nf} &= \frac{a \ln(\mathcal{J}_0 / \mathcal{J}_1)}{\mathcal{J}_0^{\frac{1}{2}} - \mathcal{J}_1^{\frac{1}{2}}} \\ \bar{r}_{wf} &= \frac{6a}{\ln(\mathcal{J}_0 / \mathcal{J}_1)} \left(\frac{1}{\mathcal{J}_1^{\frac{1}{2}}} - \frac{1}{\mathcal{J}_0^{\frac{1}{2}}} \right) \end{aligned} \right\} \quad (45)$$

Chain transfer

When chain transfer is appreciable the relations become more complicated and, even in the case of termination by disproportionation, cannot be expressed by substitution of \mathcal{T} for \mathcal{J} . The relative importance of transfer and termination is involved, and thus, in general, the results are less useful practically.

Intrinsic viscosities

The intrinsic viscosity of the total polymer is given by equations (46) and (47) for disproportionation and combination, respectively.

$$[\eta] = KM_0^\alpha \Gamma(2 + \alpha) \bar{r}_{nf}^\alpha \left(-\frac{1}{\ln z} \right)^{1+\alpha} \frac{(1-z)^\alpha}{\alpha} \left(\frac{1}{z^2} - 1 \right) \quad (46)$$

$$[\eta] = KM_0^\alpha \frac{\Gamma(3 + \alpha)}{2^{1+\alpha}} \bar{r}_{nf}^\alpha \left(-\frac{1}{\ln z} \right)^{1+\alpha} \frac{(1-z)^\alpha}{\alpha} \left(\frac{1}{z^2} - 1 \right) \quad (47)$$

Here z is defined by $z = (\mathcal{J}_1 / \mathcal{J}_0)^{\frac{1}{2}} = C_1 / C_0$. (48)

From these equations it follows that we may define a factor $F_2(z, \alpha)$ which may be used to obtain the final number-average from intrinsic viscosity measurements as already described, and which is the same for termination by disproportionation and combination. We find that

$$F_2(z, \alpha) = \alpha (-\ln z)^{1+\alpha} (1-z)^{-1} (1/z - 1)^{-\alpha} \quad (49)$$

Plots of this function for $\alpha = 0.76$ and 0.66 are shown in Figure 2. As would be expected, F_2 deviates from unity rather more markedly than F_1 .

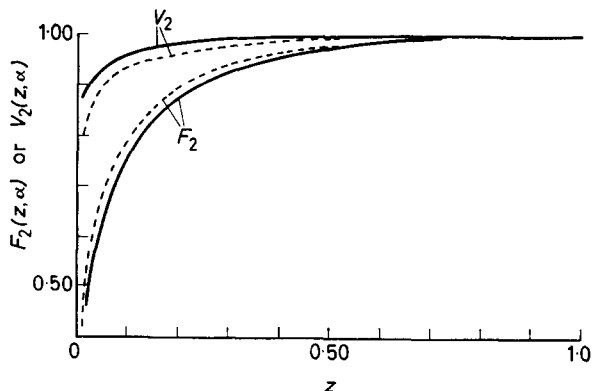


Figure 2— $F_2(z, \alpha)$ and $V_2(z, \alpha)$ as functions of z (second-order decay of initiator). Full curves: $\alpha = 0.76$; broken curves: $\alpha = 0.66$

Calculation of $k_p k_i^{-1}$

Estimation of the quantity $k_p k_i^{-1}$ may be carried out from measurements of $\bar{\omega}_i$ and \bar{r}_i in a manner similar to that described above. The relevant equations are (50) and (51).

$$\left. \begin{array}{l} \text{For disproportionation } \bar{r}_i \bar{\omega}_i / a^2 = V_2(z, \alpha) \\ \text{For combination } \bar{r}_i \bar{\omega}_i / 2a^2 = V_2(z, \alpha) \end{array} \right\} \quad (50)$$

where
$$V_2(z, \alpha) = -\frac{\ln z}{1-z} \left(-\frac{1-z^2}{z \ln z} \right)^{1/2} \quad (51)$$

Graphs of the function $V_2(z, \alpha)$ for $z=0.76$ and 0.66 are given in *Figure 2*.

THE CASE WITHOUT RESTRICTION ON LIFETIMES

General

The situation is much more complicated if assumption (a) is relaxed, i.e. if the halflife of the initiator is comparable to the life of the kinetic chain. To obtain the total radical concentration $[R]$ it then becomes necessary to solve the general equation

$$d[R]/dt = nk_1 C_0 e^{-k_1 t} - k_t [R]^2 \quad (52)$$

which applies for first-order decomposition of the initiator (the only case we consider).

This Riccati-type equation can be transformed to the more familiar form equation (54) by making the substitutions:

$$\left. \begin{array}{l} [R] = (1/k_t y) (dy/dt) \quad (a) \\ u = 2(nC_0 k_1 / k_t)^{1/2} e^{-k_1 t / 2} \quad (b) \end{array} \right\} \quad (53)$$

$$d^2 y / du^2 + (1/u) (dy/du) - y = 0 \quad (54)$$

Equation (54) is a modified Bessel equation (for functions of order zero with purely imaginary argument) and for present purposes the solution may be written in terms of the standard functions $I_0(u)$, $K_0(u)$ in the form

$$y = I_0(u) + \lambda K_0(u) \quad (55)$$

where λ is an integration constant determined by the boundary conditions*. The reader may consult ref. 3 for a discussion of the Bessel function $I_n(u)$, $K_n(u)$. It should be noted that various authors have denoted by $K_n(u)$ a function differing from that in the above reference by omission of a factor $\cos n\pi$. This changes the sign of the functions for odd integral n . We follow the usage of ref. 3, according to which the $I_n(u)$ and $K_n(u)$ satisfy identical recurrence formulae. Initially $[R]=0$, i.e. $dy/dt=0$, and hence from equation (55)

$$\lambda = -I_1(u_0) / K_1(u_0) \quad (56)$$

*The general solution of equation (54) contains two arbitrary constants, but only the ratio of these (λ) remains after substitution into (53a). This would be anticipated since the solution of (52) contains only one arbitrary constant.

where $I_1(u)$, $K_1(u)$ are the modified Bessel functions of order one³. By employing equation (53a) we may now derive expression (57), which gives the total free radical concentration as a function of u

$$[R] = -\frac{uk_1}{2k_t} \cdot \frac{I_1(u) + \lambda K_1(u)}{I_0(u) + \lambda K_0(u)} \quad (57)$$

The $[R]/t$ relation may be obtained simply from equation (57) with the aid of equation (53b).

The monomer conversion ΔM and the number-average degree of polymerization can be calculated without difficulty. We find

$$\begin{aligned} \Delta M &= k_p [M] \int_0^t [R] dt = \frac{k_p [M]}{k_t} \ln \frac{y}{y_0} \\ &= \frac{k_p [M]}{k_t} \ln \left\{ \frac{I_0(u) + \lambda K_0(u)}{I_0(u_0) + \lambda K_0(u_0)} \right\} \end{aligned} \quad (58)$$

The total number of chains started is $nC_0(1 - e^{-k_1 t})$, so that we obtain for the overall number-average at time t (assuming disproportionation)

$$\bar{r}_{n,t} = \frac{k_p [M]}{nk_t C_0 (1 - e^{-k_1 t})} \ln \left\{ \frac{I_0(u) + \lambda K_0(u)}{I_0(u_0) + \lambda K_0(u_0)} \right\} \quad (59)$$

Strictly, this includes growing chains as well as finished polymer molecules, but except at very short times the latter will be greatly in excess. Separation of the two species may be effected by recourse to equation (52). The number of finished polymer molecules is $\int_0^t k_t [R]^2 dt$, which from equation (52) is given by

$$\int_0^t k_t [R]^2 dt = n(C_0 - C_1) - [R] \quad (60)$$

and thus may be evaluated by use of equation (57). If termination is by combination, the mean degree of polymerization, except at very short times, is twice the value given by equation (59). Equation (60) may be used in this case also, the number of finished polymer molecules being $\frac{1}{2} \int_0^t k_t [R]^2 dt$.

The extension of these results to systems in which chain transfer is important will be obvious since the number of polymer molecules produced by transfer is proportional to $\int_0^t [R] dt$ which has already been evaluated (cf. ref. 58).

According to equation (58), $\Delta M \rightarrow \infty$ as $u \rightarrow 0$, i.e. as $t \rightarrow \infty$, since $K_0(u) \rightarrow \infty$. This could not be deduced from the relations given earlier in the paper [equations (13), (18), (21)] in view of assumption (a). The present result is not surprising since it is well-known that, in principle, the photochemical after-effect in free radical polymerization becomes infinite if there is zero rate of initiation in the dark.

Equations (56) to (59) allow calculation of $[R]$, ΔM and $\bar{r}_{n,t}$ in the general case from tabulated values of the Bessel functions, e.g. those given by Sibagaki⁴. If the relevant values of u_0 and u are either $\gg 1$ or $\ll 1$ it is

more convenient to use algebraic expansions of the functions instead of tabulated values, and we now discuss briefly some cases which may arise.

$u_0, u \gg 1$

In many cases of practical interest both u_0 and u will be $\gg 1$. It is then convenient to use asymptotic expansions for the Bessel functions. These are given in ref. 3 and their use leads to the following expressions for $[R]$, \bar{r}_{nj} and ΔM , in which terms in $1/u_0^2$, $1/u^2$ and higher powers are omitted.

$$\lambda = (e^{2u_0/\pi}) (1 - 3/4u_0) \quad (61)$$

$$[R] = \frac{uk_1}{2k_t} \left(1 + \frac{1}{2u}\right) \frac{e^{2(u_0-u)} - \left(1 - \frac{3}{4u} + \frac{3}{4u_0}\right)}{e^{2(u_0-u)} + \left(1 + \frac{1}{4u} + \frac{3}{4u_0}\right)} \quad (62)$$

$$\begin{aligned} \Delta M &= \bar{r}_{nj} n C_0 (1 - e^{-k_1 t}) \\ &= \frac{k_p [M]}{k_t} \ln \left\{ \left(\frac{u_0}{u}\right)^{\dagger} \frac{e^{u_0-u} + \left(1 + \frac{1}{4u} + \frac{3}{4u_0}\right) e^{-(u_0-u)}}{2 + 1/u_0} \left(1 - \frac{1}{8u} + \frac{1}{8u_0}\right) \right\} \end{aligned} \quad (63)$$

If $(u_0 - u) \gg 1$, equation (62) can be reduced to

$$[R] = \frac{uk_1}{2k_t} = \left(\frac{nk_1 C_0}{k_t}\right)^{\dagger} e^{-k_1 t/2} \quad (64)$$

(neglecting terms in $1/u$, etc.). This value of $[R]$ corresponds to the stationary state value for a slowly decaying initiator, as would be expected for the conditions $u_0, u, (u_0 - u) \gg 1$. Similarly equation (63) yields the values of $\Delta M (= \sum r [P_r])$, \bar{r}_{nj} given in equations (13) and (14), respectively.

On the other hand, if $u_0, u \gg 1$ but $(u_0 - u) \ll 1$ equation (62) becomes

$$[R] = (uk_1/2k_t) (u_0 - u) = nk_1 C_0 t \quad (65)$$

which illustrates the initial growth of radical concentration, linear in time, before significant termination has occurred. Under the same conditions we may obtain from equation (63)

$$\left. \begin{aligned} \Delta M &= \frac{1}{2} nk_p [M] C_0 k_1 t^2 \\ \bar{r}_{nj} &= \frac{1}{2} k_p [M] t \end{aligned} \right\} \quad (66)$$

$u_0, u \ll 1$

If $u \ll 1$ the appropriate limits are given below, in which terms in u^3 and higher powers are omitted³.

$$\begin{aligned} I_0(u) &= 1 + \frac{u^2}{4}; & K_0(u) &= -\left(\ln \frac{u}{2} + \gamma\right) - \frac{u^2}{4} \left(\ln \frac{u}{2} + \gamma - 1\right) \\ I_1(u) &= \frac{u}{2}; & K_1(u) &= -\frac{1}{u} - \frac{u}{2} \left(\ln \frac{u}{2} + \gamma - \frac{1}{2}\right) \end{aligned} \quad (67)$$

Here γ is Euler's constant ($= 0.5772 \dots$). For $u_0, u \ll 1$ we obtain from relations (56) to (59):

$$\left. \begin{aligned} \lambda &= \frac{1}{2}u_0^2 \\ [\mathbf{R}] &= \frac{k_1}{4k_t} \cdot \frac{u_0^2 - u^2}{1 - \frac{1}{2}u_0^2 \ln \frac{1}{2}u} \\ \Delta M &= \bar{r}_n n C_0 (1 - e^{-k_1 t}) = \frac{k_p [\mathbf{M}]}{k_t} \ln \frac{1 + \frac{1}{2}u^2 - \frac{1}{2}u_0^2 \ln \frac{1}{2}u}{1 + \frac{1}{2}u_0^2 - \frac{1}{2}u_0^2 \ln \frac{1}{2}u_0} \end{aligned} \right\} \quad (68)$$

If the reaction is carried out for a sufficiently long time, $k_1 t \gg 1$ and $u/u_0 \ll 1$. In these circumstances equations (68) become:

$$\left. \begin{aligned} [\mathbf{R}] &= 1/k_t \\ \Delta M &= \bar{r}_n n C_0 = \frac{k_p [\mathbf{M}]}{k_t} \ln t \end{aligned} \right\} \quad (69)$$

These limiting relations may be verified by simple calculation. They would, of course, apply to the case in which k_1 is very large, so that initiation would occur in a short 'burst', the exact profile of which is unimportant.

If the reaction time is short so that $k_1 t \ll 1$, equation (68) can be reduced to equation (66) as would be expected. Evaluation of the logarithmic term in equation (68) is most easily effected in this case by using Taylor's theorem.

$u_0 \gg 1$, no restriction on u

It may easily happen that while $u_0 \gg 1$ the values of u at times for which ΔM is required are not large enough to allow the use of asymptotic expansions. In this case, we obtain from equations (58) and (59) by using the asymptotic expansions for the functions of u_0

$$\Delta M = \bar{r}_n n C_0 (1 - e^{-k_1 t}) = (k_p [\mathbf{M}]/k_t) \left\{ u_0 + \frac{1}{2} \ln (u_0/2\pi) + \ln K_0(u) \right\} \quad (70)$$

If appropriate, $K_0(u)$ may be evaluated from equation (67).

Examples

Figure 3 shows the $\Delta M/\log t$ curves calculated from equations (63) and (70) using the values of the constants indicated. These are such that the stationary state treatment would be expected to hold for much of the

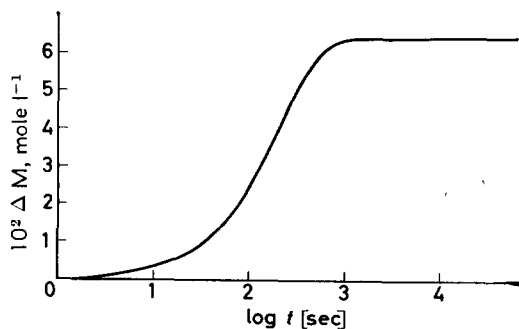


Figure 3 — Conversion / time curve calculated from expressions (63) and (70) using the following values: $C_0 = 10^{-4}$, $[\mathbf{M}] = 10$ mole l^{-1} ; $n = 1$; $k_1 = 10^{-2}$ sec $^{-1}$; $k_p = 100$, $k_t = 10^7$ mole $^{-1}$ l. sec $^{-1}$. The curve calculated from equations (1) and (13) is very similar except that it is more nearly horizontal for $\log t > 3$

reaction. That this is so is illustrated by the fact that values of ΔM calculated from equation (13) are very close to those in *Figure 3*. At very short times (< 1 sec) equation (13) gives results which are too high (not apparent from *Figure 3*) while at very long times equation (13) incorrectly predicts a finite limit for ΔM . However, the extent of the agreement indicates that the viscosity corrections in equations (25) and (34) may be expected to apply in regions of practical interest.

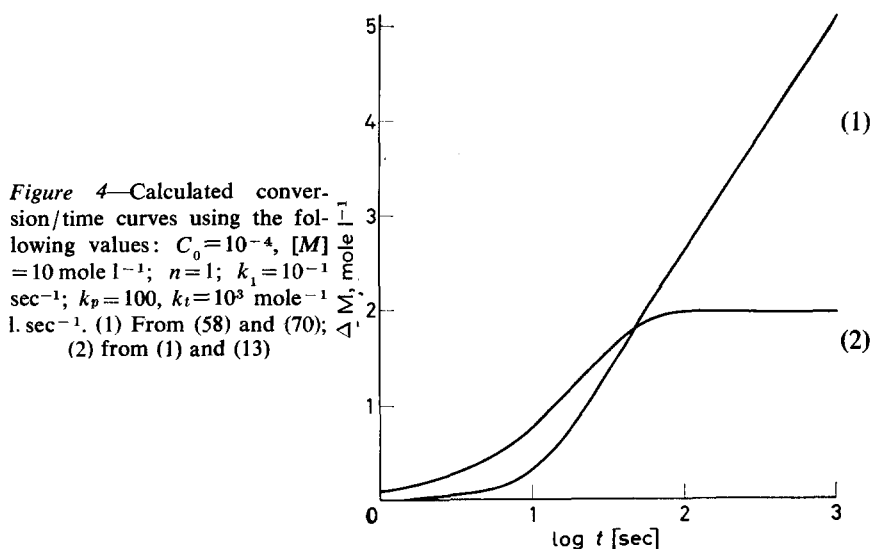


Figure 4—Calculated conversion/time curves using the following values: $C_0 = 10^{-4}$, $[M] = 10$ mole l^{-1} ; $n = 1$; $k_1 = 10^{-1}$ sec^{-1} ; $k_p = 100$, $k_t = 10^3$ mole $^{-1}$ $l. sec^{-1}$. (1) From (58) and (70); (2) from (1) and (13)

If the parameters are such that the stationary state approximation is not valid, equation (13) is, of course, inapplicable. This is illustrated in *Figure 4* which differs from *Figure 3* in that a larger value of k_1 and a smaller value of k_t have been used. The stationary state curve (2) is a very poor approximation.

The author is pleased to thank Alan Bamford for assistance with the calculation of the curves.

*Department of Inorganic, Physical and Industrial Chemistry,
University of Liverpool*

(Received May 1964)

REFERENCES

- ¹ BAMFORD, C. H., EASTMOND, G. C. and MALTMAN, W. R. *Trans. Faraday Soc.* In press
- ² BAMFORD, C. H., BARB, W. G., JENKINS, A. D. and ONYON, P. F. *The Kinetics of Vinyl Polymerization by Radical Mechanisms*, Chapter 7. Butterworths: London, 1958
- ³ WHITTAKER, E. T. and WATSON, G. N. *Modern Analysis*, p 372 et seq. Cambridge University Press: London, 1927
- ⁴ SIBAGAKI, W. *0.01% Tables of Modified Bessel Functions*. Baifukan: Tokyo, 1955. This author uses the alternative definition of $K_n(u)$ mentioned on page 72, the functions being always positive

Thermal Conductivities of Polymers I— Polyvinyl Chloride

R. P. SHELDON and Sister K. LANE

The thermal conductivities of unplasticized and plasticized samples of polyvinyl chloride have been measured in the range 15° to 98°C. At a temperature above about 25°C the thermal conductivity decreases with increasing plasticizer concentration, a simple relationship holding between the two quantities at this temperature. The results indicate that thermal conductivity increases with temperature, reaching a maximum in the neighbourhood of the glass-temperature, and then begins to decrease.

A KNOWLEDGE of the thermal conductivities of polymers is of interest both from the point of view of industry with its concern for the fabrication and application of materials and also from an academic viewpoint where there is an interest in the interrelation of physical properties and structure. It is apparent that an understanding merely of the chemical nature of a polymer will not suffice for this information since in the first place only a limited amount of data is available, thus permitting no more than a general appreciation of such factors as the influence of polar and non-polar groups, etc., and in the second place we may presume a further dependence upon the actual physical state. Regarding the latter it would be reasonable to expect contributions dependent upon such variables as the nature and extent of crystallinity, molecular orientation, the position of the glass-temperature with reference to the operating temperature, the presence of additives, etc. Since considerations of this kind further demand a recognition of different mechanisms of heat conduction it is perhaps opportune to review briefly at this stage the current theories of heat conduction.

Ignoring, for the purposes of the present discussion, metallic conduction which will be applicable only to specialized applications of polymeric systems, e.g. metal-filled resins, two mechanisms of heat conduction have been proposed corresponding to two distinct classes of materials¹. Molecular transmission or molecule-to-molecule transfer of energy is accomplished by the excitation of adjacent groupings, i.e. by the translation, rotation or vibration of energized groups (and presumably these too will differ in efficiency). Such a process is diffusional in nature and comparatively slow, contributing to the lower thermal conductivity of an amorphous or molecular solid. The second mode of heat conduction is one involving lattice energy vibrations within a crystalline structure, in which thermal excitation creates waves of disturbance in the form of primary lattice imperfections known as phonons². This gives rise to a more efficient transfer of heat and one which is considered applicable to valency and ionic solids. In any given material, particularly if the material is a polymer involving either an intrinsic heterogeneity of structure or an imposed heterogeneity through the presence of additives, both mechanisms of heat conduction may be operating at the same time. Moreover, since polymers

in general have strongly temperature-dependent properties the relative contribution of each mechanism may vary with temperature.

At the time of the commencement of the present studies little information on the thermal conductivities of polymers was available, particularly as a function of temperature and although the last two or three years have seen a significant increase in the amount of available data much work still remains to be carried out for a comprehensive appreciation of the subject. The present paper, which is the first in a series, describes work which has taken place using plasticized and unplasticized polyvinyl chloride (PVC). An interpretation of the results has been made in terms of separate contributions of individual components and suggestions are made for the extension of the results to other systems.

EXPERIMENTAL

Materials

The samples of PVC were kindly supplied by B.X. Plastics Ltd and had compositions as shown in *Table 1*. A separate sample of the di alphanyl

Table 1. Composition of PVC samples

<i>Code No.</i>	<i>1</i>	<i>2</i>	<i>3</i>	<i>4</i>	<i>5</i>	<i>6</i>
Plasticizer conc. %w/w	0	20	26	30	36	40

The samples also included less than two per cent 'thio tin' stabilizer and about 0.2 per cent stearic acid lubricant.

phthalate plasticizer used in the formulation of these compositions was also supplied by B.X. Plastics Ltd.

Apparatus and technique

(1) *Thermal conductivity*—The apparatus used in the determination of thermal conductivity was identical to that described by Kline³, being a cylindrical cell technique in which the polymer is in the form of a tube (i.d. = 0.25 in., o.d. = 0.50 in., length \approx 8 in.). Through the centre of the tube is inserted a copper tube containing an electrically heated wire embedded in an aluminium-filled epoxy resin. The polymer sample is surrounded along its length by a copper jacket through which water at temperatures in the range 15° to 98°C is pumped from a temperature-controlled bath. The temperature across the polymer was measured by means of previously calibrated copper-constantan thermocouples inserted at each side of the sample. The actual temperatures themselves were obtained through p.d. measurements using a Thermocouple Potentiometer Type P4 (Croydon Precision Instrument Co.). The thermal conductivity could then be obtained from the appropriate form of Fourier's equation for steady-state conditions

$$k = (q/2L \cdot \Delta t) \ln (r_2/r_1) \quad (1)$$

where k is the thermal conductivity, q is the heat flux (obtained from a knowledge of the voltage across, and the current through, the heater wire), L is the specimen length, Δt is the temperature difference across the

specimen, and r_2 and r_1 are its external and internal radii respectively.

(2) *Density*—The density of the di alphanyl phthalate was determined using a density bottle and was found to be 0.944 g cm^{-3} at 25°C .

Densities of PVC samples were obtained with the aid of a density gradient column containing a mixture of carbon tetrachloride and hexane. Since, presumably due to a slow extraction of plasticizer, the plasticized sample densities changed slowly with time, measurements were made as a function of time and plotted graphically, from which an estimate of the 'zero time density' could be made. The validity of this approach was confirmed by a separate determination using sample No. 4 in a conventional water displacement method which gave exact agreement ($\pm 0.001 \text{ g cm}^{-3}$) with the result for a small piece of polymer using the aforementioned technique⁴.

(3) *Confirmation of isotropy*—Fourier's equation as presented above is strictly applicable to an isotropic condition. That the latter applied with the present samples was confirmed by X-ray diffraction analysis which showed weak but recognizable ring patterns due to scattering from crystalline regions.

(4) *Sound velocity*—A convenient way of determining the thermal conductivity of a liquid is through the measurement of the velocity of sound in a liquid and applying an equation due to Bridgman⁵

$$k = 3k_b V (d/m)^{2/3} \quad (2)$$

where k_b is Boltzmann's constant, V is the velocity of sound, m is the mass of one molecule of the liquid, and d is its density.

The velocity of sound in di alphanyl phthalate was determined at 25°C using an acoustic interferometer cell similar to that described by Hubbard and Loomis⁶ and was found to be 1416 m sec^{-1} . From this the thermal conductivity of the plasticizer was calculated to be $1.93 \times 10^{-4} \text{ cal cm}^{-1} \text{ sec}^{-1} (\text{C}^\circ)^{-1}$.

RESULTS

The thermal conductivities of the various samples of PVC are shown as a function of temperature in *Figure 1*. From this the individual values at 25°C were obtained and plotted as a function of plasticizer concentration as shown in *Figure 2*. It might be mentioned at this stage that the method was evaluated by comparison of a measurement upon a standard sample of atactic polymethyl methacrylate with a value obtained separately on the same material using the slab method. The value of $4.60 \times 10^{-4} \text{ cal cm}^{-1} \text{ sec}^{-1} (\text{C}^\circ)^{-1}$ at 25°C compares favourably with the value of $4.5 \times 10^{-4} \text{ cal cm}^{-1} \text{ sec}^{-1} (\text{C}^\circ)^{-1}$ quoted at the same temperature for the second technique⁷.

Figure 3 shows the densities of PVC samples as a function of plasticizer concentration at 25°C .

DISCUSSION

Figure 1 shows that the behaviour of unplasticized PVC is quite different from that of the plasticized material. It should also be mentioned that the

Figure 1—Thermal conductivities of PVC as a function of plasticizer concentration and temperature

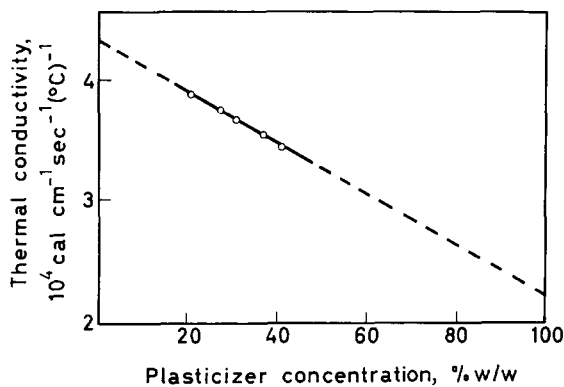
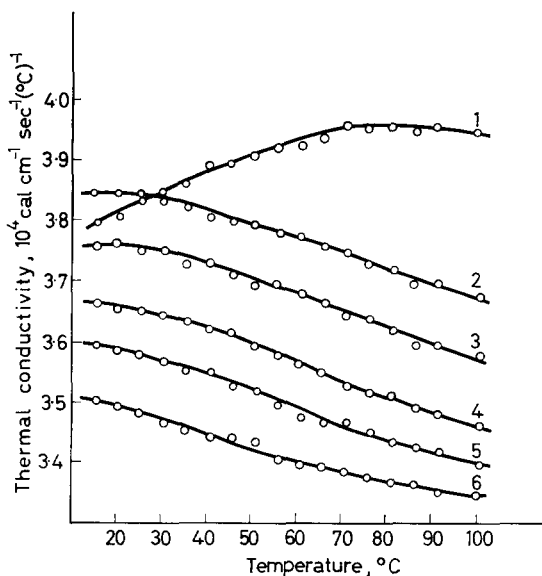
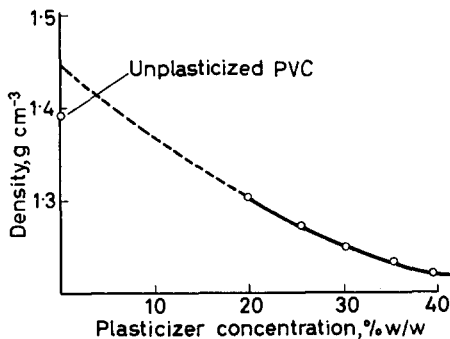


Figure 2—Thermal conductivity as a function of plasticizer concentration at 25°C

Figure 3—Density of PVC as a function of plasticizer concentration at 25°C



values for the unplasticized polymer agree satisfactorily with those of Hennig and Knappe⁸, and particularly well with those of Eiermann and Hellwege⁹ who used a non-steady state method for their thermal conductivity measurements, and that the latter workers similarly present results indicative of a maximum in the thermal conductivity of PVC at the higher temperatures. Moreover, results of measurements on three plasticized (unspecified) samples are again in tentative agreement with those of the present work in that the values for the plasticized samples are generally lower, the difference depending upon the concentration, at temperatures above about 25°C and that there is some evidence, albeit slight in the present results, for a tendency towards maxima in the results and that the maxima themselves tend towards lower temperatures the higher the plasticizer concentration.

This general behaviour may be qualitatively understood on the views of Uberreiter and Nens¹⁰ who suggest, for polymers in general, that at temperatures below the brittle-point conduction is mainly due to longitudinal waves propagated along main chains and that propagation in this way proceeds more easily the higher the temperature. Above the brittle-point they consider that transverse vibrations tend to dampen the longitudinal wave motion causing a decrease in the thermal conductivity. It might also be mentioned that these authors extend their views to predict an increase again at higher temperatures.

Returning to *Figure 1*, the maximum in the curve for the unplasticized sample of PVC is seen to occur in the neighbourhood of the glass-temperature reported to be at 82°C¹¹ as would be expected on the above theory. Presumably, the lowering of the maximum with increase of plasticizer concentration corresponds simply to a lowering of the glass-temperature. Closer examination of the curves relating to the more highly plasticized samples indicates at a higher temperature a tendency towards minima suggestive of some support for the suggestions of Uberreiter and Nens for behaviour at temperatures substantially above the glass-temperature. It should be pointed out, however, that this tendency is not apparent in the results presented by Eiermann and Hellwege.

Figure 2 shows that within the range of plasticizer concentration used a rectilinear relationship obtains between thermal conductivity at 25°C and plasticizer concentration. Extrapolation to zero concentration produces a higher value for the unplasticized PVC than the value obtained experimentally, i.e. 4.33×10^{-4} compared with 3.85×10^{-4} cal cm⁻¹ sec⁻¹ (°C)⁻¹. This discrepancy was at first attributed to evidence of the Horsley effect in which the presence of plasticizer in PVC is believed to produce an increase in the extent of crystallization¹². That the presence of certain liquids can produce crystallization is well known with other polymers¹³. As well as an improvement in the resolution of the X-ray diffraction photographs of plasticized polymer other evidence apparently in support of this contention appears in *Figure 3* in which it is seen that the extrapolated value for the unplasticized sample of PVC is again higher than the experimentally determined value of density as would be expected for a more crystalline polymer. (In support of the rather long extrapolation shown in *Figure 3*

it should be mentioned that analysis of the curve within the experimental region shows that the second differential of the curve is constant and this constant was used for purposes of extrapolation.) However, further consideration shows that although this interpretation may be partly true and, if it were, might lead to a separate evaluation of crystalline and amorphous contributions to thermal conductivity as will be described in another context in the second paper in this series, another but not exclusive explanation of the discrepancy lies in a consideration of the individual curves for each system, together with the results of Eiermann and Hellwege. Since the position of the maxima with respect to temperature depends upon the plasticizer concentration then there will be overlap of the curves at the lower temperatures. It follows therefore that curves corresponding to *Figure 2* at lower temperatures will exhibit maxima also. This then explains why, at 25°C which is presumably above the glass-temperature for any of the plasticized samples, there is a simple relationship between thermal conductivity and concentration for these samples since the curves show some parallelism, whilst the unplasticized sample with the higher glass-temperature appears to show an anomaly. Extension of these considerations may be made to density, or to any physical property, to explain corresponding apparent anomalies.

Extrapolation of the results in *Figure 2* in an opposite direction enables a value to be quoted for the thermal conductivity of di alphanyl phthalate of $2.25 \times 10^{-4} \text{ cal cm}^{-1} \text{ sec}^{-1} (\text{°C})^{-1}$ which, considering the long extrapolation and the approximations of the Bridgman theory, compares favourably with the value of $1.93 \times 10^{-4} \text{ cal cm}^{-1} \text{ sec}^{-1} (\text{°C})^{-1}$ obtained from sound velocity measurements. In fact, if the latter value was used as the basis of the rectilinear relationship, very small errors indeed would result for the interpolation of thermal conductivities of plasticized PVC in the practical range of plasticization. Extending this conclusion to plasticized polymers in general it would seem to indicate a simple way, provided the apparatus was available, for deducing thermal conductivities once that of the parent polymer is known. It should be emphasized, however, that care must be exercised in this in particular at temperatures which are some distance away from the glass-temperature of the parent polymer, in the light of the above discussion concerning overlap of the thermal conductivity curves of the plasticized samples at the lower temperatures.

The authors wish to thank Mr P. B. Blakey for his assistance in the X-ray diffraction analysis.

*Polymer Research Laboratories,
Department of Chemical Technology,
Institute of Technology, Bradford*

(Received May 1964)

REFERENCES

- ¹ SINNOTT, M. J. *The Solid State for Engineers*. Wiley: New York, 1961
- ² SEITZ, F. *Imperfections in Almost Perfect Crystals: A Synthesis*. Department of Physics, University of Illinois, 1950

THERMAL CONDUCTIVITIES OF POLYMERS I

- ³ KLINE, D. E. *J. Polym. Sci.* 1961, **50**, 441
- ⁴ GARDNER, R. R. Private communication
- ⁵ BRIDGMAN, P. W. *Proc. Amer. Acad. Arts Sci.* 1923, **59**, 141
- ⁶ HUBBARD, J. C. and LOOMIS, A. L. *Phil. Mag.* 1928, **5**, 1177
- ⁷ STEPHENSON, C. E. (I.C.I. Ltd). Private communication
- ⁸ HENNIG, J. and KNAPPE, W. 'Polymer Preprints', American Chemical Society, 1963, **4**, 647
- ⁹ EIERMANN, K. and HELLWEGE, K. H. *J. Polym. Sci.* 1962, **57**, 99
- ¹⁰ UBERREITER, K. and NENS, S. *Kolloidzshr.* 1951, **123**, 92
- ¹¹ TOBOLSKY, A. V. *Properties and Structure of Polymers*. Wiley: New York, 1960
- ¹² HORSLEY, R. A. *Plastics Progress*, **1957**, 77
- ¹³ See e.g. BLAKEY, P. B. and SHELDON, R. P. *Nature, Lond.* 1962, **195**, 172

Book Reviews

Dislocations

J. FRIEDEL. International Series of Monographs on Solid State Physics, Vol. 3. Pergamon: London; Gauthier-Villars: Paris, 1964. xxi+491 pp. 6½ in.×9 in. 120s

ORIGINALLY published in French in 1956, Professor FRIEDEL's book has been translated into English and extended to include a number of recent developments in the field. It now appears as a valuable addition to this series of solid state monographs.

The French edition originated from a series of lectures given by the author; the present edition retains much of the character of lecture notes and probably accounts for the somewhat staccato nature of the English. A great deal of the theory is discussed in relation to illustrations in the text of which there are some 250 line diagrams and 30 plates. This is of considerable help in obtaining a clear physical picture of the properties of dislocations.

The text is divided into three parts; the first deals with the general properties of dislocations and includes definitions and discussions on elastic theory and motion of dislocations, dislocation climb, imperfect dislocations and the relations between dislocations and crystal growth, vacancies and interstitial atoms. Part two is concerned with the properties of dislocation networks, covering elastic limits, cold working, grain boundaries, creep and cleavage. The third part deals largely with the interactions of dislocations with impurity defects, and concludes with a chapter discussing the role of dislocations in relation to such topics as X-ray scattering, electron microscopy, semiconductivity, thermal conductivity and optical and magnetic properties.

Although the bulk of dislocation theory appears in the classic texts of ten years ago this volume is a useful addition to the literature, and provides a dual supplement to the older texts. In the first place it contains a useful account of recent work, including the important development of the direct observation of dislocations, together with a number of excellent illustrations which demonstrate the appearance of dislocations when observed by various techniques. Secondly, the subject matter is treated in a rather different manner, going into some aspects of the background theory in considerable detail.

Dislocation theory is most completely understood in its applications to metals and ionic crystals, and this book is written primarily for the metallurgist. Although the observation and properties of dislocations in molecular crystals, and polymer crystals in particular, where the theory is more speculative, are not discussed, this book should provide useful background information on the general features of dislocations for the worker interested in the physics and chemistry of the organic solid state.

In general the book is well produced. There are, however, a small number of mistakes, most of which, fortunately are obvious on a careful reading of the text. The subject index is very short for a book of this size, but when combined with the detailed contents pages it provides a satisfactory means of finding information on specific topics.

G. C. EASTMOND

Fibre Structure

J. W. S. HEARLE and R. H. PETERS. Butterworths: London, 1963. 667 pp. 5½ in. by 9 in. 126s

THIS book started life as a series of lectures given to students in the Manchester College of Science and Technology in 1959. It is aimed primarily at the technologist who requires knowledge of fibre structure in order to carry out his own work more effectively. It is also intended to summarize existing knowledge and the sources of that knowledge in order to provide a springboard for future research workers in the

BOOK REVIEWS

field. The lectures were given by a well chosen team drawn from industrial laboratories and research institutes in both the U.K. and the U.S.A. and from Universities. This diversity is apparent in the changing style and content as the reader passes from chapter to chapter. It has also, one suspects, been the bane of the editors' life and has accounted for the long period of gestation so that few references to work published after 1960 are given.

The book is thorough and treats the subject in three ways. In the first five chapters the chemical structure of fibres is discussed. The main chapter headings are cellulose, polypeptides and proteins and synthetic polymers and copolymers. A small chapter tagged on the end describes the knowledge of tactic polymers in existence in those days and points to the first casualty brought about by the delay in publishing.

The fine structure of fibres is the second theme, and this is developed in the next six chapters. The beginning of this section contains a general introduction largely devoted to the micellar theory and its subsequent development to the fringed fibril structure proposed by one of the editors. The next two chapters deal with observed structure in plant, animal and synthetic fibres. These two chapters contain excellent photographs taken by both optical and electron microscopes. Two further chapters discuss the non-crystalline and the crystalline state respectively. These provide the second casualty caused by delay. The author of the second chapter (A. Keller) has been forced to admit to second thoughts and both chapters should be understood to refer to the knowledge available early in 1960. This middle section is completed by chapters on the cell structure of natural fibres and the surface structure of fibres.

The final section reinforces the work of the two preceding ones by describing, chapter by chapter, the detailed structure of specific fibres including cotton and other vegetable fibres, various types of synthetic and man-made fibres, animal fibres, glass and asbestos. A final short chapter by one of the editors makes it clear why the fibre technologist and scientist should bother with the preceding six hundred pages.

The book is excellently produced and well illustrated. It is, however, too long and in many places a firmer hand by the editors would have avoided unnecessary repetition. At least I had thought that removing obvious repetitions was an essential part of their work until I came in the last chapter to Table 19.2 and Figure 19.9. These are minor variants on Table 13.2 and Figure 13.5. They are sufficiently identical to annoy the man who has himself paid six guineas for the book and yet the reviewer was intrigued by the differences between the tables. They confirmed his belief that technologists do not normally know quantitative measures of the properties of their materials to three significant figures. The chapter on fibres from condensation polymers gives a very clear account of the production of synthetic fibres by melt extrusion and drawing. It is only included in this book by stretching the definition of fibre structure rather far. It will be a pity if anyone wanting this knowledge overlooks this account because he has been misled by the title of the book, since the chapter does not deserve to be lost in this way. The reviewer suggests a method of overcoming this difficulty in the second edition, confident that the book will be so successful. Re-edit this book and the companion volume of *Physical Properties of Textile Fibres* [cf. *Polymer, Lond.* 1964, 5, 313 for review], complete the trilogy by a volume on methods of manufacture and by hard, but quite possible, pruning produce the three volumes for the length and price of the two.

K. W. HILLIER

Dictionary of Plastics

J. A. WORDINGHAM and P. REBOUL. Newnes: London, 1964. 211 pp. 5 in. by 7½ in. 30s

A DICTIONARY of plastics? A Glossary of Terms used in the Plastics Industry would be more accurate, although it would still be surprising to find entries such as atom, pH and sulphuric acid. Indeed, one wishes that the space allotted to terms like these had been devoted to others which could have been usefully amplified. For example, the descriptions of abrasion resistance as 'the degree to which a product will withstand surface wear and rubbing', and of resin as 'an amorphous substance or mixture, of

Book Reviews

Dislocations

J. FRIEDEL. International Series of Monographs on Solid State Physics, Vol. 3. Pergamon: London; Gauthier-Villars: Paris, 1964. xxi+491 pp. 6½ in.×9 in. 120s

ORIGINALLY published in French in 1956, Professor FRIEDEL's book has been translated into English and extended to include a number of recent developments in the field. It now appears as a valuable addition to this series of solid state monographs.

The French edition originated from a series of lectures given by the author; the present edition retains much of the character of lecture notes and probably accounts for the somewhat staccato nature of the English. A great deal of the theory is discussed in relation to illustrations in the text of which there are some 250 line diagrams and 30 plates. This is of considerable help in obtaining a clear physical picture of the properties of dislocations.

The text is divided into three parts; the first deals with the general properties of dislocations and includes definitions and discussions on elastic theory and motion of dislocations, dislocation climb, imperfect dislocations and the relations between dislocations and crystal growth, vacancies and interstitial atoms. Part two is concerned with the properties of dislocation networks, covering elastic limits, cold working, grain boundaries, creep and cleavage. The third part deals largely with the interactions of dislocations with impurity defects, and concludes with a chapter discussing the role of dislocations in relation to such topics as X-ray scattering, electron microscopy, semiconductivity, thermal conductivity and optical and magnetic properties.

Although the bulk of dislocation theory appears in the classic texts of ten years ago this volume is a useful addition to the literature, and provides a dual supplement to the older texts. In the first place it contains a useful account of recent work, including the important development of the direct observation of dislocations, together with a number of excellent illustrations which demonstrate the appearance of dislocations when observed by various techniques. Secondly, the subject matter is treated in a rather different manner, going into some aspects of the background theory in considerable detail.

Dislocation theory is most completely understood in its applications to metals and ionic crystals, and this book is written primarily for the metallurgist. Although the observation and properties of dislocations in molecular crystals, and polymer crystals in particular, where the theory is more speculative, are not discussed, this book should provide useful background information on the general features of dislocations for the worker interested in the physics and chemistry of the organic solid state.

In general the book is well produced. There are, however, a small number of mistakes, most of which, fortunately are obvious on a careful reading of the text. The subject index is very short for a book of this size, but when combined with the detailed contents pages it provides a satisfactory means of finding information on specific topics.

G. C. EASTMOND

Fibre Structure

J. W. S. HEARLE and R. H. PETERS. Butterworths: London, 1963. 667 pp. 5½ in. by 9 in. 126s

THIS book started life as a series of lectures given to students in the Manchester College of Science and Technology in 1959. It is aimed primarily at the technologist who requires knowledge of fibre structure in order to carry out his own work more effectively. It is also intended to summarize existing knowledge and the sources of that knowledge in order to provide a springboard for future research workers in the

BOOK REVIEWS

field. The lectures were given by a well chosen team drawn from industrial laboratories and research institutes in both the U.K. and the U.S.A. and from Universities. This diversity is apparent in the changing style and content as the reader passes from chapter to chapter. It has also, one suspects, been the bane of the editors' life and has accounted for the long period of gestation so that few references to work published after 1960 are given.

The book is thorough and treats the subject in three ways. In the first five chapters the chemical structure of fibres is discussed. The main chapter headings are cellulose, polypeptides and proteins and synthetic polymers and copolymers. A small chapter tagged on the end describes the knowledge of tactic polymers in existence in those days and points to the first casualty brought about by the delay in publishing.

The fine structure of fibres is the second theme, and this is developed in the next six chapters. The beginning of this section contains a general introduction largely devoted to the micellar theory and its subsequent development to the fringed fibril structure proposed by one of the editors. The next two chapters deal with observed structure in plant, animal and synthetic fibres. These two chapters contain excellent photographs taken by both optical and electron microscopes. Two further chapters discuss the non-crystalline and the crystalline state respectively. These provide the second casualty caused by delay. The author of the second chapter (A. Keller) has been forced to admit to second thoughts and both chapters should be understood to refer to the knowledge available early in 1960. This middle section is completed by chapters on the cell structure of natural fibres and the surface structure of fibres.

The final section reinforces the work of the two preceding ones by describing, chapter by chapter, the detailed structure of specific fibres including cotton and other vegetable fibres, various types of synthetic and man-made fibres, animal fibres, glass and asbestos. A final short chapter by one of the editors makes it clear why the fibre technologist and scientist should bother with the preceding six hundred pages.

The book is excellently produced and well illustrated. It is, however, too long and in many places a firmer hand by the editors would have avoided unnecessary repetition. At least I had thought that removing obvious repetitions was an essential part of their work until I came in the last chapter to Table 19.2 and Figure 19.9. These are minor variants on Table 13.2 and Figure 13.5. They are sufficiently identical to annoy the man who has himself paid six guineas for the book and yet the reviewer was intrigued by the differences between the tables. They confirmed his belief that technologists do not normally know quantitative measures of the properties of their materials to three significant figures. The chapter on fibres from condensation polymers gives a very clear account of the production of synthetic fibres by melt extrusion and drawing. It is only included in this book by stretching the definition of fibre structure rather far. It will be a pity if anyone wanting this knowledge overlooks this account because he has been misled by the title of the book, since the chapter does not deserve to be lost in this way. The reviewer suggests a method of overcoming this difficulty in the second edition, confident that the book will be so successful. Re-edit this book and the companion volume of *Physical Properties of Textile Fibres* [cf. *Polymer, Lond.* 1964, 5, 313 for review], complete the trilogy by a volume on methods of manufacture and by hard, but quite possible, pruning produce the three volumes for the length and price of the two.

K. W. HILLIER

Dictionary of Plastics

J. A. WORDINGHAM and P. REBOUL. Newnes: London, 1964. 211 pp. 5 in. by 7½ in. 30s

A DICTIONARY of plastics? A Glossary of Terms used in the Plastics Industry would be more accurate, although it would still be surprising to find entries such as atom, pH and sulphuric acid. Indeed, one wishes that the space allotted to terms like these had been devoted to others which could have been usefully amplified. For example, the descriptions of abrasion resistance as 'the degree to which a product will withstand surface wear and rubbing', and of resin as 'an amorphous substance or mixture, of

BOOK REVIEWS

intermediate or high molecular weight, which is insoluble in water but soluble in some organic solvents and which at ordinary temperatures is either a very viscous liquid or a solid which softens gradually on heating', are unhelpful and confusing respectively. Coal is mentioned, but not oil; acetal resin is given, but not acetal copolymer, polyacetal or polyformaldehyde; and coefficient of thermal expansion is defined as a change in *mass* of material. Nevertheless, the treatment of most subjects is well done—the main fabricating techniques are illustrated by good diagrams—and there are useful charts on such topics as maximum working temperatures, classification of plasticizers, and the general properties of plastics colorants. Recently introduced materials, e.g. polyimides and phenoxies, are included, and appendices give lists of trade names, British Standards, and books and films available. Users of plastics and those working in the plastics industry itself will find this book a useful addition to their library.

J. M. J. ESTEVEZ

Newer Methods of Polymer Characterization

Edited by BACON KE. Wiley: New York and London, 1964. 722 pp. 6½ in. by 9¼ in. 185s

THIS book is the sixth volume in the series of 'Polymer Reviews' produced under the general editorship of Professor H. F. Mark and Dr E. H. Immergut.

The editor, Dr B. Ke, is to be congratulated for enlisting the support of 16 other internationally-known authors. Between them the team has produced 16 chapters, each dealing with one aspect of polymer characterization.

It can be said immediately that in the reviewer's opinion the book is thoroughly to be recommended to polymer research workers as a useful account of the major physical methods and as a stimulant to the general development of polymer research.

The subjects dealt with are as follows: the measurement of stereo-regularity; preparative fractionation (though only one technique—that of elution chromatography—is treated); light scattering and osmometry in solutions at high temperatures; density-gradient centrifugation; elasto-osmometry; monomolecular film studies; orientation studies by light scattering from polymers in the solid state and by X-ray diffraction and infra-red methods; flow birefringence; differential thermal analysis and thermal measurements during mechanical deformation; high resolution n.m.r. spectroscopy and infra-red spectra obtained with deuterated polymers and with polarized radiation; electron diffraction and small-angle X-ray diffraction; fluorescence techniques and optical rotary dispersion.

This is an imposing list of topics; not surprisingly the treatments vary appreciably in general importance and in length (from 10 to 104 pages). There is some unevenness in quality of content and of style of writing though the overall standard is high and the editorial brief to authors has been well observed. Thus each contribution contains a short account of the theory of the technique concerned, it describes the experimental details when this is profitable, concentrates on giving a wide range of examples of practical application of the technique and gives an assessment of the potentialities of the method in polymer research.

One minor complaint the reviewer has in this connection is that giving the authors free rein to present their own opinions and 'personal flavours' has in one or two instances led to somewhat biased conclusions as to the relative importance of particular techniques. This may well be regarded as not altogether undesirable except that in the absence of editorial comment or a summarizing chapter the reader will sometimes need to exercise his own judgement as to the choice of techniques best suited to his particular problem.

A further general criticism is that the title of the book scarcely justifies all the contents. For example, flow birefringence and monolayer studies, though interesting in themselves, can hardly be regarded as methods of characterization of polymers. The same is true of thermal measurements during deformation; the relation between the results of such measurements and polymer structure is indirect.

A few points of detail require comment. On p 442 it is suggested that 'the deforma-

BOOK REVIEWS

intermediate or high molecular weight, which is insoluble in water but soluble in some organic solvents and which at ordinary temperatures is either a very viscous liquid or a solid which softens gradually on heating', are unhelpful and confusing respectively. Coal is mentioned, but not oil; acetal resin is given, but not acetal copolymer, polyacetal or polyformaldehyde; and coefficient of thermal expansion is defined as a change in *mass* of material. Nevertheless, the treatment of most subjects is well done—the main fabricating techniques are illustrated by good diagrams—and there are useful charts on such topics as maximum working temperatures, classification of plasticizers, and the general properties of plastics colorants. Recently introduced materials, e.g. polyimides and phenoxies, are included, and appendices give lists of trade names, British Standards, and books and films available. Users of plastics and those working in the plastics industry itself will find this book a useful addition to their library.

J. M. J. ESTEVEZ

Newer Methods of Polymer Characterization

Edited by BACON KE. Wiley: New York and London, 1964. 722 pp. 6½ in. by 9¼ in. 185s

THIS book is the sixth volume in the series of 'Polymer Reviews' produced under the general editorship of Professor H. F. Mark and Dr E. H. Immergut.

The editor, Dr B. Ke, is to be congratulated for enlisting the support of 16 other internationally-known authors. Between them the team has produced 16 chapters, each dealing with one aspect of polymer characterization.

It can be said immediately that in the reviewer's opinion the book is thoroughly to be recommended to polymer research workers as a useful account of the major physical methods and as a stimulant to the general development of polymer research.

The subjects dealt with are as follows: the measurement of stereo-regularity; preparative fractionation (though only one technique—that of elution chromatography—is treated); light scattering and osmometry in solutions at high temperatures; density-gradient centrifugation; elasto-osmometry; monomolecular film studies; orientation studies by light scattering from polymers in the solid state and by X-ray diffraction and infra-red methods; flow birefringence; differential thermal analysis and thermal measurements during mechanical deformation; high resolution n.m.r. spectroscopy and infra-red spectra obtained with deuterated polymers and with polarized radiation; electron diffraction and small-angle X-ray diffraction; fluorescence techniques and optical rotary dispersion.

This is an imposing list of topics; not surprisingly the treatments vary appreciably in general importance and in length (from 10 to 104 pages). There is some unevenness in quality of content and of style of writing though the overall standard is high and the editorial brief to authors has been well observed. Thus each contribution contains a short account of the theory of the technique concerned, it describes the experimental details when this is profitable, concentrates on giving a wide range of examples of practical application of the technique and gives an assessment of the potentialities of the method in polymer research.

One minor complaint the reviewer has in this connection is that giving the authors free rein to present their own opinions and 'personal flavours' has in one or two instances led to somewhat biased conclusions as to the relative importance of particular techniques. This may well be regarded as not altogether undesirable except that in the absence of editorial comment or a summarizing chapter the reader will sometimes need to exercise his own judgement as to the choice of techniques best suited to his particular problem.

A further general criticism is that the title of the book scarcely justifies all the contents. For example, flow birefringence and monolayer studies, though interesting in themselves, can hardly be regarded as methods of characterization of polymers. The same is true of thermal measurements during deformation; the relation between the results of such measurements and polymer structure is indirect.

A few points of detail require comment. On p 442 it is suggested that 'the deforma-

BOOK REVIEWS

tion [of a rubber-elastic material] probably consists of a large decrease in entropy with elongation, the internal energy probably remaining practically constant (ref.). The first part of this quotation is badly written and the second part is incorrect. The suggestion that the internal energy remains practically constant during deformation is contradicted by experiment (as the author goes on to say) and in the reference mentioned (Treloar, p 24).

Discussion of glass transition temperatures of polymers has often given rise to controversy. It is a subject needing more than normal care and statements such as the 'glass transition involves motion of short-chain segments in the amorphous region, and is related to the brittleness of a polymer' (p 350) seem ill-advised especially since this remark is not amplified. What is meant by 'short-chain'? Is this consistent, for example, with the data given on p 395 which show that for atactic polypropylene T_g is an increasing function of molecular weight up to $M_n=50\ 000$ approximately?

The treatment of differential thermal analysis does not mention explicitly that it is a non-equilibrium technique.

The general production of the book (layout, printing, diagrams etc.) is of a very high standard and only four misprints were detected. An author index, however, would have been useful.

The price (185s) is high but the merits of the book should ensure its inclusion in the libraries of all polymer research groups.

E. R. HOWELLS

Elastic Liquids: An Introductory Vector Treatment of Finite-Strain Polymer Rheology

A. S. LODGE. Academic Press: New York and London, 1964. xii + 389 pp.
6½ in. by 9¼ in. 75s

AS THE author says in his Preface, the aim of *Elastic Liquids* is to introduce scientists, engineers and mathematicians to phenomenological theories of viscoelastic liquids and solids subjected to large changes of shape.

It is directed at final year honours students and postgraduates. The book can be studied by those with only a fairly elementary knowledge of mathematics (except for the final chapter, no facility in tensor analysis is required) though it is probably fair to say that only those with appreciable mathematical talent will get maximum benefit. For them, this is an authoritative book written in a beautiful, logical manner which should stimulate fruitful research in the practically important field of polymer rheology.

There is a great deal of value even for those readers possessing limited mathematical talent for it is easy to read around the mathematics to see the results which emerge from the initial physical assumptions.

The book is well designed for the teaching of rheology. The mathematics is gradually developed from an elementary starting point and the first seven chapters each have examples at the end with detailed solutions given later in the book (chapter 11).

Chapters 1 to 8 deal with the formulation of equations of state for various physically ideal materials subjected to uniform stress and strain and with the calculation of the basic rheological properties of these materials. The foundation is laid for the extension of this process to other materials with different equations of state.

Chapters 9 and 10 describe normal stress differences in shear flow and other important elastic effects observed in concentrated polymer solutions.

The final chapter considers non-uniform states of stress and strain; it is an analysis mathematically more difficult than that earlier in the book and owes much to the work of OLDROYD. This is the only section which the reader is likely to find elusive as regards physical interpretation.

The production of the book is excellent and the price (75s) is very reasonable by present standards.

It is to be expected that *Elastic Liquids* will come to be regarded as a standard

BOOK REVIEWS

tion [of a rubber-elastic material] probably consists of a large decrease in entropy with elongation, the internal energy probably remaining practically constant (ref.). The first part of this quotation is badly written and the second part is incorrect. The suggestion that the internal energy remains practically constant during deformation is contradicted by experiment (as the author goes on to say) and in the reference mentioned (Treloar, p 24).

Discussion of glass transition temperatures of polymers has often given rise to controversy. It is a subject needing more than normal care and statements such as the 'glass transition involves motion of short-chain segments in the amorphous region, and is related to the brittleness of a polymer' (p 350) seem ill-advised especially since this remark is not amplified. What is meant by 'short-chain'? Is this consistent, for example, with the data given on p 395 which show that for atactic polypropylene T_g is an increasing function of molecular weight up to $M_n=50\ 000$ approximately?

The treatment of differential thermal analysis does not mention explicitly that it is a non-equilibrium technique.

The general production of the book (layout, printing, diagrams etc.) is of a very high standard and only four misprints were detected. An author index, however, would have been useful.

The price (185s) is high but the merits of the book should ensure its inclusion in the libraries of all polymer research groups.

E. R. HOWELLS

Elastic Liquids: An Introductory Vector Treatment of Finite-Strain Polymer Rheology

A. S. LODGE. Academic Press: New York and London, 1964. xii + 389 pp.
6½ in. by 9¼ in. 75s

AS THE author says in his Preface, the aim of *Elastic Liquids* is to introduce scientists, engineers and mathematicians to phenomenological theories of viscoelastic liquids and solids subjected to large changes of shape.

It is directed at final year honours students and postgraduates. The book can be studied by those with only a fairly elementary knowledge of mathematics (except for the final chapter, no facility in tensor analysis is required) though it is probably fair to say that only those with appreciable mathematical talent will get maximum benefit. For them, this is an authoritative book written in a beautiful, logical manner which should stimulate fruitful research in the practically important field of polymer rheology.

There is a great deal of value even for those readers possessing limited mathematical talent for it is easy to read around the mathematics to see the results which emerge from the initial physical assumptions.

The book is well designed for the teaching of rheology. The mathematics is gradually developed from an elementary starting point and the first seven chapters each have examples at the end with detailed solutions given later in the book (chapter 11).

Chapters 1 to 8 deal with the formulation of equations of state for various physically ideal materials subjected to uniform stress and strain and with the calculation of the basic rheological properties of these materials. The foundation is laid for the extension of this process to other materials with different equations of state.

Chapters 9 and 10 describe normal stress differences in shear flow and other important elastic effects observed in concentrated polymer solutions.

The final chapter considers non-uniform states of stress and strain; it is an analysis mathematically more difficult than that earlier in the book and owes much to the work of OLDROYD. This is the only section which the reader is likely to find elusive as regards physical interpretation.

The production of the book is excellent and the price (75s) is very reasonable by present standards.

It is to be expected that *Elastic Liquids* will come to be regarded as a standard

BOOK REVIEWS

rheological textbook and if it is widely taken up by university teachers, as it deserves to be, the general advance will be greater even than that achieved by the author's own notable researches.

E. R. HOWELLS

Crystalline Olefin Polymers, Part II
(High Polymer Series, Volume 20)

R. A. V. RAFF and K. W. DOAK. Wiley: New York and London, 1964. 675 pp.
6 in. by 9 in. 169s

THE high polymer series of Interscience continues to provide us with a number of important textbooks which now cover a large part of the polymer field. Naturally, in an area of knowledge which is growing so quickly, such books tend to become out of date and require revision. The present work constitutes the second part of a book which aims at widening and consolidating the previous textbook on *Polythene* by RAFF and ALLISON. It is a measure of the rapidity of development in the polyolefin field that a new work should have become necessary after only eight years. As in other cases, the need to have the book written with reasonable speed makes it necessary to have different chapters contributed by selected experts in the respective fields.

This second part of *Crystalline Olefin Polymers* covers two groups of topics, one concerned with 'Properties' and one with 'Technology'. Among the properties covered are Brittleness (perhaps not an ideal term applied to polyolefins), Stress Cracking, Electricals, Permeability, and (inevitably) Miscellaneous. Under 'Technology' are included Chemical Modification, Irradiation, Degradation, Processing, and Applications. From the reviewer's viewpoint the parts on Stress Cracking, Permeability, and Irradiation and Degradation are of a particularly high standard and should be consulted by any person wishing to learn about these matters. The chapter on Brittleness, although containing many interesting results, seems more superficial in its coverage. It also includes the results of OHLBERG *et al.* (p 21) on the relation between impact strength and spherulite size for Ziegler polyethylene which, in the reviewer's experience, it has not been possible to confirm.

The chapters on Processing and Application represent a workmanlike and comprehensive effort to cover these large fields. For example, the section on extrusion starts with a short but useful description of extrusion theory and then goes on to cover film, sheet, pipe, monofil, etc. The application of polyolefins is discussed, perhaps rather formally, in terms of the polymer properties and requirements for each particular field of use. There seemed to be little tie-up between the section here, dealing with rheological requirements, and the chapter on 'Rheology' in Part I of the same work.

These minor defects reflect the inevitable speed and pressure under which a work of this sort has to be written. They should not deter any worker who is concerned with polyolefins from consulting or purchasing the book. Indeed, the very difficulties which may generate its imperfections also make it of particular importance. The problem of keeping up to date with one's own and with contiguous fields of work besets us all. The appearance of this generally authoritative and extensive survey is likely to give valuable assistance to all those who want to keep abreast of the many rapid developments of the crystalline polyolefins.

R. N. HAWARD

Premix Molding

R. B. WHITE. Reinhold Publishing Corporation: New York; Chapman and Hall: London, 1964. xi+201 pp. 6 in. by 9 in. \$12.00 or 96s

THE advantages of incorporating certain particulate fillers into thermosetting moulding compositions have long been recognized, and the useful combination of strength,

BOOK REVIEWS

rheological textbook and if it is widely taken up by university teachers, as it deserves to be, the general advance will be greater even than that achieved by the author's own notable researches.

E. R. HOWELLS

Crystalline Olefin Polymers, Part II
(High Polymer Series, Volume 20)

R. A. V. RAFF and K. W. DOAK. Wiley: New York and London, 1964. 675 pp.
6 in. by 9 in. 169s

THE high polymer series of Interscience continues to provide us with a number of important textbooks which now cover a large part of the polymer field. Naturally, in an area of knowledge which is growing so quickly, such books tend to become out of date and require revision. The present work constitutes the second part of a book which aims at widening and consolidating the previous textbook on *Polythene* by RAFF and ALLISON. It is a measure of the rapidity of development in the polyolefin field that a new work should have become necessary after only eight years. As in other cases, the need to have the book written with reasonable speed makes it necessary to have different chapters contributed by selected experts in the respective fields.

This second part of *Crystalline Olefin Polymers* covers two groups of topics, one concerned with 'Properties' and one with 'Technology'. Among the properties covered are Brittleness (perhaps not an ideal term applied to polyolefins), Stress Cracking, Electricals, Permeability, and (inevitably) Miscellaneous. Under 'Technology' are included Chemical Modification, Irradiation, Degradation, Processing, and Applications. From the reviewer's viewpoint the parts on Stress Cracking, Permeability, and Irradiation and Degradation are of a particularly high standard and should be consulted by any person wishing to learn about these matters. The chapter on Brittleness, although containing many interesting results, seems more superficial in its coverage. It also includes the results of OHLBERG *et al.* (p 21) on the relation between impact strength and spherulite size for Ziegler polyethylene which, in the reviewer's experience, it has not been possible to confirm.

The chapters on Processing and Application represent a workmanlike and comprehensive effort to cover these large fields. For example, the section on extrusion starts with a short but useful description of extrusion theory and then goes on to cover film, sheet, pipe, monofils, etc. The application of polyolefins is discussed, perhaps rather formally, in terms of the polymer properties and requirements for each particular field of use. There seemed to be little tie-up between the section here, dealing with rheological requirements, and the chapter on 'Rheology' in Part I of the same work.

These minor defects reflect the inevitable speed and pressure under which a work of this sort has to be written. They should not deter any worker who is concerned with polyolefins from consulting or purchasing the book. Indeed, the very difficulties which may generate its imperfections also make it of particular importance. The problem of keeping up to date with one's own and with contiguous fields of work besets us all. The appearance of this generally authoritative and extensive survey is likely to give valuable assistance to all those who want to keep abreast of the many rapid developments of the crystalline polyolefins.

R. N. HAWARD

Premix Molding

R. B. WHITE. Reinhold Publishing Corporation: New York; Chapman and Hall: London, 1964. xi+201 pp. 6 in. by 9 in. \$12.00 or 96s

THE advantages of incorporating certain particulate fillers into thermosetting moulding compositions have long been recognized, and the useful combination of strength,

BOOK REVIEWS

lightness and durability that can be achieved by a proper choice of resin and filler is well exemplified by the glass fibre reinforced polyester laminates developed during the last 20 years. More recently a variety of glass-filled thermoplastics with enhanced strength and stiffness have become commercially available.

Despite these and other related technical advances, there is a notable lack of published work on the quantitative, or even general, relationships that might be expected to obtain between the physical properties of a filled composite and the characteristics of the filler. Here one has in mind such parameters as particle size, size distribution, particle geometry, orientation, surface and chemical interaction. It seems that, outside the rubber field, the study of the role of fillers in modifying polymer properties is a rather neglected area of basic polymer science. A typical problem of practical importance in the processing of fibre-filled materials concerns the flow of filler particles in a medium of high and varying viscosity, namely the difficulty of ensuring and maintaining reasonably uniform distribution and controlled orientation of the fibres during moulding and similar operations. This problem is particularly acute in the materials which form the subject of the volume under review.

Premix Molding describes the processing, properties and applications of fibre-reinforced polyester moulding compositions. The term 'premix' (U.S. nomenclature) can be applied to a variety of reinforced thermosetting resins but those based on polyester resins are most common, and they are known in the U.K. as 'dough moulding compounds'. These consist essentially of an unsaturated polyester resin, containing about 30 per cent styrene or similar monomer, together with a finely divided inorganic filler such as calcium carbonate and a proportion, usually about 20 per cent, of chopped fibres (normally glass) of 0.25 to 0.50 in. length; other components, e.g. catalyst, inhibitor, pigment, mould lubricant, are present in minor amounts.

Premixes, although reasonably stable on storage, are fast-curing at elevated temperatures and can be handled on conventional compression or transfer equipment to give mouldings having many of the desirable properties associated with polyester-glass laminates, e.g. excellent insulation properties, good strength retention on exposure to high temperatures, dimensional stability and low water-absorption. At present the main applications of such mouldings are electrical, but their good shock-resistance and ability to carry heavy metal inserts is leading to many other uses. Certain deficiencies evident in earlier products of this type have now been eliminated by improved formulations, although care is still needed in the moulding of these materials to obtain optimum properties in the final article.

As indicated by the title a considerable portion of this book is devoted to a discussion of moulding procedures, correct mould design, reasons for moulding faults and methods for remedying them. This part is clearly written and profusely illustrated, and should be of value to anyone with an interest in moulding: techniques are described for delineating resin flow and fibre orientation, for detecting voids and fibre degradation.

In addition to the topics mentioned, there are chapters dealing with the manufacture of premixes, finishing, quality control, specifications and costs. A list is given of U.S. manufacturers of materials and equipment and the book ends with a reasonably complete bibliography of publications on premix materials up to the beginning of 1964. The author himself has made a number of contributions to the technology of premixes and he is to be congratulated on having provided a lucid survey of the field. Two minor criticisms are that the book could be improved by a rather more detailed discussion of chemical and physical aspects of these materials and by the inclusion of relevant patents in the bibliography.

P. F. ONYON

BOOK REVIEWS

rheological textbook and if it is widely taken up by university teachers, as it deserves to be, the general advance will be greater even than that achieved by the author's own notable researches.

E. R. HOWELLS

Crystalline Olefin Polymers, Part II
(High Polymer Series, Volume 20)

R. A. V. RAFF and K. W. DOAK. Wiley: New York and London, 1964. 675 pp.
6 in. by 9 in. 169s

THE high polymer series of Interscience continues to provide us with a number of important textbooks which now cover a large part of the polymer field. Naturally, in an area of knowledge which is growing so quickly, such books tend to become out of date and require revision. The present work constitutes the second part of a book which aims at widening and consolidating the previous textbook on *Polythene* by RAFF and ALLISON. It is a measure of the rapidity of development in the polyolefin field that a new work should have become necessary after only eight years. As in other cases, the need to have the book written with reasonable speed makes it necessary to have different chapters contributed by selected experts in the respective fields.

This second part of *Crystalline Olefin Polymers* covers two groups of topics, one concerned with 'Properties' and one with 'Technology'. Among the properties covered are Brittleness (perhaps not an ideal term applied to polyolefins), Stress Cracking, Electricals, Permeability, and (inevitably) Miscellaneous. Under 'Technology' are included Chemical Modification, Irradiation, Degradation, Processing, and Applications. From the reviewer's viewpoint the parts on Stress Cracking, Permeability, and Irradiation and Degradation are of a particularly high standard and should be consulted by any person wishing to learn about these matters. The chapter on Brittleness, although containing many interesting results, seems more superficial in its coverage. It also includes the results of OHLBERG *et al.* (p 21) on the relation between impact strength and spherulite size for Ziegler polyethylene which, in the reviewer's experience, it has not been possible to confirm.

The chapters on Processing and Application represent a workmanlike and comprehensive effort to cover these large fields. For example, the section on extrusion starts with a short but useful description of extrusion theory and then goes on to cover film, sheet, pipe, monofils, etc. The application of polyolefins is discussed, perhaps rather formally, in terms of the polymer properties and requirements for each particular field of use. There seemed to be little tie-up between the section here, dealing with rheological requirements, and the chapter on 'Rheology' in Part I of the same work.

These minor defects reflect the inevitable speed and pressure under which a work of this sort has to be written. They should not deter any worker who is concerned with polyolefins from consulting or purchasing the book. Indeed, the very difficulties which may generate its imperfections also make it of particular importance. The problem of keeping up to date with one's own and with contiguous fields of work besets us all. The appearance of this generally authoritative and extensive survey is likely to give valuable assistance to all those who want to keep abreast of the many rapid developments of the crystalline polyolefins.

R. N. HAWARD

Premix Molding

R. B. WHITE. Reinhold Publishing Corporation: New York; Chapman and Hall: London, 1964. xi+201 pp. 6 in. by 9 in. \$12.00 or 96s

THE advantages of incorporating certain particulate fillers into thermosetting moulding compositions have long been recognized, and the useful combination of strength,

Communications and Notes

Thermal Transitions of Synthetic and Biological Polymers in Bulk and in Solution

IN A recent communication to this Journal Moraglio *et al.*¹ reported some very small thermal transitions in polystyrene occurring in the bulk phase as well as in solution. Using a sensitive dilatometric technique Moraglio and Danusso located a transition region some 8°C wide and centred at about 50°C both for the bulk polymer and for toluene solutions of 0.5 to 1.0 per cent concentration; one of their published curves for the bulk polymer is reproduced as curve P in *Figure 1*. Bianchi and Rossi confirmed the location of the solid-state transition by measuring the internal pressure at different temperatures, whilst Liquori and Quadrifoglio observed optical density anomalies around 50°C in solutions of isotactic polystyrene in decalin.

Moraglio *et al.* recognized the essentially intramolecular nature of these phenomena, but considered that the basic molecular process would not be a major conformational change 'analogous to helix-coil shape transitions . . . in proteins'. They suggested instead some unspecified molecular change whose effects would appear equally in solution or in the bulk material. In view both of the smallness of the transitions in polystyrene and of their location well below the glass-transition point (*ca.* 105°C) it seems likely that only very local molecular motions are involved, e.g. the β - and γ -mechanisms studied in polymer viscoelasticity². In polystyrene the phenyl groups are thought to be responsible for the small β -transition and the even smaller γ -transition has been attributed³ to the presence of adjacent $-\text{CH}_2-$ groups resulting from head-to-head polymerization. The measurements of Illers and Jenckel⁴ show the β -transition (at 1 cycle/sec) lying between 40° and 50°C and it may be suggested that this mechanism underlies the phenomena discussed above.

However, the main point we wish to make in this Note is that the phenomena of solution- and bulk-transitions occurring at the same temperatures is also found in the protein systems collagen-saline⁵ and keratin-water⁶ where the solution mechanism at least is certainly a helix-coil transition.

Optical rotation or viscosity measurements on dilute solutions prepared from mammalian collagen⁷ show a pronounced helix-coil transition over a very narrow range of temperature; von Hippel and Wong⁸ have shown that ΔT , the difference in temperature between the points at which the transition is one quarter and three quarters complete, is only $2 \pm 0.5^\circ\text{C}$. The location of this transition is in the range 35° to 40°C for dilute saline solutions near to neutrality. Measurements of the apparent specific volume of the bulk material in dilute saline show a small and narrow volume transition in the

same region of temperature. The curve C in *Figure 1* is an example of such a 'minor' transition for kangaroo tail tendon in 0.9 per cent saline solution (the 'major' transition in this system occurs at a higher temperature and consists of melting of the crystalline phase). There is thus a formal identity with the situation in polystyrene.

The comparable behaviour of keratin is less clear, partly because the native material is insoluble, and measurements of the thermal stability of solutions have therefore to be carried out on α -helix-forming proteins extracted after reduction of the disulphide bonds responsible for the original insolubility. In this way optical rotatory dispersion measurements⁹ showed a very broad helix-coil transition at pH 9.1, centred on 55°C and with a ΔT of approximately 23°C.

Specific volume measurements on solid keratin immersed in water⁶ also showed a transition region between about 45° and 65°C, having a qualitative resemblance to the behaviour reported by Moraglio and Danusso for bulk polystyrene. Curve K in *Figure 1* illustrates a typical result for Corriedale wool in water.

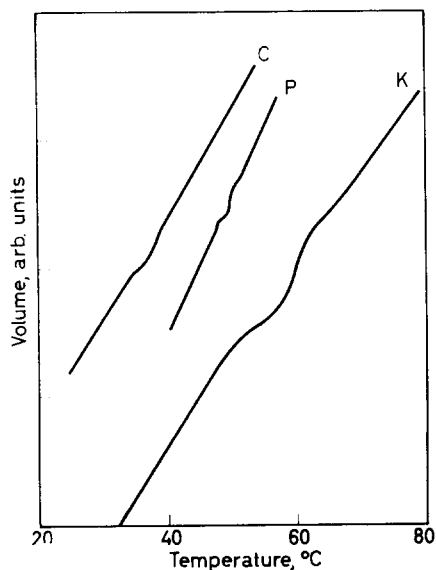


Figure 1—Minor thermal expansion transitions in bulk polymer. C—Collagen-saline solution; P—Polystyrene (after Moraglio *et al.*¹); K—Keratin-water

Notwithstanding the obvious structural differences between the three polymer systems considered, it is seen that in polystyrene and collagen, and perhaps also in keratin, the solution behaviour can be detected in the solid state. It may be considered that on statistical grounds there will be regions where the molecular packing is exceptionally open and the local free volume so large that the molecular segments experience little interaction from neighbouring molecules. The material in these regions will undergo any transition which occurs in a dilute solution, and this will be detected if a sufficiently sensitive technique is used. The extent of these regions may be small and dependent on the thermal history of the specimen, varying for

instance between specimens which have been abruptly quenched from a higher temperature or more slowly annealed. This would account for the smallness and variability of the phenomena described. Nevertheless, phenomena of this type may be expected to be found quite generally in either glassy or partly crystalline polymers.

One difference between the situations in polystyrene and in collagen is that the solution transition for collagen is a first-order effect involving helix-coil transformations of every tropocollagen molecule in the solution. The smallness of the bulk transition thus indicates that only a small fraction of the molecules can be involved. Nevertheless, if this fraction is directly involved in carrying the mechanical stresses, it may be crucial in certain physiological situations. For example, in collagen the phenomena of stress relaxation and length recovery show marked changes¹⁰ at approximately 38°C, the temperature of the transition in question. Permanent damage to the tissue may then be produced by straining at temperatures much above this value, which is significantly very close to normal deep-body temperatures.

A polymer which could provide a clear test of the foregoing ideas is poly(cyclohexyl methacrylate). This gives a well defined viscoelastic transition below the glass-transition point which has been shown¹¹ to arise from alternation of the cyclohexane ring between two isomeric chair forms of the molecule. Other polymers containing the cyclohexyl group exhibit similar 'β-mechanisms' at the same frequency-temperature combinations, indicating that the mechanism is operating independently of the environment. On this supposition, dilatometry of the polymer in bulk or in dilute solution should reveal the same transition, as with the materials discussed above.

P. MASON
B. J. RIGBY

*Division of Textile Physics,
C.S.I.R.O. Wool Research Laboratories,
Ryde, Sydney, Australia.*

(Received October 1964)

REFERENCES

- ¹ MORAGLIO, G., DANUSSO, F., BIANCHI, V., ROSSI, C., LIQUORI, A. M. and QUADRIFOGLIO, F. *Polymer, Lond.* 1963, **4**, 445
- ² FERRY, J. D. *Viscoelastic Properties of Polymers*. Wiley: New York, 1961
- ³ ILLERS, K. H. and JENCKEL, E. *J. Polym. Sci.* 1959, **41**, 528
- ⁴ ILLERS, K. H. and JENCKEL, E. *Rheol. Acta*, 1958, **1**, 322
- ⁵ MASON, P. and RIGBY, B. J. *Biochim. biophys. Acta*, 1963, **66**, 448
- ⁶ MASON, P. *Textile Res. J.* In press
- ⁷ DOTY, P. and NISHIHARA, T. in *Recent Advances in Gelatin and Glue Research* (ed. G. STAINSBY). Pergamon: London, 1958
- ⁸ VON HIPPEL, P. H. and WONG, K-Y. *Biochemistry*, 1963, **2**, 1399
- ⁹ HARRAP, B. S. *Austral. J. biol. Sci.* 1963, **16**, 231
- ¹⁰ RIGBY, B. J., HIRAL, N., SPIKES, J. D. and EYRING, H. *J. gen. Physiol.* 1959, **43**, 265
- ¹¹ HEIJBOER, J. *Kolloidzshr.* 1956, **148**, 36

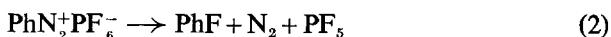
A 'Living' Polymer after Cationic Initiation

ALL the 'living' systems of the Szwarc type studied in detail to date have involved anionic initiation^{1,2}. Previous workers have suggested that catalysts such as triphenylmethyl hexachloroantimonate³ and phosphorus pentafluoride⁴ when used to catalyse the polymerization of bulk tetrahydrofuran (THF) may lead to 'living' systems. No evidence beyond continued polymerization upon addition of further monomer to the equilibrium monomer-polymer mixture was presented.

We report here a study of a 'living' system arising after cationic initiation of THF using a new catalyst, benzenediazonium hexafluorophosphate (PhN_2PF_6)*. The use of this particular compound itself as an initiator for the polymerization of cyclic ethers has not been reported previously, although its use as a convenient laboratory source of phosphorus pentafluoride by thermal decomposition at 160° is recommended⁵. Since this study has so far been confined to the termination process, or lack of it, it is not possible at the present time to say whether initiation is due to phenyl carbonium ion formed by solvent (monomer) induced decomposition according to the equation



or if the initiation is of the type occurring in phosphorus pentafluoride catalysed polymerizations with a solvent induced decomposition similar to the thermal decomposition



Benzenediazonium hexafluorophosphate has proved to be a very active initiator for the polymerization of THF in bulk at 25° and has led to very tough crystalline polymers with higher intrinsic viscosities than have been reported previously^{4,6,7}. The variation of intrinsic viscosity with catalyst concentration is shown in *Figure 1*. It is clear that a linear relation exists between $\log [\eta]$ and $\log [\text{PhN}_2\text{PF}_6]$, as it should for a 'living' system⁸. PhN_2PF_6 has a limited solubility in THF and it is impossible to extend the work to higher catalyst concentrations than those reported. The deviation at high catalyst concentration shown in *Figure 1* is thought to be due to the solubility limit having been reached.

We have demonstrated in other ways that polymerizations initiated with PhN_2PF_6 do not terminate. They are summarized in *Table 1*. The first experiment clearly shows that upon the addition of further monomer to an equilibrium monomer-polymer mixture, polymerization continued and the intrinsic viscosity increased. It is significant that both the initial and final intrinsic viscosity values fall very close to the curve shown in *Figure 1*, even though it was impossible to obtain good mixing upon addition of the THF. A clearer example of this increase in viscosity is illustrated in the second experiment, where mixing was easily accomplished.

Addition of more catalyst to an equilibrium monomer-polymer mixture (experiment 3) had the expected effect of lowering the intrinsic viscosity

*Distributed in crude form by Qzark-Mahoning Company, Tulsa, Oklahoma, U.S.A., under the trade name Phosfluorogen 'A' and conveniently purified by dissolving in water at 30° and crystallizing at 5° (dec. 152-9°).

COMMUNICATIONS AND NOTES

without affecting the yield. This effect can be explained by assuming that the additional PhN_2PF_6 reacts with the THF remaining at equilibrium to initiate new chains and that the equilibrium between polymer and monomer is then reached at a lower molecular weight.

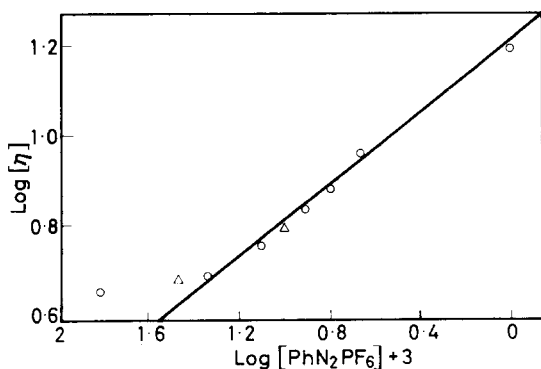


Figure 1—Effect of variation of PhN_2PF_6 concentration on intrinsic viscosity: O, from bulk THF polymerizations in which all polymerizations reached after 24–48 h at 25°C the same equilibrium 75 per cent conversion previously reported^{4,6}; Δ, from experiment 2, Table 1

It is not necessary to add more of the same monomer in order to continue polymerization. As experiment 4 illustrates, upon addition of another cyclic ether polymerization continued and a soluble, rubbery polymer resulted. Since the homopolymer of the oxetane is very insoluble, and the yield and character of the polymer obtained in experiment 4 were quite different from those of parallel homopolymerization experiments, growth of a THF-oxetane copolymer apparently continued on the polytetrahydrofuran chains already present.

Table 1. Experiments demonstrating lack of termination in polymerizations initiated with PhN_2PF_6

Expt No.*	PhN_2PF_6 conc. (moles l ⁻¹ THF × 10 ³)		Polymer yield (per cent)		Reaction time (days)		Intrinsic viscosity (Benzene at 25°, dl/g)	
	Init.	Final	Init.	Final	Before addn	After addn	Before addn	After addn
1	29.6	10.2	75	75	1	1	4.8	5.9
2	4.56	1.82	9.4	25.6†	5	2	7.2	13.0
3	3.88	5.70	12.1	12.9	3‡	2	5.7	3.9
4	3.85	—	—	85 §	3	2	—	—

*1: THF added to THF polymerized in bulk.

2: THF added to THF polymerized in 40.3 per cent w/w solution in benzene.

3: Catalyst added to THF polymerized in 42.3 per cent w/w solution in benzene.

4: 3,3-bis-(chloromethyl)oxetane (6.93 g) added to THF (9.33 g) polymerized in 56.1 per cent w/w solution in benzene.

†The increase in percentage yield is due to the increased molar concentration of THF in benzene brought about by adding pure THF to a benzene solution. Thus, since at equilibrium the same molar concentration of monomer must be reached* (our data suggest that in benzene at 25° this value is approximately 4.5 moles THF l⁻¹), a greater percentage of the THF becomes available for polymerization.

‡In this case the sample ampoule was allowed to continue polymerizing until the experiment finished and they were then worked up simultaneously.

§Based on both monomers. Yields in excess of those observed for THF homopolymerizations have been reported¹⁰ for THF-3,3-bis-(chloromethyl)oxetane copolymerizations.

We wish to acknowledge helpful and stimulating discussion with Professor C. E. H. Bawn and Professor M. Szwarc. One of us (M.P.D.) is indebted to Imperial Chemical Industries for an I.C.I. Postdoctoral Fellowship and the other (P.D.) to the American Association of University Women for the award of the Marie Curie Fellowship for 1964-65.

M. P. DREYFUSS
P. DREYFUSS

Department of Inorganic, Physical and Industrial Chemistry,
University of Liverpool

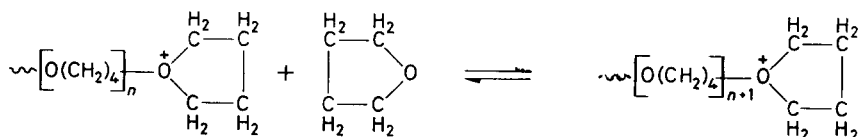
(Received October 1964)

REFERENCES

- 1 SZWARC, M. *Advanc. Polym. Sci.* 1960, **2**, 275
- 2 PLESCH, P. H. *The Chemistry of Cationic Polymerization*, p 555. Pergamon: Oxford, 1963
- 3 BAWN, C. E. H., BELL, R. and LEDWITH, A. Chemical Society Anniversary Meeting, Cardiff, 1963
- 4 SIMS, D. *J. chem. Soc.* 1964, 864
- 5 SORENSEN, W. and CAMPBELL, T. W. *Preparative Methods of Polymer Chemistry*, p 253. Interscience: New York, 1961
- 6 BELL, R. *Ph.D. Thesis*, University of Liverpool, 1963
- 7 MUETTERTIES, E. L. *U.S. Patent No. 2 856 370* (1958)
- 8 WAACK, R., REMBAUM, A., COOMBES, J. D. and SZWARC, M. *J. Amer. chem. Soc.* 1957, **79**, 2026
- 9 BRODY, H., LADACKI, M., MILKOVICH, R. and SZWARC, M. *J. Polym. Sci.* 1957, **25**, 221
- 10 WORSFOLD, D. J. and BYWATER, S. *J. Polym. Sci.* 1957, **26**, 299
- 11 BYWATER, S. and WORSFOLD, D. J. *J. Polym. Sci.* 1962, **58**, 571
- 12 SAIGUSA, T., IMAI, H., HIRAI, S. and FURUKAWA, J. *Kogyo Kagaku Zasshi*, 1962, **65**, 699; *Chem. Abstr.* 1962, **57**, 15346^c

Monomer-Polymer Equilibrium and Ceiling Temperature for Tetrahydrofuran Polymerization

TETRAHYDROFURAN (THF) readily yields high polymer under the influence of typical Friedel-Crafts type catalysts¹⁻⁴. Meerwein¹ observed that the maximum possible degree of conversion to polymer at room temperature was around 70 per cent and therefore suggested that the propagation reaction involved oxonium ions with a monomer-polymer equilibrium, i.e.



More quantitative evaluation of this phenomenon was hindered by the fact that, as in many cationic polymerizations⁴, the active catalyst was of uncertain composition and only the overall reaction rates could be studied. In order to overcome these difficulties we have developed the use of salts of the stable triphenylmethyl⁵ and tropylium⁶ carbonium ions as cationic

We wish to acknowledge helpful and stimulating discussion with Professor C. E. H. Bawn and Professor M. Szwarc. One of us (M.P.D.) is indebted to Imperial Chemical Industries for an I.C.I. Postdoctoral Fellowship and the other (P.D.) to the American Association of University Women for the award of the Marie Curie Fellowship for 1964-65.

M. P. DREYFUSS
P. DREYFUSS

Department of Inorganic, Physical and Industrial Chemistry,
University of Liverpool

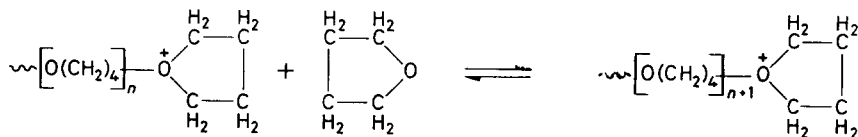
(Received October 1964)

REFERENCES

- ¹ SZWARC, M. *Advanc. Polym. Sci.* 1960, **2**, 275
- ² PLESCH, P. H. *The Chemistry of Cationic Polymerization*, p 555. Pergamon: Oxford, 1963
- ³ BAWN, C. E. H., BELL, R. and LEDWITH, A. Chemical Society Anniversary Meeting, Cardiff, 1963
- ⁴ SIMS, D. *J. chem. Soc.* **1964**, 864
- ⁵ SORENSEN, W. and CAMPBELL, T. W. *Preparative Methods of Polymer Chemistry*, p 253. Interscience: New York, 1961
- ⁶ BELL, R. *Ph.D. Thesis*, University of Liverpool, 1963
- ⁷ MUETTERTIES, E. L. *U.S. Patent No. 2 856 370* (1958)
- ⁸ WAACK, R., REMBAUM, A., COOMBES, J. D. and SZWARC, M. *J. Amer. chem. Soc.* 1957, **79**, 2026
- BRODY, H., LADACKI, M., MILKOVICH, R. and SZWARC, M. *J. Polym. Sci.* 1957, **25**, 221
- ⁹ WORSFOLD, D. J. and BYWATER, S. *J. Polym. Sci.* 1957, **26**, 299
- BYWATER, S. and WORSFOLD, D. J. *J. Polym. Sci.* 1962, **58**, 571
- ¹⁰ SAIGUSA, T., IMAI, H., HIRAI, S. and FURUKAWA, J. *Kogyo Kagaku Zasshi*, 1962, **65**, 699; *Chem. Abstr.* 1962, **57**, 15346^e

Monomer-Polymer Equilibrium and Ceiling Temperature for Tetrahydrofuran Polymerization

TETRAHYDROFURAN (THF) readily yields high polymer under the influence of typical Friedel-Crafts type catalysts¹⁻⁴. Meerwein¹ observed that the maximum possible degree of conversion to polymer at room temperature was around 70 per cent and therefore suggested that the propagation reaction involved oxonium ions with a monomer-polymer equilibrium, i.e.



More quantitative evaluation of this phenomenon was hindered by the fact that, as in many cationic polymerizations⁴, the active catalyst was of uncertain composition and only the overall reaction rates could be studied. In order to overcome these difficulties we have developed the use of salts of the stable triphenylmethyl⁵ and tropylium⁶ carbonium ions as cationic

COMMUNICATIONS AND NOTES

polymerization initiators. Polymerizations initiated in this manner are characterized by (i) rapid initiation involving complete use of catalyst, (ii) little or no termination except at higher temperatures, (iii) highly reproducible reaction rates and molecular weights. Such systems can thus be classified as containing 'living' polymers according to the nomenclature devised by Szwarc⁷ for some anionic polymerizations.

For THF polymerization triphenylmethyl hexachloroantimonate ($\text{Ph}_3\text{C}^+\text{SbCl}_6^-$) is particularly useful as initiator and facilitates study of the monomer-polymer equilibrium. The data in *Table 1* show clearly that

Table 1. Polymerization of THF at 25°C*

$10^3 \times [\text{Ph}_3\text{C}^+\text{SbCl}_6^-]$ M	Weight of polymer recovered†	$[\eta]^\ddagger$ dl/g
1.37	6.44	3.55
2.06	6.85	2.88
2.74	6.35	2.70
3.53	6.71	2.06
4.93	6.57	1.76
8.00	6.29	1.64

*10.0 ml of THF used for each experiment.

†Each reaction left for approximately 48 h.

‡Measured in benzene at 25.0°C.

the degree of conversion of monomer to polymer reached a constant (equilibrium) value at 25°C independent of initiator concentration.

At 50°C (*Table 2*) there was a significant termination reaction which

Table 2. Polymerization of THF at 50°C*

$10^4 \times [\text{Ph}_3\text{C}^+\text{SbCl}_6^-]$ M	Reaction time	Weight of polymer recovered (g)	$10^4 \times [\text{Ph}_3\text{C}^+\text{SbCl}_6^-]$ M	Reaction time	Weight of polymer recovered (g)
4.0	7.7 h	5.47	1.0	30.8 h	4.20
4.0	5 weeks	7.93	0.6	46.6 h	3.46
3.0	24 h	7.30	0.5	61.5 h	2.88
2.6	24 h	7.40	0.4	79.9 h	2.38
2.0	15.4 h	4.90	0.4	5 weeks	2.62
1.3	23.6 h	4.75			

*20.0 ml THF used for each experiment.

destroyed all the active ends before true equilibrium was reached unless the catalyst concentration was greater than ca. 10^{-3} M. The chain stopping reaction became progressively more important as the temperature was increased.

Using appropriate catalyst concentrations it was possible to measure directly the equilibrium conversion at a series of temperatures above 50°C and the results are shown in *Figure 1*. Extrapolation of this curve leads to a value of 60° to 70°C for the ceiling temperature of high polymer formation from monomeric THF. From kinetic measurements at 25° and 50°C the heat of polymerization of THF can be calculated as (-4.0 ± 1.0) kcal/mole (liquid monomer-dissolved polymer) in close agreement with the value (-5.2) kcal/mole estimated from thermodynamic constants⁹.

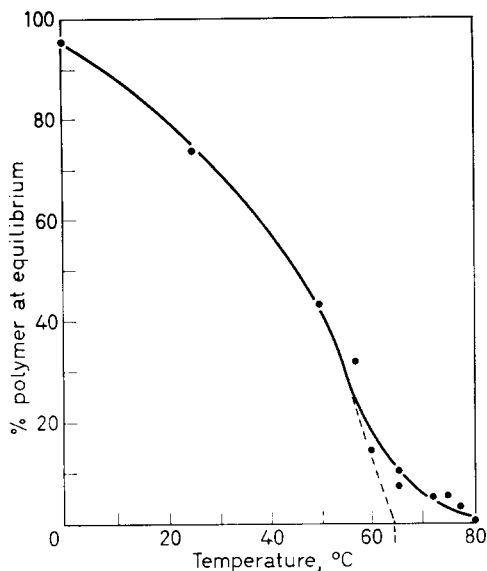


Figure 1—Measurement of ceiling temperature for THF polymerization

Using PF_5 as initiator Sims⁸ has reported similar equilibrium data at temperatures up to 50°C with $\Delta H_x = -4.3$ kcal/mole. However, with PF_5 as initiator much higher molecular weights are obtained and the degree of conversion is greater (at high temperatures) than with $\text{Ph}_3\text{C}^+\text{SbCl}_6^-$. These results suggest that the depropagation reaction is affected in some way when using PF_5 at temperatures above 50°C and under these conditions the

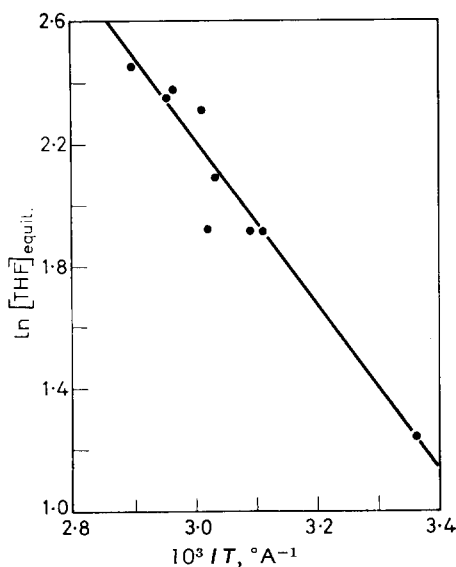


Figure 2—Equilibrium polymerization of THF

system would not possess a true monomer-polymer equilibrium. From the general theory of equilibrium polymerization⁹ it can be shown that

$$\ln [\text{THF}]_{\text{equil.}} = \frac{1}{T} \cdot \frac{\Delta H_x}{R} - \frac{\Delta S_x^0}{R}$$

and hence a plot of $\ln [\text{THF}]_{\text{equil.}}$ versus $1/T$ should be a straight line of slope $\Delta H_x/R$. Figure 2 shows this plot for data obtained in the present work and substantiates the conclusion that a true equilibrium exists. The value of ΔH_x obtained in this manner is $-(5.3 \pm 1.0)$ kcal/mole. Significantly the data of Sims, using PF_5 as initiator, do not give a linear $\ln [\text{THF}]_{\text{equil.}}$ versus $1/T$ plot above 50°C .

The authors are grateful to D. Richardson for help in determining equilibrium monomer concentrations.

C. E. H. BAWN
R. M. BELL
A. LEDWITH

*Department of Inorganic, Physical and Industrial Chemistry,
University of Liverpool*

(Received October 1964)

REFERENCES

- ¹ MEERWEIN, H., DELFS, D. and MORSCHER, H. *Angew. Chem.* 1960, **72**, 927
- ² HACHIHAMA, Y. and SHONE, T. *Technol. Rep. Osaka Univ.* 1959, **9**, 337
- ³ MUETTERIES, E. L. *U.S. Patent No. 2 856 370* (1958)
- ⁴ *Cationic Polymerization*. Edited by P. H. PLESCH. Pergamon: Oxford, 1963
- ⁵ BAWN, C. E. H., BELL, R. M. and LEDWITH, A. Chemical Society Anniversary Meeting, Cardiff, 1963
- ⁶ BAWN, C. E. H., FITZSIMMONS, C. and LEDWITH, A. *Proc. chem. Soc.* Dec. 1964, 391
- ⁷ SZWARC, M. *Advanc. Polym. Sci.* 1960, **2**, 275
- ⁸ SIMS, D. *J. chem. Soc.* 1964, 864
- ⁹ DANTON, F. S. and IVIN, K. *Quart. Rev. chem. Soc. Lond.* 1958, **12**, 61

Monomer Reactivity Ratios of a Ternary System

THE reactivity ratios were determined for the ternary system of (a) styrene, (b) 2-ethylhexyl acrylate, (c) glycidyl acrylate, and are reported in Table 2.

Copolymer composition was determined by elemental analysis for styrene-2-ethylhexyl acrylate (S-EHA) and by % Epirane oxygen determination¹ for styrene-glycidyl acrylate (S-GA) and 2-ethylhexyl acrylate-glycidyl acrylate (EHA-GA) copolymers.

With this information, the reactivity ratios were determined by graphic solution of the copolymer equation². The Q and e values³ for glycidyl acrylate were calculated from experimentally determined reactivity ratios and published Q and e values for styrene⁴ and 2-ethylhexyl acrylate⁵.

system would not possess a true monomer-polymer equilibrium. From the general theory of equilibrium polymerization⁹ it can be shown that

$$\ln [\text{THF}]_{\text{equil.}} = \frac{1}{T} \cdot \frac{\Delta H_x}{R} - \frac{\Delta S_x^0}{R}$$

and hence a plot of $\ln [\text{THF}]_{\text{equil.}}$ versus $1/T$ should be a straight line of slope $\Delta H_x/R$. Figure 2 shows this plot for data obtained in the present work and substantiates the conclusion that a true equilibrium exists. The value of ΔH_x obtained in this manner is $-(5.3 \pm 1.0)$ kcal/mole. Significantly the data of Sims, using PF_5 as initiator, do not give a linear $\ln [\text{THF}]_{\text{equil.}}$ versus $1/T$ plot above 50°C .

The authors are grateful to D. Richardson for help in determining equilibrium monomer concentrations.

C. E. H. BAWN
R. M. BELL
A. LEDWITH

*Department of Inorganic, Physical and Industrial Chemistry,
University of Liverpool*

(Received October 1964)

REFERENCES

- ¹ MEERWEIN, H., DELFS, D. and MORSCHER, H. *Angew. Chem.* 1960, **72**, 927
- ² HACHIHAMA, Y. and SHONE, T. *Technol. Rep. Osaka Univ.* 1959, **9**, 337
- ³ MUETTERIES, E. L. *U.S. Patent No. 2 856 370* (1958)
- ⁴ *Cationic Polymerization*. Edited by P. H. PLESCH. Pergamon: Oxford, 1963
- ⁵ BAWN, C. E. H., BELL, R. M. and LEDWITH, A. Chemical Society Anniversary Meeting, Cardiff, 1963
- ⁶ BAWN, C. E. H., FITZSIMMONS, C. and LEDWITH, A. *Proc. chem. Soc.* Dec. 1964, 391
- ⁷ SZWARC, M. *Advanc. Polym. Sci.* 1960, **2**, 275
- ⁸ SIMS, D. *J. chem. Soc.* 1964, 864
- ⁹ DANTON, F. S. and IVIN, K. *Quart. Rev. chem. Soc. Lond.* 1958, **12**, 61

Monomer Reactivity Ratios of a Ternary System

THE reactivity ratios were determined for the ternary system of (a) styrene, (b) 2-ethylhexyl acrylate, (c) glycidyl acrylate, and are reported in Table 2.

Copolymer composition was determined by elemental analysis for styrene-2-ethylhexyl acrylate (S-EHA) and by % Epirane oxygen determination¹ for styrene-glycidyl acrylate (S-GA) and 2-ethylhexyl acrylate-glycidyl acrylate (EHA-GA) copolymers.

With this information, the reactivity ratios were determined by graphic solution of the copolymer equation². The Q and e values³ for glycidyl acrylate were calculated from experimentally determined reactivity ratios and published Q and e values for styrene⁴ and 2-ethylhexyl acrylate⁵.

COMMUNICATIONS AND NOTES

Reactivity ratios calculated from published and determined Q and e values agree closely with experimental results.

Table 1. Monomer feed and copolymer composition

System	M	m	M	m	M	m
Styrene 2-EHA	0.865	0.871	0.551	0.601	0.384	0.476
	0.0543	0.0544	0.218	0.204	0.326	0.274
Styrene GA	0.865	0.846	0.625	0.629	0.385	0.490
	0.0781	0.0936	0.273	0.270	0.469	0.383
2-EHA GA	0.489	0.493	0.353	0.352	0.1902	0.179
	0.0781	0.0729	0.273	0.276	0.508	0.524

M denotes mole fraction in monomer mixture.
 m denotes mole fraction found in polymer.

Table 2. Monomer reactivity ratios

System	Q	e	r (exp.)	r (calc.)
Styrene 2-EHA	1.0	-0.8	r_{12}	0.91
	0.41	0.39	r_{21}	0.29
Styrene GA*	1.0	-0.8	r_{13}	0.73
	0.47	0.49	r_{31}	0.25
2-EHA GA*	0.41	0.39	r_{23}	0.98
	0.47	0.49	r_{32}	1.08

*The Q and e values were calculated from experimentally obtained r values.

EXPERIMENTAL

The monomers used were redistilled under reduced pressure prior to use. Polymerizations were carried out to 5 to 10 per cent conversion by rapidly heating a solution in xylene of two monomers and 0.1 per cent initiator to 138°C and then maintaining this temperature for three minutes. Polymerization was then quenched by external cooling and addition of alcohol. The polymers were purified by repeated precipitations and washings. All samples were dried for 24 hours at 60°C and 20 mm of mercury pressure prior to analysis.

J. T. KHAMIS

Continental Can Company, Inc.,
Corporate R & D Laboratories,
Chicago, Illinois

(Received November 1964)

REFERENCES

- DURBETAKI, A. J. *Analyt. Chem.* 1956, **28**, 2000
- BILLMEYER, F. W. *Textbook of Polymer Chemistry*, Chap. 24. Interscience: New York and London, 1957
- ALFREY, Jr, T. and PRICE, C. C. *J. Polym. Sci.* 1947, **2**, 101
- YOUNG, L. J. *J. Polym. Sci.* 1961, **54**, 411
- Rohm & Haas Company. Unpublished results

*Proton Magnetic Resonance Study of the Polystyrene
'Transition' in Solution*

THE demonstration by Reiss and Benoit¹ of the irregular variation of the second virial coefficient and radius of gyration of polystyrene in solution as a function of temperature was the first of a series of experiments showing that the intramolecular structure of chain polymer molecules in solution may require a more detailed model than the random coil picture commonly adopted. Other measurements on polystyrene exhibiting similar variation with temperature were reported by Schmitt and Kovacs² who studied changes in specific volume in solution, by Moraglio and Danusso³ who detected changes in specific volume of the bulk material, by Bianchi and Rossi⁴ who found irregularities in the temperature dependence of the internal pressure $(\partial E/\partial V)_T$ of the bulk polymer, and by Liquori and Quadrioglio⁵ who noted changes in the ultra-violet spectrum of polystyrene solutions.

Of particular importance was the measurement of the decrease in depolarization of scattered light of a polystyrene solution by Weill and Reiss⁶. This result showed that the correlation in orientation between benzene rings along the polymer chain changes relatively abruptly in the temperature interval between 50° and 80°C.

We have investigated the change of polystyrene structure in solution as a function of temperature by measuring the width at half height ($\delta W_{\frac{1}{2}}$) of the proton magnetic resonance peaks of the phenyl rings on polystyrene molecules. The experiments were carried out on the amorphous extract and soluble isotactic portions of a sample prepared with a titanium tetrachloride, aluminium triisobutyl catalyst in accordance with a previously described recipe^{7*}.

The measurements were carried out as a function of temperature on a Varian† A-60 (60 mc.) proton magnetic resonance apparatus on solutions of the polymer in carbon tetrachloride and decalin.

Solutions were used of varying concentration (from 4 per cent to 15 per cent). In no case studied were the results found to be concentration dependent. While carrying out the experiments, regular checks of an internal standard were made to ensure that the magnetic field in the spectrometer was kept uniform. The experiments were repeated at different times and with duplicate samples to reduce the possibility of experimental error. The significant results are summarized in *Figure 1*. In all cases the decrease in line width is more rapid between 40° and 80°C which is consistent with the phenomena observed by previous authors¹⁻⁶. For the isotactic polymer, the effect takes place in a narrower range, between 50° and 60°C. The widths of proton magnetic resonance peaks of polystyrene in solution are determined by unresolved spin-spin splitting and by the time dependence of the magnetic dipole interaction of the hydrogen nuclei. The narrower the peak, the more rapid are the motions of the chain segments, and it

*The authors wish to express their gratitude to Dr W. Burlant and Mr R. Taylor of the Ford Scientific Laboratory for having synthesized the material.

†Varian Associates—Palo Alto, California.

becomes clear that there is an unusually rapid increase of mobility of units of the polymer chain with temperature in the 40° to 80°C (50° to 60°C) temperature interval.

It is to be noted that the widths of the n.m.r. lines of the isotactic fraction of the polymer are less than for the amorphous fraction. This can be attributed, in part, to the stereochemical homogeneity of the isotactic chain as opposed to the partially random character of isotactic, heterotactic and syndiotactic sequences in the amorphous part. What appears to be significant to us is that the abruptness of the change with temperature is

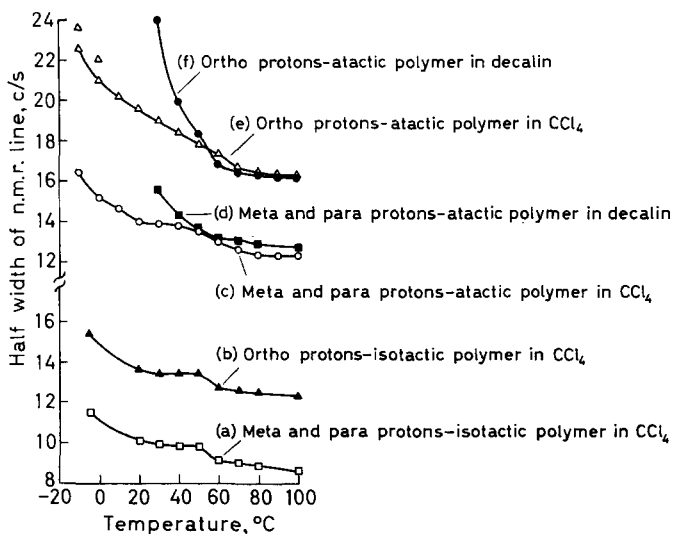


Figure 1—The line widths of proton magnetic resonance peaks of phenyl protons on polystyrene as a function of temperature. The ordinate is the width of the peak at half height in cycles per second

greater for the isotactic polymer. It would seem that the phenomenon observed in the amorphous material is a consequence of the same sort of structure change as that which occurs in the isotactic polymer but the effect is diluted by the presence of chain sequences which do not exhibit any change of this type.

It is known that isotactic polystyrene crystallizes in a helical form. Most of the crystalline polymer does not dissolve under the conditions of these experiments and the soluble fraction may be less regular in structure than the insoluble crystalline material, but nevertheless it contains a considerable fraction of isotactic sequences in each chain. This has been confirmed on our sample by comparing the infra-red spectrum with that reported for isotactic polystyrene⁸.

It is not certain that the conformations of a polymer chain in solution are the same as those in the solid, but it is probable that conformational arrangements close to that of the solid are present in considerable excess over the other geometric possibilities, at least at low temperatures.

The changes which take place in magnetic resonance and depolarization of scattered light⁶ can be accounted for by assuming that the van de Waals forces between neighbouring phenyl rings on polystyrene create structures of groups of chain units of temporary stability, but which break up and reform relatively rapidly. The temperature interval of 50° to 60°C represents a 'melting range' in the sense that the cooperative stabilization of these chain units is no longer effective above 60°C. This explanation is consistent with the measurements and seems to be a reasonable one on the basis of present information.

It is clear from *Figure 1* that the resonance peaks become much broader at lower temperatures. This can arise from increased solvent viscosity, greater impediment to hindered rotation, and nearness of approach to the precipitation point. The relative importance of these and other factors has not been assessed as yet.

KANG-JEN LIU
R. ULLMAN

*Scientific Laboratory,
Ford Motor Company,
Dearborn, Mich., U.S.A.*

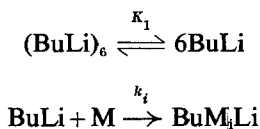
(Received October 1964)

REFERENCES

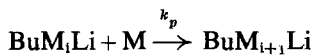
- ¹ REISS, C. and BENOIT, H. *C.R. Acad. Sci., Paris*, 1961, **253**, 268
- ² SCHMITT, A. and KOVACS, A. J. *C.R. Acad. Sci., Paris*, 1962, **255**, 677
- ³ MORAGLIO, G. and DANUSSO, F. *Polymer, Lond.* 1963, **4**, 445
- ⁴ BIANCHI, U. and ROSSI, C. *Polymer, Lond.* 1963, **4**, 447
- ⁵ LIQUORI, A. and QUADRIFOGLIO, F. *Polymer, Lond.* 1963, **4**, 448
- ⁶ WEILL, G. and REISS, C. *C.R. Acad. Sci., Paris*, 1963, **256**, 2816
- ⁷ OVERBERGER, C. G., ANG, F. and MARK, H. J. *Polym. Sci.* 1959, **35**, 381
- ⁸ TAKEDA, M., IIMURA, K., YAMADA, A. and IMAMURA, Y. *Bull. chem. Soc. Japan*, 1960, **33**, 1219

*The Kinetics of the Polymerization of Styrene Initiated by
n-Butyl Lithium*

PREVIOUS work¹ on the polymerization of styrene in benzene initiated by *n*-butyl lithium has shown that the initiation process is



and that, when all the *n*-butyl lithium has been converted into polystyryl lithium, the propagation reaction is



The changes which take place in magnetic resonance and depolarization of scattered light⁶ can be accounted for by assuming that the van de Waals forces between neighbouring phenyl rings on polystyrene create structures of groups of chain units of temporary stability, but which break up and reform relatively rapidly. The temperature interval of 50° to 60°C represents a 'melting range' in the sense that the cooperative stabilization of these chain units is no longer effective above 60°C. This explanation is consistent with the measurements and seems to be a reasonable one on the basis of present information.

It is clear from *Figure 1* that the resonance peaks become much broader at lower temperatures. This can arise from increased solvent viscosity, greater impediment to hindered rotation, and nearness of approach to the precipitation point. The relative importance of these and other factors has not been assessed as yet.

KANG-JEN LIU
R. ULLMAN

*Scientific Laboratory,
Ford Motor Company,
Dearborn, Mich., U.S.A.*

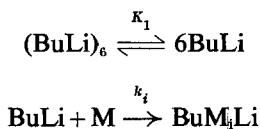
(Received October 1964)

REFERENCES

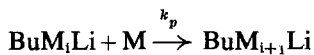
- ¹ REISS, C. and BENOIT, H. *C.R. Acad. Sci., Paris*, 1961, **253**, 268
- ² SCHMITT, A. and KOVACS, A. J. *C.R. Acad. Sci., Paris*, 1962, **255**, 677
- ³ MORAGLIO, G. and DANUSSO, F. *Polymer, Lond.* 1963, **4**, 445
- ⁴ BIANCHI, U. and ROSSI, C. *Polymer, Lond.* 1963, **4**, 447
- ⁵ LIQUORI, A. and QUADRIFOGLIO, F. *Polymer, Lond.* 1963, **4**, 448
- ⁶ WEILL, G. and REISS, C. *C.R. Acad. Sci., Paris*, 1963, **256**, 2816
- ⁷ OVERBERGER, C. G., ANG, F. and MARK, H. J. *Polym. Sci.* 1959, **35**, 381
- ⁸ TAKEDA, M., IIMURA, K., YAMADA, A. and IMAMURA, Y. *Bull. chem. Soc. Japan*, 1960, **33**, 1219

*The Kinetics of the Polymerization of Styrene Initiated by
n-Butyl Lithium*

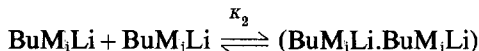
PREVIOUS work¹ on the polymerization of styrene in benzene initiated by *n*-butyl lithium has shown that the initiation process is



and that, when all the *n*-butyl lithium has been converted into polystyryl lithium, the propagation reaction is



the active centres, BuM_iLi , being in dynamic equilibrium with an inactive dimeric form



At concentrations of polystyryl lithium greater than 10^{-4} mole litre $^{-1}$, the rate of disappearance of monomer is first order with respect to the monomer and half order with respect to the total lithium atom concentration showing that the above equilibrium lies well over to the right hand side.

If, as in our work², the monomer disappears both by reaction with the monomeric *n*-butyl lithium and the active centres, no such simple kinetics are observed. Instead the monomer concentration/time curves are sigmoidal indicating that of the two reactions competing for styrene that between the active centres and the monomer is preferred. As a result, some *n*-butyl lithium may remain at the end of the polymerization. In this Note, we demonstrate that the previous four-reaction scheme proposed by Worsfold and Bywater¹ is adequate to describe the polymerization occurring under these more complex conditions. Our original analytical approach involved, as Bywater³ pointed out, a number of inconsistent approximations. Consequently for our present purpose, we have used a numerical method of solving the equations governing the kinetic behaviour of the system. Following our previous symbolism, these are :

$$\frac{d(X+2Y)}{dt} = \frac{k_i}{(6K_1)^{1/6}} (a_0 - X - 2Y)^{1/6} M$$

$$\frac{-dM}{dt} = \frac{d(X+2Y)}{dt} + k_p X \cdot M$$

$$X = \{[1 + 8K_2(X+2Y)]^{1/2} - 1\} / 4K_2$$

where $X = \sum_i [\text{BuM}_i\text{Li}]$

$$Y = \sum_{i,j} [(\text{BuM}_i\text{Li} \cdot \text{BuM}_j\text{Li})]$$

$$a_0 = 6 [(\text{BuLi})_6] + X + 2Y$$

In writing these equations, we have had to retain the assumptions that the two equilibria are rapidly maintained and that the concentration of the monomeric *n*-butyl lithium is negligible. The three simultaneous equations were solved using a digital computer (DEUCE) to give values of the concentrations, M and $(X+2Y)$, at pre-selected times for different sets of the parameters $k_i/(6K_1)^{1/6}$, k_p and K_2 . Since M and $(X+2Y)$ were known as functions of time for various initial concentration conditions— M from dilatometric measurements and $(X+2Y)$ from optical density determinations—it was possible to compare the predicted and experimental concentration/time curves directly. This comparison showed immediately that, if the numerical values of the three parameters were chosen so as to be

consistent with the findings of Worsfold and Bywater, all our results were qualitatively reproduced on the basis of their mechanism—the fact of our using toluene as solvent rather than benzene being of no consequence. *Figures 1, 2 and 3*, on which we plot our runs obtained at 15°C, illustrate the results found using the values:

$$k_i/(6K_1)^{1/6} = 5 \times 10^{-6} \text{ litre}^{1/6} \text{ mole}^{-1/6} \text{ sec}^{-1}$$

$$k_p = 10 \text{ litre mole}^{-1} \text{ sec}^{-1}$$

$$K_2 = 2 \times 10^6 \text{ litre mole}^{-1}$$

$$\epsilon_{550\text{m}\mu} = 108 \text{ litre mole}^{-1} \text{ cm}^{-1}$$

The value of the extinction coefficient has to be specified in order to convert the predicted $(X+2Y)$ concentration terms to optical densities at the wavelength used in our measurements.

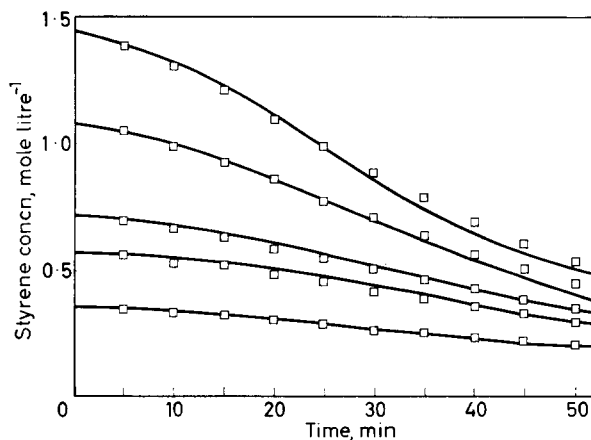


Figure 1—Comparison of calculated and experimental dependence of monomer consumption on the initial monomer concentration at a constant initial *n*-butyl lithium concentration of 0.029 mole litre⁻¹. Temperature 15°C.
□ calculated results; — experimental

It must be emphasized that the values of k_p and K_2 quoted above are *not* necessarily the true values appropriate to the polymerization at 15°C but merely one pair from a large set which, at this particular value of $k_i/(6K_1)^{1/6}$, lead to a satisfactory fit of the experimental and calculated monomer/time curves. In fact, we find that if any two or all three of the parameters are varied* such that

$$\{k_i/(6K_1)^{1/6}\}^{1/2} \{k_p/K_2^{1/2}\}$$

remains constant, the calculated monomer/time curve is unaffected. (An analogous situation is found in the case of free-radical initiated polymeriza-

*In our calculations, we did not investigate variations greater than one order of magnitude.

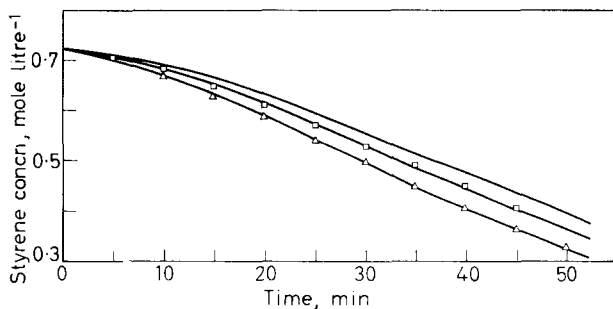


Figure 2—Comparison of calculated and experimental dependence of monomer consumption on the initial *n*-butyl lithium concentration at a constant initial monomer concentration of 0.722 mole litre⁻¹. Temperature 15°C. — Mean experimental result for initial *n*-butyl lithium concentration from 0.008 to 0.070 mole litre⁻¹; □ Calculated for $[n\text{-Bu Li}]_0 = 0.008$ mole litre⁻¹; △ Calculated for $[n\text{-Bu Li}]_0 = 0.070$ mole litre⁻¹

tion; using conventional symbols, the disappearance of monomer is determined essentially by the parameter $(k_i/k_t)^{1/2} k_p$ and not by the individual values of the rate constants.) On the other hand, the rate of formation of the lithiated polystyrenes is determined primarily by the quantity

$$k_i/(6K_1)^{1/6}$$

It follows, therefore, that the procedure which we have employed can establish no more than probable values for the two composite quantities and hence, by division, the two ratios $k_p/K_2^{1/2}$ and $k_i/(6K_1)^{1/6}$.

Since our objective in this work was the demonstration of the essential validity of the four-reaction mechanism under our conditions, we have not

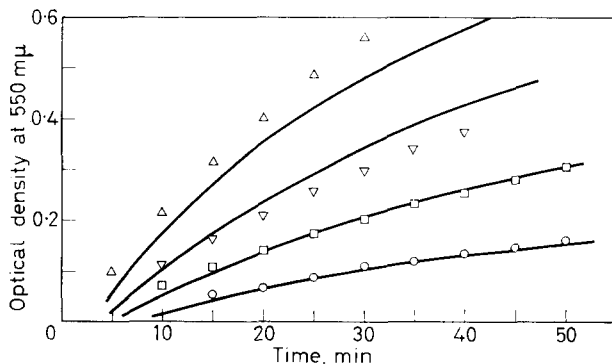


Figure 3—Comparison of calculated and experimental dependence of the optical density/time curves on the initial monomer concentration at a constant initial *n*-butyl lithium concentration of 0.071 mole litre⁻¹. — Experimental results; calculated results for initial monomer concentrations of: △ 1.08, ▽ 0.54, □ 0.36 and ○ 0.18 mole litre⁻¹

COMMUNICATIONS AND NOTES

attempted to obtain the best values of these ratios by a statistical procedure. It is sufficient for our purposes that our 'best' value of $k_p/K_2^{1/2}$ at the 'Worsfold and Bywater' value of $k_i/(6K_1)^{1/6}$ of 5×10^{-6} litre^{1/6} mole^{-1/6} sec⁻¹ is 7×10^{-3} litre^{1/2} mole^{-1/2} sec⁻¹ in good agreement with the result 6.2×10^{-3} litre^{1/2} mole^{-1/2} sec⁻¹ quoted by these authors.

Table 1. Comparison of calculated and observed concentration/time data for 30°C.
 $M_0 = 27.4 \times 10^{-3}$ mole litre⁻¹; $a_0 = 1.18 \times 10^{-3}$ mole litre⁻¹

Time min	[Styrene] mole litre ⁻¹ × 10 ³		[Polystyryl lithium] mole litre ⁻¹ × 10 ⁵	
	Observed	Calculated	Observed	Calculated
0	27.4		0	
5	26.5	26.8	3.1	6.1
10	—	25.8	—	12.1
20	22.9	23.3	21.6	23.1
30	20.8	20.4	31.1	32.5
40	17.8	17.6	40.1	40.6
50	—	14.9	—	47.4
60	13.0	12.5	51.5	53.1
70	10.8	10.4	56.1	57.8
80	9.1	8.6	59.6	61.6
90	7.3	7.0	62.5	64.7
100	5.9	5.8	64.7	67.2

Finally we show a comparison of predicted and experimental data for 30°C in Table 1. The experimental results are those of Worsfold and Bywater who, in this case, followed the disappearance of styrene in the presence of *n*-butyl lithium. The calculated data were obtained using the same programme employed to simulate our own findings with values of $k_p/K_2^{1/2}$ and $k_i/(6K_1)^{1/6}$ of 1.8×10^{-2} litre^{1/2} mole^{-1/2} sec⁻¹, and 2.3×10^{-5} litre^{1/6} mole^{-1/6} sec⁻¹ respectively. The agreement is most satisfactory.

R. C. P. CUBBON

Research Department,
 British Nylon Spinners Ltd,
 Pontypool, Monmouthshire

D. MARGERISON

Department of Inorganic, Physical and Industrial Chemistry,
 University of Liverpool

(Received November 1964)

The authors wish to thank Drs D. J. Worsfold and S. Bywater for supplying the above experimental data. They also wish to acknowledge the help given by the Staff of the Department of Numerical Analysis, The University of Liverpool.

REFERENCES

- 1 WORSFOLD, D. J. and BYWATER, S. *Canad. J. Chem.* 1960, **38**, 1891
- 2 CUBBON, R. C. P. and MARGERISON, D. *Proc. Roy. Soc. A*, 1962, **268**, 260
- 3 BYWATER, S. Private communication

Cold-drawing and Crystallization of Polyethylene Terephthalate

If polyethylene terephthalate is extruded either as a fibre or film and then constrained to cool rapidly, the polymer may be obtained in an amorphous state. If it is then heated at temperatures some 40°C or more above the glass temperature of approximately 70°C, rapid crystallization occurs. This is clearly shown in differential thermal analysis studies of the amorphous material where an exothermic process is seen to occur at these temperatures with a peak maximum at about 145°C^{1,2}.

If the polymer is first cold-drawn at room temperature before being submitted to differential thermal analysis, no characteristic crystallization peak is detected and the thermogram bears a close resemblance to that for a cold-drawn specimen which had been subsequently heated and which, being recognized as crystalline from X-ray diffraction studies, has led to the suggestion that cold-drawn polyethylene terephthalate may also be crystalline². It has therefore been suggested that heating such a specimen merely results in a reorganization of the crystalline phase. It has also been reported that during the heating of the cold-drawn polymer, some longitudinal (i.e. in the direction of drawing) contraction occurs².

On the basis of these results and indications it was decided to investigate the process of cold-drawing in more detail. For this purpose, samples of amorphous film with a thickness of 2.0×10^{-2} cm were cold-drawn (draw ratio $\approx \times 4$) at room temperature in a Hounsfield tensometer and then heated in an air oven at constant elongation using a draw-frame for a period of 20 minutes, this time having been found to be adequate for the attainment of a state of apparent equilibrium, at temperatures in the range 50° to 242°C. At the same time separate pieces were freely mounted for purposes of determining the extent of contraction. The results of the latter investigation expressed as a percentage of the original (drawn) length are shown in *Figure 1*. It is clear that the value for the contraction is greater

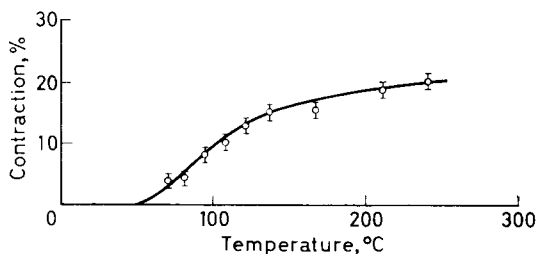


Figure 1—Contraction of cold-drawn polyethylene terephthalate

the higher the temperature and, implicitly, that the tendency to contract is also greater for the samples held at constant elongation. X-ray diffraction photographs were obtained for the samples held in the draw-frame and a selection of these is shown in *Figure 2*. The results are best described by reference to the reflections from the $0\bar{1}1$ and the $01\bar{1}$ planes on the one hand and the 010 and the $0\bar{1}0$ planes on the other³. The greater separation

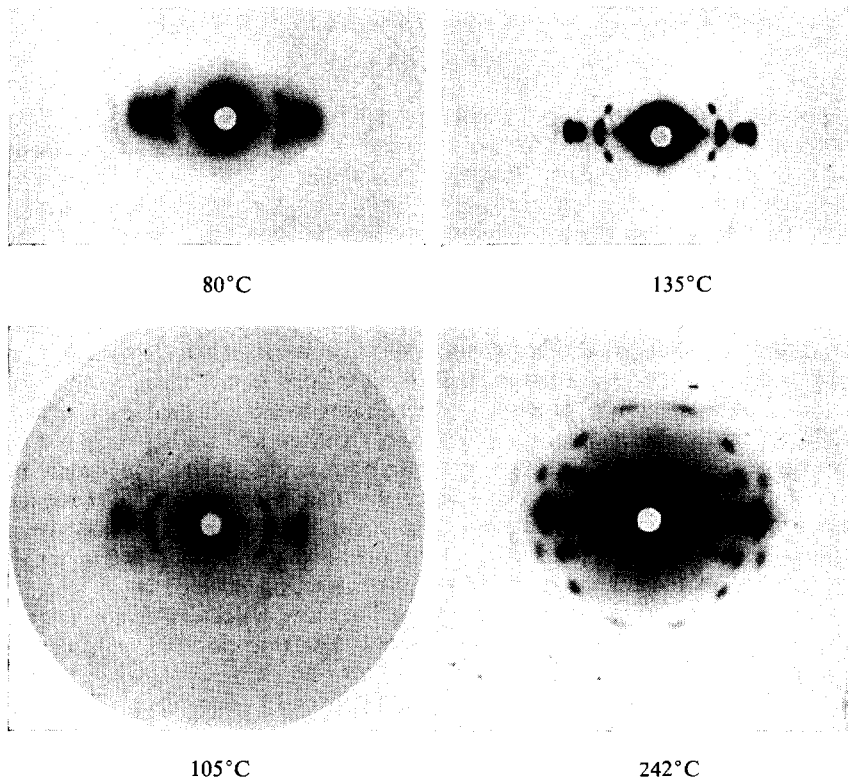


Figure 2—X-ray diffraction patterns for cold-drawn polyethylene terephthalate (after heating at various temperatures under constant strain)

of the former and the smaller separation of the latter corresponds to the smaller angle of tilt in the $\bar{2}30$ plane with respect to the fibre axis⁴. Since the reflections due to the 010 and $0\bar{1}0$ planes approach each other and also the equator, with increase of oven temperature, whereas the reflections from the other planes move away from each other then we may presume a smaller angle of inclination of the crystalline material to the fibre axis with an increase of temperature. At the same time there is an improvement in the diffuseness as the temperature is raised, which is a feature of both crystallite growth and disappearance of crystal defect. It should also be mentioned that at temperatures above about 100°C polymer which has been allowed to contract freely produces an X-ray photograph of improved resolution but with loss of orientation, or if only allowed to contract partially arcs characteristic of poorer orientation are obtained. Before considering an explanation of these phenomena, two further points are of relevance; first, it should be mentioned that diffuse X-ray diffraction photographs have been obtained not only from cold-drawn amorphous polymer but also from cold-drawn crystalline material, but in the latter case substantial orientation is retained on heating, even in the absence of a maintained elongation⁵. Secondly, whereas it might appear that the differential

thermal analysis results are at variance with those of specific heat studies on polymer drawn at the glass temperature where pronounced crystallization was indicated⁶, it is in fact pointed out that as a result of the difference in drawing conditions the two sets of results are regarded as compatible⁷.

It is clear that a postulated mechanism for the cold-drawing and crystallization processes must be capable of explaining both the results of the X-ray diffraction studies and those from differential thermal analysis, and to this end the following proposals are made. It is suggested that the process of cold-drawing of amorphous polymer at this relatively low temperature corresponds to an uncoiling and drawing out of the randomly arranged molecules. The increased mobility associated with this together with the possibility of a local heating effect⁸ allows appreciable crystallization and some orientation with respect to the fibre axis while permitting a simultaneous extension of chains in amorphous regions of the polymer. The diffuseness of the diffraction picture is presumably a result of strain. Subsequent heating at relatively high temperatures under conditions of free contraction causes a disappearance of internal strain, resulting from the effect of temperature on chain mobility, whereas for samples held at constant elongation not only do we have the latter condition but also there is a superimposed anisotropic stress resulting from a tendency of the amorphous regions in particular to contract. This has a further tendency towards tilting of the crystalline regions which will be greater the higher the temperature. In this way a higher orientation of crystalline regions with respect to the fibre axis is produced. That complete disorientation does not occur on heating cold-drawn crystallized material suggests that in this case much less orientation of amorphous regions has taken place. The latter contention is well supported by other work⁹. If this view of strain induced crystallization is not accepted and it is suggested that crystallinity develops only upon heating, it would seem a curious coincidence that energy effects associated with relaxation balance those due to crystallization as seen by differential thermal analysis. Moreover, it is not readily apparent why less oriented regions would crystallize first as would be indicated by the subsequent higher degrees of orientation observed at the higher temperatures. On balance therefore, it would seem that the process of low temperature drawing produces substantial crystallization with the crystalline material in a state of strain, and that this latter condition may be effectively relieved upon heating.

Since preparing this Note our attention has been drawn to recent work on the heating of normal polyethylene terephthalate fibre in which disorientation is described in general terms of a lateral expansion effect¹⁰. It is felt that this interpretation is in keeping with the mechanisms proposed above.

P. R. BLAKEY
R. P. SHELDON

*Institute of Technology,
Bradford*

(Received November 1964)

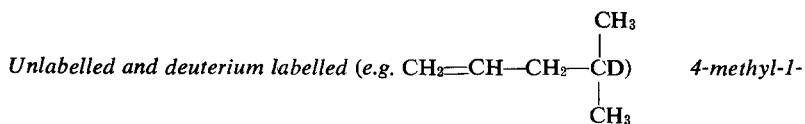
COMMUNICATIONS AND NOTES

REFERENCES

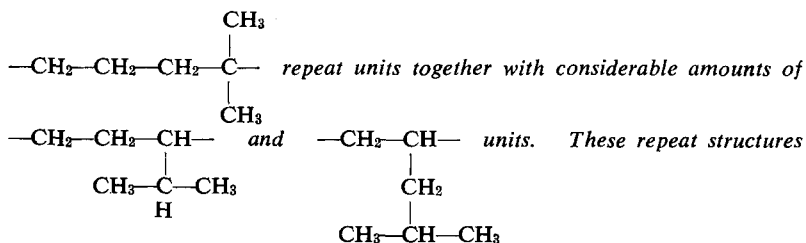
- ¹ SCOTT, N. D. *Polymer, Lond.* 1960, **1**, 114
KE, B. *J. appl. Polym. Sci.* 1962, **6**, 624
- ² HUGHES, M. A. and SHELDON, R. P. *J. appl. Polym. Sci.* 1964, **8**, 1541
- ³ DAUBENY, R. DE P., BUNN, C. W. and BROWN, C. J. *Proc. Roy. Soc. A*, 1954, **226**, 531
- ⁴ BUNN, C. W. Private communication
- ⁵ BLAKEY, P. R. and SHELDON, R. P. *J. Polym. Sci.* 1964, **A2**, 1043
- ⁶ SMITH, C. W. and DOLE, M. J. *J. Polym. Sci.* 1956, **20**, 37
- ⁷ HUGHES, M. A. and SHELDON, R. P. In preparation
- ⁸ MARSHALL, I. and THOMPSON, A. B. *Proc. Roy. Soc. A*, 1954, **221**, 541
- ⁹ KOSLOV, P. V., KABANOV, V. A. and FROLOVA, A. A. *Dokl. Akad. Nauk S.S.S.R.*, 1959, **125**, 118
CHAPPELL, F. P. *Polymer, Lond.* 1960, **1**, 409
STEIN, R. S. and NORRIS, F. H. *J. Polym. Sci.* 1956, **21**, 381
PRESTON, J. M. and TSEIN, P. C. *J. Soc. Dy. Col.* 1950, **66**, 361
- ¹⁰ WLOCHOWICZ, A. *Polimery*, 1963, **8**, 238

Intramolecular Hydride Shift Polymerization by Cationic Mechanism III—Structure Analyses of Deuterated and Non-deuterated Poly-4-methyl-1-pentene

G. G. WANLESS and J. P. KENNEDY



pentene were polymerized by aluminium chloride catalyst in alkyl chloride at -130° and -78°C , and the structure of the products was investigated. Thus, the solid polymers were pyrolysed in high vacuum and the composition and relative distribution of gaseous fractions were determined. The oily fractions were analysed by mass spectroscopy supported by infra-red and nuclear magnetic resonance techniques. The analysis of the data indicates that cationically obtained poly-4-methyl-1-pentene consists mainly of

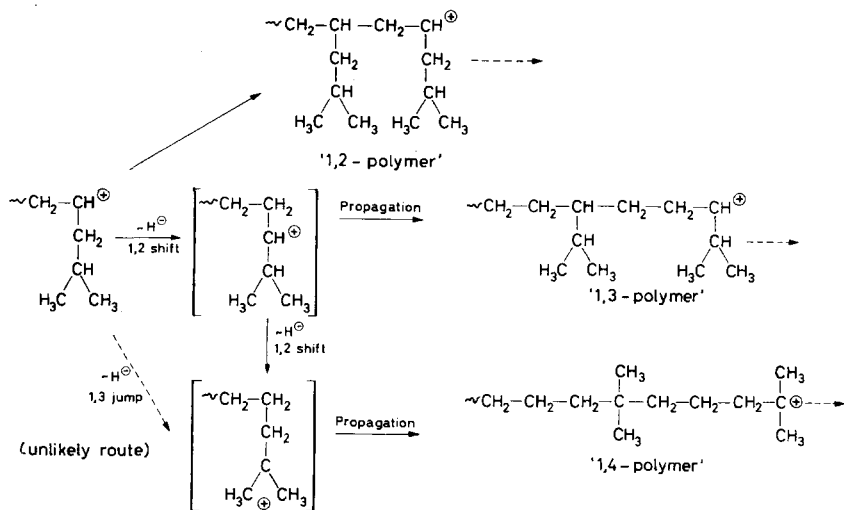


suggest that the cationic polymerization of 4-methyl-1-pentene proceeds by composite hydride shift and conventional mechanisms. More particularly, the analysis of deuterated cationic poly-4-methyl-1-pentene indicates that a succession of $1 \rightarrow 2$ hydride shifts occur and not $1 \rightarrow 3$ hydride jumps. The analytical techniques are presented and the polymerization mechanisms are discussed.

THE cationic isomerization (i.e. hydride shift) polymerization of 3-methyl-1-butene has been discussed in great detail by several groups¹⁻⁹. Among other facts, it has been established that the low temperature polymerization of this monomer gives a crystalline product with α, α' -dimethyl propane type repeat units¹. The structure of the next homologue, cationically obtained poly-4-methyl-1-pentene has been investigated by nuclear magnetic resonance (n.m.r.) spectroscopy. Thus, Edwards and Chamberlain² found that poly-4-methyl-1-pentene obtained at -73°C gave a rather simple n.m.r. spectrum indicating the presence of mainly CH_3- and $-\text{CH}_2-$ groups. Examination of band widths led these workers to suspect that groups other than geminal methyls and isolated methylene might also be present in

these samples. The n.m.r. spectrum of polymers prepared at 0°C more clearly indicated the presence of pendant isopropyl groups in the polymer.

The cationic polymerization (i.e. propagation) of 4-methyl-1-pentene can proceed by at least the following mechanisms:



These equations and formulae define the terminology used in this paper, i.e. 1,2-propagation or 1,2-polymer, 1,3-propagation or 1,3-polymer, and 1,4-propagation or 1,4-polymer.

In the course of our fundamental studies on the structure of cationically obtained hydrocarbon polymers, we developed special techniques which were employed to investigate the complex structure of poly-4-methyl-1-pentene. More particularly, this paper discusses structure analysis of deuterated and non-deuterated poly-4-methyl-1-pentene based mainly on quantitative mass spectroscopic techniques supported by n.m.r. and infrared (i.r.) spectroscopy and gas analysis of pyrolysates. Attempts are made to assign characteristic identification 'codes' to specific polymer structures which then could be correlated with polymerization mechanism. Another purpose of this paper is to provide analytical reality for multiple hydride shift isomerization polymerization.

EXPERIMENTAL

(A) Materials

4-Methyl-1-pentene (Phillips Petroleum Co., 99 mole per cent) was stored over molecular sieves and freshly distilled before use. Gas chromatographic analysis indicated the presence of two minor impurities (total amount less than 0.1 mole per cent).

4-Methyl-1-pentene-4d₁ (i.e. $\text{CH}_2=\text{CH}-\text{CH}_2-\overset{\text{CH}_3}{\underset{|}{\text{C}}}-\text{CH}_3$)₂ was purchased from New England Nuclear Co. Gas chromatographic analysis

indicated the presence of 0.8 per cent pentane and 0.8 per cent unidentified material. The monomer contained 2.80 mole per cent undeuterated material by mass spectroscopy.

The source and purity of aluminium chloride catalyst, methyl and ethyl chloride solvent has been described^{8,9}.

(B) *Polymerization conditions*

Deuterated and undeuterated poly-4-methyl-1-pentenes have been prepared by essentially the same technique. Thus precooled aluminium chloride in ethyl chloride catalyst solutions (about 0.15 molar) were added dropwise to a mixture of 5 ml monomer in 20 ml methyl chloride stirred at -78°C or in ethyl chloride at -130°C . Polymerization started immediately after catalyst addition, and the product was insoluble in the reaction medium. The reaction was terminated by the introduction of cold methanol. The polymer was washed several times with methanol and dried *in vacuo* at 50°C . The Ziegler-Natta type polymer was prepared with aluminium alkyl-titanium halide complex catalyst.

(C) *Vacuum depolymerization of polymers and analytical techniques*

Procedures have been defined (a) for direct pyrolysis within the mass spectrometer solids inlet systems and (b) using a separate all-glass apparatus^{4,11}. A gas fraction, a 'gasoline-like' fraction containing dimers and trimers and a heavy 'gas-oil' fraction containing a mixture of C_6 to C_{31} olefins and minor amounts of higher boiling products were obtained. The last fraction frequently represented 60 to 80 wt per cent of the total sample. These fractions make possible the study of dimers, trimers, tetramers and pentamers of the various polymer samples. All fractions were analysed by nuclear magnetic resonance, gas chromatography, mass spectroscopy and i.r. spectroscopy.

Infra-red spectra were obtained on a Perkin-Elmer No. 521 grating spectrometer.

Gas chromatographic analyses on the C_1 to C_5 gas fractions were carried out using a 25 ft \times $\frac{1}{4}$ in. column packed with 30 per cent, 2,5-hexanedione on Chromasorb P support, at 0°C .

The n.m.r. spectra were obtained, using a Varian A-60 spectrometer, at 175° to 200°C . Samples were either undiluted or dissolved in hexachlorobutadiene.

Mass spectra were taken on a 12 in. radius, 60° magnetically-scanned spectrometer¹¹. Special conditions were used to acquire spectra which are as 'simple' as possible, i.e. which include the minimum of 'smothering' effect at lower molecular weights due to cumulative fragmentation. These conditions include (a) optimum tuning of all parameters for most favourable mass discrimination, (b) ionization chamber temperature of 145°C , and (c) a nominal electron beam energy of 10 eV. The relative effects of altering these parameters on wide-cut olefin mixtures are shown, in part, in *Figure 1*.

(D) *Calculation for deuterated oligomers*

By using identical pyrolysis procedures, 'gas-oil' fractions were prepared from both the deuterated and non-deuterated polymers of 4-methyl-1-pentene and their mass spectra were taken. Each spectrum is isotope

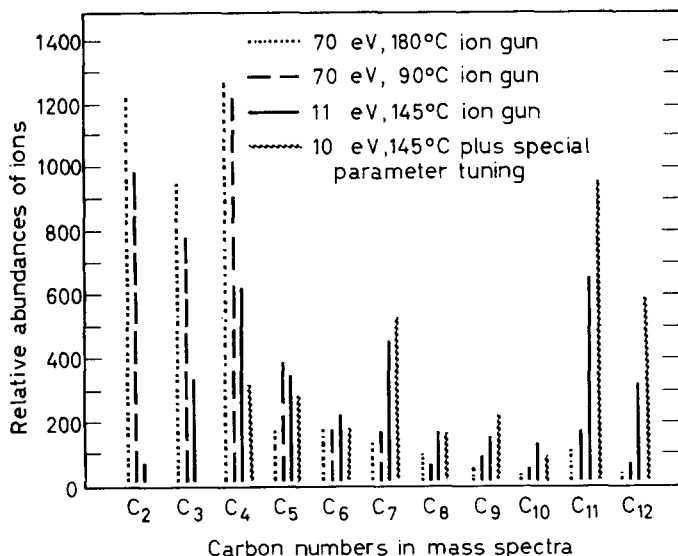


Figure 1—Special M.S. conditions facilitate recognition of polymer 'codes' [Ziegler-Natta poly-4-methyl-1-pentene]

corrected throughout the entire mass range to adjust for natural deuterium content and ^{13}C content. Each sample is adjusted to common sample size by summing all of the mass peaks at each carbon number.

Table 1. Mass spectral calculation—deuterated olefin distribution at carbon No. 15

1 <i>m/e</i>	2 <i>DP</i>	3 <i>m/e</i>	4 <i>NDP</i>	5 <i>Subtract</i>	6 <i>Residue</i>	7 <i>Subtract</i>	8 <i>Residue</i>
203	—	200					
204	—	201					
205	4.9	202	2.9	-1.7	3.2	-2.4	0.8
206	4.8	203	4.0	-2.3	2.5	-2.9	—
207	8.2	204	4.9	-2.8	5.4	-7.1	—
208	14.6	205	12.1	-6.9	7.7	-6.6	1.1
209	28.6	206	11.1	-6.4	22.2	-21.3	0.9
210	43.5	207	36.0	-20.6	22.9	-32.6	—
211	88.8	208	55.1	-31.6	57.2	-24.7	32.5
212	187	209	41.8	-23.9	163.1	-163.1	—
213	158	210	275.9	-158	—	—	0.0
214	53	211	145.8	—	0.0	—	—
215	9.2	212	6.5	—	—	—	—
216	3.2	213	7.6	—	—	—	—
	603.8		603.7				

Notes:

Col. 2 Abundances of deuterated product (DP).

.. 4 Abundances of non-deuterated product (NDP).

.. 5 Scale column 4 (the reference) so that m/e 210 = 158, and subtract from column 2.

.. 7 Scale column 4 so that m/e 210 = 163.1, and subtract from column 6.

Result: The terms 158, 163.1 and 32.5 are taken to represent the relative abundances of the deuterated olefins which contain, respectively 3, 2 and 1 deuterium atoms at carbon No. 15. Since there is no residual at m/e 210, there must be no C_{11} olefins present in the deuterated product which contain no deuterium atoms.

INTRAMOLECULAR HYDRIDE SHIFT POLYMERIZATION III

It is assumed that the mass spectral pattern at a given carbon number of the non-deuterated polymer will be essentially the same as the mass spectral pattern for each of the deuterated olefins in the deuterated sample, at the same carbon number. Since there is, on the average, one deuterium for eleven hydrogens, this assumption should be acceptable. It is also justified by the results.

The non-deuterated polymer can be used as a model to estimate the relative amounts of the deuterated olefins. By subtracting the non-deuterated ('reference') spectrum from the deuterated spectrum at corresponding carbon numbers, deuterated olefins can be successively subtracted from the mixture. Repetition of this process is carried out until the residual spectrum vanishes. In this way, the olefin mixture is 'sorted out'. A sample calculation for C_{15} olefins is shown in *Table 1*.

RESULTS

 (A) *Composition of gases obtained by vacuum pyrolysis*

This method has already been used successfully in our earlier structure studies of poly-3-methyl-1-butene^{3,4}. *Table 2* shows the composition of

Table 2. Major components of light gases from depolymerization of 4-methyl-1-pentene polymers

Component	I Ziegler-Natta	II Friedel-Crafts (-78°C)	III Friedel-Crafts (-130°C)
Per cent of charge	7.4%	6.5%	7.4%
Ethane	—	3.7 mole %	3.3 mole %
Ethylene	0.7 mole %	9.1	10.0
Propane	30.7	20.6	18.2
Propylene	2.4	8.7	8.9
Ratio of $C_3/C_3=$	13	2.4	2.0
Isobutane	6.2	3.4	3.9
<i>n</i> -Butane	0.3	3.8	3.6
Ratio of <i>i</i> -C ₄ / <i>n</i> -C ₄	20	0.9	1.1
1-Butene	0.1	2.1	2.0
Isobutylene	55.4	20.2	22.3
Isopentane	}	1.2	1.0
<i>tr</i> -2-Butene			
<i>cis</i> -2-Butene			
	1.0	11.6	11.6
1-Pentene	—	1.0	0.9
2-Me-1-butene	—	1.3	1.2
<i>tr</i> -2-Pentene	—	0.2	0.1
<i>cis</i> -2-Pentene	0.5	1.6	1.7
2-Me-2-butene	—	1.8	1.4
Neopentane	—	0.2	0.2
4-Me-1-pentene	1.7	3.1	3.1

gases obtained by vacuum pyrolysis⁴ of Ziegler-Natta type and cationic poly-4-methyl-1-pentene prepared at -78° and -130°C .

(B) *Principal i.r. features of gas oils from polymer pyrolysis*

With 3-methyl-1-butene polymers⁴, it has been possible to correlate, in part, the types of olefins formed on pyrolysis with the mechanisms of polymerization. This technique was also applicable to poly-4-methyl-1-pentene. Table 3 gives the absorbance values for the dominant olefin types found in various poly-4-methyl-1-pentene samples on vacuum pyrolysis.

Table 3. Principal olefin types in gas oils from depolymerization of 4-methyl-1-pentene polymers

Olefin types	Absorbance values			Ratio $\frac{\text{CH}_2=\text{CH}-}{\text{CH}_2=\text{C}}$
	$\text{CH}=\text{CH}$	$\text{CH}_2=\text{CH}$	$\text{CH}_2=\text{C}$	
Band location, cm^{-1}	963	906	884	
Cationic poly-4-methyl-1-pentene	0.393	1.11	0.506	2.18
Cationic poly-4-methyl-1-pentene-4d ₁	0.235	1.14	0.601	1.91
Ziegler-Natta poly-4-methyl-1-pentene	0.183	Not found	0.77	

The other essential features of the i.r. spectra of the gas oils from these polymers are:

- (1) The CD stretch peak at 2136 cm^{-1} in the deuterated product is absent in the non-deuterated sample.
- (2) The band at 733 cm^{-1} and a shoulder at 750 cm^{-1} is present in the non-deuterated product. These bands are considered due to three and two consecutive methylene groups, respectively. In the deuterated product, these peaks are essentially absent.
- (3) In the deuterated product, no peaks are found at low wave numbers which could correspond to the presence of deuterium atoms on the olefin sites.

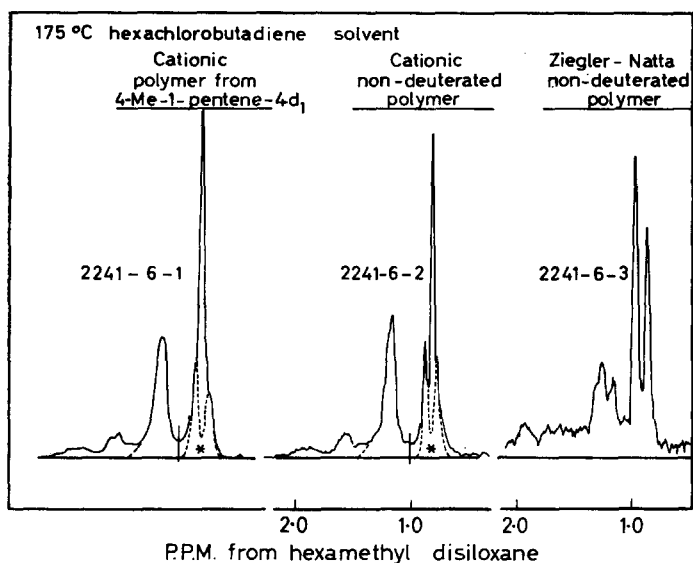
(C) *The n.m.r. spectra of gas oils*

Figure 2 presents the n.m.r. spectra of the gas oil fractions of the deuterated and non-deuterated cationic products and of the Ziegler-Natta product. By area measurement we find that ratios of $\beta\text{CH}_3/\beta\text{CH}_2$ hydrogen atoms are as follows:

	$\frac{\beta\text{CH}_3}{\beta\text{CH}_2}$
Cationic poly-4-methyl-1-pentene	1.27
Cationic poly-4-methyl-1-pentene-4d ₁	1.57
Ziegler-Natta poly-4-methyl-1-pentene	1.95

The two shoulders on the cationic βCH_3 peaks are considered to be due to polymer types which contain isopropyl groups, i.e. due to either or both the 1,2 and the 1,3 polymers. Using the βCH_3 peaks of the Ziegler-Natta

polymer as a model, we can scale the 'isopropyl' peak to match the shoulders in the n.m.r. spectra of the two cationic products. Thus, by subtracting the



* Dashed areas are scaled, using the Ziegler-Natta spectrum as a reference

Figure 2—60 Mc/s n.m.r. spectra of gas oils from vacuum pyrolysis of polymers of 4-methyl-1-pentene

scaled isopropyl peaks from the spectra of the cationic products, the contribution of the 1,4-structure can be obtained. This leads to the following estimate of product type ratios:

	$\frac{[1,4]}{([1,2] + [1,3]) + [1,4]}$
Cationic poly-4-methyl-1-pentene	0.53
Cationic poly-4-methyl-1-pentene-4d ₁	0.66

In principle, the same results should be obtained from $\beta\text{CH}_3/\beta\text{CH}_2$ ratios. To arrive at realistic theoretical ratios of $\beta\text{CH}_3/\beta\text{CH}_2$ n.m.r. areas, the molecular weight distribution of the wide-cut olefin samples must be considered.

Few mass spectral sensitivity data are available for calculation of molecular weight distributions of such wide-cut samples of iso-olefins. However, by assuming that the specific sensitivity of a given olefin is three per cent less than that of a similar olefin which is 14 mass units lighter, one can calculate a first approximation olefin distribution using the 10 eV mass spectra. This olefin distribution is shown for non-deuterated cationic poly-4-methyl-1-pentene in *Table 4*.

Table 4. First approximation molecular weight distribution, C₈ to C₃₀ gas oil from vacuum pyrolysis of poly-4-methyl-1-pentene

Olefins	%	Olefins	%	Olefins	%	Olefins	%
C ₈	8.0	C ₁₃	4.7	C ₁₉	1.6	C ₂₅	0.96
C ₉	18.9	C ₁₄	4.0	C ₂₀	1.5	C ₂₆	0.97
C ₁₀	16.7	C ₁₅	6.9	C ₂₁	2.7	C ₂₇	1.15
C ₁₁	7.7	C ₁₆	4.9	C ₂₂	1.9	C ₂₈	1.1
C ₁₂	6.4	C ₁₇	3.0	C ₂₃	1.2	C ₂₉	0.75
		C ₁₈	2.8	C ₂₄	1.3	C ₃₀	0.78
							99.91

The $\beta\text{CH}_3/\beta\text{CH}_2$ ratios for all olefins from C₈ to C₃₀ which would be expected for each polymerization mechanism are calculated. These values are then weighted according to the molecular weight distribution of Table 4. These calculations give the following results:

	Theoretical n.m.r. $\beta\text{CH}_3/\beta\text{CH}_2$ area ratios for olefin distribution shown in Table 4
1,2 mechanism	2.505
1,3 mechanism	2.505
1,4 mechanism	1.129

Using these values and the experimental area ratios shown above, the same product type ratio can be calculated:

	$\frac{[1,4]}{([1,2] + [1,3]) + [1,4]}$
Cationic 4-methyl-1-pentene	0.32*
Cationic 4-methyl-1-pentene-4d ₁	0.60

(D) Mass spectra of gas oils from pyrolysis

The relative abundances of the series obtained from the cationic non-deuterated product are plotted in Figure 3 (solid line). The corresponding distribution of C_nH_{2n} ions from the Ziegler-Natta product is plotted in Figure 4. Table 5 shows the distribution of deuterated olefins at each carbon number for the cationic deuterated product (for calculation see Experimental part). The sums of the various deuterated olefin ion abundances at each carbon number are plotted in Figure 3 (broken line). For all three mass spectra (Figures 3 and 4), the sums of the ion abundances are the same.

Another way of expressing the data is to record the relative olefin ion abundances as a percentage of all of the ions at each cycle of 14 mass units. This is shown in Table 5.

The sums of these percentages representing all of the various deuterated olefins at each carbon number are plotted in Figure 5.

*The 0.32 value disagrees with i.r. and M.S. data, as well as with n.m.r. data by the subtraction method. No explanation can be offered for this discrepancy at present.

INTRAMOLECULAR HYDRIDE SHIFT POLYMERIZATION III

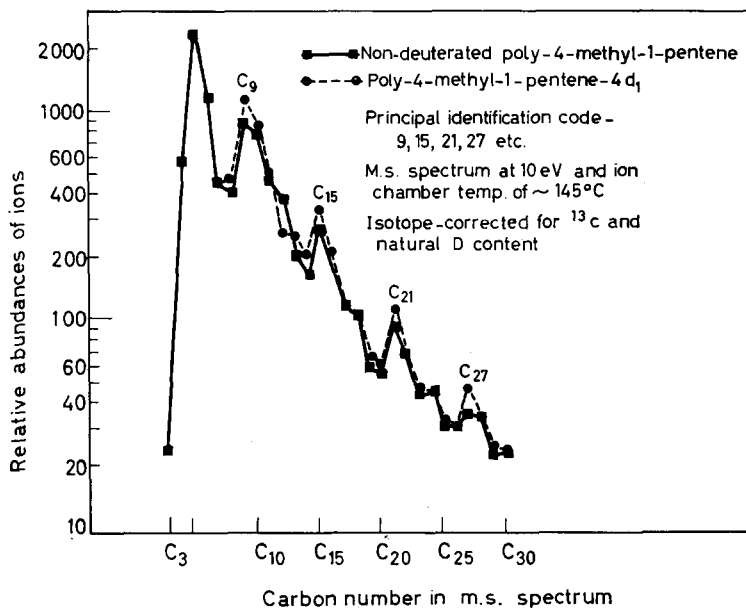


Figure 3—Olefin distribution in oils from vacuum depolymerization of cationic poly-4-methyl-1-pentene

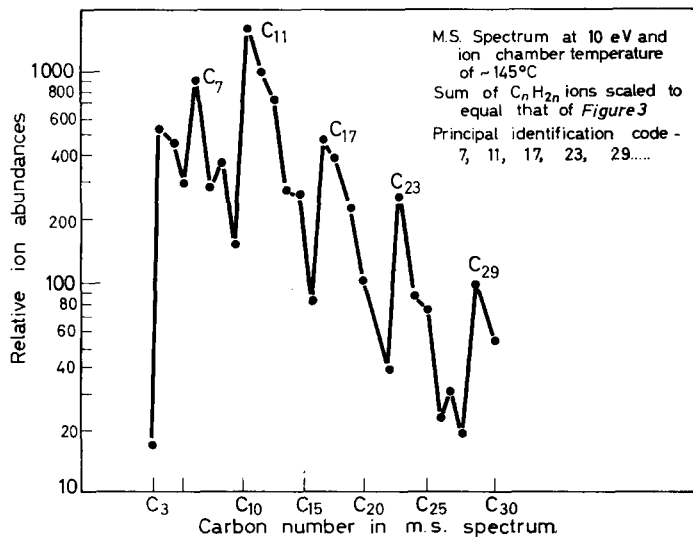


Figure 4—Olefin distribution in oils from vacuum depolymerization of Ziegler-Natta poly-4-methyl-1-pentene

Table 5. Distribution of deuterio-olefins in dimers, trimers, tetramers, pentamers (Gas o from vacuum depolymerization of poly-4-methyl-1-pentene-1-4d₁)

Carbon No.	D ₅ =	D ₄ =	D ₃ =	D ₂ =	D ₁ =	D ₀ =	Ratios			
							D ₅ /D ₄ =	D ₄ /D ₃ =	D ₃ /D ₂ =	D ₂ /D ₁ =
C ₃₀	23.5%	15.3%					1.54			
29	20.6	20.0	1.0				1.03			
28	23.5	23.4					1.00			
27	21.8	31.4	5.6				0.69			
26	17.0	20.8	1.4				0.82			
25	13.3	20.8	5.5				0.64			
24		24.4	14.9					1.64		
23		25.8	16.6					1.55		
22		25.8	21.4	0.91				1.20		
21		17.6	34.5	5.7				0.51		
20		19.5	19.6	2.7				1.00		
19		16.6	20.8	6.0				0.80		
18			32.1	11.0					2.79	
17			29.9	16.0					1.87	
16			30.4	21.6	0.1				1.41	
15			26.2	27.1	5.4				0.97	
14			23.4	17.5	3.4				1.34	
13			21.4	18.6	2.9				1.15	
12				28.0	7.7					3.64
11				26.0	9.9					2.62
10				27.6	11.8	0.3				2.34
9				27.2	8.4	3.5				3.24
8				18.9						
7				17.4						
6					28.9					
5					39.4					
4					52.5					
3					57.4					

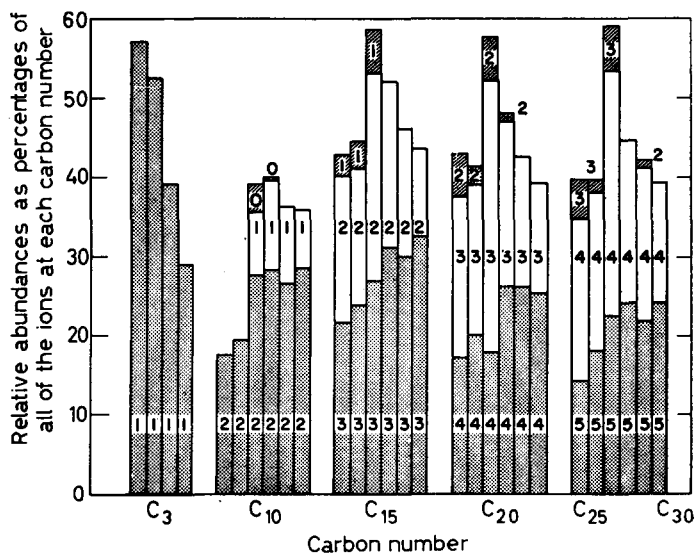


Figure 5—Distribution of deuterio-olefins

INTRAMOLECULAR HYDRIDE SHIFT POLYMERIZATION III

The ratios of deuterated olefins at each carbon number are recorded in Table 5 and plotted in Figure 6.

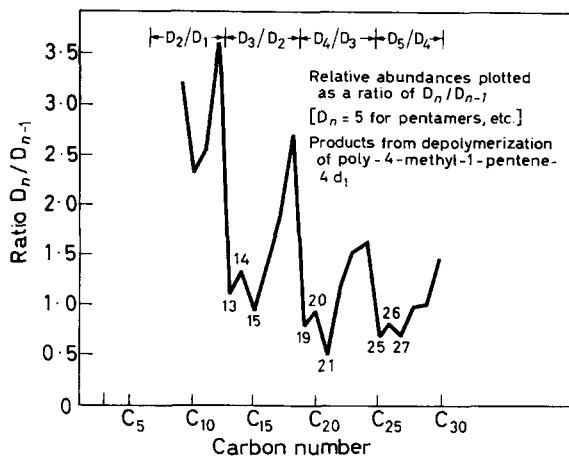


Figure 6—First approximation distribution of deuterio-olefins

From the mass spectral data, an estimation of the proportions of the three types of polymers is made and recorded in Table 6. For the non-deuterated cationic sample, this is done by measuring the relative ion abundances at twelve selected locations in the spectrum. The justification for this is given in the Discussion.

Table 6. Estimation of polymer composition from mass spectra of gas-oil depolymerizates

(A) Gas oils from poly-4-methyl-1-pentene

—1,2 polymer—		—1,3 polymer—		—1,4 polymer—	
C No.	Relative* abundance	C No.	Relative* abundance	C No.	Relative* abundance
29	24.5%	28	36.5%	27	39.0%
23	20.5	22	32.6	21	46.9
17	19.5	16	33.1	15	47.4
11	21.3	10	36.3	9	42.4
Ave.	21.5%		34.6%		43.9%

(B) Gas oil from poly-4-methyl-1-pentene-4d₁

29	23.1%	28	32.4%	27	44.4%
23	20.0	22	29.5	21	50.6
17	17.0	16	31.5	15	51.5
11	19.4	10	34.4	9	46.2
Ave.	19.9%		32.0%		48.2%

*No adequate sensitivity data are available for the various olefin types, and no approximations were applied.

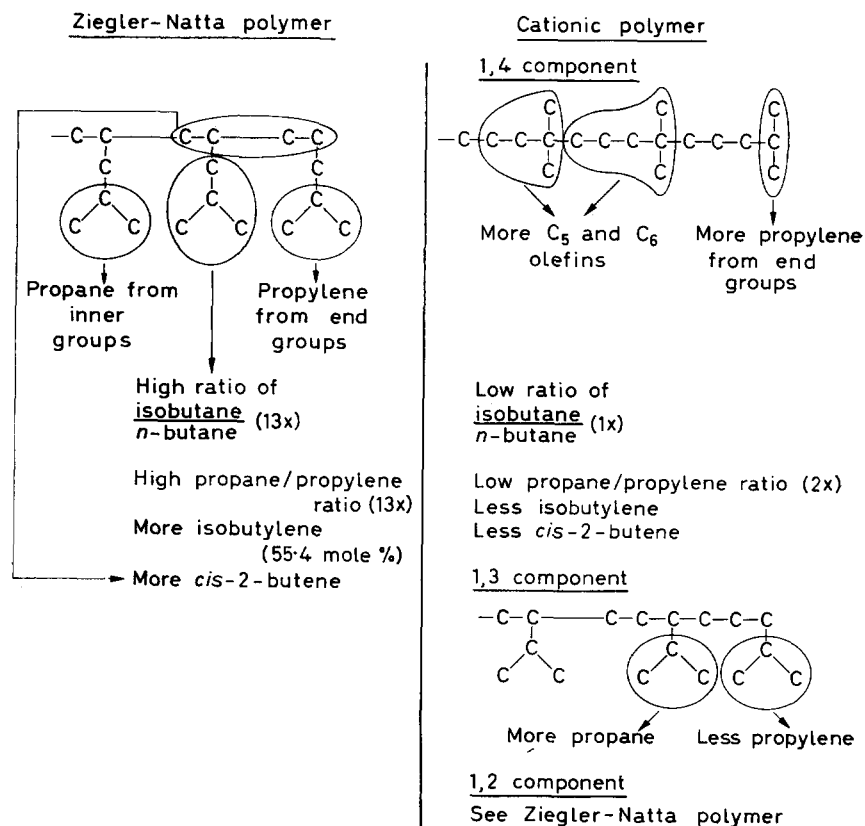
The procedure is the same for the cationic, deuterated product, except that the sums of the various deuterated olefins at the same selected locations are used.

DISCUSSION

(A) *Composition of gases from vacuum pyrolysis*

The quantitative analysis of gas compositions from vacuum pyrolysis of cationic 3-methyl-1-butene polymers showed that the products contained about 27 mole per cent maximum of 1,2 polymer and the balance (73 mole per cent) 1,3 polymer⁴. Similar studies with cationic 4-methyl-1-pentene polymers show that the polymers are more complex. No more than 62 mole per cent of the product is formed by the 1,4 process. The balance is 1,3 and 1,2 polymers in decreasing amounts. No quantitative estimates on these amounts will be placed by this method, because of lack of suitable reference polymers.

The gas composition of Table 2 can be explained at least qualitatively by the following cleavage patterns:



(B) *Infra-red and n.m.r. spectra of pyrolysates (gas oils)*

In a previous publication⁴, we showed that vacuum pyrolysis of various poly-3-methyl-1-butene samples produced characteristic olefin types which could be analysed by i.r. spectroscopy and correlated with polymerization mechanism. This technique was used in this work to characterize pyrolysates of Ziegler-Natta and cationic poly-4-methyl-1-pentene. The summary of our i.r. analyses of pyrolysates of these polymers is shown in *Table 7*.

Table 7. Correlation of polymerization mechanism and olefin types in pyrolysates

<i>Ziegler-Natta</i>	<i>Cationic</i>
Poly-3-methyl-1-butene ⁴	
Mechanism: 1,2 process	Mechanism: largely 1,3 process
Pyrolysis yields: CH ₂ =C< and —CH=CH—	Pyrolysis yields: mostly CH ₂ =CH—
Poly-4-methyl-1-pentene	
Mechanism: 1,2 process	Mechanism: largely 1,4 process
Pyrolysis yields: CH ₂ =C< and —CH=CH—	Pyrolysis yields: mostly CH ₂ =CH—; the concurrent 1,3 and 1,2 processes yield on pyrolysis CH ₂ =CH— and —CH=CH—

The formation of the various types of unsaturations characterized by i.r. techniques can be explained by simple β -scissions as shown with the set of equations in *Table 8*.

Consequently, the relative amounts of these olefin types in the pyrolysates can be used to estimate the propagation types in cationic poly-4-methyl-1-pentene by the following relationship:

$$\frac{[\text{CH}_2=\text{CH—}]}{[\text{CH}_2=\text{C}<]} \sim \frac{[1,4] + [1,3]}{[1,2]}$$

From *Table 3*, this ratio is 1.9 to 2.2, average 2.05, which gives

$$\begin{aligned} [1,2] \text{ structure} &= 33 \text{ per cent} \\ [1,4] + [1,3] \text{ structure} &= 67 \text{ per cent} \end{aligned}$$

(No sensitivity data are applied. Above estimates are based on equal sensitivities for both olefin types.)

In addition, the band at 733 cm⁻¹ and the shoulder at 750 cm⁻¹ in the non-deuterated cationic product indicate three and two consecutive methylene groups. These suggest the presence of 1,4 and 1,3 structures.

The 1,4 structure is demanded by the n.m.r. findings. The results taken at 60 Mc/s, and at 175° to 200°C, using hexachlorobutadiene solvent, are more completely resolved than earlier spectra. By means of the subtraction method (above), the following n.m.r. ratio is obtained.

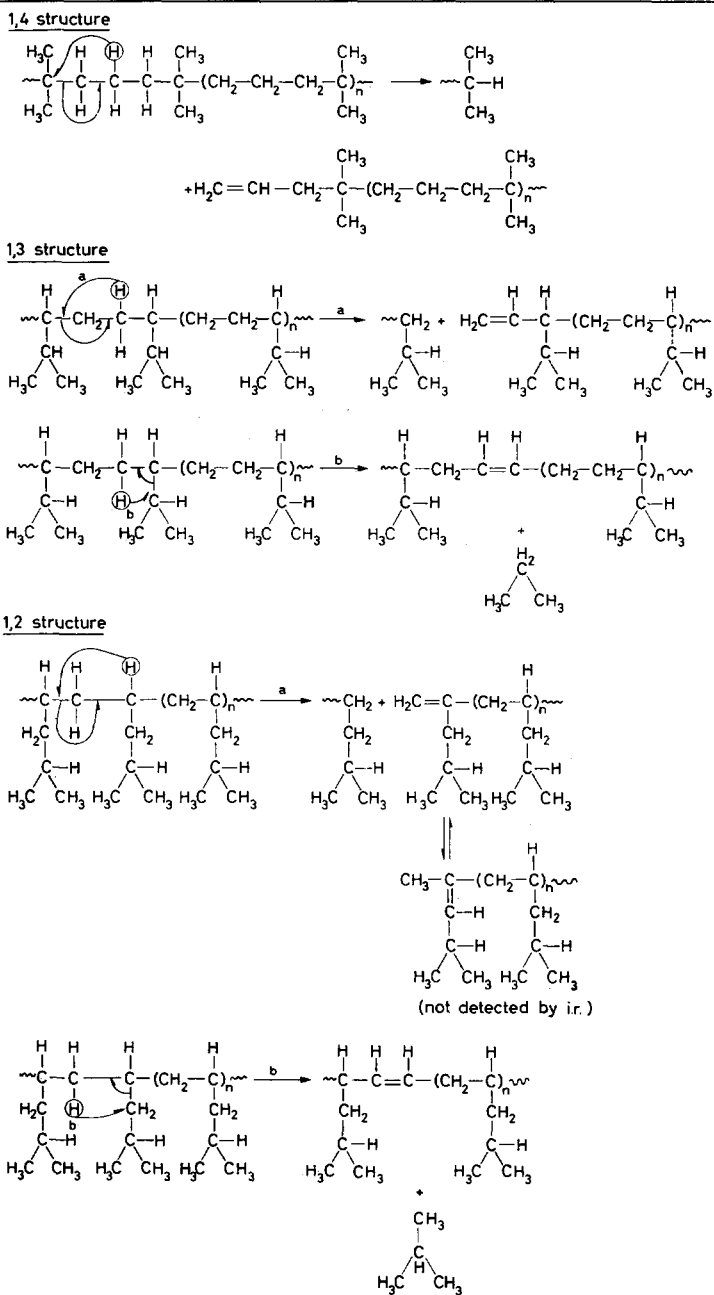
$$\frac{[1,4]}{([1,2] + [1,3]) + [1,4]} = 0.53 \text{ to } 0.60, \text{ average } 0.60$$

This result taken together with the above i.r. results would lead to the

following approximate polymer composition:

[1,4] structure 60, [1,3] structure 7, [1,2] structure 33 per cent.

Table 8. Characteristic olefin types obtained on vacuum pyrolysis of poly-4-methyl-1-pentene



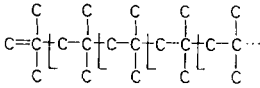
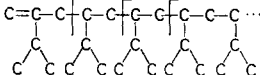
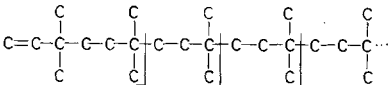
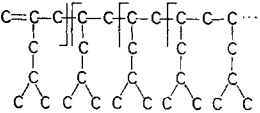
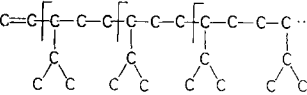
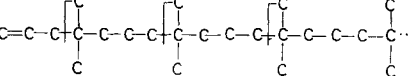
INTRAMOLECULAR HYDRIDE SHIFT POLYMERIZATION III

(C) *Mass spectra of gas oils from pyrolysis of cationic and Ziegler-Natta polymers*

(1) *The analysis of mass spectra of polymers of 4-methyl-1-pentene*—It has been demonstrated⁴ that mass spectral cracking patterns of polymers are characteristic, and can be used for empirical identifications of structures. Briefly, it was found that within cracking patterns of wide-boiling olefin mixtures from vacuum pyrolysis, certain predictable 'dominances' occur. These dominances or 'codes' were correlated successfully with proposed polymer structures, which in turn could reflect polymerization mechanisms⁴.

In a few cases studied, we have been able to predict a numerical code of selected polymer structures. Examples of structures and codes for six cases are listed in *Table 9*. The code sequences are obtained by operating from each end of a chain. This produces two sequences in each case, although in practice one sequence may prove to be dominant, and if so it is marked ('D'). Thus, the principal code of the mass spectrum of polyisobutylene pyrolysate (gas oil) is the expected 4,8,12,16-sequence. The relatively simple

Table 9. Polymer structures and mass spectral codes

<u>(a) Isobutylene</u>	M.S. code sequence
	<p>(a) 5, 9, 14, 19, 23....</p> <p>(b) 4, 8, 12, 16, 20.... ('D')</p>
<p><u>(b) 3-methyl-1-butene polymers</u></p> <p><u>1,2 structure</u></p> 	<p>9, 14, 19, 24, 29....</p>
<p><u>1,3 structure</u></p> 	<p>(a) 10, 15, 20, 25, 30.... ('D')</p> <p>(b) 8, 13, 18, 23, 28....</p>
<p><u>(c) 4-methyl-1-pentene polymers</u></p> <p><u>1,2 structure</u></p> 	<p>(a) 7, 13, 19, 25, 31....</p> <p>(b) 11, 17, 23, 29, 35.... ('D')</p>
<p><u>1,3 structure</u></p> 	<p>(a) 8, 14, 20, 26, 32....</p> <p>(b) 10, 16, 22, 28, 34.... ('D')</p>
<p><u>1,4 structure</u></p> 	<p>(a) 9, 15, 21, 27, 33....</p> <p>(b) 9, 15, 21, 27, 33....</p>

case of 3-methyl-1-butene polymers has been explained satisfactorily^{3,4}.

The application of these codes is of special interest with poly-4-methyl-1-pentene because there is no authentic model for the 1,3 polymer, and because n.m.r. data cannot distinguish between 1,2 and 1,3 structures.

The structure of dimers, trimers, tetramers and pentamers obtained by vacuum pyrolysis of unlabelled and deuterated poly-4-methyl-1-pentene have been investigated. These products are contained in the wide-cut gas oils (pyrolysates) which contained also small amounts of olefins beyond C₃₂.

Figure 3, solid line, shows the relative abundances of the olefin peaks for the cationic polymer and Figure 4 shows the same for the Ziegler-Natta polymer. For the deuterated cationic polymer (Figure 3, broken line) the sum of the various deuterated olefins is plotted at each carbon number.

The codes observed experimentally together with the corresponding mechanisms are shown in Table 10.

Table 10. Estimated composition of various poly-4-methyl-1-pentenenes, from codes

Type of poly-4-methyl-1-pentene	Experimental M.S. codes (Figs. 3, 4)	Expected mechanism (Table 9)	Estimated composition* (from Table 6)
Ziegler-Natta	7,11,17,23,29 . . .	1,2	100%
Cationic (non-deuterated)	9,15,21,27 . . .	1,4	43-48
	10,16,22,28 . . .	1,3	32-35
	7,11,17,23,29 . . .	1,2	20-21.5

*No calibration data applied.

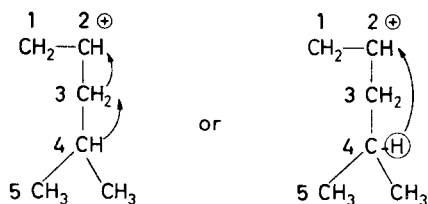
Table 11 is a compilation of our analytical results. It shows the percentage composition of various contributing structures in cationic poly-4-methyl-1-pentene estimated from (a) quantitative gas chromatography of gaseous fragments, (b) quantitative i.r. and n.m.r. spectroscopy of liquid pyrolysates, and (c) from characteristic mass spectroscopic codes (dominances). In view of the complicated techniques and extensive calculations employed, the reasonable agreement between i.r. and n.m.r. results and mass spectroscopic data is indeed gratifying.

Table 11. Composition of cationic 4-methyl-1-pentene polymers by various methods

Method	1,2	1,3	1,4	Remarks
(a) Composition of pyrolytic gases	Present	May be present	62% max.	Qualitative at present due to lack of calibrations
(b) Combination of i.r. and n.m.r. (subtraction technique)	33%	7%	60%	Based on assumption that olefin sensitivities are equal
(c) Application of characteristic 'codes' to M.S. olefin distributions	20-22%	32-35%	43-48%	No calibrations applied

(2) *Analysis of the deuterated mass spectrum and location of the deuterium atoms in the polymer*—According to our findings, an important portion of the cationic polymerization of 4-methyl-1-pentene leads to 1,4

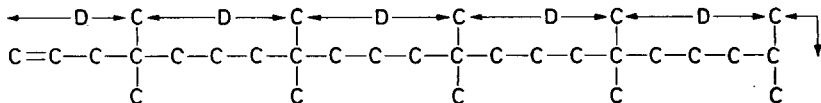
polymer and most likely proceeds by intramolecular hydride migration. The question then arises whether hydride involves a hydride jump or two consecutive hydride shifts, i.e.



The presence of 1,3 polymer in the cationic product which most likely was formed by 1,3 propagation in turn suggests a multiple hydride shift mechanism for the 1,4 polymer. No 1,3 polymer could form if propagation were to proceed by hydride jumps from C_4 to C_2 . A detailed study of the mass spectrum of the deuterated poly-4-methyl-1-pentene provides further and more conclusive evidence for the multiple hydride shift mechanism.

The following experimental facts and arguments corroborate this proposition:

- (a) The calculated distributions (above) and the results (*Figure 5*) show that the distribution of deuterium is not uniform along the polymer backbone.
- (b) The deuterium distributions are cyclical.
- (c) The total percentage deuterium contents (*Figure 5*) are maximum at carbon 9,15,21,27. The second most abundant maxima are found at carbon to 10,16,22,28, and the third at 7,11,17,23,29. These findings can be related to the mechanism-composition estimates given in *Table 11*.
- (d) These results can be explained readily by assuming random scissions next to branches¹². In particular, they indicate that the methyl groups contain few if any deuterium atoms. As an example consider the elimination of a three-carbon fragment from a given C_{30} olefin. On the average, there will be one D atom for each six carbon atoms:



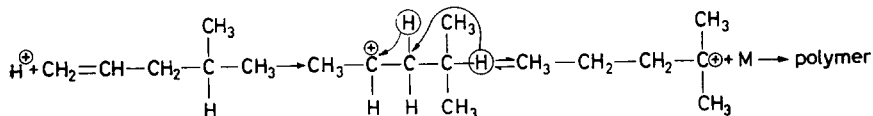
(Note that the end group is similar for 1,2 and 1,3 as well as 1,4 structures.)

- (e) The data of *Table 5* and *Figure 5* are replotted as ratios in *Figure 6*. The ratio of olefins containing 5 and 4 deuterium atoms drop sharply from C_{30} to C_{29} olefin. This indicates that the D atom is still on the end tertiary carbon and that CH_3D is eliminated predominantly. Loss

of another carbon changes the ratio little, but the effect is substantial on going to a 27-carbon fragment. Over this range, the relative D_5 and D_4 olefin ratios have changed sharply (see *Table 5*). Since formation of a C_{27} olefin by loss of C_3H_6 fragment increases the total deuterium content (*Figure 5*), it is evident that most of the deuterium is not on the methyl groups. This is consistent with the i.r. and n.m.r. results. The situation will be the same if a C_{27} olefin is formed by loss of C_3H_6 from a C_{30} olefin or by random scission of a long chain at the branch point.

- (f) The total deuterium content is substantially larger at C_{27} than it is at C_{26} and C_{25} , the two other methylene groups. The same sequence is observed at C_{21} , C_{20} , C_{19} , and C_{15} , C_{14} , C_{13} . Since random scission is considered to be the predominant pyrolysis mechanism in this case, this cannot be just an end-group effect. This shows that isomerization of D atoms about the methylene groups has not randomized the distribution and that there is more deuterium on carbon C_{27} than on C_{26} , and so on for the successive sequences. These results indicate that the 1,4 mechanism is in reality a succession of single hydride shifts. If it were otherwise, the ratios of D content at C_{26}/C_{27} , C_{20}/C_{21} , C_{14}/C_{15} would be expected to be higher than what they are found to be.

The sum of these considerations substantiates the theory that the 1,4 polymer component of cationic poly-4-methyl-1-pentene was formed by successive hydride shift propagation:



CONCLUSIONS

The cationic polymerization of 4-methyl-1-pentene can be best understood by considering relative carbonium ion stabilities. Polymerization initiation (most likely protonation by adventitious co-catalysts in conjunction with aluminium chloride) leads to the formation of a relatively unstable

secondary carbonium ion $-\text{CH}_2-\overset{\oplus}{\text{C}}\text{H}-\text{isoBu}$ (I) which then rearranges to

the slightly more stable secondary carbonium ion $-\text{CH}_2-\text{CH}_2-\overset{\oplus}{\text{C}}\text{H}-\text{isoPr}$ (II). The carbonium ion stabilizing effect of the isopropyl group is believed to be higher than that of the isobutyl group. Finally, cation II rearranges

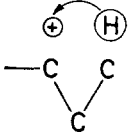
to the considerably more stable tertiary ion $-\text{CH}_2-\text{CH}_2-\text{CH}_2-\overset{\oplus}{\text{C}}(\text{CH}_3)-\text{CH}_3$

(III) which is the most important propagating species.

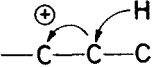
The overall polymerization (propagation) mechanism can be regarded as a competition between a number of possibilities. Thus, the initially formed secondary cation I could be consumed by conventional propagation

leading to 1,2 structure or by single hydride shift giving cation II. The latter then can either propagate to 1,3 structure or it can rearrange by another single hydride shift and give cation III. Cation III, the major propagating species, attacks an incoming monomer and gives cation I so that the cycle can start again.

Finally, at least theoretically, the possibility exists that cation I might be

consumed by a  hydride jump. However, in the light of our

experiments with deuterated poly-4-methyl-1-pentene this hydride jump step is rather unlikely, and the 1,4 structure is most likely formed by two

consecutive hydride shifts: . The situation is summarized in

the diagram shown at the outset. The unlikely hydride jump route is indicated by the dotted arrow.

It is not surprising to find that the dominating repeat unit of cationic poly-4-methyl-1-pentene is the 1,4 structure. Previously, we have shown¹ that practically pure, crystalline poly- α,α' -dimethyl propane, i.e. isomerized poly-3-methyl-1-butene, can readily be obtained even at -130°C , indicating that the rate determining step cannot be the hydride shift. Apparently, the activation energy of hydride shifts is very low, and this step proceeds rapidly even at very low temperatures. Therefore, it is rather interesting to find conclusive evidence for the occurrence of 1,2 and 1,3 structures which must have been formed without a hydride shift or with a single hydride shift, respectively. Apparently, at -78°C conventional (i.e. 1,2) propagation by cation I and propagation involving cation II are fast enough to compete with multiple hydride shifts and 1,2 and 1,3 structures appear. Attempts were made to obtain polymers at lower temperatures (-100° to -150°C) and to 'freeze out' these competing steps. However, the molecular weights of these products were much lower than the polymer synthesized at -78°C and they were not investigated further.

It is also interesting to note that cation III is able to propagate at all since this species is more stable than the secondary cation I which is formed upon initial attack. Apparently, however, the new C—C bond which is created provides sufficient driving force to compensate the difference between carbonium ion stabilities.

The authors are grateful to Dr J. J. Elliott for discussions of infra-red spectra and to Mr R. M. Thomas for discussions on polymerization theory.

*Esso Research and Engineering Co.,
Linden, N.J., U.S.A.*

(Received May 1964)

REFERENCES

- ¹ KENNEDY, J. P. and THOMAS, R. M. *Makromol. Chem.* 1962, **53**, 28
- ² EDWARDS, W. R. and CHAMBERLAIN, N. F. *J. Polym. Sci. Part A*, 1963, **1**, 2299-2308
- ³ KENNEDY, J. P., MINCKLER, Jr, L. S., WANLESS, G. G. and THOMAS, R. M. *J. Polym. Sci. Part C*, 1963, No. 4, 289-296
- ⁴ KENNEDY, J. P. and MINCKLER, Jr, L. S., WANLESS, G. G. and THOMAS, R. M. *J. Polym. Sci.* In press
- ⁵ KENNEDY, J. P., MINCKLER, Jr, L. S., WANLESS, G. G. and THOMAS, R. M. *J. Polym. Sci.* In press
- ⁶ KENNEDY, J. P. and THOMAS, R. M. *Makromol. Chem.* 1963, **64**, 1
- ⁷ KETLEY, A. D. *Polymer Letters*, 1963, **1**, 313
- ⁸ KENNEDY, J. P., MINCKLER, Jr, L. S. and THOMAS, R. M. *J. Polym. Sci. Part A*, 1964, **2**, 367
- ⁹ KENNEDY, J. P. *J. Polym. Sci. Part A*, 1964, **2**, 381
- ¹⁰ WANLESS, G. G. *J. Polym. Sci.* 1962, **62**, 263-279 and references given therein
- ¹¹ WANLESS, G. G. and GLOCK, Jr, G. A. *A.S.T.M. E-14*. Tenth Annual Mass Spectrometry Conference, 3-8 June 1962, pp 269-278. New Orleans, La
- ¹² SIMHA, R. and WALL, L. A. 'The mechanism of polymer formation and decomposition' in P. H. EMMETT (Ed.), *Catalysis*, Vol. VI, p 303. Reinhold: New York, 1958

APPENDIX

In this paper we are trying to do two things:

(I) *Assay the relative amounts of 1,2; 1,3 and 1,4 structures in cationic poly-4-methyl-1-pentene.*

This can be done fairly well. In this connection *Table 9* will clarify *Figure 5*. Note that:

- (1) C_{29} and C_{25} come *essentially* from 1,2 polymers.
- (2) C_{28} and C_{26} come *essentially* from 1,3 polymers.
- (3) C_{27} fragments come *essentially* from 1,4 polymers.

(II) *Determine the mechanism of the 1,3 hydride shift:*

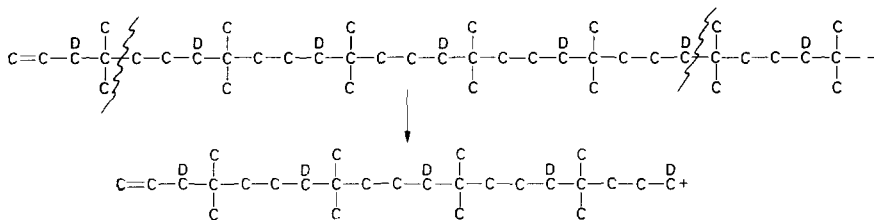
- (i) *Table 12* shows that *only* this (1,4) mechanism requires any shift of D atoms.
- (ii) The most probable D content for C_{27} fragments should be 4 and not 5, if the C_{27} fragments are formed by breaking a piece from either end of a chain. But our calculations (*Table 5* and *Figure 6*) show that the D_5/D_4 ratio is quite substantial for C_{25} to C_{27} fragments, i.e. 0.6 to 0.8. This proves, we believe, that many of the C_{27} fragments (and also

INTRAMOLECULAR HYDRIDE SHIFT POLYMERIZATION III

Table 12. Produce structures resulting from one 'sequence', i.e. C₃₀ to C₃₅ in cationic poly-4-methyl-1-pentene-4d₁

		<i>Most probable number of D atoms</i>
C29		5
C28		5
(1,2) (1,3) (1,4)	C27 (1,4)	4
	or	4
C26		4
C25		4

C₂₆, C₂₅, . . .) must be sliced out of longer chains by double scissions, i.e.



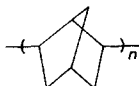
Representation of C₂₇ fragment with 5 D atoms—resulting from one 1,2 shift of D atoms

(iii) To obtain C₂₆ and C₂₅ fragments with 5 D atoms is harder to explain even on the basis of the 1,2 shift mechanism, but it is impossible to explain on the basis of the 1,3 shift mechanism. Thus, if 1,3 shifts occurred, there is no way in which one could obtain a C₂₅ fragment with 5 D atoms, and the D₅/D₄ ratio should then become zero:

Cationic Transannular Polymerization of Norbornadiene

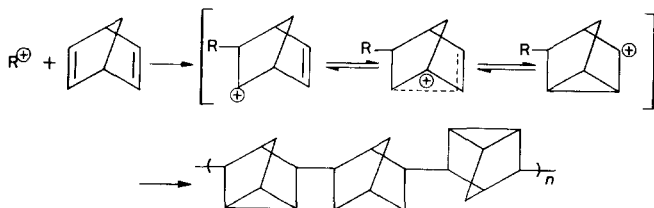
J. P. KENNEDY and J. A. HINLICKY

The cationic polymerization of norbornadiene [bicyclo-(2,2,1)-heptadiene-2,5] has been investigated. Polymerizations using aluminium chloride catalyst in ethyl chloride and methylene chloride solvent were carried out at -123 , -78 , 0 and $+40^{\circ}\text{C}$. Only the product synthesized at -123°C was completely soluble, the rest contained considerable amounts of crosslinked material. The structure of the soluble product was determined by infra-red and n.m.r. spectroscopy. The repeat unit of the polymer is a 2,6-disubstituted nortricyclene unit

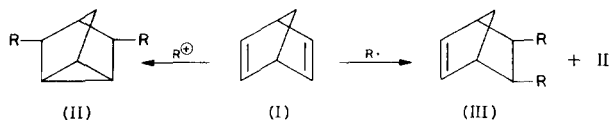


The polymerization apparently proceeds by an intramolecular transannular reaction between carbon atoms 3 and 5

IN THE course of our studies on cationic isomerization polymerization, we proposed the following reaction mechanism for the carbonium ion polymerization of norbornadiene [bicyclo-(2,2,1)-hepta-2,5-diene]:



This conclusion was derived chiefly from the study of small molecule chemistry of norbornadiene under carbonium ion attack. Thus Winstein and Shatavsky¹ and Schmerling *et al.*² showed that norbornadiene (I) gives almost exclusively nortricyclenes (II) under cationic conditions, whereas the reaction is less specific and tends to give chiefly mixtures of 2,6-nortricyclenes and 3,4-bicycloheptenes (III) under free radical conditions:



Also, we theorized that norbornadiene is closely related to butadiene and therefore would polymerize under cationic conditions to a predominantly '1,4-structure', e.g. to give a product consisting of polynortricyclene repeat units. Although the interatomic distance between the 3-5 and/or 2-6 carbons of norbornadiene was calculated to be about 1.6 times larger than that between the 2-3 carbons of butadiene³, there was likelihood for some measure of transannular conjugation in norbornadiene too. Our ultra-violet (u.v.) and infra-red (i.r.) spectroscopic studies corroborated this expectation.

Butadiene polymerizes readily with cationic initiators to give a predominantly 1,4-structure⁴. Thus we expected that cationic polymerization of norbornadiene will proceed by a transannular reaction and give predominantly poly-2,6-nortricyclene, as shown above.

Indeed, results of our low temperature polymerization of norbornadiene with aluminium chloride catalyst in ethyl chloride diluent seem to corroborate this expectation.

The polymerization of norbornadiene with aluminium chloride in hydrocarbon solvent at ambient temperature did not yield polymer⁵.

Polymerizations of norbornadiene with Ziegler-type catalysts have been reported, but the structure of the products was not investigated in detail⁶. It seems to be reasonable to expect a similar enchainment, particularly with acidic Ziegler-type catalyst. In a recent publication, Zutty⁷ investigated the free radical polymerization of this diene and the structure of the polymer. It was concluded that the product consisted largely of polynortricyclene repeat units. Graham *et al.*⁸ who polymerized 2-carbethoxy-norbornadiene came to similar conclusions.

Apparently just about the same time Zutty proposed the probable polymerization mechanism of norbornadiene with free radical initiators, we independently postulated a substantially identical reaction mechanism and polymer structure obtainable with cationoid initiators.

EXPERIMENTAL

Norbornadiene [bicyclo(2,2,1)-hepta-2,5-diene] monomer (Matheson Coleman and Bell) was distilled before use. Gas chromatographic analysis indicated better than 98 per cent purity, and the presence of four or five minor impurities.

Polymerizations were carried out in a dry box⁹ in stirred glass reactors. For the experiment at -123°C , 10.14 g norbornadiene was diluted with 65 ml ethyl chloride. This mixture is homogeneous and remains liquid even at this low temperature. The catalyst was aluminium chloride dissolved in ethyl chloride, and its concentration was 0.191 mole/l. Polymerization started immediately after catalyst introduction. The reaction was terminated by introducing precooled *n*-propanol. The product was washed thoroughly with methanol, filtered and dried *in vacuo* at 60°C . Yield was 1.753 g or 17.25 per cent. This material was soluble in toluene, benzene, ether and carbon tetrachloride. Its number average molecular weight (vapour phase osmometer) was 5462 indicating a degree of polymerization of about 60.

Polymerizations at -78° and 0° were run under substantially similar

conditions. The polymerization at $+40^{\circ}$ was carried out with 5.63 g monomer in 80 ml methylene chloride under reflux conditions.

The soluble fraction was determined by extracting with refluxing benzene for eight hours. Number average molecular weights were obtained by osmometry.

X-ray studies were carried out with a Norelco diffractometer (goniometer scanning), the i.r. spectra were obtained with a Baird instrument using a sodium chloride prism and the usual potassium bromide pellet technique, and the u.v. spectrum was obtained using a Cary instrument. A Varian 60 n.m.r. spectrometer was used.

RESULTS AND DISCUSSION

Table 1 compiles some pertinent facts obtained in polymerization experiments. None of the polymers melted up to 285°C , and they started to decompose on heating before melting. When heated in nitrogen atmosphere decomposition was accompanied by the evolution of heavy yellow fumes. The powders could not be moulded. Their cast films were clear and transparent but extremely weak and brittle. The product obtained at -123°C was tested for crystallinity, but X-ray studies revealed only one rather diffuse halo at 5.5 \AA indicating an amorphous hydrocarbon. Only the polymer synthesized at -123°C was soluble in common solvents. The amorphous X-ray diffraction pattern coupled with high solubility indicates a random linear structure for the polymer as indicated in the introduction. The other products were only partially soluble, and the insoluble portion swelled in solvents. Evidently, these materials were partially crosslinked.

Table 1. Polymerization results

Temperature, $^{\circ}\text{C}$	-123	-78	0	+40
Solvent	$\text{C}_2\text{H}_5\text{Cl}$	$\text{C}_2\text{H}_5\text{Cl}$	$\text{C}_2\text{H}_5\text{Cl}$	CH_2Cl_2
Monomer conc., mole/l.	1.39	1.39	1.39	0.688
Catalyst* conc., mole/l.	0.191	0.151	0.151	0.161
Amount of catalyst added, ml	14	4.5	4.0	6.0
Reaction time, min	37	25	29	4
Yield, %	17.2	42.0	71.0	30.2
Benzene-soluble fraction, %	100	72.5	34.5	59
Mol. wt (of soluble fraction)	5 519 5 405	8 676	3 676 3 678	2 976
Melting behaviour	----- Decomposes before it melts -----			
Crystallinity (X-ray)	Amorphous			

*The catalyst was aluminium chloride dissolved in ethyl chloride.

The structure of the polymers was investigated by i.r. and n.m.r. spectroscopy. *Figure 1* shows representative spectra of products obtained at -123° and $+40^{\circ}\text{C}$. The broad band at 12.4μ which appeared in all spectra has been assigned to the 2,6-disubstituted nortricyclene structure^{2,7,10}. This strong band became increasingly prominent with decreasing temperature, and it was stronger in the soluble fraction than in the insoluble one. It is equally significant that no bands appeared in the 6.0 to 6.5μ region

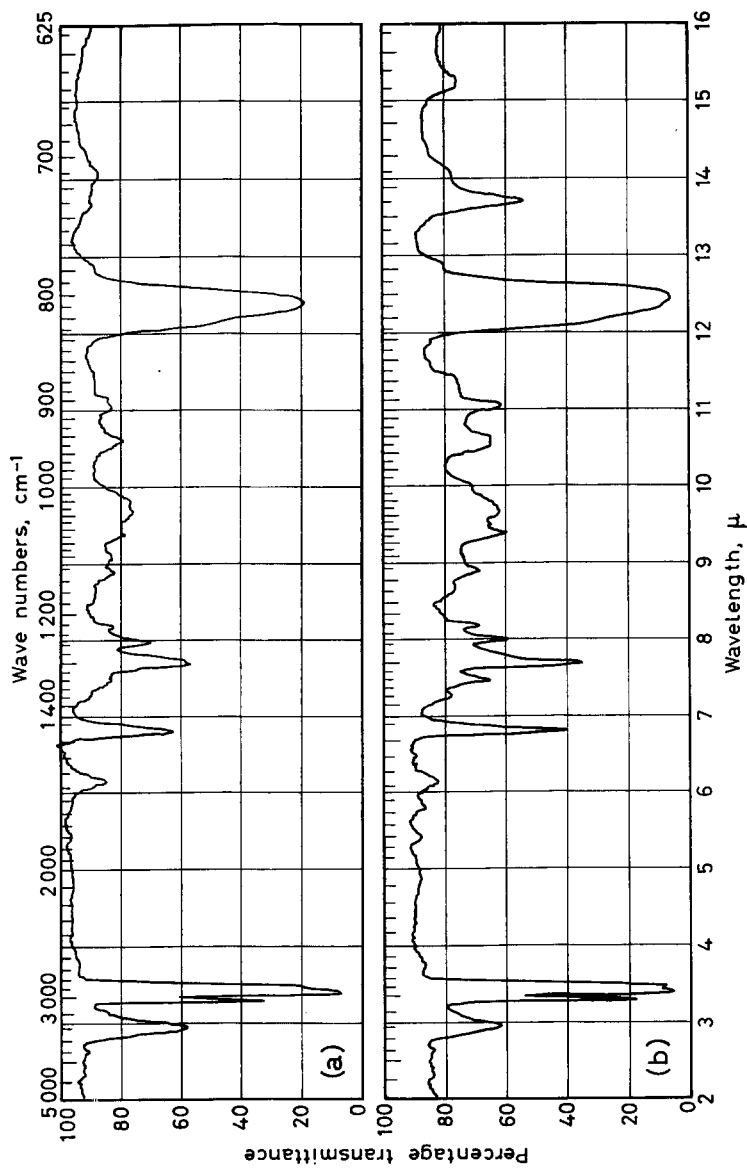


Figure 1(a)—Infrared spectrum of polymerization obtained at +40°C

Figure 1(b)—Infrared spectrum of polynortricyclene obtained at -123°C

indicating the absence of unsaturation. (The band at 6.15μ is water from potassium bromide, and it appears only in conjunction with the 2.8μ band.)

A very strong symmetrical band increasingly develops at 13.7μ as the temperature is lowered. As shown in *Figure 2*, the net absorbance of this band increases more or less linearly with decreasing temperature from $+40^\circ$ to -123°C . Similarly, according to *Table 1*, the amount of benzene-soluble fraction seems also to increase with decreasing temperatures. Apparently, therefore, the band at 13.7μ is related to some form of regularity in the polymer chain. It is interesting to note that this region of the spectrum is where long chains of methylene groups absorb.

The methylene bending mode at 6.82μ is perfectly symmetrical in the lowest temperature sample indicating a symmetrical structure. However, as the temperature is increased, the band is distinctly split into a doublet

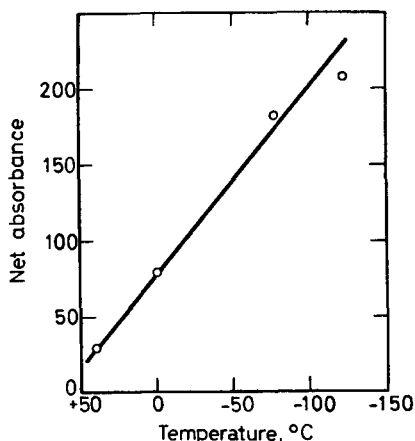


Figure 2—Effect of temperature on net absorbance of i.r. band at 13.7μ

indicating that a more asymmetrical arrangement appeared (crosslinking). Also this band is quite different in the spectra of the soluble and insoluble fractions of the $+40^\circ$ sample. The insoluble fraction shows peaks at 6.75 and 6.80μ , whereas the soluble fraction shows a maximum of 6.80μ and only a shoulder at 6.85μ . The shift to higher frequencies with the insoluble fraction would indicate more strain on the bending motion of the $-\text{CH}_2-$ group.

A band appears at about 7.70μ which, as the polymerization temperature is progressively increased, splits into a distinct doublet of about equal intensity at 7.70 and 7.75μ . The band at 7.75μ is only an unresolved shoulder on the 7.70μ band of much stronger intensity in the spectrum of the low temperature samples. This band may, therefore, be also related to enhanced disorder, and could indicate increased crosslinking as the temperature is increased. An i.r. band is observed in this region for mono-substituted ring systems which splits into two or more bands as the number of substitutes is increased.

A small band was always noted at 14.1μ . At first glance this could be attributed to a small amount of unsaturation. However, this assignment

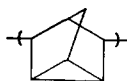
cannot be correct because (a) the intensity of this band remained constant at every temperature level investigated from -123° to $+40^{\circ}\text{C}$, (b) the intensity, if anything, was higher in the lowest temperature product, and (c) polynorbornadiene does not absorb in the 6.0 to 6.5μ region, although 2-methylcyclopentene, an unsaturated structure which would appear if simple 2,3-type polymerization occurred, shows a band in this region. Hence, this band is more likely analogous to those arising from substituted ring systems in this region, thus



A band appears at 11.5μ in the spectrum of the highest temperature sample. A band is usually observed in this region for multisubstituted ring systems. The bands at 5.8μ and 9.8μ indicate the presence of carbonyl and hydroxyl impurities, respectively, due to acetone and methanol washings during sample preparation.

N.m.r. spectroscopy corroborated the i.r. findings. The soluble sample obtained at -123°C has been studied. Significantly, there was practically no absorption in the olefin region of 4.5 to 6.5 p.p.m. All protons appeared as rather broad and unresolved bands in the area between 0.5 and 2.0 p.p.m. downfield from the trimethylsilane internal standard. A distinct broad peak appeared at 0.9 p.p.m. The area ratio between this band and the rest of the absorbing area is about 5:3. The peak at 0.9 p.p.m. could indicate the two bridge protons on C_7 , plus the three tertiary protons of the cyclopropane ring (C 1, 2 and 6).

In conclusion then it appears that the soluble portion of these products consists of linear chains having 2,6-disubstituted nortricyclene repeat units, e.g.



Such a polymer structure could also be expected by considering the possibility of transannular conjugation of the double bonds in the monomer. In fact we found that the u.v. spectrum of pure norbornadiene showed a single strong band at $232\text{m}\mu$. Absorption in this region is attributed to conjugated double bonds¹¹. Similarly the i.r. spectrum contained strong bands at 6.10 , 6.25 and 6.48μ indicating unsaturation. The normal position of an olefin band is around 6.1μ and absorptions above 6.2μ are usually associated with conjugated double bonds. The peak at 6.48μ was found to be the strongest one of the three olefin bands which most likely indicates some measure of conjugation. By analogy butadiene shows its double bond at 6.3μ . This band is about 0.2μ displaced from the normal position toward

lower frequencies due to conjugation. Cyclopentenes absorb around 6.1 and 6.2μ , when unsubstituted at the double bond, and hence a band at around 6.5μ would be in line with the position expected if conjugative effects were present. The nortricyclene repeat unit indicates that polymerization takes place by an intramolecular transannular rearrangement. The polymerization proceeds with great rapidity even at very low temperatures so that the driving force of the reaction must be appreciable, and the homoallylic carbonium ion transition state must be quite stable.

Crosslinking takes place only at higher temperatures indicating that it involves reactions of higher activation energy. It could be that crosslinking occurs by consecutive '2,3-type' reactions:

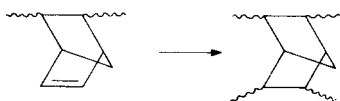


Figure 3 shows the effect of temperature on the number average molecular weights of the benzene-soluble polymer fraction. The molecular weights

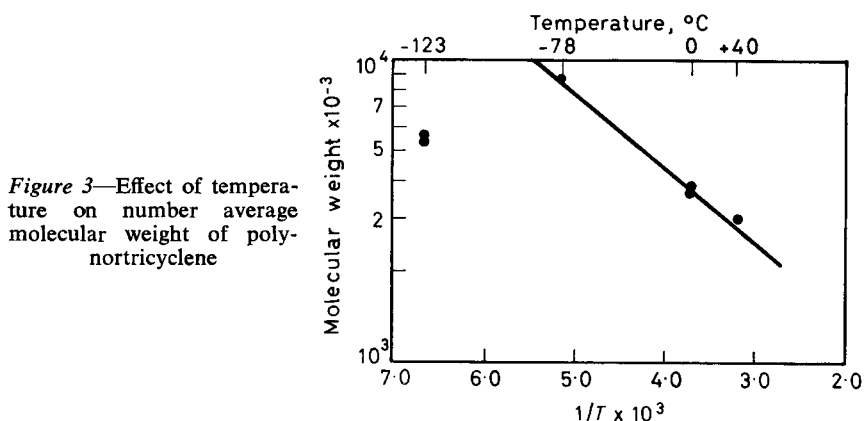


Figure 3—Effect of temperature on number average molecular weight of polynortricyclene

increase linearly with reciprocal temperature between $+40^{\circ}$ and -78°C ($E_{\text{DP}} = 1.14$ kcal/mole). This inverse relation is common for most ionic, particularly cationic, polymerizations. At very low temperatures, -123°C , the molecular weights seem to decrease and there seems to be a preferred temperature range around -78°C where the molecular weights show a maximum. This phenomenon, however, could be due to the low conversion at -123°C .

The authors thank Dr W. Naegele for the interpretation of n.m.r. spectra.

*Chemicals Research Division and Analytical Research Division,
Esso Research and Engineering Company,
Linden, New Jersey, U.S.A.*

(Received May 1964)

REFERENCES

- ¹ WINSTEIN, S. and SHATAVSKY, M. *Chem. & Ind.* 1956, 59
- ² SCHMERLING, L., LUVISI, J. P. and WELCH, R. W. *J. Amer. chem. Soc.* 1956, **78**, 2819
- ³ WILCOX, C. F., WINSTEIN, S. and McMILLAN, W. C. *J. Amer. chem. Soc.* 1960, **82**, 5450
- ⁴ FERINGTON, T. E. and TOBOLSKY, A. V. *J. Polym. Sci.* 1958, **31**, 25
- ⁵ *Austral. Pat. Appl.* 32 649/57 to duPont (11/1/1957)
- ⁶ *U.S. Pat. No.* 3 066 123 to Esso Research & Engineering Co. (11/27/1962)
- ⁷ ZUTTY, N. L. *J. Polym. Sci.*, Part A, 1963, **1**, 2231
- ⁸ GRAHAM, P. J., BUHLE, E. L. and PAPPAS, N. *J. org. Chem.* 1961, **26**, 2658
- ⁹ KENNEDY, J. P. and THOMAS, R. M. *Advances in Chemistry Series*, 1962, **34**, 111
- ¹⁰ ROBERTS, J. D. *J. Amer. chem. Soc.* 1950, **72**, 3116
- ¹¹ JAFFE, H. H. and ORCHIN, M. *Theory and Applications of Ultraviolet Spectroscopy*, Chapter 10. Wiley: New York, 1962

Multiple Glass Transitions of Block Polymers

R. J. ANGELO, R. M. IKEDA and M. L. WALLACH

High molecular weight, block copolymers of styrene, butadiene and isoprene were prepared in tetrahydrofuran solution by anionic polymerization techniques employing sodium- α -methylstyrene initiation. Selected samples were characterized by dilute solution techniques and found to be genuine block copolymers with narrow molecular weight distributions and little composition heterogeneities. The multiphase nature and the mechanical response of the polymers were investigated by torsion pendulum analyses.

The two phase nature of the styrene-butadiene block copolymers was evident from the two glass transitions characteristic of the individual segment types, polystyrene and polybutadiene. The purity of the phase separations was indicated by the invariance of the butadiene T_g with copolymer composition and the equality of the mechanical response of two copolymers with identical compositions but inverted monomer sequences, i.e. ABA versus BAB. Variations in the magnitude of the butadiene loss peak and the step character of the log modulus/temperature curves were also determined as functions of the composition.

Some effects of macrophase size were observed by comparing the mechanical behaviour of a physical blend of homopolymers with a block copolymer of the same composition. The temperature variation of the modulus was greatly affected above the butadiene T_g .

The compatibility of similar soft segments, polybutadiene and polyisoprene was also investigated. Block terpolymers of styrene, butadiene and isoprene were compared to a physical mixture of styrene-butadiene and styrene-isoprene block copolymers. Although the blending of the two soft diene segments in the physical mixture was substantial, it was not as complete as that obtained through terpolymerization where some indication of the effect of segment position on the blending was also noted.

GLASS transition temperatures have been of considerable interest in describing the mechanical behaviour of copolymer systems. For amorphous, random copolymers, the situation is understood and well-documented¹. Such polymers form a single thermodynamic phase and consequently exhibit a single glass transition for the main polymer chain. The transition temperatures for such polymers vary with copolymer compositions and the variations can often be predicted.

There is less complete understanding of glass transition phenomena for graft and block copolymers. If the homopolymer segments form a single thermodynamic phase, then the copolymer should behave like a random copolymer and show a single glass transition, whose temperature is composition dependent. However, if the homopolymer segments form separate phases, then the copolymer should exhibit two transitions, each characteristic of a given homopolymer phase. Experience with physical mixtures^{2,3} illustrates the extreme requirements for polymer-polymer solubility and

one would expect most high molecular weight graft and block copolymers to exhibit two transitions—each characteristic of a given homopolymer phase. Although some data which illustrate these points appear in the literature^{2,4,5}, a thorough demonstration has not been possible due to the lack of well-characterized samples.

The advent of controlled block copolymerization, through suitable anionic catalysis⁶, provides a means to synthesize the desired block copolymers. Such polymers should meet at least two requirements. The first, and most important, is the assurance of sharp block segments—i.e. the absence of significant areas with random sequences of comonomers. The second, is that the samples be essentially free of homopolymer. To eliminate possible ambiguities, the molecular weight distributions of the polymers should be fairly narrow and the degrees of polymerization of the segments should be sufficiently large so that the T_g s would be insensitive to further increases in DP . Anionic polymerization techniques discussed by numerous workers⁶⁻⁹ demonstrate the means by which polymers can be tailored to these requirements. We report the synthesis and characterization of a series of block co- and ter-polymers and their torsion pendulum analyses.

EXPERIMENTAL

(A) Polymer preparation

The need for high purity in anionic polymerizations has been discussed⁷⁻⁹ previously. High vacuum techniques which are suitable for the purification of the starting materials as well as the polymerization process itself have been described^{7,9}.

(1) *Apparatus*—A high vacuum line equipped with four manifolds and an outlet to a polymerization flask was utilized. A two-stage mercury diffusion pump with mechanical prepump was employed. The vacuum line could be rapidly pumped to 10^{-5} torr and maintained from 10^{-5} to 10^{-6} torr.

The polymerization flask was designed so that reasonable size polymerizations could be conducted (10 to 50 g polymer), adequate stirring could be provided, high vacuum conditions could be maintained and ease of polymer isolation could be assured. A three-necked, 500 ml round-bottom flask with an enclosed, magnetic-driven stirring device was constructed. A standard taper glass cap (5 cm diameter) was mounted from the centre neck of the flask. A double-bladed (slightly less than 5 cm wide) glass stirrer, equipped with a glass enclosed magnetic stirrer head was mounted between the cap and the bottom of the flask. The stirrer was balanced and centred by using tungsten wire tips into slight indentations in the head and bottom of the flask. Efficient stirring from an external magnetic source was thus provided.

(2) *Materials*. (a) *Styrene*—Eastman White Label styrene was extracted twice with ten per cent sodium hydroxide solution followed by two extractions with distilled water. After drying over magnesium sulphate for 20 to 30 minutes, the monomer was vacuum distilled under a nitrogen

atmosphere. A centre cut (*ca.* 50 ml) was collected over calcium hydride and placed directly on to the vacuum line. The styrene was then distilled twice on the vacuum line using standard degassing techniques in each step. The purified distillate was collected over calcium hydride in a calibrated receiver and frozen until needed for the polymerization. Prior to the polymerization, the solidified monomer was melted, degassed and a 5 ml forecut taken. Styrene was then vaporized through the vacuum line into the polymerization vessel at the desired rate. A water bath at 25° to 30°C gave smooth vaporization of the styrene. The desired volume of styrene was metered from the calibrated receiver and the volume was determined to within ± 0.5 ml. The density was 0.90 g/ml at 25°C.

(b) *Butadiene*—Phillips Research Grade (99.9 per cent) butadiene (*ca.* 50 ml) was liquefied directly into a receiver on the vacuum line. The monomer was distilled three times in the vacuum system, each time collecting the centre cut over calcium hydride. Standard degassing techniques were used. The purified product was collected in a calibrated receiver over calcium hydride and frozen with a liquid nitrogen bath until used in the polymerization. Immediately before the polymerization, a 5 ml forecut was discarded. An ice bath (0° to 5°C) gave smooth vaporization into the polymerization vessel. The volume was determined to within ± 0.5 ml. The density was 0.64 g/ml at 5°C.

(c) *Isoprene*—Phillips Research Grade isoprene was distilled at atmospheric pressure in a nitrogen atmosphere and a centre cut was collected over calcium hydride. The receiver was transferred to the vacuum line where the monomer was degassed thoroughly and distilled three successive times using calcium hydride as a drying agent. The purified monomer was collected over calcium hydride in a calibrated receiver and solidified with liquid nitrogen prior to use in the polymerization. Immediately before vaporization into the polymerization vessel, a 5 ml forecut was discarded. The volume was determined to within ± 0.5 ml. The density was 0.68 g/ml at 25°C.

(d) *Solvent*—Du Pont purified tetrahydrofuran (THF) was employed as the solvent. About one litre was transferred under nitrogen to a receiver containing sodium and biphenyl. The receiver was quickly placed on the vacuum line and stirring was started. The intense blue colour of the sodium biphenyl complex formed, whereupon the flask was cooled, evacuated and a forecut taken to a trap. The solvent was transferred by evaporation at room temperature into the cooled polymerization vessel (dry ice-acetone bath). The polymerization vessel contained 1 ml of initiator solution (α -methyl styryl tetramer¹⁰) which maintained a bright red colour during the distillation of 300 ml of solvent. Persistence of the red colour during the accumulation of solvent assured a high level of purity. If the colour dissipated, the experiment was discontinued.

(e) *Initiator*—THF solution of dianionic α -methyl styryl tetramer¹⁰ was employed as the initiator. Sodium (0.12 g) was placed into a 100 ml

graduated cylindrical tube equipped with a high vacuum stopcock and drip tip. Weighing and transfer were accomplished in an inert atmosphere. The tube was transferred to the vacuum line where a sodium mirror was deposited upon the wall of the tube. About 100 ml of THF was collected in the tube in the same fashion described for preparation of the solvent. The tube was allowed to come to room temperature, and then removed from the vacuum line and flushed with nitrogen. α -Methyl styrene (0.146 g) was introduced with a hypodermic syringe. Shaking the tube produced an immediate red colour which became more intense as the sodium mirror dissolved. The mirror was almost completely dissolved after two hours. The tube was shaken overnight and standardized the following morning. Initiator solutions were prepared every four or five days. The initiator concentrations were in the range of $2\text{--}5 \times 10^{-2}$ molar.

(3) *Typical polymerization*—A typical block copolymerization (S/B₂) of 60/40 mole per cent styrene/butadiene was carried out as follows.

The apparatus was flamed and then pumped overnight under high vacuum. The polymerization vessel, equipped with an initiator tube containing freshly prepared α -methyl styryl initiator was evacuated and cooled to -78°C (dry ice-acetone bath). Stirring was started after the addition of 1.0 ml of initiator solution. Solvent (300 ml THF) was collected in the polymerization flask during 1.1 h. A bright red colour was maintained. An additional 9.0 ml of initiator solution was added to give an intense red solution. Vaporization of styrene monomer into the stirred solvent began with no significant change of colour. After adding 1.0 ml of styrene during two minutes, the addition was stopped to determine whether any deterioration of colour could be detected. No deterioration was noticed after five minutes, and styrene addition was resumed. A total of 17.5 ml of styrene was added during 0.5 h. The solution maintained the bright red colour and became increasingly more viscous. After stirring the solution for an additional ten minutes, 1.0 ml of butadiene was vaporized into the polymerization vessel. The intense red solution immediately turned orange and then yellow upon exposure to the butadiene. The yellow colour persisted during five minutes, whereupon the addition of butadiene was resumed. A total of 9.0 ml of butadiene was added during 0.25 h. The solution remained deep yellow and became increasingly more viscous during the addition. The solution was allowed to stir for an additional 0.5 h after monomer addition without any significant change of colour. The polymerization was terminated by vaporizing 2.0 ml of glacial acetic acid into the reaction vessel. The solution immediately turned colourless and the flask was removed from the vacuum line. The viscous solution was precipitated into an excess of methanol containing an antioxidant (phenyl β -naphthylamine). The resulting white, fibrous polymer was washed three times with methanol in a blender. The polymer was dried to constant weight under vacuum at 25°C . A yield of 21.95 g of polymer having an intrinsic viscosity (in benzene at 30°C) of 0.76 dl/g was obtained. The calculated composition was 59 mole per cent of styrene, 41 mole per cent of butadiene.

A summary of the various polymerizations is given in *Table 1*. S, B and I represent polystyrene, polybutadiene and polyisoprene, respectively. The

MULTIPLE GLASS TRANSITIONS OF BLOCK POLYMERS

block polymers are denoted S/B₁, S/B₂, S/I, S/B/I, etc. The letters identify the polymer segments with the first letter indicating the centre segment (e.g. S/B/I represents a block terpolymer with polymer segments, $\text{I} \sim \text{B} \sim \text{S} \sim \text{B} \sim \text{I}$).

Table 1. Polymer preparation and characterization

(A) Styrene-Butadiene

Polymer	Monomer added (g)		Recovery %	Mole %S (Calcd)	Mole %S (n.m.r.)	[η] dl/g	$M_n \times 10^{-4}$	$\frac{M_w}{M_n}$
	S	B						
S	8.10	0.00	98	100	100	0.488	0.609	1.17
S/B ₁	15.75	2.90	97	74	72	0.71	1.05	—
S/B ₂	15.75	5.75	102	59	55	0.76	1.02	1.22
S/B ₃	15.75	8.65	100	49	43	0.82	0.845	—
S/B ₄	7.90	6.45	101	39	36	1.06	1.28	—
S/B ₅	7.90	17.30	99	19	19	2.85	3.14	—
B	0.00	19.20	101	0	0	1.19	0.914	1.08
B/S	23.80	2.70	96	80	78	1.69	1.85	—

(B) Isoprene-Styrene-Butadiene

Polymer	Monomer added (g)			Recovery %	Mole %S (Calcd)	Mole %S (n.m.r.)	[η] dl/g	$M_n \times 10^{-4}$
	S	B	I					
I	—	—	13.60	99	0	0	1.21*	—
S/I	12.06	—	7.82	92	50	51	1.02	1.11
S/B/I	15.75	4.48	5.65	99	48	53	1.60	1.43
B/S/I	15.75	4.48	5.65	102	48	50	1.08	0.778

* η_{inh} (0.5 per cent conc.)

(4) *Physical blends*—Two blends were prepared by solution techniques. The first was a blend of S and B, S//B, containing ca. 20 mole per cent styrene (n.m.r.). The second was a 50/50 weight blend of the two block polymers, S/B₃ and S/I. It is denoted S/B//S/I and contains ca. 50 mole per cent styrene (n.m.r.).

(B) Characterization

(1) *Infra-red*—The infra-red (i.r.) spectra were obtained using the Perkin-Elmer model 137 Infracord and model 21 spectrophotometers. Very thin film specimens deposited from carbon disulphide solutions on to potassium bromide pellets proved to be most satisfactory for spectra determinations.

(2) *Nuclear magnetic resonance*—The n.m.r. spectra were obtained using a Varian A-60 spectrometer. Carbon tetrachloride solutions (five per cent) were employed. Tetramethylsilane was used as an internal standard.

(3) *Viscosity*—Intrinsic viscosities were measured in benzene at 30°C using Cannon-Fenske viscometers. Flow times were kept above 100 seconds to minimize corrections.

(4) *Osmometry*—Number average molecular weights were determined with Stabin block osmometers using gauge 116 gel cellophane membranes. Osmotic heights were measured in benzene at 30°C to ± 0.005 cm with a

Gaertner micrometer slide cathetometer*. The temperature was constant to $\pm 0.04^\circ\text{C}$. Equilibrium was attained in about one to two hours. The drop curves were flat and no diffusion extrapolations were necessary. Equilibrium heights varied from 1 to 6 cm with asymmetry corrections of about 0.2 cm.

(5) *Light scattering*—Light scattering measurements were run using the modified† model VI angular dependence photometer¹¹. Dust was removed by filtration through an ultrafine biological filter. Benzene was employed as a primary standard taking the Rayleigh ratio as 22.0×10^{-6} cm at a wavelength of 5461 Å using vertically polarized incident light¹².

Angular dependence scans were obtained for polymers exhibiting a dissymmetrical radiation diagram. The ratio of the concentration to the corrected scattered intensity, C/I , was plotted against $\sin^2 \frac{1}{2}\theta$ (where θ is the angle of observation) and extrapolated to zero angle. Then $(C/I)_{\theta=0}$ was plotted against C and extrapolated to zero concentration. For lower molecular weight polymers (i.e. S) exhibiting no dissymmetry only 90° scattering data were collected. Molecular weights were calculated from the Debye¹³ equation. It was assumed that the depolarization correction factor was negligible.

(6) *Ultracentrifugation*—Sedimentation velocity measurements were run at 44 770 rev/min with the Spinco model E ultracentrifuge employing schlieren optics. The determinations were made at $C=0.5$ per cent in THF at 30°C .

(7) *Torsion pendulum*—The compound torsion pendulum used in these studies was similar to those described elsewhere¹⁴. In such an instrument the samples are clamped rigidly at the bottom and the upper clamp assembly acts as the inertia member and is suspended by a thin torsion wire. The medium for thermostatic control was dry nitrogen and could be cooled or heated as desired. Free oscillations (ca. 1 c/s) were used exclusively. The temperature range covered was from -160°C to about 100°C with measurements taken at varying intervals (1° to 10°).

The test specimens of the polymers were prepared by pressing thin (10 to 20 mils) films in a Carver press. The pressing was conducted at temperatures ranging from 25°C for homopolybutadiene to 150°C for homopolystyrene. 0.250 in. \times 2.00 in. strips were then cut from the film for torsion pendulum analysis.

In computing the torsion modulus, G' , loss modulus, G'' , and internal friction, Q^{-1} , the appropriate form factor¹⁵ was used for our thin samples (ca. 10 to 20 mils \times 0.250 in. \times 1.00 in.). Corrections were made for the slight tensile stress on the samples¹⁶ and also for the modulus component due to the torsion wire.

*With homopolybutadiene the data were taken in THF at 30°C .

†The modifications introduced recently by W. J. Pangonis of this laboratory consisted of an intense AH-4 high pressure mercury vapour lamp, a sensitive EMI end-on photomultiplier tube and a signal amplification system.

RESULTS AND DISCUSSION

 (A) *Polymer microstructure*

The microstructure of the polymers was investigated using i.r. and n.m.r. spectroscopy.

(1) *Infra-red*—The i.r. analysis of the polybutadiene by the method of Richardson¹⁷ gave 90 per cent 1,2-, 10 per cent *trans*-1,4- and little or no *cis*-1,4-content. The method of Silas *et al.*¹⁸ gave 88 per cent 1,2-, 12 per cent *trans*-1,4- and little or no *cis*-1,4-content. The i.r. spectra of the butadiene copolymers indicated the same type of diene microstructure.

The i.r. analysis of polyisoprene, by the method of Richardson and Sacher¹⁹, revealed about 90 per cent external unsaturation (3,4- and 1,2-structure) and 10 per cent internal unsaturation (probably *trans*-1,4-). The ratio of 3,4/1,2 unsaturation was about 3/2. The i.r. spectra of the isoprene copolymers indicated the same type of diene microstructure.

(2) *Nuclear magnetic resonance*—The compositions of the styrene-butadiene copolymers were obtained from integration of the proton peaks and use of the equation, where X_s denotes the mole fraction styrene,

$$X_s = \frac{6 (\text{Aromatic H})}{5 (\text{Total H}) - 2 (\text{Aromatic H})}$$

Two commercially available styrene-butadiene copolymers were analysed in this fashion and gave the following results: Copo* 1505 (4.9 mole per cent styrene). Found: 4.9 mole per cent. Naugapol† 1019F (13.7 mole per cent styrene). Found: 12.0 mole per cent. It should be recognized that butadiene polymers and copolymers prepared by free radical catalysis have considerably different diene microstructure from those prepared by anionic catalysis. Polybutadienes prepared in emulsion have approximately 80 per cent 1,4- (largely *trans*-) and 20 per cent 1,2-structure²⁰, whereas the anionic butadiene compositions described in this paper consist of about 90 per cent 1,2- and 10 per cent *trans*-1,4-structure.

All of the styrene anionic block copolymers gave two well-resolved aromatic proton peaks at 397 c/s (*ortho* H) and 426 c/s (*mèta* and *para* H) in the ratio of 2/3. The two commercial styrene-butadiene random copolymers gave only one aromatic proton peak at 435 c/s.

Analysis of homopolybutadiene in the olefinic proton region (~ 300 c/s) gave a value of 96 per cent 1,2- and 4 per cent 1,4-structure. Analysis of homopolybutadiene in the allylic proton region (~ 120 c/s) gave a value of 91 per cent 1,2- and 9 per cent 1,4-structure. The n.m.r. spectra of butadiene copolymers indicated the same type of microstructure as the homopolymer.

Analysis of homopolyisoprene in the olefinic and allylic proton regions gave 55 per cent 3,4-, 29 per cent 1,2-, 16 per cent 1,4- and 58 per cent 3,4-, 31 per cent 1,2-, 11 per cent 1,4-addition, respectively. The n.m.r.

*Copolymer Rubber and Chemical Corporation.

†Naugatuck Chemical Division, U.S. Rubber Co.

spectra of isoprene copolymers also indicated the same type of microstructure as the homopolymer.

(B) *Solution properties*

(1) *Homopolymers*—The osmometric and light scattering molecular weights for homopolystyrene and homopolybutadiene are given in *Table 1*. As evidenced by the values of M_w/M_n (i.e. S: 1.17, B: 1.08), the molecular weight distributions are quite narrow.

(2) *Block copolymers*—The osmometric and viscosity data for the block copolymers are also given in *Table 1*. The number average molecular weights are generally high enough to preclude the presence of much low molecular weight homopolymeric impurity. This was verified by ultracentrifugation (on S/B₂ and S/B₄) which revealed only one sharp schlieren peak. Although M_n for S/B₁₋₄ remains fairly constant, the intrinsic viscosity and the second virial coefficient increase as the copolymer becomes richer in butadiene (*Figure 1*). This is due to expansion of the end caps caused by a strong repulsive effect of styrene on butadiene and to the fact that benzene is a better solvent for polybutadiene.

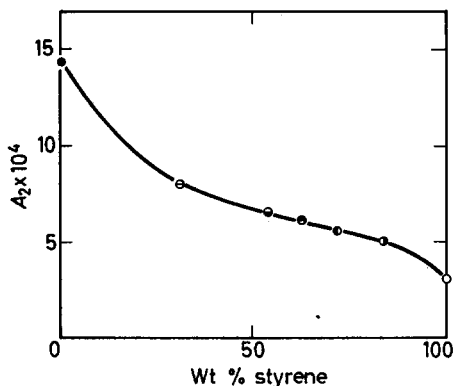


Figure 1—Osmometric second virial coefficient versus copolymer composition. Measurements were done in benzene at 30°C for copolymers S/B₁₋₅ and for homopolystyrene; for homopolybutadiene data were taken in THF at 30°C

In order to verify that the copolymers had sharp block segments of high enough \overline{DP} , and that the samples had narrow molecular weight distributions and were essentially free of homopolymer, a selected styrene-butadiene block copolymer (S/B₂) was completely characterized by light scattering. No fractionation or extraction was attempted.

Observations of the effect of composition heterogeneity on the light scattering characteristics of GR-S rubber were first reported by Tremblay *et al.*²¹. Subsequent theoretical work was done by Stockmayer *et al.*²² and the experimental application of the theory to block copolymers of styrene and methylmethacrylate was reported by Krause²³. Extensive theoretical work was done independently by Benoit and co-workers²⁴⁻²⁶ and successfully applied experimentally to a variety of block and graft copolymers.

Light scattering measurements were made on S/B₂ in five solvents with

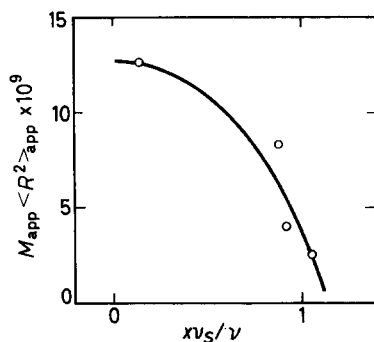
MULTIPLE GLASS TRANSITIONS OF BLOCK POLYMERS

 Table 2. Refractive index increments, apparent molecular weights and radii of gyration for block copolymer S/B₂

Solvent	Refractive index	(dn/dc) _S cm ³ /g	(dn/dc) _B cm ³ /g	(dn/dc) _{S/B₂} cm ³ /g	M _{app}	$\langle R^2 \rangle_{app} \times 10^{-4} \text{ \AA}^2$
Tetrahydrofuran	1.40	0.198	0.132	0.179	134 000	6.12
Chloroform	1.45	0.158	0.083	0.138	133 000	2.98
Benzene	1.50	0.108	0.011*	0.082	124 000	2.12
Bromoform	1.60	-0.005*	-0.115	-0.028	124 000	10.3
1-Bromonaphthalene	1.66	-0.091	-0.185	-0.044	123 000	—

*Calculated.

Figure 2—Product of apparent molecular weight and apparent radius of gyration versus refractive index increment variable: x is the weight per cent styrene, v_s is dn/dc of homopolystyrene and v is dn/dc of the copolymer



systematically varying indices of refraction (1.40 to 1.66). The results are given in Tables 2 and 3. We find from dn/dc measurements that there is 58 mole per cent (79 wt %) styrene and 42 mole per cent (21 wt %) butadiene in good agreement with the stoichiometric and the n.m.r. results. For the

 Table 3. Molecular weights and radii of gyration for S/B₂ and its component blocks

Structural Parameter	S	B	S/B ₂
M _w	87 200	21 200	124 000
R (Å)	179	348	275

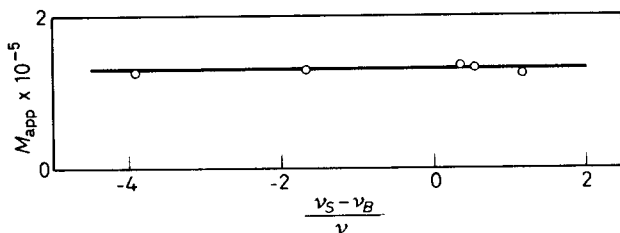


Figure 3—Apparent molecular weight versus refractive index increment variable: v_s is dn/dc of homopolystyrene, v_B is dn/dc of homopolybutadiene and v is dn/dc of the copolymer

copolymer $M_w=124\ 000$, $M_n=102\ 000$, and $M_w/M_n=1.22$. Therefore, the distribution of molecular weights is reasonably narrow. For the component blocks $(M_w)_S=87\ 200$ and $(M_w)_B=21\ 200$. Since

$$(M_w)_{SB} > 0.79(M_w)_S + 0.21(M_w)_B$$

the sample is primarily block polymer. The latter relation becomes an identity for a mixture of homopolymers²⁴. When the product of the apparent molecular weight and the square of the radius of gyration is plotted against the refractive index increment function, $0.79v_s/v$ (where v_s is dn/dc of homopolystyrene and v is dn/dc of the copolymer), a downward concavity indicates block copolymer²⁵. Our data, showing such a

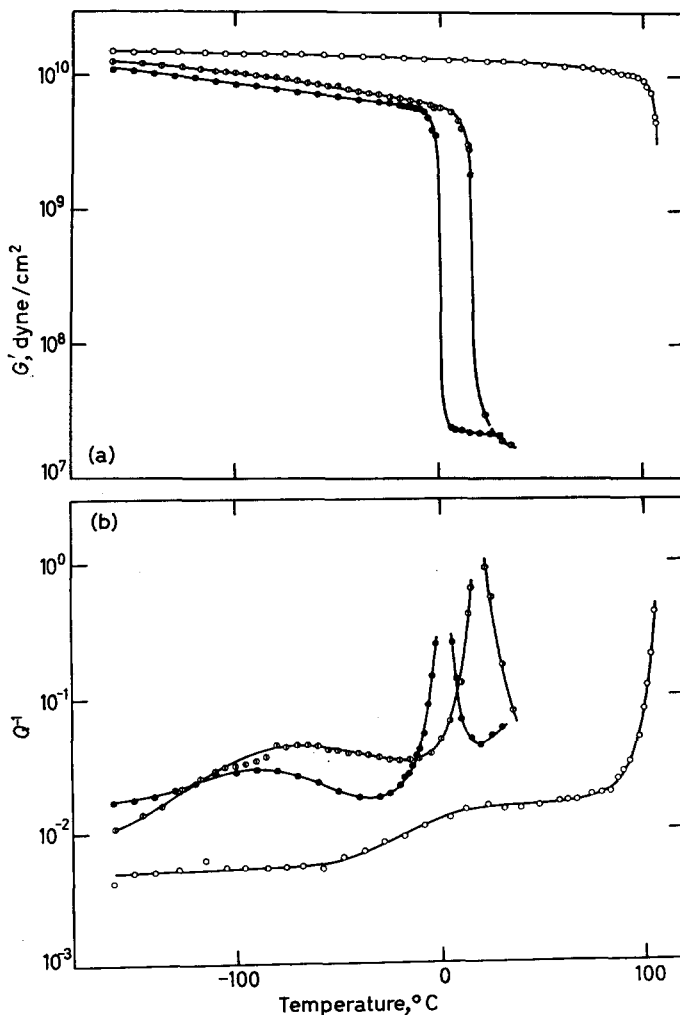


Figure 4—Homopolymers: temperature dependence of the torsion modulus, G' , and internal friction, Q^{-1} ; \circ Polystyrene, \bullet Polybutadiene and \odot Polyisoprene

downward concavity, are plotted in *Figure 2**. A mixture of homopolymers or a random copolymer would give upward concavity²⁵. Radii of gyration (R) derived from *Figure 2* are given in *Table 3*. We note that $R_B^2 > R_S^2$ whereas for a random copolymer R_B^2 would be equal to R_S^2 .

As indicated by the linearity in *Figure 3*, M_{app} is independent of the refractive index increments. Thus, there is little composition heterogeneity indicating that we have well-tailored blocks with insignificant quantities of homopolymer. A random copolymer or a mixture would give a parabola with upward concavity²⁴.

We conclude, therefore, that the polymers are genuine block copolymers.

(C) Torsion pendulum analysis

(1) *Homopolymers*—*Figure 4* shows the temperature variation of the shear modulus and internal friction of the homopolymers, B(polybutadiene), S(polystyrene) and I(polyisoprene). The curves are typical of amorphous polymers.

The internal friction data are very similar to those reported in the literature for several poly- α -olefins²⁷. In each case there is a broad, low temperature dispersion peak. For B and I these low temperature maxima are near -90°C and -70°C , respectively. For S the peak appears as a shoulder with a maximum in the 20° to 40°C range. The large, higher temperature peaks are all indicative of the glass transitions of the respective samples. For S, the fall-off of the internal friction at temperatures greater than 100°C was not measured due to experimental difficulties. Similar data are available in the literature²⁸, indicating the glass transition at a temperature slightly greater than 100°C . For B and I samples, the 'glass' peaks occur near 0°C and 15°C , respectively. Since no corroborating data exist to relate these internal friction maxima with the glass transition as determined by other means, linear expansion coefficient measurements were undertaken on sample B. The apparatus and methods used were similar to those reported by Dannis²⁹. The results showed one abrupt change in the expansion coefficient at $-9^\circ \pm 1^\circ\text{C}$. The 10°C discrepancy is not unusual in these two types of measurements. Since both measurements indicated but one transition in this temperature range, the internal friction maximum is accepted as indicative of the glass transition.

(2) *Block copolymers*—In *Figure 5* are plotted the shear modulus data for a series of butadiene-styrene block copolymers of varying composition. The 'step' character of these curves is very reminiscent of those reported for physical mixtures of homopolymers^{2, 3, 30}. The first step occurs near the glass transition of the polybutadiene segments and the second near the glass transition of the polystyrene. Also in *Figure 5* are plotted some of the corresponding internal friction data. Two of the curves have been omitted for clarity. Here, again the 'two-phase' nature of the block copolymer samples is quite evident.

For comparison purposes the blended sample of polystyrene and polybutadiene was prepared. Whereas the block copolymers pressed into clear

*The theoretical equations involving R^2 do not take account of the effect of the nature of the solvent on the chain configurations which alter the coefficients in the $M_{app} < R^2 >_{app}$ vs. v_s/v_0 function. This accounts for the scatter in *Figure 2*.

films, attempts to press clear specimens from this material failed. Temperatures as high as 235°C were attempted without success. The opacity of this film sample clearly indicated phase separation on a macro scale.

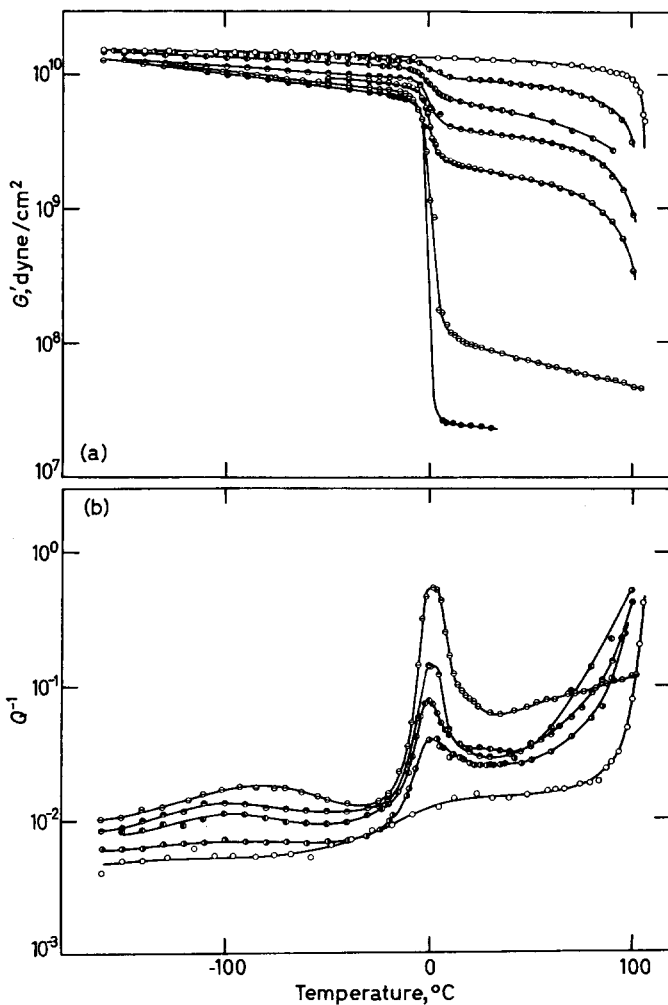


Figure 5—Styrene-butadiene block copolymers: temperature dependence of the torsion modulus, G' , and internal friction, Q^{-1} : \circ Polystyrene, \bullet S/B₁, \circ S/B₂, \bullet S/B₃, \circ S/B₄, \bullet S/B₅, and \bullet Polybutadiene

The data obtained are compared to those of copolymer, S/B₅, in Figure 6. The loss data, G'' , are very similar over the entire temperature range (-160°C to 100°C) but only a portion is plotted in Figure 6(a). This plot illustrates the great similarity in size and shape of the peaks, and the closeness of the maxima on the temperature scale. The modulus data,

[Figure 6(b)], show a striking difference. Although the positions of the modulus drops are nearly the same, the magnitudes differ by a factor of ten.

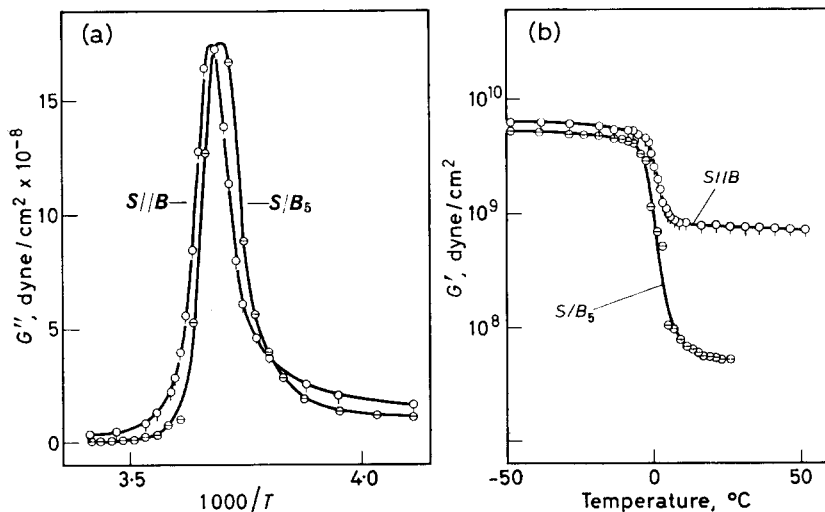


Figure 6—Comparison of a physical blend and a block copolymer: \ominus S/B₅, \circ S//B: (a) Loss modulus, G'' , versus $1/T$, (b) Temperature dependence of the torsion modulus, G'

Data were collected on sample B/S to examine the effect of segment position in the polymer molecule. Whereas the other polymers had polystyrene centre segments, sample B/S had polybutadiene as its centre

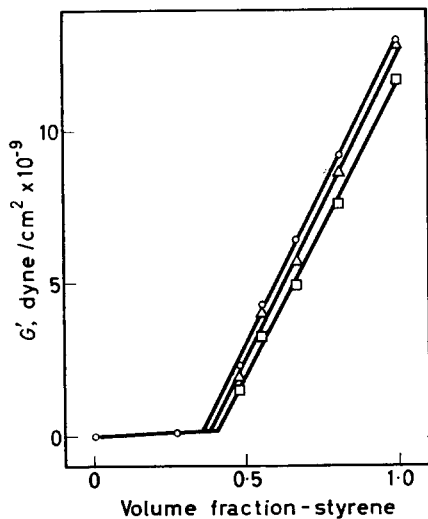


Figure 7—Torsion modulus versus copolymer composition; \circ 25°C, Δ 50°C, \square 75°C

segment. The results were compared with those of S/B₁. Except for the small differences expected from the slight composition variance, the mechanical behaviour of the specimens appeared identical.

For given temperatures between the glass peaks of the two homopolymers, plots of the shear moduli versus compositions show an interesting result. This can be seen in *Figure 7*. For the larger styrene contents, the shear modulus appears to be a linear function of the volume fraction of polystyrene. A simplified model assuming parallel bonding of Maxwell elements predicts a linear dependence between the modulus of pure polystyrene and that of the pure polybutadiene. The failure of this simplified model may be expected, but more sophisticated treatments also fail in that they do not predict linear behaviour over such a large composition range³¹. Further examination of the two-phase system reveals a possible explanation. At the high polystyrene contents, one would expect a dispersion of 'soft' phases in a continuous 'hard' medium. As the composition changes, the roles of the components would switch and the material would behave as a uniform dispersion of 'hard' phases in a 'soft' continuum.

(3) *Terpolymers*—Styrene-butadiene block copolymers illustrate viscoelastic behaviour of block copolymers composed of segments of rather different character. The two-phase nature of such specimens is evident. In this case, the invariance of the individual phase transitions with composition is also adequately demonstrated. On the other hand, the behaviour of block copolymers composed of segments of similar character has received very little attention. Baer⁵ recently reported on block copolymers of styrene and α -methylstyrene, which appear to be single-phase materials, exhibiting a single glass transition. The mechanical behaviour of block copolymers with very similar segments, butadiene and isoprene, was of interest here. A styrene-isoprene block copolymer, S/I, and two styrene-butadiene-isoprene block terpolymers, S/B/I and B/S/I, were prepared for this purpose. Polystyrene segments were included not only to provide an added variable—i.e. separation of the 'soft' segments on the chain—

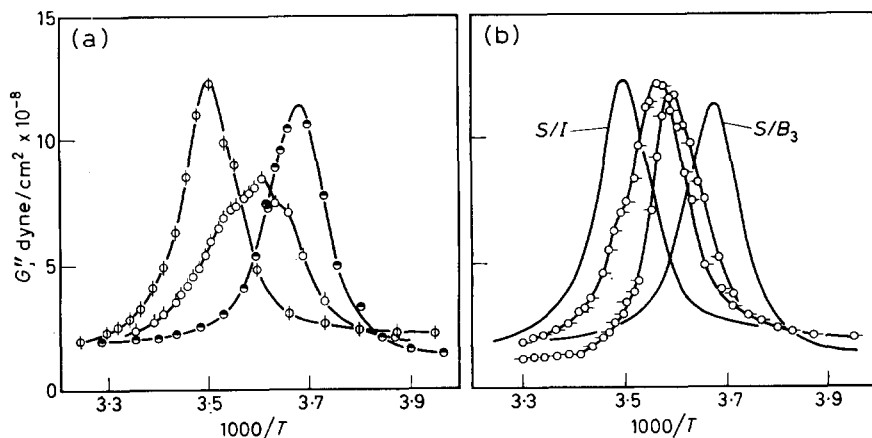


Figure 8—Terpolymers and blends: loss modulus versus $1/T$. ϕ S/I, \circ S/B//S/I, \bullet S/B₃, \circ B/S/I, \circ S/B/I; (a) Comparison of a blend and two block copolymers, (b) Comparison of the block terpolymers and two block copolymers

but also to impart a certain amount of stiffness to the specimens at temperatures above the transition regions of 'soft' segments. The latter was an experimental expedient used to ensure precise, reproducible results.

In Figure 8(a) are plotted the loss modulus data for copolymers, S/B₃ and S/I, and also comparable data for a physical mixture or blend, S/B//S/I. In all of these samples the styrene content was about 50 mole per cent. The data for the S/B₃ and S/I specimens suggest that one should be able to verify, experimentally, the existence of a double loss peak if two 'soft' phases were formed in the physical mixture. Such was not so. The data for the blend reveal a broad, low peak having structure which may be explained by assuming that only a portion of the polyisoprene and polybutadiene segments were able to blend into a single phase. This would account for the large centre peak with its maximum between those for the pure polyisoprene and polybutadiene phases. The remainder of the 'soft' segments were kept from blending, possibly because of inadequate mixing techniques or possibly because of the large polystyrene segments, and could account for the shoulders on both sides of the blend peak.

In Figure 8(b) data are presented for the two terpolymer samples. Sample S/B/I contains polybutadiene and polyisoprene segments adjacent to each other on the polymer chain. This proximity provided unhindered phase blending of the two soft segments as indicated by the sharp symmetrical peak located between those for the homopolymer phases. In sample B/S/I, the centre polybutadiene segment is separated from the polyisoprene chains by the stiff polystyrene segments. The loss modulus data show basically one peak, but careful examination reveals that the peak is broader than that for S/B/I and a shoulder appears near 10°C ($3.5 \times 10^{-3} \text{ }^\circ\text{K}^{-1}$). These results indicate slight imperfections in the blending of the two soft segments as influenced by their relative positions in the polymer chain.

The authors would like to thank Dr F. P. Gay of our laboratory for many valuable discussions and Dr R. R. Garrett of the Elastomer Chemicals Department for the linear expansion measurements.

*E. I. du Pont de Nemours & Co., Inc.
Film Department, Experimental Station,
Wilmington, Delaware, U.S.A.*

(Received June 1964)

REFERENCES

- ¹ NIELSEN, L. E. *Mechanical Properties of Polymers*, p 27, Reinhold: New York, 1962
- ² NIELSEN, L. E. *J. Amer. chem. Soc.* 1953, **75**, 1435
- BUCHDAHL, R. and NIELSEN, L. E. *J. Polym. Sci.* 1955, **15**, 1
- ³ JENCKEL, E. and HERWIG, H. U. *Kolloidzshr.* 1956, **148**, 57
- ⁴ HUGHES, L. J. and BROWN, G. L. *J. appl. Polym. Sci.* 1961, **5**, 580; 1963, **7**, 59
- RE MBAUM, A., ELLS, F. R., MORROW, R. C. and TOBOLSKY, A. V. *J. Polym. Sci.* 1962, **61**, 155
- RE MBAUM, A., MOACANIN, J. and CUDDIHY, E. *J. Polym. Sci.* 1963, **C4**, 529
- TOBOLSKY, A. V. and REMBAUM, A. *J. appl. Polym. Sci.* 1964, **8**, 307
- ⁵ BAER, M. *J. Polym. Sci.* 1964, **A2**, 417

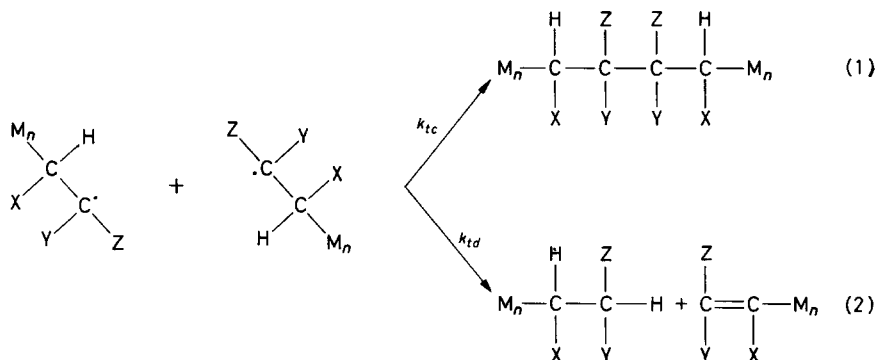
- ⁶ SZWARC, M. *Nature, Lond.* 1956, **178**, 1168
 SZWARC, M., LEVY, M. and MILKOVICH, R. *J. Amer. chem. Soc.* 1956, **78**, 2656
 SZWARC, M. and REMBAUM, A. *J. Polym. Sci.* 1956, **22**, 189
⁷ WENGER, F. *Makromol. Chem.* 1960, **36**, 200; 1963, **64**, 151
 WENGER, F. *J. Polym. Sci.* 1962, **60**, 99
 SCHLIEK, S. and LEVY, M. *J. phys. Chem.* 1960, **64**, 883
⁸ BRODY, H., LADACKI, M., MILKOVICH, R. and SZWARC, M. *J. Polym. Sci.* 1957, **25**, 221
 OROFINO, T. A. and WENGER, F. *J. chem. Phys.* 1961, **35**, 532
⁹ MORTON, M., MILKOVICH, R., MCINTYRE, D. B. and BRADLEY, J. L. *J. Polym. Sci.* 1963, **A1**, 443
¹⁰ LEE, C. L., SMID, J. and SZWARC, M. *J. phys. Chem.* 1962, **66**, 904
¹¹ BAUM, F. J. and BILLMEYER, F. W. *J. opt. Soc. Amer.* 1961, **51**, 452
¹² CANTOW, H. J. and SCHULZ, G. V. *Z. phys. Chem.* 1954, **1**, 365
¹³ DEBYE, P. *J. appl. Phys.* 1944, **15**, 338
 DEBYE, P. *J. Phys. Colloid Chem.* 1947, **51**, 18
¹⁴ ILLERS, K. H. and JENCKEL, E. *Kolloidzshr.* 1958, **160**, 97
¹⁵ WANG, C. *Applied Elasticity*. McGraw-Hill: New York, 1953
¹⁶ INOUE, Y. and KOBATAKI, Y. *Kolloidzshr.* 1958, **159**, 18
¹⁷ RICHARDSON, W. S. *J. Polym. Sci.* 1954, **13**, 229
¹⁸ SILAS, R. S., YATES, J. and THORNTON, V. *Analyt. Chem.* 1959, **31**, 529
¹⁹ RICHARDSON, W. S. and SACHER, A. *J. Polym. Sci.* 1953, **10**, 353
²⁰ CONDON, F. E. *J. Polym. Sci.* 1953, **11**, 139
 MEYER, A. W. *Industr. Engng Chem. (Industr.)*, 1949, **41**, 1570
²¹ TREMBLAY, R., RINFRET, M. and RIVEST, R. *J. chem. Phys.* 1952, **20**, 523
²² STOCKMAYER, W. H., MOORE, Jr, C. D., FIXMAN, M. and EPSTEIN, B. N. *J. Polym. Sci.* 1955, **16**, 517
²³ KRAUSE, S. *J. phys. Chem.* 1961, **65**, 1618
²⁴ BUSHUK, W. and BENOIT, H. *Canad. J. Chem.* 1958, **36**, 1616
²⁵ LENG, M. and BENOIT, H. *J. Chim. phys.* 1961, **58**, 479
²⁶ BENOIT, H. and WHIPPLER, C. *J. Chim. phys.* 1960, **57**, 524
²⁷ WOODWARD, A. E., SAUER, J. A. and WALL, R. A. *J. chem. Phys.* 1959, **30**, 854
 WOODWARD, A. E., SAUER, J. A. and WALL, R. A. *J. Polym. Sci.* 1961, **50**, 117
²⁸ NEWMAN, S. and COX, W. P. *J. Polym. Sci.* 1960, **46**, 29
²⁹ DANNIS, M. L. *J. appl. Polym. Sci.* 1959, **1**, 121
³⁰ TOBOLSKY, A. V. *Properties and Structure of Polymers*, p 82. Wiley: New York, 1960
³¹ KERNER, E. H. *Proc. Roy. Soc. B*, 1956, **69**, 808
 LANDEL, R. F. *Trans. Soc. Rheol.* 1958, **2**, 53
 SMALLWOOD, H. M. *J. appl. Phys.* 1944, **15**, 758

Radiochemical Studies of Free Radical Vinyl Polymerization III—Bulk Polymerization of Styrene, *p*-Methoxystyrene and *p*-Chlorostyrene*

G. AYREY, F. G. LEVITT and R. J. MAZZA

Azoisobutyronitrile-¹⁴C has been used to initiate polymerization of styrene, p-methoxystyrene and p-chlorostyrene at 60° and 80°C. Rates and efficiencies of initiation have been measured and are compared with values obtained previously in similar systems. Factors affecting the bimolecular termination of polymer radicals are discussed and it is shown that polar effects are important in polymer radical-radical interactions. For styrene and p-chlorostyrene termination is by combination, but with p-methoxystyrene 19 per cent and 47 per cent of polymer radicals are terminated by disproportionation at 60° and 80° C respectively.

PAIRS of polymer radicals can interact either by combination (reaction 1), or by disproportionation (reaction 2).



It has been suggested that the mode of termination in specific instances is governed by steric factors, the availability and reactivity of hydrogen atoms adjacent to the radical site, reaction temperature, and polymer radical reactivity. The relative importance and interdependence, or even relevance, of these various factors have not been well defined and it is certainly not possible to predict with any certainty the mode of reaction of a particular pair of polymer radicals.

Accurate information on this type of reaction was rarely available from studies of reaction kinetics. However, the advent of isotopic tracer techniques¹⁻³ introduced a powerful tool for the investigation of these and other polymerization processes.

*Joint contribution from the Isotope Unit and the Department of Chemistry, Queen Elizabeth College (University of London), Campden Hill Road, London W.8.

Studies previously reported give some indication of the effects of temperature and radical structure. Thus, in the polymerization of methyl methacrylate it has been shown that mutual termination of polymer radicals occurs by both combination and disproportionation^{1,2,4}, the importance of the latter reaction increasing with increasing temperature². Polymethyl methacrylate radicals have hydrogen atoms available for the disproportionation reaction at both the penultimate carbon atom in the chain and at the α -methyl group. This multiplicity of sites together with the steric effects of the methyl and ester groups on the α -carbon may account for the observed tendency to disproportionation but it is also possible that the electron withdrawing power of the ester group has some effect.

Polystyrene radicals are known to terminate solely by combination at temperatures up to 70°C^{1,2,4-8} and the present work has extended this range to 80°. In this instance the steric effects are not so marked and there are only two hydrogen atoms available for the disproportionation reaction. Further, the polystyrene radical is inherently much less reactive than that of polymethyl methacrylate because of resonance stabilization by the phenyl group.

The difference between polystyrene and polymethyl methacrylate radicals is too great to permit a detailed comparison of the effects of radical reactivity on the mode of termination. The present work was undertaken, therefore, in an attempt to isolate the effect of radical reactivity through a correlation of the well known effects of nuclear aromatic substituents with the modes of termination of nuclear substituted polystyrene radicals.

The monomers chosen for this study were *p*-methoxystyrene and *p*-chlorostyrene since it was thought unlikely that these monomers would give rise to complicating chain transfer reactions. Methoxy is an effective electron donating group (Hammett $\sigma = -0.268$) while the chloro substituent has the opposite effect (Hammett $\sigma = +0.226$). Styrene was also polymerized at 80° since comparable results have not previously been reported at this temperature.

Use of azoisobutyronitrile-¹⁴C (AIBN-¹⁴C) to initiate polymerization also enabled us to calculate rates and efficiencies of initiation⁹ and these results are compared with earlier results for similar systems³.

RESULTS

Rates of polymerization (R_p) were measured dilatometrically. Number average molecular weights (\bar{M}_n) were measured osmotically in toluene solutions and in the case of styrene only were calculated from the limiting viscosity number. Specific activities of polymers (a_p) and of the initiator ($a_i = 2.13 \times 10^8$ c sec⁻¹ mole⁻¹ for results in *Table 2*, and 1.00×10^8 c sec⁻¹ mole⁻¹ for results in *Tables 1* and *3*) were determined by liquid scintillation counting.

The results of these measurements together with monomer concentration $[M]_0$, initiator concentration $[I]_0$ and time of reaction (t), are recorded in *Tables 1*, *2* and *3* for styrene, *p*-methoxystyrene and *p*-chlorostyrene respectively.

STUDIES OF FREE RADICAL VINYL POLYMERIZATION III

 Table 1. AIBN-¹⁴C initiated polymerization of styrene at 80°C

Expt No.	Temp. °C	[M] ₀	[I] ₀	t	R _p	\bar{M}_n	a _p
		mole l ⁻¹	mole l ⁻¹ × 10 ³	sec × 10 ⁻³	mole l ⁻¹ sec ⁻¹ × 10 ⁴	× 10 ⁻⁵	c sec ⁻¹ g ⁻¹ × 10 ⁻³
1	80	8.20	0	13.500	0.104	9.330	0
2	80	8.20	1.75	1.050	~1.96	1.200	0.779
3	80	8.20	3.62	1.050	2.62	0.824	1.19
4	80	8.19	6.00	1.050	3.81	0.689	1.50

 Table 2. AIBN-¹⁴C initiated polymerization of *p*-methoxystyrene at 60° and 80°C

Expt No.	Temp. °C	[M] ₀	[I] ₀	t	R _p	\bar{M}_n	a _p
		mole l ⁻¹	mole l ⁻¹ × 10 ³	sec × 10 ⁻³	mole l ⁻¹ sec ⁻¹ × 10 ⁴	× 10 ⁻⁵	c sec ⁻¹ g ⁻¹ × 10 ⁻²
5	60	7.16	—	21.960	0.033	4.898	—
6	60	7.16	3.40	15.120	0.537	2.715	6.34
7	60	7.16	3.69	12.600	0.590	2.455	6.44
8	60	7.15	7.73	9.600	0.777	1.742	9.55
9	60	7.14	13.5	7.200	1.05	1.496	12.7
10	60	7.13	21.6	5.412	1.37	1.073	16.9
11	60	7.13	24.6	4.080	1.36	1.080	19.2
12	80	7.03	—	30.720	0.160	2.528	—
13	80	7.03	0.961	2.400	1.62*	2.023	7.06
14	80	7.03	2.28	3.870	2.24*	1.308	11.0

*Rates measured gravimetrically.

 Table 3. AIBN-¹⁴C initiated polymerization of *p*-chlorostyrene at 60° and 80°C

Expt No.	Temp. °C	[M] ₀	[I] ₀	t	R _p	\bar{M}_n	a _p
		mole l ⁻¹	mole l ⁻¹ × 10 ³	sec × 10 ⁻³	mole l ⁻¹ sec ⁻¹ × 10 ⁴	× 10 ⁻⁵	c sec ⁻¹ g ⁻¹ × 10 ⁻²
15	60	7.60	—	27.480	0.078	—	—
16	60	7.60	7.12	10.466	0.928	2.455	3.67
17	60	7.59	13.5	10.980	1.08	1.831	4.97
18	60	7.56	37.5	4.451	1.95	1.194	7.62
19	60	7.50	89.3	3.127	3.02	0.659	13.9
20	60	7.41	162	2.656	3.86	0.490	19.9
21	80	7.46	—	36.300	0.291	3.160	—
22	80	7.46	2.62	1.927	3.27*	1.756	5.28
23	80	7.46	6.47	2.285	5.15*	1.039	8.25
24	80	7.45	9.26	1.560	6.27*	0.955	9.75

*Rates measured gravimetrically.

DISCUSSION

(1) The initiation reaction

Rates of initiation were calculated via equation (3)

$$R_{i,\text{cat.}} = (R_p/\nu) ([I]_0/[I]_{\text{av.}}) \quad (3)$$

where ν , the mean kinetic chain length, is obtained from the specific activity of the polymer, a_p , the specific activity of the initiator, a_i , and the molecular weight of the monomer, m , according to equation (4).

$$\nu = a_i / 2m \cdot a_p \quad (4)$$

This calculation takes into account the fact that two radicals are produced from each molecule of initiator but does not allow for any thermal initiation $R_{i\text{therm}}$, which may occur; $R_{i\text{cat}}$, therefore, is the rate of initiation by AIBN-¹⁴C only. At 60°C $R_{i\text{therm}}$ is sufficiently small to be neglected but at 80° it may become significant. This aspect is discussed further in section (2). The factor $[I]_0/[I]_{\text{av}}$ allows for the fall off in rate during the course of the reaction because of loss of initiator; $[I]_{\text{av}}$ is the mean initiator concentration during the reaction period⁹. It has previously been shown that AIBN does not become attached to polymer via chain transfer reactions at temperatures up to 60°. Such reactions seem equally unlikely at 80° and the data plotted in *Figures 4 to 6* tend to support these observations, since the plots are more or less linear (see p 162). Similarly, it is unlikely that any initiation could occur via hydrogen abstraction. Finally, it was demonstrated that loss of low molecular weight polymer during precipitation was insignificant.

Initiator efficiencies, f , were calculated using equation (5)

$$R_{i\text{cat}} = 2fk_d [I]_0 \quad (5)$$

where k_d is the first order rate constant for decomposition of the initiator. In the present work values of k_d were taken as $1.20 \times 10^{-5} \text{ sec}^{-1}$, and $1.54 \times 10^{-4} \text{ sec}^{-1}$, at 60° and 80° respectively.

The use of the former has been justified previously¹⁰ and we consider that the value at 80° which is based on careful experimentation^{11,12} is the most reliable one available. Values calculated from Arrhenius relationships tend to be somewhat lower, viz. $1.03 \times 10^{-5} \text{ sec}^{-1}$ and $1.43 \times 10^{-4} \text{ sec}^{-1}$ ¹³ or $1.11 \times 10^{-5} \text{ sec}^{-1}$ and $1.49 \times 10^{-4} \text{ sec}^{-1}$ ¹⁴ at 60° and 80° respectively. However, such relationships embrace data of very variable quality, and as seen above are not themselves concordant.

Values of $R_{i\text{cat}}$, $R_{i\text{cat}}/[I]_0$ and f obtained from the data of *Tables 1 to 3* are recorded in *Tables 4 and 5*.

If our chosen values of k_d are too high (see above) then the recorded values for f are too low by a commensurate amount.

At 60°C values for $R_{i\text{cat}}/[I]_0$ previously reported for a variety of monomers range from 1.02×10^{-5} to 1.53×10^{-5} with a mean value of 1.23×10^{-5} , and values for f range³ from 0.43 to 0.70 with a mean of 0.53. The values recorded in *Table 4* all fall well within this range and are in harmony with the accepted view that a substantial amount of initiator is lost in wasteful side reactions.

There are indications that at 80°C (*Table 5*) efficiencies are somewhat higher, possibly reflecting a greater ease of escape of initiator radicals from the solvent cage due to increased thermal excitation. As pointed out above, such an observation is dependent upon the chosen value of k_d and possibly even higher values of f may obtain. The only relevant

STUDIES OF FREE RADICAL VINYL POLYMERIZATION III

information in the literature is an observed value of $f=0.88$ for 1-azocyclohexane carbonitrile initiated polymerization of styrene at 80°C^{15} . Unfortunately thermal decomposition of this compound is probably too slow at 60° , and photochemical decomposition at 60° has not been reported, so that direct comparison is not possible at the present time.

 Table 4. Rates and efficiencies of initiation at 60°C

Expt No.	Monomer	$[\text{I}]_0$ mole l^{-1} $\times 10^3$	$R_{i \text{ cat.}}$ mole l^{-1} sec^{-1} $\times 10^3$	$\frac{R_{i \text{ cat.}}}{[\text{I}]_0}$ sec^{-1} $\times 10^5$	f
6	<i>p</i> -MeOStyrene	3.40	4.68	1.37	0.57
7	"	3.69	5.15	1.40	0.58
8	"	7.73	9.88	1.28	0.53
9	"	13.5	17.5	1.30	0.54
10	"	21.6	30.0	1.39	0.58
11	"	24.6	33.6	1.36	0.57
16	<i>p</i> -ClStyrene	7.12	10.0	1.41	0.59
17	"	13.5	15.9	1.18	0.49
18	"	37.5	42.2	1.12	0.47
19	"	89.3	118	1.32	0.55
20	"	162	216	1.34	0.56

 Table 5. Rates and efficiencies of initiation at 80°C

Expt No.	Monomer	$[\text{I}]_0$ mole l^{-1} $\times 10^3$	$R_{i \text{ cat.}}$ mole l^{-1} sec^{-1} $\times 10^7$	$\frac{R_{i \text{ cat.}}}{[\text{I}]_0}$ sec^{-1} $\times 10^4$	f
2	Styrene	1.75	3.44	1.96	0.64
3	"	3.62	6.73	1.86	0.60
4	"	6.00	12.7	2.14	0.70
13	<i>p</i> -MeOStyrene	0.961	1.73	1.80	0.58
14	"	2.28	4.11	1.80	0.59
22	<i>p</i> -ClStyrene	2.62	5.53	2.11	0.69
23	"	6.47	14.0	2.16	0.70
24	"	9.26	19.1	2.06	0.67

(2) The termination reaction

Provided that polymer molecules are formed solely by mutual interaction of pairs of polymer radicals via reactions (1) and (2), determination of the mode of termination is simply a matter of obtaining the number of initiator fragments per polymer molecule^{1,2}. If a labelled initiator such as AIBN-¹⁴C is used, this number may be determined with the aid of equation (6).

$$n = 2a_p \bar{M}_n / a_i \quad (6)$$

The specific activities of polymer and initiator can be determined with good accuracy by liquid scintillation counting. The determination of \bar{M}_n by osmotic pressure measurements, however, is fraught with difficulties

resulting from solute diffusion¹⁶ and even interpretation of the data¹⁷. We have attempted to surmount these difficulties by use of cellulose acetate membranes¹⁸ and by use of an unequivocal method for extrapolation of the data¹⁹.

Apart from errors in \bar{M}_n , the value of n may be too large if: (i) termination by combination of a polymer radical with an initiator radical occurs, or (ii) if chain transfer to initiator takes place. The monomers considered in this paper were all relatively reactive, their concentrations were high and temperatures were moderately high. Also polymerizations were stopped after about ten per cent conversion. All these factors militate against primary radical termination. Further, the order of overall polymerization with respect to initiator is 0.5 (Figures 1, 2 and 3), hence it

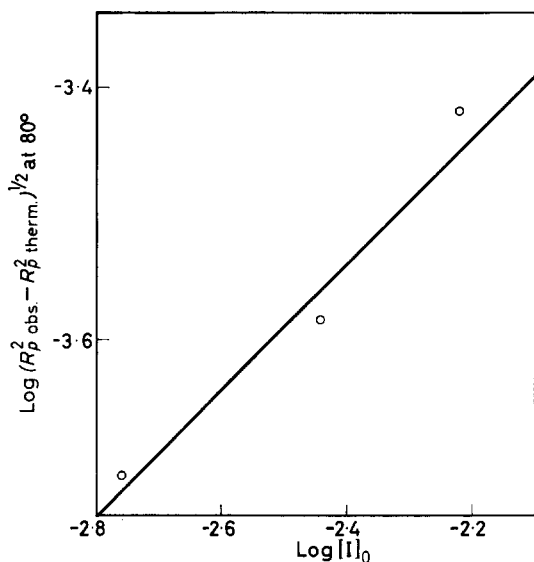


Figure 1—Dependence of rate of polymerization on initiator concentration for styrene at 80°C. Points are experimental. Line is drawn with a theoretical slope of $\frac{1}{2}$

is considered that termination via (i) is insignificant. There is no evidence in the literature that AIBN participates in transfer reactions. Such transfer reactions require that plots of reciprocal degree of polymerization $1/\bar{P}_n$ against R_p should be curved since

$$\frac{1}{\bar{P}_n} = C_M + \frac{(k_t/k_p^2) R_p}{[M]_0^2} + C_I \frac{(k_t/k_p^2 f k_d) R_p^2}{[M]_0^3} \quad (7)$$

where C_M and C_I are transfer constants for monomer and initiator respectively. There is no evidence of curvature in Figures 4, 5 and 6, therefore process (ii) may be disregarded.

The value of n may be too small if: (iii) transfer to monomer occurs, or (iv) if initiation occurs via processes other than addition of initiator radicals to the monomer double bond. The intercepts on plots of $1/\bar{P}_n$ against R_p are a measure of chain transfer to monomer (cf. equation 7).

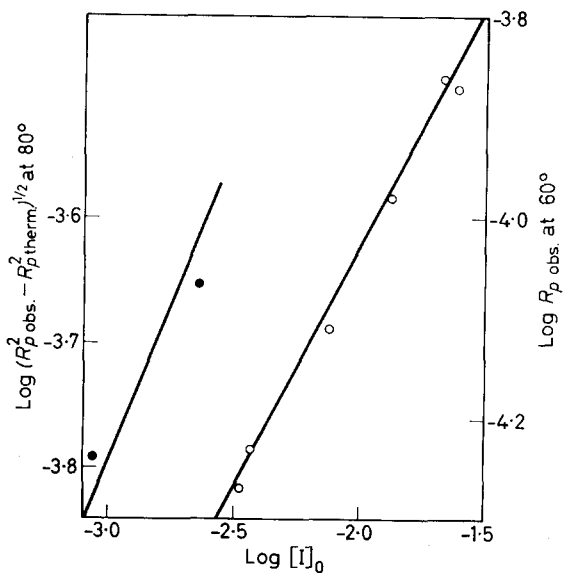


Figure 2—Dependence of rate of polymerization on initiator concentration for *p*-methoxystyrene at 60° and 80°C. Points are experimental. Lines are drawn with a theoretical slope of $\frac{1}{2}$

In Figures 4, 5 and 6, these intercepts are very small and consequently process (iii) may be neglected. There is abundant evidence that AIBN cannot initiate polymerizations by hydrogen abstraction, and initiation via the ionizing β -particles is also known to be insignificant. At 60°C thermal

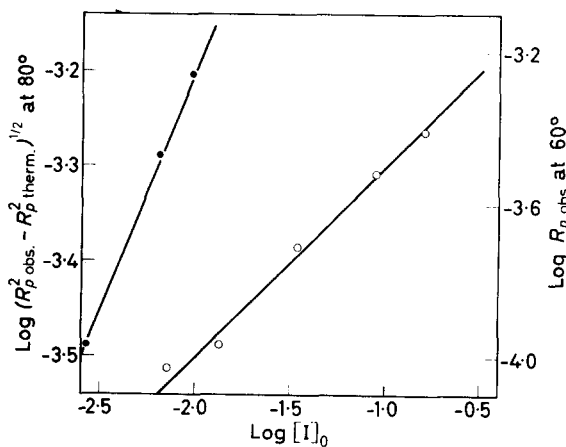


Figure 3—Dependence of rate of polymerization on initiator concentration for *p*-chlorostyrene at 60° and 80°C. Points are experimental. Lines are drawn with a theoretical slope of $\frac{1}{2}$

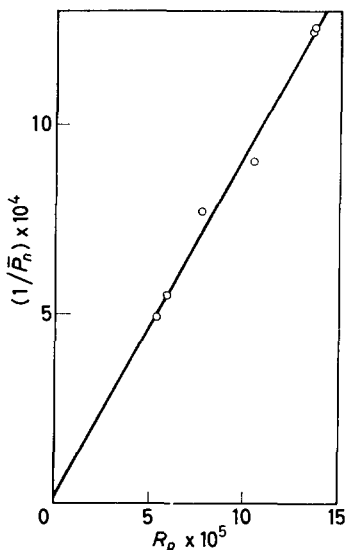


Figure 4—Plot of reciprocal degree of polymerization against rate for *p*-methoxystyrene at 60°C

initiation is unimportant but at 80° such initiation, particularly of the substituted styrenes, may be significant (expts 12 and 21), hence a correction to the value of n was attempted.

Without specifying the mode of thermal initiation but assuming bimolecular termination and that the steady state approximation holds, it is possible to derive an expression for the rate of thermal initiation, $R_{i\text{therm.}}$.

$$R_{i\text{therm.}} = \frac{2R_p^2 \text{therm.}}{[M]_0^2} \times \frac{k_t}{k_p^2} \quad (8)$$

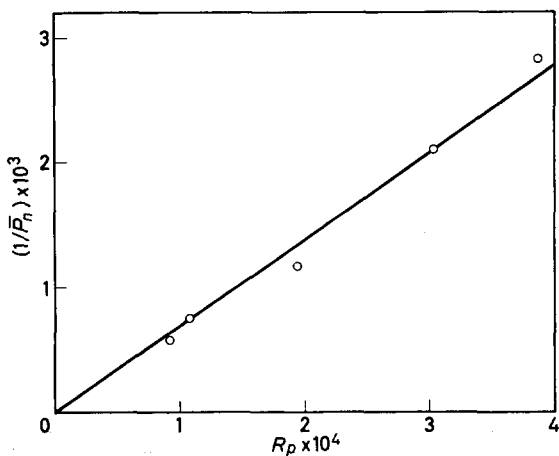


Figure 5—Plot of reciprocal degree of polymerization against rate for *p*-chlorostyrene at 60°C

where $k_t = (k_{td} + k_{tc})$ is the termination rate constant and k_p is the rate constant for the propagation step. The ratio k_t/k_p^2 is constant for a particular monomer at a given temperature and may be determined either from the slope of plots of $1/\bar{P}_n$ against R_p (cf. equation 7) or from rates of initiation determined radiochemically and use of equation (9).

$$R_{i\text{cat.}} = \frac{2(R_{p\text{obs.}}^2 - R_{p\text{therm.}}^2)}{[M]_0^2} \cdot \frac{k_t}{k_p^2} \quad (9)$$

If it is now assumed that thermal initiation occurs solely via monoradical formation* then the fraction of chain ends not containing an initiator fragment is given by $R_{i\text{therm.}}/(R_{i\text{cat.}} + R_{i\text{therm.}})$. Consequently the observed value of n may be corrected to give a value, $n_{\text{corr.}}$, via equation (10).

$$n_{\text{corr.}} = n \left(1 - \frac{R_{i\text{therm.}}}{R_{i\text{cat.}} + R_{i\text{therm.}}} \right)^{-1} \quad (10)$$

This equation will hold provided that $R_{i\text{cat.}}$ does not change more than a few per cent during the course of the experiment.

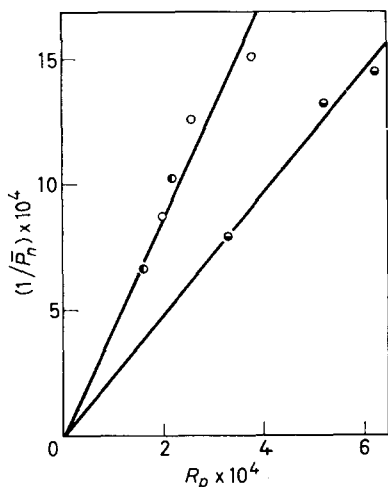


Figure 6—Plots of reciprocal degrees of polymerization against rates at 80°C.

○ styrene, ● p-methoxystyrene,
● p-chlorostyrene

It must be acknowledged that, in this paper, $R_{i\text{therm.}}$ is based upon one measurement only, and consequently is likely to have a wide margin of error so that the corrections made by application of equation (10) are merely approximations. However, they serve to show that even at 80°C thermal initiation does not vitiate the results which are recorded in *Tables 6, 7 and 8*.

The results in *Tables 6 and 8* indicate that both poly-styrene and poly-*p*-chlorostyrene radicals are terminated via combination reactions. On the other hand, the results in *Table 7* suggest that some poly-*p*-methoxystyrene

If thermal initiation occurs via formation of diradicals, it will have no effect on the number of chain ends in the final product when termination is by combination. However, since diradical initiation is not now considered plausible, we have assumed monoradical initiation.

Table 6. Values of n and k_t/k_p^2 derived for styrene at 80°C

Expt No.	Temp. °C	$\bar{M}_n \times 10^{-5}$	n	$n_{\text{corr.}}$	k_t/k_p^2 mole l^{-1} sec	k_t/k_p^{2*} mole l^{-1} sec
2	80	1.200	1.87	1.88	302	
3	80	0.824	1.96	1.96	331	
4	80	0.689	2.07	2.07	297	
						296

*From slope of Figure 6.

Table 7. Values of n and k_t/k_p^2 derived for *p*-methoxystyrene at 60° and 80°C

Expt No.	Temp. °C	$\bar{M}_n \times 10^{-5}$	n	$n_{\text{corr.}}$	k_t/k_p^2 mole l^{-1} sec	k_t/k_p^{2*} mole l^{-1} sec
6	60	2.715	1.62	1.63	418	
7	60	2.455	1.48	1.49	380	
8	60	1.742	1.56	1.56	420	
9	60	1.496	1.78	1.78	407	
10	60	1.073	1.70	1.70	410	
11	60	1.080	1.95	1.95	465	
						455
13	80	2.023	1.34	1.36	164	
14	80	1.308	1.35	1.36	204	
						218

*From slope of Figures 4 and 6.

radicals are terminated by disproportionation. The fraction of radicals undergoing disproportionation is given by $(2-n)/n$ and for this system is 0.19 at 60° and 0.47 at 80°C.

In the systems reported here two factors affecting the termination reaction, viz. steric effects and the number of hydrogen atoms on the β -carbon atom, have been kept constant. Thus it is possible to examine more closely the remaining factors which govern the mode of termination.

The values of k_t/k_p^2 collected together in Tables 6, 7 and 8 show that both *p*-methoxystyrene and *p*-chlorostyrene are slightly more reactive monomers than styrene ($k_t/k_p^2 \approx 700$ mole l^{-1} sec at 60°) and therefore must both have somewhat less reactive polymer radicals than styrene because of the additional resonance structures possible due to the substituent groups. This fact seems to rule out any explanation for the disproportionation reaction in general terms of radical reactivity. Hence, the specific importance of the electron donating properties of the *p*-methoxy group require explanation.

Szwarc²⁰ recently pointed out that, although free radicals are neutral species, changes in structure may invoke slightly nucleophilic or electrophilic character resulting in a wide spectrum of possible responses. Earlier indications of 'polar' effects in free radical reactions were evident in appli-

STUDIES OF FREE RADICAL VINYL POLYMERIZATION III

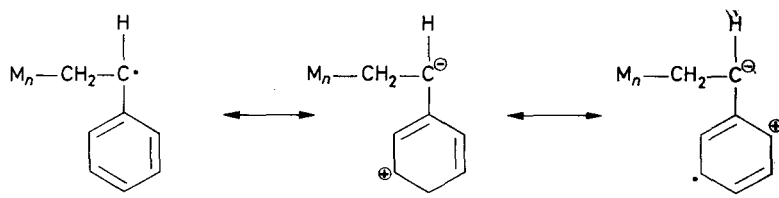
 Table 8. Values of n and k_t/k_p^2 derived for *p*-chlorostyrene at 60° and 80°C

Expt No.	Temp. °C	$\bar{M}_n \times 10^{-5}$	n	$n_{\text{corr.}}$	k_t/k_p^2 mole l^{-1} sec	k_t/k_p^{2*} mole l^{-1} sec
16	60	2.455	1.80	1.81	336	
17	60	1.831	1.82	1.82	391	
18	60	1.194	1.82	1.82	318	
19	60	0.659	1.83	1.83	364	
20	60	0.490	1.95	1.95	398	
						401
22	80	1.756	1.85	1.86	109	
23	80	1.039	1.71	1.72	146	
24	80	0.955	1.86	1.87	137	
						145

*From slope of Figures 5 and 6.

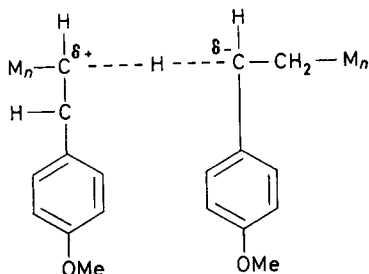
cations of the Hammett equation to radical copolymerizations of styrene with substituted styrenes²¹ and to the effects of substituents on the rates of decomposition of various dibenzoyl peroxides²². For copolymerization in particular it was recognized that radical reactivity was dependent upon both polar and non-polar factors²³. The Alfrey-Price *Q-e* scheme was an important attempt to separate these factors and is still widely used for predicting behaviour in co-polymerizations. More recently, Bamford and Jenkins have discussed the weaknesses inherent in the *Q-e* scheme and have proposed a new scheme, more widely applicable to a variety of polymer radical-substrate reactions²⁴⁻²⁶. Their scheme is intended to place the separation of polar and non-polar contributions on a more secure experimental basis²⁷, and they have tabulated derived reactivity parameters for a large number of monomers²⁶. The scheme has been applied by Bevington to show that polar effects are important in the reactions of the benzoyloxy radical²⁸. Thus, there is abundant evidence pointing to the importance of polar effects in radical-molecule reactions.

Currently, there are insufficient data to permit a comparable separation of polar and non-polar factors in radical-radical interactions. The present work is considered to be a demonstration that polar effects have an important role in mutual termination reactions. The polystyrene radical, by virtue of the phenyl group, is essentially an electronegative radical:



This effect is considerably enhanced by the *p*-methoxy group, and there could, therefore, be an increased tendency for electrostatic repulsion

between poly-*p*-methoxystyrene radicals. Such repulsion would manifest itself as an increase in the energy requirements for combination. Further, the highly electronegative character of the radical should lead to a polarization of the transition state for disproportionation



and this polarization lowers the potential energy barrier for disproportionation. Thus, two factors may operate to assist the disproportionation reaction in this instance, though such factors have no importance in the other two systems studied.

The importance of polar effects in other termination reactions remains obscure but it is significant that in copolymerization of styrene and methyl methacrylate, termination is largely cross-termination by combination². Since polar effects are important for the alternating effect in copolymerization²³, and in the light of the present work, it seems reasonable to suppose that the electronegative polystyrene radical and the electropositive polymethyl methacrylate radical are mutually attracting and give rise to the observed results. We hope to investigate other examples of cross-termination reactions shortly.

EXPERIMENTAL

Materials

Azoisobutyronitrile-¹⁴C—This was prepared from 1,3-[¹⁴C]-acetone diluted with inactive AIBN and the radiochemical purity established as described in part I⁴. Similarly, *styrene* was purified by standard procedures⁴.

p-Methoxystyrene—*p*-Methoxyphenylmagnesium bromide was prepared from *p*-bromoanisole, and converted to *p*-methoxyphenylmethyl carbinol by reaction with acetaldehyde²⁹. The crude alcohol was fractionally distilled through an 18 in. Vigreux column (b.pt 83° to 90°C/0.1 mm Hg) and shown by gas-liquid chromatography (GLC) to be approximately 85 per cent pure. A pyridine solution of the alcohol (2.5 mole/l.) was treated with acetyl chloride to yield the acetate (b.pt 80°/0.2 mm Hg). GLC analysis showed that the only impurity was a trace of the carbinol. The acetate was pyrolysed in a stream of nitrogen at 500° on a 12 in. × ½ in. column of glass helices. The product was washed with 2*N* hydrochloric acid, ten per cent sodium hydroxide and water, dried over calcium sulphate and distilled *in vacuo*. Further purification was effected by passage through an alumina column in petroleum ether (b.pt 30° to 40°C) followed by fractional distillation through the 18 in. Vigreux column. A pure fraction had b.pt 37.5° to 39°/0.3 mm Hg. $\epsilon^{260} = 2.37 \times 10^4$ (cf. lit. value³⁰

STUDIES OF FREE RADICAL VINYL POLYMERIZATION III

$\epsilon^{258} = 1.92 \times 10^4$); GLC analysis revealed no impurities; the overall yield was approximately 25 per cent.

p-Chlorostyrene—*p*-Chlorobenzaldehyde was reacted with methyl magnesium iodide to yield *p*-chlorophenylmethyl carbinol (b.pt 77°C/0.2 mm Hg; 99 per cent pure by GLC). The acetate was prepared as above (b.pt 65°C/0.2 mm Hg; 97 per cent pure by GLC) and pyrolysed to yield *p*-chlorostyrene which was purified as above to give a fraction (b.pt 22°C/0.15 mm Hg; no impurity detectable by GLC. $\epsilon^{255} = 1.95 \times 10^4$, cf. lit. value³⁰ $\epsilon^{253} = 1.97 \times 10^4$), in overall yield of about 25 per cent.

Gas liquid chromatography

GLC analyses were performed on a Pye argon chromatograph using a 4 ft \times 4 mm column packed with Celite and either ten per cent Apiezon L grease or ten per cent silicone oil as the stationary phase. Column temperature was 150°C in all cases.

Polymerization procedure

Polymerizations were carried out in Pyrex dilatometers of bulb capacity approximately 6 ml and 10 ml. Monomers were distilled in a pot still at room temperature and $< 10^{-4}$ mm of mercury immediately before use. A known weight of AIBN was washed into the weighed dilatometer by the required volume of monomer. The contents of the dilatometer were degassed three times by cycles of freezing in liquid nitrogen, pumping at $< 10^{-4}$ mm and thawing to room temperature. Finally the dilatometer was sealed at $< 10^{-4}$ mm and re-weighed before immersion in an oil bath at $60^\circ \pm 0.1^\circ$ or $80^\circ \pm 0.1^\circ$ C.

Concentrations were calculated at 60° and 80°C using the densities shown in Table 9, measured dilatometrically on the pure monomers. Observed volume contractions for 100 per cent polymerizations, determined by gravimetric estimates of polymer yields, are also recorded in the Table 9.

Table 9

Monomer	Density ($g\ cm^{-3}$)		Volume contraction for 100% polymerization (%)	
	at 60°	at 80°	at 60°	at 80°
Styrene	—	0.852	—	18.46
<i>p</i> -Chlorostyrene	1.053	1.033	16.51	—
<i>p</i> -Methoxystyrene	0.961	0.944	12.93	—

Polymerizations were stopped at about ten per cent conversion, the contents of the dilatometers washed out with benzene and the polymers precipitated by slow addition of a tenfold excess of methanol containing 0.01 per cent calcium chloride. The mixtures were allowed to stand overnight at 0°C, then the polymers were collected in sintered glass crucibles, and dried to constant weight in a vacuum oven at 50° to 60°C (2 to 3 days). After polymer yields had been determined, further purification was affected by re-precipitation of one per cent (w/v) benzene solutions by addition of methanol. Two precipitations were adequate for complete

removal of uncombined initiator residues, and negligible loss of polymer was detected.

Radiochemical assay

The radiochemical assay of initiators and polymers was carried out by liquid scintillation counting. Redistilled AnalaR toluene was used as solvent, and the phosphor solution contained 3 g 2,5-diphenyloxazole (PPO) and 0.3 g 1,4-bis-2-(4-methyl-5-phenyloxazolyl)-benzene (dimethyl POPOP) per litre. Most of the assays were performed in an Ekco type N664A counter and each sample was counted alone and with added toluene-¹⁴C internal standard. Count-rates were corrected for background count and counter efficiency, and reproducibility was about ± 3 per cent (expressed as standard deviation). The polystyrene samples formed at 80°C were assayed in a Tri-Carb scintillation spectrometer type 3314 and in this case quench corrections were made by the channels ratio method³¹ with an improved reproducibility of about ± 1 per cent.

Molecular weight measurements

Molecular weights of unfractionated polymers were determined after the final precipitation. Osmotic pressures, π , were measured on toluene solutions of polymers by a static equilibrium procedure at 25°C. The osmometers used were a new type similar to those of Breitenbach and Forster³² but with larger cell capacity of ~ 2.5 ml. They had a total membrane area of approximately 8 cm² and were designed for filling and emptying through the 1 mm measuring capillary with a syringe and long cannula. We found this arrangement very convenient for handling radioactive solutions. Some trouble was experienced with diffusion of low molecular weight material but satisfactory cellulose acetate membranes were eventually selected from large batches prepared by Vaughan's method¹⁸. The number average molecular weights \bar{M}_n were obtained by linear extrapolations of $(\pi/c)^{1/2}$ as functions of concentration, c , to zero concentration as described previously¹⁹.

With styrene at 80°C molecular weights were obtained from the relationship³³

$$\bar{M}_n = 1.78 \times 10^5 [\eta]^{1.37}$$

Limiting viscosity numbers $[\eta]$ were measured in benzene solutions at 25°C using Ubbelohde dilution viscometers.

The authors gratefully acknowledge that this research was partly supported by grants to G.A. from the Department of Scientific and Industrial Research for assistance; and from the University of London Central Research Fund for purchase of Gas Chromatography apparatus. We are also indebted to Professor C. H. Bamford, F.R.S., for helpful suggestions during the preparation of this paper.

Queen Elizabeth College,
University of London

(Received June 1964)

REFERENCES

- ¹ BEVINGTON, J. C., MELVILLE, H. W. and TAYLOR, R. P. *J. Polym. Sci.* 1954, **12**, 449
- ² BEVINGTON, J. C., MELVILLE, H. W. and TAYLOR, R. P. *J. Polym. Sci.* 1954, **14**, 464
- ³ AYREY, G. *Chem. Rev.* 1963, **63**, 645
- ⁴ AYREY, G. and MOORE, C. G. *J. Polym. Sci.* 1959, **36**, 41
- ⁵ FUNT, B. L. and PASIKA, W. *Canad. J. Chem.* 1960, **38**, 1865
- ⁶ HENRICI-OLIVÉ, G. and OLIVÉ, S. *J. Polym. Sci.* 1960, **48**, 329
- ⁷ KOLTHOFF, I. M., O'CONNOR, P. R. and HAUSEN, J. L. *J. Polym. Sci.* 1955, **15**, 459
- ⁸ HENRICI-OLIVÉ, G. and OLIVÉ, S. *Makromol. Chem.* 1963, **68**, 120
- ⁹ BEVINGTON, J. C., BRADBURY, J. H. and BURNETT, G. M. *J. Polym. Sci.* 1954, **12**, 469
- ¹⁰ BEVINGTON, J. C. *Trans. Faraday Soc.* 1955, **51**, 1392
- ¹¹ TALAT-ERBEN, M. and BYWATER, S. *J. Amer. chem. Soc.* 1955, **77**, 3712
- ¹² LEWIS, F. M. and MATHESON, M. S. *J. Amer. chem. Soc.* 1949, **71**, 747
- ¹³ VAN HOOK, J. P. and TOBOLSKY, A. V. *J. Amer. chem. Soc.* 1958, **80**, 779
- ¹⁴ BAMFORD, C. H., BARB, W. G., JENKINS, A. D. and ONYON, P. F. *The Kinetics of Vinyl Polymerization by Radical Mechanisms*, p 220. Butterworths: London, 1958
- ¹⁵ BARTON, A. F., BEVINGTON, J. C. and WAHID, A. *Makromol. Chem.* 1963, **67**, 195
- ¹⁶ ALLEN, P. W. and PLACE, M. A. *J. Polym. Sci.* 1957, **26**, 386
- ¹⁷ ALLEN, P. W., AYREY, G., MERRETT, F. M. and MOORE, C. G. *J. Polym. Sci.*, 1956, **22**, 549
- ¹⁸ VAUGHAN, M. F. *Nature, Lond.* 1959, **183**, 43
- ¹⁹ BRISTOW, G. and PLACE, M. A. *J. Polym. Sci.* 1962, **60**, S21
- ²⁰ SZWARC, M. *The Transition State*, p 91. *Spec. Publ. No. 16*. The Chemical Society: London, 1962
- ²¹ WALLING, C., BRIGGS, E. R., WOLFSTEIN, K. B. and MAYO, F. R. *J. Amer. chem. Soc.* 1948, **70**, 1537
- ²² SWAIN, C. G., STOCKMAYER, W. H. and CLARKE, J. T. *J. Amer. chem. Soc.* 1950, **72**, 5426
- ²³ MAYO, F. R. and WALLING, C. *Chem. Rev.* 1950, **46**, 191
- ²⁴ BAMFORD, C. H., JENKINS, A. D. and JOHNSTON, R. *Trans. Faraday Soc.* 1958, **55**, 418
- ²⁵ BAMFORD, C. H. and JENKINS, A. D. *J. Polym. Sci.* 1961, **53**, 149
- ²⁶ BAMFORD, C. H. and JENKINS, A. D. *Trans. Faraday Soc.* 1963, **59**, 530
- ²⁷ BAMFORD, C. H. and EASTMOND, G. C. *Ann. Rep. chem. Soc. Lond.* 1963, **60**, 100
- ²⁸ BEVINGTON, J. C. *Radical Polymerization*, p 89. Academic Press: New York, 1961
- ²⁹ *Organic Syntheses*, Coll. Vol. III, p 200
- ³⁰ SAUNDERS, W. H. and WILLIAMS, R. A. *J. Amer. chem. Soc.* 1957, **79**, 3712
- ³¹ (a) BAILLE, L. A. *Internat. J. appl. Radiation and Isotopes*, 1960, **8**, 1
- ³¹ (b) BRUNO, G. A. and CHRISTIAN, J. E. *Analyt. Chem.* 1961, **33**, 650
- ³² BREITENBACH, J. W. and FORSTER, E. L. *Ost. ChemZtg.* 1955, **56**, 93
- ³² BREITENBACH, J. W. and FORSTER, E. L. *Mikrochim. Acta*, 1956, 1-6, 982
- ³³ MAYO, F. R., GREGG, R. A. and MATHESON, M. S. *J. Amer. chem. Soc.* 1956, **73**, 1691

Book Reviews

The Proceedings of the Tihany Symposium on Radiation Chemistry

JÁNOS DOBÓ (Editor). Publishing House of the Hungarian Academy of Sciences: Budapest, 1964. 482 pp. 6 in. by 9 in. U.S. \$14.00

THIS symposium was held at Tihany, Hungary, in September 1962. There were about eighty participants, mainly from European countries.

The proceedings are divided into four roughly equal sections devoted to General and Organic compounds, Polymeric systems, Aqueous solutions, and finally Dosimetry and Miscellaneous papers. In all, there are about fifty papers and short reviews covering a large variety of topics in radiation chemistry.

In the first section, possibly the most interesting paper is by Voevodsky on the mechanism of radiation effects in organic solids, in which the use of e.s.r. techniques in this field is emphasized. A survey of ionic mechanisms in radiation chemistry by Burns, and a short paper by Swallow on recent developments in radiation chemistry at the Imperial College of Science and Technology are interesting. Many of the other papers in this section (and indeed in the book) are concerned with chemical reactions induced by radiation, some of which, the authors suggest, may become technologically important with the advent of cheap sources of radiation; this may be particularly true for chain reactions where G values of approximately 10^4 may be obtained.

The section concerned with Polymeric systems is the longest in the book. There is a short review by Chapiro and three papers (by Hardy *et al.*, by Zurakowska-Orszagh and by Bensasson *et al.*) concerned with solid state polymerization. Three other papers are concerned with initiation of polymerization by radiation, and the remainder with the effect of radiation on polymer structure, either in the solid state or in solution.

The section on Aqueous solutions has eleven short papers (four to ten pages) on a variety of aspects. Bednar discusses the problems associated with concentrated solutions, with particular reference to sodium nitrate solutions, and two papers (Haissinsky and Zagorski) deal with alkaline solutions.

The last section has eight papers, three of which deal with problems of dosimetry, and the rest deal with miscellaneous aspects.

The book as a whole is quite well produced, but suffers occasionally from peculiarities in the translation. Further, since it appears that the decision to publish the proceedings was taken at the end of the conference, it would not be surprising if many of the more important papers are duplicated in the literature. In spite of this, however, the book provides a variety of papers on many subjects of interest to radiation and polymer chemists.

V. J. ROBINSON

Infrared Spectroscopy of High Polymers

R. ZBINDEN. Academic Press: New York and London, 1964. xii + 264 pp.
6 in. by 9¼ in. 76s

THE aim of the author of this book, according to the preface, is 'to assist both the spectroscopist in interpreting the spectra of high polymers and the polymer scientist in using infra-red spectroscopy for the elucidation of chemical and physical structure of polymers'. The emphasis is, however, decidedly on the first objective. The first chapter on characteristic features of polymer spectra gives a brief account of polymer structure, of orientation in polymers and its manifestation in dichroic properties and of crystallinity, followed by examples of polymer spectroscopy applied to analytical problems.

The second chapter contains a comprehensive treatment (64 pages) of the selection rules for chain molecules. It commences with a brief summary of the theory of groups and their representations, and goes on to apply the theory to symmetry opera-

tions and groups. Numerous tables are given which clarify the treatment. This is indeed a feature of the whole book and much labour must have gone to the computing and graphical representation of numerical examples. The normal modes of vibration are considered for isolated chains and for crystalline polymers, of finite as well as of infinite extent. The selection rules for these vibrations are derived, and there is a section on the temperature dependence of transitions involving lattice vibrations. The chapter ends with illustrations from several polymers, and the interpretation of the spectrum of polyethylene is dealt with in some detail.

Chapter III deals with numerical calculations of vibrations in chain molecules, for linear and for planar zig-zag chains. The treatment includes the case of alternating masses (as in vinyl polymers) and finite as well as infinite chains. Many numerical examples for finite chains are given in graphical form. Chapter IV is on the closely related subject of vibrational interaction; the treatment does not include interaction between chains. The examples are chiefly from the spectra of normal paraffins, where the short chain length results in many 'interaction' bands having appreciable intensity (they are of zero intensity in an infinite straight chain). It would be interesting to see the application of the theory to the hydrocarbon portions of polyamide chains.

The last chapter on orientation measurements deals with experimental techniques, the use of polarized radiation and a very thorough classification of orientation types and of orientation parameters with the relevant expressions for dichroic ratios. The section on techniques includes a discussion of sources of error in measurements of dichroism, but more might have been said about the effect of the elliptical polarization which in general is produced when the electric vector of the radiation incident on the specimen is neither parallel nor perpendicular to the fibre axis. The table of orientation types on pages 190 to 194 with examples of polar diagrams and intensity ellipsoids etc. will be very useful. The reviewer greatly regrets, however, that the term 'perfect *uniaxial* orientation' (all chains perfectly aligned along *z* axis, but chains rotated around their own axes so that all equivalent functional groups or crystallite faces point in the same direction) is used to describe a polymer which could be optically *biaxial*. The chapter ends with an interesting discussion of some dichroic effects observed in polyethylene and in polystyrene. An appendix to the book gives a guide to the literature for individual polymers.

The treatment is clear and adequate, references being given in the few cases where a full derivation is not given. The book can be thoroughly recommended, but is not a reference book on the spectra of high polymers, the subject being strictly indicated by the title. A surprising omission, which it is to be hoped will be remedied in a second edition, is the absence of any discussion of the spectroscopic effects of hydrogen bonding.

A. ELLIOTT

Manufacture of Plastics, Volume I

W. MAYO SMITH (Editor). Reinhold: New York; Chapman and Hall: London, 1964.
xiii + 560 pp. 6 in. by 9½ in. \$18.00 or 144s

FOR some time there has been a need for a text which brings together, within handy compass, reasonably detailed descriptions of the manufacturing techniques currently used for the main classes of plastics materials. The book under review appears, at first sight, to answer this need. It contains a wealth of data, diagrams and illustrations, and the editor states in his preface: 'A lack of detailed manufacturing know-how has existed in the literature up to the present time; and it is the purpose of this volume (and the volumes to follow) to overcome the deficiency in the literature as well as in published patents'. The scope of Volume I is indicated by the chapter headings, which include: Polyethylene (127 pp), Polypropylene, Polyvinyl acetate, Polyvinyl alcohol, Polyvinyl acetal resins, Vinyl and vinylidene chloride polymers and copolymers, Acrylic polymers, Melamines, Styrene polymers, ABS plastics, Polyurethanes, Epoxy resins, Nylon and Penton.

It is therefore somewhat disappointing to find, on closer inspection, that the book discloses little that has not been published previously in one form or another, and in this respect the editor's avowed purpose is only partly fulfilled. Nevertheless the aim

Book Reviews

The Proceedings of the Tihany Symposium on Radiation Chemistry

JÁNOS DOBÓ (Editor). Publishing House of the Hungarian Academy of Sciences: Budapest, 1964. 482 pp. 6 in. by 9 in. U.S. \$14.00

THIS symposium was held at Tihany, Hungary, in September 1962. There were about eighty participants, mainly from European countries.

The proceedings are divided into four roughly equal sections devoted to General and Organic compounds, Polymeric systems, Aqueous solutions, and finally Dosimetry and Miscellaneous papers. In all, there are about fifty papers and short reviews covering a large variety of topics in radiation chemistry.

In the first section, possibly the most interesting paper is by Voevodsky on the mechanism of radiation effects in organic solids, in which the use of e.s.r. techniques in this field is emphasized. A survey of ionic mechanisms in radiation chemistry by Burns, and a short paper by Swallow on recent developments in radiation chemistry at the Imperial College of Science and Technology are interesting. Many of the other papers in this section (and indeed in the book) are concerned with chemical reactions induced by radiation, some of which, the authors suggest, may become technologically important with the advent of cheap sources of radiation; this may be particularly true for chain reactions where G values of approximately 10^4 may be obtained.

The section concerned with Polymeric systems is the longest in the book. There is a short review by Chapiro and three papers (by Hardy *et al.*, by Zurakowska-Orszagh and by Bensasson *et al.*) concerned with solid state polymerization. Three other papers are concerned with initiation of polymerization by radiation, and the remainder with the effect of radiation on polymer structure, either in the solid state or in solution.

The section on Aqueous solutions has eleven short papers (four to ten pages) on a variety of aspects. Bednar discusses the problems associated with concentrated solutions, with particular reference to sodium nitrate solutions, and two papers (Haissinsky and Zagorski) deal with alkaline solutions.

The last section has eight papers, three of which deal with problems of dosimetry, and the rest deal with miscellaneous aspects.

The book as a whole is quite well produced, but suffers occasionally from peculiarities in the translation. Further, since it appears that the decision to publish the proceedings was taken at the end of the conference, it would not be surprising if many of the more important papers are duplicated in the literature. In spite of this, however, the book provides a variety of papers on many subjects of interest to radiation and polymer chemists.

V. J. ROBINSON

Infrared Spectroscopy of High Polymers

R. ZBINDEN. Academic Press: New York and London, 1964. xii + 264 pp.
6 in. by 9¼ in. 76s

THE aim of the author of this book, according to the preface, is 'to assist both the spectroscopist in interpreting the spectra of high polymers and the polymer scientist in using infra-red spectroscopy for the elucidation of chemical and physical structure of polymers'. The emphasis is, however, decidedly on the first objective. The first chapter on characteristic features of polymer spectra gives a brief account of polymer structure, of orientation in polymers and its manifestation in dichroic properties and of crystallinity, followed by examples of polymer spectroscopy applied to analytical problems.

The second chapter contains a comprehensive treatment (64 pages) of the selection rules for chain molecules. It commences with a brief summary of the theory of groups and their representations, and goes on to apply the theory to symmetry opera-

tions and groups. Numerous tables are given which clarify the treatment. This is indeed a feature of the whole book and much labour must have gone to the computing and graphical representation of numerical examples. The normal modes of vibration are considered for isolated chains and for crystalline polymers, of finite as well as of infinite extent. The selection rules for these vibrations are derived, and there is a section on the temperature dependence of transitions involving lattice vibrations. The chapter ends with illustrations from several polymers, and the interpretation of the spectrum of polyethylene is dealt with in some detail.

Chapter III deals with numerical calculations of vibrations in chain molecules, for linear and for planar zig-zag chains. The treatment includes the case of alternating masses (as in vinyl polymers) and finite as well as infinite chains. Many numerical examples for finite chains are given in graphical form. Chapter IV is on the closely related subject of vibrational interaction; the treatment does not include interaction between chains. The examples are chiefly from the spectra of normal paraffins, where the short chain length results in many 'interaction' bands having appreciable intensity (they are of zero intensity in an infinite straight chain). It would be interesting to see the application of the theory to the hydrocarbon portions of polyamide chains.

The last chapter on orientation measurements deals with experimental techniques, the use of polarized radiation and a very thorough classification of orientation types and of orientation parameters with the relevant expressions for dichroic ratios. The section on techniques includes a discussion of sources of error in measurements of dichroism, but more might have been said about the effect of the elliptical polarization which in general is produced when the electric vector of the radiation incident on the specimen is neither parallel nor perpendicular to the fibre axis. The table of orientation types on pages 190 to 194 with examples of polar diagrams and intensity ellipsoids etc. will be very useful. The reviewer greatly regrets, however, that the term 'perfect *uniaxial* orientation' (all chains perfectly aligned along *z* axis, but chains rotated around their own axes so that all equivalent functional groups or crystallite faces point in the same direction) is used to describe a polymer which could be optically *biaxial*. The chapter ends with an interesting discussion of some dichroic effects observed in polyethylene and in polystyrene. An appendix to the book gives a guide to the literature for individual polymers.

The treatment is clear and adequate, references being given in the few cases where a full derivation is not given. The book can be thoroughly recommended, but is not a reference book on the spectra of high polymers, the subject being strictly indicated by the title. A surprising omission, which it is to be hoped will be remedied in a second edition, is the absence of any discussion of the spectroscopic effects of hydrogen bonding.

A. ELLIOTT

Manufacture of Plastics, Volume I

W. MAYO SMITH (Editor). Reinhold: New York; Chapman and Hall: London, 1964.
xiii + 560 pp. 6 in. by 9½ in. \$18.00 or 144s

FOR some time there has been a need for a text which brings together, within handy compass, reasonably detailed descriptions of the manufacturing techniques currently used for the main classes of plastics materials. The book under review appears, at first sight, to answer this need. It contains a wealth of data, diagrams and illustrations, and the editor states in his preface: 'A lack of detailed manufacturing know-how has existed in the literature up to the present time; and it is the purpose of this volume (and the volumes to follow) to overcome the deficiency in the literature as well as in published patents'. The scope of Volume I is indicated by the chapter headings, which include: Polyethylene (127 pp), Polypropylene, Polyvinyl acetate, Polyvinyl alcohol, Polyvinyl acetal resins, Vinyl and vinylidene chloride polymers and copolymers, Acrylic polymers, Melamines, Styrene polymers, ABS plastics, Polyurethanes, Epoxy resins, Nylon and Penton.

It is therefore somewhat disappointing to find, on closer inspection, that the book discloses little that has not been published previously in one form or another, and in this respect the editor's avowed purpose is only partly fulfilled. Nevertheless the aim

BOOK REVIEWS

of providing a reference work on manufacturing methods has been accomplished to some extent. The qualification is necessary in view of the serious defects in presentation evident throughout the book. Briefly, these are that editorial control over the contributors has been, to say the least, inadequate and that many of the contributions are written in a style which is virtually unreadable.

The difficulties of securing uniformity of presentation in a cooperative work are well known, but there is little excuse for the wide variations that are found between individual chapters in the manner of treatment and in arrangement of topics that are common to nearly all of them. Glaring inconsistencies obtrude in such important matters as nomenclature, symbolism, units, reference citations, tabulation of properties, test methods, etc. Some of the information presented is irrelevant and occasionally meaningless, as in the graphs on pp 440 and 441, the abscissae of which lack both scales and units. There are also many examples of unnecessary and irritating duplication of subject matter in separate chapters, as in those dealing with polyvinyl acetate and its derivatives. The style of writing in some parts of the book makes one suspect that manufacturers' literature has been utilized extensively and in a novel way, namely by abstracting the sentences and randomizing them. The result, although soporific to a degree, is not a happy one.

Despite these strictures there are one or two commendable articles, notably those on Polyurethanes, Nylon and Polyethylene. The most useful contribution is that of Louis Basel on Polymer plant engineering (65 pp). This deals with the handling, processing and design problems associated with the production of monomers and polymers, together with aspects such as plant layout, safety and packaging. To many this chapter will give some insight into the type of problem encountered when the relatively simple bench operations of polymer chemistry are translated to the ton scale. Perhaps for this alone, the book can be recommended for library purchase. It should, however, be kept well out of the reach of embryo technical authors.

P. F. ONYON

Cationic Polymerization of 3-Methylbutene-1 IV—Molecular Weight/ Intrinsic Viscosity Relationship for Poly-3-methylbutene-1

I. H. BILLICK* and J. P. KENNEDY

The relation between intrinsic viscosity and molecular weight for amorphous poly-3-methylbutene-1 obtained by low temperature cationic polymerization has been determined by light scattering technique. The relationship in diisobutylene solution at 20°C is $[\eta]=4.2 \times 10^{-4} M_w^{0.63}$, where $[\eta]$ denotes intrinsic viscosity in 100 ml/g and M_w is the weight average molecular weight.

ALTHOUGH a considerable amount of work has been carried out with poly-3-methylbutene-1 synthesized by cationic catalysts, intrinsic viscosity values were only used to express relative molecular weights¹. In the course of our fundamental polymerization studies, we decided to determine the relationship between weight average molecular weight and intrinsic viscosity for cationic poly-3-methylbutene-1. The present paper presents the experimental work and the data used to obtain this relationship.

EXPERIMENTAL

Materials

All measurements and investigations were carried out with amorphous poly-3-methylbutene-1 obtained with aluminium chloride catalyst in methyl chloride solvent at low temperatures.

Diisobutylene solvent was used. After distillation, a total of 0.02 wt per cent impurities were detectable by gas chromatography. Prior to use, the solvent was filtered through a Millipore membrane filter.

The iso-octane used for determination of the molecular weights by light scattering was a commercial spectro- or chromatographic grade product and was used without further purification.

Fractionation

Polymer fractionation was carried out using the two-step fractional precipitation technique of Flory². Benzene was used as solvent and acetone served as precipitant. Polymer fractions were recovered by evaporation of the solvent-nonsolvent mixture followed by redissolution in benzene and freeze-drying. A total of six fractions were obtained.

*Intrinsic viscosity*³

Intrinsic viscosity measurements were made on all six fractions, using a special dilution viscometer of the Ubbelohde type. Temperature was maintained at $20.00^\circ \pm 0.05^\circ\text{C}$ in a well stirred constant temperature water bath.

*Present address: National Bureau of Standards, Washington, D.C.

The viscometer which holds about 25 ml of solution was constructed so that a known volume of solution could be removed and replaced with solvent. This permitted a series of viscosities to be run at various known dilutions. The dilution factor for the viscometer was obtained by the U.S. Testing Company.

Stock solutions were made at various concentrations depending on the expected viscosity of the polymer. The concentration was chosen so that at least four dilutions were obtained and the lowest relative viscosity was not less than 1.15. This restriction held for fractions 1-5 while the lowest relative viscosity for fraction 6 was about 1.10.

The viscometer had a flow time of about 165 seconds for diisobutylene. The measured flow times of the solutions were corrected for kinetic energy factors using calibration factors obtained by the U.S. Testing Company. The data are shown in *Table 1*.

Table 1. Intrinsic viscosity data for poly-3-methylbutene-1

Fraction	$[\eta]$ (100 ml/g)	k_1	k_2	$k_1 + k_2$
1	0.87	0.32	0.14	0.46
2	0.60	0.30	0.22	0.52
3	0.57	0.39	0.14	0.53
4	0.53	0.35	0.14	0.49
5	0.34	0.29	0.19	0.48
6	0.18	0.43	0.15	0.58

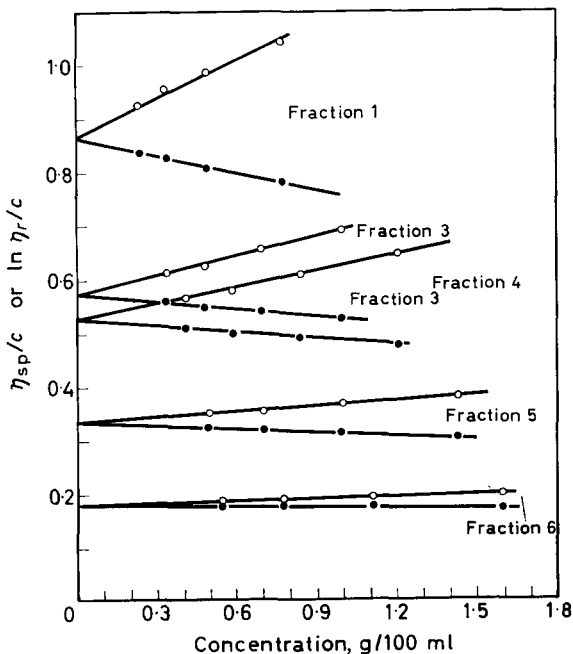


Figure 1—Intrinsic viscosity plots of poly-3-methylbutene-1

Values of η_{sp}/c , and $(\log \eta_r)/c$ were calculated in the usual manner, where c denotes concentration in g/100 ml, and η_{sp} , η_r have their usual meanings³.

Figure 1 is a plot of these values versus concentration for five fractions. The intrinsic viscosities $[\eta]$ are obtained from the intercepts at zero concentration and the Huggins constants, k_1 and k_2 , from the slopes. According to equations (1) and (2):

$$\eta_{sp}/c = [\eta] + k_1 [\eta]^2 c \quad (1)$$

$$(\ln \eta_r)/c = [\eta] - k_2 [\eta]^2 c \quad (2)$$

To a good approximation³ $k_1 + k_2 = 0.5$, within experimental error.

Light scattering^{4,5}

In order to obtain the molecular weights of the fractions, light scattering was measured from dilute solutions of the polymer in iso-octane. Since preliminary experiments showed that the molecular weight (and, therefore, probably molecular dimensions) was comparatively low, even for fraction 1, it was decided to use the dissymmetry method⁶, rather than the complete angular distribution methods of Zimm⁷.

When applying the dissymmetry method, the following equation holds

$$\frac{Kc}{R_{90}} = \frac{1}{M} \frac{1}{P(90)} + 2A_2c \quad (3)$$

where c is the concentration, M_w is the weight average molecular weight, A_2 is the second virial coefficient, R_{90} is Rayleigh's ratio at 90° , $P(90)$ is the particle scattering factor at 90° , $K = 2\pi n_0^2 (dn/dc)^2 / N\lambda^4$, n_0 is the refractive index of the solvent, λ is the wavelength of light *in vacuo*, and dn/dc is the refractive index increment. In practice R_{90} , dn/dc and $P(90)$ are determined experimentally.

The quantity $P(90)$ is a correction factor dependent on the size, shape and size distribution of the polymer in solution. When the particles are small, as here, the value of $P(90)$ can be assumed to be independent of the latter two. By measuring the excess scattering of light at two angles symmetrical about 90° , usually 45° and 135° , a dissymmetry ratio, $Z = (\text{scattering at } 45^\circ) / (\text{scattering at } 135^\circ)$, can be calculated. In the implementation of equation (3) the intrinsic dissymmetry, Z , is obtained by extrapolating a plot of $1/(Z-1)$ versus c to zero concentration. By use of data in the literature⁶, values of $P(90)$ can be obtained. For the highest molecular weight, fraction 1, $1/P(90)$ was less than 1.08.

Values for dn/dc at the two wavelengths of light, 546 $m\mu$ and 436 $m\mu$, used in the light scattering experiments, were determined for the poly-3-methylbutene-1-iso-octane system. A Brice-Phoenix differential refractometer⁸ was used for all measurements. A constant temperature bath was used to maintain the cell in the refractometer at 28.9°C . Calibration was accomplished using polystyrene-cyclohexane and data from the literature⁹.

For the purpose of obtaining dn/dc an unfractionated sample of polymer was used. The values of dn/dc obtained for the system of interest are 0.118 at 546 $m\mu$ and 0.119 at 436 $m\mu$.

Light scattering was carried out on a Brice-Phoenix light scattering photometer¹⁰ with a chart recorder. Solutions at various concentrations were obtained dust free by filtration, through a Silas 03 filter, directly into an acetone washed, dust free, semi-octagonal cell. The measurement procedure outline in the instruction manual¹¹ was followed.

However, the calibration constants furnished by the manufacturer were not used. Rather, the photometer was calibrated by measuring the excess scattering of an 0.5 per cent solution of Cornell standard polystyrene in toluene. The values of the turbidity for this system at the two wavelengths

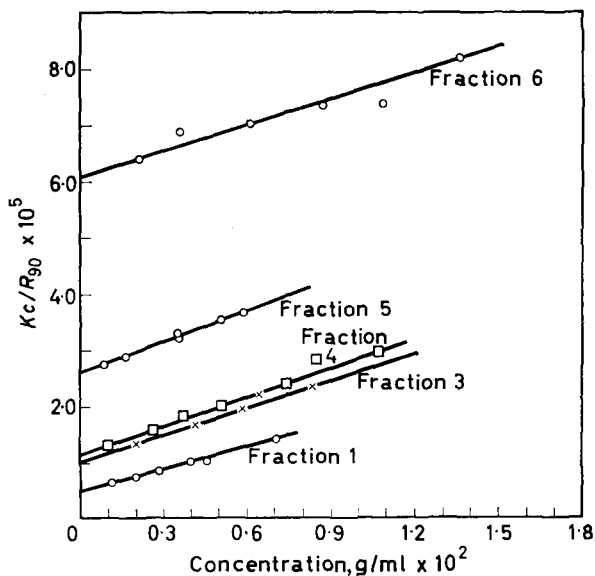


Figure 2—Light scattering of poly-3-methylbutene-1 at 436 mμ

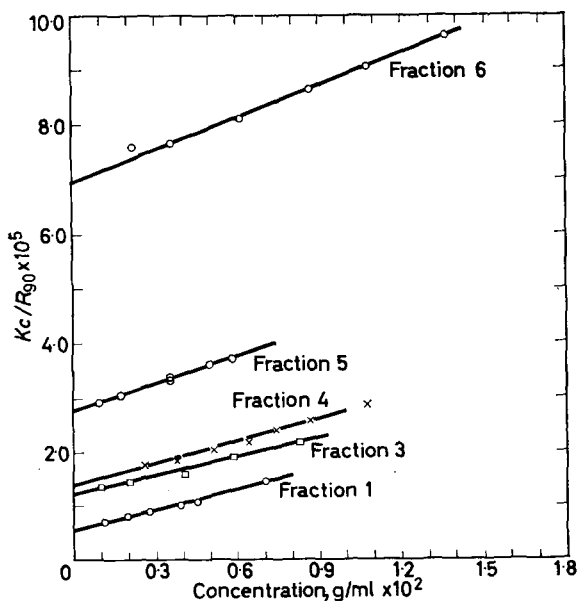


Figure 3—Light scattering of poly-3-methylbutene-1 at 546 mμ

of interest were those suggested as being reliable by Kratochvil *et al.*¹².

Measurements were carried out at the angles 0°, 45°, 90°, 135° at both wavelengths. Values of Kc/R_{90} were calculated using the above mentioned data and procedures¹¹. In these calculations, it has been assumed that the depolarization was negligible. In addition, a comparison of the data obtained at the two different wavelengths indicated that neither absorption nor fluorescence was present.

Figures 2 and 3 are plots of the data according to equation (3). Table 2 summarizes the values of M_w and A_2 obtained from these plots. In both Figures 2 and 3, the data for fraction 2 have been omitted for the sake of clarity.

Table 2. Weight average molecular weights and second virial coefficients for poly-3-methylbutene-1 in iso-octane

Fraction	$M_w \times 10^{-5}$			$A_2 \times 10^3$		
	546	436	Ave.	546	436	Ave.
1	1.85	2.04	1.95	0.56	0.56	0.56
2	1.09	1.05	1.07	0.79	0.78	0.78
3	0.86	0.90	0.88	0.64	0.66	0.65
4	0.81	0.85	0.83	0.76	0.78	0.77
5	0.37	0.39	0.38	0.83	0.87	0.85
6	0.15	0.17	0.16	0.90	0.75	0.88

MOLECULAR WEIGHT / INTRINSIC VISCOSITY
RELATIONSHIP

Given values of molecular weight and intrinsic viscosity, the constants of the well-known relationship

$$[\eta] = K'M_v^a \tag{4}$$

can be determined. While the value of the molecular weight in this equation is the viscosity average, this can be assumed to be equal, within experi-

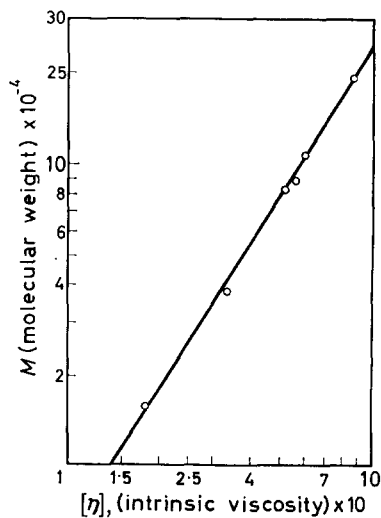


Figure 4—Log molecular weight versus log intrinsic viscosity for poly-3-methylbutene-1 in diisobutylene at 20°C

mental error, to the weight average for the fractions used. A plot of $\log [\eta]$ versus $\log M_w$ permits evaluation of K' and a . *Figure 4* is plot of this type and equation (4) can now be written as

$$[\eta] = 4.2 \times 10^{-4} M_w^{0.63} \quad (5)$$

where $[\eta]$ is the intrinsic viscosity of poly-3-methylbutene-1 in diisobutylene at 20°C.

It is interesting to note that the values for K' and a for polyisobutylene-diisobutylene are 3.6×10^{-4} and 0.64, respectively¹³. Indeed, one might conclude the two systems are equal, within experimental error.

Finally, caution should be exercised in the application of equation (5) obtained from *Figure 4* outside the experimental range for which the equation was derived. Errors in extrapolated molecular weights or intrinsic viscosities may become significant particularly toward the lower values¹⁴.

*Analytical Research Division and Chemicals Research Division,
Esso Research and Engineering Company,
Linden, New Jersey, U.S.A.*

(Received June 1964)

REFERENCES

- ¹ KENNEDY, J. P., MINCKLER Jr, L. S. and THOMAS, R. M. *J. Polym. Sci. Part A*, 1964, **2**, 367
- ² FLORY, P. J. *J. Amer. chem. Soc.* 1943, **65**, 372
- ³ ONYON, P. F. in *Techniques of Polymer Characterization*. Edited by ALLEN, P. W. Butterworths: London, 1959
- ⁴ PEAKER, F. W. in *Techniques of Polymer Characterization*. Edited by ALLEN, P. W. Butterworths: London, 1959
- ⁵ STACEY, K. A. *Light Scattering in Physical Chemistry*. Butterworths: London, 1956
- ⁶ DOTY, P. and STEINER, R. F. *J. chem. Phys.* 1950, **18**, 1211
- ⁷ ZIMM, B. H. *J. chem. Phys.* 1948, **16**, 1093 and 1099
- ⁸ BRICE, B. A. and HALWER, M. *J. opt. Soc. Amer.* 1951, **41**, 1033
- ⁹ O'MARA, J. H. and MCINTYRE, D. *J. phys. Chem.* 1959, **63**, 1435
- ¹⁰ BRICE, B. A., HALWER, M. and SPEISER, R. *J. opt. Soc. Amer.* 1950, **40**, 768
- ¹¹ Brice-Phoenix Operation Manual OM-1000A
- ¹² KRATOCHVIL, J. P., DEZELIC, GJ., KERKER, M. and MATYEVIC, M. *J. Polym. Sci.* 1962, **57**, 59
- ¹³ FLORY, P. J. *J. Amer. chem. Soc.* 1943, **65**, 372
- ¹⁴ COHN-GINSBERG, E., FOX, T. G and MASON, H. F. *Polymer, Lond.* 1962, **3**, 97

Lower Critical Solution Phenomena in Polymer-Solvent Systems

G. ALLEN and C. H. BAKER

The phase boundary curves in the region of the lower critical solution temperatures (LCST) have been established for the systems; polystyrene + cyclopentane, polypropylene oxide + n-pentane, and polyisobutene + isopentane. In every case the molecular weight of the polymer has a profound effect on the location of the LCST in a particular solvent. The effect of hydrostatic pressure on the LCST of solutions of two samples of polyisobutene in isopentane was investigated over a pressure range of two to twenty five atmospheres, and concentrations up to six per cent by weight of polymer. The shapes of the phase boundary curves were unaltered by the increase in pressure and the pressure coefficient of the LCST was $\sim 0.5 \text{ deg. atm}^{-1}$ for each molecular weight.

It is usual for the mutual solubility of a polymer and a poor solvent to increase with temperature so that complete miscibility is reached at an upper critical solution temperature (UCST). Hitherto studies of polymer-solvent miscibility have been confined to relatively small ranges of temperature and pressure, usually below the normal boiling point of the solvent. Recently it has been established¹ that hydrocarbon polymers show partial immiscibility with hydrocarbon solvents if the temperature is raised sufficiently above the normal boiling point of the solvent. Immiscibility occurs if the temperature is raised above a lower critical solution temperature (LCST) and such behaviour appears to be a very widespread phenomenon in polymer solutions.

The extent to which a polymer solution must be heated so as to bring about phase separation at or near to a LCST depends partly on the chemical nature of the two components but also on the relative molecular sizes of solvent and solute. Hence the molecular weight of the polymer affects the situation of a LCST in any particular solvent. Polymers of low molecular weight (about 10^4) undergo phase separation within 20° or 30° of the solvent's gas-liquid critical temperature, while polymers of high molecular weight ($> 10^6$) separate at temperatures as much as 120° below the gas-liquid critical temperature². A recent thermodynamic study of polyisobutene in *n*-pentane has shown that the nearness of a polymer-solvent system to a LCST can be related to the negative heats of mixing found in various systems^{2,3}.

This paper reports further studies on LCSTs in polymer solutions and the effect of molecular weight on the LCSTs of the three polymer-solvent systems; polystyrene + cyclopentane, polypropylene oxide + *n*-pentane and polyisobutene + isopentane. The effect of hydrostatic pressure on the LCSTs of the polyisobutene + isopentane system has also been established.

EXPERIMENTAL

Materials

Six samples of polystyrene were used. These are denoted as PS 1 to 6 and had mean molecular weights 5 900, 13 800, 33 100, 64 900, 99 100 and 600 000 respectively. Sample PS 1 was a gift from BX Plastics Ltd. Sample PS 2 was prepared by benzoyl peroxide initiation in benzene solution at 80°C, while samples PS 3 to 6 were prepared by an anionic mechanism involving initiation by a sodium-naphthalene complex in dioxan.

Eight samples of polypropylene oxide were used and these are denoted by PPO 1 to 8. The respective molecular weights were 2 025, 5 300, 16 000, 40 000, 45 000, 220 000, 420 000 and 680 000. Sample PPO 1 was a gift from the I.C.I. Dyestuffs Division, while samples PPO 2 to 8 were prepared by various members of this department using $\text{AlMe}_3/\text{H}_2\text{O}$ or $\text{ZnEt}_2/\text{H}_2\text{O}$ as catalysts.

All the molecular weights were determined viscometrically in benzene solution at 25°C using an Ubbelohde dilution viscometer. The intrinsic viscosity/molecular weight relationships used were:

$$[\eta] = 4 \cdot 17 \times 10^{-4} M_v^{0.60}$$

and

$$[\eta] = 1 \cdot 12 \times 10^{-4} M_v^{0.77}$$

for polystyrene⁴ and polypropylene oxide⁵ respectively.

Only two samples of polyisobutene were used. These are denoted by PIB 1 and 2, and had weight-average molecular weights $2 \cdot 25 \times 10^6$ and 62 000 respectively. (These samples are identical with samples IV and VB used in a thermodynamic study reported elsewhere².)

The solvents were obtained by careful fractionation of commercial products. Gas chromatograms of the final products showed that all but about 0.5 per cent of the impurities, which were principally pentane isomers, had been removed. The boiling points and gas-liquid critical temperatures of the final products were:

<i>Solvent</i>	<i>B.pt °C</i>	<i>T^c °C</i>
Cyclopentane	49.14 ± 0.02 (49.262)	238.10 (238.60)
<i>n</i> -Pentane	36.02 ± 0.07 (36.074)	196.84 (196.62)
Isopentane	27.84 ± 0.02 (27.852)	187.30 (187.8)
Isobutane	—	134.9

The values in parentheses are those quoted by the American Petroleum Institute⁶.

Some observations were made also on the phase behaviour of the system polypropylene oxide + isobutane. The isobutane was a commercial sample which was about 96 per cent pure and was used without further purification.

Procedure

The experimental work falls conveniently into two parts: the establishment of the temperature/weight fraction of polymer (T, w) phase boundary curves for the polymer plus solvent systems, and the determination of the dependence of the LCST of the polyisobutene + isopentane system on the applied hydrostatic pressure.

(1) *(T, w) phase equilibria studies*—The polymer solutions used in the phase boundary studies were prepared in sealed tubes under high vacuum conditions. The mixtures were gently stirred to accelerate solution of the polymer at room temperature, although the higher molecular weight polypropylene oxide solutions had to be heated above 50°C first to melt the partially crystalline polymer.

The homogeneous solutions were then heated slowly, at about 0.2° per hour, in a stirred 1-litre bath of silicone oil. This in turn was heated by circulating the vapour of a boiling solvent through the vapour jacket surrounding the silicone oil bath, the boiling point of the solvent being controlled by a manostat. Solvents used for this purpose were:

benzene (40 to 80°C); chlorobenzene (80 to 130°C);

bromobenzene (130 to 156°C); and nitrobenzene (156 to 206°C).

The few separation temperatures measured above 206°C were determined in an air thermostat.

The temperatures of phase separation were found by heating up the tubes until a definite opalescence was observed. In polymers of lower molecular weight two distinct liquid layers would separate out from the cloudy solution, but the viscosities of the higher molecular weight polymer solutions were usually too great to allow two liquid layers to form readily. In this way phase boundary curves were established over composition ranges up to polymer weight fractions of about 0.3, while the solutions were under their own vapour pressure.

(2) *(P, T) studies*—Since the LCST of polyisobutene + isopentane solutions is located conveniently at 54°C¹ for a molecular weight $M_w = 2 \times 10^6$, this system was chosen for an investigation of the effect of hydrostatic pressure on the LCST. Using the same samples as for the *(T, w)* studies, solutions of polyisobutene in isopentane were prepared in sealed Pyrex tubes of the type shown in *Figure 1*. A weighed piece of polymer was inserted into D and the tube then evacuated. Solvent was then distilled in so as to fill B, C and about one quarter of D. The tube was sealed off under vacuum at the constriction E and reweighed to ascertain the amount of solvent. The polymer and solvent were then allowed to mix by draining all the solvent into D. After dissolution of the polymer the solution was drained

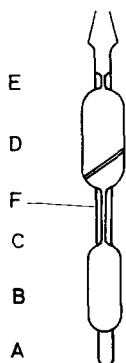


Figure 1—Experimental cell used in *(P, T)* studies

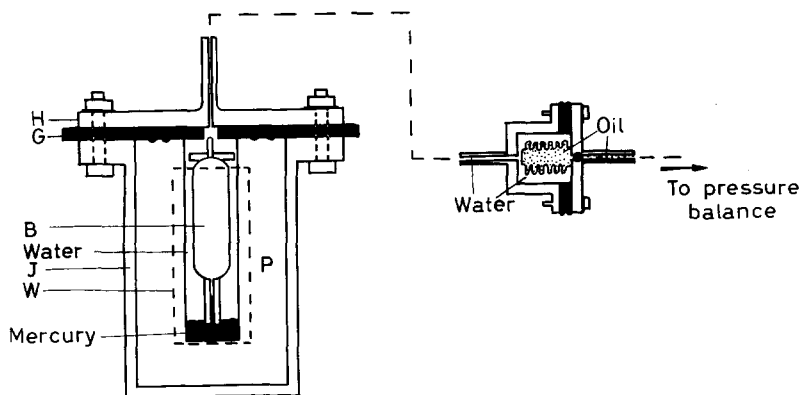


Figure 2—The pressure vessel and copper bellows arrangement

back so as to fill B and C. The cell B was then detached by snapping the capillary at F, some 8 cm from the tip of the glass rod A.

The experimental cell was then examined in the pressure vessel shown in Figure 2. A Perspex cylinder P was held in a tightly fitting copper jacket, J, which had two windows, W, about 1.5 cm wide and 8 cm long, cut out on opposite sides so that the Perspex cylinder might be seen. The experimental cell B was accommodated in a hole 8.5 cm deep and 1.3 cm in diameter drilled out along the axis of the pressure block. The top of the Perspex pressure chamber was sealed off by a neoprene gasket G and brass disc H which was bolted down on to the collar at the top of the copper jacket surrounding the Perspex block. Hydrostatic pressure was applied to the solution in the cell B from a Budenburg pressure balance via the copper bellows arrangement shown in Figure 2. This enabled the oil pressure from the balance to be transmitted via the water, which completely filled the system to the left of the bellows arrangement, to the solution which was kept in the cell by the mercury seal at the bottom of the capillary neck.

The pressure vessel and cell were immersed in a water thermostat bath controlled to $\pm 0.05^\circ$. Pressure, some 100 lb/in² above the vapour pressure of the solution, was then applied at the normal temperature* of phase separation of the particular solution being studied. The pressure vessel was then thermostated some 2° above this temperature. The rod A prevented the top of the experimental cells from heating up quicker than the lower regions due to conduction by the brass disc H, and so reduced density gradients and heterogeneity inside the cell. The applied pressure was lowered gradually in steps of 5 lb/in² until faint light scattering could be observed.

On lowering the pressure further the solution would become increasingly cloudy and within a range of about 40 lb/in² the appearance of the

*The terms 'normal temperature of phase separation' and 'normal LCST' have been chosen to describe the temperature of phase separation or LCST of a solution which is in equilibrium with a vapour phase, as in the (T , w) studies. However, these terms have only been used when it is necessary to distinguish between such a system and a totally condensed one in which there is no vapour space.

solution for either molecular weight sample would change from that of perfect clarity to one of intense grey-brown opacity.

The precipitation pressure was taken to be that at which cloudiness was first observed, and this boundary condition could be easily detected by exerting a slight extra pressure on the balance table with the hand which would immediately remove the opalescence in the region of incipient phase separation. Reproducibility of the precipitation pressure was within $\pm 15 \text{ lb/in}^2$ for every solution studied and often within $\pm 5 \text{ lb/in}^2$. As soon as the precipitation pressure had been determined the applied pressure was increased by about 100 lb/in^2 to prevent a polymer-rich phase from settling; once such separation had occurred and there were two liquid layers, quantitative measurements became impossible. The temperature was then raised by 1° or 2° , and after allowing two hours for thermal equilibration the new precipitation pressure was measured.

RESULTS

The results of (T, w) studies are shown in *Figures 3, 4 and 5* for polystyrene + cyclopentane; polypropylene oxide + *n*-pentane; and polyisobutene + isopentane respectively. The reproducibilities of the separation temperatures varied with the molecular weights of the polymer and the viscosities of the solutions; they were usually better than 0.5°C but were one degree for PS 6 and PPO 8 above $w_2 = 0.01$ and for PIB 1 above $w_2 = 0.05$.

One of the solutions PPO 1 ($w_2 = 0.1034$) remained homogeneous even though it was maintained at a temperature well above the expected separation temperature. In this case the solution had expanded so as to fill the tube completely and eliminate the vapour space thus producing a pressure higher than the normal vapour pressure. This prompted the

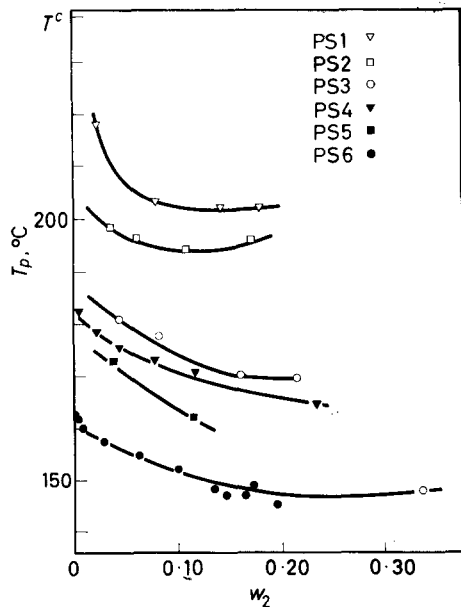


Figure 3— (T, w) phase diagram for the system: polystyrene + cyclopentane

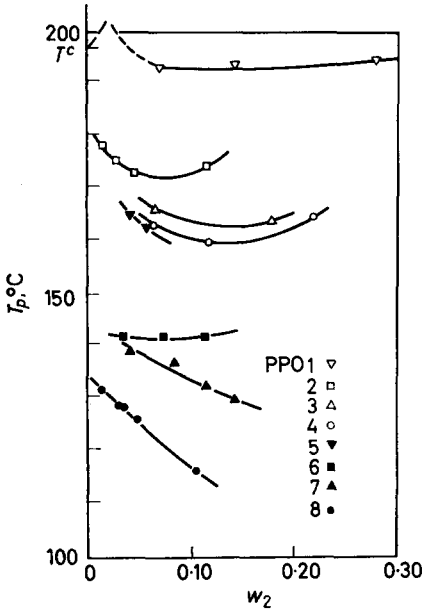


Figure 4—(T, w) phase diagram for the system: polypropylene oxide + *n*-pentane

subsequent investigation of the effect of pressure on LCSTs. Solutions of both samples of polyisobutene were investigated at concentrations of up to $w_2 = 0.06$, over temperature and pressure ranges of about 12 degrees and 400 lb/in², respectively. The results are shown in *Figures 6 and 7*. Phase separation temperatures are raised appreciably by relatively small pressure increases, and in the range studied the effect of pressure upon the phase separation temperature is independent of the concentration. The dashed lines in *Figures 6 and 7* represent the vapour pressures of the pure solvent at the corresponding temperatures and, therefore, to a close approximation, represent also the pressure under which the polymer solutions would exist if there were a vapour space in the cell⁷.

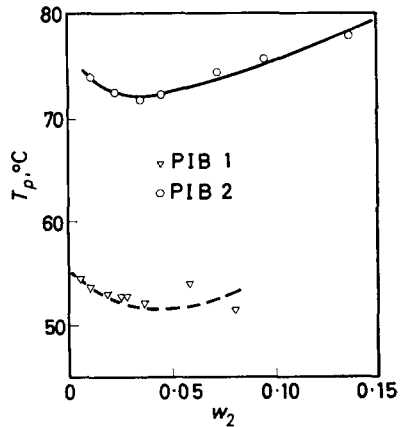


Figure 5—(T, w) phase diagram for the system: polyisobutene + isopentane

LOWER CRITICAL SOLUTION PHENOMENA

Figure 6—Effect of temperature upon the precipitation pressure (P_p) for the system: polyisobutene (PIB 1)+isopentane, at various concentrations

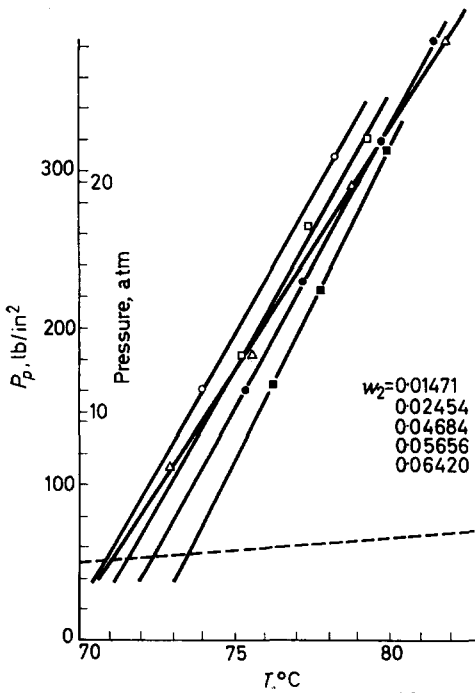
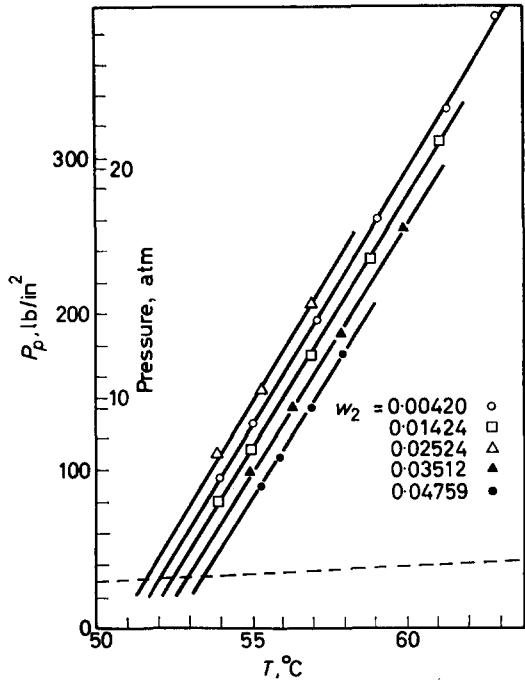


Figure 7—Effect of temperature upon the precipitation pressure (P_p) for the system: polyisobutene (PIB 2)+isopentane, at various concentrations

An expansion of the system of the order of 0.1 per cent occurred when a solution of sample PIB 2 ($w_2=0.04$) underwent phase separation at 79.40°C. This was estimated by observations of the mercury meniscus in the capillary neck of the cell while the pressure was lowered; first when the system was homogeneous *and then* after phase separation had occurred.

DISCUSSION

In polymer-solvent systems the degree of polymerization affects the location of both the lower and upper critical solution temperatures; as the molecular weight increases the range of total miscibility decreases. A complete set of data is not available for any system showing both phenomena but the comparison of UCST data for polystyrene+cyclohexane⁸ and the results shown in *Figure 3* for polystyrene+cyclopentane suggests that the LCST is more sensitive to molecular weight variation.

Table 1

Polystyrene \bar{M}_v	Critical temperatures of polystyrene solutions	
	UCST (°C) in cyclohexane ⁸	LCST (°C) in cyclopentane*
1.3×10^6	31.2	150
2.5×10^5	27.8	164
8.9×10^4	23.6	172
4.3×10^4	19.2	178

*Estimated from *Figure 3*.

Inspection of the (T, w) LCST phase boundary curves shows that the critical concentration w_c is not very sensitive to change in molecular weight. At an UCST the Flory-Huggins equation predicts, at least qualitatively, the shift to lower concentration observed experimentally as the molecular weight of the polymer is increased. The curves shown in *Figures 1 to 3* are distinguished from UCST curves also by their breadth. This could be due to a fairly wide molecular weight distribution in the polymer sample giving rise to fractionation between the two liquid phases. Other workers⁹ have reported, however, similar broad curves at the LCSTs of methyl acetate+monodisperse polystyrene.

Thus although the possibility of fractionation cannot be excluded from our own work, there does appear to be a difference in behaviour of the critical concentrations at the two critical temperatures of a solution.

A wide variation in curvature of the phase boundary is encountered in the polypropylene oxide + *n*-pentane system. This feature could be connected with the fact that these polymer samples vary in crystallizability (and, by implication, in stereoregularity) according to their source. Polyisobutene does not exhibit this type of isomerism and high resolution n.m.r. spectra of the polystyrene samples showed qualitatively that they were all of a similar degree of tacticity. The qualitative observations on polypropylene oxide + isobutane are also of interest because they provide an example of a system which does not quite attain complete miscibility. The more usual type of liquid-liquid immiscibility found in polymer solutions is depicted in *Figure 8(a)*; a range of temperature exists within which complete

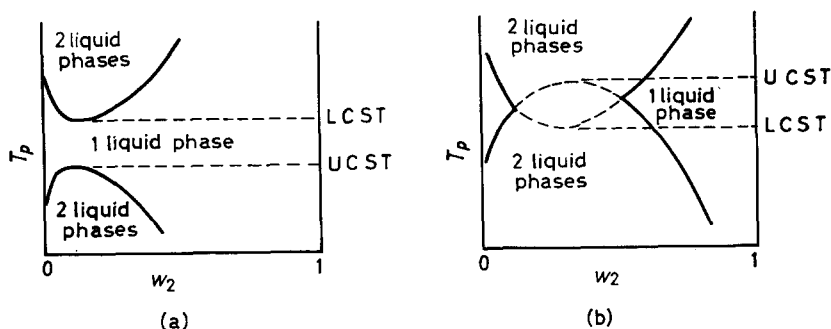


Figure 8—(a) Typical phase diagram for a polymer and a moderately poor solvent; (b) Phase diagram for a polymer and a very poor solvent

miscibility occurs above an UCST and below a LCST. Examples of this type of system are: polystyrene + cyclohexane (30°C and 180°C); polystyrene + cyclopentane (6°C and 150°C); polyisobutene + benzene (23°C and 160°C). The range of total miscibility will decrease, however, with decreasing solvent power and in a very poor solvent the boundary curves are expected to overlap as in Figure 8(b) so that complete miscibility is never observed. From a comparison of the critical constants of *n*-pentane and isobutane together with the location of the LCST in *n*-pentane, the LCST of polypropylene oxide ($\bar{M}_v = 1.3 \times 10^5$) + isobutane should occur in the range 50° to 70°C. In fact liquid-liquid immiscibility was found above and below this range of temperature and maximum swelling was observed at approximately 65°C, suggesting that the phase boundary curve is of the type shown in Figure 8(b).

The pressure coefficient of a critical solution temperature T_c is given by the relation

$$dT_c/dP = (\partial^2 V / \partial \phi_2^2)_{T_c} / (\partial^2 S / \partial \phi_2^2)_{T_c}$$

where ϕ_2 is the volume fraction of polymer. At a LCST $(\partial^2 S / \partial \phi_2^2)_{T_c}$ is necessarily positive and, since negative volumes of mixing are observed in this region, so is the volume coefficient. In agreement with this analysis the pressure coefficients for solutions of PIB 1 and 2 in isopentane are respectively 0.46 ± 0.01 and 0.40 ± 0.01 deg. atm⁻¹. At an UCST $(\partial^2 S / \partial \phi_2^2)_{T_c}$ must be negative and so dT_c/dP will be opposite in sign to $(\partial^2 V / \partial \phi_2^2)_{T_c}$. Ham, Bolen and Hughes¹⁰ found that the volume change on mixing for polystyrene + cyclohexane was small and positive, i.e. $(\partial^2 V / \partial \phi_2^2)_{T_c}$ negative. Accordingly dT_c/dP should be positive and was, in fact, observed to be 0.005 deg. atm⁻¹ at the UCST of the system¹⁰. Since the magnitude of $(\partial^2 V / \partial \phi_2^2)_{T_c}$ at the UCST and LCST do not differ by more than a factor of ten, it is clear that $(\partial^2 S / \partial \phi_2^2)_{T_c}$ is very much smaller at the LCST and some two orders of magnitude less than the value predicted from the Flory-Huggins equation.

Within the pressure and temperature ranges investigated the actual shape of the phase boundary curve is not affected by increasing the pressure.

Our apparatus would not withstand pressures greater than 400 lb/in² but from the work of Ehrlich *et al.*^{11,12} on polyethylene + *n*-alkane systems it is probable that at much higher pressures the linear (P, T) plots of *Figures 6 and 7* will eventually curve to give a maximum critical solution pressure.

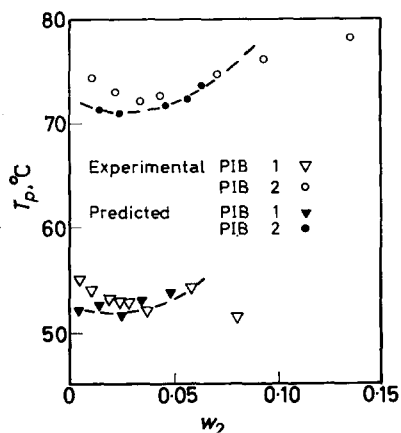


Figure 9—Comparison between (T, w) phase diagrams directly determined for polyisobutene and isopentane, and those derived by extrapolation of the (P, T) plot.

Extrapolation of the (P, T) plots back to the line representing the vapour pressure of the solvent provides an alternative method of estimating the normal phase separation temperature at each concentration. In *Figure 9*, temperatures obtained in this way are compared with the results obtained directly from (T, w) studies. Although more tedious than the direct method, the ease and sensitivity of detection of the onset of phase separation by this pressure technique provides a more accurate method of studying viscous media. Furthermore, control of solvent power by pressure can be effected in virtually isothermal conditions without the addition of a non-solvent and in an apparatus of reasonable bore the pressure is distributed uniformly thereby reducing problems of mixing. Thus, in view of the strong influence of molecular weight on the location of a LCST, these factors can be incorporated with some advantage into the design of an apparatus for polymer fractionation. Not only do these observations offer a new fractionation method but also the range of solvents may be extended to include compressed gases. Fractionation studies on the system polyisobutene + isopentane will be reported in another paper.

The origin of LCST phenomena is not adequately described by current theories of polymer solutions. From an experimental standpoint three factors govern the appearance of a LCST:

- the relative sizes of solute and solvent molecules
- the location of the critical temperature of the solvent, and
- the chemical natures of polymer and solvent.

The pattern of behaviour is consistent with an equation of the Flory-Huggins type in which the parameter χ is a function of temperature and composition² and also pressure. The relative sizes of polymer and solvent will influence primarily the Flory-Huggins configurational entropy of mixing

and account for part of the influence of molecular weight on the phase separation temperature. The suggestion² is that, as the critical temperature is approached, χ increases rapidly to cause phase separation because the solvent becomes expanded. In relation to the solubility parameters of the system, χ increases with $(\delta_1 - \delta_2)^2$; for a given solvent near its gas-liquid critical temperature δ_1 is sensitive both to temperature and pressure and δ_2 is controlled essentially by the chemical nature of the solute. A comprehensive assessment of the usefulness of the Flory-Huggins equation in the neighbourhood of the LCST requires a more extensive study of vapour pressures and heats of mixing under the appropriate conditions.

*Chemistry Department,
The University,
Manchester 13*

(Received July 1964)

REFERENCES

- ¹ FREEMAN, P. I. and ROWLINSON, J. S. *Polymer, Lond.* 1960, **1**, 20
- ² BAKER, C. H., BROWN, W. B., GEE, G., ROWLINSON, J. S., STUBLEY, D. and YEADON, R. E. *Polymer, Lond.* 1962, **3**, 215
- ³ DELMAS, G., PATTERSON, D. and SOMEYNOKY, T. J. *Polym. Sci.* 1962, **57**, 79
- ⁴ PEPPER, D. C. *Sci. Proc. Dublin Soc.* 1951, **239**, 25
- ⁵ JONES, M. N. *Ph.D. Thesis*, University of Manchester, 1962
- ⁶ American Petroleum Institute, *Research Project 44*. Carnegie Press: Pittsburgh, 1953
- ⁷ JORDAN, T. E. *Vapour Pressures of Organic Compounds*. Interscience: New York, 1954
- ⁸ SHULTZ, A. R. and FLORY, P. J. *J. Amer. chem. Soc.* 1952, **74**, 4760
- ⁹ MYRAT, C. and ROWLINSON, J. S. Private communication, Imperial College, London, 1962
- ¹⁰ HAM, J., BOLEN, M. C. and HUGHES, J. C. *J. Polym. Sci.* 1962, **57**, 25
- ¹¹ EHRLICH, P. and GRAHAM, E. P. *J. Polym. Sci.* 1960, **45**, 246
- ¹² EHRLICH, P. and KURPEN, J. J. *J. Polym. Sci. A*, 1963, **1**, 3009

The Thermal Degradation of Polypropylene Promoted by Organic Halogen Compounds

A. R. CAVERHILL and G. W. TAYLOR

The thermal degradation of polypropylene is promoted by certain halogenated compounds at temperatures above 220°C. In the chlorinated methanes, the activity increases with degree of chlorination. It is suggested that these compounds take part in a chain transfer process, involving attack of radicals derived from the polypropylene on the halogenated compound, followed by further reactions of the radicals produced from the halogenated compound, the fate of these radicals being dependent on the temperature.

IN A recent plant operation, it was found that traces of perchloroethylene markedly reduced extrusion pressures in the spinning of isotactic polypropylene filaments. The present paper describes laboratory experiments designed to explain this observation.

Further semi-technical work showed that the chloro- and bromo-methanes, and a variety of other alkyl halides, reduced the extrusion pressure. By contrast, chloro- and bromo-benzene were inactive, though benzyl chloride was very active. Accordingly, the chloromethanes were selected for laboratory study.

The polymer was 'Propathene' powder, of intrinsic viscosity 3.0 dl/g. Samples of polymer (5 g) were heated in evacuated sealed tubes in the presence of the halogenated compounds. In general, the dose of halogenated compound was measured in a gas burette. The extent of degradation was measured by determination of melt flow index, and these values were converted into intrinsic viscosities.

EVALUATION OF THE CHLOROMETHANES

These were used at a concentration of 10^{-3} mole per mole of polymer repeat unit; this is about 0.3 wt per cent for carbon tetrachloride. The samples were heated for 20 min in a vapour bath at 282°C. The compounds used, and final polymer viscosities, are shown in *Table 1*.

Table 1. Effect of chloromethanes on degradation of polypropylene

<i>Compound</i>	<i>I.V. (dl/g)</i>	<i>Compound</i>	<i>I.V. (dl/g)</i>
None	1.9	Carbon tetrachloride	0.4
Methylene chloride	1.8	Dichlorodifluoro-	
Chloroform	0.4	methane	2.0

The data of *Table 1* showed that a high degree of chlorination was necessary for promotion of degradation. Other work had suggested that bromo compounds were more effective than chloro compounds; the result for the dichlorodifluoromethane suggests that, in turn, chlorine compounds are more effective than fluoro compounds.

By heating at a lower temperature (259°C), it was found that carbon tetrachloride was more effective than chloroform.

EFFECT OF CONCENTRATION OF CARBON TETRACHLORIDE

Again, the samples were heated for 20 min at 282°C. The additive concentrations and polymer viscosities are shown in *Table 2*.

Table 2. Effect of concentration of carbon tetrachloride on degradation of polypropylene

CCl_4 concn (mole/polymer repeat unit) $\times 10^4$	I.V. (dl/g)	CCl_4 concn (mole/polymer repeat unit) $\times 10^4$	I.V. (dl/g)
None	1.9	1.8	0.7
0.8	1.0	3.5	0.4
1.0	0.8	10	Too low to measure

These results show that the extent of polymer degradation in a given time depends on the concentration of carbon tetrachloride.

EFFECT OF TIME

In this experiment, the temperature was 244°C, and the carbon tetrachloride concentration 4×10^{-4} mole per mole of polymer repeat unit. The data, given in *Table 3*, show that, during the early part of the heating period, there is a sharp drop in intrinsic viscosity. This is followed by a decreased rate of degradation.

Table 3. Effect of time on degradant action of carbon tetrachloride

Heating time (min)	0	15	30	45
I.V. (dl/g)	3.0	1.64	1.56	1.3

EFFECT OF TEMPERATURE

Various concentrations of carbon tetrachloride were used over a range of temperatures. The data are shown in *Table 4*. The heating time was 20 min.

Table 4. Effect of temperature on activity of carbon tetrachloride

Temp. (°C)	Additive concn (mole/polymer repeat unit) $\times 10^4$	I.V. (dl/g)	Temp. (°C)	Additive concn (mole/polymer repeat unit) $\times 10^4$	I.V. (dl/g)
197	0	2.93	244	0	2.82
197	8	2.74	244	8	1.13
197	220	2.67	259	0	2.87
223	0	2.92	259	4	0.48
223	8	1.98			

THE THERMAL DEGRADATION OF POLYPROPYLENE

The above results show that (a) carbon tetrachloride is active as low as 223°C, but essentially inactive at 197°C, and (b) the activity markedly increases as the temperature is raised.

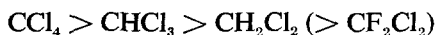
FATE OF CARBON TETRACHLORIDE

In this experiment, the volatile reaction products were analysed. Polypropylene (5 g) and carbon tetrachloride (0.1 g) were heated in a break-seal tube at 282°C for 30 min. The volatile products, analysed by gas chromatography and mass spectrometry, consisted mainly of equal parts of chloroform and methylene chloride, with traces of carbon tetrachloride and possibly methyl chloride. In addition, water, carbon dioxide and traces of acetic acid were detected.

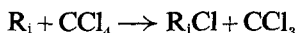
In another experiment, it was shown that carbon tetrachloride alone was stable under these conditions.

DISCUSSION

It has been found that a variety of halogenated hydrocarbons are active in reducing the molecular weight of polypropylene heated in the absence of air in the temperature range 240° to 280°C. In the chlorinated methanes, the activity ranking is as follows:

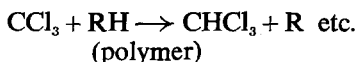


This is also the ranking found when these compounds are used as chain transfer agents in vinyl polymerization reactions¹. The activity does not, however, originate in the thermal decomposition of the chlorinated compound; carbon tetrachloride has been shown to be stable in the temperature region under consideration. In the presence of polypropylene carbon tetrachloride is successfully dechlorinated to chloroform, methylene chloride, and probably methyl chloride. These products are most easily explained in terms of radical attack on the tetrachloride, the radical originating from the thermal decomposition of a 'weak link' in the polymer chain:



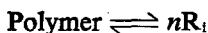
In this context, a 'weak link' is some intrusive element in a polymer structure which is generally considered to be the source of initiation of thermal degradation².

At temperatures in the region of 280°C, the CCl_3 radical undergoes further reactions as follows



At lower temperatures, the rate of this reaction falls, and presumably the chlorinated radicals undergo other reactions, for example recombination.

Even in the absence of these further reactions of CCl_3 , the above mechanism leads to a fall in molecular weight of the polymer. In the absence of chlorinated compound, the radicals derived from the scission of 'weak links' usually recombine



The effect of the halogenated compound is to upset this equilibrium, stabilizing R_1 by converting it to R_1Cl . This is a form of chain transfer. At very low temperatures (e.g. 200°C) the low rate of chlorine abstraction by R_1 , coupled with the high melt viscosity favouring geminate recombination of R_1 (these are probably formed in pairs), results in the halogenated compound having no effect on the change in molecular weight of the polymer.

At a given temperature, the molecular weight initially falls rapidly. This is followed by a much slower rate of fall. This behaviour is to be expected if the driving force of the process, that is, the generation of radicals from the scission of 'weak links' in the polymer, is rapidly exhausted.

*I.C.I. Fibres Ltd,
Research Department,
Hookstone Road, Harrogate*

(Received August 1964)

REFERENCES

- ¹ BAMFORD, C. H., BARB, W. G., JENKINS, A. D. and ONYON, P. F. *Kinetics of Vinyl Polymerization by Radical Mechanisms*, p 239. Butterworths: London, 1958
- ² GRASSIE, N. *Chemistry of High Polymer Degradation Processes*, p 73. Butterworths: London, 1956

The Use of Frictional Coefficients to Evaluate Unperturbed Dimensions in Dilute Polymer Solutions*

J. M. G. COWIE and S. BYWATER

It has been shown that the unperturbed dimensions of polymer molecules can be estimated from a knowledge of the frictional coefficients in any given solvent. The method involves a graphical procedure based on the simple relation

$$[\eta] = K_f M^{\frac{1}{2}} + 0.201 P_0 B A^{-2} M$$

which is similar to an equation developed by Stockmayer and Fixman relating intrinsic viscosity and molecular weight. The method is tested experimentally using data obtained from dilute solution measurements on polystyrene and polymethylmethacrylate.

IN ANY investigation of the dilute solution properties and structural characteristics of polymer molecules, it is important to obtain an estimation of the coil dimensions in the absence of specific solvent interaction. This has been accentuated in recent years when, during studies on stereoregular polymers, it was observed that the molecular dimensions of species with differing tacticities, which were generally regarded as being indistinguishable in good solvents, showed marked differences when dissolved in θ solvents^{1,2}. Thus the unperturbed dimension is a sensitive indication of stereochemical differences which are often swamped by strong interactions with the solvent. The unperturbed root mean square end-to-end distance $\langle R_0^2 \rangle^{\frac{1}{2}}$ may be obtained from light scattering measurements in a θ solvent. Such solvents may not, however, be readily available, and a graphical method can then be used if data in a thermodynamically good solvent are available. The original procedure proposed by Flory and Fox³, and Schaeffgen, which requires a knowledge of the $[\eta]/M$ relation, has recently been modified by Stockmayer and Fixman⁴ to the simple equation

$$[\eta] = KM^{\frac{1}{2}} + 0.51 \Phi_0 B M \quad (1)$$

where $\Phi_0 = 2.87 \times 10^{21}$, B is a solvent-polymer interaction parameter, and the unperturbed dimension of the macromolecule can be calculated from

$$K = \Phi_0 A^3 \quad (2)$$

$$A = [\langle R_0^2 \rangle / M]^{\frac{1}{2}} \quad (3)$$

The authors plot $[\eta] M^{-\frac{1}{2}}$ against $M^{\frac{1}{2}}$, yielding K as intercept on the ordinate. The unperturbed dimension of a flexible linear polymer molecule in any solvent can thus be estimated from equation (1), assuming that draining effects are negligible.

*Issued as N.R.C. No. 8376.

It is the purpose of this paper to point out that it is possible to obtain $\langle R_0^2 \rangle^\dagger$ from a knowledge of the frictional coefficient and that a relation analogous to equation (1) can be derived in a similar manner.

The frictional coefficient f_0 is related to the sedimentation coefficient S by

$$f_0 = M(1 - \bar{v}_2 \rho) / S_0^0 N_A \quad (4)$$

and is usually expressed as the intrinsic frictional coefficient $[f]$, where

$$[f] = f_0 / \eta_0 \quad (5)$$

η_0 being the solvent viscosity in poises.

It has been shown by Stockmayer and Albrecht⁵ that $[f]$ is related to molecular weight by

$$[f] = K_f M^{\dagger \alpha_f} \quad (6)$$

where

$$K_f = P_0 [\langle R_0^2 \rangle / M]^\dagger \quad (7)$$

and

$$\alpha_f = 1 + 0.609 z - \dots \quad (8)$$

Here P_0 is a constant whose limiting value, derived by Kurata and Yamakawa⁶, is 5.2, and z can be defined⁷ as

$$z = 0.330 BM^\dagger / A^3 \quad (9)$$

Thus substitution of equations (7), (8) and (9) into equation (6) with subsequent rearrangement gives the relation

$$[f] = K_f M^\dagger + 0.201 P_0 B A^{-2} M \quad (10)$$

Thus a plot of $[f] M^{-\dagger}$ against M^\dagger will have K_f as intercept, and $\langle R_0^2 \rangle^\dagger$ may then be obtained from equation (7). It should be noted that equation (8) is not a closed expression, and terms beyond the first power of z have been dropped.

The procedure has been tested using frictional coefficients derived from sedimentation measurements using polystyrene and polymethylmethacrylate (PMMA), and the results are compared with unperturbed dimensions measured directly from light scattering and indirectly from viscosity data.

EXPERIMENTAL

Samples

The preparation of polystyrene samples with very narrow molecular weight distributions has been described previously⁸. These have \bar{M}_w / \bar{M}_n ratios less than 1.1 and are equivalent to well fractionated material. Atactic PMMA was prepared by heating a 20 per cent solution of methylmethacrylate in benzene at 60°C for three hours using azobisisobutyronitrile as catalyst. A sample of PMMA which was ~80 per cent isotactic was prepared by Dr D. M. Wiles by the butyllithium initiated polymerization of methylmethacrylate in toluene solution at -30°C. Both PMMA samples were fractionated using a previously detailed technique⁹.

Light scattering

Light scattering measurements on polystyrene in cyclohexane were

carried out in a SOFICA P.G.D. instrument using unpolarized blue light ($\lambda = 4358 \text{ \AA}$). Cylindrical cells were used and were immersed in a thermostatically controlled bath containing benzene, the temperature of which was maintained at $35.0^\circ \pm 0.2^\circ \text{C}$. The bath temperature was measured by thermocouple at the entrance space for the cell and not in the thermometer well of the instrument. Solutions were clarified by passing them through a fine grade sinter glass filter, equipped with a water jacket, into a pre-heated cell. Solutions were prevented from precipitating during filtration by circulating water at 40°C through the filter jacket. Scattered intensities were measured at various angles from 45° to 135° , while the response of the instrument was kept constant by repeated reference to a glass standard previously calibrated against the 90° scattering of pure benzene at that particular temperature. Zimm plots were constructed and the coil size measured in the usual manner. Molecular weights could be calculated from

$$\frac{1}{\bar{M}_w} = \frac{2\pi^2}{\lambda^4 N_A R_B} \times n_B^2 \left(\frac{dn}{dc} \right)^2 I_B \left(\frac{c}{I_\theta} \right)_{\theta=0}^{c=0} \quad (11)$$

where N_A is Avogadro's number, I_B is the scattering intensity of standard benzene, n_B the refractive index of benzene, $(dn/dc) = 0.1814^{10}$, and R_B is the Rayleigh ratio for benzene, taken¹¹ as 49×10^{-6} . Values of \bar{M}_w obtained for narrow distribution polystyrene samples dissolved in toluene were within three per cent of similar measurements made on a Brice Phoenix photometer³, when this value of R_B was used. As the Brice Phoenix instrument was previously calibrated by three independent methods¹² which were in good agreement, it is felt that this value for R_B is most reliable. Details of molecular weight measurements for PMMA samples are given elsewhere².

Sedimentation velocity

A Spinco model E ultracentrifuge with a temperature control unit was used to measure the sedimentation coefficients (S_0^0) of polystyrene in cyclohexane and toluene at 35°C , and PMMA in nitromethane at 30°C . Runs of short duration were made at 59 780 rev/min, and were followed by means of phase plate schlieren optics. Values of (S_0^0) were calculated from the initial slopes of $\ln r$ against t as described previously¹³, thus minimizing pressure effects. Samples of polystyrene in cyclohexane were examined in detail, according to the method of Billick¹⁴, in order to estimate the effect of pressure on the sedimentation coefficient. A value of 1.66×10^{-9} for μ , the pressure correction factor, was obtained for this system which is in good agreement with previous determinations by Wales¹⁵ and Billick¹⁴, and sedimentation constants corrected for pressure were within three per cent of the values obtained by measuring the initial slope. Fractions of polystyrene in toluene and PMMA in nitromethane behaved similarly and the data were treated accordingly.

Partial specific volume

A Sprengel-Ostwald pycnometer, having a volume of approximately 21 ml was used to determine solution densities. The partial specific volume (\bar{v}_2) for atactic PMMA in nitromethane at 30°C was found to be 0.837 ml/g

and 0.824 ml/g for ~ 80 per cent isotactic PMMA. A value of 0.928 ml/g for polystyrene in cyclohexane at 35°C was used¹⁰ and the measurement on polystyrene in toluene at 35°C gave $\bar{v}_2 = 0.919$ ml/g.

Viscosity

Viscosity measurements were made using a Cannon-Ubbelohde semi-micro viscometer designed to have negligible kinetic energy correction. The viscometer was reproducibly positioned by means of a triple point suspension system in a constant temperature bath controlled to 0.01°C. The capillary size was chosen to ensure solvent flow times in excess of 200 sec.

RESULTS

Polystyrene

The relations between the sedimentation coefficient and molecular weight, and intrinsic viscosity and molecular weight were derived from double logarithmic plots and were found to be

$$S_0^2 = 1.50 \times 10^{-15} \bar{M}_w^{0.5} \quad (12)$$

$$[\eta] = 8.60 \times 10^{-4} \bar{M}_w^{0.5} \quad (13)$$

for polystyrene in cyclohexane and

$$S_0^2 = 2.70 \times 10^{-15} \bar{M}_w^{0.45} \quad (14)$$

for polystyrene in toluene, all being measured at 35°C.

Intrinsic frictional coefficients were calculated for both solvents and are shown in *Table 1*.

Table 1. Intrinsic frictional coefficients for polystyrene in toluene and cyclohexane at 35°C

Sample	$\bar{M}_w \times 10^{-5}$	$[f] \times 10^5$ Toluene	$[f] \times 10^5$ Cyclohexane
S1159	4.95	—	2.67
M2	4.60	3.66	2.63
S108	2.30	2.38	1.89
M4	1.25	1.71	1.48
S102	0.84	1.35	1.24
M1	0.57	1.11	0.95
M3	0.27	—	0.66

In *Figure 1* is shown a plot of $[f] M^{-1}$ against $M^{\frac{1}{2}}$, in which the data can be extrapolated to a common intercept of $K_f = 4.00 \times 10^{-8}$. *Figure 1* also shows results obtained by Cantow¹⁶, for polystyrene in cyclohexane, these being in good agreement with the present results. The value of the parameter A (equation 3) was found to be 0.78×10^{-8} when P_0 was taken as 5.1, which compares favourably with the results obtained from light scattering measurements in this and other laboratories (see *Table 2*).

Heterogeneity corrections

The parameter A obtained from *Figure 1* should be comparable with that calculated from the viscosity data using equation (1). This can readily

THE USE OF FRICTIONAL COEFFICIENTS

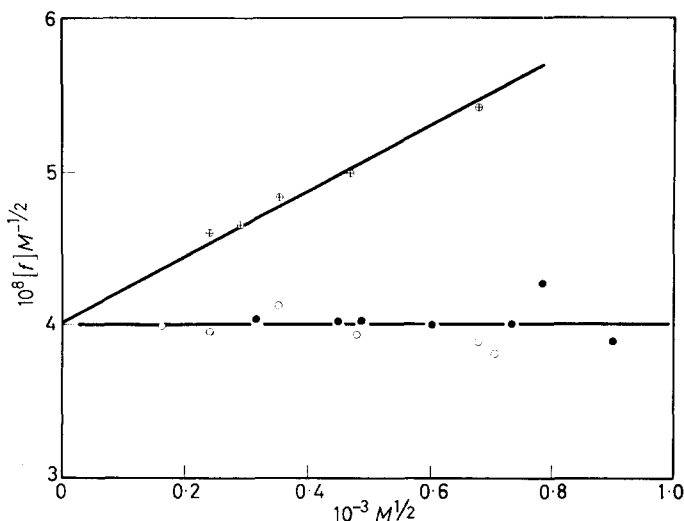


Figure 1—Variation of $[f] M^{-1/2}$ with $M^{1/2}$ for polystyrene in toluene \oplus , and polystyrene in cyclohexane, this work \circ , Cantow \bullet ; at 35°C

Table 2. Unperturbed dimensions for polystyrene in cyclohexane at 35°C

Sample	$\bar{M}_w \times 10^{-6}$	$\langle R_0^2 \rangle_z^\dagger A$	$\left[\frac{\langle R_0^2 \rangle_z^\dagger}{\bar{M}_w} \right]^\dagger \times 10^8$
S108	0.238	396	0.811
J3	0.574	580	0.766
M5	1.24	854	0.767
M6	1.91	1098	0.790
NBS*	4.0	1506	0.753
K. & C.†	3.2	1300	0.727
Average value of $A = 0.796 \times 10^{-8}$			

*See reference 10.

†See reference 17.

be obtained from K_θ in equation (13), and calculation of $\langle R_0^2 \rangle^\dagger$ then requires knowledge of the 'constant' Φ_0 whose limiting value is 2.87×10^{21} as computed by Kurata and Yamakawa⁶. However, it has been shown by Flory and his co-workers¹⁸ that the correct averages to be used in the relation

$$[\eta] = \Phi_0 \langle R^2 \rangle_n^{3/2} / \bar{M}_n \quad (15)$$

are number averages, and these authors proposed introduction of a factor to correct for sample heterogeneity when the ratio $\langle R^2 \rangle^\dagger / \bar{M}_w$ was determined from light scattering measurements. Thus equation (2) can be written

$$K = (\Phi_0 q_z) A^3 \quad (16)$$

where⁷

$$q_z = [(h+1)/(h+2)]^{3/2} \Gamma(h+3/2) (h+1)^{-1/2} \Gamma(h+1)^{-1} \quad (17)$$

For sharp fractions, such as are used here with $\bar{M}_w / \bar{M}_n \sim 1.1$, a value of $h \simeq 10$ can be used and Φ_0 becomes 2.5×10^{21} . For normally fractionated

material a value of $h=4$ is more representative and Φ_0 can then be reduced to 2.1×10^{21} , a value obtained experimentally by several workers. A similar correction¹⁹ for P_0 can be made reducing P_0 to 5.1 for $h=10$ and 4.95 for $h=4$. Thus when $h=10$, one obtains $A=0.70 \times 10^{-8}$ from the viscosity data, which is about ten per cent lower than both that obtained using frictional coefficients and the average of the light scattering values.

Polymethylmethacrylate

Sedimentation velocity measurements on PMMA fractions of differing stereoregularity gave the relations

$$S_0^0 = 1.29 \times 10^{-15} \bar{M}_w^{0.435} \quad (18)$$

for atactic fractions and

$$S_0^0 = 1.22 \times 10^{-15} \bar{M}_w^{0.425} \quad (19)$$

for (~ 80 per cent) isotactic fractions.

Intrinsic frictional coefficients were calculated and plotted according to equation (10) (see *Figure 2*). Values of $[f]$ are listed in *Table 3*.

Table 3. Sedimentation and intrinsic frictional coefficients for atactic and isotactic PMMA in nitromethane at 30°C

Sample	$\bar{M}_w \times 10^{-5}$	$[f] \times 10^5$	$S_0^0 \times 10^{13}$
<i>Atactic</i>			
R1	2.25	1.61	2.5
R2	1.68	1.36	2.2
R3	1.45	1.28	2.0
R4	0.91	0.98	1.6
R5	0.73	0.83	1.5
<i>Isotactic</i>			
D1	5.83	3.71	3.4
D2	3.64	2.86	2.8
D3	2.24	2.12	2.3
D4	1.64	1.75	2.0
D5	0.97	1.31	1.6

Calculation of A , assuming $P_0=4.95$ ($h=4$), gave 0.74×10^{-8} for isotactic and 0.56×10^{-8} for atactic PMMA respectively. The difference is quite marked and reflects the variation of the unperturbed dimension with tacticity which has been observed in PMMA using viscosity and light scattering measurements². The values may be compared with data reported by Sakurada *et al.*²⁰ for PMMA in various θ solvents. These authors examined isotactic PMMA in a methylethyl ketone-isopropanol mixture which had a θ temperature of 30.3°C. From viscosity measurements they calculated a value of $A=0.68 \times 10^{-8}$ using $\Phi_0=2.87 \times 10^{21}$ and, if this is corrected for heterogeneity (assuming $h=4$), A becomes 0.75×10^{-8} in good agreement with the value reported here. Atactic PMMA does not give such a good correlation as interpolation of Sakurada's results yields $A=0.66 \times 10^{-8}$ corrected for heterogeneity, which is about 17 per cent higher than that calculated from frictional coefficients.

Schulz and Kirste²¹ carried out light scattering measurements on atactic PMMA in butyl chloride and found the θ temperature to be $\sim 35^\circ\text{C}$. Using their data one can calculate $A = 0.54 \times 10^{-8}$ which is in close agreement with the value quoted here, even allowing for the small changes due

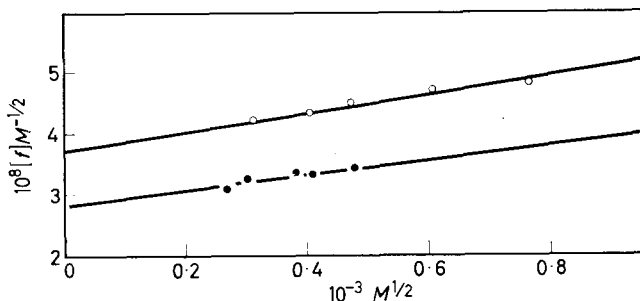


Figure 2—Plot of $[f] M^{-1/2}$ against $M^{1/2}$ for PMMA in nitromethane at 30°C . Atactic samples \bullet , and ~ 80 per cent isotactic samples \circ

to the temperature difference. Krause and Cohn-Ginsberg²² used an extrapolation procedure³ on viscosity data at 30°C and obtained $A = 0.61 \times 10^{-8}$, whereas similar measurements⁴ made in this laboratory² show $A = 0.59 \times 10^{-8}$ at 32°C . With the exception of Sakurada's data these results are within 11 per cent of each other, but Schulz is the only worker who has actually measured $\langle R_0^2 \rangle^{1/2}$ directly by light scattering.

DISCUSSION

Intrinsic frictional coefficients have been derived exclusively from sedimentation measurements in this investigation. However, it is also possible to calculate $[f]$ from diffusion measurements, but in the absence of suitable diffusion data the method has not been tested. It should be applicable, nevertheless, to this type of plot, thus extending its usefulness. It has been noticed when using equations (1) and (10) that the plot may curve towards the abscissa at molecular weights $> 10^6$ when measurements are made in good solvents. The effect may be due to the neglect of higher terms in the expansion of α . Stockmayer and Fixman⁴ have used a simple closed expression for the expansion factor α , and equation (8) is an equivalent expression if terms beyond the first power are dropped. The slopes of the lines obtained from both equations were found to be the same, indicating the equivalence of the two expressions. Thus when using this type of graphical procedure to obtain $\langle R_0^2 \rangle^{1/2}$, it is advisable to use data in which α is not too large, thus ensuring a more accurate extrapolation. Equation (1) is probably easier to use, as viscosity measurements are much more readily carried out. One advantage, however, of equation (10) seems to be that P_0 is less sensitive than Φ_0 to both heterogeneity and excluded volume corrections, thus a more reliable value for the parameter A should be obtained. This appears to be true for polystyrene in cyclohexane, where

the average experimentally determined parameter is in good agreement with that calculated from equation (10). Moreover, the differences involved are not so serious if considered in the light of possible corrections for sample heterogeneity. Krigbaum and Carpenter¹⁷ have dealt with this and found the difference between corrected and uncorrected A values to be about ten per cent. Thus fractions of well defined molecular weight distribution would be required to give the most accurate results.

The method may therefore be used to estimate the unperturbed dimensions in the absence of a suitable θ solvent, or when the molecular weights are too low to allow accurate determination of the coil size by light scattering techniques. It is probably best used as a plot, complementary to the Stockmayer-Fixman equation.

The authors wish to thank Drs D. J. Worsfold and D. M. Wiles for preparing the samples, and Mr P. M. Toporowski for measurements on the ultracentrifuge.

- *Division of Applied Chemistry,
National Research Council,
Ottawa, Ontario, Canada*

(Received August 1964)

REFERENCES

- ¹ For review see *Newer Methods of Polymer Characterization*, Chapter 1. Interscience: New York, 1964
- ² BYWATER, S., COWIE, J. M. G. and WILES, D. M. Paper presented at the 12th Canadian High Polymer Forum, St Marguerite, P.Q., 1964
- ³ FLORY, P. J. and FOX, T. G. *J. Amer. chem. Soc.* 1951, **73**, 1904
- ⁴ STOCKMAYER, W. H. and FIXMAN, M. *J. Polym. Sci. Part C*, 1963, **1**, 137
- ⁵ STOCKMAYER, W. H. and ALBRECHT, A. C. *J. Polym. Sci.* 1958, **32**, 215
- ⁶ KURATA, M. and YAMAKAWA, H. *J. chem. Phys.* 1958, **29**, 311
- ⁷ KURATA, M. and STOCKMAYER, W. H. *Fortschr. HochpolymerForsch.* 1963, **3**, 196
- ⁸ COWIE, J. M. G., WORSFOLD, D. J. and BYWATER, S. *Trans. Faraday Soc.* 1961, **57**, 705
- ⁹ COTTAM, B. J., WILES, D. M. and BYWATER, S. *Canad. J. Chem.* 1963, **41**, 1905
- ¹⁰ MCINTYRE, D., WIMS, A., WILLIAMS, L. C. and MANDELKERN, L. *J. phys. Chem.* 1962, **66**, 1932
- ¹¹ SICOTTE, Y. and RINFRET, M. *Trans. Faraday Soc.* 1962, **58**, 1090
- ¹² SIRIANNI, A. F., WORSFOLD, D. J. and BYWATER, S. *Trans. Faraday Soc.* 1959, **55**, 2124
- ¹³ COWIE, J. M. G. and TOPOROWSKI, P. M. *Polymer, Lond.* 1964, **5**, 601
- ¹⁴ BILLICK, I. H. *J. phys. Chem.* 1962, **66**, 1941
- ¹⁵ WALES, M. and REHFELD, S. J. *J. Polym. Sci.* 1962, **62**, 179
- ¹⁶ CANTOW, H.-J. *Makromol. Chem.* 1959, **30**, 169
- ¹⁷ KRIGBAUM, W. R. and CARPENTER, D. K. *J. phys. Chem.* 1955, **59**, 1166
- ¹⁸ NEWMAN, S., KRIGBAUM, K. R., LAUGIER, C. and FLORY, P. J. *J. Polym. Sci.* 1954, **14**, 451
- ¹⁹ GOUNLOCK, E. V., FLORY, P. J. and SCHERAGA, H. A. *J. Polym. Sci.* 1955, **16**, 383
- ²⁰ SAKURADA, I., NAKAJIMA, A., YOSHIZAKI, O. and NAKAMAE, K. *Kolloidzshr.* 1962, **186**, 41
- ²¹ SCHULZ, G. V. and KIRSTE, R. Z. *phys. Chem.* 1961, **30**, 171
- ²² KRAUSE, S. and COHN-GINSBERG, E. *Polymer, Lond.* 1962, **3**, 565

Thermal Conductivities of Polymers

II—Polyethylene

R. P. SHELDON and Sister K. LANE

The thermal conductivities of a series of polyethylenes of different densities have been measured in the range 15° to 98°C. The thermal conductivity is found to decrease with increase of temperature and decrease of density. The results have been analysed by two methods for the separate evaluation of the contributions of the amorphous and crystalline fractions, and in both cases the thermal conductivity is found to decrease with increase of temperature. Measurements on irradiated polymer indicate a decrease with crosslinking for small extents of the latter.

IN A previous paper¹ which was devoted to the thermal conductivities of unplasticized and plasticized polyvinyl chloride, discussion was thereby restricted to a material which is considered to be largely amorphous in character. In a series of measurements carried out in the range 15° to 98°C, the results support the view that the thermal conductivity of any one particular specimen increases with increase of temperature, reaches a maximum in the vicinity of the glass-temperature and then decreases, at least in the initial stages, with further increase of temperature. In general, this is characteristic of an amorphous polymer and is the behaviour to be expected upon the basis of mechanisms for the conduction process proposed by Uberreiter and Nens following their work with amorphous polystyrene². For a crystalline polymer the nature of the results may be somewhat different in that there may be separate contributions of the crystalline and amorphous phases to the overall thermal conductivity and the temperature dependence of these contributions may be quite different. It is clear that polyvinyl chloride is not very suitable for study along these lines.

A polymer which is more suitable for this approach is polyethylene, since not only may it be obtained in a range of degrees of crystallinity but it is also readily available in bulk form suitable for investigation. At the time of commencement of the work described in this paper, although some information had been published on the thermal conductivity of polyethylene no attempt had apparently been made to analyse the results for an assessment of the individual contributions of the two phases. However, more recently Eiermann has made this approach³ using an equation adapted from one relating to the electrical conductivity of a two-phase system and which had been derived by Maxwell⁴. The results of the present work on five samples of polyethylene of differing density have received a similar treatment, and at the same time a second approach has been made using an equation based upon what is believed to be a more realistic concept of the polymer texture although this in turn involves some approximation⁵. The results themselves have been obtained over the same temperature range as for the polyvinyl chloride. Some mention is also made of results obtained on one sample which was subsequently irradiated with γ -rays.

EXPERIMENTAL

Materials

The samples of polyethylene were kindly supplied by I.C.I. Ltd, having properties as shown in *Table 1*. They were received in block form and so were machined on a lathe to a shape suitable for insertion into the thermal conductivity apparatus. For the purposes of drilling a special drill was made from a $\frac{1}{4}$ in. twist drill which was brazed on to a silver steel rod in order to produce a central hole in the 8 in. long test piece.

It should be mentioned that density measurements were made after machining and also after a complete experimental run and in all cases the agreement was within 0.002 g/cm^3 of the values quoted in *Table 1*.

Table 1. Densities of polyethylene samples at 25°C

<i>Sample</i>	<i>A</i>	<i>B</i>	<i>C</i>	<i>D</i>	<i>WNG 14</i>
Density (g/cm^3)	0.940	0.948	0.951	0.935	0.918

Sample B was irradiated in the Fuel Rod Assembly at Harwell in two stages, being given doses of 11 and 30 megarads respectively. The thermal conductivity was determined after each irradiation.

Apparatus and technique

(1) *Thermal conductivity*.—The apparatus and technique used in the measurement of thermal conductivity was identical to that previously described^{1,6} being one involving a cylindrical cell under steady state conditions. Measurements were made on all samples including the one which had been irradiated, in the temperature range 15° to 98°C .

(2) *Confirmation of isotropy*.—Fourier's equation used in the thermal conductivity calculations is of a form appertaining to isotropic material. That this condition obtains was confirmed by X-ray diffraction analysis which showed sharp ring patterns characteristic of isotropic crystalline material. It might be mentioned that birefringence techniques, although offering the apparent advantages of speed and simplicity, were not convenient for this purpose because of impressed surface orientation resulting from the action of cutting a specimen.

RESULTS

The thermal conductivities of the various samples of polyethylene are shown expressed as a function of temperature in *Figure 1*. The values for sample B after an irradiation of 11 megarads (density 0.947 g/cm^3 at 25°C , with a gel-fraction of 43.6 per cent and a molecular weight between crosslinks of 9.6×10^4 as determined by swelling in xylene), were parallel to those for the original sample but approximately $0.15 \times 10^{-4} \text{ cal/cm sec } ^\circ\text{C}$ lower at all temperatures. The corresponding values after a further irradiation dose of 30 megarads (density 0.946 g/cm^3 at 25°C , with a gel-fraction of 76.1 per cent and a molecular weight between crosslinks of 1.0×10^4) were again parallel but approximately $0.3 \times 10^{-4} \text{ cal/cm sec } ^\circ\text{C}$ lower than the un-irradiated sample values.

DISCUSSION

Figure 1 shows that the value of thermal conductivity decreases with an increase of temperature in the range of temperatures used, and also decreases with the density of polyethylene at any particular temperature. The latter trend which is more clearly seen in Figure 2 for a plot of thermal conductivity at 25°C against density is presumably a consequence of the different degrees of crystallinity associated with the different samples, being a reflection of the superior mechanism for conduction in crystalline material. (It would be interesting in this context, where an alternative direct

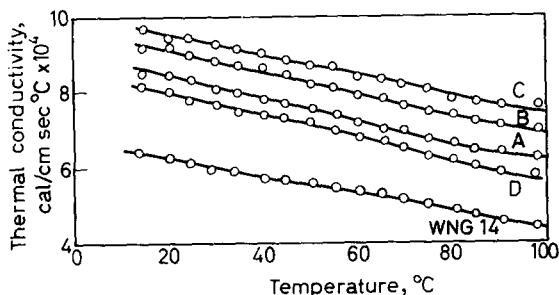


Figure 1—Thermal conductivities of polyethylenes versus temperature

dependence upon density might be proposed, to carry out measurements on a polymer such as poly-4-methyl-pentene-1 where the crystalline density is reported to be lower than that of the amorphous⁷ value.) The temperature dependence of the thermal conductivity of polyethylene is similar to that previously reported for polyvinyl chloride¹. The decrease in this case may, however, be attributed to one or more of a number of factors. For example, the experimental temperature range is sufficiently above the glass-temperature for a decrease to be expected on the basis of the amorphous content contribution to thermal conductivity. Indeed, work at lower temperatures with polyethylene has shown a maximum in the thermal conductivity expressed as a function of temperature³ just as in the case of polyvinyl chloride. Against this it should be remembered that an increase of thermal conductivity with temperature for amorphous polymers has been predicted at temperatures much higher than that of the glass-temperature². A second influence of temperature may result from a decrease in the thermal conductivity of crystalline material as has been found for low molecular weight paraffin by Eucken⁸. A further influence might be expected as a result of incipient melting as the 'apparent' melting-point is approached.

Before discussing this aspect in more detail in the light of an analytical treatment of the experimental results in terms of separate contributions of the amorphous and crystalline fractions some mention should be made of the agreement between the present results and those of other workers.

In general, where comparison is made on the basis of similarity of density of the polyethylene samples studied in the various laboratories it can be said that the agreement is very good. This is particularly true for

the results of Eiermann³ and Knappe⁹, which were obtained by quasi-stationary state methods, for high density polymer although small differences are apparent for low density material. On the other hand good agreement is observed between the present results and those of Kline⁶ who studied a lower density polyethylene, although the downward trend of

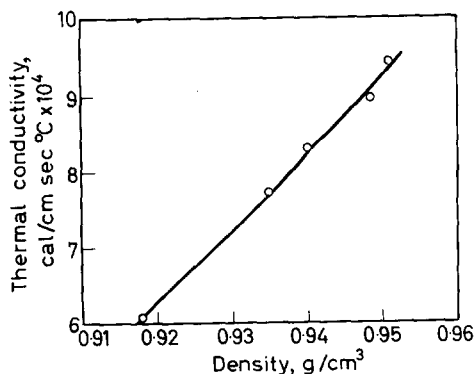


Figure 2—Thermal conductivities of polyethylenes at 25°C versus density

values is sharper at higher temperatures in the latter case. This general agreement would suggest further that in view of, presumably, the different sources and conditioning histories of the various samples studied any influence of larger scale texture on thermal conductivity may be small.

Some mention may also be made at this stage of the results obtained on irradiated polymer which have been reported earlier. It would appear that the fall in thermal conductivity is presumably a consequence of a decrease in density rather than from the production of crosslinks, although this may not be true at higher degrees of crosslinking. Much more prolonged irradiation should throw light on this aspect, since it is known that following an initial fall in the density of polyethylene, there follows a progressive increase on irradiation¹⁰. Even so interpretation may well be complicated by other possible simultaneous changes in chemical and physical properties.

Returning to the problem of analysis of the results in terms of separate contributions of amorphous and crystalline fractions the first approach was made along the lines indicated by Eiermann³ using an equation adapted from one derived by Maxwell⁴ relating to the electrical conductivity of a two-phase system. The transformed equation has the form

$$k = \frac{2k_a + k_c + 2x_v(k_c - k_a)k_a}{2k_a + k_c - x_v(k_c - k_a)} \quad (1)$$

where k is the overall thermal conductivity, k_a and k_c , the thermal conductivities of the amorphous and crystalline fractions respectively, and x_v is the volume fraction degree of crystallinity.

Using values of x_v obtained in the usual way from a knowledge of the densities of the polymer and interpolating the corresponding values of k from the curves shown in *Figure 1*, the resulting equations were solved in pairs for a series of temperatures to provide individual values for k_a and k_c at the same temperatures. The means for k_a are shown plotted as a

function of temperature in *Figure 3*. Following the procedure adopted by Eiermann for purposes of comparison of results the reciprocal thermal conductivities of the crystalline phase are similarly presented as a function of temperature in *Figure 4*.

The values for k_a are somewhat lower than those of Eiermann but are of an order to be expected from the extrapolation of isothermals of conductivity expressed as a function of density or degree of crystallinity. Attention is drawn to the fact that the values show a trend of a decrease with increase of temperature which is not unexpected for amorphous material. The values of $1/k_c$ are also lower than those presented by

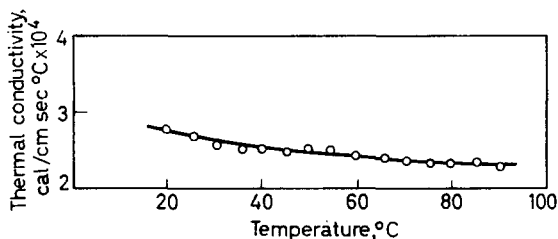


Figure 3—Thermal conductivity of amorphous polyethylene versus temperature (Eiermann equation)

Eiermann, but on the other hand if we ignore the extreme pairs of points on the graph for the purposes of plotting (there is some little justification for this for the higher temperature results due to uncertainties in the degree of crystallinity), then as found by Eiermann the results follow a T^{-1} law with the straight line passing approximately through the absolute zero point on the temperature scale. It is seen therefore that there is a certain amount of agreement between the two sets of results.

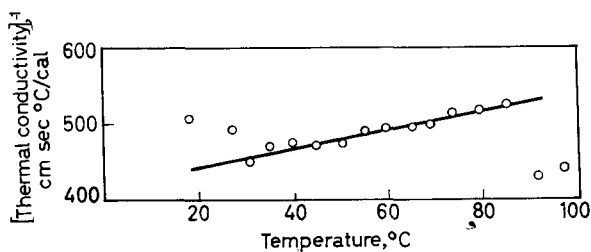


Figure 4—Reciprocal thermal conductivity of crystalline polyethylene versus temperature (Eiermann equation)

However, as mentioned previously, a second approach has been made in the analysis of the experimental results. The main reason for doing this is because of reservations on the applicability of the Maxwell model to polyethylene. In this model the second phase is imagined to exist as small spheres, their radii being small compared with the distance between spheres and consequently their total volume being a small fraction of the whole. Although there is still some difference of opinion as to the nature of the

texture of polyethylene, it is felt that the above model must be very approximate. The second approach depends upon a model which may be considered more closely to represent the 'fringed micelle' concept of structure but even this involves approximations which will be discussed later. In this model cubes, which represent one phase, of side a are on common centres with cubes of a second phase of side b , so that the total volume fraction of the first phase is $(a/b)^3$. The resistivity of the system in terms of the separate contributions of the individual phases may then be calculated⁵. It is pointed out that interferences which would necessitate the application of field theory have been ignored for the purposes of this calculation. Converting the expression in the appropriate way for thermal conductivity considerations the final equation has the form

$$\frac{1}{k} = \frac{(x_v)^{1/3} (1/k_c k_a)}{(1/k_c) [1 - (x_v)^{2/3}] + (1/k_a) (x_v)^{2/3}} + \frac{1}{k_a} [1 - (x_v)^{1/3}] \quad (2)$$

This equation was solved for interpolated values from *Figure 1* at a number of temperatures, by taking a series of arbitrary values for k_c in a range of order indicated by general extrapolation of curves of the form of *Figure 3*. The value of k_c which resulted in the minimum deviation in the calculated values for k_a was then adopted. For example, at 25°C a value of 1.90×10^{-3} cal/cm sec °C for k_c produces an average value with a coefficient of variation of one per cent of 2.23×10^{-4} cal/cm sec °C for k_a . Following the initial analysis of the results obtained at 25°C it was found that the value for k_c together with the experimental values of k for the various samples gave an approximately linear logarithmic relationship with degree of crystallinity and this observation was used to ease the subsequent laborious calculations for the results at higher temperatures. *Figures 5* and *6* show the relationships between k_a and $1/k_c$ as before with temperature. From *Figure 5*, although the absolute values are slightly lower, it is seen that the general behaviour is as obtained with the Eiermann treatment,

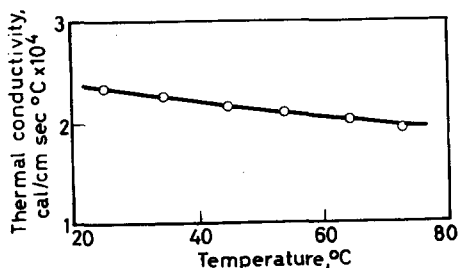


Figure 5—Thermal conductivity of amorphous polyethylene versus temperature

i.e. k_a decreases with increase of temperature. Similarly, the results for $1/k_c$ follow a T^{-1} law but, in this instance, with a more approximate approach towards absolute zero. On the other hand closer agreement with the actual values reported by Eiermann in the experimental temperature range is achieved. Although, in the above analysis, the cubes of side a have been identified with the crystalline phase, there is no mathematical reason for doing this. It was found, however, that if the identity is reversed and the

analysis is carried out as before, then completely unrealistic values were obtained for the thermal conductivity of the amorphous phase. Whether this is support for the model and in turn for a fringed micelle concept is not clear. It would presumably require refinement of the treatment with an extension to other possible models before an opinion on this aspect could be given.

Comparing the results of the two approaches it would appear that on the whole those obtained by the second analysis are more consistent in

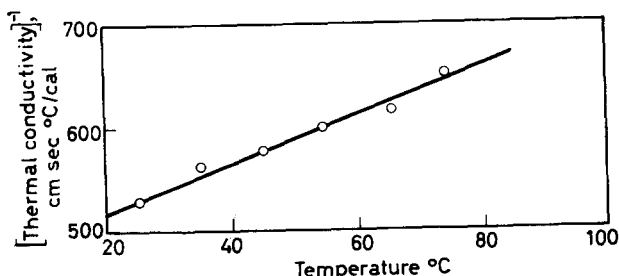


Figure 6—Reciprocal thermal conductivity of crystalline polyethylene versus temperature

themselves. It is conceded, however, that the model neglects the possibility of irregularly shaped crystallites, if they exist at all, together with a size distribution, as well as the probability of non-linear flow lines. Perhaps an easier way to assess the usefulness of the model would be to carry out measurements on samples which extend the density range so that extrapolation to the completely amorphous and crystalline conditions is not subject to so much uncertainty. As mentioned previously, doing this with the present results gives reasonable agreement and the value of k_a compared with that for polyvinyl chloride¹ and polymethyl methacrylate¹¹ is of an order to be expected if we draw conclusions from the rather sparse information concerning organic liquids¹² in that the more polar the liquid the greater it appears is the thermal conductivity.

The authors gratefully acknowledge the assistance of R. Roberts, R. W. Vale, P. R. Blakey and S. W. Smethurst in various aspects of this work.

*Polymer Research Laboratories,
Department of Chemical Technology,
Institute of Technology, Bradford*

(Received September 1964)

APPENDIX A

DERIVATION OF EQUATION (2)

From a model of a cube (of side a) of material A, on a common centre with a larger cube (of side b) of material B, it is seen that the volume of $A = a^3$ and the residual volume of $B = b^3 - a^3$.

If p and r are the resistivities of A and B respectively, then the resistance of A is

$$R_1 = p/a \quad (\text{i})$$

and the resistance of the centre slab of residual B of width a is

$$R_2 = ra/b^2 - a^2 \quad (\text{ii})$$

The parallel resistance of both volumes is

$$R_3 = R_1 R_2 / (R_1 + R_2) = apr / (pb^2 - pa^2 + ra^2) \quad (\text{iii})$$

The resistance of slabs length $(b - a)$ is $R_4 = r(b - a)/b^2$ (iv)

therefore the total resistance $R_t = R_3 + R_4$

$$= \frac{apr}{p(b^2 - a^2) + ra^2} + \frac{r(b - a)}{b^2} \quad (\text{v})$$

The overall resistivity of the system, and implicitly an array of similar systems is therefore $= bR_t$, which in terms of conductivity may be expressed as

$$\frac{1}{k} = \frac{(x_v)^{1/3} (1/k_c k_a)}{(1/k_c) [1 - (x_v)^{2/3}] + (1/k_a) (x_v)^{2/3}} + \frac{1}{k_a} [1 - (x_v)^{1/3}] \quad (2)$$

where k , k_a and k_c are the conductivities of the overall system, material B and material A severally, and x_v is the volume fraction $(a/b)^3$ of A.

REFERENCES

- ¹ SHELDON, R. P. and LANE, K. *Polymer, Lond.* 1965, **6**, 63
- ² UBERREITER, K. and NENS, S. *Kolloidzshr.* 1951, **123**, 92
- ³ EIERMANN, K. American Chemical Society *Polymer Reprints*, 1963, **2**, 637
- ⁴ MAXWELL, J. C. *Treatise on Electricity and Magnetism*, Vol. I. Oxford University Press: London, 1873
- ⁵ MIDGLEY, D. Private communication (see Appendix)
- ⁶ KLINE, D. E. *J. Polym. Sci.* 1961, **50**, 441
- ⁷ GRIFFITH, J. H. and RANBY, B. G. *J. Polym. Sci.* 1960, **44**, 369
- ⁸ EUCKEN, A. *Ann. Phys., Lpz.* 1911, **34**, 185
- ⁹ KNAPPE, W. *Z. Phys.* 1960, **12**, 508
- ¹⁰ CHARLESBY, A. and ROSS, M. *Proc. Roy. Soc. A*, 1953, **217**, 122
- ¹¹ See e.g. SHOULBERG, R. H. and SHETTER, J. A. *J. appl. Polym. Sci.* 1962, **6**, S32
- ¹² LANGE, N. A. (Ed.). *Handbook of Chemistry*. Handbook Pub. Co.: Ohio, 1956; *Handbook of Chemistry and Physics*. Chemical Rubber Pub. Co.: Cleveland, 1962-63

The Bulk Crystallization Kinetics of Polypropylene and Polybutene

M. GORDON* and I. H. HILLIER†

The crystallization kinetics of polypropylene and polybutene have been investigated dilatometrically. The results, when analysed in terms of the Avrami equation, yield values of the Avrami exponent of 2.5 ± 0.1 and 3.13 ± 0.13 respectively. Values of 2.5 and 3 indicate the diffusion controlled growth of sporadically nucleated spherulites for polypropylene, and the constant radial growth of instantaneously nucleated spherulites for polybutene. In contrast to the behaviour of many other polymers, the exponent is here temperature independent and compatible with the simple Avrami picture. Also, dilatometry and optical microscopy show some degree of correlation. The exponent is found to be 3 ± 0.05 when polypropylene is crystallized from 'seeds'. The temperature dependence of the Avrami rate constants is also discussed.

THE crystallization kinetics of bulk polymers has been interpreted in terms of the Avrami equation¹

$$\chi_t = \chi_\infty [1 - \exp(-zt^n)] \quad (1)$$

where χ is the crystallinity, t the time, z a rate constant depending upon the nucleation and growth rates, and n an integer depending upon the shape of the growing entities. For spherulites growing with a constant radial rate, the value of n would ideally be three or four, corresponding to instantaneous and sporadic nucleation respectively². In terms of the measured dilatometric heights (h_t), equation (1) becomes

$$[h_0 - h_t]/[h_0 - h_\infty] = 1 - \exp[-zt^n] \quad (2)$$

where h_0 and h_∞ are the dilatometric heights at zero and infinite time respectively.

Recent work on a number of polymers³⁻⁶ has cast doubt as to the validity of this equation, for although it fits the crystallization of many polymers with low standard deviations, the value of n is rarely found to be three or four. Frequently, n is non-integral, and dependent upon temperature. Both polypropylene and polybutene readily crystallize to give well-defined spherulites and show only a slight degree of secondary crystallization. They are thus good systems for investigating the validity of the Avrami equation.

EXPERIMENTAL

Isotactic polypropylene (having viscosity average degree of polymerization $P_v = 9.8 \times 10^3$) given by Shell Research Ltd, and polybutene given by Cabot

*Present address: Department of Pure and Applied Chemistry, University of Strathclyde, Glasgow, C.1.
†Present address: Institute for the Study of Metals, University of Chicago, Illinois, U.S.A.

Corpn were used. The construction of the dilatometers containing less than 100 mg of polymer, and details of the temperature stability have been given in a previous paper³.

Evaluation of dilatometric data

Dilatometric data are usually⁷ fitted to equation (2) by plotting

$$\ln [-\ln (h_t - h_\infty)/(h_0 - h_\infty)] \text{ versus } \ln t$$

The slope of this line gives the value of the exponent n . However, this method of representation is too insensitive for testing the Avrami equation. In this work we have fitted data to equation (2) by a least squares procedure on the Mercury computer, using a minimization programme⁸ to find the optimum values of n and z . A fit of 70 experimental points takes about two minutes on this computer. This procedure gives the standard deviation (σ), and also the individual deviations of the experimental points from the calculated values. The latter are graphically represented in the form of difference plots, percentage difference between the calculated and observed shrinkages at the experimental times being calculated on the total range of shrinkage covered by a given run.

RESULTS

Polypropylene

Previous workers studying the crystallization of this polymer^{9,10} quote the best *integral* value of the Avrami exponent as three, although the data of Griffith and Rånby show deviations from the theoretical curve towards the end of the crystallization (see their Figure 2). Parrini and Corrieri⁷ found that the value of n depends upon molecular weight and crystallization temperature, varying from 2.8 to 4.1. These values were obtained by the conventional logarithmic plot, and so little measure of the goodness of the fit is available. Owing to the slight degree of secondary crystallization, the value of $(h_0 - h_\infty)$ was made a further adjustable parameter when fitting the Avrami equation (2) to the data analysed in this work. *Table 1*

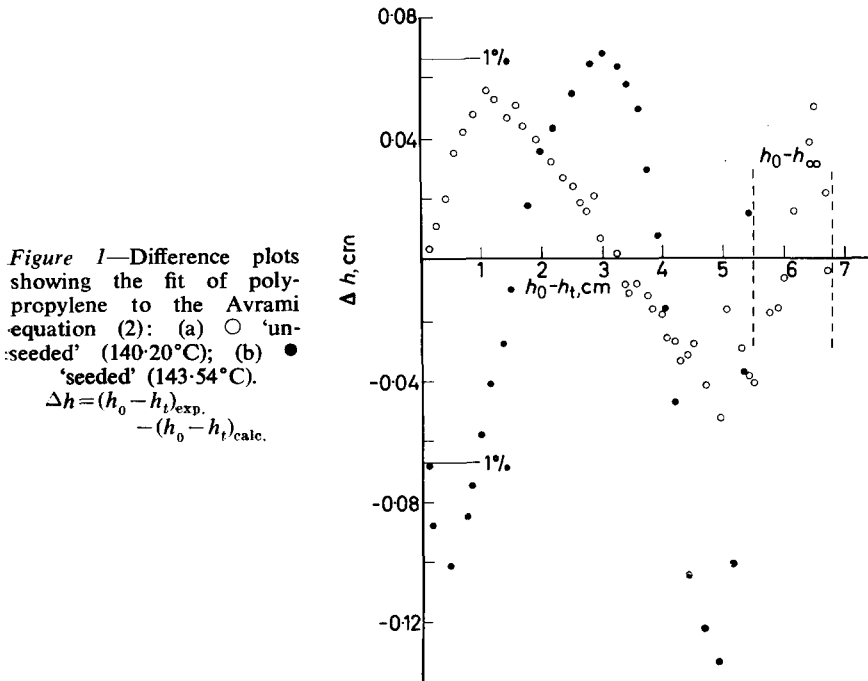
Table 1. Fit of Avrami equation (2) to polypropylene

Temp. °C	No. of points	n	z (time, min)	$(h_0 - h_\infty)$ cm		σ %
				Exptl value	Optimum value	
134.08	44	2.48	1.44, -4	5.88	6.12	1.00
135.50	62	2.52	5.44, -5	5.77	5.86	0.81
137.04	77	2.54	2.52, -5	5.77	5.60	0.34
138.98	71	2.60	5.64, -6	6.23	6.24	1.26
140.20	71	2.48	3.38, -6	6.71	6.73	0.47
143.54	33	2.46	5.07, -7	6.94	6.88	0.45
149.30	20	2.40	3.74, -8	6.97	6.88	1.15

Analysis of 'seeded' runs

x_s/x_∞	Temp. °C	No. of points	n	z (time, min)	$(h_0 - h_\infty)$ cm	σ %
0.14	147.94	61	3.00	8.03, -7	5.60	—
0.09	143.54	55	2.95	4.00, -6	5.59	—

shows the result of the least-squares fits to seven runs. In only one run is the difference between the final experimental measurement taken, and the optimum value of $(h_0 - h_\infty)$ greater than three per cent of $(h_0 - h_\infty)$. The remarkably low standard deviations (0.34–1.26 per cent) show that the crystallization is well fitted by the Avrami equation. The difference plot of a representative run (*Figure 1a*) shows that the deviations are still highly



systematic, although it was found that the pattern varied in different runs (perhaps because h_∞ has been treated as an adjustable parameter). The value of the Avrami exponent is 2.5 ± 0.1 (*Table I*) over a temperature range which varies the Avrami rate constant (z) by a factor of 4×10^3 . In other polymers, the temperature dependence of n has made interpretation difficult^{4,5}. The total contraction observed increases (*Table I*) by about 20 per cent when the temperature of crystallization is greater than 140°C, but the constancy of the value of n indicates that there is no change in mechanism when this change in contraction occurs. (This effect cannot be due to any irreversible systematic degradation of the polymer since the results remained reproducible throughout the investigation.) Although a similar result has been observed with polydecamethylene terephthalate⁴ no complete explanation of it has been given. It is probably due to a change in crystal modification at 140°C. It has been reported¹¹ that polypropylene spherulites exhibit positive birefringence below 134°C, and negative birefringence above 138°C, the form observed between these two temperatures

being a fibrillar mixture. The transition observed dilatometrically at approximately 140°C may be due to this change from the fibrillar mixture to negatively birefringent spherulites.

The results of two 'seeded' runs³, starting from initial seed crystallinity χ_s , analysed according to the Avrami equation, the value of $(h_0 - h_\infty)$ corresponding to the final experimental point, is shown in *Table 1*. The optimum value of n is very close to three, but the standard deviations are somewhat larger than in the unseeded runs.

Polybutene-1

Previous workers^{1,2} report that the crystallization kinetics of polybutene is described by the Avrami equation with the best *integral* value of n of four. The fit (their Figure 5) is not good after 50 per cent of the process has been completed, and no standard deviations indicating the goodness of the fit are given. *Table 2* shows the fit of eight runs to the Avrami equation (2).

Table 2. Fit of Avrami equation (2) to polybutene

Temp. °C	No. of points	n	z (time, min)	$(h_0 - h_\infty)$ cm		σ %
				Exptl value	Optimum value	
97.31	33	3.06	3.47, -6	1.95	1.96	0.94
98.47	47	3.09	9.84, -7	1.82	1.86	0.83
98.88	47	3.19	3.93, -7	1.94	1.93	0.95
100.62	32	3.00	1.38, -7	2.36	2.27	1.42
101.54	35	3.00	6.27, -8	2.48	2.46	0.64
103.10	32	3.23	2.15, -8	2.07	1.95	1.10
105.81	34	3.15	5.97, -10	2.53	2.49	0.96
107.08	17	3.13	5.31, -11	2.69	2.63	0.91

Again $(h_0 - h_\infty)$ was made an adjustable parameter owing to the slight degree of secondary crystallization present. In two runs only did the final experimental point taken differ from the adjusted value of $(h_0 - h_\infty)$ by more than three per cent. The very low standard deviations (0.64–1.42 per cent) show the good fit of the data to the Avrami equation. The residual deviations are again systematic, but do not follow the same pattern in all the runs. The value of n in all the runs is very close to three (*Table 2*) corresponding on the simple Avrami picture to linear radial growth of spontaneously nucleated spheres. There is, however, a definite tendency for n to be slightly greater than three, which is possibly due to some degree of sporadic nucleation. As for polypropylene, the total contraction observed changes sharply as the crystallization temperature is varied (in this case at approximately 100°C). Again, this has no effect on the value of the Avrami exponent, indicating that no change in the crystallization mechanism occurs.

DISCUSSION

Despite the large number of investigations in which the crystallization kinetics of a variety of polymers has been successfully, if usually rather crudely, fitted to the Avrami equation (2), no clear pattern has emerged

when the parameters z and n (and their temperature dependence) are examined. A more rigorous investigation of polymethylene has shown³ that the primary and secondary crystallization processes must and can be exactly separated from each other, and that the simple Avrami equation (2) gives a less satisfactory account of measurements on polymethylene than a modified Avrami model involving growth of single crystal lamellae without non-coherent secondary nucleation. On the other hand, the present measurements show that the crystallization behaviour of polypropylene and polybutene-1 to the straightforward Avrami equation (2) cannot be faulted by rigorous analysis over wide temperature ranges. In particular the parameter n turns out to be constant at permissible values (3 and 2.5) independently of temperature (contrast Table 3 of ref. 3 for polymethylene) and does not systematically fall during the course of a run (contrast Figure 3, ref. 3). Furthermore, the standard deviations found when applying the Avrami equation (2) to polypropylene and polybutene-1 are appreciably lower than for the same equation applied to polymethylene.

The distinction between the behaviour of polymethylene on the one hand, and polypropylene and polybutene-1 on the other, is supported by other evidence. No spherulites could be resolved in microscope investigations of polymethylene³, while our samples of polypropylene and polybutene-1 gave spherulites similar to those observed by others¹³. The Avrami exponent of $n=3$ is consistent with a linear growth rate of the spherulites, which is usually observed when examining thin films under the microscope. The Avrami exponent of $n=2.5$ implies spheres born sporadically and growing at a radial rate proportional to t^{-1} (owing to diffusion control). It is pleasing that the only case in the literature for which this rate law appears to have been observed under the microscope is, in fact, for polypropylene¹³. This argument is weakened by the fact that we find our own specimen of polypropylene to give well-defined spherulites under the microscope which undoubtedly grow with a linear rate law. However, correlation between dilatometric measurements on bulk specimens and microscope measurements on thin films is often not achieved, probably because of the strains induced by spreading a polymer into a thin film¹⁴. Moreover, diffusion control of growth can be abolished in our bulk specimens by the process of seeding, and the Avrami exponent n is then found to be three (Table 1) which is consistent with the linear growth rate.

This change in the radial growth rate, from a dependence upon t^{-1} , to a constant value on 'seeding' may originate from some order (or 'memory') remaining in the amorphous regions after partial melting, so that subsequent growth is no longer diffusion controlled. An acceleration of growth has been observed when polymethylene is crystallized from 'seeds'³. It is noteworthy that polypropylene is the only polymer studied to date which shows an increase in the Avrami exponent when crystallization occurs from 'seeds'. The difference plot (Figure 1b) shows that the greatest deviations occur towards the end of the crystallization when the experimental contraction lags far behind the calculated value. This is to be expected as the 'memory' effect will be smaller, the greater the distance from the 'seed' nucleus. The temperature dependence of the Avrami rate constants z (Tables 1 and 2) is shown in Figures 2 and 3, where $\log z$ is plotted against

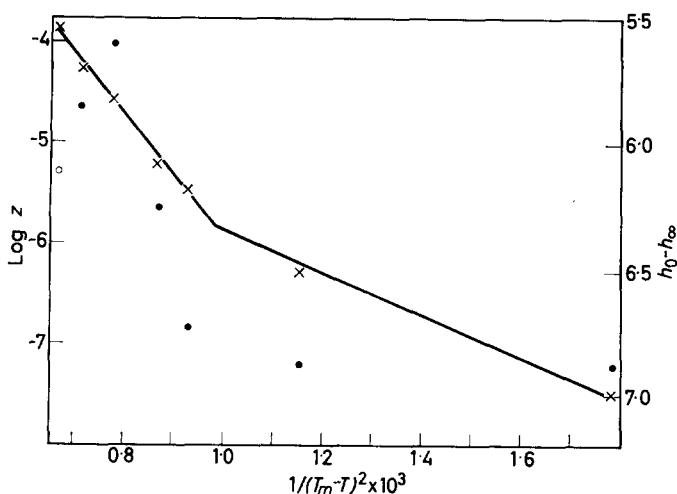


Figure 2—Temperature dependence of polypropylene rate constants:
 × $\log z$; ● $h_0 - h_\infty$

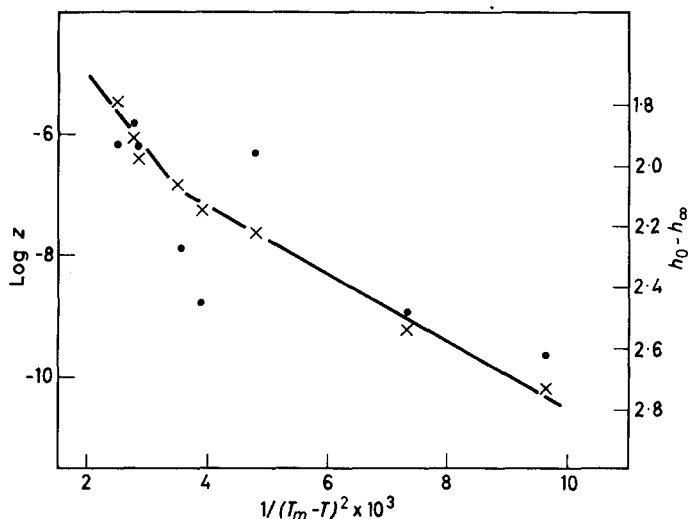


Figure 3—Temperature dependence of polybutene rate constants:
 × $\log z$; ● $h_0 - h_\infty$

$1/(T_m - T)^2$ corresponding to growth by a process of three-dimensional secondary nucleation. In both polymers, it appears that these plots have two straight portions, although for polypropylene this cannot be said unequivocally as there are only two points on one straight portion. The kinks cannot be located exactly, but occur in the regions where the total contraction also changes sharply (also shown in *Figures 2 and 3*). It has been shown² that the slope of these plots depends upon the free surface energies of the critical secondary nucleus. The change in slope observed

here probably represents a difference in the surface free energies involved in forming the critical secondary nucleus of two different crystal modifications with different densities. The sign of the effect agrees with this interpretation, since the modification of higher surface energy should be formed at higher degrees of supercooling.

The calculations were performed on the Mercury Computer of the University of London Computer Unit. We thank the Director for these facilities.

*Chemistry Department,
Imperial College of Science and Technology,
London, S.W.7.*

(Received August 1964)

REFERENCES

- ¹ AVRAMI, M. *J. chem. Phys.* 1939, **7**, 1103
- ² MANDELKERN, L. *Growth and Perfection of Crystals*, pp 467-497. Chapman and Hall: London, 1958
- ³ GORDON, M. and HILLIER, I. H. *Trans. Faraday Soc.* 1964, **60**, 763
- ⁴ SHARPLES, A. and SWINTON, F. L. *Polymer, Lond.* 1963, **4**, 119
- ⁵ BANKS, W., GORDON, M., ROE, R. -J. and SHARPLES, A. *Polymer, Lond.* 1963, **4**, 61
- ⁶ BANKS, W. and SHARPLES, A. *Makromol. Chem.* 1963, **59**, 233
- ⁷ PARRINI, P. and CORRIERI, G. *Makromol. Chem.* 1963, **62**, 83
- ⁸ ROSEN BROCK, H. H. *Computer J.* 1960, **3**, 175
- ⁹ GRIFFITH, J. H. and RANBY, B. G. *J. Polym. Sci.* 1959, **38**, 107
- ¹⁰ MARKER, L., HAY, P. M., TILLEY, G. P., EARLY, R. M. and SWEETING, O. J. *J. Polym. Sci.* 1959, **38**, 33
- ¹¹ PADDEN, F. J. and KEITH, H. D. *J. appl. Phys.* 1959, **30**, 1485
- ¹² BOOR, J. and MITCHELL, J. C. *J. Polym. Sci. A*, 1963, **1**, 59
- ¹³ PADDEN, F. J. and KEITH, H. D. *J. appl. Phys.* 1964, **35**, 1286
- ¹⁴ BANKS, W., HAY, J. N., SHARPLES, A. and THOMSON, G. *Polymer, Lond.* 1964, **5**, 163

Note

Internal Pressure of Crystalline Polymers

IT HAS previously been shown¹ that the internal pressure (P_i) of a crystalline polymer, polyethylene oxide, is much lower than that of the melt. However, with some other crystalline polymers it has been found that the value of P_i was higher than expected (*Table 1(a)*)². The internal pressure of polyethylene, for example, was found to be of the order of 120 cal/cm³ at room temperature. If this is so, and the internal pressure of the material increased on melting as previously demonstrated for polyethylene oxide, then the value of P_i for molten polyethylene would be greatly in excess of that given by the empirical relationship Internal Pressure (P_i)/Cohesive Energy Density (CED) ~ 1.4 shown earlier³ for non-polar polymers lacking specific interactions since the CED of polyethylene estimated by extrapolation of data for hydrocarbons cannot be much greater⁴ than 70 cal/cm³.

To investigate this problem measurements have been carried out on two further samples of polyethylene, two paraffin hydrocarbons and two polyethers, polyoxymethylene and polytetramethylene oxide.

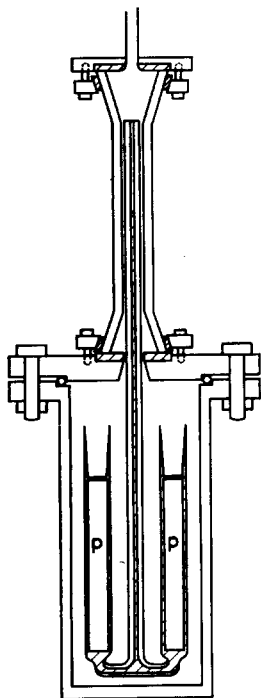


Figure 1—Pressure vessel assembly

NOTE

EXPERIMENTAL

The apparatus used was similar to that described earlier³ but having a modified pressure vessel fitted with a Pyrex glass pressure tube through which changes in the height of mercury in the cell capillary could be measured with a cathetometer (see *Figure 1*). The apparent thermal expansivity, compressibility or thermal pressure coefficient could all be measured at will on the same sample. Corrections for compressibility and expansivity of mercury and glass were applied as previously described⁴.

MATERIALS

Polyethylene—Two samples were used. These were Allied Chemicals Grades 6 (mol. wt 2 000) and 617 (mol. wt 1 500).

Dotriacontane as supplied by L. Light & Co. was redistilled under reduced pressure. Vapour phase chromatography indicated purity better than 99 per cent.

Eicosane as supplied by L. Light & Co. was treated similarly and had a purity better than 99 per cent.

Polytetramethylene oxide (Teracol 30) a sample supplied by Du Pont de Nemours had a molecular weight (end group assay) of 3 000.

All the above polymers were cast into rods using a vertical zone refining machine operating under a high vacuum and at a speed of about 6 in. per

Table 1(a)

Sample	$\alpha \times 10^4$ (°C) ⁻¹	T °C	$\beta \times 10^5$ (atm) ⁻¹	γ atm/°C	ρ at T g/ml	P_i cal/cm ³
Nylon 66	2.4	37	1.67	14.4*	—	107.6
Nylon 11	4.3	37	3.86	11.1*	—	83.2
Polytetrafluoro- ethylene	2.5	37	2.87	8.72*	—	64.9
Alkathene 7	7.05	37	4.61	15.30*	—	114.8
Rigidex 9	4.0	37	2.8	14.28*	—	107.2

Table 1(b)

Polyethylene 6	4.09	32.8	2.64	15.48*	0.914	114.7
	4.46	47.9	2.93	15.10*	0.892	117.4
	6.72	116	8.52	7.89*	0.802	74.0
Polyethylene 617	7.34	116	8.67	8.47*	0.799	79.8
	<i>Dotriacontane</i>					
C ₃₂ H ₆₆	6.0	37	3.20*	18.80	0.934	141.1
	8.10	50	4.42*	18.33	0.923	143.0
	7.53	74	8.27*	9.11	0.778	74.7
Eicosane C ₂₀ H ₄₂	4.79	16	2.72*	17.60	0.993	123.5
	5.11	47	5.46*	9.35	0.771	72.4
Polytetramethylene oxide	5.85	16	3.27*	11.90	1.060	125.3
	7.29	71	6.85*	10.64	0.935	88.6
Delrin 150	5.52	32	2.89*	19.07	1.42	122.0

*Computed from the relation $\gamma = \alpha/\beta$.

NOTE

hour. Usually a suitable rod was cast after one pass, sections cut at random showing no internal voids.

Polyoxymethylene, Delrin 150, was supplied in the form of an extruded rod by Polypenco and was used without further treatment.

RESULTS

The results are summarized in *Table 1(b)*, the values of P_i are estimated to be accurate to ± 3 per cent below and ± 2 per cent above the melting point.

With the polymers examined, some difference in (dp/dt) was observed when using increasing or decreasing pressures. However, this effect was reduced after several cycles, the difference being less than one per cent in the results published.

All the results obtained show that the internal pressure of the crystalline solid is greater than that of the melt, the values for polyethylene being in good agreement with values recently published⁵. The only materials which might differ from this behaviour are Delrin, where unfortunately the internal pressure of the high molecular weight liquid cannot readily be obtained although the CED has been estimated⁶ as 104 cal/cm³ and ratio P_i /CED is greater than unity, and Nylon 11 which has a rather low value of P_i in the solid state; the internal pressure of the liquid is almost certainly higher than this.

Measurements are to be continued on other polymers and, in particular, further samples of polyethylene oxide, preliminary results for which appear to support the results previously published for this polymer.

This text and accompanying illustration are Crown Copyright, reproduced with permission of the Controller of Her Majesty's Stationery Office.

D. SIMS

*Ministry of Aviation,
Explosives Research and Development Establishment,
Waltham Abbey, Essex*

(Received November 1964)

REFERENCES

- ¹ ALLEN, G. and SIMS, D. *Polymer, Lond.* 1964, **4**, 105
- ² STOKOE, A. and WILKINS, P. Unpublished results
- ³ ALLEN, G., SIMS, D. and WILSON, J. G. *Polymer, Lond.* 1960, **1**, 467
- ⁴ ALLEN, G., GEE, G. and WILSON, J. G. *Polymer, Lond.* 1960, **1**, 456
- ⁵ MARTYNYNK, M. M. and SEMENCHENKO, V. K. *Colloid. J. of U.S.S.R.* 1963, **25**, 150
- ⁶ BOYD, R. J. *Polym. Sci.* 1961, **50**, 133

The Infra-red Spectrum of Syndiotactic Polypropylene

I. J. GRANT and I. M. WARD

The infra-red spectrum of syndiotactic polypropylene is reported, and comparison made with that of the isotactic polymer. It is concluded that several of the absorption bands in the range 1500 cm^{-1} to 200 cm^{-1} are characteristic of the portions of chains in the syndiotactic helical configuration, and therefore give an empirical measure of the stereoregularity.

IN A previous publication¹ the infra-red (i.r.) spectra of isotactic and atactic polypropylene were described. Assignments for the principal vibrations were attempted following the preliminary analysis of the isotactic polypropylene spectrum proposed by Peraldo². Similar attempts have also been made by Krimm³, Tobin⁴, and Liang, Lytton and Boone⁵. With the exception of Tobin it is assumed that the multiplicity of absorptions arises from the interactions between modes of vibration of different units within a chain molecule rather than between units belonging to different chain molecules.

The present communication describes the measurement of the i.r. spectrum of syndiotactic polypropylene and considers the general assignment of absorptions in both the isotactic and syndiotactic polymers.

EXPERIMENTAL

Preparation of samples

The spectrum of isotactic polypropylene was obtained from a standard commercial grade moulding powder and the atactic polymer spectrum was obtained from a polymer prepared with a non-stereospecific catalyst. The syndiotactic spectrum was obtained from an experimental sample of polymer prepared by a method similar to that described by Natta *et al.*⁶. To confirm that this polymer was primarily syndiotactic high resolution proton magnetic resonance (p.m.r.) spectra and X-ray diffraction spectra were obtained. *Figure 1* is a high resolution p.m.r. spectrum of the syndiotactic polypropylene used for the i.r. spectra. This p.m.r. spectrum was obtained from a 15% w/v solution of the polymer in orthodichlorobenzene at 140°C using a Varian Associates A60 spectrometer. This spectrum shows the presence of equivalent methylene protons only, as would be expected for syndiotactic polymer⁷, the more complicated ABC₂ type spectrum for isotactic polymer being absent within the sensitivity of the spectrometer. In a similar manner the X-ray diffraction photographs showed reflections identical to those described by Natta *et al.*⁸ for syndiotactic polymer and complete absence of reflections expected for isotactic polymer.

Measurement of i.r. spectra

The i.r. spectrum of isotactic polypropylene was recorded using films of thickness 0.15 mm to 1.0 mm. The i.r. spectra of the syndiotactic and

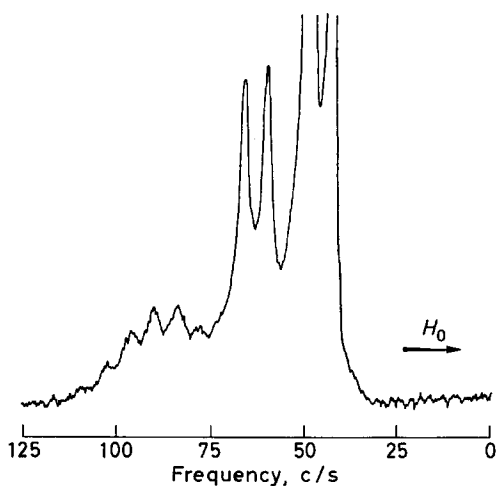


Figure 1—60 Mc/s proton magnetic resonance spectrum of a 15 per cent w/v solution of syndiotactic polypropylene in ortho-dichlorobenzene at 140°C

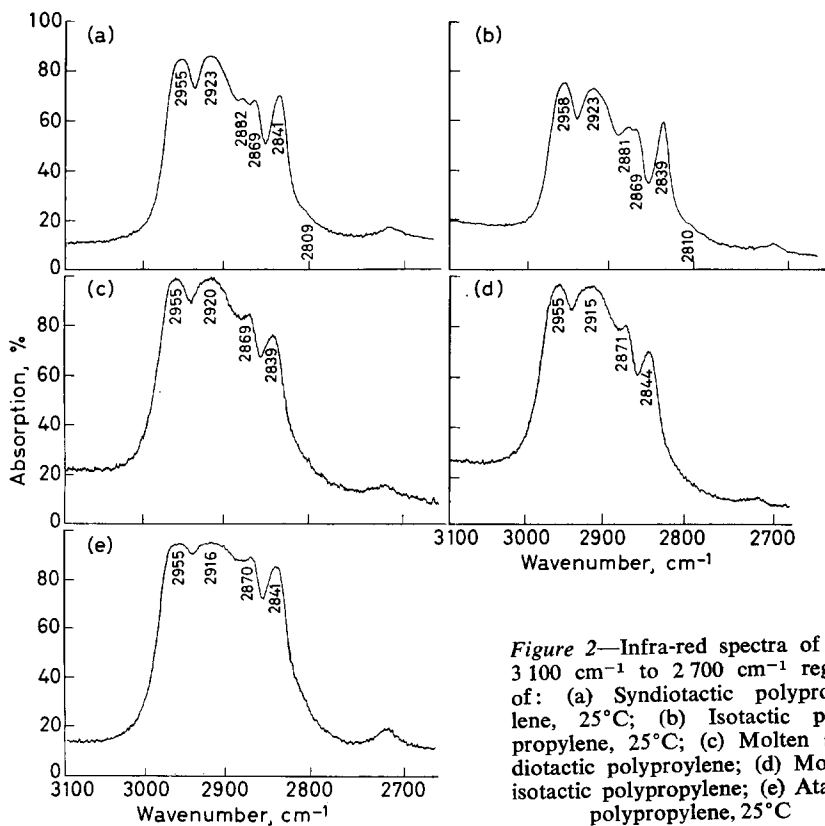


Figure 2—Infra-red spectra of the 3100 cm^{-1} to 2700 cm^{-1} region of: (a) Syndiotactic polypropylene, 25°C; (b) Isotactic polypropylene, 25°C; (c) Molten syndiotactic polypropylene; (d) Molten isotactic polypropylene; (e) Atactic polypropylene, 25°C

THE INFRA-RED SPECTRUM OF SYNDIOTACTIC POLYPROPYLENE

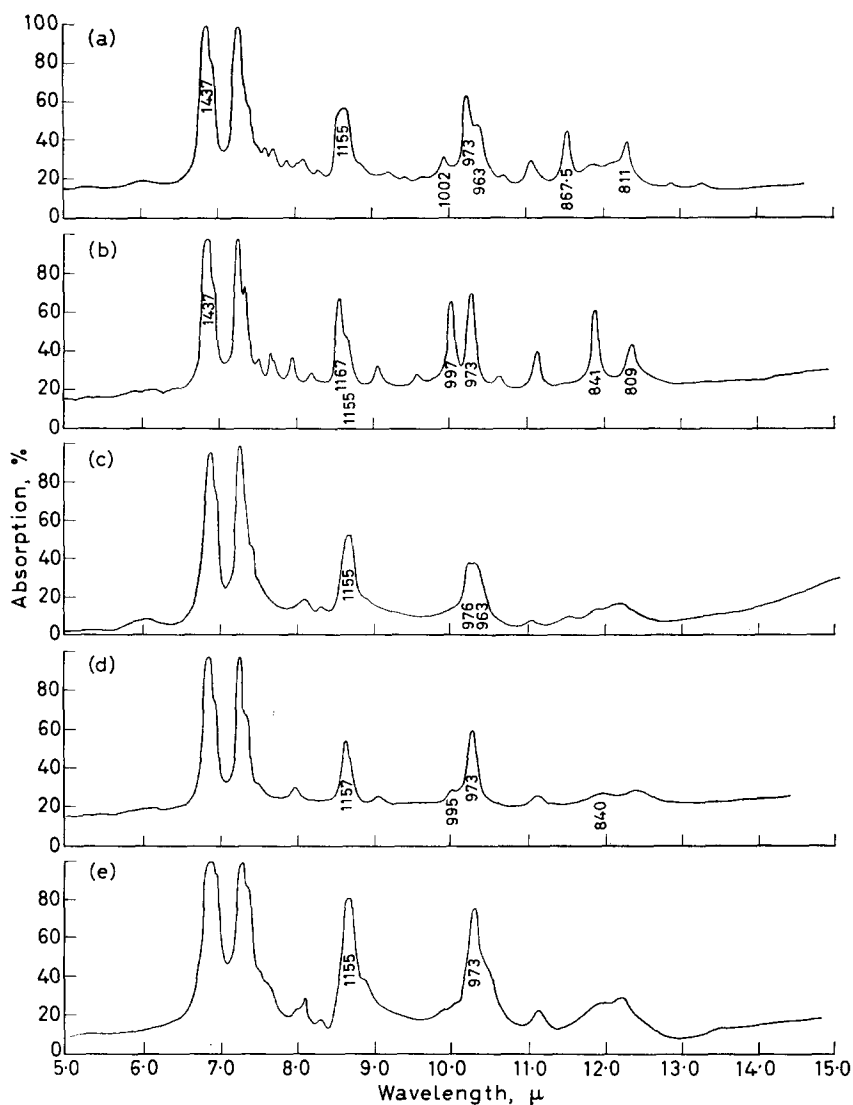


Figure 3—Infra-red spectra of the 2000 cm^{-1} to 666 cm^{-1} region of: (a) Syndiotactic polypropylene, 25°C; (b) Isotactic polypropylene, 25°C; (c) Molten syndiotactic polypropylene; (d) Molten isotactic polypropylene; (e) Atactic polypropylene, 25°C

atactic polymer samples were recorded using films of thickness 0.15 mm to 0.3 mm supported between rocksalt plates of 4 mm thickness in the 4000 cm^{-1} to 666 cm^{-1} spectral region. In the 666 cm^{-1} to 222 cm^{-1} region the syndiotactic spectrum was recorded using unsupported films of 0.5 mm to 1.0 mm thickness. The molten spectra of syndiotactic and isotactic polypropylene were obtained from films supported between rocksalt plates

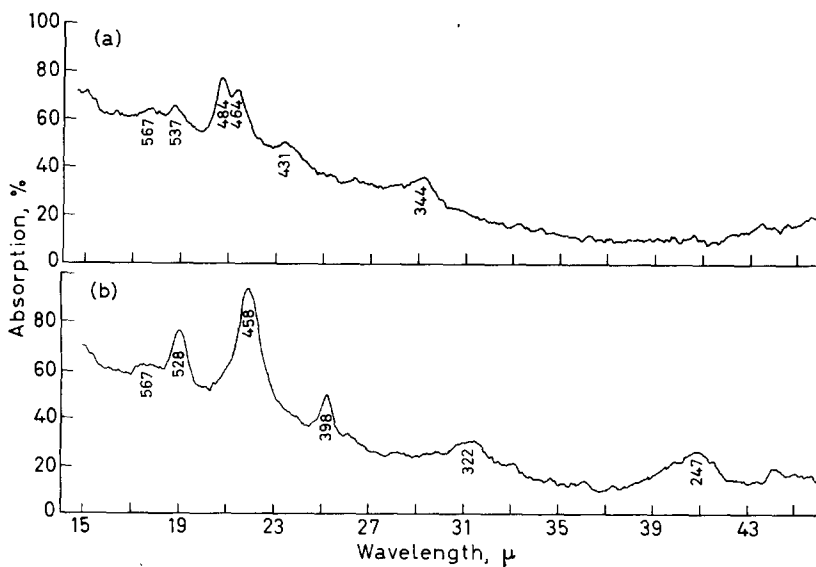


Figure 4—Infra-red spectra of the 666 cm^{-1} to 222 cm^{-1} region of: (a) Syndiotactic polypropylene, 25°C ; (b) Isotactic polypropylene, 25°C

placed in a thermostatically controlled oven maintained at a temperature 20° above the melting point of the polymer.

The i.r. spectra were measured using a Grubb Parsons single beam spectrometer Type S3 equipped with a rocksalt prism for the region 1500 cm^{-1} to 666 cm^{-1} and a lithium fluoride prism for the region 4000 cm^{-1} to 1500 cm^{-1} . In addition spectra were obtained for the range 666 cm^{-1} to 222 cm^{-1} using a Grubb Parsons DM4 Spectrometer (with the cooperation of Dr A. E. Martin). In the region 4000 cm^{-1} to 666 cm^{-1} the spectrometer was calibrated against gas samples contained in a 10 cm gas cell and in the region 666 cm^{-1} to 222 cm^{-1} atmospheric water vapour was used to calibrate the instrument.

RESULTS

The i.r. spectra of syndiotactic, isotactic and atactic polypropylene along with the spectra of molten syndiotactic and molten isotactic polypropylene are shown in Figure 2 for the 3100 cm^{-1} to 2700 cm^{-1} region and in Figure 3 for the 2000 cm^{-1} to 666 cm^{-1} region. Figure 4 shows the spectra of syndiotactic and isotactic polypropylene for the 666 cm^{-1} to 222 cm^{-1} spectral region.

The frequencies of the absorption bands together with indications of their intensity and tentative assignment are listed in Tables 1 and 2 for syndiotactic and isotactic polypropylene respectively. Table 1 also records the frequencies observed in the molten spectrum together with indications of their intensities.

DISCUSSION

(i) Comparison of solid phase spectra

It can be seen that although the principal internal carbon-hydrogen stretching and bending vibration absorptions of the isotactic and syndiotactic

THE INFRA-RED SPECTRUM OF SYNDIOTACTIC POLYPROPYLENE

Table 1. Characteristics of syndiotactic polypropylene absorption bands

Frequency cm^{-1}	Relative strength	Frequency above <i>m.pt</i>	Relative strength	Tentative assignment
2955	S	2955	S	Asymm. —CH ₃ stretching
2923	S	2920	S	Asymm. —CH ₂ stretching
2882	Sh.	—	—	2X—CH ₂ bending
2869	Sh.	2869	Sh.	Symm. —CH ₃ stretching
2841	S	2839	S	Symm. —CH ₂ stretching
2809	W	2809	W	—CH stretching
1461	S	1457	S	Asymm. —CH ₃ bending
1437	Sh.	1437	Sh.	—CH ₂ bending
1376	S	1378	S	Symm. —CH ₃ bending
1369	Sh.	1369	Sh.	
1347	Sh.	—	—	
1332	W	—	—	
1311	W	—	—	
1290	W	—	—	
1262	W	—	—	
1242	W	—	—	
1229	W	1229	W	
1200	W	1205	W	
1162	M	—	—	
1154	M	1155	M	—CH ₃ wagging (amorphous)
1128	W	—	—	
1083	W	—	—	
1061	W	—	—	
1034	W	—	—	
1002	M	—	—	
976	S	972	M	
963	M	961	M	
935	W	—	—	
905	W	899	W	
868	M	868	vW	
839	W	835	W	
811	M	816	W	
775	W	—	—	
750	W	—	—	
567	W	*		Water vapour absorption
537	W	*		
484	M	*		
469	M	*		
431	W	*		
344	W	*		

(S—strong, M—medium, W—weak, Sh.—shoulder, *—not determined in this work.)

polymers are very similar, there are considerable differences in the range 1500 cm^{-1} to 220 cm^{-1} . It is particularly noticeable that the absorptions at 1167 cm^{-1} , 997 cm^{-1} and 841 cm^{-1} which are considered by some workers^{1,9} to be associated with the threefold helix of isotactic polypropylene are absent from the spectrum of the syndiotactic polymer. The spectrum of the syndiotactic polymer does, however, contain a considerable

Table 2. Characteristics of isotactic polypropylene absorption bands

Frequency cm^{-1}	Relative strength	Frequency above <i>m.pt</i>	Assignment (Ref. 1)
2958	S	2956	Asymm. —CH ₃ stretching (A and E modes)
2923	S	2915	Symm. —CH ₃ stretching
2881	S	—	2X—CH ₂ bending
2869	S	2871	Symm. —CH ₃ stretching
2839	S	2844	Symm. —CH ₂ stretching
2810	W	2810	—CH stretching
1458	S	1451	Asymm. —CH ₃ bending (A and E modes)
1440	Sh.		—CH ₂ bending (E)
1377	S	1373	Symm. —CH ₃ bending (E)
1360	M	1353	—CH bending (E)
1329	W	1317	—CH ₂ wagging (E)
1303	W		—CH bending (A)
1297	W		—CH ₂ twisting (E)
1255	W	1248	—CH wagging (A)
1219	W		—CH wagging (E)
1168	S		
1153	Sh.	1150	—CH ₃ wagging (amorphous)
1103	W	1100	
1045	W		
997	S	996	
972	S	971	
940	W		
899	W	897	
841	S	830	
809	M	810	
567	W	*	Water vapour absorption
528	M	*	
458	S	*	Assignments of these bands not attempted by McDonald and Ward ¹
398	M	*	
322	W	*	
247	W	*	

(S—strong, M—medium, W—weak, Sh.—shoulder, *—not determined in this work.)

number of absorptions which are not present in the molten spectrum. These occur at 1 332, 1 311, 1 290, 1 262, 1 242, 1 162, 1 128, 1 083, 1 034, 1 002, 935, 867.5 and 811 cm^{-1} and we consider that they are characteristic of the syndiotactic helix.

The number of fundamental vibrations for a repeat unit of a polypropylene helix is $(3N-4)$ where N is the number of atoms in one complete turn of the helix. For isotactic polypropylene, with three monomer units in one complete turn of the helix¹⁰, $(3N-4)=(3 \times 27-4)=77$ modes of vibration and for syndiotactic polypropylene with a binary helix⁷ consisting of four monomer units in a complete turn this analysis yields $(3 \times 36-4)=104$ modes of vibration. Comparison of the unpolarized spectra of isotactic and syndiotactic polypropylene, shown in *Figures 2 and 3*, clearly shows that there are many more external vibrations in the syndio-

tactic spectrum compared with the isotactic spectrum. The $(3N-4)$ analysis for the number of fundamental modes of vibration indicates that the ratio of the number of isotactic modes to syndiotactic modes is $77/104=0.74$. In the spectral range $4\,000\text{ cm}^{-1}$ to 220 cm^{-1} , for unpolarized spectra, there are 30 isotactic absorption bands and 39 syndiotactic absorption bands which yield an isotactic to syndiotactic ratio of 0.77. The close agreement of calculated and observed ratios suggests that this approach to assigning the modes of vibration in a syndiotactic polypropylene helix is substantially correct.

(ii) *Comparison of molten and atactic spectra*

Comparison of molten isotactic, molten syndiotactic and atactic spectra shows that, in the first place, the three are approximately similar. Several absorption bands which are characteristic either of the isotactic or syndiotactic polymer disappear or are reduced in intensity on melting but return to their original intensity upon cooling. One common feature of these spectra is the bands at $1\,155\text{ cm}^{-1}$ and 973 cm^{-1} which retain their original intensity on melting. These two bands are found in the i.r. spectra of all steric forms of polypropylene whether in a solid or in a molten state suggesting that these bands derive from the chemical rather than the structural nature of polypropylene.

Subsidiary differences are observed between the molten spectra and that of the atactic polymer. It is interesting to note that the molten syndiotactic and atactic spectra are very closely similar and differ significantly from the molten isotactic spectrum. For example in both the molten syndiotactic and atactic spectra the absorption *ca.* 973 cm^{-1} appears as a doublet² with peaks at 976 and 963 cm^{-1} and bands in the $1\,200\text{ cm}^{-1}$ region appear to be very similar. This suggests first that the pattern of stereoregularity in the atactic polymer, although not sufficiently regular to allow crystallization is nearer to that in a syndiotactic rather than an isotactic polymer; and secondly that certain absorptions are observed in the molten state which are characteristic of the chain configurations of syndiotactic and isotactic polymers, even though the absorptions characteristic of the different types of helix are no longer present. This interpretation was confirmed by the similarity of the p.m.r. spectra of syndiotactic and atactic polymers.

(iii) *Conclusion*

In the previous publication from this laboratory¹ McDonald and Ward following Peraldo² and Krimm³ assumed that both the internal and external modes of vibration would be affected by the intramolecular interactions. On the other hand, Liang, Lytton and Boone⁵ assumed that only the external modes of vibration would be affected.

These unpolarized spectra of syndiotactic polypropylene do not throw any further light on this particular controversy. The present investigation does, however, suggest that the approach of considering several of the absorptions in the $1\,500$ to 220 cm^{-1} region as arising from interactions within the helix to be a correct one. Furthermore, in syndiotactic polymer, as

in isotactic polymer, certain absorptions characterize the portions of chains existing in the helical configuration and therefore give an empirical measure of the stereoregularity. This measure will depend on the presence of at least four monomer units being alternately d and l substituted, as against three being identically substituted in the isotactic case.

(Received August 1964)

Research Department,
ICI Fibres Ltd,
Hookstone Road, Harrogate

REFERENCES

- ¹ McDONALD, M. P. and WARD, I. M. *Polymer, Lond.* 1961, **2**, 341
- ² PERALDO, M. *Gazz. chim. ital.* 1959, **89**, 798
- ³ KRIMM, S. *Advanc. Polym. Sci.* 1960, **2**, 51
- ⁴ TOBIN, M. C. *J. phys. Chem.* 1960, **64**, 216
- ⁵ LIANG, C. Y., LYTTON, M. R. and BOONE, C. J. *J. Polym. Sci.* 1961, **54**, 523
- ⁶ NATTA, G., PASQUON, I. and ZAMBELLI, A. *J. Polym. Sci., Part C, Polymer Symposia* No. 4, p 411
- ⁷ TINCHER, W. C., American Chemical Society Division of Polymer Chemistry, Papers presented at Atlantic City Meeting Vol. III, p 142, 1962
- ⁸ NATTA, G., PASQUON, I., CORRADINI, P., PERALDO, M., PEGORARO, M. and ZAMBELLI, A. *Atti. Accad. Lincei*, 1960, **28**, 539
- ⁹ BRADER, J. J. *J. appl. Polym. Sci.* 1960, **3**, 370
- ¹⁰ NATTA, G., CORRADINI, P. and CESARI, M. *Atti Accad. Lincei*, 1956, **21**, 365

Application of Irreversible Thermodynamics to the Kinetics of Polymer Crystallization from Seeded Nuclei

R.-J. ROE* and W. R. KRIGBAUM

The kinetics of crystallization of polymers from a melt containing seeded nuclei is treated theoretically by applying irreversible thermodynamics to a model for semi-crystalline polymers. The latter model was previously shown to be useful in predicting the equilibrium degree of crystallinity and the initial Young's modulus of such materials.

Comparison of the theoretical result with experimental crystallization kinetics data obtained with fractionated linear polyethylene, containing a small amount of seed crystallinity due to partial melting, shows that the overall course of the crystallization, and the fractional value of the Avrami constant, can be explained successfully. The slight disagreement between theory and the experimental data arising during the very early stages, and that observed during the last part of the crystallization process, is discussed in terms of the assumptions involved in applying irreversible thermodynamics in the linear approximation to the present system.

BY APPLICATION of statistical thermodynamics to a system consisting of a semi-crystalline linear polymer, it was shown previously¹ that the equilibrium degree of crystallinity attainable at a given temperature can be predicted in terms of such parameters as the heat of fusion, flexibility of the polymer chains, and the density of crystal nuclei originally present. The general validity of this concept was further attested in a subsequent publication² in which the modulus of such semi-crystalline polymers calculated from the model was found to agree well with experimental values.

The method is now extended, by use of irreversible thermodynamics, to apply to the kinetic process of crystallization of such polymer systems. The crystallization process consists, in general, of two distinct steps: first, the formation of incipient nuclei from amorphous melt and, second, the subsequent growth of these nuclei into stable crystallites. The theoretical aspects of nucleus formation have been considered fairly extensively by other workers (see Mandelkern³ for references). In this work we confine our considerations to the second step of crystal growth from pre-formed nuclei, and develop a theory to predict the rate of growth as a function of time (or the extent of crystallization).

THEORY

The driving force for the crystallization comes from the free energy gradient $-\partial F/\partial\omega$, or the change in the total free energy F of the system accompanying the increase in the degree of crystallinity ω . In crystallization of

*Present address: Electrochemicals Department, E. I. du Pont de Nemours and Co., Niagara Falls, New York.

bulk polymers, strain is imposed on the amorphous chains connecting crystallites. As a result, the molar free energy of the amorphous region increases and gradually offsets the free energy decrease arising from the growth of the crystalline region. As crystallization proceeds, therefore, the free energy gradient decreases progressively, and this is reflected in the gradual decline of the crystallization rate.

We assume that when the nuclei were first formed they were interconnected by polymer chains each consisting of N equivalent, flexible links. If $n/2$ links at each end of the chain crystallize by subsequent deposition on the nuclei, the crystallinity ω will be

$$\omega = n/N \quad (1)$$

The free energy change for the crystallization of n units from each of a mole of chains is given by

$$\Delta F = -n(\Delta H_f - T\Delta S_f) - T\Delta S_D \quad (2)$$

where ΔH_f and ΔS_f are the molar heat and entropy changes associated with the fusion of equivalent links from a perfect crystal and ΔS_D is the entropy change caused by the deformation of the remaining amorphous part of the chain (for details see the previous paper¹). When the number of nuclei, hence N , is constant, both ω and F are functions of n only. The free energy gradient, or the driving force for the crystallization, is then given by

$$-(\partial\Delta F/\partial\omega)_{N,T,p} = -N(\partial\Delta F/\partial n)_{N,T,p} \quad (3)$$

According to the theory of irreversible thermodynamics developed by De Groot⁴, Prigogine⁵ and others, the velocity v of a rate process of a system which is not very far removed from equilibrium is linearly related to the affinity A of the system. If ξ is the parameter characterizing the extent of change, then v and A are defined by

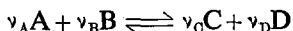
$$v = d\xi/dt \quad (4)$$

$$A = -(\partial F/\partial\xi)_{T,p} \quad (5)$$

and therefore

$$d\xi/dt = -\gamma(\partial F/\partial\xi)_{T,p} \quad (6)$$

where γ is a proportionality constant. For example, in a chemical reaction



one can define ξ as the increase in the number of moles of a product, say D, divided by the stoichiometric coefficient ν_D , and then the affinity becomes

$$A = \nu_A\mu_A + \nu_B\mu_B - \nu_C\mu_C - \nu_D\mu_D \quad (7)$$

where μ_S are the chemical potentials.

For the present problem we choose as the extent of reaction parameter, ξ , the crystallinity ω . Then, within the range of applicability of equation (6), we have

$$d\omega/dt = -\gamma(\partial\Delta F/\partial\omega)_{N,T,p} \quad (8)$$

ΔF was calculated as a function of n in the previous treatment¹ for several

slightly different crystallization models. At temperatures not very far below the melting point, gaussian statistics still furnish a good approximation for the amorphous chains, so that ΔF for the folded chain model is given by

$$\Delta F = -n\Delta H_f (1 - T/T_M^0) + (3/2) RT [n/(N-n)] \quad (9)$$

where T_M^0 is the melting point of a large perfect crystal and R is the gas constant. After substitution of equation (9) into (8), the latter may be integrated to give

$$Bt = (\omega - \omega_0) + [(1 - \omega_\infty)/2] \times \ln [(2 - \omega_\infty - \omega)(\omega_\infty - \omega_0)/(2 - \omega_\infty - \omega_0)(\omega_\infty - \omega)] \quad (10)$$

with

$$B = \Delta H_f (1 - T/T_M^0) \gamma / N^2 \quad (11)$$

In equation (10) ω_0 is the crystallinity at time $t=0$ and ω_∞ is the equilibrium crystallinity, which is given by the condition¹

$$(\partial F / \partial n)_{N,T,p} = 0 \quad (12)$$

so that

$$\omega_\infty = 1 - \{[3R/2\Delta H_f N] (1/T - 1/T_M^0)\}^{1/2} \quad (13)$$

DISCUSSION

Comparison is made in *Figure 1* between the theory and experimental data. The latter were obtained by Banks, Gordon and Sharples⁶ with a fractionated linear polyethylene sample which had contained a residual seed crystallinity of 3.53 per cent before the sample was allowed to crystallize at 127.5°C. The curve in *Figure 1* was calculated from equation (10) with values of parameters $\omega_0 = 0.0353$, $\omega_\infty = 0.350$ and $B = 0.02 \text{ min}^{-1}$. The

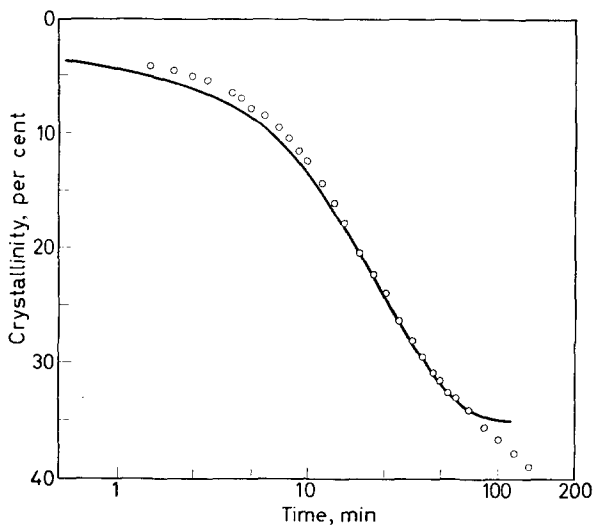


Figure 1—Crystallization kinetics calculated from the present theory (solid line) compared with experimental data (circles) obtained with seeded polyethylene by Banks, Gordon and Sharples⁶

agreement is satisfactory in most of the crystallinity range below 35 per cent. In order to assess the slight deviation in the early part, and the very pronounced one beyond the 35 per cent crystallinity, we will examine some of the underlying assumptions employed in arriving at equation (10).

A more exact expression for ΔF than (9) was also derived in the previous work¹ by the use of inverse Langevin, instead of the gaussian, statistics for the chain conformation. When the inverse Langevin expression for ΔF was substituted in equation (8), and the integration performed numerically on a computer, the result gave a curve which was almost indistinguishable from the one shown in *Figure 1* after the value of B had been adjusted slightly. We thus feel that the gaussian entropy expression is a sufficiently good approximation for the present purpose.

For the theory of irreversible thermodynamics in the linear approximation to apply to a system, the following two conditions have to be met: first, the system should not be too far removed from equilibrium and, second, the mechanism of the physical or chemical process considered should not change during the course of the process. The validity of these two conditions in the present problem will now be examined.

(1) Prigogine *et al.*⁷ have shown that if the affinity A is defined by equation (7) for a chemical reaction, the linear law represented by relation (6) holds as long as A is small compared to RT . The same criterion cannot be applied literally to our problem, since there is some arbitrariness involved in the choice of the extent of reaction ξ . Identification of ξ with either ω , n or the specific volume of the polymer, all lead to the same equation (8), but the values of A given by (5) differ by numerical factors. In a chemical reaction the fundamental process is concerned with the single molecules which enter into the reaction. Therefore, for the criterion of $A \ll RT$ to apply to our problem, we may define ξ with respect to the smallest unit which can be transferred in one step from amorphous melt to the surface of a growing crystallite. If we assume that such a unit consists of ρ statistical links, we have

$$A/RT = \rho [(\Delta H_f/RT)(1 - T/T_M^0) - 3/\{2N(1 - \omega)^2\}] \quad (14)$$

For polyethylene one statistical link consists of about ten methylene units⁸, and ΔH_f is around 10 kcal per mole of statistical links. With $T = 400^\circ\text{K}$ (127°C) and $T_M^0 = 410^\circ\text{K}$ the ratio A/RT decreases from about 0.3ρ at $\omega = 0$ to zero at $\omega = \omega_\infty$. If the size of the unit being transferred at the solid/liquid interface is comparable to that of a statistical link, so that ρ is of order unity, we should expect a moderate deviation from the linear law (8) in the early phase of the crystallization when ω is less than ten per cent. With increasing ω the ratio A/RT becomes smaller, so that the linear law is obeyed progressively more exactly.

(2) The proportionality constant γ in equation (6) is a measure of the resistance which must be overcome if the process is to occur under the driving force, and if the mechanism of the process changes the value of γ will be altered. In the crystallization of polymers, at least when the crystallinity is small, the rate is controlled by the activated transfer of chain units from the melt to the crystallite surface. However, there appears

to be a growing body of evidence which suggests that the nature of the process changes as the equilibrium degree of crystallinity is approached. For example, it has been suggested that during the latter stages, chain units which were already incorporated in the crystallites begin to rearrange in a process called secondary crystallization. Fischer and Schmidt⁹ have demonstrated that secondary crystallization is accompanied by an increase in the fold period. A second consideration arises from the observation of Keith and Padden¹⁰ that less crystallizable molecules (by virtue of branching or lower molecular weight) are rejected during the initial stages, so that the final stage would be concerned primarily with the crystallization of these rejected species.

In either of these circumstances it is probable that the value of N no longer remains constant. If the crystallization is performed at constant temperature and pressure, ΔF is now a function of two variables, n and N . If we define a new variable by

$$v \equiv 1/N \quad (15)$$

then

$$\omega = n/N = nv \quad (16)$$

and

$$d\omega/dt = n(dv/dt) + v(dn/dt) \quad (17)$$

The rate of change of v and n with time can then be related to the free energy gradients by applying the formalism of irreversible thermodynamics,

$$\left. \begin{aligned} dv/dt &= L_{11}(\partial\Delta F/\partial v)_n + L_{12}(\partial\Delta F/\partial n)_v \\ dn/dt &= L_{21}(\partial\Delta F/\partial v)_n + L_{22}(\partial\Delta F/\partial n)_v \end{aligned} \right\} \quad (18)$$

We now have three linear coefficients L_{11} , L_{22} and L_{12} ($=L_{21}$), which cannot be evaluated at the moment directly from the physical nature of the system, and are therefore to be regarded as purely adjustable parameters. By judicious choice of these parameters we had some success in fitting the experimental curve beyond 35 per cent crystallinity but, because the interpretation of these parameters is uncertain, it appears to be unprofitable to describe this result in further detail.

Crystallization kinetics has hitherto been interpreted mostly in terms of the Avrami¹¹ equation

$$\omega/\omega_\infty = 1 - \exp[-Zt^m] \quad (19)$$

where Z and m are constants. The above equation was derived on the assumption that the retardation of crystal growth arises solely from the impingement of growing crystallites or, in other words, from the decrease in the available amorphous space for the crystallites to grow into. On this premise the constant m was predicted to be an exact integer 1, 2, 3 or 4 (or half integers for diffusion-controlled growth). Careful analysis of experimental results has, however, shown¹² that in the crystallization of polyethylenes from an unseeded, completely amorphous melt, the value of m is never integral, varying from 2.7 to 3.9. Extension of the Avrami theory to the case of seeded crystallization leads¹³ to the expectation that the value of m is still integral, but reduced by 1.0. It is observed⁶, however,

that when the sample is seeded, the constant m decreases to a more or less uniform value of about 1.3. Thus, it is clear that the derivation of the Avrami equation based solely on volume considerations¹¹ is not adequate to explain the detailed course of both seeded and unseeded crystallizations. The effect of seeding by partial melting is to leave a large number of minute crystallites which act as nuclei in the subsequent crystallization process. In this case the growth of these nuclei into full crystallites probably does not involve the process of secondary nucleation, which is usually considered to be rate-controlling in unseeded crystallization. In the present treatment we have assumed that the process of crystallization is governed by the activated transfer of chain units from the melt on to a crystallite, and that the retardation of the rate as crystallization progresses arises from the gradual decrease in the free energy gradient which acts as the driving force of the process, until the final equilibrium crystallinity, as determined by the number of original nuclei, is approached. The analysis of the theoretical curve in *Figure 1* in terms of the Avrami equation leads to an m value of about 1.2 in good agreement with the experimental values. Any attempt to rationalize the fractional values of m in unseeded crystallization in terms of geometrical considerations has to postulate *ad hoc* variations of the primary nucleation rate and/or the shape of the growing crystallites. From the viewpoint of the present treatment it would appear that the real cause lies in the retardation of the growth rate of crystallites already incorporated in the expanding spherulites, by a mechanism similar to the one considered here.

Support of the U.S. Army Research Office (Durham) under grant 31-134-G202 is gratefully acknowledged.

*Department of Chemistry,
Duke University,
Durham, North Carolina*

(Received August 1964)

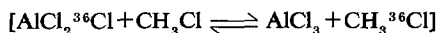
REFERENCES

- ¹ ROE, R.-J., SMITH, Jr, K. J. and KRIGBAUM, W. R. *J. chem. Phys.* 1961, **35**, 1306
- ² KRIGBAUM, W. R., ROE, R.-J. and SMITH, Jr, K. J. *Polymer, Lond.* 1964, **5**, 533 and 636
- ³ MANDELKERN, L. *Crystallization of Polymers*. McGraw-Hill: New York, 1964
- ⁴ DE GROOT, S. R. *Thermodynamics of Irreversible Processes*. Interscience: New York, 1951
- ⁵ PRIGOGINE, I. *Introduction to Thermodynamics of Irreversible Processes*. C. C. Thomas: Springfield, Illinois, 1955
- ⁶ BANKS, W., GORDON, M. and SHARPLES, A. *Polymer, Lond.* 1963, **4**, 289
- ⁷ PRIGOGINE, I., OUTER, P. and HERBO, I. *J. phys. Colloid Chem.* 1948, **52**, 321
- ⁸ VOL'KENSHTEIN, M. V. *Configurational Statistics of Polymeric Chains*, p 428. Interscience: New York, 1963
- ⁹ FISCHER, E. W. and SCHMIDT, G. *Angew. Chem.* 1962, **1**, 488
- ¹⁰ KEITH, H. D. and PADDEN, Jr, J. *J. appl. Phys.* 1964, **35**, 1270 and 1286
- ¹¹ AVRAMI, M. *J. chem. Phys.* 1939, **7**, 1103; 1940, **8**, 212; 1941, **9**, 177. See also Mandelkern, ref. 3
- ¹² BANKS, W., GORDON, M., ROE, R.-J. and SHARPLES, A. *Polymer, Lond.* 1963, **4**, 61
- ¹³ HOFFMAN, J. D., WEEKS, J. J. and MURPHY, W. M. *J. Res. Nat. Bur. Stand. A.* 1959, **63**, 67

Consequences of Chlorine Exchange between Methyl Chloride and Aluminium Chloride in Cationic Polymerization

J. P. KENNEDY and F. P. BALDWIN

The chlorine exchange reaction at -24.2°C between aluminium chloride and methyl chloride



has been investigated. Exchange with solid aluminium chloride is very much faster than that with dissolved aluminium chloride. When considered in the light of the cationic polymerization of isobutylene in methyl chloride diluent, the data suggest that in the presence of solid aluminium chloride, methyl chloride might be chemically involved in initiation; but it is not likely to be a co-catalyst in a completely homogeneous system.

THE tetrachloroaluminate complex $\text{R}^+(\text{AlCl}_4)^-$ or the dimeric form $\text{R}^+(\text{Al}_2\text{Cl}_7)^-$ is frequently cast as the initiating species in cationic polymerizations using aluminium chloride catalyst in alkyl chloride diluents (or catalyst solvents)¹⁻⁵. These complexes have also been postulated to participate in chain transfer reactions involving alkyl halides⁶.

The existence of such ion pairs at respectably high concentrations would lead one to suspect that halogen exchange between the alkyl chloride and dissolved aluminium chloride should be a relatively fast process. Accordingly, as part of our work on cationic polymerization, it seemed worthwhile to investigate this exchange reaction. Our experimental method allowed for observations both in hetero- and homo-geneous systems.

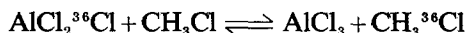
EXPERIMENTAL

Catalyst solution was prepared by dissolving commercially available aluminium chloride-³⁶Cl in non-radioactive methyl chloride. Aluminium chloride-³⁶Cl supplied by New England Nuclear Corporation was a statistical mixture of $\text{AlCl}_2^{36}\text{Cl}$. 133 mg of the anhydrous salt was refluxed (b.pt -24.2°C) in 20 ml methyl chloride ($d_{-24^{\circ}} = 1.005 \text{ g/cm}^3$). At suitable time intervals some of the alkyl halide was distilled off and condensed in preweighed counting vials containing 15 ml of phosphor solution. Phosphor solution consisted of 4 g of 2,5-diphenyl oxazole and 0.05 g *p*-bis-(2,5 phenyl oxazole)-benzene dissolved in 1000 ml toluene. The methyl chloride vapours were led through a bed of potassium hydroxide pellets to remove adventitious H^{36}Cl formed by traces of water in the system. The vials were capped immediately, and the condensed methyl chloride was determined by weighing. Finally, the vials were sealed with wax and tape. A liquid scintillation spectrometer (Packard Tricarb, Model 314X) was used for radioactive counting.

RESULTS AND DISCUSSION

(1) *The Exchange reaction*

Table 1 compiles the results of the isotope exchange



It will be noted that exchange is fairly rapid up to about 320 minutes, but thereafter, the exchange rate drops rapidly and becomes very slow when

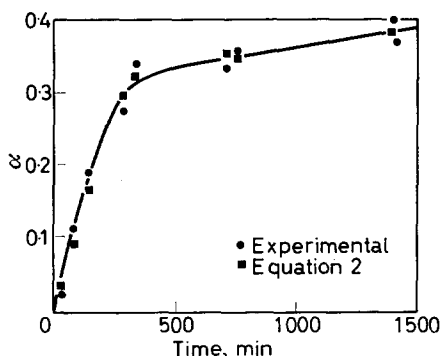


Figure 1—Rate of isotope exchange

about 40 per cent exchange has occurred. The abruptness of this rate change is shown in Figure 1 where the ratio

$$\alpha = W^*/W_0$$

(where W^* is the weight of $\text{AlCl}_2^{36}\text{Cl}$ exchanged, and W_0 is the original weight of $\text{AlCl}_2^{36}\text{Cl}$) is plotted versus time.

Table 1. Results of isotope exchange experiment

No. of vial	Time of 'cut'	g CH_3Cl collected	DPM*	CPM** g CH_3Cl	Corrected total CPM $\times 10^{-5}$ ***
1	5	0.5940	5 591	1 235	0.257
2	21	0.7025	18 891	35 400	6.867
3	60	0.7025	78 033	146 400	27.66
4	120	0.6048	120 857	263 500	48.69
5	270	0.4647	140 736	408 000	73.88
6	320	0.3428	131 131	504 000	90.18
7	702	0.4076	158 283	511 000	91.26
8	741	0.3690	154 571	552 000	97.84
9	1 393	0.1264	58 311	607 500	106.63
10	1 397	0.1975	85 337	569 000	100.50
Values for complete exchange				1 335 000	266.00

*DPM denotes disintegrations per minute. The blank was 18 DPM. Counting efficiency was 0.759.
 **CPM denotes counts per minute (corrected DPM).
 ***Denotes corrected for CH_3Cl removed by sampling during experiment.

While this behaviour might be construed as characteristic of a system of opposing reactions, no such explanation is possible here. The enormous excess of methyl chloride in the experiment requires a kinetic isotope effect of about 10^3 to explain the data on the basis of kinetic equilibrium between forward and reverse reactions. This is most unreasonable.

Observations made during the course of the experiment hold the key to this behaviour. When the ampoule into which aluminium chloride had been sublimed was crushed in the presence of methyl chloride, various sized flakes were produced. Drastic decrease in exchange of rate occurred 350 to 400 minutes later, coincidentally with the visual disappearance of solid material. Hence, an explanation of the exchange data assumes a fast heterogeneous reaction and a slow homogeneous reaction. This general phenomenon has been observed by others in similar systems⁷⁻⁹.

While it is impossible in such an ill-defined solid-liquid system to arrive at exact kinetic expressions describing the homogeneous and heterogeneous reactions, it is possible to establish at least a lower limit for the order of difference between the two. In a very general way, we can set the rate of exchange in the heterogeneous reaction as being proportional to some fraction F of the total weight W of aluminium chloride present as solid at any particular instant of time. Thus we have

$$dW^*/dt = k_1 F(t) W(t) \quad (1)$$

where F and W are unknown functions of time. One can then approximate the integrated form of equation (1) by a series to give

$$\alpha = W^*/W_0 = 1.66 \times 10^{-3} t - 2.29 \times 10^{-6} t^2 + 9.35 \times 10^{-10} t^3 \quad (2)$$

Equation (2) yields a multiple correlation coefficient of 0.999 (see *Figure 1*).

Differentiation of equation (2) and evaluation at $t=0$ leads to

$$\left| \frac{dW^*}{dt} \right|_{t=0} = k_1 F W_0 = 1.66 \times 10^{-3} W_0 \quad (3)$$

giving a pseudo first order rate constant multiplied by the fraction of the solid which is available at the surface for reaction of $1.66 \times 10^{-3} \text{ min}^{-1}$. A conventional first order plot of the data, *Figure 2*, indicates a pseudo first order rate constant k_2 for the homogeneous exchange reaction of $8.06 \times 10^{-5} \text{ min}^{-1}$. The ratio of hetero- to homo-geneous reaction rate is

$$k_1 F / k_2 = 20.5 \quad (4)$$

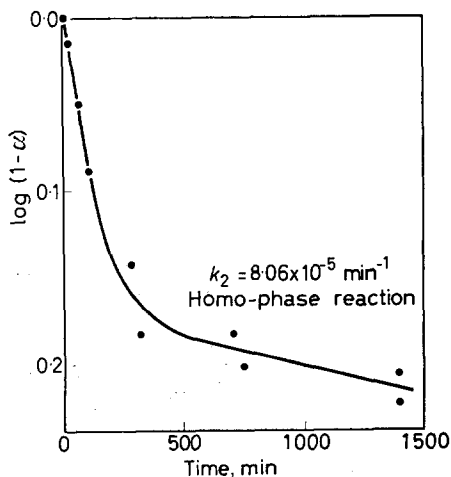
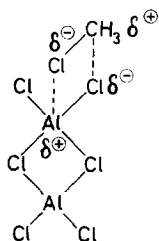


Figure 2—First order plot of the ratio of ^{36}Cl not exchanged

Necessarily, F must be considerably less than unity, hence, the heterogeneous reaction must be at least about two orders of magnitude greater than the homogeneous reaction. This enhancement of rate might be construed as reflecting the strong polarizing effect of the ionic lattice of the aluminium chloride crystal¹⁰ or the influence of a surface 'sludge'. At any rate, the results imply that whether the reaction be alkylation or polymerization, the presence of solid aluminium chloride can be expected to influence rate and possibly mechanism. Consequently, in cationic surface reactions one might envisage particulate ('heterogeneous') gegenions associated with the carbonium ion and the exact nature of the gegenion should have important bearing on reaction details.

We propose that the surface exchange reaction proceeds by a concerted ionic mechanism. Presumably, the methyl chloride molecule is so strongly polarized at the ionic surface that its chlorine atom loses its specific identity and it leaves the site with an exchanged chlorine atom, thus



Such a concerted heterogeneous ionic exchange should be much faster than a conventional homogeneous S_N2 type substitution. The sluggishness of the homogeneous exchange reaction suggests that ionized compounds either do not exist or, if they do, the degree of ionization is extremely low.

These facts suggest that methyl chloride could act as co-catalyst in the low temperature aluminium chloride catalysed polymerization of isobutene provided solid aluminium chloride surfaces are present in the system, but it is probably not a co-catalyst in the usual sense in a completely homogeneous system.

A recent paper¹¹ which appeared during the proof-reading of our manuscript corroborates and expands our findings. Thus Trotter investigated, among other things, the exchange and isomerization reactions occurring in the *n*-propyl bromide-aluminium chloride system. He postulated that if halogen exchange proceeds by an ionic mechanism *n*-propyl \rightarrow isopropyl rearrangement should take place. According to the data, only a very limited amount of exchange ($n\text{-PrBr} \rightarrow n\text{-PrCl} + i\text{-PrCl}$) took place for a short while; however, the concurrent isomerization ($n\text{-PrBr} \rightarrow i\text{-PrBr}$) proceeded for a long time until an apparent equilibrium was reached. It was stated that 'aluminium chloride dissolved in seven minutes in pure *n*-propyl bromide' which is just about the time when exchange stopped. Similarly, in another experiment with the *n*-propyl iodide-aluminium chloride system, continuous slow halogen exchange was observed throughout the experiment; however, in this run 'the catalyst did not dissolve completely (in *n*-propyl iodide) and the system remained heterogeneous

throughout the reaction'. Trotter concluded that the unrearranged reaction products were evidence for a non-ionic exchange mechanism.

An alternative explanation is that exchange and isomerization do not proceed by the same mechanism. Consequently, the data might indicate that halogen exchange proceeds only on aluminium chloride surfaces and that this process becomes extremely slow or stops altogether in the absence of solid. Isomerization could occur by some other mechanism and proceed in the homogeneous medium as well.

*Esso Research & Engineering Co.,
Chemicals Research Division,
Linden, N.J., U.S.A.*

(Received September 1964)

REFERENCES

- ¹ ZLAMAL, Z., AMBROZ, J. and AMBROZ, L. *Chem. Listy*, 1955, **49**, 1606
- ² ZLAMAL, Z., AMBROZ, L. and VESELY, K. *J. Polym. Sci.* 1957, **24**, 285
- ³ AMBROZ, L. and ZLAMAL, Z. *J. Polym. Sci.* 1958, **30**, 381
- ⁴ PLESCH, P. H. *Z. Elektrochemie*, 1956, **60**, 325
- ⁵ KENNEDY, J. P. and THOMAS, R. M. *J. Polym. Sci.* 1961, **55**, 311
- ⁶ KENNEDY, J. P. and THOMAS, R. M. *J. Polym. Sci.* 1961, **49**, 189
- ⁷ WALLACE, C. H. and WILLARD, J. E. *J. Amer. chem. Soc.* 1950, **72**, 5275
- ⁸ BLAU, M. and WILLARD, J. E. *J. Amer. chem. Soc.* 1951, **73**, 442
- ⁹ BLAU, M., CARNALL, W. T. and WILLARD, J. E. *J. Amer. chem. Soc.* 1952, **74**, 5762
- ¹⁰ THOMAS, C. A. *Anhydrous Aluminium Chloride in Organic Chemistry*. Reinhold: New York, 1941
- ¹¹ TROTTER, P. J. *J. org. Chem.* 1963, **28**, 2093

The Effect of Crystallization Conditions and Temperature on the Polymorphic Forms of Polyethylene

J. G. FATOU*, C. H. BAKER and L. MANDELKERN

Experimental evidence (using wide-angle X-ray and dilatometric techniques) is presented to indicate development of a second crystalline form as a result of further crystallization from the melt, and the temperature interval covering its formation and disappearance. Three fractionated samples of polyethylene of viscosity average molecular weights 12 500, 425 000 and 1 000 000 and an unfractionated sample of Marlex 50 of molecular weight 180 000 were used. The extra reflections reported were not observed with rapidly cooled samples.

WIDE angle X-ray diffraction studies of linear polyethylenes and polymethylenes have shown that besides the reflections assigned to the orthorhombic structure by Bunn¹ extra reflections are also sometimes observed^{2,3}. These extra reflections, which are particularly noticeable in cold worked samples, have been attributed by Teare and Holmes³ to a triclinic structure and correspond to Bragg spacings of 4.56, 3.80 and 3.55 Å. The appearance of these reflections has also been observed in molecular weight fractions of Marlex 50 which have been crystallized at low undercoolings under controlled conditions⁴. Volume/temperature studies of these fractions have failed to disclose any evidence for the presence of a second crystalline phase. It has not been possible, thus far, to ascertain whether this crystalline modification of polyethylene is formed by further crystallization from the residual melt or by a crystal-crystal type of transition. The temperature range in which this form appears is not known, nor is its thermodynamic stability. Since this modification appears subsequent to crystallization at low undercoolings, it is important that its stability relative to the more abundant orthorhombic form be determined. In the present paper, we present experimental evidence which indicates that the second crystalline form develops as a result of further crystallization from the melt. The temperature interval over which it forms and disappears is also delineated.

EXPERIMENTAL

Three fractionated samples of polyethylene of viscosity average molecular weights of 12 500, 425 000 and 1 000 000 and an unfractionated Marlex 50 sample of molecular weight 180 000 were utilized in this study. The method of fractionation and characterization has been previously described⁵. Various crystallization procedures were adopted. In one set of experiments the samples were crystallized at 130°C for a period of 40 days and then cooled down to room temperature over a period of 24 hours. Studies of

*Present address: Physical Chemistry Section, Departamento de Plasticos (C.S.I.C.), Madrid, Spain.

the crystallization kinetics of polyethylene fractions⁶ indicate that after this extended time interval no further significant crystallization will occur at the elevated temperature. The degree of crystallinity reached in all cases was determined from specific volume values measured at 25°C by the gradient column technique, assuming additivity of the volumes of the respective phases and using the specific volume relationships given by Chiang and Flory⁷. In accord with previous results⁵ the degree of crystallinity at 25°C for samples thus crystallized decreases from 90 to 78 per cent as the molecular weight of the fractions increases from 12 500 to 1 000 000. In another procedure all four samples were rapidly crystallized by quenching from the melt to an ice-water mixture. The degrees of crystallinity at 25°C that developed following this procedure decreased from 77 to 56 per cent over the same molecular weight range. We can also note, parenthetically,

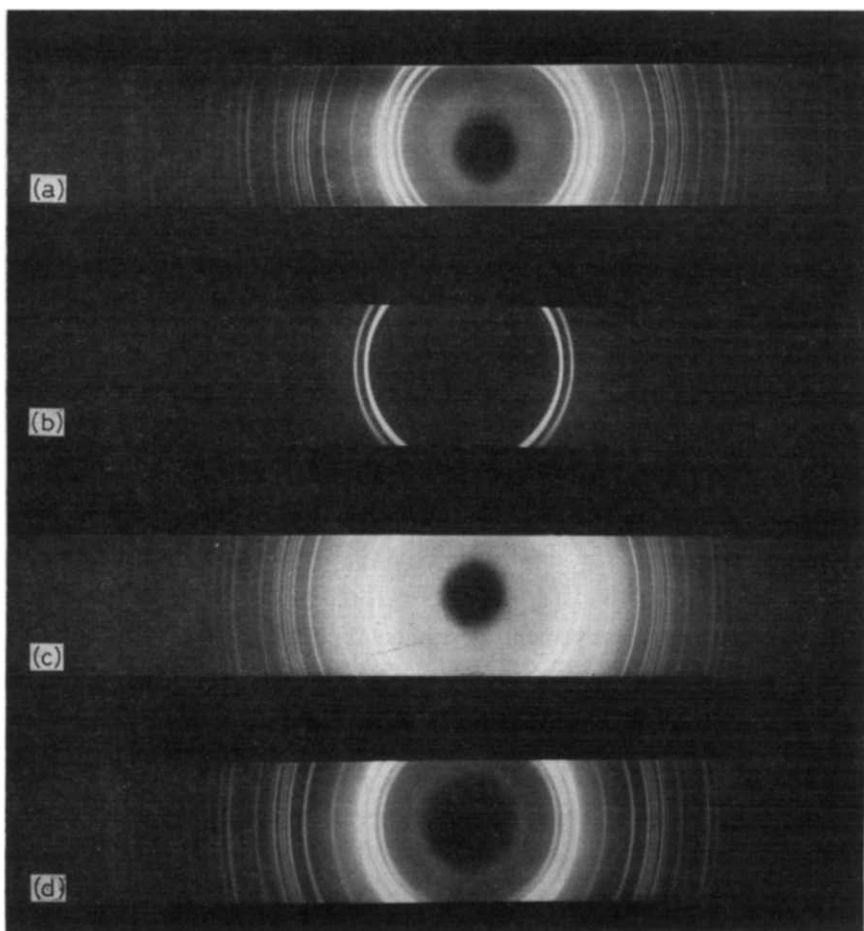


Figure 1—Powder photographs for polyethylene fraction R-2-9 (mol. wt 12 500) (a) crystallized at 130°C; (b) quenched; (c) single crystals; (d) quenched and annealed at 130°C

the relatively low level of crystallinity that can be obtained from a high molecular weight fraction. 'Single crystals' of the unfractionated Marlex 50 and the lowest molecular weight fraction were prepared by crystallization from an 0.5 per cent xylene solution at 90°C. Crystallization was allowed to take place for two days and the system was then cooled gradually to room temperature over a 24 hour period.

The dilatometric procedures that were employed have been previously described⁵. Wide angle X-ray diffraction patterns were obtained at room temperature using a Norelco powder camera with Ni filtered CuK_α radiation. Confirmatory experiments were also obtained using a Norelco diffractometer. In one set of experiments to be described below, the X-ray diffraction pattern was studied as a function of temperature. A specially designed sample holder, the details of which will be reported elsewhere⁸, was utilized for this purpose.

RESULTS AND DISCUSSION

Typical X-ray powder patterns of the lowest molecular weight fraction crystallized under various conditions are illustrated in *Figure 1*. Similar results are obtained for molecular weight fractions of *M* up to 1 000 000.

The wide-angle diffraction patterns for all the samples crystallized in the bulk for 40 days at 130°C included the extra reflections that have been attributed to the triclinic structure. The lowest molecular weight fraction displayed the sharpest reflections and was devoid of any halo. The reflections observed for the highest molecular weight sample were more diffuse and a broad halo is displayed. The extra lines are clearly discerned in patterns (a) and (d) of *Figure 1*. The extra reflections were not observed in either the samples rapidly cooled from the melt [*Figure 1*(b)] or those crystallized from dilute solution [*Figure 1*(c)]. The quenched sample of the lowest molecular weight fraction was then annealed at 130°C for 24 hours and cooled to room temperature over an additional 24 hour period. Subsequent examination of the sample by X-ray diffraction revealed that the extra reflections now appeared in the sample [*Figure 1*(d)] while prior to annealing they were not observed. The results of the X-ray diffraction experiments are summarized in *Table 1*.

Table 1

Sample	Mol. wt	(a)	(b)	(c)	(d)
Marlex 50	180 000	e	n	n	—
Fraction R-2-9	12 500	e	n	n	e
Fraction R-3-9	425 000	e	n	—	—
Fraction P-M-3	1 000 000	e	n	—	—

(a) Crystallized at 130°C for 40 days and cooled over 24 hours.

(b) Quenched in ice-water.

(c) Single crystals from 0.5 per cent xylene at 90°C for two days.

(d) Quenched, annealed 24 hours at 130°C then cooled to room temperature.

e Extra lines observed.

n No extra lines observed.

These results indicate that the second crystalline form appears below 130°C only when the subsequent cooling rate is relatively slow. Further experiments were then performed to determine the temperature range of formation and disappearance of this crystalline modification.

Samples which had been crystallized under the conditions which yield the extra reflections were annealed at temperatures between 60° and 130°C for a period of 24 hours and then quenched into ice-water. It was found that the previously observed extra reflections progressively weakened as the annealing temperature was increased. At annealing temperatures of about 85° or 90°C the extra lines became very weak so as to be almost undetectable. In the range of 90° to 95°C it was impossible to state definitely whether or not the lines were present. However, when the samples were heated above 100°C and then quickly cooled the extra reflections completely disappeared. These observations demonstrate that the polymorphic form disappears at about 95°C and this process takes place over a relatively wide temperature range below this point.

Since the above X-ray patterns were taken at room temperature, after the sample was heated, a corollary set of experiments was performed as the sample showing the extra reflections was heated. Geiger counter observations over the range 2θ from 18° to 26°, were made in sequential order at the following temperatures: room temperature, 50°, 75°, 85°, 95°, 102°, 130° and 85°C over a period of three hours. The traces observed for the molecular weight sample $M=12\,500$ initially crystallized at 130°C for 40 days are illustrated in *Figure 2*. In confirmation of the previous conclusion, the diffraction patterns of this molecular weight sample show the gradual disappearance of the innermost peak (at $2\theta=19^\circ 20'$). The slight shoulders on the [200] peak (at $2\theta=24^\circ$) which are present initially also gradually disappear as the temperature is increased. This effect, however, is much less noticeable.

It has previously been suggested that the polymorph develops by further crystallization, as a partially crystalline sample is cooled from 130°C to room temperature⁴. The results discussed above support this view. A further substantiation of this conclusion is found in a detailed dilatometric analysis of the crystallization process. After the cessation of crystallization at 130°C, the dilatometers were quickly transferred to a thermostat at 125°C and the decrease in specific volume was studied as a function of time until a stationary value was reached. This process was repeated by lowering the temperature in five degree intervals down to 25°C⁵. *Figure 3* summarizes the increased crystallinity calculated for the decreasing temperature intervals for fractions of four different molecular weights. The density changes have been converted to degree of crystallinity at each temperature. A definite discontinuity is seen to exist in the plot in the range of 90° to 100°C. However, fusion curves do not show, unequivocally, a definite transition in this temperature interval^{5,9}. This could be attributed to annealing of the orthorhombic form or the melting and recrystallization of the polymorphic form to the orthorhombic one.

Independent of the polymorphism, the loss peaks observed in dynamic mechanical experiments at 90° to 95°C¹⁰ and the enhanced irradiation crosslinking efficiency observed for polyethylene in this temperature

THE EFFECT OF CRYSTALLIZATION CONDITIONS ON POLYETHYLENE

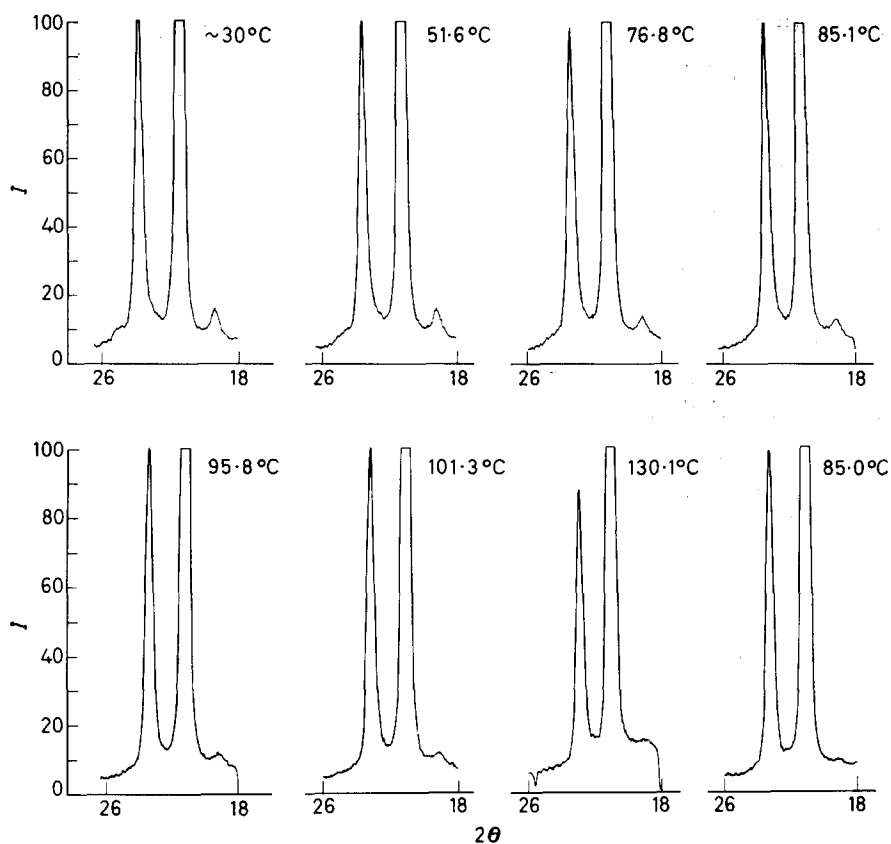


Figure 2—Diffraction patterns at various temperatures, of polyethylene sample R-2-9 (mol. wt 12 500) initially crystallized at 130°C

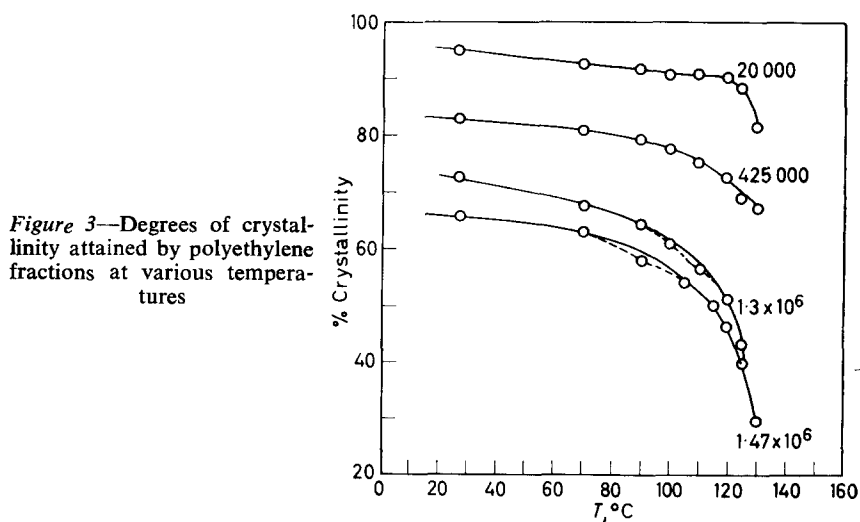


Figure 3—Degrees of crystallinity attained by polyethylene fractions at various temperatures

range^{11,12} have been attributed to the onset of molecular motions of the chain units within the crystalline regions. Moreover, Takayanagi¹⁰ has reported a discontinuity in the linear expansion coefficient of the *a* dimension of the polyethylene unit cell at about 90°C. It is not clear at present as to whether these observations are intimately related with or are independent of the disappearance of the extra reflections and the melting of the polymorphic form. However, it should be noted in this connection that the 'single crystals' in which the polymorphic form has not as yet been developed also display the changes in dynamic mechanical properties and crosslinking efficiency in the range of 90° to 95°C.

This work was supported by a grant from the U.S. Army Research Office (Durham) and a contract with the Division of Biology and Medicine, Atomic Energy Commission.

*Department of Chemistry and Institute of Molecular Biophysics,
Florida State University,
Tallahassee, Florida*

(Received September 1964)

REFERENCES

- ¹ BUNN, C. W. *Trans. Faraday Soc.* 1939, **35**, 489
- ² TURNER JONES, A. *J. Polym. Sci.* 1962, **62**, 553
- ³ TEARE, P. W. and HOLMES, D. R. *J. Polym. Sci.* 1957, **24**, 496
- ⁴ POLLACK, S. S., ROBINSON, W. H., CHIANG, R. and FLORY, P. J. *J. appl. Phys.* 1962, **33**, 237
- ⁵ FATOU, J. G. and MANDELKERN, L. *J. phys. Chem.* 1965, **69**, 417
- ⁶ FATOU, J. G. and MANDELKERN, L. To be published
- ⁷ CHIANG, R. and FLORY, P. J. *J. Amer. chem. Soc.* 1961, **83**, 2857
- ⁸ BAKER, C. H. and MANDELKERN, L. To be published
- ⁹ BOYER, R. F. *Rubber Reviews*, 1963, **36**, 1303
- ¹⁰ TAKAYANAGI, M. *Mem. Fac. Engng Kyushu Univ.* 1963, **23**, No. 3
- ¹¹ KITAMARU, R., FATOU, J. G. and MANDELKERN, L. *J. Polym. Sci.* 1964, **2B**, 511
- ¹² KITAMARU, R. and MANDELKERN, L. *J. Amer. chem. Soc.* 1964, **86**, 3529

Cocrystallization in Copolymers of α -Olefins I—Copolymers of 4-Methylpentene with Linear α -Olefins

A. TURNER JONES

The helical chain conformations in homopolymers of isotactic olefins, branched and unbranched, are shortly discussed with a view to predicting the degree to which cocrystallization may occur in random copolymers due to isomorphism of monomer units, and particularly in relation to copolymers of 4-methylpentene with linear α -olefins, pentene, hexene, octene, decene and octadecene. In accordance with prediction, it is shown that copolymers with pentene and hexene show a high degree of isomorphism and cocrystallization. Copolymers with the higher α -olefins show increasing disruption of the poly-4-methylpentene crystallinity with side-chain length and comonomer content, but octene and decene units can enter the poly-4-methylpentene crystal lattice to some extent, while octadecene units do not. Degrees of crystallinity, lattice parameters and melting points have been measured, and crystal phases in pentene copolymers are discussed. Although the polymerization conditions were designed to give random copolymers, evidence is adduced to show that copolymerization has taken place but not entirely randomly; chains of varying composition and degrees of blocking are undoubtedly present.

ISOTACTIC copolymers which are well crystalline over a wide range of composition have been described by Natta¹ for copolymers of styrene and the ring-substituted styrenes, and by Reding and Walter² for 4-methylpentene with 3-methylbutene. Some copolymers of 4-methylpentene with pentene-1, hexene-1, octene-1 and octadecene-1 made by polymerization of mixtures of monomers containing 10 to 25 per cent unbranched α -olefin have been described by Campbell³ as well crystalline, high melting and readily forming films and fibres; the actual polymer compositions are not given. Hewitt and Weir⁴ have measured dynamic mechanical properties of 4-methylpentene (4MP) copolymers containing hexene-1 (10 and 50 per cent by monomer charge ratio) and pentene-1 (50 per cent) and concluded that crystallinity was present in all three copolymers and that crystals contained mixed monomer units.

This paper describes an X-ray investigation of the cocrystallizing behaviour of isotactic copolymers of 4-methylpentene with the unbranched olefin comonomers, pentene-1, hexene-1, octene-1, decene-1 and octadecene-1 over a wide range of copolymer composition. At each composition the crystal phases were identified and unit cell dimensions, degrees of crystallinity and melting points measured.

CRYSTALLIZATION IN α -OLEFIN COPOLYMERS—
THEORETICAL CONSIDERATIONS

Natta¹ has discussed isomorphism and solid solution formation in mixtures of isotactic polymers with macromolecular chains of similar chemical nature and structure. In the same paper he discusses 'isomorphism phenomena among monomeric units' and 'isodimorphism'. The former occurs when copolymerizing monomer units are able to replace each other isomorphously in the unit cell of the homopolymers, which must have an analogous crystal structure, the same identity period and only very slightly different lattice constants. Copolymers of styrene and *o*-fluorostyrene (both with 3_1 helices) form such a system. Here the physical properties, e.g. lattice dimensions, melting point and crystallinity, vary in a strictly continuous way as a function of composition. He describes as 'isodimorphic' those systems which are crystalline over the whole composition range, even though the homopolymers have different crystal structures, e.g. copolymers of styrene (3_1 helix) and *p*-fluorostyrene (4_1 helix), which at each composition show the crystallinity of the homopolymer of the major component, although the polystyrene lattice becomes deformed owing to incorporation of the larger monomer units; the melting point curve is linear with composition.

Mixed crystal formation of either of the above types, the 'chain' type or the 'monomeric unit' type, may be expected to occur in any copolymer of similar chemical and stereochemical structure with nearly identical repeat units and similar three-dimensional packing, provided the dimensions of the cells in cross section perpendicular to the fibre axis (transverse dimensions) do not differ by more than perhaps ten per cent (as required for isomorphism in monomeric crystals), giving roughly 20 per cent tolerance in the unit cell cross-section area. With isotactic polyolefins the tolerance limits may be expected to be somewhat wider than this.

In the crystallites the chains are all coiled into helices and only differ in helix type, repeating unit, and in the size of their pendant side-chains. Provided the side-chains are of similar size and shape, theoretically the helix of the second component can fit into the lattice of the major component by coiling or uncoiling. All known crystalline isotactic polyolefins of type $-(CH_2-CHR)-$, branched and unbranched, have helices lying in the range 3_1 to 4_1 . Some polymers, e.g. polypentene-1⁵, have crystal forms with both 3_1 and 4_1 helices which are not energetically very different, hence modification to any type of helix in this range is not likely to involve large energy changes. This allows a greater tolerance of repeat units, since these can also be adjusted by coiling or uncoiling of the helices, and in transverse dimensional limits since the uncoiling of a helix results in an increase in cross-sectional area occupied per chain. This is frequently accompanied by flattening of the helix also, and hence a further increase in transverse area occurs. A high degree of isomorphism, both of the 'chain' type and the 'monomeric' type, and hence also of block polymers, may be manifested in copolymers from monomers whose homopolymers crystallize in crystallographically different cells and with different helices and side-by-side packings, by suitable adjustment of the side-by-side packing and helix type to allow for the different sizes and the distribution of the two monomer units. This may involve phase changes at intermediate

compositions to helices and crystal forms quite different from those of either homopolymer. Various degrees of cocrystallization may be observed depending upon the degree of compatibility of the side chains, and copolymers containing chains of mixed type, homopolymer, blocked, random etc. may show a very complicated crystal phase behaviour. Different degrees and types of isomorphism and cocrystallization will be more fully discussed in Part II of this paper (to be published later).

In considering whether cocrystallization is likely to occur in any olefin copolymer system, the helical chain conformations are best described not by the usual description as numbers of monomer units and turns per crystallographic repeat, but by the number of monomer units per turn of the helix and the length parallel to the fibre axis per turn (l_t) and per monomer unit (l_m). An 11_3 helix is thus described as 3.67. The various stages in the uncoiling of a helix from 3_1 to 4_1 through, for instance, helices usually described as 3_1 , 7_2 , 11_3 , 37_{10} , 4_1 then show a continuous numerical change 3.0, 3.5, 3.67, 3.7, 4.0; the large and irregular changes in the true identity periods, while crystallographically important, do not reflect the very gradual changes in helical conformation.

It is useful to compare the homopolymer crystal phases from the points of view of the above helix parameters, the cross-sectional area occupied per chain and the crystal density. By taking the cross-sectional area per chain the chains are effectively being treated as cylinders which can readily pack side-by-side in various transverse lattices; it also reflects the side-chain length and branching. These parameters are listed in *Table 1* for the homopolymer crystal forms of poly-4-methylpentene (P4MP) and the poly- α -olefins under investigation, together with their unit cell dimensions and melting points.

Table 1. Homopolymer crystal phases—unit cell and helix parameters

Character	Poly 4MP	Polypentene ^a		Polyhexene ^a either/or		Polydecene ^a	Polyocta- decene ^a
		I	II _a	O	M		
Symmetry	T	M	M	O	M		O
Unit cell constants	<i>a</i>	18.60	11.2*	19.3	11.7	22.2	7.5
	<i>b</i>	18.60	20.85*	16.9	26.9	8.9	70.4
	γ	90°	90°	116°	90°	94.5°	90°
(Fibre repeat)	<i>c</i>	13.86	6.49	7.08	13.7	13.2	6.7
Helix—monomer units per turn	3.5	3.0	4.0	3.5			Not helical
l_t —length parallel to <i>c</i> per turn	6.93	6.49	7.08	6.85			
l_m —length parallel to <i>c</i> per monomer unit	1.98	2.15	1.77	1.95			1.68
Transverse area per chain, Å ²	85	58.5	74	79	98		264
Crystal density, g/cm ³	0.83	0.92	0.90	0.91	0.73		0.95
Melting point, °C	248	120*	80*	—	—	40	72

All lengths in Å. T = tetragonal, M = monoclinic, O = orthorhombic.

* a_0 and b_0 (*a* and *b* projected perpendicular to *c*).

Crystallization in copolymers of 4MP with unbranched α -olefins—theoretical

In considering *Table 1* the following further points about the homopolymers should be noted. Polyhexene which is amorphous when unoriented possesses a 3.5 helix in oriented fibres⁶. In crystalline polydecene and

polyoctadecene the side chains are not helically disposed⁸. Crystallinity has not been obtained in oriented fibres of polyoctene-1 and it is not known if the chain conformation is helical or not.

Examination of *Table 1* suggests that a high degree of cocrystallizing compatibility might be expected in copolymers of 4MP with pentene or hexene. Although the polypentene and P4MP unit cells are quite different, the side chains derived from pentene units are the same length (three carbon atoms) and the relevant parameters, cross-sectional area per chain, and number of monomer units per turn, l_m and l_t are reasonably close for P4MP and the Type II form of polypentene. Moreover, the latter can exist in stable helices both more tightly coiled (3.0) and more open (4.0) than the 3.5 helix of P4MP.

Polyhexene possesses a closely similar helical chain to P4MP (3.5) and the same total number of carbon atoms in the side chain. The extra length of side chain (1 carbon atom) could be expected to fit readily into the open P4MP structure and a high degree of cocrystallization is expected. As the side chain of the unbranched α -olefin comonomer unit becomes longer, the likelihood of cocrystallization becomes progressively lower, especially when the chain conformation of the poly- α -olefin is no longer helical and the homopolymer structures are no longer sterically similar.

EXPERIMENTAL

Polymerizations were carried out with stereospecific catalysts based on titanium chloride and the procedures adopted, which will be described elsewhere⁹, were designed to give copolymers henceforward described as 'random' in which the two monomer units were as randomly distributed as possible. This is not easily achieved where the rates of polymerization of the two monomers are widely different; 4-methyl-pentene in fact polymerizes less rapidly than the linear α -olefins because of the steric hindrance offered by the growing P4MP chains to incoming monomer units because of the methyl branch in the 4-position. In practice it is necessary to consider the possibility that the polymer formed may be (a) random, (b) blocked or (c) consist of a mixture of homopolymers, or be mixtures of all three. In addition there may be chains present which consist of either a simple AB block structure, or ABABAB polymers of varying block length, or chains of sliding composition. A mixture of chains of different types or chains with sliding composition is likely to result from systems where one monomer polymerizes faster than the other and no attempt is made to keep the composition of the reaction mixture constant throughout the polymerization which is taken to high conversion.

The estimation of linear α -olefin content of these copolymers is based on the intensity of the absorption band due to the $-\text{CH}_2-$ rocking vibration in linear hydrocarbons where the $-\text{CH}_2-$ groups are present in the *trans* configuration.

The wavelength of this vibration increases with the number of $-\text{CH}_2-$ groups from 13.58μ in pentene-1 copolymers to 13.88μ in octadecene-1 copolymers. The copolymerized α -olefin content is determined by a measurement of the intensity of this absorption and an internal thickness measurement of total hydrocarbon absorption at 2.27μ .

X-ray photographs were taken with Unicam 3 cm radius cylindrical cameras and Cu K_{α} radiation, and crystallinity determinations were obtained as further described later by diffractometry with a Philips PW 1010 diffractometer, with pulse height analysis and proportional counter. Melting points were determined optically by the disappearance of birefringence and by X-rays. Fibres were obtained from copolymers of all compositions by drawing strips of pressed sheets at temperatures between 20°C and the melting point of the copolymer.

Copolymers of 4MP with hexene, octene, decene and octadecene

Figure 1 shows the variation in crystallinity with composition, which throughout this paper is expressed in mole per cent, for the above four copolymer systems. All copolymers were slow cooled from 240°C at 6°C per hour. The crystal form in all four series was basically that of 4MP homopolymer only, with reduction in degree of crystallinity as the

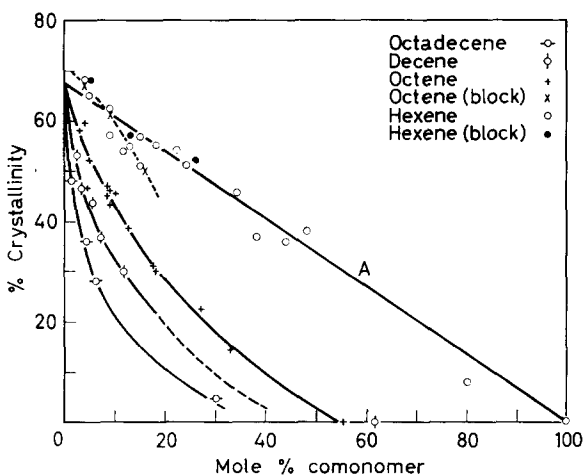


Figure 1—Copolymers of 4MP with hexene, octene, decene, octadecene; crystallinity (slow cooled from 240°C) versus mole % comonomer

comonomer content increased and, in some systems, changes in the a dimension of the tetragonal lattice and some small changes in relative intensities, more particularly loss of weak reflections. The degrees of crystallinity were measured by an extension of the method originally devised for polyethylene¹⁰ and similar to that used by Natta *et al.* for polypropylene¹¹. As shown in Figures 2(a) and 2(e), a linear background was drawn in between 2° and 32° of 2θ on a diffractometer curve of an annealed specimen and the area under the peaks was divided as shown into amorphous (A) and crystalline (C) areas. The degree of crystallinity was taken simply as $C/(A + C)$ with no further corrections. Composite correction factors to take account of the effect of Lorentz factors etc. on the relative areas were not considered very practicable or useful; since the composition

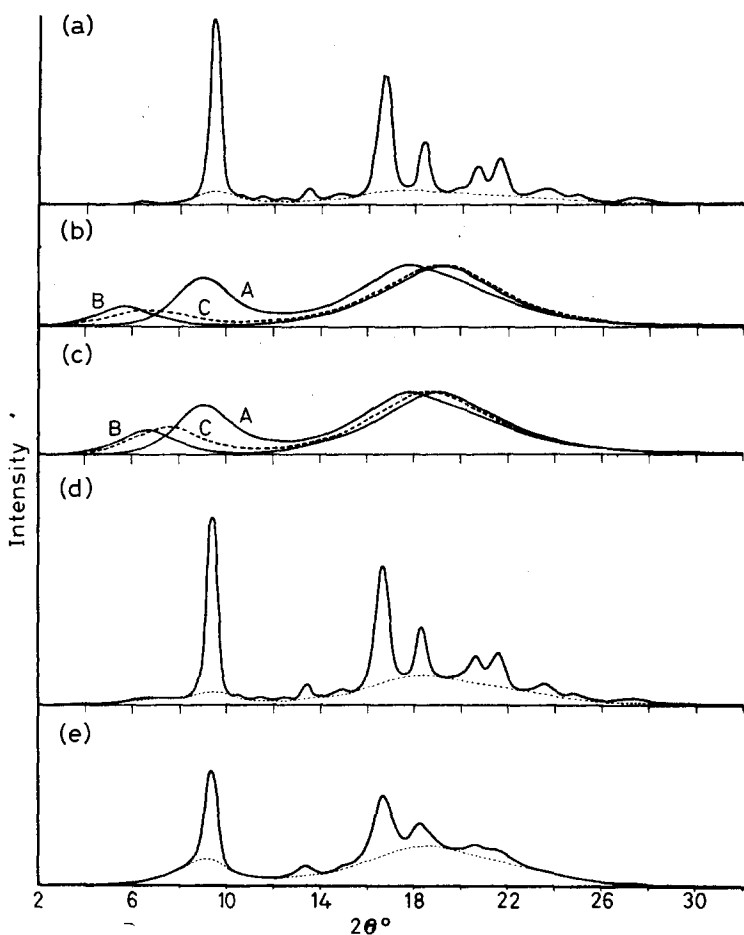


Figure 2—X-ray diffractometer scans: (a) 4MP homopolymer, (b) Amorphous polymers—4MP homopolymer A; polydecene B; copolymer containing 62 mole % decene C, (c) Amorphous polymers—4MP homopolymer A; polyoctene B; copolymer containing 55 mole % octene C, (d) 'Block' copolymer containing 16% octene, (e) 'Random' copolymer containing 18% octene

of the amorphous phase changes with comonomer content this must give a progressively changing amorphous intensity distribution with 2θ . Thus the crystallinities cannot be regarded as absolute but relative; maximum consistency in the placing of the amorphous curve under the P4MP crystalline peaks was aimed at by making this curve touch the minima between the peaks as in Figures 2(a) and 2(e).

Figure 1 shows that as the comonomer unit increases in size, incorporation of a given number of comonomer molecules has an increasingly disruptive effect on the crystallinity. In the decene and octadecene series the crystallinity would be expected to rise again at the low 4MP end of the range

since polydecene and polyoctadecene are crystalline^{12,6} but this part of the range was not investigated.

Copolymers of 4MP with octene, decene, octadecene

If no copolymerization had taken place and the materials were mixtures of homopolymers, the degree of crystallinity would be expected to be approximately the sum of the crystallinities of the homopolymers crystallizing separately, and the crystallinity versus composition curve approximately linear between the crystallinities of the homopolymers. In the octene, decene and octadecene copolymers, the observed reduction in crystallinity is much more drastic than this and it may be concluded that copolymerization has taken place as intended. The observed persistence of crystallinity up to a comonomer content of 30 per cent (even in the octadecene series a little is still present) may result either from the presence of 4MP rich chains and non-random (blocked) chains, or from a limited degree of isomorphism, perhaps also combined with a non-random distribution. In a random copolymer, where no isomorphous replacement occurs, a 1:2 ratio of monomer units would normally be expected to result in an amorphous polymer. Evidence is given later which suggests that, while copolymerization has taken place effectively in all chains, there is some spread in comonomer content of the chains at all compositions.

The effect of copolymerized α -olefin units in reducing the degree of crystallinity will depend upon the degree of randomness in their distribution and may be due to the inclusion of comonomer units within the P4MP crystal lattice and hence introduction of imperfections, particularly if the unit is too large to be easily accommodated. Alternatively it may be due to a reduction in crystallite size because the fold length and fold regularity is limited when comonomer units have to be incorporated into the amorphous regions between lamellae, or to both of these factors.

In Figure 3 the variation in tetragonal a -axis spacing with composition is shown for unoriented samples slow cooled from 240°C under vacuum

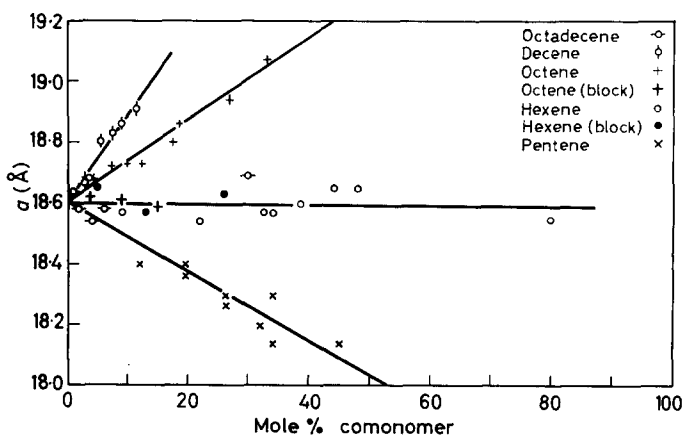


Figure 3— a -axis spacing of tetragonal P4MP cell versus mole % comonomer

at 6°C per hour. With octene and decene as comonomers, a expands progressively over the composition range examined—the expansion being greater for the larger decene-1 unit—but with octadecene-1 no expansion was observed. X-ray fibre diagrams show that the fibre repeat c does not change measurably in any of the systems. These results suggest that the octadecene units cannot be incorporated into the P4MP crystal lattice, as indeed would be *a priori* very unlikely owing to the very large difference in size of the side chains as shown by the cross-sectional area per chain (Table 1). Hence the disruption of crystallinity is due to the need to incorporate the large octadecene units in the amorphous regions. In this system then the presence of a little crystallinity at a 30 per cent comonomer content must indicate lack of randomness.

It appears that octene and decene units can be included at least to some extent within the P4MP crystallites, and that the lattice is able to expand to accommodate them. It is just possible that the expansion of the lattice could result from the presence of the longer comonomer side chains without their actually entering the crystalline regions, but fibre diagrams of the octene copolymer series suggest that this is not so. Fibres drawn at 100°C from copolymers containing 27 per cent and 33 per cent octene units were highly oriented and the stronger P4MP reflections were well defined, but the weak 4MP reflections were lost. This must result from disorder in the crystallites produced by incorporation of octene units. In the decene series specimens containing ten per cent decene units showed some streaks on the layer lines, again indicating disorder in the crystallites, although there was very little loss of detail in the P4MP pattern in spite of the low crystallinity. It appears that at least some decene units are entering the lattice. In both systems the crystallinity may arise from chains which are richer in 4MP than the overall copolymer composition, but this does not affect the above conclusions.

It is somewhat surprising that side chains which are six or eight carbon atoms long do not disrupt the lattice completely when replacing side chains three carbon atoms long, even though the P4MP crystals have a very open structure with a density of only 0.83 g/cm³^{1,3}, and hence might be expected to accommodate additional carbon atoms in the side chains. The fact that in polydecene the side chains are believed not to be disposed helically would not in itself prevent the inclusion of some decene units in the helical P4MP chains, except where runs of several decene units are present, when a marked disruption of the crystal lattice might be expected.

Copolymers of 4MP with hexene

The crystallinities of the 4MP-hexene copolymers decrease approximately linearly with molar composition between 65 per cent (at 100 per cent 4MP) and 0 per cent for hexene homopolymer. Provided copolymerization has taken place (as already shown for the octene and decene copolymers), and the polymers are not mixtures of homopolymers or copolymers of very long block length (further evidence for this is given later), then the linearity of the composition/crystallinity curve shows that the 4MP portion of each copolymer is crystallizing to the same extent as in 4MP homopolymer (~65 per cent). Moreover, Figure 3 shows that, within experimental error,

the tetragonal a -axis remains unchanged at 18.60 Å from that in 4MP homopolymer, and that the c -axis is also unchanged. Hence, as forecast from *Table 1* above, isotactically placed hexene units readily replace 4MP units in the P4MP crystal lattice, with no distortion of the 3.5 helix or change in cell dimensions.

Variations in crystallinity result from different methods of polymerization (e.g. bulk or diluent) which in themselves may give different distributions of hexene units in the copolymers, or different amounts of atactic polymer and hence different maximum crystallinities. Crystallinities of all specimens lay close to the linear curve of *Figure 1* indicating a high degree of isomorphism of the two monomer units.

The linearity of the crystallinity/composition curve requires some discussion. Even though polyhexene itself is amorphous, copolymers containing a low concentration of randomly distributed, isotactically placed hexene units (which are isomorphously incorporated into the P4MP lattice) would be expected to show the same overall crystallinity as 4MP homopolymer, instead of the observed linear decrease with hexene content. This would be followed by a steeper drop at high hexene contents, when the influence of the irregular conformation of hexene chain sequences becomes more effective; but this is not observed, although one or two points lie above the linear crystallinity curve.

That hexene-1 units add in the main isotactically is clear, otherwise the disruption in crystallinity would be expected to be as great or greater than that observed in the decene and octadecene copolymers. The failure to maintain maximum crystallinity at low hexene contents suggests that either a range of chain compositions is present, with hexene-rich chains reducing the crystallinity more than would occur in a completely random copolymer, or that the hexene units are not randomly distributed along each chain or both. While single, or perhaps two, consecutive hexene units could be incorporated into the P4MP lattice, a few short runs of a critical length, perhaps three or more units, might cause marked disruption of crystallinity because they preferentially take up a random conformation as in hexene homopolymer.

Oriented fibres were obtained at all compositions, and the X-ray photographs showed no loss of detail, i.e. disappearance of weak reflections, up to 34 per cent hexene. In view of the failure to crystallize polyhexene itself, the presence of crystallinity, even though rather low (8 per cent), in the copolymer containing 80 per cent hexene (4 mol. hexene to 1 mol. 4MP) is surprising. Moreover, in oriented fibres of the same copolymer the crystallinity was considerably more highly developed, with no lattice parameter changes from those of P4MP; the very weak reflections had disappeared, but the stronger ones were sharp and well developed [see *Figure 4(f)*]. Although the crystallizing chains may have a 4MP content somewhat higher than one in four it is nevertheless clear that the 4MP units (which crystallize very readily in 4MP homopolymer) are having a marked influence in constraining the hexene units to crystallize both in the unoriented specimens and even more strongly in the drawn fibres. Polyhexene-1 itself crystallizes to a small degree when extended and held under tension⁶, which presumably aids the formation of a helical conformation. It appears

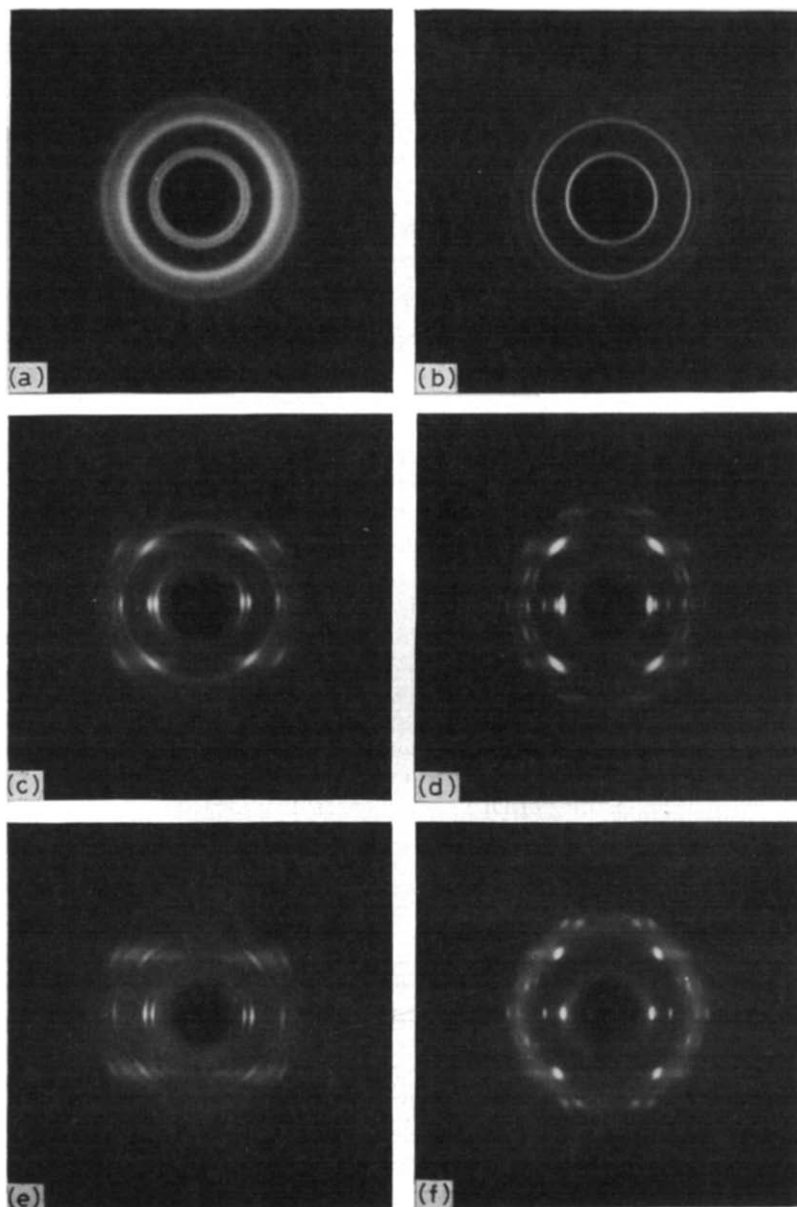


Figure 4—X-ray diffraction patterns: (a) to (d) 4MP pentene copolymer with 34% pentene; (a) powder, unannealed, showing P4MP and II crystal forms; (b) powder, annealed, showing P4MP form only; (c) fibre drawn 20°C showing well oriented II and poorly oriented P4MP forms; (d) fibre drawn 120°C showing P4MP form, principally; (e) polypentene-1 fibre showing Type IIb form; (f) 4MP-hexene copolymer (20 per cent 4MP); fibre drawn 60°C

that polyhexene-1 is not basically poorly isotactic, but requires some extra impetus to crystallize, which is supplied by the presence of 4MP units well distributed along the chains, and it is the steric effect of the methyl branch in the 4-position which, even when adjacent to hexene units with unbranched side chains, tends to favour a helical and therefore crystallizable conformation of the main chain. The fact that both homopolymers crystallize in a 3.5 helix must be a strongly contributing factor. A side-by-side packing similar to that in P4MP is favoured, rather than that in polyhexene itself, and as both units have six carbon atoms in the side chain the crystal density is the same as for P4MP.

It appears then that hexene units can readily replace 4MP units isomorphously in the 4MP lattice, but the picture is complicated by the fact that polyhexene, while presumably isotactic, is amorphous. At the low hexene end of the composition range, the crystallinity is reduced more than would be expected for a truly random copolymer, but at the high hexene end, the crystallinity is higher than would be expected owing to the presence of 4MP units.

FURTHER EVIDENCE FOR COPOLYMERIZATION

'Block' and 'random' copolymers

Evidence that copolymerization has taken place in these linear α -olefin copolymers is provided by a comparison of their X-ray diffraction scans with those of homopolymer mixtures or copolymers of long block length based on the same monomers. Polymers of the latter type were prepared by polymerizing hexene and octene after the 4MP polymerization to form a tail or mixture. These would be expected to give diffractometer scans showing intensity distributions which are effectively the sum of those from each homopolymer diffracting separately. *Figure 2(c)* shows the diffractometer scans of amorphous (practically atactic) P4MP, amorphous polyoctene and a 'randomly' polymerized copolymer containing 55.5 per cent octene which was also amorphous. The copolymer scan shows a low angle maximum at $2\theta = 7.4^\circ$ which cannot be derived satisfactorily from the sum of the respective homopolymer maxima at 6.7° and 9.0° adjusted to the correct proportions, but lies between the two maxima indicating that copolymerization has taken place. The copolymer containing 62 per cent decene shows the effect even more clearly because the homopolymer maxima are better resolved. *Figure 2(d)* shows that the low angle polyoctene maximum at 6.7° is present in the block copolymer containing 15 per cent octene-1, but not in the 'random' copolymer of equivalent composition. The same effects cannot be seen so clearly in the hexene-1 copolymers where the two homopolymer amorphous maxima are closer together but are nevertheless detectable. Moreover, the tetragonal a -axis dimension does not differ from that in 4MP homopolymer in the octene 'block' copolymers (see *Figure 3*).

Figure 1 gives the crystallinities of some 'block' hexene and octene copolymers annealed under the same conditions as the 'random' copolymers. At the same molar composition the octene-1 'block' copolymers develop a higher crystallinity than the 'random' copolymers and lie close to the theoretical crystallinity line, A, which indicates separate crystallization of the P4MP portion and confirms that the 'random' copolymers contain

crystallinity disrupting units in the P4MP chains. The crystallinities of the 'block' hexene copolymers also lie close to the theoretical curve; here, owing to the high degree of isomorphism of the monomer units the distribution of these units is immaterial to the crystallinity developed.

Effect of thermal treatment on copolymer crystallinity

Figure 5 compares the degree of crystallinity of copolymers containing up to 30 mol. per cent hexene, octene and octadecene both as powders as made, and after slow cooling at 6°C per hour from 250°C, i.e. from above the melting point. As the comonomer content rises the

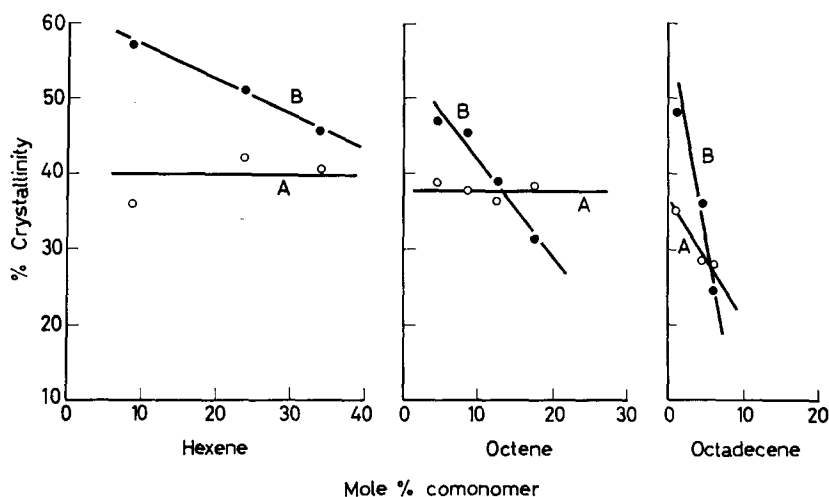


Figure 5—Crystallinity versus composition for 4MP copolymers with hexene, octene, octadecene; A powders as made; B slow cooled at 6°C per hour from 240°C

increase in crystallinity produced on annealing becomes progressively less until a crossover point is reached where the crystallinity actually decreases on annealing. This behaviour is consistent with copolymerization. At the crossover point it appears that the large side chains of the comonomer unit increase the chain entanglements in the melt and thus do not permit the initial crystalline order to be regained. In this series the crossover point occurred as might be expected at a progressively lower comonomer content as the length of the side chain increased, but the precise position would be expected to vary with the crystallinity initially developed in the unannealed powders.

Melting points

Final melting points show an overall progressive decrease from that of 4MP homopolymer (245° to 248°C) as the comonomer content increases and as the length of the side chains of the comonomer increases (see Figure 6). This is consistent with the X-ray evidence that copolymerization has taken place and comonomer units have been incorporated into the

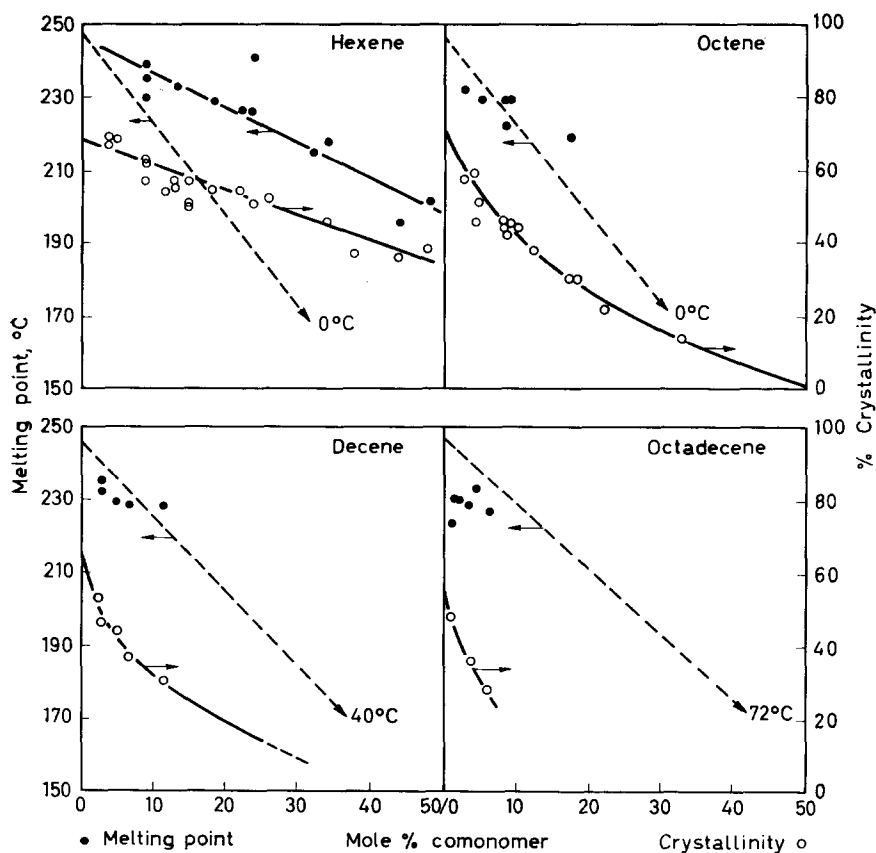
COCRYSTALLIZATION IN COPOLYMERS OF α -OLEFINS I


Figure 6—Melting points and crystallinity versus composition for 4MP copolymers with hexene, octene, decene and octadecene

polymer chains. The final melting points are for all the copolymers much higher than would be expected for a random distribution of comonomer units, even if complete isomorphous replacement occurred. The linear variation with composition to be expected for such systems is shown by dotted lines in Figure 6 where the theoretical melting points of polyhexene and polyoctene have been taken as $\sim 0^\circ\text{C}$. Where the copolymerized α -olefin units are either not incorporated in the crystal lattice (octadecene), or incorporated to a limited extent with distortion of the lattice (octene, decene), the depression of melting point would be expected to be considerably greater than that represented by the dotted line. This would be in accordance with their much reduced crystallinities, but is not, however, observed. It is clear that the copolymers are not completely random and homogeneous, and must contain 4MP rich chains and/or 4MP blocks. The high melting material cannot, however, be separated into a physically distinct phase (under the microscope) so that the presence of a small amount of 4MP homopolymer can be excluded. This high melting material must

therefore contain some comonomer units. There is no optical evidence, either, for free polyhexene, polyoctene, etc. at the high 4MP end of the composition range (up to 50 per cent hexene). On the optical evidence, therefore, all the chains are to some degree copolymerized but possess a range of comonomer compositions and degrees of blocking.

Fractionation

To characterize more precisely the distribution of compositions between chains, and of comonomer units along the chains, careful fractionation is required and is currently being undertaken. A copolymer containing 22 per cent hexene (crystallinity 54 per cent) has been crudely fractionated into three parts; a portion precipitated from xylene solution on cooling from 138° to 20°C (62 per cent); the portion precipitated from the cold xylene solution with methanol (32 per cent); highly soluble residue (6 per cent). The crystallinities of these fractions were 63, 41.5 and about 10 per cent respectively, and their hexene contents 10 and 33 per cent (too little material was available for a determination on the residue). These results confirm that chains with a wide range of chain compositions are present. Even the very soluble residue was not hexene homopolymer, since it showed some crystallinity, but had a high hexene content as the diffraction pattern showed differences from the normal form of P4MP which must be modified crystallographically by the presence of the large proportion of hexene units.

Conclusions

Evidence derived from degrees of crystallinity, lattice spacings and melting points shows that hexene units are highly isomorphic with 4MP units in the P4MP crystal lattice, while octene and decene units can enter the lattice to some degree causing expansion of the lattice and reduction in crystallinity. Octadecene units do not enter the lattice. All polymer chains show some degree of copolymerization, but there is a wide range of comonomer compositions and/or degrees of blocking in the chains of each copolymer.

CRYSTALLINITY IN COPOLYMERS OF 4-METHYLPENTENE WITH PENTENE

Crystallinity determinations

Percentage crystallinities were determined as for the copolymers already discussed, and must be regarded as relative and not absolute. The fitting of an appropriate amorphous curve to the diffraction scan of polypentene Type II⁵ is difficult because of the multiplicity of strong crystalline peaks. As a result of this the crystallinity determinations on copolymers of high pentene content are likely to be low relative to the values at the high 4MP end of the range (see *Table 2*). Even more is this true in the middle composition range, where more crystalline peaks are present from two or more phases.

Identification of crystalline phases

This series of copolymers differs from those already discussed in that the linear α -olefin comonomer itself gives a highly crystalline homopolymer.

COCRYSTALLIZATION IN COPOLYMERS OF α -OLEFINS I

Table 2. Crystal phases, degrees of crystallinity, and unit cell dimensions of 4MP-pentene copolymers

Copolymer	P4MP	A	B	C	D	E	Poly-pentene I Ib	
Mole % pentene	0	11	34	45	67	83	100	
Crystalline phases§								
Unannealed P4MP II	xxx } Nil }	xxx } xx }	xxx } xx }	xx } xx }	xx } xx }	— } xxx }	Nil } xxx }	
Annealed(s) P4MP II	xxx } Nil }	xxx } — }	xxx } trace }	xxx } x }	xx } xxx }	? } xxx }	Nil } xxx }	
Crystallinity % (s)	68	59	45	40	43	47	50	
Unit cell dimensions								
Fibres								
P4MP form	<i>a</i>	18·60†	18·45†	18·35‡	18·10‡	17·80‡	17·75‡	—
	\AA^2	86·5	85·0	84·5	82·0	79·5	78·5	—
II form*	<i>a</i>			21·8		20·5	20·3	19·60
	<i>b</i>			18·1		17·3	17·25	16·75
	γ			115° 30'		115°	115° 8'	115° 20'
	<i>b</i> *			0·0946		0·0988	0·0990	0·1015
	\AA^2			86·5		80·5	79·5	73·2
Unannealed, unoriented								
II	<i>b</i> *	—	0·0922	0·0930	0·0972	0·0964	0·0986	
P4MP	<i>a</i>		~19·0	~19·0				

All lengths in \AA . (s) denotes slow cooled from 240°C at 6°C per hour.

*Fibres showing II form were all drawn at 20°C.

†Drawn at 200°C.

‡Drawn at 120°C.

\AA^2 denotes transverse area per chain.

§The number of crosses indicates the rough proportion of P4MP and II phases present, but does not indicate degrees of crystallinity. (Unoriented specimens.)

High crystallinity, 40 to 60 per cent (see Figure 7) was also observed in the copolymers over the whole composition range after slow cooling from 240°C at 6°C per hour. Powders as originally prepared were 30 to 40 per cent crystalline. The crystalline phase distribution appeared rather complex at first sight; at the ends of the composition range, the crystallinity was predominantly that of the homopolymer of the major constituent, but the X-ray patterns change with composition and with the thermal and mechanical treatment applied. Careful examination of X-ray patterns of unoriented specimens, and more particularly of oriented fibres, showed that the patterns could be satisfactorily accounted for by the presence in varying proportions of two principal crystal forms closely related to those of 4MP homopolymer and polypentene Type I Ib⁵ (henceforward called the P4MP and II forms) when allowance was made for gradual spacing and intensity changes with composition. Other crystal forms were present in only minor amounts.

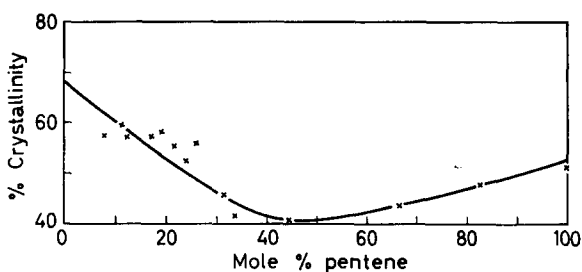


Figure 7—Copolymers of 4MP and pentene; crystallinity versus composition

The identification of crystal forms is complicated by overlapping of reflections and in particular by the overlapping (after cell expansion or contraction) of the strong 200 reflection of the P4MP form, which in the homopolymer is at a spacing of 9.3 Å, and the 200 reflection of the two strong reflections of the polypentene IIb form, 200 and 020, which in the homopolymer occur at spacings of 8.87 Å and 7.59 Å respectively. The presence of form II was identified in unoriented specimens of high 4MP content by the 020 reflection of lower spacing.

Results and discussion of X-ray investigation

Table 2 summarizes the degrees of crystallinity and crystal phases present for five copolymers of varying composition together with unit cell dimensions.

At the high 4MP end of the series copolymers containing up to ~25 per cent pentene (copolymer A and others not listed) examined as powders as made, without thermal treatment, showed both the P4MP form and the II form. On slow cooling from 240°C the II form disappeared and only the P4MP pattern was seen. On drawing fibres from pressed sheets at temperatures up to 200°C, only oriented P4MP crystallinity developed.

At the high pentene end (83 per cent pentene—sample E), no P4MP form was distinctly observed in unoriented specimens (annealed or unannealed) and the X-ray patterns closely resembled that of the IIb form of crystalline polypentene. On drawing fibres between 20° and 120°C the X-ray patterns showed highly oriented IIb polypentene only (repeat unit 7.1 ± 0.08 Å), with a little Type I polypentene (repeat unit 6.5 Å) developing in increasing proportion as the temperatures of draw rose. At 120°C an additional crystal phase could be distinguished which appeared to be a modified P4MP form with tetragonal unit cell, $a = \sim 17.8$ Å, and repeat unit between 6.9 and 7.1 Å; in some drawn specimens weak intermediate layer lines typical of P4MP were present with repeat 13.85 Å indicating some P4MP in addition.

In the intermediate composition range (copolymers B, C and D) both the P4MP and the II forms were present in roughly equal proportions [see Figure 4(a)], but on slow cooling from 240°C, apart from the expected increase in overall crystallinity, the relative proportion of II increased considerably in sample D (67 per cent pentene), but the proportion of P4MP increased considerably in samples B and C (34 and 45 per cent pentene),

[Figure 4(b)]. On cold drawing sample D only oriented II developed, but at higher temperatures (65° and 120°C), while the amount of crystalline II increased, increasing proportions of P4MP form developed; there was evidence for the presence of some 'tetragonal' 4MP phase also. Although cold drawing sample C gave poorly oriented II and P4MP, drawing at higher temperatures gave highly oriented P4MP and only a trace of II. Sample B gave poorly oriented P4MP and highly oriented II on cold drawing [Figure 4(c)], but well oriented P4MP form with only a small amount of well oriented II at 120°C [Figure 4(d)].

As the proportion of 4MP in the copolymer decreased the *a* unit cell dimension of the tetragonal P4MP form in the drawn fibres decreased (Table 2), but the *c* axis repeat remained constant within experimental error. Similarly, as the proportion of pentene units decreased, the equatorial unit cell dimensions of the II form increased, but the *c* axis repeat remained constant.

True isomorphous replacement, with only a gradual change in lattice dimensions to accommodate comonomer units of slightly different size, naturally cannot be expected in this system since the unit cells of the homopolymer crystal forms are quite different. Nevertheless the different relative proportions of the two principal forms which can be developed in the same specimen by different conditions of drawing and thermal treatment, as well as the high overall crystallinity observed in these copolymers over the whole composition range (both unannealed and annealed) show that at least a proportion of chains containing monomer units of both types are capable of crystallizing in either of the two principal forms, with lattice parameters suitably adjusted. The marked expansion of the poly-pentene transverse unit cell dimensions with increasing proportion of 4MP comonomer units is the expected consequence of the inclusion of the larger 4MP unit. Although a less drastic reduction in the P4MP equatorial cell dimensions might be expected, since the lattice can tolerate the inclusion of smaller monomer units without disruption, the structure is already very open ($d_{\text{cryst.}} = 0.83 \text{ g/cm}^3$) and inclusion of smaller pentene side groups would reduce the density to an abnormally low value. Thus the lateral contraction of the cell shown by the fibres (Table 2) is not unexpected.

The inclusion of comonomer units in the two basic homopolymer crystal forms is shown, not only by the gradual change in cell dimensions with increasing comonomer contents, but also in each phase by a gradual change in relative intensities of the reflections in oriented specimens, by the disappearance of weak reflections which characterize the fine detail of the structure, and by the appearance of streaks on the layer lines indicating disorder in the unit cell.

The presence of the P4MP and II forms at the high pentene and high 4MP ends of the composition range respectively show that the copolymers are not random with statistically homogeneous chains; these forms must arise from chains richer in 4MP or pentene than the overall copolymer composition. Nevertheless the copolymer compositions cannot be described by a basically two-phase system of '4MP-rich' and 'pentene-rich' chains with the two types varying in proportion. Such a system would inevitably tend to phase separate into a high melting P4MP phase and a low melting

polypentene II phase on slow cooling from the melt, whereas even up to ~ 45 per cent pentene, only a little of the polypentene II form develops, as already described. To some extent, however, the overall compositions could be accounted for by a contribution from a system of this type. Melting point data provide further evidence on the composition of the polymer chains.

Melting points

The upper melting point curve P given in *Figure 8* shows the temperatures at which the last traces of birefringence disappear in annealed specimens.

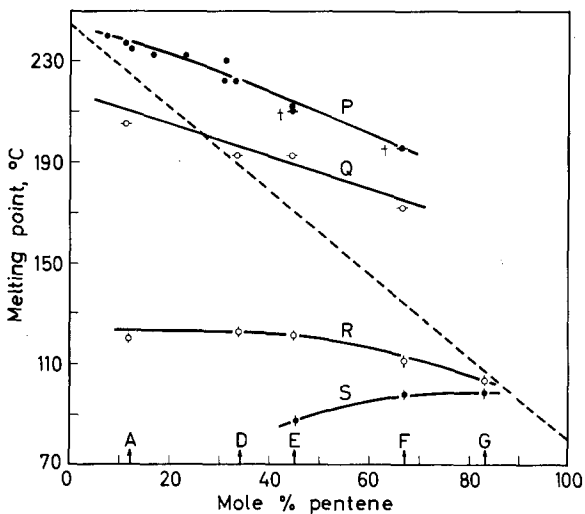


Figure 8—Copolymers of 4MP and pentene; final melting points versus composition. Curve P—P4MP form, annealed, melting point determined optically (points marked † determined by X-rays); Q—P4MP form, unannealed (by X-rays); R—polypentene II form, unannealed (by X-rays); S—polypentene II form, annealed (by X-rays).

As for the hexene series of copolymers, at high 4MP contents the final melting points drop gradually with increasing pentene content, but remain higher than would be expected for a completely random copolymer showing isodimorphism¹ (broken line *Figure 8*), and hence indicate the presence of chains richer in 4MP than the copolymer composition or blocked chains. As the melting of the II form tends to be masked by the marked increase in birefringence shown by the P4MP form on heating and the spherulitic texture in the high pentene and middle composition ranges is not well developed even after slow cooling, melting points were also determined by X-rays where necessary, on both unannealed and annealed specimens of copolymers A to E (see *Figure 8*). The final melting points of the P4MP and II forms were taken respectively as the temperatures at which the P4MP (200) and the II (020) peaks disappeared; the melting of both phases

took place over wide temperature ranges of some 20° to 30°C for II and 50° to 70°C for P4MP. All these melting points are shown in *Figure 8* (curves Q, R and S).

Figure 8 shows that the final melting points of the II form (curve R) in the unannealed copolymers are well above that of pentene homopolymer, 80°C, although they drop gradually from a roughly constant value of 120°C at the high 4MP end as the pentene content increases beyond 50 per cent. The presence of 4MP units in the II lattice is thus confirmed. The lattice dimensions of both the P4MP and II phases (b^* —*Table 2*) are markedly expanded in these unannealed specimens as might be expected. The effective disappearance of this form II on slow cooling from the melt in copolymers A and B, and the development of a II form in copolymers C and D of lowered melting point (curve S), indicates that chains containing both monomer units have been transferred from the II to the P4MP lattice. In C this process is particularly apparent from the marked increase in intensity of the P4MP peak at $\sim 120^\circ\text{C}$ which accompanies the melting of the II phase. The higher melting points of the unannealed specimens are not just due to a long tail caused by a small proportion of higher melting crystallites. In D the bulk of the crystalline material in the unannealed and annealed specimens melts at $\sim 100^\circ$ to 105°C and $\sim 90^\circ\text{C}$ respectively. At 67 per cent pentene the P4MP peak is of rather low intensity and the increase in proportion of form II on annealing shows that the crystallization process is becoming increasingly dominated by pentene-rich chains. This is reflected in the increase in form II melting point (after annealing) with increasing pentene content, showing that chains richer in 4MP are now being incorporated into the II lattice.

Conclusions

The X-ray and melting point data are consistent with a high degree of copolymerization of 4MP and pentene units but show that the copolymers are not homogeneous and, at each overall composition, contain chains with a range of comonomer compositions and/or degrees of blocking. Copolymer chains not too rich in either pentene or 4MP units can exist in either the 4MP or the II lattice, indicating a marked degree of isodimorphism. In the intermediate composition range the cross-sectional area per chain deduced from the cell dimensions (*Table 2*) is closely similar in either the P4MP or the polypentene II forms at a given copolymer composition so that neither crystal form is favoured on grounds of side-by-side packing density. The crystal form produced is determined by the thermal or drawing treatment applied. Drawing fibres at low temperatures tends to favour the production of the polypentene II form (homopolymer melting point 80°C) whereas high temperatures develop the P4MP form (homopolymer melting point 245° to 258°C). At the lower temperatures chains containing a higher proportion of pentene units have the greater mobility and crystallize into the II form. At higher draw temperatures, where many of these chains would (in a homogeneous polymer) be 'melted', the chains containing a higher proportion of 4MP units—or 4MP blocks—have now sufficient mobility to crystallize and in so doing can also incorporate pentene-rich chains into the P4MP lattice. It is not unreasonable

to envisage chains containing quite long blocks of polypentene-1 being thus included. At the high pentene end, however, most of the chains are too rich in pentene to be stable in this lattice, and only a small amount of the P4MP crystal form can be formed. Separation into phases on crystallization certainly occurs (as also shown under the microscope), but the same polymer chains can enter different phases under different conditions of crystallization. In fibres drawn at low temperatures the II form tends to become highly oriented while the P4MP type crystallinity shows relatively low orientation, indicating that physical phase separation has occurred.

Isodimorphism occurs, as predicted earlier in this paper from the crystallographic constants and helical chain forms of the three homopolymer crystal phases, between the P4MP crystal lattice and that of the polypentene II and not with the type I form.

The author's thanks are due to: Mr R. P. Palmer for many useful discussions and for the optical melting point data, Dr K. J. Clark who made the copolymers, Messrs R. G. J. Miller and M. E. A. Cudby for infra-red copolymer composition determinations, Mrs K. W. Small for fractionation work and to Miss J. M. Aizlewood and Mr D. R. Beckett who carried out the experimental work and helped in the calculations.

*I.C.I. Plastics Division,
Welwyn Garden City, Herts.*

(Received September 1964)

REFERENCES

- ¹ NATTA, G. *Makromol. Chem.* 1960, **35**, 94
- ² REDING, F. P. and WALTER, E. R. *J. Polym. Sci.* 1959, **37**, 555
- ³ CAMPBELL, T. W. *J. appl. Polym. Sci.* 1961, **5**, 184
- ⁴ HEWITT, W. A. and WEIR, F. E. *J. Polym. Sci.* 1963, **A1**, 1239
- ⁵ TURNER JONES, A. and AIZLEWOOD, J. M. *Polymer Letters*, 1963, **B1**, 471
- ⁶ TURNER JONES, A. *Makromol. Chem.* 1964, **71**, 1
- ⁷ NATTA, G. and CORRADINI, P. *Makromol. Chem.* 1955, **16**, 213
- ⁸ DANUSSO, F. and GIANOTTI, G. *Makromol. Chem.* 1963, **61**, 164
- ⁹ CLARK, K. J. and PALMER, R. P. *Soc. chem. Ind. Monogr.* In press
- ¹⁰ MATTHEWS, J. L., PEISER, H. S. and RICHARDS, R. B. *Acta cryst., Camb.* 1949, **2**, 85
- ¹¹ NATTA, G., CORRADINI, P. and CESARI, M. *Atti Accad. Lincei*, 1957, **22**, 11
- ¹² REDING, F. P. *J. Polym. Sci.* 1956, **21**, 547
- ¹³ GRIFFITH, J. H. and RANBY, B. G. *J. Polym. Sci.* 1960, **44**, 369

Kinetics and Mechanism of Trioxan Polymerization

L. LEESE and M. W. BAUMBER

The work of Kern and Jaacks on polymerization of trioxan in methylene chloride has been extended by a study in ethylene dichloride. Kinetics have been investigated chemically and by adiabatic calorimetry, and results indicate that during an induction period soluble low molecular weight polymer is produced which eventually forms crystal nuclei. These initiate an accelerating reaction whose rate depends on the area of crystal surface available for polymer deposition or formation and equations have been obtained which describe the observed kinetics. The kinetics arguments are supported by photomicrographs of crystals at various stages of polymerization, which indicate a progressive increase in the size of the original crystals rather than constant formation of fresh nuclei. The evidence strongly suggests that polymerization takes place at the growing crystal surface.

TRIOXAN may be polymerized cationically, and the general features of the reaction catalysed by boron trifluoride in methylene chloride at 30°C have been described by Kern and Jaacks¹. Polymerization is preceded by an induction period during which formaldehyde gas is produced; when this has reached a certain pressure polymerization begins and proceeds at an accelerating rate. Kern and Jaacks interpret their results in terms of ring opening by boron trifluoride without the need for a co-catalyst. The open chain species so formed immediately decompose to give formaldehyde, which continues to be formed until the equilibrium



is established. Polymerization then begins. The subsequent acceleration in rate is attributed to an increase in the rate of chain initiation and the absence of a step terminating the kinetic chain, but Kern and Jaacks do not give a kinetic analysis of their results.

Work in this laboratory has been concerned with polymerization of trioxan in ethylene dichloride solution and considerable progress has been made in interpreting the kinetics obtained.

EXPERIMENTAL

Materials

Trioxan was obtained from Synthite Ltd. Ethylene dichloride was obtained from May and Baker Ltd.

Boron trifluoride diethyl etherate was B.D.H. material, used without purification.

Purification of material and drying technique

Solutions of trioxan in ethylene dichloride were purified and dried in

one process by passage through a 3 ft by 1 in. glass column packed with activated alumina. Batches of 2 l. of dried solution were stored under dry nitrogen and dispensed from an automatic burette.

Water contents were determined using a standard Karl Fischer titration on 10 ml samples of solution.

Adiabatic calorimetry

(a) *General procedure*—The reaction of boron trifluoride etherate with solutions of trioxan in ethylene dichloride was studied by adiabatic calorimetry.

The calorimeter consisted of a 2 in. diameter straight-sided Dewar flask, of capacity 400 ml, closed with a rubber stopper. The stopper was bored to take a Beckmann thermometer set for 50°C and a glass paddle stirrer which was driven at constant speed. A third inlet carried a delivery tube fitted with the female half of a spherical joint, 18/9 BS, which could be closed with a small rubber stopper. This inlet was used for addition of reagents.

Before use all glassware was cleaned by being soaked in permanganic acid followed by water, and dried in an air oven at 130°C. It was then flushed with dry nitrogen.

161 ml (\equiv 200 g) of dried solution was dispensed into a 250 ml flask where the temperature was raised to just over 50°C; the solution was transferred to the Dewar flask via the delivery tube under a pressure of dry nitrogen. The temperature of the solution was controlled so that the Beckmann thermometer read approximately 3° (total scale, 6°). The apparatus was then immersed in an oil bath maintained at $50^\circ \pm 0.1^\circ$ C.

Experiments were conducted by obtaining a cooling curve for the solution over a time interval of six minutes, then injecting the appropriate quantity of catalyst below the surface of the solution using an 'Agla' microsyringe fitted with a long needle.

The temperature was estimated to 0.001° and a temperature/time curve was plotted.

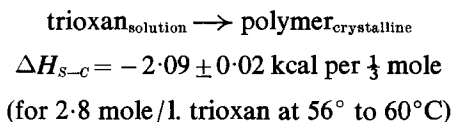
(b) *Thermal capacity of equipment*—The thermal capacities of the equipment and solutions were determined by the method of mixing.

The heat capacity of ethylene dichloride at 50°C may be estimated from data in the literature², i.e. 20°C, 0.301 cal/g; 60°C, 0.319 cal/g; 50°C, 0.314 cal/g (calc.).

(c) *Heat capacity of trioxan solution*—The heat capacities of trioxan solutions (estimated by the method of mixing) are higher than that of pure ethylene dichloride. A calibration curve of heat capacity against trioxan concentration was used in the work described below.

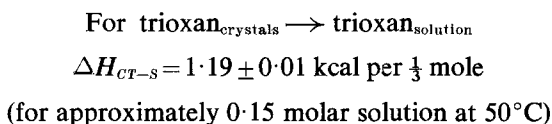
(d) *Heat of polymerization*—Polymerization of trioxan is an exothermic reaction; the heat of polymerization was determined in a preliminary experiment by comparing heats of reaction with a gravimetric determination of the amount of polymer formed. The reaction was 'killed' by addition of tri-*n*-butylamine after a temperature rise of 5°C had been recorded. Cooling corrections, in this and other experiments, were applied graphically.

For the reaction



This result was used to convert the heats of reaction obtained in later experiments into weights of polymer precipitated. It should be noted that small errors in the values for the heat capacities of the calorimeter and solutions will have very small effects on the polymer weights derived from the thermochemical measurements. Since the same volume of solution was always used, such errors tend to cancel out except for the effect of trioxan concentration on heat capacity.

(e) *Heat of solution*—The integral heat of solution of trioxan was determined by breaking a small glass ampoule containing the purified solid into ethylene dichloride contained in the calorimeter.



Determination of formaldehyde

Formaldehyde and low molecular weight polymer were determined by the sulphite method³. A correction was applied for the presence of catalyst residues.

Photomicrography

Samples were removed at intervals from a polymerizing solution, and the reaction was quenched in a large excess of solvent containing tri-*n*-butylamine.

The polymer was allowed to settle or centrifuged off, and washed three times with fresh solvent. Specimens were prepared by allowing a drop of suspension to dry on a microscope slide.

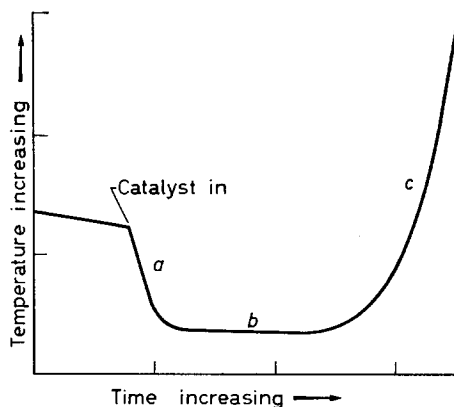


Figure 1—Temperature/time curve (schematic): *a* Endothermic reaction, *b* Athermal reaction, and *c* Exothermic (polymerization) reaction

DISCUSSION AND RESULTS

A characteristic time/temperature curve for trioxan polymerization is illustrated in *Figure 1*.

After the addition of catalyst, reaction takes place in three well defined stages, corresponding to (a) endothermic, (b) athermal and (c) exothermic processes.

Stages (a) and (b) correspond to the induction period described by Kern and Jaacks¹ while stage (c) corresponds to precipitation of crystalline polymer.

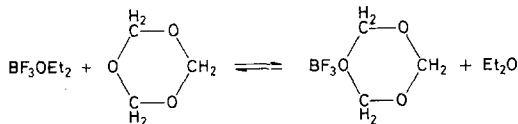
(a) Endothermic process

The rate of heat absorption during the endothermic process is a function of the catalyst and trioxan concentrations.

The total heat absorbed is much less affected by experimental variables, being unaffected by catalyst concentration over a tenfold range and increasing only slightly as the trioxan concentration is increased from 0.7 to 5.6 mole/l.

It seems natural to associate the endothermic reaction with depolymerization of opened trioxan rings to produce formaldehyde gas. In order to establish this the thermochemistry of the process must be considered.

When boron trifluoride etherate is added to a solution of trioxan in ethylene dichloride rapid exchange of boron trifluoride between ether and trioxan will occur.



Such an exchange will have a relatively low heat of reaction which can be neglected in view of the small quantities of boron trifluoride etherate used in the experiments. Similar equilibria between mixtures of ethers and boron trifluoride have been described by Craig and Richards⁴.

The heat absorption results from the overall reaction



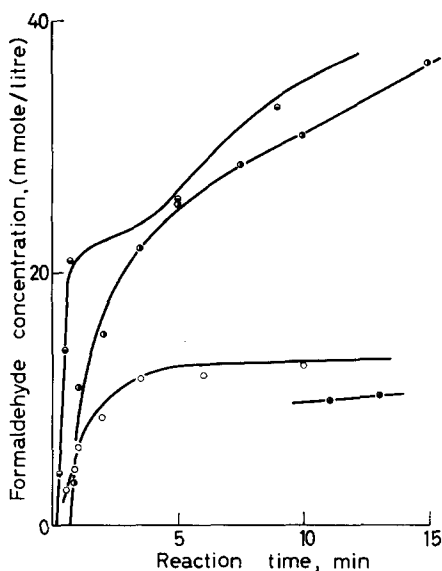
where P_n represents any soluble linear polymer formed. This is true irrespective of the exact mechanism of ring opening.

The production of formaldehyde and oligomer during early stages of the reaction at constant catalyst concentration, which represents the total amount of ring opening, is illustrated in *Figure 2*.

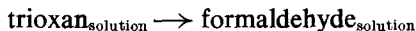
A rapid rate of ring opening is succeeded by a much slower reaction, which then accelerates as insoluble polymer begins to form. At a trioxan concentration of 1.4 mole/l. ring opening practically ceases after the first stage of the reaction, the formaldehyde concentration levelling off at 12.5 m mole/l. At a trioxan concentration of 0.7 mole/l. with less than 2.0 m mole/l. of catalyst, the final formaldehyde concentration varies between 9.8 and 10.4 m mole/l. and the mean heat of reaction is

$$\Delta H_{ss} = 13.7 \pm 1 \text{ kcal/mole of formaldehyde produced}$$

Figure 2—Decomposition of trioxan. Catalyst concentration 1.6 m mole/l. of boron trifluoride etherate. Trioxan concentrations, mole/l.: \oplus 0.7; \circ 1.37; \bullet 2.5; \ominus 2.8

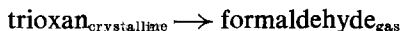


If the formation of oligomers in the decomposition reaction is neglected for low trioxan and catalyst concentrations, this is the heat of the reaction



The integral heat of solution of trioxan at 50°C in ethylene dichloride (0.15 mole/l. trioxan), as determined in the calorimeter already described, is 1.19 ± 0.1 kcal per $\frac{1}{3}$ mole.

Hence neglecting the heat of solution of formaldehyde in ethylene dichloride, which should be small³, the heat of the reaction



at 50°C is $13.7 + 1.2 = 14.9$ kcal per $\frac{1}{3}$ mole trioxan from our measurements. This is in good agreement with the value of

$$\Delta H_{G-CT} = -15 \text{ kcal}$$

given by Walker³ for the polymerization of formaldehyde to trioxan.

By using the measured value of ΔH_{SS} in conjunction with the observed total heat absorptions, apparent concentrations of formaldehyde after completion of the endothermic reaction have been calculated for differing concentrations of trioxan (Table I).

There is an increasing discrepancy between the titrated formaldehyde concentration and the heat change as trioxan concentration is increased, and the comparison of curves such as those in Figure 2 with the temperature/time curves shows that ring opening continues to occur without formation of solid polymer during the athermal process.

(b) *Athermal process*

Throughout this stage of the reaction, formaldehyde monomer and

Table 1

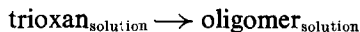
[T] mole/l. trioxan	[T] [†] mole/l. [‡]	Average heat absorbed cal/l.	[F] (Calc.) m mole/l. formaldehyde	Titrateable formaldehyde m mole/l.	Solid polymer formation
0.70	0.89	138	—	10.08	—
1.40	1.12	167	—	12.20	—
2.08	1.28	196	14.3	—	+
2.50	1.36	197	14.4	—	+
2.77	1.41	186	13.6	36.8	+
3.06	1.45	—	—	33.2	+
3.47	1.51	196	14.3	—	+
5.56	1.77	219	16.0	35.6	+

oligomeric cations or zwitterions must be produced simultaneously. The relative proportions of monomer and oligomer produced may be estimated as follows:

Let N_0 be the total number of mole/l. of trioxan rings opened since the start of the reaction. Then the total heat change per l. is

$$Q_{\text{total}} = [F]\Delta H_{SS} + (3N_0 - [F])Q_R$$

where [F] is the concentration of formaldehyde and Q_R is the heat of the reaction

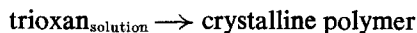


The rate of heat production will be

$$\frac{dQ_{\text{total}}}{dt} = (\Delta H_{SS} - Q_R) \times \frac{d[F]}{dt} + 3Q_R \frac{dN_0}{dt}$$

$$\simeq 0$$

during the athermal process. Q_R may be estimated from the heat of the reaction



which was measured directly

$$\Delta H_{S-c} = -2.09 \pm 0.02 \text{ kcal per } \frac{1}{3} \text{ mole}$$

Hence for the heat of polymerization of formaldehyde gas to crystalline polymer we find

$$\Delta H_{G-c} = -(2.09 + 13.7) = -15.8 \text{ kcal}$$

As expected this is higher than the value of 15 kcal given by Walker³ as a reasonable estimate of the heat of polymerization of formaldehyde to partially crystalline polyoxymethylene glycols.

The heat of fusion of 100 per cent crystalline polyoxymethylene is given⁵ as 1.76 kcal per base mole, so that neglecting the heat of mixing of polymer and solvent

$$Q_R \simeq -0.3 \text{ kcal per base mole}$$

Hence

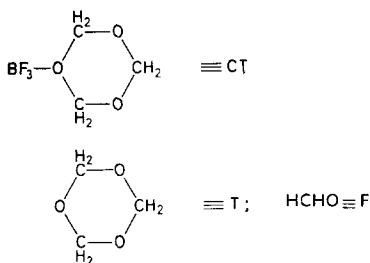
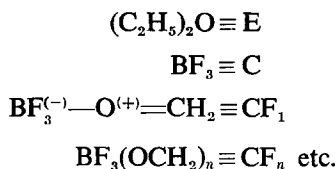
$$\frac{d[F]}{dt} \bigg/ \frac{dN_0}{dt} \simeq 0.06 \simeq 0$$

i.e. most of the ring opening during the athermal reaction occurs without liberation of formaldehyde.

Such a small value of Q_R implies that the entropy of reaction is either positive or very small, but this is not unlikely for a ring opening. On the basis of the above discussion, the values for $[F]$ given in *Table 1* represent concentrations of formaldehyde at which formation of oligomer is the main consequence of opening of trioxan rings.

The dependence of this concentration on trioxan concentration can be derived from a reaction scheme based on that put forward by Kern and Jaacks¹.

The following symbolism will be adopted.

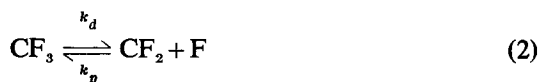


The reaction scheme can now be written :

(a) Complex formation

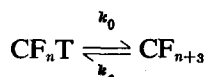


(b) Ring opening and depolymerization



As formaldehyde accumulates in solution, the reverse reactions (1) to (4) will increase in importance, and higher species such as CF_4 , CF_5 , etc.,

will form. However, reactions analogous to (1) can take place for all species after CF, and CF₂; at equilibrium there will be a general reaction.



$$\text{i.e. } [\text{CF}_{n+3}]/[\text{CF}_n\text{T}] = k_o/k_c$$

Now consider reactions (2), (3) and (4). At equilibrium, neglecting possible differences between values of k_p and k_d for different values of n ,

$$[\text{F}] = (k_d/k_p) [\text{CF}_2]/[\text{CF}_1]$$

$$= (k_d/k_p) [\text{CF}_3]/[\text{CF}_2]$$

$$[\text{CF}_1][\text{T}] = (k_I/k_T) [\text{CT}][\text{F}]$$

$$[\text{F}]^3 = (k_d^2/k_p^2) (k_T/k_I) ([\text{CF}_3]/[\text{CT}]) [\text{T}]$$

$$= (k_d^2/k_p^2) (k_T/k_I) (k_o/k_c) [\text{T}]$$

The dependence of [F] on [T][†] is in reasonable agreement with experiment (*Table 1*, columns 2, 4 and 5).

Several features of this reaction scheme are worth noting: (a) The data given in *Table 1* do not represent true equilibrium values of (F), which will only be reached when a complete distribution of oligomer molecular weights has been obtained. (b) A quasi-equilibrium concentration of formaldehyde is reached very rapidly, and this probably corresponds with the formation of the species CF₃. Further reaction takes place relatively slowly (see *Figure 2*).

The net rate of ring opening is greatly reduced after the first stage of the reaction, and this is not in agreement with the mechanism of Kern and Jaacks¹ who suggest that the presence of oligomeric zwitterions accelerates the reaction. The general argument does not depend on the exact mode of operation of the catalyst, but our results suggest that the BF₃ initiator is much more effective in ring opening in homogeneous systems than the zwitterions. This is because the possibility of ring closure exists for all oligomers with more than three molecules of formaldehyde.

INITIAL KINETICS OF RING OPENING

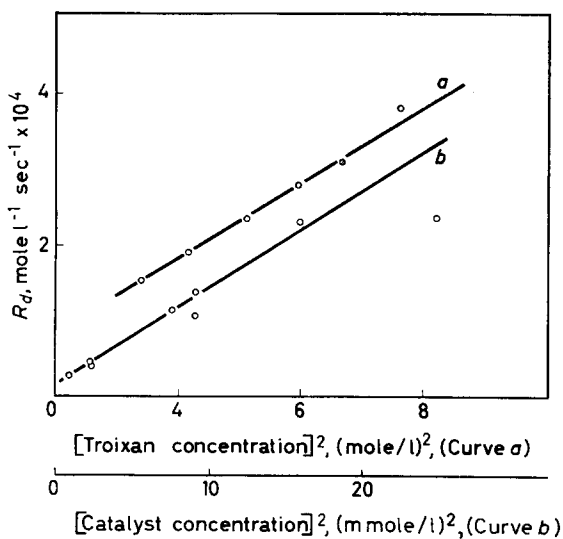
Ring opening of trioxan by Bronsted acids in aqueous solution has been studied by a number of workers, and a simple mechanism in which the rate-determining step is unimolecular decomposition of the conjugate acid of trioxan has been proposed⁶.

Rates of heat absorption obtained in our experiments give a measure of the rate of the ring opening reaction in relatively anhydrous conditions.

Rates of formaldehyde production in mole l.⁻¹ sec⁻¹ (R_d) obtained from the thermal data are illustrated in *Figure 3*. R_d is approximately proportional to C_0^2 and [T]² where C_0 is the initial catalyst concentration and [T] is the monomer concentration.

Preliminary experiments indicate that R_d is also inversely proportional to the water concentration and to the concentration of added ether.

Figure 3—Rates of formaldehyde production (calculated from thermochemistry), R_d mole l^{-1} sec $^{-1}$: *a* Effect of trioxan concentration. Catalyst concentration, 2.0 m mole/l. boron trifluoride etherate; water concentration, 8.2 m mole/l. *b* Effect of catalyst concentration. Trioxan concentration, 0.7 mole/l.; water concentration, 5.0 m mole/l.



These kinetics may be explained on the basis of competition for boron trifluoride between trioxan, water and ether, leading to formation of an equilibrium concentration of the initiating species, which then decomposes unimolecularly. However, insufficient evidence is available to eliminate other possible mechanisms and the problem requires further attention. The difficulty of interpreting the kinetics of the ring opening process may be circumvented in discussing the polymerization reaction by taking the initial rate of the endothermic process as a direct measure of the number of active species present in the system.

During the athermal reaction, ring opening occurs either at the active end of an oligomeric cation, or via a small quantity of initiating species CT in equilibrium with it. Both mechanisms involve the assumption that ring opening by the oligomers is a slow process.

As the reaction continues, the number of oligomer molecules will increase, and the average molecular weight of ionic species will also increase, until the solubility limit of the oligomers is reached. This limit is about 35 m mole/l. of total formaldehyde, and is practically independent of trioxan concentration (Table I).

It seems likely that the value of 60 m mole/l. quoted by Kern and Jaacks¹ for the formaldehyde concentration in equilibrium with linear polymer in methylene chloride at 30°C represents a similar solubility limit.

(c) Exothermic reaction

When the solubility limit is reached the induction time for polymerization ends and the overall reaction becomes exothermic. This is because the heat of crystallization of polyoxymethylene is included in the heat of polymerization. The induction time referred to throughout this discussion is the time between addition of the catalyst and the beginning of the exothermic reaction.

Since the concentration of soluble polymer at the precipitation point is constant, the inverse of the induction time represents the rate of formation of soluble polymer. In agreement with this, the induction time is inversely proportional to the product of the initial rate R_d and the trioxan concentration (Figure 4).

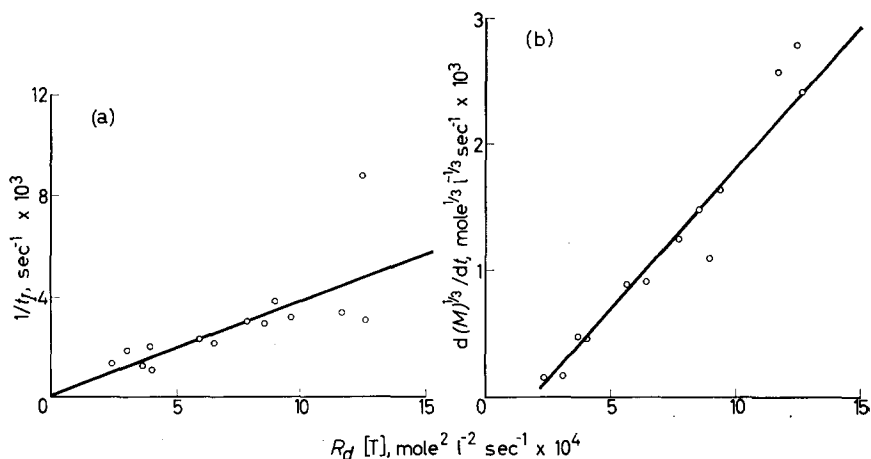


Figure 4(a)—Reciprocal induction times—dependence on R_d

Figure 4(b)—Linear growth rates' from Figures 10 and 11—dependence on R_d

At the precipitation point, the polymerization begins to accelerate, and this is associated with the continuous increase in the quantity of solid polymer present. Using the measured value of the heat of formation of crystalline polymer in conjunction with the temperature/time curves, the polymerization kinetics have been studied.

Since the heat of crystallization is a large part of the heat of reaction, it seemed likely that crystal growth would play an important part in the polymerization. The crystallization process itself was also investigated, by examination of batches of crystals removed at intervals from polymerizing solutions.

Figure 5 shows a batch of such crystals which consists of uniform, regular hexagons, very similar to those prepared by solution crystallization of polyoxymethylene⁷. The dark shadow on each crystal suggests that the crystals are pyramids or bipyramids resting on one face. The dark lines probably represent actual terraces on the crystal surface. Samples taken at higher conversion contain larger crystals, less regular and partially agglomerated. The crystals are thicker, resembling twisted piles of platelets.

Dr A. Keller⁸ has shown that such agglomerates may be broken down by ultrasonic vibrations to give fragments of hexagons. X-ray diffraction shows that the polymer is highly crystalline, with polymer chains oriented perpendicular to the plane of the hexagons.

Under carefully controlled conditions in the presence of water to reduce the overall rate of polymerization and molecular weight of product, a series of six batches of regular hexagons was obtained from a single solution (Figure 5). The widths were measured (mean of twelve crystals per batch)

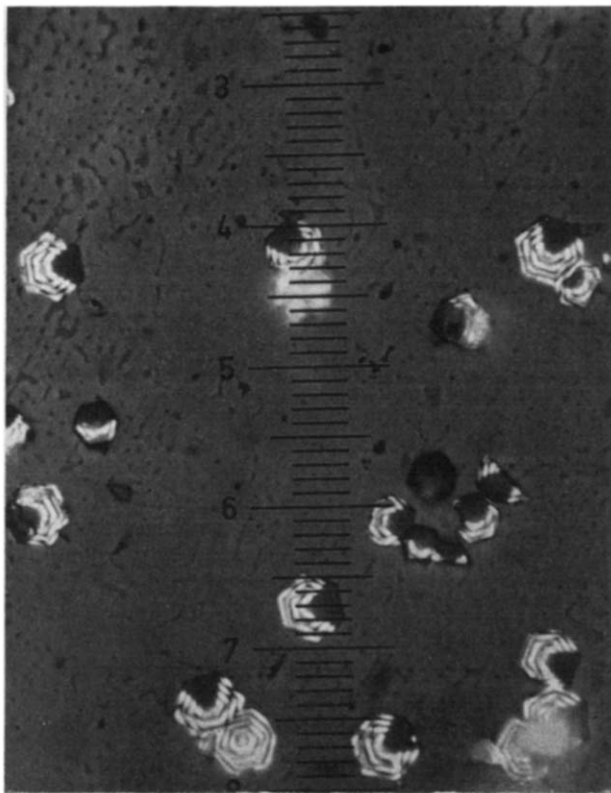


Figure 5—Polyoxymethylene crystals. Photomicrograph, reflected light; 1 small division represents 2 microns. Reaction conditions: temperature 50°C, trioxan concentration 2.78 mole/l., catalyst concentration 1.4 m mole/l., boron trifluoride etherate

and Figure 7 shows the proportionality between the width and the time of growth.

If a fixed number of crystal hexagons forms at the precipitation point and these then grow at constant linear growth rates on their sides and faces, the mass of polymer formed in time t can be obtained.

Consider a segment of a regular hexagon (Figure 8). Let the segment thickness be y and its width, $\frac{1}{2}x$. Then

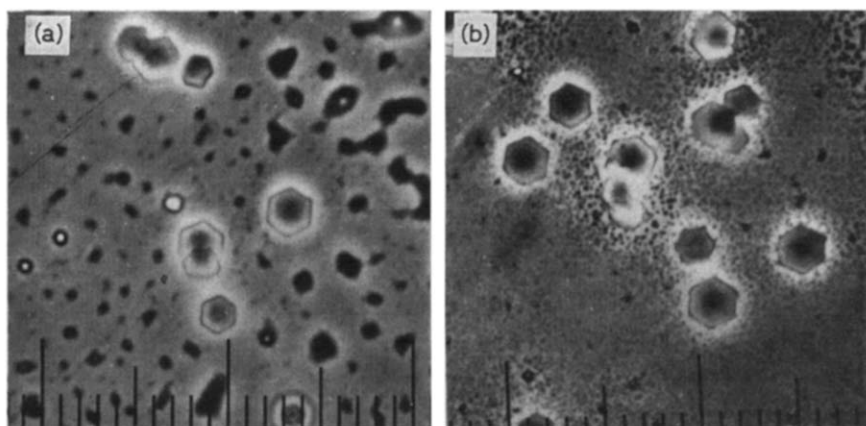
$$b = \frac{1}{2}x \tan 30^\circ = x/2\sqrt{3}$$

Consider small increments $dx/2$ and dy of width and thickness. The total volume added will be

$$dV = (x^2/4\sqrt{3}) dy + (xy/\sqrt{3}) d\frac{1}{2}x \quad (1)$$

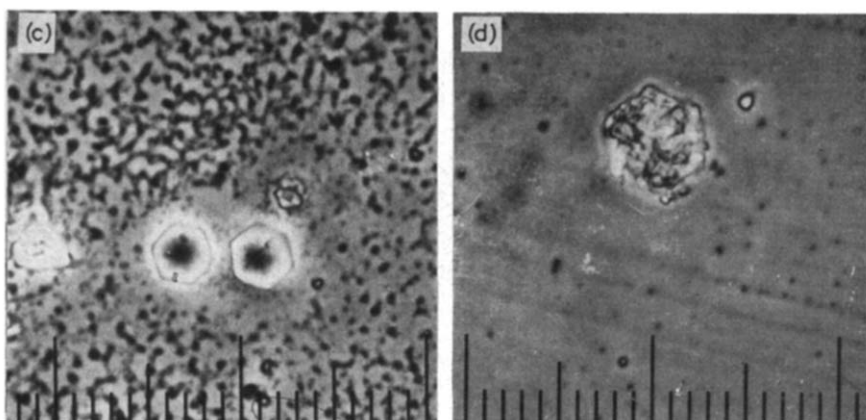
neglecting second order differentials. Now assume that both width and thickness change linearly with time, i.e.

$$dx/dt = Gx \quad \text{and} \quad dy/dt = Gy$$



(a) Time 41 min, width 3.8 microns

(b) Time 44 min, width 4.6 microns

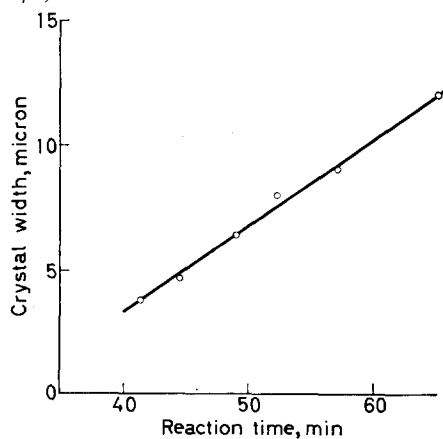


(c) Time 48.5 min, width 6.4 microns

(d) Time 65 min, width 12.0 microns

Figure 6—Growth of polyoxymethylene crystals. Photomicrograph, transmitted light. Reaction conditions: temperature 50°C, trioxan concentration 2.44 mole/l., catalyst concentration, 1.9 m mole/l., boron trifluoride etherate

Figure 7—Growth of polyoxymethylene crystals



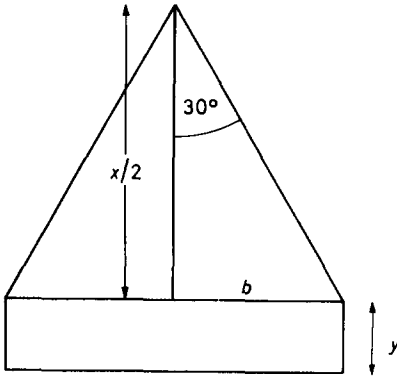


Figure 8—Segment of regular hexagon

Integrating and neglecting the size of the nuclei

$$x = Gx(t - t_0) \text{ and } y = Gy(t - t_0)$$

where t_0 is the induction time. Now the increment of mass corresponding to dV_{total} is simply

$$dM = \rho dV_{\text{total}}$$

where ρ is the crystal density. Substituting for dx , dy , x and y in (1) we have

$$dV = (3/4\sqrt{3}) G^2(x) Gy(t - t_0)^2 dt \quad (2)$$

i.e., integrating between t_0 and t ,

$$M = (\rho/4\sqrt{3}) G^2(x) Gy(t - t_0)^3$$

and for N_0 complete hexagons

$$M = N_0 (3/2\sqrt{3}) \rho G^2(x) Gy(t - t_0)^3 \quad (3)$$

where N_0 is the initial number of nuclei.

The relative rate of growth of the two types of face is constant, i.e.

$$(Gy/Gx) = R$$

$$M = N_0 (3/2\sqrt{3}) \rho R G^3(x) (t - t_0)^3 \quad (4)$$

and one linear growth rate characterizes the whole crystallization process.

The instantaneous rate of polymerization obtained from equation (4) is

$$dM/dt = (9/2\sqrt{3}) N_0 \rho R G^3(x) (t - t_0)^2 \quad (5)$$

This may be compared with the instantaneous surface area of the crystals which, for the segment already discussed, is

$$A = \{G^2(x) (1 + R)/2\sqrt{3}\} (t - t_0)^2$$

and for N_0 hexagons

$$A_N = \sqrt{3} N_0 G^2(x) (1 + R) (t - t_0)^2 \quad (6)$$

i.e. comparing (5) and (6)

$$dM/dt = \{1.5 \rho R Gx/(1 + R)\} A_N$$

Since R is small for flat hexagons (~ 0.1).

$$dM/dt \simeq 1.5\rho R Gx A_N = 1.5\rho G y A_N$$

i.e. the instantaneous rate of polymerization is proportional to the surface available for deposition. This treatment neglects the possible pyramidal nature of the crystals, but since the pyramidal angle is small this is probably justified.

The growth of fresh polymer on existing crystals has been demonstrated by 'seeding' a solution of trioxan with a polymerizing suspension.

A clear demarcation line between polymer formed before and after mixing can be seen in the electron micrograph (*Figure 9*) kindly supplied by Dr A. Keller.

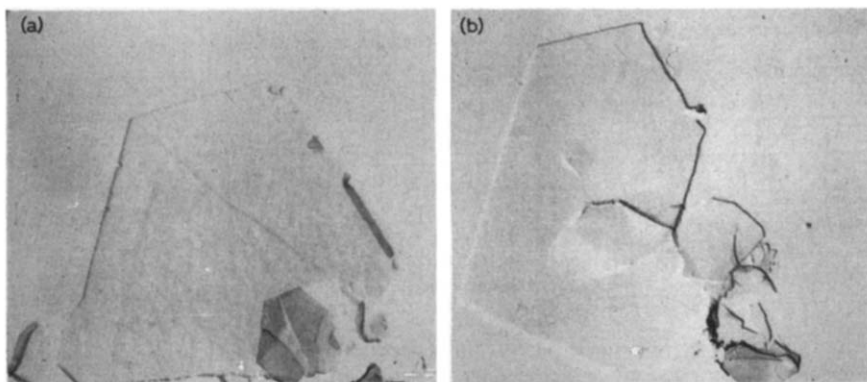


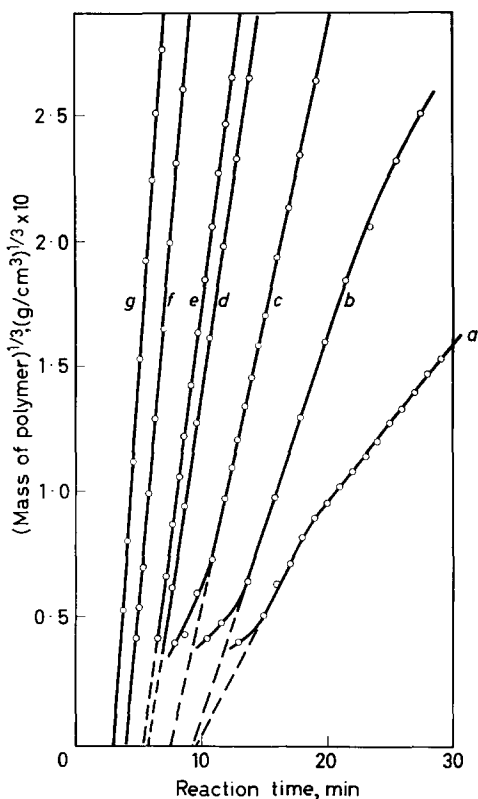
Figure 9—Growth of polyoxymethylene crystals. Electron micrographs $24\,000\times$ (A. Keller). Effect of seeding: (a) seeded polymerization. Reaction conditions: temperature 70°C , trioxan concentration 2.78 mole/l., catalyst concentration, 0.2 m mole/l. of fluoroboric acid; (b) unseeded polymerization. Reaction conditions: temperature 70°C , trioxan concentration 5.6 mole/l., catalyst concentration, 0.8 m mole/l. of boron trifluoride etherate

The polymerization kinetics are plotted in accordance with the cubic equation (4) in *Figures 10* and *11*. Good agreement is obtained, over considerable variations in catalyst and trioxan concentrations, for the first 0.1 to 10 per cent of polymerization.

Below 0.1 per cent deviations would be expected owing to nucleation phenomena, and above 10 per cent conversion the reduction in trioxan might affect the linear growth rate, or some process other than crystallization might become rate-controlling as the total surface area of the crystals becomes relatively large.

The temperature rise in these experiments (from 2° to 3°C) constitutes a source of error, since it should produce some acceleration of the reaction. However, this effect is small (approximately 10 per cent for a 3° temperature rise if the activation energy is 19 kcal, as stated by Okamura *et al.*⁹) compared with the observed accelerations. Moreover, the cubic equation given above also applies to the results of Kern and Jaacks, where polymerization in methylene chloride solution was studied dilatometrically at constant temperature.

Figure 10—Crystal polymer deposition (calculated from thermochemistry). Test of cubic equation; effect of trioxan concentration. Catalyst concentration 2.0 m mole/l. of boron trifluoride etherate. Water concentration 8.2 m mole/l.: Trioxan concentrations, mole/l.: a 1.67, b 2.09, c 2.50, d 2.78, e 3.06, f 3.34, g 3.47



The slopes of the lines in *Figures 10* and *11* give values of the expression $(\frac{1}{2}\rho N_0 R)^{\frac{1}{3}} Gx$ for various values of trioxan and catalyst concentration.

Since precipitation of crystals begins at a constant polymer concentration, N_0 may reasonably be regarded as constant. If R is also constant the slopes are a measure of Gx , the linear growth rate. The slopes increase with the square of the catalyst concentration and the cube of the initial trioxan concentration. They are thus related to the initial net rate of ring opening as measured by the endothermic reaction in the same way as inverse induction times, the slopes depending linearly on the product of the initial rate and the trioxan concentration (*Figure 14*).

However, trioxan is consumed many times more rapidly in the later stages of heterogeneous polymerization reaction than at any time during the induction period, including the initial endothermic reaction. The net rate of ring opening in the presence of solid crystalline polymer is much higher than the homogeneous rate, and this suggests that the reactions are occurring in different environments.

It seems likely that polymerization occurs on chains already attached to the solid surface, the transfer of charge by the growing cation to a new monomer molecule taking place at a growth step on the crystal surface. If nucleation of a new crystal face is a rate-determining step during the first ten per cent of the polymerization, the observed kinetics are accounted for.

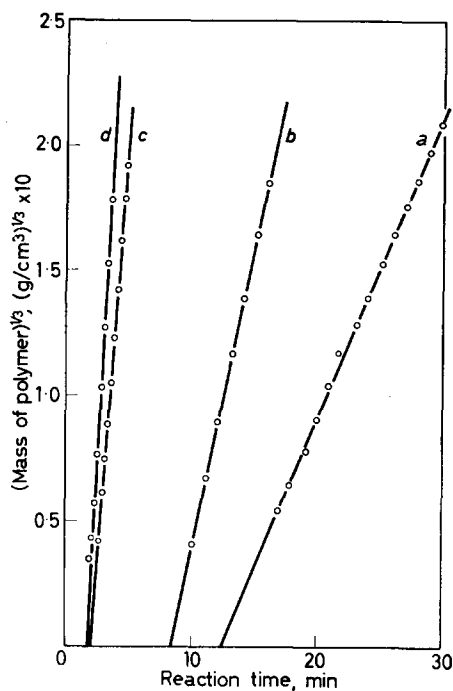


Figure 11 — Crystalline polymer deposition (calculated from thermochemistry). Test of cubic equation; effect of catalyst concentration. Trioxan concentration 2.5 mole/l. Water concentration 4.2 m mole/l. Catalyst concentrations, m mole/l. of boron trifluoride etherate *a* 1.0, *b* 1.5, *c* 2.5; *d* 3.0

Topochemical polymerizations of this kind are thought to occur during sublimation polymerization of trioxan¹⁰, and recently a similar mechanism has been proposed for the polymerization of trioxan during crystallization from solutions in liquid paraffin¹¹.

Attention should also be drawn to the patent literature, where seeded polymerizations are described.

Polymer of 100 per cent crystallinity is produced by this technique in the polymerization of formaldehyde¹².

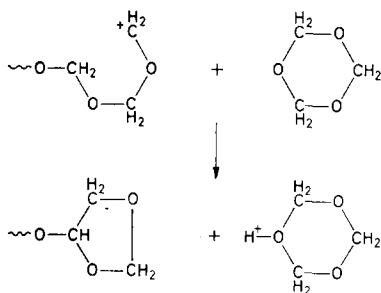
Trioxan polymerization is more rapid than in the unseeded reaction, and the product has higher molecular weight¹³. These effects correspond to our observations of the importance of crystallization during polymerization.

Comparable behaviour might be expected for other polymerizations in which similar conditions are fulfilled, viz.

- (a) A crystalline product is formed, insoluble in the reaction medium.
- (b) The heat of reaction is small compared with the heat of crystallization.

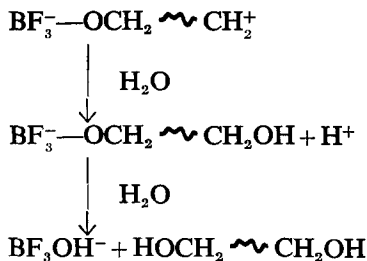
The above general description of the kinetics does not require a detailed analysis of the chemistry of the initiation, growth and termination steps. This information is difficult to obtain because of the complicated kinetics involved, and because of the difficulty in measuring true molecular weights.

In the experiments described above molecular weights were low (of the order of 5 000) and were probably limited by transfer reactions of various kinds. Transfer with water, or to monomer via reactions such as



are possible.

It seems likely that the initiating reaction changes during the course of the polymerization from the zwitterion mechanism outlined previously to one involving polymeric cations with gegenions such as OH^- and BF_3OH^- , i.e.



Such reactions would be favoured by the separation of charge necessarily brought about by crystallization of the oligomeric zwitterions.

Practical assistance was received from Messrs J. Caley, R. Ransome and T. Taylor-Brown.

Photomicrography was undertaken by Mr C. B. Bucknall.

It is a pleasure to acknowledge the continued encouragement and advice of Mr E. B. Atkinson and Dr R. R. Smith, and the authors thank the directors of Bakelite-Xylonite Ltd for permission to publish this work.

Reference to B.P. 914 046 is by permission of the Controller of H.M. Stationery Office.

An abbreviated form of the foregoing results was presented at the Polymer Physics Meeting at Shrivenham (this Journal, 1964, 5, 380).

*B.X. Plastics Ltd, Research Station,
Lawford Place, Lawford,
Nr Manningtree, Essex*

(Received September 1964)

REFERENCES

- ¹ KERN, W. and JAACKS, V. J. *J. Polym. Sci.* 1960, **48**, 399
- ² *Handbook of Chemistry and Physics*. Chemical Rubber Publishing Co.: Cleveland, Ohio, 1963
- ³ WALKER, J. F. 'Formaldehyde', 3rd ed., pp 52, 180, 194 and 486. Reinhold: New York, 1964

- ⁴ CRAIG, R. A. and RICHARDS, R. E. *Trans. Faraday Soc.* 1963, **59**, 1962
- ⁵ INOUE, M. *J. Polym. Sci.* 1963, **1 Pt A**, 2697-2709
- ⁶ WITHEY, R. J. and WHALLEY, E. *Trans. Faraday Soc.* 1963, **59**, 901-906
- ⁷ RENEKER, D. H. and GEIL, P. H. *J. appl. Phys.* 1960, **31**, 1916
- ⁸ KELLER, A. Private communication
- ⁹ OKAMURA, S. *et al. J. Polym. Sci.* 1963, **4 Pt C**, 827-838
- ¹⁰ KERN, W. and JAACKS, V. *Makromol. Chem.* 1962, **52**, 38
- ¹¹ BACCAREDDA, M., BUTTA, E. and GUISTI, P. *J. Polym. Sci.* 1963, **4 Pt C**, 953
- ¹² E.I. Du Pont Co. Ltd. *U.S. Pat. No. 3 000 861*
- ¹³ Celanese Corpn of America, *Brit. Pat. No. 914 046*

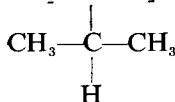
Intramolecular Hydride Shift Polymerization by Cationic Mechanism V—The Effect of Temperature and Monomer Concentration on the Structure and Molecular Weight of Poly-3-methylbutene-1

J. P. KENNEDY, W. W. SCHULZ, R. G. SQUIRES* and R. M. THOMAS

The effects of temperature, monomer concentration and monomer conversion on the molecular weight and structure (1,3 versus 1,2 contribution) of poly-3-methylbutene-1 obtained with aluminium chloride and aluminium bromide catalysts in ethyl chloride, methyl bromide and n-pentane solvents have been investigated. A near-infra-red method which allows the quantitative determination of 1,3-type enchainment in cationic poly-3-methylbutene-1 has been developed and is described. Decreasing the polymerization temperature increases the molecular weight of poly-3-methylbutene-1 in all systems studied. The linear relationship of logarithm of molecular weights plotted against $1/T$ for polymers obtained with aluminium chloride in ethyl chloride changes its slope from $E_{DP} = -2.5$ kcal/mole in the range of $+10^\circ$ to -80°C to about $E_{DP} = -0.35$ at lower temperatures.

Product composition measured by the structure ratios (the ratio of 1,3 monomer units to 1,2 monomer units in the polymer) also changes with temperature. The logarithm of the structure ratio increases linearly with reciprocal temperature in the range $+100^\circ$ to -100°C . The gegenion strongly affects the slope of the product composition curves, whereas the polarity of the medium is less important in this region. At lower temperatures the structure ratio increases more rapidly with reciprocal temperature, and at -130°C essentially pure crystalline 1,3-poly-3-methylbutene-1 is obtained. Under the experimental conditions employed, monomer concentration and monomer conversion do not affect the structure ratio. These results are discussed and a kinetic model is proposed which involves competition between propagation to form 1,2-enchainment and intramolecular hydride shift to form 1,3-enchainment.

THE cationic low temperature polymerization of 3-methylbutene-1 proceeds by intramolecular hydride shift mechanism, and the product is a polymer of the α,α -dimethyl propane type¹⁻⁶. In the course of fundamental studies of the cationic polymerization of 3-methylbutene-1, it was of interest to investigate simultaneously the effect of temperature, monomer concentration and/or conversion on the molecular weight and the structure of the products. Earlier studies² showed that the ratio of the amount of 1,3-polymer $[-\text{CH}_2-\text{CH}_2-\text{C}(\text{CH}_3)_2-]$ to 1,2-polymer $[-\text{CH}_2-\text{CH}-]$ increases with



*Present address: School of Chemical Engineering, Purdue University, W. Lafayette, Indiana.

decreasing temperature and that about 30 per cent 1,2-polymer is present in polymer prepared at -80°C . Essentially pure, crystalline 1,3-polymer is obtained when the polymerization is carried out at -130°C ¹. Below -130°C , the rate of polymerization becomes extremely slow⁷.

In the present study, poly-3-methylbutene-1 samples were prepared with aluminium chloride and aluminium bromide catalysts in polar and non-polar solvents at various temperatures and at various monomer concentrations. Both the structure of the polymers and the number average molecular weights were determined. An infra-red (i.r.) method was developed and used to measure quantitatively the amount of 1,3-enchainment of cationic poly-3-methylbutene-1.

EXPERIMENTAL

Materials, procedures and polymerization

Most of the materials used, their source and purity, together with the low temperature polymerization technique have been described previously^{8,9}. Polymerizations at 0°C and at higher temperatures were performed in *n*-pentane solvent in ceramic-lined steel bombs. In these experiments, the monomer and *n*-pentane solvent were placed in the bombs with a sealed glass vial containing the aluminium bromide catalyst in *n*-pentane solution. After thermo-equilibration in a suitable bath at the selected temperature, the catalyst vial was broken by shaking the bomb vigorously.

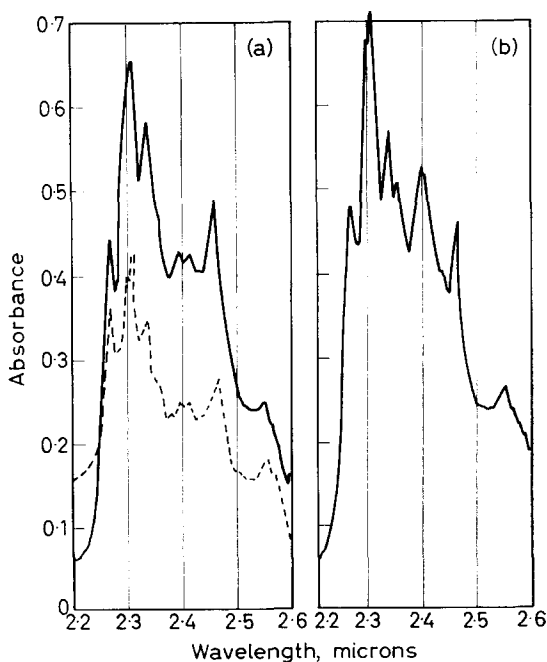
The effect of monomer conversion and monomer concentration on molecular weight and amount of 1,3-enchainment were studied by polymerizing 3-methylbutene-1 in ethyl chloride at various concentrations with aluminium chloride catalyst at -115° and -80°C . Polymer recovery and purification were performed as previously described⁸. Intrinsic viscosities were determined in diisobutene solution at 20°C ¹⁰, and number average molecular weights determined osmotically in *o*-dichlorobenzene solution at 120°C . The amount of 1,3-enchainment in the polymer was determined by means of near-infra-red spectra recorded with a Cary Model 14 spectrophotometer over the wavelength range of 2.6 to $2.2\ \mu$ as described below.

Infra-red method to determine percentage of 1,3-structure in cationic poly-3-methylbutene-1

Previous i.r. studies showed that quantitative estimates of the relative amounts of 1,2- and 1,3-structures in cationic poly-3-methylbutene-1 cannot be made in the 3 to $16\ \mu$ region³. N.m.r. spectroscopy is valuable in characterizing the pure 1,3-structure but, unfortunately, is of little value for the quantitative measurement of the 1,2-structure.

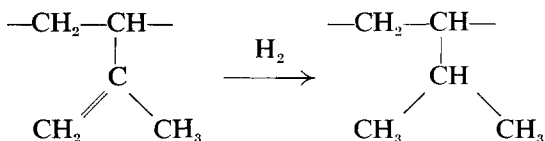
Careful evaluation of near-infra-red combination bands in the range of 2.2 to $2.6\ \mu$ revealed differences in band intensities for various poly-3-methylbutene-1 samples (*Figure 1*). In particular, low temperature cationic polymer exhibits a strong band at $2.403\ \mu$ [*Figure 1(b)*], the intensity of which diminishes as the polymerization temperature increases. The spectra of hydrogenated 3,4-polyisoprene as well as Ziegler-Natta type poly-3-methylbutene-1 show a small peak at this wavelength, the intensity of which is approximately equivalent to the neighbouring peak at $2.418\ \mu$ [*Figure 1(a)*].

Figure 1 — Near-infra-red spectra of various poly-3-methylbutene-1 samples: (a) hydrogenated 3,4-polyisoprene (—), Ziegler-Natta poly-3-methylbutene-1 (---); (b) crystalline cationic poly-3-methylbutene-1



The high intensity of the 2.403μ band in crystalline cationic polymer is believed to be caused by a quaternary carbon vibration, since this band is also prominent in spectra of polyisobutylene and polyisobutylene oxide. The 2.403μ band was used to estimate quantitatively 1,3-structure in polymer samples. A base line was drawn between the minimum at 2.37μ and the shoulder at 2.43μ of the recorded spectrum, and the extinction coefficient of the 2.403μ band was determined above this line.

Soluble crystalline cationic poly-3-methylbutene-1, synthesized at -130°C was used as a calibration standard for 100 per cent 1,3-structure and soluble hydrogenated 3,4-polyisoprene.



prepared by Wilke catalyst¹¹ as a standard for 0 per cent 1,3-structure. The calibration curve, which was used to determine unknown amounts of 1,3-contribution in polymer samples, was obtained by co-dissolving various weight ratios of cationic crystalline poly-3-methylbutene-1 and hydrogenated 3,4-polyisoprene in carbon tetrachloride and determining the extinction coefficient at 2.403μ . The total polymer concentration ranged from 0.02 to 0.03 g/ml. A plot of extinction coefficients in $\text{ml g}^{-1} \text{cm}^{-1}$ against per cent 1,3 composition was linear over the whole composition range from 0 to 100 per cent 1,3-structure (Figure 2).

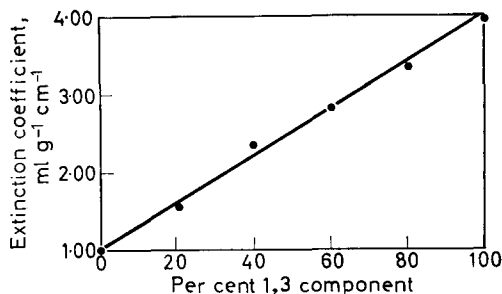


Figure 2—Calibration curve for 1,3-component in cationic poly-3-methylbutene-1

The polymer was dissolved in spectrograde carbon tetrachloride which was also used in the reference path. Polymer concentrations were kept between 0.02 and 0.03 g/ml, at which concentration level convenient absorbance values were obtained with cells of 1 cm path length. No solubility difficulties were encountered in this concentration range.

The peak at 2.354μ is useful as internal standard. The extinction coefficients for the two reference polymers at a concentration of 0.027 g/ml differed by $0.543 \text{ ml g}^{-1} \text{ cm}^{-1}$ or 2.7 per cent. An average extinction coefficient value of 19.8 for this concentration introduces a maximum error of 1.35 per cent.

A better reference compound for the 0 per cent 1,3-structure would have been a Ziegler-Natta isotactic poly-3-methylbutene-1. Unfortunately, due to its insolubility in common solvents at room temperature, this polymer could not be used in our solution studies. However, by dissolving the isotactic Ziegler-Natta polymer in 1,3-hexachlorobutadiene at 200°C and cooling the solution rapidly, an i.r. spectrum was obtained which was virtually identical to that of hydrogenated 3,4-polyisoprene. The spectrum of the isotactic polymer (broken line) and that of the soluble reference compound are shown in *Figure 1(a)*.

RESULTS AND DISCUSSION

Table 1 and *Figures 3(a)*, *3(b)* and *4* show the effect of temperature on molecular weight and structure (amount of 1,3-enchainment) of cationic poly-3-methylbutene-1. More specifically, *Table 1* contains pertinent experimental details whereas *Figures 3* and *4* show the effect of temperature under various experimental conditions on structure and the number average molecular weights.

Figures 3(a) and *3(b)* are plots of the number average molecular weights versus reciprocal polymerization temperature for aluminium bromide and aluminium chloride catalyst systems, respectively. Earlier results obtained in an almost identical system⁸ showed that the viscosities of the polymer product were quite unaffected by monomer conversion in the range 20 to 98 per cent. Thus, it was not surprising to find that in spite of conversion ranging from about 10 to 97 per cent, the plot of the number average molecular weights versus $1/T$ gave reasonably defined straight lines down to about -80°C . The slopes of these curves of the Arrhenius type obtained in the three different polymerization series (aluminium chloride in ethyl chloride, aluminium bromide in methyl bromide, and aluminium bromide

HYDRIDE SHIFT POLYMERIZATION BY CATIONIC MECHANISM V

Table 1. The effect of temperature on the molecular weight and structure (amount of 1,3-component) of cationic poly-3-methylbutene-1

Temp., °C	$1/^\circ K \times 10^3$	Conversion %	\overline{M}_n	% 1,3- component	Structure ratio P(1,3)/P(1,2)	
I. Polymerization with $AlCl_3$ in C_2H_5Cl†						
1st run						
-20	4.05	95	5 000	79	3.76	
-45	4.39	92.3	10 000	82	4.56	
-80	5.18	90.5	10 000	82	4.56	
-100	5.78	62.5	21 000	85	5.67	
-130	7.0	10.2	24 000	104	∞	
2nd run (3 months later)						
+10	3.52	75.0	1 877	2 059	81	4.26
0	3.67	69.0	2 314	2 525	83	4.88
-20	4.03	47.0	2 958	3 801	81	4.26
-40	4.30	91.4	5 130	5 647	87	6.68
-60	4.70	97.3	9 751	8 340	84	5.25
{ -80	{ 5.18	{ 90.3	{ 16 789	{ 11 621	{ 86	{ 6.15
{ -80	{ 5.18	{ 63.0	{ —	{ 10 719	{ 87	{ 6.68
{ -80	{ 5.18	{ 21.5	{ —	{ 13 489	{ 86	{ 6.15
-100	5.78	43.0	14 380	17 320	91	10.1
-115	6.35	17.7	21 162	13 816	98	49.0
-130	7.0	10.9	—	19 990	103	∞
II. Polymerization with $AlBr_3$ in CH_3Br‡						
-25	3.69	37.2	2 958	—	—	
-13*	3.85	73.5	3 558	82	4.55	
-26*	4.05	79.2	4 782	88	6.3	
-29*	4.10	73.5	4 892	88	6.3	
-39.5	4.30	11.6	5 320	87	6.2	
-45*	4.39	92.1	—	87	6.2	
-66*	4.82	49.7	5 881	84.5	5.45	
-77	5.1	22.8	8 228	93	13.2	
III. Polymerization with $AlBr_3$ in <i>n</i>-pentane§						
+100	2.68	26.2	538	63	1.70	
+50	3.10	52.6	920	70	2.33	
0	3.67	69.3	1 604	77	3.25	

*Maximum temperature during polymerization.

 †Monomer concentration: 3.1 mole/l.; catalyst concentration: 5.7×10^{-2} mole/l.

 ‡Monomer concentration: 3.43 mole/l.; catalyst concentration: 5.46×10^{-2} mole/l.

 §Monomer concentration: 1.1 mole/l.; catalyst concentration: 5.46×10^{-2} mole/l.

in *n*-pentane) are within what is considered to be experimental error. In the range from +100° to -80°C, the overall activation energies calculated from the molecular weight data are about identical ($E_{DP} = -1.5$ to -2.5 kcal/mole) indicating that variations in the aluminium halide and polarity of solvent do not significantly affect the overall energetics of polymerization in this temperature range.

The two series with aluminium bromide catalyst, one in methyl bromide and the other in *n*-pentane solvent [Figure 3(a)] show that molecular weights

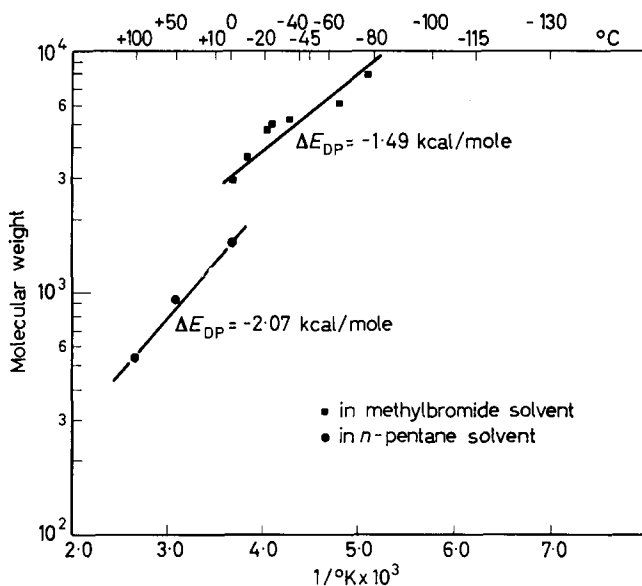


Figure 3(a)—The effect of temperature on the molecular weight of poly-3-methylbutene-1 obtained with aluminium bromide catalyst

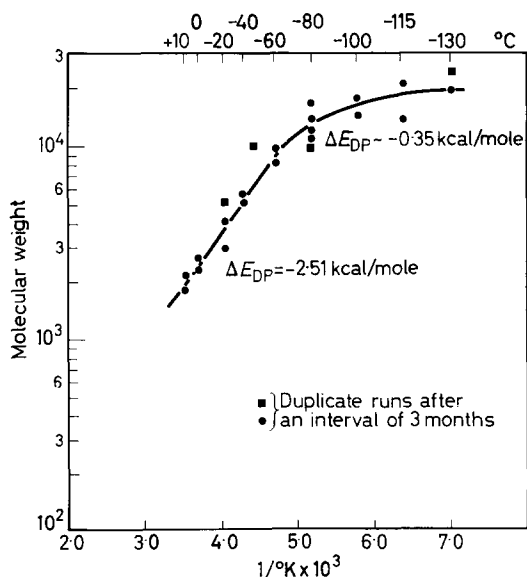


Figure 3(b)—The effect of temperature on the molecular weight of poly-3-methylbutene-1 obtained with aluminium chloride catalyst

increase somewhat with changes in the dielectric constant (d.c.) and/or polarity of the solvent at least in the region of d.c. ~ 1.8 (for *n*-pentane) to ~ 9.8 (for methyl bromide at -80°C). Earlier research showed that the medium greatly affects polymerization rate but only moderately influences

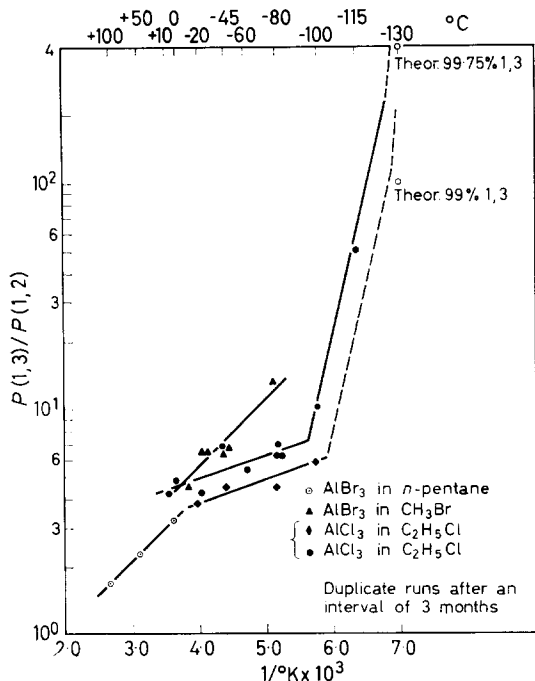


Figure 4—The effect of temperature on the structure of cationic poly-3-methylbutene-1

molecular weights⁸. This is generally true in cationic polymerization systems¹².

Comparing the data shown in Figures 3(a) and 3(b), it is evident that the molecular weights obtained with aluminium chloride are higher than those obtained with aluminium bromide catalyst at the same temperature level. This effect could be due, at least partly, to the higher d.c. of ethyl chloride (~ 16.0) used in conjunction with aluminium chloride, than that of the methyl bromide (~ 9.8) used with aluminium bromide.

A break in the slope of the curve in Figure 3(b) is observed at about -80°C . The apparent overall activation energy calculated from the molecular weights is about -2.5 kcal/mole in the range $+10^{\circ}$ to -80°C , and drops to about -0.35 kcal/mole from -80° to -130°C . A similar phenomenon has already been described and discussed in connection with the isobutene-ethyl chloride-aluminium chloride system⁹. A possible explanation of this phenomenon in terms of a proposed kinetic model will be discussed subsequently.

The effect of temperature on the structure of cationic poly-3-methylbutene-1 is shown in Figure 4. This plot shows the logarithm of the structure ratio $P(1,3)/P(1,2)$ versus the reciprocal temperature for various experimental conditions. The structure ratio $P(1,3)/P(1,2)$ or $P(1,3)/(1.0 - P(1,3))$ is the ratio of the number of 1,3 monomer units in the polymer to the number of 1,2 monomer units. The fraction of 1,3 polymer is determined directly by near-infra-red spectroscopy as described above.

According to the data in Figure 4, the plot of the structure ratio versus

$1/T$ gives straight lines for all three systems investigated in the temperature range from $+100^\circ$ to -100°C . The lines obtained for aluminium chloride in ethyl chloride solvent in two duplicate experiments with an interval of approximately three months are reproduced satisfactorily, having almost identical slopes in the range of 0° to about -90°C . At $\sim -90^\circ\text{C}$ there is a break in the curve, the slope increasing sharply. The curves obtained with aluminium bromide catalyst, either in *n*-pentane in the range from $+100^\circ$ to 0°C or in methyl bromide in the range from 0° to -80°C are also linear.

We found that aluminium bromide is a poor catalyst for the polymerization of 3-methylbutene-1 at temperatures lower than -100°C . Indeed, uncommonly large amounts of catalyst were required to initiate a small amount of polymerization even at -100°C . Lack of polymerization with aluminium bromide at low temperatures is probably due to slow initiation. Thus, the aluminium bromide line can only be shown down to -80°C and a break in this line, if there is any, was not observed because of this experimental difficulty. The data in *Figure 4* will also be analysed later in terms of the proposed kinetic model.

Table 2 shows the effect of monomer concentration and monomer conversion on the molecular weight and structure of poly-3-methylbutene-1 at -115° and -80°C . These two temperature levels were selected to lie below (-115°) and above (-80°C) the break in the $\log P(1,3)/P(1,2)$ versus

Table 2. The effect of monomer concentration, monomer conversion and molecular weight on the structure (amount of 1,3-component) of cationic poly-3-methylbutene-1

Temp., $^\circ\text{C}$		-115°			
[M] mole/l.	Conversion %	\bar{M}_n	% 1,3- component	Structure ratio $P(1,3)/P(1,2)$	
10.3 (undiluted monomer)	1.9		94	15.7	
10.3	3.9	9 100	98.5	65.7	
10.3	9.2	8 503	96	24	
5.0	4.25	10 118	96.5	27.6	
5.0	5.5	11 769	96.5	27.6	
3.1	5.85	10 613	101	∞	
1.5	18.4	13 650	101	∞	
0.75	16.9		105	∞	
0.75	23.3	11 912	98.5	65.7	
Temp., $^\circ\text{C}$		-80°			
[M] mole/l.	Conversion %	\bar{M}_n	% 1,3- com- ponent	Structure ratio $P(1,3)/P(1,2)$	
10.3 (undiluted monomer)	16.7	7 546	6 947	87	6.7
5.0	22.9	10 381	10 083	87	6.7
3.1	21.5	8 598	6 957	86	6.15
3.1	63			87	6.7
3.1	90.3			86	6.15
1.5	6.7		10 651	87	6.7
0.75	38.9	13 824	11 470	89	8.1

1/°K curve (see *Figure 4*). The polymerizations at -115°C were expected to be particularly sensitive to the possible effect of monomer concentration because the slope of the curve is very steep at this temperature level. It was considered desirable to carry out another series of polymerizations at -80°C , since monomer diffusion (which will be postulated to be important at -115°C) could have obscured concentration effects at -115°C .

Thus, *Table 2* indicates that at -80°C the structure ratio is approximately constant and independent both of changes in percentage conversion from 16.7 to 90, and of changes in monomer concentration from 0.75 to 10.3 mole/l. (undiluted monomer). Also, at a constant monomer concentration of 3.1 mole/l., a variation of percentage conversion from 21.5 to 90.3 produced no corresponding change in structure ratio.

At -115°C , the data are difficult to interpret due to experimental error. Since in the range from 98 to 100 per cent 1,3-enchainment the structure ratios would increase from 49 to ∞ , a ± 2 per cent error in the data would completely mask the effect of monomer concentration on structure ratio. Thus in this low temperature region, the effect of monomer concentration on structure ratio remains indefinite.

At both -115°C and -80°C , the effect of monomer concentration and percentage conversion on molecular weight is small. Similar percentage conversion versus molecular weight (inherent viscosity) data have been previously reported⁸ according to which the molecular weights rapidly increase to a plateau at low conversions and they remain essentially unchanged with increasing conversions.

POLYMERIZATION MECHANISM

Attempts were made to explain all the experimental results by a uniform polymerization mechanism. Such a theory should explain the following significant facts:

(a) The linear dependence of the structure ratio on reciprocal absolute temperature at high temperatures ($+100^{\circ}$ to -100°C) (*Figure 4*).

(b) The change in slope of the structure ratio curve at approximately -100°C (*Figure 4*).

(c) Formation of crystalline 1,3-poly-3-methylbutene-1 at -130°C .

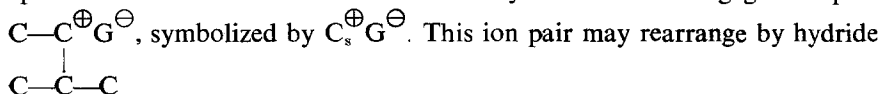
(d) The independence of structure ratio on monomer concentration at high temperatures.

(e) The linear relationship of the logarithm of molecular weight with reciprocal absolute temperature [*Figures 3(a) and 3(b)*].

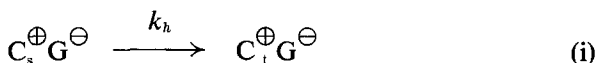
(f) The change in slope of this linear dependence at approximately -80°C [*Figure 3(a)*].

The following mechanism is proposed.

Polymerization starts by initiation which probably occurs by protonation of the monomer by the aluminium chloride cocatalyst system, the cocatalyst being provided by adventitious impurities (water) in the system. The first species formed on initiation is a secondary carbonium ion-gegenion pair



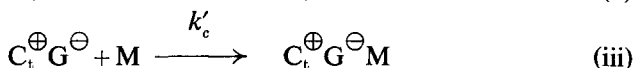
shift and give a tertiary carbonium ion-gegenion pair: $C-C-C^{\oplus}G^{\ominus}$, or $C_t^{\oplus}G^{\ominus}$. This rearrangement involves an energetically favourable hydride shift. The rate of this rearrangement is probably extremely fast and it is characterized by the rate constant k_h , i.e.



The back-reaction is highly unlikely to occur and will be ignored. However, both ion pairs can react with monomer M to form an intermediary ternary complex:



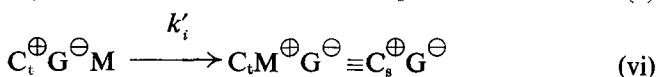
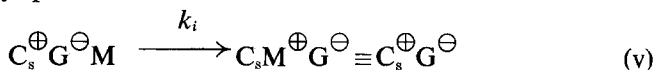
and



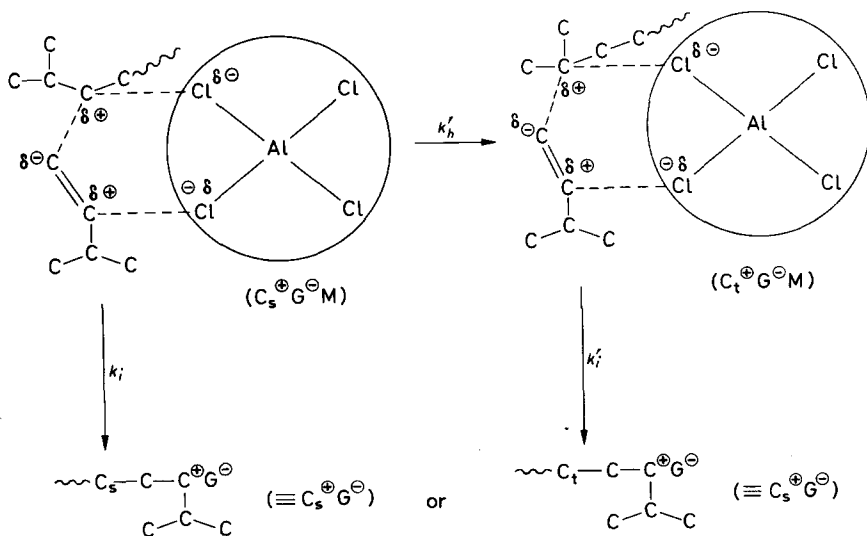
The secondary carbonium ion of the ternary complex can rearrange to the tertiary carbonium ion



Again the back-reaction can be ignored because of energetic considerations (see above). Both intermediary ternary species can incorporate the complexed monomer and both of these events then, necessarily, lead back to the initial secondary species:

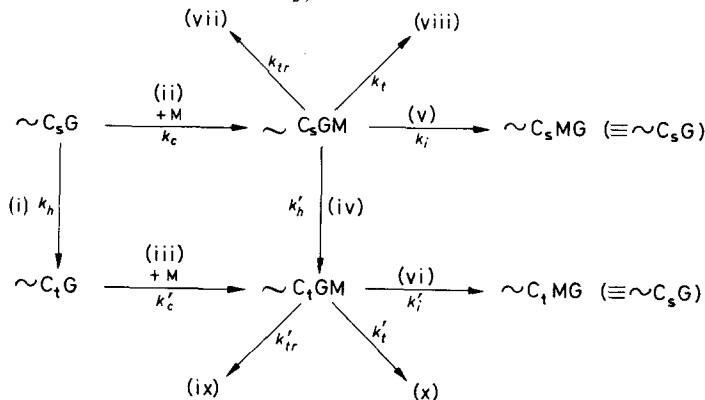


The chemistry of these two reactions can be visualized as follows:



The ternary complexes are probably also involved in chain transfer [equations (vii) and (ix)] and termination reactions [equations (viii) and (x)], events which do not affect the structure of the final polymer but determine the molecular weight and conversion, respectively.

The model can be summarized in the following scheme (charge symbols are omitted for the sake of clarity):



where the rate constants k_c and k'_c , k_h and k'_h , k_i and k'_i , k_{tr} and k'_{tr} , k_t and k'_t refer to complex formation, hydride shift, incorporation, transfer, and termination, respectively.

Thus the tertiary carbonium ion complex is formed either by direct hydride shift from the secondary complex [reaction (iv)], or by complex formation from $C_t G$ [reaction (iii)] in which a hydride shift has previously occurred by reaction (i). The reverse reactions in (i) and (iv) are insignificant. Once the hydride shift has occurred, the newly formed tertiary complex is rapidly consumed by propagation as shown in equation (vi).

The formation of $C_s G$ during the initiation step is assumed to be very rapid compared with the subsequent propagation steps, so that the concentration of chain carriers would be initially equal to the catalyst concentration and would thereafter decrease as catalyst was removed from the system by termination. Thus, if the catalyst concentration is initially low enough, the concentration of chain carriers may fall to zero while excess monomer still remains, and the polymerization will stop at low percentage conversions. Such a mechanism is obviously non-steady state with regard to $C_s G$ and $C_t G$.

The concentrations of the ternary complexes $[C_s GM]$ and $[C_t GM]$, however, which are zero initially, are assumed rapidly to reach a small steady state value which will not appreciably change as the reaction proceeds. If we assume that $k_i \gg (k_t + k_{tr})$ and $k'_i \gg (k'_t + k'_{tr})$, which is reasonable in view of the high molecular weight polymer formed, in this steady state region:

$$\frac{d [C_s GM]}{dt} \simeq 0 = k_c [C_s G] [M] - (k_i + k'_i) [C_s GM] \quad \text{(xi)}$$

and

$$\frac{d [C_t GM]}{dt} \simeq 0 = k'_c [C_t G] [M] + k'_h [C_s GM] - k'_i [C_t GM] \quad \text{(xii)}$$

Structure ratio

The structure ratio, $P(1,3)/P(1,2)$ is determined by the relative propagation rate of tertiary to secondary species; the transfer and termination reactions should have little or no influence on $P(1,3)/P(1,2)$. Thus:

$$dP(1,3)/dt = k'_i [C_tGM] \quad (xiii)$$

$$dP(1,2)/dt = k_i [C_sGM] \quad (xiv)$$

Consequently the structure ratio is proportional to the relative rate of 1,3 and 1,2 incorporation

$$P(1,3)/P(1,2) = k'_i [C_tGM] / k_i [C_sGM] \quad (xv)$$

Eliminating $[C_tGM]$ and $[C_sGM]$ with the use of equations (xi) and (xii) gives

$$\frac{P(1,3)}{P(1,2)} = \frac{k'_h}{k_i} + \frac{(k_i + k'_h) k'_c}{k_i k_c} \frac{[C_tG]}{[C_sG]} \quad (xvi)$$

We now focus our attention on the ratio $[C_tG]/[C_sG]$. If the activation energy for reaction (ii) is larger than the activation energy for reaction (i), then at high temperature ($> -100^\circ\text{C}$) reaction (ii) would predominate. Since reactions (ii) and (iii) are almost identical and expected to be rapid in this temperature range, we conclude that $[C_tG] \ll [C_sG]$. Thus, the second term in equation (xvi) becomes negligible and $P(1,3)/P(1,2) = k'_h/k_i$. Thus the structure ratio is independent of monomer concentration, as is clearly indicated by the data at -80°C in *Table 2*.

In other words, in the temperature range $+10^\circ$ to -100°C , and possibly from $+100^\circ$ to -100°C , the product ratio $P(1,3)/P(1,2)$ is determined by the competition between hydride shift governed by k'_h and incorporation characterized by k_i . Consequently, from $\log P(1,3)/P(1,2)$ versus $1/T$ in *Figure 4*:

$$\begin{aligned} \Delta E = E_{1,2} - E_h &= 0.5 \text{ kcal/mole in the AlCl}_3 \text{ in C}_2\text{H}_5 \text{ system,} \\ &1.33 \text{ kcal/mole in the AlBr}_3 \text{ in CH}_3\text{Br system and} \\ &1.48 \text{ kcal/mole in the AlBr}_3 \text{ in } n\text{-pentane system.} \end{aligned}$$

These orders of magnitude indicate that the overall activation energy difference between 1,2 propagation and hydride shift is very small and that these two processes are truly competing for the ternary complexes.

The effect of the gegenion on the hydride shift polymerization of 3-methylbutene-1 is revealed by the different slopes of the product ratio lines in the range $+100^\circ$ to -100°C obtained with aluminium bromide and aluminium chloride catalyst. The slopes of the two lines obtained with aluminium bromide catalyst are practically identical (1.33 in *n*-pentane and 1.48 kcal/mole in methyl bromide) indicating that the polarity of the medium has little or no effect on overall product distribution. However, the difference between the slopes of the aluminium bromide and aluminium chloride curves is about 1.0 kcal/mole which is more significant. This could mean that the larger AlBr_4^\ominus gegenion interferes more with 1,2 propagation than the smaller AlCl_4^\ominus gegenion, perhaps by blocking the way of the

incoming monomer molecule. Also, due to this steric effect, the overall rate of polymerization and particularly 1,2 propagation could be slowed down in the presence of the more bulky AlBr_4^- gegenion so that the $\text{sec.C}^+ \rightarrow \text{tert.C}^+$ rearrangement would become more important. This would explain the fact that more 1,3-enchainment is obtained with aluminium bromide than with aluminium chloride catalyst at identical temperatures.

It has been reported¹ earlier that crystalline, completely rearranged, i.e. 100 per cent 1,3-poly-3-methylbutene-1 is obtained at -130°C . Our present i.r. studies coupled with n.m.r. evidence also indicate that polymers synthesized at -130°C are pure 1,3 products. Completely pure or 100 per cent 1,3 polymer would give a product ratio of $+\infty$. The plotting of product ratios above 99 is meaningless since the 1 per cent interval between 99 and 100 per cent 1,3 product would correspond to the range 99 to $+\infty$ in the $\log P(1,3)/P(1,2)$ plot. The experimental value of 98 per cent 1,3 obtained for the polymer synthesized at -115°C , which corresponds to a product ratio of $(98/2) 49$ is, however, valid and significant.

Linear extrapolation to -130°C of product ratios obtained in the range $+100^\circ$ to -100°C (Figure 4) would give values far below those determined by experiment. For example, extrapolation of the aluminium chloride curve to -130°C would give a product ratio of nine corresponding to only 90 per cent 1,3 polymer. This value is obviously lower than the experimental one. It can be concluded confidently that a break exists in the $\log P(1,3)/P(1,2)$ versus $1/T$ line at low temperatures, probably around -100°C .

This change in slope may be explained as follows. It is conceivable that diffusion of monomer to the growing chain end may become important at low temperatures (i.e. $< -100^\circ\text{C}$). Diffusion control would greatly decrease the effective monomer concentration retarding reactions (ii) and (iii), which are monomer dependent. The rate of the competing hydride shift [reaction (i)] should not be affected by diffusion. Thus at low temperatures, reaction (i) would begin to predominate over reaction (ii) and the effect of the competition between these two reactions on $P(1,3)/P(1,2)$ would become increasingly important. In this region, where the rates of reactions (ii) and (iii) are slow relative to the rate of reaction (i), we would expect $[\text{C}_t\text{G}] \gg [\text{C}_s\text{G}]$. Thus, the second term in equation (xvi) would predominate. Note that in this region the logarithm of molecular weight may be monomer dependent since $[\text{C}_t\text{G}]/[\text{C}_s\text{G}]$ may be a function of monomer concentration. As was already pointed out, however, experimental error obscures any monomer dependence which might exist in this range. The slope of the logarithm of molecular weight versus $1/T$ curves in the range -100° to -130°C would reflect the effect of temperature on both the kinetic rate constants in the second term of equation (xvi) and on the diffusion coefficient. The apparent activation energy in this temperature range, calculated from Figure 4, is about 6 kcal/mole, which is a reasonable value for $E_{\text{diffusion}}$.

Thus, 1,3 polymer formation by the reaction routes (i), (iii) and (vi), becomes increasingly predominant at low temperatures and at $\sim -130^\circ\text{C}$ essentially pure 1,3-poly-3-methylbutene-1 is formed.

Molecular weight

In general, molecular weights are controlled by the relative rate of propagation reactions to the rates of chain transfer and termination reactions. By the proposed model, all of these processes, propagation, chain transfer, and termination originate with the activated ternary complexes. Thus, once the steady states of the activated ternary complexes are reached, the degree of polymerization should be unaffected by monomer concentration. Similarly, while diffusion should control the rates of reactions (ii) and (iii), the relative rates of reactions (v) and (vi) to reactions (vii), (viii), (ix), and (x) should be independent of diffusion.

Thus,

$$\text{Molecular weight} = \frac{k_i [C_sGM] + k'_i [C_tGM]}{(k_t + k_{tr}) [C_sGM] + (k'_t + k'_{tr}) [C_tGM]} \quad (\text{xvii})$$

Eliminating $[C_sGM]$ and $[C_tGM]$ with the use of equations (xi) and (xii) gives:

$$\text{Molecular weight} = \frac{k_c [C_sG] + k'_c [C_tG]}{k_1 [C_sG] + k_2 [C_tG]} \quad (\text{xviii})$$

where k_1 and k_2 are complicated functions of the proposed rate constants. In the high temperature region where $[C_sG] \gg [C_tG]$, molecular weight = k_c/k_1 . Similarly, at low temperatures where due to diffusion $[C_tG] \gg [C_sG]$, molecular weight = k'_c/k_2 . In both cases, molecular weights are monomer independent. Thus, a break in the log molecular weight versus $1/T$ curve is predicted at the transition temperature (-100°C) between the two regions. Such a break can be seen in *Figure 3(b)*. The significance of the slope of these lines in *Figure 3(b)* depends on the predominating rate constants in the k_1 and k_2 functions.

If we assume, however, that $k_i = k'_i$, $k_{tr} = k'_{tr}$, and $k_t = k'_t$, the denominator of equation (xviii) can be reduced to $\{(k_t + k_{tr})/k_i\} \{k_c [C_sG] + k'_c [C_tG]\}$. The second factor then cancels with the numerator of equation (xviii) giving

$$\text{Molecular weight} = k_i / (k_t + k_{tr}) \quad (\text{xix})$$

over the entire temperature region. This would indicate that the break in the slope of *Figure 3(a)* is caused by the effect of temperature on k_i and k_{tr} . In this case, if chain transfer is the molecular weight controlling process at lower temperatures, as has previously been proposed⁹, the activation energy calculated from *Figure 3(a)* would be $E_i - E_{tr} = -2.5$ kcal/mole and $E_i - E_{tr} = -0.35$ kcal/mole where transfer predominates.

Chemicals Research Division and

Analytical Research Division,

Esso Research and Engineering Company,

Linden, N.J., U.S.A.

(Received September 1964)

REFERENCES

- ¹ KENNEDY, J. P. and THOMAS, R. M. *Makromol. Chem.* 1962, **53**, 28
- ² KENNEDY, J. P., MINCKLER Jr, L. S., WANLESS, G. G. and THOMAS, R. M. *J. Polym. Sci. Part A*, 1964, **2**, 1441

HYDRIDE SHIFT POLYMERIZATION BY CATIONIC MECHANISM V

- ³ KENNEDY, J. P., MINCKLER Jr, L. S., WANLESS, G. G. and THOMAS, R. M. *J. Polym. Sci. Part A*, 1964, **2**, 2093
- ⁴ KENNEDY, J. P., MINCKLER Jr, L. S., WANLESS, G. G. and THOMAS, R. M. *J. Polym. Sci. Part C*, 1963, No. 4, 289
- ⁵ KETLEY, A. *Polymer Letters*, 1963, **1**, 313
- ⁶ EDWARDS, W. R. and CHAMBERLAIN, N. F. *J. Polym. Sci. Part A*, 1963, **1**, 2299
- ⁷ KENNEDY, J. P. *J. Polym. Sci. Part A*, 1964, **2**, 381
- ⁸ KENNEDY, J. P., MINCKLER Jr, L. S. and THOMAS, R. M. *J. Polym. Sci. Part A*, 1964, **2**, 367
- ⁹ KENNEDY, J. P. and THOMAS, R. M. in 'Polymerization and polycondensation processes', *Advances in Chemistry Series No. 34*, Chap. 7. American Chemical Society: Washington, D.C.
- ¹⁰ BILICK, I. H. and KENNEDY, J. P. *Polymer, Lond.* 1965, **6**, 175
- ¹¹ WILKE, G. *Angew. Chem.* 1956, **68**, 306
- ¹² PEPPER, D. C. *Quart. Rev. chem. Soc., Lond.* 1954, **8**, 88

Light Scattering and Ultra-violet Absorption Studies on Dilute Aqueous Solutions of Poly-4-vinylpyridinium Chloride

D. O. JORDAN, T. KURUCSEV and R. L. DARSKUS*

The discontinuous concentration of viscosity, streaming birefringence and conductance of dilute aqueous solutions of poly-4-vinylpyridinium chloride is attributed, on the basis of light scattering and spectra measurements, to the extensive hydrolysis of the poly-ions in dilute solution. The decrease in the charge on the poly-ion consequent on the hydrolysis produces changes in the shape and size which may explain the observed hydrodynamic properties.

THE discontinuous concentration dependence of the viscosity, streaming birefringence and conductance of dilute aqueous solutions of poly-4-vinylpyridinium chloride has recently been described^{1,2}. The presence of similar discontinuities is also suggested by the published reduced viscosity data at low concentrations for many strong and weak polyelectrolytes; the effects observed for poly-4-vinylpyridinium chloride solutions have therefore been assumed to represent a general property of polyelectrolyte solutions. By analogy with the behaviour of micelle-forming soaps and detergents, the discontinuities were explained tentatively in terms of the reversible aggregation of the poly-ions in solution. For such aggregation to occur, however, it is necessary to assume the presence of attractive forces between poly-ion segments which is contrary to accepted theories of polyelectrolyte solutions. We have now determined the size of the polyvinylpyridinium ions in solution and find no direct evidence for aggregation. The spectra of dilute solutions of poly-4-vinylpyridinium chloride suggest that extensive hydrolysis of the polyelectrolyte ions occurs. This has been confirmed by electrochemical measurements. The previously published hydrodynamic properties have therefore been re-interpreted in terms of the varying degree of hydrolysis of the polyvinylpyridinium ions.

EXPERIMENTAL

Several preparations of poly-4-vinylpyridine (PVP) were made by emulsion polymerization³ of freshly distilled 4-vinylpyridine (Light and Co.) with either benzoyl peroxide or azobisisobutyronitrile as initiator. The polymer samples were fractionated by precipitation from methanol solution with toluene, the fractions redissolved in tertiary butanol and freeze dried.

The purity of the samples was determined by potentiometric titration⁴ with *p*-toluene sulphonic acid in glacial acetic acid solution using a silver/silver chloride reference electrode and a glass indicator electrode. In this system the products of the titration do not precipitate. Satisfactory titration end points (± 1 per cent) compared with the potentiometric equivalence points were also obtained visually using crystal violet as indicator. The

*Present address: Institut für physikalische Chemie der Universität, Mainz, Western Germany.

impurity present in the samples (8 to 12 per cent) was assumed to be water, an assumption consistent with the results of elementary analysis and with the slightly hygroscopic nature of the polymer.

The fractions were characterized by their intrinsic viscosities in ethanol at 25°C determined with Ostwald capillary viscometers. The solution viscosities of the high molecular weight fractions ($[\eta] > 1\ 000$ ml/g) were found to decrease with time. This instability of solutions of PVP has been observed previously^{3,5} and explained in terms of degradation due to the presence of peroxides in the polymer chains. Oxidative degradation is probably an additional factor contributing to this instability since the effect was found to diminish by keeping the solutions under nitrogen. None of the polymer fractions used in the study discussed below showed any detectable variation of the viscosity with time.

Poly-4-vinylpyridinium chloride (PVP-HCl) was prepared by the partial neutralization of PVP with dilute hydrochloric acid solution. The dissolution of the samples generally required several days. Concentrations (c) for both PVP and PVP-HCl are expressed as grammes of uncharged polymer per millilitre of solution.

Light scattering measurements were made with a modified P.C.L.—Peaker light scattering apparatus^{6,7}. A narrow spectrometer slit and four additional apertures were introduced into the optical system to ensure a more precise definition of the scattering volume and a reduction in stray light. The effect of fluctuations in the intensity of the light source was reduced by directly measuring the ratio of the photocurrents due to the incident and scattered rays. This photocurrent ratio measuring device (manufactured by EILCO, South Australia) was tuned to receive only the 100 c/s component of the photocurrent. Since the mercury arc source (Mazda 250 W type ME/D) was run from a 50 c/s a.c. supply, the d.c. component of the photomultiplier tube dark current was eliminated.

Scattering cells, which were of rectangular shape and had a volume of 4 ml, were constructed from 3.5 mm thick glass. The cells were held in an outer cell of blackened brass which contained distilled water while measurements were being made. Unpolarized light of 436 m μ was used. After traversing the scattering cell, the primary beam was absorbed by red glass. With this arrangement the Fresnel correction⁸ was rendered negligible. The scattered light was observed through a semicircular glass window cemented to the outer cell. The range of angles through which observation was possible was from 27° to 140°.

The dependence of the scattering volume on the angle of observation, θ , was determined empirically using dilute solutions of sodium dichlorofluoresceinate. The deviations from proportionality to $1/\sin \theta$ were less than three per cent. The instrument was calibrated with benzene using the mean value of 47×10^{-6} cm⁻¹ for the reduced scattering intensity^{8,9}. The refractive index correction was taken to be n^2 .

Clarification of the PVP-HCl solutions was carried out using a Spinco model E ultracentrifuge with an SW-39 swinging bucket rotor at 100 000 g for two hours. In preliminary experiments, when these solutions were clarified in fixed angle rotors at 20 000 g, 'striations' were sometimes observed similar to those reported previously¹⁰.

Specific refractive increments were determined with a double prism differential refractometer of the type described by Cecil and Ogston¹¹.

Spectrophotometric measurements were made using a Unicam SP 500 instrument with constant temperature attachment. The photoelectric response of the instrument was tested in the wavelength range 215 to 500 m μ by standard potassium chromate solution¹². Some of the measurements were repeated on an Optica recording spectrophotometer. The extinction coefficients, defined by $K = (1/l) \log(I_0/I)$, where l is the optical path length through the solution, were found to be independent of time.

Conductance measurements were made using a cell designed to avoid errors due to adsorption of the solute on the electrodes. The concentration was changed by adding polyelectrolyte solution or solvent to the cell in an atmosphere of purified nitrogen. The bridge employed has been described previously¹³. Measurement of pH was made with a Cambridge pH-meter using an 'alkacid' glass electrode.

RESULTS AND DISCUSSION

The curve relating the relative viscosity with concentration of aqueous solutions of PVP at various degrees of neutralization cuts the concentration axis at a finite value of the concentration, γ_0 , below which the viscosity of the solution is indistinguishable from that of the solvent^{1,2}. A similar effect is observed for the magnitude of the birefringence of the solutions and, further, the curve relating the specific conductance with concentration exhibits a sharp change of slope at the same critical concentration, γ_0 ^{1,2}. This discontinuous variation of solution properties with concentration must be related to changes in either the size or shape (or both) of the poly-ion kinetic unit in solution. An interpretation of these results was given^{1,2} on the basis of the first of these alternatives, thus assuming that aggregation of the poly-ions occurred at concentrations greater than γ_0 , such aggregation being enhanced by the presence of added electrolyte (i.e. γ_0 is displaced to lower concentrations on the addition of electrolyte). A direct test of this interpretation is possible by determining the molecular weight of the polymer in solution under the following conditions: (i) in the uncharged state in a solvent where no aggregation would occur, (ii) in the partially neutralized and therefore charged state at concentrations above γ_0 , and (iii) at the same degree of neutralization but at a concentration below γ_0 . Light scattering measurements have therefore been made on solutions satisfying these conditions.

The weight average molecular weights were equated to the reciprocal of the ratio $Kc/R(\theta)$ at zero angle and zero polymer concentration⁸ and extrapolations were effected by Zimm plots¹⁴. No corrections for depolarization were applied. The degree of polymerization of the PVP sample in ethanol obtained from light scattering measurements on four solutions in the concentration range 0.6 to 2.8×10^{-4} g/ml was 21 000. Viscosity measurements on the same sample of PVP in ethanol solution gave a value, calculated by the method of Berkowitz, Yamin and Fuoss³, of 16 000 which is regarded as being in reasonable agreement with the light scattering result. The degree of polymerization of the sample of PVP 56 per cent neutralized with hydrochloric acid in aqueous 0.2 M sodium chloride calculated from

light scattering measurements on five solutions in the concentration range 2 to 10×10^{-4} g/ml was 16 000. This range of concentration lies well above the critical concentration for this solvent. The lower value obtained for the degree of polymerization of the polyelectrolyte in sodium chloride solution, compared with that obtained for the uncharged polymer in ethanol from light scattering measurements, is almost certainly due to the neglect of preferential interactions in the three-component system¹⁵. However, even though the values of the degree of polymerization obtained lack precision owing to the nature of the solutions and to the low concentration range studied, these measurements are sufficient to indicate that no aggregation of the poly-ions has occurred in the presence of sodium chloride compared with the corresponding uncharged molecules in ethanol.

Light scattering measurements have also been made on solutions of 50 per cent neutralized PVP at concentrations 0.18 and 0.29×10^{-4} g/ml in pure water as solvent. These concentrations lie well below γ_0 for PVP for this degree of neutralization in pure water. Light scattering measurements at such low concentrations are subject to considerable error owing to the low intensity of the scattered light and the consequential large corrections for solvent scattering; the extrapolation to zero angle and zero polymer concentration therefore proved to be somewhat arbitrary. However, the value obtained for the degree of polymerization, 30 000, even though approximate is in accordance with the conclusion reached above that there is no aggregation of the poly-ion on increasing the concentration through the critical concentration, γ_0 .

An alternative explanation of the discontinuous concentration dependence of solution properties was suggested from spectral studies. The ultra-violet spectra of aqueous PVP-HCl solutions were found to be concentration dependent, as is shown in *Figure 1*, which gives the spectra of solutions of

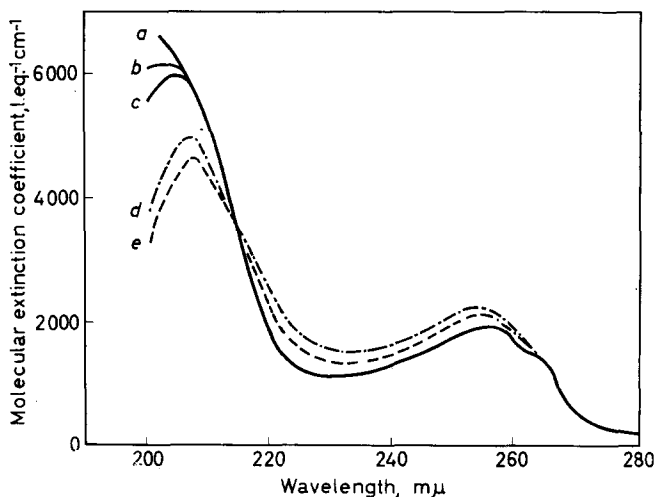


Figure 1—Absorption spectra of aqueous PVP-80 per cent hydrochloric acid at different concentrations: *a* 0.77, *b* 1.44, *c* 1.88, *d* 3.50, *e* 4.23×10^{-5} g/ml

DILUTE AQUEOUS SOLUTIONS OF POLY-4-VINYLPYRIDINIUM CHLORIDE

an 80 per cent neutralized PVP fraction in pure water. The molecular extinction coefficients are expressed in terms of the number of gramme atoms of nitrogen per litre of polymer solution. In *Figure 2* the variation of the extinction coefficient for these solutions is shown for two different wavelengths and the discontinuous nature of the deviations from Beer's law is revealed. The concentration at which the change in slope occurs at these wavelengths has been studied as a function of temperature, degree of neutralization and molecular weight of the polymer and of the concentration of sodium chloride. This study has shown that the position of the point of discontinuity in the curves relating extinction coefficient and concentration may be identified with the critical concentration, γ_{cs} , previously identified by hydrodynamic methods.

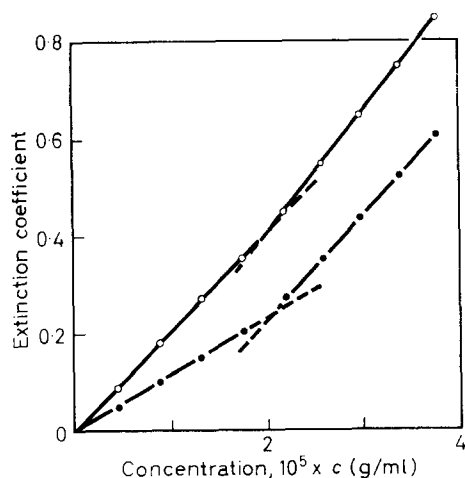


Figure 2—Variation of optical density with concentration of PVP-80 per cent hydrochloric acid at two different wavelengths: \circ 255 m μ , \bullet 225 m μ

The ultra-violet absorption spectra of solutions of PVP in ethanol and in 0.1 M hydrochloric acid are shown in *Figure 3*. These spectra are considered to represent the extremes of uncharged polymer and fully ionized poly-electrolyte respectively. The molecular extinction coefficients were independent of concentration under these conditions.

Comparison of the spectra shown in *Figures 1* and *3* suggests that the concentration dependence of the spectral activity of PVP-HCl solutions could be attributed to the variation of the degree of hydrolysis of the pyridinium groups. If it be assumed that the molecular extinction at some convenient wavelength, e.g. 255 m μ or 225 m μ , is a linear function of the fraction of ionized pyridinium groups, the degree of hydrolysis of the poly-ions may be calculated as a function of concentration. From the results obtained (*Figure 4*) it is evident that PVP-HCl in pure water as solvent is extensively hydrolysed with only 15 to 20 per cent of the pyridinium groups remaining in the charged form in very dilute solution. Similar high values for the degree of hydrolysis have been obtained from conductance measurements. If the poly-ion at high dilutions is hydrolysed to a large extent, the contribution of the poly-ion to the conductance may be neglected and if the

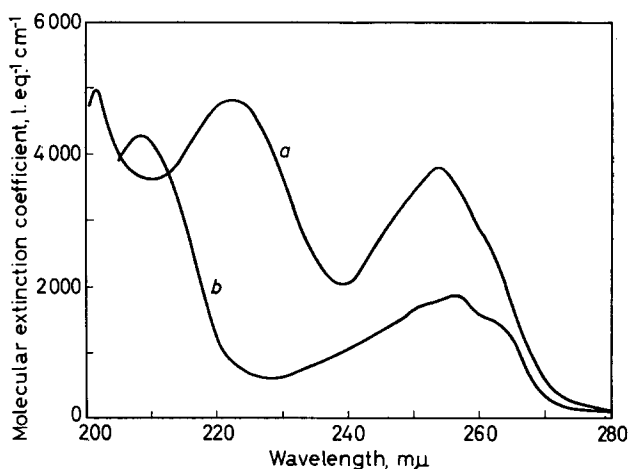


Figure 3—Absorption spectra of PVP in different solvents: a 0.1 M hydrochloric acid, b ethanol

effect of counterion binding is also neglected the conductance of the solution may be attributed, to a first approximation, to that of the hydrogen and chloride ions only. The errors introduced by the two assumptions are to some extent mutually compensatory. The values of the degree of hydrolysis calculated in this way (Figure 4) again indicate that 80 to 85 per cent of the pyridinium groups are hydrolysed. Further evidence for the extensive hydrolysis of PVP-HCl in aqueous solution has been obtained from pH measurements.

On the basis of the above results it would appear that the previously described discontinuous dependence of hydrodynamic properties on concentration^{1,2} is caused by changes in the shape of the kinetic unit in solution

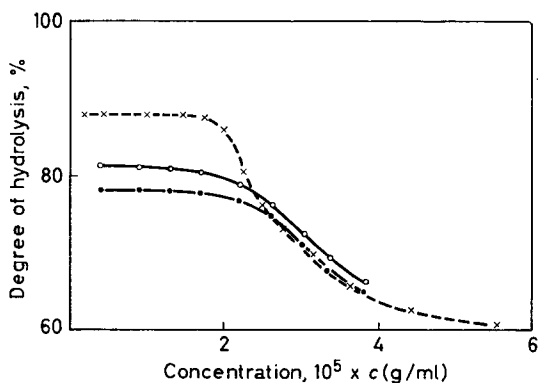


Figure 4—Variation of the degree of hydrolysis of PVP-80 per cent hydrochloric acid with concentration: X, determined from conductance measurements (sample E6); determined from molecular extinction coefficients, O, at 225 mμ, ● at 255 mμ (sample R1)

due to changes in the degree of hydrolysis¹⁶ and hence in the charge of the poly-ion as the concentration is altered. Owing to the experimental difficulties of observing the properties of very dilute solutions, the nature of the kinetic unit at concentrations below γ_0 has not been studied in detail. However, the intrinsic viscosity in ethanol of one fraction of PVP is 410 ml/g, while the same material in its polyelectrolyte form in pure water at a concentration below γ_0 has a reduced viscosity of less than 40 ml/g (extrapolation to give the intrinsic viscosity is not possible for the polyelectrolyte in pure water as solvent). A similar marked reduction of the intrinsic viscosity has been observed for styrene-maleic acid copolymers¹⁷ in transferring from a θ solvent to an acid aqueous solution. Accordingly, the polyelectrolyte at concentrations below γ_0 must be regarded as a tightly coiled structure. Since water is a non-solvent for uncharged PVP and since below the point of discontinuity only about 15 per cent of the original electrolyte groups will carry charges, this contraction of the polymer to well below the size that corresponds to a random chain configuration may be attributed to the hydrophobic bonding mechanism discussed by Kauzmann¹⁸ for proteins. The polyelectrolyte unit at very low charge may thus be regarded as being an essentially spherical structure from the interior of which water is excluded. Coagulation of this system would be prevented by the presence of the charges on the particles. The apparent constancy of the degree of hydrolysis below γ_0 (Figure 4) could be explained if the remaining charged groups were buried inside the compact structure, either as such or intramolecularly hydrogen bonded, and thus inaccessible to the solvent.

The hydrodynamic behaviour previously described^{1,2} can be satisfactorily interpreted on the basis of the change in shape accompanying dilution. Thus the maxima observed in the curve relating reduced viscosity with concentration for solutions of PVP-HCl in pure water may be explained in the following way. With increasing dilution there will be two opposing effects. The poly-ions will at first expand on dilution due to the decrease in the screening effect of the counterions on the intramolecular electrostatic repulsion but as dilution proceeds, hydrolysis will increase with a consequential decrease in the number of charged groups, and hence a decrease in the intramolecular repulsion leading finally to a contraction of the poly-ion. At very low concentrations (corresponding to γ_0) where hydrolysis is high, the polyelectrolyte will collapse to a compact sphere such that the viscosity contribution will approach the Einstein limit. The increase of γ_0 for PVP-HCl with temperature¹ and the decrease on the addition of hydrochloric acid and sodium chloride² is also in agreement with the hydrolysis mechanism.

We wish to acknowledge the assistance of Mr B. C. Simpson who carried out many of the spectral measurements, and the award of a Commonwealth Postgraduate Scholarship to R.L.D.

*Department of Physical and Inorganic Chemistry,
The Johnson Laboratories, University of Adelaide,
Adelaide, South Australia.*

(Received October 1964)

REFERENCES

- ¹ JORDAN, D. O. and KURUCSEV, T. *Polymer, Lond.* 1960, **1**, 193
- ² JORDAN, D. O. and KURUCSEV, T. *Polymer, Lond.* 1960, **1**, 202
- ³ BERKOWITZ, J. B., YAMIN, M. and FUOSS, R. M. *J. Polym. Sci.* 1958, **28**, 69
- ⁴ BURLEIGH, J. E., MCKINNEY, O. F. and BARKER, M. G. *Analyt. Chem.* 1959, **31**, 1684
- ⁵ FITZGERALD, L. B. and FUOSS, R. M. *J. Polym. Sci.* 1954, **14**, 329
- ⁶ BOSWORTH, P., MASSON, C. R., MELVILLE, H. W. and PEAKER, F. W. *J. Polym. Sci.* 1952, **9**, 565
- ⁷ OVERALL, D. W. and PEAKER, F. W. *Makromol. Chem.* 1959, **33**, 222
- ⁸ See, for example, STACEY, K. A. *Light Scattering in Physical Chemistry*. Butterworths: London, 1956
- ⁹ CONNON, D. J. *J. Colloid Sci.* 1960, **15**, 408
- ¹⁰ See, for example, HUQUE, M. M., JAWORZY, J. and GORING, D. A. *J. Polym. Sci.* 1959, **39**, 9
- ¹¹ CECIL, R. and OGSTON, A. G. *J. sci. Instrum.* 1951, **28**, 253
- ¹² HAUPT, G. W. *J. opt. Soc. Amer.* 1952, **42**, 441
- ¹³ INMAN, R. B. and JORDAN, D. O. *Biochim. biophys. Acta*, 1960, **42**, 421
- ¹⁴ ZIMM, B. H. *J. chem. Phys.* 1948, **16**, 1093 and 1099
- ¹⁵ VRIJ, A. and OVERBEEK, J. TH. G. *J. Colloid Sci.* 1962, **17**, 570
- ¹⁶ ALFREY, T. and MORAWETZ, H. *J. Amer. chem. Soc.* 1952, **74**, 436
- ¹⁷ DANNHAUSER, W., GLAZE, W. H., DUELTGEN, R. L. and NINOMIYA, K. *J. phys. Chem.* 1960, **64**, 954
- ¹⁸ KAUZMANN, W. *Advances in Protein Chemistry*, 1956, **14**, 1

Yield Stress Behaviour of Polymethylmethacrylate

J. A. ROETLING

The yield stress behaviour of polymethylmethacrylate over a fairly wide range of strain rates and temperatures is described by the Ree-Eyring modification of the Eyring viscosity theory. Two rate processes are involved and the activation energies determined for these processes are in good agreement with values reported from other types of measurements. The two processes observed probably correspond to different degrees of freedom of the asymmetric molecular segments.

TENSILE stress/strain curves, obtained at constant rate of straining on unoriented polymers, frequently exhibit a well defined maximum stress at a strain which may be considerably less than the break or rupture strain. A well known characteristic of this maximum or yield stress is that the time rate of change of stress is zero although the strain is increasing at a constant rate*. That is, the yield point has the appearance of a momentary condition of pure viscous flow. Generally the yield stress increases with increase in strain rate but the apparent viscosity decreases. Possibly because of this obvious non-linearity, the yield stress behaviour of polymers has not received as much attention as have other types of mechanical behaviour. However, Robertson¹ has shown that the variation of the yield stress of polybisphenol-A carbonate with strain rate and temperature can be described by the Eyring² viscosity equation. Similar studies at this laboratory have indicated that the Eyring model is applicable to a number of polymers, although it is frequently necessary to assume that two processes are involved, these being combined as in the Ree-Eyring³ modification of the theory. It is the purpose of this paper to present the results obtained on polymethylmethacrylate (PMMA) and to compare these with results that have been reported for other types of measurements.

THE MODEL

At the yield point of a stress/strain curve, a condition momentarily exists wherein the deformation is proceeding at a constant strain rate but the time rate of change of stress is zero. Because this set of conditions exists, it is possible to analyse the motion of the molecular segments in a manner very similar to Eyring's approach to viscosity†. Therefore, following the procedure of Eyring, one may derive an equation relating the yield stress to the strain rate and temperature.

*In some cases necking may start at the yield point, but up to yield the strain and rate appear to be uniform over the length of the specimen.

†From tensile work recovery type measurements on PMMA, it has been observed that a plot of recovered energy as a function of input energy has zero slope at the point corresponding to the yield point. Therefore, at the yield point, energy is being dissipated, or otherwise being made unavailable, at the same rate that energy is being supplied to the system. Since PMMA is not known to undergo any changes (such as crystallite formation) which might inhibit recovery, this suggests that the deformation process at this point is nearly purely dissipative. However, the assumption of a purely dissipative process is not essential to the analysis which follows.

This equation may be extended, as was done by Ree and Eyring³, to the case where more than one species of flow unit exists on the shear surface. In this case it is assumed that all species of flow units move at the same average rate, the stresses being additive. This allows for the possibility of more than one process being involved in the flow, but whether the processes actually correspond to different species of flow units or to a single species possessing several degrees of freedom is a matter of interpretation and as such need not be considered at this point.

Following the procedure outlined above, one arrives at an equation of the form

$$(\sigma/T) = \sum_i (1/A_i) \sinh^{-1} \{(C_i \dot{\epsilon}/T) \exp(\Delta H_i/RT)\} \quad (1)$$

where σ denotes yield stress (dynes cm⁻²), $\dot{\epsilon}$ is strain rate (sec⁻¹), T is the temperature (°K) and the A_i , C_i and ΔH_i are constants. The ΔH_i are the activation energies of the various processes involved and the C_i contain the entropies. Two approximations which are sometimes useful in working with the above equation are:

$$\sinh X \simeq X, \text{ if } X \leq 0.25 \quad (2)$$

and

$$\sinh X \simeq \frac{1}{2} \exp(x), \text{ if } X \geq 3.5 \quad (3)$$

Considering a single process, the first of these approximations applies in the Newtonian flow region. In a region where the second approximation applies, the yield stress will increase linearly with the log of the strain rate. If more than one process is involved in the flow but the second approximation applies to all of the processes, the total stress will again increase linearly with the logarithm of the strain rate. If measurements happen to be confined to this region, it is not possible to determine whether more than one process is involved. If more than one process is involved, the apparent activation energy in this region, ΔH_0 , is related to the activation energies of the individual processes by

$$\Delta H_0 = [\sum_i (\Delta H_i/A_i)] / [\sum_i (1/A_i)] \quad (4)$$

Because of this it is important that a wide range of rates and temperatures be examined or it may not be possible to separate the processes, if indeed more than one is involved. Further, the apparent activation energy obtained from a combination of two or more processes may appear unrelated to activation energies obtained from other types of measurements.

In the tensile measurements on PMMA which are described below, it has been necessary to assume that two processes are involved. Primarily as a matter of convenience, the higher activation energy process will be referred to as the α -process and the lower energy process as the β -process.

EXPERIMENTAL

Some physical characteristics of the PMMA sample used in this investigation are given in *Table I*. This sample contained none of the stabilizers, lubricants, etc. which are frequently found in commercially available material. Also, no comonomer was used in its preparation, whereas many

YIELD STRESS BEHAVIOUR OF POLYMETHYLMETHACRYLATE

commercial 'PMMA' samples are copolymers, albeit the MMA content is high.

Test specimens were injection-moulded bars, the test sections of which were approximately square in cross section (about 0.6 cm × 0.6 cm). A long (11.2 cm) test specimen with rather sharply flared ends was used in order to minimize end effects. Strain and strain rates were calculated from the

Table 1. Sample characterization

[η] Acetone	0.436	\bar{M}_w	3.22×10^5
\bar{M}_r Acetone	2.3×10^5	\bar{M}_n	1.60×10^5
[η] Benzene	0.670	\bar{M}_w/\bar{M}_n	2.01
\bar{M}_v Benzene	2.56×10^5		

crosshead displacement, which was measured as a function of time. Yield strains obtained in this manner at low strain rates were in good agreement with values obtained using an extensometer at the same rate. Yield stresses were based on the calculated cross section at the yield strain, this calculation involving the assumption of no change in volume. The small error in the stress, which results from failure to take volume change into account, results in a correspondingly small error in the constants A_i , but does not affect the remaining constants. Yield stress at constant strain rate was measured as a function of strain rate and temperature over approximately six decades of rate and at temperatures from 30° to 90°C. The usual precautions¹ to ensure adequate instrument response, particularly at the higher test rates, were observed. Since PMMA will usually fracture before yielding when tested at low temperatures and moderate to high strain rates, it was not possible to measure the yield stress over the entire range of available rates at all temperatures.

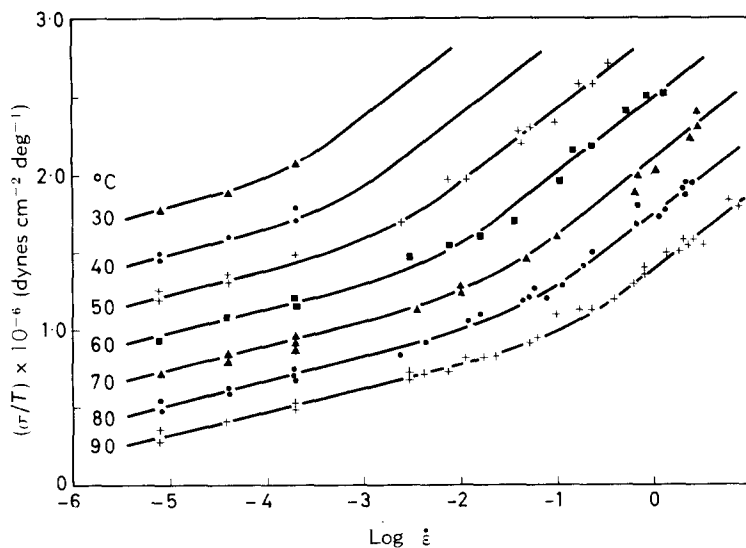


Figure 1—PMMA measurements in the region covered by equation (3)

The results of the measurements on the PMMA sample are shown in *Figure 1*, where the quantity (σ/T) is plotted against $\log \dot{\epsilon}$. The ratio σ/T was plotted in preference to stress since this should give a family of parallel curves in the region where the approximation given by equation (3) applies to both processes. The solid curves drawn through the data were calculated from equation (1) using the constants given in *Table 2*. It is seen that the fit of the equation to the data is quite good. This does not mean, however,

Table 2. PMMA constants

Process	α	β	A	15×10^{-6}	7.2×10^{-6}
ΔH (kcal/mole)	81	24	$\log_e C$	-90	-25

that these constants necessarily give the best fit. The constants were first estimated by assuming that equation (3) was applicable to both processes at the highest strain rates but that at the lowest rates and highest temperatures the stress was due primarily to the α -process. The estimates thus obtained were used in equation (1) to calculate the stress as a function of rate and temperature and the resultant curves were then compared with the data. From this comparison the estimated values of the constants were revised and the process repeated until a reasonably good fit was obtained. The availability of a digital computer made this a fairly rapid procedure and the values given in *Table 2* were obtained in only three or four trials. However, it is apparent that a better method would be highly desirable. Also in view of specimen to specimen variability, a wider range of rates and temperatures would improve the accuracy with which the constants can be determined.

DISCUSSION

In comparing the results obtained from the above described yield stress measurements with the results reported for other types of measurements on PMMA, it should be borne in mind that rather large differences may, and probably do, exist among the PMMA samples used by various investigators. Unfortunately, the composition of the samples used is frequently unknown. As mentioned above, 'PMMA' samples frequently contain a few per cent of a second material as a copolymer, plus various additives. In addition, the molecular weight of cast sheet, which is frequently used, is more than an order of magnitude greater than that of moulding powder. How much influence these factors have is uncertain, but some are known to affect physical properties. In addition to these sample differences, care must be exercised in interpreting the slope of an Arrhenius rate plot as an 'activation energy'. As was recently demonstrated by McCrum and Morris⁵, such apparent activation energies may be somewhat in error as the result of variation of equilibrium compliances (or moduli) with temperature.

One of the more interesting comparisons that may be made is with the creep measurements of Sherby and Dorn⁶ who measured the change in creep rate due to a sudden temperature change. Except for a relatively minor difference in temperature dependence, the equation which they applied to their measurements was similar to that obtained from equation (1) under the condition that equation (3) applies to both processes. When this approximation is valid, an apparent activation energy of 43 kcal/mole is obtained

from the yield stress measurements (i.e. using the constants given in Table 2). From creep measurements at low temperatures (-10° to $+40^{\circ}\text{C}$), where this approximation is also reasonable (for the creep rates reported), Sherby and Dorn obtain an apparent activation energy of 48 kcal/mole, which agrees fairly well. At temperatures above 40°C , the apparent activation energy obtained from the creep measurements increased with increase in temperature and reached a maximum of about 100 kcal/mole at 140°C . This is essentially what would be expected from equation (1). At the lower temperatures the approximation given by equation (3) applies to both processes, but as the temperature is increased a point is reached where equation (3) still applies to the α -process but equation (2) applies to the β -process. At this point the α -process is dominant, equation (1) is again very similar to the equation used with the creep data, and the apparent activation energy is nearly equal to ΔH_{α} . It appears, therefore, that the creep data can also be described as the resultant of two processes having activation energies of roughly 20 kcal/mole and 100 kcal/mole. Except that ΔH_{α} from the creep measurement appears to be somewhat higher than the value obtained from the yield stress (100 as compared to 80 kcal/mole) the two measurements are in good agreement. This difference, if real, could be due to sample differences since the material used in the creep experiments appears to be cast sheet and hence to have much higher molecular weight. A comparison of constants other than activation energy was not made since these were not strictly comparable. This is because equation (1) applies to a pure viscous or 'steady state' flow whereas the creep involved only anelastic flow. As a result, equation (1) may be applied to the creep data but, as no other provision has been made for the effect of restoring forces, some of the 'constants' must be made variable to account for the variation of creep rate with time.

In addition to the above, other types of measurements have yielded comparable results. From dielectric measurements, the values of ΔH_{β} and ΔH_{α} have been reported^{7,8} to be about 20 to 23 kcal/mole and near 100 kcal/mole respectively. Dynamic mechanical measurements^{9,10} have given similar results and Deutsch *et al.* obtained a value of about 80 kcal/mole for ΔH_{α} from tensile modulus measurements. This last is essentially the same as obtained from the yield stress. The measurements in this case were similar except for making use of a different region of the stress/strain curve, but whether or not the samples were similar in molecular weight is not known.

Exceptionally poor agreement is obtained when the results of the yield stress measurements are compared with those obtained from creep compliance measurements¹¹ by means of the time/temperature shifting technique. However, there appears to be a good reason for this difference. The creep compliance measurements gave an apparent activation energy which increased from about 50 kcal/mole at 60°C to a maximum of about 250 kcal/mole at 110°C and then decreased to about 30 kcal/mole at 160°C . If, as indicated by other measurements, there are two processes involved in creep, then the contribution to the compliance of the high activation energy process may be 'frozen' out at low temperatures but go to completion in

very short times at high temperatures. Here one would expect the apparent activation energy, as obtained from the time/temperature shifting, to approach the value for the β -process at both very high and very low temperatures. At some intermediate temperatures the time dependent compliance will be affected by both processes and the apparent activation energy will go through a maximum. However, in a region where two processes having different activation energies are both contributing significantly to the time rate of change of the compliance, the time/temperature shifting technique is not valid and, except over a short time interval, difficulty will be experienced in superimposing curves obtained at different temperatures. Because of this it is difficult to estimate the maximum apparent activation energy that might be expected. Thus the difference in results is a reflection of the difference in the methods of data analysis used. Poor agreement would also be expected with viscosity measurements obtained¹¹ by subtracting the creep recovery curve from the creep curve since the material used in the present study, like that used by Sherby and Dorn, showed no nonrecoverable flow. It appears, therefore, that any differences between creep and creep recovery curves of PMMA of a molecular weight of 2×10^5 or higher (at temperatures $\leq 100^\circ\text{C}$) may be due to failure to allow sufficient time for the creep to attain a steady state.

In considering the molecular motions connected with the observed dispersion, it has long been recognized that the α -process is associated with the glass transition and hence is usually ascribed to 'main chain motion'. Having made this assignment, it is necessary to find some other motion to connect with the β -process and the side chain offers the most obvious choice. There have been many good reasons for ascribing the β -process to 'side chain motion', and certainly the side chain is involved, but the important question of how it is involved has remained. Usually the β -process is considered as a rotation of the side chain, or a portion thereof, relative to the main chain. Integrated infra-red absorbance measurements, made by Havriliak¹² on syndiotactic PMMA as a function of temperature, have indicated that the ester side chain may exist in one of two discrete positions. The variation of the integrated absorbance ratio with temperature, at temperatures above the glass transition temperature, indicated an energy difference of about 0.8 kcal/mole between the two positions. However, below the glass temperature this ratio was constant and by rapid quenching could be 'frozen' at a value corresponding to a higher temperature, indicating that a rather large potential barrier separates the two sites. From these infra-red measurements plus dielectric studies, Havriliak concluded that the β -dispersion could not be due to a side-chain rotation relative to the main chain but is probably due to either a twisting or rotation of the main chain about its longitudinal axis. Thus it appears probable that the observed dispersions are due to different degrees of freedom of the molecular segments, the β -process corresponding to a rotation about the longitudinal axis of the segment and the α -process probably involving a rotation about an axis perpendicular to the longitudinal axis.

From Havriliak's observations that no side-chain rotation occurs below the glass temperature and that a 'supercooled' sample also showed no change (over 24 hours) at a temperature of 100°C (at which temperature the

relaxation time for the β -process should be very short), it appears that side-chain rotation, if related to either process, may be more nearly associated with the α -process. This suggests that side-chain rotation may occur only at a bend in the main chain (i.e. when a segment rotates relative to its immediate neighbours in the same chain). It is also quite possible that the increase in free volume above the glass temperature is directly related to conformational changes such as those noted.

The author is greatly indebted to Mr W. W. Moore for assistance in data collection and reduction, to Mr L. R. DeFonso for computational assistance and to Dr S. Havriliak for many stimulating discussions during the course of this work.

*Rohm and Haas Company,
Research Laboratories,
P.O. Box 219, Bristol, Pa*

(Received October 1964)

REFERENCES

- ¹ ROBERTSON, R. E. *J. appl. Polym. Sci.* 1963, **7**, 443
- ² GLASSTONE, S., LAIDLER, K. J. and EYRING, H. *The Theory of Rate Processes*, pp 480-483. McGraw-Hill: New York, 1941
- ³ REE, T. and EYRING, H. *J. appl. Phys.* 1955, **26**, 793
- ⁴ BALLOU, J. W. and ROETLING, J. A. *Text. Res. J.* 1958, **28**, 631
- ⁵ MCCRUM, N. G. and MORRIS, E. L. *Proc. Roy. Soc. A*, 1964, **281**, 258-273
- ⁶ SHERBY, O. D. and DORN, J. E. *J. Mech. Phys. Solids*, 1958, **6**, 145
- ⁷ STUART, H. A. *Die Physik der Hochpolymeren*, Vol. 4. Springer: Berlin, 1956
- ⁸ DE BROUCHERE, L. and OFFERGELD, G. *J. Polym. Sci.* 1958, **30**, 105
- ⁹ BECKER, G. W. *Kolloidzshr.* 1955, **140**, 1
- ¹⁰ DEUTSCH, E., HOFF, E. A. W. and REDDISH, W. *J. Polym. Sci.* 1954, **13**, 565
- ¹¹ BUECHE, F. *J. appl. Phys.* 1955, **26**, 738
- ¹² HAVRILIAK, S. Unpublished data

Thermal Degradation of an Aromatic Polypyromellitimide in Air and Vacuum III—Pyrolytic Conversion into a Semiconductor

S. D. BRUCK

The pyrolytic conversion of poly[N,N'-(p,p'-oxydiphenylene) pyromellitimide] to semiconducting products is discussed as supported by data on electron paramagnetic resonance (e.p.r.) absorption, specific resistivity, weight loss, density, and composition. Specific resistivities as low as 10 to 0.05 ohm cm were obtained by vacuum pyrolysis between 620° and 850°C with a simultaneous increase in density to 1.65 g/cm³. The region between 575° and 620°C was characterized by no further appreciable weight loss, increase in density, and a sharp drop in the specific resistivity. These changes could be related to an internal reorganization of the polymer to semiconducting products, for which an activation energy of 25 ± 3 kcal was calculated. The development of semiconduction in the pyrolysates occurs well below the graphitization temperature and with the retention of considerable quantities of nitrogen and oxygen. The results are explained in terms of increased mobility of current carriers facilitated by enhanced π -orbital overlap, which in turn arises from a molecular reorganization and fusion process at sufficiently high temperatures.

PREVIOUS publications¹⁻⁴ dealt with the thermal degradation of poly-[N,N'-(p,p'-oxydiphenylene)pyromellitimide] in air and vacuum and with the nature of the volatile degradation products. When subjected to vacuum pyrolysis this polymer does not volatilize completely but yields a residue that constitutes approximately 60 per cent of the original sample weight and which retains the dimensional integrity of a film.

Several years ago Winslow and his colleagues demonstrated that the non-volatile pyrolytic degradation products of polyvinylidene chloride and pre-oxidized polyvinylbenzene exhibit semiconducting properties (specific resistivity $< 10^7$ ohm cm), and showed that this phenomenon is accompanied by remarkable changes in the electron paramagnetic resonance (e.p.r.) absorption of the pyrolysis products^{5,6}. Recently, Topchiev reported that the pyrolytic condensation product of polyacrylonitrile exhibits semiconducting properties⁷. Similar observations have also been made with non-pyrolytic polymers, including polymers of phthalocyanine⁸, polyphenyleneaminoquinone⁷, polyphenylenequinone⁷, and the iodine complex of poly-*p*-phenyl⁹. Among non-polymeric organic substances, Kepler¹⁰ recently reported very high conductivity (specific conductivity of 100 ohm⁻¹ cm⁻¹) for salts of tetracyanoquinodimethane (TCNQ). In 1953 Eley *et al.*¹¹ published semiconductivity data for several organic substances including coronene, anthracene, isodibenzanthrone, and also plasma albumin, fibrinogen and edestin. These last three materials are of biochemical importance and their study was stimulated by the suggestion of Albert Szent-Györgyi that mobile electrons in proteins could lead to semiconduction in living systems¹².

The object of this paper is to discuss the pyrolytic conversion of poly[*N, N'*-(*p, p'*-oxydiphenylene)pyromellitimide] to semiconducting products in terms of data on e.p.r. absorption, specific resistivity, weight loss, density and composition.

EXPERIMENTAL DETAILS

For pyrolysis and e.p.r. absorption studies approximately 32 mg film (0.002 inch thick) samples of poly[*N, N'*-(*p, p'*-oxydiphenylene)pyromellitimide] were used (so-called 'H'-film of E. I. du Pont de Nemours and Company, Inc.). The film sample (cylindrical in shape) was placed in a quartz tube (length: 12 in., outside diameter: $\frac{3}{8}$ in.) which was equipped with a vacuum stopcock and a joint for connection to a high vacuum manifold. After evacuation to a pressure of approximately 5×10^{-6} torr, a preheated electric furnace was raised and the sample pyrolysed for specific periods. Accurate temperature control of $\pm 1^\circ\text{C}$ was maintained by means of chromel-alumel thermocouples and an electronic thermoregulator. At the end of the pyrolysis the vacuum stopcock was closed and the tube containing the pyrolysed sample was placed in a Dewar flask filled with liquid nitrogen.

The e.p.r. absorption measurements were conducted within one to three hours after the completion of the pyrolysis. The evacuated quartz tube was transferred from its storage Dewar flask into a Dewar assembly containing liquid nitrogen and situated between the poles of the electromagnet of the microwave equipment. The e.p.r. absorption measurements were carried out at a frequency of 9 140 Mc/s. The derivative curve that appeared on the recorder was manually integrated with a planimeter and the results expressed in arbitrary units. Calibration with a crystal of 2,2-diphenyl-1-picrylhydrazyl and subsequent correction for the geometrical shape factor of the sample showed that one arbitrary unit corresponds to approximately $3.5 \times 10^{14} \pm 20$ per cent spins. In order to avoid complications arising from the small variations of sample weights in each experiment, the relative e.p.r. absorptions were corrected to the overall average weight (32.6 mg) of all samples used in the e.p.r. studies.

Specific resistivity measurements were carried out by the radio frequency induction method (50 Mc/s) at atmospheric pressure and at room temperature, as described by Poehler and Liben¹³. This method is applicable only to samples having relatively low specific resistivities and hence the measurements were restricted to the region of < 100 ohm cm. In order to utilize fully the induction method it is essential that the film samples be reasonably flat. Therefore, separate pyrolysis experiments were carried out at 620°, 700°, 800° and 850°C in a quartz tube equipped with a quartz plunger. The weight of this plunger prevented the film samples from 'curling up' during the pyrolysis and facilitated the retention of their original flat shape.

Density measurements were carried out by the flotation method.

Elemental microanalyses were performed by the Schwarzkopf Micro-analytical Laboratory, Woodside 77, New York.

RESULTS AND DISCUSSION

The relative e.p.r. absorption (in arbitrary units) as a function of time of pyrolysis at various temperatures and the corresponding weight loss are

THERMAL DEGRADATION OF AN AROMATIC POLYPYROMELLITIMIDE III

 Table I. Summary of e.p.r. absorption data on the pyrolysates of poly-
 [*N,N'*-(*p,p'*-oxydiphenylene) pyromellitimide]

Temperature (°C)	Time (h)	Wt of sample (mg)	Wt of pyrolysate (mg)	Weight loss %	Relative e.p.r. absorption* (arb. units)	No. of spins (per g pyrolysate) (±20%)	Δ <i>H</i> (points of max. slope) (gauss)
550	1.0	34.3	24.7	28.0	113	1.6 × 10 ¹⁸	6.7
550	2.0	32.2	21.9	32.0	151	2.4 × 10 ¹⁸	7.5
550	3.0	31.3	21.2	32.3	463	7.6 × 10 ¹⁸	6.6
550	3.5	33.9	22.7	33.0	1987	3.0 × 10 ¹⁹	6.6
550	4.0	33.2	22.0	33.7	1215	1.9 × 10 ¹⁹	6.9
550	4.5	33.1	21.5	35.0	1393	2.2 × 10 ¹⁹	6.4
550	5.0	33.6	21.7	35.4	1164	1.9 × 10 ¹⁹	5.5
550	6.0	32.2	20.7	35.7	261	4.4 × 10 ¹⁹	6.3
575	0.5	34.4	24.1	29.9	379	5.5 × 10 ¹⁹	7.6
575	1.0	31.7	—	—	593	—	7.6
575	1.5	33.5	22.3	33.4	2318	3.6 × 10 ¹⁹	6.5
575	2.0	33.3	20.6	38.1	2235	3.8 × 10 ¹⁹	5.3
575	3.0	34.8	21.5	38.2	3170	5.1 × 10 ¹⁹	6.2
575	4.0	32.8	20.4	37.8	2675	4.6 × 10 ¹⁹	5.8
575	5.0	31.2	19.4	37.8	2456	4.4 × 10 ¹⁹	6.6
590	0.25	33.9	23.5	30.7	1141	1.7 × 10 ¹⁹	8.2
590	0.5	33.7	22.0	34.7	1677	2.7 × 10 ¹⁹	6.7
590	1.0	33.7	22.3	33.8	1804	2.8 × 10 ¹⁹	6.5
590	1.5	33.0	21.4	35.2	2709	4.4 × 10 ¹⁹	5.7
590	2.0	33.4	20.7	38.0	2683	4.5 × 10 ¹⁹	4.7
590	2.5	33.8	—	—	3029	—	6.5
590	3.0	33.6	21.0	37.5	2861	4.8 × 10 ¹⁹	7.4
620	0.5	30.2	19.6	35.1	1551	2.7 × 10 ¹⁸	7.4
620	1.0	31.4	20.3	35.4	1921	3.3 × 10 ¹⁹	7.1
620	2.0	29.4	18.3	37.8	3052	5.2 × 10 ¹⁸	4.5
620	3.0	30.2	19.1	36.8	3387	6.2 × 10 ¹⁹	6.8
620	6.0	30.5	18.3	40.0	2922	5.5 × 10 ¹⁹	6.2

* The relative e.p.r. absorption was corrected to the overall average weight (32.6 mg) of the samples.

illustrated on *Figures 1 to 4* and summarized in *Table 1*. In general, there is an increase in the microwave absorption with increasing times of pyrolysis. The spin concentration is in the order of 10^{19} spins per gramme of pyrolysate. Most of the weight loss occurs during the early part of the

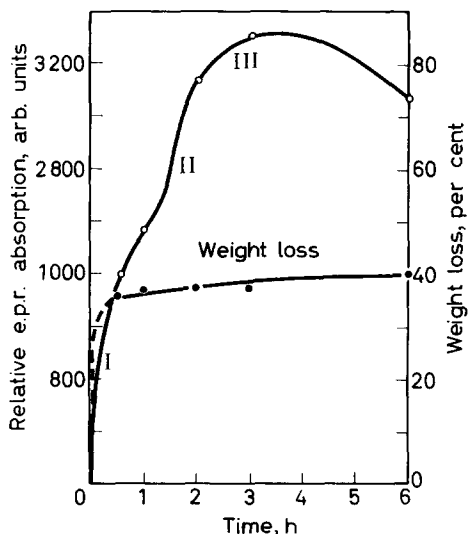


Figure 1—Relative e.p.r. absorption of poly[*N,N'*-(*p,p'*-oxydiphenylene) pyromellitimide] as a function of time of pyrolysis at 620°C

heating and only small changes in weight are observed beyond approximately one hour of pyrolysis at 620°, 590° and 575°C, except in the case of the pyrolysis carried out at 550°C. This is in agreement with the thermogravimetric studies¹⁻⁴. Each e.p.r. absorption versus time curve shows a distinct inflection that occurs during the early part of the pyrolysis. This becomes more pronounced as the temperature of the pyrolysis *decreases*, and roughly corresponds to the levelling off in weight loss. These e.p.r. absorption curves may thus conveniently be divided into three parts (as

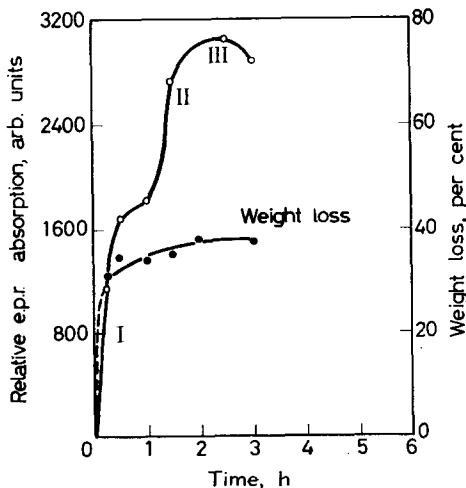


Figure 2—Relative e.p.r. absorption of poly[*N,N'*-(*p,p'*-oxydiphenylene) pyromellitimide] as a function of time of pyrolysis at 590°C

THERMAL DEGRADATION OF AN AROMATIC POLYPYROMELLITIMIDE III

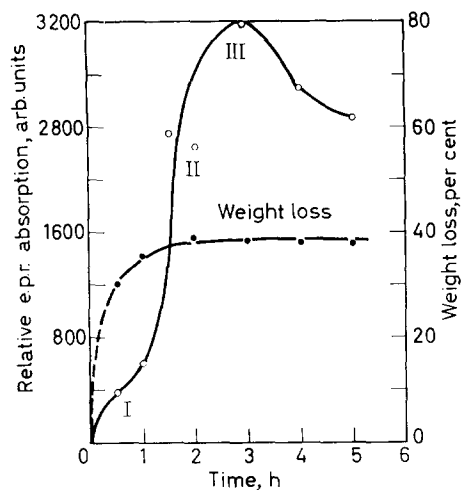


Figure 3—Relative e.p.r. absorption of poly[*N,N'*-(*p,p'*-oxydiphenylene) pyromellitimide] as a function of time of pyrolysis at 575°C

Figure 4—Relative e.p.r. absorption of poly[*N,N'*-(*p,p'*-oxydiphenylene) pyromellitimide] as a function of time of pyrolysis at 550°C

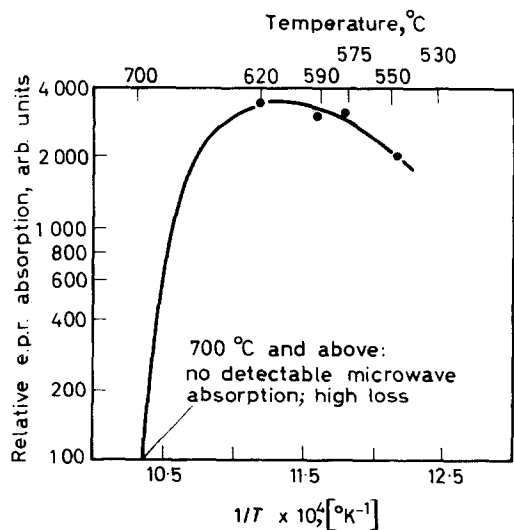
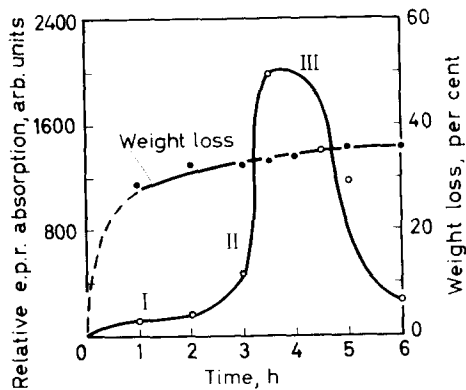


Figure 5—Relative e.p.r. absorption of poly[*N,N'*-(*p,p'*-oxydiphenylene) pyromellitimide] as a function of temperature of pyrolysis

indicated on the figures by Roman numerals). The significance of these regions will be discussed in a later part of this paper.

Figure 5 illustrates the maximum e.p.r. absorption (at a given temperature) as a function of progressively higher temperatures. There is a gradual increase in the microwave absorption with temperature up to 620°C which is followed by a drastic drop. A similar phenomenon was observed by Winslow and his co-workers with pyrolysates of polydivinylbenzene and polyvinylidene chloride⁵, and by Uebersfeld *et al.*¹⁴, Bennett *et al.*¹⁵, and Ingram *et al.*¹⁸ with coals and carbonaceous solids. This drop in the e.p.r. absorption coincides with a sharp decrease in specific resistivity.

Separate experiments were needed to provide resistivity measurements on the pyrolysis products of the polyimide film (see experimental details). Specific resistivity ($= 1/\text{specific conductivity}$) data were obtained on samples pyrolysed at 620°, 700°, 800° and 850°C by the radio frequency induction method (50 Mc/s) as described by Poehler and Liben¹³. The general integrity of the material is retained during heating in a vacuum except for some shrinkage. The pyrolysed film also retains some of its strength although no tensile measurements were conducted in this work.

The specific resistivity as well as density data are illustrated in Figure 6. During the early part of the pyrolysis the density of the original sample drops from 1.426 g/cm³ to approximately 1.330 g/cm³ which coincides

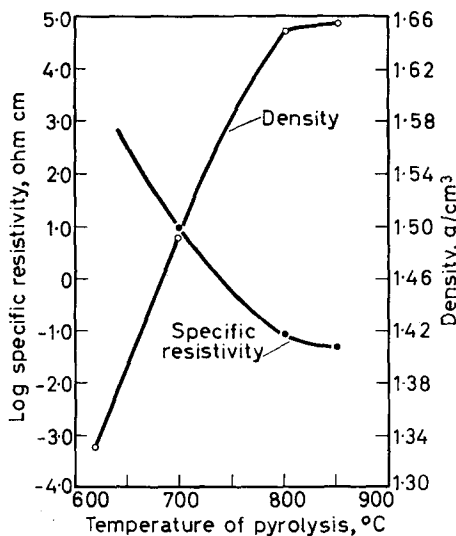


Figure 6—Specific resistivity and density of poly[*N,N'*-(*p,p'*-oxydiphenylene) pyromellitimide] film as a function of temperature of pyrolysis

with the general weight loss by the polymer. During this early period carbon monoxide is given off as the result of the cleavage of the carbonyl groups^{3,4} which is probably accompanied by limited polycondensation of the aromatic rings. Between 620° and 800°C a large increase in density is observed, reaching a plateau at 1.65 g/cm³ with a simultaneous decrease in the specific resistivity. Increased semiconduction (specific resistivity $< 10^7$ ohm cm) appears throughout this region with a levelling off at approximately 5×10^{-2} ohm cm. In this connection it should be noted that

THERMAL DEGRADATION OF AN AROMATIC POLYPYROMELLITIMIDE III

Mrozowski^{17,18}, while studying the electrical properties of carbons, observed a similar rapid drop in resistivity when the carbon was heated to 1 000°C. Essentially no change in resistivity was observed during additional heating up to 2 000°C. Heating from 2 000° to 3 000°C caused a further drop in resistivity from 10^{-2} to the limiting value of 10^{-3} ohm cm as graphitization set in.

Table 2 compares the specific resistivity data of the pyrolysis products of poly[*N, N'*-(*p, p'*-oxydiphenylene)pyromellitimide] with those of polydivinylbenzene as reported by Winslow and co-workers⁵. Although the

Table 2. Specific resistivity of poly[*N, N'*-(*p, p'*-oxydiphenylene)pyromellitimide] (PPMI) and preoxidized polydivinylbenzene (PDVB) pyrolysates as a function of temperature of pyrolysis

Polymer	Vacuum pyrolysis		Sp. resistivity ohm cm, 25°C	Reference
	Temp. (°C)	Time (h)		
PPMI	620	1	*	Bruck (this work)
PPMI	700	1	10	Bruck (this work)
PPMI	800	1	9×10^{-2}	Bruck (this work)
PPMI	850	1	5×10^{-2}	Bruck (this work)
PDVB	500	not given	$10^{1.5}$	Winslow <i>et al.</i> ⁵
PDVB	600	not given	$10^{1.2}$	Winslow <i>et al.</i>
PDVB	700	not given	10^6	Winslow <i>et al.</i>
PDVB	800	not given	1	Winslow <i>et al.</i>
PDVB	1000	not given	10^{-2}	Winslow <i>et al.</i>

*Too high for accurate measurement by induction method.

trend is similar in both cases, it appears that the pyrolysate of the polyimide develops semiconduction at a lower temperature than does polydivinylbenzene. This may be due to the greater number of aromatic rings in the repeat unit of the polyimide in comparison to polydivinylbenzene, the increased tendency of the polyimide to form a polynuclear condensation product, and the consequent earlier development of optimum overlap of π -orbitals. The significance of this will be discussed in greater detail below.

Table 3 summarizes the data on the specific electroconductivities of selected synthetic and pyrolytic polymers and compares these to the specific electroconductivity of TCNQ, a synthetic organic material with the highest conductivity so far reported¹⁰. The high specific electroconductivities of the pyrolysates of poly[*N, N'*-(*p, p'*-oxydiphenylene)pyromellitimide] are among the highest of polymeric materials, and compare favourably even with non-polymeric TCNQ.

In the light of the above experimental evidence, the relative e.p.r. absorption versus time curves (Figures 1 to 4) mentioned earlier may now be discussed in greater detail. The region (II) immediately following the early inflection is characterized by drastic changes: (a) essentially no more weight loss occurs; (b) the density increases, and (c) a sharp drop in the specific resistivity takes place. Apparently an essentially chemical change is superseded by a predominantly physical change within the pyrolysate. This physical change most likely consists of a reorganization and fusion of aromatic rings resulting in increased unsaturation, and facilitating optimum overlap of π -orbitals. That conjugation by *itself* is not sufficient to bring

Table 3. Specific electroconductivity of salts of non-polymeric tetracyanoquinodimethane and selected synthetic and pyrolytic polymers

Sample	Preparation		Sp. electroconductivity* $\text{ohm}^{-1} \text{cm}^{-1}, 25^\circ \text{C}$	Reference
	Synthetic	Pyrolytic		
Tetracyanoquinodimethane	Yes	—	10^2	Kepler ¹⁰
Poly[N,N'-(p,p'-oxydiphenylene)pyromellitimide]	—	Yes	0.2×10^2	Bruck (this work)
Poly(divinylbenzene)	—	Yes	10^2	Winslow <i>et al.</i> ⁵
Poly(acrylonitrile)	—	Yes	10^{-5} to 10^{-7}	Topchiev ⁷
Poly(p-phenylene) iodine complex	Yes	—	4×10^{-5}	Mainthia <i>et al.</i> ⁹
Poly(phenyleneaminoquinone)	Yes	—	7×10^{-7} to 9×10^{-7}	Topchiev ⁷
Poly(phenylenequinone)	Yes	—		
Polymeric copper phthalocyanine	Yes	—	2.5×10^{-2}	Marvel and Rassweiler ⁸

*Specific electroconductivity = $1/(\text{Sp. resistivity})$.

THERMAL DEGRADATION OF AN AROMATIC POLYPYROMELLITIMIDE III

about semiconduction may be seen from the fact that many conjugated molecules are typical insulators. A certain critical condensation of poly-conjugated regions must take place before π -orbital overlap develops to a degree sufficient to permit electronic conduction.

From the above combined evidence it would appear that region (II) of the e.p.r. absorption versus time curves (Figures 1 to 4) is distinctly related to the final transformation of the pyrolysate into semiconducting products. In an attempt to gain further insight into this process, the rates of the e.p.r. absorption ($d\text{e.p.r.}/dt$) were calculated from the e.p.r. absorption versus

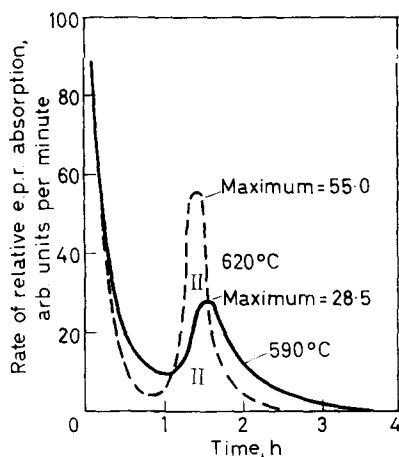
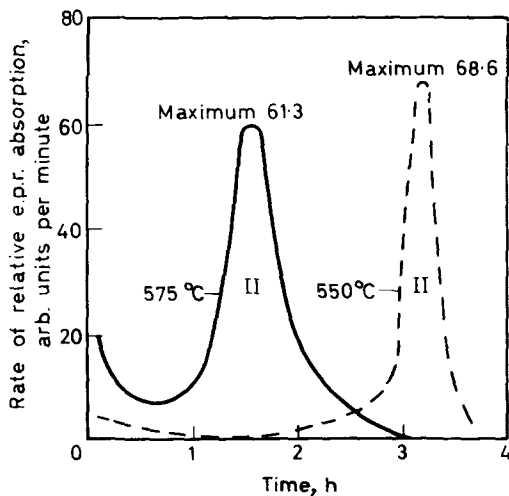


Figure 7—Rate of relative e.p.r. absorption as a function of time of pyrolysis of poly[*N,N'*-(*p,p'*-oxydiphenylene) pyromellitimide] at 620°C and 590°C

time curves with an electronic computer, and are illustrated in Figures 7 and 8. The maxima (II) in the rate curves appear between 90 and 100 minutes for the pyrolyses carried out at 620°, 590° and 575°C. On the other hand, in the pyrolysis at 550°C, the maximum rate of e.p.r. absorption for region (II) appears at approximately 195 minutes. It is possible

Figure 8—Rate of relative e.p.r. absorption as a function of time of pyrolysis of poly[*N,N'*-(*p,p'*-oxydiphenylene) pyromellitimide] at 575°C and 550°C



to demonstrate an Arrhenius type relationship between the logarithm of the maximum rates of the e.p.r. absorption of region (II) and the inverse of the absolute temperature of the pyrolyses, as indicated on *Figure 9*. The maximum rates of e.p.r. absorption for region (II) at the three higher temperatures fall on an approximately straight line, the slope of which yields an activation energy of 25 ± 3 kcal. The maximum rate at 550°C does not fall on the straight line. It is quite possible that this lower temperature is inadequate to bring about the proper degree of polycondensation with sufficient π -orbital overlap for the development of a semiconducting network.

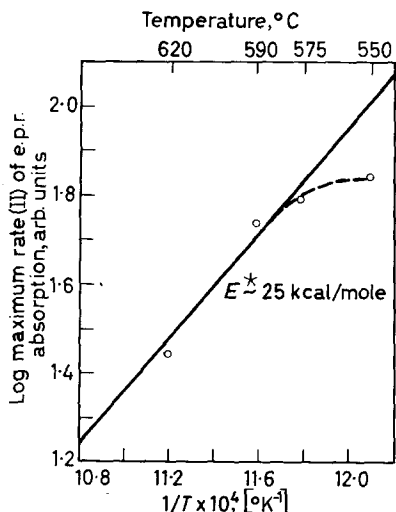


Figure 9—Arrhenius plot for relative e.p.r. absorption of poly[*N,N'*-(*p,p'*-oxydiphenylene) pyromellitimide]

Due to the fact that the transformation of the pyrolysate into a semiconducting system apparently occurs in a rather narrow temperature range, only four points were available for the construction of the plot. Consequently, an unequivocal proof of this apparent Arrhenius type relationship must await further work in this area.

The relative e.p.r. absorption versus time curve (*Figure 1*) shows a drastic drop in the e.p.r. absorption beyond approximately three hours of pyrolysis at 550°C . This is unlike the situation at the higher pyrolytic temperatures (*Figures 2 to 4*) where the curves appear either to level off or to show less drastic downward changes. This is interpreted to mean that at the higher pyrolytic temperatures a continuous network of polyconjugated regions can develop with consequent free radical mobility, whereas at the lower temperature of 550°C such a continuous network does not form. The diminishing of the microwave absorption arises from the pairing of some of the free radicals. This situation should not be confused with the previously discussed sudden drop in e.p.r. absorption above 620°C (*Figure 5*), which phenomenon has been attributed to the onset of semiconduction.

Elemental microanalyses of the pyrolysates indicate progressive carbonization with increasing temperature (*Table 4*). It should be noted, however, that up to 700°C considerable amounts of nitrogen and oxygen are retained

THERMAL DEGRADATION OF AN AROMATIC POLYPYROMELLITIMIDE III

 Table 4. Elemental microanalyses of poly[*N,N'*-(*p,p'*-oxydiphenylene)pyromellitimide] before and after pyrolysis in a vacuum

Vacuum pyrolysis		Elemental microanalysis (%)			
Temperature (°C)	Time (h)	C	H	O	N
NO	NO	67.5	2.8	21.0	7.9
575	1	77.2	3.9	11.0	8.0
575	3	76.9	3.4	11.9	7.4
575	5	76.5	3.2	12.1	7.4
590	1	79.0	3.2	9.5	8.0
590	2	78.2	3.3	11.3	7.7
590	3	78.7	3.2	10.0	7.9
620	3	78.0	3.5	11.1	7.4
620	6	78.9	3.1	12.0	7.2
800	1	77.7	3.2	12.8	7.0

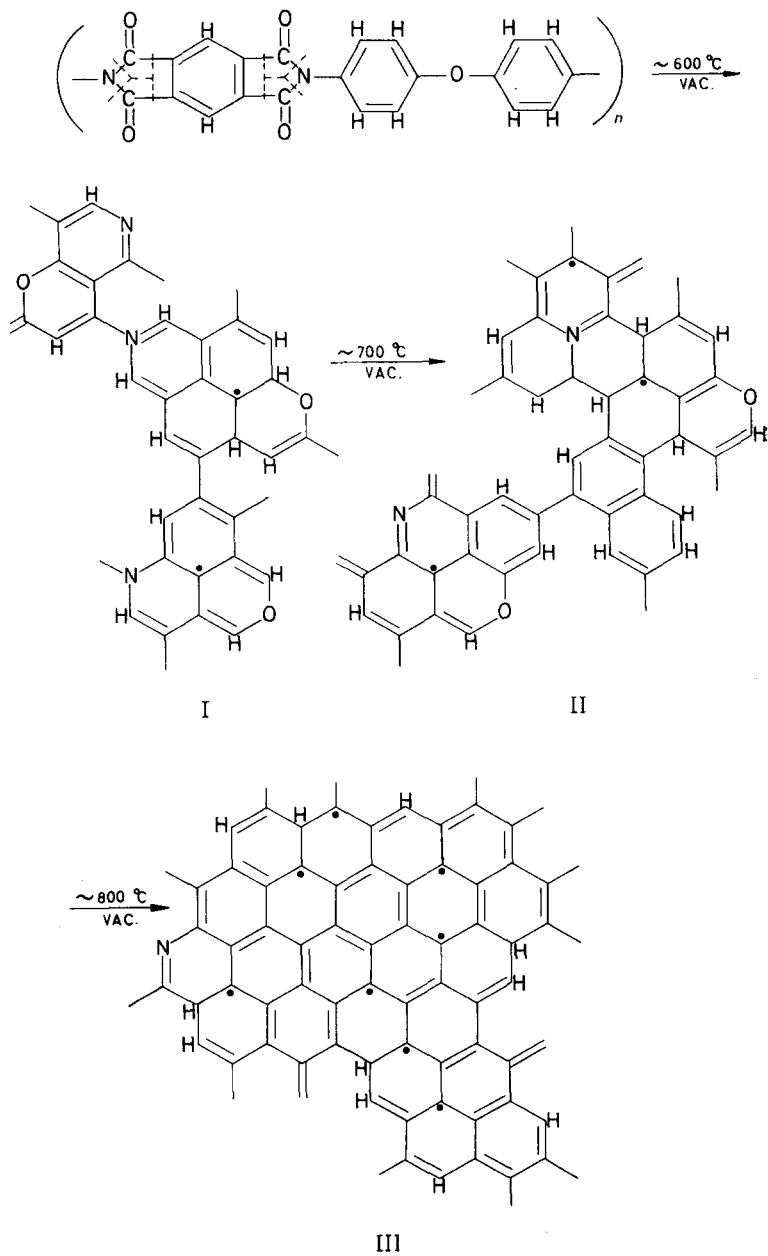
by the pyrolysates. Previous publications¹⁻⁴ have confirmed that carbon monoxide and carbon dioxide are the major degradation products of the pyrolysis, the former most likely arising from the cleavage of the carbonyl groups of the polyimide, whereas the latter originates from a polyamide type of impurity. In the range of 700° to 850°C increased carbonization takes place, and had the pyrolysis been continued at higher temperatures (1 000° to 3 000°C) graphitization would probably have resulted. The fact that semiconduction was observed in samples prepared in the temperature range of 620° to 850°C, and which contained considerable quantities of nitrogen and oxygen, indicates that graphitization is not an essential requirement for semiconduction in pyrolytic polymers.

Based on the above experimental evidence, the pyrolytic conversion of poly[*N,N'*-(*p,p'*-oxydiphenylene)pyromellitimide] to semiconducting products may be illustrated by the scheme shown on page 330.

Most of the weight loss takes place during the early part of the pyrolysis with the cleavage of the carbonyl groups and the formation of semi-isolated regions of condensed polynuclear systems (I). However, as was discussed above, such semi-isolated regions are not sufficient to bring about enough π -orbital overlap to cause semiconduction. During the second stage of the pyrolysis (II) there is an increasing reorganization of the pyrolysate, and the semi-isolated condensed ring systems gradually merge into a continuous network of fused aromatic rings in which an increasingly effective π -orbital overlap develops. At this stage semiconduction sets in (specific resistivity $<10^7$ ohm cm). Further growth in the network of fused polynuclear regions and increasing unsaturation (III) give rise to a still larger increase in semiconductivity.

The specific electroconductivity, σ , may be expressed by the relationship $\sigma = enu$, where e is the electronic charge, n the concentration of current carriers, and u denotes mobility of the carrier.

The above experimental data and discussion support the view that electroconductivity in pyrolytic polymers depends not only on the movement of current carriers *within the individual molecules* but also on the



movement of electrons *from one molecule to another*. Topchiev⁷ showed an exponential dependence of specific electroconductivity on temperature [$\sigma = \sigma_0 \exp(-\Delta E/2kT)$] for the pyrolysis product of polyacrylonitrile, and for the non-pyrolytic polyphenyleneaminoquinone and polyphenylenequinone. If the increase in electroconductivity were due only to an increase in the concentration of current carriers, this would be accompanied by a sharp drop in the differential thermal electromotive force⁷. On the other hand, if the concentration of current carriers is independent of temperature, then the thermal electromotive force will be only weakly dependent on temperature, in agreement with Topchiev's findings. Hence, he concluded that the observed change in specific electroconductivity relative to temperature arises from an increase in the *mobility* rather than in the *number* of current carriers.

An increase in the mobility of current carriers is facilitated by enhanced π -orbital overlap which in turn is brought about by a molecular reorganization and fusion process at sufficiently high temperatures. Eley¹¹ reported that a definite activation energy is associated with crystalline organic materials exhibiting semiconduction and suggested that the excited orbitals of π -electrons in the isolated molecule are combined in mobile orbitals stretching throughout the crystal.

Huggins¹⁹ recently emphasized the great difficulties in attempting to derive quantitative correlations between electrical conductivity of polymeric systems and chemical and physical structures, and pointed out some of the serious experimental problems which have retarded progress in this area. Only by examination of many more polymeric semiconductors of sufficient purity can one hope to arrive at valid proof of the theoretical arguments that have been advanced.

This work is supported by the Bureau of Naval Weapons, Department of the U.S. Navy, under Contract NOW 62-0604-c.

The author thanks Dr E. L. Cochran and Mr V. A. Bowers for the e.p.r. absorption measurements, Dr T. O. Poehler for the specific resistivity measurements, and Mr S. J. Burdick for technical assistance in some phases of this work. The author appreciates the continued encouragement of Dr W. G. Berl.

*Applied Physics Laboratory,
The Johns Hopkins University,
8621 Georgia Avenue,
Silver Spring, Maryland, U.S.A.*

(Received October 1964)

REFERENCES

- ¹ BRUCK, S. D. *Polymer, Lond.*, 1964, **5**, 435
- ² BRUCK, S. D. *Polymer Preprints*, p 148, 147th National Meeting, American Chemical Society, 5 to 10 April 1964, Philadelphia, Pa
- ³ BRUCK, S. D. *Polymer, Lond.*, 1965, **6**, 49
- ⁴ BRUCK, S. D. *Polymer Preprints*, p 466, 148th National Meeting, American Chemical Society, 30 August to 4 September 1964, Chicago, Illinois
- ⁵ WINSLOW, F. H., BAKER, W. O. and YAGER, W. A. *J. Amer. chem. Soc.* 1955, **77**, 4751

S. D. BRUCK

- ⁶ WINSLOW, F. H., BAKER, W. O., PAPE, N. R. and MATREYEK, W. J. *Polym. Sci.* 1955, **16**, 101
- ⁷ TOPCHIEV, A. V. *J. Polym. Sci.* 1963, **A1**, 591
- ⁸ MARVEL, C. S. and RASSWEILER, J. H. *J. Amer. chem. Soc.* 1958, **80**, 1197
- ⁹ MAINTHIA, S. B., KRONICK, P. L., UR, H., CHAPMAN, E. F. and LABES, M. M. *Abstract of papers*, p 11Q, 144th National Meeting, American Chemical Society, 31 March to 5 April 1963, Los Angeles, California
- ¹⁰ KEPLER, R. G. *Abstract of papers*, p 10Q, 144th National Meeting, American Chemical Society, 31 March to 5 April 1963, Los Angeles, California
- ¹¹ ELEY, D. D., PARFITT, G. D., PERRY, M. J. and TAYSUM, D. H. *Trans. Faraday Soc.* 1953, **49**, 79
- ¹² SZENT-GYÖRGYI, A. *Nature, Lond.* 1941, **148**, 157
- ¹³ POEHLER, T. O. and LIBEN, W. *Proc. Inst. elect. electron. Engrs.* 1964, **52**, 731
- ¹⁴ UEBERSFELD, J., ETIENNE, A. and COMBRISSE, J. *Nature, Lond.* 1954, **174**, 614
- ¹⁵ BENNETT, J. E., INGRAM, D. J. E. and TAPLEY, J. G. *J. chem. Phys.* 1955, **23**, 215
- ¹⁶ INGRAM, D. J. E., TAPLEY, J. G., JACKSON, R., BOND, R. L. and MURNAGHAN, A. R. *Nature, Lond.* 1954, **174**, 798
- ¹⁷ MROZOWSKI, S. *Phys. Rev.* 1952, **85**, 609
- ¹⁸ MROZOWSKI, S. *Phys. Rev.* 1952, **86**, 1056
- ¹⁹ HUGGINS, C. M. *Abstract of papers*, p 12Q, 144th National Meeting, American Chemical Society, 31 March to 5 April, 1963, Los Angeles, California

Entropy of Stereoregularity in Aldehyde Polymerization

A. M. NORTH and D. RICHARDSON*

A variation in the free energy of polymerization in stereoregular and random polymerizations has been observed as a change in the ceiling temperature of aldehyde polymerization. The change, from -31°C for atactic cationic polymerization of acetaldehyde and propionaldehyde to -39°C for isotactic polymerization, is of the magnitude predicted from considerations of entropy of stereoregularity. Failure to obtain an accurate measure of the heat of polymerization has so far obviated attempts to use ceiling temperatures as an exact measure of chain stereospecificity.

IT HAS been suggested¹ that the stereo-disorder of a polymer chain should contribute an increment to the total polymer entropy, and that such an increment (named the entropy of stereoregularity) should also appear in the entropy of polymerization. Calculation of this entropy has yielded a value of $1.38 \text{ cal deg}^{-1}$ for the difference between perfectly random polymer and perfectly stereospecific polymer. This quantity represents a variation of about six per cent in the entropy of polymerization, and as such should be experimentally observable.

In order to verify this hypothesis we have studied the addition polymerization of acetaldehyde and propionaldehyde. These monomers are particularly suited to studies of this nature, since they can be polymerized to atactic polymers using homogeneous acidic initiators, and to stereospecific polymers using homogeneous initiators derived from metal alkyls or metal alkoxides²⁻⁵. We have chosen a study of the ceiling temperature for polymerization as an indirect measurement of the entropy of polymerization.

In a system of initial monomer concentration, $[M]$, the ceiling temperature is given by

$$T_c = \Delta H_p^0 / (\Delta S_p^0 + R \ln [M])$$

where ΔH_p^0 and ΔS_p^0 are the standard state enthalpy and entropy of polymerization respectively. The theory outlined in ref. 1 predicted that

$$\frac{1}{T_{c_0}} = \frac{1}{T_c} - \frac{1.38}{\Delta H^0} + \frac{\delta\Delta S}{\Delta H^0} \quad (1)$$

where T_{c_0} is the ceiling temperature for absolutely random polymer, ΔH^0 is assumed to be independent of the polymer type formed, and $\delta\Delta S$ is the entropy of stereoregularity of the polymer under study.

The aim of the present work was to test the hypothesis that stereoregularity could produce an observable alteration in polymerization ceiling temperature, and to ascertain whether such an observation can be used to calculate the probability of tactic placement during the polymerization.

*Present address: Chemistry Department, University of Manitoba, Winnipeg, Canada.

EXPERIMENTAL

Materials

Acetaldehyde—Crude paraldehyde was shaken with sodium hydroxide pellets and then distilled through a 1 m column packed with Fenske helices. The fraction boiling at 120°C was collected, dried with Linde molecular sieves, 4A, and depolymerized by adding $\frac{1}{2}$ per cent syrupy phosphoric acid and warming to 60°C on total reflux for one hour. The acetaldehyde produced was distilled through the column described above using a reflux ratio 8:1 (b. pt 20·8°C). All distillations were carried out under rigorously dried nitrogen.

The distillate was sealed in collection vessels fitted with breakseals, and stored in the dark at -80°C. Aliquot portions of the monomer were out-gassed on the vacuum line, prepolymerized by 'freezing polymerization'⁶, and distilled into reaction vessels as required.

Propionaldehyde—B.D.H. propionaldehyde was treated with Linde molecular sieves, type 4A, and sodium hydroxide pellets, and then fractionally distilled under dry nitrogen. The fraction, boiling point 48·5°C at 770 mm of mercury pressure, was collected and stored as described for acetaldehyde.

Triethyl aluminium—Supplied by Shell Petrochemicals Ltd, triethyl aluminium was used without further purification. Calibrated ampoules of the alkyl were filled under vacuum. Analysis of the hydrolysis products using gas-liquid chromatography showed that the alkyl contained 7·9 per cent diethyl aluminium hydride.

Trichloroacetic acid—This was purified by repeated crystallization from benzene, followed by pumping for 24 hours at a pressure of 10^{-5} mm of mercury, and a temperature of 20°C.

Procedure

All experiments were conducted under an air pressure of less than 10^{-5} mm of mercury, using conventional vacuum procedures.

Low temperature experiments were performed in a Townson and Mercer Minus Seventy thermostat. The temperature fluctuation was $\pm 0\cdot1^\circ\text{C}$ at -30°C, and was less than this at lower temperatures.

Residual comonomer compositions were analysed using a Perkin-Elmer 800 gas-liquid chromatograph.

Percentage conversions, monomer to polymer, in bulk polymerizations initiated by triethyl aluminium, were carried out by sealing monomer and an initiator ampoule in a closed vessel. The initiator ampoule was broken when the system attained thermal equilibrium, and then quenched with methanol after a predetermined time. Unchanged monomer was then removed by volatilization under vacuum at the temperature of the experiment.

Reproducible estimates of the acid catalysed conversion could not be obtained using this procedure. In these cases both the instability of the polymer and the presence of other non-volatile products introduced considerable errors. In these cases the viscosity of the polymerization mixture was monitored by use of a falling ball inside the reaction vessel.

RESULTS

The cationic polymerization

It was noted that for both monomers the viscosity of the polymerization mixtures increased by a factor greater than ten over a period of five hours at temperatures below -34°C . With acetaldehyde the viscosity increase was slight at -32°C , and not observable at -30°C . The ceiling temperature for cationic polymerization of acetaldehyde is thus taken to be $-31^{\circ} \pm 1^{\circ}\text{C}$. With propionaldehyde a marked viscosity increase over five hours was noted at -34°C , and a slight increase was noted at -32°C . Above -32°C only crystalline cyclic oligomers and condensation products were formed. The ceiling temperature for this polymerization is thus estimated to be $-31^{\circ} \pm 2^{\circ}\text{C}$.

The metal alkoxide polymerization

The use of aluminium trialkyl as initiator leads to a propagating metal alkoxide intermediate. The percentage conversions acetaldehyde to polyacetaldehyde (measured after two hours reaction initiated by 2.45×10^{-1} mole litre $^{-1}$ triethyl aluminium) are illustrated in *Figure 1*. On the same figure are illustrated the percentage conversions propionaldehyde to polypropionaldehyde (estimated after five hours reaction initiated by 1.74×10^{-1} mole litre $^{-1}$ triethyl aluminium). In both cases the ceiling temperature was assigned a value of $-39^{\circ} \pm 1.0^{\circ}\text{C}$. This value is 8° lower than that for the cationic polymerizations, a temperature variation several times larger than the most pessimistic estimation of the experimental error. Infra-red spectroscopy confirmed that all the products obtained were polyethers.

Two mixtures of acetaldehyde and propionaldehyde were prepared. These contained 68 mole per cent and 50 mole per cent acetaldehyde. The polymer yields after 20 hours reaction (triethyl aluminium 1.75×10^{-1} mole litre $^{-1}$)

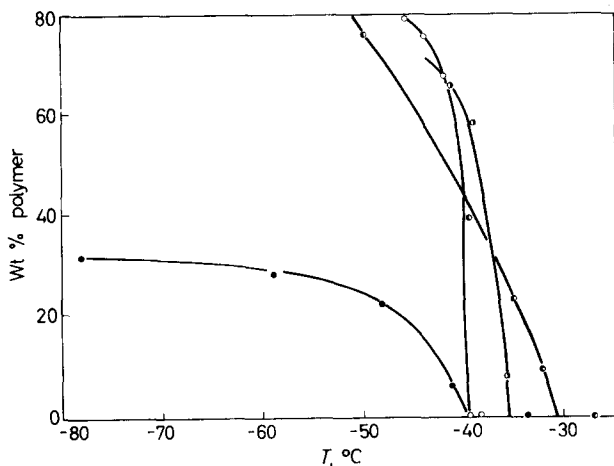


Figure 1—Weight percentage of polymer in polymerizations initiated by triethyl aluminium: ● acetaldehyde, ○ propionaldehyde, ● acetaldehyde:propionaldehyde 1:1, ○ acetaldehyde:propionaldehyde 68:32

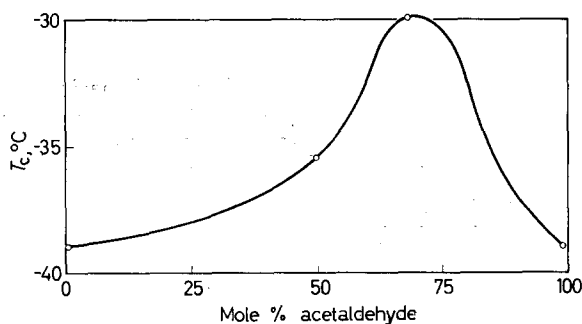


Figure 2—Variation of T_c with monomer feed composition

are also illustrated in *Figure 1*, and a curve of ceiling temperature against monomer composition is drawn in *Figure 2*. It is noteworthy that the maximum in the metal-alkoxide propagating copolymerization ceiling temperature occurs at a temperature remarkably close to that for the acid-catalysed polymerization. Copolymer compositions were obtained by monitoring $d[\text{Acetaldehyde}]/d[\text{Propionaldehyde}]$ and $[\text{Acetaldehyde}]/[\text{Propionaldehyde}]$ using the gas-liquid chromatograph. Plots of

$$r_2 = r_1 \frac{d[A]}{d[P]} \left(\frac{[P]}{[A]} \right)^2 + \frac{[P]}{[A]} \left(\frac{d[A]}{d[P]} - 1 \right) \quad (2)$$

are illustrated in *Figure 3*. The experimental error is considerable, but it is quite certain that r_2 (monomer 1 being propionaldehyde) is greater than r_1 . Within the large experimental error the mean reactivity ratios are $r_2 = 1.0$, $r_1 = 0.5$.

Using these analysis data, the maximum ceiling temperature occurs at a polymer composition of 74 mole per cent acetaldehyde.

Attempts to measure the heat of polymerization using an adiabatic calorimeter, as described by Biddulph and Plesch⁷, were unsuccessful due to the high heat of initiation and low rate of polymerization.

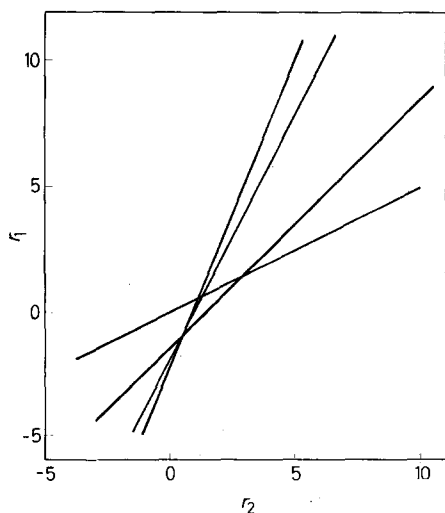


Figure 3—Determination of r_1 and r_2

DISCUSSION

These measurements show that the introduction of two types of monomer unit into a polymer chain raises the ceiling temperature for polymerization. In this respect it is immaterial whether the two units are different stereoisomers of a single chemical type, or are different chemical species.

If a heat of polymerization (calculated from bond strengths⁸) is taken as 5 kcal mole⁻¹, then the difference in the entropies of cationic and metal-alkoxide homopolymerizations is 0.7 cal deg⁻¹ for both monomers. If it is further assumed that the acid-catalysed reaction is perfectly random, application of the data of Table 1, ref. 1, shows that the alkoxide-catalysed reaction is not perfectly stereospecific. On the basis of these assumptions the probability of isotactic placement in these polymerizations at -40°C is 0.8. Very approximate verification of this is yielded by the partial solubility of the polymer in acetone, a solvent which dissolves atactic but not isotactic polymer.

Although accurate calorimetric measurements of ΔH^0 have not proved possible, geometrical examination of molecular models and use of acceptable intermolecular interaction potentials⁹ suggests that the difference in ΔH^0 between isotactic and atactic polymerizations is negligible. Since such an examination is not at all rigorous, the results can be interpreted only as showing a definite variation in the free energy of polymerization. This variation most probably arises in the entropy term.

The copolymerization of acetaldehyde and propionaldehyde (metal alkoxide catalysed) is particularly interesting in that the growing acetaldehyde chain reacts indiscriminately with either monomer, whereas the growing propionaldehyde chain reacts preferentially with acetaldehyde. This effect is presumably due to steric causes, and cannot be explained in terms of electron density on the monomer carbonyl group. A further peculiarity of the copolymerization is that, if these composition analyses are correct, the maximum disorder in the chain is not achieved with a 50-50 mole per cent *chain* composition. A complete theory of the disorder effects in such four-unit chains (monomer *A* in a *D* configuration, monomer *A* in an *L* configuration, and the *D* and *L* configurations of monomer *B*, all four types appearing in a copolymerization for which the reactivity ratio product $r_A r_B \neq 1$) is not yet available, and it is not clear whether the copolymer contains large blocks of a single unit, or whether the stereospecificity decreases at moderately high acetaldehyde mole percentages.

While the general conclusion that the entropy of stereoregularity is an observable quantity seems well verified, its accuracy as a means of estimating the probability of tactic placement cannot yet be tested with these monomers.

One of us (D.R.) acknowledges receipt of a maintenance grant from the D.S.I.R. and of a University of Liverpool Leverhulme Fellowship during the pursuance of this work.

*Department of Inorganic, Physical and Industrial Chemistry,
Donnan Laboratories,
University of Liverpool.*

(Received October 1964)

REFERENCES

- ¹ NORTH, A. M. and RICHARDSON, D. *Polymer, Lond.* 1964, **5**, 227
- ² VOGL, O. *J. Polym. Sci.* 1960, **46**, 261
- ³ FURUKAWA, J., SAEGUSA, T. and FUJII, H. *Makromol. Chem.* 1961, **44-46**, 398
- ⁴ NATTA, G., MAZZANTI, G., CORRADINI, P. and BASSI, I. *Makromol. Chem.* 1960, **37**, 156
- ⁵ ISHIDA, S. I. *J. Polym. Sci.* 1962, **62**, 1
- ⁶ LETORT, M. and DUVAL, X. *C.R. Acad. Sci., Paris*, 1943, **216**, 58 and 608
- ⁷ BIDDULPH, R. H. and PLESCH, P. H. *Chem. & Ind.* **1959**, 1482
- ⁸ COTTRELL, T. L. *The Strengths of Chemical Bonds*. Butterworths: London, 1958
- ⁹ BAWN, C. E. H., JANES, W. H. and NORTH, A. M. *J. Polym. Sci.* 1964, **C4**, 427

Some Grafting Reactions Involving Poly(olefin sulphones)

E. C. EATON* and K. J. IVIN

Some grafting reactions involving poly(olefin sulphones) have been briefly investigated. Conditions are described under which (a) rather small amounts of poly(hexene-1 sulphone) may be grafted on to polyethylene and polypropylene, (b) substantial amounts of poly(hexene-1 sulphone) may be grafted on to poly(cyclopentene sulphone) and (c) substantial amounts of polystyrene may be grafted on to poly(butene-1 sulphone). In the last case AZBN as initiator gives a well-defined copolymer.

THERE appears to be virtually no information in the literature concerning grafting of polysulphones on to other polymers or vice versa. This paper describes the results of an exploratory investigation of the following systems:

System	Substrate polymer	Graft monomer(s)
A	Polyethylene	Hexene-1 + sulphur dioxide
B	Polypropylene	Hexene-1 + sulphur dioxide
C	Poly(cyclopentene sulphone)	Hexene-1 + sulphur dioxide
D	Poly(butene-1 sulphone)	Styrene

All systems were either initially heterogeneous or became so during the course of the grafting reaction. The products were extracted with suitable solvents to remove homopolymers and examined by means of chemical analysis, i.r. spectra and viscosity measurements.

SYSTEMS A AND B

Branch points were formed by irradiation of films of the substrate polymer in air with X-rays. This treatment is known to produce peroxides and hydroperoxide groups in the polymer¹. Hydroperoxides are good initiators for the formation of polysulphones even at -78°C ; peroxides are initiators at higher temperatures (50°C). The formation of hydroperoxides was confirmed by the appearance of a peak at 2.9μ in the i.r. spectrum². They were removed by treatment with liquid sulphur dioxide as shown by the disappearance of the 2.9μ peak and by a much reduced ability to graft acrylonitrile at 100°C ; no peaks attributable to $\text{S}=\text{O}$ bonds appeared in the i.r. spectrum. To prevent premature reaction of the hydroperoxide groups in the grafting experiments, the monomers were distilled on to the irradiated films in the order hexene-1, sulphur dioxide. Even so, very little grafting occurred and very little homopolymer, i.e. poly(hexene-1 sulphone), was formed. The highest amount of grafting (4 per cent by weight) was

*Present address: Synthite Ltd, Birmingham.

obtained with a sample of polyethylene which had been irradiated for 60 hours with 45 kVp X-rays and reacted with a 1:1 mixture of hexene-1 and sulphur dioxide at 50°C.

SYSTEM C

It was found that considerable grafting occurred when 0.12 g poly(cyclopentene sulphone) was heated for 3 h with 0.012 mole hexene-1, 0.06 mole sulphur dioxide and 14 mg azobisisobutyronitrile (AZBN) at 50°C. After extraction of the poly(hexene-1 sulphone) with toluene, the original polymer was found to have gained 20 per cent in weight, with a corresponding change in the i.r. spectrum. No grafting occurred at 25° when ultra-violet light was used to initiate the reaction.

SYSTEM D (AZBN AS INITIATOR)

This system was investigated in more detail than the others. Tests showed that poly(butene-1 sulphone) and polystyrene could be separated quantitatively by extraction of the latter with toluene. The i.r. peaks at 7.66, 8.17, 8.87 μ (polysulphone) and at 6.7 and 9.75 μ (polystyrene) provide a ready method of analysis.

0.4 g of the polysulphone was heated with 4.2 g styrene and 23 mg AZBN at 60° for 3 h. The polysulphone was swollen by the styrene but did not dissolve; free styrene was therefore present as a second phase. The weights, compositions and limiting viscosity numbers of the extracts of the resultant polymer are shown in *Figure 1*. A good separation into two pure

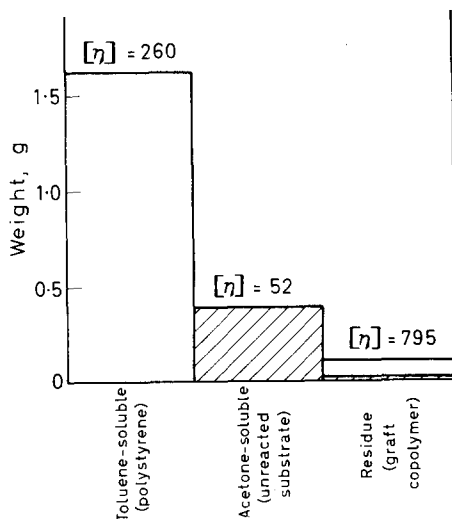


Figure 1—Polymer distribution after heating poly(butene-1 sulphone) with styrene and AZBN. Viscosities (ml g⁻¹) in chloroform. Hatched area denotes proportion of poly(butene-1 sulphone)

homopolymers and a graft copolymer was achieved. Only 2 to 3 per cent of the initial polysulphone underwent grafting, but this was grafted to about ten times its original weight; the remainder was unchanged in molecular weight. $[\eta]$ of the graft copolymer is markedly higher than those of the homopolymers. On hydrolysis of the graft copolymer (refluxed with

0.25N caustic soda for 4 h) the residue was indistinguishable (by i.r. spectrum) from polystyrene and had lost about 9 per cent of its weight, as expected. Its $[\eta]$ had fallen to 657 ml g⁻¹ compared with 795 ml g⁻¹ for the graft copolymer. It was confirmed that the hydrolysis treatment had no effect on $[\eta]$ of an ordinary sample of polystyrene.

In converting the viscosities to molecular weights (M) we are faced with some difficulties. First, the $[\eta]/M$ relation is not known for poly-(butene-1 sulphone) in chloroform; the relation for poly(hexene-1-sulphone) in chloroform³ may be taken as a reasonable approximation, $[\eta] = 5.9 \times 10^{-3} M^{0.73}$ ml g⁻¹. Secondly, the values of $[\eta]$ above 500 ml g⁻¹ are probably too low since no shear corrections were made. Thirdly, the graft polymer molecules are not linear, but it is necessary to assume an $[\eta]/M$ relation intermediate between that of the two linear homopolymers. For polystyrene in chloroform⁴, $[\eta] = 10.7 \times 10^{-3} M^{0.74}$ ml g⁻¹. Since the graft copolymer consists predominantly of polystyrene, no serious error is likely to be caused by the use of a suitably weighted $[\eta]/M$ relation.

The recovery of a large proportion of unchanged polysulphone shows that the transfer reaction between polystyryl radicals and polysulphone molecules does not occur to any great extent. Thus the grafts are probably terminated by combination⁵ with another growing graft or with an ungrafted polystyryl radical. If graft points were formed singly by attack of a radical from AZBN, then subsequent hydrolysis of the graft copolymer should reduce the molecular weight only to the extent caused by the removal of 9 per cent by weight of polysulphone. The fall in molecular weight appears to be somewhat greater than this ($[\eta]$ decreased from 795 to 657 ml g⁻¹) and may be accounted for by supposing that some of the catalyst molecules decompose sufficiently close to a given polysulphone molecule to enable both radicals to attack it, so forming two graft points on the same molecule. This will lead to two polystyrene molecules in the hydrolysis products and hence to a further reduction in molecular weight.

From the viscosity and composition data, and with the assumptions already mentioned, it may be estimated that each graft copolymer molecule contains on average 2 to 2.5 molecules of the original polysulphone. This is understandable if termination occurs by combination of two grafted polystyryl radicals within the swollen polysulphone. More than two molecules of polysulphone will be incorporated in a given copolymer molecule if two graft points are occasionally formed on the same polysulphone molecule, as seems likely (see above).

The polystyrene chains in the graft copolymer molecules are evidently about four times as long as in the homopolymer produced simultaneously. This is accountable in terms of the 'gel' effect. The growth of the graft occurs in a viscous gel where the termination reaction may well be diffusion-controlled and have a lower rate constant than for reaction in the pure styrene phase¹. The homopolymer is formed, at least in part, in the latter phase and will thus have a lower molecular weight.

An attempt was made to study this system in homogeneous solution in order to test these ideas. To this end an equal volume of methyl ethyl ketone was added to the styrene. However, on heating with AZBN at 60°, no graft copolymer was formed. The reason for this is not clear.

SYSTEM D (X-RAYS AS INITIATOR)

Irradiation of 1.34 g polysulphone with 1.44 g styrene for 8 h with 45 kVp X-rays gave the result summarized in *Figure 2*. 70 per cent of the styrene

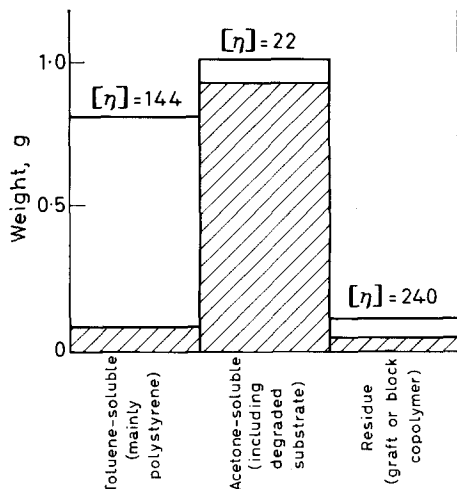


Figure 2—Polymer distribution after irradiating poly(butene-1 sulphone) and styrene with X-rays. (cf. *Figure 1*)

was polymerized compared with only 5 per cent in the absence of polysulphone. It is well known that the G value for the production of radicals from styrene is low on account of the protecting action of the benzene rings¹. Most of the branch-points will therefore be produced by interaction of the X-rays with the polysulphone. However, it is clear from the degradation of the polysulphone ($[\eta]$ of acetone-soluble fraction is 22 ml g⁻¹ compared with 52 ml g⁻¹ for the original polymer) and from the greater complexity of the products (*Figure 2*) that main-chain fission as well as side-chain fission is likely to be involved. Thus the product almost certainly contains block copolymer in addition to graft copolymer. It is interesting to note that the toluene-soluble fraction in *Figure 2* has about the same overall composition as the toluene-insoluble graft copolymer in *Figure 1*. The difference in solubility presumably stems from the difference in molecular weight and structure of the copolymers.

E.C.E. is indebted to B.I.P. Chemicals Ltd for making it possible to undertake this work.

*Department of Physical Chemistry,
The University, Leeds 2*

(Received September 1964)

REFERENCES

- 1 CHAPIRO, A. *Radiation Chemistry of Polymeric Systems*. Wiley: New York, 1962
- 2 BELLAMY, L. J. *The Infra-red Spectra of Complex Molecules*, 2nd ed., p 122. Methuen: London, 1958
- 3 IVIN, K. J., ENDE, H. A. and MEYERHOFF, G. *Polymer, Lond.* 1962, **3**, 129
- 4 BAWN, C. E. H., FREEMAN, R. F. J. and KAMALIDDIN, A. R. *Trans. Faraday Soc.* 1950, **46**, 1107
- 5 BEVINGTON, J. C., MELVILLE, H. W. and TAYLOR, R. P. *J. Polym. Sci.* 1954, **12**, 449

Pyrolysis—Hydrogenation—GLC of Poly- α -olefins

J. VAN SCHOOTEN and J. K. EVENHUIS

Pyrolysis—hydrogenation—GLC experiments on polyethylene, polypropylene, hydrogenated natural rubber, polybutene-1, polyisobutylene, poly-3-methylbutene-1, poly-4-methylpentene-1, polystyrene and poly- α -methylstyrene are discussed with special emphasis on the mechanisms by which the volatile fragments are formed. It is shown that intramolecular hydrogen exchange reactions of the radicals formed on pyrolysis occur mainly with the fifth carbon atom but also with some others. Splitting off of side groups becomes increasingly important as their size increases.

IN RECENT years analysis of the volatile pyrolysis products of polymers has been developed into a versatile technique for polymer characterization which is widely used. The direct combination of polymer pyrolysis and GLC is introduced by Lehrle and Robb^{1,2} in 1959 and this technique has since received increasing attention.

Pyrolysis—GLC analysis can be used for several purposes:

- (i) for identification of unknown samples, in a similar way as spectroscopic techniques, by comparing the pyrogram of the unknown compound with a collection of model pyrograms of known polymers;
- (ii) for quantitative analysis of copolymer composition after calibration by means of an absolute method;
- (iii) for obtaining information on the molecular structure of polymers or copolymers, e.g. about copolymer 'blockiness';
- (iv) for studying the reaction mechanism of thermal degradation.

This paper describes work on pyrolysis—GLC of poly- α -olefins: polyethylene, polypropylene, polybutene-1, polyisobutene, poly-3-methylbutene-1, poly-4-methylpentene-1, polystyrene, poly- α -methylstyrene, and completely hydrogenated natural rubber. The last-mentioned polymer was included because of its regular structure and because it is a model for the ideally alternating ethylene—propylene copolymer. The relation between polymer structure and the structure of the pyrolysis products and the mechanism by which these products have been formed will be stressed.

EXPERIMENTAL

Apparatus and method

The pyrolysis apparatuses described in the literature either use a heated pyrolysis chamber³⁻⁵ or a platinum spiral or dish which is heated direct by an electric current⁶⁻⁸. For analytical applications the latter technique is most convenient because it is both rapid and simple and has therefore been chosen for the present investigation.

On pyrolysis, the polymers studied largely yield unsaturated products. In order to reduce the number of peaks in the chromatograms and because many more saturated model hydrocarbons were available for calibration

than unsaturated ones we hydrogenated the pyrolysis products before they entered the GLC-column.

The principle of our apparatus is shown in *Figure 1*. The pyrolysis unit consists of a glass tube in three sections:

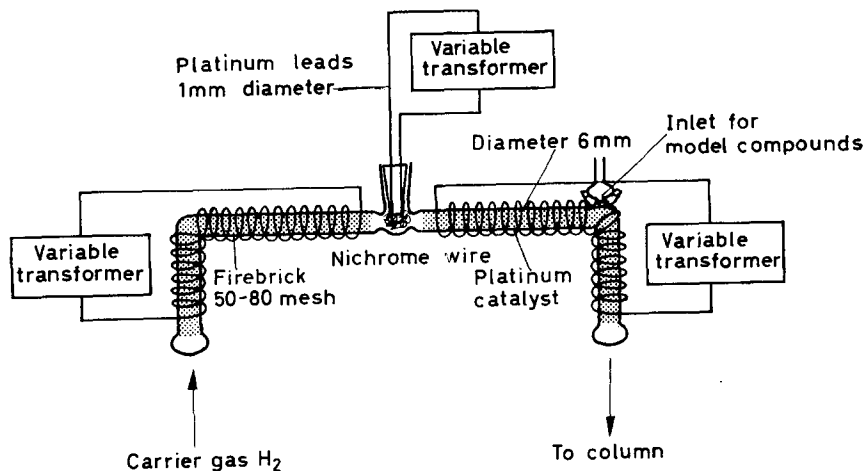


Figure 1—Schematic diagram of pyrolysis unit

(a) one filled with firebrick*, 50–80 mesh, externally heated to warm up the carrier gas to about 100°C. This prevents condensation of the higher-molecular-weight degradation products, before they enter the column;

(b) a small chamber, containing a Nichrome wire on which the polymer is to be pyrolysed. The wire is 0.25 mm thick and 100 mm long, wound in a spiral, 5 mm long and 2.5 mm in diameter. Its resistance is about 2 ohms;

(c) a hydrogenation section, containing a platinum-on-alumina catalyst (0.75 per cent by weight Pt-on-Al₂O₃, 30–50 mesh), and connected with the chromatographic column. This section is kept at about 200°C. The catalyst is first reduced with hydrogen at 400°C. All olefins, but also benzene and substituted benzenes like toluene, ethylbenzene, cumene, etc., are completely hydrogenated to the corresponding alkanes or cycloalkanes.

The chromatographic analysis is carried out with Apiezon-L as the liquid phase and ground firebrick (50–80 mesh) as the solid support. A flame-ionization detector is used with a collecting voltage of about 90 V. The signal obtained is amplified and fed to a recording millivoltmeter having a range of 0 to 0.3 mV.

The temperature is programmed linearly by a simple technique: the temperature of the oil bath in which the column is placed is increased at a rate of 0.75°C/min by pulling the contact of a contact thermometer upwards at constant speed by means of a synchronous motor with attached gear box†. To obtain a constant flow rate of the carrier gas, a Moore diaphragm-type flow controller is employed‡.

*Sil-O-Cel, manufacturer Johns Mansville, New York.

†Manufacturer of synchronous motor and gear box: Erwin Halstrup, Kirchzarten, Schwarzwald, Germany.

‡Moore Products Co., Philadelphia, U.S.A., type No. 63 BUL.

Procedure

A small sample (0.4 mg) is placed on the Nichrome wire, which is heated for a few seconds by an electric current controlled by means of a variable transformer. For the polymers discussed the voltage used was about 4 V. The actual pyrolysis is completed in less than a second and proceeds at a temperature estimated to be about 500°C.

Our apparatus and procedure have proved to yield a good resolution of the chromatograms, the range of detectable hydrocarbons extending to the C₁₃ group. Some details are given in *Table 1*.

Table 1. Operational conditions of chromatograph

Column length	m	7	Pressure head	atm	1.5 to 2
Bore	mm	3	Column temperature		
Column material		16.7% w Apiezon-L on firebrick 50-80 mesh	range	°C	90-170
		Hydrogen	Rate of temperature increase	°C/min	0.75
Carrier gas			Sample	mg	0.4
Flow rate	l./h	2.5	Time of pyrolysis	s	< 1

Samples

Pyrolysis experiments have been carried out with the following polymers:

(1) *Polyethylene samples*—(a) Polymethylene (laboratory sample synthesized from diazomethane); (b) a high-density polyethylene of density 0.96.

(2) *Polypropylene samples*—Six commercial samples from different manufacturers were used.

(3) *Hydrogenated natural rubber*—This sample was prepared from masticated natural rubber, without previous purification, by hydrogenation in cyclohexane solution at a hydrogen pressure of 250 atm and a temperature of up to 185°C with nickel-on-guhr containing 60 per cent of nickel as the catalyst⁹.

(4) *Polybutene-1, poly-3-methylbutene and poly-4-pentene-1*—These samples were prepared with the aid of Ziegler-Natta catalysts containing γ -titanium chloride and an alkylaluminium compound. The polybutene-1 samples were an amorphous polymer, obtained by extraction with ether, a highly crystalline isotactic extraction residue, m.pt 118°C and a total sample of medium crystallinity.

The poly-3-methylbutene-1 and poly-4-methylpentene-1 samples were highly crystalline, m.pt 260°C and 230°C respectively.

(5) *Polyisobutene*—A commercial polymer containing one or two per cent of isoprene.

(6) *Polystyrene*—A commercial sample.

(7) *Poly- α -methylstyrene*—Prepared according to Swarc *et al.*¹⁰ using living α -methylstyrene tetramer with sodium counter ions as the initiator; molecular weight \bar{M}_n 380 000.

Identification of peaks

The peaks in the pyrograms were identified in three ways:

(a) Retention 'times' [measured as *distance* (mm) from the appearance

of the methane peak] were compared with those of available model compounds. This procedure is quite straightforward and simple, as long as the desired model compounds are available.

(b) With the aid of the retention distances of the model compounds and their normal boiling points, taken from existing tables^{11,12}, we constructed curves of retention distance versus boiling point in a similar way as reported by Polgar, Holst and Groennings¹³ (see *Figure 2*). With the Apiezon-L substrate, separation is mainly according to boiling point, but with a clearly

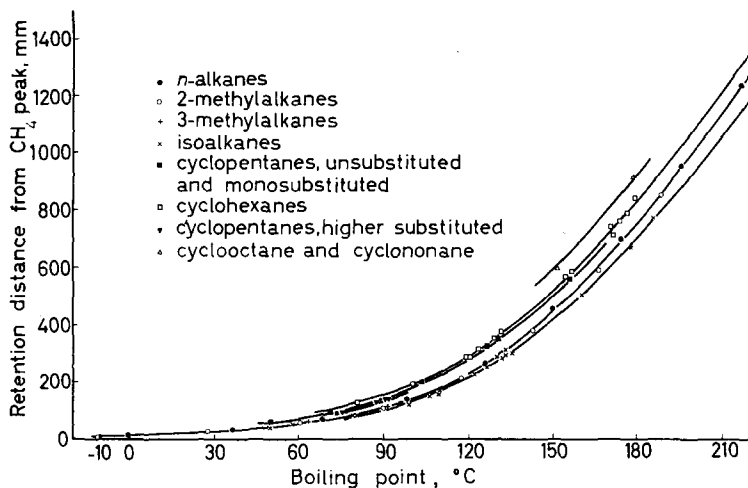


Figure 2—Retention distance from CH_4 peak versus boiling point of alkanes and cyclanes

discernible type selectivity. Compared to the *n*-alkanes of equal boiling temperature the cycloalkanes are retarded and the highly substituted isoalkanes appear somewhat earlier. Retention distances of compounds that are not available can thus be estimated when their boiling points are known. The result is that for peaks not corresponding with an available model compound one usually has to choose between only a few possibilities. The choice is made on the basis of knowledge of the structure of the polymer and the mechanism of pyrolysis.

(c) Three polypropylene pyrolysis products from a large-scale pyrolysis experiment have been isolated with the aid of preparative GLC and identified by infra-red and mass-spectrometric analysis. One peak was found to consist of 30 to 40 per cent of a C_{10} -alkane and 70 to 60 per cent of 1,3,5-trimethylcyclohexane. The infra-red spectrum was similar to that of 1-*cis*-3-*cis*-5-trimethylcyclohexane. The isoalkane was most probably the expected 2,4,6-trimethylheptane. A second set of two distinctly separate peaks (with retention distances of 710 and 718 in our apparatus, which were not resolved in the preparative GLC) was found by its mass and infra-red spectra to correspond to 4,6-dimethylnonane. Probably the two separate peaks in our pyrogram correspond to the stereoisomers: one for the DL- or LD- structures and one for the DD- or LL-structures. A similar

PYROLYSIS-HYDROGENATION-GLC OF POLY- α -OLEFINS

phenomenon was observed for a third component: it corresponded with the peaks with retentions 830 and 845 in our pyrogram and was found to be 2,4,6-trimethylnonane.

To illustrate the way in which the above identification procedures were applied, detailed data about the pyrograms of polybutene-1 and polystyrene are given in *Tables 2* and *3*.

Table 2. Components from the pyrolysis of polybutene-1

Retention distance in mm from CH ₄ -peak	Expected boiling point, °C		Possible components		Peak height, cm	Peak surface area, cm ²	
	Alkanes	Cyclanes	Structure	Boiling point, °C			
0	—	—	C ₁	—	9	1.6	
1	—	—	C ₂	—	37	9.3	
4	—	—	C ₃	—	24	7.1	
8	—	—	iC ₄	-11.7	0.2	0.1	
13	—	—	nC ₄	-0.5	96	34	
23	28	—	iC ₅	27.9	26	9.9	
30	36	—	nC ₅	36.1	3.1	1.3	
52	59-61	—	2MC ₅	60.3	0.2	0.1	
59	63-66	—	3MC ₅	63.3	1.4	0.7	
66	68-71	55-59	nC ₆	68.7	6.6	3.5	
107	88-91	77-81	2MC ₆	90.0	0.5	0.4	
117	90-93	80-84	3MC ₆	91.9	3.1	2.4	
137	97-100	87-92	nC ₇	98.4	32	28.1	
223	117-121	108-111	3MC ₇	118.9	18.2	21.8	
262	125-129	115-119	nC ₈	125.7	0.3	0.4	
321	134-138	124-129	3,5MC ₇	136.0	3.7	5.7	
373	141-145	128-133	3MC ₈ /4EC ₇	144.2/141.2	0.4	0.6	
454	150-154	140-144	nC ₉	150.9	0.5	1.0	
486	154-158	144-147	3M5EC ₇	158.2	0.3	0.5	
514	157-161	147-150		—	—	0.2	0.3
537	159-163	150-153		—	—	0.3	0.5
572	162-166	154-157	4EC ₈	163.6	0.3	0.5	
625	167-171	159-164	3MC ₉	167.8	0.5	1.0	
807	183-187	176-180	5EC ₉ or 3,7MC ₉	183.0	2.9	6.8	
				181.7			
942	193-198	187-192	3M5EC ₉	194.7	15.4	58	
1080	204-208	196-200	3,7M5EC ₉	—	1.6	9.3	
Σ						204.9	

DISCUSSION OF RESULTS

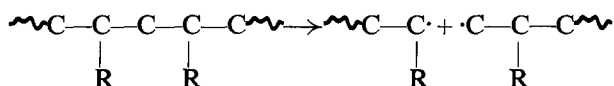
Degradation mechanism

For a fruitful discussion of the results it is desirable to recall first the main features of the mechanism of thermal degradation of hydrocarbon polymers as developed by Simha, Wall and co-workers^{14,15}. According to these authors the pyrolysis is a radical chain reaction comprising initiation, depropagation, hydrogen transfer and termination reactions.

Table 3. Components from the pyrolysis of polystyrene

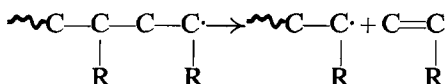
Retention distance in mm from CH ₄ -peak	Expected boiling point, °C		Possible component		Peak height, cm	Peak surface area, cm ²
	Alkanes	Cyclanes	Structure	Boiling point, °C		
0	—	—	C ₁	—	0	0
1	—	—	C ₂	—	8.6	3.0
124	94-98	80-84	CyC ₆	80.7	3.6	2.6
190	112-115	100-103	MCyC ₆	100.9	12.4	12.4
372	141-145	128-133	ECyC ₆	131.8	683	955
567	164-168	154-157	<i>i</i> -PCyC ₆	154.8	1.8	4.3
580	165-169	155-158	<i>n</i> -PCyC ₆	156.7	1.0	2.5
						979.8

The *initiation* reaction is mostly the thermal cleavage of the polymer backbone into two radicals

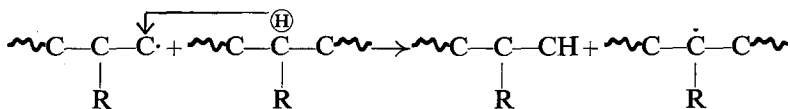


The initiation may occur at the chain ends or at random somewhere along the chain.

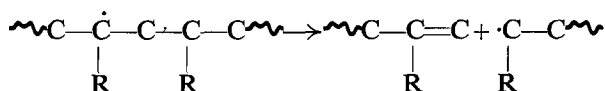
When these radicals decompose under β -scission, monomers are split off. For vinylpolymers, this reaction is called *unzipping* or *depropagation*



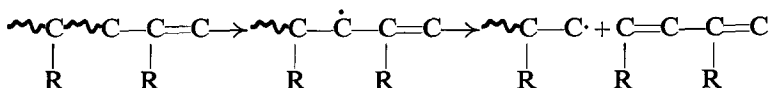
The hydrogen transfer reactions may be intermolecular or intramolecular. *Intermolecular hydrogen transfer* will preferentially abstract tertiary hydrogen atoms



The radical formed may decompose, giving an α' -olefin and a new radical:



The α -methylene hydrogen in the α' -olefin is even more easily abstracted than a tertiary hydrogen and by a second intermolecular hydrogen abstraction an allyl radical may be formed, which on β -scission gives a substituted butadiene, showing up as a methylalkane in hydrogenation-GLC:

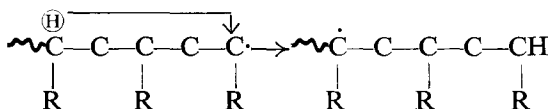


Since C—C bonds in β -position to a double bond are appreciably weaker than normal saturated C—C bonds the α' -olefin may also decompose and give a substituted allyl radical $\cdot\text{C}=\text{C}-\text{C}$, which yields a 2-methylalkane

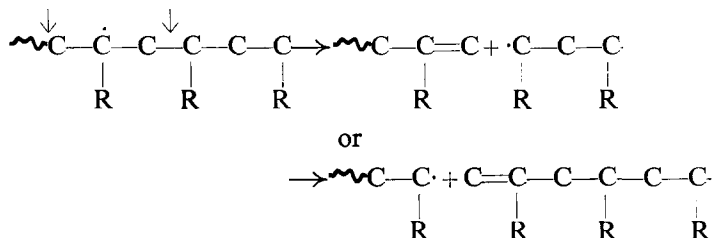


on hydrogenation.

Intramolecular hydrogen transfer has also been taken into consideration by Wall *et al.*¹⁵ in discussing the kinetics of the pyrolysis of branched polyethylenes and other polymeric hydrocarbons, e.g.



The newly formed radical may then decompose by β -scission into volatile fragments:



Polymers for which the rate of unzipping or depropagation is high compared with the initiation and transfer reactions give a high yield of monomer on pyrolysis and volatilize to a great extent. When depropagation is slow the polymers volatilize incompletely, giving a large number of decomposition products.

Discussion of the pyrograms

The main features of the pyrograms of the various polyhydrocarbons will now be discussed in relation to their structure, giving special attention to the way in which the volatile fragments have been formed.

The experimental results are summarized in *Figures 3 to 11*, where peak areas are given for the main fragments. The peak area per carbon atom of the fragments is a measure of the frequency with which the particular fragment is formed as illustrated for polyethylene in *Figure 3*.

(1) *Polyethylene*: $\text{---CH}_2\text{---CH}_2\text{---}_n$ —The pyrogram of a linear polyethylene*, e.g. polymethylene, contains only very small peaks for branched and cyclic alkanes and very large n -alkane peaks. Surface areas of the various n -alkane peaks are given in *Figure 3*. The largest peaks in the pyrogram are those for propane, n -hexane, n -heptane, n -decane and n -undecane, indicating important hydrogen exchange reactions followed by β -scission with the fifth (C_3 and $n\text{-C}_6$), ninth ($n\text{-C}_7$ and $n\text{-C}_{10}$) and thirteenth ($n\text{-C}_{11}$ and $n\text{-C}_{14}$) carbon atoms. Hydrogen transfer with the sixth carbon

*Characteristics of the pyrograms of polyethylenes with short-chain branching will be discussed in a following publication.

atom would account for the rather large $n\text{-C}_4$ peak, but this peak could also be due to intermolecular chain transfer reactions*.

Direct exchange with higher-numbered carbon atoms will be less likely, since it would require an increasingly higher entropy of activation. However, since the experiments suggest that such exchange reactions do occur, they must probably take place in two or more steps.

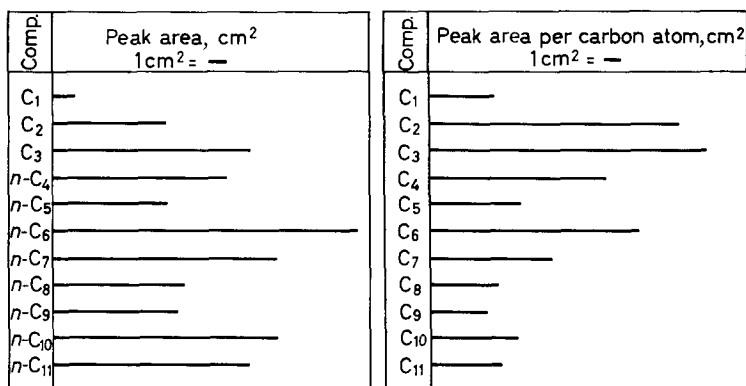


Figure 3—Areas of the main peaks in the pyrogram of polyethylene



(2) *Polypropylene*: $-\text{ECH}_2\text{CH}(\text{CH}_3)-$ _n—Identical pyrolysis patterns have been found for various polypropylene samples. The surface areas of the main peaks in the pyrogram of polypropylene are shown in *Figure 4*.

Depolymerization is much more important for polypropylene than for polyethylene, as shown by the large propane peak. Two other very large

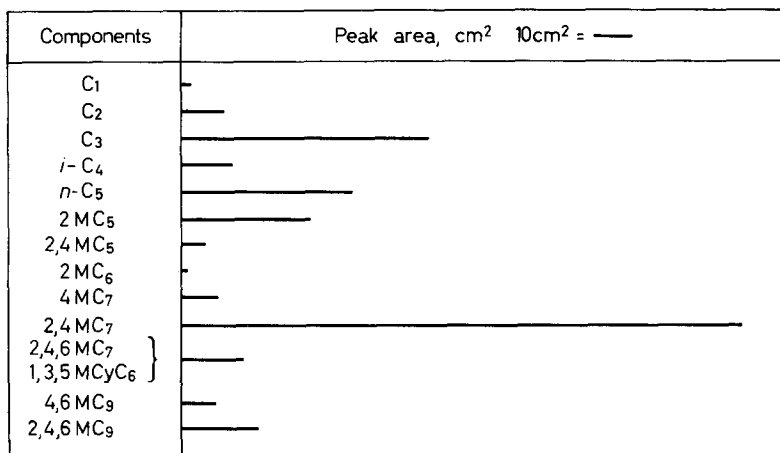
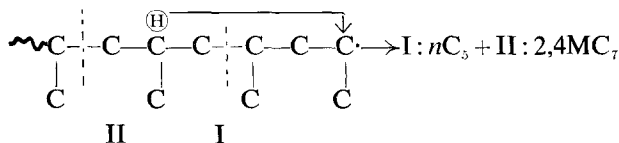


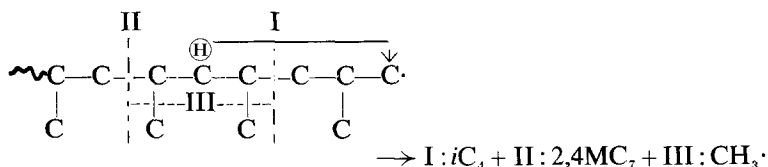
Figure 4—Areas of the main peaks in the pyrogram of polypropylene

*Willbourn¹⁶ estimates that for high-pressure polyethylene polymerization hydrogen transfer with the fifth carbon atom is favoured by 3 to 5 kcal over that with the fourth or sixth carbon atom. When, however, the sixth carbon atom carries a tertiary and the fifth carbon atom a secondary hydrogen, the difference will certainly be less.

peaks can be interpreted as originating from intramolecular hydrogen transfer with the fifth carbon atom of the secondary radical:



The primary radical gives in this way



The isobutane and especially the methane peaks are rather small, indicating that this reaction is not very frequent for the primary radical. For this radical hydrogen transfer with the sixth carbon atom might be more important, as the 2MC_5 peak could be explained in this way (see

Table 4. Products expected from intramolecular hydrogen transfer during pyrolysis of polypropylene (main observed peaks underlined)

	Number of the hydrogen-donating carbon atom				
	5	6	7	8	9
Secondary radical:	$n\text{C}_5$	CH_4	4MC_7	CH_4	$4,6\text{MC}_9$
$\sim \text{C}-\text{C}-\text{C}-\text{C}-\text{C}-\text{C}-\text{C} \cdot$ C C C C	<u>$2,4\text{MC}_7$</u>	<u>2MC_5</u> 4MC_7^* <u>$4,6\text{MC}_9$</u>	$2,4,6\text{MC}_9$	$2,4\text{MC}_7$ $4,6\text{MC}_9^*$ <u>$4,6,8\text{MC}_{11}$</u>	$2,4,6,8\text{MC}_{11}$
Primary radical:	$i\text{C}_4$	2MC_5	CH_4	$2,4\text{MC}_7$	CH_4
$\sim \text{C}-\text{C}-\text{C}-\text{C}-\text{C}-\text{C} \cdot$ C C C	<u>2MC_5^*</u> <u>$2,4\text{MC}_7$</u> <u>CH_4</u>	<u>$2,4,6\text{MC}_7$</u>	$2,4\text{MC}_5$ $2,4\text{MC}_7^*$ <u>$2,4,6\text{MC}_9$</u>	$2,4,6,8\text{MC}_9$	$2,4,6\text{MC}_7$ $2,4,6\text{MC}_9^*$ <u>$2,4,6,8\text{MC}_{11}$</u>

*Formed after hydrogen exchange with a methyl group.

Table 4). Another possibility is that this peak should be ascribed to intermolecular hydrogen transfer reactions (formation of 2-methylpentadiene)*.



(3) *Hydrogenated natural rubber*: $-\text{E}-\text{CH}_2-\text{CH}_2-\overset{\text{CH}_3}{\text{C}}-\text{CH}_2-$ \exists $_n-$ The surface areas of the main peaks of hydrogenated natural rubber are given in Figure 5. The 'unzipping' reaction, which would yield equal amounts of ethane and propane† in the hydrogenated pyrolysate, evidently takes place to some extent, but is less important than the hydrogen transfer reactions. The large number of peaks reflects the many possible hydrogen transfer reactions for this polymer. This is further illustrated in Table 5.

*A recent paper by Voigt²¹, published after this work was finished, ascribes one of the larger peaks in the polypropylene pyrogram to 4-methylpentene-1 (or -2). This would point to intramolecular hydrogen transfer with the third carbon atom.

†Hydrogenated natural rubber is the completely alternating ethylene-propylene copolymer.

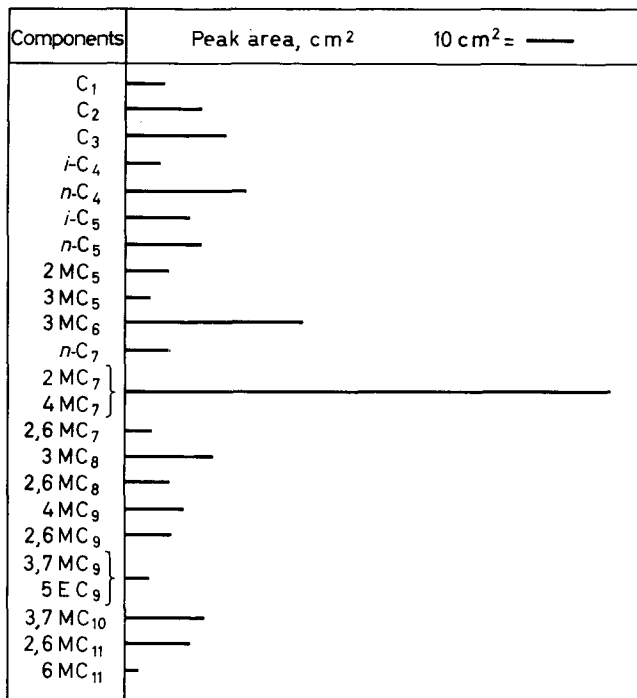


Figure 5—Areas of the main peaks in the pyrogram of hydrogenated natural rubber

All compounds mentioned in *Table 5* are indeed detected. Also in this case, however, hydrogen transfer from the fifth carbon atom predominates, as indicated by the large *n*C₄, 3MC₆ and 2MC₇ peaks, followed by transfer from the ninth carbon atom, which is shown by the size of the 3MC₈, the 3,7MC₁₀ and the 2,6MC₁₁ peaks. Transfer reactions with the other carbon atoms seem to occur, but only to a minor extent. The iso-C₅ peak may also be due to intermolecular hydrogen transfer in the same way as discussed for polyethylene (*n*C₄) and polypropylene (2MC₅).

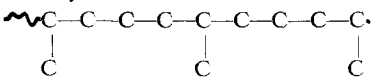
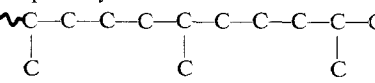
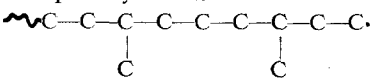
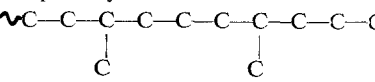


(4) *Polybutene-1*: $-\text{ECH}_2-\overset{\text{C}_2\text{H}_5}{\underset{|}{\text{CH}}}-\text{E}-\text{CH}_2-\text{CH}_2-$ —Three polybutene-1 samples of varying degree of isotacticity were investigated and gave identical pyrograms. The surface areas of the main peaks are given in *Figure 6*. The large *n*-butane peak shows that unzipping is here an important reaction, as it was for polypropylene.

The primary products expected from intramolecular hydrogen transfer are shown in *Table 6*. Hydrogen transfer from the fifth carbon atom is again the main reaction. Part of the ethane peak may be due to direct splitting off of the ethyl side group, as some of the minor peaks can easily be ascribed to consecutive reactions after removal of the ethyl group, e.g. the C₃, *n*C₆, *n*C₉, 3,7MC₉ and the 3M5EC₁₁ peaks. Two other peaks, the

PYROLYSIS-HYDROGENATION-GLC OF POLY- α -OLEFINS

Table 5. Products expected from intramolecular hydrogen transfer during pyrolysis of hydrogenated natural rubber (main observed peaks underlined)

	Number of the hydrogen-donating carbon atom				
	5	6	7	8	9
Secondary radical: 	$\frac{nC_4}{2MC_7}$	$\frac{nC_5}{3MC_8}$ $\frac{nC_7^*}{CH_4}$	$\frac{nC_7}{4MC_9}$	$\frac{2MC_7}{6MC_{11}}$ $\frac{CH_4}{CH_4}$	$\frac{3MC_8}{2,6MC_{11}}$
First primary radical: 	$\frac{iC_4}{2MC_7}$ $\frac{CH_4}{CH_4}$	$\frac{iC_5}{2,6MC_7}$	$2MC_5$ $2,6MC_8$ $\frac{2MC_7^*}{CH_4}$	$\frac{2MC_7}{2,6MC_9}$	$2,6MC_7$ $2,6MC_{11}$ $\frac{CH_4}{CH_4}$
Second primary radical: 	$\frac{nC_4}{3MC_6}$	$\frac{iC_5}{3MC_8}$ $\frac{CH_4}{CH_4}$	$3MC_5$ $2,6MC_8$	$\frac{3MC_6}{3,7MC_9}$ $3MC_8^*$ $\frac{CH_4}{CH_4}$	$\frac{3MC_8}{3,7MC_{10}}$
Third primary radical: 	C_3 $\frac{3MC_6}{nC_5}$ $\frac{CH_4}{CH_4}$	$\frac{nC_5}{4MC_7}$	$2MC_5$ $4MC_9$ $\frac{CH_4}{CH_4}$	$\frac{3MC_6}{2,6MC_9}$	$\frac{4MC_7}{3,7MC_{10}}$ $4MC_9^*$ $\frac{CH_4}{CH_4}$

*Formed after hydrogen exchange with a methyl group.

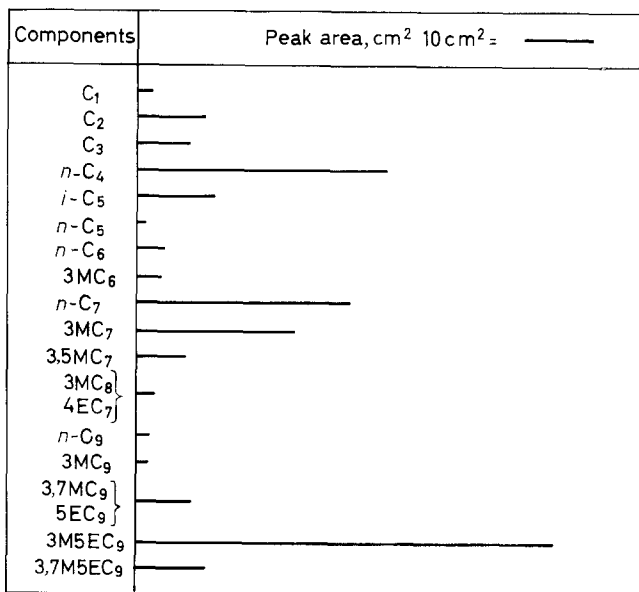


Figure 6—Areas of the main peaks in the pyrogram of polybutene-1

Table 6. Products expected from intramolecular hydrogen transfer during pyrolysis of polybutene-1 (main observed peaks are underlined)

	Number of the hydrogen-donating carbon atom		
	5	6	7
Primary radical 	C_2 iC_5 <u>$3M5EC_9$</u> <u>$3MC_7$</u>	$3MC_7$ $3,7M5EC_9$	$3,5MC_7$ <u>$3M5,7EC_{11}$</u>
Secondary radical 	nC_7 <u>$3M5EC_9$</u> C_2	$3MC_7$ $5EC_9$ $5,7EC_{11}$	$5EC_9$ <u>$3M5,7EC_{11}$</u>

$3MC_7$ and $3MC_9$ ones, may similarly be ascribed to reactions involving intermolecular hydrogen transfer.



(5) *Polyisobutylene*: $\cdot EC-CH_2\dot{E}_n$ —For polyisobutylene, ‘unzipping’ is by far the principal reaction, as follows from the large iC_4 peak (see Figure 7). This has been found earlier^{17,18} and was then ascribed to the absence of easily abstractable hydrogen atoms. However, several of the peaks in the pyrogram can again be ascribed to intramolecular hydrogen transfer reactions, followed by β -scission. Hydrogen transfer with a methylene group then gives methane, neopentane and 2,2,4,4,6-pentamethyl-

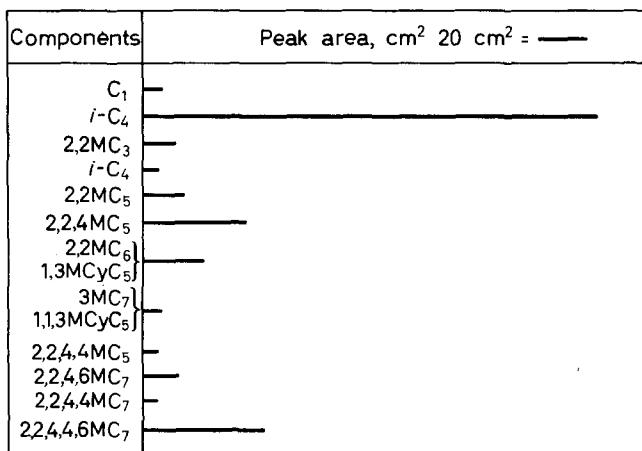
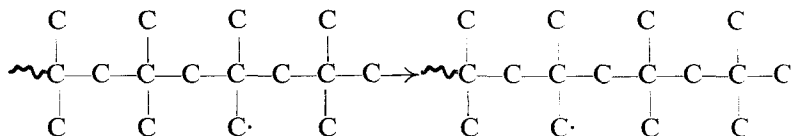


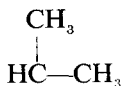
Figure 7—Areas of the main peaks in the pyrogram of polyisobutylene

heptane, while hydrogen transfer with a methyl group gives methane, neopentane and 2,2,4-trimethylpentane.

A second transfer reaction may give 2,2,4,4-tetramethylpentane (2,2,4,4MC₅) and 2,2,4,4,6-pentamethylheptane (2,2,4,4,6MC₇):



and all these compounds were indeed detected.



(6) *Poly-3-methylbutene-1*: $-\text{ECH}_2-\text{CH}_3-$ The surface areas of the main peaks in the pyrogram of poly-3-methylbutene-1 are shown in *Figure 8*. The large isopentane peak can be ascribed to 'unzipping' and most of the other peaks are satisfactorily explained by intramolecular hydrogen transfer reactions. The propyl group may have been split off direct or as a consecutive reaction to intramolecular hydrogen transfer. The number of favourable transfer reactions is larger with this polymer, because of the large number of tertiary hydrogen atoms, which also increases the occurrence of consecutive transfers before bond rupture occurs. Products which may have been formed in this way are shown in *Table 7*.

Comparison of the expectations expressed in *Table 7* with the pyrogram (*Figure 6*) shows that intramolecular hydrogen transfer actually occurs. Some minor peaks can be explained as stemming from consecutive reactions after removal of the side group (e.g. 2-methylhexane) or of a methyl group

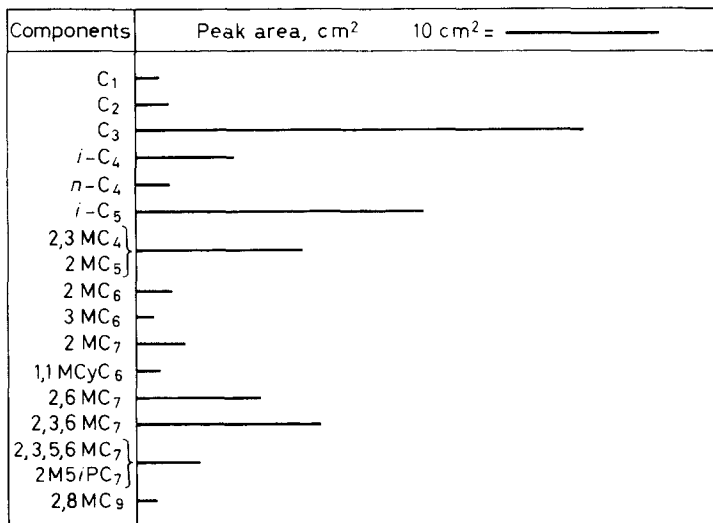
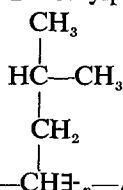


Figure 8—Areas of the main peaks in the pyrogram of poly-3-methylbutene-1

Table 7. Products expected from intramolecular hydrogen transfer during pyrolysis of poly-3-methylbutene-1 (main observed peaks are underlined)

	Number of the hydrogen-donating carbon atom		
	5	6	7
Primary radical: 	C_3 $\underline{2,3MC_4}$ $2,3,6MC_7$ $2,3,8M5iPC_9$	$\underline{2,3,6MC_7}$ $2,3,7,8M5iPC_9$ $\underline{CH_4}$	$2,3,5,6MC_7$ $2,3,8M5iPC_9$ $\underline{C_3}$
Secondary radical: 	$\underline{2,6MC_7}$ $2,3,8M5iPC_9$ $\underline{CH_4}$	$2,3,6MC_7$ $\underline{2,8M5iPC_9}$ $2,10M5,7iPC_{11}$	$2,8M5iPC_9$ $2,3,10M5,7iPC_{11}$ $\underline{CH_4}$

from the secondary radical originally formed (e.g. 2-methylheptane), or after intramolecular hydrogen transfer (e.g. 2-methylpentane and 2,8-dimethylnonane).



(7) Poly-4-methylpentene-1: $-ECH_2-CH-)_n-$ A survey of the main degradation products of poly-4-methylpentene-1 is given in Figure 9. We see

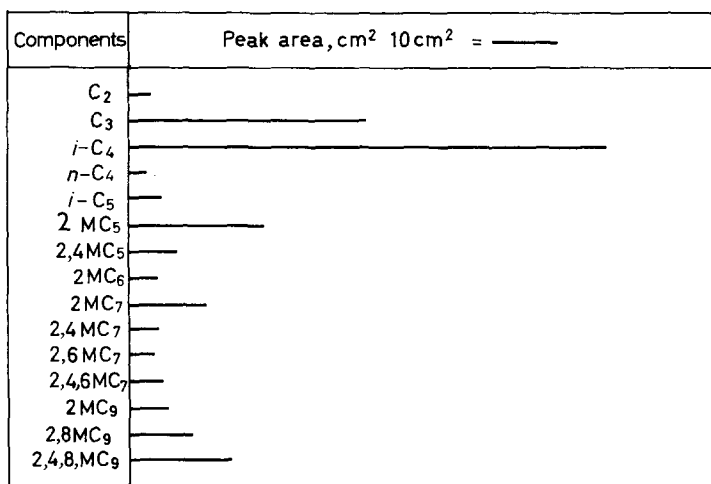


Figure 9—Areas of the main peaks in the pyrogram of poly-4-methylpentene-1

PYROLYSIS-HYDROGENATION-GLC OF POLY-2-OLEFINS

that not only the whole side group but also the isopropyl group is easily removed (C₃ peak). This parallels observations made on degradation by high-energy irradiation¹⁹. The 2-methylpentane peak, which in size follows the propane peak, should probably be ascribed to unzipping.

Peaks expected from intramolecular hydrogen transfer are listed in Table 8.

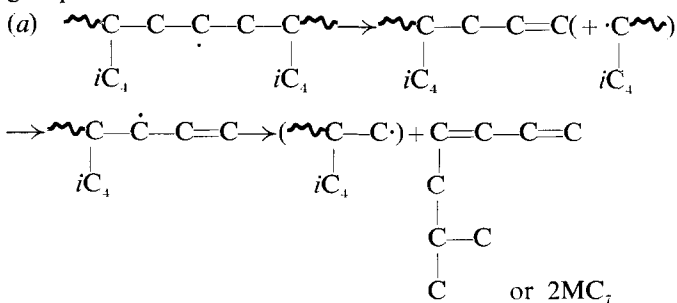
The peaks in this table that fall in the range detected in our experiments are indeed rather large. Most of the remaining peaks in the pyrogram are

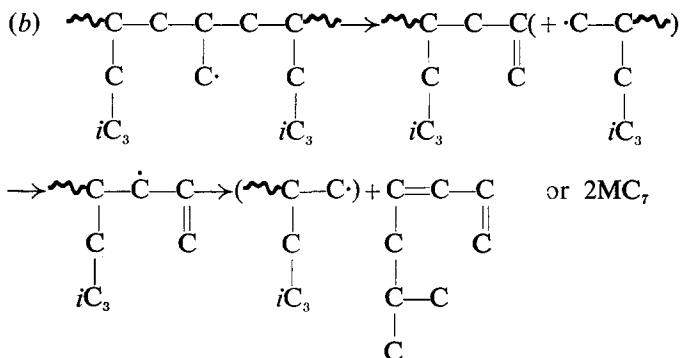
Table 8. Products expected from intramolecular hydrogen transfer during pyrolysis of poly-4-methylpentene-1 (main observed peaks are underlined)

	Number of the hydrogen-donating atom	
	5	6
Primary radical: $\begin{array}{ccccccccccc} & & & & 6 & 5 & & & & & \\ \sim & C & - & C & - & C & - & C & - & C & - & C & - & C & - & C & \cdot \\ & & & & & & & & & & & & & & & \\ & C & & C & & C & & 5C & & C & & C & & & & \\ & & & & & & & & & & & & & & & \\ & C & - & C & - & C & - & C & - & 6C & - & C & - & C & - & C_3 \\ & & & & & & & & & & & & & & & \\ & C & & C & & C & & C & & C & & C & & & & \end{array}$	$\begin{array}{c} CH_4 \\ \underline{iC_4} \\ \underline{2,4MC_3} \\ \underline{2,4,8MC_9} \\ 2,4,10M6iBC_{11} \\ \underline{C_3} \end{array}$	$\begin{array}{c} C_3 \\ \underline{iC_4} \\ \underline{2,4,8MC_9} \\ 2,4,10M6iBC_{11} \end{array}$
Secondary radical: $\begin{array}{ccccccccccc} & & & & 6 & 5 & & & & & \\ \sim & C & - & C & - & C & - & C & - & C & - & C & - & C & \cdot \\ & & & & & & & & & & & & & & \\ & C & & 6C & & C & & C & & C & & & & & \\ & & & & & & & & & & & & & & \\ & C & - & C & - & C & - & 5C & - & C & - & C & - & C & \\ & & & & & & & & & & & & & & \\ & C & & C & & C & & C & & C & & C & & & \end{array}$	$\begin{array}{c} \underline{iC_4} \\ 2,8MC_9 \\ 2,4,8M6iBC_{11} \end{array}$	$\begin{array}{c} CH_4 \\ 2,4,8MC_9 \\ 2,8M6iBC_{11} \\ 2,12M6,8iBC_{13} \end{array}$

formed by consecutive reactions after removal of the side group or part of it. In this way the 2-methylalkanes and 2,4- and 2,6-dimethylheptane may have been formed.

The large 2-methylheptane peak may have to be ascribed to 2-methylheptadiene formed after direct splitting off of the isobutyl or propyl side group:





(8) *Polystyrene and poly- α -methylstyrene*—These two polymers give the simplest pyrograms as nearly complete depolymerization to monomer occurs (see *Figures 10 and 11*). This is in agreement with results obtained by Madorsky and co-workers^{18, 20}.

Components	Peak area, cm ² 100 cm ² = ———
C ₂	
CyC ₆	
MCyC ₆	
ECyC ₆	—————
<i>i</i> -PCyC ₆	
<i>n</i> -PCyC ₆	

Figure 10—Areas of the main peaks in the pyrogram of polystyrene

PYROLYSIS PATTERN AND POLYMER STRUCTURE

From the results discussed a few general conclusions can be drawn as regards the relation between polymer structure and detectable pyrolysis products:

(a) The depolymerization reaction in the pyrolysis of polyolefins increases with branching but is relatively insensitive to the size of the branches (see *Table 9*; compare polyethylene, hydrogenated natural rubber, polypropylene, polybutene-1, poly-3-methylbutene-1 and poly-4-methylpentene-1).

Components	Peak area, cm 200 cm = ———
CyC ₆	
<i>i</i> -PCyC ₆	—————

Figure 11—Areas of the main peaks in the pyrogram of poly- α -methylstyrene

(b) The depolymerization reaction predominates over hydrogen transfer reactions in the absence of tertiary hydrogen atoms. (Compare polyisobutylene with polybutene-1.)

PYROLYSIS-HYDROGENATION-GLC OF POLY- α -OLEFINS

(c) With increasing size of the branches we find an increasing amount of splitting-off of the alkyl side group. (Compare polypropylene, polybutene-1, poly-3-methylbutene-1 and poly-4-methylpentene-1.)

(d) Intramolecular hydrogen transfer is an important reaction in the pyrolysis of all saturated polyolefins and takes place predominantly, although not exclusively, with the hydrogen of the fifth carbon atom.

Apart from these conclusions there is one further aspect that deserves some attention. The pyrolysis products above carbon number 13 are not detected by our pyrolysis-GLC technique. The larger fragments formed under the conditions of our experiments condense for the greater part in the pyrolysis or hydrogenation section or are trapped in the GLC column. As was to be expected, the percentage of detectable products formed differs widely for the various polymers.

This is illustrated in *Table 9*, where the total sum of the peak surface areas is given for the various polymers investigated. We have assumed that poly- α -methylstyrene is pyrolysed completely to monomer and that the

Table 9. Total peak surface area of detected pyrolysis fragments

<i>Polymer</i>	<i>Total peak surface area</i>	<i>Percentage of sample detected</i>	<i>Percentage of sample detected as monomer</i>
Polyethylene	75	5	0.3
Polypropylene	315	23	3.8
Hydrogenated natural rubber	210	15	1.5
Polybutene-1	205	15	2.5
Polyisobutylene	455	33	12.2
Poly-3-methylbutene-1	165	12	1.9
Poly-4-methylpentene-1	230	17	1.9
Polystyrene	980	70	68.6
Poly- α -methylstyrene	1390	100	98.5

sensitivity of the detection per carbon atom is constant for the various fragments. The percentage of the sample that has been converted to detectable fragments can then be calculated.

It is seen that the yield of detectable products is higher for those polymers that are known to produce a large amount of monomer: polystyrene and polyisobutylene.

Of the poly- α -olefins the largest yield is found for polypropylene and it is more than fourfold that for polyethylene.

Thanks are due to Dr G. J. van Amerongen of this laboratory for the samples of polybutene-1, poly-3-methylbutene-1 and poly-4-methylpentene-1 and to Dr P. H. van der Mey for the poly- α -methylstyrene sample.

The authors are indebted to Messrs H. de Ruyter and W. G. van Wijk for the infra-red and mass-spectrometric identification of the three polypropylene peaks isolated with preparative GLC.

Koninklijke/Shell-Laboratorium, Amsterdam,
Badhuisweg 3, Amsterdam N,
The Netherlands

(Received October 1964)

REFERENCES

- ¹ LEHRLE, R. S. and ROBB, J. C. *Nature, Lond.* 1959, **183**, 1890
- ² BARLOW, A., LEHRLE, R. S. and ROBB, J. C. *Polymer, Lond.* 1961, **2**, 27
- ³ BARRAL II, E. M., PORTER, R. S. and JOHNSON, J. F. *Analyt. Chem.* 1963, **35**, 73
- ⁴ ETTRE, K. and VÁRADI, P. F. *Analyt. Chem.* 1963, **35**, 69
- ⁵ HEWITT, G. C. and WHITMAN, B. T. *Analyst*, 1961, **86**, 643
- ⁶ COBLER, J. G. and SAMSEL, E. P. *SPE Trans.* 1962, **2**, 145
- ⁷ STANLEY, C. W. and PETERSON, W. R. *SPE Trans.* 1962, **2**, 298
- ⁸ ETTRE, K. and VÁRADI, P. F. *Analyt. Chem.* 1962, **34**, 752
- ⁹ VAN SCHOOTEN, J., DUCK, E. W. and BERKENBOSCH, R. *Polymer, Lond.* 1961, **2**, 357
- ¹⁰ SWARC, M. *et al. J. Amer. chem. Soc.* 1956, **78**, 2656
- ¹¹ FERRIS, S. W. *Handbook of Hydrocarbons*. Academic Press: New York, 1955
- ¹² 'Selected values of properties of hydrocarbons', American Petroleum Institute, *Research Project 44*
- ¹³ POLGAR, A. G., HOLST, J. J. and GROENNINGS, S. *Analyt. Chem.* 1962, **34**, 1226
- ¹⁴ SIMHA, R., WALL, L. A. and BLATZ, P. J. *J. Polym. Sci.* 1950, **5**, 615
- ¹⁵ WALL, L. A. and STRAUSS, S. J. *Polym. Sci.* 1960, **44**, 313
- ¹⁶ WILLBOURN, A. H. *J. Polym. Sci.* 1959, **34**, 592
- ¹⁷ See, for example, JELLINEK, H. H. G. *Pure appl. Chem.* 1962, **4**, 419
- ¹⁸ WALL, L. A. *J. Res. Nat. Bur. Stand.* 1948, **41**, 315
- ¹⁹ (a) HARLEN, F. *et al. J. Polym. Sci.* 1955, **18**, 589
(b) BOYLE, D. A., SIMPSON, W. and WALDRON, J. D. *Polymer, Lond.* 1961, **2**, 323 and 335
- ²⁰ MADORSKY, S. L. and STRAUSS, S. J. *J. Res. Nat. Bur. Stand.* 1948, **41**, 417
- ²¹ VOIGT, J. *Kunststoffe*, 1964, **54**, 2

The Calculation of Unperturbed Polymer Dimensions from Perturbed Ones

C. F. CORNET

It is shown that unperturbed polymer dimensions cannot be derived reliably from perturbed ones by means of existing theoretical relations. Each polymer-solvent combination seems to obey its own specific α/z relation. Therefore unperturbed dimensions can only be calculated from perturbed ones with the aid of α/z relations into which additional parameters, depending on both the polymer and the solvent, are introduced.

DIMENSIONS of polymer molecules in solution can be determined experimentally, though not very accurately, by techniques such as light-scattering dissymmetry measurements or dilute solution viscometry. In most solvents the configuration and consequently the dimensions of the polymer molecules are perturbed by the influences of the polymer-solvent interaction and by the excluded-volume effect. 'Unperturbed' polymer dimensions can only be determined by measurements in a so-called θ -solvent, in which the second virial coefficient A_2 is zero.

Many attempts have been made to find a relation between the degree of perturbation of the polymer coils and some polymer-solvent interaction parameter, but agreement between theory and experiment has always been poor. An excellent review was recently given by Kurata and Stockmayer¹. G. V. Schulz *et al.*² gave a lucid comparison between theoretical and experimental results for polymethyl methacrylate (cf. also refs. 3 and 4).

The aim of this paper is to investigate whether unperturbed dimensions can be obtained from perturbed ones with sufficient accuracy.

RELATIONS BETWEEN THE DEGREE OF PERTURBATION AND THE POLYMER-SOLVENT INTERACTION

The degree of perturbation can be expressed as the expansion factor z defined as the ratio of the root-mean-square (r.m.s.) values of the perturbed and unperturbed radii of gyration

$$z = (\overline{S^2} / \overline{S_0^2})^{1/2} \quad (1)$$

The polymer-solvent interaction is usually expressed by the parameter z . If the size and shape of a polymer segment can be taken approximately equal to the size and shape of a solvent molecule z can be written⁵⁻⁷

$$z = 2 \left(\frac{3}{2\pi} \right)^{3/2} \left(\frac{6\overline{S_0^2}}{M} \right)^{-3/2} \frac{A_2 M^{1/2}}{N_0 h(z)} \quad (2)$$

where M is the molecular weight of the polymer, N_0 is Avogadro's number, A_2 is the second virial coefficient, and $h(z)$ is some function of z , which is not precisely known.

Flory⁸⁻¹⁰ was the first to relate the expansion factor α and some polymer-solvent interaction parameter in a closed expression. He considered the polymer coil to be represented by a spherically symmetrical Gaussian distribution of unconnected segments around its mass centre. He calculated the Gibbs free energy as a function of α and found a relation which reads in terms of z (see also refs. 5 and 7)

$$\alpha^5 - \alpha^3 = 2.60 z \quad (3)$$

Flory stated that this expression is open to question, because the assumptions on the segment distribution do not hold rigorously. Several authors¹¹⁻¹⁴ have tried to establish an α/z relation without making these assumptions. These so-called exact derivations do not differ much from each other and all give the same results. The authors calculate the probabilities of all configurations either by attaching to each configuration a weight depending on the total potential energy of all unconnected segment pairs or by correcting for the probability that two unconnected segments occupy the same volume. In these calculations additivity of the potential energy of segment pairs is assumed. All authors but one¹³ only consider the contribution of pairs of segments.

The exact calculations result in the slowly converging series expansion

$$\alpha^2 = 1 + \frac{4}{3} z - \frac{6.28}{3} z^2 + \dots \quad (4)$$

the quadratic term in which was derived by Fixman¹³.

Actually, the expansion factor α used in equation (4) does not correspond to the definition given by equation (1), because in equation (4) α is defined as the ratio of the r.m.s. perturbed and unperturbed end-to-end distances (instead of radii of gyration). We shall not distinguish between these two α values, however, because the difference is probably not large.

Owing to the very slow convergence of the exact series expansion and the mathematical difficulty of obtaining the higher terms it cannot be applied to experiments unless z is very small. Attempts have therefore been made to find a closed expression.

Assuming that Flory's result, equation (3), is essentially correct, Stockmayer^{5,7} replaced the RHS of equation (3) by the second term of the exact series and obtained

$$\alpha^5 - \alpha^3 = \frac{4}{3} z \quad (5)$$

Fixman^{15,16} and Ptitsyn¹⁷ independently derived an expression approximated by

$$\alpha^3 - 1 = 2z \quad (6)$$

Using an equivalent ellipsoid model of uniformly distributed unconnected segments Kurata, Stockmayer and Roig¹⁸ found

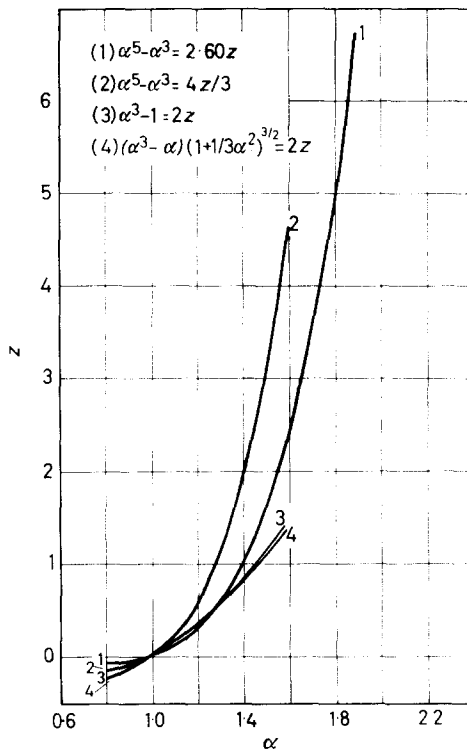
$$(\alpha^3 - \alpha) (1 + 1/3 \alpha^2)^{3/2} = 2z \quad (7)$$

UNPERTURBED POLYMER DIMENSIONS FROM PERTURBED ONES

COMPARISON WITH EXPERIMENTAL DATA

The α/z relations given by equations (3), (5), (6) and (7) are shown in Figure 1. There appears to be a not inconsiderable difference between the various functions. We therefore plotted the z -values calculated from a number of experimental literature data versus the corresponding α -values.

Figure 1—Plots of z versus α



The experimental data on α - and z -values were taken from several sources. Schulz² measured α - and A_2 values for polymethyl methacrylate solutions both near the θ -temperature and in good solvents by light-scattering measurements. Oth and Desreux¹⁹ determined molecular weights, second virial coefficients and radii of gyration of polystyrene in good non-polar and polar solvents and in poor polar solvent mixtures by light-scattering measurements. Kinsinger and Hughes^{20, 21} used light-scattering measurements to find M , A_2 and \overline{S}_0^2 for isotactic polypropylene in a good solvent. They also give²¹ a value for \overline{S}_0^2 . The possible errors involved are estimated to be ± 20 per cent in the value of z and ± 10 per cent in the value for α , except for the Schulz α -values, which are in very good agreement with his own viscometric data; we assume these α -values to be accurate within ± 5 per cent.

In all cases the data pertained to polymers with a fairly narrow molecular weight distribution.

The z -values were deduced by using equation (2) and—arbitrarily—

Flory's closed expression¹⁰ for $h(z)$, which, in the symbols used here, reads

$$h(z) = h(3^{3/2}z\alpha^{-3}) = 1 - \frac{3^{3/2}z\alpha^{-3}}{2! 2^{3/2}} + \frac{\{3^{3/2}z\alpha^{-3}\}^2}{3! 3^{3/2}} - \dots \quad (8)$$

Combination of equations (1) and (2) gives

$$(z/\alpha^3) h(z) = 1.095 \times 10^{-24} A_2 M^2 (\overline{6S^2})^{-3/2} \quad (9)$$

Now $(z/\alpha^3) h(z)$ can be found from experimental data.

The quantity $(z/\alpha^3) h(z)$ was calculated for a number of values of z/α^3 , using a sufficient number of terms in the $h(z)$ series expansion [equation (8)], and plotted in *Figure 2*. For a given value of $(z/\alpha^3) h(z)$ the value of

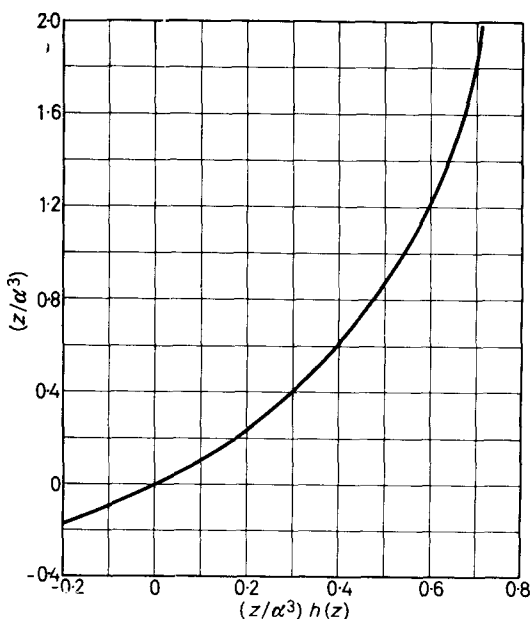


Figure 2— (z/α^3) as a function of $(z/\alpha^3) h(z)$ according to equation (8)

(z/α^3) may be read from this plot. The value of α is known from experiment and thus z can now be calculated. The 'experimental' values of z so obtained have been plotted against α in *Figure 3*.

It appears that every polymer-solvent combination seems to obey its own specific α/z relationship.

CONCLUSION

From *Figure 3* we cannot conclude that there is a general relationship between α and z ; the use of any such relationship may give rise to large errors. In other words, in the present state of knowledge it is impossible to calculate reliable unperturbed dimensions from experimentally determined perturbed ones, without the introduction of additional parameters*.

*After this work was completed, the author came across an article by Burchard¹¹, which tends to confirm his conclusions.

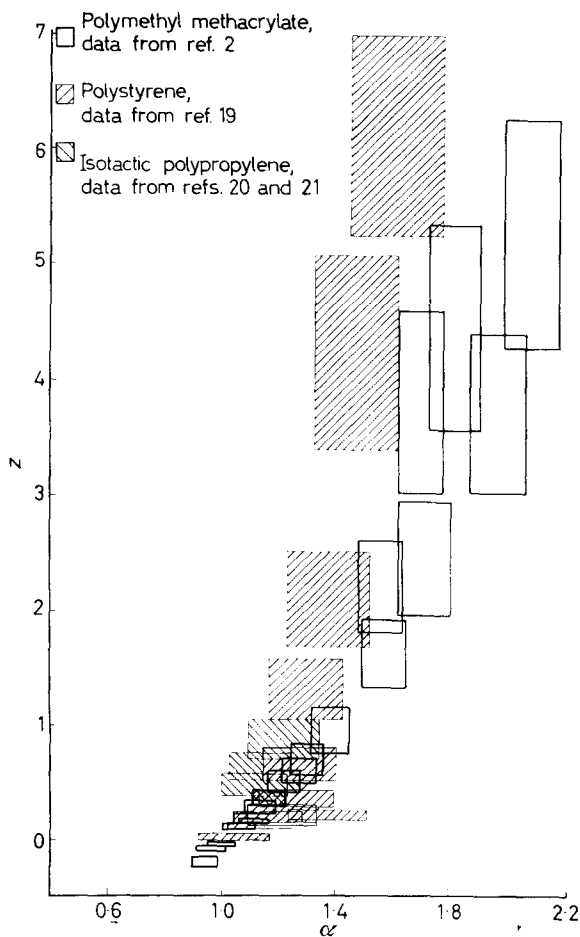


Figure 3—Plots of experimental α - and z -values

Koninklijke/Shell-Laboratorium, Amsterdam,
 Badhuisweg 3, Amsterdam N,
 The Netherlands

(Received October 1964)

REFERENCES

- ¹ KURATA, M. and STOCKMAYER, W. H. *Fortschr. Hochpolymer.-Forsch.* 1963, **3**, 196
- ² SCHULZ, G. V. and KIRSTE, R. *Z. phys. Chem.* 1961, **30**, 171
- ³ SCHULZ, G. V. and BAUMANN, H. *Makromol. Chem.* 1963, **60**, 120
- ⁴ SCHULZ, G. V., HAUG, A. and KIRSTE, R. *Z. phys. Chem.* 1963, **38**, 1
- ⁵ STOCKMAYER, W. H. *J. Polym. Sci.* 1955, **15**, 595
- ⁶ ZIMM, B. H. *J. chem. Phys.* 1946, **14**, 164
- ⁷ STOCKMAYER, W. H. *Makromol. Chem.* 1959, **35**, 54
- ⁸ FLORY, P. J. *J. chem. Phys.* 1949, **17**, 303
- ⁹ FLORY, P. J. and FOX JR, T. G. *J. Amer. chem. Soc.* 1951, **73**, 1904; *J. Polym. Sci.* 1950, **5**, 745
- ¹⁰ FLORY, P. J. *Principles of Polymer Chemistry*, Ch. X, XII and XIV. Cornell University Press: Ithaca, 1953

- ¹¹ BUECHE, F. *J. chem. Phys.* 1953, **21**, 205
- ¹² ZIMM, B. H., STOCKMAYER, W. H. and FIXMAN, M. *J. chem. Phys.* 1953, **21**, 1716
- ¹³ FIXMAN, M. *J. chem. Phys.* 1955, **23**, 1656
- ¹⁴ KURATA, M., YAMAKAWA, H. and TERAMOTO, E. *J. chem. Phys.* 1958, **28**, 785
- ¹⁵ FIXMAN, M. *J. chem. Phys.* 1962, **36**, 3123
- ¹⁶ STOCKMAYER, W. H. and FIXMAN, M. *J. Polym. Sci. C*, 1963, **1**, 137
- ¹⁷ PITTSYN, O. B. *Vysokomol. Soed.* 1961, **3**, 1673; *Polymer Sci. U.S.S.R.* 1962, **3**, 1061
- ¹⁸ KURATA, M., STOCKMAYER, W. H. and ROIG, A. *J. chem. Phys.* 1960, **33**, 151
- ¹⁹ OTH, J. and DESREUX, V. *Bull. Soc. chim. Belg.* 1954, **63**, 285
- ²⁰ KINSINGER, J. B. and HUGHES, R. E. *J. phys. Chem.* 1959, **63**, 2002
- ²¹ KINSINGER, J. B. and HUGHES, R. E. *J. phys. Chem.* 1963, **67**, 1922
- ²² BURCHARD, W. *Z. phys. Chem.* 1964, **42**, 293

Crystallization of Polyamides

II—Nylon 6 and Nylon 66

J. H. MAGILL

A comparison is made between the rates of spherulitic growth in Nylon 6 and Nylon 66 polymers. Theoretical equations describing the growth rates are presented using the concept of molecular chain folding within the fibrils or lamellae comprising the spherulites. These equations adequately describe the rate of spherulite growth in these two polyamides, which occurs by a coherent two-dimensional mechanism. Crystal surface free energies are given.

NYLON 6 and Nylon 66 crystallize spherulitically when cooled from the molten state¹. Both polymers form positively birefringent spherulites at supercoolings (ΔT^*) in excess of 20°C below their respective thermodynamic melting points (T_m^*). At comparable ΔT^* for similar molecular weights, Nylon 66 spherulites grow many times faster than Nylon 6 spherulites^{2,3}. The purpose of this communication is to examine the crystallization kinetics of these two similar polyamides in the light of recently developed concepts of crystallization^{4,5}.

RESULTS AND DISCUSSION

Table 1 contains some isothermal spherulite growth rates² obtained on a $\bar{M}_n = 24\,700$ Nylon 6 sample which was fused (prior to crystallization) at 270°C for half an hour. It is assumed that molecular chain folding occurs in the growing fibrils or lamellae comprising the spherulites. Growth can

Table 1. Spherulitic crystallization rates (G) for Nylon 6

Temperature (°K)	363	368	374	380	390	397.5	408	414	421
G (μ /min)	22.5	36.6	38.4	66.5	94.3	116.0	146.3	146.3	126.3
Temperature (°K)	430	445	457	457.5					
G (μ /min)	107.4	59.0	18.3	14.4					

be perpetuated by either coherent or non-coherent nucleation mechanisms around a central nucleus. Spherulite growth (G) can be described by an equation of the form

$$G = G_0 \exp(-\Delta F_\eta^*/RT) \exp(-\Delta G^*/RT) \quad (1)$$

where G_0 may be considered a constant. ΔG^* is the free energy of crystal formation and ΔF_η^* expresses the temperature dependence of the segmental jump rate from potential wells in the liquid side to the growing crystal front.

An analysis of these Nylon 6 results (in a manner similar to that used for polychlorotrifluoroethylene³) clearly indicates that a ΔT^{-1} (two-dimensional surface nucleation) law is preferred to a ΔT^{-2} (three-

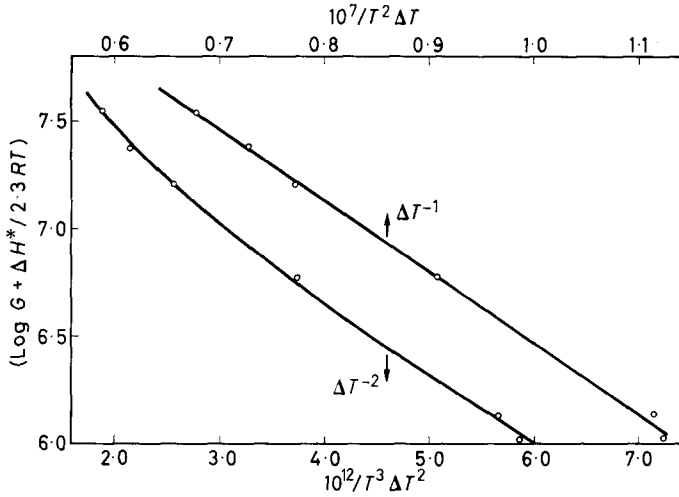


Figure 1—Determination of the ΔT law for Nylon 6 (radial growth rate data) with $T_m = 227^\circ\text{C}$

dimensional surface nucleation as illustrated in Figure 1). The plot of $[\log G + \Delta H^*/2.3RT]$ is linear for the ΔT^{-1} plot, but distinct curvature is apparent in the ΔT^{-2} plot, using the G values to the right of the maximum of Figure 2. For the purpose of this analysis, ΔF_n^* was replaced by ΔH^* taken to be 10.8 kcal per mole of repeat units of Nylon 6°. It is necessary to include the temperature dependence of this term, in the manner indicated, to establish the exact nature of the growth mechanism. From the slope of the linear ΔT^{-1} plot (Figure 1) it was deduced that the product of the lateral surface free energy (σ) and chain end fold surface free energy (σ_e) was about 480 erg²/cm⁴ for crystal growth.

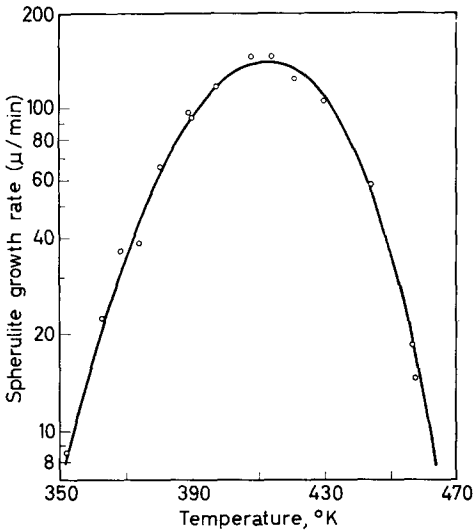


Figure 2—Spherulite growth rates for Nylon 6, $\bar{M}_n = 24\,700$ and calculated curve corresponding to these experimental points

CRYSTALLIZATION OF POLYAMIDES II

An alternative approach utilizes all the experimental results on both sides of the maximum. The best curve is fitted by computer to an equation of the form

$$G = G_0 \exp(-\Delta F_{\eta}^*/RT) \exp(-BT_m^2/T^2\Delta T) \quad (2)$$

or

$$G = G'_0 \exp(-\Delta F_{\eta}^*/RT) \exp(-B'T_m/T\Delta T) \quad (3)$$

Equation (3) is a less exact form derived from (2). The first exponential term of equations (2) or (3) can be expressed⁷ as $\exp[-A/R(T-T_0)]$ which utilizes a reference temperature $T_0 \sim T_g$ rather than 0°K as employed in equations (2) and (3); whence (2) and (3) become

$$G = G_0 \exp[-A/R(T-T_0)] \exp[-BT_m^2/T^2\Delta T] \quad (4)$$

and

$$G = G_0 \exp[-A'/R(T-T_0)] \exp[-B'T_m/T\Delta T] \quad (5)$$

The values in *Table 1* were least squared with equations (4) and (5) using $T_m = 500^\circ\text{K}$ and $T_m = 503^\circ\text{K}$. The significant molecular parameters are presented in *Table 2*.

Table 2. Parameters governing the crystallization of Nylon 6 spherulites by a secondary, two dimensional nucleation mechanism

T_m	Equation (4)		Equation (5)	
	500°K	503°K	500°K	503°K
$A \times 10^{-3}$	1.29	1.50	1.56	1.84
$B \times 10^{-2}$	2.98	3.40	2.96	3.38
$G_0 \times 10^{-6}$	2.43	6.92	2.14	6.33
T_0 °K	276	269	270	263
$\sigma\sigma_e$	465	520	465	520

G_0 is expressed above in μ/min and $\sigma\sigma_e$ in erg^2/cm^4 . The calculated curve is shown with the experimental points in *Figure 2*.

Using the somewhat empirical relationship⁴

$$\sigma / \Delta h_f b_0 = \alpha \text{ (constant)} \quad (6)$$

where Δh_f is the heat of fusion and b_0 the interplanar spacing of the crystal monolayers, a reasonable estimate can be made for σ taking $\alpha = 0.1$. For Nylon 6, this lateral surface free energy is about $8 \text{ erg}/\text{cm}^2$, whence σ_e is 60 to $65 \text{ erg}/\text{cm}^2$ approximately. These values are of similar magnitude to those found for other polymers. Interesting, too, is the correspondence of G_0 values among these polymers. Nylon 6, polyethylene⁵ and polychlorotrifluoroethylene⁵ all have values around $10^5 \text{ cm}/\text{sec}$.

Table 3

	Equation (4)	Equation (5)
$A \times 10^{-2}$	0.76	1.67
$B \times 10^{-2}$	2.07	2.04
$G_0 \times 10^{-4}$	3.42	2.57
T_0 °K	334	318
$\sigma\sigma_e$	325	320

For Nylon 66 the results are somewhat different. An analysis of spherulite growth rates⁸ through the maximum, using equations (5) and (6), gave (for a $T_m = 545^\circ\text{K}$) the following values (*Table 3*). A heat of fusion⁶ of 48 cal/g was used in the calculation of $\sigma\sigma_e$. From equation (6) σ was derived to be 8.0 to 8.5 erg/cm², whence σ_e must be 40 erg/cm² approximately. A similar result follows from an analysis of McLaren's spherulitic growth rates⁹ for this polymer. From the slope of $[\log G + \Delta H^*/2.3RT]$ versus $[1/T^2\Delta T]$, $\sigma\sigma_e$ is found to be about 360 erg²/cm⁴. This corresponds to a σ of about 8.5 erg/cm², and a σ_e of 40 to 45 erg/cm² in good agreement with the results of *Table 3*.

Earlier², it was suggested that the faster rate of crystallization of Nylon 66 over Nylon 6 might arise because of some configurational differences between these two polymer molecules. Nylon 66 molecules, being symmetrical, can be accommodated in the crystal lattice with greater ease than Nylon 6 which must pack in antiparallel arrays to favour complete hydrogen bonding. A definitive explanation still cannot be given for this difference in rate. However, it is worth noting that a lower G_0 (1.55×10^3 cm/sec) is found for Nylon 66 than for Nylon 6. Furthermore the work of chain folding, q , which reflects the molecular chain stiffness of the polymer has been expressed as

$$q = 2A_0\sigma_e \quad (7)$$

where A_0 is the molecular cross section of the polymer chain. From Bunn's unit cell structures^{10,11}, A_0 for Nylon 6 was calculated to be 17.7 Å² and for Nylon 66 as 17.6 Å². Since σ_e for Nylon 66 is less than σ_e for Nylon 6, then, using equation (7), the q values for these polymers must be in the same order. Initial moduli measurements have not been made on lactam-free dry polymers at equal supercoolings to bear comparison with these results. Although the theoretical modulus of Nylon 66 has been calculated¹², that for Nylon 6 would be comparable in such a derivation because of the assumptions and procedures involved. The melt viscosity¹³ and apparent activation energy for viscous flow of lactam-free Nylon 6 is found to be greater than that of Nylon 66 of similar molecular weight and molecular weight distribution at corresponding temperatures above their respective melting points. This experimental result bears comparison with the results above.

Clearly further experimental work is necessary to provide alternative derivations of σ and σ_e values. In particular, the analysis of dilatometric measurements of homogeneous nucleation experiments¹⁴ using dispersed polymer droplets (and long period X-ray measurements on isothermally crystallized bulk polymers or single crystals) should yield, in conjunction with the present rate data, consistent and reliable values of σ and σ_e and so permit a definitive solution to the problem of rate difference in these two polymers. For the present, however, it is clear that a coherent two-dimensional secondary nucleation mechanism with chain folding adequately describes the rate of spherulite growth in these two polyamides.

In all instances the derived T_0 values are approximately equal to, or less than, the observed glass temperatures for these two polymers. For Nylon 66, using equation (4), T_0 is found to equal T_g but this close agreement is

believed to be fortuitous. Noteworthy too is the fact that the Nylon 6 rate curve reaches a maximum ($T_{\max.}$) about 138°C, while Nylon 66 peaks about 141°C giving the ratio $T_{\max.}/T_m$ for Nylon 6 about 0.82 and for Nylon 66 around 0.76 in fair agreement with the values¹⁵ obtained for Nylon 5.6 (0.85) and Nylon 9.6 (0.87).

This work was supported in part by the U.S. Office of Naval Research under Contract Number Nonr 2693 (00). Gratitude is also expressed to Mr B. Hazlett for least square calculations.

Mellon Institute,
4400 Fifth Avenue, Pittsburgh 13,
Pennsylvania, U.S.A.

(Received November 1964)

REFERENCES

- ¹ KHOURY, F. J. *Polym. Sci.* 1957, **26**, 373; 1958, **33**, 389
- ² MAGILL, J. H. *Polymer, Lond.* 1962, **3**, 43; 1962, **3**, 655
- ³ BURNETT, B. B. and McDEVIT, W. F. *J. appl. Phys.* 1957, **28**, 1101
- ⁴ HOFFMAN, J. D. and LAURITZEN, Jr, J. I. *J. Res. Nat. Bur. Stand. A.* 1961, **65**, 297
- ⁵ HOFFMAN, J. D. and WEEKS, J. J. *J. chem. Phys.* 1962, **37**, 1723
- ⁶ DOLE, M. and WUNDERLICH, B. *Makromol. Chem.* 1959, **34**, 29
- ⁷ MAGILL, J. H. *ONR Report No. 12*, September 1964
- ⁸ LINDERGREN, C. R. *J. Polym. Sci.* 1961, **50**, 181
- ⁹ McLAREN, J. V. *Polymer, Lond.* 1963, **4**, 175
- ¹⁰ BUNN, C. W. and GARNER, E. V. *Proc. Roy. Soc. A*, 1947, **189**, 39
- ¹¹ HOLMES, D. R., BUNN, C. W. and SMITH, D. J. *J. Polym. Sci.* 1955, **17**, 159
- ¹² TRELOAR, L. R. G. *Polymer, Lond.* 1960, **1**, 95
- ¹³ CHAPMAN, C. B. Private communication
- ¹⁴ CORMIA, R. L., PRICE, F. P. and TURNBULL, D. J. *J. chem. Phys.* 1962, **37**, 1333
- ¹⁵ MAGILL, J. H. *J. Polym. Sci.*, Part A, 1965, **3**, 1195

The Determination of Unperturbed Dimensions of Polymer Molecules by Viscometry of Moderately Concentrated Solutions

C. F. CORNET

It is demonstrated that unperturbed dimensions of high-molecular-weight polymer coils can be determined from viscosity data of moderately concentrated polymer solutions by assuming that a uniform total segment density is attained at the so-called critical concentration. The root-mean-square end-to-end distance is given by

$$\overline{(R^2)}^{1/2} = 2.84 \times 10^{-8} (M/c_{cr})^{1/3}$$

M and c_{cr} denote the molecular weight and the critical concentration, respectively.

THE dimensions of a polymer chain in dilute solution are influenced by two factors: the polymer-solvent interaction and the intramolecular excluded-volume effect. The energy of interaction between polymer segments and the molecules of a good solvent tends to increase the chain dimensions, because by expansion more polymer-solvent contacts are created. The intramolecular excluded-volume effect also increases the dimensions (see e.g. ref. 1, pp 423-426 and 523-530).

According to Flory's definition a chain has its unperturbed dimensions in a θ -solvent, in which the second virial coefficient is zero. It can be proved that these unperturbed dimensions approximate the statistically determined random-flight dimensions; at θ -conditions, therefore, the excluded volume effect is compensated by a positive polymer-solvent interaction energy (see e.g. ref. 1, pp 423-426; 595-602 and 519-534).

Unperturbed chain dimensions can be determined by methods such as light-scattering or dilute-solution-viscosity measurements on polymers dissolved in θ -solvents. They can, in principle, also be calculated from perturbed dimensions, provided sufficient data are available.

Direct measurement of unperturbed dimensions by the above-mentioned methods is, however, not simple and sometimes even impossible. Starting from the supposition that polymer molecules in concentrated solutions are in the unperturbed state, we have developed a method to determine the unperturbed dimensions from viscosity data on such solutions. It is based on the assumption that a uniform distribution of the polymer segments throughout a polymer solution is attained at the so-called critical concentration. This concentration is determined by a break in a plot of the

logarithm of the viscosity versus the logarithm of the concentration. The method is discussed in the present paper.

DISCUSSION OF EXPERIMENTAL DATA

Plots of the logarithm of the viscosity of polymer melts versus the logarithm of the molecular weight have been reported²⁻⁴ to consist of two straight intersecting lines. The same has been observed for plots of the log viscosity of polymer solutions of equal concentration versus the log molecular weight⁵⁻⁷. Very recently Onogi *et al.*⁸ and the author have independently obtained log viscosity versus log concentration plots for polymer solutions which also showed two straight intersecting lines. The points of intersection are called the critical molecular weight and critical concentration, respectively. *Figure 1* illustrates the usual appearance of such plots.

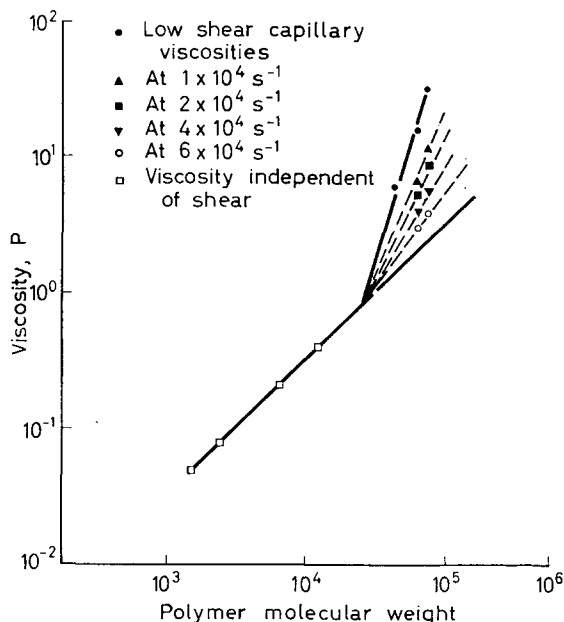


Figure 1—Solution viscosities of polyisobutenes (49.3 per cent by weight of polymer in cetane at 100°C) dependence on rate of shear (after Porter and Johnson⁵)

Figure 1 also illustrates that polymer melts or solutions of fixed concentration show non-Newtonian behaviour^{3-5, 7, 9} at *molecular weights* higher than a critical value but are essentially Newtonian below this value. The author recently observed that polymer solutions at *concentrations* higher than the critical one show non-Newtonian flow, while at low concentrations the viscosity is much less dependent on shear.

Closer inspection of accurate measurements on solutions of a poly- α -methylstyrene sample in toluene reveal that a plot of the log viscosity versus the log concentration for polymer solutions does not really consist of two straight intersecting lines but of one smooth line which is curved up to a certain concentration (hereafter also called the critical concentration) and

practically straight from there onwards (see *Figure 2*). Curves of this shape have recently been reported by Utracki and Simha¹⁰.

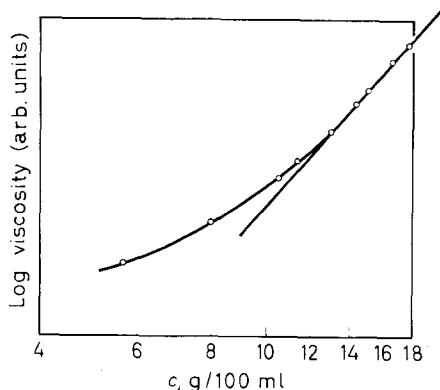


Figure 2—Viscosity versus concentration of a poly- α -methylstyrene sample. Viscosities measured with a Schulten-Sparks²⁹ capillary viscometer

What we have called the critical concentration in a log viscosity versus log concentration plot is therefore in reality a rather narrow region where the curve becomes practically a straight line.

THEORETICAL INTERPRETATION

Discussion of literature data

The existence of a critical concentration or molecular weight is thought to be due to entanglement of polymer molecules²⁻⁵. Some investigators have tried to find a relation between the concentration of the polymer and its molecular weight at the critical point. Porter and Johnson⁷, who studied plots of the log viscosity versus the log molecular weight of many polymer solutions of fixed concentration, state that the product $c.M_{cr}$ of the critical molecular weight and the concentration is constant for a given polymer. Tager *et al.*⁸ came to the same conclusion. Both studies are limited to rather low-molecular-weight materials. These statements are not in agreement with that of Onogi *et al.*^{8,11}, who show that $c_{cr}.M^{0.5}$ is constant, and with Ferry *et al.*¹² finding that $c.M^{0.68}$ is related to the log viscosity. However, Onogi and Ferry used high-molecular-weight polymers in their studies.

Utracki and Simha¹⁰ show that the curves in a plot of the logarithm of some viscosity function versus the logarithm of the reduced concentration c/γ for different molecular weight samples of a given polymer coincide, if the 'shift parameters' γ are adjusted to the molecular weights in such a way that $\gamma.M^b$ is constant. The exponent b is 0.47 or 0.64, depending on the solvent used. It seems reasonable to assume that the shift parameter γ is approximately proportional to the critical concentration c_{cr} , so that $c_{cr}.M^{0.47 \text{ to } 0.64}$ is constant. Utracki and Simha used polystyrene samples of various polydispersities and of medium molecular weights.

From these combined data it would seem that the product $c_{cr}M^{0.5}$ is constant for material of sufficiently high molecular weight, while $c_{cr}M$ is constant for low-molecular-weight polymers.

These phenomena may be explained in the following way: in a polymer melt or solution the total volume available per polymer molecule, V , is given by

$$V = M / (cN_0) \quad (1)$$

where M is the weight of one mole of polymer in grammes, c is the polymer concentration in g/ml and N_0 is Avogadro's number.

There are reasons to suppose that the volume V in a critically concentrated solution, or in a polymer melt of the critical molecular weight, is a constant fraction of the effective volume V' of the isolated unperturbed polymer coil itself (see Appendix). We therefore write

$$V = p.V' \quad (2)$$

where p is a constant.

We know that the effective molecular volume V' of a polymer of *high* molecular weight is related to the molecular weight M by

$$V' = b^3 M^{3/2} \quad (3)$$

where b is a constant (see ref. 13, p 243). In consequence, as

$$V_{cr} = M / c_{cr}N_0 = pb^3 M^{3/2} \quad (4)$$

we find, as Onogi^{8,11} did, that $c_{cr}M^{0.5}$ is constant for high-molecular-weight polymers.

If the molecular weight of a polymer is *very low*, according to mathematical calculations¹⁴ the mean square unperturbed end-to-end distance \overline{R}_0^2 is related to M as follows

$$(\overline{R}_0^2)^{1/2} = \text{constant} \times M^{(1+\delta)/2} \quad (5)$$

where δ will be larger than 0.20 for chains with less than two hundred segments and will decrease with increasing molecular weight. We see that for very low-molecular-weight polymers (taking arbitrarily $\delta = 0.33$) V' is proportional to $(\overline{R}_0^2)^{3/2}$ and so to M^2 . We now find via equations (1) and (2) that $c_{cr}M$ is constant, in agreement with Porter and Johnson⁷ and Tager *et al.*⁶.

We can qualitatively arrive at the same conclusion from the relation (see e.g. ref. 1, p 418)

$$(\overline{R}_0^2)^{1/2} = C.l.n^{1/2} \quad (6)$$

where C is a constant exceeding unity, l is the length of a segment and n the number of segments. This equation gives too high values for $(\overline{R}_0^2)^{1/2}$ if n is very small, as is evident if we put n equal to unity. $(\overline{R}_0^2/n)^{1/2}$ must therefore be smaller than follows from equation (6) for low values of n and must approach asymptotically to $C.l$ for increasing n . This is illustrated in *Figure 3*, where the lower part of the curve indicates that the exponent

of n in equation (6) must be higher than a half for low n and that it approaches this value for high n .

If the assumption expressed in equation (2) is correct, it should be possible to estimate polymer molecular dimensions of materials having sufficiently high molecular weight from the value of the critical concentration*.

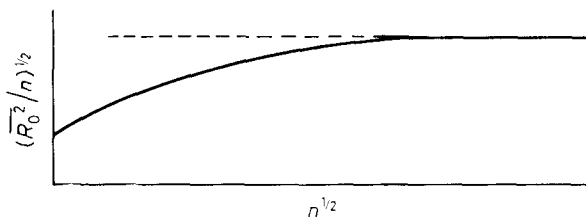


Figure 3— $(R_0^2/n)^{1/2}$ as a function of $n^{1/2}$ —see equation (6) and following text

Discussion of results based on a new model

Let us consider a critically concentrated polymer solution more closely. In a very dilute solution the polymer coils are isolated [Figure 4(a)]. If the solution becomes more concentrated there is some penetration of the coils [Figure 4(b)]. At a certain concentration there is so much penetration that the total segment density becomes uniform throughout the solution [Figure 4(c)]. At still higher concentrations we suppose the segment density to remain uniform, gradually increasing with concentration.

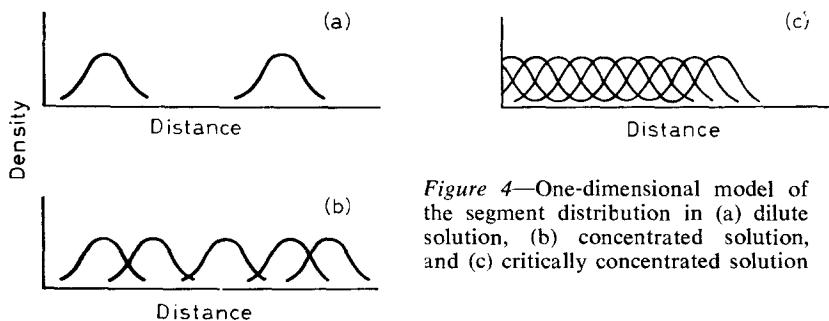


Figure 4—One-dimensional model of the segment distribution in (a) dilute solution, (b) concentrated solution, and (c) critically concentrated solution

In terms of this model the critical concentration presumably corresponds to the situation where the solution just attains a uniform polymer segment

*This has already been tried by Onogi *et al.*⁴, but in our opinion these authors did not approach the problem correctly, because they used the equivalent hydrodynamic volume of a polymer coil, which is the volume of the sphere that shows the same hydrodynamic behaviour as the corresponding polymer coil in an infinitely dilute solution. Onogi *et al.* used this equivalent hydrodynamic volume in the case of a fairly concentrated solution, which seems artificial. That nevertheless they obtain good results is probably due to compensation of the error introduced by this approach (which happens to be small) by the use of an unrealistic model for the space filling of the polymer coils at the critical concentration.

density. The model would then be supported qualitatively by the form of the log viscosity versus log concentration curve (see *Figure 2*).

We can now calculate the average coil dimensions at the critical concentration from the value of this concentration c_{cr} and the molecular weight M , if we make the following supplementary assumptions (see Appendix):

- (1) The polymer molecules are all linear and of equal length and chemical composition.
- (2) The distribution of polymer segments around the centre of gravity of a coil is Gaussian and has a spherical symmetry at the critical concentration.
- (3) The centres of gravity of the coils are arranged in a regular lattice.
- (4) The uniform segment density is attained when the segment density in the centre of gravity of a coil equals the density at a position halfway between two such centres.

We calculate the segment density in a certain point by inserting the numbers of polymer coils and the distances from their centres of gravity to the point concerned in the Gaussian distribution functions. By equalizing the densities in a lattice point and a point halfway between two of them we find the root-mean-square (r.m.s.) end-to-end distance of the coils

$$(\overline{R^2})^{1/2} = K (M/c_{cr})^{1/3} \quad (7)$$

where K is a constant depending on the type of lattice. The constant K has a value of $3.04 \times 10^{-8} \text{ mole}^{1/3}$ for a face-centred cubic (f.c.c.) lattice, $2.64 \times 10^{-8} \text{ mole}^{1/3}$ for a body-centred cubic (b.c.c.) lattice and $2.45 \times 10^{-8} \text{ mole}^{1/3}$ for a simple cubic lattice.

In order to determine the value of the constant K for an actual polymer solution, we assumed that the arrangement of the centres of gravity of the coils is like a close array of randomly packed spheres. We found that the particle density of such random arrays indicates an 'average structure' somewhere between a b.c.c. and a f.c.c. lattice, if we take the effect of a slight heterodispersity into account (see Appendix). Accordingly we used $K = 2.84 \times 10^{-8} \text{ mole}^{1/3}$ in our calculations.

Now the question arises to what degree the coil dimensions are perturbed in a critically concentrated solution. Let us consider this situation for a solution where the polymer segment density is uniform. If there were neither an excluded volume effect nor a polymer-solvent interaction, the coils would approximate their θ or unperturbed extensions because of maximum entropy, hence of minimum Gibbs free energy, in that configuration. In actual fact, however, both effects are at work. But with a solution of uniform segment density, no alteration of the number of polymer-solvent contacts can be forced by shrinking or expansion of the coils, nor can the excluded volume influence the coil dimensions, because any change in the number of intramolecular polymer-polymer contacts will be counterbalanced by an opposite change in the number of intermolecular contacts. In consequence, the heat content of a coil is independent of its configuration and since the entropy is still a maximum for the random flight configuration

UNPERTURBED DIMENSIONS OF POLYMER MOLECULES

the coils will be very near to their unperturbed dimensions at the critical point*.

Table 1. $(\bar{R}_0^2/M)^{1/2}$ values from different sources

$\bar{M}_w \times 10^{-3}$	$c_{cr} \times 10^2$	Remarks	$\left[\frac{\bar{R}_0^2}{\bar{M}_w} \right]^{1/2} \times 10^{11}$	$\left[\frac{\bar{R}_0^2}{M} \right]^{1/2} \times 10^{11}$	Remarks
			from c_{cr}	from lit.	
1 230	4.61	polystyrene in toluene; data from ref. 8	764	760 670 735	light-scattering; ref. 19 intrinsic viscosity; ref. 20 intrinsic viscosity; ref. 1 p 61
587	6.85		759		
282	10.22		750		
157	13.25		758		
96.8	7.80	polyvinyl alcohol in water; data from ref. 8	982	950 948	intrinsic viscosity; ref. 20 ref. 21
88.0	8.25		978		
70.4	9.30		975		
48.4	10.83		986		
28.2	14.70		975		
103.2	9.54	polyvinyl chloride in cyclohexanone; data from ref. 8	908	720 780-940	intrinsic viscosity; ref. 20 intrinsic viscosity; ref. 22
78.2	10.95		908		
60.6	12.43		908		
46.3	14.22		908		
380	12.50	poly- α -methylstyrene in toluene; data from our measurements	667	655	intrinsic viscosity; ref. 20
502	1.55	polyisoprene in <i>n</i> -heptane; data† from our measurements	1 278	970-1 370	light-scattering; ref. 23
1 074	0.72		1 453		
810	1.59	ethylene-propylene copolymer in a θ -mixture; data from our measurements	1 169	1 010	estimated from data‡ in refs. 17 and 18

*The first polyisoprene sample had been masticated by milling. The two samples probably differ in polydispersity and perhaps also in degree of branching.

†Our sample contained 37% m of propylene. We calculated the reference value of $(\bar{R}_0^2/M)^{1/2}$ by interpolation between the values of the homopolymers mentioned in refs. 17 and 18.

Our final relation between the unperturbed dimension and the critical concentration is therefore

$$(\bar{R}_0^2)^{1/2} = 2.84 \times 10^{-8} (M/c_{cr})^{1/3} \quad (8)$$

Table 1 compares some values for $(\bar{R}_0^2/M)^{1/2}$, where $(\bar{R}_0^2)^{1/2}$ is derived from critical concentration measurements with values for $(\bar{R}_0^2/M)^{1/2}$ from other sources. There appears to be fair agreement between our experimental values for the unperturbed end-to-end distances and those found by means of other techniques.

Since the perturbed dimensions can be determined from the intrinsic viscosity it appears possible to determine both perturbed and unperturbed dimensions by viscosity measurements on one polymer-solvent system.

*This assumption is supported by findings of Maron *et al.*^{15,16}, who showed that the total effective volume of polymer in a solution at higher concentrations is independent of the quality of the solvent used. Only unperturbed dimensions can be solvent-independent; perturbed dimensions never can.

Effects of polydispersity and branching

Although the segment distribution function of a branched chain is higher and narrower than that of a linear chain of the same molecular weight, there is no essential difference between the two distributions, so that the calculation can be applied unchanged (see ref. 1, pp 523–530; refs. 24 and 25).

Preliminary calculations indicate that the influence of polydispersity may be of some importance, but that the errors are not very large for molecular weight distributions of moderate width.

The author is very grateful to Mr J. van Schooten for many helpful discussions.

Koninklijke/Shell-Laboratorium, Amsterdam,
Badhuisweg 3, Amsterdam N,
The Netherlands

(Received November 1964)

APPENDIX

THE MOLECULAR DIMENSIONS AT THE CRITICAL
CONCENTRATIONS*The model*

The viscosity* of a polymer solution is determined by the influence of the individual molecules and by their interactions, the entanglement phenomena. In a very dilute solution the viscosity is determined by the action of the individual coils only. A more concentrated solution has a higher viscosity as well as a stronger concentration dependence of the viscosity, because the low-shear regions of low-segment density between the polymer coils become increasingly smaller and less effective with increasing concentration. As soon as the segment density is uniform, there are no longer any regions of easy shear and we assume that the concentration dependence of the viscosity remains essentially constant from there on.

Therefore the attainment of a uniform segment distribution is supposed to coincide with the critical concentration.

Calculations of dimensions

The statistically determined average segment density in an isolated polymer coil i at a distance r_i from its centre of gravity is approximately given by a Gaussian distribution function (see ref. 1, pp 519–534 and ref. 24).

$$\rho_i = C \exp(-9r_i^2/\overline{R}^2) \quad (9)$$

where \overline{R}^2 is the mean square end-to-end distance of the total chain, and C is a constant, depending on \overline{R}^2 .

*We do not account for the viscosity of the solvent itself here; strictly speaking, we ought to write relative viscosity or specific viscosity instead of the viscosity of the solution. In addition, we only consider zero shear viscosity, because any shear would disturb the array of penetrating coils. We therefore measured the viscosities of polymer solutions at very low shear or extrapolated to zero shear.

The total segment density in any point of the lattice in which the centres of gravity of the polymer coils are thought to be arranged is now

$$\rho_{\text{total}} = \sum_i \rho_i = C \sum_i \exp(-9r_i^2/\bar{R}^2) \quad (10)$$

This summation should include all chains of the lattice, but because ρ decreases very rapidly with increasing r , we may neglect the contribution of coils far enough from the lattice point concerned.

If the centres of gravity were arranged according to a f.c.c. lattice, i.e. the cubic closest packing of spheres, with a lattice constant $a\sqrt{2}$, then the distance between nearest neighbours would be a . The total segment density in the centres of gravity would then be almost exclusively determined by the following molecules. The one whose centre of gravity we consider:

$r_1 = 0$;

12 chains with distances r_2 to r_{13} equal to a ;

6 chains with distances r_{14} to $r_{19} = a\sqrt{2}$; and

24 chains with distances r_{20} to $r_{43} = a\sqrt{3}$.

The density in any centre of gravity is then

$$\begin{aligned} \rho_{\text{centre}} = C \left[1 + 12 \exp\left(\frac{-9\{a\}^2}{\bar{R}^2}\right) + 6 \exp\left(\frac{-9\{a\sqrt{2}\}^2}{\bar{R}^2}\right) \right. \\ \left. + 24 \exp\left(\frac{-9\{a\sqrt{3}\}^2}{\bar{R}^2}\right) \right] \quad (11) \end{aligned}$$

The segment density ρ_{half} at a position halfway between two neighbouring centres would be

$$\begin{aligned} \rho_{\text{half}} = C \left[2 \exp\left(\frac{-9\{\frac{1}{2}a\}^2}{\bar{R}^2}\right) + 4 \exp\left(\frac{-9\{\frac{1}{2}a\sqrt{3}\}^2}{\bar{R}^2}\right) \right. \\ + 4 \exp\left(\frac{-9\{\frac{1}{2}a\sqrt{5}\}^2}{\bar{R}^2}\right) + 8 \exp\left(\frac{-9\{\frac{1}{2}a\sqrt{7}\}^2}{\bar{R}^2}\right) \\ + 6 \exp\left(\frac{-9\{3a/2\}^2}{\bar{R}^2}\right) + 4 \exp\left(\frac{-9\{\frac{1}{2}a\sqrt{11}\}^2}{\bar{R}^2}\right) \\ \left. + 12 \exp\left(\frac{-9\{\frac{1}{2}a\sqrt{13}\}^2}{\bar{R}^2}\right) + 8 \exp\left(\frac{-9\{\frac{1}{2}a\sqrt{15}\}^2}{\bar{R}^2}\right) \right] \quad (12) \end{aligned}$$

From $\rho_{\text{centre}} = \rho_{\text{half}}$ we find

$$a = 0.438 (\bar{R}^2)^{1/2} \quad (13)$$

A relation between the lattice constant $a\sqrt{2}$, the weight of one mole of polymer M and the critical concentration c_{cr} is easily found

$$a\sqrt{2} = (4M/c_{cr}N_0)^{1/3} \quad (14)$$

where $N_0 = 6.02 \times 10^{23}$ mole⁻¹. Combination gives

$$(\bar{R}^2)^{1/2} = 3.04 \times 10^{-8} (M/c_{cr})^{1/3} \quad (15)$$

A similar calculation for coils arranged in a b.c.c. lattice gives

$$\begin{aligned} \rho_{\text{centre}} &= C \left[1 + 8 \exp\left(\frac{-9 \{a\}^2}{R^2}\right) + 6 \exp\left(\frac{-9 \{2a/\sqrt{3}\}^2}{R^2}\right) \right] = \\ \rho_{\text{half}} &= C \left[2 \exp\left(\frac{-9 \{\frac{1}{2}a\}^2}{R^2}\right) + 6 \exp\left(\frac{-9 \{\frac{1}{2}a(11/3)^{1/2}\}^2}{R^2}\right) \right. \\ &\quad \left. + 6 \exp\left(\frac{-9 \{\frac{1}{2}a(19/3)^{1/2}\}^2}{R^2}\right) + 8 \exp\left(\frac{-9 \{3a/2\}^2}{R^2}\right) \right] \quad (16) \end{aligned}$$

The distance between nearest neighbours is again a ; so the lattice constant is $2a/\sqrt{3}$. We then obtain

$$(\bar{R}^2)^{1/2} = 2.64 \times 10^{-8} (M/c_{cr})^{1/3} \quad (17)$$

For a simple cubic lattice in which the distance between nearest neighbours a equals the lattice constant we find via

$$\begin{aligned} \rho_{\text{centre}} &= C \left[1 + 6 \exp\left(\frac{-9 \{a\}^2}{R^2}\right) + 12 \exp\left(\frac{-9 \{a\sqrt{2}\}^2}{R^2}\right) \right. \\ &\quad \left. + 8 \exp\left(\frac{-9 \{a\sqrt{3}\}^2}{R^2}\right) + 6 \exp\left(\frac{-9 \{2a\}^2}{R^2}\right) \right. \\ &\quad \left. + 24 \exp\left(\frac{-9 \{a\sqrt{5}\}^2}{R^2}\right) \right] = \rho_{\text{half}} \end{aligned}$$

and

$$\begin{aligned} \rho_{\text{half}} &= C \left[2 \exp\left(\frac{-9 \{\frac{1}{2}a\}^2}{R^2}\right) + 8 \exp\left(\frac{-9 \{\frac{1}{2}a\sqrt{5}\}^2}{R^2}\right) \right. \\ &\quad \left. + 18 \exp\left(\frac{-9 \{3a/2\}^2}{R^2}\right) + 8 \exp\left(\frac{-9 \{\frac{1}{2}a\sqrt{13}\}^2}{R^2}\right) \right. \\ &\quad \left. + 16 \exp\left(\frac{-9 \{\frac{1}{2}a\sqrt{17}\}^2}{R^2}\right) \right] \quad (18) \end{aligned}$$

that

$$(\bar{R}^2)^{1/2} = 2.45 \times 10^{-8} (M/c_{cr})^{1/3} \quad (19)$$

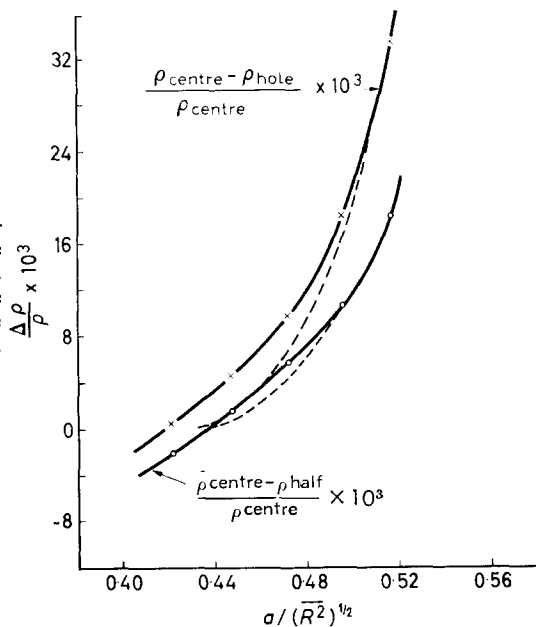
Justification of the various assumptions

To assume that the density distribution of the segments around the centres of gravity is Gaussian and spherically symmetrical is of course incorrect.

At the critical concentration, however, the coils are approximately in their unperturbed state and then the distribution will be fairly near to a Gaussian one. From *Figure 5* which gives the dependence of the densities in three points of a f.c.c. lattice on the reduced distance between nearest neighbours $a/(\bar{R}^2)^{1/2}$ if a Gaussian distribution is assumed, it appears that the density outside the centres of gravity will exceed that in these centres if $a/(\bar{R}^2)^{1/2}$ is less than the critical value (see also below). The real situation is likely to be different from this purely mathematical model. We suppose that the Gaussian character of the distribution as well as its spherical symmetry will

be disturbed to such an extent that the total segment density will approach asymptotically to a uniform distribution throughout the solution. This situation is qualitatively represented by the broken lines in *Figure 5*.

Figure 5—Differences in segment density between some points in a f.c.c. lattice as a function of the ratio of the nearest neighbour distance to the r.m.s. end-to-end distance



In a real polymer solution there will, of course, be no regular arrangement of the coils. We suppose that there is a random structure similar to that of rigid spheres in a random close packing.

It is possible to derive the density of such a random packing of spheres by measurements on arrays of metal balls. Scott^{26,27} found a value of 0.64 for the effective volume fraction ϕ of a closely packed random array of monodisperse metal balls. Rutgers²⁸ obtained the same result by means of similar tests; for a system under shear he reported a volume fraction of about 0.67. We suggest using a higher ϕ -value, however, because there is always some heterodispersity in polymer systems causing a higher effective packing density.

Therefore we used in our calculations a ϕ -value intermediate between that of a f.c.c. lattice ($\phi=0.74$) and a b.c.c. lattice ($\phi=0.68$). The value for K is then 2.84×10^{-8} , so that

$$(\overline{R^2})^{1/2} = 2.84 \times 10^{-8} (M/c_{cr})^{1/3} \quad (20)$$

A pre-requisite for our assumption that the segment density is uniform when the densities in the centre of gravity of a coil and in a point halfway between two neighbouring centres are equal, is that at the critical point the density in any point of the lattice equals that in a centre of gravity of a coil. We checked this for the density in the centre of the octahedron 'hole'

of the f.c.c. lattice. If the distance between nearest neighbours is $a=0.438(\bar{R}^2)^{1/2}$, as was calculated for the critical point (see equation (13)), we find for the density ρ_{hole} in the octahedron hole

$$\rho_{\text{hole}} = C \left[6 \exp \left(\frac{-9 \left\{ \frac{1}{2} a \sqrt{2} \right\}^2}{R^2} \right) + 8 \exp \left(\frac{-9 \left\{ \frac{1}{2} a \sqrt{6} \right\}^2}{R^2} \right) + 24 \exp \left(\frac{-9 \left\{ \frac{1}{2} a \sqrt{10} \right\}^2}{R^2} \right) \right] = 3.461 C \quad (21)$$

The values for ρ_{centre} and ρ_{half} are $3.468 C$ and $3.469 C$, respectively. As these three densities are almost identical, the simplifying assumption of equal densities in only two points of the lattice should be a very good approximation.

REFERENCES

- ¹ FLORY, P. J. *Principles of Polymer Chemistry*. Cornell University Press: Ithaca, 1953
- ² PORTER, R. S. and JOHNSON, J. F. *J. appl. Polym. Sci.* 1960, **3**, 194
- ³ PORTER, R. S. and JOHNSON, J. F. *J. appl. Polym. Sci.* 1960, **3**, 200
- ⁴ PORTER, R. S. and JOHNSON, J. F. *Trans. Soc. Rheol.* 1962, **6**, 107
- ⁵ PORTER, R. S. and JOHNSON, J. F. *Polymer, Lond.* 1962, **3**, 11
- ⁶ TAGER, A. A., DREWAL, W. E. and TRAJANOWA, H. G. *Dokl. Akad. Nauk, S.S.S.R.* 1963, **151**, 140
- ⁷ PORTER, R. S. and JOHNSON, J. F. *Trans. Soc. Rheol.* 1963, **7**, 241
- ⁸ ONOGI, S., KOBAYASHI, T., KOJIMA, Y. and TANIGUCHI, Y. *J. appl. Polym. Sci.* 1963, **7**, 847
- ⁹ PORTER, R. S. and JOHNSON, J. F. *S.P.E. Trans.* 1963, **3**, 18
- ¹⁰ UTRACKI, L. and SIMHA, R. *J. Polym. Sci. A*, 1963, **1**, 1089
- ¹¹ ONOGI, S., KOBAYASHI, T., KOJIMA, Y. and TANIGUCHI, Y. *Trans. Soc. Rheol.* 1962, **6**, 390
- ¹² JOHNSON, M. F., EVANS, W. W., JORDAN, I. and FERRY, J. D. *J. Colloid Sci.* 1952, **7**, 498
- ¹³ TOMPA, H. *Polymer Solutions*, Butterworths: London, 1956
- ¹⁴ FLUENDY, M. A. D. and SMITH, E. B. *Quart. Rev. chem. Soc., Lond.* 1962, **16**, 241
- ¹⁵ MARON, S. H., NAKAJIMA, N. and KRIEGER, I. M. *J. Polym. Sci.* 1959, **37**, 1
- ¹⁶ MARON, S. H. and CHIU, T. T. *J. Polym. Sci. A*, 1963, **1**, 2651
- ¹⁷ KINSINGER, J. B. and HUGHES, R. E. *J. phys. Chem.* 1959, **67**, 1922
- ¹⁸ HOEVE, C. A. J. *J. chem. Phys.* 1961, **35**, 1266
- ¹⁹ OTH, J. and DESREUX, V. *Bull. Soc. chim. Belg.* 1954, **63**, 285
- ²⁰ KURATA, M. and STOCKMAYER, W. H. *Fortschr. Hochpolymer.-Forsch.* 1963, **3**, 196
- ²¹ BURCHARD, W. Communicated at the 'Makromolekulares Kolloquium' in Freiburg, W. Germany, 1964
- ²² SATO, M., KOSHIISHI, Y. and ASAHINA, M. *J. Polym. Sci. B*, 1963, **1**, 233
- ²³ BRISTOW, G. M. *J. Polym. Sci. A*, 1963, **1**, 2261
- ²⁴ DEBIJE, P. and BUECHE, F. *J. chem. Phys.* 1952, **20**, 1337
- ²⁵ STOCKMAYER, W. H. and FIXMAN, M. *Ann. N.Y. Acad. Sci.* 1953, **57**, 334
- ²⁶ SCOTT, G. D., CHARLESWORTH, A. M. and MAK, M. K. *J. chem. Phys.* 1964, **40**, 611
- ²⁷ SCOTT, G. D. *Nature, Lond.* 1960, **188**, 908
- ²⁸ RUTGERS, R. *Nature, Lond.* 1962, **193**, 465
- ²⁹ SCHULKEN Jr, R. N. and SPARKS, M. L. *J. Polym. Sci.* 1957, **26**, 227

Proton Spin-Lattice Relaxation in Polybutene-1 Oxides

A Comparison with Related Polymers

T. M. CONNOR and D. J. BLEARS*

T_1 measurements have been made for polybutene-1 oxides (PBO) of molecular weights 500, 1 000, 2 000 and 2×10^6 over wide temperature ranges. PBO 500 and 2 000 have also been studied in solution in the non-magnetic solvent carbon disulphide. Two T_1 minima were observed in all cases corresponding to chain backbone and sidechain motions. The dilution measurements enable the relaxation times at infinite dilution, $(T_1)_\infty$, to be determined and also indicate, on the basis of BPP theory, that the most important contributions to T_1 are from intramolecular interactions, as is usually assumed when analysing polymer T_1 measurements. Activation energies, Q , calculated from the slopes of T_1 curves for the solutions show a marked molecular weight dependence, and extrapolation to infinite dilution enables quantities Q_∞ to be obtained, which are in the order PBO 500 > PBO 2 000.

Comparisons have been made between the activation parameters and temperatures of T_1 minima obtained for high molecular weight PBO and a number of other oxide polymers of the type $-\text{ECHR}-\text{CH}_2-\text{O}-\text{R}_n$. Other polymers of the types $-\text{ECHR}-\text{CH}_2-\text{R}_n$ and $-\text{ECHR}-\text{O}-\text{R}_n$ are also compared. The activation energies, which are assumed not to vary with temperature were calculated from slopes (Q^\pm), and from areas under curves of $1/T_1$ against $1/T \times 10^3$ ($\langle Q \rangle$). Also included for comparison are barrier heights, E , for methyl group rotation derived from Stejskal and Gutowsky's quantum mechanical tunnelling calculations. A number of interesting trends are shown by the results obtained such as a rise in the temperatures of T_1 minima for polymers of the type $-\text{ECHR}-\text{CH}_2-\text{O}-\text{R}_n$ as R becomes more bulky, the temperatures being in the order $\phi > t\text{-Bu} > \text{Et} > \text{Me} > \text{H}$. In some respects, the simplest member of this series, polyethylene oxide, and polyethylene, the simplest member of the series $-\text{ECHR}-\text{CH}_2-\text{R}_n$, appear to be anomalous. The effect of introducing an extra oxygen atom into the chain monomer unit seems to be the expected one of increasing chain mobility.

MEASUREMENTS have been made of the proton spin-lattice relaxation time, T_1 , as a function of temperature for polybutene-1 oxides (PBOs) of molecular weights 500, 1 000, 2 000 (\bar{M}_n) and $\sim 2 \times 10^6$ (\bar{M}_w). For this polymer there is the possibility of at least two types of molecular motion¹⁻⁶, one involving the chain backbone (setting in at the glass transition temperature) and another involving motion of the sidechain (methyl or methylene group rotations), and T_1 measurements have been made in order to study them. T_1 s for PBOs of molecular weights 500 and 2 000 were measured in solution in the non-magnetic solvent carbon disulphide. Many oxide polymers have now been studied by nuclear resonance techniques⁵⁻⁸,

*The Chemistry Department, The University, Manchester.

which raises the possibility of comparing the results obtained (correlation times and activation parameters) with those of this study. Also spin-lattice relaxation measurements have been made on various polymers, such as polyethylene, which are identical to the oxide polymers except that the chain does not contain oxygen atoms⁴. It is thus possible to make qualitative comparisons of the effects of sidechain groups of different sizes, and also to show the effect of the addition of an oxygen atom to the chain monomer units.

EXPERIMENTAL AND RESULTS

The T_1 s were measured using conventional pulse techniques^{7,9}, the temperature being varied with a gas-flow cryostat¹⁰.

The low molecular weight polymers were obtained from the Dow Chemical Co.¹¹, and are viscous liquids with hydroxyl end groups. The high molecular weight sample was made by polymerizing butene-1 oxide with zinc diethyl catalyst in dioxan solution under high vacuum conditions for one week at room temperature¹². The molecular weight was determined from light scattering experiments giving $\bar{M}_w = 2 \times 10^6$, for an amorphous sample. Solutions of PBO 500 and 2 000 were made up in analytical reagent grade carbon disulphide, and these and the solid samples were sealed off *in vacuo* after degassing to remove dissolved oxygen. Carbon disulphide was chosen as a solvent since it is magnetically inert, apart from very small percentages of ¹³C and ³³S nuclei. Results for pure PBOs 500, 1 000, 2 000 and 2×10^6 are shown in Figure 1, where $\log T_1$ (T_1 in seconds) is plotted against $1/T \times 10^3$. Figures 2 and 3 show similar results for PBO 500 and 2 000 solutions respectively.

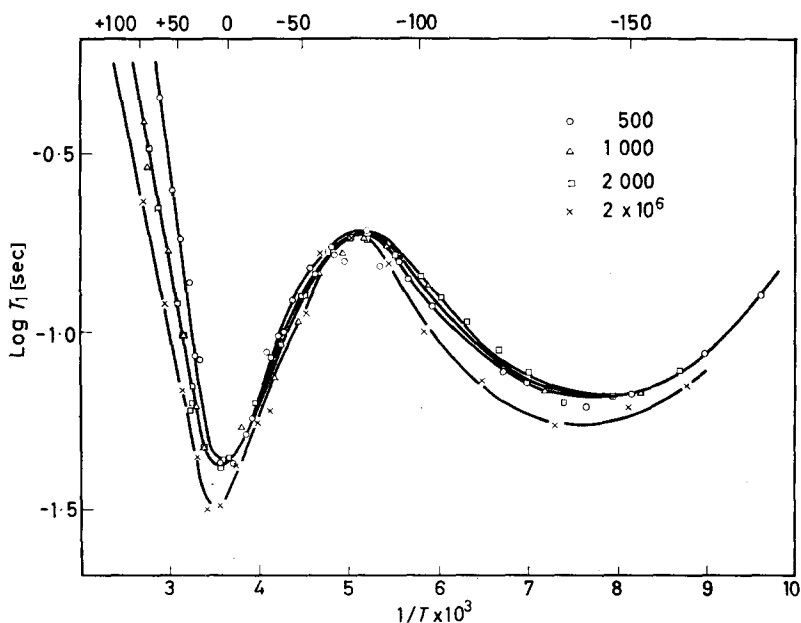


Figure 1— $\log T_1$ against $1/T \times 10^3$ for PBOs 500, 1 000, 2 000 and 2×10^6

PROTON SPIN-LATTICE RELAXATION IN POLYBUTENE-1 OXIDES

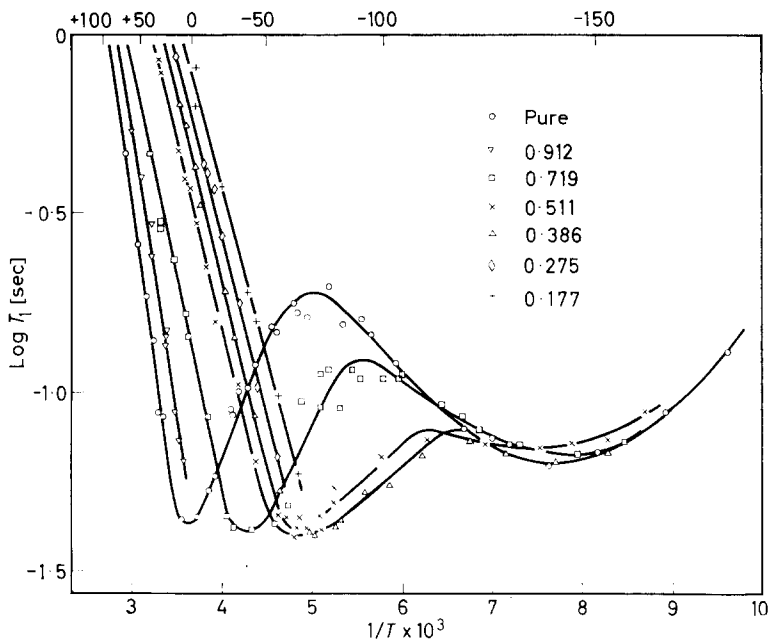


Figure 2— $\text{Log } T_1$ against $1/T \times 10^3$ for PBO 500 solutions in carbon disulphide

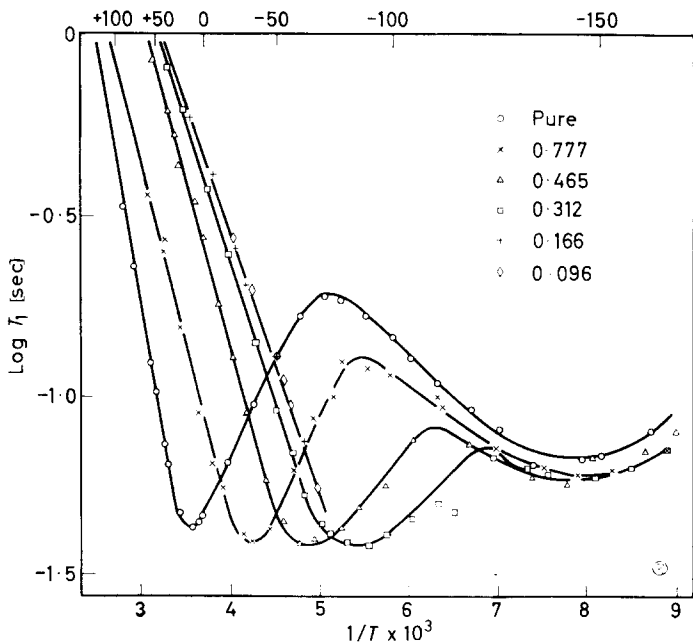


Figure 3— $\text{Log } T_1$ against $1/T \times 10^3$ for PBO 2000 solutions in carbon disulphide

DISCUSSION

The concentration dependence of T_1

Figure 1 shows that change of molecular weight has little effect on the relaxation properties of PBO, apart from a small decrease in T_1 with increasing chain length in the high temperature region. This is similar to results found for unmethylated polypropylene oxides⁵ (PPOs) and is in contrast to those for polyethylene oxides^{7,13} (PEOs) where there are great differences in T_1 for different chain lengths, these variations apparently being related to the degrees of crystallinity of the polymers. Such complicating effects due to changing crystallinity do not seem to occur for PBOs or PPOs although both these polymers may exist in stereoregular forms. No information on this point is available for PBOs although PPO fractions of varying stereoregularity have been prepared^{14,15} whose densities increase as the isotacticity increases. The expected two minimum values of T_1 are always observed and are presumably to be assigned to a chain backbone motion (high temperature minimum) and methyl group rotation (low temperature minimum) by analogy with a number of other polymers¹⁻⁸.

Figures 2 and 3 illustrating the variation of T_1 with dilution show that the low temperature minimum is little affected by concentration, as is also found for PPOs⁵. This is consistent with this minimum being caused by an intramolecular process such as a methyl group rotation. (It is not possible to decide whether the methylene group of the ethyl sidechain also contributes to this minimum. Selective deuteration^{3,5} of the methylene and methyl groups might enable an assignment to be made.) The high temperature minimum is concentration dependent, however, and its position shifts to lower temperatures as the volume fraction of polymer decreases. Also, the value of T_1 at a given temperature above the minimum (where⁸ $\omega\tau \ll 0.616$) increases markedly as the concentration is decreased. If it is assumed that T_1 for polymers may be divided into components caused respectively by inter- and intra-molecular interaction, we may write

$$T_1^{-1} = (T_1^{-1})_{\text{inter}} + (T_1^{-1})_{\text{intra}} \quad (1)$$

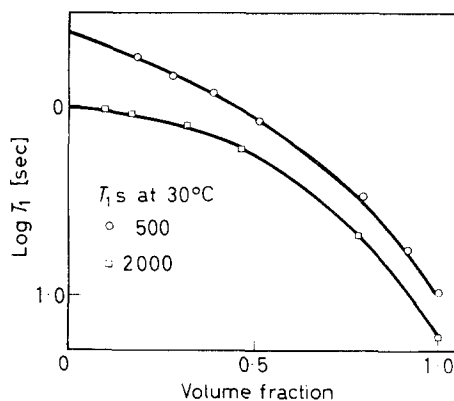
We may also define⁵ another quantity $(T_1)_{\infty}$ which is the value of $(T_1)_{\text{intra}}$ at infinite dilution and which may be determined by extrapolation of T_1 to zero volume fraction of polymer. Since measurements have been carried out to quite low concentrations (~ 0.1 vol. fraction) this quantity may be determined with some certainty for PBO 500 and 2 000, by plotting $\log T_1$ against concentration as shown in Figure 4. Considering reasonable limits of error the values of $(T_1)_{\infty}$ shown in Table 1 are found at 30°C.

Table 1. Relaxation times for PBOs at 30°C

<i>Mol. wt</i>	T_1 (sec)	$(T_1)_{\infty}$ (sec)	$(T_1)_{\infty}/T_1$	$\eta_{30}^{\text{PBO}}/\eta_{30}^{\text{CS}_2^*}$
500	0.105	2.51 ± 0.24	24.5	259
2 000	0.062	0.98 ± 0.07	15.6	1 204

* $\eta_{30}^{\text{CS}_2} = 0.343$ cP; $\eta_{30}^{\text{PBO500}} = 88.8$ cP; $\eta_{30}^{\text{PBO2000}} = 413$ cP.

Figure 4—Values of $\log T_1$ at 30°C for solutions of PBO 500 and 2000 in carbon disulphide as a function of concentration



No entirely satisfactory model of polymer relaxation behaviour under these conditions is available⁵ and so Bloembergen–Purcell–Pound theory¹⁶ will be used which applies approximately to small molecules^{17,18}. It has been shown that on this basis^{5,19}

$$(T_1)_\infty/T_1 \sim \eta_{30}^{\text{PBO}}/\eta_{30}^{\text{CS}_2} \quad (2)$$

where η_{30}^{PBO} and $\eta_{30}^{\text{CS}_2}$ are respectively the solute and solvent viscosity at 30°C. Values of this viscosity ratio and the experimental ratio $(T_1)_\infty/T_1$ are also shown in Table I, with values of T_1 for the pure polymers at 30°C. In each case $(T_1)_\infty/T_1 \neq \eta_{30}^{\text{PBO}}/\eta_{30}^{\text{CS}_2}$ as might be expected in view of the inadequate model assumed. Apart from other simplifications, the approximation of assuming that the mean molecular correlation time, τ , is proportional to the macroscopic viscosity used in deriving equation 2 is clearly not correct. Not only are the numerical magnitudes different, but as molecular weight increases $(T_1)_\infty/T_1$ decreases, whereas $\eta_{30}^{\text{PBO}}/\eta_{30}^{\text{CS}_2}$ increases. It is thus difficult to decide on the relative importance of intermolecular and intramolecular contributions to T_1 on this basis. The contribution $(T_1)_\infty$ at infinite dilution will be considerably different from $(T_1)_{\text{intra}}$ due to the great difference in viscosity of solvent and solute.

The variation of T_1 with temperature in the neighbourhood of the minima may be described by an expression of the form^{16,20}

$$1/T_1 = (A + NB) f(\omega\tau) \quad (3)$$

where A and B are approximately temperature independent constants giving the magnitude of intramolecular and intermolecular contributions respectively. N is the number of spins/cm³ which is proportional to the volume fraction and $f(\omega\tau)$ is defined as

$$f(\omega\tau) = \tau / (1 + \omega^2\tau^2) + 4\tau / (1 + 4\omega^2\tau^2) \quad (4)$$

where ω is the resonance frequency. Equation (3) is derived on the assumption of a single molecular correlation time, τ , which is the same for inter- and intra-molecular interactions. The quantity $f(\omega\tau)$ has a constant value at the minimum condition ($\omega\tau = 0.616$), so that if intermolecular interactions

were predominant then $(T_1)_{\min.}$ would be approximately proportional to N^{-1} . Thus as N decreased we should expect $(T_1)_{\min.}$ to increase, by a factor of about ten in this case. In fact $(T_1)_{\min.}$ is not proportional to N^{-1} and actually decreases slightly for both PBO 500 and PBO 2 000 as the dilution increases. It thus appears that intermolecular interactions are not at all important in determining T_1 , an assumption frequently made in discussions of polymer relaxation^{5,8}. We can thus omit the term in NB in equation (3). The interpretation of the observed trends might be slightly modified if a distribution of correlation times which was changing with dilution was present. This would make $f(\omega\tau)$ concentration dependent. However, it seems unlikely that the possible variations in $(T_1)_{\min.}$ due to this cause⁸ could alter the conclusion that intermolecular interactions are not important in this case.

Activation parameters. Comparison with other polymers

It will be observed from *Figures 2 and 3* that the slopes of the curves of $\log T_1$ against $1/T \times 10^3$ for the high temperature minimum in the region where $\omega\tau \ll 0.616$ get smaller as dilution increases. Activation energies may be calculated from these slopes⁸ (assuming a single correlation time) and plotted as a function of concentration as shown in *Figure 5*.

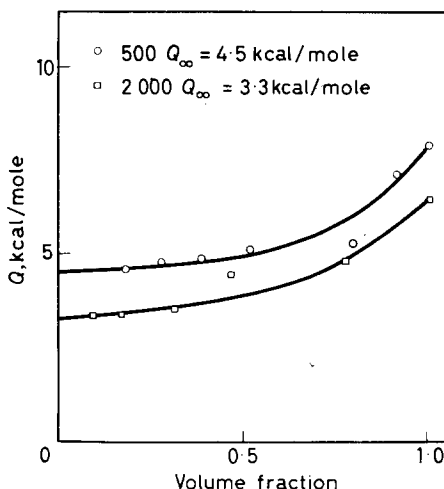


Figure 5—Activation energies as a function of concentration for PBO 500 and 2000 solutions in carbon disulphide ($\omega\tau \ll 0.616$)

Extrapolating to infinite dilution gives the values $Q_\infty = 4.5$ kcal/mole for PBO 500 and $Q_\infty = 3.3$ kcal/mole for PBO 2000. Similar behaviour was found for PPO, Q_∞ becoming smaller as the chain length was decreased when molecular weights of 250, 400 and 2000 were examined. These changes in activation energies show a sharp dependence on molecular weight, although the trends might be considerably modified if a distribution of correlation times which changed with concentration was present⁵.

Apart from polybutene-1 oxide, a number of other oxide polymers have been studied by nuclear resonance, enabling correlation times and activation parameters of molecular motions to be determined. Also, similar quantities

can be derived from results on a number of related polymers which do not contain oxygen atoms in the chain backbone. The positions of minima in the curves of $\log T_1$ against reciprocal temperature give the temperatures at which τ is given by $\omega\tau=0.616$. Activation parameters may be determined from the experimental results by a number of different methods⁸. In the comparisons which follow it is assumed that the activation energies (Q) are constant over the temperature ranges considered. This is known to be a considerable approximation for the motions causing the high temperature minima⁸, but since data are not usually available to take account of possible changes in Q , this assumption will be made as a basis for comparison. The temperature dependence of Q arises since the motion setting in at the glass transition temperature, T_g , of the polymer is a cooperative phenomenon. The rate of change of Q is greatest at temperatures just above T_g and falls off at higher temperatures, Q often reaching a fairly constant value at high temperatures. Since the T_1 minimum temperature may be as much as 70°C higher⁵ than T_g , Q will be changing slowly with temperature in the region of the minimum. The motions of sidechain groups, which according to available evidence cause the low temperature minima^{3,5}, probably do not require such a high degree of cooperation, and the approximation of constant Q s may be better in these cases. There are unfortunately no independent measurements to support this conclusion since dielectric studies, which show Q to be temperature dependent in the high temperature minimum region, do not give information about methyl or phenyl group rotations.

In *Table 2* the temperatures at which the high and low temperature minima occur are shown and also Q s calculated by various methods.

For the high temperature minima, Q has been derived from the slopes of the $\log T_1$ versus $1/T \times 10^3$ curves⁸. These values are denoted by Q^+ and Q^- according to whether the slope is derived from the curve on the high or low temperature side of the minimum respectively. Activation energies, $\langle Q \rangle$, were also derived from the expression⁸

$$\left\langle \frac{1}{Q} \right\rangle = \frac{2\omega}{3\pi AR} \int_0^{\infty} \left(\frac{1}{T_1} \right) d \left(\frac{1}{T} \right) \quad (5)$$

where the integral represents the area under a curve of $1/T_1$ versus $1/T \times 10^3$. For the low temperature minimum a further quantity is listed, E , which is the barrier height for methyl group rotation derived from Stejskal and Gutowsky's calculations in a manner previously described for polyacetaldehyde (PAA). In cases where data are available, i.e. PPO, PAA and polymethylene oxide (PMO), the activation energies have been calculated taking account of distributions of correlation times in a manner described previously⁸. The quantity β in *Table 2* is the Fuoss-Kirkwood distribution parameter. For PPO and polystyrene oxide (PSO) data are given for amorphous (A) and crystalline samples (X). The data for PSO and polytertiarybutylethylene oxide (PBEO) will be described more fully elsewhere²³ when a comparison with dielectric and mechanical data will be given. The data on all the polymers mentioned so far are derived from

Table 2. Activation parameters for polybutene-1 oxide and related polymers

Polymer	High temp. min. °C	Q^\pm , $\langle Q \rangle$ kcal/mole	Low temp. min. °C	Q^\pm , $\langle Q \rangle$ kcal/mole	Notes
PEO	0	4.6 Q^+	—	—	30 Mc/s $Q^+ > 70^\circ\text{C}$
PPO	+ 1 (A) + 21 (X)	$9.2 Q^+$ $6.5 Q^+$ $10.5 \langle Q \rangle$ $7.4 \langle Q \rangle$	$\beta \begin{cases} 0.7 \\ 1.0 \\ 0.7 \\ 1.0 \end{cases}$ — 136 (A) — 119 (X)	$1.8 Q^+$ $1.1 Q^-$ $1.7 \langle Q \rangle$ $3.6 E$	30 Mc/s Q_s for amorphous sample only
PBO	+ 14.5	$5.7 Q^+$ $3.4 Q^-$ $5.8 \langle Q \rangle$	— 140	$1.2 Q^+$ $1.1 Q^-$ $1.4 \langle Q \rangle$ $3.5 E$	30 Mc/s. Low temp. Q_s for mol. wt 500
PBEO	+ 95	$5.7 Q^+$ $3.2 Q^-$	— 112	$2.3 Q^+$ $1.8 Q^-$ $2.1 \langle Q \rangle$ $4.5 E$	30 Mc/s
PSO	+ 109 (A) + 127 (X)	8.3 Q^-	— 93 (A) — 108 (X)	Small min.	30 Mc/s
PMO	+ 12	$6.4 Q^+$ $9.9 Q^-$ $10.3 \langle Q \rangle$	—	—	30 Mc/s. Highly crystalline sample
PAA	+ 43.5	$13.9 Q^-$ $\beta=0.53$	— 100	$3.6 Q^+$ $1.2 Q^-$ $2.2 \langle Q \rangle$ $4.6 E$	30 Mc/s
PE	— 23	$1.6 Q^-$ $2.5 \langle Q \rangle$	—	—	21.5 Mc/s
PP	+ 84	$4.6 Q^+$ $4.8 Q^-$	— 112	$1.6 Q^+$ $1.4 Q^-$ $1.7 \langle Q \rangle$ $4.4 E$	21.5 Mc/s $4.8 Q^-$ for CD_3 cmpd
PS	+ 207	10.4 Q^-	— 13	Small min.	21.5 Mc/s

measurements made at 30 Mc/s. Three further polymers are also included in Table 2, polyethylene (PE), polypropylene (PP) and polystyrene (PS) for which measurements were made at 21.5 Mc/s^{3,4}. The difference between the frequencies is not sufficient to alter qualitative conclusions drawn about the positions of T_1 minima. All the tabulated quantities refer to polymers with a fairly high molecular weight, i.e. $> 10^4$ and usually $\sim 10^6$, except for the Q_s derived from PBO from the low temperature minimum. These data are derived from PBO 500 since the T_1 data show little molecular weight dependence in this temperature region and the measurements extend to lower temperatures than they do for the high molecular weight compound. The low temperature minima for PSO and PS were insufficiently

well defined to allow calculation of the activation energies. The limits of error for the tabulated temperatures are of the order of $\pm 3^\circ\text{C}$ for the positions of the high temperature minima (except for PEO where the uncertainty is larger) and $\pm 6^\circ\text{C}$ for the low temperature minima. The errors involved in calculating Q s are hard to estimate since there is an element of uncertainty in the operations of taking slopes of experimental lines or measuring areas under bell-shaped curves whose tails may not be well defined. The probable error in the $\langle Q \rangle$ s resulting from uncertainties in the areas is $\sim \pm 15$ per cent while values of Q^\pm may be in error by more than this amount when the slopes are not well defined by the experimental points.

The data in *Table 2* exhibit a number of interesting trends which may be discussed under the headings of high and low temperature minima.

(1) *High temperature minima*—For amorphous polymers of general formula $-\text{ECHR}-\text{CH}_2-\text{O}\ddot{\text{X}}_n$ the temperatures of the T_1 minima rise as the size of the group R increases the temperatures being in the order $\phi > t\text{-Bu} > \text{Et} > \text{Me} > \text{H}$. The ease of chain backbone motion is thus decreased as the size of substituent groups increases, as might be expected. The values of Q show a similar although not so well defined trend. Apart from the difficulties mentioned earlier due to the possible temperature dependence of Q s, there is also the fact that the effect of distributions of correlation times on the values of Q cannot always be taken into account due to lack of sufficient data. Q^+ for PEO is quoted for the region above the softening point of 70°C . The minimum at $\sim 0^\circ\text{C}$ is broad and ill-defined, and measurements of the slope in this region would correspond to a value of Q^+ very much smaller than 4.6 kcal/mole. Similar trends are shown by polymers of the form $-\text{ECHR}-\text{CH}_2\ddot{\text{X}}_n$ which do not contain a chain hetero-atom. The temperatures of T_1 minima and the Q^- s are in the order $\phi > \text{CH}_3 > \text{H}$, the bulky groups again inhibiting chain backbone motion. This observation also applies to the polymers PAA and PMO which are of the form $-\text{ECHR}-\text{O}\ddot{\text{X}}_n$ where the T_1 minimum temperatures and Q s are in the order $\text{CH}_3 > \text{H}$. This is in spite of the fact that the PMO sample was highly crystalline whereas the PAA is amorphous. For PPO and PSO where amorphous and crystalline fractions were studied the more efficient molecular packing resulting in increased crystallinity apparently inhibits molecular motion, raising the T_1 minimum temperatures by $\sim 20^\circ\text{C}$ in each case.

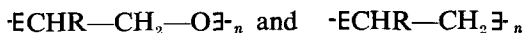
The introduction of the hetero-atom, oxygen, into the chain apparently sometimes facilitates backbone motion as shown by the relative minimum positions, i.e. $\text{PP} > \text{PPO}$ and $\text{PS} > \text{PSO}$. However, when $\text{R} = \text{H}$, $\text{PEO} > \text{PE}$, the trend being reversed. Although PEO and PE are chemically the simplest members of their respective series, it is more difficult to interpret their T_1 data than it is for polymers with more complicated structures. PE shows a distinct minimum in the region of its softening point⁴ ($\sim 136^\circ\text{C}$) whilst PEO shows a rather indistinct minimum in the same region ($\sim 70^\circ\text{C}$). (The PE sample consisted of linear Rigidex 35 pellets). The softening point data indicate that the presence of an oxygen atom facilitates molecular motions in contrast to the n.m.r. data. However, there is some doubt as to the precise origins of the T_1 minima quoted in *Table 2* for PE and PEO. It has

been suggested²⁴ that the minimum in PE may be connected with spin-diffusion mechanisms, coupling to the lattice presumably occurring as a result of chemical (e.g. the presence of CH₃ groups) or morphological defects. However, it seems unlikely that CH₃ group rotation can be responsible for the coupling, since this should be most effective at a much lower temperature than -40°C as shown by the low temperature minimum data in Table 2, where the highest minimum temperature is -100°C for PAA. It is thus difficult to make a valid comparison of PE and PEO on the basis of the T_1 data.

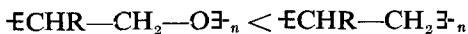
As expected⁸, the highest values of Q obtained are for those cases where a distribution of correlation times has been considered, i.e. PPO, PMO and PAA. The extra CH₂ group in PPO results in $\langle Q \rangle$ s and minimum temperatures in the order PAA > PPO. High activation energies were also found in similar temperature regions by dielectric studies on PAA and PMO^{22, 25}.

(2) *Low temperature minima*—Since the motions causing the low temperature minima are primarily intramolecular phenomena, it might be expected that trends in the tabulated quantities would be less obvious than they are for the parameters associated with the backbone motion. However, the barriers to methyl and phenyl group reorientation are presumably influenced to some extent by the chain packing, and significant differences are observed particularly in the temperatures of T_1 minima for methyl group rotation. For polymers of the type $\text{-CHR-CH}_2\text{-O-}$, the minimum temperatures are in the order PSO > PBEO > PPO > PBO, which might be expected on a simple molecular picture. The phenyl group, being the most bulky, reorients with the greatest difficulty. In PBEO, the methyl groups in the *t*-butyl group probably interfere with each other making the minimum temperature higher than that for PBO or PPO. In PBO the methyl group is probably freer to rotate than in PPO since it is further removed from the backbone chain. The $\langle Q \rangle$ s for this series are also in the order PBEO > PPO > PBO, no value being available for PSO. The amorphous sample of PPO has its minimum at a lower temperature than the crystalline sample, repeating a trend observed for the high temperature minima of PPO and PSO. This trend is reversed for PSO, although the significance of the small minima found for this polymer is not clear.

The minimum temperatures for



are in the order



particularly for the pair PSO, PS. The value of $\langle Q \rangle$ for PAA is the largest measured, as is the case for Q^- for the high temperature minimum. This seems a little surprising since the sample used was amorphous.

The values of E quoted are all higher than the values of $\langle Q \rangle$ given. This is expected in general since the calculation of the reorientation rate from which E is derived includes a contribution from quantum mechanical tunnelling, which becomes more important at lower temperatures. However, for the cases considered here the temperatures are such that according to

the calculations, the contribution due to tunnelling is small, the reorientation rate having reached almost the limiting classical value. There is thus a poor agreement between the classical quantity $\langle Q \rangle$ and E , which may be due to the unsatisfactory nature of the assumptions made in calculating the reorientation rate²¹. This tunnelling theory has also been found unsatisfactory when used to explain T_1 s obtained for solid ethylene²⁶. It will be noticed that the value of $\langle Q \rangle$ is similar to Q^+ and Q^- in all cases and that often $Q^+ > \langle Q \rangle > Q^-$. This observation also applies to values of Q^+ , Q^- and $\langle Q \rangle$ obtained in the high temperature region, and gives added grounds for thinking that the assumptions on which equation (5) is based are justified^{8, 27}.

The authors thank Dr G. Allen for helpful comments and advice. This research forms part of the programme of the National Physical Laboratory, and is published by permission of the Director.

*The Basic Physics Division,
The National Physical Laboratory,
Teddington, Middlesex*

(Received December 1964)

REFERENCES

- ¹ KAWAI, T. *J. phys. Soc., Japan*, 1961, **16**, 1220
- ² HIRAI, A. and KAWAI, T. *Mem. Coll. Sci. Univ. Tokyo*, 1961, **29**, No. 3
- ³ POWLES, J. G. and MANSFIELD, P. *Polymer, Lond.* 1962, **3**, 336 and 339
- ⁴ HUNT, B. I., POWLES, J. G. and WOODWARD, A. E. *Polymer, Lond.* 1964, **5**, 323
- ⁵ CONNOR, T. M., BLEARS, D. J. and ALLEN, G. *Trans. Faraday Soc.* To be published
- ⁶ CONNOR, T. M. *Polymer, Lond.* 1964, **5**, 265
- ⁷ ALLEN, G., CONNOR, T. M. and PURSEY, H. *Trans. Faraday Soc.* 1963, **59**, 1525
- ⁸ CONNOR, T. M. *Trans. Faraday Soc.* 1964, **60**, 1574
- ⁹ CARR, H. Y. and PURCELL, E. M. *Phys. Rev.* 1954, **94**, 630
- ¹⁰ CONNOR, T. M. *Brit. J. appl. Phys.* 1963, **14**, 396
- ¹¹ *Choosing the Right Polyglycol*, Dow Chemical Co., 1962
- ¹² POWELL, E. *Ph.D. Thesis*. University of Manchester, 1963
- ¹³ CONNOR, T. M., READ, B. E. and WILLIAMS, G. *J. appl. Chem.* 1964, **14**, 74
- ¹⁴ STANLEY, E. and LITT, M. *J. Polym. Sci.* 1960, **43**, 453
- ¹⁵ ALLEN, G., BOOTH, C. and JONES, M. N. *Polymer, Lond.* 1964, **5**, 195 and 257
- ¹⁶ BLOEMBERGEN, N., PURCELL, E. M. and POUND, R. V. *Phys. Rev.* 1948, **73**, 679
- ¹⁷ MONIZ, W. B., STEELE, W. A. and DIXON, J. A. *J. chem. Phys.* 1963, **38**, 2418
- ¹⁸ BLEARS, D. J. *Ph.D. Thesis*, University of Manchester, 1964
- ¹⁹ ABRAGAM, A. *Principles of Nuclear Magnetism*. Oxford University Press: London, 1961
- ²⁰ KUBO, R. and TOMITA, K. *J. phys. Soc., Japan*, 1954, **9**, 888
- ²¹ STEJSKAL, E. O. and GUTOWSKY, H. S. *J. chem. Phys.* 1958, **28**, 388
- ²² READ, B. E. and WILLIAMS, G. *Polymer, Lond.* 1961, **2**, 239
- ²³ ALLEN, G. and BLEARS, D. J. To be published
- ²⁴ MCCALL, D. W. and DOUGLASS, D. C. *Polymer, Lond.* 1963, **4**, 433
- ²⁵ WILLIAMS, G. *Trans. Faraday Soc.* 1963, **59**, 1397
- ²⁶ RUSHWORTH, F. A. *13th Ampère Colloquium, Leuven*, 1964
- ²⁷ READ, B. E. and WILLIAMS, G. *Trans. Faraday Soc.* 1961, **57**, 1979

Communications and Notes

The Stress Strain Relation of Swollen Rubbers

WHEN an elastic material is deformed the elastically stored energy and the degree of deformation are related by the following equation

$$W = C_1 (\lambda_x^2 + \lambda_y^2 + \lambda_z^2) + C_2 (\lambda_x^{-2} + \lambda_y^{-2} + \lambda_z^{-2}) + \text{constant} \quad (1)$$

where W is the elasticity stored energy per unit volume, λ_x , λ_y and λ_z are the principal extension ratios and C_1 and C_2 are constants. This relationship was derived by Mooney¹ for reversible isometric deformations. On elongating an elastic material the condition of constant volume requires that $\lambda_y = \lambda_z = \lambda_x^{-1/2} = \lambda^{-1/2}$. Imposing this condition and differentiating equation (1) yields a relation between the tension and the extension ratio

$$\tau / (\lambda - \lambda^{-2}) = 2C_1 + 2C_2 \lambda^{-1} \quad (2)$$

in which τ is the tension per unit area of the undeformed sample, and λ is the extension ratio of elongation.

There is much experimental evidence¹⁻⁵ that this relationship is applicable to elongation of elastomers at least in the range of extension ratios of about 1.2 to 3. However, this evidence results from experiments in which elastic equilibrium was not attained. The difficulty of reaching equilibrium conditions is acknowledged by some authors and is discussed by Ciferri and Flory². In the experience of this writer elongation-retraction cycles show considerable hysteresis even when measurements of tension and elongation are delayed until no further creep occurs.

To the extent that the condition of reversibility is not fulfilled, agreement between experimental results and equation 2 must be regarded as an empirical observation. This has been recognized in the literature by at least one author⁶. It follows that the expression for the stored energy function, from which equation 2 is derived, need not be restricted to reversible deformations either.

It is of interest to examine what the consequences are of disregarding another restriction of equation 1, namely the condition of constant volume. In particular we assume that equation 1 not only describes the increase in stored energy on elongating a rubber but also on swelling it. Such application of the stored energy function was recently also employed by Gee *et al.*⁷.

In the following paragraphs the volume fraction of polymer in swollen rubber is designated by v_r . Subscripts carried by the various symbols refer to the condition of the undeformed material: d for dry rubber; s for swollen rubber. A second subscript, carried by the symbols for extension ratios, denotes the type of deformation considered: e for elongation; s for swelling; and p for swelling plus elongation.

For a swollen elongated sample, the stored elastic energy per unit volume of dry rubber is given by

$$W_d = C_{1d} [(\lambda_x)_{dp}^2 + (\lambda_y)_{dp}^2 + (\lambda_z)_{dp}^2] + C_{2d} [(\lambda_x)_{dp}^{-2} + (\lambda_y)_{dp}^{-2} + (\lambda_z)_{dp}^{-2}] + \text{constant}$$

Since

$$\lambda_{dy} = \lambda_{se} \lambda_{ds}$$

$$(\lambda_x)_{ds} = (\lambda_y)_{ds} = (\lambda_z)_{ds} = v_r^{-1/3}$$

and

$$W_s = W_d v_r$$

it follows that in simple extension

$$W_s = C_{1d} v_r^{1/3} (\lambda_{se}^2 + 2\lambda_{se}^{-1}) + C_{2d} v_r^{5/3} (\lambda_{se}^{-2} + 2\lambda_{se}) + \text{constant}$$

The tension τ_s per unit area of initial (i.e. swollen) cross section is obtained by differentiating W_s with respect to λ_{se} . This operation and the use of the relation $\tau_d = \tau_s v_r^{-2/3}$ yields

$$\frac{1}{2} \tau_d v_r^{1/3} (\lambda_{se} - \lambda_{se}^{-2})^{-1} = C_{1d} + C_{2d} v_r^{4/3} \lambda_{se}^{-1}$$

Because statistical theory predicts that the product on the LHS of the above equation is independent of v_r , it has become customary to define C_{1s} and C_{2s} by the relation

$$\frac{1}{2} \tau_d v_r^{1/3} (\lambda_{se} - \lambda_{se}^{-2})^{-1} = C_{1s} + C_{2s} \lambda_{se}^{-1}$$

it follows that

$$C_{1s} = C_{1d} \tag{3}$$

and

$$C_{2s} = C_{2d} v_r^{4/3} \tag{4}$$

The term $2C_1$ of equation 2 is usually identified with the corresponding term νRT of the statistical theory of elasticity, although it is not theoretically justified². It follows from equation 3 that C_1 should be the same for a particular sample whether rubber is swollen or dry. This has indeed been found experimentally^{2, 3, 5, 8, 9}.

The physical significance of C_2 has been discussed by several authors^{2-5, 10, 11}, but still remains obscure^{8, 12}. In these discussions much significance is attached to the observation that the value of C_2 is smaller for a rubber in the swollen state than in the dry state, and that it decreases with increasing degree of swelling. These observations have been cited by Ciferri and Flory² in support of their view that departures from statistical theory (i.e. non-zero values of C_2) are attributable to the difficulty of attaining elastic equilibrium in elongated dry rubber specimens. Equation 4 predicts that C_{2s} should be proportional to the 4/3 power of v_r . This has been found empirically by Mullins and Thomas for a variety of solvents (equation 7.46 of ref. 8 and equation 7 of ref. 5).

Thus, experimental confirmation of equations 3 and 4 lends credence to the assumption on which its derivation is based and to its corollary that the decrease of C_2 with increasing degree of swelling is a consequence of the geometry relating to the elongation of a network that has been isotropically 'prestrained' by imbibition of solvent. While this conclusion does not contribute to a ready interpretation of the physical significance of C_2 , it does cast doubt on the suggestion of Ciferri and Flory that the C_2 term arises from hysteresis.

Because C_{2d} can be interpreted as a measure of the departure from statistical theory¹⁰, it is important to recognize that this parameter does not appear to change on dilution of a rubber network.

B. M. E. VAN DER HOFF

*Research and Development Division,
Polymer Corporation Ltd,
Sarnia, Canada*

(Received December 1964)

REFERENCES

- ¹ MOONEY, M. *J. appl. Phys.* 1940, **11**, 582
- ² CIFERRI, A. and FLORY, P. J. *J. appl. Phys.* 1959, **30**, 1498
- ³ GUMBRELL, S. M., MULLINS, L. and RIVLIN, R. S. *Trans. Faraday Soc.* 1953, **49**, 1495
- ⁴ CIFERRI, A. *J. Polym. Sci.* 1961, **54**, 149
- ⁵ MULLINS, L. *J. appl. Polym. Sci.* 1959, **2**, 257
(Equation 7 of this paper contains an error. The first term on the RHS of this equation should read C_1 (dry), as can be concluded from the text.)
- ⁶ MASON, P. *Trans. Faraday Soc.* 1959, **55**, 1461
- ⁷ BOOTH, C., GEE, G., HOLDEN, G. and WILLIAMSON, G. R. *Polymer, Lond.* 1964, **5**, 343
- ⁸ MULLINS, L. and THOMAS, A. G. *The Chemistry and Physics of Rubber-like Substances*. Edited by L. BATEMAN. Chapter 7. MacLaren: London, 1963
- ⁹ MULLINS, L. *J. appl. Polym. Sci.* 1959, **2**, 1
- ¹⁰ THOMAS, A. G. *Trans. Faraday Soc.* 1955, **51**, 569
- ¹¹ TRELOAR, L. R. G. *The Physics of Rubber Elasticity*, Chapter 8, Section 10. Clarendon Press: Oxford, 1958
- ¹² GEE, G. Discussion of a paper by L. D. LOAN, 'Techniques of polymer science'. Society of Chemical Industry *Monograph No. 17*: London, 1963

Correction of Errors in Polymer Testing using Diffracted Ultrasonic Waves

RECENTLY techniques have been used to measure the velocity and attenuation of mechanical waves in polymers even near their softening point in order to determine the complex elastic constants of the material.

One technique involves the launching of a longitudinal wave in a liquid, mode changing it to a shear wave when it encounters a parallel slab of the solid at an oblique angle and its subsequent re-transformation to a longitudinal wave on emergence. Certain errors arise in using these techniques which have been disregarded in the past. This letter discusses corrections which may be applied to reduce these errors.

There is an effect of attenuation on the direction of propagation of the wave in the specimen which causes a departure from Snell's law expressed in the form

$$k_i \sin \theta_i = k_s \sin \theta_t$$

where k_s is the real part of the complex wave number for the attenuating specimen, k_i is the wave number, i.e. $2\pi/\text{wavelength}$ for the liquid path, assumed non-attenuating and θ_i, θ_t are the angles of incidence and refraction respectively at the interface; this departure can be calculated using the theory of Born and Wolf¹ and an example is illustrated in the graph of $F(\theta)$ where θ_i , calculated from the above expression, has to be multiplied

Because C_{2d} can be interpreted as a measure of the departure from statistical theory¹⁰, it is important to recognize that this parameter does not appear to change on dilution of a rubber network.

B. M. E. VAN DER HOFF

*Research and Development Division,
Polymer Corporation Ltd,
Sarnia, Canada*

(Received December 1964)

REFERENCES

- ¹ MOONEY, M. *J. appl. Phys.* 1940, **11**, 582
- ² CIFERRI, A. and FLORY, P. J. *J. appl. Phys.* 1959, **30**, 1498
- ³ GUMBRELL, S. M., MULLINS, L. and RIVLIN, R. S. *Trans. Faraday Soc.* 1953, **49**, 1495
- ⁴ CIFERRI, A. *J. Polym. Sci.* 1961, **54**, 149
- ⁵ MULLINS, L. *J. appl. Polym. Sci.* 1959, **2**, 257
(Equation 7 of this paper contains an error. The first term on the RHS of this equation should read C_1 (dry), as can be concluded from the text.)
- ⁶ MASON, P. *Trans. Faraday Soc.* 1959, **55**, 1461
- ⁷ BOOTH, C., GEE, G., HOLDEN, G. and WILLIAMSON, G. R. *Polymer, Lond.* 1964, **5**, 343
- ⁸ MULLINS, L. and THOMAS, A. G. *The Chemistry and Physics of Rubber-like Substances*. Edited by L. BATEMAN. Chapter 7. MacLaren: London, 1963
- ⁹ MULLINS, L. *J. appl. Polym. Sci.* 1959, **2**, 1
- ¹⁰ THOMAS, A. G. *Trans. Faraday Soc.* 1955, **51**, 569
- ¹¹ TRELOAR, L. R. G. *The Physics of Rubber Elasticity*, Chapter 8, Section 10. Clarendon Press: Oxford, 1958
- ¹² GEE, G. Discussion of a paper by L. D. LOAN, 'Techniques of polymer science'. Society of Chemical Industry *Monograph No. 17*: London, 1963

Correction of Errors in Polymer Testing using Diffracted Ultrasonic Waves

RECENTLY techniques have been used to measure the velocity and attenuation of mechanical waves in polymers even near their softening point in order to determine the complex elastic constants of the material.

One technique involves the launching of a longitudinal wave in a liquid, mode changing it to a shear wave when it encounters a parallel slab of the solid at an oblique angle and its subsequent re-transformation to a longitudinal wave on emergence. Certain errors arise in using these techniques which have been disregarded in the past. This letter discusses corrections which may be applied to reduce these errors.

There is an effect of attenuation on the direction of propagation of the wave in the specimen which causes a departure from Snell's law expressed in the form

$$k_l \sin \theta_i = k_s \sin \theta_t$$

where k_s is the real part of the complex wave number for the attenuating specimen, k_l is the wave number, i.e. $2\pi/\text{wavelength}$ for the liquid path, assumed non-attenuating and θ_i, θ_t are the angles of incidence and refraction respectively at the interface; this departure can be calculated using the theory of Born and Wolf¹ and an example is illustrated in the graph of $F(\theta)$ where θ_t , calculated from the above expression, has to be multiplied

by the correction factor $F(\theta)$. A loss function is shown along the abscissa and the graph has been computed for $k_s = 3k_l$, a typical relation applicable to the highly attenuating region near the softening point of a polymer.

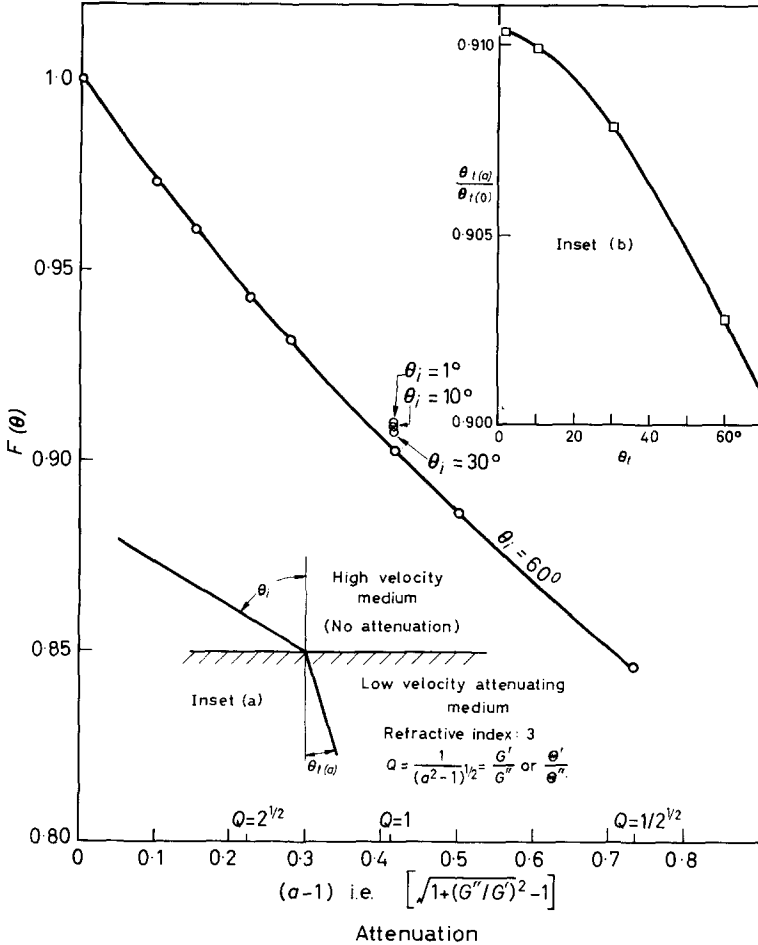


Figure 1. Effect of attenuation on refraction. *Inset (a)* Ratio of angles $\theta_{t(a)}/\theta_{t(0)}$ (with and without attenuation) for angle of incidence $\theta_i = 60^\circ$. *Inset (b)* Variation of $\theta_{t(a)}/\theta_{t(0)}$ with θ_t where $a = 2^{1/2}$, $Q = 1$. θ is the bulk modulus $+ \frac{4}{3}G$. G is the modulus of rigidity

It is to be noted that the error in the angle can rise as high as 20 per cent for values of loss tangent likely to be encountered in practice.

A further error arises from obliquity of energy flow even at the rather lower attenuations in the specimen. The polymer slab in this method of test is quite near to the piezoelectric radiator and also to the piezoelectric pick-up, say each at a distance d which is less than the extent of the Fresnel region a^2/λ , where a is the radius of the radiator and λ is the wavelength in the liquid. Consequently the specimen surface is not irradiated by a simple

plane wave but by a multiplicity of wave fronts. Some estimate of the inclination of the wave components carrying most of the energy can be obtained by adapting a calculation by Bradfield and Goodwin² which applies to circumstances such as above when the polymer slab is not too thick. The extra phase lag of the energy picked up at the second parallel and coaxial transducer is, for a typical geometry, about $\pi/4$ radians compared with the centre-to-centre radiation which is phase shifted by about $4\pi d/\lambda$ radians, say 200π . The inclination of the mean energy path to this centre-to-centre direction is therefore about 0.05 radians, i.e. about $2\frac{1}{2}$ degrees. Due to attenuation in the polymer, the component wave with the shortest path length will be favoured. This will alter the direction of the energy and hence the length of the path travelled. A correction for this can be computed and will therefore have to be applied in attempting to evaluate the velocity in the polymer accurately; this correction will not be likely to be the same for different thicknesses of polymer specimen.

This work is part of the programme of the National Physical Laboratory and is published with permission of the Director. The valuable help of Miss A. M. Nunn in the Born and Wolf computation is acknowledged.

G. BRADFIELD

*National Physical Laboratory,
Teddington, Middlesex*

(Received April 1965)

REFERENCES

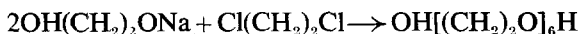
- ¹ BORN, W. and WOLF, E. *Principles of Optics*, p 612. Pergamon: Oxford, 1959
- ² BRADFIELD, G. and GOODWIN, E. T. *Phil. Mag.* 1961, **6**, 1065

Model Polyethers I—Synthesis by the Williamson Reaction

T. P. HOBIN

Model polyalkylene ethers $\text{H}[(\text{CH}_2)_x\text{O}]_y(\text{CH}_2)_x\text{H}$ and *trialkylene glycols* $\text{OH}[(\text{CH}_2)_x\text{O}]_3\text{H}$, where $x=4, 5, 6$ and 10 and $y=2, 3$ and 4 have been synthesized by the Williamson reaction. Attempts to prepare the corresponding compounds where $x=3$ were only partly successful.

HIBBERT¹⁻³ used the Williamson reaction for the stepwise synthesis of a series of pure polyethylene glycols, thus

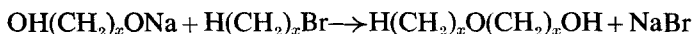


He used the product in a similar reaction with its chlorinated derivative to give $\text{OH}[(\text{CH}_2)_2\text{O}]_{18}\text{H}$, and so on.

Model polymethylene and polyethylene oxides and their derivatives have since been prepared by various other methods⁴⁻¹⁰ but there is little available information concerning model polyalkylene oxides having greater numbers of recurring methylene units.

In the present work trialkylene glycols were prepared from monosodium salts of glycols in reactions with their corresponding dibromoalkanes and model polyethers having alkoxy end-groups were prepared from alkoxy-alcohols and alkoxyalkylhalides by the reactions outlined below.

(a) Preparation of alkoxyalcohols



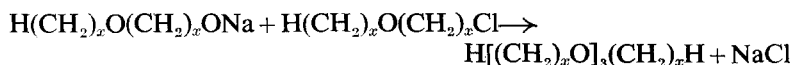
(b) Preparation of alkoxyalkylhalides



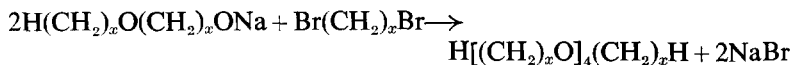
(c) Diethers



(d) Triethers



(e) Tetraethers



The purities of the products were checked by vapour phase chromatography and infra-red spectroscopy. Where appropriate, the following measurements were made: melting point, boiling point, density, refractive index and molecular weight.

EXPERIMENTAL

(1) *Synthesis*

(a) *Triglycols*—A three- to five-fold excess of glycol was used to act as solvent and to reduce the likelihood of the formation of disodium salts. The monosodium salt was formed by addition of a hot saturated aqueous solution of sodium hydroxide with rapid stirring, after which half of an equivalent of dibromoalkane was added dropwise with stirring whilst the temperature was not allowed to exceed 90°C or to fall below 60°C. After the addition the temperature was raised to 150°C to complete the reaction. The product was cooled and sufficient water added to dissolve all the inorganic salts. The lower aqueous layer was then discarded and the upper layer was vacuum distilled until most of the excess glycol had been removed. The residue was cooled, dissolved in ether and washed with water before being subjected to further vacuum distillation. The crude triglycol fraction was purified by fractional distillation through a Vigreux column.

(b) *Hepta-pentenediol*—Sodium was added to a two-fold excess of triptentane diol containing an equal volume of dibutylether. The mixture was heated under reflux to form the monosodium salt, which was then reacted with half of an equivalent of dibromopentane. The excess triptentane diol was removed by vacuum distillation and the residual hepta-pentane diol was distilled under high vacuum. The boiling point was 320° to 330° under high vacuum.

(c) *Alkoxyalcohols*—A two-fold excess of diol was used. To this was added powdered sodium hydroxide, with stirring, followed by half of an equivalent (based on NaOH) of alkyl halide, added dropwise. For trimethylene and tetramethylene derivatives the temperatures were maintained at 50° to 60° during the reaction in order to reduce side reactions involving hydrolysis or dehydrohalogenation of the alkyl halide. Reactions of higher alkylene derivatives were carried out on a steam bath. In each case the temperature was finally raised to 130° to complete the reaction. The alkoxyalcohols, which are insoluble in water but soluble in ether, were isolated from the excess glycols by dissolution in ether followed by extraction with water. The residue was distilled and the crude alkoxyalcohol fraction was further purified by aqueous washing of the ethereal solution before being subjected to fractional distillation. Propoxypropanol contained a persistent impurity and copious washings with water were required to remove it. Butoxybutanol also contained an impurity but this could not be removed by washing or fractional distillation.

(d) *Alkoxyalkyl halides*—The method used for the preparation of these was developed from that described by Hibbert². Alkoxyalcohol dissolved in 1.2 equivalents of pyridine was stirred at 0°C whilst two equivalents of thionylchloride were added dropwise. The product was heated under reflux for 30 minutes and, after cooling, the upper layer was decanted from the dark, viscous lower layer and added to two per cent aqueous sodium hydroxide solution containing ice. The organic layer was separated and again washed with sodium hydroxide solution, followed by water. It

was dried over calcium chloride and fractionally distilled. The alkoxyalkylhalide cut was used in subsequent reactions without further purification.

(e) *Diethers*—These were prepared by the technique described for the synthesis of alkoxyalcohols except that the glycols were replaced by the corresponding alkoxyalcohols. The reactants were finally heated to 150° to complete the reactions. After cooling the products were washed with water and vacuum distilled. The crude diethers were re-distilled several times from sodium (until they showed no further reactivity towards sodium) before being purified by fractional vacuum distillation.

(f) *Triethers*—Sodium was added to a two-fold excess of alkoxyalcohol contained in four times its volume of the corresponding dialkylether (as solvent). An exception to this was the decamethylene derivative, which was prepared in di-*n*-amyl ether. The mixtures were heated under reflux until the sodium had reacted (two days). The product was then stirred on a steam bath whilst an equivalent of alkoxyalkyl halide was added. The mixture was finally heated under reflux for eight hours. After cooling, the inorganic salts were extracted with water and the residue was distilled under vacuum. The crude tri-ether fraction was re-distilled several times from sodium (until no longer reactive to sodium). It was finally purified by fractional distillation under vacuum.

(g) *Tetraethers*—The preparation of these was identical to the preparation of the triethers, except that half of an equivalent of dibromoalkane was used instead of one equivalent of alkoxyalkylhalide. The work-up was as before except for the decamethylene derivative; the latter was not very volatile and hence was purified by crystallization from (a) methanol (b) ether.

(2) *Characterization*

The model polyethers and the trialkyleneglycols gave the anticipated infra-red spectra and no unexpected absorptions were detected. Vapour phase chromatography on those that were sufficiently volatile showed that they were essentially pure substances. The impurity peaks, when evident, were close to the major peaks and the impurities were generally more volatile; they may have been isomeric species arising from isomeric impurities in the raw materials.

Molecular weights were estimated from measurements of the depression of freezing point of benzene; they are liable to an error of about five per cent for every 100 units of molecular weight but the agreement with the calculated molecular weights was better than this. The molecular weights of compounds containing hydroxy groups were ascertained by end-group analysis (acetylation).

Densities at 20°C were determined in a pycnometer. Densities at 60°C were determined in a small dilatometer; they were not as accurate as those obtained at 20°C.

Refractive index measurements were used in conjunction with density measurements and the calculated molecular weights to determine the mole-

Table 1. Intermediates

Compound	Yield %	B. pt/mm Hg	YPC purity %	Molec. wt		Refractive index D line 20°	Microanalyses													
				calc.	obs.		calc.			obs.										
							C	H	Cl*	C	H	Cl*								
Propoxypropanol		174-6/760	96			1.411														
Propoxypropyl chloride		88/15																		
Butoxybutanol	75	212-14/760	80																	
Butoxybutylchloride	75	196-200/760	97																	
Pentyloxypentanol	62	249-51/760	>99	174	178	1.432														
Pentyloxypentylchloride	57	95-100/3	99																	
Hexyloxyhexanol	74	280-282/760	97	202	213	1.441														
Hexyloxyhexylchloride	69	110/1.0	98																	
Decyloxydecanol	47	202/2.0 (M.pt 42°C)	98	314	316	1.4390 (60°)														
Decyloxydecylchloride	25	170-80/0.7																		

*Halogens estimated by oxygen flask method.

Table 2. Trialkyleneglycols OH $[(CH_2)_xO]_y H$

x	y	Compound	Yield %	Melting point °C	Boiling point °C/mm Hg	Refractive index n_D^{20}	Molec. wt		Microanalyses											
							calc.	obs.	calc.			obs.								
									C	H	Cl*	C	H	Cl*						
3	3	Tri-propane-1,3-diol	Insignificant	33	182-184°															
4	3	Tri-butane-1,4-diol	31		2.0-2.4	1.4484	234	238												
5	3	Tri-pentane-1,5-diol	51	29	188-190° 0.8-1.0	1.4495	276	283												
5	7	Hepta-pentane-1,5-diol	64% (crude yield)	36-38	320-330 at high vacuum	1.4538														
6	3	Tri-hexane-1,6-diol	48	56	209-210° 0.8-0.9	1.4538	318	317												
10	3	Tri-decane-1,10-diol	70	80	290-300° 1.0	1.4518	486	473												

MODEL POLYETHERS I

cular refractivities. The values so obtained are in good agreement with those calculated from atomic refraction equivalents (taking $C=2.418$, $H=1.100$ and $O=1.643$).

(3) *Summarized experimental data*

The experimental data are summarized in *Tables 1 to 3*.

Table 3. Model polyethers $H[(CH_2)_xO]_y(CH_2)_zH$

Row	x	y	Name	Yield %	Estimated purity (by VPC) %	Boiling point °C/mm Hg	Melting point °C	Density g/ml 20°C
1	3	2	4,8-dioxaundecane	58	100	180/760	—	0.836
2	3	3	4,18,12-trioxapentadecane	4	91	240-250/760	—	
3	3	4	4,8,12,16-tetraoxanonadecane	<1				
4	4	2	5,10-dioxatetradecane	26	99	234-236/760	—	0.843
5	4	3	5,10,15-trioxanonadecane	43	98	137/1.4	—	0.878
6	4	4	5,10,15,20-tetraoxatetradecane	16	>99	190/1.0	—	0.895
7	5	2	6,12-dioxaheptadecane	53	97	120/0.2	—	0.843
8	5	3	6,12,18-trioxatricosane	70	97	160/0.3	—	0.870
9	5	4	6,12,18,24-tetraoxanonacosane	50		200/0.2	—	0.890
10	6	2	7,14-dioxaicosane	58	>99	130/0.4	—	0.842
11	6	3	7,14,21-trioxaheptacosane	16	96	184/0.6	—	0.867
12	6	4	7,14,21,28-tetraoxatetriacontane	40		260/1.5	20.5	0.879
13	10	2	11,22-dioxadotriacontane	50		233/0.3	40	0.819 (60°C)
14	10	3	11,22,33-trioxatritetracontane	65		310-330/2	50	0.834 (60°C)
15	10	4	11,22,33,44-tetraoxatetrapentacontane	42		—	59	0.850 (60°C)

Row	Refractive index n (sodium D line) 20° unless otherwise stated	$\frac{n^2-1}{n^2+2} \times \frac{M}{d}$	Sum of atomic refractivities	Mol. wt M (calc.)	Mol. wt (obsd)	Analysis			
						Found		Calculated	
						C	H	C	H
1	1.4090	47.3	47.1	160	162				
2									
3									
4	1.4226	61.0	60.9	202	195	70.7	12.8	71.2	13.0
5	1.4357	81.6	81.0	274	307	69.8	12.6	70.0	12.5
6	1.4393	102	101	346	388	69.4	12.3	69.3	12.2
7	1.4318	75.0	74.8	244	246	73.4	13.2	73.7	13.2
8	1.4416	100	99.5	330	303	72.8	12.7	72.7	12.8
9	1.4471	125	124	416	394	71.8	12.3	72.0	12.6
10	1.4379	89.2	88.6	286	266	75.6	13.6	75.4	13.4
11	1.445	119	118	386	390	74.6	13.0	74.5	13.0
12	1.451	149	147	486	501	74.2	12.8	74.0	12.9
13	1.4370 (60°C)	145	144	454	501	79.0	13.9	79.2	13.8
14	1.4416 (60°C)	193	193	610	574	79.0	13.9	78.6	13.5
15	1.4457 (60°C)	240	242	766	808	77.3	13.8	78.2	13.4

Table 1 gives data for the intermediates. These were not specially purified and physical constants are only given for those that happened to be reasonably pure.

Table 2 gives data for the trialkylene glycols. These were rather hygroscopic but not very soluble in water; they were soluble in most polar solvents. The only unsuccessful attempt at synthesis was that of trimethylene glycol. All attempts to synthesize this resulted in the formation

of considerable quantities of volatile byproducts and very little material of boiling point higher than the starting material was obtained.

Table 3 gives data for the model polyethers. At temperatures above their melting points these were soluble in most organic solvents. Again, all syntheses were successful except for some of those in the trimethylene series. Quite a few of the preparations were carried out only once and on a small scale and so better yields than those quoted may be possible.

(4) Discussion

The Williamson reaction, which was known to be satisfactory for the synthesis of model polyethylene glycols has been found to be equally satisfactory for the preparation of model polyethers and trialkyleneglycols containing sequences of 4, 5, 6 and 10 methylene units, but not so satisfactory for those containing sequences of 3 units. It is probably relevant in this connection that propane diol decomposes at its boiling point¹¹. This decomposition is probably enhanced by alkali—the presence of which is unavoidable in the Williamson synthesis.

A few of the compounds listed in the tables have already been reported in the literature, namely, propoxypropanol¹², butoxybutanol¹³⁻¹⁵, butoxybutylchloride¹⁵, tri-butanediol¹⁶ and 5,10-dioxatetradecane^{14, 15, 17}. The data cited for these are in reasonable agreement with those in the literature.

It is not possible to use a Williamson reaction between disodium salts of glycols and dibromoalkanes to synthesize high polyethers because:

- (a) the insolubility of the monosodium salts of diols makes it very difficult to convert them into disodium salts,
- (b) the dibromoalkanes are susceptible to dehydrohalogenation and to hydrolysis in the alkaline medium.

It should be possible to prepare higher model polyethers than those described by the use of correspondingly higher intermediates. They may be rather involatile for purification by distillation but other methods, e.g. fractional crystallization or zone refinement, should be effective.

The author is grateful to the E.R.D.E. Analytical Services for the following measurements: Infra-red spectra, vapour phase chromatography, microanalysis and hydroxyl determinations.

*Explosives Research and Development Establishment,
Waltham Abbey, Essex*

(Received December 1964)

REFERENCES

- ¹ HIBBERT, H. and PERRY, S. Z. *Canad. J. Res. B*, 1936, **14**, 77-83
- ² HIBBERT, H., FORDYCE, R. and LOVELL, E. L. *J. Amer. chem. Soc.* 1939, **61**, 1905-1909
- ³ HIBBERT, H. and FORDYCE, R. *J. Amer. chem. Soc.* 1939, **61**, 1910-1911
- ⁴ GRESHAM, W. F. and BROOKS, R. E. *U.S. Pat. No. 2 449 469* (1948)
- ⁵ AUBERSTEIN, P. *Mémorial des Poudres*, 1959, **41**, 57-64
- ⁶ PUTHOFF, M. E. and BENEDICT, J. H. *Analyt. Chem.* 1961, **33**, 1884-1887

MODEL POLYETHERS I

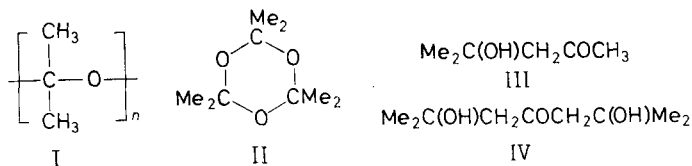
- ⁷ HENGLEIN, F. A. and FRANK, R. *Makromol. Chem.* 1962, **54**, 10-23
- ⁸ HEAD, F. S. H. *J. chem. Soc.* **1963**, 2972-2976
- ⁹ RIEMSCHEIDER, P. and GROSS, P. *Mh. Chem.* 1960, **91**, 48-56
- ¹⁰ REMPP, P. *Bull. Soc. chim. Fr.* **1957**, 844-847
- ¹¹ *Handbook of Chemistry and Physics*, 44th ed., p 1180. The Chemical Rubber Publishing Co.: Cleveland, Ohio, 1962
- ¹² SEARLES, S. and BUTLER, C. F. *J. Amer. chem. Soc.* 1954, **76**, 56-58
- ¹³ PISTOR, H. J. *German Pat. No. 802 817* (1951)
- ¹⁴ *Brit. Pat. No. 654 771* (1951)
- ¹⁵ REMPP, P. *Bull. Soc. chim. Fr.* **1957**, 844-847
- ¹⁶ SIEBER, G. *German Pat. No. 1 106 306* (1959)
- ¹⁷ TALLMAN, R. C. *J. Amer. chem. Soc.* 1934, **56**, 126-129

Polyacetone

V. C. E. BURNOP

Unstable acetone polyacetals and a stable acetone-propylene block copolymer have been briefly reported in the literature during the last few years. Attempts to repeat some of this work, or to prepare acetone polyacetals by other methods have failed. However, pure molecular sieve dried acetone and anionic initiators at -78°C were found to deposit triacetone dialcohol (2,6-dimethyl-2,6-dihydroxy-heptan-4-one) which has similar solubility characteristics and melting point to a 'polyacetone' of the literature. The condensation of acetone to diacetone alcohol and triacetone dialcohol is favoured by low temperatures and is easily reversible. If not completely neutralized at the reaction temperature, the triacetone dialcohol retained sufficient catalyst to promote decomposition at room temperature, where the equilibrium concentration of acetone is about 90 per cent. This behaviour could be mistaken for the spontaneous decomposition of an acetone polyacetal to monomer.

ON THERMODYNAMIC grounds, acetone is unlikely to polymerize to a polyacetal, I, except at low temperatures, and perhaps not at all^{1,2}.



The cyclic trimer of acetone, II, is also unknown, and although compounds containing $\text{---O---CMe}_2\text{---O---}$ or $\text{---CMe}_2\text{---O---CMe}_2\text{---}$ groups can be prepared, they are exceptionally unstable to acids. Until recently, all known self condensation reactions of acetone involved formation of carbon to carbon bonds, as in diacetone alcohol III or triacetone dialcohol IV. This contrasts with the behaviour of aldehydes, which give polyacetals, cyclic trimers, and the aldol condensation. Formaldehyde gives a trimer and polyacetal with greater thermal stability than those from other aldehydes. Leaving aside thermodynamic arguments, it is apparent that the stability of a system of alternating carbon and oxygen atoms is reduced by substitution, and that structures such as I and II would be among the least stable. Construction of I with molecular models shows it to be strained and hindered.

Kargin *et al.*¹ prepared polyacetone, I, by condensing acetone and magnesium simultaneously on to a surface at -196°C . The vitreous deposit polymerized when the temperature rose sufficiently to allow ordered rearrangement of the monomer molecules. The polymer was a white elastomer, decomposing to acetone within 10 to 12 hours at room temperature. Okamura *et al.*^{3,4} obtained a yellow unstable elastomer in 0.2 to 1.2 per cent yield by irradiating acetone at -136° to -196°C with a cobalt-60

source. The product contained carbonyl groups, and had an irritating smell, and was not a pure polyacetal. Both Kargin and Okamura observed that the addition of traces of vinyl acetate to the acetone gave a more stable product. Interrupting the C—O sequence by vinyl groups would retard the unzipping of the polyacetal chain. Kawai⁵ claimed an unstable waxy acetone polymer (m.pt 60° to 70°C), using organometallic initiators at -70° to -78°C. Furukawa⁶⁻⁸ reported a 1 to 2 per cent yield of a thermally stable highly crystalline, block copolymer of acetone and propylene using as initiator a mixture of titanium halide, aluminium triethyl and an inorganic acetate.

These polymers were characterized by decomposition to acetone, and by i.r. absorption attributed to ether linkages. The polymers of Furukawa¹¹ and Okamura absorbed in the 1 150 to 1 000 cm^{-1} region, consistent with the polyacetal structure. Kawai's polymer did not absorb in the 1 300 to 1 000 cm^{-1} region, and bands at 985 and 855 cm^{-1} were described as 'characteristic' without explanation; bands due to the C—O—C linkage were claimed to be present but were not identified, and an unexplained reference to cyclic ethers is quoted. The polymer also showed strong OH absorption explained as due to end groups, but not consistent with any substantial degree of polymerization. It is concluded that, on this evidence, Kawai's product was not a polyacetal.

Furukawa's copolymer of acetone and propylene contained 84 per cent acetone, calculated from the oxygen content. It was, unexpectedly, soluble in water, and was hydrolysed to acetone by dilute hydrochloric acid. The thermal stability could be explained by random copolymerization, but the high crystallinity of the polymer is attributed to polyacetone blocks. To prevent unzipping, the polyacetone blocks would of necessity be capped at both ends by stabilizing groups. The means by which this was achieved is not apparent from the information disclosed.

The anionic copolymerization of acetone and ketenes at -60° to -78°C gives polyesters of β -hydroxy acids^{9,10}. These are the only reported polymerizations involving the acetone carbonyl group which give substantial yields of products; for instance, acetone and dimethyl ketene give a 50 per cent yield of polyester.

This paper reports attempts to prepare polymers or copolymers of acetone by novel or published methods. It was difficult to reproduce, with confidence, the conditions used by previous authors as few preparative details are disclosed. For instance, no acetone purification procedures are described, although these must be critical, especially the method of drying.

EXPERIMENTAL

(a) Acetone purity

AR-acetone was redistilled after drying with anhydrous calcium sulphate (drierite), and with Linde molecular sieve 5A for about an hour. It was found that long contact between acetone and the molecular sieve produced some mesityl oxide.

(b) Acetone irradiation

Acetone was sealed in a Pyrex glass tube *in vacuo* and irradiated at

POLYACETONE

-196°C using a cobalt-60 source, giving a dose of 3.4×10^6 rads over six hours. Evaporation of the acetone under reduced pressure at -30°C gave 0.5 per cent of a yellow acrid-smelling oil, insoluble in petroleum ether and not solid at -80°C. The product was not sufficiently stable to be characterized.

(c) *Kawai's method and other ionic initiations*

Following Kawai, acetone was stored in sealed tubes at -78°C with lithium and aluminium alkyls. Several other possible initiators and comonomers were also used (*Table 1*). The initiators were introduced into the tubes in a dry box filled with nitrogen, and the acetone and other reagents via a vacuum manifold. Examination of the tubes at intervals up to four weeks showed, usually, no apparent change such as viscosity, and no polymer separated when the solutions were poured into cold petroleum

Table 1. Attempted polymerizations of acetone at -78°C

(A) Homopolymerizations			
<i>Expt. No.</i>	<i>Initiator</i>	<i>% Initiator (wt/vol. acetone)</i>	
1	AlCl ₃	2.5	
2	TiCl ₄	2.0	
3	Na (dissolved)	0.1 to 1.0	
4	Mg(OAc) ₂	2.5	
5	<i>tert</i> -BuLi	0.01 to 0.1	
6	<i>n</i> -BuLi	0.01 to 0.1	
7	Mg-pinacol complex	By solution of 0.5% Mg	
8	AlEt ₃	0.5	
(B) Copolymerizations			
<i>Expt. No.</i>	<i>Initiator (% wt/vol)</i>		<i>Comonomer*</i>
9	Na	(1.0)	Methyl styrene
10	Na	(1.0)	Styrene
11	BF ₃ Et ₂ O	(1.0)	Maleic anhydride
12	AcClO ₄	(1.0)	Maleic anhydride
13	BF ₃ Et ₂ O	(1.0)	Acetone diethyl ketal
14	FeCl ₂	(2.0)	Acetone diethyl ketal
15	Al <i>iso</i> -propoxide	(4.0)	Acrylamide
16	BF ₃ Et ₂ O	(1.0)	Propylene oxide
17	FeCl ₃	(4.0)	Propylene oxide
18	Al <i>iso</i> -propoxide	(4.0)	Propylene oxide
19	BF ₃ Et ₂ O	(1.0)	Vinyl acetate
20	BF ₃ Et ₂ O	(1.0)	Methylmethacrylate
21	BF ₃ Et ₂ O	(1.0)	Ethyl vinyl ether

*2.0 g. if solid, or 2.0 ml if liquid, of comonomer to 10 ml acetone.

ether. On the other hand, reaction mixtures containing lithium alkyls or dissolved sodium deposited white crystalline solids (experiments 3, 5, 6 and 10, *Table 1*), which were filtered off under nitrogen in cold (-78°C) sintered glass funnels and washed with hexane. When exposed in the funnels to air at room temperature, the solids began to decompose after about one hour, and gave a liquid filtrate and a small solid inorganic residue, containing alkali metal, on the filter plate. Fractional distillation separated the filtrates into acetone, mesityl oxide, and diacetone alcohol, III, identified by i.r. spectrum and dehydration to mesityl oxide. Mesityl oxide was identi-

Table 2. Decomposition products of solids from acetone 'polymerization'

Expt. No.	Catalyst	Catalyst concentration	% Yield of solid	% Diacetone-alcohol in decomp. solids
3	Na	0.3 N	14	*
5	<i>tert</i> -BuLi	0.1 N	53	40
10†	Na	0.5 N	35	13 to 16

*Liquid fraction of reaction mixture contained 8 per cent diacetone alcohol.

†The styrene present did not take part in the reaction.

fied by i.r. spectrum and 2,4-dinitrophenylhydrazone, m.pt 202°C. Details are given in Table 2. The solid was therefore not a polyacetal. Other preparations (e.g. experiments 3, 5 and 6, Table 1) using acetone alone or diluted with hexane and lithium alkyls or sodium as initiators showed separation of a solid at -78° after a few hours. The reaction tubes were opened and the solids filtered off in an atmosphere of carbon dioxide to neutralize alkali present. In these conditions the solid (yield about 30 per cent) was stable and when recrystallized from hexane had m.pt 58°C. Its i.r. spectrum showed strong CO and OH bands. The solid proved to be triacetone dialcohol IV, previously characterized by Conolly¹².

Analysis

Found: C 62.5, H 10.4 per cent; C₉H₁₈O₃ requires 62.1, and 10.3 per cent. 2,4-Dinitrophenylhydrazone—orange, m.pt 169°C.

Found: C 53.5, H 6.0, N 16.7 per cent;

C₁₅H₂₀O₅N₄ requires 53.6, 6.0 and 16.7 per cent.

The filtrates from the reaction mixtures consisted of acetone, III and IV. Kawai's insoluble waxy polymer could not be detected. Pure triacetone dialcohol IV was stable at room temperature indefinitely, but grinding with a trace of aqueous alkali caused rapid decomposition to the equilibrium mixture consisting mainly of acetone. The properties of IV are compared with Kawai's polymer in Table 3. There is at least a superficial resemblance. Figure 1 compares the i.r. spectra. Above 1350 cm⁻¹ the spectra are similar in shape but relatively displaced.

The possibility of detecting the polyacetal by n.m.r. spectroscopy was considered. The n.m.r. spectra of the acetals 2,2-dimethoxypropane, V, and

Table 3. Comparison of Kawai's polymer and triacetone dialcohol

Character	Kawai's polymer	Triacetone dialcohol
(i) Appearance	White wax	Crystalline deposit
(ii) Melting point	60° to 70°C	59°C
(iii) Decomposition temp. (foaming)	230°C	230°C
(iv) Decomposition	Decomposes at room temp. when exposed to air for several hours	Decomposes to acetone etc. in a few hours at room temperature if trace of alkali present
(v) I.r. spectrum	OH, CO(?) present	OH, CO present
(vi) Solubilities	Soluble in methanol, chloroform, dioxan, precipitated by hexane	Soluble in methanol, chloroform, dioxan, sparingly soluble in hexane

POLYACETONE

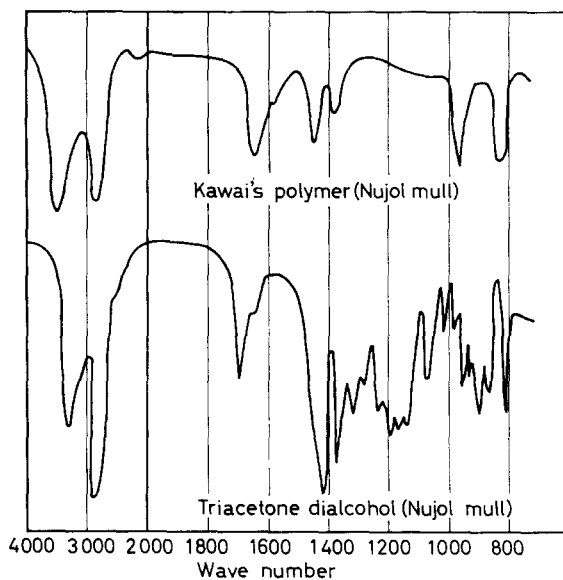
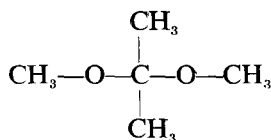
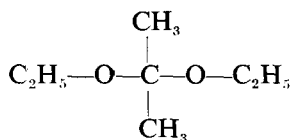


Figure 1—The i.r. spectra of 'polyacetone'

2,2-diethoxypropane, VI, were compared with those of acetone, diacetone alcohol, III, and triacetone dialcohol, IV.



V



VI

The chemical shift of 1.24 p.p.m. due to the acetal group $\text{—CMe}_2\text{O—}$ was too close to that of methyl groups α to the hydroxyl group of the alcohols (1.20 p.p.m. for III, 1.26 p.p.m. for IV) to allow detection of a polyacetal in the reaction mixture.

If 0.1 per cent of sodium is dissolved in acetone containing 0.5 per cent water and cooled, triacetone dialcohol is still formed but crystallizes out less easily. Equilibrium conditions are given in Table 4. The equilibria were frozen by passing carbon dioxide into the reaction mixture. No immediate precipitate of sodium salt formed, but on warming to room temperature there was a transient gel stage followed by precipitation of sodium carbonate

Table 4. Composition of equilibrium mixtures of condensation products of acetone. Catalyst: 0.1 per cent sodium

Temperature	0°C	-40°C	-78°C
Density	0.847	0.913	—
Wt % diacetone alcohol	20.8	33.6	28.8
Wt % triacetone dialcohol	2.0	14.2	5.4*

*This is the solubility in the reaction mixture since solid dialcohol had separated.

or bicarbonate. The components of the reaction mixture were separated by distillation.

(d) *Attempts to repeat Furukawa's acetone-propylene copolymerization*

2 ml of 25 per cent w/v aluminium triethyl in petroleum ether was added cautiously to 0.15 g of titanium trichloride (Strauffer Chemicals Corpn) and 0.5 g powdered anhydrous sodium acetate. The mixture was diluted with 30 ml pure dry heptane in a vessel attached to a vacuum manifold, cooled in liquid nitrogen and pumped out. Teflon sleeves were fitted to ground glass joints to avoid contamination by grease. 250 ml propylene (Phillips Research Grade), measured at room temperature and pressure, was transferred during one hour on a vacuum line into the catalyst mixture, now at -78°C , followed by 10 ml of acetone over one and a half hours. The reaction mixture was kept at -78°C for 24 hours, with shaking, then poured into 200 ml of methanol. After standing overnight, the solid deposit was filtered off. The filtrate was evaporated at about 200 mm of mercury pressure, and gave a further residue of solid. The combined solids, dried *in vacuo*, were continuously extracted with chloroform. The chloroform extract gave 0.10 g of a vaseline-like material, insoluble in water, and giving no 2,4-dinitrophenylhydrazone in acid alcoholic solution. A repeat

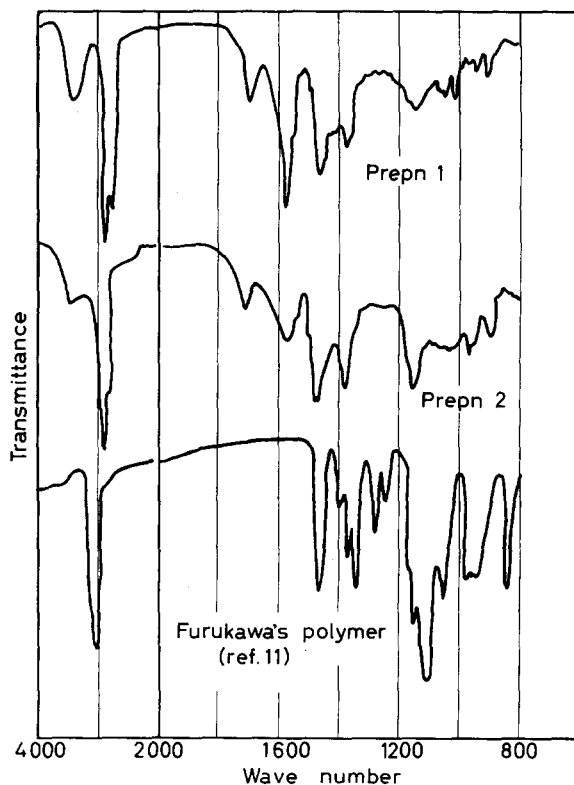


Figure 2—The i.r. spectra of acetone-propylene reaction products

experiment, in which the ingredients of the catalyst were added to the heptane to avoid the vigorous reaction at this stage of the first preparation, gave a similar result.

The i.r. spectra of these products were not identical but neither showed ether bands. They were quite different from that of Furukawa's polymer (Figure 2).

(e) *Attempted copolymerizations by radical anions*

Catalysts were prepared by dissolving 0.09 g lithium, 0.29 g sodium or 0.47 g potassium in a mixture of 20 ml α -methyl styrene and 50 ml tetrahydrofuran. 2 ml portions of these catalysts were added to 20 ml α -methyl styrene at -78° followed by 100 ml acetone. The colour of the radical ion was immediately discharged. No polymer could be isolated after 24 hours reaction time at -78° . Air was excluded throughout. Similar experiments, using the alkali metal ketyls from benzophenone as initiators, were also unsuccessful.

The author wishes to thank Mr J. M. Jones who carried out most of the experimental work described in this paper, and also Mr E. Kendrick for the n.m.r. measurements.

Esso Research Ltd,
Abingdon, Berks.

(Received December 1964)

REFERENCES

- ¹ KARGIN, V. A., KABANOV, P., ZUBOV, V. P. and PAPISOV, I. M. *Dokl. Akad. Nauk S.S.S.R.* 1960, **134**, 1098
- ² ELIAS, H.-G. *Chimia*, 1962, **16**, 161
- ³ OKAMURA, S., HAYASHI, K. and MORI, S. *Isotopes and Radiation (Japan)*, 1961, **4**, 70
- ⁴ OKAMURA, S., HAYASHI, K., MORI, S., SOBUA, H., TABATA, Y. and SHIBANO, H. *Jap. Pat. No. 16 341* (1963)
- ⁵ KAWAI, W. *Bull. chem. Soc. Japan*, 1962, **35**, 516
- ⁶ FURUKAWA, J., SAEGUSA, T., TSURUTA, T., OHTA, S. and WASAI, G. *Makromol. Chem.* 1962, **52**, 230
- ⁷ FURUKAWA, J. *Polymer, Lond.* 1962, **3**, 495
- ⁸ FURUKAWA, J., SAEGUSA, T. and OHTA, S. *Jap. Pat. No. 20 987* (1963)
- ⁹ Montecatini. *Ital. Pat. No. 631 585* (1962), *Brit. Pat. No. 950 507* (1963)
- ¹⁰ Imperial Chemical Industries Ltd. *Brit. Pat. No. 931 144* (1962)
- ¹¹ FURUKAWA, J. and SAEGUSA, T. *Polymerization of Aldehydes and Oxides*, p 414. Interscience: New York, 1963
- ¹² CONNOLLY, E. E. *J. chem. Soc.* **1944**, 338

The Free Radical and Anionic Polymerization of Some N-substituted Maleimides

R. C. P. CUBBON

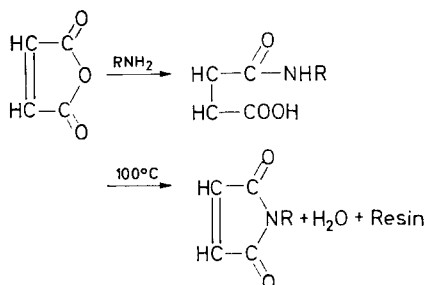
Eight N-substituted maleimide monomers have been prepared and polymerized by free radical initiators and n-butyl lithium, a typical anionic initiator. X-ray studies indicate that both types of initiator give rise to polymers which have a predominantly threo di isotactic configuration.

THE susceptibility of *N*-substituted maleimides to polymerization and copolymerization by free radical initiators has been known for some time¹⁻³. The anionic polymerization of these monomers has not previously been reported, except for the polymerization of maleimide by sodium ethoxide⁴. In the present work eight *N*-substituted maleimides have been prepared containing both linear and branched substituents. The effect of the substituent and the type of initiator on the polymer properties has been examined.

EXPERIMENTAL

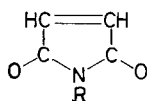
Preparation of the monomers

The *N*-alkyl maleimides were prepared by the reaction of the required primary amine with maleic anhydride in xylene⁵.



At temperatures above 100°C the *N*-alkyl maleamic acid cyclizes to yield the *N*-alkyl maleimide in 30 to 40 per cent yield. The monomers were purified by drying over anhydrous sodium sulphate and redistilling under reduced pressure of nitrogen. *N*-ethyl maleimide was recrystallized from benzene and *N*-isobutyl maleimide from aqueous alcohol. The purity of the monomers was established by gas-liquid chromatographic analysis. The properties of the monomers which were prepared are recorded in *Table 1*.

N-phenyl maleimide was prepared by the ring closure of *N*-phenyl maleamic acid with acetic anhydride and sodium acetate⁶. The monomer was purified by three recrystallizations from water.

Table 1. Properties of the *N*-alkyl maleimides,

<i>R</i>	<i>M.pt</i> ($^{\circ}\text{C}$)	<i>B.pt</i> ($^{\circ}\text{C}/\text{mm}$)
Ethyl	45.5	86/18
Isopropyl	~ 20	75/10
<i>n</i> -Butyl	~ 20	103/20
Isobutyl	42.5	
<i>t</i> -Butyl	—	104/18
<i>n</i> -Octyl	37.5	
Benzyl	50	120/5

Free radical polymerization procedure

The required quantities of monomer and benzene were introduced into a Carius tube with the accurately weighed amount of azo-bis-isobutyronitrile (0.02 to 0.05 per cent by weight based on the monomer). The contents of the tube were then outgassed under vacuum, purged and sealed under oxygen free nitrogen. The tube was maintained at 100°C for the required time, usually from 5 to 15 hours. The polymers were recovered by precipitation in methanol. Another free radical initiator which was employed was the potassium persulphate-sodium bisulphite aqueous system⁷.

n-Butyl lithium initiated polymerizations

These polymerizations were carried out in toluene and tetrahydrofuran (THF) using a pentane/heptane solution of *n*-butyl lithium supplied by the Foote Mineral Co. Toluene was freed from sulphur compounds by washing with sulphuric acid and dried by refluxing over sodium wire in an atmosphere of nitrogen. The toluene was distilled off the sodium under nitrogen as required. THF was dried over sodium wire in an atmosphere of nitrogen until the addition of a small amount of naphthalene yielded the dark green colour of sodium naphthalene. The THF was distilled from this sodium naphthalene solution as required.

In a typical experiment, the dry solvent was distilled under nitrogen into a reaction vessel equipped with a vacuum sealed stirrer, a nitrogen inlet and outlet and a rubber serum cap. The monomer was introduced and the reaction vessel was cooled to the required temperature. The polymerization was initiated by injecting the *n*-butyl lithium solution through the serum cap with a hypodermic syringe. The polymerization was terminated by the addition of methanol and the deep red coloration was discharged with a few drops of dilute hydrochloric acid.

RESULTS

Free radical polymerization

Polymerization with azo-bis-isobutyronitrile gave 70 to 80 per cent yields of polymers with inherent viscosities in the range 0.3 to 0.8 (0.5 per cent solutions in dimethyl formamide). The reactivity of the monomers decreased with increasing size of the substituent. The potassium persulphate-sodium bisulphite initiator gave higher yields of polymer, but the inherent viscosities were much lower.

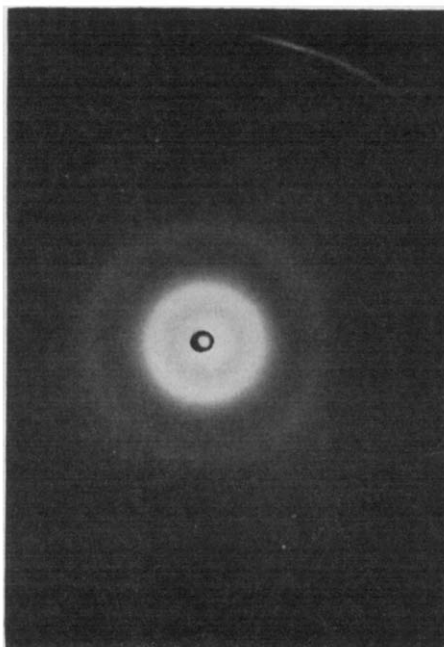
THE POLYMERIZATION OF SOME *N*-SUBSTITUTED MALEIMIDES

The poly-*N*-substituted maleimides were found to be high melting polymers as shown by the penetrometer softening points recorded in *Table 2*. The polymers in fact softened over a range of temperature. Examination of poly-*N*-*n*-butyl maleimide fibres on a hot plate showed that the brittle fibre begins to exhibit rubberlike properties at 200° to 210°C. The actual melting point of the poly-*N*-*n*-butyl maleimide is about 60°C higher at 270°C.

Table 2. Penetrometer softening points of the free radical initiated poly-*N*-substituted maleimides

$\left[\begin{array}{c} \text{H} \quad \text{H} \\ \quad \\ \text{---C---C---} \\ \quad \\ \text{O} \quad \text{N} \quad \text{C} \quad \text{O} \\ \quad \quad \\ \quad \quad \text{R} \end{array} \right]_n$	<i>Penetrometer S.pt</i> (°C)
Ethyl	265
Isopropyl	238
<i>n</i> -Butyl	210
Isobutyl	176
<i>t</i> -Butyl	204
<i>n</i> -Octyl	137
Benzyl	110
Phenyl	> 330

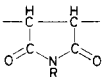
Figure 1—X-ray spectrum of poly-*N*-ethyl maleimide



X-ray powder photographs (*Figure 1*) showed that the polymers had two marked interplanar spacings, which are recorded in *Table 3*. It is apparent from *Table 3* that the spacing of ~5 Å common to all the poly-*N*-substituted maleimides prepared must be associated with the repeat unit

of the polymer backbone. The larger spacing which increases with the size of the substituent must represent the spacing between the polymer chains. The crystallinity of the polymers was not improved by annealing. Melt spun fibres showed only slight signs of orientation and were too brittle to draw.

Table 3. Interplanar spacings of the poly-*N*-substituted maleimides

	Interplanar spacings (Å)	
Ethyl	4.9	10.6
Isopropyl	4.9	10.8
<i>n</i> -Butyl	5.1	11.3
Isobutyl	5.1	13.1
<i>t</i> -Butyl	5.4	12.2
Phenyl	5.3	14.2
Benzyl	5.0	14.9
<i>n</i> -Octyl	4.8	18.9

Anionic polymerization

The *n*-butyl lithium initiated polymerization of *N*-ethyl maleimide was found to show a marked dependence on the nature of the solvent and the temperature. Table 4 shows that in toluene polymerization only takes place below 0°C and lowering the temperature increases the rate of polymerization and the molecular weight.

The polymerizations in toluene were heterogeneous and were accompanied by the formation of a dark red colouration. The red colour of the reaction mixture persisted after the addition of methanol or water, but was discharged by the addition of a few drops of dilute hydrochloric acid.

Table 4. The effect of temperature on the *n*-butyl lithium initiated polymerization of *N*-ethyl maleimide in toluene
(Initial monomer concentration = 0.27 mole l⁻¹)

Temp. (°C)	[<i>n</i> -Butyl lithium] (mole l ⁻¹)	Reaction time (hours)	Yield of polymer (%)	Inherent viscosity in dimethyl formamide
0	0.01	3	—	—
-20	0.01	3	20	0.115
-40	0.01	3	22	0.167
-70	0.02	‡	20	0.172

In THF at -70°C the *n*-butyl lithium initiated polymerization of *N*-ethyl maleimide proceeded much more rapidly than in toluene and 90 to 95 per cent yields of polymer were obtained. The poly-*N*-ethyl maleimide and poly-*N*-*n*-butyl maleimide obtained in this way were found to be insoluble in dimethyl formamide, unlike the polymers prepared in toluene. In fact, no solvent could be found for these polymers indicating that crosslinking had taken place. Poly-*N*-isobutyl maleimide and poly-*N*-phenyl maleimide

prepared in THF were soluble in dimethyl formamide. The anionic initiated polymers showed the same softening points, X-ray and infra-red spectra as the corresponding free radical initiated polymers.

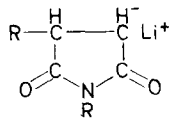
DISCUSSION

The ready free radical initiated homopolymerizations of maleimide⁴ and the *N*-substituted maleimides are in marked contrast with the extremely reluctant polymerization of maleic anhydride⁸. The high heat of polymerization of maleimide⁹ indicates that steric repulsions between neighbouring groups in the polymer chains are not very large, and thus it is unlikely that the difficulty of the homopolymerization of maleic anhydride is a result of steric hindrance. It has been suggested that release of strain in the ring on opening the double bond may contribute to the ease of polymerization of maleimide⁹.

The susceptibility of the *N*-substituted maleimides to polymerization by *n*-butyl lithium is not unexpected, since methyl methacrylate¹⁰ and *N,N'*-disubstituted acrylamides¹¹ are readily polymerized by this initiator. The inability of this initiator to polymerize the *N*-substituted maleimides at 0°C or above must be a result of the predominance of side reactions of the *n*-butyl lithium with the imide groups. Similar behaviour has been observed in the alkyl lithium initiated polymerizations of methyl methacrylate¹⁰ and acrylonitrile¹², these being monomers which also contain functional groups.

The crosslinking of the poly-*N*-ethyl maleimide and poly-*N-n*-butyl maleimide prepared in THF could arise from the attack of the propagating carbanions on the imide groups of the polymer. The absence of crosslinking in poly-*N*-isobutyl maleimide and poly-*N*-phenyl maleimide prepared under the same conditions indicates that the bulkier substituents on these polymers hinder attack on the imide groups. The enhancement of the rate of the *n*-butyl lithium initiated polymerizations on changing the solvent from toluene to THF appears to be a common feature of alkyl lithium initiated polymerizations¹³.

The deep red colour accompanying the anionic polymerization of maleimide and the *N*-substituted maleimides is worthy of some comment. By analogy with the anionic polymerizations of *N,N'*-disubstituted acrylamides which are not coloured, the propagating species



would not be expected to be coloured. Furthermore, this carbanion will almost certainly be sufficiently basic to accept a proton from methanol, while the red coloured species can only be destroyed by a strong acid. Tawney and co-workers⁴ have proposed that the colour is produced by the reaction of base with residual unsaturation in the polymers. This seems to be borne out by the fact that when poly-*N*-alkyl maleimides dissolved in dimethyl formamide are treated with alkali a red colour is obtained similar to that observed in the polymerizations.

The configuration of the poly-*N*-substituted maleimides obtained by both free radical and anionic initiation is of some interest. The five-membered maleimide ring is planar and hence there are the possibilities of *cis* and *trans* enchainment. Examination of Courtauld Models shows that there is considerable steric hindrance to the formation of polymers containing the *cis* configuration. Assuming that *trans* opening of the double bonds takes place exclusively, then three types of polymer can be formed: (i) all the rings are on the same side of the backbone chain (threo di isotactic polymer), (ii) the rings are on alternate sides of the backbone chain (threo di syndiotactic polymer), and (iii) the rings may be randomly distributed on either side of the backbone chain.

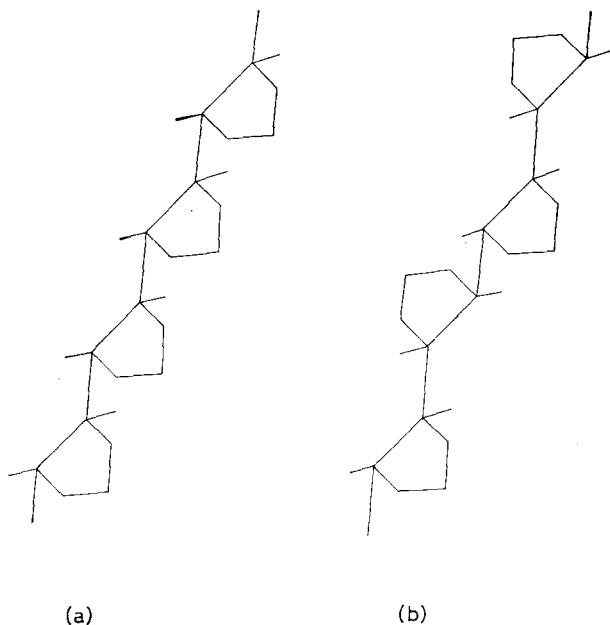


Figure 2—(a) Threo di isotactic configuration; (b) Threo di syndiotactic configuration

The threo di isotactic and the threo di syndiotactic polymers are represented diagrammatically in *Figure 2*. Inspection of models shows that the threo di isotactic polymers can form a 3_1 helix in which the repeat distance is 4.7 Å. The diameter of the helix with no substituents on the nitrogen is ~ 10 Å. Changing the substituent does not affect the repeat distance of the 3_1 helix, but does, of course, alter the distance between the chains. Thus it is apparent that the X-ray data recorded in *Table 3* can be accounted for if the polymers have a threo di isotactic configuration. The lack of sharpness of the X-ray spectra (*Figure 1*) and the failure to obtain oriented fibres suggests that the polymers are not completely stereoregular. It seems likely that the polymers are predominantly threo di isotactic with occasional threo di syndiotactic placements which disrupt the crystallinity to some extent.

The tendency for *trans* opening of the double bond to take place is exemplified in the stereospecific *trans* addition of hydrogen bromide to cyclohexene^{14,15}. The stereochemistry of polymers prepared from some other 1,2-disubstituted cyclic monomers presents a rather confused picture. The cationic polymerizations of indene and 4,5-dihydro-2-methyl furan in the presence of optically active cocatalysts gave non-crystalline optically inactive polymers¹⁶. This result might be accounted for if internally compensated threo di syndiotactic polymers were formed, or alternatively the polymers could be atactic. Free radical initiated poly-indene and poly-acenaphthylene were found to be amorphous¹⁷, but in more recent work the preparation of crystalline polyacenaphthylene by anionic, free radical and cationic initiation has been described¹⁸. Natta and co-workers¹⁹ have recently succeeded in polymerizing cyclobutene to give two types of crystalline polymer which have been identified as erythro di isotactic and erythro di syndiotactic. Thus with cyclobutene *cis* opening of the double bond takes place. Natta and co-workers²⁰ have also polymerized benzofuran with cationic initiators in the presence of optically active compounds. Under these conditions an asymmetric synthesis occurs and optically active poly-benzofuran is obtained. This must be a di isotactic polymer since the syndiotactic polymers are internally compensated. Whether *cis* or *trans* addition occurs in this polymerization could not be established, because of the failure of the polybenzofuran to crystallize. These results show that there is no general rule of *trans* addition in the polymerization of 1,2-disubstituted cyclic monomers. The type of addition obtained is a function of the monomer and perhaps also of the type of initiator.

The polymerization conditions employed in the preparation of the poly-*N*-substituted maleimides do not normally lead to stereoregular polymers. It seems likely that the stereospecificity arises as a result of the geometry of the monomer unit, which requires *trans* opening of the double bonds and leads to the formation of the helix. The influence of a helical conformation of a polymer chain on the mode of propagation has been observed in the polymerization of *N*-carboxy anhydrides to polypeptides²¹. Inspection of models indicates that there is little freedom of rotation of the 3₁ helix, and so when a threo di isotactic sequence occurs, the polymer will probably adopt the helical conformation in solution. It follows that if the rate of isotactic placement preserving the symmetry of the helix is faster than the syndiotactic placements a stereospecific polymerization results²².

The author wishes to thank British Nylon Spinners Ltd for permission to publish this work.

Research Department,
British Nylon Spinners Ltd,
Pontypool, Mon.

(Received January 1965)

REFERENCES

- ¹ U.S. Pat. No. 2 306 918 (29.12.1942)
- ² U.S. Pat. No. 2 669 555 (16.2.1954)

- ³ COLEMAN Jr, L. E. and CONRADY, J. A. *J. Polym. Sci.* 1959, **38**, 241
- ⁴ TAWNEY, P. O., SNYDER, R. H., CONGER, R. P., LEIBBRAND, K. A., STITELER, C. H. and WILLIAMS, A. R. *J. org. Chem.* 1961, **26**, 15
- ⁵ COLEMAN Jr, L. E., BORK, J. F. and DUNN, H. J. *org. Chem.* 1959, **24**, 135
- ⁶ *U.S. Pat. No. 2 444 536* (6.7.1948)
- ⁷ BACON, R. G. R. *Trans. Faraday Soc.* 1946, **42**, 410
- ⁸ LANG, J. L., PAVELICH, W. A. and CLAREY, H. D. *J. Polym. Sci.* 1963, **A1**, 1123
- ⁹ JOSHI, R. M. *Makromol. Chem.* 1963, **62**, 140
- ¹⁰ WILES, D. M. and BYWATER, S. *Polymer, Lond.* 1962, **3**, 175
- ¹¹ BUTLER, K., THOMAS, P. R. and TYLER, G. J. *J. Polym. Sci.* 1960, **48**, 357
- ¹² MILLER, M. L. *J. Polym. Sci.* 1962, **56**, 203
- ¹³ CUBBON, R. C. P. and MARGERISON, D. *Progress in Reaction Kinetics*, Volume III. Ed. PORTER, G. Pergamon: Oxford. In press
- ¹⁴ GOERING, H. L., ABELL, P. I. and AYCOCK, B. F. *J. Amer. chem. Soc.* 1952, **74**, 3588
- ¹⁵ GOERING, H. L. and SIMS, L. L. *J. Amer. chem. Soc.* 1955, **77**, 3465
- ¹⁶ SCHMITT, G. J. and SCHUERCH, C. J. *J. Polym. Sci.* 1961, **49**, 287
- ¹⁷ YAMADA, A., YANAGITA, M. and KOBAYASHI, E. *J. Polym. Sci.* 1962, **61**, S14
- ¹⁸ MOACANIN, J. and REMBAUM, A. *J. Polym. Sci.* 1964, **B2**, 979
- ¹⁹ NATTA, G., DALL'ASTA, G., MAZZANTI, G. and MOTRONI, G. *Makromol. Chem.* 1963, **69**, 163
- ²⁰ NATTA, G., FARINA, M., PERALDO, M. and BRESSAN, G. *Makromol. Chem.* 1961, **43**, 68
- ²¹ IDELSON, M. and BLOUT, E. R. *J. Amer. chem. Soc.* 1958, **80**, 2387
- ²² SZWARC, M. *Chem. & Ind.* 1958, 1589

The Fine Structure of Cotton Fibre as Revealed by Swelling During Methacrylate Embedding

J. DLUGOSZ

Water-swollen cotton fibres, accommodated to the embedding medium by means of a solvent exchange technique, were embedded in a mixture of methyl methacrylate and n-butyl methacrylate and sectioned with a diamond knife. Examination of the sections under the electron microscope showed that the swelling effect of the water on the fibres was subsequently enhanced by an enormous additional swelling that occurred during the polymerization of the embedding medium. This additional swelling is explained by the assumption that the polymerization reaction proceeds in the medium permeating the fibre at a faster rate than in the external medium. In consequence, monomer diffuses from outside into the fibre.

Since the methacrylate embedding technique can disperse the cellulose to a great extent, it provides a suitable method for studying the structure of the cotton fibre.

A GREAT deal of effort goes into attempts to improve the properties of the cotton fibre by various chemical finishing processes. Since reactions designed to introduce crosslinking agents into cellulose proceed via swelling of the cotton, an understanding of the swelling mechanism of the cotton fibre is of great importance to anyone engaged in this field of research. Swelling is intimately connected with the fine structure of the fibre; hence a study of the cotton in the swollen state should shed light on its fine structure.

Although in the past the cotton fibre has been the subject of many studies, it is only recently that the advent of modern microtomes has facilitated a more direct study of its fine structure. Of particular value is the availability of diamond knives with which tough materials like mature cotton fibres can be cut into sections only a hundred or so Ångström units thick. As shown by Rollins, Moore and Tripp¹, not only can the fine structure of unmodified cotton fibre be studied, but it is also possible by suitable techniques to observe the effect of crosslinking reactions.

This paper presents results of the examination of sections of cotton fibre. It will be shown that if fibres are first swollen in water, and then after a suitable solvent exchange embedded in methacrylates, an enormous additional swelling is obtained.

EXPERIMENTAL

Cotton cloth that had been desized, pressure boiled, bleached in sodium hypochlorite and acid washed was cut into small pieces approximately 5 mm × 5 mm. Prior to being embedded, some of the pieces were dried in an oven at 100°C while others were soaked in water at room temperature. The methacrylate embedding was carried out as follows. The monomers, supplied by Imperial Chemical Industries Ltd, were freed from inhibitor by washing in dilute alkali, washing in distilled water, and drying with

anhydrous sodium sulphate. The embedding medium was a 4:1 mixture by volume of *n*-butyl methacrylate and methyl methacrylate catalysed with benzoyl peroxide (approximately two per cent). The oven-dried cotton was placed directly in gelatin capsules containing the embedding medium. The water-swollen cotton was first passed through a series of water-acetone mixtures of ascending concentration of acetone, finishing with pure acetone. The acetone was then replaced with methacrylates by soaking the sample in several changes of the monomers. Finally the sample was placed in the catalysed embedding medium. The polymerization was effected in the oven at temperatures ranging from 50° to 75°C. Embedding was also done in Petri dishes so that the progress of polymerization could be followed with the aid of a low-power optical microscope. Samples both dry and water-swollen were also embedded in Araldite, Durcupan and gelatin according to standard techniques².

Sections were cut on an LKB Ultratome microtome fitted with a diamond knife, collected in the usual way on specimen grids, and examined in the electron microscope. The sections embedded in methacrylates were sometimes subjected to one of the following treatments.

(1) The embedding medium was dissolved from the section by immersing the grid in a suitable solvent, e.g. methyl ethyl ketone, amyl acetate, or amyl alcohol. After several washes in pure solvent the specimen was shadowed by the evaporation *in vacuo* of a platinum-carbon pellet³.

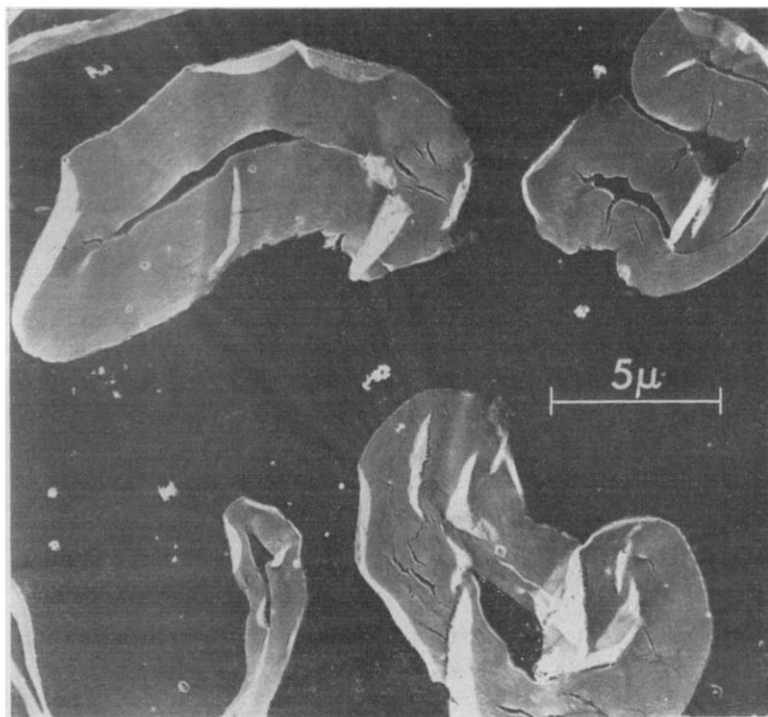


Figure 1—Dry fibres. Cross section shadowed after dissolution of embedding medium. Magnification $\times 4500$; reproduced without reduction

(2) (a) The cellulose was dissolved from the section, leaving the embedding medium intact, by floating the grid, section downwards, on the surface of a solution of cuprammonium hydroxide (supplied by the British Drug Houses Ltd to the British Cotton Industry Research Association's specification⁴). The sections were rinsed first in ammonia, then in a solution of Rochelle salt, and finally in distilled water.

(b) Another way of dissolving the cellulose was by floating the grids on the surface of 72 per cent sulphuric acid, and rinsing in distilled water.

(3) Some sections were stained by floating the grids on the surface of five per cent phosphotungstic acid.

RESULTS

Figure 1 shows a shadowed cross section of the oven-dried fibre embedded in methacrylates. Apart from general contours very little of the fibre structure can be seen in such a section.

However, a cross section of an originally water-swollen fibre embedded in methacrylates after solvent replacement contains a wealth of detail. *Figure 2* shows that the wall of the fibre has separated into concentric layers, or lamellae, of remarkably uniform thickness. The lamellae are seen in the micrograph as discontinuous rings; evidently they are split up.

In *Figure 2* the darker areas correspond to the cellulose and the lighter ones to the embedding medium. That this is so can be proved by treating

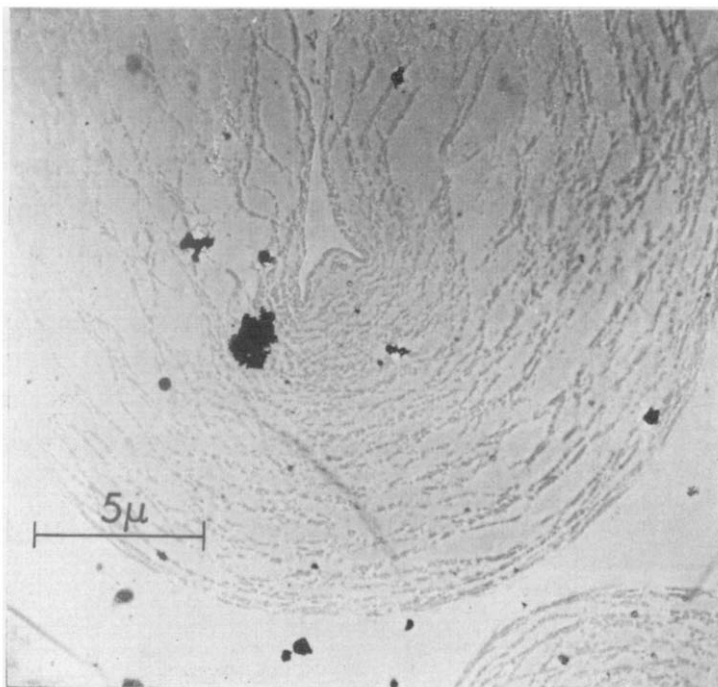


Figure 2—Cross section of a swollen fibre. Magnification $\times 4500$; reproduced without reduction

the sections with solvents. If a section is treated with a solvent for the embedding medium, *Figure 3* results, showing the cotton cellulose. If, however, a solvent for cellulose is used, the resulting electron micrograph (*Figure 4*) shows the embedding medium with many holes; each of these originally contained cellulose. Kling⁵ and co-workers published electron micrographs similar to *Figure 2*, but they mistakenly interpreted the light areas as corresponding to swollen lamellae and the dark areas as representing some noncellulosic interlammellar substances of unspecified chemical composition; hence most of their conclusions are perforce wrong.

Staining the cross sections with phosphotungstic acid reveals that the fibre wall is composed of very thin fibrils which will be called microfibrils. These can be seen in *Figure 5*, which is a micrograph, taken at higher magnification, of such a stained cross section; it shows parts of two lamellae. The thickness of the microfibrils has been estimated to be about 80 Å, although microfibrils having thickness of about 40 Å have also been observed. It is not yet known whether the 80 Å microfibrils eventually split into the thinner 40 Å microfibrils.

Figure 6 shows a shadowed longitudinal section from which the embedding medium has been dissolved. It illustrates how in some regions the dispersion

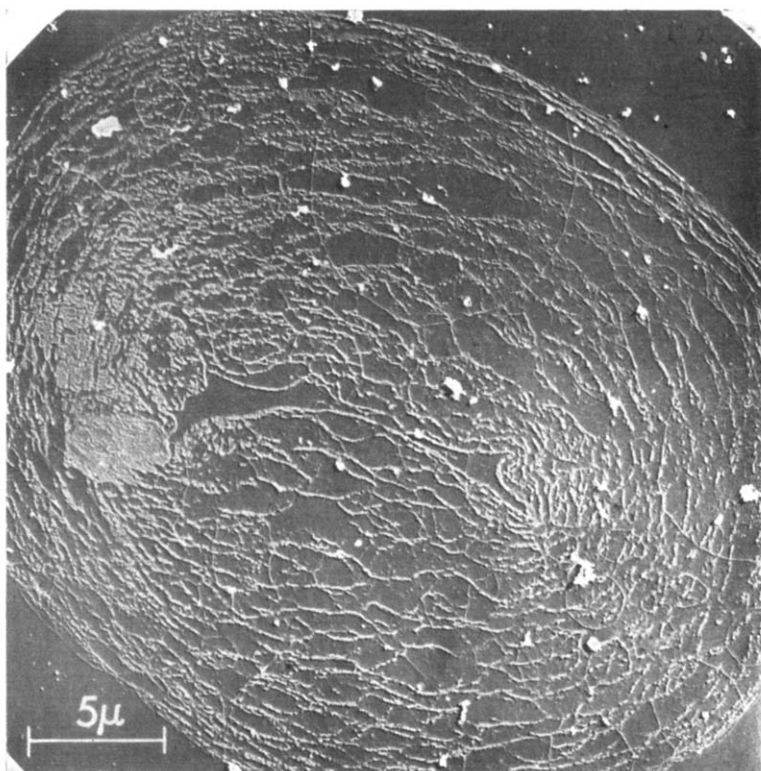


Figure 3—Swollen fibre. Cross section shadowed after dissolution of embedding medium. Magnification $\times 3600$; reproduced without reduction

of cellulose progressed to such an extent that individual microfibrils may be discerned, while in other regions the microfibrils are united to form quite thick bundles.

Fibres recovered by dissolving polymerized embeddings exhibit appearance and properties different from those of ordinary cotton, even after continuous extraction in boiling solvents for three weeks. Even sections as thin as 300 Å cannot be washed completely free from the embedding medium by such extraction. These facts suggest that some grafting, as well as homopolymerization, has taken place.

The dispersed state of the structure, as seen in *Figures 2 to 6*, might at first sight be taken to represent the true structure of the fibre in its water-swollen state, since the water of swelling was replaced by acetone which, in turn, was replaced by embedding medium in the course of preparation of the sections. However, the cross-sectional swelling of the cotton fibre on immersion in water is only about 30 per cent, whereas on embedding it may be as much as 10 000 per cent. This enormous additional swelling occurs only with the methacrylates as the embedding medium; in other media, e.g. in gelatin or epoxy resin, no distension of the fibre structure is observed, the sections having an appearance similar to that shown in *Figure 1*. Thorough pre-swelling in water followed by an efficient solvent replacement is a necessary condition for the occurrence of the phenomenon, which, however, is not due to simple diffusion, since it is not brought

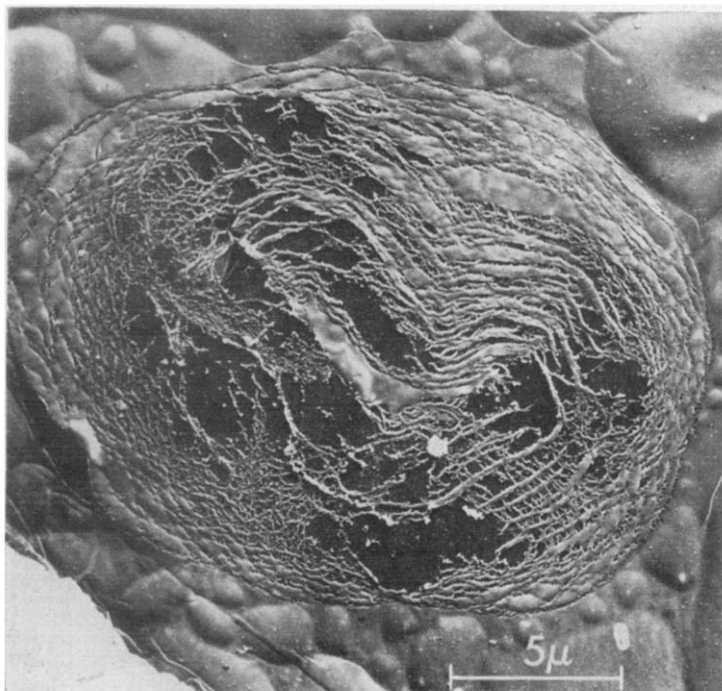


Figure 4—Swollen fibre. Cross section shadowed after dissolution of cellulose. Magnification $\times 4500$; reproduced without reduction

about even by soaking the fibres in methacrylate monomers for several weeks.

It therefore follows that this additional swelling is due to and occurs during the polymerization of the methacrylate embedding medium. It will therefore be called 'polymerization swelling'. In order to follow its progress, the polymerizing preparation was removed from the oven at intervals and examined. It was then observed that the swelling occurred rather rapidly after a period of induction of several hours during which no appreciable swelling could be detected. The appearance of polymerization swelling coincided with a sharp rise in the viscosity of the external medium. This suggests that the polymerization swelling may be connected with the well-known auto-acceleration effect⁶ and may occur by the same mechanism.

DISCUSSION

It is well known that the bulk polymerization of methyl methacrylate proceeds initially as a first-order reaction; at about 25 per cent conversion, when the viscosity of the system increases markedly, the reaction accelerates. The auto-acceleration is believed to be brought about by a decrease in the termination rate caused by the rise in the viscosity of the polymerizing medium. This explanation is supported by the finding of Trommsdorff *et al.*⁷ that the polymerization is hastened if the viscosity of the monomer is increased by the dissolution in it of its (or other) polymer.

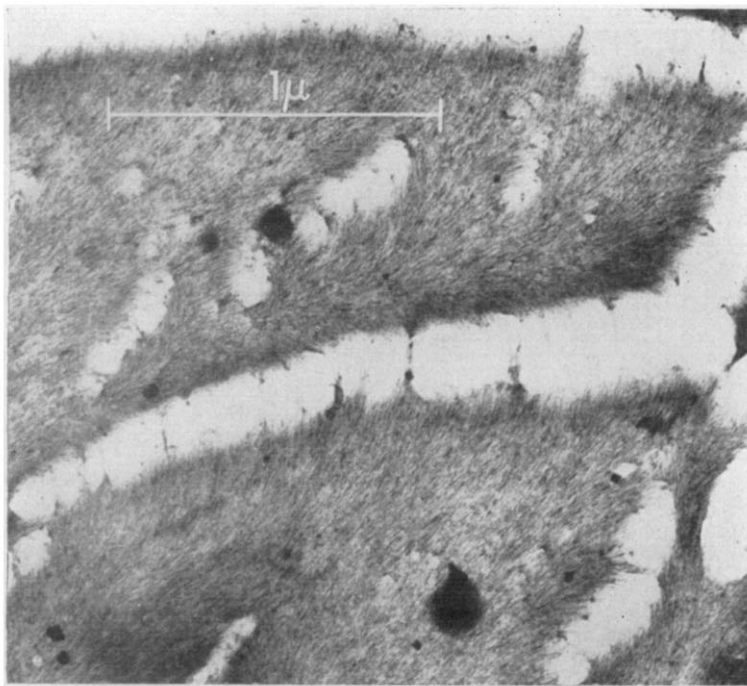


Figure 5—Cross section of a small part of a swollen fibre. Section stained with phosphotungstic acid. Magnification $\times 44\ 000$; reproduced without reduction

THE FINE STRUCTURE OF COTTON FIBRE

Similar conditions exist in the medium permeating the cotton fibre; the presence of cellulose, while not appreciably affecting the reactions of initiation and propagation, impedes chain termination. Movement and growth of a macroradical are restricted to the spaces that were originally accessible to water and are now filled with monomer. A macroradical in the fibre is to some extent isolated from other macroradicals by cellulose; the probability of its colliding and reacting with another macroradical is reduced and hence its lifetime is increased, during which it continues to add on monomer molecules and so grows longer. Thus the rate of polymerization is higher and auto-acceleration occurs earlier than in the external medium.

In a system comprising a cotton fibre impregnated with catalysed methyl methacrylate monomer and immersed in it, the external medium is in communication with the medium in the fibre; during polymerization, therefore, a gradient of concentration of monomer is developed across the boundary of the fibre. Monomer tends to diffuse through the outermost lamella into the medium in the first interlamellar space and to dilute it. This results in a swelling pressure which causes the outermost lamella to expand and to separate from the rest of the fibre. The tension in the

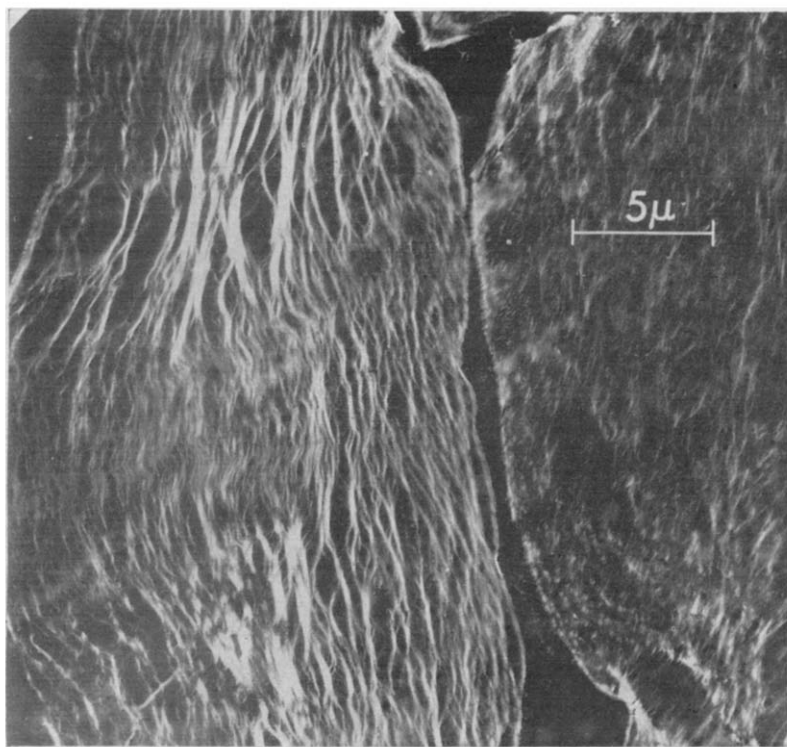


Figure 6—Longitudinal section of a swollen fibre. Section shadowed after dissolution of embedding medium. Magnification $\times 3600$; reproduced without reduction

expanding lamella splits it up. The now open structure of the outermost lamella facilitates the diffusion of monomer. Consequently, a concentration gradient is set up across the second lamella, which, in its turn, expands and splits up. In this way the dispersion of cellulose is propagated, layer by layer, towards the lumen.

Monomer must evidently be driven into the fibre under the influence of a considerable concentration gradient to account for the rapidity with which polymerization swelling is propagated. Continuous removal, by polymerization, of molecules from the diffusing monomer tends to maintain the gradient and swelling of the polymer so generated continues to expand the fibre. The following factors are thought to contribute to this state of affairs.

(1) The medium within the expanding part of the fibre, containing polymer of higher molecular weight and hence being more viscous, polymerizes faster than the external medium.

(2) The restricted mobility of the polymer molecules confined to grow in the spaces that have been opened by swelling the fibre in water may result in the existence of long-lived macroradicals. On being brought into contact with the diffusing monomer, these trapped radicals would resume their polymerization.

(3) The viscoelastic flow of cellulose during polymerization swelling involves first the breaking of van der Waals and hydrogen bonds and, as stress concentrations exceed chemical bond strength, probably the scission of cellulose chains. Now the breaking of primary valence bonds results in the production of free radicals. This additional source of initiation, by further increasing the rate of polymerization, would tend to increase the concentration gradient; the grafted polymer chains, though attached at one end to cellulose, can still participate in the swelling phenomena.

The polymerization swelling occurs some hours after the polymerization reaction has started. Evidently it is only after auto-acceleration has begun in the medium permeating the fibre but before it has done so in the external medium that the concentration gradient, and hence the swelling pressure, may become high enough to disrupt the fibre. The polymerization swelling ceases when, with the onset of auto-acceleration in the external medium, the monomer concentrations within and without the fibre equalize.

It is thus seen that the polymerization swelling is likely to be a complex phenomenon involving diffusion, polymerization, and viscoelastic flow, which taking place simultaneously, determine its progress. For instance, when a piece of cotton fabric rather than a single fibre is embedded, the polymerization swelling is not uniform throughout the sample; only the fibres lying along the edge of the fabric tend to be swollen along their entire length, while in those disposed at right angles to the edge the swelling decreases away from the edge. This is readily explained: just as the presence of cellulose hastens the polymerization in the medium within the fibre, so the presence of the fabric hastens, though to a less extent, the polymerization of the part of the medium that fills inter-fibre spaces. Thus, except at the edges of the fabric, the time is reduced during which the concentrations of monomer in the medium within and without the fibres may differ appreciably.

CONCLUSIONS

It has long been known that biological specimens, when embedded in methacrylates, may suffer serious distortion, which has been called 'polymerization damage' or 'polymerization explosion' because it results in the separation of cells or even in the disruption of the contents of a single cell⁸. Cotton fibres, being so susceptible to this damage and showing it readily, are suitable specimens with which to study the methacrylate embedding method, should such a study be undertaken in an effort to find how to eliminate this damage.

This disruptive tendency of the methacrylate embedding medium is nevertheless found useful in structural studies of materials lacking inherent contrast. The methacrylate embedding technique disperses the structural building units of cellulose to a considerable extent, without at the same time altering their relative positions, and thus provides an exploded view of the fibre, so that its architecture can be studied. In particular, the technique sheds light on the problem of water accessibility; it shows where in the fibre the imbibed water goes. At the same time it reveals the shape and the size of the cellulose crystallites. It is generally understood that the water swelling of cellulose is intercrystalline; the crystalline regions are impermeable to water on account of the very regular van der Waals and hydrogen bonding that arises from the regular arrangement of the molecules. Evidently the microfibrils, the thinnest supermolecular building units into which the fibre splits during polymerization swelling, may be identified as the crystalline regions of cotton cellulose.

The structure of the cotton fibre may therefore be pictured as an array of elastic crystalline microfibrils held together principally by hydrogen bonds formed between the hydroxyl groups residing on the surfaces of microfibrils. This bonding is weak since it is irregular, depending on the degree of perfection with which the microfibrils are aligned with respect to one another; a whole range of bond strengths is thus thought to exist in the inter-microfibrillar spaces. This variable bonding probably accounts for the properties of cotton fibre that are usually ascribed to the so-called amorphous regions of cellulose.

The very strong lateral cohesive forces operating within a microfibril may be either entirely of the secondary type or may, in part at least, be due to primary chemical bonds, i.e. either the cellulose chains are parallel to each other and to the axis of the microfibril, or they form regular folds or spirals. It may prove possible to decide with the aid of the electron microscope which type of molecular arrangements does in fact obtain. Since polymerization swelling is bound to result in the breaking of some of the microfibrils, the examination of the broken ends at sufficiently high magnification may give the answer to this question.

The author is indebted to Mr R. J. E. Cumberbirch and Drs F. E. Holmes and A. R. Urquhart for helpful discussion and criticism of the manuscript.

*The Cotton Silk and Man-made Fibres Research Association,
Shirley Institute, Didsbury, Manchester*

(Received February 1965)

REFERENCES

- ¹ ROLLINS, M. L., MOORE, A. T. and TRIPP, V. W. *Text. Res. J.* 1963, **33**, 117
- ² GLAUERT, M. G. in *Techniques for Electron Microscopy* (Ed. KAY, D.), pp 179-186. Blackwell: Oxford, 1961
- ³ KRANITZ, M. and SEAL, M. *Fifth Internat. Congr. Electron Microscopy, Philadelphia*, FF7 (1962)
- ⁴ CLIBBENS, D. A. and LITTLE, A. H. *J. Text. Inst.* 1936, **27**, T285
- ⁵ KLING, W., LANGNER-IRLE, C. and NEMETSCHKEK, T. *Melliand Textilber.* 1958, **39**, 879
- ⁶ BAMFORD, C. H., BARB, W. G., JENKINS, A. D. and ONYON, P. F. *Kinetics of Vinyl Polymerization by Radical Mechanism*, p 76. Butterworths: London, 1958
- ⁷ TROMMSDORFF, E., KOHLE, E. and LAGELLY, P. *Makromol. Chem.* 1948, **1**, 169
- ⁸ BORYSKO, E. J. *Biophys. Biochem. Cytol.* 1956, **2**, No. 4, suppl. 3

Stress-whitening in High-impact Polystyrenes

C. B. BUCKNALL and R. R. SMITH

The behaviour of high-impact polystyrene under stress is studied by stretching thin films of the polymer on the microscope stage. Both phase-contrast and polarized light microscopy reveal the formation of bands at right angles to the applied stress. These bands are shown to contain oriented polymer and are identified with the crazes observed in untoughened polystyrene. A theory of toughening is proposed which accounts for the temperature dependence of impact strength.

THE fracture of rubber-toughened polystyrene is usually preceded by an opaque whitening of the stressed area. *Figure 1* shows an example of the phenomenon in a tensile specimen which failed at an elongation of 35 per cent. Whitening is first observed at an elongation of about two per cent (i.e. near the yield point) and intensifies as the strain is increased. In impact tests more rapid local whitening takes place near the fracture surface. In both cases the appearance of stress-whitening is associated with the absorption of a large amount of energy: when stress-whitening is suppressed by testing at very high strain rates or at low temperatures both impact strength and breaking elongation fall drastically. The aim of the present paper is to establish the mechanism of energy absorption by investigating the causes of stress-whitening.

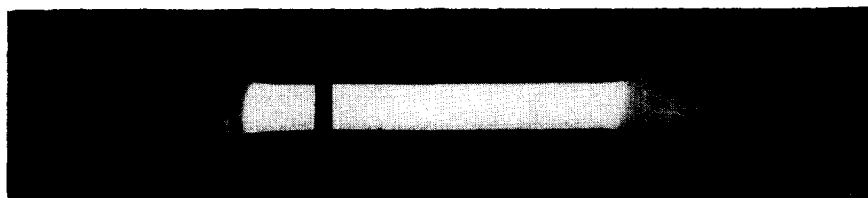


Figure 1—A stress-whitened bar of high-impact polystyrene

Previous theories of toughening attributed the whitening effect to large numbers of small cracks formed at right angles to the applied stress. Merz, Claver and Baer suggested that elongation and energy absorption proceed by the widening of these microcracks and buckling of the polystyrene against the resistance of rubber particles spanning the cracks¹. There is, however, a serious objection to this theory. In unmodified polystyrene the first effect of a tensile stress is not cracking but crazing, and it is difficult to see why crazing should not also precede cracking in toughened polystyrene.

Crazes, or silver cracks, are very similar to void cracks in appearance, but quite different in other respects. The distinction was first made by Sauer, Marin and Hsiao^{2,3}, who pointed out that polystyrene is capable of bearing considerable loads even after crazes have extended across the entire cross section of the specimen. From X-ray diffraction evidence, the high modulus of crazed polystyrene and the failure of fully oriented material to craze when stretched in the orientation direction, they concluded that crazes are composed of oriented polymer interspersed by voids. Similar conclusions were reached by Bessonov and Kuvshinskii⁴, who showed that the interference pattern from a craze does not change on removing the load.

Later workers confirmed these views. Kambour⁵ measured the refractive indices of crazes by the critical angle method and showed they contain about 50 to 60 per cent polymer. Spurr and Niegisch⁶ published electron micrographs of cross sections through crazes which showed conclusively that they contain material in mechanical continuity with surrounding polymer, and Kambour⁷ showed that the voids present are 20 to 200 Å in diameter.

Both the initiation and propagation of crazes are activated. The number of crazes formed in a specimen depends not only on the stress but also on the temperature and time for which it is applied⁶, and the rate of craze propagation increases with temperature in accordance with the Arrhenius equation⁸.

EXPERIMENTAL

Experiments consisted of stretching thin films of toughened polystyrene on a microscope stage and following the changes taking place during stretching by means of polarized light and phase contrast. Polarized light shows up changes in molecular orientation and phase contrast shows up changes in refractive index.

Specimens between 5 and 10 microns thick were microtomed by Traylor's method⁹ from a notched Izod bar to give a section $\frac{1}{2}$ in. square with a notch in the middle of one side. These specimens were warmed in a glycerol bath to release strains introduced during cutting, washed in methanol, and mounted as shown in *Figure 2*.

Specimens were attached to the stretching device by four Sellotape strips and immersed in a glycerol solution of mercuric potassium iodide between two glass cover slips. The refractive index of the solution was 1.59, matching that of polystyrene, so that the rubber particles, which have

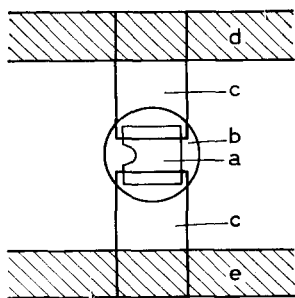


Figure 2—Mounting of specimen in stretching device. (a) the specimen; (b) glass cover slips; (c) Sellotape strips; (d) fixed bar; (e) movable bar

a lower refractive index, were clearly visible in the phase contrast microscope. The stretching device is illustrated in *Figure 3*. It consists of two long bars pivoted at one end and joined at the other end by a screw which can be turned to force the bars apart. One of the bars is fixed to a frame which clips on to the microscope stage. Specimens are mounted halfway between the screw and the pivot with the notch on the same side as the screw so that the greatest stress is applied at the tip of the notch.

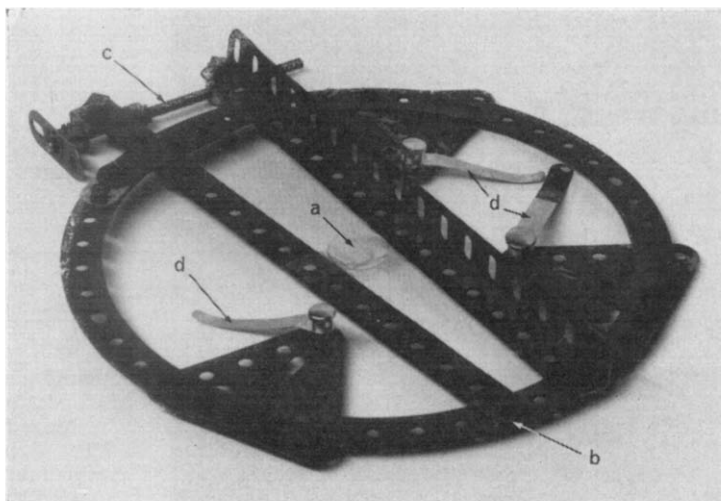


Figure 3—The stretching device: (a) the specimen; (b) pivot; (c) screw; (d) microscope stage clips

RESULTS

When a stress is applied to the specimen by turning the screw, as described above, distinct whitening takes place near the notch. Further stretching causes the whitened area to extend over almost the entire specimen. Finally a tear is initiated at the notch and the specimen fails.

Photomicrographs of a whitened area in the early stages of stretching are shown in *Figure 4*. Under polarized light the prominent feature is a series of parallel bright bands about 50 microns long at right angles to the applied stress. These bands pass through distinct maxima and minima of brightness on rotation of the microscope stage. It is concluded that the bands are birefringent and therefore that they contain oriented molecules.

Bands are observed in identical positions under phase contrast conditions. They are more difficult to see because of the background of rubber particles also made visible by this technique. The bands are light under positive contrast and dark under negative contrast, indicating a reduction in refractive index.

Figure 5 shows the sequence of events in a single area, from first application of stress to final rupture of specimen. Each stage was photographed under both phase contrast and polarized light. The polystyrene used had a

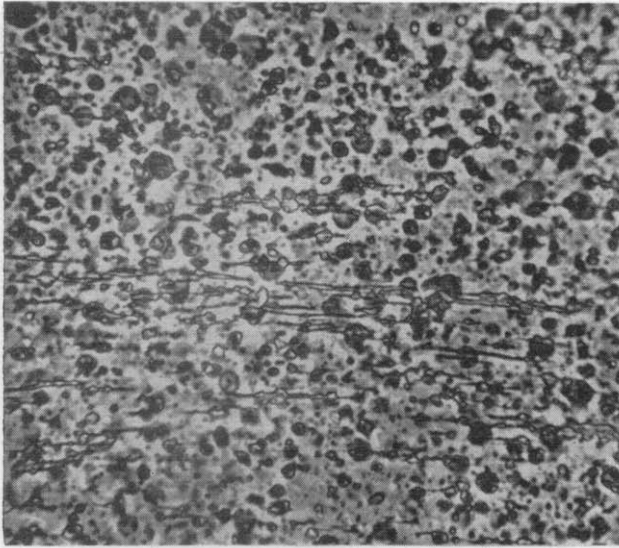
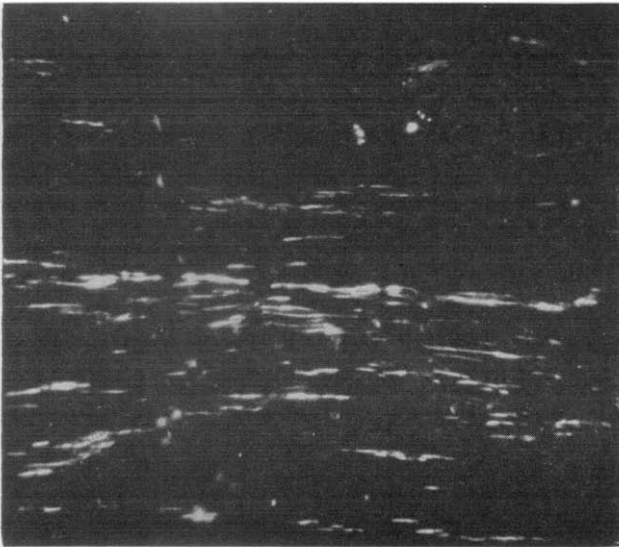


Figure 4 — Photomicrographs of a toughened polystyrene film after stretching in the vertical direction.

Top: negative phase contrast, showing the rubber particles as dark circles.

Bottom: the same area under polarized light. Magnification: $\times 250$. Reproduced without reduction

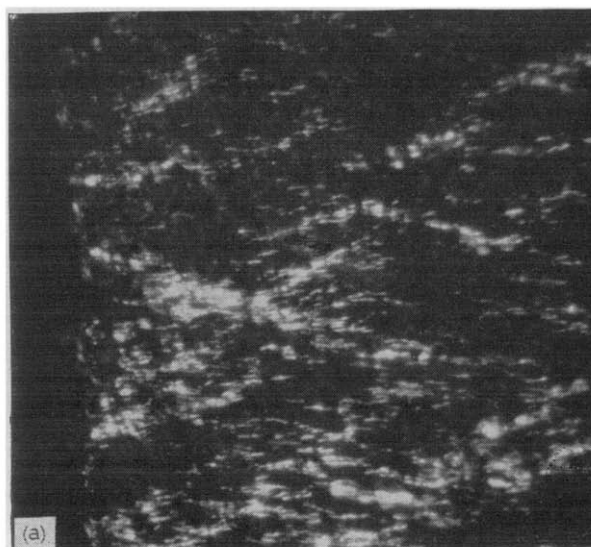
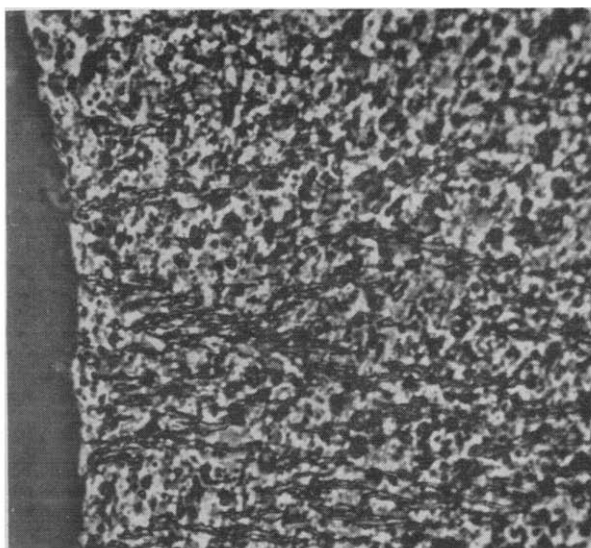


higher rubber content than that shown in *Figure 4* and the bands are correspondingly shorter, the average length being about 10 microns.

The curve of the notch can be seen on the left hand side of each photograph. Two small projections into the notch enable direct measurements of strain to be made. Bands spread from the notch until they cover the major part of the area under study. No void cracks are visible before the specimen begins to break, at an elongation of 45 per cent. The microcrack

Figure 5—Photomicrographs of a toughened polystyrene film during stretching in the vertical direction.

Top: negative phase contrast. Bottom: polarized light. (a) 1 per cent strain. Magnification: $\times 250$. Reproduced without reduction



theory of toughening therefore does not apply to this material even at high elongations. It is interesting to note that the point at which failure finally occurred coincides with the point at which bands first appeared.

Both the stress-whitening and the bands disappear completely on heating. This is useful in eliminating any bands formed accidentally during cutting. Heating the specimen under strain renders the rubber particles faintly visible in polarized light, as dark ellipses against a brighter background of oriented polystyrene. Using a specimen strained in this way an attempt was made to determine the points of origin of the bands in relation to

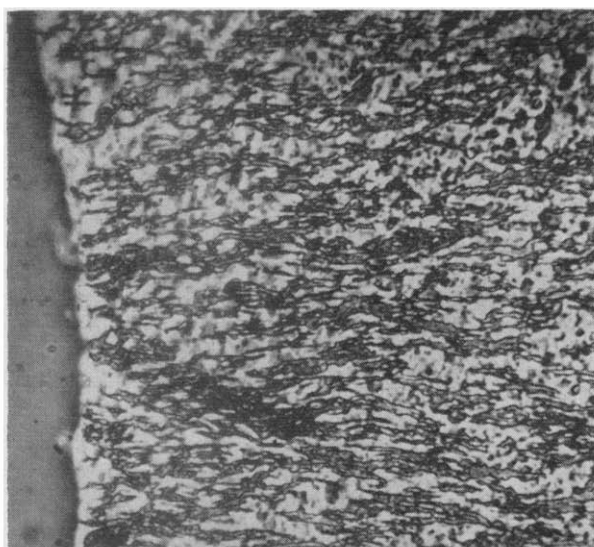
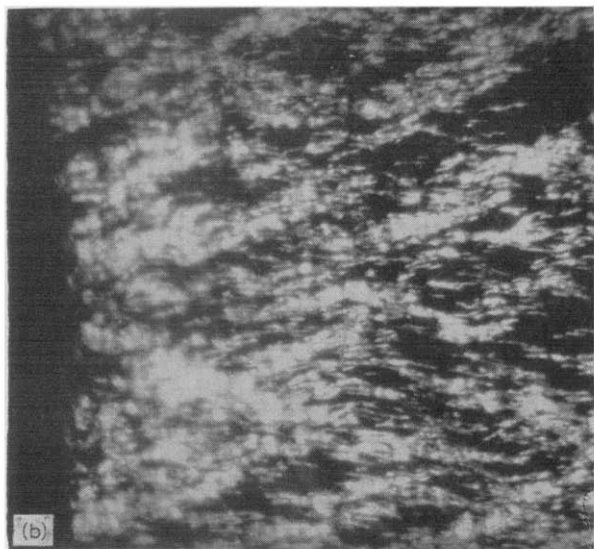


Figure 5—Photomicrographs of a toughened polystyrene film during stretching in the vertical direction.



Top: negative phase contrast. Bottom: polarized light. (b) 10 per cent strain. Magnification: $\times 250$. Reproduced without reduction

the position of the rubber particles. Under phase contrast conditions the rubber particles are too prominent to permit clear observation of the bands.

Although the bands are more prominent under polarized light, the problem remains a difficult one. Bands are formed randomly over the field of view in a fraction of a second. The points of origin appear to be near the rubber/polystyrene interface, but this cannot be regarded as established.

Both the lengthening of existing bands and the establishment of new ones are involved in the extension of the specimen. Both processes proceed intermittently and both continue for some time after the imposition of an

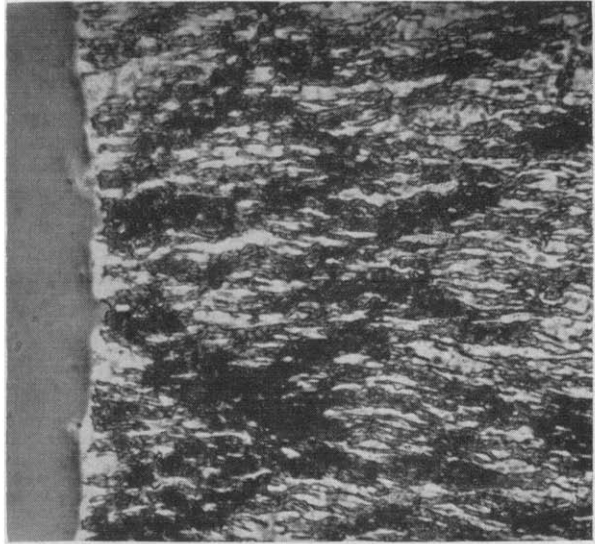
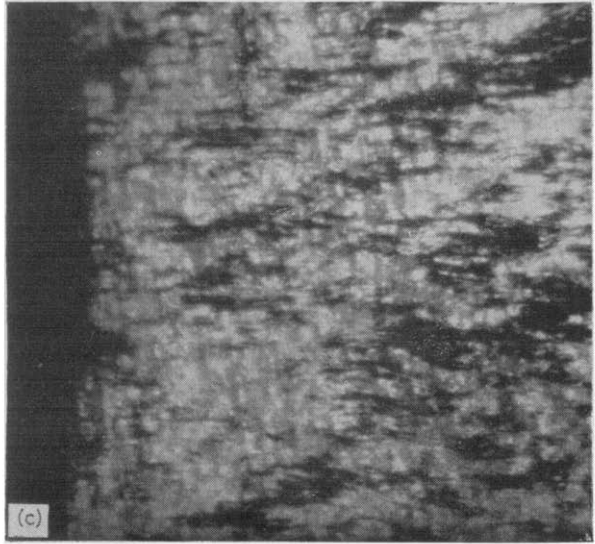


Figure 5—Photomicrographs of a toughened polystyrene film during stretching in the vertical direction.

Top: negative phase contrast. Bottom: polarized light. (c) 44 per cent strain. Magnification: $\times 250$. Reproduced without reduction



added stress, suggesting that they are activated.

DISCUSSION

The bands observed in stress-whitened films of toughened polystyrene are similar in several respects to the crazes formed in unmodified polystyrene under stress. They are birefringent, low in refractive index, capable of bearing load, healed by heat, and formed after an induction period. We therefore conclude that crazing and stress-whitening are simply different aspects of the same phenomenon.

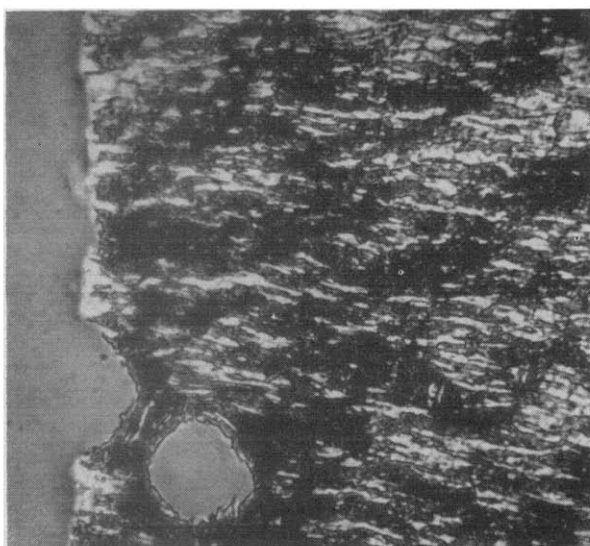
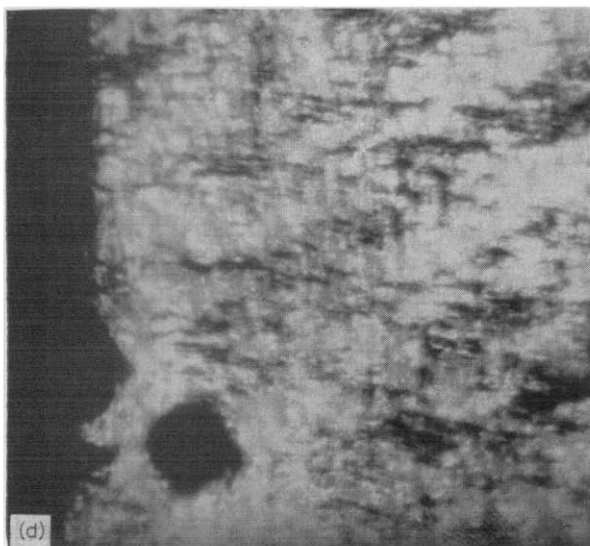


Figure 5—Photomicrographs of a toughened polystyrene film during stretching in the vertical direction.



Top: negative phase contrast. Bottom: polarized light. (d) beginning of failure. Magnification: $\times 250$. Reproduced without reduction

The differences between toughened and untoughened polystyrene lie in the maximum size and concentration of the craze-bands. The decrease in length with increase in rubber content was noted above. In untoughened polystyrene the crazes may be a millimetre or two long. In toughened polystyrene the crazes are much shorter, but the number formed before the specimen fails is very much greater, so that the fraction of material converted into craze matter is considerably higher. This higher conversion into craze matter accounts for the higher breaking elongation of toughened polystyrene. On the assumption that energy is absorbed in forming craze

matter, it also accounts for the higher fracture energy of these materials.

When a stress is applied to toughened polystyrene rapid relaxation takes place in the rubber, provided that it is above its glass temperature, and a non-uniform stress field is set up in the polystyrene. The present work supports the view that crazes are initiated at points of maximum stress concentration. Since neither the relaxation of the rubber nor the initiation of craze bands takes place instantaneously, brittle fracture occurs under conditions of rapid loading, when the stress level reaches a high value before a significant amount of crazing has taken place.

Raising the temperature increases the rates both of stress relaxation in the rubber and of craze initiation and propagation in the polystyrene. This is the most important consequence of the activated nature of crazing. The overall effect on the impact strength of a commercial toughened polystyrene is shown in *Figure 6*. The graph can be divided into three parts: below

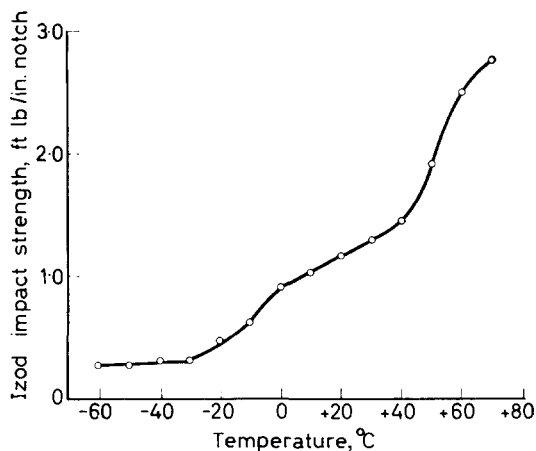


Figure 6—Graph of Izod impact strength against temperature for a toughened polystyrene containing grafted GR-S

-30°C specimens break without stress-whitening at about the same impact strength as untoughened polystyrene; between -30°C and $+40^{\circ}\text{C}$ a small but increasing amount of stress-whitening is observed near the notch, and the impact strength rises steadily; above $+40^{\circ}\text{C}$ dense stress-whitening occurs around the final part of the crack, and both the impact strength and the extent of whitening increase rapidly with temperature. At all temperatures the major part of the energy appears to be absorbed in initiating a crack. Above -30°C local crazing at the base of the notch precedes crack formation, so that a greater deformation of the specimen and therefore an increased input of energy is required to initiate a crack. The immediate cause of this increase is the second-order transition in the rubber between -30° and $+10^{\circ}\text{C}$, but it should be noted that the impact strength continues to increase at temperatures well above this transition range, an effect which is to be expected in view of the activated nature of crazing. The dense stress-whitening occurring above $+40^{\circ}\text{C}$ indicates that at higher temperatures energy is also absorbed in propagating the crack, apparently as a result of decreasing crack velocity. It is planned to cover

this and other points connected with the fracture of toughened polymers more fully in a future paper.

The function of the rubber particles cannot simply be to initiate crazes by providing points of stress concentration. Improving the bond between rubber and polystyrene by grafting is well known to be important in determining the impact resistance of toughened polystyrene, and it is therefore clear that the rubber is required to sustain tensile stress at some stage in the crazing process.

Except at low temperatures tensile failure is likely to occur in the rubber only at high local strains, i.e. after crazing has taken place in the surrounding polystyrene. Kambour has shown that crazing requires the existence of triaxial tensile stresses, which are concentrated near the tip of the craze. These stresses, acting on poorly bonded rubber particles in the path of an advancing craze, probably cause mechanical breakdown at the rubber/resin interface and so generate voids large enough to weaken the structure seriously.

The craze theory of toughening is similar to the microcrack theory in its treatment of the rubber phase but differs from the older theory in its treatment of the polystyrene phase. Three advantages are gained. First, the high breaking elongations of toughened polystyrenes are explained more convincingly. Taking the polymer content of craze matter as 50 per cent, a theoretical maximum elongation of 100 per cent is predicted provided that no necking occurs. Secondly, the variation of impact strength with temperature is explained. Thirdly, a single theory of fracture covers both toughened and untoughened polystyrene. The difference between the two materials lies simply in the amount of craze matter formed before fracture.

The experiments described above were confined to toughened polystyrene, but there is no reason why the conclusions should not apply equally to ABS, toughened PVC or toughened PMMA. All of these materials exhibit stress-whitening, and it would be surprising if the mechanism of whitening and energy absorption were different from that in polystyrene.

The authors thank the directors of Bakelite Xylonite Limited for permission to publish this work.

*Bakelite Xylonite Ltd, Research Station,
Lawford Place, Nr Manningtree, Essex*

(Received February 1965)

REFERENCES

- ¹ MERZ, E. H., CLAVER, G. C. and BAER, M. *J. Polym. Sci.* 1956, **22**, 325
- ² SAUER, J. A., MARIN, J. and HSIAO, C. C. *J. appl. Phys.* 1949, **20**, 507
- ³ HSIAO, C. C. and SAUER, J. A. *J. appl. Phys.* 1950, **21**, 1071
- ⁴ BESSONOV, M. I. and KUVSHINSKII, E. V. *Plast. Massy*, 1961, (5), 57; *Soviet Plastics Engl. Transl.* 1961, (5), 49
- ⁵ KAMBOUR, R. P. *Nature, Lond.* 1962, **195**, 1299
- ⁶ SPURR, O. K. and NIEGISCHE, W. D. *J. appl. Polym. Sci.* 1962, **6**, 585
- ⁷ KAMBOUR, R. P. *Polymer, Lond.* 1964, **5**, 143
- ⁸ STERNSTEIN, S. S. and SIMS, K. J. *Amer. chem. Soc. Polymer Preprints*, 1964, **5**, 422
- ⁹ TRAYLOR, P. A. *Analyt. Chem.* 1961, **33**, 1629

Communication

*Determination of Number-average Molecular Weights of Polyamides in 90 per cent Formic Acid by Thermoelectric Differential Vapour Pressure Lowering**

THE determination of the number-average molecular weights of polymers by thermoelectric differential vapour pressure lowering has recently become practicable by the introduction of commercially available instruments^{1,2}. Its applicability to high polymers has also been demonstrated³.

The two presently available commercial instruments are restricted essentially to non-corrosive solvents which do not react with the material of the vapour chamber. For example, aluminium (used in one of the commercial instruments) is attacked by acids, and to a lesser extent by chloroform, whereas nickel-plated brass (used in another commercial apparatus) is damaged by formic acid.

Many polymers, especially polyamides, readily dissolve in 90 per cent formic acid at room temperature. Although this solvent is widely used for viscosity measurements which are important to the proper characterization of polymers, viscosity data alone do not permit the direct calculation of molecular weights without prior calibration by an absolute method.

The object of this communication is to report the determination of the number-average molecular weights of polyamides in 90 per cent formic acid by thermoelectric differential vapour pressure lowering with a modified version of a commercially available apparatus, and thereby extend the usefulness of this technique.

The basic equipment in this work was the Isothermal Distillation Molecular Weight Apparatus of Arthur H. Thomas Co., Philadelphia, Pennsylvania¹ the vapour chamber of which (originally nickel-plated brass) was gold-plated in our laboratories for use with corrosive solvents.

Commercially available microsyringes were unsatisfactory with formic acid since they invariably dripped and/or leaked, especially when placed inside the warm vapour chamber. Therefore, new drip- and leak-proof precision syringes were designed and fabricated in our laboratories, as described in detail elsewhere⁴.

Poly(terephthaloyl *trans*-2,5-dimethylpiperazine) was prepared by the method of Morgan and Kwolek⁵.

Polycaprolactam (Nylon-6) was a commercial fibre sample from which the finish and delustrant (titanium dioxide) were removed.

The technique used in the determination of number-average molecular

*This work was supported by the Bureau of Naval Weapons, Department of the U.S. Navy, under Contract N0w 62-0604-c.

weights by thermoelectric differential vapour pressure lowering is well known and hence does not require detailed elaboration.

First a calibration curve is established for the solvent using a known substance. In the present work mannitol was chosen. The calibration constant, K ($= 1\,470$ ohm per molal for 90 per cent formic acid), is obtained by plotting the reduced difference in resistance versus the molal concentration of the calibrating compound. A similar plot is obtained with the unknown solution using weight concentrations. From the Clausius-Clapeyron equation, the number-average molecular weight of the unknown can be expressed as

$$M_n = \frac{[\Delta R/m]_{m \rightarrow 0}}{[\Delta R/c]_{c \rightarrow 0}} = \frac{K}{[\Delta R/c]_{c \rightarrow 0}}$$

where ΔR is the change in resistance in ohms, c is the concentration of solute in g/kg of solvent, m is the molal concentration of the calibrating compound, and K is the calibration constant for the solvent.

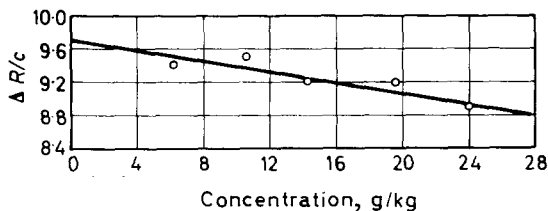


Figure 1—Response curve for tartaric acid in 90 per cent formic acid at 37°C plotted as reduced difference in resistance versus concentration

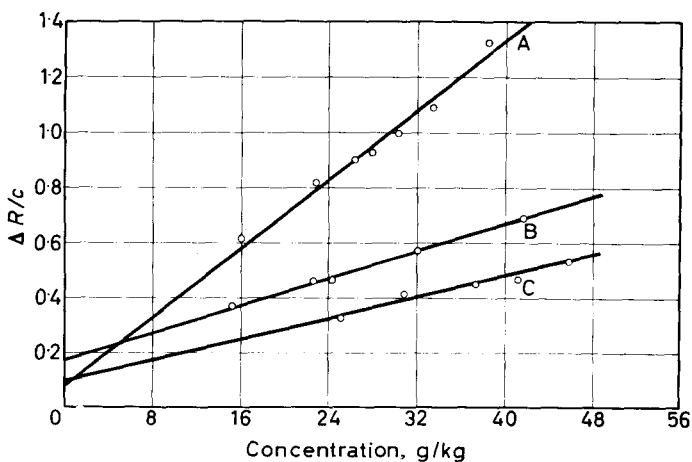


Figure 2—Response curves for: (A) Polycaprolactam; (B) and (C) Poly(terephthaloyl *trans*-2,5-dimethylpiperazine) in 90 per cent formic acid at 37°C plotted as reduced difference in resistance versus concentration

The applicability of 90 per cent formic acid was first determined with tartaric acid. Figure 1 is a plot of the reduced difference in resistance,

$\Delta R/c$, versus concentration. The experimentally determined molecular weight is 151.6 which is within one per cent of the theoretical 150.1. The differential vapour pressure lowering data for one sample of polycaprolactam (Nylon-6) and for two samples of poly(terephthaloyl *trans*-2,5-dimethylpiperazine) are illustrated in *Figure 2*. The calculated number-average molecular weights are in good agreement with those obtained by other methods, as summarized in *Table 1*. No precise data could be obtained at 37°C in 90 per cent formic acid with a sample of poly(terephthaloyl *trans*-2,5-dimethylpiperazine) having a number-average molecular weight of 21 000 because the solubility of the sample limited the preparation of solutions of sufficient concentrations to give proper instrumental response.

Table 1. Molecular weight determinations in 90 per cent formic acid

No.	Solute	Method		Theoretical
		Vapour pressure lowering	End group and viscosity	
1	Polycaprolactam	18 000	19 000	—
2	PDMP*	8 500	9 100	—
3	PDMP	14 600	13 400	—
4	Tartaric acid	151.6	—	150.1

*PDMP denotes poly(terephthaloyl *trans*-2,5-dimethylpiperazine).

The sensitivity of the thermoelectric differential vapour pressure lowering method is inversely related to the heat of vaporization of the solvents⁶. Water, with its high heat of vaporization ($\Delta H_{\text{vap.}} = 575.8$ cal/g at 37°C) is least sensitive, whereas carbon tetrachloride ($\Delta H_{\text{vap.}} \sim 51$ cal/g at 37°C) is among the most sensitive solvents. On the other hand, the calculated heat of vaporization of 90 per cent formic acid at 37°C is approximately 178 cal/g. Despite the presence of water and the corrosive nature of the solvent, precision within one per cent may be obtained with low molecular weight substances, whereas with polyamides having number-average molecular weights of 5 000 to 20 000, accuracy within five to ten per cent is indicated.

Difficulties were experienced with certain other polyamides which were prepared in poor solvents from which the polymer precipitates instantaneously. The number-average molecular weights of some of these polymers as determined by thermoelectric differential vapour pressure lowering were considerably lower than those indicated by end-group analyses and by viscosity measurements. The problem is most likely due to the formation of an excessively large fraction of low molecular weight material during the initial part of the polycondensation which becomes entrapped in the precipitate. In these cases the removal of this low molecular weight fraction from the polymer by dialysis in a suitable solvent is necessary to ensure reasonable molecular weight data by the thermoelectric differential vapour

COMMUNICATION

pressure method. Similar discrepancies were also reported by Morgan and Kwolek⁷ in the number-average molecular weights of 6-10 polyamides prepared by interfacial polycondensation.

The authors thank Mr C. Dixon Smith of the Applied Physics Laboratory of The Johns Hopkins University for his efforts in gold plating the equipment, and Mrs Ardith I. Bailey for typing this manuscript.

S. D. BRUCK

H. E. BAIR

*Applied Physics Laboratory,
The Johns Hopkins University,
8621 Georgia Avenue,
Silver Spring, Maryland, U.S.A.*

(Received March 1965)

REFERENCES

- ¹ Arthur H. Thomas Company, Philadelphia, Pennsylvania, U.S.A. *Bull.* Vol. 1 (No. 3), September 1963
- ² Mechrolab, Inc., Mountain View, California, U.S.A. Series 300 Vapor Pressure Osmometer
- ³ BILLMEYER Jr, F. W. and KOKLE, V. *J. Amer. chem. Soc.* 1964, **86**, 3544
- ⁴ BRUCK, S. D. and RECTOR, R. R. *Rev. sci. Instrum.* 1965, **36**, 239
- ⁵ MORGAN, P. W. and KWOLEK, S. L. *J. Polym. Sci. A*, 1964, **2**, 181
- ⁶ WILSON, A., BINI, L. and HOFSTADER, R. *Analyt. Chem.* 1961, **33**, 135
- ⁷ MORGAN, P. W. and KWOLEK, S. L. *J. Polym. Sci. Part A*, 1963, **1**, 1147

The Effect of pH on the Polymerization of Acrylamide in Water

D. J. CURRIE, F. S. DAINTON and W. S. WATT

The rate constants of propagation (k_p) and mutual termination (k_t) for the free-radical polymerization of acrylamide in water at pH 1, 5.5 and 13 have been measured using cobalt-60 γ -ray initiation and a steel rotating sector. k_p and k_t both diminish by about one order of magnitude as the pH is changed from 1 to 13 and $k_p/k_t^{1/2}$ is almost constant.

THE polymerization of acrylamide in pure water and acidic aqueous solution has been extensively investigated¹⁻⁶, but for various purposes it was necessary to know the dependence on pH of the individual rate constants of propagation, k_p , and mutual termination, k_t . Because of the lack of a photosensitizer which could be used in alkaline solution without contributing directly or indirectly to termination, it was decided to initiate the reaction by irradiation with cobalt-60 γ -rays and to use a recording dilatometer for remote following of the reactions.

EXPERIMENTAL

The cobalt source, dosimetric methods, steel sector and recording dilatometer (capacitance type) have already been described⁷. The methods used for preparation of the solutions, including their de-aeration, the filling of the dilatometers and the purification of the reagent were either identical or closely similar to those used previously¹⁻³.

RESULTS AND DISCUSSION

The following results relate to experiments at 25°C and for which the extent of polymerization was always less than ten per cent:

(i) Using dose-rates, I , of 1.13×10^{17} and 3.54×10^{15} eV l⁻¹ sec⁻¹ the intensity exponent x in the expression $R_p = \alpha I^x$ was found to be 0.49 ± 0.05 and to fit exactly on the curve previously published¹. The ratios of the rates of polymerization at fast sector speeds relative to those in which the γ -rays fall continually on the dilatometer confirmed this value which was unaffected by changing the pH of the solution in the range 1 to 13.

(ii) The rate of polymerization at constant dose-rate and pH was proportional to monomer concentration in the range 3.0 to 0.7 M. At natural pH and below a concentration of 0.7 the rate was approximately proportional to $[m_1]^{1.3}$. Since an exponent of unity is found for photo-chemical initiation², the fractional exponent must be due to the different nature of the chain initiation process when γ -rays are used. We attribute it to the ability of acrylamide in the concentration range 0.05 to 0.6 M to scavenge primary species produced in the water radiolysis which would otherwise largely revert to water. Evidence for this kind of effect has become increasingly available. Solutes other than acrylamide can behave in this

way in this concentration range, notably hydrion, hydroxide ion and nitrous oxide⁸. The consequence of this effect is that G_i , the number of polymerization chains initiated per 100 eV energy absorbed by solution at the natural pH=5.5, will increase in the lower concentration range from a value $G_H + G_e + G_{OH} \approx 5.2$ at $[m_1]=0.05$ M to a limiting value of about 7.5 at $[m_1] \geq 0.7$ M, thus giving an apparent monomer exponent greater than unity. At pH 1 and 13, H^+ or OH^- ions are present in sufficient concentration to ensure that the number of initiating species available to react with the monomer is already at a high level. We conclude therefore that the correct rate equation is $R_p = (G_i I / k_t)^{1/2} k_p [m_1]$ with $G_i \approx 7.5$ for pH 1 and pH 13 and 7 and 7.5 at pH 5.5 and $[m_1]=0.2$ and 0.4 respectively. The values of $k_p/k_t^{1/2}$ obtained in this way are shown in *Table 1*.

(iii) The results of a typical set of sector experiments at pH 5.5 are shown in *Figure 1* and comparable sets were obtained for pH 1 (perchloric acid) and pH 13 (sodium hydroxide) at 0.2 and 0.4 M monomer concentrations,

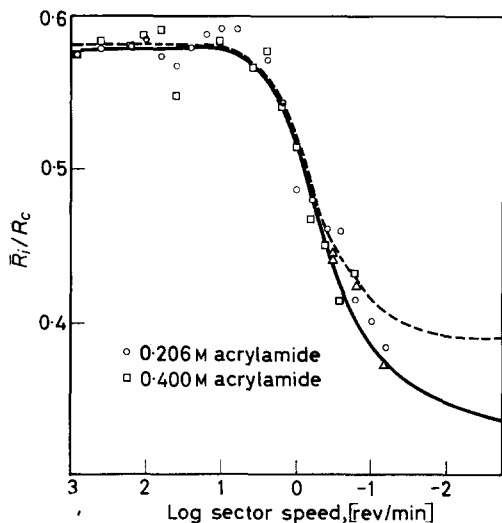


Figure 1—A typical sector curve for solutions containing 0.206 M and 0.400 M acrylamide at pH 5.5 and 25°C using a 1 in 3 sector. \bar{R}_i is the average rate of polymerization under intermittent irradiation and R_c the rate of polymerization under continual irradiation at the same distance from the source. The triangles are data obtained when penumbra errors were minimized by manual control. The full line represents theory for no penetration of steel sector by γ -rays and the broken line the theoretical curve for 0.6 per cent transmission

at the same dose-rate. To obtain the chain lifetimes, τ , the data in each set were fitted to a theoretical curve⁹ which allowed for the fact that 0.6 per cent of the γ -ray beam was transmitted through the steel of the sector thereby causing the rate with the sector in the 'closed' position to be 8 per cent of that with it open. The contraction versus time traces were linear at high sector speeds but at very low sector speeds the effect of individual pulses of radiation could be seen in the form of discontinuities in these traces. To minimize 'penumbra' error¹⁰ at very low irradiation times some experiments (indicated by triangles in *Figure 1*) were carried out in which the sector was not in constant slow revolution but rotated rapidly between the 'open' and 'closed' positions and vice-versa.

(iv) A post-irradiation polymerization is expected in this system^{1,2}. At pH 1 and 5.5 this amounted to < 2 per cent of the rate of the radiation-induced reactions. At pH 13 this post-effect was entirely absent, in agreement with the previously expressed view that this effect is associated with the

THE EFFECT OF pH ON POLYMERIZATION OF ACRYLAMIDE IN WATER

partial imidization of the growing polymer chains², a process which is known to be acid catalysed and therefore likely to be suppressed in alkaline solution.

The values of $k_p/k_t^{\frac{1}{2}}$, k_t [$=(\tau^2 G_i I)^{-1}$] and k_p are shown in *Table 1*. Those at pH 1 are in excellent accord with the values (shown in parentheses)

Table 1. $k_p/k_t^{\frac{1}{2}}$, k_t and k_p for acrylamide in water

pH	1	5.5	13
$k_p/k_t^{\frac{1}{2}}, M^{-\frac{1}{2}} sec^{-\frac{1}{2}}$	4.2 ± 0.2 (4.7 ± 0.5)	3.3 ± 0.3	4.0 ± 0.5
$k_t \times 10^{-6}, M^{-1} sec^{-1}$	16.3 ± 0.7 (14.5 ± 2.0)	3.3 ± 0.6	1.0 ± 0.2
$k_p \times 10^{-4}, M^{-1} sec^{-1}$	1.72 ± 0.3 (1.8 ± 0.15)	0.6 ± 0.1	0.4 ± 0.1

obtained by Dainton and Tordoff² referring to a 0.12 M perchloric acid medium. Evidently $k_p/k_t^{\frac{1}{2}}$ is relatively insensitive to changes of pH but both k_p and k_t diminish as the pH is increased, in contrast to the sharp change which is found in the polymerization of methacrylic acid¹¹. It may be that these effects are connected with the hydrolysis of the amide group which is known to occur in alkaline media and which may cause the growing polymer radical to acquire increasing amounts of negative charge as the pH is increased. The development of this charge may influence k_p and k_t either by increasing electrostatic repulsion between growing radicals or by altering the flexibility, configuration and mobility of the radicals in the polar solvent.

We thank the Rockefeller Foundation for the provision of the cobalt source; General Electric Research for the award of a scholarship to D.J.C. and D.S.I.R. for a studentship awarded to W.S.W.

*Department of Physical Chemistry,
The University,
Leeds, 2*

(Received February 1965)

REFERENCES

- ¹ COLLINSON, E., DAINTON, F. S. and MCNAUGHTON, G. S. *Trans. Faraday Soc.* 1957, **53**, 476 and 489
- ² DAINTON, F. S. and TORDOFF, M. *Trans. Faraday Soc.* 1957, **53**, 499 and 666
- ³ ARMSTRONG, D. A., COLLINSON, E. and DAINTON, F. S. *Trans. Faraday Soc.* 1959, **55**, 1375
- ⁴ TRUDEL, G. J. *Ph.D. Thesis* University of Leeds, 1959
- ⁵ SMITH, D. R. *Ph.D. Thesis* University of Leeds, 1961
- ⁶ ZAHIR, S. *Ph.D. Thesis* University of Leeds, 1960
- ⁷ COLEBOURNE, N., COLLINSON, E., CURRIE, D. J. and DAINTON, F. S. *Trans. Faraday Soc.* 1963, **59**, 1357
- ⁸ DAINTON, F. S. and WATT, W. S. *Proc. Roy. Soc. A*, 1963, **275**, 447
- ⁹ DAINTON, F. S. and LOGAN, S. R. *Trans. Faraday Soc.* 1965, **61**, 715
- ¹⁰ MELVILLE, H. W. and BURNETT, G. M. *Technique of Organic Chemistry*, Vol. VIII, p 133. (Edited by A. WEISSBERGER.) Interscience: New York, 1953
- ¹¹ BURNS, W. G. and DAINTON, F. S. *Trans. Faraday Soc.* 1950, **46**, 411
- ¹² KATCHALSKY, E. and BLAUER, G. *Trans. Faraday Soc.* 1951, **47**, 1360
- ¹³ BLAUER, G. *Trans. Faraday Soc.* 1960, **56**, 606

The Composition and Temperature Dependence of Polymer–Solvent Interaction Parameters

D. PATTERSON and S. N. BHATTACHARYYA

The contribution of free-volume changes on mixing to polymer–solvent interaction parameters is discussed in terms of a corresponding states approach to the configurational thermodynamic properties of oligomers and their mixtures. Expressions for κ and χ are derived in a form identical with the empirical expansions in ϕ_2 proposed by Flory, Orfino and others. The observed qualitative feature of an increase of κ and χ with polymer concentration is predicted as well as the temperature dependence of these parameters which, as shown by the presence of the Lower Critical Solution Temperature in polymer solutions, does not agree with predictions of most current theories.

MOST theories of the thermodynamics of non-dilute polymer solutions (e.g. the Flory–Huggins theory) are extensions of the theory of regular solutions of spherical molecules, the combinatorial factor in the partition function being re-evaluated to allow for the different sizes of polymer and solvent molecules. The remainder of the partition function, which leads to the ‘interaction’ parameters κ and χ , is taken over essentially unchanged from regular solution theory, a contact between a solvent molecule and a polymer segment being assumed similar to one between two spherical molecules. This feature in the Flory–Huggins theory leads to κ and χ independent of concentration. It is found, however, that these parameters usually vary markedly throughout the entire concentration range even for simple non-polar systems*: (1) κ increases with increasing polymer volume fraction, ϕ_2 , as shown by calorimetric studies of the following systems: polyisobutylene(PIB)–benzene^{2a}, –toluene^{2a}, –chlorobenzene^{2a}, –heptane^{2b}, polydimethylsiloxane–benzene^{2c}, natural rubber–benzene^{2d}. (2) As found from osmotic and vapour pressure studies, χ is constant or even decreasing for a few systems: natural rubber–benzene^{2d}, polystyrene–toluene^{3a}, polyethylene–heptane^{3b} at 109°C. However, χ usually increases with ϕ_2 : PIB–benzene^{4a, b}, polyisobutylene of high molecular weight–pentane^{4c}, polybutadiene–benzene^{4b}, polydimethylsiloxane–benzene^{2c}, polystyrene–cyclohexane^{4d, e}. Furthermore, it is well known that coexistence curves are usually too ‘flat’ and the critical concentration too high as compared with Flory theory predictions, and these features may be explained⁵ by assuming an increasing value of χ . (3) The entropy of dilution usually appears considerably lower than the Flory–Huggins value at low concentrations, but

*After completing the manuscript we noticed the extensive review article, reference 21, on the variation of these parameters which contains most of the references cited here as well as others to heats found from the temperature variation of the free energy and for polar systems.

approaches it at high concentrations, or even becomes greater as in the well-known rubber-benzene system.

The variation of κ and χ has been described^{4,6} through the following Flory-Orofino empirical equations for the heat and the non-combinatorial part of the free energy of dilution:

$$\Delta\bar{H}_1/RT = \sum_{i=1}^{\infty} \kappa_i \phi_2^{i+1} = \kappa \phi_2^2 \quad (1)$$

$$\Delta\bar{G}_1(\text{non-comb.})/RT = \sum_{i=1}^{\infty} \chi_i \phi_2^{i+1} = \chi \phi_2^2 = \Delta\mu_1/RT \quad (2)$$

the combinatorial contribution being the well-known

$$\Delta\bar{G}_1(\text{comb.})/RT = \ln(1 - \phi_2) + (1 - 1/r) \phi_2 \quad (3)$$

The Flory-Huggins theory gives no reason for the existence of a non-combinatorial contribution to the entropy

$$\begin{aligned} \Delta\bar{S}_1(\text{non-comb.})/RT &= \sum_{i=1}^{\infty} (\kappa_i - \chi_i) \phi_2^{i+1} \\ &= \sum_{i=1}^{\infty} [\psi_i - 1/(i+1)] \phi_2^{i+1} \end{aligned} \quad (4)$$

and the unexplained experimental findings¹⁻³ may be roughly summarized as:

$$\kappa_2 > 0; \quad \chi_2 > 0; \quad \psi_1 - \frac{1}{2} < 0; \quad \psi_2 - \frac{1}{3} > 0 \quad (5)$$

The usual polymer solution thermodynamics predicts neither the Lower Critical Solution Temperature (LCST) found in polymer solutions⁷ nor the correct temperature dependence of χ and κ which must be: (1) χ decreases with T increasing, rising again as the LCST is approached⁴. (2) The dependence of κ has not been adequately investigated, but from the temperature dependence of χ it must decrease with increase of T becoming negative somewhere below the LCST. The temperature dependence of χ and κ shows that the non-combinatorial contribution to $\Delta\bar{S}$, becomes more and more negative as T increases, and it is this negative contribution to the entropy of mixing which brings about the LCST. A more complete theory⁸ gives at least a qualitative prediction⁹ of the temperature dependence, and we apply it here to the related composition dependence of the interaction parameters.

PRIGOGINE POLYMER SOLUTION THERMODYNAMICS

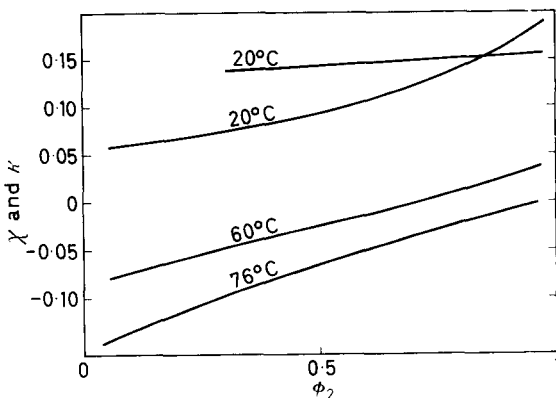
The excess heat and the excess non-combinatorial free energy of a polymer solution contain⁹ two contributions: the first, I, is due to the difference in (a) force fields (δ factor), and (b) sizes (ρ factor) between a polymer segment and a solvent molecule or solvent segment. The second, II, arises from changes of volume and hence 'free volume' of the component liquids on mixing and is of particular importance when the components are composed of molecules of different chain lengths, hence most of all in polymer solutions. During the mixing process the free volume changes of the polymer and the solvent are opposite in sign. Conceivably the total V^E could be zero although the contribution II would still exist. Thus this effect is

improperly treated by the usual correction to constant volume of results at constant pressure.

Effects I(b) and II are treated for the first time by the Prigogine theory⁸, which may be used in full generality (the average potential corresponding state theory, requiring for its application considerable thermodynamic information about polymer and solvent), or one may make use of a special form of the theory obtained by assuming a cell model for the solution. The latter approach was used for the discussion⁹⁻¹¹ of certain polymer-solvent systems, and the new contribution II is apparently dominant when the 'chemical' difference between polymer and solvent is small, for instance in the PIB-alkane systems, or *a fortiori* in systems containing polydimethylsiloxane and an oligomer of dimethylsiloxane. The cell model successfully predicts, *inter alia*, the LCST⁹ and, qualitatively, the correct temperature dependence of κ , χ and ψ .

The relative importance of contribution II led us to examine¹² the thermodynamics of mixtures of normal alkanes of widely differing chain lengths. These might serve as models not only of polyethylene-alkane systems but also of systems where small chemical differences between polymer and solvent exist. Both the composition and temperature dependence of the excess functions of *n*-alkane mixtures do in fact display the same 'polymer solution behaviour' as described in relations (5). Thus Figure 1 shows the variation of κ for the C₆-C₁₆ system at three tempera-

Figure 1— κ (lower curves) and χ (upper curve) versus ϕ_2 for hexane-hexadecane



tures as calculated from excess heat data of McGlashan and Morcom¹³ and Holleman¹⁴, C₁₆ being the 'polymer', and of χ at 20°, using data of McGlashan and Williamson¹⁵. At concentrations less (greater) than that at the 'crossover' of χ and κ , the entropy of dilution is less (greater) than the Flory-Huggins value. There is a very satisfactory body of thermodynamic information for the *n*-alkanes so that the average potential theory⁸ can be applied. Actually, however, a modification due essentially to Hijmans¹⁶ was used, and it was found that contribution II alone qualitatively explained the excess functions and their observed dependences, including now that on the concentration. Contribution I, in this case the effect of different end and middle segments, could be ignored in a qualitative treat-

ment and the whole of the thermodynamic parameters associated with changes of free volume on mixing molecules of different lengths. We now examine the effect of these changes on the composition and temperature dependence of κ and χ in polymer solutions generally. Since we are more interested in the significance of these dependences than in a quantitative fit of experimental data, the contribution I is ignored ($\delta, \rho=0$).

DERIVATION OF THE FLORY-OROFINO EXPRESSIONS

Hijmans¹⁶ used a corresponding states principle to treat the configurational thermodynamic quantities of a homologous series of linear chain molecule liquids characterized by a molecular length parameter n , which could be the number of atoms in the chain backbone. Thus

$$U(T, n) = U_0(n) \times U^*(T^*) \quad (6)$$

$$S(T, n) = S_0(n) \times S^*(T^*) \quad (7)$$

$$C_p(T, n) = S_0(n) \times C_p^*(T^*) \quad (8)$$

$$V(T, n) = V_0(n) \times V^*(T^*) \quad (9)$$

Here the starred reduced quantities are functions of the reduced temperature given by:

$$T^* = T/T_0; \quad T_0 = U_0(n)/S_0(n) \quad (10)$$

and the reduction parameters with subscript 0 are functions only of n . As n increases, T^* decreases, approaching an asymptotic limit for the infinite polymer. T^* may be considered as a measure of the free volume. The role of the segment is played by a spherical reference molecule characterized by energy and distance interaction constants ε and σ ; three 'effective numbers of segments' are defined:

$$U_0(n) = N\varepsilon q \quad (11)$$

$$S_0(n) = Nkc \quad (12)$$

$$V_0(n) = N\sigma^3 r \quad (13)$$

c gives the number of external degrees of freedom of the molecule, and r and q have the usual polymer solution meanings. Thus $q \simeq r$, and in a lattice model, for infinite coordination number¹,

$$z \rightarrow \infty, \quad q \rightarrow r \quad (14)$$

A polymer series is predicted to follow the corresponding states principle provided it fulfils certain plausible conditions⁸. V/T data for a variety of oligomers and polymers can in fact be put in reduced form¹⁷. The same is true for configurational energies of the n -alkanes¹⁶, but the configurational C_p only roughly fulfilled the principle¹² and only qualitative agreement between predicted excess functions and experiment was obtained¹². The following treatment must thus be considered as speculative and the predictions of qualitative, rather than quantitative, significance.

Consider two members of the homologous series n_1 and n_2 with $n_2 \gg n_1$, so that 2 may be taken to be the polymer and 1 the solvent; n_1 might equal

unity. An example of such a simple solution would be polyethylene in an *n*-alkane solvent or, possibly, PIB-*n*-alkane. Each liquid and, by assumption, the mixture, follows equations 6 to 9. For the mixture¹²

$$U(T) = \langle U_0 \rangle \times U^*(\langle T^* \rangle) \quad (15)$$

where

$$\langle U_0 \rangle = x_1 U_{0,1}(n_1) + x_2 U_{0,2}(n_2) \quad (16)$$

$$\langle T^* \rangle = \langle U_0 \rangle / \langle S_0 \rangle = X_1 T_1^* + X_2 T_2^* \quad (17)$$

or

$$\langle T^* \rangle - T_1^* = X_2 (T_2^* - T_1^*) \quad (18)$$

and

$$X_2 = x_2 U_{0,2}(n_2) / \langle U_0 \rangle \quad (19)$$

It is evident from equation 11 that X_2 is the surface fraction⁸ of polymer which becomes the volume fraction when $z \rightarrow \infty$

$$X_2 \rightarrow \phi_2 \quad (20)$$

The molar excess heat at 1 atm is given by

$$H^E \simeq U^E = \langle U_0 \rangle U^*(\langle T^* \rangle) - x_1 U_{0,1}(n_1) U^*\{T_1^*(n_1)\} - x_2 U_{0,2}(n_2) U^*\{T_2^*(n_2)\} \quad (21)$$

The heat of dilution of the solution is found using

$$\Delta \bar{H}_1 = H^E - x_2 \partial H^E / \partial x_2 \quad (22)$$

Performing the differentiation and using equations 15 to 19, one finds

$$\Delta \bar{H}_1 = U_{0,1} [U^*(\langle T^* \rangle) - U^*(T_1^*) + X_2 (T_1^* - T_2^*) \partial U^*(\langle T^* \rangle) / \partial \langle T^* \rangle] \quad (23)$$

The identical form of the Flory-Orofino equation 1 may be obtained by (a) expanding $U^*(\langle T^* \rangle)$ and $\partial U^*(\langle T^* \rangle) / \partial \langle T^* \rangle$ around $U^*(T_1^*)$ and $\partial U^*(T_1^*) / \partial T_1^*$, using equation 18, and (b) replacing X_2 by ϕ_2 through assumption 20. We have finally

$$\kappa_i = \frac{(-1)^i i}{(i+1)!} \left(\frac{U_{0,1}}{RT} \right) (T_1^* - T_2^*)^{i+1} \frac{\partial^i C_p^*(T_1^*)}{\partial T_1^{*i}} \quad (24)$$

In practice, however, one does not obtain the parameters U_0 , S_0 , etc., directly; rather one finds¹⁶ ratios of these parameters to those for a reference homologue, R , e.g. $U_{0,1}/U_{0,R}$. For the alkanes the reference homologue was heptane. Similarly, the reduced quantities are found multiplied by the corresponding reduction parameter of R . Equation 24 can be rewritten to involve only these experimentally accessible quantities:

$$\kappa_i = (-1)^i B_i (T_1^* T_{0,R})^i \frac{\partial^i \{C_p^*(T_1^*) S_{0,R}\}}{\partial \{T_1^* T_{0,R}\}^i} \quad (25)$$

with

$$B_i = \frac{i}{(i+1)!} \frac{S_{0,1}/S_{0,R}}{R} \left(1 - \frac{T_{0,1}/T_{0,R}}{T_{0,2}/T_{0,R}} \right)^{i+1} \quad (26)$$

where B_i is a positive constant for any 1-2 pair, which may be evaluated, at least for the alkanes, from data in ref. 16.

We may also set up an expression analogous to equation 21 but with $G_{(\text{non-comb.})}$ replacing H .

$$\begin{aligned} \Delta \overline{G}_1(\text{non-comb.}) &\simeq \Delta \overline{F}_1(\text{non-comb.}) = \Delta \mu_1(\text{non-comb.}) \\ &= U_{0,1} [F^*(\langle T^* \rangle) - F^*(T_1^*)] \\ &\quad + X_2 (T_1^* - T_2^*) \partial F^*(\langle T^* \rangle) / \partial \langle T^* \rangle \end{aligned} \quad (27)$$

The differentiations throughout keep P^* constant.

Then, equation 2 is found with

$$\chi_i = (-1)^{i-1} B_i (T_1^* T_{0,R})^i \partial^{i-1} \{C_p^* S_{0,R} / T_1^* T_{0,R}\} / \partial (T_1^* T_{0,R})^{i-1} \quad (28)$$

One may verify that equation 28 gives equation 25 through the Gibbs-Helmholtz relation

$$\kappa_i = -T \partial \chi_i / \partial T$$

It may be also noted that the single curve of C_p^* versus T^* gives both the temperature and concentration dependence of the thermodynamic parameters, because changes of both composition and temperature are expressed by a change of reduced temperature. It is of interest to write κ_i and χ_i in terms of thermodynamic data for a particular solvent. The first two parameters are:

$$\kappa_1 = - \frac{(1 - T_{0,1}/T_{0,2})^2}{2R} T \frac{\partial C_p}{\partial T} \quad (29)$$

$$\kappa_2 = \frac{(1 - T_{0,1}/T_{0,2})^3}{3R} T^2 \frac{\partial^2 C_p}{\partial T^2} \quad (30)$$

$$\chi_1 = \frac{(1 - T_{0,1}/T_{0,2})^2}{2R} C_p \quad (31)$$

$$\chi_2 = - \frac{(1 - T_{0,1}/T_{0,2})^3}{3R} T^2 \frac{\partial C_p / T}{\partial T} \quad (32)$$

SIGNS AND MAGNITUDES OF κ_i AND χ_i

(a) Cell theories

The cell model has been used by Prigogine and his collaborators in two forms: a model using a smoothed potential whose depth depends on the liquid volume and intermolecular distance according to a 6-12 law, and a harmonic potential model. Both models predict a reduced heat capacity which is linear in reduced temperature at lower reduced temperatures, and then goes off to infinity presumably as the critical point is approached. In the lower temperature range¹²

$$C_p^* S_{0,R} = \frac{21 \cdot 0}{z} \frac{S_{0,R}}{U_{0,R}} (T^* T_{0,R}) \quad (33)$$

and hence equation 25 shows that only the κ_1 , χ_1 and ψ_1 exist. They are:

$$2\chi_1 = -2\kappa_1 = (\frac{1}{2} - \psi_1) = (21 \cdot 0 / z^2) (T / r_1) \quad (34)$$

as given in the synopsis of ref. 9 if $\delta, \rho = 0$. The non-combinatorial contribution to the entropy and heat is thus negative and to the free energy, positive. Although the temperature dependence of the parameters is qualitatively correct⁹, the prediction of composition-independent κ and χ is certainly generally invalid. At higher temperatures the positive curvature of the reduced heat capacity gives $\kappa_2 > 0$, $\chi_2 < 0$ with $\kappa_1 < 0$.

(b) *Corresponding states theory*

On the other hand, experimental data¹⁸ show that in reality the configurational heat capacity for polyatomic liquids can at first decrease with increasing T and pass through a minimum before rising again, going to infinity at the critical point. Using heptane as the reference alkane we show in Figure 2 $C_p^*S_0(T)$ versus $T_1^*T_0(T)$ obtained from heats of vaporization

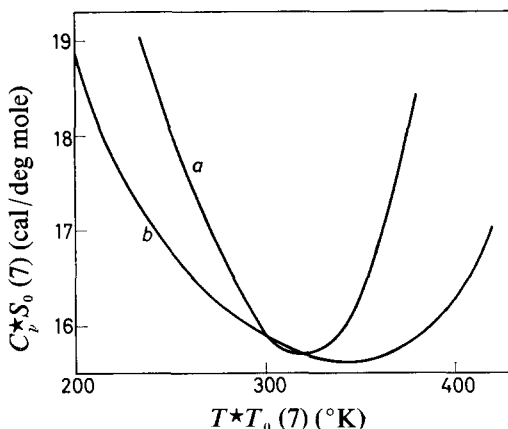


Figure 2—Reduced configurational heat capacity versus reduced temperature (a) curve from heats of vaporization (b) curve for heptane from gas and liquid heat capacities

of the alkanes from C_3 to C_{16} at 25°C and at their normal boiling points, as described in ref. 12, and used there to predict the thermodynamics of n -alkane mixtures. Also shown are the data for heptane obtained¹² from heat capacities of liquid and gaseous heptane. Since $R=7$, $T_1^*T_0(T)$ and $C_p^*S_0(T)$ are in fact just the experimental temperature and configurational heat capacity for heptane. Although the corresponding states principle is not totally obeyed for the alkanes (as shown by the lack of coincidence of the two curves; also see ref. 12), it appears that:

$$\begin{aligned}
 C_p^*S_0(T) &> 0 \\
 \partial C_p^*S_0(T) / \partial T_1^*T_0(T) &< 0 \text{ at low } T \\
 &> 0 \text{ at high } T \\
 \partial^2 C_p^*S_0(T) / \partial^2 T_1^*T_0(T) &> 0
 \end{aligned} \tag{35}$$

The signs of higher derivatives are uncertain.

It is likely that other homologous series besides the n -alkanes will behave as in relations 35 rather than follow the cell model predictions, possibly if¹² the molecules have rotational isomers as for the alkanes (*trans* and

gauche forms). The relations 35 lead to a qualitative prediction that the composition dependence of the parameters is as given by conditions 5. Thus from relations 35 and equations 25 or 29 and 30, it is clear that at low temperature $\kappa_1 > 0$; $\kappa_2 > 0$ while higher κ_i are uncertain. At high temperatures, $\kappa_1 < 0$; $\kappa_2 > 0$. Using relations 35 and equation 28 for the χ_i , one finds that χ_1 , χ_2 and χ_3 are all positive at lower temperatures, while at higher temperatures only χ_1 can be said with certainty to be positive. From equation 28 or 31 χ_1 follows C_p^* or C_p and thus decreases with increasing temperature attaining a minimum, and then increases. Comparison of the predicted composition and temperature dependence with that observed as given in relations 5 is good, and convinces us of the qualitative validity of the approach.

Table 1. Temperature dependence of parameters

$T, ^\circ K$	κ_1	κ_2	χ_1	χ_2	ψ_1	ψ_2
300	+0.3	1.7	0.85	0.4	-0.1	1.6
330	-0.28	2.6	0.84	0.2	-0.5	2.7
350	-0.9	3.2	0.88	0.0	-1.3	3.5

In Table 1 we show the calculated magnitudes of the parameters at various temperatures using equation 25 for a model polymer solution: an alkane of infinite molecular weight in heptane. An analytical expression for $U^*U_0(T)$ in terms of $T^*T_0(T)$ is given in ref. 12 and hence $C_p^*S_0(T)$ and its derivatives are found. $S_{0,1}/S_{0,R} = T_{0,1}/T_{0,R} = 1$ since $R=7$. Both $U_0(n)/U_0(T)$ and $S_0(n)/S_0(T)$ are linear functions of n (see ref. 16) so that their ratio $T_0(n)/T_0(T)$ may be extrapolated to give $T_{0,2}/T_{0,R}$ for the required infinite alkane. $\Delta\bar{H}_1$ and $\Delta\bar{G}_1$ may be found from equations 23 and 27 and so κ and χ can be calculated. These parameters are plotted in Figure 3 as functions of ϕ_2 ; values cannot be found at the higher concen-

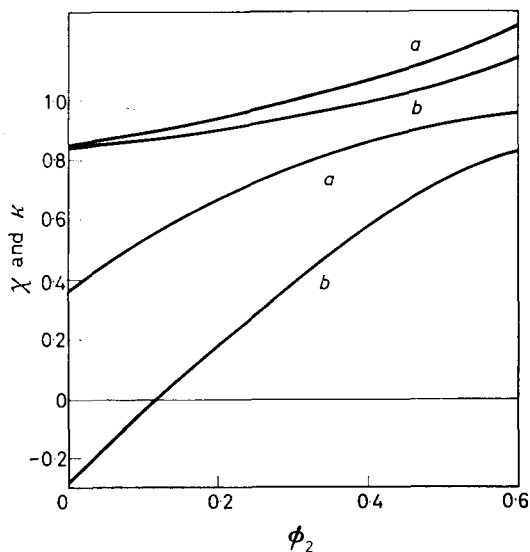


Figure 3— κ (lower curves) and χ (upper curves) versus ϕ_2 for polyethylene - heptane: (a) 300°K, (b) 330°K

trations since they correspond to U^*U_0 (7) data at reduced temperatures lower than those available from ref. 12.

The above values are presented to give a qualitative picture only. In particular, χ_1 is predicted much too large. The same feature was found in our treatment of *n*-alkane mixtures, where due to this incorrect prediction χ remained larger than κ throughout the composition range (as here) and hence with increase of ϕ_2 , $\Delta\bar{S}_1$ was predicted to remain less than the Flory value, in disagreement with *Figure 1*.

Contribution II with δ , $\rho \neq 0$ might be introduced as was done in the cell model treatment⁹. However, the mathematical complexity is greatly increased and the effect seems to be mainly on κ_1 and χ_1 ; it seems inappropriate to introduce these new parameters in the present discussion.

In our treatment the higher κ_i and χ_i arise through the role played by free volume changes in the non-combinatorial part of the partition function. On the other hand, this part has been accepted traditionally as adequate, and the κ_i and χ_i are supposed to compensate for an error in the combinatorial factor arising from the Flory-Huggins assumption of random mixing, or neglect of correlations between probabilities of occupation of lattice sites by polymer segments. Improvements have been made using the cell model by taking into account short-range correlations (Huggins-Miller-Guggenheim theory¹); the desired increase of κ and χ may be obtained by making z unrealistically small, ~ 3 to 5. The necessity of this small effective value of z may be explained at least qualitatively by taking into account long-range correlations¹⁹ which seem to give a possible treatment of the κ and χ dependence on composition. However, an approximate extension²⁰ to concentrated solutions of the theory of dilute and (hence non-homogeneous) solutions suggests that κ and χ should be independent of ϕ_2 above very moderate concentrations. The complete explanation of the higher κ_i and χ_i may combine various effects, including that of non-homogeneity of the solution and that of a possible order in the pure polymeric liquid²¹. One justification of our adding another effect to the discussion may be that the free volume approach seems to predict both the composition and the temperature dependence of κ and χ .

Part of the work for this article was completed at the University of Montreal, and was supported by the Paint Research Institute of the Federation of Societies for Paint Technology, whose aid is gratefully acknowledged.

*Centre de Recherches sur les Macromolécules,
Strasbourg, France
Indian Association for the Cultivation of Science,
Calcutta, India*

(Received February 1965)

REFERENCES

- ¹ TOMPA, H. *Polymer Solutions*, Ch. 4. Butterworths: London, 1956
^{2a} SENEZ, M. and DAoust, H. *Canad. J. Chem.* 1962, **40**, 734

- ^{2b} SENEZ, M. *Ph.D. Thesis*, University of Montreal, 1961
- ^c NEWING, M. J. *Trans. Faraday Soc.* 1950, **46**, 613
- ^d GEE, G. and ORR, W. J. C. *Trans. Faraday Soc.* 1946, **42**, 507
- ^{3a} BAWN, C. E. H., FREEMAN, R. F. J. and KAMALIDDIN, A. R. *Trans. Faraday Soc.* 1950, **46**, 677
- ^b VAN DER WAALS, J. and HERMANS, J. J. *Rec. Trav. chim. Pays-Bas*, 1950, **69**, 971
- ^{4a} FLORY, J. and DAOUST, H. J. *Polym. Sci.* 1957, **25**, 429
- BAWN, C. E. H. and PATEL, R. D. *Trans. Faraday Soc.* 1956, **52**, 1664
- ^b JESSUP, R. S. J. *Res. Nat. Bur. Stand.* 1958, **60**, 47
- ⁻ BAKER, C. H., BROWN, W. B., GEE, G., ROWLINSON, J. S., STUBLEY, D. and YEADON, R. E. *Polymer, Lond.* 1962, **3**, 215
- ^d KRIGBAUM, W. R. and GEYMER, D. A. J. *Amer. chem. Soc.* 1959, **81**, 1959
- ^o REHAGE, G. and MEYS, H. J. *Polym. Sci.* 1958, **30**, 271
- ⁵ Ref. 1, p 177
- ⁶ OROFINO, T. A. and FLORY, P. J. *J. chem. Phys.* 1957, **26**, 1067
- ⁷ FREEMAN, P. I. and ROWLINSON, J. S. *Polymer, Lond.* 1959, **1**, 20
- ⁸ PRIGOGINE, I. (with the collaboration of BELLEMANS, A. and MATHOT, V.). *The Molecular Theory of Solutions*, Chs. 16 and 17. North Holland Publishing Co.: Amsterdam, 1957
- ⁹ DELMAS, G., PATTERSON, D. and SOMCYNKY, T. J. *Polym. Sci.* 1962, **57**, 79
- ¹⁰ DELMAS, G., PATTERSON, D. and BOHME, D. *Trans. Faraday Soc.* 1962, **58**, 2116
- ¹¹ BATAILLE, P. and PATTERSON, D. J. *Polym. Sci.* 1963, **A1**, 3265
- ¹² BHATTACHARYYA, S. N., PATTERSON, D. and SOMCYNKY, T. *Physica, 's Grav.*, 1964, **30**, 1276
- ¹³ MCGLASHAN, M. L. and MORCOM, K. W. *Trans. Faraday Soc.* 1961, **59**, 581
- ¹⁴ HOLLEMAN, T. *Thesis*, University of Amsterdam, 1964
- ¹⁵ MCGLASHAN, M. L. and WILLIAMSON, A. G. *Trans. Faraday Soc.* 1961, **57**, 588
- ¹⁶ HIJMANS, J. *Physica, 's Grav.* 1962, **27**, 433
- ¹⁷ SIMHA, R. and HAVLIK, A. J. *J. Amer. chem. Soc.* 1964, **86**, 197
- ¹⁸ ROWLINSON, J. S. *Liquids and Liquid Mixtures*, Figure 8.4. Butterworths: London, 1959
- ¹⁹ KURATA, M. *Ann. N.Y. Acad. Sci.* 1961, **89**, 635
- STAVERMAN, A. J. *Rec. Trav. chim. Pays-Bas*, 1950, **69**, 163
- ²⁰ FIXMAN, M. J. *J. chem. Phys.* 1961, **35**, 889
- ²¹ BOOTH, C., GEE, G., JONES, M. N. and TAYLOR, W. D. *Polymer, Lond.* 1964, **5**, 353

The Structure of the Gamma Form of Polycaproamide (Nylon 6)

E. M. BRADBURY*, L. BROWN†, A. ELLIOTT‡ and D. A. D. PARRY‡

The X-ray diffraction pattern of the gamma form of polycaproamide (Nylon 6) has been photographed from oriented fibres treated with aqueous hydriodic acid from which the iodine was subsequently removed in a solution of sodium thiosulphate. Reciprocal space coordinates and relative intensities have been measured. A model for the structure is proposed in which hydrogen bonds between parallel (like-directed) chains form sheets of molecules, with a random variation of chain sense from sheet to sheet. Very good agreement between the X-ray reflection intensities calculated for this model and the observed ones is found. The model predicts a layer line streak, which is also observed. Anisotropic temperature factors are found necessary.

POLYCAPROAMIDE (Nylon 6) $[\text{NH}(\text{CH}_2)_5\text{CO}]_n$ is known to exist in at least two well-marked crystalline forms. The better-known α form has been investigated by Holmes, Bunn and Smith¹ who find that the polymer has a sheet structure of alternately directed fully extended chains connected by hydrogen bonds ('antiparallel sheet'). Alternate sheets are displaced along the chain axis, an arrangement which gives four chains in a monoclinic unit cell. Holmes *et al.* found evidence of a second modification which they called the β form, and suggested that the difference between the two forms was in the packing arrangement of the chains.

New experimental evidence on the polymorphism of Nylon 6 was obtained by Ueda and Kimura² and by Tsuruda, Arimoto and Ishibashi³, who showed that when oriented fibres of Nylon 6 are treated with aqueous potassium iodide containing iodine (the iodine being subsequently removed by means of a solution of sodium thiosulphate) a new form is obtained without loss of orientation. This, the γ form, has been shown by Kinoshita⁴ to be characterized by a somewhat contracted chain repeat length, compared with the fully extended form. It occurs in other polyamides. Kinoshita suggested that the hydrogen bonds in the γ form were formed between *parallel* chains, and that a tilting of the amide groups occurred in order to form a linear hydrogen bond. In consequence, the chains were somewhat contracted. The nature of the γ form has been well established by Kinoshita⁵ in polyheptamethylene pimelamide (Nylon 7), where the positions of the atoms have been determined by X-ray crystallographic methods.

The structure of the γ form in Nylon 6 has recently been examined by Vogelsohn⁶, using X-ray diffraction. He concludes that the γ form (obtained by iodine treatment) is identical with the β form of Holmes, Bunn and Smith which occurs (usually as a minor component) in melt-spun specimens. We are in agreement with this conclusion. Although the term ' β ' was used

*Physics Department, Portsmouth College of Technology

†Acetate & Synthetic Fibres Laboratory, Courtaulds Ltd, Coventry

‡Biophysics Department, 26-29, Drury Lane, King's College, London W.C.2

earlier than ' γ ', we propose to use the latter designation because it is used in most of the literature on the structure of this form, and it would be confusing now to use the historically more correct one.

The unit cell of γ Nylon 6, deduced from the X-ray diffraction pattern, has sometimes been described as hexagonal or pseudo-hexagonal, the implication being that there is only one chain passing through the unit cell, and Vogelsong's two alternative structures are based on this premise. He does, however, state that there is some distortion from the rhombohedral symmetry which he adopts, but treats it as having a negligible effect on the Fourier transform of the molecule. In the two structures which he gives, all chains are parallel, and no attempt is made to reconcile this with the fact that the γ form is derived, without loss of orientation, from the α form in which the crystallites contain equal numbers of oppositely directed chains. In one of his structures, hydrogen-bonded sheets are formed. In the other, regarded as the one which more closely approximates to the actual structure, the hydrogen bonds alternate between the 100 and 010 planes, and this would lead to a hexagonally shaped unit cell. It is noted that, in the other structure (all hydrogen bonds along 100) an anisotropic thermal expansion would be expected, and so some reflections should be resolved at a suitable temperature. The fact that this was not seen in observations made up to the melting point is regarded as evidence against the structure. As will be described later, we have in fact found the expected splitting, not on raising but on lowering the temperature. For some time we have been examining the i.r. spectra and the X-ray diffraction patterns of the Nylon 6 structures and have published our view that essentially the unit cell in the γ form is orthorhombic in shape (Bradbury and Elliott⁷) with

$$\begin{aligned}a &= 4.82 \text{ \AA} \\b &= 7.82 \text{ \AA} \\c &= 16.70 \text{ \AA (fibre axis)}\end{aligned}$$

Arimoto⁸ has described experiments with doubly oriented Nylon 6. X-ray diffraction and measurement with polarized i.r. radiation show convincingly that in the α form the NH and C=O bonds lie approximately in the plane of the rolled specimen. When the specimen is treated with iodine (subsequently removed) to obtain the γ form, these same bonds are perpendicular rather than parallel to the rolled plane. This shows that there is a preferred plane in which the hydrogen bonds are formed, and is not compatible with Vogelsong's structure in which the hydrogen bonds are equally divided between two planes at 60°. Arimoto proposes a structure for the γ form with hydrogen-bonded sheets of parallel chains, with the chain direction alternating from sheet to sheet. This regular form is discussed below.

The measurements and considerations which lead us to propose a different structure from either of Vogelsong's (though with a chain conformation similar to his structure with all hydrogen bonds along 100) will now be described. Our structure also differs from that of Arimoto.

EXPERIMENTAL

Specimen preparation

Drawn Nylon 6 fibres were immersed in hydriodic acid to which 20 per

cent of iodine had been added, and after some hours the iodine was removed in an aqueous solution of sodium thiosulphate. It was found easier to remove iodine when hydriodic acid was used than with aqueous potassium iodide. The fibres were treated whilst held taut.

The X-ray diffraction photographs from which the unit cell dimensions were measured were taken in 3 cm and in 5.73 cm cylindrical cameras; when necessary, tilted fibres were used (for the higher order layer lines). Photographs were taken at various temperatures up to 190°C and down to -125°C. As might be expected, some of the changes observed were not completely reversible. The distribution of intensity of the diffraction pattern was little changed (see, however, below) and the dimensional changes could be attributed, in the main, to changes in the intermolecular distances. Though clearly not identical, the corresponding structures under the various conditions appear to be sufficiently alike to be given the common designation ' γ '. Measurements of the x and y coordinates on the films were made using a measuring machine with a cross-slide in which a no-parallax setting device was used in place of a microscope (Elliott and Dickson⁹). Reciprocal space coordinates were calculated directly, this being in our opinion a more satisfactory method than using a Bernal chart, if high accuracy is required. Since the unit cell is nearly hexagonal in cross section, high accuracy is required for indexing the reflections.

Measurements of relative intensities were made by photometering the arcs on cylindrical films in a radial direction on a Joyce-Loebl microdensitometer. The areas under the curves were measured, and these are referred to subsequently as I_{obs} . For the 00 l reflections, the same procedure was not appropriate, and the relative intensities were measured on a diffractometer. These intensities were then scaled so that, when the observed and calculated intensities for the whole diffraction pattern were compared, the best fit was obtained.

The measurement of the two strongest reflections, 110 and 020 presented some difficulty, for these are so much stronger than the other reflections on cylindrical films that the densitometer cannot accurately span the gap in optical density. Recourse was had to a camera in which the film is curved to a circular cone of semi-angle 45°, used with a toroidal reflecting system (Elliott¹⁰). The geometry of the conical camera is such as to favour reflections of high Bragg angle, and this made measurement of the 110, 020 and 026 reflections possible on the same film. This arrangement was not available at the time when most of the measurements were made, otherwise the whole diffraction pattern would have been photographed in this way.

The corrections to be applied to density measurements of fibre photographs for disorientation etc. have recently been examined in some detail by Dr Struther Arnott, who has kindly allowed us to make use of his calculations. The details are given in the Appendix. The corrections to be made are: (1) Lorentz factor, (2) Polarization factor, (3) Disorientation factor, (4) Temperature factor, (5) Specimen to spot distance factor, (6) Obliquity of incidence on film, (7) Microdensitometer trace factor, and (8) Scale factor. The combined Lorentz, polarization and disorientation factor for non-meridional reflections, by which the observed intensities are to be multiplied, is

$$\frac{\rho (-\rho^4/4 + \rho^2 \cos^2 \mu + \rho^2 \zeta \sin \mu - \zeta^2)^{\frac{1}{2}}}{2 - \rho^2 + \rho^4/4}$$

where μ is the angle of tilt of the specimen, $\zeta = \lambda l/c$ and

$$\rho = \lambda \{h^2/a^2 + k^2/b^2 + l^2/c^2\}^{\frac{1}{2}}$$

For meridional reflections, the corresponding factor is

$$\mathbf{k} \frac{\sin^2 \theta \cos \theta}{(2 - \rho^2 + \rho^4/4)^{\frac{1}{2}}}$$

where \mathbf{k} is a scale factor (to be determined either from powder photographs of an unoriented specimen or by comparison of the observed and calculated intensities. The latter method was used).

The temperature factor used was an anisotropic one, as is discussed in the section on the verification of the structure.

For cylindrical films the specimen-to-spot distance varies only if the displacement of the spot from the 000 reflection has a component in a direction parallel to the cylindrical axis. If this component is z , the integrated optical density is multiplied by the factor $(R^2 + z^2)^{\frac{1}{2}}$, where R is the camera radius.

These factors correct data obtained with cameras of different radii. Corrections 6 and 7 were small and were not applied. The latter arises from the fact that with films taken on a cylindrical camera the microdensitometer trace is not in general normal to the arc on the photograph. These corrections (valid for tilted fibres as well as for those normal to the X-ray beam) when applied to integrated optical density measurements appear to eliminate the most serious errors in measuring relative structure amplitudes from fibre photographs.

The unit cell

As will appear later, we believe that there is no crystallographic unit cell, only a statistical one. Most of the reflections can be indexed with a near-hexagonal cell, and photographs of fibres which have been annealed at 190°C and then cooled to room temperature (the procedure adopted by Vogelsong) show that these fibres are nearer to the hexagonal shape than those which have not been so treated. They are, however, decidedly not hexagonal or pseudo-hexagonal; the 110 and 020 reflections (indexed for the orthorhombic cell given above) are clearly separated in *Figure 4(b)*. There is, moreover, a decided sharpening of the $h00$ compared with other reflections showing at once that the order in the a axis direction is increased by annealing, and suggesting that this may be the direction of the hydrogen bonds. The strong, sharp 200 spot is easily seen in *Figure 4(b)*. The annealed specimens do not have any reflections which require a unit cell with two chains passing through it, and a monoclinic cell with one chain would suffice. However, the dimensions are such that two adjacent sides together with the shorter diagonal form an isosceles triangle, and this is reminiscent of an orthorhombic arrangement. To prevent confusion, the indexing in this paper is that appropriate to the larger, orthorhombic-shaped unit cell even when no reflections appear which require this larger cell.

STRUCTURE OF THE GAMMA FORM OF POLYCAPROAMIDE (NYLON 6)

Specimens which have not been annealed show the weak 101 and very weak 103 reflections of the orthorhombic cell, which disappear on heating. The former may be seen on an unheated specimen photographed at -125°C [Figure 1(a)] where the departure from hexagonality is very marked. The very strong 111 and 021 reflections are clearly separated. The orthorhombic shape remains, however. Even when these reflections cannot be resolved,

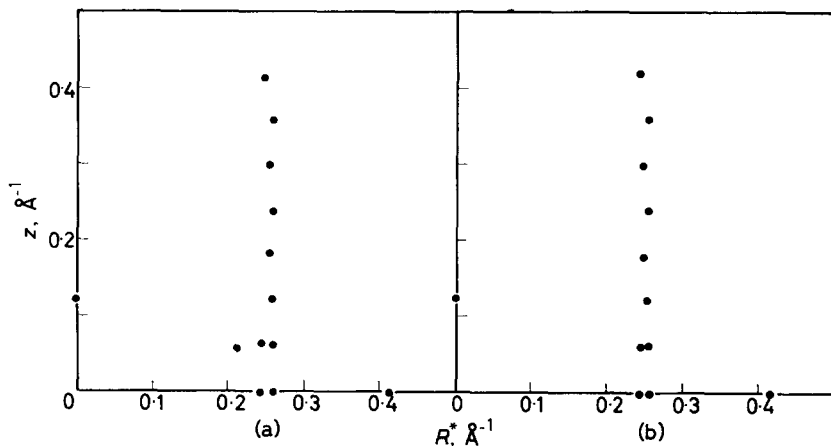
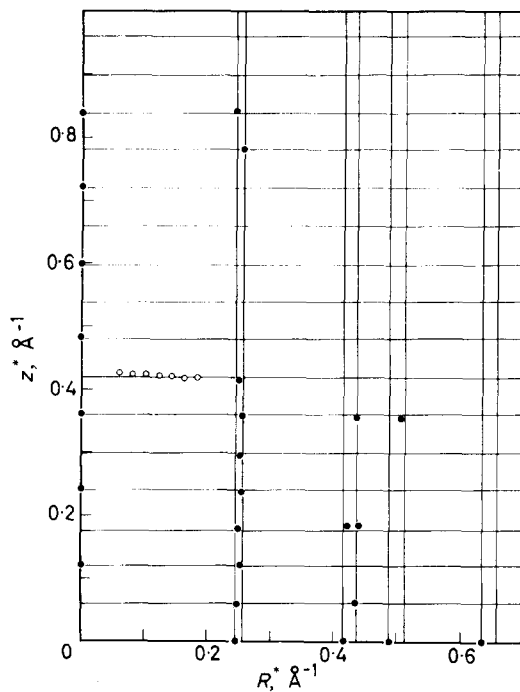


Figure 1—Part of reciprocal lattice of Nylon 6 (γ form); (a) Unheated specimen, photographed at -125°C ; (b) Specimen which has been heated to 195°C *in vacuo*, photographed at -115°C

Figure 2—Reciprocal lattice of Nylon 6 (γ form), from specimens photographed at room temperature which have previously been heated to 195°C *in vacuo*



evidence of the non-hexagonal shape is found in the (unresolved) $11l$ and $02l$ row lines. As shown in *Figures 1* and *2* the reciprocal lattice points are staggered, the staggering being a direct consequence of the way in which the intensity distribution favours sometimes row $11l$, sometimes row $02l$ (see *Table 6*). *Table 1* shows the lengths of the axes measured on photographs taken under different conditions. The a axis length is practically unaffected by temperature changes (less than one per cent), the c axis by about one per cent, but the b axis changes by over four per cent. This behaviour supports our belief that the hydrogen bonding is along the a axis.

Table 1. Unit cell dimensions (Å) in the γ form of Nylon 6 under various conditions

Film No.	Treatment	Temp. of observation °C	a	b	c
2144A	Heated to 195°C	23	4.83	8.07	16.67
2141A	"	-115	4.81	7.84	16.67
2093A	"	23	4.81	7.94	16.58
2094A	"	23	4.82	8.00	16.61
2139A	Not heated	-125	4.84	7.75	16.74
1794A	"	23	4.82	7.91	16.72

NOTE: a measured from 200 reflection, b and c from 026.

The suggestion that hydrogen bonds are formed between parallel chains is very reasonable in view of the contraction of the c axis in the γ form. It would then be expected (as proposed by Arimoto⁸) that there would be an *antiparallel* arrangement of sheets, neighbouring sheets being alternately 'up' and 'down'. This would give a unit cell containing two chains, and could be orthorhombic. It would allow the transition from the oriented α form to the oriented γ form with a small re-arrangement of the chains, chiefly of rotation round the c axis. However, the intensity data are not compatible with such a structure. Calculation shows that a strong 107 reflection is expected (see *Table 6*, footnote), and we have found that this reflection is either very weak or absent. There is, however, a strong streak on the seventh layer line, extending from near the meridian to the $11l$ row line [*Figure 4(c)*]. This shows that there is disorder of some kind in the structure. The streak is shown on the reciprocal lattice net of *Figure 2*. The most likely arrangement in these circumstances is a random direction of chain sense in the several hydrogen-bonded layers which comprise the crystallite, with a parallel arrangement of chains in the layer. This would account for the features of the diffraction pattern of the annealed form described above. For consider a fully ordered arrangement of the orthorhombic cell. Of those reflections which distinguish this cell from a near-hexagonal one with one chain, the only ones in the region of reciprocal space where they are observable are those on the seventh layer line, as is shown by calculations we have made. As the regular sequence of 'up' and 'down' layers is lost, the reflections with h or k odd and k or h even become smeared out into streaks, and since these reflections have appreciable intensity only on the layer line $l=7$, it is on this line only that a streak is observed. The reflections corresponding to the near-hexagonal cell remain

STRUCTURE OF THE GAMMA FORM OF POLYCAPROAMIDE (NYLON 6)

sharp, and their intensities are unchanged. It will be noticed that, although we suppose that there is still some order in the structure (for each hydrogen-bonded layer is supposed to contain only one sense of chain) the diffraction pattern is the same as if there were complete randomness of chain sense. (This occurs in poly-L-alanine, and leads to a diffraction pattern of sharp reflections and streaks.)

It is not so easy to account for the appearance of 101 and 103 reflections on specimens which have not been heated [Figure 1(a)]. Possibly the development of the parallel-chain hydrogen bonded sheet is imperfect, with a few chains forming hydrogen bonds to chains in neighbouring sheets (as in one of Vogelsong's structures). This might give rise to weak reflections corresponding to an imperfectly developed larger cell. On annealing it would be expected that the regular, parallel chain type of sheet would be produced. The partly irreversible contraction of the *b* axis which occurs on annealing is of interest in this connection.

Atomic positions

The positions of the atoms in the hydrogen bonded sheet have been determined from wire models ($1 \text{ \AA} \equiv 2 \text{ in.}$) which have been described elsewhere (Bradbury *et al.*¹¹). It was assumed that the hydrocarbon portion

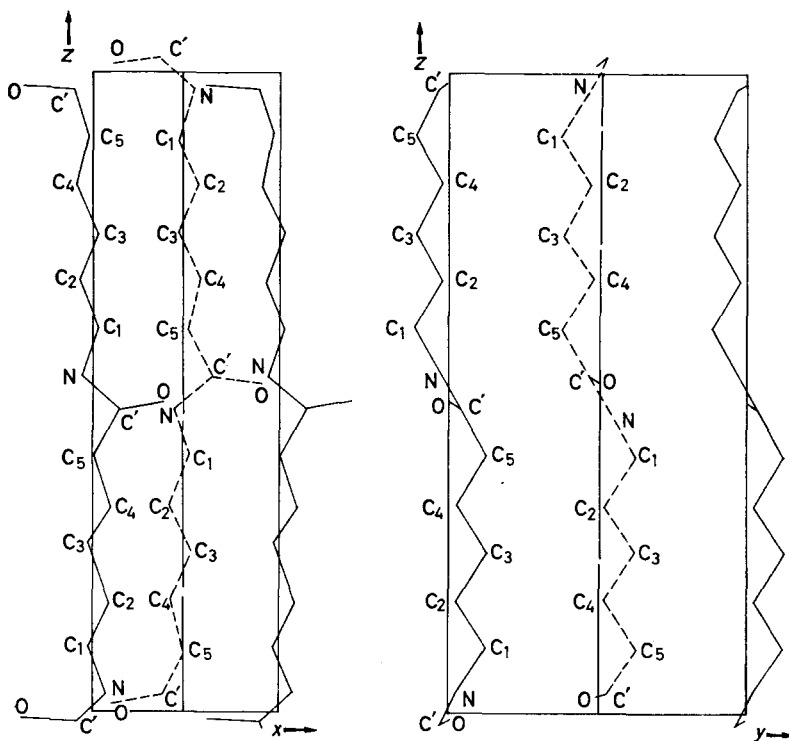


Figure 3—Arrangement of atoms in unit cell of Nylon 6 (γ form). All chains within any hydrogen-bonded sheet are parallel, but the chain sense varies randomly from sheet to sheet

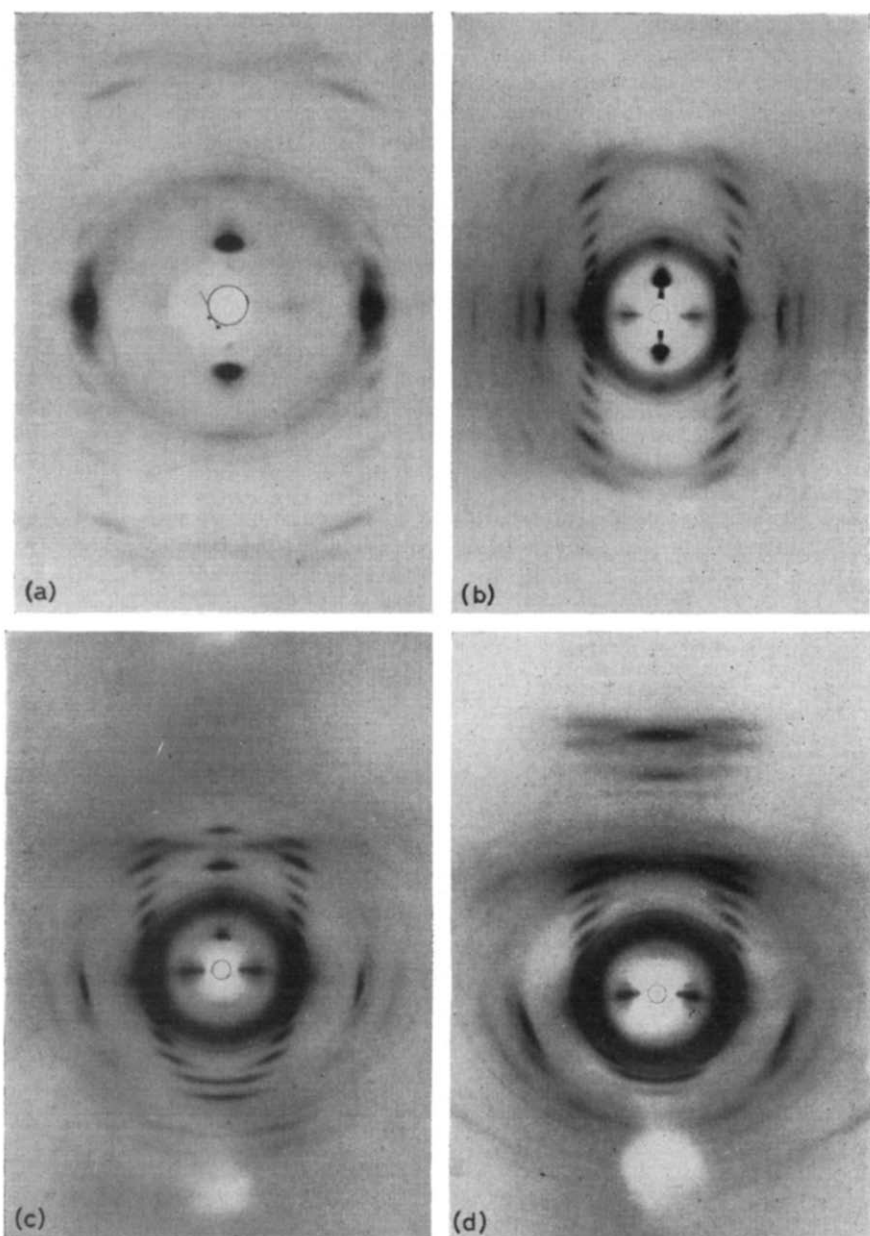


Figure 4—(a) Nylon 6 (γ form) unheated fibres photographed at -125°C (5.73 cm camera, $\text{Cu } K\alpha$ radiation). (b) Nylon 6 (γ form) photographed at room temperature after heating to 195°C *in vacuo* (3 cm cylindrical camera, $\text{Cu } K\alpha$ radiation). (c) Specimen as in (b), fibres tilted in equatorial plane of camera $18^{\circ} 4'$ from normal to X-ray beam. (d) As (c), with angle of tilt $40^{\circ} 20'$

STRUCTURE OF THE GAMMA FORM OF POLYCAPROAMIDE (NYLON 6)

 Table 2. Atomic coordinates ($x, y, z, \text{\AA}$) for the γ form of Nylon 6

 $a=4.82 \text{\AA}$ $b=7.82 \text{\AA}$ $c=16.70 \text{\AA}$ (fibre axis)

Atom	x	y	z
C'	-0.68	-0.23	-0.40
O	-1.90	-0.15	-0.27 ⁵
N	0.24	0.21	0.46 ⁵
C ₁	-0.11	0.97	1.67
C ₂	0.38	0.19	2.92
C ₃	-0.08	0.93	4.19
C ₄	0.43	0.18	5.42
C ₅	0.08	0.97	6.71

 Atoms at $x, y, z; -x, -y, z+c/2; x+a/2, y+b/2, z$

 and at $-x+a/2, -y+b/2, z+c/2$.

 These chains may be randomly replaced by chains in which the atomic coordinates are $x, -y, -z,$
 $-x, y, -z+c/2; x+a/2, -y+b/2, -z$
 and at $-x+a/2, y+b/2, -z+c/2$.

 Table 3. Bond lengths (\AA) and angles ($^\circ$) calculated from coordinates of Table 2

C'—O	1.23	O—C'—N	126
C'—N	1.34	C'—N—C ₁	122
C ₁ —N	1.47	N—C ₁ —C ₂	109
C ₁ —C ₂	1.55	C ₁ —C ₂ —C ₃	109
C ₂ —C ₃	1.54	C ₂ —C ₃ —C ₄	109
C ₃ —C ₄	1.53	C ₃ —C ₄ —C ₅	109
C ₄ —C ₅	1.55	C ₄ —C ₅ —C'	109
C ₅ —C'	1.56	C ₅ —C'—O	119

would be fully extended, and that (since 00*l* reflections are observed only when *l* is even) the chain has a two-fold screw axis. The most linear arrangement of the NH...O atoms was taken. In order to find the displacement along the *c* axis of the 'up' sheets relative to the 'down' sheets the 00*l* intensities were computed and compared with the observed ones, the displacement being adjusted until the best fit was obtained. The strength of the 00.14 reflection [see Figure 4(d)] shows that the heavy atoms in one type of sheet must have heavy atoms in the other type of sheet at nearly the same *z* value. Although there are seven arrangements which satisfy this condition, the one chosen was outstandingly better than the others when the 00*l* reflections were considered.

The coordinates adopted are given in Table 2 and the corresponding chain conformation is shown in Figure 3. Table 3 gives the bond lengths and angles calculated from the coordinates of Table 2.

Verification of the structure

A good deal of support for the structure was obtained from optical transform photographs, but in the latter stages computation was done on an Elliott 803 machine. The scattering powers of C, O, CH₂ and NH were taken to be 6, 8, 8 and 8, and the variation of scattering power with $(1/\lambda) \sin \theta$ was calculated by the method of Vand, Eiland and Pepinsky¹².

At an early stage it became evident, from comparison of the 00*l* intensities (observed and calculated), that the temperature factor for these reflections would be lower than that used by Vogelsong, who found a value of 10 for *B* in the temperature factor, $\exp[-B(\sin\theta/\lambda)^2]$. In structures where the chains are almost fully extended and where there are sheets of molecules formed by hydrogen bonds it is to be expected that anisotropic temperature factors will be found. We have accordingly assumed that a relation of the following kind would hold

$$I_{\text{calc.}} = |F|^2 \exp\left[-\frac{\alpha h^2}{4a^2} - \frac{\beta k^2}{4b^2} - \frac{\gamma l^2}{4c^2}\right]$$

and have determined the best values of α , β and γ from the data. In the isotropic case $\alpha = \beta = \gamma = B$ and the expression can be reduced to the usual one. The factors are to be chosen so as to give the best fit between observed quantities and those deduced from the model structure. In single crystal work the practice is to multiply the observed intensities by the Lorentz and polarization factors. These are then compared with the calculated intensity $I_{\text{calc.}}$. This is justifiable, for all reflections from a single crystal produce a photographic image whose densities are simply related to their intensities. In fibre diffraction photographs this is not so, for disorientation affects the reflections to very different degrees, depending on which part of the pattern is under consideration. In consequence, many reflections are below the threshold value and are recorded as of zero intensity, whereas others in a more favourable region (near the meridian) are registered even though they may have a lower $|F|$ value. Correction in such cases is clearly impossible. It would seem that with data derived from fibre photographs a better procedure might be to apply the corrections to $|F|^2$ and then compare these with the observed intensity $I_{\text{obs.}}$ (or alternatively $|F|$ and $I_{\text{obs.}}^{1/2}$ may be compared). The observed data, imperfect though they are, are the sole means whereby the model structure may be compared with the polymer, and to distort them by multiplying by large corrections seems unsatisfactory. We have treated the question empirically by using four different procedures.

Case a—The values of $|F|^2$ were multiplied by the anisotropic temperature factor (4) while the values of $I_{\text{obs.}}$ (integrated optical densities) were multiplied by the Lorentz (1), polarization (2), disorientation (3), specimen-to-spot distance (5) and scale factors (8).

Case b—The values of $|F|^2$ were multiplied by the anisotropic temperature factor (4) and divided by (1), (2), (3), (8) and (5). The results were compared with $I_{\text{obs.}}$.

Case c—Procedure *a* was used, replacing $|F|^2$ by $|F|$ and $I_{\text{obs.}}$ by $I_{\text{obs.}}^{1/2}$.

Case d—Procedure *b* was used with the modification introduced into *c*.

These procedures were examined by finding the values of α , β and γ in the temperature factor which gave a minimum when $\sum w\Delta^2$ is determined for the recorded reflections. Here w is the weighting factor applied to each reflection and Δ is the difference in the compared values (intensities or amplitudes, as appropriate). Since the 110 and 020 reflections are so much more intense than the next strongest, it was decided not to make use of these reflections in calculating reliability factors. The effect of including

STRUCTURE OF THE GAMMA FORM OF POLYCAPROAMIDE (NYLON 6)

reflections which are much stronger than the others is of course to diminish this factor, but the result is not very meaningful. A least squares solution was computed for each procedure and for each of these, three different weighting factors were used: (1) w proportional to the observed intensity or amplitude, (2) $w=1$ in all cases, (3) w proportional to the reciprocal of the observed intensity or amplitude.

Table 4. Temperature factors obtained from different cases, with different weighting factors w
 α , β and γ refer to temperature factors in the a , b and c axial directions

Case	(a)			(b)		
	α	β	γ	α	β	γ
$w \propto I_{obs.}$	7.55	26.7	3.52	8.55	7.55	8.95
$w=1$	8.40	32.8	3.64	15.1	19.5	8.50
$w \propto \frac{1}{I_{obs.}}$	6.55	35.4	3.48	12.4	31.2	7.76

Case	(c)			(d)		
	α	β	γ	α	β	γ
$w \propto I_{obs.}^{\frac{1}{2}}$	6.86	32.0	3.04	12.14	21.6	7.76
$w=1$	6.0	33.2	2.96	10.48	28.2	7.52
$w \propto \frac{1}{I_{obs.}^{\frac{1}{2}}}$	4.64	32.4	2.72	6.56	31.8	7.04

Table 5. Reliability factors (per cent) in different cases, with different weighting factors w

Case	(a)	(b)	Case	(c)	(d)
$w \propto I_{obs.}$	23.8	16.4	$w \propto I_{obs.}^{\frac{1}{2}}$	13.4	11.8
$w=1$	23.1	15.0	$w=1$	13.5	11.8
$w \propto \frac{1}{I_{obs.}}$	23.5	17.8	$w \propto \frac{1}{I_{obs.}^{\frac{1}{2}}}$	13.5	11.8

The 'reliability factor' R was calculated in each of the twelve cases. This factor is the sum of the differences between observed and calculated quantities (without regard to sign) divided by the sum of the observed quantities. The values of the anisotropic temperature factors are given in Table 4, and the R values in Table 5. The temperature factors vary a good deal from case to case, and so have little absolute significance. However, the very marked anisotropy of the temperature factor is striking, and is as we would expect in a polymer in which the molecules are arranged in hydrogen-bonded sheets. There is a special reason for the very high values of β , the

part of the temperature factor which depends on k . In *Figure 3* the y/z projection shows that profiles of two kinds of sheet (containing respectively all 'up' or all 'down' chains) are very similar but not identical. So the distance between two neighbouring like sheets will not be quite the same as that between unlike sheets. A random occurrence of the two kinds of sheet will result in random displacement of the sheets from the positions they would occupy in a regular lattice. This will lead to a large value of β .

The results are clearly not greatly dependent on the weighting factor adopted. We have thought it preferable to put $w=1$ in the final assessment of the structure, so as to avoid giving an unduly large weight either to very large or to very small intensities. For reasons given above, we prefer to

Table 6. Calculated, corrected intensities for the γ form of Nylon 6 compared with observed intensities

hkl	$I_{\text{calc. corr.}}$	$I_{\text{obs.}}$	hkl	$I_{\text{calc. corr.}}$	$I_{\text{obs.}}$
110	962	907	220	10	17
020	404	503	040		
111	379	366	221	37	
021	294	312	041		29
112			222		
022	93	100	042	4	—
113	100	86	223	7	6
023			043		
114			224		
024	64	62	044	4	—
115			225	4	—
025	42	50	045		
116			226		
026	124	130	046	22	8
117	84	76	227	12	—
027			047		
118	8	—	228		
028			048	2	—
200	76	106	310	3	14
130			240		
201			311	4	9
131	50	32	241		
202			342		
132	1	—	242	0	—
203			343		
133	11	12	243	0	—
204			344		
134	1	—	244	0	—
205			315		
135	8	—	245	0	—
206			316		
136	36	11	246	4	4
207			317	2	—
137	4	—	247		
208			318		
138	12	—	248	1	—
002	24	12	11·12	11	15
004	4	3	02·13	22	31
006	1	1	11·14	24	27
008	0	—	107	108*	—

*For a regular succession of 'up' sheets and 'down' sheets.
 Note: When (as in most cases) two reflections are not resolved the intensities are given the index of the component with the stronger calculated intensity. The calculated intensities of the two components have been added.

compare $I_{\text{obs.}}$ (or its square root) with the intensity which is calculated for the actual spot on the film [cases (b) or (d)]. Comparison of intensities rather than amplitudes emphasizes the discrepancies between observed and calculated quantities, and so *Table 6* shows the results for case (b), including the 110 and 020 reflections which were not used in calculating R . It may be remarked again that the meridional reflections have been measured separately and scaled to fit the calculated values. Because of the very great enhancement of meridional intensities compared with those of other reflections it is difficult to use any other procedure. The very high intensity of 002 on fibre photographs (although $|F|$ for this reflection is not large) is of course a consequence of this enhancement. In considering the significance of R , it must be remembered that with three components of the temperature factor to be chosen the degree of fit is naturally better than it would be when the temperature factor is isotropic. Even when some allowance is made for this, however, the fit between observed and calculated quantities is so much better than for either of Vogelsong's structures that we are in no doubt of the greater validity of the structure which we propose. The regular structure proposed by Arimoto cannot occur as a major constituent form of the γ form, for the strong 107 reflection predicted for it has not been observed. The expected intensity of this reflection lies between that of 026 and 117. Instead of the 107 reflection a strong layer line streak is seen [*Figure 4(c)*]. It is, of course, conceivable that a different method of making the γ form of Nylon 6 would result in a regular alternation of chain sense between one sheet and the next. Finally, although the model on which our calculations are based is one in which the sheets have a random chain sense, it may be that a degree of disorder less than complete randomness would suffice to account for the X-ray diffraction pattern.

We are indebted to Mr A. W. Porter for his care in taking the X-ray photographs. One of us (D.A.D.P.) wishes to acknowledge the receipt of a grant from the Department of Scientific and Industrial Research which enabled him to take part in the work. We also wish to thank Sir John Randall for facilities during the later stages of the work.

*Biophysics Dept., King's College,
London W.C.2*

(Received February 1965)

REFERENCES

- ¹ HOLMES, D. R., BUNN, C. W. and SMITH, D. J. *J. Polym. Sci.* 1955, **17**, 159
- ² UEDA, S. and KIMURA, T. *Chem. High Polymers, Tokyo*, 1958, **15**, 243
- ³ TSURUDA, M., ARIMOTO, H. and ISHIBASHI, M. *Chem. High Polymers, Tokyo*, 1958, **15**, 619
- ⁴ KINOSHITA, Y. *Makromol. Chem.* 1959, **33**, 1
- ⁵ KINOSHITA, Y. *Makromol. Chem.* 1959, **33**, 21
- ⁶ VOGELSONG, D. C. *J. Polym. Sci. A*, 1963, **1**, 1055
- ⁷ BRADBURY, E. M. and ELLIOTT, A. *Polymer, Lond.* 1963, **4**, 47
- ⁸ ARIMOTO, H. *J. Polym. Sci. A*, 1964, **2**, 2283
- ⁹ ELLIOTT, A. and DICKSON, J. H. *Laboratory Instruments*, 2nd ed., p 145. Chapman & Hall: London, 1959
- ¹⁰ ELLIOTT, A. *J. sci. Instrum.* 1965, **42**, 312
- ¹¹ BRADBURY, E. M., BROWN, L., ELLIOTT, A., FRASER, R. D. B. and HANBY, W. E. *J. molec. Biol.* 1962, **5**, 230
- ¹² VAND, V., EILAND, P. F. and PEPINSKY, R. *Acta cryst., Camb.* 1957, **10**, 303

APPENDIX

THE GEOMETRY OF DIFFRACTION OF CRYSTALLINE FIBRES

STRUTHER ARNOTT

THE diffraction from crystalline fibres has many of the properties of that from rotated single crystal specimens. The geometrical relationships involved when this diffraction is recorded on a flat film perpendicular to the primary X-ray beam, or on a cylindrical film coaxial with the single crystal rotation axis, have been described in *International Tables for Crystallography*, Vol. II, 4.3. Those results will, in the following, be adapted and amended for the usual experimental arrangements of fibre crystallography.

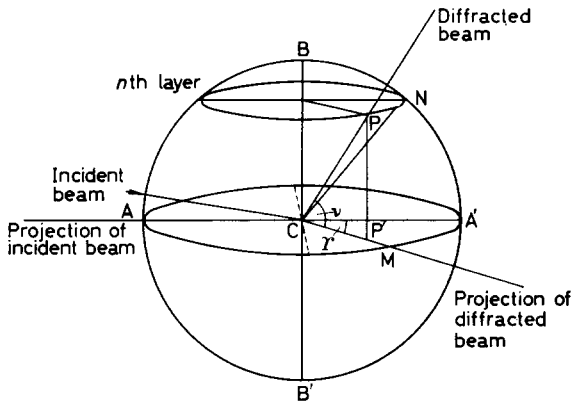


Figure 5—Perspective diagram. BB' is fibre axis direction, P a reciprocal lattice point in reflecting position ξ, ϕ', ζ . Angular coordinates of diffracted beam are ν, Υ (note $\hat{MCP} = \hat{P'CM}$)

Figure 5 shows the geometrical principles of diffraction in the general case of a fibre with its axis tipped μ degrees towards the incident beam of X-rays. P is a reciprocal lattice point (with cylindrical polar coordinates ξ, ϕ', ζ) in a reflecting position and P' its projection on the equatorial plane. If the angles ν and Υ are defined as in Figure 5 it can be shown that

$$\sin \nu = -\sin \mu + \zeta \quad (1)$$

$$\cos \Upsilon = (2 \cos^2 \mu + 2\zeta \sin \mu - \rho^2) / \cos \mu (\cos^2 \mu + 2\zeta \sin \mu - \zeta^2)^{\frac{1}{2}} \quad (2)$$

The diffraction is commonly observed in one of four systems:

(a) on a plane film normal to CO (see Figure 6) and distant D from O ;

- (b) on a cylindrical film of radius r with axis in the plane ACB and passing through C perpendicular to the incident beam or
- (c) with axis through C perpendicular to B'B and to the X-ray beam;
- (d) on a conical film with axis CO and angle α and with the specimen to apex distance equal to d .

In these cases CP, the diffracted beam, will intersect the film where:

(a) $X_1 = D \cos Y \sin Y / (\cos v \cos Y \cos \mu + \sin v \sin \mu)$
 $Y_1 = D$ and
 $Z_1 = D (\sin v \cos \mu - \cos v \cos Y \sin \mu) / (\cos v \cos Y \cos \mu + \sin v \sin \mu)$

(b) $X_2 = r \cos v \sin Y / R^\ddagger$
 $Y_2 = r (\cos v \cos Y \cos \mu + \sin v \sin \mu) / R^\ddagger$
 $Z_2 = r (\sin v \cos \mu - \cos v \cos Y \sin \mu) / R^\ddagger$

where $R = (\cos^2 v \cos^2 Y + \sin^2 v \sin^2 \mu + \cos^2 v \cos^2 Y \cos^2 \mu + \sin v \cos v \cos Y \sin \mu \cos \mu)$

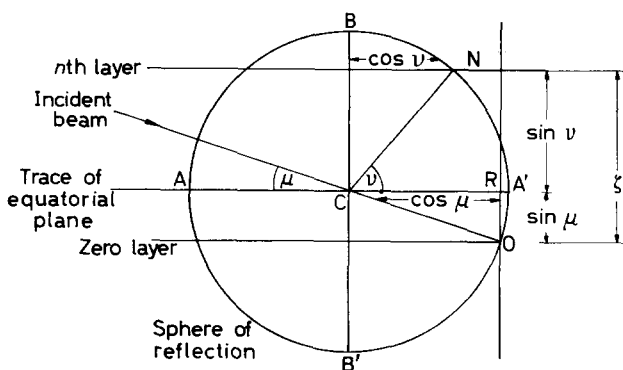


Figure 6—Section of sphere of reflection through the plane MAA'. Incident beam in the plane, O is the reciprocal lattice origin

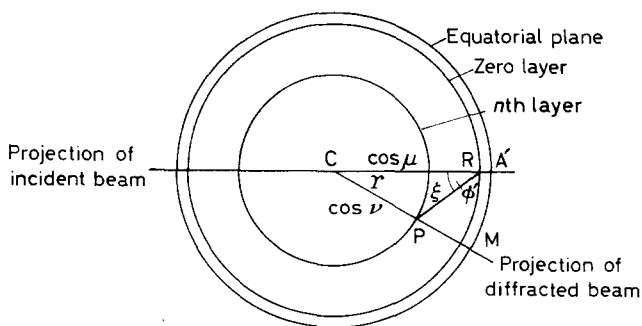


Figure 7—Plan of sphere of reflection. R is the projection of the fibre axis on the equatorial plane

(c) $X_3 = r \cos v \sin Y / (\sin^2 v + \cos^2 v \cos^2 Y)^\ddagger$
 $Y_3 = r (\cos v \cos Y \cos \mu + \sin v \sin \mu) / (\sin^2 v + \cos^2 v \cos^2 Y)^\ddagger$
 $Z_3 = r (\sin v \cos \mu - \cos v \cos Y \sin \mu) / (\sin^2 v + \cos^2 v \cos^2 Y)^\ddagger$

$$\begin{aligned}
 (d) \quad X_4 &= K \cos \nu \sin Y \\
 Y_4 &= K \cos \nu \cos Y \\
 Z_4 &= K \sin \nu
 \end{aligned}$$

where $K = d [\cos \nu \cos Y \mp (\sin^2 \nu + \cos^2 \nu \sin^2 Y)] / (2 \cos^2 \nu \cos^2 Y - 1)$

and physically represents the distance from the specimen to the diffraction spot on the film.

Equations (1) and (2) and the previous relationships a, b, c, d can be used to relate the diffraction record to the coordinates of the appropriate reciprocal lattice point and the angle (μ) by which the fibre is tilted into the X-ray beam. (In cases b, c and d measurements are made on the flattened out films) whence the film coordinates for the four cases in the same order as before are:

$$\begin{aligned}
 x_1 = X_1 &= D (-\zeta^2 + \zeta\rho^2 \sin \mu + \rho^2 \cos^2 \mu - \frac{1}{4}\rho^4)^{\frac{1}{2}} / \cos \mu (1 - \frac{1}{2}\rho^2) \\
 y_1 = Z_1 &= D (\zeta - \frac{1}{2}\rho^2 \sin \mu) / \cos \mu (1 - \frac{1}{2}\rho^2)
 \end{aligned} \quad (3)$$

$$\begin{aligned}
 x_2 &= (\pi r / 180) \tan^{-1} (X_2 / Y_2) \\
 &= (\pi r / 180) \tan^{-1} \{ (-\zeta^2 + \zeta\rho^2 \sin \mu + \rho^2 \cos^2 \mu - \frac{1}{4}\rho^4)^{\frac{1}{2}} / \cos \mu (1 - \frac{1}{2}\rho^2) \} \\
 y_2 = Z_2 &= r (\zeta - \frac{1}{2}\rho^2 \sin \mu) / (\cos^2 \mu - \zeta^2 + \zeta\rho^2 \sin \mu - \frac{1}{4}\rho^4 \sin^2 \mu)^{\frac{1}{2}}
 \end{aligned} \quad (4)$$

$$\begin{aligned}
 x_3 = X_3 &= r \{ (-\zeta^2 + \zeta\rho^2 \sin \mu + \rho^2 \cos^2 \mu - \frac{1}{4}\rho^4) / (\cos^2 \mu + \zeta^2 \\
 &\quad + \zeta\rho^2 \sin \mu - \rho^2 \cos^2 \mu + \frac{1}{4}\rho^4) \}^{\frac{1}{2}} \\
 y_3 &= (\pi r / 180) \tan^{-1} (Z_3 / Y_3) \\
 &= (\pi r / 180) \tan^{-1} \{ (\zeta \mp \frac{1}{2}\rho^2 \sin \mu) / \cos \mu (1 - \frac{1}{2}\rho^2) \}
 \end{aligned} \quad (5)$$

In the case of the opened out conical film, which becomes a circle with a segment of angle $2\pi(1 - \sin \frac{1}{2}\alpha)$ cut out, it is convenient to use polar coordinates and

$$\begin{aligned}
 R &= K\rho (2 - \frac{1}{2}\rho^2)^{\frac{1}{2}} \\
 \phi &= \{ \sin (\frac{1}{2}\alpha) \} \tan^{-1} \{ (-\zeta^2 + \zeta\rho^2 \sin \mu + \rho^2 \cos^2 \mu - \frac{1}{4}\rho^4)^{\frac{1}{2}} / (\zeta - \frac{1}{2}\rho^2 \sin \mu) \}
 \end{aligned} \quad (6)$$

R is the distance of the reflection from the centre of the opened out film and ϕ is the angle between R and the meridian.

The integrated intensity (I_i) recorded is a function not only of the ideal intensity $I = |F|^2$ ($|F|$ is the structure amplitude) but also of a number of geometrical factors, the most important of which take account of the polarization of the X-ray beam (P) and the differing relative reflection opportunities of the various reciprocal lattice points (L) (this is the Lorentz factor in conventional single crystal diffraction)

$$I = I_i \times P \times L \quad (7)$$

where $P = 2 / (2 - \rho^2 + \frac{1}{4}\rho^4)$.

The value of L will now be considered. It is convenient first of all to consider the most general case of a disoriented polycrystalline specimen—

the powder case—where any reciprocal lattice point is distributed over a spherical shell, the ‘disorientation sphere’, of radius ρ , thickness $\Delta\rho$, and volume $4\pi\rho^2\Delta\rho$ (see *Figure 8*). The part of this shell which lies in a reflecting

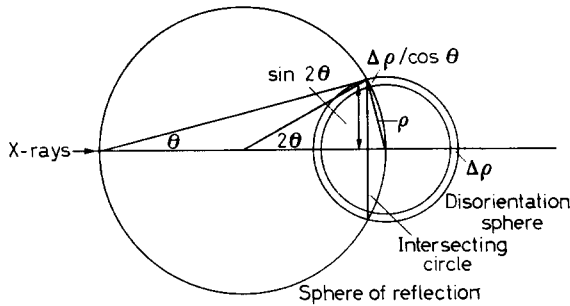


Figure 8—The diffraction geometry (in elevation) for a completely disoriented polycrystalline specimen

position is the circular annulus of radius $\sin 2\theta$ and thickness $\Delta\rho/\cos \theta$ which lies on the sphere of reflection perpendicular to the incident X-ray beam. Its area is $2\pi \sin 2\theta (\Delta\rho/\cos \theta)$. The relative reflection opportunity of this lattice point is therefore

$$2\pi \sin 2\theta (\Delta\rho/\cos \theta) / 4\pi\rho^2\Delta\rho = \frac{1}{2} \frac{\sin 2\theta}{\rho \cos \theta}$$

We note that this expression is the length of the circumference of the intersecting circle divided by the area of the disorientation sphere and a factor $\cos \theta$ which arises because of the shell thickness.

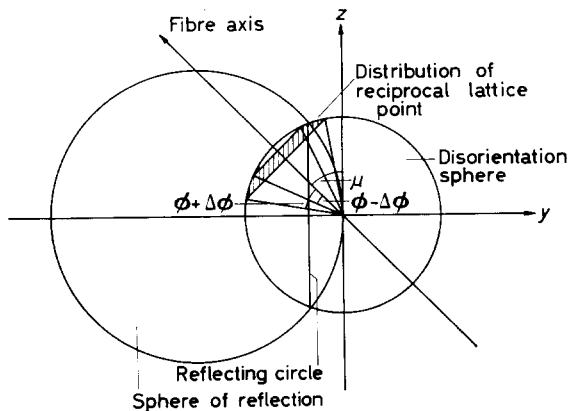


Figure 9—The diffraction geometry (in elevation) for a well oriented crystalline fibre

With a well oriented crystalline fibre the reciprocal lattice ‘point’ will be distributed over only that part of the disorientation sphere (see *Figure 9*) which is a belt lying between the cones

$$x^2 + (y \cos \mu - z \sin \mu)^2 = (y \sin \mu + z \cos \mu)^2 \tan^2 (\phi \pm \Delta\phi)$$

The area of the belt is $2\pi\rho^2 \sin \phi \sin \Delta\phi$. That part of the distribution which is in a reflecting position is an arc of the reflecting circle of length

$$\sin 2\theta [\sin^{-1} (\tan \mu/2 \cos \theta - \cos (\phi - \Delta\phi)/\cos \mu \cos \theta) - \sin^{-1} (\tan \mu/2 \cos \theta - \cos (\phi + \Delta\phi)/(\cos \mu \cos \theta))]$$

and the relative reflection opportunity is therefore

$$\frac{\sin 2\theta [\sin^{-1} (\tan \mu/2 \cos \theta - \cos (\phi - \Delta\phi)/\cos \mu \cos \theta) - \sin^{-1} (\tan \mu/2 \cos \theta - \cos (\phi + \Delta\phi)/(\cos \mu \cos \theta))]}{2\pi\rho^2 \sin \phi \sin \Delta\phi \cos \theta}$$

$$= \frac{[\sin^{-1} (\tan \mu/2 \cos \theta - \cos (\phi - \Delta\phi)/\cos \mu \cos \theta) - \sin^{-1} (\tan \mu/2 \cos \theta - \cos (\phi + \Delta\phi)/(\cos \mu \cos \theta))]}{2\pi\rho \sin \phi \sin \Delta\phi}$$

Now, $L^{-1} \rightarrow (\frac{1}{2}\pi) (-\frac{1}{4}\rho^4 + \zeta\rho^2 \sin \mu + \rho^2 \cos^2 \mu - \zeta^2)^{-\frac{1}{2}}$ as $\Delta\phi \rightarrow 0$

This limiting value of L^{-1} has been found to be an acceptable approximation in all the cases of well oriented fibres we have studied.

Further geometrical factors arise when the quantity measured is not itself the integrated intensity. The measure of intensity commonly obtained from diffraction patterns of crystalline fibres is the area under a densitometer trace across the centre of each diffraction arc. This area requires to be multiplied by the effective length of the arc to become proportional to the integrated intensity. For the small diffraction angles which usually occur in diffractograms from crystalline fibres the effective arc length may be considered to be proportional to ρ .

*M.R.C. Biophysics Research Unit,
University of London King's College,
26-29 Drury Lane, London, W.C.2*

*Thermal Degradation of Piperazine Polyamides I—Poly(terephthaloyl trans-2,5-dimethylpiperazine) and Poly(oxalyl trans-2,5-dimethylpiperazine)**

S. D. BRUCK

The thermal degradation of two heterocyclic polyamides, poly(terephthaloyl trans-2,5-dimethylpiperazine) and poly(oxalyl trans-2,5-dimethylpiperazine), is discussed in terms of rates, activation energies and degradation products. These piperazine polyamides are stable in a vacuum up to approximately 420°C, but beyond this temperature essentially total volatilization takes place. From the rates of degradation an activation energy of 64 kcal/mole was calculated for both polymers, but poly(oxalyl trans-2,5-dimethylpiperazine) volatilizes approximately two to three times faster than poly(terephthaloyl trans-2,5-dimethylpiperazine). The addition of trace amounts of sulphuric acid to poly(terephthaloyl trans-2,5-dimethylpiperazine) prior to its pyrolysis reduced the activation energy of degradation to 55 kcal/mole. Mass spectrometric analysis of the volatile degradation products indicates the appearance of large quantities of carbon monoxide and lesser amounts of water, carbon dioxide, hydrocarbons, hydrogen, pyrazines and pyrroles. The character of the rate curves, the nature of the volatile degradation products, and an activation energy of 64 kcal/mole point to a random thermal free radical degradation. In contrast to the behaviour of aliphatic polyamides, the amide linkages in both poly(terephthaloyl trans-2,5-dimethylpiperazine) and poly(oxalyl trans-2,5-dimethylpiperazine) are quite resistant to acid-catalysed hydrolytic breakdown at elevated temperatures.

IN previous publications¹⁻⁴ the thermal degradation of an aromatic poly-pyromellitimide was discussed. The interest in this and other ring-containing polymers is stimulated by recent technological demands for non-metallic materials that are stable at high temperatures⁵⁻⁷. A considerable number of aromatic and heterocyclic polymers have recently been reported including poly(1,3,4-oxadiazoles)⁸, polybenzothiazoles⁹, polybenzimidazoles¹⁰, and polyquinoxalines¹¹, some of which show outstanding thermal stabilities. On the other hand, polyamides have received less attention from the point of view of thermal stability, probably because aliphatic polyamides do not, in general, possess high melting points, have fairly low activation energies, and

*This work was supported by the Bureau of Naval Weapons, Department of the Navy, under Contract NOW 62-0604-c.

are susceptible to oxidative as well as hydrolytic degradation. However, the preparations of fully aromatic¹² and heterocyclic^{13, 14} polyamides have recently been reported. The high melting points ($> 400^{\circ}\text{C}$) of some of these polymers and their structural features indicate that they may well possess interesting thermal properties.

The object of this paper is to discuss the thermal degradation of two heterocyclic polyamides, poly(terephthaloyl *trans*-2,5-dimethylpiperazine) and poly(oxalyl *trans*-2,5-dimethylpiperazine), in terms of rates, activation energies and degradation products, and to determine the effect of trace amounts of acidic catalysts on the course of the degradation.

EXPERIMENTAL DETAILS

Instrumentation

Both programmed and isothermal degradation studies were carried out in a vacuum ($\sim 10^{-4}$ mm of mercury) with a Cahn RG electrobalance by a method described in detail in previous publications¹⁻⁴.

Degradation studies for mass spectrometry

Degradation studies for mass spectrometric analyses were carried out in separate experiments with approximately 10 mg samples which were first pre-heated at 100°C for 30 minutes under a vacuum of $\sim 10^{-5}$ mm of mercury with continuous pumping to remove adsorbed gases and moisture; while maintaining this vacuum, the system then was sealed for the actual pyrolyses at 475°C . A fractionation technique was employed (liquid nitrogen, dry ice-acetone) in admitting the degradation products (volatile at room temperature) into the mass spectrometer.

Viscosity measurements

The inherent viscosities $[(\ln \eta_{\text{rel}})/c]$, where $c = 0.5$ g/100 ml] were determined in *m*-cresol at 30°C . Intrinsic viscosities $([\eta] = \lim_{c \rightarrow 0} \eta_{\text{inh}})$ were determined in a 40:60 mixture by weight of sym-tetrachlorethane: phenol at 30°C .

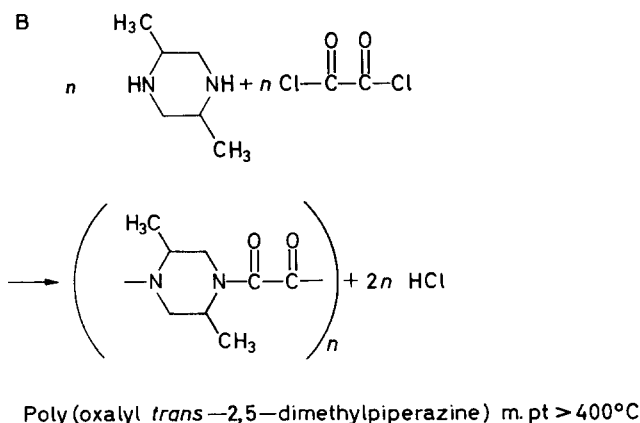
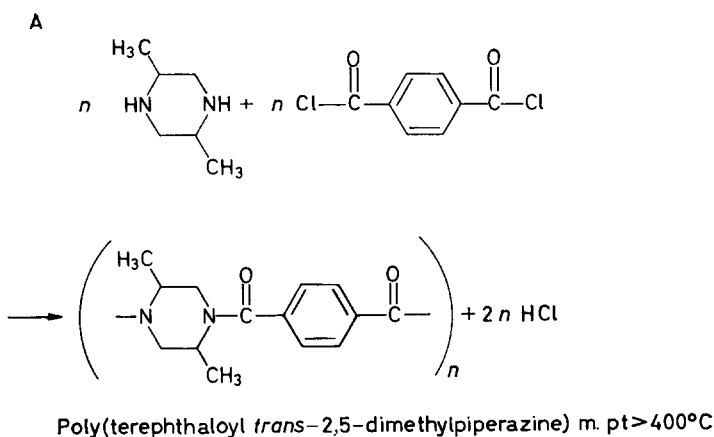
Materials

Poly(terephthaloyl *trans*-2,5-dimethylpiperazine) and poly(oxalyl *trans*-2,5-dimethylpiperazine) were prepared by the low-temperature solution condensation method of Morgan and Kwolek¹³ with excess diamine as the acceptor. The number-average molecular weights of the polymers were in the range of 25 000 to 30 000 as determined by end-group/viscosity data and also indicated by thermo-electric differential vapour pressure lowering in 90 per cent formic acid¹⁵.

RESULTS

Poly(terephthaloyl *trans*-2,5-dimethylpiperazine) and poly(oxalyl *trans*-2,5-dimethylpiperazine) are prepared according to the following reactions¹³:

THERMAL DEGRADATION OF PIPERAZINE POLYAMIDES I



The inherent viscosity in *m*-cresol (30°C) of poly(terephthaloyl *trans*-2,5-dimethylpiperazine) was 2.1, while that of poly(oxalyl *trans*-2,5-dimethylpiperazine) was 2.3.

The first series of experiments was carried out by programmed thermogravimetry at a heating rate of 4°C/min in a vacuum ($\sim 10^{-4}$ mm of mercury). Figure 1 illustrates the results for poly(terephthaloyl *trans*-2,5-dimethylpiperazine), poly(oxalyl *trans*-2,5-dimethylpiperazine), and a sample of poly(terephthaloyl *trans*-2,5-dimethylpiperazine) that had been treated with a two per cent solution of sulphuric acid for 24 hours and dried at 75°C for three hours prior to the pyrolysis. The data indicate that under a programmed rate of heating of 4°C/min poly(terephthaloyl *trans*-2,5-dimethylpiperazine) and poly(oxalyl *trans*-2,5-dimethylpiperazine) show no appreciable weight loss until about 430°C and 420°C, respectively. On the other hand, the sulphuric acid-treated sample of poly(terephthaloyl *trans*-2,5-dimethylpiperazine) showed an early weight loss of approximately 15 per

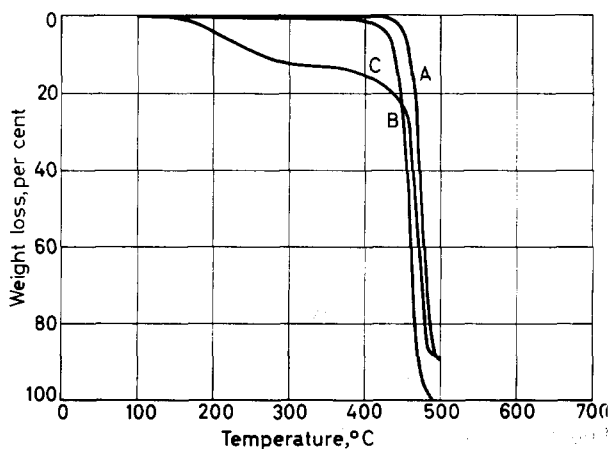


Figure 1—Thermal degradation of (A) poly(terephthaloyl *trans*-2,5-dimethylpiperazine), (B) poly(oxalyl *trans*-2,5-dimethylpiperazine) and (C) sulphuric acid-treated poly(terephthaloyl *trans*-2,5-dimethylpiperazine) in a vacuum by programmed thermogravimetry of 4°C/min

cent which was followed by a progressively rapid degradation commencing at about 400°C. This early weight loss between 100°C and 300°C may be at least partly due to the removal of water rather than polymer degradation, since the analytical results in *Table 2* indicate that the sulphuric acid-treated polymer retains an unusually large amount of water. In this connection it should be noted that a similar early rapid weight loss of approximately 15 per cent was also reported by other investigators¹⁶ during the pyrolysis of sulphuric acid-treated aliphatic polyamides. They associated this with

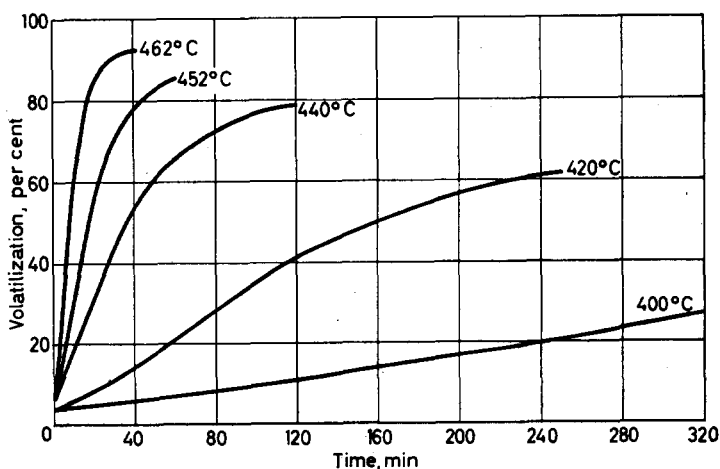


Figure 2—Thermal degradation of poly(terephthaloyl *trans*-2,5-dimethylpiperazine) in a vacuum at various temperatures

THERMAL DEGRADATION OF PIPERAZINE POLYAMIDES I

polymer degradation, although at least part of the weight loss could have been due to the evaporation of water that was not removed during the drying of the acid-treated sample. These piperazine polymers undergo almost total volatilization in a vacuum, unlike the aromatic polypyromellitimide discussed in previous publications¹⁻⁴.

The second series of experiments was conducted under isothermal conditions in a vacuum ($\sim 10^{-4}$ mm of mercury) between 400° and 500°C. Figures 2, 3 and 4 show, respectively, the percentage volatilization as a function of time at various temperatures of poly(terephthaloyl *trans*-2,5-

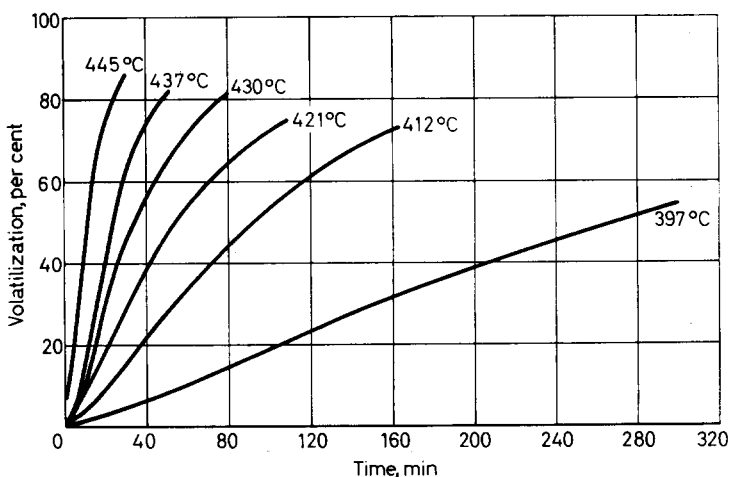


Figure 3—Thermal degradation of poly(oxalyl *trans*-2,5-dimethylpiperazine) in a vacuum at various temperatures

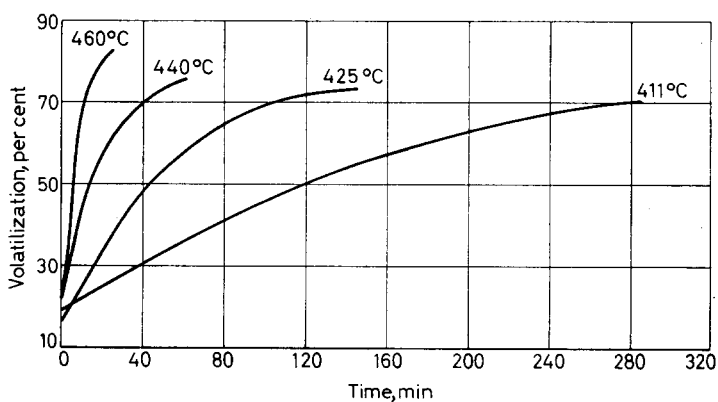


Figure 4—Thermal degradation of sulphuric acid-treated poly(terephthaloyl *trans*-2,5-dimethylpiperazine) in a vacuum at various temperatures

dimethylpiperazine), poly(oxalyl *trans*-2,5-dimethylpiperazine), and the sulphuric acid-treated sample of poly(terephthaloyl *trans*-2,5-dimethylpiperazine). Thermal equilibrium was reached usually within 15 to 20 minutes from the time the pre-heated furnace was positioned around the sample tube. Zero time signifies the start of the isothermal heating period. In Figures 5 to 9 the rates of volatilization are plotted against the percentage of volatilization. These rates were calculated from the volatilization/time

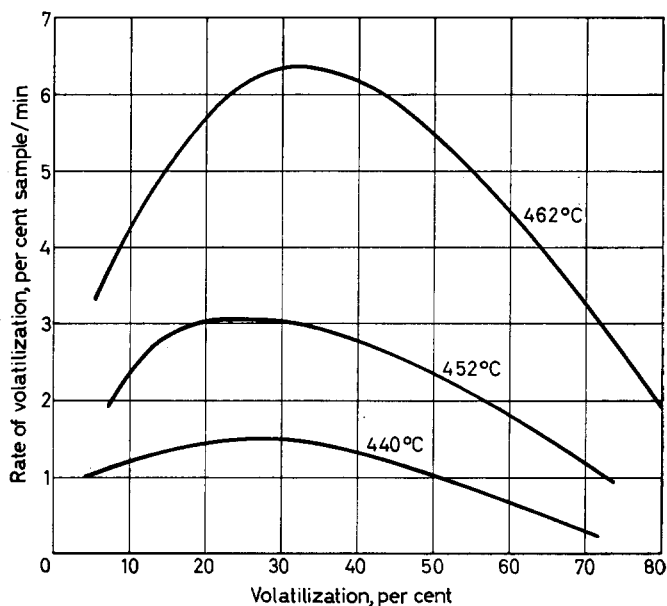


Figure 5—Rates of thermal degradation of poly(terephthaloyl *trans*-2,5-dimethylpiperazine) in a vacuum at 462°, 452° and 440°C

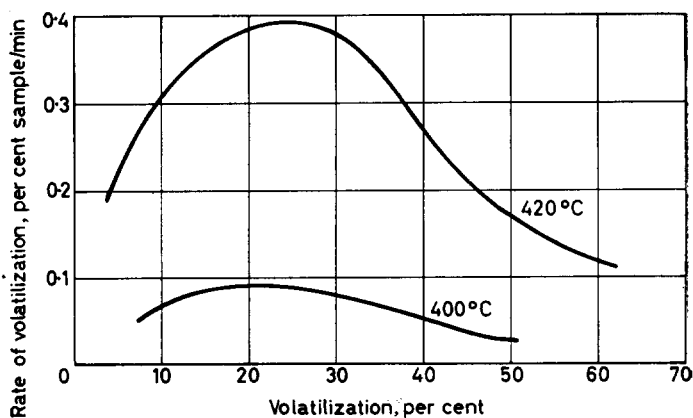


Figure 6—Rates of thermal degradation of poly(terephthaloyl *trans*-2,5-dimethylpiperazine) in a vacuum at 420° and 400°C

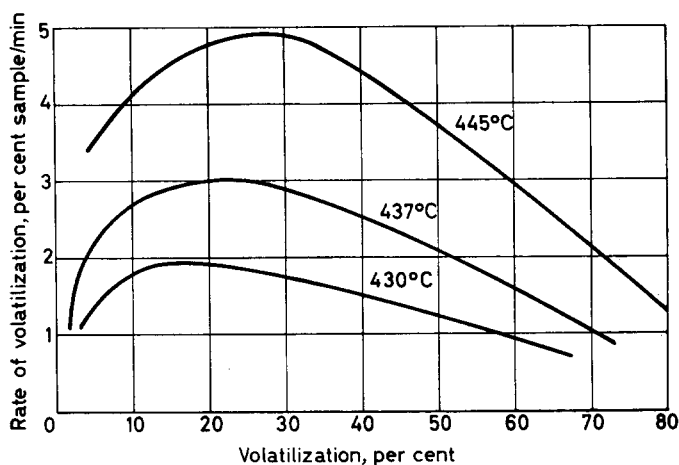


Figure 7—Rates of thermal degradation of poly(oxalyl *trans*-2,5-dimethylpiperazine) in a vacuum at 445°, 437° and 430°C

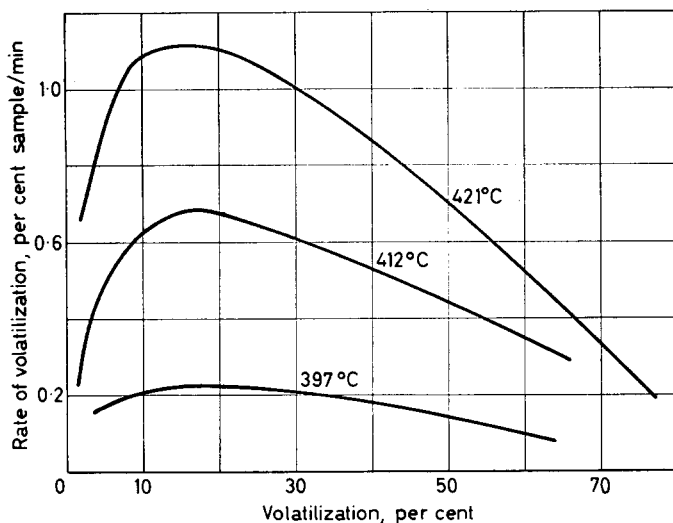


Figure 8—Rates of thermal degradation of poly(oxalyl *trans*-2,5-dimethylpiperazine) in a vacuum at 421°, 412° and 397°C

curves with the aid of an electronic computer. The data indicate the appearance of distinct maxima between 15 and 30 per cent volatilization in the case of the untreated samples.

The activation energies were obtained from the maximum rates of degradation using the well-known Arrhenius relationship ($k = Se^{-E/RT}$, where k is the rate constant, S is a frequency factor, E is the activation energy, R is the gas constant, and T denotes the absolute temperature). By plotting the logarithm of the maximum rates (here expressed in per cent of sample volatilized per minute) against the inverse of the absolute temperatures, straight

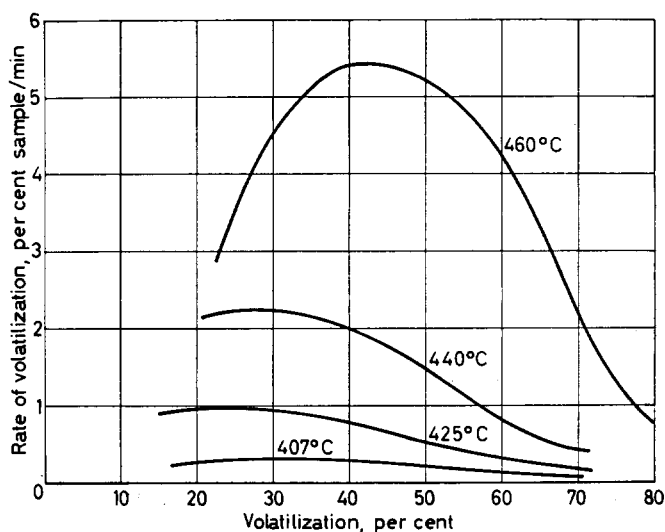


Figure 9—Rates of thermal degradation of sulphuric acid-treated poly(terephthaloyl *trans*-2,5-dimethylpiperazine) in a vacuum at 460°, 440°, 425° and 407°C

line relationships were obtained, as seen in *Figure 10*. The slopes of these lines gave activation energies of 64 kcal/mole for the thermal degradation of both poly(terephthaloyl *trans*-2,5-dimethylpiperazine) and poly(oxalyl

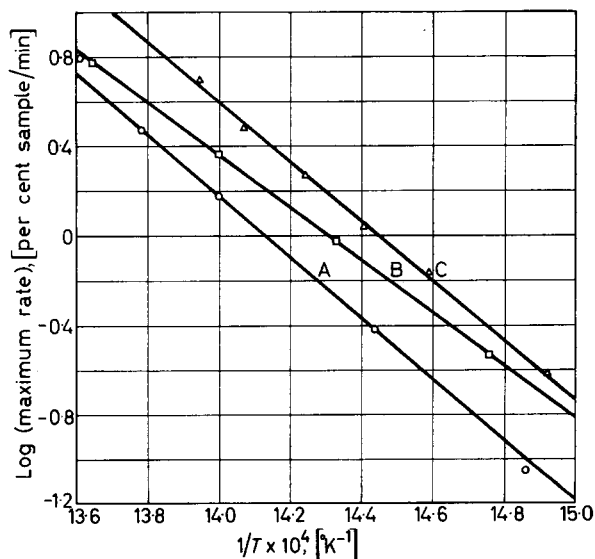


Figure 10—Arrhenius plot for thermal degradation in a vacuum of (A) poly(terephthaloyl *trans*-2,5-dimethylpiperazine), (B) sulphuric acid-treated poly(terephthaloyl *trans*-2,5-dimethylpiperazine) and (C) poly(oxalyl *trans*-2,5-dimethylpiperazine)

THERMAL DEGRADATION OF PIPERAZINE POLYAMIDES I

trans-2,5-dimethylpiperazine) and an activation energy for 55 kcal/mole for the thermal degradation of the sulphuric acid-treated sample of poly(terephthaloyl *trans*-2,5-dimethylpiperazine). In view of the early rapid weight loss of the sulphuric acid-treated sample, and because below 400°C the rates of degradation were complicated by side reactions, only four experimental points were available for the construction of the Arrhenius plot for this sample. Although the activation energies of poly(terephthaloyl *trans*-2,5-dimethylpiperazine) and poly(oxalyl *trans*-2,5-dimethylpiperazine) are the same, the maximum rates of degradation of the latter polymer are approximately two to three times faster. Table 1 summarizes the data on maximum rates and activation energies.

Table 1. Rates and activation energies for the thermal degradation in a vacuum of piperazine polyamides

Polymer	Pyrolysis temp. °C	Max. rate % sample/min	Activation energies kcal/mole
Poly(<i>t</i> -2,5-DMePip-T)*	462	6.342	64
	452	3.000	
	440	1.500	
	420	0.388	
	400	0.084	
Poly(<i>t</i> -2,5-DMePip-T) (H ₂ SO ₄ -treated)	460	5.400	55
	440	2.300	
	425	0.940	
	407	0.300	
Poly(<i>t</i> -2,5-DMePip-2)†	445	4.920	64
	437	3.000	
	430	1.880	
	421	1.110	
	412	0.678	
	397	0.229	

*Poly(*t*-2,5-DMePip-T) = poly(terephthaloyl *trans*-2,5-dimethylpiperazine).

†Poly(*t*-2,5-DMePip-2) = poly(oxalyl *trans*-2,5-dimethylpiperazine).

The thermal degradation profiles (Figure 4) of the sulphuric acid-treated sample of poly(terephthaloyl *trans*-2,5-dimethylpiperazine) indicate weight losses of up to 17 per cent (at least some of which is probably due to the removal of water) during the heating period required to reach isothermal conditions. Furthermore, the maxima in the rate curves (Figure 9) occur at somewhat higher conversions in comparison with the untreated samples.

To determine the degradation products volatile at room temperature, separate pyrolysis experiments were carried out in a closed system which had been evacuated to approximately 10⁻⁵ mm of mercury prior to sealing. Table 2 summarizes the results in mole per cent. The chief degradation product is carbon monoxide with lesser quantities of carbon dioxide, hydrogen, hydrocarbons, pyrazines and pyrroles. Ammonia was detected only in those samples which had not been treated with sulphuric acid prior to the pyrolyses. Water is probably not a product of the pyrolysis but rather

Table 2. Mass spectrometric analysis of degradation products volatile at room temperature of piperazine polyamides during pyrolysis in a vacuum (475°C, 1 h, $\sim 10^{-5}$ mm of mercury)

Component	Poly(<i>t</i> -2,5-DMePip-1) Mole %		Poly(<i>t</i> -2,5-DMePip-2) Mole %	
	Untreated	H ₂ SO ₄ - treated	Untreated	H ₂ SO ₄ - treated
Carbon monoxide	32.3	16.3	75.1	39.0
Carbon dioxide	10.2	2.9	3.3	11.1
Water	21.6	60.8	0.5	33.4
Ammonia	7.8	—	0.1	—
Hydrogen	*	4.0	5.4	2.5
Methane	8.6	5.4	6.9	3.6
Ethane	2.6	1.6	2.4	2.2
Propene	—	—	2.1	1.9
<i>n</i> -Butane	4.6	1.5	1.2	1.5
Butylene	—	—	0.6	0.8
2,5-Dimethylpyrazine	4.9	5.4	1.7	3.3
2-Methylpyrazine	—	—	0.4	0.1
Pyrrole	1.4	0.6	0.2	0.2
1-Methylpyrrole	0.3	0.3	0.1	0.2
2-Methylpyrrole	0.3	—	0.4	0.1
Benzoic acid	0.4	0.2	—	—
Benzaldehyde	0.3	0.1	—	—
<i>p</i> -Xylene	0.3	0.3	—	—
Benzonitrile	0.3	0.1	—	—
Toluene	1.3	0.6	—	—
Benzene	1.8	0.6	—	—
Phenol	0.9	0.3	—	—
Acetic acid	—	—	—	0.2
Total volatiles at room temperature, %	87.4	56.8	25.5	28.7
Total non-volatiles at room temperature, %	3.2 (est.)	29.8	73.5	68.3
Residue, %	9.4	13.4	1.0 (est.)	3.0

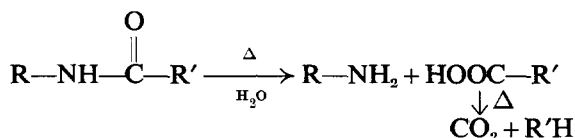
*Hydrogen present but not accurately determined due to instrumental difficulties.

originates from adsorbed moisture held by hydrogen bonds. The significance of these results will be discussed below.

DISCUSSION

The thermal degradation of both poly(terephthaloyl *trans*-2,5-dimethylpiperazine) and poly(oxalyl *trans*-2,5-dimethylpiperazine) gives rise to large quantities of carbon monoxide with only lesser amounts of carbon dioxide. The ratio of carbon monoxide to carbon dioxide is approximately 3.3 to 1 for poly(terephthaloyl *trans*-2,5-dimethylpiperazine), and 22.6 to 1 for poly(oxalyl *trans*-2,5-dimethylpiperazine). The increased production of carbon monoxide reflects the degradation of the oxalyl groups in the latter polymer. The appearance of large quantities of carbon monoxide is unlike the situation with aliphatic polyamides, where thermal degradation in a vacuum produced large quantities of carbon dioxide but only trace amounts (0.4 mole per cent or less) of carbon monoxide^{16,17}. With aliphatic poly-

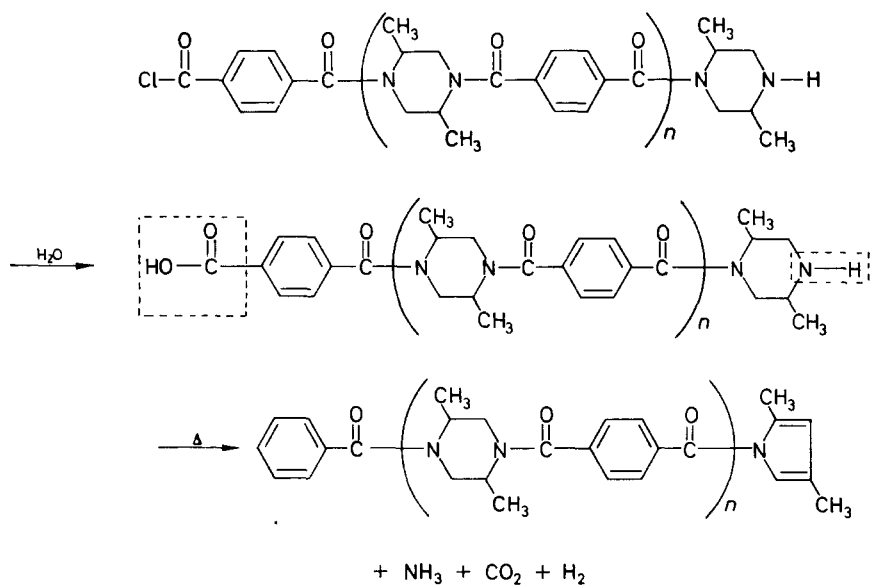
amides, carbon dioxide was shown by Straus and Wall^{16,17} to arise most probably from the hydrolytic breakdown of the peptide groups according to the following reaction



The addition of trace amounts of acids to aliphatic polyamides further increased the production of carbon dioxide, as expected from the above hydrolytic scheme.

It was of interest with the poly(terephthaloyl *trans*-2,5-dimethylpiperazine) sample that had been treated with sulphuric acid that there was an actual *decrease* in the production of carbon dioxide, with the ratio of carbon monoxide to carbon dioxide changing from 3.3 to 5.5. On the other hand, some increase in the production of carbon dioxide was observed with the sulphuric acid-treated poly(oxalyl *trans*-2,5-dimethylpiperazine) sample. This probably indicates the effect of a hydrolytic type degradation with the latter polymer. In neither case was any ammonia detected, in contrast to the untreated polymers.

The appearance of small quantities of ammonia with the untreated samples suggests the participation of end groups in the thermal degradation process. A possible mechanism for the evolution of ammonia may be illustrated by the transformation of the piperazine end groups of poly(terephthaloyl *trans*-2,5-dimethylpiperazine) to pyrroles, the latter having actually been identified among the volatile degradation products. The thermal degradation of the free carboxyl end groups will result in the evolution of carbon dioxide.

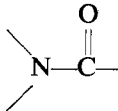


The apparent absence of ammonia from the sulphuric acid-treated samples is puzzling and the resolution of this problem must await the results of further investigation.

The presence of pyrazine and hydrogen in the volatile degradation products of both poly(terephthaloyl *trans*-2,5-dimethylpiperazine), and poly(oxalyl *trans*-2,5-dimethylpiperazine) indicates the dehydrogenation of the piperazine rings. Further degradation of these rings could give rise to the various hydrocarbons that were present in the volatile products, since the benzene groups in poly(terephthaloyl *trans*-2,5-dimethylpiperazine) are not expected to cleave at 475°C.

In addition to the degradation products volatile at room temperature, pyrolysis of the polymers produces oily materials (soluble in acetone) that were deposited in the combustion tube immediately next to the hot zone (Table 2). With poly(terephthaloyl *trans*-2,5-dimethylpiperazine) these degradation products constituted less than ten per cent by weight of the original sample, whereas with poly(oxalyl *trans*-2,5-dimethylpiperazine) they represented more than 70 per cent of the polymer. The i.r. spectra of these oily degradation products resembled those of the polymers but no further separation or analysis was attempted.

Simha and Wall¹⁸ have shown on theoretical grounds that for a random thermal degradation, the maxima in the rate curves should occur at about 26 per cent conversion. The character of the rate curves of both untreated poly(terephthaloyl *trans*-2,5-dimethylpiperazine) and poly(oxalyl *trans*-2,5-dimethylpiperazine), and the nature of the volatile degradation products point to a random thermal free radical degradation, with possibly a minor influence by hydrolytic mechanism. An activation energy of 64 kcal/mole for the thermal degradation in a vacuum of both piperazine polyamides suggests that the initiation of the degradation occurs at the C—N bond of the amide groups. It appears that, in contrast to the behaviour of aliphatic

polyamides, the  linkages of poly(terephthaloyl *trans*-2,5-dimethylpiperazine) and poly(oxalyl *trans*-2,5-dimethylpiperazine) are quite resistant to acid-catalysed hydrolytic breakdown at elevated temperatures.

The author thanks Mr S. J. Burdick for technical assistance in some phases of the work, and Mrs Ardith I. Bailey for typing the manuscript. The mass spectrometric analyses were carried out by Mr William H. Dorko of the National Bureau of Standards.

*Applied Physics Laboratory,
The Johns Hopkins University,
8621 Georgia Avenue,
Silver Spring, Maryland, U.S.A.*

(Received March 1965)

REFERENCES

- ¹ BRUCK, S. D. *Polymer, Lond.* 1964, **5**, 435
- ² BRUCK, S. D. *Polymer, Lond.* 1965, **6**, 49
- ³ BRUCK, S. D. *Polymer, Lond.* 1965, **6**, 319
- ⁴ BRUCK, S. D. in *Vacuum Microbalance Techniques*, Vol. IV (edited by P. M. WATERS) Plenum Press: New York, 1965
- ⁵ BRUCK, S. D. *J. chem. Educ.* 1965, **42**, 18
- ⁶ BAWN, C. E. H. *New Scientist*, 1964, No. 375, 224
- ⁷ WALLENBERGER, F. T. *Angew. Chem.* 1964, **76**, 484
- ⁸ FRAZER, A. H., SWEENEY, W. and WALLENBERGER, F. T. *J. Polym. Sci.* 1964, **A2**, 1157
- ⁹ HERGENROTHER, P. M., WRASIDLO, W. and LEVINE, H. H. *Polymer Preprints*, 1964, **5**, 153, 147th National Meeting, American Chemical Society, Philadelphia, Pa, April 1964
- ¹⁰ LEVINE, H. H., DELANO, C. B. and KJOLLER, K. J. *Polymer Preprints*, 1964, **5**, 160, 147th National Meeting, American Chemical Society, Philadelphia, Pa, April 1964
- ¹¹ STILLE, J. K. and WILLIAMSON, J. R. *Polymer Preprints* 1964, **5**, 185, 147th National Meeting, American Chemical Society, Philadelphia, Pa, April 1964
- ¹² PRESTON, J. and DOBINSON, F. *J. Polym. Sci.* 1964, **B2**, 1171
- ¹³ MORGAN, P. W. and KWOLEK, S. L. *J. Polym. Sci.* 1964, **A2**, 181
- ¹⁴ MORGAN, P. W. and KWOLEK, S. L. *J. Polym. Sci.* 1964, **A2**, 209
- ¹⁵ BRUCK, S. D. and BAIR, H. E. *Polymer, Lond.* 1965, **6**, 447
- ¹⁶ STRAUS, S. and WALL, L. A. *J. Res. nat. Bur. Stand.* 1958, **60**, 39
- ¹⁷ STRAUS, S. and WALL, L. A. *J. Res. nat. Bur. Stand.* 1959, **63A**, 269
- ¹⁸ SIMHA, R. and WALL, L. A. *J. phys. Chem.* 1952, **56**, 707

Propagation Reactions in the Copolymerization of Styrene and *p*-Chlorostyrene by Perchloric Acid

G. R. BROWN and D. C. PEPPER

The kinetics of the homopolymerization of *p*-chlorostyrene by perchloric acid in ethylene dichloride have been found to be similar to those of styrene but with a lower value of the propagation rate constant at 25°: $k_p = 290 \text{ l. mol}^{-1} \text{ min}^{-1}$. The copolymer compositions in copolymerization with styrene yield values of the reactivity ratios

$$r_1 (\text{styrene}) = 2.0 \pm 0.2, \quad r_2 = 0.43 \pm 0.05$$

very similar to values found with Friedel-Crafts catalysts. Combination of these results with the value of the homopropagation rate constant for styrene, $k_{11} = 1050$, under the same conditions yields values for the cross-propagation constants

$$k_{12} = 525 \text{ l. mol}^{-1} \text{ min}^{-1} \quad \text{and} \quad k_{21} = 670 \text{ l. mol}^{-1} \text{ min}^{-1}$$

The propagating species derived from styrene is therefore more reactive than that from *p*-chlorostyrene, i.e. the opposite effect to that expected if the propagating species were a free carbonium ion. A complex mechanism for the propagation reaction is indicated.

THE kinetics of polymerization of styrene by perchloric acid are most simply interpreted¹⁻³ on the hypothesis that initiation is very fast, there is no termination, and consequently the overall rates yield the propagation rate constant directly.

If so, a combination of homopolymerization kinetics and copolymer compositions can in principle yield the cross-propagation constants and hence the relative reactivities of the growing species as well as those of the two monomers.

In this study the cross-propagation constants have been derived by this method for styrene and *p*-chlorostyrene at 25°C. They indicate that the more reactive monomer (styrene) yields also the more reactive propagating species, the reverse of the behaviour found in most free radical polymerizations, and expected also in propagation by 'free' carbonium ions.

EXPERIMENTAL

Materials

p-Chlorostyrene (Koch) was washed with ten per cent aqueous sodium hydroxide, dried over calcium hydride and distilled *in vacuo* using a 2 ft pear column with reflux head. First and last fractions showed slight impurities (GLC, 5 ft SAIB column at 190°) but the middle fraction used (b.pt 49°/2 mm) only traces. This material was stored over calcium hydride *in vacuo* and subjected to molecular distillation immediately before use.

Perchloric acid was obtained by distillation *in vacuo* at 50°C from a mixture of 32 ml of concentrated analytical reagent grade sulphuric acid and 8 ml of analytical reagent grade 72 per cent aqueous perchloric acid, the anhydrous acid being condensed into ampoules, sealed off under vacuum and stored in liquid nitrogen. The catalyst solutions were prepared by breaking the ampoules into ethylene dichloride in an atmosphere of dry nitrogen.

Techniques

Rates of polymerization were measured in a double-limb annular dilatometer of the type described by Pepper and Reilly³.

Copolymerizations were carried out at 25°C in glass-stoppered test tubes under dry nitrogen, the monomers being weighed in from syringes, followed by catalyst solution to give a final concentration of monomers 5 per cent v/v and perchloric acid about 1.5×10^{-4} molar. The reactions were stopped with methanol after about 20 per cent conversion and unchanged monomers and solvents removed by steam distillation followed by pumping in a vacuum oven at 50°C. The copolymer compositions were determined by chlorine analysis using Schoninger's method⁴. All polymers were white and brittle solids.

RESULTS

Polymerization of *p*-chlorostyrene

The reactions (all at initial monomer concentration of 5 per cent v/v $\equiv 0.39$ M) were found to be of the first order in monomer concentration over the whole observable range 10 to 90 per cent of conversion. The observed first order constants were proportional to the perchloric acid concentration (Figure 1) over the whole range studied (0.24 to 1.2 mM).

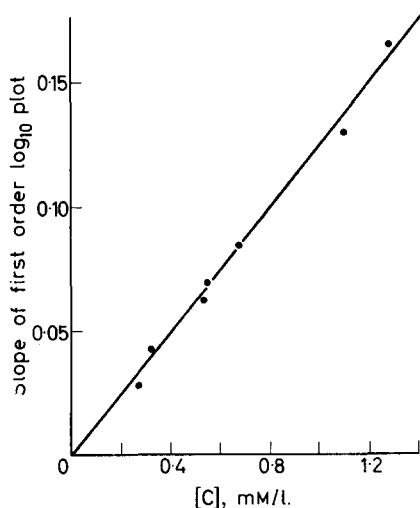


Figure 1—Effect of catalyst concentration

THE COPOLYMERIZATION OF STYRENE AND *p*-CHLOROSTYRENE

The derived rate constant, identified with that of propagation, is $290 \text{ l. mol}^{-1} \text{ min}^{-1}$ at 25°C .

Copolymerization with styrene at 25°C

The copolymer composition curve is shown in *Figure 2*, where the mole fractions are corrected values calculated according to Overberger *et al.*⁵

Figure 2—Copolymer composition curve

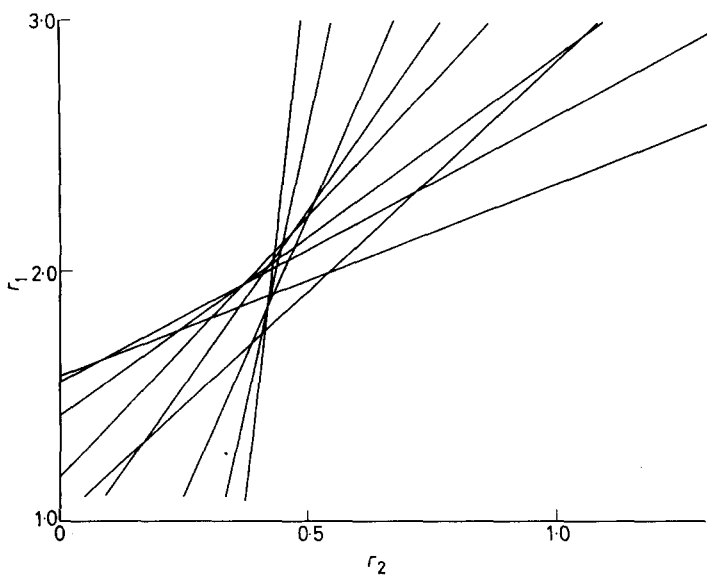
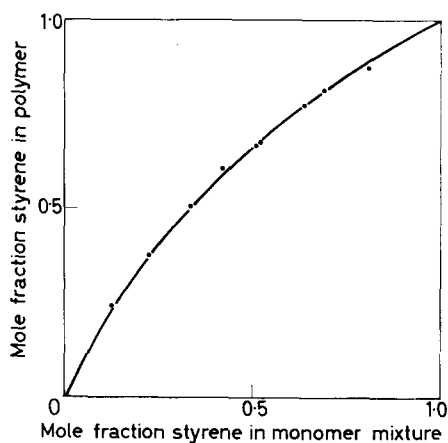


Figure 3—Mayo-Lewis plot

Reactivity ratios were calculated using the integrated form of the Mayo-Walling equation, the Mayo and Lewis plot being shown in *Figure 3*. The derived values

$$r_1 (\text{styrene}) = 2.0 \pm 0.20; \quad r_2 = 0.43 \pm 0.05$$

are weighted means calculated by the graphical adaptation of the Joshi and Kapur method.

A few molecular weights (\bar{M}_n) were measured in solution in benzene using a Mechrolab vapour pressure osmometer, with the following results:

Mole fraction styrene	0	0.376	0.662	0.770
\bar{M}_n	1 385	1 460	1 360	1 460

DISCUSSION

The simple first order kinetics of polymerization of *p*-chlorostyrene are similar to those found earlier for styrene². The rate constant will therefore be similarly identified with that of propagation. Its value 290 l. mol⁻¹ min⁻¹ is then to be compared with that of 1 020 l. mol⁻¹ min⁻¹ found for styrene under the same conditions of monomer concentration, solvent and temperatures, or more realistically with the value 1 050 l. mol⁻¹ min⁻¹, if the rates are to be compared in solutions of identical dielectric constant ($\epsilon=9.83$).

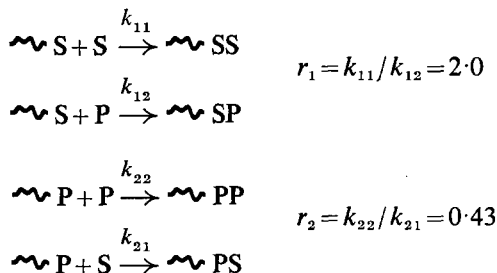
The lower rate shown by *p*-chlorostyrene accords with general expectations from the deactivating effect of the chlorine substituent.

The reactivity ratios are very similar to values previously found for these monomers with other initiators of 'cationic' polymerization, e.g.

Initiator	r_1 (styrene)	r_2 (<i>p</i> -chlorostyrene)	Ref.
HClO ₄	2.0	0.43	This work
I ₂	2.5	0.45	6
BF ₃ .Et ₂ O	1.4	0.55	7
Ten different F.C. halides, mean values	2.1	0.40	8

The copolymerization of these monomers with perchloric acid, as with most of the above initiators, is thus approximately 'ideal', in that $r_1 \approx 1/r_2$, and largely unaffected by the nature of the initiator. This is far from true with some other monomer pairs in cationic copolymerization; the reason for simple behaviour in the present system may be connected with the general close similarity of the two monomers.

The various propagation constants can now be derived as follows:



where S and P denote styrene and *p*-chlorostyrene respectively. From the homopolymerizations, $k_{11}=1\,050$ and $k_{22}=290$. Hence $k_{12}=525$ and $k_{21}=670$ (units of all k are l. mol⁻¹ min⁻¹).

It is clear that the more reactive monomer (styrene) gives the more reactive propagating species, and that the relative reactivities of these species depend only slightly on the monomer being attacked, i.e. $k_{11}/k_{21}=1.6$ (compared with styrene) and $k_{12}/k_{22}=1.8$ (compared with *p*-chlorostyrene).

This same behaviour has been deduced by Kanoh *et al.*⁶ in the iodine-initiated copolymerization of this pair of monomers. With isobutyl vinyl ether and 2-chloroethyl vinyl ether they found the 'normal' behaviour, that the more reactive monomer (IBVE) gives the *less* reactive propagating species, which is to be expected on grounds of carbonium ion stability, if the reacting species is a free carbonium ion. They conclude that the abnormal behaviour of the styrene-type monomers can be explained if the propagating species are ion-pairs, to which monomer must be coordinated, and polarized, in the transition state.

The present results with perchloric acid confirm the 'abnormal' behaviour of these styrene-type monomers. It does not seem possible, however, to make any detailed interpretation at present, since evidence about the nature of the propagation species is conflicting. Hitherto the choice has seemed to lie between free carbonium ions or ion-pairs, but Gandini and Plesch^{9,10} have found evidence (from the absence of conductance and characteristic spectra) that neither of these species is present *during* the polymerization of styrene by perchloric acid. They call the propagating species 'pseudo cationic' and regard it as a perchlorate ester, stabilized by coordinated monomer molecules. Such a species might conceivably have the higher reactivity indicated by our results, but until its existence is more firmly established it seems premature to speculate further.

Trinity College,
Dublin

(Received March 1965)

REFERENCES

- ¹ PEPPER, D. C. and REILLY, P. J. *Proc. chem. Soc.* **1961**, 200
- ² PEPPER, D. C. *J. Polym. Sci.* 1962, **58**, 639
- ³ PEPPER, D. C. and REILLY, P. J. *Proc. Roy. Soc. A*, in press
- ⁴ SCHONINGER, W. *Mikrochim. Acta*, 1955, **1**, 123
- ⁵ OVERBERGER, C. G., EHRIG, R. J. and TANNER, D. J. *Amer. chem. Soc.* 1954, **76**, 773
- ⁶ KANO, N. *et al. Makromol. Chem.* 1963, **63**, 115
- ⁷ SAOTOME, K. and IMOTO, M. *J. chem. Soc. Japan*, 1959, **62**, 1130
- ⁸ OVERBERGER, C. G. *et al.* quoted by D. C. PEPPER, Chap. XXX of G. A. OLAH. *Friedel-Crafts and Related Reactions*, Vol. II, Pt II, p 1338. Interscience: London, 1964
- ⁹ GANDINI, A. and PLESCH, P. H. *Proc. chem. Soc.* **1964**, 240
- ¹⁰ GANDINI, A. and PLESCH, P. H. *J. Polym. Sci. Part B*, 1965, **3**, 127

The $n \rightarrow \pi^$ Transition of the Carbonyl Group and Polymer Stereoregularity*

W. M. PASIKA and R. BRANDON

*The u.v. spectra of dilute solutions of atactic and isotactic poly(*N,N*-dimethylacrylamide) have been studied. Hyperchromaticity has been observed for the $n \rightarrow \pi^*$ absorption band. It is suggested that this effect may be due to vibronic effects or more likely to a developing helical conformation in solution.*

CHARACTERIZATION of the u.v. spectra of low molecular weight compounds has received considerable attention from experimental and theoretical spectroscopists. The electronic absorption spectra of synthetic vinyl polymers, however, have not been studied to any extent despite the fact that there are a large number of such polymers which contain chromophoric groups. As part of a general study and because electronic absorption spectra are sensitive to the environment of and structural variations in a molecule, we decided to examine the u.v. spectra of atactic and isotactic poly(*N,N*-dimethylacrylamide).

EXPERIMENTAL

Atactic poly(*N,N*-dimethylacrylamide) was prepared at room temperature by photo-decomposing 2,2'-azobis(2-methylpropionitrile) in a monomer-toluene solution. The usual precautions for such a free radical preparation were taken. The polymer was purified by repeated precipitations in several two litre volumes of diethyl ether, after which the polymer was dried on a high vacuum line.

Isotactic poly(*N,N*-dimethylacrylamide) was prepared in a dry box at room temperature, using a commercial lithium butyl preparation as initiator. The required number of millilitres of lithium butyl-hexane solution was put into the polymerization flasks and the hexane driven off with dry nitrogen. To this flask toluene was added and after solution was effected the *N,N*-dimethylacrylamide poured in. Polymer precipitated immediately. The heterogeneous mixture was allowed to remain in the dry box overnight. The next day methanol was added to destroy any active centres and to dissolve the polymer. Isolation and purification were effected as with the atactic modification.

Evidence that different steric modifications had been prepared could be ascertained from the melting points of the samples. The atactic polymer samples had melting points in the range 155°C to 185°C, whereas the isotactic ones had melting points in the range 250°C to 270°C. This difference in melting point range is comparable to that reported by Butler, Thomas and Tyler¹; atactic 100°C, isotactic 300°C. Also, qualitatively it was observed that the isotactic polymer dissolved more slowly than the atactic one. This observation is in agreement with the general experience of others who have worked with polymers of differing steric modification.

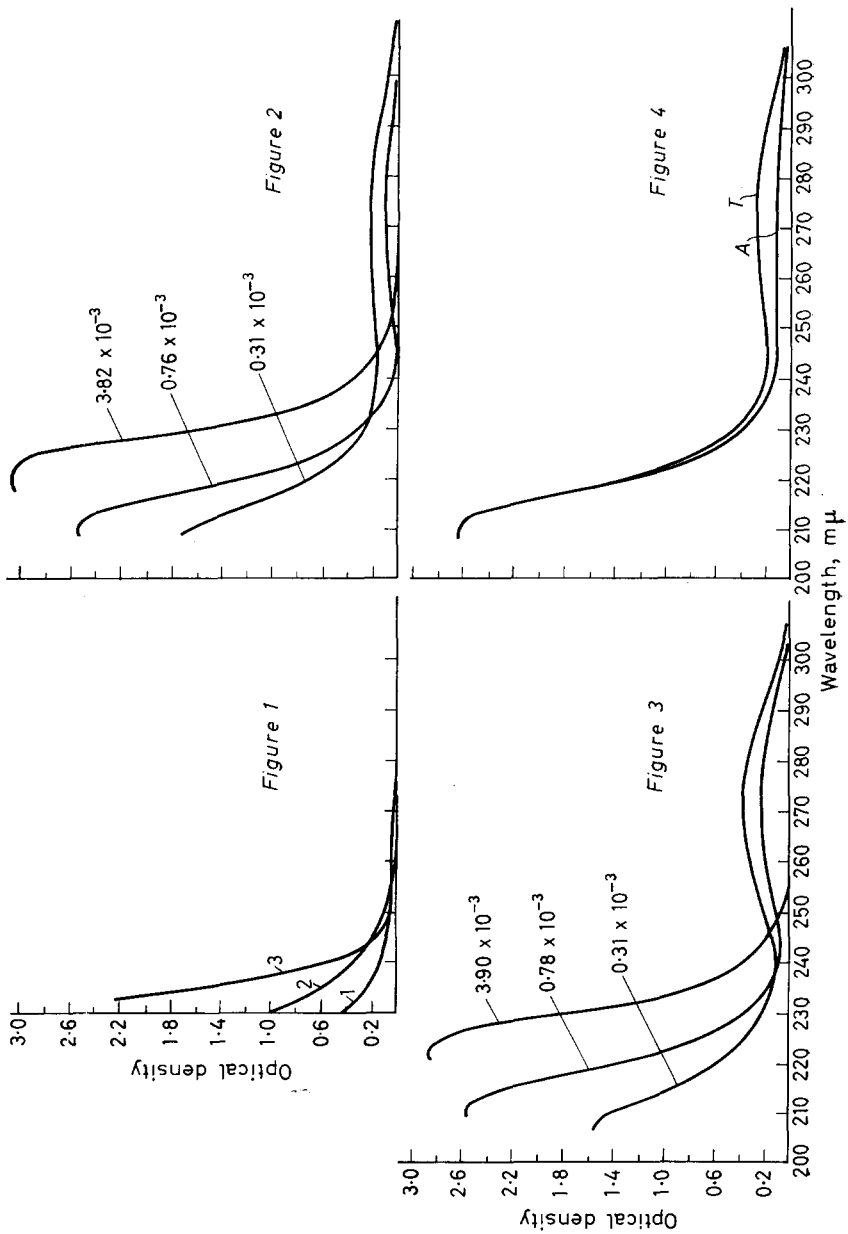


Figure 1—Spectra of *N,N*-dimethylacetamide in (1) methanol, conc. 1.6×10^{-3} M; (2) hexane, conc. 4.87×10^{-3} M; (3) methanol, conc. 2.0×10^{-2} M

Figure 2—Ultra-violet spectra of atactic poly(*N,N*-dimethylacrylamide) in methanol at the molar concentrations indicated

Figure 3—Ultra-violet spectra of tactic poly(*N,N*-dimethylacrylamide) in methanol at the molar concentrations indicated

Figure 4—Ultra-violet spectra of atactic (*A*) and tactic (*T*) poly(*N,N*-dimethylacrylamide) methanol solutions, 0.78×10^{-3} gMC in polymer and 15.6×10^{-3} M in water

Ultra-violet spectra were obtained at room temperature with the aid of a Unicam SP-500 spectrophotometer using 1 cm quartz cells.

Purification of *N,N*-dimethylacrylamide was by fractionation under vacuum and *N,N*-dimethylacetamide by fractionation at atmospheric pressure.

Solvents used were redistilled analytical reagent grade methanol, spectroscopic grade hexane and doubly distilled water.

Micro amounts of water were measured with the aid of a microlitre syringe.

RESULTS

The u.v. spectra of *N,N*-dimethylacetamide in methanol and in hexane are shown in Figure 1. Spectra of atactic and isotactic poly(*N,N*-dimethylacrylamide) in methanol are reproduced in Figures 2 and 3. In Figure 4 are shown the spectra of methanol solutions of atactic and isotactic poly(*N,N*-dimethylacrylamide) which contained small amounts of water.

The spectra of atactic and isotactic poly(*N,N*-dimethylacrylamide) indicate a decrease in the intensity of the absorption in the $220 \text{ m}\mu$ region as the gram-molar concentration (gMC) is lowered. (gMC refers to the molar concentration of monomeric residue.) These spectra also reveal a broad peak of low intensity (maximum $270 \text{ m}\mu$) which did not shift upon dilution or decrease in intensity but decidedly *increased* in intensity. For both the atactic and isotactic poly(*N,N*-dimethylacrylamide) the optical density (OD) at $270 \text{ m}\mu$ for a 3.90×10^{-3} gMC was < 0.01 but on dilution to 0.31×10^{-3} gMC the OD increased for the atactic sample to 0.20 and for the isotactic sample to 0.39.

The spectra of *N,N*-dimethylacetamide in methanol and hexane reveal no broad absorption in the region of $270 \text{ m}\mu$.

The addition of water to methanol solutions of atactic and isotactic poly(*N,N*-dimethylacrylamide) has no effect on the absorption in the $220 \text{ m}\mu$ region but increases the absorption in the region $240 \text{ m}\mu$ to $250 \text{ m}\mu$.

DISCUSSION

The fact that the poly(*N,N*-dimethylacrylamide) used in this study had a melting point some 50°C higher than Butler, Thomas and Tyler¹ reported for their sample would suggest that samples of lower tacticity can be prepared. Therefore it would be expected that our atactic sample might show some isotactic characteristics. The isotactic sample no doubt would not be 100 per cent isotactic.

The model compound *N,N*-dimethylacetamide did not show any absorption in the 270 $m\mu$ region in either hexane or methanol solutions. One would not expect the *N,N*-dimethylacetamide to have absorption characteristics different from the monomer residue of the polymer chain—that of a saturated dimethyl substituted amide. Therefore, if no unusual effects were operative in our polymeric system we would expect to see no evidence for a transition in the 270 $m\mu$ region.

The fact that the polymer samples in dilute solution absorbed at 270 $m\mu$ would suggest that this absorption is a property of the polymer structure. Since the absorption is greater for the isotactic polymer sample and since we cannot rule out the presence of a certain degree of isotacticity in the atactic sample, it is not unreasonable to assign the 270 $m\mu$ absorption band to the presence of isotacticity.

It is generally agreed that the electronic absorption bands possessed by carbonyl functions in the 220 $m\mu$ and 270 $m\mu$ region belong to the $V \leftarrow N$ or $\pi \rightarrow \pi^*$ transition and the $Q \leftarrow N$ or $n \rightarrow \pi^*$ transition respectively. That the broad weak absorption detected at 270 $m\mu$ is one associated with an $n \rightarrow \pi^*$ transition can be ascertained by observing what happens to the spectrum when water is added to the methanol solution of polymer. Complexation of the lone pair electrons by the strong hydrogen bonding water molecules should cause a hypsochromic or blue shift of the absorption band responsible for the $n \rightarrow \pi^*$ transition. Small amounts of water added to the methanol solutions of atactic and isotactic poly(*N,N*-dimethylacrylamide) increased the absorption in the region 240 to 250 $m\mu$. This fact is demonstrated quantitatively in *Table 1* where the ratio *R* of the OD at 245 $m\mu$

Table 1. Ratio (*R*) of absorption at 245 $m\mu$ to that at 270 $m\mu$ of poly(*N,N*-dimethylacrylamide) polymer samples. R_1 is the ratio of *R* for the system with water to that without water, indicating the effect of water on the absorption in the region, 245 $m\mu$

Sample	245 $m\mu$	270 $m\mu$	$R = \frac{OD\ 245\ m\mu}{OD\ 270\ m\mu}$	R_1
(a) Isotactic H_2O	0.190	0.270	0.705	$\frac{R_a}{R_b} = \frac{0.705}{0.446} = 1.58$
(b) Isotactic	0.107	0.240	0.446	
(c) Atactic H_2O	0.119	0.099	1.20	$\frac{R_c}{R_d} = \frac{1.20}{0.244} = 4.92$
(d) Atactic	0.020	0.082	0.244	

to the OD at 270 $m\mu$ is listed for polymer-methanol solutions with and without water. R_1 , indicative of this effect of water, is the ratio of *R* for the system with water to that without.

Since solution of *N,N*-dimethylacetamide did not show any absorption in the 270 $m\mu$ region it is tempting to put forward the explanation that it is the isotacticity or proximity of neighbouring groups which might cause vibronic effects allowing the $n \rightarrow \pi^*$ transition to occur. As dilution of the sample is effected more amide groups are allowed the particular freedom of motion responsible for the vibronic effects and absorption in the 270 $m\mu$ region increases.

A large number of X-ray studies on various isotactic polymer samples indicates that these steric modifications exist in the solid state in the form of helices. The suggestion that these same materials exist in solution as helices has also been made (but not proved). If this is so, the hyperchromism we observed in our samples could alternatively be interpreted in the 'light' of the absorption characteristics of stacked chromophores.

It has been suggested that hyperchromism and hypochromism are a direct result of the geometric arrangement of chromophores with respect to one another^{2,3}. If the chromophores are so arranged that the transition moments of a particular transition are parallel to one another, then hypochromism occurs. If the transition moments are lined up end on end then hyperchromism occurs. Experimental evidence for these concepts has been obtained for only one system to date, namely deoxyribonucleic acid (DNA)^{2,4} which can occur as either a helix or a random coil. In the helix the $\pi \rightarrow \pi^*$ transition moments of the bases are parallel and hence hypochromism is observed² for the absorption band associated with $\pi \rightarrow \pi^*$ transition on going from the random coil to the helical configuration. The $n \rightarrow \pi^*$ transition moments of the bases, on the other hand, are perpendicular to the $\pi \rightarrow \pi^*$ transition moments, that is, the transition moments are lined up. Hyperchromism, therefore, is expected and has been observed⁴ for the absorption band associated with the $n \rightarrow \pi^*$ transition of the DNA bases.

It is known that isotactic poly(*N,N*-di-*n*-butylacrylamide) exists in the solid state as a 3_1 helix⁵. It is not unreasonable to expect that poly(*N,N*-dimethylacrylamide) might have a helical configuration in solution and chromophore stacking.

Hyperchromaticity with dilution was very evident for the $n \rightarrow \pi^*$ absorption band in our polymer solution spectra. This could mean that on dilution the poly(*N,N*-dimethylacrylamide) macromolecule changed its configuration in such a way that the chromophores and, therefore, the transition moments associated with the $n \rightarrow \pi^*$ transition lined up linearly producing the observed hyperchromaticity. Hyperchromaticity is thus a result of chromophore stacking, chromophore stacking a result of helicity and helicity a result of isotacticity.

It is a pleasure to thank Professor C. E. H. Bawn for his interest and for facilities provided during the course of the above research.

*Donnan Laboratories,
University of Liverpool*

(Received April 1965)

REFERENCES

- ¹ BUTLER, K., THOMAS, P. R. and TYLER, G. J. *J. Polym. Sci.* 1960, **48**, 357
- ² TINOCO JR, I. J. *Amer. chem. Soc.* 1960, **82**, 4785
- ³ TINOCO JR, I. J. *chem. Phys.* 1960, **33**, 1332
- ⁴ KASHA, M. *Light and Life*. Edited by W. D. McELROY and B. GLASS, p 31. Johns Hopkins Press: Baltimore, 1961
- ⁵ BADAMI, D. V. *Polymer, Lond.* 1960, **1**, 273

Communication and Note

The Polymerization of Ethylene Oxide by Some Organozinc Compounds

EPOXIDES have been polymerized¹⁻⁸ with the products from reactions between dialkylzincs, R_2Zn , and alcohols, $R'OH$, and both alkylzinc alkoxides^{2,8}, $RZnOR'$, and zinc alkoxides^{1,4,5,7}, $Zn(OR')_2$, have been suggested to be catalytically active, although it has also been stated⁵ that ethylzinc alkoxides are not catalysts. The catalyst has usually been prepared in the presence of the epoxide, but since epoxides form complexes^{9,10} with dialkylzincs it is possible that the catalytically active materials result from an alcoholysis reaction involving both the epoxide and the dialkylzinc, and it was therefore of interest to examine the reactions with ethylene oxide of some alcoholysis products preformed in the absence of monomer. The results of preliminary spectroscopic studies, using a high ratio of organozinc compound to ethylene oxide in an attempt to detect products formed in the early stages of the reaction, are described in the present Communication.

The products from alcoholyses of dialkylzincs have been studied by i.r. spectroscopy^{5,8}, but more recent investigations of the methanolysis¹¹ and *t*-butanolysis¹² of dimethyl- and diphenyl-zinc by proton magnetic resonance spectroscopy have shown that the systems are more complex than was previously believed¹³. Thus the monomethanolysis products, empirically $RZnOMe$, exist in benzene solution as mixtures involving equilibria between R_2Zn , aggregates of the type $(RZnOMe)_n$ which, particularly when $R=Ph$, probably contain appreciable contributions from complexes $[R_2Zn, Zn(OMe)_2]_m$, and species which are empirically $R_6Zn_7(OMe)_8$. The latter can be prepared directly from R_2Zn and methanol in the molar ratio 7:8; a higher proportion of methanol yields zinc methoxide. The *t*-butanolysis products appear to contain only aggregates of true organozinc alkoxides $(RZnOBu^t)_n$.

For the polymerization experiments a mixture of the organozinc compound (equivalent to 0.3 g atom l^{-1} of zinc, and approximately so for suspensions of insoluble compounds), ethylene oxide (2 g mole l^{-1}), and benzene (or hexadeuteriobenzene for phenylzinc compounds) was prepared *in vacuo* in a sample tube which could be sealed and inserted in a Varian A-60 proton magnetic resonance spectrometer. Where possible the spectrum was measured initially and then at intervals between which the sample was maintained at an appropriate temperature, usually 40°C or 70°C. Polymerization was indicated by a decrease in the intensity of the resonance at τ 7.85 (measured relative to that at 2.80 due to the benzene or the proton impurity in the hexadeuteriobenzene) due to ethylene oxide, and a corresponding increase in the intensity of the resonance at τ 6.50 due to

the polymer, and, except for reactions involving zinc *t*-butoxide, by an increase in viscosity. For some experiments the benzene was omitted, and the organozinc compounds, at similar concentrations, were allowed to react with undiluted ethylene oxide: polymerization occurred more rapidly than in the presence of benzene, and in some cases the formation of a white solid product was so rapid that spectroscopic measurements could not be made. All the mixtures were initially homogeneous except for those containing zinc alkoxides which are insoluble in both benzene and ethylene oxide. The polymers were not isolated.

Polymerization of ethylene oxide had proceeded to the extent of only 35 per cent even after it had been heated with dimethylzinc in benzene at 130°C for 42 days. The intensity of the resonance at τ 10.62 due to dimethylzinc did not change, indicating a negligible reaction (cf. ref. 9) with the monomer and suggesting that polymerization was a consequence of adventitious catalysis. With 'MeZnOMe', conversion of monomer to polymer was 40 per cent after 84 days at 70°C, but with 'Me₆Zn₇(OMe)₈' conversion was quantitative after two days at 70°C; there was no spectroscopic evidence for consumption of methyl or methoxyl residues. This increased activity as the proportion of methoxyl groups is increased suggests that zinc methoxide should be particularly active, and this was found to be so. Thus zinc methoxide prepared by treatment of dimethylzinc in benzene with an excess of methanol at 20°C and subsequent removal of the volatile materials, finally at 20°C and 10⁻⁵ mm of mercury, had caused complete polymerization of ethylene oxide in benzene after 2½ hours at 20°C. However, the zinc methoxide prepared in this way contains unreacted methylzinc residues, and is solvated by methanol. Both impurities can be removed at 180°C and 10⁻⁵ mm of mercury, and the product is then even more reactive, causing quantitative polymerization of the undiluted monomer within minutes; the reaction starts at a temperature below 0°C, is strongly exothermic, and gives a product which is a white solid at room temperature. The greater reactivity of the methoxide which has been heated at 180°C and 10⁻⁵ mm of mercury is probably due to the removal of methanol of solvation, since the less active form can be regenerated by soaking the more active material in methanol and then pumping at 20°C and 10⁻⁵ mm of mercury; heating at 180°C and 10⁻⁵ mm of mercury restores the activity.

Initially the proton magnetic resonance spectrum of the supernatant liquid in polymerizations catalysed by zinc methoxide which has been pumped at 20°C and 10⁻⁵ mm of mercury showed only a monomer resonance, but as polymerization proceeded bands of low intensity appeared at τ 6.10 and 6.83, on each side of the absorption due to the polymer. These may have been due to species of the form MeOZn(OCH₂CH₂)_nOMe which would arise by insertion⁴ of monomer units at the zinc-oxygen bond, since benzene solutions of the products empirically MeZn(OCH₂CH₂)_nOMe, for which $n=1$ and 2, formed by treatment of dimethylzinc with the mono-methyl ethers of ethylene glycol and diethylene glycol respectively, show resonances in similar positions, e.g. when $n=1$, $\tau=6.13$ (triplet), 6.72 (triplet), and 6.87 (singlet) in the intensity ratio 2:2:3, and when $n=2$, $\tau=6.04$ (triplet), 6.54 (sextet), and 6.83 (singlet) in the ratio 2:6:3, thus

indicating that the absorption in the τ 6.10 region is due to the protons of the methylene group nearest to the zinc, and that at 6.83 to terminal methoxyl groups. This observation is in agreement with a recent report⁴ that treatment of propylene oxide with a catalyst prepared *in situ* from diethylzinc and ¹⁴C-methanol yields a polymer containing radiocative methoxyl end groups. The species 'MeZn(OCH₂CH₂)_nOMe', for which $n=0,1$ and 2 , are all of similar, low reactivity towards ethylene oxide.

Unlike dimethylzinc, diphenylzinc reacts comparatively rapidly with ethylene oxide, and as polymerization proceeds the proton magnetic resonance spectrum of the solution in hexadeuteriobenzene changes from that characteristic¹⁰ of a diphenylzinc etherate (two groups of bands centred at, respectively, τ 2.4 and 2.7 with intensities in the ratio 2:3 due to the aromatic protons, and a singlet at τ 7.82 due to the ethylene oxide) to a more complex one containing additional multiplets at τ 2.0 and 7.2 which are tentatively assigned, respectively, to the *o*-aromatic and the benzylic protons in a system of the type PhZn(OCH₂CH₂)_nPh, thus providing further evidence for transfer of a group, in this case phenyl, from the organozinc compound to the monomer. The species 'PhZnOMe' and 'Ph₆Zn₇(OMe)₈' are progressively more active than diphenylzinc, and all the members of the phenylzinc series are more active than the corresponding methyl compounds.

The *t*-butanolysis products show rather different activity. Thus whereas (MeZnOBu')_n is more active than 'MeZnOMe' but less active than 'Me₆Zn₇(OMe)₈', in the phenyl series (PhZnOBu')_n is more active towards ethylene oxide than 'Ph₆Zn₇(OMe)₈', and rapidly leads to the formation of a transparent gel from the benzene solution, and an opaque white solid from the undiluted monomer. This is contrary to the position with di-*n*-butylzinc, which yields⁸ more active catalysts with *p*- than with *t*-alcohols.

Treatment of dimethylzinc with an excess of *t*-butanol in benzene at 70°C gives only (MeZnOBu')_n, in agreement with the report⁵ that diethylzinc fails to react with more than one molar equivalent of *t*-butanol even at 80°C, but similar treatment of diphenylzinc readily yields the insoluble zinc *t*-butoxide. After being pumped at 20°C and 10⁻⁵ mm of mercury this material is a poor catalyst, but if the pumping is carried out at 90°C and 10⁻⁵ mm the product is more reactive towards ethylene oxide, although in benzene only a low polymer is formed: at the end of the reaction the proton magnetic resonance spectrum shows bands at τ 6.48 due to polymer, and at τ 8.88 due to *t*-butoxyl residues presumably present as chain end groups, the relative intensities of the bands indicating the presence of one *t*-butoxyl group for every twelve monomer units in the chain. If the catalyst is pumped at 180°C and 10⁻⁵ mm of mercury the subsequent reaction with ethylene oxide in benzene is faster, but the number of monomer units in the polymer decreases to approximately four per *t*-butoxyl group. This behaviour is consistent with the formation of a greater number of active sites on the zinc *t*-butoxide, either by removal of *t*-butanol or solvation, and/or breakdown of the surface. All forms of the zinc *t*-butoxide eventually yield solid polymers when caused to react with undiluted ethylene

oxide, but the reaction is much slower than that with similarly treated zinc methoxide.

These results support earlier observations^{4,5} that zinc alkoxides are catalysts for the polymerization of epoxides, and that a group is transferred from the zinc to an end of the polymer chain, possibly by a process involving coordination^{4,8} of an epoxide molecule on to the zinc followed by insertion of a monomer unit into a zinc-oxygen bond, rather than by a simple anionic reaction initiated by an alkoxyl anion. They also suggest that in some cases, e.g. with the $(RZnOBu)_n$ systems for which the spectra did not indicate consumption of the organozinc compound, the first product of a reaction with ethylene oxide may be catalytically much more active than the initial material, and that reactions involving diarylzincs and their *t*-alcoholysis products are potentially capable of yielding catalysts of different reactivity from those obtained from dialkylzincs, possibly as a consequence of the greater strength¹⁰ of the coordinate bond between the monomer and the arylzinc system. These aspects are being further investigated.

J. MALCOLM BRUCE
D. W. FARREN

*Department of Chemistry,
The University,
Manchester 13*

(Received April 1965)

REFERENCES

- ¹ BORROWS, E. T. and STEWART, D. G. *Brit. Pat. No. 785 053* (1957) and *U.S. Pat. No. 2 870 099* (1959); quoted by FURUKAWA, J. and SAEGUSA, T. in *Polymer Reviews*, 1963, **3**, 332 (Interscience: New York)
- ² STEWART, D. G., WADDAN, D. Y. and BORROWS, E. T. *Brit. Pat. No. 785 229* (1957) and *U.S. Pat. No. 2 870 100* (1959), quoted in ref. 1
- ³ INOUE, S., TSURUTA, T. and FURUKAWA, J. *Makromol. Chem.* 1962, **53**, 215
TSURUTA, T., INOUE, S., YOSHIDA, N. and FURUKAWA, J. *Makromol. Chem.* 1962, **53**, 230
- ⁴ INOUE, S., TSURUTA, T. and YOSHIDA, N. *Makromol. Chem.* 1964, **79**, 34
- ⁵ ISHIMORI, M. and TSURUTA, T. *Makromol. Chem.* 1963, **64**, 190
- ⁶ TSURUTA, T., INOUE, S., YOSHIDA, N. and YOKOTA, Y. *Makromol. Chem.* 1965, **81**, 191
- ⁷ IMAI, H., SAEGUSA, T. and FURUKAWA, J. *Makromol. Chem.* 1965, **81**, 92
- ⁸ GARTY, K. T., GIBB, T. B. and CLENDINNING, R. A. *J. Polym. Sci. A*, 1963, **1**, 85
- ⁹ THIELE, K.-H. *Z. anorg. Chem.* 1962, **319**, 183
- ¹⁰ ALLEN, G., BRUCE, J. M. and HUTCHINSON, F. G. *J. chem. Soc.* In press
- ¹¹ ALLEN, G., BRUCE, J. M., FARREN, D. W. and HUTCHINSON, F. G. Unpublished work
- ¹² BRUCE, J. M., FARREN, D. W. and RABAGLIATI, F. M. Unpublished work
- ¹³ See also COATES, G. E. and RIDLEY, D. *J. chem. Soc.* 1965, 1870

A Comparison of the Linearity of High Density Polyethylene and Polymethylene

POLYMETHYLENE, obtained by the decomposition of diazomethane, has long been considered to consist of entirely linear, unbranched chains. It is characterized by the higher density (0.98) reported for polymethylene¹ in contrast to the 0.95 to 0.97 range which brackets the high density com-

oxide, but the reaction is much slower than that with similarly treated zinc methoxide.

These results support earlier observations^{4,5} that zinc alkoxides are catalysts for the polymerization of epoxides, and that a group is transferred from the zinc to an end of the polymer chain, possibly by a process involving coordination^{4,8} of an epoxide molecule on to the zinc followed by insertion of a monomer unit into a zinc-oxygen bond, rather than by a simple anionic reaction initiated by an alkoxyl anion. They also suggest that in some cases, e.g. with the $(RZnOBu)_n$ systems for which the spectra did not indicate consumption of the organozinc compound, the first product of a reaction with ethylene oxide may be catalytically much more active than the initial material, and that reactions involving diarylzincs and their *t*-alcoholysis products are potentially capable of yielding catalysts of different reactivity from those obtained from dialkylzincs, possibly as a consequence of the greater strength¹⁰ of the coordinate bond between the monomer and the arylzinc system. These aspects are being further investigated.

J. MALCOLM BRUCE
D. W. FARREN

*Department of Chemistry,
The University,
Manchester 13*

(Received April 1965)

REFERENCES

- ¹ BORROWS, E. T. and STEWART, D. G. *Brit. Pat. No. 785 053* (1957) and *U.S. Pat. No. 2 870 099* (1959); quoted by FURUKAWA, J. and SAEGUSA, T. in *Polymer Reviews*, 1963, **3**, 332 (Interscience: New York)
- ² STEWART, D. G., WADDAN, D. Y. and BORROWS, E. T. *Brit. Pat. No. 785 229* (1957) and *U.S. Pat. No. 2 870 100* (1959), quoted in ref. 1
- ³ INOUE, S., TSURUTA, T. and FURUKAWA, J. *Makromol. Chem.* 1962, **53**, 215
TSURUTA, T., INOUE, S., YOSHIDA, N. and FURUKAWA, J. *Makromol. Chem.* 1962, **53**, 230
- ⁴ INOUE, S., TSURUTA, T. and YOSHIDA, N. *Makromol. Chem.* 1964, **79**, 34
- ⁵ ISHIMORI, M. and TSURUTA, T. *Makromol. Chem.* 1963, **64**, 190
- ⁶ TSURUTA, T., INOUE, S., YOSHIDA, N. and YOKOTA, Y. *Makromol. Chem.* 1965, **81**, 191
- ⁷ IMAI, H., SAEGUSA, T. and FURUKAWA, J. *Makromol. Chem.* 1965, **81**, 92
- ⁸ GARTY, K. T., GIBB, T. B. and CLENDINNING, R. A. *J. Polym. Sci. A*, 1963, **1**, 85
- ⁹ THIELE, K.-H. *Z. anorg. Chem.* 1962, **319**, 183
- ¹⁰ ALLEN, G., BRUCE, J. M. and HUTCHINSON, F. G. *J. chem. Soc.* In press
- ¹¹ ALLEN, G., BRUCE, J. M., FARREN, D. W. and HUTCHINSON, F. G. Unpublished work
- ¹² BRUCE, J. M., FARREN, D. W. and RABAGLIATI, F. M. Unpublished work
- ¹³ See also COATES, G. E. and RIDLEY, D. *J. chem. Soc.* 1965, 1870

A Comparison of the Linearity of High Density Polyethylene and Polymethylene

POLYMETHYLENE, obtained by the decomposition of diazomethane, has long been considered to consist of entirely linear, unbranched chains. It is characterized by the higher density (0.98) reported for polymethylene¹ in contrast to the 0.95 to 0.97 range which brackets the high density com-

mercial polyethylenes. The assumption that polymethylene is completely linear and that all other polyethylenes contain some side chains has been accepted, and formed the basis for an important composition of matter patent issued to A. W. Larcher and D. C. Pease in the U.S.A.². In that patent it is contended that polyethylenes with densities in the range of 0.95 to 0.97 have branches, but at a frequency less than 1 per 200 carbons. Present day spectroscopic techniques, however, have never been sensitive enough to detect such differences in branching between polymethylene and high density polyethylene.

It is also known that the density of ethylene polymers is influenced by the molecular weight of the sample³. We present experimental evidence in this Note which shows that when the effect of molecular weight on density is eliminated the densities of polymethylene and high density polyethylene are essentially the same. Based on this evidence there is no difference in branching frequency between these two polymers.

In order to eliminate molecular weight as a variable, a comparison was made between fractions of polyethylene and polymethylene. For fractionation, 20 g of polymethylene was prepared from diazomethane⁴. Although the boron trifluoride-etherate decomposition of diazomethane gives predominantly very high molecular weight material, we were able to obtain three fractions using a fractional extraction technique. Densities of the fractions were obtained from samples moulded and annealed under strictly comparable conditions.

Table 1 lists the densities, viscosities and calculated molecular weights⁵ determined for three fractions obtained from polymethylene.

Table 1

<i>Polymethylene fraction</i>	<i>Annealed density</i>	<i>Inherent viscosity</i>	<i>Calc. mol. wt</i>	<i>Density of linear polyethylene of corresponding mol. wt</i>
Fraction 1	0.962	1.97	88.6×10^3	0.956
Fraction 2	0.950	2.42	117×10^3	0.954
Fraction 3	0.936	4.14	247×10^3	—
Whole polymer	0.929	>14	—	—

The data from fraction 1 were discarded since the first fraction included all the shortest chains and was undoubtedly of very wide distribution. Fraction 2 was in the range where comparison of its molecular weight and density to the plot in work published earlier could be made³. Fraction 3 was already of such high molecular weight that it could be compared only by extrapolation of Tung's plot beyond reasonable limits. Because of the high average molecular weight, the whole polymer exhibited a density far lower than the 0.98 value reported earlier by Bunn¹.

Since the annealed density of fraction 2 was 0.950, and the density of the commercial low pressure process polyethylene fraction of equal molecular weight was 0.954, we have concluded that the commercial sample is

at least as linear as polymethylene itself. Thus the difference between polymethylene and commercial linear polyethylene homopolymer is only a difference in molecular weight. This large difference in molecular weight is the direct cause of the physical property differences observed, rather than any linearity differences in the polymer.

P. E. HINKAMP
L. H. TUNG

*Petrochemicals Research Laboratory,
The Dow Chemical Company,
Midland, Michigan, U.S.A.*

(Received April 1965)

REFERENCES

- ¹ BUNN, C. W. *Polyethylene*. Edited by A. RENFREW and P. MORGAN, p 98. Iliffe & Sons: London, 1957
- ² LARCHER, A. W. and PEASE, D. C. *U.S. Pat. No. 2 816 883* (1957)
- ³ TUNG, L. H. *S. P. E. J.* 1958, **14**, No. 7, 25
- ⁴ KANTOR, S. W. and OSTHOFF, R. C. *J. Amer. chem. Soc.* 1953, **75**, 931
- ⁵ TUNG, L. H. *J. Polym. Sci.* 1957, **24**, 333

Gamma Irradiation Polymerization of Acrylonitrile in the Presence of Solid Additives

F. PROVOOST

An attempt has been made to polymerize acrylonitrile under gamma irradiation both at 26°C and at -78°C in the presence of additives having various electric properties, chemical compositions and specific surface areas. In the liquid phase the rate of polymerization is greatly increased by the presence of additives having a large specific surface area. The factors responsible for this are discussed and the probable mechanism considered.

THE catalytic influence of solid additives in radiochemical polymerization has already been investigated for several monomers, which, in the homogeneous phase (no additive), polymerize via a cationic mechanism¹⁻³. The additives generally used have a small specific surface area. Not many studies were devoted to catalytic effects in anionic polymerizations³.

Several authors^{9,10} have shown that acrylonitrile initiated by gamma irradiation most likely polymerizes via an anionic mechanism at very low temperature and via a radical mechanism at room temperature.

In this work, an attempt was made to polymerize acrylonitrile under gamma irradiation, both at 26°C and at -78°C, in the presence of additives with various electric properties (semi-conductors and insulators), chemical composition and specific surface area. It has been shown that the rate of polymerization induced by γ -irradiation of acrylonitrile is noticeably increased only in the presence of additives with a large specific surface area.

EXPERIMENTAL

(1) Additives

Table I gives some data on the preparation, composition and surface area of the additives used. The additives CA 3/173, CA 3/185, CS 1/174, LMS 5A and EC 7/18 are microporous^{11,12}; the specific surface area of the others is less than 20 m² g⁻¹.

The impregnated additives were prepared in the following way¹³⁻¹⁵.

Solutions of Ni (NO₃)₂ and Zn (NO₃)₂ were mixed with gamma alumina CA 3/185 or alpha alumina Al₂O₃ · 240, and evaporated to dryness under continuous stirring. After about four hours these mixtures were heated to 600°C and kept at this temperature for four more hours.

At 600°C the nitrates are decomposed to their oxides, the carrier remaining microporous. When the additives are impregnated in this way, the specific surface area does not change (less than one per cent, Table I, CA 3/173 + Fe₂O₃) and one obtains a catalyst finely dispersed at random on the large surface area carrier^{16,17}.

All catalysts are degassed *in vacuo* immediately before use.

Table 1. Characteristics of the additives

Additive	Preparation	Ref.	Composition	Surface area, m ² g ⁻¹ (BET)
ZnO IV	Zn(NO ₃) ₂ + Cr ₂ O ₃	14	ZnO + Cr ₂ O ₃ (2.1% Cr)	—
NiO IV	Ni(NO ₃) ₂ + (NH ₄) ₂ CrO ₄	15	NiO + Cr ₂ O ₃ (5% Cr)	1.04
α-Al ₂ O ₃ . 240	Al ₂ O ₃ UCB calc. 1380°C, 240 mesh	—	α-Al ₂ O ₃ (99.9%) max. 30 p.p.m. Fe	11.57
α-Al ₂ O ₃ . 130	Al ₂ O ₃ UCB calc. 1380°C, 130 mesh	—	Al ₂ O ₃ (99.9%)	17.83
SR Al ₂ O ₃ . 150	Al ₂ O ₃ Degussa 150 mesh	—	Techn. product 1270 p.p.m. Fe, 2 400 Si	0.1
ZnO UCB	ZnO UCB p.a.	—	ZnO	5.03
CA 3/173	AlCl ₃ + NH ₄ OH	21	γ-Al ₂ O ₃ . (gel)	187.2
CA 3/173 + Fe ₂ O ₃	CA 3/173 + Fe(OH) ₃	—	γ-Al ₂ O ₃ + Fe ₂ O ₃ (5%)	187.0
CA 3/185	AlCl ₃ + NH ₄ OH	21	γ-Al ₂ O ₃ . (gel)	150.6
LMS 5A	Linde molecular sieves 5A	Union Carbide	Ca-aluminosilicate	365.3
ES 1/174	SiO ₂	21	SiO ₂	625.0
EC 7/18	Active coal	—	Coal	1 003.0
CA 3/185 + NiO	CA 3/185 + Ni(NO ₃) ₂	—	γ-Al ₂ O ₃ + NiO (7.5%)	—
CA 3/185 + ZnO	CA 3/185 + Zn(NO ₃) ₂	—	γ-Al ₂ O ₃ + ZnO (10%)	—
α-Al ₂ O ₃ + ZnO	α-Al ₂ O ₃ + Zn(NO ₃) ₂	—	α-Al ₂ O ₃ + ZnO (10%)	—

(2) *Monomer acrylonitrile*

The monomer is first dried over Linde molecular sieves 5A and distilled *in vacuo* immediately before use. The quantity of monomer is determined by weight, not by volume.

(3) *Polymerization*

The polymerization is carried out in Pyrex bulbs, filled *in vacuo*. These bulbs must previously be cleaned with nitric acid and rinsed with boiling water.

After irradiation the bulbs are immediately broken and the unreacted monomer is recovered by distillation. The irradiations are made in the 'Gamma Cell 220' with a cobalt-60 source. The present dose rate at room temperature is 3.28×10^5 rads h⁻¹ and for the irradiations at -78°C it is 2.3×10^5 rads h⁻¹.

(4) *Determinations*

The quantity of polymer is determined by the difference of the initial and final weights of the monomer. A blank run (A 110) showed that in

GAMMA IRRADIATION POLYMERIZATION OF ACRYLONITRILE

this way more than 99.5 per cent of the unreacted monomer can be recovered, which corresponds to an error of 0.06 per cent h^{-1} for an 8 h irradiation and 20 per cent conversion. The amount of polymer could not be determined by solvent extraction. Only 50 to 60 per cent of the polymer can be extracted from the microporous additives by dimethyl formamide. With the non-microporous additives 90 per cent of the polymer can be extracted.

RESULTS AND DISCUSSION

 (1) *Small-surface additives*

The influence of additives with a small-surface area (less than $20 \text{ m}^2 \text{ g}^{-1}$) on the rate of polymerization of acrylonitrile under gamma irradiation appears to be very small in the liquid phase at room temperature and at -78°C (Table 2), whereas for isobutene, an important influence was

Table 2. Influence of small-surface area additives

Run	Additive* 0.50 g	Acrylo- nitrile g	Dose Mrads	Irradia- tion temp. $^\circ\text{C}$	Polymer g	Conver- sion %
A4	—	0.9432	1.64	26	0.1081	11.5
A11	—	1.2845	1.64	26	0.1487	11.6
A2	NiO IV	1.0242	1.64	26	0.0961	9.4
A3	ZnO IV	1.0533	1.64	26	0.0843	8.0
A6	$\alpha\text{-Al}_2\text{O}_3 \cdot 24\text{O}$	1.0683	1.64	26	0.1492	14.0
A32	—	1.5758	3.69	-78	0.0276	1.7
A5	—	1.6239	3.69	-78	0.0284	1.8
A26	$\alpha\text{-Al}_2\text{O}_3 \cdot 24\text{O}$	1.0220	3.69	-78	0.0224	2.2
A31	$\alpha\text{-Al}_2\text{O}_3 \cdot 24\text{O}$	1.0573	3.69	-78	0.0205	2.0
A27	ZnO . UCB	1.0650	3.69	-78	0.0152	1.4
A34	$\alpha\text{-Al}_2\text{O}_3 \cdot 15\text{O}$	1.0688	3.84	-78	0.0319	2.98
A35	SR . $\text{Al}_2\text{O}_3 \cdot 15\text{O}$	1.1295	3.84	-78	0.0241	2.10

*ZnO IV and NiO IV are degassed at 200°C , the other additives at 400°C . Dose rate: $2.3 \times 10^5 \text{ rads } h^{-1}$.

observed¹. At 26°C (liquid phase and radical mechanism) the catalytic influence is very small when 1 g of monomer is polymerized in the presence of 0.5 g of solid. At -78°C the influence of ZnO and $\alpha\text{-Al}_2\text{O}_3$ is dubious, the polymerization rate being very low. In fact, there is a small increase of the reaction rate, with 0.5 g alumina and 1 g of monomer (A 31, A 26), and a small decrease for 0.5 g ZnO and 1 g of monomer. For larger quantities of $\alpha\text{-Al}_2\text{O}_3$ per 1 g of monomer, inhibition is observed (A 29, A 33) (Table 3). The nature and specific area of the solid as well as the weight ratio solid/monomer are thus important factors. Without additives it was supposed that at this temperature the polymerization would proceed via an ionic mechanism⁹. In an earlier study³ an increase in the rate of polymerization of β -propiolactone was observed in the presence of ZnO. This monomer was also supposed to polymerize via an anionic mechanism²². A recent study¹⁹ mentioned a decrease for the rate of polymerization of acrylonitrile

Table 3. Influence of the surface of $\alpha\text{-Al}_2\text{O}_3 \cdot 24\text{O}$

Run	$\frac{g \alpha\text{-Al}_2\text{O}_3}{g \text{AN}}$	$\frac{\text{Surf. m}^2}{g \text{AN}}$	Dose Mrads	Conversion % h^{-1}
A29	9.09	104.5	3.69	0
A33	1.9517	22.6	3.84	0.08
A31	0.4650	5.4	3.69	0.12
A26	0.4880	5.6	1.85	0.14
A30	0.0468	0.5	3.69	0.11

Additive degassed at 400°C. Irradiation temperature: -78°C . Dose rate: 2.3×10^5 rads h^{-1} .

and methyl methacrylate in the presence of a semi-conductor type n (e.g. ZnO) but an increase for some p semi-conductors.

(2) Large-surface additives

Different types of additives were studied. For gamma alumina, the effects of polymerization temperature, degassing temperature of the solid and addition of NiO and ZnO were more thoroughly investigated.

Effect of nature and surface of additive—Microporous additives markedly enhance the rate of the γ -irradiation polymerization of acrylonitrile at -78°C (Table 4). When 1 g of acrylonitrile is polymerized in the presence of 0.5 g of such additives as alumina ($150 \text{ m}^2 \text{ g}^{-1}$), silica ($625 \text{ m}^2 \text{ g}^{-1}$), LMS 5A ($365.3 \text{ m}^2 \text{ g}^{-1}$), the polymerization rate increases up to thirty times, for active coal ($1003 \text{ m}^2 \text{ g}^{-1}$) only four times (Table 3). A similar effect was observed⁵ in the polymerization of ethylene initiated by gamma irradiation at 31°C . The enhanced catalytic influence of silica was also observed^{6,7} for styrene at -78°C .

Several comments can be made on these observations. The most obvious explanation of the catalytic influence could be found in the absorption of monomer on the surface. The additive can so affect one or more elementary steps in the polymerization reaction. Increases in rate of polymerization in

Table 4. Influence of surface and nature of large-surface area additives

Run	Additive degassed at 400°C	$\frac{g \text{Add.}}{g \text{AN}}$	$\frac{\text{Surf. m}^2}{g \text{AN}}$	Dose Mrads	Conversion % h^{-1}
A46	CA 3/173	0.4253	79.6	0.45	3.47
A52	CA 3/173	0.4249	79.7	0.54	3.04
A57	CA 3/185	0.5405	68.1	0.69	3.26
A53	LMS 5A	0.4595	167.9	0.54	2.78
A48	CS 1/174	0.4659	291.2	0.46	3.24
A50	CS 1/174	0.4670	291.9	0.54	4.39
A49	EC 7/18	0.4435	444.8	0.46	0.61
A51	EC 7/18	0.4424	443.7	0.54	0.30
A32	—	—	—	3.69	0.11
A110	CA 3/185	0.4650	70.0	—	0.06

Irradiation temperature: -78°C . Dose rate: 2.3×10^5 rads h^{-1} .

heterophase systems are ascribed to increases in the rate of initiation or to decreases in termination rate constants²³. The difference in rate of polymerization in the presence of the small and the large surface area additives could now be found in their different absorption capacities of the monomer acrylonitrile. It was suggested¹⁸ that the increase should be due to the removal of polar impurities from the monomer by the additives. This explanation also is only compatible with the surface effect.

Besides this, a more specific effect of the nature of the additive is observed. Although active coal has the largest specific surface area, its catalytic influence is smaller than that of other additives. This effect could be ascribed to the conductivity of the additives; it has been observed that insulators present the most interesting activation possibilities in radiochemical processes⁸. The conductivity of the additives used was not measured.

Influence of irradiation temperature on polymerization rate—The influence of temperature on the polymerization rate of acrylonitrile definitely increases in the presence of porous alumina (Table 5). When the irradiation

Table 5. Influence of irradiation temperature

Run	Additive 0.5 g	Irradiation temp. °C	Conversion % h ⁻¹
A95	CA 3/185	26	53.9
A96	CA 3/185	-18	15.2
A57	CA 3/185	-78	3.3
A4	—	26	23.0
A11	—	26	23.2
A98	—	-18	4.96
A32	—	-78	0.11
A5	—	-78	0.12

Degassing temperature of additive: 400°C. 1 g monomer acrylonitrile. Dose rate: 2.28×10^4 rads h⁻¹.

temperature increases, the influence becomes smaller. At very low temperature (-78°C) acrylonitrile polymerizes via an anionic mechanism. It is possible that for this mechanism the large-surface additives such as gamma alumina have a greater effect than for a radical one; a progressive transition from ionic into a radical mechanism should thus exist between -78°C and 26°C. The same effect was investigated for the heterophase polymerization of isobutene. The mechanism changed¹ from ionic to radical between -20°C and 0°C. Another explanation is that at low temperature more acrylonitrile is adsorbed, and so more monomer initiated.

Influence of degassing temperature—The degassing temperature of the additive appears to be very important. We have observed that gamma alumina degassed at 400°C becomes greyer than at 200°C. This might be an indication for a change in the conductivity of alumina, and thus for the important change of the reaction rate when the degassing temperature was changed (Table 6). Degassing the additive at 400°C increases the degree

F. PROVOOST

Table 6. Influence of degassing temperature and supported additives

Run	Additive 0.5 g	Degassing temp. °C	Dose Mrads	Conversion % h ⁻¹
A32	—	—	3.69	0.11
A109	—	—	1.596	0.14
A57	CA 3/185	400	1.824	3.26
A60	CA 3/185	200	1.824	2.01
A111	CA 3/185	200	1.368	2.11
A61	CA 3/185 + NiO	200	1.824	1.49
A205	CA 3/185 + NiO	200	1.596	1.08
A78	CA 3/185 + ZnO	200	1.824	2.25
A106	CA 3/185 + ZnO	200	1.596	2.24
A63	α -Al ₂ O ₃ · 24O + ZnO	200	3.69	0.10
A62	α -Al ₂ O ₃ · 24O	200	3.69	0.10

Irradiation temperature: -78°C. Dose rate: 2.28×10^4 rads h⁻¹.

of conversion for acrylonitrile by more than 50 per cent over this at 200°C. The above-mentioned degassing temperatures do not change the porosity and the specific surface area of the additives¹¹.

Influence of supported additives—Alumina was impregnated with ZnO and NiO in turn. Due to the presence of the surface of the alumina, active ZnO or NiO catalyst with a large surface is formed¹⁶. It is most probable that ZnO and NiO, calcined at 600°C and degassed at 200°C *in vacuo*, are semi-conductors of the type n and p respectively; however, their electrical properties were not investigated.

An increase in the polymerization rate (10 per cent) was noted with the ZnO and a decrease (25 per cent) with the NiO. For impregnated small-surface area additives, the polymerization rate of acrylonitrile was too low to observe any difference (A 63 and A 62, Table 5). The same effect with these supported additives was observed²⁰ in the polymerization of vinylchloride at -78°C. In a recently published study¹⁹ an increase in the rate of polymerization of acrylonitrile in the presence of a p semi-conductor was observed and the rate was not further increased by addition of ZnO (n semi-conductor). The carrier is not catalytically indifferent but may modify the catalyst¹⁶. This might be an explanation for the observed difference. A fundamental comparative examination of the structures of catalysts is necessary to explain this phenomenon.

CONCLUSION

The rate of polymerization of acrylonitrile initiated by gamma irradiation in the liquid phase is strongly increased by the presence of some additives with a large specific surface area. Several factors are responsible:

- (1) A high specific surface area is a requisite. Nevertheless, this condition is not sufficient by itself. The influence on the polymerization rate at

- 78°C is greater for alumina and silica (30 times) than for active coal (only 4 times), although alumina has the lowest specific surface area. The nature of the additive plays a role.
- (2) Catalytic influence decreases when the irradiation temperature increases.
 - (3) The degassing temperature of the additive plays an important part; the rate is higher after degassing the additive at 400°C than at 200°C.
 - (4) ZnO supported on microporous alumina increases the rate of polymerization, whereas NiO decreases it.

The author is much indebted to Dr C. David* and Dr V. Mathot for valuable discussions, to Dr R. Constant for his interest in this work, and to Ir M. De Proost for the gamma irradiations.

He also wishes to thank the management of the 'Studiecentrum voor Kernenergie' for permitting publication of this study.

Studiecentrum voor Kernenergie,
Mol-Donk, Belgium

(Received March 1965)

REFERENCES

- ¹ DAVID, C., PROVOOST, F. and VERDUYN, G. *J. Polym. Sci. Part C*, 1963, **1**, 1135
- ² DALTON, F. L., GLAWITSCH, G. and ROBERTS, R. *Polymer, Lond.* 1961, **2**, 419
- ³ DAVID, C., PROVOOST, F. and VERDUYN, G. *Polymer, Lond.* 1963, **4**, 391
- ⁴ DALTON, F. L. and HAYOKAWA, K. *Polymer, Lond.* 1963, **4**, 283
- ⁵ MECHELYNCK-DAVID, C. and PROVOOST, F. *Internat. J. appl. Radiation and Isotopes*, 1961, **10**, 191
- ⁶ CHARLESBY, A. and MORRIS, J. *Proc. Roy. Soc.* 1963, **273**, 387
- ⁷ CHARLESBY, A. and MORRIS, J. *J. Polym. Sci. Part C*, 1963, **4**, 1127
- ⁸ COEKELBERGS, R., CRUCQ, A. and FRENNET, A. *Advanc. Catalysis*, 1962, **13**, 55
- ⁹ SOBUE, H. and TABATA, Y. *J. Polym. Sci.* 1960, **43**, 459
- ¹⁰ CHAPIRO, A. *Radiation Chemistry of Polymeric Systems*. Interscience: New York, 1962
- ¹¹ COEKELBERGS, R., GOSSELAIN, P., JULIENS, J., SCHOTSMANS, L. and VAN DER VENNE, M. Communication presented to the Conference of the AIEA at Warsaw on The Use of Active Sources of Irradiation
- ¹² COEKELBERGS, R., GOSSELAIN, P. and SCHOTSMANS, L. Proceedings of the Second United Nations International Conference on the Peaceful Uses of Atomic Energy, Geneva, September 1958
- ¹³ SELWOOD, P. W. *Advanc. Catalysis*, 1951, **3**, 59
- ¹⁴ ROMERO-ROSSI, F. and STONE, F. S. *Actes du deuxième Congrès International de Catalyse, 1960*. Editions Technip: Paris, 1961
- ¹⁵ DRY, M. E. and STONE, F. S. *Disc. Faraday Soc.* 1959, **28**, 193
- ¹⁶ DE BOER, J. H. *Advanc. Catalysis*, 1957, **9**, 137
- ¹⁷ SCHUIT, G. C. A. and VAN REYEN, L. L. *Advanc. Catalysis*, 1958, **10**, 244
- ¹⁸ WILLIAMS, F. *Quart. Rev. chem. Soc., Lond.* 1963, **17**, 2
- ¹⁹ MEZHIROVA, L. P., SCHEINKER, A. P. and ABKIN, A. D. *Dokl. Akad. Nauk S.S.S.R.* 1963, **153**, 1378
- ²⁰ Unpublished data
- ²¹ Belg. Pat. No. 573 657 to SBA and PCM
- ²² GRESHAM, T. L., JANSEN, J. E. and SHAVER, W. F. *J. Amer. chem. Soc.* 1948, **70**, 998
- ²³ WORRALL, R. and PINNER, S. H. *J. Polym. Sci.* 1959, **34**, 229

*Present address: Université Libre de Bruxelles, Service de Chimie générale II.

The Ultra-violet Degradation of Scissioning Copolymers

C. H. KUIST and L. D. MAXIM

A description is given of investigations into the u.v. degradation of the vinyl acetate-ethyl acrylate copolymer system. Also included are reactivity ratios calculated from the literature. AZBN was used to initiate polymerization. A possible extension to all scissioning systems is indicated.

THE ultra-violet (u.v.) degradation of polymeric materials has received considerable study in recent years, due primarily to the increased utilization of these materials in applications involving sunlight exposure. Most of the studies of the kinetics or mechanisms of u.v. degradation have been on homopolymers, whereas most of the applications involve copolymers. It is the purpose of this paper to describe some investigations of the u.v. degradation of copolymer systems. The copolymer of vinyl acetate and ethyl acrylate was chosen for the experimental work, as the kinetics of homopolymer degradation have been described¹ and this copolymer system is of some industrial importance.

In a linear copolymer of monomers A and B there are ten possible types of monomer-monomer contacts: A—A, A—B and B—B together with the permutations of these due to 'head-to-head' and 'tail-to-tail' contacts. In scissioning vinyl polymers such as vinyl acetate, the mole per cent of 'head-to-head' contacts is so small² that their influence on the overall degradation kinetics may be ignored in this treatment. Therefore, it is assumed that only three types of linkages exist and may be ruptured.

The rate of rupture of each type of linkage is proportional to the number (concentration) of each type present per molecule.

If we let η , ψ and θ , represent the number of A—A, A—B and B—B links respectively unbroken per molecule, then:

$$-d\eta/dt = k_{AA}\eta \quad (1)$$

and
$$-d\psi/dt = k_{AB}\psi \quad (2)$$

and
$$-d\theta/dt = k_{BB}\theta \quad (3)$$

The number of links of each type broken (s) is given by:

$$s_\eta = f_{AA}P_0 - \eta \quad (4)$$

$$s_\psi = f_{AB}P_0 - \psi \quad (5)$$

$$s_\theta = f_{BB}P_0 - \theta \quad (6)$$

where f_{AA} , f_{AB} and f_{BB} represent the original fraction of A—A, A—B and B—B linkages respectively in a molecule of $DP = P_0$. Integrating equations 1, 2 and 3 and substituting 4, 5 and 6, we obtain:

$$s_\eta = f_{AA}P_0(1 - e^{-k_{AA}t}) \quad (7)$$

$$s_{\psi} = f_{AB}P_0(1 - e^{-k_{AB}t}) \quad (8)$$

$$s_{\theta} = f_{BB}P_0(1 - e^{-k_{BB}t}) \quad (9)$$

The total number of scissions per mer (α) is the sum of equations 7, 8 and 9, divided by P_0

$$\alpha = [s_{\eta} + s_{\psi} + s_{\theta}] / P_0 \quad (10)$$

or

$$\alpha = f_{AA}(1 - e^{-k_{AA}t}) + f_{BB}(1 - e^{-k_{BB}t}) + f_{AB}(1 - e^{-k_{AB}t}) \quad (11)$$

For the condition $k_{ij}t \ll 1$

$$(1 - e^{-k_{ij}t}) \simeq k_{ij}t \quad (12)$$

Figure 1 shows the percentage error introduced by this approximation as a function of the product kt .

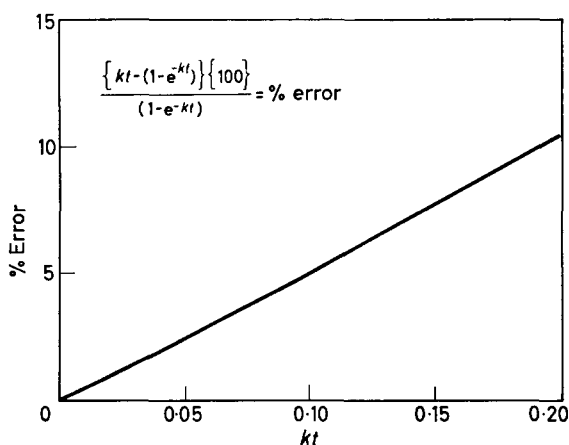


Figure 1—Error introduced by the approximation in equation 12

Allowing the condition of equation 11 to hold for equation 12

$$\alpha \simeq f_{AA}k_{AA}t + f_{BB}k_{BB}t + f_{AB}k_{AB}t \quad (13)$$

Dividing through by t (note that $\alpha/t = \bar{k}$, the observed kinetic constant)

$$\bar{k} = f_{AA}k_{AA} + f_{BB}k_{BB} + f_{AB}k_{AB} \quad (14)$$

Equation 14 indicates that, for the condition $k_{ij} \ll 1$, the observed kinetic constant is the weighted sum of the individual constants for each linkage. Rearranging equation 14 to a linear form

$$[\bar{k} - (f_{AA}k_{AA} + f_{BB}k_{BB})] = k_{AB}f_{AB} \quad (15)$$

A plot of the quantity in brackets of equation 15 versus f_{AB} is linear with a slope of k_{AB} .

The fraction of the various types of linkages (f_{AA} , f_{AB} and f_{BB}) can be calculated if certain simplifying assumptions are made. One assumption is that the effect of penultimate units is negligible. A second is that the

THE ULTRA-VIOLET DEGRADATION OF SCISSIONING COPOLYMERS

following equations describe only the instantaneous sequence ratio. This condition may be approached experimentally by limiting the reaction to very low conversion. If reactions are carried to completion, it would be necessary to integrate these equations over the entire range of composition. Lastly, the assumption of steady state is made. *Table 1* summarizes³ the reaction considerations of the steady state condition in the copolymerization of two monomers, A and B.

Table 1

Growing chain	Adding monomer	Rate constant	Reduction product	Rate
—m _a ·	M _a	k ₁₁	—m _a m _a ·	k ₁₁ [m _a ·] [M _a]
—m _a ·	M _b	k ₁₂	—m _a m _b ·	k ₁₂ [m _a ·] [M _b]
—m _b ·	M _a	k ₂₁	—m _b m _a ·	k ₂₁ [m _b ·] [M _a]
—m _b ·	M _b	k ₂₂	—m _b m _b ·	k ₂₂ [m _b ·] [M _b]

The instantaneous probability of finding an A—A unit becomes

$$P_{AA} = \frac{k_{11} [m_a \cdot] [M_a]}{k_{11} [m_a \cdot] [M_a] + k_{22} [m_b \cdot] [M_b] + k_{12} [m_a \cdot] [M_b] + k_{21} [m_b \cdot] [M_a]} \quad (16)$$

Similarly for a B—B unit

$$P_{BB} = \frac{k_{22} [m_b \cdot] [M_b]}{k_{11} [m_a \cdot] [M_a] + k_{22} [m_b \cdot] [M_b] + k_{12} [m_a \cdot] [M_b] + k_{21} [m_b \cdot] [M_a]} \quad (17)$$

and an A—B unit

$$P_{AB} = \frac{k_{12} [m_a \cdot] [M_b] + k_{21} [m_b \cdot] [M_a]}{k_{11} [m_a \cdot] [M_a] + k_{22} [m_b \cdot] [M_b] + k_{12} [m_a \cdot] [M_b] + k_{21} [m_b \cdot] [M_a]} \quad (18)$$

In the steady state, the rate of reaction of chains ending in m_a· with monomer M_b must be equal to the rate of reaction of chains ending in m_b· with M_a⁴. Expressing this steady state assumption mathematically, we have

$$[m_b \cdot] = \frac{k_{12} [M_b]}{k_{21} [M_a]} [m_a \cdot] \quad (19)$$

Using accepted nomenclature, we can define the following quantities:

$$r_a = k_{11}/k_{12} \quad \text{and} \quad r_b = k_{22}/k_{21} \quad (20)$$

The mole fractions of the two monomers in the feed, *f_a* and *f_b*, are:

$$f_a = [M_a]/([M_a] + [M_b]) \quad (21)$$

and

$$f_b = [M_b]/([M_a] + [M_b]) \quad (22)$$

Substituting relationships 19, 20, 21 and 22 in equations 16, 17 and 18, we obtain the following results:

$$\frac{1}{f_{aa}} = 1 + \frac{r_b}{r_a} \left(\frac{1-f_a}{f_a} \right)^2 + \frac{2}{r_a} \left(\frac{1-f_a}{f_a} \right) \quad (23)$$

$$\frac{1}{f_{bb}} = 1 + \frac{r_a}{r_b} \left(\frac{1-f_b}{f_b} \right)^2 + \frac{2}{r_b} \left(\frac{1-f_b}{f_b} \right) \quad (24)$$

$$\frac{1}{f_{ab}} = 1 + \frac{r_a}{2} \left(\frac{1-f_b}{f_b} \right) + \frac{r_b}{2} \left(\frac{1-f_a}{f_a} \right) \quad (25)$$

where f_{aa} represents the mole fraction of A—A linkages in the copolymer, etc.

It is often of more interest to relate the fraction of various types of linkages to the mole fraction of comonomer in the copolymer (F_a), rather than to the mole fraction comonomer in the feed (f_a). The relationship between these quantities is

$$F_a = \frac{(r_a f_a^2 + f_a f_b)}{(r_a f_a^2 + 2f_a f_b + r_b f_b^2)} \quad (26)$$

Reactivity ratios r_a and r_b may either be determined experimentally or calculated from the Alfrey-Price parameters⁵.

$$r_a = (Q_a/Q_b) \exp \{ -e_a (e_a - e_b) \} \quad (27)$$

and

$$r_b = (Q_b/Q_a) \exp \{ -e_b (e_b - e_a) \} \quad (28)$$

where Q represents a constant proportional to the reactivity of the monomer, and e represents a constant proportional to the polar character of the radical adduct.

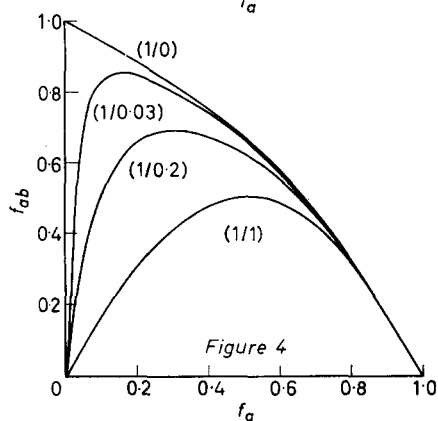
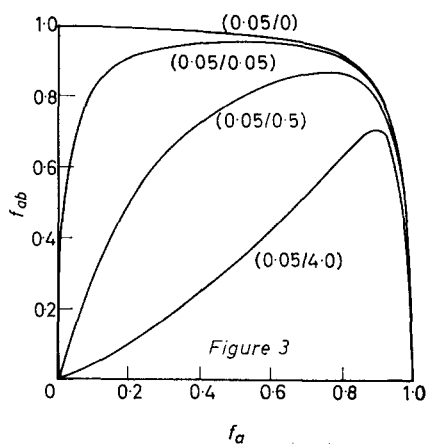
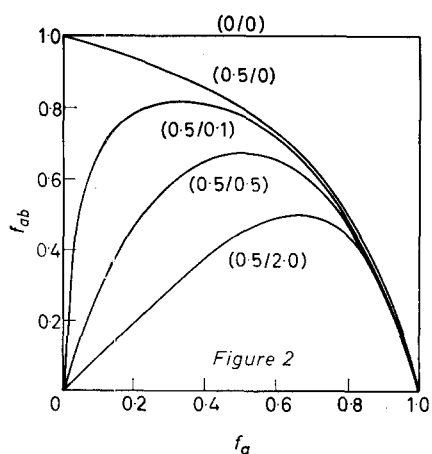
RESULTS AND DISCUSSION

Figures 2, 3 and 4 show calculated values of the mole fraction of A—B links f_{ab} as a function of the mole fraction of component A in the feed (f_a) for various indicated values of reactivity ratios. It can be seen that fixing r_a determines an envelope within which the calculated family of curves must fall. The parameter r_b specifies the exact location of the curve within this envelope.

The polymers used in this study were a series of copolymers of vinyl acetate and ethyl acrylate. Reactivity ratios were calculated from published Q and e values. The values for vinyl acetate⁶ are: $Q=0.028$, and $e=-0.3$.

The values used for ethyl acrylate⁷ are: $Q=0.34$, and $e=0.58$. The reactivity ratios calculated from these data are: $r_a=0.064$, and $r_b=7.3$. Figure 5 shows the mole fraction of A—A, A—B and B—B linkages as a function of the mole fraction vinyl acetate (a) in the feed. Equations 23, 24 and 25 were used in these calculations. Figure 6 shows the mole fraction of the various linkages as a function of the mole fraction of vinyl acetate (F_a) in the copolymer.

Copolymers of various ratios of vinyl acetate to ethyl acrylate were polymerized in ethyl acetate using azobisisobutyronitrile initiator. Conversions were limited to 4 to 6 per cent. In a typical reaction, to produce a 50/50 copolymer 90.0 parts by weight of vinyl acetate were added to 10.0 parts by weight ethyl acrylate, 0.2 parts by weight of azobisisobutyronitrile and 40.0 parts by weight of ethyl acetate and the mixture heated to reflux for two hours. Then 0.2 parts by weight of hydroquinone in 10 parts by weight ethyl acetate were added and the mixture cooled. The conversion of this reaction was found to be 5.5 per cent. The polymer was then isolated by successive precipitations using *n*-hexane. These



Figures 2, 3, 4—Fraction ab linkages as a function of mole fraction monomer a in feed. Values in parentheses are reactivity ratios, r_a/r_b

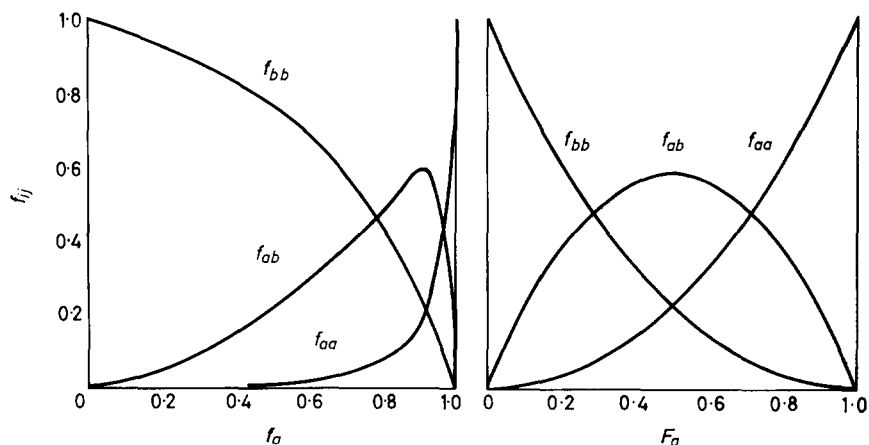


Figure 5 (on left)—Mole fractions of A—A, B—B and A—B linkages as functions of the mole fraction of vinyl acetate (a) in the feed, with the vinyl acetate—ethyl acrylate (b) system, when $r_a=0.064$, $r_b=7.3$. Figure 6 (on right)—Mole fraction of the various linkages as a function of the mole fraction of vinyl acetate (F_a) in the copolymer

copolymers were then exposed as thin (*ca.* 0.001 in.) films to u.v. radiation using an exposure cabinet previously described¹ and the osmotic molecular weights were measured at successively increasing exposure times. Kinetic constants for homopolymer degradation have been reported previously⁸.

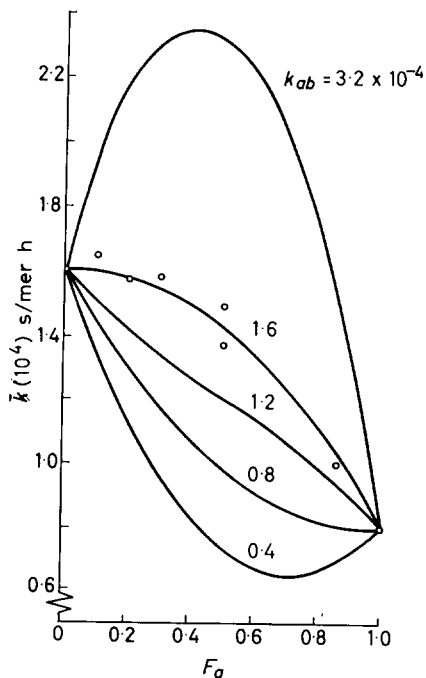
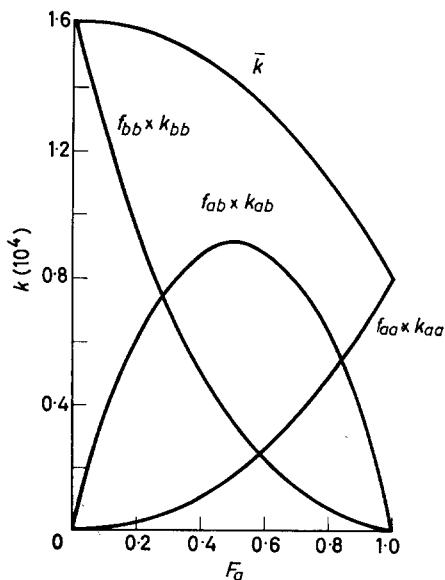


Figure 7—Variation of scissioning constant with mole fraction of monomer A in the copolymer

Figure 8—Contributions of the individual bond types to the scissioning constant k



The variation of the scissioning constant with composition is shown in *Figure 7*. The lines are calculated from equations 14, 23, 24 and 25 and the open circles represent the experimental data. *Figure 8* shows the contribution of each term in equation 14, assuming a value for k_{AB} of 1.6×10^{-4} scissions per mer hour. The value for k_{AB} can be estimated by fitting curves as was done in *Figure 6* or more directly by means of equation

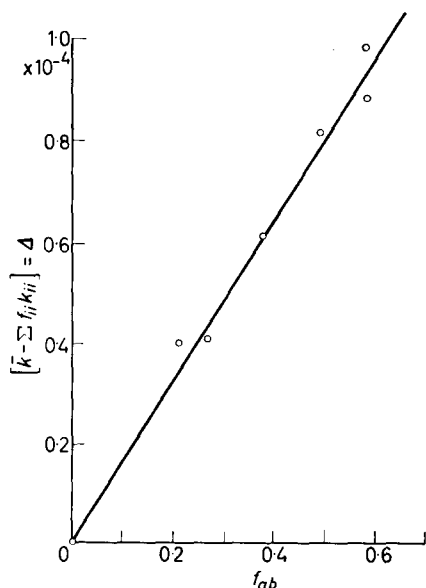


Figure 9—Agreement of experimental data with the model proposed in equation 15

15. *Figure 9* shows the variation of the parameter Δ with calculated values of the fraction of inter-mer bonds (f_{AB}). The slope of the line (k_{AB}) is 1.6×10^{-4} scissions per mer hour. This value is approximately the same as for the acrylate-acrylate linkages. Further insight into the nature of the AB bonds could be gained by studying the effect of wavelength of irradiation on the scission constant.

The extension of this approach to more complex cases may be made. Terpolymers of A, B and C monomers could be characterized by determination of the following constants: k_{AA} , k_{AB} , k_{AC} , k_{BB} , k_{BC} , k_{CC} . With this approach, it should be possible to describe the behaviour of all scissioning systems.

The authors are indebted to R. H. Marchessault for osmotic molecular weight measurements and F. A. Bovey for very helpful discussions.

*National Starch and Chemical Corporation,
1700 West Front Street,
Plainfield, New Jersey, U.S.A.*

(Received April 1965)

REFERENCES

- ¹ MAXIM, L. D. and KUIST, C. H. '*Official Digest*', 1964, **36**, 723
- ² FLORY, P. J. and LEUTNER, F. S. *J. Polym. Sci.* 1948, **3**, 880
See also *ibid.* 1950, **5**, 267
- ³ FLORY, P. J. *Principles of Polymer Chemistry*, p 178. Cornell University Press: Ithaca, New York, 1953
- ⁴ ALFREY, T., BOHRER, J. J. and MARK, H. *High Polymers*, Vol. VIII, 'Copolymerization' p 9. Interscience: New York, 1952
- ⁵ ALFREY, T. and PRICE, C. C. *J. Polym. Sci.* 1947, **2**, 101
- ⁶ PRICE, C. C. *J. Polym. Sci.* 1948, **3**, 772
- ⁷ Rohm & Haas Co., *Laboratory Report SP-251*, 1962
- ⁸ MAXIM, L. D. and KUIST, C. H. *American Chemical Society, Polymer Preprints*, 1963, **4**, 352

Polymers of Halogen-substituted 1-Olefins

K. J. CLARK and T. POWELL

The preparation of polymers of ω -halo-olefins and their copolymers with 4-methylpentene-1, using a Ziegler-type catalyst, is described and discussed. Polymerization, as opposed to participation in an irreversible reaction with the aluminium component of the catalyst, is favoured by increase in the size of the halogen atom, and its distance from the polymerizing double bond, and also by its attachment to primary rather than secondary or tertiary carbon atoms.

THE Ziegler-catalysed polymerization of 1-olefins bearing halogen atoms in the side chain has been described for few cases, e.g. trifluoroalkyl substituted ethylenes¹, halostyrenes² and chloroprene³. The nature and brevity of this list, and the widely-observed catastrophic deactivating effect of treating Ziegler catalysts with polar monomers such as halo-olefins, has suggested that only special cases (involving de-activated halogen atoms) may be polymerized by Ziegler-type catalysts, and that the polymerization of simple 1-olefin structures bearing halogen atoms in the aliphatic side-chain is not possible because of irreversible interaction of the halide with one or both of the components of the Ziegler catalyst. Recently a method for suppressing this activity, involving the deliberate introduction of basic components into the reaction mixture, has been described⁴ by R. Bacskai, and in this paper we describe our own findings in this field.

For the preparation of polymers of alkenyl halides it is clearly necessary to employ active Ziegler catalysts, whose components are substantially inactive towards the various types of alkyl halide groups possible. It was found that TiCl_3 , as prepared by the aluminium sesquihalide reduction of TiCl_4 , was relatively inert towards many alkyl halides, and our studies were therefore confined to the use of this material as catalyst. Examination of the reaction of a series of model alkyl halides (*n*-, *sec*- and *tert*-butyl chlorides, bromides and iodides) with four possible co-catalysts for TiCl_3 (AlEt_3 , AlBu_3^i , AlEt_2Cl and AlEtCl_2) and, where possible, the subsequent polymerization activity of the resultant catalyst-co-catalyst combination, showed that the real obstacle to the polymerization of halo-olefins lay in their reactivity with aluminium (halo) alkyls. Frequently mixing of these two components led to the formation of yellow-coloured solutions, or insoluble complexes, and thereby complete loss of co-catalyst activity, but the survey revealed significant trends in activities. Thus the activity of the alkyl halide RX in the deactivating reaction could be graded in the order $\text{RX} = \text{primary} < \text{secondary} < \text{tertiary}$ and $\text{X} = \text{I} < \text{Br} < \text{Cl}$, and that of the aluminium-derived co-catalyst in the order $\text{AlR}_3 < \text{AlR}_2\text{Cl} < \text{AlRCl}_2$. Furthermore the survey afforded some evidence that the reaction occurring on mixing AlEt_2Cl and a normal alkyl halide could be suppressed by conducting the operation in the presence of a high concentra-

tion of vinyl double bonds. Thus, whereas the irreversible yellowing reaction took place on mixing *n*-butyl chloride or 11-chloro-undecene-1 and AlEt_2Cl in petroleum ether, so that, on the subsequent addition of 4-methylpentene-1 and TiCl_3 , no polymerization took place, no deactivating reaction took place on mixing these components in 4-methylpentene-1, and polymerization took place on the subsequent addition of TiCl_3 . Under the most favourable conditions both allyl chloride and bromide reacted irreversibly with the aluminium alkyl; allyl iodide did not react noticeably in this manner, but suppressed the polymerization of 4-methylpentene-1.

On the basis of these results the copolymerization of a series of ω -halo-1-olefins with 4-methylpentene-1, using the catalyst system $\text{AlEt}_2\text{Cl-TiCl}_3^5$ was undertaken. In the belief that the highest possible concentration of vinyl double bonds should be employed to suppress the halide reaction, early experiments were carried out in bulk 4-methylpentene-1, and copolymers containing ~ 5 per cent w/w chlorine (i.e. ~ 26 per cent w/w halo-olefin) were obtained from solutions of undecylenyl chloride (26 per cent w/w) in 4-methylpentene-1. Soxhlet extraction gave fractions soluble in ether, petrol (b.pt 40° to 60°C), petrol (b.pt 60° to 80°C) and insoluble containing 6.3, 4.2, 3.9 and 4.0 per cent chlorine, respectively. It was then found that the procedure used for the preparation in diluent at 50°C of copolymers of 4-methylpentene-1 with linear 1-olefins⁶ gave excellent results in the copolymerization of a range of ω -halo-1-olefins (excluding allyl halides) with 4-methylpentene-1 (Table 1).

Table 1. Copolymerization of 4-methylpentene-1 with halo-olefins, by Ziegler catalysis

Diluent† (120 ml), AlEt_2Cl (4.5 mm), TiCl_3 (1.5 mm), 50°C . A solution (40 g) of halo-olefin in 4-methylpentene-1 added as an initial charge (14 g), followed by feed of the remainder over 2 h. Polymers isolated by the addition of *n*-BuOH, washing with excess *n*-BuOH, and drying at 60°C *in vacuo*

Halo-olefin in feed, wt%	Copolymer			
	Yield, g	Appearance	Halogen found, wt%	Halo-olefin in copolymer, wt%
4-Iodobutene-1, 20	4.4	White powder	18.9	27
5-Chloropentene-1, 13*	3	White powder	6.3	18.5
5-Bromopentene-1, 17	6.6	White powder	12.6	23.4
11-Chloro-undecene-1, 15	21	White powder	2.4	12.7
11-Chloro-undecene-1, 25	15	White shreds	5.4	28.6
11-Bromo-undecene-1, 14	17.5	White powder	5.1	14.8
11-Bromo-undecene-1, 27	15	White shreds	11.2	32.6
11-Iodo-undecene-1, 17	23	White powder	8.5	18.7

*Half-scale.

†Saturated aliphatic hydrocarbon fraction b.pt 180° to 200°C .

Addition of allyl chloride and bromide to established bulk polymerizations of 4-methylpentene-1 at 20°C gave vigorous exothermic reactions and 1,4-poly(4-methylpentene-1) as product. Addition of allyl iodide made no visible difference to the polymerization mixture, but stopped polymerization. No iodine was found in the isolated isotactic poly(4-methylpentene-1).

Experiments on the homopolymerization of ω -halo-olefins (Table 2) supported the earlier findings from model experiments. Thus, in the poly-

Table 2. Homopolymerization of halo-olefins by Ziegler catalysis

Halo-olefin, g	Diluent, ml	Al Alkyl, mm	TiCl ₃ , mm	Temp., °C	Duration, h	Final appearance of reactions	Yield, g	Halogen, wt%		R.V.†
								Found	Calc.	
4-Bromobutene-1,1,3	3,3-DMP*,40	AlEt ₂ Cl,3	3	20 & 40	1½	Catalyst degraded	Nil			
4-Bromobutene-1,1,3	Petrol,40	AIBu ₃ ,3	3	30	20	Unchanged	Nil			
4-Iodobutene-1,7,8	3,3-DMP,20	AlEt ₂ Cl,3	3	20 & 40	4	Brown slurry	3	68	69.8	
5-Bromopentene-1,4,5	Petrol,50	AlEt ₂ Cl,1.5	1.5	20 & 35	4	Catalyst degraded	Nil			
5-Bromopentene-1,9	3,3-DMP,40	AlEt ₂ Cl,3	3	20	½	Catalyst degraded	Nil			
5-Iodopentene-1,6,2	3,3-DMP,20	AlEt ₂ Cl,1.5	1.5	40	3	Catalyst eventually degraded	1.2	54.8	64	
11-Chloro-undecene-1,4,5	Petrol,50	AlEt ₂ Cl,1.5	1.5	25	1	Catalyst degraded	Nil			
11-Chloro-undecene-1,9	Petrol,40	AIBu ₃ ,3	3	30	20	Coagulated particles	0.6	15	18.8	2.53
11-Chloro-undecene-1,7,2	Petrol,20	AlEt ₂ Cl,4.5	1.5	20	3½		0.3	18.5	18.8	
11-Bromo-undecene-1,5,4	+ 3,3-DMP,20 Petrol,50	AlEt ₂ Cl,1.2	1.2	35	3	Catalyst eventually degraded	2.8	28	34.3	1.75
11-Iodo-undecene-1,8,4	Petrol,50	AlEt ₂ Cl,1.5	1.5	20	4½	Brown slurry	7	41.5	45	3.9

*3,3-Dimethylpentene-1.

†1 per cent CHCl₃ at 25°C. Solution viscosity.

‡A saturated aliphatic fraction b.p. 180° to 200°C.

merization of the undecylenyl halides, using $\text{AlEt}_2\text{Cl-TiCl}_3$, yields of the polymers of 11-iodo-, -bromo- and -chloro-undecene-1 were 83 per cent, 52 per cent (with delayed degradation of the polymerization mixture) and nil (immediate degradation), respectively. Some limited success was achieved in the polymerization of the chloride in the presence of a non-polymerizable vinylic compound, 3,3-dimethylpentene-1. In this medium, using $\text{AlEt}_2\text{Cl-TiCl}_3$, polymers of 4-iodobutene-1 and 5-iodopentene-1 were obtained, but the corresponding bromides both underwent the halide reaction under these conditions. Using $\text{Al}(\text{Bu})_3\text{-TiCl}_3$ in a high boiling petrol fraction, a low yield of poly(11-chloro-undecene-1) was obtained.

In conclusion, results from homo- and co-polymerization studies show that the preparation of polymers of ω -halo-1-olefins is favoured by increase in the size of the halogen atom and its distance from the polymerizing double bond, and its attachment to primary rather than secondary or tertiary carbon atoms. The principle underlying these preferences is clearly the decrease in the probability of ionic reaction of the carbon-halogen bond with the aluminium-based component of the catalyst. TiCl_3 may be considered to be relatively inert to attack by carbon-halogen bonds. In addition the ability of diethyl aluminium chloride to participate in the deactivating ionic reaction with carbon halogen bonds appears to be reduced in the presence of vinylic double bonds, suggesting the formation of some kind of labile olefin-aluminium alkyl complex.

*I.C.I. Plastics Division,
Welwyn Garden City, Herts.*

(Received May 1965)

REFERENCES

- ¹ OVERBERGER, C. G. and DAVIDSON, E. B. *J. Polym. Sci.* 1962, **62**, 23
- ² NATTA, G., DANUSSO, F. and SIANESI, D. *Makromol. Chem.* 1958, **28**, 253
- ³ E. I. Du Pont de Nemours and Co. *Brit. Pat. No. 776 326* (1957)
- ⁴ BACSKAI, R. *Chem. Engng News*, 14 September 1964, **42**, 55
- ⁵ Imperial Chemical Industries Ltd. *Brit. Pat. No. 942 297* (1963)
- ⁶ Imperial Chemical Industries Ltd. *Belg. Pat. No. 646 737* (1964) and Society of Chemical Industry Symposium on Chemistry of Polymerization Processes, 22 and 23 April 1965, London

The Dynamic Mechanical Properties of some Iodine-substituted 1-Olefin Polymers

J. A. E. KAIL

Measurements of the dynamic mechanical properties of three iodine-substituted 1-olefin polymers have been made over the temperature range of -180°C to $+90^{\circ}\text{C}$ and in a frequency range of 80 c/s to 500 c/s using a resonant cantilever beam method. The polymers studied were poly(4-iodobutene-1), which gave a glass transition temperature (T_g) of $+70^{\circ}\text{C}/239$ c/s, poly(5-iodopentene-1) with a T_g of $+30^{\circ}\text{C}/50$ c/s and poly(11-iodoundecene-1) with a T_g of $-6^{\circ}\text{C}/211$ c/s. The results from these polymers have been compared with those of the corresponding poly- α -olefins where the iodine has been replaced by a methyl group. The introduction of the iodine has caused the relaxation processes found present in the poly- α -olefins to move to higher temperature, the shift being more pronounced as the length of the side chain is decreased. The increased mass of the iodine atom over that of the methyl group is thought to be the major contributing factor behind the shift of the observed relaxation processes.

THE segmental motion of polymers has been widely studied over the past ten years using the three complementary techniques of nuclear magnetic resonance¹, dielectric² and dynamic mechanical³ spectroscopy. Although a great deal of dynamic mechanical information is available concerning the effect that the substitution of various organic groupings has upon the thermal motion of various elastomers^{4,5}, the effect of halogen substitution has been mainly limited to the surfeit of results upon poly(vinyl chloride)⁶ and poly(tetrafluoroethylene)⁷ together with the few reported observations upon poly(vinyl fluoride)⁴, poly(vinylidene chloride)⁴, poly(chlorotrifluoroethylene)⁴, halogen-substituted polystyrene⁸, polychloroprene⁹ and the α -chloroacrylic series⁵ of polymers. The reason for the brevity of this list has been the inability to synthesize halogen-substituted polymers; however, a method has been reported whereby halogen-substituted olefin polymers were made using a modified Ziegler-type catalyst¹⁰. These polymers have recently been synthesized in these laboratories using a Ziegler catalyst¹¹ and this paper reports the dynamic mechanical behaviour of three such iodine-substituted olefin-1 polymers.

EXPERIMENTAL

Five halogen-substituted polyolefins were successfully made using a Ziegler catalyst as described by Clark and Powell¹¹ in the previous paper. However, the small yield of poly(11-chloroundecene-1) and the inability to mould a suitable sample of poly(11-bromoundecene-1) prevented any dynamic mechanical measurements being made on them. It was found that if these polymers were taken to too high a temperature, the halogen was driven off; this therefore meant that a certain amount of care had to be exercised in producing samples suitable for measurement. *Table 1* lists the samples tested and the conditions under which they were moulded.

Table 1. Samples tested and moulding conditions

Polymer	Monomer repeat unit	Moulding conditions
Poly(4-iodobutene-1)	$\begin{array}{c} \text{CH}_2-\text{CH} \\ \\ (\text{CH}_2)_2 \\ \\ \text{I} \end{array}$	Dried at 60°C under vacuum. Powder mixed with 50% 'Tufknit' and pressed at 60°C into a suitable reed ¹²
Poly(5-iodopentene-1)	$\begin{array}{c} \text{CH}_2-\text{CH} \\ \\ (\text{CH}_2)_3 \\ \\ \text{I} \end{array}$	Powder compressed into reed at 20°C
Poly(11-iodoundecene-1)	$\begin{array}{c} \text{CH}_2-\text{CH} \\ \\ (\text{CH}_2)_9 \\ \\ \text{I} \end{array}$	Filled with 67% 'Tufknit' and pressed into reed at 20°C ¹²

The use of 'Tufknit' for dynamic mechanical measurements has been described by Sandiford and Thomas who have shown that it affects only the intensity and not the positions of the loss processes¹².

The dynamic flexural modulus (E') and losses ($\tan \delta$) of the iodo-polymers were determined from the value of the resonant frequency of vibration (fundamental mode) and the bandwidth using a cantilever beam apparatus and method described by Robinson¹³. The measurements were made over a temperature range of -180°C to $+90^\circ\text{C}$ and in a frequency range of 80 c/s to 500 c/s. The dynamic moduli of the filled samples have not been quoted because of the uncertainty involved in calculating such a value in a two-phase system¹².

RESULTS

Each polymer shows two relaxation processes which manifest themselves

Table 2. Summary of results

Polymer	$T_g, ^\circ\text{C}/\text{measuring frequency, c/s}$	$T_{sub}, ^\circ\text{C}/\text{measuring frequency, c/s}$	
Poly(4-iodobutene-1)	+70/239	-90/375	} Figure 1
Poly(pentene-1)*	-3/80	-130/300	
Poly(5-iodopentene-1)	approx. +30/50	-98/208	} Figure 2
Poly(hexene-1)*	-23/170	-130/500	
Poly(11-iodoundecene-1)	-6/211	-120/392	} Figure 3
Poly(dodecene-1)*	-6/150	-145/520	

*Results of Clark, Turner-Jones and Sandiford¹⁴.

Figure 1—Mechanical loss versus temperature of poly-(4-iodobutene-1) filled with 50 per cent 'Tufknit' (+) compared with that of an unfilled sample of poly-(pentene-1)²⁰ (full line)

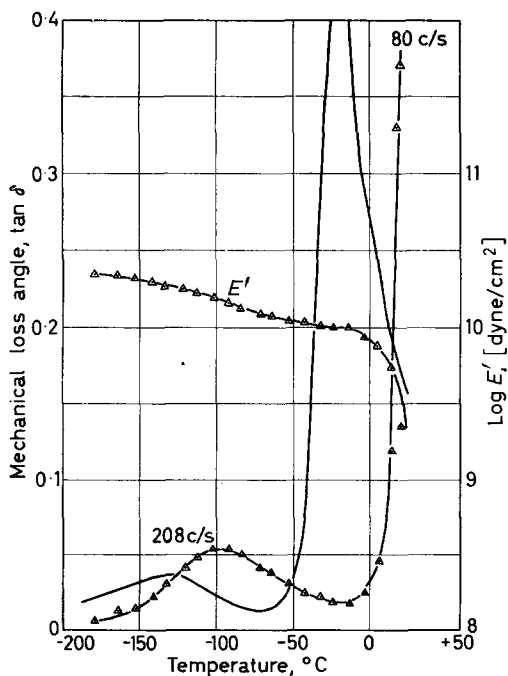
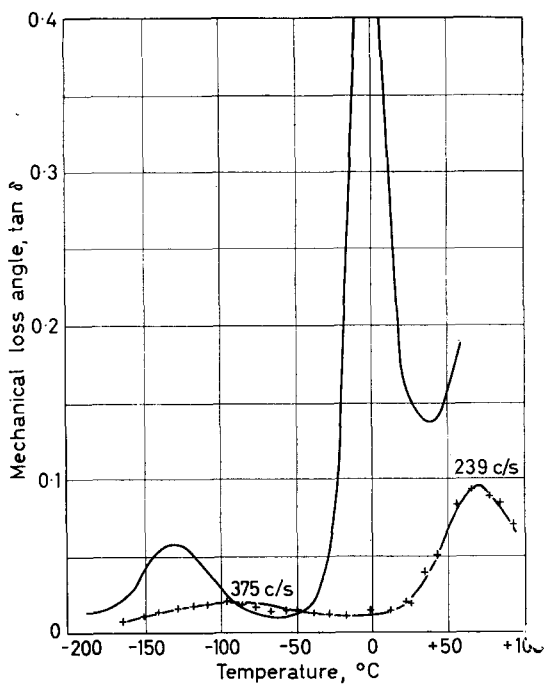


Figure 2—Mechanical loss and dynamic modulus E' versus temperature of poly(5-iodopentene-1) (Δ) compared with the mechanical losses of a 50 per cent 'Tufknit' filled poly-(hexene-1)¹² (full line)

as maxima in the mechanical loss angle ($\tan \delta$) versus temperature plot. The temperature at which the $\tan \delta$ maximum of the more intense peak occurred has been called here the glass transition temperature, T_g , and is thought to be the temperature at which the polymer main chain acquires considerable mobility. The less intense peak occurred at lower temperatures in all cases considered here. The results of the three polyiodo-olefins have been compared with those of the corresponding poly- α -olefin where the iodine has been replaced by a methyl group. These results are summarized in *Table 2*.

The temperature dependence of the dynamic flexural modulus E' , for the unfilled poly(5-iodopentene-1) is also shown on *Figure 2*. The temperature positions of the two dispersions of the dynamic modulus plot correspond to the two loss processes of the poly(5-iodopentene-1). The three iodopolymers were found to be amorphous by X-ray analysis¹⁵.

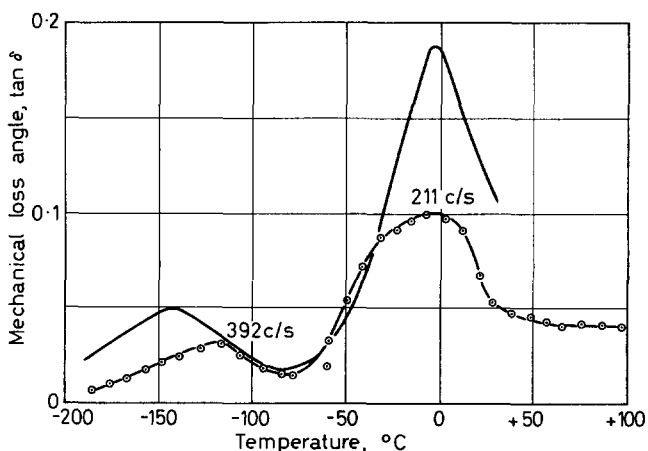


Figure 3—Mechanical loss versus temperature of poly(11-iodo-undecene-1) (○) filled with 67 per cent 'Tufknit' compared with that of an unfilled sample of poly(dodecene-1)²⁰ (full line)

DISCUSSION

For the purpose of this discussion these results have been compared with the corresponding poly- α -olefin, as mentioned earlier. The dynamic mechanical behaviour of the poly- α -olefins has been summarized by Clark and co-workers¹⁴. Dynamic mechanical observations by Willbourn¹⁶, and by Lawson, Sauer and Woodward¹⁷ suggest that the low temperature relaxation process is probably caused by re-orientation of $-(CH_2)_n-$ segments where $3 < n < 10$, whereas the high temperature relaxation is a manifestation of the onset of main chain mobility (the so-called glass/rubber transition) in the amorphous phase. There is no reason not to suppose that the losses observed in the iodopolymers are caused by similar types of relaxation mechanisms which have been 'modified' by the presence of the iodine.

The general effect of the iodine is to cause the relaxation process to shift to higher temperatures, the magnitude of the shift depending upon the length of the side chain. As would perhaps have been expected, the glass/

rubber transition is extremely sensitive to the length of the side chain. Poly(11-iodoundecene-1) exhibits the same T_g as poly(dodecene-1), by which it may be inferred that the iodine is too far removed from the main chain to be able to modify its relaxation processes. However, when moved into closer proximity, the effect is very noticeable and consequently the T_g of poly(5-iodopentene) is 53°C higher than poly(hexene-1) and that of poly(4-iodobutene) is 73°C higher than poly(pentene-1).

Factors affecting main chain flexibility and hence the glass transition of polymers, have been adequately reviewed by Boyer¹⁸. Among others it is known that main chain flexibility is reduced by polar side groups near the main chain, bulky inflexible side groups and steric hindrance. However, the effect of mass of the side group has not previously been studied as generally a heavy group is usually bulky and often causes steric hindrance and, in such cases, it is difficult to separate the various effects. The iodopolymers are in a unique position in that although the mass of the iodine (atomic weight 127) is greatly in excess of the methyl group it replaces (molecular weight 15), its 'bulk' or van der Waals radius (2.15 Å for iodine) is comparable to that of a methyl group (2.0 Å)¹⁹.

Unfortunately iodine is also polar and it seems probable, therefore, that the shift of the relaxation processes of the iodopolymers to higher temperatures is a consequence of the polarity imparted to the structure and/or the increased mass caused by the presence of the iodine. It is difficult to deduce which effect is dominant; however, further evidence presented here suggests that the mass of the iodine is a major factor contributing to the increased glass transition temperatures.

The secondary loss process of all three iodopolymers shows a shift to higher temperatures in the order poly(4-iodobutene-1) (40°C shift), poly(5-iodopentene-1) (32°C shift) and poly(11-iodoundecene-1) (25°C shift). Perhaps the most surprising result here is the increase in the low temperature loss peak of the poly(11-iodoundecene-1). It is thought, as stated earlier, that this low temperature dispersion is a result of motion of small groups of methylene units. Therefore, even if one assumes that the main chain and iodine effectively 'lock' the side chain ends, there should still be at least seven consecutive methylene units capable of producing the typical 'low temperature' dispersion seen in the poly- α -olefins. [Note that poly(nonene-1) with a side group length of seven CH₂ units and poly(decene-1) with eight CH₂ units both display a low temperature transition¹⁴ at -160°C.]

Remembering that these iodopolymers are amorphous, the increase in the low temperature dispersion of the poly(11-iodoundecene-1) can only be caused by the presence of the iodine. As pointed out above, there is no reason to expect a shift in temperature of the dispersion if we consider the iodine as fixed relative to the main chain. Consequently, neither the increase in polarity nor the slight increase in volume of the iodine compared with the methyl group can adequately explain this observation.

In conclusion, therefore, it appears that the greater mass of the iodine is the major contributing factor to the differences observed between the dynamic mechanical relaxations of the iodopolymers studied here and their corresponding polyolefins.

The author wishes to thank D. J. H. Sandiford and Miss A. Turner-Jones for their cooperation and permission to use some of their unpublished results.

I.C.I. Plastics Division,
Welwyn Garden City, Herts.

(Received May 1965)

REFERENCES

- ¹ For example POWLES, J. G. *Polymer, Lond.* 1960, **1**, 219
- ² For example CURTIS, A. J. *Progress in Dielectrics*, Vol. II, pp 29-76. Wiley: New York, 1960
- ³ For example WOODWARD, A. E. and SAUER, J. A. *Fortschr. HochpolymerForsch.* 1958, **1**, 114
- ⁴ SCHMIEDER, K. and WOLF, K. *Kolloidzshr.* 1953, **134**, 149
- ⁵ HOFF, E. A. W., ROBINSON, D. W. and WILLBOURN, A. H. *J. Polym. Sci.* 1955, **18**, 161
- ⁶ For example SCHMIEDER, K. and WOLF, K. *Kolloidzshr.* 1952, **127**, 65
- ⁷ For example McCURUM, N. G. *J. Polym. Sci.* 1959, **34**, 355
- ⁸ ILLERS, K. H. and JENCKEL, E. *J. Polym. Sci.* 1959, **41**, 528
- ⁹ YIN, T. P. and PARISER, R. *J. appl. Polym. Sci.* 1963, **7**, 667
- ¹⁰ BACSKAI, R. *Chem. Engng News*, 14 September 1964, **42**, 55
- ¹¹ CLARK, K. J. and POWELL, T. *Polymer, Lond* 1965, **6**, 531
- ¹² SANDIFORD, D. J. H. and THOMAS, D. A. *Kolloidzshr.* 1962, **181**, 4
- ¹³ ROBINSON, D. W. *J. sci. Instrum.* 1955, **32**, 2
- ¹⁴ CLARK, K. J., TURNER-JONES, A. and SANDIFORD, D. J. H. *Chem. & Ind.* **1962**, 2010
- ¹⁵ TURNER-JONES, A. Unpublished results
- ¹⁶ WILLBOURN, A. H. *Trans. Faraday Soc.* 1958, **54**, 717
- ¹⁷ LAWSON, K. D., SAUER, J. A. and WOODWARD, A. E. *J. appl. Phys.* 1963, **34**, 2492
- ¹⁸ BOYER, R. F. *Rubb. Chem. Technol.* 1963, **36**, 1303
- ¹⁹ PAULING, L. *Nature of the Chemical Bond*, Ch. V. Cornell University Press: New York, 1939
- ²⁰ SANDIFORD, D. J. H. Unpublished results

The Vapour Pressure of a Swollen Crosslinked Elastomer

G. GEE, J. B. M. HERBERT and R. C. ROBERTS

The use of vapour pressure measurements in the study of the configurational free energy changes involved in the isotropic dilation of a network was investigated, with the conclusion that the assumptions implicit in this approach require further study.

THE absorption of a liquid by a crosslinked polymer is in most respects similar to the swelling of a linear polymer, but with the essential difference that it requires a deformation of the network. Theoretical treatments of the phenomenon rest on the assumption that the free energies of mixing and network deformation are additive¹. The success of these analyses in accounting for the effect of crosslinking on maximum swelling gives strong support to this assumption, and has led to the general acceptance of swelling measurements as a convenient and reliable method of estimating degree of crosslinking². There is, however, abundant evidence to show that current theories of the free energy of mixing are least reliable when applied to conditions of saturation³, and it therefore seemed desirable to measure the effect of crosslinking at a lower level of liquid concentration. This can in principle be done readily, by comparing the vapour pressures, at the same concentration, of two polymers which are identical except that one is crosslinked.

Let μ_1^c and μ_1^u be the chemical potentials of the liquid in crosslinked (^c) and uncrosslinked (^u) samples at equal concentrations*, and p_1^c, p_1^u the vapour pressures. Then

$$\mu_1^c - \mu_1^u = RT \ln (p_1^c / p_1^u) \quad (1)$$

Further, if G_c is the configurational free energy of the network and n_1 the number of moles of liquid absorbed, the hypothesis of additivity of free energies requires

$$\mu_1^c - \mu_1^u = \delta G_c / \delta n_1 \quad (2)$$

If we confine our attention to isotropic swelling, the absorption by 1 cm³ of dry polymer of n_1 moles of liquid of molar volume V_1 will increase the linear dimensions by a factor λ , where $\lambda^3 = 1 + n_1 V_1$ whence

$$dn_1 = (3/2) (\lambda / V_1) d\lambda^2 \quad (3)$$

Combining equations (1), (2) and (3) the network free energy per cm³ of polymer is given by

$$G_c = \frac{3RT}{2V_1} \int_1^{\lambda^3} \lambda \ln (p^c / p^u) d\lambda^2 \quad (4)$$

*'Equal concentrations' has been interpreted here as equal volume fractions, since the theoretical equations used relate free energy with volume rather than weight composition. The two are not quite equivalent since the densities of the two polymers differ.

The equation has been cast in this form because the statistical theory of rubber elasticity requires⁴

$$G_c = (3/2) (\rho RT / M_c) (\lambda^2 - 1) \quad (5)$$

where M_c is the molecular weight between junction points, and ρ the density of the polymer. If equations (4) and (5) both hold,

$$\lambda \ln (p^c / p^u) = \rho V_1 / M_c \quad (6)$$

The accuracy of equation (5) has been questioned by Wall and Flory⁵, who introduced a further term arising from the random distribution of crosslinks over the total volume:

$$G_c = (3/2) (\rho RT / M_c) (\lambda^2 - 1 - \ln \lambda) \quad (5')$$

whence

$$\lambda \ln (p^c / p^u) = (\rho V_1 / M_c) (1 - 1/2\lambda^2) \quad (6')$$

Further doubts concerning the accuracy of the statistical theory arise from the departure of experimental stress/strain curves from the predicted form. In a recent discussion of this problem⁶, it has been suggested that the configurational free energy of a single chain can be expressed over a limited range of deformation by an equation of the form

$$G_c = a (\lambda^2 - 1) + b (\lambda^{-2} - 1) \quad (5'')$$

Since in isotropic swelling each chain will, to a first approximation, be deformed in the same ratio, this equation gives a third alternative for the network free energy, and leads to

$$\lambda \ln (p^c / p^u) = A - B / \lambda^4 \quad (6'')$$

It is clear that determination of $\lambda \ln (p^c / p^u)$ over a range of composition is in principle capable of distinguishing among the alternatives. This is particularly desirable since other types of measurement have not proved decisive. The additional term in equation (5') vanishes for any deformation of the dry polymer, and measurements of equilibrium swelling can usually be interpreted equally well by either (5) or (5'). A general difficulty, which is particularly troublesome with equation (5''), is that in analysing any mechanical deformation of a polymer, we have to relate the deformations of first the network and then the individual chains to that of the bulk. Evidence about the chain free energy is therefore never clear-cut. In contrast, when a polymer swells isotropically, it is plausible to assume that each chain is extended in the ratio λ , where λ^3 is the ratio swollen volume: dry volume.

In this paper we report an experimental study of the quantity $\lambda \ln (p^c / p^u)$. This is unfortunately inherently difficult, since it is clear that the magnitude to be expected for a normal vulcanizate will lie between 0.01 and 0.1.

EXPERIMENTAL

Materials

Natural rubber (crepe 100 parts) was mill-mixed with dicumyl peroxide (4.5 parts), and part of the stock press cured (45 min at 160°C). Cured and uncured samples were acetone extracted in a Soxhlet under nitrogen in the dark, and stored *in vacuo*.

Benzene, after preliminary purification, was recrystallized four times and fractionally distilled (b.pt $80.2^{\circ}\text{C}/764$ mm mercury; vapour pressure at 25°C , 95.6 mm (lit. 95.3)).

Microbalances

The balances had the same basic design as those used by Whytlaw-Gray *et al.*, the construction of which has been reviewed by Bradley⁷. They were calibrated using a set of small accurately weighted lengths of platinum wire, the calibrations being such as to ensure that no errors arose from the unavoidable slight inequalities in the balance arms. During the course of the experimental work, balances were constructed having sensitivities of from 4 to 20 mg/cm deflection of the beam, depending on the load to be measured.

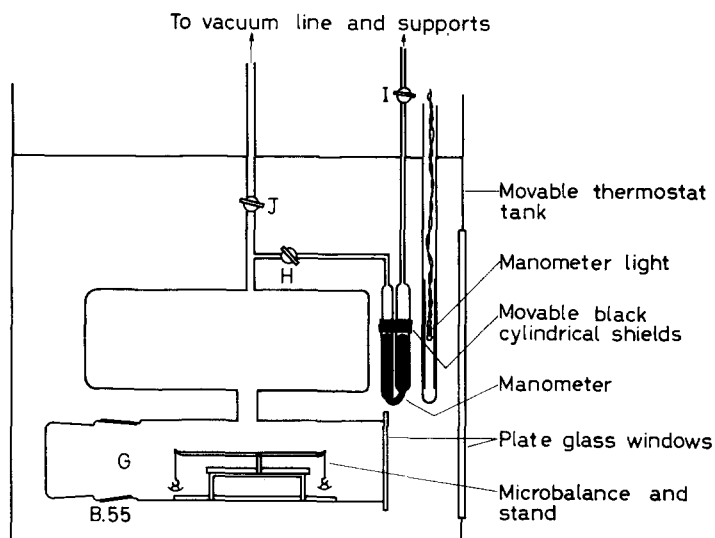


Figure 1—Microbalance cell and manometer

General arrangement

The general plan of the apparatus is shown in Figure 1. The balances were rigidly secured to a brass stand which was mounted in a cylindrical cell, G. This was closed at one end by a B55 stopper which allowed easy removal and replacement of the balance and at the other end by a one-quarter inch plate glass window, permanently fixed in place with Araldite. The cell communicated with a large reservoir of about 800 cm^3 , constructed from 3 in. diameter tubing, which served to minimize pressure changes caused by the absorption of benzene by the samples. Pressure in the system was measured on a mercury manometer constructed from 15 mm diameter Veridia tubing.

The whole apparatus was immersed in water in a well-lagged tank fitted with a long one-quarter inch plate glass observation window. The bath was well stirred and thermostatically controlled at $25^{\circ} \pm 0.004^{\circ}\text{C}$.

The thermostat tank was supported in a frame and could be lowered completely clear of the cell to facilitate removal of the balance. The deflection of the microbalance beam and the height of the mercury in the manometer were measured on a cathetometer. Care was taken to ensure that both the cell window and that of the tank when in its raised position were vertical and parallel to each other to avoid refraction errors in the height and deflection measurements.

Experimental procedure

Two kinds of measurement were made:

(1) A single weighed piece of crosslinked rubber (12 to 150 mg) was approximately balanced by a platinum wire. Benzene was then introduced or removed in stages, allowing equilibrium to be obtained each time (8 to 24 h). The weight absorbed was determined from the balance deflection, and the corresponding vapour pressure read on the manometer. Desorption measurements showed complete absence of hysteresis.

(2) The balance was loaded with samples of crosslinked and uncrosslinked rubbers, matched in weight within 5 μg . Benzene was introduced or removed in stages and the difference of uptake determined as a function of vapour pressure.

Supplementary measurements

(1) Density measurements, by density bottle and by flotation in water/methanol gave: crosslinked 0.915 g cm^{-3} , uncrosslinked 0.908 g cm^{-3} .

(2) Equilibrium swelling of the crosslinked material was determined by immersing *ca.* 0.5 g samples in benzene for 48 h, and re-weighing after rapid surface drying.

RESULTS

The results of the two sets of measurements are shown in *Figures 2* and *3*. The observed difference of weight between uncrosslinked and crosslinked samples was expressed as a difference in volume fraction. If ϕ_1^u and ϕ_1^c are the volume fractions of liquid in the two samples at a fixed vapour pressure, $\Delta\phi \equiv \phi_1^u - \phi_1^c$. *Figure 2* gives a plot of $\Delta\phi$ against ϕ_1^c , in which the full line is our empirical smoothing of the data, as used in subsequent calculations.

Figure 3 gives the experimental points, and the smoothed curve, of vapour pressure against ϕ_1^c . By combining the smoothed curves of *Figures 2* and *3* we obtain values of $\Delta p (=p^c - p^u)$ at a given volume fraction of rubber ϕ_2 . Then since $\lambda = \phi_2^{-1/3}$, the results can be expressed in the form of a plot of $\lambda \ln(p^c/p^u)$ against λ^2 . The points plotted in *Figure 4* have been obtained in this way, at intervals of $\lambda^2 - 0.1$: they do not represent unsmoothed experimental measurements. The final point, at $\lambda^2 = 2.21$, represents the equilibrium swelling of the polymer, determined in a separate experiment. For this point p^c is of course equal to the saturation vapour pressure of the pure liquid. The corresponding value of p^u was evaluated by means of the Flory-Huggins equations, which has been shown to hold accurately for

THE VAPOUR PRESSURE OF A SWOLLEN CROSSLINKED ELASTOMER

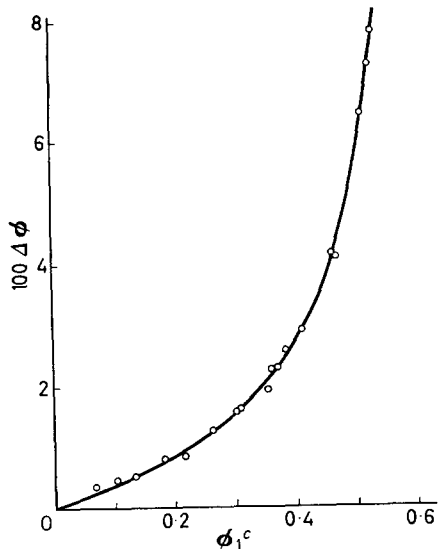


Figure 2—Isopiestic measurements;
 $\Delta\phi = \phi_1^u - \phi_1^c$ at 25°C

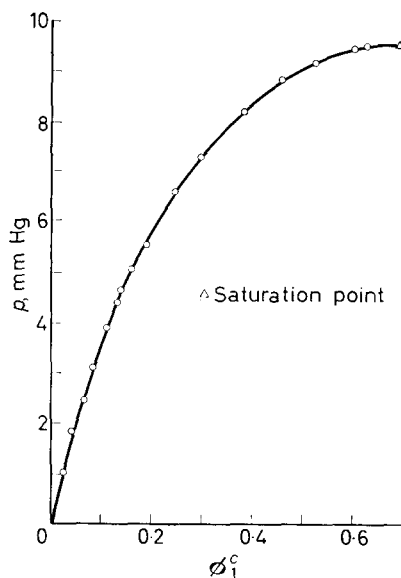


Figure 3—Vapour pressure of
 crosslinked rubber system at 25°C

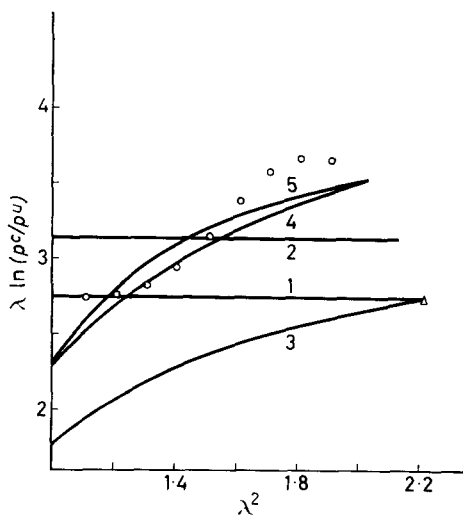


Figure 4—Evaluation of $\lambda \ln(p^c/p^u)$.
 Points \circ calculated from smoothed
 curves of Figures 2 and 3; Δ from
 saturation. Calculated curves: 1,2
 equation (6) ($\rho V_1/M_c = 0.0275,$
 0.0315); 3,4 equation (6') ($\rho V_1/M_c$
 $= 0.0356, 0.0465$); 5 equation (6'')
 ($A = 0.0392, B = 0.0160$)

this system over a very wide concentration range⁸. For saturation this gives

$$\ln(p^u/p^c) = \ln \phi_1 + \phi_2 + \chi \phi_2^2 \quad (7)$$

Our values of p^u (obtained from p^c and Δp) give a mean value of $\chi = 0.43_2$, calculated from the most reliable range of ϕ_1 (0.2 to 0.5). Hence from equation (7), $\ln(p^c/p^u)$ at saturation = 0.0185.

DISCUSSION

The five curves drawn in *Figure 4* were derived from equations (6), (6') and (6''). Since it is apparent that none of them fits the experimental points, it is necessary to consider critically the reliability of the measurements.

The saturation value is subject to two uncertainties. The measured concentration should be reliable to one per cent, corresponding to three per cent in the derived value of $\lambda \ln(p^c/p^u)$. An error of +0.010 in χ would change $\lambda \ln(p^c/p^u)$ by -5 per cent. To raise the saturation value to the level of curve 3 requires $\chi = 0.403$, which is within the range of values which have been reported for natural rubber and benzene, but is certainly not consistent with the present measurements.

Uncertainties in the isopiestic measurements are much more difficult to assess. *Figure 2* shows a satisfactory absence of excessive scatter, but the values near the origin are clearly subject to considerable uncertainty. Values of $\lambda \ln(p^c/p^u)$ calculated from these points instead of from the smoothed curve are substantially higher and suggest a sharp minimum in the region of $\lambda^2 \sim 1.2$. The experimental uncertainty is high at these very low degrees of swelling, and no great significance can be attached to the values. Over the main part of the concentration range ($\phi_1^c = 0.25$ to 0.55, corresponding to $\lambda^2 = 1.2$ to 1.7) there seems no doubt that $\lambda \ln(p^c/p^u)$ is larger than the saturation value and increases markedly with λ^2 . Permissible alternative smoothings of the data change the position and steepness of the slope somewhat but leave no doubt that the curve must pass through a maximum to reach the saturation point.

This maximum is perhaps the most striking and unexpected feature of the results. Bearing in mind the relatively small deformations involved, it seems very unlikely that it can be a property of the configurational free energy of the network. The alternative explanation is that it arises from a difference of mixing free energy of the two polymers at equal swelling. Such a maximum would be observed if, in the neighbourhood of saturation, the mixing free energy of the crosslinked polymer falls below that of the uncrosslinked polymer. This suggestion recalls another well-established phenomenon. The chemical potential of a liquid in a polymer with which it is only partially miscible falls below the theoretical (Flory-Huggins) curve as saturation is approached, and the degree of swelling is greater than predicted³ [*Figure 5(a)*]. In the present case we have previous evidence to show that μ^u is accurately described by the Flory-Huggins equation⁸; the maximum now observed in *Figure 4* implies that the mixing part of μ^c falls below the Flory-Huggins line near saturation [*Figure 5(b)*]. If this explanation is correct, the currently accepted method of estimating crosslinking from swelling measurements depends on a false assumption.

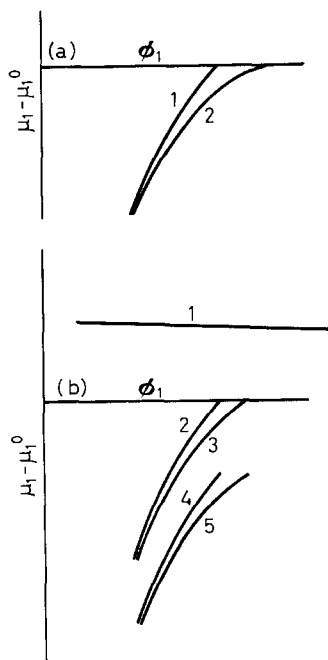


Figure 5—Schematic representation of departures from Flory-Huggins equation. (a) Linear polymer in a non-solvent: 1 theory, 2 expt; (b) crosslinked polymer: 1 network contribution; 2,3 total (theory, expt); 4,5 mixing term (theory, expt)

Turning now to the main part of *Figure 2*, we have to account for the rise in $\lambda \ln(p^c/p^u)$ with λ^2 . A complication which cannot be overlooked is the possibility that the Flory-Huggins parameter χ is changed by the chemical modification involved in the process of crosslinking. If $\chi^c \neq \chi^u$, there will be an additional term in $\lambda \ln(p^c/p^u)$ equal to $(\chi^c - \chi^u)/\lambda^2$, and potentially large enough to change very significantly both the absolute value and the concentration dependence of $\lambda \ln(p^c/p^u)$. Thus if $\chi^c - \chi^u = -0.020$ the points in *Figure 2* should be raised by $2/\lambda^2$ to get the network contribution: this has the effect of bringing the level to 4.0 ± 0.2 between $\lambda^2 = 1.2$ and 2.0 , falling to 3.0 at saturation. While it seems scarcely likely that χ^c and χ^u can differ as widely as this, it is apparent that great caution is needed in relating these experimental observations to theoretical equations. The evidence as it stands suggests that equation (5) is inadequate and favours instead (5') or possibly (5''). This clearly should not be taken as well-established.

CONCLUSIONS

This investigation was undertaken with the aim of using vapour pressure measurements to study the configurational free energy changes involved in the isotropic dilation of a network. The main conclusion is that the assumptions implicit in this approach require further study. These same assumptions are involved in conventional determinations of crosslinking from swelling. There is reason to suspect that such measurements over-estimate the degree of crosslinking.

*Department of Chemistry,
The University,
Manchester 13*

(Received April 1965)

REFERENCES

- ¹ FLORY, P. J. *Principles of Polymer Chemistry*, p 577. Cornell University Press: Ithaca, 1953
- ² See e.g. MULLINS, L. *et al. J. Polym. Sci.* 1956, **19**, 225, 237; 1960, **43**, 13; *J. appl. Polym. Sci.* 1959, **2**, 1, 257
- ³ GEE, G. *Trans. Faraday Soc.* 1946, **42B**, 33
BOOTH, C., GEE, G., HOLDEN, G. and WILLIAMSON, G. R. *Polymer, Lond.* 1964, **5**, 343
- ⁴ TRELOAR, L. R. G. *The Physics of Rubber Elasticity*, Chapter 4. Clarendon Press: Oxford, 1958
- ⁵ WALL, F. T. and FLORY, P. J. *J. chem. Phys.* 1950, **18**, 108; 1951, **19**, 1435
- ⁶ GEE, G. *Proceedings of the Natural Rubber Conference, Cambridge 1964* (in press)
- ⁷ BRADLEY, R. S. *J. sci. Instrum.* 1953, **30**, 84
- ⁸ GEE, G. and ORR, W. J. C. *Trans. Faraday Soc.* 1946, **42**, 507

The Polymerization of Vinylcarbazole by Electron Acceptors II

L. P. ELLINGER*

The polymerization of vinylcarbazole in the presence of methylmethacrylate is now shown to yield polyvinylcarbazole and some copolymer of very much higher molecular weight. The formation of the copolymer occurs mainly during the early stage of the polymerization, is retarded by anthracene, and is ascribed to bimolecular thermal initiation. The polyvinylcarbazole formation is not markedly affected by anthracene, and is regarded as proceeding by mesomeric polarization.

The polymerization is also initiated by ω -N,N-dialkylaminoalkyl cyanides, the rate depending strongly on size of dipole and being greatest with dimethylaminoacetoneitrile. The results are held to support a dipolar mechanism.

The formation of oligomers of vinylcarbazole in the presence of chloranil in acetone solution in the dark under conditions of complete charge transfer is described. The steric consequences of partial and of complete charge transfer on vinyl monomers are discussed.

THE initiation of the polymerization by organic electron acceptors has been shown to be possible using compounds which range widely in their electron affinity¹, and not to be limited only to such stronger acceptors as chloranil, tetranitromethane or maleic anhydride^{2,3}. The less electrophilic initiators included acrylonitrile and methylmethacrylate (MMA)¹, and it was a feature that the main product was polyvinylcarbazole essentially free of the initiating comonomer. With acrylonitrile a little copolymer was indeed isolated as a separate product by virtue of its insolubility in benzene, in which polyvinylcarbazole is soluble (except possibly for a very high molecular weight polymer). The polymerization in the presence of MMA was exceptional in yielding benzene-soluble polymer of very high molecular weight which, in bulk polymerization, varied with the MMA concentration in a characteristic manner¹.

The polymerization with MMA has now been examined in greater detail, especially since it could be shown spectroscopically that the polymer of very high molecular weight contains polymethyl methacrylate which was not readily found by a hydrolytic determination.

The initiation by these acceptors, under conditions under which complete electron transfer is thought not to apply, has been ascribed to sufficient activation by an increase in the mesomeric polarization of the *N*-vinyl group, which would be expected to follow the partial removal of one of the lone pair electrons on the nitrogen¹. The polarization of the *N*-vinyl group should be increased also by bringing it into contact with sufficiently strongly dipolar molecules, even if the latter are not over all electron acceptors. The ω -dialkylaminoalkyl cyanides are such compounds, and they have been examined as initiators^{2,3}.

*Now at The Distillers Co. Ltd, Great Burgh, Epsom, Surrey.

With the stronger organic acceptors in bulk and in non-ionizing solvents, vinylcarbazole shows colours which are typical of the formation of (solvated) ion pairs, and which on addition of ionizing solvent change characteristically to show the more intensive colouration of the ion radicals^{1,4}. Mixtures of vinylcarbazole with the weaker acceptors are either colourless or become coloured only slowly, any colouration fading on addition of ionizing solvent¹. The u.v. absorption spectrum of vinylcarbazole was found to be intensified according to the electron affinity of the acceptor, but no spectroscopic interaction could be observed in the i.r. spectrum even with the strongest acceptors studied. The cryoscopic behaviour of vinylcarbazole in the presence of maleic anhydride, or of tetrachlorethylene, in benzene (representing stronger and weaker acceptors) has now been examined for such interaction. Benzene was chosen as solvent in view of its large cryoscopic constant, and the relatively high solubility in it of the solutes. The position is complicated in the case of the maleic anhydride, which is known from u.v.⁹ and n.m.r.¹⁰ spectroscopic evidence to form a complex with benzene, although details of the equilibrium involved are not known.

Vinylcarbazole in methanolic solution containing chloranil or tetranitromethane has been shown to form 1,2-*trans*-dicarbazylcyclobutane and 9'-(1'-methoxyethyl)carbazole in daylight, but only the latter in the dark^{1,5}. The conditions under which these products are formed have been examined more closely, as have the reactions which occur under similar conditions in acetone solution.

MATERIALS

Vinylcarbazole (BASF Chemicals Ltd) once recrystallized grade, once recrystallized from methanol before use⁷.

Chloranil (L. Light & Co. Ltd) recrystallized from benzene.

Maleic anhydride (Griffin & George Ltd) recrystallized from benzene.

Tetrachlorethylene (Griffin & George Ltd) was washed repeatedly with concentrated aqueous caustic soda and water, dried over magnesium sulphate, and fractionated, a cut b.pt 121° to 122°C being used.

Methyl methacrylate (I.C.I. Ltd) was fractionated *in vacuo* for removal of stabilizer.

N,N-Dimethylaminoacetonitrile (L. Light & Co. Ltd) was washed with water and distilled, b.pt 136° to 137°C.

2-(*N,N*-Diethylamino)propionitrile (L. Light & Co. Ltd) was distilled under argon, b.pt 54° to 58°C at 2 mm.

3-(*N,N*-Diethylamino)butyronitrile (L. Light & Co. Ltd) was distilled under argon, b.pt 112° to 116°C at 40 to 45 mm mercury.

Anthracene (Hopkins & Williams Ltd) purified grade, was sublimed twice and recrystallized from benzene, m.pt 217°C.

Benzene (Griffin & George Ltd) AR grade.

Toluene (Griffin & George Ltd).

Methylene dichloride (Griffin & George Ltd) redistilled grade.

Argon and nitrogen ('White Spot' grade) (British Oxygen Co. Ltd).

EXPERIMENTAL

Well cleaned glass equipment was used, but no attempt was made to remove moisture films.

Unless otherwise stated polymerization was carried out in an oil bath, so that very little daylight reached the reaction mixture.

Control experiments on the same sample of monomer and under the same conditions, other than the presence of additive, were used freely.

Modified conditions of precipitation¹ were used for the isolation of the MMA-initiated polymer of high molecular weight to ensure more effective removal of residual monomer. The reaction product was dissolved in benzene (5 ml per g monomer), and the hot benzene solution was added with stirring to boiling methanol (6 ml per g monomer). The precipitated polymer was reprecipitated twice under similar conditions. The polymer was fractionated at ambient temperature by adding methanol with stirring to the benzene solution of the polymer.

Initiations in day-artificial light refer to exposure of the solution in Pyrex glass vessels to laboratory illumination (daylight and fluorescent strip light) at ambient temperature. The dimer was isolated by filtration, while monomer and 9-(1'-methoxyethyl)carbazole were precipitated from the solution by the addition of water to the methanol solution.

Irradiations were carried out with stirring and generally with ice-water cooling in a ventilated box lined with aluminium foil. A 500 W projector lamp sited outside the Pyrex reactor was used as intense source of tungsten light, and an Engelhard-Hanovia low pressure discharge mercury lamp, let into the reactor to allow direct irradiation, as u.v. source.

The i.r. spectra were determined in methylene dichloride solution. The limit of detection of polymethyl methacrylate in the polymer was 0.2 per cent.

Relative viscosities were determined at 20°C in one per cent benzene solutions of the polymers using an Ostwald viscometer, type A for relative viscosities below and type B for relative viscosities above 2.5.

RESULTS

(a) Polymerization initiated by MMA

The i.r. spectroscopic examination of polyvinylcarbazole polymerized in the presence of MMA showed that the quantity of polymethyl methacrylate incorporated in the polymer and its molecular weight both increased with the concentration (in the range 1 to 10 per cent) of MMA present in

Table 1. Polymerization of vinylcarbazole in the presence of MMA.
Temperature: 80°. Atmosphere: air

Polymerization		Polymer		
MMA on monomer, %	Time, h	Yield, %	Relative viscosity	Polymethyl methacrylate, %
1	27.5	23.3	2.07	2
2	25.3	23.2	5.30	6
5	24.0	39.6	8.04	9

the original mixture, though the results were subject to appreciable variability.

With increasing polymerization period the proportion of polymethyl methacrylate in the product and its molecular weight declined.

Table 2. Polymerization of vinylcarbazole in the presence of MMA.
Temperature: 82°. Atmosphere: nitrogen

Polymerization			Polymer		
Expt No. KE	MMA on monomer, %	Time, h	Yield, %	Relative viscosity	Polymethyl methacrylate, %
38 (I)	5	4	—	—	26.6
		6	—	38.6	24.2
		23	—	4.03	5.4
		30	—	3.34	4.1
40 (I)	10	65	4.6	6.19	11.4
		113	11.5	4.26	4.2
		257	35.3	2.22	2.6

The products contained less than one per cent of vinylcarbazole monomer, except the product 40 (II), which contained 3.8 per cent.

Preliminary fractionations of other samples of polymers containing polymethyl methacrylate having indicated that these can be separated into polyvinylcarbazole homopolymer, and into material which contains polymethyl methacrylate and which appears to be copolymer, sample KE 40 (II) (Table 2) was selected for fractionation.

Table 3. Fractionation of polyvinylcarbazole polymerized in presence of methyl methacrylate. Polymer sample No. KE 40 (II) (Table 2)

Solution		Fractionation					
Polymer, g	Benzene solution, ml	Methanol added, ml	Polymer fraction,		Relative viscosity	Polymethyl methacrylate	
			g	%		content, %	recovery, %
1.0005	100	15	0.4405	44.0	—	<0.2	<2.0
		3	0.0686	6.8	—	<0.2	<0.4
		3	0.0408	4.1	—	5.0	4.8
		85	0.1217	12.2	—	7.0	19.2
		50	0.1690	16.9	—	11.0	44.3
		400	0.0065	0.6	—	0.7	0.1
4.9993	500	67	1.7235	32.5	1.71	0.2	1.6
		23	0.8466	16.9	1.65	1.3	5.2
		28.8	0.3612	7.2	1.36	0.3	0.3
		1000	1.663	33.3	15.65	11.3	89.6

The mother liquor from the second fractionation was evaporated, and a residue (0.166 g) containing 80.5 per cent vinyl carbazole (2.7 per cent on original material) and 0.5 per cent polymethyl methacrylate was isolated.

POLYMERIZATION OF VINYL CARBAZOLE BY ELECTRON ACCEPTORS II

Thus essentially pure polyvinylcarbazole, of a molecular weight somewhat higher than that of homopolymer obtained with the aid of other organic electron acceptors, is a major product, while the polymethyl methacrylate appears to be contained in copolymer of very much higher molecular weight than the homopolymer though of greater solubility in benzene-methanol.

Anthracene has been shown to be a retarder of the free radical initiated polymerization of both vinylcarbazole^{6,7} and MMA⁸.

Table 4. Effect of anthracene upon polymerization of vinylcarbazole in the presence of MMA. MMA: 5.0 per cent w/w on monomer. Temperature: 82°C. Atmosphere: nitrogen

Polymerization		Polymer		
Anthracene on monomer, %	Time, h	Yield, %	Polymethyl methacrylate content, %	Relative viscosity
Nil	48	24.0	14.9	15.7
1	48	9.9	8.2	2.1
Nil	120	31.4	9.2	10.9
1	102	41.2	0.7	1.29
10	120	44.1	0.2	1.21

The bulk polymerization of vinylcarbazole in the presence of 5 to 10 per cent MMA was not found to be sensitive to oxygen, but in toluene solution oxygen affected the polymerization, the effect decreasing with the concentration of the solution. In bulk polymerization both the rate of polymerization and the (very high) molecular weight of the gross product were closely similar, whether the reaction was carried out under air or nitrogen. In toluene solution under nitrogen the relative viscosity of the gross product fell with increasing dilution (25 per cent w/w solution, relative viscosity of polymer 1.9 to 2.0, 12.5 per cent w/w solution, relative viscosity of polymer 1.5 to 1.6). Under air the fall in molecular weight of the polymer was much greater, and the more dilute solution became yellow as the polymerization progressed.

(b) Polymerization initiated by ω-N,N-dialkylaminoalkyl cyanides

N,N-Dimethylaminoacetonitrile proved an effective initiator²³ especially under an inert atmosphere, under which the mixtures remained almost

Table 5. Bulk polymerization of N-vinylcarbazole in the presence of ω-N,N-dialkylaminoalkylnitriles

Polymerization			Polymer		
N,N-(dialkylaminoalkyl) nitrile, g	Atmosphere	Time, h	Yield, %	Relative viscosity	
Dimethylaminoaceto	0.575	Air	21	7.3	1.168
Dimethylaminoaceto	0.5	Air	120	14.2	1.166
Dimethylaminoaceto	0.5	Nitrogen	22	33.0	1.161
Dimethylaminoaceto	0.5	Nitrogen	144	63.5	1.144
Diethylaminopropio	0.5	Air	120	0.26	—
Diethylaminopropio	0.5	Nitrogen	144	6.1	1.146
Diethylaminobutyro	0.5	Nitrogen	144	0.016	—

colourless. In the presence of oxygen the mixtures became progressively more yellow with this and with the other cyanides studied.

(c) *Cryoscopic behaviour of vinylcarbazole-acceptor-benzene mixtures*

The cryoscopic behaviour of vinylcarbazole, of tetrachlorethylene and of maleic anhydride were essentially normal up to concentrations of 0.5, 1.0 and 0.25 mole/l. respectively. At concentrations above 0.25 mole/l. the depression produced by maleic anhydride became increasingly smaller than normal. Of the ternary systems, the one including tetrachlorethylene shows no evidence of complex formation or association up to the maximum concentration studied, but at and above concentrations of 0.25 mole/l. for each solute, the depressions for the system including maleic anhydride became progressively smaller than calculated from the results of the component binary systems.

Table 6. Depression of freezing point of benzene by vinylcarbazole, maleic anhydride or tetrachlorethylene, and by binary mixtures of vinylcarbazole and one of the latter. Cryoscopic constant of benzene: 5120

Solute	Conc., mole/l.	Depression of freezing point, °C	Molecular weight	
			Calc.	Actual
Vinylcarbazole	0.1	0.59	191	193.25
	0.25	1.50	188	
	0.4	2.43	186	
	0.5	2.95	191	
Maleic anhydride	0.1	0.57	100	98.06
	0.2	1.14	100	
	0.25	1.45	99	
	0.4	2.09	110	
	0.5	2.49	115	
Tetrachlorethylene	0.1	0.57	170	165.85
	0.25	1.5	163	
	0.5	2.995	162	
	1.0	5.86	165	

Vinylcarbazole, mole/l.	Maleic anhydride, mole/l.	Tetrachlor- ethylene, mole/l.	Depression,		Difference	
			obs. °C	calc. °C	obs. °C	% on calc.
0.1	0.1	Nil	1.24	1.16	+0.08	+6.9
0.25	0.25	Nil	2.84	2.95	-0.09	-3.1
0.4	0.4	Nil	4.19	4.52	-0.33	-7.9
0.5	0.5	Nil	4.71	5.44	-0.73	-13.4
0.1	Nil	0.1	1.18	1.16	+0.02	+1.7
0.25	Nil	0.25	3.05	3.00	+0.05	+1.7
0.5	Nil	0.5	5.96	5.945	+0.015	+0.25

(d) *Effect of electron acceptors on vinylcarbazole in methanol*

A solution of vinylcarbazole in methanol acquires a characteristic brown-mauve colour on the addition of chloranil; with tetranitromethane the colour is yellow. On exposure to day and artificial light needles of 1,2-*trans*-dicarbazylcyclobutane separate from the solution at a rate which

POLYMERIZATION OF VINYL CARBAZOLE BY ELECTRON ACCEPTORS II

becomes gradually slower, while the intensity of the colouration of the solution fades. Some 9-(1'-methoxyethyl)carbazole was isolated from the illuminated solutions upon dilution with water.

Table 7. Formation of 1,2-*trans*-dicarbazylcyclobutane in methanol solution in day-fluorescent light. Vinylcarbazole: 1.29% w/v. Temperature: ~20°C

Chloranil, % w/v	Tetranitromethane, % w/v	Reaction time, h	1,2- <i>trans</i> -dicar- bazylcyclobutane, %
0.013	Nil	48	11.9
0.013	Nil	120	17.5
0.013	Nil	600	6.3
Nil	0.013	48	2.6

Irradiation of methanol solutions of vinylcarbazole by intense tungsten light was examined in the presence and absence of chloranil.

Table 8. Intense tungsten light irradiation of methanol solutions of vinylcarbazole in the presence and absence of chloranil. Vinylcarbazole: 10 g. Methanol: 750 ml

Chloranil g	Irradiation		Product		
	Time, h	Temp., °C	Dicarbazyl- cyclobutane, g	9-(1'-Methoxy- ethyl)-carbazole, g	Unchanged vinylcarbazole
0.1	2.5	65	1.1	4.07	—
0.1	2.5	~10	0.717	Nil	Some
Nil	4	~10	Nil	Nil	Only product

Upon addition of tetrachlorethylene (0.0128 per cent, 0.064 per cent, 2.0 per cent w/v) or acrylonitrile (0.064 per cent w/v) (as examples of the weaker acceptors) to methanol solutions of vinylcarbazole (1.31 per cent w/v) these remained colourless, and on irradiation in day and artificial light at ~20°C only traces of methanol-insoluble material separated over a period of two months.

Irradiations by intense tungsten light in the presence of chloranil (0.013 per cent w/v) and of one mole (on vinylcarbazole) of acrylonitrile yielded 1,2-*trans*-dicarbazylcyclobutane; no condensation product of vinylcarbazole and acrylonitrile could be isolated.

Only unchanged monomer was obtained following irradiation by the u.v. light from an Engelhard-Hanovia quartz low pressure discharge mercury lamp at ~20° for 5 to 12 h of methanol solutions of vinylcarbazole (1.3 per cent) and chloranil (0.013 per cent). There was some fading of the original brown-mauve colouration of these solutions.

(e) Effect of electron acceptors on vinylcarbazole in acetone

The colour of solutions containing vinylcarbazole and chloranil in acetone is similar (brown-mauve) to that of similar solutions in methanol. In the dark oligomers of vinylcarbazole are formed in such solutions, both at

ambient temperature and at the boiling point. These are fairly soluble in acetone (polyvinylcarbazole of higher molecular weight is only slightly soluble in acetone), and they are precipitated by the addition of water or of methanol.

After 22 days at ambient temperature in the dark a mixture of oligomers m.pt 115° to 204°C (all melting above vinylcarbazole) was obtained from a solution of vinylcarbazole (1.3 per cent) and of chloranil (0.013 per cent) in acetone. From the oligomer mixture a colourless product m.pt 120° to 125°C was isolated by precipitation and extraction with methanol. No monomer could be isolated from this product, nor from that of the following experiment nor from other similar experiments, indicating high conversion. (Found C, 84.3; H, 6.2. $(2C_{14}H_{11}N)CH_3OH$ requires C, 83.3; H, 6.22 per cent). Peaks in the i.r. spectrum at 1090, 1375 cm^{-1} , seen also in the i.r. spectrum of 9-(1'-methoxyethyl)carbazole, indicate one methoxy group for each two carbazyl groups.

A product which is apparently largely the tetramer (Found C, 85.3; H, 5.8; N, 7.1 per cent; mol. wt (in camphor) 785. $(4C_{14}H_{11}N)CH_3OH$ requires C, 85.1; H, 5.9; N, 7.0 per cent; mol. wt 772) was isolated from a similar reaction mixture containing also one mole equivalent (on vinylcarbazole) of acrylonitrile and boiled for 16 h in the dark. No inclusion of acrylonitrile in the product could be detected.

In day-fluorescent light and in the presence of chloranil 1,2-*trans*-dicarbazylcyclobutane was formed in better yield than in methanol solution. With acrylonitrile or MMA as electron acceptors, no colour was developed nor was dimerization observed on exposure to light; essentially pure vinylcarbazole was the sole product isolated.

Table 9. Effect of day-fluorescent light upon vinylcarbazole in acetone in presence of electron acceptors. Temperature: $\sim 20^\circ C$

Solution					Time, h	1,2- <i>trans</i> -dicarbazylcyclobutane, yield, %
Vinylcarbazole, g	Chloranil, g	Acrylonitrile, g	MMA, g	Acetone, ml		
1	0.01	—	—	75	22	43
9.65	—	2.65	—	100	11	Nil
9.65	—	—	5.0	100	26	Nil

DISCUSSION

The results with MMA are now seen to be closely similar to those obtained with other weak organic electron acceptors, and especially with acrylonitrile¹.

Fractionation of the polymer samples obtained with MMA shows these to consist of a mixture of homopolymer, and of material containing in addition to polyvinylcarbazole up to 30 per cent polymethyl methacrylate. The homopolymer has a molecular weight slightly higher than that of polyvinylcarbazole prepared in the presence of other weak electron acceptors; the molecular weight of the polymer containing polymethyl methacrylate is very much higher. The latter is, despite its much higher molecular weight, more soluble in benzene-methanol than the homopolymer. No polymethyl methacrylate homopolymer could be separated from this

fraction, and in view of the conditions of its separation and molecular weight, the polymethyl methacrylate is considered to be present as copolymer with vinylcarbazole.

The high molecular weight copolymer is formed mainly during the first part of the polymerization. This copolymerization is thought to have similarities to the thermal copolymerization of styrene and MMA¹⁷. Thus it proceeds at an appreciable rate at a temperature (80°C) at which, by comparison, the thermal homopolymerization of vinylcarbazole is negligible (judged by controls), and that of MMA¹⁴ is also considered to be much slower^{14, 16}. The rate of thermal copolymerization of styrene-MMA is also much greater than the corresponding rates of the individual monomers suggest. This has been ascribed to thermal bimolecular initiation¹⁷. In the present case the rates of polymerization of vinylcarbazole⁷ and of MMA¹⁴⁻¹⁶ are not very reproducible, and this may be the explanation of an appreciable variation observed in the formation of the copolymer, and consequently of the vinylcarbazole homopolymer.

The effect of anthracene is consistent with the copolymerization proceeding by free radical initiation, since free radical initiated polymerization of both monomers is known to be retarded by anthracene⁶⁻⁸.

It is suggested that a high degree of order due to dipolar interaction between molecules in the molten phase is responsible for the very high molecular weight of the copolymer²², rather than hindrance of chain termination due to the high viscosity of the medium.

The relatively high molecular weight of the homopolymer (compared with that of polyvinylcarbazole obtained in the presence of other weak electron acceptors) is thought to be ascribable to the high viscosity of the medium due to the early formation of the very viscous copolymer. When this copolymerization is repressed by anthracene, the molecular weight of the homopolymer is lowered, even though its rate of formation is not decreased (*Tables 3 and 4*).

If the homopolymerization of vinylcarbazole involves complete charge transfer to the MMA, corresponding homopolymerization of the latter would be expected, since anionically initiated polymerization of MMA is known¹⁸. More rigorous examination is still required to prove completely the absence of polymethyl methacrylate homopolymer from the product. Absence would support the view that partial electron transfer only applies under the conditions of these polymerizations.

In considering the ω -*N,N*-dialkylaminoalkylcyanides, *N,N*-dimethylaminoacetonitrile is seen to present a dipole of a length closely similar to that of the $>N-CH=CH_2$ group, whereas the other nitriles are longer, albeit otherwise similar, dipoles. The observed initiating power of *N,N*-dimethylaminoacetonitrile, especially when compared with its longer relatives, may thus be considered as supporting the case for initiation of vinylcarbazole by a mechanism involving increased mesomeric polarization.

The results of the cryoscopic determinations indicate that in a non-ionizing solvent such as benzene, there is a distinct interaction between the stronger organic acceptors and vinylcarbazole (at least above a lower limit of concentrations), but with a weaker acceptor, such as tetrachloroethylene, there is no indication of complex formation with vinylcarbazole

up to the highest concentration studied. The results with solutions of vinylcarbazole in methanol or acetone reveal a notable difference between the weaker and stronger organic electron acceptors. No colour forms on addition of MMA, acrylonitrile or tetrachlorethylene (in methanol), and on exposure of solutions containing these weaker acceptors to daylight, only unchanged vinylcarbazole could be isolated.

When chloranil was added to similar solutions, the intense brown-mauve colouration ascribed to the chloranil cation radical developed quickly, and on exposure to day and fluorescent light, 1,2-*trans*-dicarbazylcyclobutane was formed in both solvents, accompanied in the methanol solution by some 9-(1'-methoxyethyl)carbazole. In the dark methanolysis occurred in the methanol solution, and in acetone vinylcarbazole oligomers were formed.

If the interaction of vinylcarbazole with the weaker acceptors in the absence of solvent or in non-ionizing solvents were to result in solvated ion pairs or in ionic species, the required electron transfer should be promoted in ionizing solvents such as methanol and acetone. In the absence of such an effect, the interaction, in the absence of solvent or in non-ionizing solvent, is regarded as amounting to only partial charge transfer.

The formation in the dark of vinylcarbazole oligomers (in acetone solution by chloranil) occurs under conditions under which vinylcarbazole cation radicals are considered to be formed. The low molecular weights of these products are notable. Comparison with the degree of polymerization of the polyvinyl carbazole obtained by tropylium hexachloroantimonate or tropylium tetrafluoroborate in methylene dichloride, which is also believed to involve formation of vinylcarbazole cation radicals¹², will be of interest.

The occurrence and characteristic features of polymerization by charge transfer will be determined by the amount of activation required for initiation to occur, and upon the factors determining the propagation and termination reactions.

The degree of charge transfer required for initiation will depend on the nature of the monomer, and there are indications that this requirement can vary appreciably. If mesomeric polarization is insufficient, complete charge transfer is necessary before polymerization can occur. Thus isobutylvinyl ether polymerizes rapidly even at 0°C in the presence of tropylium salts in methylene dichloride¹², but does not polymerize with weaker organic acceptors even on heating²². Acenaphthylene is another monomer requiring apparently a strong acceptor for initiation^{12, 22}.

Initiation of vinylcarbazole by mesomeric polarization appears to be possible, and to be necessary, if polymer of more than a very low degree of polymerization is to be obtained. Some of the reasons have been discussed, and attention has been drawn to the limiting effect of mesomerism in the $>N-CH=CH_2$ upon free rotation of the bond linking the nitrogen atom and the vinyl group¹. The restriction of free rotation should increase with increasing charge transfer, and upon the loss of an electron from the nitrogen, the nitrogen bonds should approach coplanarity¹³.

The degree of steric hindrance produced must depend on the shape and size of the molecule bearing the vinyl group and the nature of the reaction. The shape of the vinylcarbazole molecule is such that with the vinyl group

forced into the plane of the carbazole ring, steric hindrance especially to reaction with another large molecule such as vinylcarbazole must be severe, and must be greater for the dimer (and for higher stages) than for the monomer.

This effect may contribute to the low degree of polymerization of polyvinylcarbazole obtained under conditions indicating complete charge transfer, compared with the much higher molecular weight obtained in the presence of weak acceptors and of dipolar molecules.

These steric considerations apply to the activated intermediates involved in the initiation and propagation stages, and should not be applicable to conventional cationic polymerization.

Under conditions of partial charge transfer, polymerization is much slower than when complete charge transfer is indicated, especially at lower temperatures¹². That complete charge transfer can occur under favourable conditions with vinylcarbazole is indicated by the earlier and present results, and is supported also by the preparation of Wurster cations from related compounds¹⁹. It is notable that the oxidative step by which the latter are formed is slow. This should be reflected in the polymerization kinetics, indicating whether complete charge transfer is essential to the polymerization.

The photochemical dimerization of vinylcarbazole appears to have features similar to the photochemical formation of cyclobutanes studied by Bryce-Smith²¹ and by Schenck *et al.*²⁰. The latter authors note (without supporting data) the preparation of a cyclobutane dimer from acenaphthylene in the presence of chloranil²⁰. In the present instance also, there is some evidence of dissociation of the dimer (presumably after much of the chloranil has been destroyed). No open chain dimer which might be considered as intermediate in cyclobutane formation or dissociation has been identified, so that despite the large substituent groups both reactions appear to be concerted. The role of chloranil in this dimerization still requires elucidation.

The author wishes to thank Mr E. Freeman for experimental assistance, Professor C. E. H. Bawn and Dr A. Ledwith, Liverpool University, for their encouragement and valuable discussions, the Ministry of Aviation for their support of this work, and the British Oxygen Company Limited for permission to publish this paper.

*The British Oxygen Company Limited,
Scientific Centre,
Deer Park Road, London, S.W.19*

(Received April 1965)

REFERENCES

- ¹ ELLINGER, L. P. *Polymer, Lond.* 1964, **5**, 559
- ² SCOTT, H., MILLER, G. A. and LABES, M. M. *Tetrahedron Letters*, 1963, No. 17, 1073
- ³ ELLINGER, L. P. *Chem. & Ind.* 1963, 1982
- ⁴ BRIEGLEB, G. *Elektronen-Donator-Acceptor-Komplexe*, p 186. Springer: Berlin, 1961
- ⁵ ELLINGER, L. P., FEENEY, J. and LEDWITH, A. *Mh. Chem.* 1965, **96**, 131
- ⁶ HORT, E. V. and GRAHAM, D. E., to General Aniline & Film Corp. *U.S. Pat. No.* 2883393 (1959)
- ⁷ ELLINGER, L. P. *J. appl. Polym. Sci.* In press
- ⁸ SINITSYNA, Z. A. and BAGDASAR'YAN, K. S. *Zt. fiz. Khim.* 1958, **32**, 2614
- ⁹ BARB, W. G. *Trans. Faraday Soc.* 1953, **49**, 143
- ¹⁰ ARBUZOV, B. A., SANITOV, Y. Y. and KONOVALOV, A. P. *Izvest. Akad. Nauk S.S.S.R., Ser. Fiz.* 1963, **27**, No. 1, 82
- ¹¹ ALFREY Jr, T. and KAPUR, S. L. *J. Polym. Sci.* 1949, **4**, 215
- ¹² BAWN, C. E. H., FITZSIMMONS, C. and LEDWITH, A. *Proc. chem. Soc., Lond.* 1964, 391
- ¹³ WHELAND, G. W. *Resonance in Organic Chemistry*, p 512. Wiley: New York, 1955
- ¹⁴ WALLING, C. and BRIGGS, E. R. *J. Amer. chem. Soc.* 1946, **68**, 1141
- ¹⁵ BAMFORD, C. H. and DEWAR, M. J. S. *Proc. Roy. Soc. A*, 1949, **197**, 356
- ¹⁶ MACKAY, M. H. and MELVILLE, H. W. *Trans. Faraday Soc.* 1949, **45**, 323; 1950, **46**, 63
- ¹⁷ WALLING, C. J. *Amer. chem. Soc.* 1949, **71**, 1930
- ¹⁸ BEAMAN, R. G. *J. Amer. Chem. Soc.* 1948, **70**, 3115
- ¹⁹ LEDWITH, A. and SAMBHI, M. *Chem. Comm.* 1965, **4**, 64
- ²⁰ SCHENCK, G. O., HARTMANN, I. and METZNER, W. *Tetrahedron Letters*, 1965, **6**, 347
- ²¹ BRYCE-SMITH, D. and GILBERT, A. *Tetrahedron Letters*, 1964, **4**, 3471
- ²² ELLINGER, L. P. Unpublished results
- ²³ ELLINGER, L. P. to British Oxygen Co. Ltd. *Brit. Pat. Appl. No.* 31654/64

Pyrolysis—Hydrogenation—GLC of Alpha Olefin Copolymers

J. VAN SCHOOTEN and J. K. EVENHUIS

Pyrolysis—hydrogenation—GLC has been applied to copolymers of ethylene with propylene and butene-1, to propylene—butene-1 copolymers and to partly unsaturated ethylene—propylene terpolymers. Copolymers of ethylene with up to about ten per cent by weight of butene-1, hexene-1 and octene-1 have been used to interpret the pyrograms of Ziegler, and of high-pressure, polyethylene. The method is shown to provide information both about the composition and about the structure, degree of alternation, head-to-head or head-to-tail arrangement, etc., of copolymers.

Quantitative methods of analysis are described for ethylene—propylene copolymers and for ethylene—propylene—dicyclopentadiene terpolymers.

In a previous paper¹ we described the application of pyrolysis—hydrogenation—GLC to a number of poly- α -olefins.

In the present paper we wish to report similar experiments on a number of α -olefin copolymers and the application of the method to quantitative copolymer analysis.

EXPERIMENTAL

The sample, about 0.4 mg, is pyrolysed at a temperature of about 500°C on a Nichrome spiral in a stream of hydrogen, which serves as the carrier gas. The pyrolysis products are then led over a hydrogenation catalyst and all products are thus converted into saturated hydrocarbons, which are separated by a GLC column with flame ionization detection. The procedure and the apparatus used have been described in detail previously¹. The following samples were used in the present investigation:

(1) *Ethylene—propylene copolymers*—Prepared with various catalyst systems based on TiCl_3 , VCl_3 or VOCl_3 in combination with an alkylaluminium or alkylaluminium halide, and of varying overall composition. Besides saturated ethylene—propylene copolymers we investigated a number of unsaturated terpolymers, most of which contained dicyclopentadiene as the third monomer. As before¹, a sample of hydrogenated natural rubber was included as a model for ideally alternating ethylene—propylene copolymer.

(2) *Ethylene—butene copolymers*—Prepared with a catalyst containing TiCl_3 and AlEt_3 . As a special type of ethylene—butene copolymer a few hydrogenated polybutadienes were investigated as well. These varied in 1.4/1.2 ratio, corresponding to varying ethylene/butene ratios in the hydrogenated product.

(3) *Propylene—butene copolymers*—Prepared with a TiCl_3 — AlEt_3 catalyst.

(4) *Ethylene—hexene-1 copolymer*—Containing ten per cent by weight of hexene-1, prepared with γ - TiCl_3 and an alkylaluminium halide.

(5) *Ethylene-octene-1 copolymer*—Containing ten per cent by weight of octene-1, also prepared with γ -TiCl₃ and an alkylaluminium halide.

(6) A sample of *commercial Ziegler-type polyethylene*, density 0.945, a sample of *high-pressure polyethylene* and a *linear polyethylene* (polymethylene).

ETHYLENE-PROPYLENE COPOLYMERS

(A) Relation between structure and pyrogram

(1) *Degree of alternation*—Two copolymers of the same overall composition may differ widely in the way in which the two types of monomer units are distributed in the polymer molecule.

The two extremes of a one-to-one ethylene-propylene copolymer are, on the one hand, the completely alternating copolymer, and on the other the block copolymer in which the molecule consists of one long block of ethylene units and one long block of propylene units. The former type of ethylene-propylene copolymer is structurally identical with completely hydrogenated natural rubber, whereas the latter type of copolymer will in many respects behave like an intimate mixture of the two homopolymers. A third idealized copolymer is one where the monomer sequence-length distribution corresponds to a random insertion of the two monomers.

As has been shown before^{2,3}, the pyrogram of a copolymer depends on the sequence-length distribution. For ethylene-propylene copolymers this is illustrated in *Figure 1*, where the main peaks of the pyrogram of a copolymer containing about 50% M ethylene have been compared with those of the pyrograms of hydrogenated natural rubber and of a 1:1 molar mixture of polyethylene and polypropylene. It will be seen that the copolymer, in which the monomer distribution is near random, gives a pyrogram with peak heights intermediate between the two extremes. The

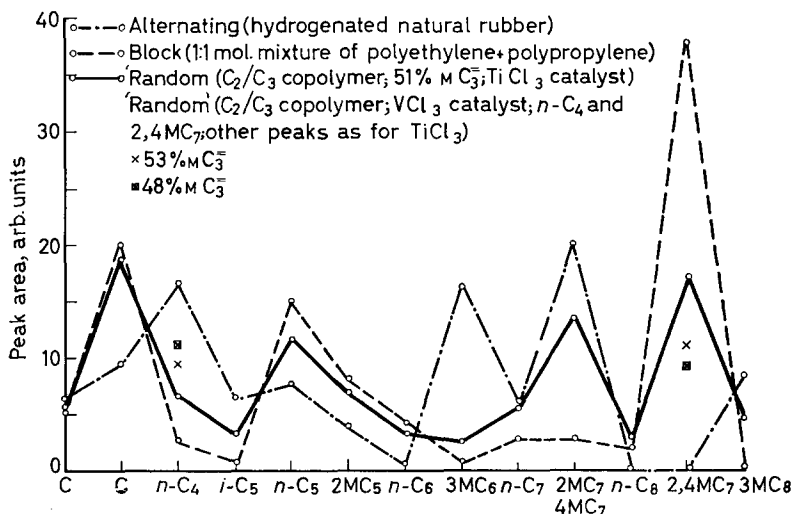


Figure 1—Pyrograms of ethylene-propylene copolymers

same figure also shows that the curves for the copolymer prepared with a γ - TiCl_3 -containing catalyst differ from those prepared with a VCl_3 -containing catalyst only in the $n\text{-C}_4$ and the $2,4\text{MC}_7$ peaks*.

Differences in the degree of alternation between these copolymers show up very clearly when the ratios of the heights or areas of the $2,4\text{MC}_7$ peaks to the heights or areas of the $n\text{-C}_4$ peaks are plotted versus composition.

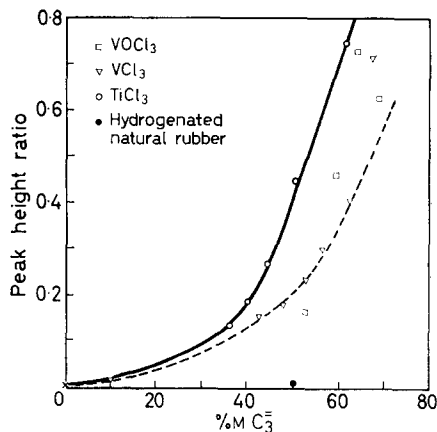
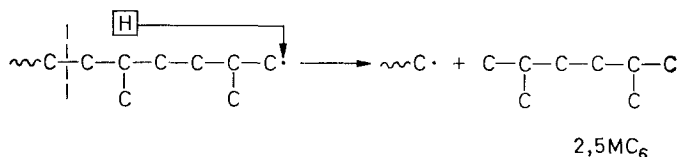


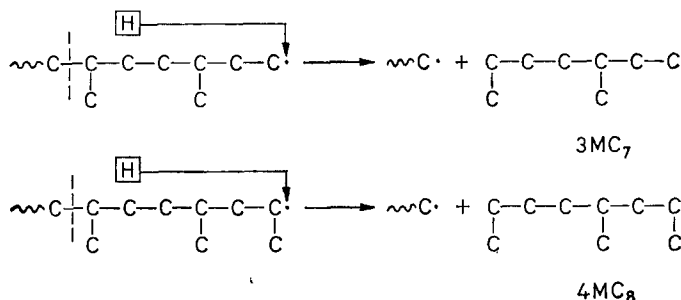
Figure 2—Ethylene-propylene copolymers. Peak height ratio $2,4\text{MC}_7/n\text{-C}_4$ as a function of propylene content

This is illustrated in Figure 2. The $2,4\text{MC}_7$ peak, which is absent from the pyrogram of hydrogenated natural rubber, is representative of the longer propylene sequences. The $n\text{-C}_4$ peak is large in the pyrogram of hydrogenated natural rubber. The results given in Figure 2 therefore show that the VCl_3 catalyst produces a higher degree of alternation than the TiCl_3 catalyst, which is in agreement with conclusions drawn from kinetic measurements⁴.

(2) *Head-to-head and head-to-tail arrangement*—In previous papers^{5,6} we have shown that ethylene-propylene copolymers prepared with VOR_3 -containing catalysts contain methylene sequences of two units, thus indicating a tail-to-tail coupling of two propylene units and/or the presence of one ethylene unit between two head-to-head propylene units. The characteristic peaks for methylene sequences of two units are the $2,5\text{MC}_6$, 3MC_7 and 4MC_8 peaks, which can be regarded as being formed by a hydrogen transfer reaction with the fifth carbon atom:



*Throughout this paper the saturated pyrolysis products are denoted by a code in which M=methyl, E=ethyl, P=propyl, Bu=butyl, Cy=cyclo and C_i =a straight chain of i carbon atoms. Thus $n\text{-C}_4$ denotes n -butane and $2,4\text{MC}_7$, 2,4-dimethylheptane.



Similarly, peaks that are characteristic of sequences of three methylene units are, for example, the 2MC_7 , 4MC_7 and 4MC_9 peaks (see pyrogram of hydrogenated natural rubber in ref. 1).

The ratios of the heights of the $2,5\text{MC}_6$ and the 4MC_9 peaks to the height of the $n\text{-C}_4$ peak are plotted versus composition in Figures 3 and 4 respectively. These figures illustrate that the copolymers prepared with a VOCl_3 -containing catalyst do indeed show different behaviour as expected, i.e. markedly higher $2,5\text{MC}_6$, 3MC_7 and $2\text{MC}_8 + 4\text{MC}_8$ peaks and smaller $2\text{MC}_7 + 4\text{MC}_7^*$ and 4MC_9 peaks than any of the copolymers prepared with the other catalyst systems. This is in fact a good illustration of the potentialities of pyrolysis-GLC in the study of polymer structure.

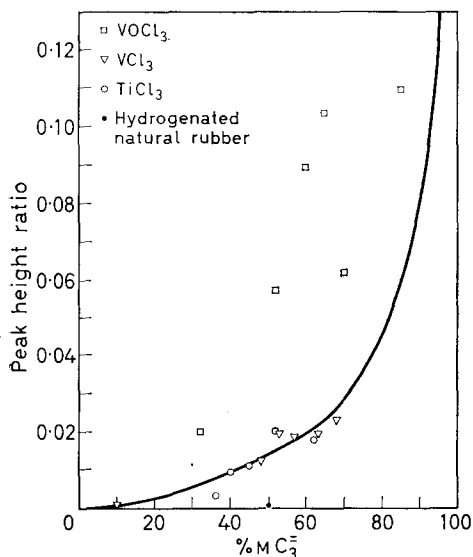


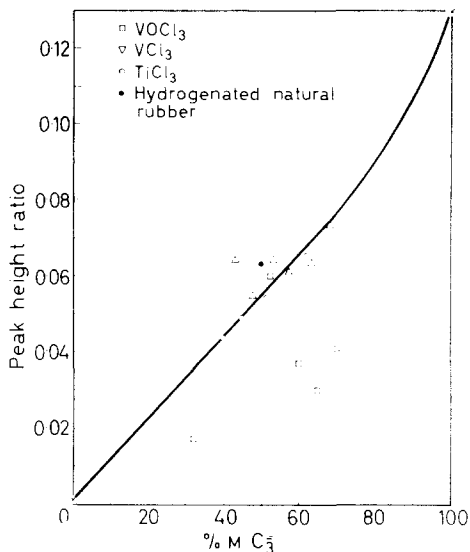
Figure 3—Ethylene-propylene copolymers. Peak height ratio $2,5\text{MC}_6/n\text{-C}_4$ as a function of propylene content

(B) Quantitative analysis of copolymer composition

The quantitative determination of the ethylene-propylene copolymer composition is usually carried out by i.r. spectroscopic measurements⁷. These measurements are accurate and quite straightforward for samples that are completely soluble in carbon tetrachloride at room temperature.

*The 2MC_7 and 4MC_7 peaks coincide.

Figure 4—Ethylene-propylene copolymers. Peak height ratio $4MC_3/n-C_4$ as a function of propylene content



For samples that are only partly soluble, however, the determination has to be carried out on thin films with the aid of calibration curves constructed by some absolute method.

Since the thin-film i.r. methods are sensitive to the degree of alternation and to the presence of polyethylene or polypropylene crystallinity as well as to composition, we have tried to determine whether a pyrolysis-hydrogenation-GLC method could be developed for this purpose.

The application of pyrolysis-GLC to the quantitative analysis of copolymers has been discussed by several authors^{2,8-10}. The analysis of ethylene-propylene copolymers by pyrolysis-GLC using the height ratio of two unidentified peaks has been described by Groten¹¹.

Since our pyrogram of polyethylene consists almost exclusively of normal alkanes and that of polypropylene of *iso*-alkanes the ratio of the peak heights of a *n*-alkane to an *iso*-alkane is expected to be a good measure of the copolymer composition.

We have therefore drawn up a number of calibration curves for various types of ethylene-propylene copolymers by the ratios* of peak heights of normal alkanes to those of *iso*-alkanes ($n-C_4$, $n-C_6$, $n-C_7$ or $n-C_8$ to $i-C_3$, $i-C_5$, $2MC_5$, $2MC_6$, $2,4MC_5$, $2MC_7 + 4MC_7$ † or $2,4MC_7$) versus propylene content as determined by i.r. analysis (using the solution method wherever possible). Some of these relationships appear to be very sensitive to the catalyst system used, either because of the effect of blockiness or because of some deviation from the regular head-to-tail arrangement of the propylene units (see, for example, Figures 2 and 4). Other relationships were much less susceptible to differences in copolymer structure and these also appeared to show better reproducibility. Of these the most suitable was the ratio $n-C_7/(2MC_7 + 4MC_7)$ (see Figure 5).

*For quantitative comparisons we prefer peak-height or peak-area ratios to peak heights or peak areas because of better reproducibility.

†See footnote on page 564.

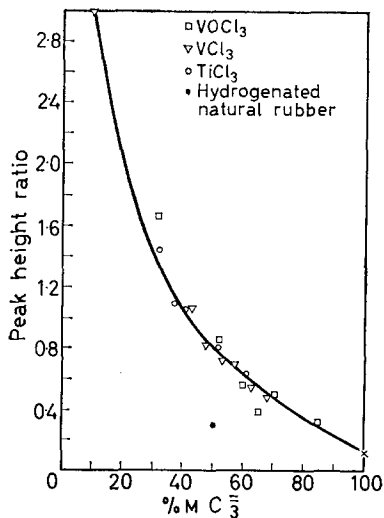
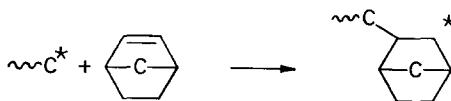


Figure 5—Ethylene-propylene copolymers. Peak height ratio $n-C_7/(2MC_7+4MC_7)$ as a function of propylene content

(C) *Unsaturated ethylene-propylene copolymers*

To obtain ethylene-propylene copolymers that can be vulcanized with conventional vulcanization recipes based on sulphur, a small amount of unsaturation is introduced into the polymer¹²⁻¹⁴. This is achieved by the use of a non-conjugated diene as a termonomer. The dienes used contain one polymerizable double bond and one that is unreactive in the polymerization. One successful termonomer in this connection is dicyclopentadiene (DCPD, structure: see *Table 1*), in which the reactive double bond is the one in the norbornene ring, and the double bond that remains present in the terpolymer and can be used for vulcanization is the one in the cyclopentene ring. Data on a number of terpolymers containing various dienes similar to DCPD and the main peaks of their pyrograms are given in *Table 1*.

The relatively low unsaturation of sample 2 shows that under the conditions of these experiments the polymerization of the norbornene double bond proceeds via a normal double bond opening and not via an opening


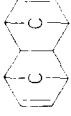


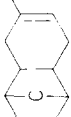

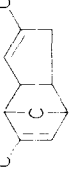


of the C—C bond next to the double bond (as was also found to be possible by Truett¹⁵ and Sartori¹⁶).

The pyrograms summarized in *Table 1* show that very large cyclic peaks are obtained from the unsaturated ring: $MCyC_5$ is found when methyl-norbornadiene is incorporated; CyC_5 when DCPD is incorporated; $MCyC_6$ and $1,2-MCyC_6$ when the addition compounds of norbornadiene with, respectively, isoprene and dimethylbutadiene are incorporated; and $MCyC_5$ when the dimer of methylcyclopentadiene is incorporated. The saturated

PYROLYSIS-HYDROGENATION-GLC OF α -OLEFIN COPOLYMERS

Table 1
Characteristic peaks in the pyrograms of a number of unsaturated terpolymers

Sample No.	1	2	3	4	5	6	7	8
% MC ₃	32	n.d.	34	34	32	35	n.d.	32
Unsaturation, C : C/1000 C	0	0.8	≤0.5	8	8.1	9.5	13	4.5
Termonomer	None	Norbornene 			DCPD 			 (dimer of MCPD)
Peak height, cm, n-C ₄	4.3	4.3-5	4.5	3.8	26.5	3.7	4.7	3.4
" " " CyC ₅	0.0	6.5	4.1	2.2	28.7	2.1	2.8	1.2
" " " MCyC ₅	0.6	1.2	1.4	4.5	2.1	2.4	2.5	9.7
" " " CyC ₆	0.35	0.5	0.5	0.6	0.9	0.7	0.5	0.5
" " " MCyC ₆	0.6	0.7	0.7	1.3	0.9	20.6	1.1	0.7
" " " ECyC ₅	0.2	0.5	0.5	3.1	1.1	—	1.2	0.4
" " " n-PCyC ₅	0.0	0.15	0.1	0.15	0.5	0.1	0.15	1.7
" " " 1,2MCyC ₆	0.0	0.0	0.0	0.5	0.0	0.0	17.8	0.0

n.d. = not determined
* Intake: ca. 16 mmole per 1000 C atoms polymer

cyclopentane rings present in the same ring systems in equal concentrations, however, give rise to peaks which are an order of magnitude smaller. Obviously, therefore, the peaks which stem from the termonomer could be used to determine its content if a suitable calibration procedure could be found.

The terpolymers were characterized by ozone absorption¹⁷, expressed as the number of double bonds per thousand carbon atoms. Consequently we subjected a number of terpolymers containing dicyclopentadiene and having different amounts of unsaturation, to pyrolysis-GLC analysis and plotted the height of the characteristic peaks (or the ratio of the heights of these peaks to the height of the $n\text{-C}_4$ peak) against unsaturation. In *Figure 6* these relationships are given for the cyclopentane peak. Similar curves were found for the methylcyclopentane or ethylcyclopentane peaks.

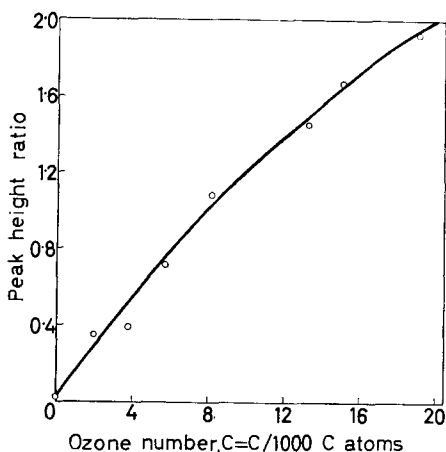


Figure 6—Ethylene-propylene-dicyclopentadiene rubbers. Peak height ratio $\text{CyC}_5/n\text{-C}_4$ versus ozone number

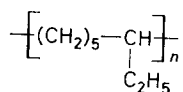
ETHYLENE-BUTENE-1 COPOLYMERS

Ethylene-butene-1 copolymers prepared by copolymerizing ethylene and butene-1 should give pyrograms with two types of peaks. On the one hand, peaks are expected which are characteristic of long sequences of one monomer, as found in the homopolymer pyrograms, and on the other, peaks which are typical of an alternating ethylene-butene copolymer—in fact exactly the same as is found for ethylene-propylene copolymers. Assuming a close analogy between the pyrogram of an alternating ethylene-butene copolymer and that of an alternating ethylene-propylene rubber the characteristic peaks in the former pyrogram would be the 3EC_6 and 3MC_9 peaks. These peaks could therefore in principle be used to find differences in degree of alternation between various types of ethylene-butene copolymers. The 3EC_6 peak, however, was found to coincide with the 3MC_7 peak, which is characteristic of long butene sequences, and so only the 3MC_9 peak remains.

Another polymer which can be regarded as an ethylene-butene copolymer is obtained by hydrogenation of polybutadienes. Polybutadienes with widely

varying 1,2 contents can be made with a lithium-butyl catalyst in isooctane with varying amounts of tetrahydrofuran. The amount of tetrahydrofuran determines the 1,2/1,4 ratio¹⁸. Each butadiene segment in 1,4 arrangement corresponds, after hydrogenation, to two ethylene units and a butadiene in 1,2 configuration to a butene unit, long sequences of 1,4 arrangement therefore give long ethylene sequences and long 1,2 sequences give long butene sequences. An alternating 1,4-1,2 butadiene polymer will have methylene sequences of five units, and a random 1,4-1,2 distribution will have isolated methylene units and sequences of 5, 9, 13 and more, methylene units; sequences of three methylene units, characteristic of an alternating ethylene-butene copolymer, will be absent, however.

On applying the rules which we have found to hold for the pyrograms of poly- α -olefins to the hydrogenated alternating 1,4-1,2 polybutadiene,



we would expect the pyrogram of this polymer to contain a rather large n -C₈ peak and a very small 3MC₉ peak, in addition to the other peaks found for ethylene-butene copolymers.

We have pyrolysed a few samples of both types of ethylene-butene-1 copolymers. A survey of the areas of the main peaks is given in *Figure 7*

Components	Peak area, arbitrary units
C ₂	—————
C ₃	—————
n -C ₄	—————
i -C ₅	—————
n -C ₅	—————
n -C ₆	—————
n -C ₇	—————
3MC ₇	—————
3EC ₆	—————
n -C ₈	—————
n -C ₉	—————
3MC ₉	—————
n -C ₁₀	—————
5EC ₉	—————
3,7MC ₉	—————
3M5EC ₉	—————
n -C ₁₁	—————

Figure 7—Areas of the main peaks in the pyrogram of an ethylene-butene-1 copolymer containing 50% M of butene-1

for one of the copolymers. Peak heights are given as a function of butene content in *Figures 8* and *9* for the directly prepared copolymers. Differences in the heights of the respective peaks for the two types of copolymers have

Figure 8—Ethylene-butene-1 copolymers. Peak heights of *n*-alkanes as functions of butene-1 content

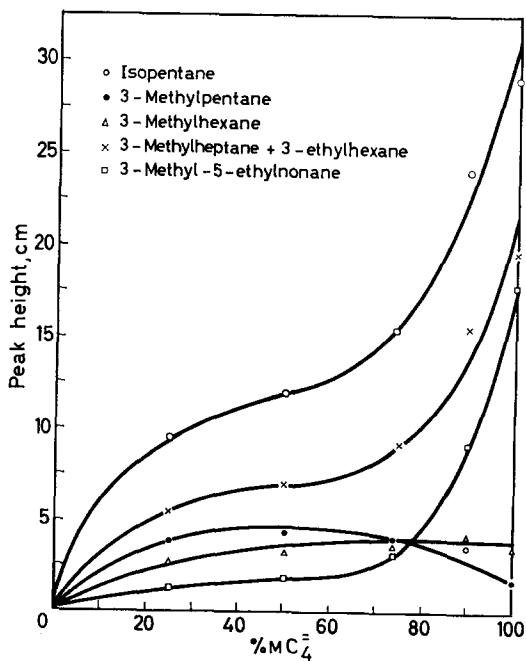
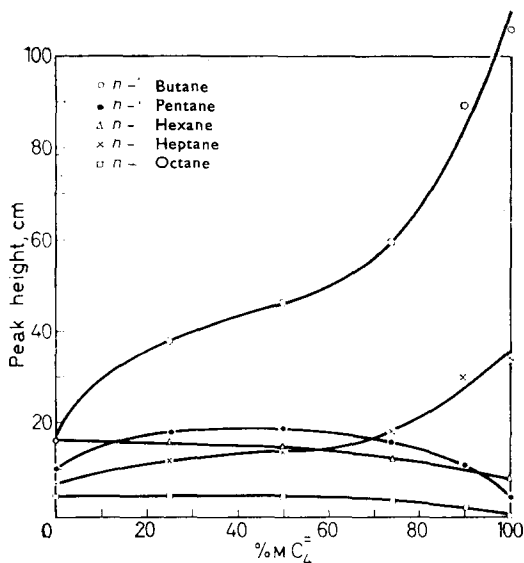
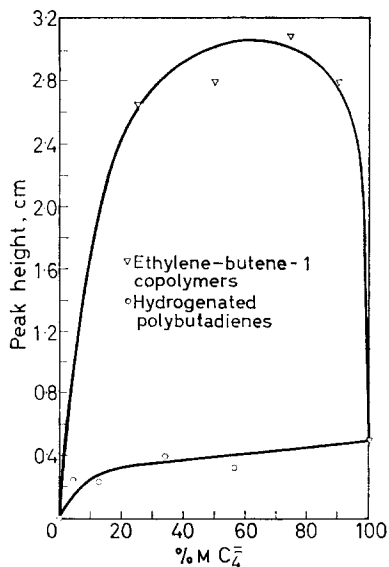


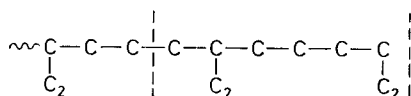
Figure 9—Ethylene-butene-1 copolymers. Peak heights of isoalkanes as functions of butene-1 content

in general been found to be only slight. One exception, however, was the considerable difference found between the 3MC₉ peaks (see Figure 10), as

Figure 10—Height of 3MC₉ peak as a function of butene-1 content



was only to be expected, considering that this peak is characteristic of butene-ethylene-butene (b-e-b) sequences:



PROPYLENE-BUTENE-1 COPOLYMERS

Three samples of propylene-butene copolymers have been studied with pyrolysis-GLC. Apart from the fragments characteristic of the homopolymers, we should expect peaks stemming from propylene-butene-1 (p-b) or b-p sequences, from p-p-b or b-p-p sequences and from p-b-b or b-b-p sequences. Characteristic peaks for the alternating copolymer should include, for example, n -C₆, 2MC₆, 3MC₆, 3,5MC₉, 2M4EC₇, 3,5,7MC₉, 2,6M4EC₇ peaks; for a $-(p-p-b)_n-$ polymer characteristic peaks would be the 2,4MC₈, 3,5MC₈ and 2,4,6MC₈ peaks; and for a $-(b-b-p)_n-$ polymer the 2M4EC₈ and 3M5EC₈ peaks. The areas of the main peaks of the pyrograms are given in Figure 11, while peak areas are given as a function of butene content in Figures 12 and 13. In Figure 12 we have given those peaks that are characteristic of sequences containing one of the monomers only: the C₃ and n -C₄ peaks from the unzipping reaction, the n -C₅ and n -C₇ peaks formed by intramolecular hydrogen transfer and composed of two propylene and two butene units respectively, and the 2,4MC₇ and 3M5EC₉ peaks, similarly formed and containing three monomer units of the same type. The last two peaks are characteristic of long

Figure 11—Areas of the main peaks in the pyrogram of a propylene-butene-1 copolymer containing 50% M of butene-1

Components	Peak area, arbitrary units
C ₂	_____
C ₃	_____
n-C ₄	_____
i-C ₅	_____
n-C ₅	_____
2MC ₅	_____
n-C ₆	_____
2MC ₆	_____
3MC ₆	_____
n-C ₇	_____
3MC ₇	_____
2,4MC ₇	_____
2,4MC ₈	_____
2M4EC ₇	_____
3,5MC ₈	_____
3M5EC ₈	_____
2,6M4EC ₇	_____
4,6MC ₉	_____
2M4EC ₈	_____
3M5EC ₈	_____
3,5MC ₉	_____
3M5EC ₉	_____

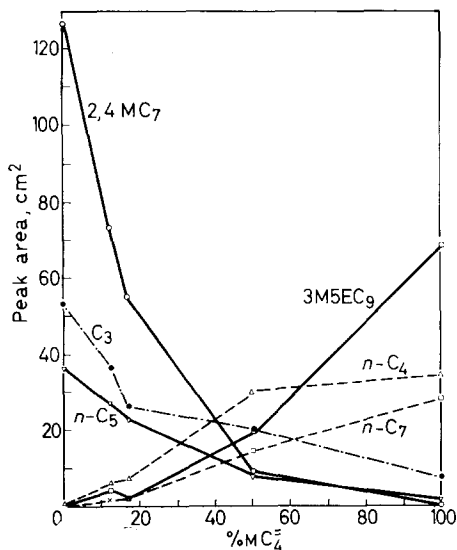
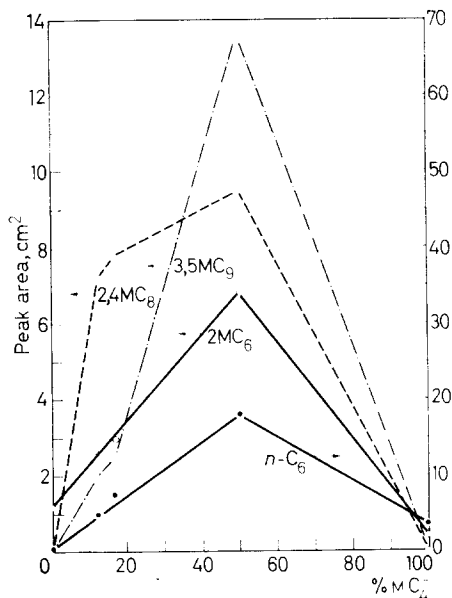


Figure 12—Propylene-butene-1 copolymers. Peak areas versus butene-1 content

propylene or butene sequences and should therefore be the most dependent on composition. In Figure 13 we have plotted the areas of several peaks which stem from a p-b or b-p sequence—the n-C₆, 2MC₆ and the 3,5MC₆ peaks—and one peak (2,4MC₈) which stems from a p-p-b or b-p-p sequence. The former peaks are a measure of the degree of alternation and should be at their maximum height at about 50% M butene, the latter peak should be at its maximum height at higher propylene contents. The shapes of the curves in Figures 12 and 13 are at least roughly in agreement with these expectations.

Figure 13--Propylene-butene-1 copolymers. Peak areas versus butene-1 content



SHORT-CHAIN BRANCHES IN POLYETHYLENE
 Short-chain branching in polyethylene has been the subject of several publications¹⁹⁻²⁵ and has been studied by i.r. spectroscopic techniques and by a combination of high-energy electron irradiation and mass spectro-

Table 2. Areas of the main iso-alkane peaks in the pyrograms of linear polyethylene, ethylene-butene-1, ethylene-hexene-1 and ethylene-octene-1 copolymers

Component	Peak area in arbitrary units			
	Linear PE	Ethylene-butene-1	Ethylene-hexene-1	Ethylene-octene-1
i -C ₄	10	20	<u>37</u>	<u>30</u>
i -C ₅	18	<u>47</u>	<u>62</u>	<u>46</u>
2MC ₅	9	<u>14</u>	<u>18</u>	<u>20</u>
3MC ₅ -CyC ₅	31	<u>54</u>	<u>46</u>	<u>76</u>
2MC ₆	14	<u>13</u>	<u>74</u>	<u>22</u>
3MC ₆	13	<u>33</u>	<u>24</u>	<u>26</u>
2MC ₇ -4MC ₇	16	<u>17</u>	<u>25</u>	<u>27</u>
3MC ₇ -3EC ₆	16	<u>67</u>	<u>64</u>	<u>32</u>
2MC ₈ -4MC ₈ -ECyC ₆	50	<u>44</u>	<u>38</u>	<u>119</u>
3MC ₈	9	<u>39</u>	<u>12</u>	<u>17</u>
4MC ₉ -5MC ₉ -4EC ₈	11	<u>21</u>	<u>51</u>	<u>36</u>
i -PCyC ₆ -BuCyC ₅			<u>94</u>	
2MC ₉ - n -PCyC ₆	40	<u>35</u>	<u>40</u>	<u>65</u>
3MC ₉	8	<u>27</u>	<u>6</u>	<u>45</u>
4MC ₁₀ -5MC ₁₀ - sec BuCyC ₆	25	<u>23</u>	<u>67</u>	<u>32</u>
2MC ₁₀ -4MC ₁₀ - n -BuCyC ₆	33	<u>30</u>	<u>47</u>	<u>102</u>
3MC ₁₀	15	<u>32</u>	<u>14</u>	<u>34</u>

metry^{21, 22}. This latter approach has shown that the short branches in high-pressure polyethylenes are mainly ethyl and *n*-butyl groups, but other short branches have also been supposed to be present²².

In order to explore the potential contribution of pyrolysis-hydrogenation-GLC to the further elucidation of structural details, we applied our technique to a number of polyethylenes and modified polyethylenes which contain small amounts of a comonomer.

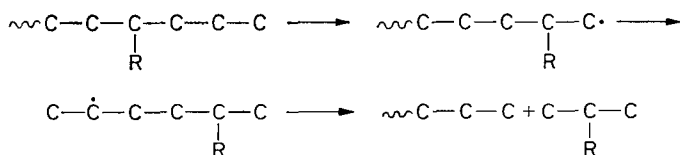
We will first discuss the pyrograms of three experimental polyethylenes containing about ten per cent by weight of butene-1, hexene-1 and octene-1 respectively, in comparison to that of a linear polyethylene. A survey of the iso-alkane peaks of the pyrograms of these polymers with their probable assignment is given in *Table 2*. The polymers have been tested also as 1 mg sample instead of the normal 0.4 mg in order to increase the size of the iso-paraffin peaks.

The effect of the comonomer on the relative sizes of the *n*-alkane peaks is given in *Table 3*. The peaks stemming from the total side group appear to be somewhat increased in intensity (*n*-C₄ peak in the polyethylene-hexene pyrogram, *n*-C₆ peak in polyethylene-octene pyrogram). The polyethylene-octene pyrogram also shows that the peak stemming from the *n*-alkane with one carbon atom less is somewhat enlarged.

Table 3. Relative sizes of *n*-alkane peaks for polyethylene and for ethylene-butene-1, ethylene-hexene-1 and ethylene-octene-1 copolymers

Peak ratio	Marlex 50	Ethylene-butene-1	Ethylene-hexene-1	Ethylene-octene-1
<i>n</i> -C ₄ - <i>n</i> -C ₇	0.71	0.86	1.15	0.86
<i>n</i> -C ₅ - <i>n</i> -C ₇	0.59	0.69	0.61	0.91
<i>n</i> -C ₆ - <i>n</i> -C ₇	0.52	1.66	1.62	1.88
<i>n</i> -C ₈ - <i>n</i> -C ₇	0.63	0.58	0.66	0.79
<i>n</i> -C ₉ - <i>n</i> -C ₇	0.67	0.63	0.62	0.75
<i>n</i> -C ₁₀ - <i>n</i> -C ₇	1.02	0.93	0.99	1.05
<i>n</i> -C ₁₁ - <i>n</i> -C ₇	1.00	0.82	0.90	0.92

This suggests that chain scission may occur both at the α - and at the β -C—C bond. Only the latter type of scission will produce methyl-substituted iso-alkanes, e.g. after intramolecular hydrogen transfer:



A list of iso-alkanes that may be expected to be formed in this way, is compared in *Table 4* with a list of those that have actually been found to be significantly increased in size in the copolymer pyrograms.

In some cases the increase in size of these peaks cannot be determined as accurately as one would wish because of the presence of a coinciding

PYROLYSIS-HYDROGENATION-GLC OF α -OLEFIN COPOLYMERS

Table 4. Expected and observed increased iso-alkane peaks in copolymer pyrograms

Ethylene-butene-1		Ethylene-hexene-1		Ethylene-octene-1		Number of backbone C atoms in fragment
Expected	Observed	Expected	Observed	Expected	Observed	
—	—	—	<i>i</i> -C ₄	—	<i>i</i> -C ₄	—
—	—	—	<i>i</i> -C ₅	—	<i>i</i> -C ₅	—
<i>i</i> -C ₅	<i>i</i> -C ₅	2MC ₆	2MC ₆	2MC ₈	2MC ₈	3
3MC ₅	3MC ₅	3MC ₇	3MC ₇	3MC ₉	3MC ₉	4
3MC ₆	3MC ₆	4MC ₈	—	4MC ₁₀	4MC ₁₀	5
3MC ₇	3MC ₇	5MC ₉	5MC ₉	5MC ₁₁	—	6
3MC ₈	3MC ₈	5MC ₁₀	5MC ₁₀	6MC ₁₂	—	7
3MC ₉	3MC ₉	5MC ₁₁	—	7MC ₁₃	—	8

peak stemming from a cyclic pyrolysis product. This product in our experiments generally gave less well reproducible peaks than the normal- and iso-alkanes. Another difficulty is that the assignments of the peaks become less certain for the heavier fragments, owing to the larger number of possible components.

However, from the data given we may conclude that the expected iso-alkanes have indeed been formed.

The experience gained with these polymers was then applied to two commercial polyethylene samples, a Ziegler polyethylene of density 0.945 and a high-pressure polyethylene of density 0.92. The sizes of the peaks of these pyrograms are given in Table 5.

Table 5. Areas of the main iso-alkane peaks in the pyrograms of linear polyethylene, Ziegler polyethylene and high-pressure polyethylene

Components	Peak area in arbitrary units		
	Linear polyethylene	Ziegler polyethylene	High-pressure polyethylene
<i>i</i> -C ₄	10	14	55
<i>i</i> -C ₅	18	70	228
2MC ₃	9	18	41
3MC ₅ -CyC ₅	31	64	234
2MC ₆	14	22	70
3MC ₆	13	28	77
2MC ₇ -4MC ₇	16	23	49
3MC ₇ -3EC ₆	16	51	246
2MC ₈ -4MC ₈ -ECyC ₆	50	85	139
3MC ₈	9	29	124
4MC ₉ -5MC ₉ -4EC ₈	11	10	50
<i>i</i> -PCyC ₆ -BuCyC ₅		37	123
3MC ₉	8	12	36
4MC ₁₀ -5MC ₁₀ - <i>sec</i> BuCyC ₆	25	25	84
2MC ₁₀ -4MC ₁₀ - <i>n</i> -BuCyC ₆	33	53	71
3MC ₁₀	15	12	35

The relative sizes of the *n*-alkane peaks are shown in *Table 6*. The iso-alkane peaks that show an increased size when compared with those of the linear polyethylene pyrogram are listed in *Table 7*.

Table 6. Relative sizes of *n*-alkane peaks for various polyethylenes

Peak ratio	Linear polyethylene	Ziegler polyethylene	High-pressure polyethylene
$n\text{-C}_4\text{-}n\text{-C}_7$	0.71	0.74	1.38
$n\text{-C}_5\text{-}n\text{-C}_7$	0.59	0.57	0.75
$n\text{-C}_6\text{-}n\text{-C}_7$	1.52	1.25	1.28
$n\text{-C}_8\text{-}n\text{-C}_7$	0.63	0.65	0.68
$n\text{-C}_9\text{-}n\text{-C}_7$	0.67	0.64	0.72
$n\text{-C}_{10}\text{-}n\text{-C}_7$	1.02	0.91	0.88
$n\text{-C}_{11}\text{-}n\text{-C}_7$	1.00	0.71	0.75

The data given in *Tables 2* and *5* show clearly that the sizes of the iso-alkane peaks increase strongly with increasing amount of short-chain branching. We find that none of the *n*-alkane peaks in the Ziegler poly-

Table 7. Iso-alkane peaks in polyethylene pyrograms

Sample	Iso-alkane peaks
Ziegler polyethylene	{ $i\text{-C}_5$, 3MC_5 , (3MC_6), 3MC_7 , 3MC_8 , (3MC_9),
High-pressure polyethylene	{ $i\text{-C}_4$, $i\text{-C}_5$, 2MC_5 , 3MC_5 , 2MC_6 , 3MC_6 , 2MC_7 - 4MC_7 , 3MC_7 , 2MC_8 - 4MC_8 , 3MC_8 , 4MC_9 - 5MC_9 , 2MC_9 , 3MC_9 , 4MC_{10} - 5MC_{10} , 2MC_{10} - 4MC_{10} , 3MC_{10}

ethylene pyrogram is significantly greater than the corresponding peak in the pyrogram of a linear polyethylene. The pattern of the increased iso-alkane peaks in the Ziegler polyethylene pyrogram strongly suggests that these peaks are mainly due to ethyl side groups. This is in good agreement with the results of electron irradiation experiments^{21, 22}. For the high-pressure polyethylene we find that the *n*-butane peak of the pyrogram shows a clear increase in size, and the *n*-pentane peak a smaller, although probably significant, increase. The increases in the *n*-butane and *n*-pentane peaks are probably due to *n*-butyl and *n*-pentyl side groups, respectively, pentyl groups being much less numerous than butyl groups. However, from the pyrograms of the ethylene-butene, ethylene-hexene-1 and ethylene-octene-1 copolymers we know that *n*-butyl side groups give a 2MC_6 peak which is at least equal to the 3MC_7 peak. In the high-pressure polyethylene pyrogram, however, the 3MC_7 peak is more than three times as large. The main part of the 3MC_7 peak, therefore, is probably due to ethyl side groups. This is in agreement with the sizes of the other 3-methylalkane peaks. We may conclude that in high-pressure polyethylene the short-chain branches are mainly ethyl and, for a smaller part, *n*-butyl groups, while also some *n*-pentyl groups may be present.

With our present knowledge of pyrolysis-hydrogenation-GLC of polymers these results can also be explained quite well when the ethyl and

butyl branches occur in clusters, as suggested by Simpson and Waldron²². In this case the increased *n*-pentane peak could possibly be due to the presence of $-\text{C}-\text{C}-\text{C}_2$ side groups.



From the above experiments we may conclude that the results obtained by pyrolysis-hydrogenation-GLC appear to be in good agreement with those obtained by i.r. and electron irradiation studies.

Koninklijke/Shell-Laboratorium,
Badhuisweg 3, Amsterdam N,
The Netherlands

(Received May 1965)

REFERENCES

- ¹ VAN SCHOOTEN, J. and EVENHUIS, J. K. *Polymer, Lond.* 1965, **6**, 343
- ² BARLOW, A., LEHRLE, R. S. and ROBB, J. C. *Polymer, Lond.* 1961, **2**, 27; *S.C.I. Monogr. No. 17* 'Techniques of Polymer Science', p 267. London, 1963
- ³ BOMBAUGH, K. J., COOK, C. E. and CLAMPITT, B. H. *Analyt. Chem.* 1963, **35**, 1834
- ⁴ NATTA, G., SARTORI, G., VALVASSORI, A., MAZZANTI, G. and CRESPI, G. *Hydrocarb. Process. Petrol. Refin.* 1962, **41**, 103
- ⁵ VAN SCHOOTEN, J., DUCK, E. W. and BERKENBOSCH, R. *Polymer, Lond.* 1961, **2**, 357
- ⁶ VAN SCHOOTEN, J. and MOSTERT, S. *Polymer, Lond.* 1963, **4**, 135
- ⁷ See, for example, CORISH, P. J. and TUNNICLIFFE, M. E. *J. Polym. Sci.* part C (Polymer Symposia), 1964, **7**, 187
- ⁸ STRASSBURGER, J., BRAUER, G. M., TRYON, M. and FORZIATI, A. F. *Analyt. Chem.* 1960, **32**, 454
- ⁹ COBLER, J. G. and SAMSEL, E. P. *S.P.E. Trans.* 1962, **2**, 145
- ¹⁰ STANLEY, C. W. and PETERSON, W. R. *S.P.E. Trans.* 1962, **2**, 298
- ¹¹ GROTEN, B. *Analyt. Chem.* 1964, **36**, 1206
- ¹² NATTA, G., CRESPI, G., MAZZANTI, G., VALVASSORI, A., SARTORI, G. and SCAGLIONE, P. *Rubb. Age, N.Y.* 1961, **89**, 636
- ¹³ NATTA, G. and CRESPI, G. *J. Polym. Sci.* 1962, **61**, 83
- ¹⁴ NATTA, G., CRESPI, G., MAZZANTI, G., VALVASSORI, A. and SARTORI, G. *Chim. e Industr.* 1963, **45**, 651
- ¹⁵ TRUETT, W. L., JOHNSON, D. R., ROBINSON, I. M. and MONTAGUE, B. A. *J. Amer. chem. Soc.* 1960, **82**, 2337
- ¹⁶ SARTORI, G., CAMPIELLI, F. and CAMELI, N. *Chim. e Industr.* 1963, **45**, 1478
- ¹⁷ BOER, H. and KOOYMAN, E. C. *Analyt. chim. Acta*, 1951, **5**, 550
- ¹⁸ KUNTZ, I. and GERBER, A. *J. Polym. Sci.* 1960, **42**, 299
KUNTZ, I. *J. Polym. Sci.* 1961, **54**, 569
- ¹⁹ WILLBOURN, A. H. *J. Polym. Sci.* 1959, **34**, 592
- ²⁰ CROSS, L. H., RICHARDS, R. B. and WILLIS, H. A. *Disc. Faraday Soc.* 1950, **9**, 235
- ²¹ HARLEN, F., SIMPSON, W., WADDINGTON, F. B., WALDRON, J. D. and BASKETT, A. C. *J. Polym. Sci.* 1955, **18**, 589
- ²² BOYLE, D. A., SIMPSON, W. and WALDRON, J. D. *Polymer, Lond.* 1961, **2**, 323 and 335
- ²³ ROEDEL, M. J. *J. Amer. chem. Soc.* 1953, **75**, 6110
- ²⁴ BRYANT, W. M. D. and VOTER, R. C. *J. Amer. chem. Soc.* 1953, **75**, 6113
- ²⁵ SCHNELL, G. *Struktur und physikalisches Verhalten der Kunststoffe*, p 609. Edited by K. A. WOLF. Springer: Berlin/Göttingen/Heidelberg, 1962

Fundamental Studies on Cationic Polymerization IV—Homo- and Co-polymerizations with Various Catalysts

J. P. KENNEDY and R. G. SQUIRES*

The homopolymerization of isobutene and the copolymerization of isobutene with isoprene ('butyl rubber') was studied with boron trifluoride, aluminium ethyl dichloride and aluminium trichloride catalysts in alkyl chloride solvent in the temperature range -30° to -146°C . Boron trifluoride yields highest molecular weight homo- and co-polymers followed by aluminium ethyl dichloride and aluminium trichloride. The molecular weights of the copolymers are about one order of magnitude lower than the corresponding homopolymers prepared under substantially identical experimental conditions. The Arrhenius plots (log DP versus reciprocal temperature) are linear for all systems investigated in the range -30° to -100°C . At $\sim -100^{\circ}\text{C}$ the slopes of the curves decrease sharply. The low temperature parts of the curves between -100° and -146°C are also linear. These observations are discussed.

ALTHOUGH the patent literature abounds in information concerning the copolymerization of isobutene with diolefins ('butyl rubber')¹, there is a dearth of information relating to the mechanisms of such polymerizations. There seems to be only one paper by Russian authors² which deals with the copolymerization of isobutene with various conjugated dienes in the presence of boron trifluoride. The work reported in the present paper attempts to elucidate some of the factors involved in the mechanisms and is another in the series reporting on the fundamentals of cationic polymerizations.

In the course of our studies, it was of interest to investigate the effect of small amounts of dienes on the molecular weight of polyisobutene in the presence of various catalyst systems. Also, we investigated the homopolymerization of isobutene in the temperature range from -30° to -146°C . Our previous studies showed that the log molecular weight versus $1/T$ plot (Arrhenius plot) is linear in the range -30° to -78°C and that it changes its slope at $\sim -100^{\circ}\text{C}$ ³. We re-investigated this phenomenon with boron trifluoride, aluminium ethyl dichloride and aluminium trichloride catalysts in the presence and absence of isoprene. Attempts were made to explain quantitatively the observed effects by expanding our previously proposed mechanism⁴.

EXPERIMENTAL

All the experiments were performed in a stainless steel dry-box under nitrogen atmosphere⁵. The origin and purity of isobutene, methyl chloride, aluminium chloride, and ethyl chloride have been described^{5,6}. Boron trifluoride (The Matheson Co.) was used without further purification. The boron trifluoride catalyst was prepared by absorbing boron trifluoride gas in methyl chloride at -78°C , determining its concentration by weight measurement and diluting it with methyl chloride to give 0.0236 mole/l. stock solution. Aluminium ethyl dichloride (Texas Alkyl, Inc.) was purified by vacuum distillation. The catalyst solution was prepared by diluting with

*Present address: School of Chemical Engineering, Purdue University, Lafayette, Indiana, 47907.

methyl chloride to give a 0.0121 mole/l. (0.125 volume per cent) stock solution. The preparation of the aluminium chloride in methyl chloride catalyst solution has been described⁵; its concentration was 1.62×10^{-2} mole/l. (0.215 wt per cent). Isoprene (Phillips, 99.6 per cent) was purified by distillation before use.

A typical polymerization experiment was carried out as follows: 5 ml (3.5 g) of isobutene in 15 ml methyl chloride or a mixture of 9.7 ml isobutene and 0.3 ml isoprene diluted with 30 ml methyl chloride (all volumes measured at -78°C) was placed in a large test tube and thermo-equilibrated. Thus, the concentrations were 3.17 moles isobutene/l. for the homopolymerizations and 3.03 moles isobutene/l. with 7.75×10^{-2} moles isoprene/l. (i.e. 3 volume per cent isoprene in isobutene) for the copolymerizations. The respective catalyst solutions were introduced from a cooled pipette. Polymerizations at -120° and -146°C were performed in ethyl chloride solvent. Polymerizations ensued instantaneously after catalyst introduction and could be observed visually. The rate of catalyst introduction was regulated in such a manner that the heat rise during reaction was never higher than 1°C . Polymerizations were carried to low conversions. The reactions were terminated by introducing cold methanol. After evaporating the unreacted monomer(s) and solvents and drying in a vacuum at 50°C , the conversions were determined. Molecular weight determination was by viscometry and has been described previously⁵.

RESULTS AND DISCUSSION

Our results are compiled in *Table 1*. *Figure 1* shows the effect of temperature on the degrees of polymerization of polyisobutene and isobutene-isoprene copolymer. These data reveal the following significant facts: (A) The nature of the catalyst affects the molecular weights of polyisobutene and isobutene-isoprene copolymers. Thus boron trifluoride yields highest molecular weight products followed by aluminium ethyl dichloride and aluminium trichloride catalysts. (B) The molecular weights of polymers obtained in the presence of 3 volume per cent isoprene in the initial monomer solution are strongly reduced with all three catalyst systems as compared to those obtained in the absence of this diene. (C) The molecular weights of all the products are strongly affected by the temperature and they increase with decreasing temperatures. This phenomenon has been discussed extensively in previous publications^{4,7}. (D) The slopes of the lines in *Figure 1* are not significantly affected by the nature of the catalyst. Within what is considered to be experimental variation, the Arrhenius lines are parallel to each other. This is also true for the three copolymerization series. However, the average slope of the homopolymerization lines and that of the copolymerization lines are slightly but significantly different. (E) The slopes of the log DP versus $1/T$ curves decrease sharply at $\sim -100^\circ\text{C}$ in all the systems investigated. Thus these curves of the Arrhenius type indicate an approximate overall activation energy (E_{DP}) of 5.6 kcal/mole for polyisobutenes and somewhat less for the copolymers in the range from -30° to -100°C , whereas below -100°C the E_{DP} drops sharply to ~ 0.73 and 0.26 kcal/mole for polyisobutenes and the copolymers, respectively.

FUNDAMENTAL STUDIES ON CATIONIC POLYMERIZATION IV

Table 1. The effect of temperature on the molecular weight of polyisobutene and butyl rubber with various catalysts

Catalyst	Temp., °C	Moles of catalyst intro- duced $\times 10^5$	Yield, g	Conv., %	Mol. wt, $\times 10^{-3}$	'DP'	Unsaturation in copolymer, mole %	
Isobutene								
BF ₃	-30	1.8	1.431	41.0	40.4	720		
		1.1	0.79	22.5	51.6	92		
		0.35	0.086	2.5	—	—		
	-50	0.58	0.398	11.4	120.4	2 150		
		0.59	0.778	22.2	148.4	2 650		
	-78	0.53	0.269	7.7	831.6	14 800		
		0.41	0.602	17.2	946.2	16 900		
	-100	0.71	0.286	8.2	5 916.0	105 500		
		0.53	0.782	22.3	—	—		
	-120	1.0	0.519	14.8	11 740.0	210 000		
		0.83	0.817	23.3	—	—		
	-146	2.0	0.431	12.3	17 970	321 000		
		1.0	0.921	26.2	—	—		
	AlEtCl ₂	-30	0.30	0.577	16.4	63.7	1 140	
-50		0.42	0.637	18.1	243.9	4 340		
-78		0.62	0.212	6.05	2 108.0	37 700		
-100		1.10	0.413	11.8	5 957.0	106 000		
		—	—	—	6 383.0	118 000		
-120		1.16	0.398	11.4	7 465.0	133 000		
-146		1.77	0.433	12.4	14 960.0	267 000		
AlCl ₃	-30	0.63	0.904	25.8	25.3	450		
	-50	0.73	0.747	21.2	105.2	1 870		
	-78	0.73	0.322	9.2	205.8	3 670		
	-100	0.56	0.352	10.0	4 498.0	80 400		
	-120	1.05	0.295	8.5	4 921.0	87 900		
	-146	1.8	0.151	4.3	9 550.0	171 000		
Isobutene-isoprene								
BF ₃	-30	1.8	—	—	—	—	—	
		4.0	1.9	27.0	12.8	228	2.61	
		1.8	2.4	34.3	27.6	494	1.59	
	-78	1.8	4.8	68.6	140.2	2 510	1.84	
		0.14	0.303	4.3	136.3	2 440	—	
		1.5	2.25	32.2	161.0	2 870	1.44	
	-100	0.13	1.146	16.7	511.0	9 130	1.08	
		1.8	0.495	7.1	925.0	16 500	1.38	
	-146	7.1	0.931	13.3	932.0	16 700	1.62	
	AlEtCl ₂	-30	2.3	1.42	20.3	45.7	816	1.04
		-50	3.1	1.081	15.5	94.2	1 680	1.29
-78		2.3	0.909	13.0	352.0	6 280	1.25	
-100		3.6	1.094	15.6	946.2	16 900	1.53	
-120		10.0	1.101	15.7	664.8	11 900	1.41	
-146		16.0	0.685	9.8	794.6	14 200	1.41	
		—	—	—	—	—	—	
AlCl ₃	-30	0.56	0.422	6.0	43.0	768	1.02	
		8.50	0.554	7.9	—	—	—	
	-50	0.62	0.502	7.2	—	—	—	
		1.25	0.596	8.5	73.6	13 100	1.24	
	-78	1.28	0.739	10.5	144.4	25 800	1.47	
	-100	2.2	0.894	12.7	452.0	80 600	1.67	
	-120	5.1	1.588	22.7	568.0	101 500	1.62	
	-146	4.9	0.938	13.4	678.0	121 000	1.57	

The fact that the nature of the catalyst does not influence the slopes of the Arrhenius lines obtained for both the homo- and co-polymerization systems indicates that the overall polymerization mechanisms, at least in

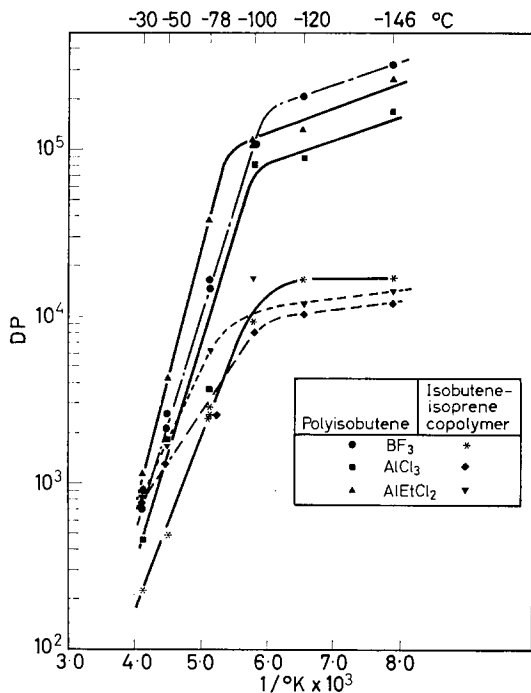
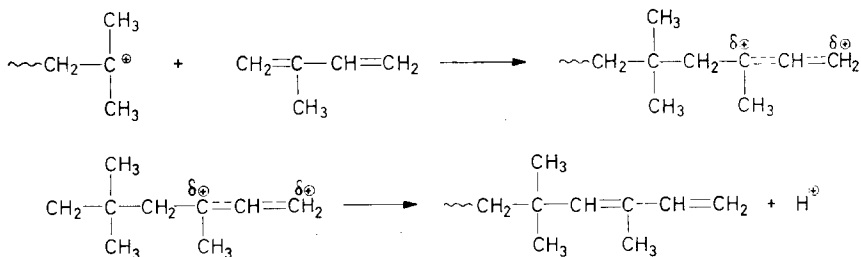


Figure 1—Effect of temperature on DP of polyisobutene and isobutene-isoprene copolymer

the three catalyst systems investigated, are quite similar and that the gegenion probably does not significantly affect major kinetic events. This is not unreasonable since we visualize the growing centre as a solvated carbonium ion which is more or less independent of the associated gegenion. This should be particularly true in solvents of high dielectric constants. However, the average slopes of the homo- and co-polymerization series are sufficiently different to indicate differences in polymerization mechanism.

The strong molecular weight depressing effect of small amounts of isoprene in the monomer mixture forcefully indicates its influence on the detailed mechanism. Isoprene, at high temperatures, reduces the DP by approximately half an order of magnitude and in the low temperature region by more than one order of magnitude. It is reasonable to assume that isoprene is a powerful chain transfer agent which could affect the kinetic chain by the following reactions:



The presence of such conjugated end-groups was corroborated experimentally. Thus, a slight but definitive u.v. absorption at $231\text{ m}\mu$ indicated conjugated unsaturation in copolymer samples prepared at -50°C .

The driving force for the first reaction is provided by the formation of the resonance stabilized substituted allyl carbonium ion and the creation of the new C—C bond. Thus according to the level of unsaturation in the copolymer in *Table I*, about 50 per cent of the available diene is incorporated at low to medium conversions in the copolymer chain from the monomer mixture containing three per cent isoprene. The second reaction is more speculative. To explain the low molecular weights obtained in the presence of isoprene, we have to assume that the rate of proton expulsion

from the allylic carbonium ion is faster than the deprotonation of $\sim\text{CH}_2\text{C}^{\oplus}$

$$\begin{array}{c} \text{CH}_3 \\ | \\ \sim\text{CH}_2\text{C}^{\oplus} \\ | \\ \text{CH}_3 \end{array}$$

the conventional chain transfer step in isobutene homopolymerization. This assumption appears to be reasonable considering the much higher molecular weights of polyisobutene than polybutadiene produced under similar cationic conditions.

The fact that polymer yields are strongly depressed in the presence of dienes as reported by the Russian authors² and often observed in our laboratories indicates that isoprene and, conceivably, butadiene and its derivatives, are not only chain transfer agents ('molecular weight poisons') but also effective terminating agents ('chain poisons'). This again can be expected from the increased stability of a substituted allyl carbonium ion at the chain end as compared to the propagating cation of the *t*-butyl type in the absence of isoprene.

Decreased polymer yields in the presence of diene can also be due to retarded initiation, i.e. the diene and the catalyst interact and yield an inactive complex ('catalyst poison'). Whether the diene interferes with the chain or with the catalyst cannot be decided from the available information.

According to our findings, the highest molecular weight homopolymer or copolymer was obtained with boron trifluoride. Aluminium ethyl dichloride and aluminium trichloride gave lower molecular weights at essentially identical conversion levels and at the same temperature. This effect of the catalyst on the molecular weights is difficult to explain.

The fact that the slopes of the log DP of polyisobutene versus $1/T$ curves decrease sharply at $\sim -90^\circ$ to -100°C has been observed previously in a number of systems^{3,4}. According to the mechanism published earlier⁴, the kinetic chain and the molecular weights are determined by the relative rates of propagation and termination and competing chain breaking processes, i.e. chain transfer to the monomer and chain transfer involving the solvent. The following equation was derived⁴

$$\text{DP} = k_1 / [(k_3 - k_4) N_m C + k_4 C] \quad (1)$$

where k_1 , k_3 and k_4 are rate constants for 'activation' of the carbonium ion

chain end, chain transfer to monomer, and chain transfer involving the solvent, respectively. N_m is the mole fraction monomer and C is the number of total moles (solvent plus monomer) per litre. In polar solvents at the inversion temperature (T_i), where $k_3 = k_4$, DP becomes independent of monomer concentration. If we assume that the rate constants k_1 , k_3 and k_4 vary with temperature according to the Arrhenius theory and if we neglect the change of C with temperature, we may differentiate equation (1) with respect to temperature to give

$$\frac{dDP}{dT} = \frac{[(k_3 - k_4) N_m C + k_4 C] k_1 \left(\frac{E_1}{RT^2} \right) - k_1 \left[k_3 \left(\frac{E_3}{RT^2} \right) - k_4 \left(\frac{E_4}{RT^2} \right) N_m C + k_4 C \left(\frac{E_4}{RT^2} \right) \right]}{[(k_3 - k_4) N_m C + k_4 C]^2} \quad (2)$$

At the inversion temperature $k_3 = k_4$, and equation (1) can be reduced to

$$DP = k_1 / k_4 C \quad (3)$$

which is independent of N_m . Similarly, when $k_3 = k_4$, equation (2) gives

$$\frac{dDP}{dT} = \frac{k_1}{k_4 C} \left[\frac{-(E_4 - E_1) - (E_3 - E_4) N_m}{RT^2} \right] \quad (4)$$

Combining (3) and (4) gives

$$\frac{d(\ln DP)}{d(1/T)} = \frac{(E_4 - E_1) + (E_3 - E_4) N_m}{R} \quad (5)$$

Therefore, at the inversion temperature, the slope of the log DP versus $1/T$ curve is a function of N_m .

Previous estimates of k_3/k_1 and k_4/k_1 as functions of temperature⁷ show that at high temperatures, far above T_i , we would expect $k_4 \gg k_3$. At temperatures far below T_i , $k_3 \gg k_4$. At high temperatures, calculations similar to those used in deriving equations (3) and (4) result in

$$DP = k_1 / k_4 C (1 - N_m) \quad (6)$$

and

$$d(\ln DP) / d(1/T) = (E_4 - E_1) / R \quad (7)$$

At low temperatures, we find that

$$DP = k_1 / k_3 C N_m \quad (8)$$

and

$$d(\ln DP) / d(1/T) = (E_3 - E_1) / R \quad (9)$$

Therefore, in temperature ranges both far above and far below T_i , the slope of the log DP versus $1/T$ plot, as indicated by equations (7) and (9), should be independent of monomer concentration.

An estimate of $(E_4 - E_1)$ and $(E_3 - E_1)$ can be made, as indicated by equation (5), by plotting the slope, S_i , measured at the inversion temperature, of the log DP versus $1/T$ curve against N_m . Figure 2, constructed using previously published data for the aluminium trichloride catalysed polymerization of isobutene in vinyl chloride solvent⁷, indicates that

$(E_4 - E_1) = 9.3$ kcal/mole and $(E_4 - E_3) = 9.0$ kcal/mole. Kennedy *et al.*⁴ reported $(E_4 - E_1) = 9.9$ kcal/mole and $(E_4 - E_3) = 7.8$ kcal/mole*.

No data are available in the high temperature region in which equation (7) applies. However, data are available at low temperatures and an estimate

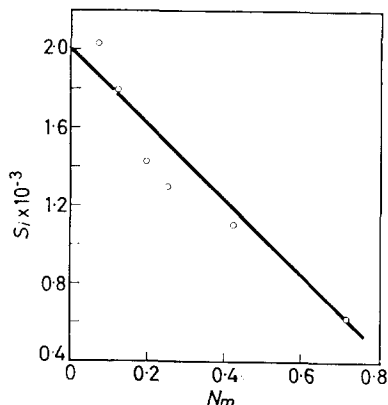


Figure 2—Effect of N_m on slope, S_i , of log DP versus $1/T$ plot at the inversion temperature

can be made of the temperature range in which the transition from equation (5) to equation (9) should occur. Since, at the inversion temperature, $k_3 = k_4$,

$$k_{04}e^{-E_4/RT_i} = k_{03}e^{-E_3/RT_i} \quad (10)$$

therefore,

$$\frac{k_{04}}{k_{03}} = e^{(E_4 - E_3)/RT_i} \quad (11)$$

At an arbitrary temperature, T ($^{\circ}\text{K}$)

$$\frac{k_4}{k_3} = \frac{k_{04}}{k_{03}} e^{-(E_4 - E_3)/RT} \quad (12)$$

Substituting (11) into (12) gives

$$\frac{k_4}{k_3} = \exp \left[\frac{(E_4 - E_3)}{R} \left(\frac{T - T_i}{TT_i} \right) \right] \quad (13)$$

Since $E_4 - E_3 \simeq 7.8$ kcal/mole and $T_i = 228^{\circ}\text{K}$, equation (13) becomes

$$\frac{k_4}{k_3} = \exp \left[\frac{17.1T - 3900}{T} \right] \quad (14)$$

The low temperature linear portion of the log DP versus $1/T$ curve represented by equation (9) exists in the region where $k_3 \gg k_4$. Deviations from this linear region should begin as k_4 becomes a non-negligible fraction of k_3 . Thus, when k_4/k_3 becomes larger than 0.02, deviations from linearity should begin to appear. From equation (14), this region corresponds to $T \sim -90^{\circ}\text{C}$. As can be seen in Figure 1 and in Figures 7 and 8 of ref. 7, at approximately -90°C , the predicted low temperature linear portion of the Arrhenius curve appears, the slope of which is independent of monomer concentration. From equation (9), this slope is equal to $(E_3 - E_1)/R$. The

*The activation energy values reported in ref. 4 have been recalculated. The corrected values are $(E_4 - E_1) = 9.9$, $(E_3 - E_1) = 2.1$ and $(E_4 - E_3) = 7.8$ kcal/mole.

data in ref. 7, while indicating qualitatively that such a trend is present, contain insufficient low temperature data points to calculate accurately $(E_3 - E_1)$ in this manner. However, the values shown in *Figure 1* indicate $(E_3 - E_1) = 0.73$ kcal/mole in the low temperature region. Kennedy *et al.*⁴ reported $(E_3 - E_1) = 2.1$ kcal/mole.

It is difficult to estimate realistically the accuracy of the calculated activation energy differences. The error in $(E_3 - E_1)$, when it is calculated from data near the inversion temperature (as was done in *Figure 2* and also by Kennedy *et al.*⁴) is larger. In this case $(E_3 - E_1)$ is a relatively small difference between two large numbers whose experimental errors are probably of the same order of magnitude as the difference between them. When $(E_3 - E_1)$ is calculated directly from the low temperature data using equation (9), its accuracy should be greatly improved. For this reason, the values of $(E_3 - E_1)$ of 0.73 kcal/mole from *Figure 1* and Kennedy's⁴ value of 2.1 kcal/mole are probably within experimental error, the true value being nearer to 0.73 kcal/mole.

Thus, the mechanism which quantitatively explains the inversion temperature in the temperature range from -35° to -78°C also explains the break in the log DP versus $1/T$ plot at -90° to -100°C . The value of $(E_3 - E_1)$ predicted by the theory from the slope of the log DP versus $1/T$ plot in the low temperature range is in agreement, within experimental error, with the $(E_3 - E_1)$ value predicted by the mechanism in the -35° to -78°C range. This is evidence that under these experimental conditions, the break in the slope of the log DP versus $1/T$ plot is due to a change in the predominant chain transfer mechanism from transfer involving the solvent at high temperature to monomer transfer at low temperature.

A similar change in the slope of the log DP versus $1/T$ curves for aluminium trichloride catalysed polymerization of isobutene in propane diluent has been reported by Kennedy and Thomas³. Substantially identical trends have been observed in numerous related experiments using various polar diluents⁷.

It is unlikely that one mechanism would explain this effect observed in many systems under different experimental conditions. Plesch⁸, for instance, has suggested that the relative rate of propagation to monomer transfer might control DP at low temperatures. Another explanation is that as the viscosity of the system increases at low temperatures, diffusion may become rate controlling by causing monomer starvation of the growing end. Other mechanisms involving the competition of various processes may be envisaged. The competition between chain transfer and termination, for example, may cause this effect in some systems. This 'freezing out' of the termination processes for polyisobutene, however, is difficult to visualize since this polymerization initiates instantaneously with aluminium trichloride catalysts and leads to high molecular weight products even at -185°C .

Our reason for supporting the proposed chain transfer competition mechanism under our particular experimental conditions is that this mechanism not only predicts a change in the DP dependence on reciprocal temperature at low temperature, but also quantitatively explains the complex inversion temperature phenomena at a higher temperature. Thus, both

effects may be successfully correlated without postulating separate and unrelated mechanisms.

The effect of isoprene comonomer on the DP of polyisobutene at various temperatures is shown in *Figure 1*. Isoprene may reduce the DP either by depressing the rate of formation of active complex, thereby decreasing the numerator of the DP expression [equation (1)] or by acting as both chain transfer agent and terminator, introducing a term involving K_3I (where I is the isoprene concentration) in the denominator of the DP expression. We thus postulate that at high temperatures where chain transfer involving the solvent predominates, the apparent activation energy for polymerization is reduced by the presence of isoprene due to an increase of E_1 . At low temperatures, chain transfer and/or termination involving isoprene predominates rather than the monomer transfer reaction. Thus, from *Figure 1*, $E_3 - E_1 = 0.26$ kcal/mole as compared to 0.73 kcal/mole for $E_3 - E_1$. However, no conclusions can be drawn concerning the relative values of E_3 and E_3 , since E_1 may also be changed by the addition of isoprene.

*Chemicals Research Division,
Esso Research and Engineering Company,
Linden, New Jersey, U.S.A.*

(Received April 1965)

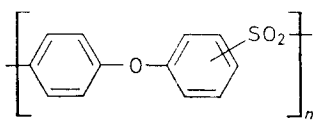
REFERENCES

- ¹ See for example, GUTERBOCK, H. *Polyisobutylene und Isobutylene Mischpolymerizate*. Springer: Berlin, 1959
- ² ANOSOV, V. I. and KOROTKOV, A. A. *Vysokomol. Soedin.* 1960, **2**, 354
- ³ KENNEDY, J. P. and THOMAS, R. M. 'Polymerization and polycondensation processes', *Advances in Chemistry Series No. 34*, Chapter 7. American Chemical Society: Washington, D. C., 1962
- ⁴ KENNEDY, J. P., KIRSHENBAUM, I., THOMAS, R. M. and MURRAY, D. C. *J. Polym. Sci.*, Part A, 1963, **1**, 331
- ⁵ KENNEDY, J. P. and THOMAS, R. M. *J. Polym. Sci.* 1960, **46**, 481
- ⁶ KENNEDY, J. P. and THOMAS, R. M. *J. Polym. Sci.* 1961, **49**, 189
- ⁷ KENNEDY, J. P. and THOMAS, R. M. *J. Polym. Sci.* 1961, **55**, 311
- ⁸ PLESCH, P. H. Private communication, Linden, 1961

Synthesis of Poly(arylene sulphones) by Polycondensation of Arylsulphonyl Chlorides under Friedel–Crafts Conditions

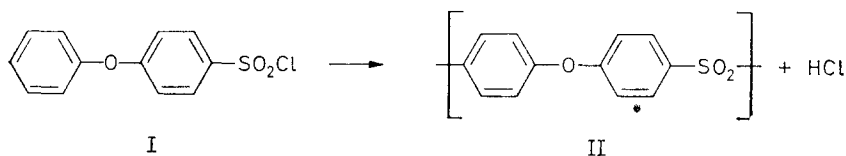
M. E. A. CUDBY, R. G. FEASEY, B. E. JENNINGS, M. E. B. JONES and J. B. ROSE

This paper reports an extension of our previous work on the synthesis of poly(arylene sulphones), and describes the preparation of these polymers by the self-condensation of certain dinuclear arylsulphonyl chlorides, catalysed by ferric chloride. In contrast with polyalkylations performed under Friedel–Crafts conditions, it is found that polysulphonylation leads to essentially linear polymers. A detailed structural examination, using i.r. and n.m.r. spectroscopy, of isomeric poly(diphenylene ether sulphones),



is also described. It is shown that the structure of this polymer, prepared by different Friedel–Crafts polysulphonylation reactions, is dependent upon the structure of the monomers.

THE synthesis of poly(arylene sulphones) by the ferric chloride-catalysed polycondensation of disulphonyl chlorides with reactive dinuclear aromatic compounds has been described in the first paper of this series¹. We now report the extension of this work to the self-condensation of certain mono-sulphonyl chlorides, e.g. *p*-phenoxybenzenesulphonyl chloride, I, which is in some respects a more convenient means for preparing polymers of high molecular weight.



As reported previously¹, this type of polycondensation proceeds smoothly using catalytic quantities of ferric chloride, and in this respect the reaction is more like a Friedel–Crafts alkylation than the conventional Friedel–Crafts reaction of acid chlorides, which is traditionally performed^{2,3} with at least one mole of ‘catalyst’ per mole of acyl or sulphonyl chloride reacted. There is, however, one significant difference between alkylation and acylation or

sulphonylation which is of particular importance in the application of these reactions to polymer synthesis. Polyalkylations, of which the condensation of benzyl chloride is a typical example, would be expected to give highly branched structures because substitution of hydrogen by alkyl groups in the benzene nucleus increases its reactivity towards electrophilic reagents⁴. Thus, in the polycondensation of benzyl chloride, rings already in the chain (which have at least two hydrogens replaced by benzyl groups) are attacked more readily by electrophilic species than the singly substituted rings at chain ends, and the observed highly branched structure results^{5,6}. In polysulphonylations, the opposite situation obtains⁴ since the sulphone groups are electron-withdrawing. Thus in the self-condensation of halides such as I, rings in the polymer chains are less reactive than the rings at chain ends. The formation of linear chains is therefore favoured, the extent of branching being dependent upon the difference in reactivity between the two types of ring. In these polysulphonylations the structure of the repeat units, e.g. II, depends on the relative activities of the three possible sites (ortho, meta or para to the ether linkage) for attack by sulphonyl chloride on the activated ring. We have examined the structures of the poly(phenylene ether sulphones) II, obtained by four different routes using i.r. and n.m.r. techniques, and have also obtained some information concerning the extent to which chain branching can occur.

RESULTS AND DISCUSSION

Polycondensation of monosulphonyl chlorides

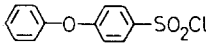
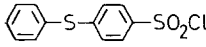
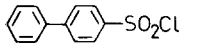
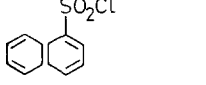
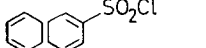
Polymers with reduced solution viscosities (RV) greater than 0.6 were not obtained from the two-component (diphenyl ether plus its 4,4'-disulphonyl chloride) system reported¹ previously, one difficulty being that small amounts of diphenyl ether were lost by vaporization, throwing the polycondensation out of balance. The use of *p*-phenoxybenzenesulphonyl chloride obviates this difficulty, and has the further advantage that this monomer, unlike diphenyl ether disulphonyl chloride, can be purified by vacuum distillation. Thus, with this single component system RVs as high as 2.0 were obtained, using the combination of melt and powder-polymerization techniques described in the experimental section.

The polycondensation of several other monosulphonyl chlorides (listed in *Table I*) was examined using the technique developed for *p*-phenoxybenzenesulphonyl chloride. α -Naphthalenesulphonyl chloride evolved hydrogen chloride only very slowly and gave a discoloured product of very low RV, and although hydrogen chloride evolution occurred readily with the β -isomer, RVs ≥ 0.1 could not be obtained. Further investigation showed that sulphur dioxide as well as hydrogen chloride was evolved during condensation of the β -sulphonyl chloride, so that in this case high polymer formation is prevented by decomposition of sulphonyl chloride groups. Polycondensation of *p*-thiophenoxybenzenesulphonyl chloride proceeded smoothly, and the polymer obtained was similar to that prepared from *p*-phenoxybenzene sulphonyl chloride in that both polymers were amorphous materials softening in the region of 240°C. *p*-Phenylbenzenesulphonyl chloride gave an insoluble, intractable polymer which was

SYNTHESIS OF POLY(ARYLENE SULPHONES) BY POLYCONDENSATION

moderately crystalline (25 per cent crystallinity by X-ray determination) with a crystal melting point of *ca.* 375°.

Table 1. Polysulphonylation with monosulphonyl chlorides

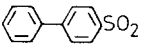
Sulphonyl chloride	FeCl ₃	Final temp. °C	Yield %	Insolubles* %	RV†
	Various up to 4wt%	Up to 260	>90	<10	Up to 2.0
	1.2	240	>90	<10	0.56
	1.3	250	95	100	—
	Various up to 4.0	Up to 290	90	0	<0.1
	"	"	90	0	<0.1

*As % of total product.

†Reduced viscosity = (t. solution - t. solvent)/t. solvent for 1% solution in dimethyl formamide at 25°.

The polycondensations of mixtures of *p*-phenoxy- and *p*-phenylbenzene sulphonyl chlorides, in which the proportion of the *p*-phenyl derivative ranged from 21 to 77 wt%, gave amorphous and readily soluble 'copolymers'. Thus, the insolubility of the 'homopolymer' from *p*-phenylbenzenesulphonyl chloride is probably due to crystallinity rather than crosslinking. The 'copolymers' had substantially higher softening points than the 'homopolymer' from *p*-phenoxybenzene sulphonyl chloride, as is shown in Table 2.

Table 2. Deformation temperatures for diphenylene-diphenylene ether sulphones

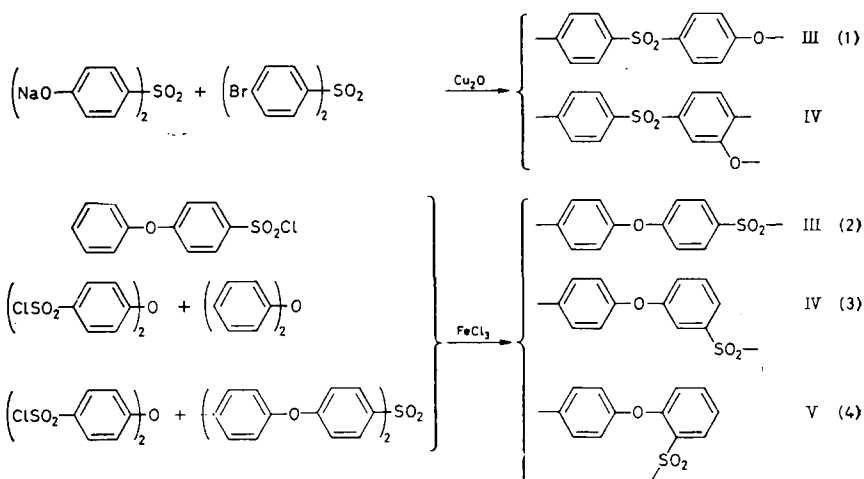
Wt % of  units	RV	T ₁₀ * °C	T ₁₀₀ * °C
0	0.64	227	234
5	0.83	232	239
29	0.77	244	259
32	1.02	256	264
38	0.98	273	284
42	1.04	286	296

*Temperatures at which 10 and 100 per cent elongation occurred for films heated at 4°/min in air under a load of 200 lb/in².

Structural investigations

The structures of the poly(phenylene ether sulphones), which were obtained as described previously by the copper-catalysed ether synthesis, reaction (1), and by the sulphonylation reactions (3) and (4) have been examined together with that of the polymer obtained by reaction (2).

Polymer from (1) would have the repeat unit III provided that reaction occurs by direct substitution, but would contain a mixture of III and IV in the unlikely event that reaction occurs via a benzyne intermediate⁷. According to the rules for orientation of electrophilic aromatic substitutions,



reactions (2) to (4) should give the repeat units III and V by substitution para and ortho to the activating ether linkage respectively, the formation of a meta substituted structure, IV, being most unlikely.

The i.r. spectra of the polymers were examined in the 11 to 15 μ region, where the aromatic C—H out-of-plane deformation bands occur. The spectra were similar and showed bands at 11.45 μ and 11.95 μ comparable to those observed for para substituted model compounds, e.g. diphenyl ether-4,4'-disulphonyl chloride, which absorb in the regions 11.35 to 11.5 μ and 11.90 to 11.99 μ . Absorption bands were not observed in the regions 12.05 to 12.3 and 12.5 μ or 13.05 and 13.28 μ characteristic of meta or ortho substitution respectively (model compounds diphenyl sulphone-3,3'-disulphonyl chloride and 2-methyldiphenyl sulphone). However, absorptions due to low proportions of such substituted nuclei would be difficult to detect among the intense absorptions due to the para substituted ones.

The n.m.r. spectra of these polymers are shown in *Figures 1 to 4*, and provide a more detailed structural picture. Thus the polymer from reaction (1) showed only a normal AB quartet (*Figure 1*) indicating a structure consisting essentially of repeat units, III, which contain only two non-equivalent types of proton (chemical shifts 3.72 and 2.99 τ). Non-equivalent protons are positioned ortho to each other as shown by the typical coupling constant (J value) of 8 c/s. Polymers obtained from reactions (2) and (4) gave very similar spectra (*Figures 2 and 4*), the observed chemical shifts being 3.75 τ and 3.00 τ with a J value of 8 c/s. However, the polymers obtained from reaction (3) (*Figure 3*) showed a more complicated n.m.r. spectrum, the AB quartet being distorted, while several additional peaks

SYNTHESIS OF POLY(ARYLENE SULPHONES) BY POLYCONDENSATION

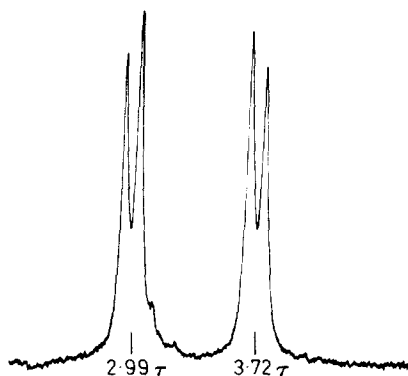


Figure 1 — The n.m.r. spectrum of polymer from the reaction

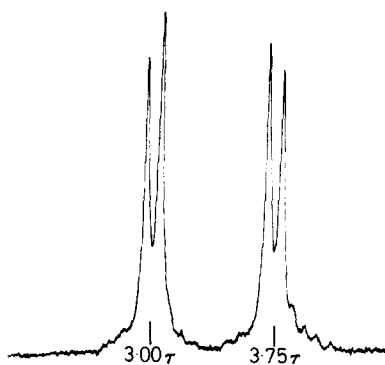
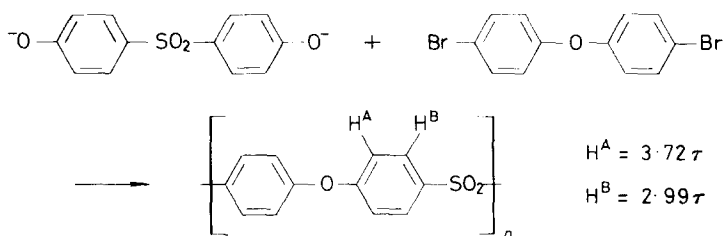
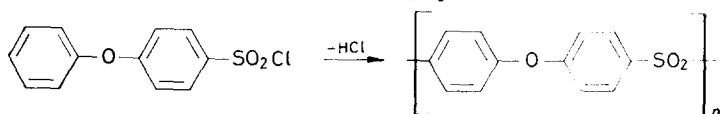


Figure 2 — The n.m.r. spectrum of polymer from the reaction



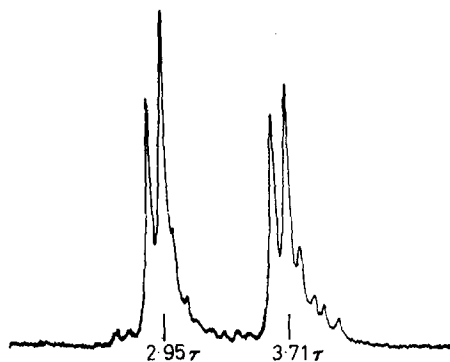


Figure 3—The n.m.r. spectrum of polymer from the reaction

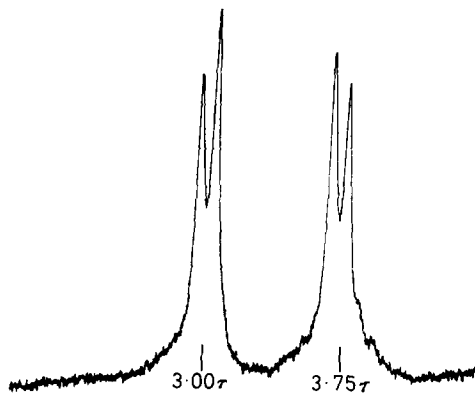
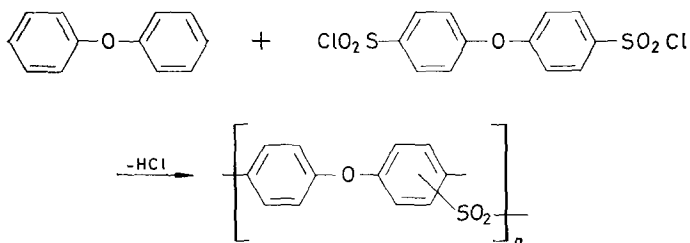
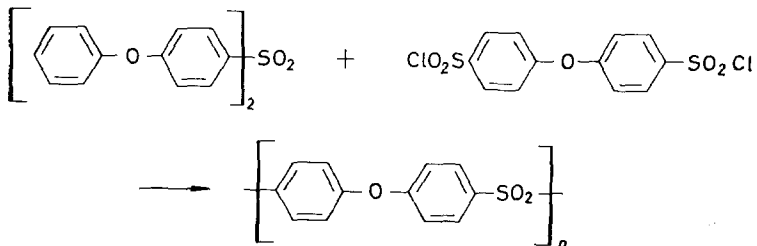


Figure 4—The n.m.r. spectrum of polymer from the reaction



appeared at the high field sides of the main resonance signals. Comparison with the spectra of model compounds suggested that these complications were due to the presence of the ortho substituted structure V. Thus 4,4'-dinitrodiphenyl ether gave the expected AB quartet (Figure 5), whereas the 2,4'-dinitro derivative gave a more complex spectrum (Figure 6) in which the AB quartet assigned to the protons in the para-disubstituted ring is shifted to higher field, due to the changed position of the nitro group in the second ring. The spectrum obtained from a mixture of 4,4'-dinitrodiphenyl ether with a small proportion of the 2,4'-isomer is shown in Figure 7. It can be seen that due to the differences in the chemical shift of the protons producing AB quartets in the two compounds, resonances have appeared to high field of the peaks assigned to the 4,4'-dinitro derivative. This is analogous to the spectrum (Figure 3) of the polymer obtained from reaction (3), indicating that in this case some ortho substitution occurs to give a polymer in which structure III predominates but V is present. The results of attempts to obtain quantitative data by measuring peak areas were not reproducible, but the proportion of the ortho substituted repeat units, V, probably does not exceed 20 per cent.

These structural determinations confirm our previous suggestion¹ that reaction (1) occurs by direct nucleophilic substitution without rearrangement according to Bunnett's⁸ addition-elimination mechanism. They also show that the structures of the polymers prepared by the polysulphonylation

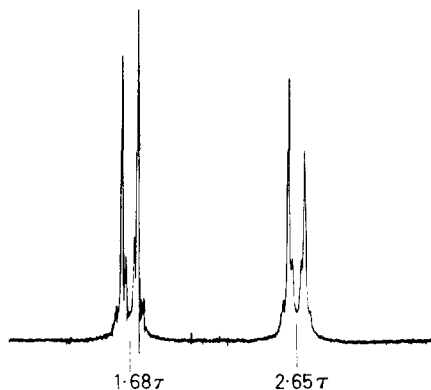
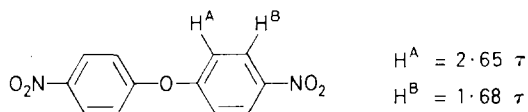


Figure 5—The n.m.r. spectrum of



reactions [(2) to (4)] are dependent upon the structures of the monomers involved. In reactions (2) and (4) sulphone linkages are invariably formed by substitution at rings linked via oxygen to rings containing sulphone or sulphonyl chloride substituents. This is not so for reaction (3), where 50 per cent of the sulphone bonds are formed by (mono) sulphonylating diphenyl

ether, and only the remaining 50 per cent by sulphonylation at rings containing *p*-sulphonylphenoxy substituents [analogous to the rings sulphonylated in reactions (2) and (4)]. The effect of electron-withdrawing ring substituents on the orientation of electrophilic substitution in an adjacent ring has been investigated^{9,10} by comparing the nitration of diphenyl with that of its 2-, 3- and 4-nitroderivatives. It was found that

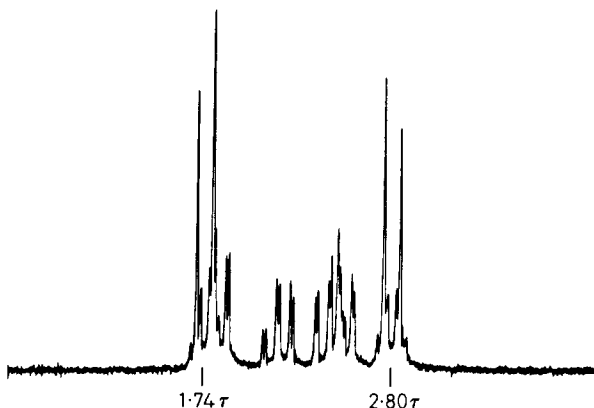
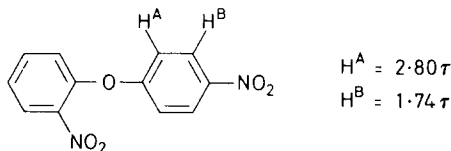


Figure 6—The n.m.r. spectrum of



the ratio of ortho to para substitution in one ring was greatly reduced by the presence of a nitro substituent in the other. Diphenyl ether has not been examined in such detail but it is known¹¹ that the electronic effects of substituents in one ring are very effectively relayed to the other. Similarly the monosulphonylation of diphenyl ether leads to a significantly higher proportion of ortho substituted units, V, than the sulphonylation of *p*-phenoxybenzenesulphonyl chloride [first step in reaction (1)], *p,p'*-diphenoxydiphenyl sulphone [first step in reaction (4)] or phenoxy groups at one end of a growing chain.

Although rings in the polymer chains are far less readily sulphonylated than phenoxy groups at chain ends, so that formation of linear polymers is favoured, the concentration of rings in the chain will of course increase at the expense of those at chain ends as polycondensation proceeds. Disubstituted rings containing ether and sulphonyl substituents can be sulphonylated in spite of deactivation by sulphonyl groups, for we found that diphenylether-4,4'-disulphonyl chloride reacts slowly with itself at 150°C in the presence of ferric chloride evolving hydrogen chloride, but only traces of sulphur dioxide. Furthermore, addition of 1 or 2 mole per cent of this disulphonyl chloride to *p*-phenoxybenzenesulphonyl chloride polycondensations gave products containing substantial quantities of insoluble polymer, showing that an excess of sulphonyl chloride groups in the system leads

to crosslinking, presumably by sulphonylation of rings in the polymer chains. Thus the formation of soluble branched chain polymers during reactions (2) to (4) is possible, especially in the final stages of these polycondensations. The most likely structure at the branching point is VI, for sulphonylation

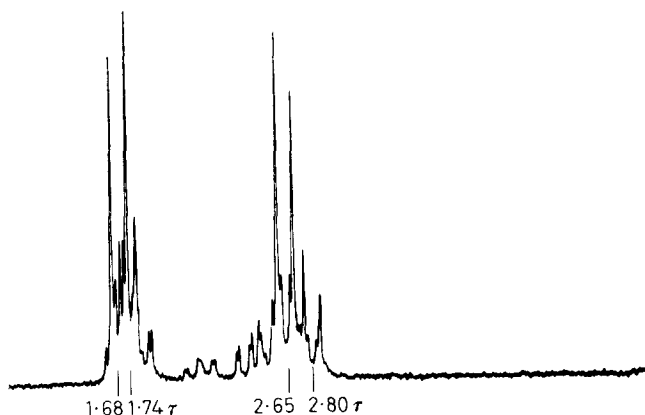
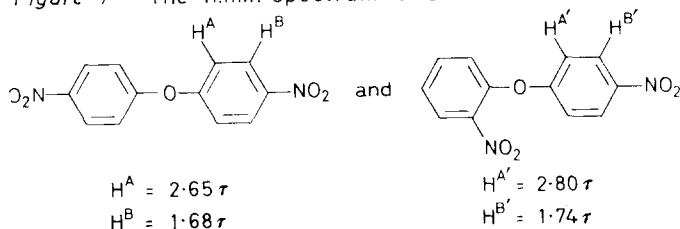
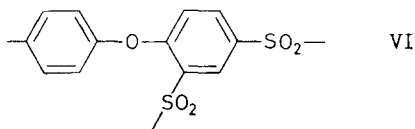


Figure 7—The n.m.r. spectrum of a mixture of



of the predominant repeat unit, III, is much more likely to occur ortho to ether than to sulphone groups. The model compound appropriate to VI is 2,2',4'-trinitrodiphenyl ether, and the n.m.r. spectrum for this compound is reproduced in *Figure 8*. This shows the AB quartet ($J=8$ c/s)



assigned to the two types of non-equivalent protons in the disubstituted ring, but the higher resonance is enhanced by addition of the high field peak of a second AB quartet ($J=8$ c/s) assigned to the two adjacent non-equivalent protons in the trisubstituted ring. The lower field resonances of this latter quartet appear as doublets with $J=2$ c/s which is characteristic of meta-splitting across an aromatic nucleus. Thus these lower-field resonances are assigned to the proton ortho to the nitro groups, as this is meta to the proton between the nitro groups, and this is the basis for our assignment of the low field part of the AB quartets to the protons adjacent to $-\text{NO}_2$.

groups in the model compounds and to $-\text{SO}_2-$ groups in the polymers. The remaining resonance in the spectrum of the trinitro compound, which is at low field (1.07τ), must be assigned to the proton placed between the $-\text{NO}_2$ groups, and as expected this is split to a doublet ($J=2\text{ c/s}$) by meta-coupling. On this basis a trisubstituted structure, VI, should give a resonance signal well to low field of the entire AB quartet, and the low molecular weight product isolated from the self-condensation of diphenyl ether-4,

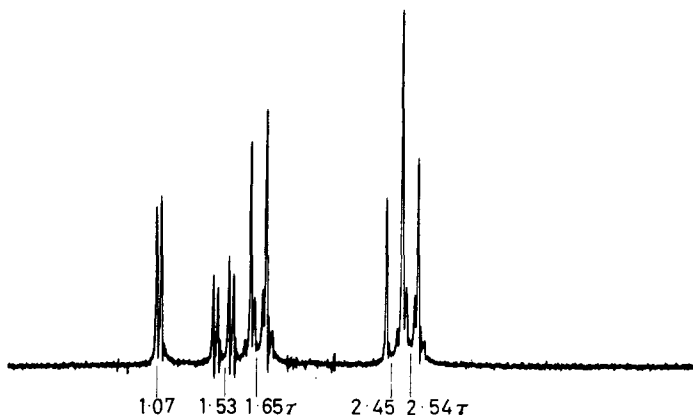
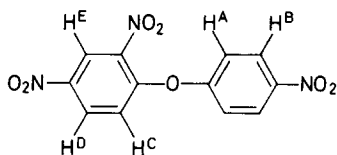


Figure 8—The n.m.r. spectrum of



$$\text{H}^A = 2.54\tau \quad \text{H}^C = 2.45\tau \quad \text{H}^E = 1.07\tau$$

$$\text{H}^B = 1.65\tau \quad \text{H}^D = 1.53\tau$$

4'-disulphonyl chloride gave a peak 0.83τ to (see Figure 9) the low field side of the quartet. Thus trisubstitution certainly occurs here, but although many polymer spectra have been run just to detect low field protons, none has been observed. Experiments with model compounds showed that the limit of quantitative estimation for low field protons was 1 in 150 other protons, the limit of detection being greater than this. The limit of detection in polymers is more difficult to assess, as only dilute solutions could be obtained in solvents suitable for n.m.r. examination, but ~ 1 in 150 should be detectable. Thus, the proportion of trisubstituted units VI, each containing

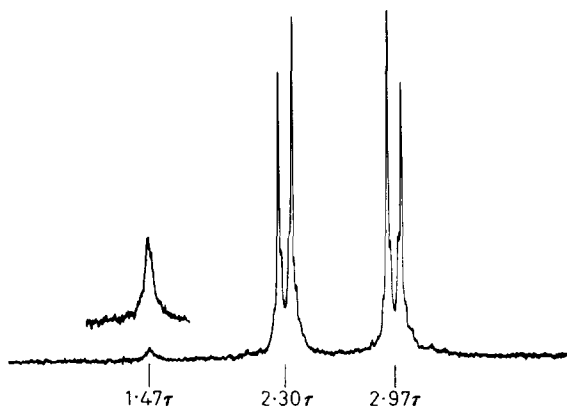
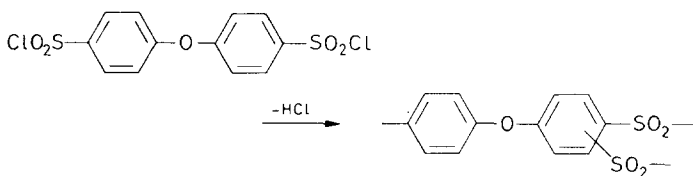


Figure 9—The n.m.r. spectrum of the low molecular weight product from the reaction



one low field proton, is less than *ca.* 5 per cent of the disubstituted ones, III or V, which have eight (higher field) protons, so that these polysulphonylations do give polymers having a predominantly linear structure.

EXPERIMENTAL

Sulphonyl chlorides

α - and β -Naphthalenesulphonyl chlorides were commercial samples purified by distillation at a pressure of 1 mm of mercury followed by recrystallization from 40° to 60° petrol. *p*-Phenyl, *p*-phenoxy- and *p*-thiophenoxybenzenesulphonyl chlorides were prepared by treating the sodium salts of the sulphonic acids with thionyl chloride in the presence of dimethylformamide¹², and purified by vacuum distillation followed by recrystallization from dry petrol ether. The *p*-phenyl, *p*-phenoxy and *p*-thiophenoxy derivatives had melting points 115° to 116°C, 42.5° to 43°C and 73.5° to 74°C respectively (literature melting points 115°C¹³, 45° to 46°C¹³ and 66° to 68°C¹⁴); they were analysed correctly for carbon, hydrogen and chlorine and had ionizable chlorine contents within 0.2 per cent of the theoretical amount.

Polymerization of monosulphonyl chlorides (Tables 1 and 2)

Weighed quantities of anhydrous ferric chloride (purified by sublimation in a stream of chlorine) and the monosulphonyl chlorides were melted under a nitrogen atmosphere and stirred to dissolve the catalyst. The temperature

was then raised to 190°C over 10 to 20 minutes, during which hydrogen chloride was evolved and the reaction mixture foamed. After cooling, the foamed mass was ground to a powder under nitrogen and then heated to ca. 200°C for 20 to 30 minutes when further evolution of hydrogen chloride occurred and the powder sintered. By the end of this stage over 75 per cent of the theoretical quantity of hydrogen chloride had been evolved. The cooled polymer was then reground under nitrogen and heated to 250°C under a vacuum of 1.5 mm for 2 to 3 h to complete the polymerization. After cooling, the product was treated with a one per cent solution of acetyl acetone in dimethyl formamide at 100°C for 10 min, filtered to remove insoluble polymer, and the filtrate poured into acetone. The precipitated polymer was washed with acetone and then dried under vacuum at 120°C.

Polycondensations of *p*-phenoxybenzenesulphonyl chloride carried out with 2.5 wt % of ferric chloride as catalyst in the presence of 1 and 2 mole % of diphenyl ether-4,4'-disulphonyl chloride gave products containing 19 and 46 per cent of insoluble polymer, respectively.

Reaction of diphenyl ether-4,4'-disulphonyl chloride with ferric chloride at 150°C

Diphenyl ether-4,4'-disulphonyl chloride (65.0 g, 0.177 M), was stirred with ferric chloride (ca. 1 g), for 20½ h at 150 ± 3°C. A stream of dry (< 5 p.p.m. v/v water) nitrogen was passed over the melt and the effluent gases were passed through a cold (ca. -80°C) trap and finally through distilled water.

Only a very small quantity (< 0.5 ml) of a liquid was retained in the cold trap. Titration of the water trap with sodium hydroxide showed it to contain 88.2×10^{-3} equivalents of acid which analysis showed to have resulted from the dissolution of 82.6 mm hydrogen chloride and 2.8 mm sulphur dioxide.

The reaction mixture was dissolved in chloroform (500 ml), and the solution was washed four times with hydrochloric acid (3N; 200 ml), and twice with water (250 ml). The chloroform solution was dried over anhydrous sodium sulphate and then evaporated to dryness. The residue was reprecipitated from 60° to 80°C petrol-acetone mixture to yield a white solid, melting range 100° to 120°C. (Found: C, 40.4; H, 2.3; O, 21.1; Cl, 18.9; S, 17.3 per cent. Empirical formula $C_{12}H_{8.1}O_{4.7}Cl_{1.9}S_{1.9}$).

The n.m.r. spectrum of this material was similar to that of the starting material except that a resonance signal was found 0.83 τ to low field of the resonance signal attributed to the protons in the starting material ortho to the sulphonyl chloride groups.

Spectral measurement

The i.r. spectra were obtained on a Grubb-Parsons GS2A double beam grating spectrophotometer, and the n.m.r. data were obtained on a Varian HA 100 spectrometer, using solutions of materials in dimethylsulphoxide.

SYNTHESIS OF POLY(ARYLENE SULPHONES) BY POLYCONDENSATION

Thanks are due to Mrs A. H. Seldon, and Messrs A. Bunn, S. Gaskin and D. Thomas for assistance with the experimental work.

Imperial Chemical Industries Ltd,
Plastics Division,
Welwyn Garden City, Herts

(Received June 1965)

REFERENCES

- ¹ JENNINGS, B. E., JONES, M. E. B. and ROSE, J. B. Paper presented at the I.U.P.A.C. Symposium on Macromolecular Chemistry, Prague 1965; to be published in *J. Polym. Sci.*
- ² FIESER, L. F. and FIESER, M. *Advanced Organic Chemistry*, p 656. Reinhold: New York, 1964
- ³ *Friedel-Crafts and Related Reactions*, Ed. G. A. OLAH, Vol. III, p 1319. Interscience: New York, 1964
- ⁴ Ref. 2 p 636
- ⁵ HAAS, H. C., INVINGSTONE, D. I. and SAUNDERS, M. *J. Polym. Sci.* 1955, **15**, 503
- ⁶ VALENTINE, L. and WINTER, R. W. *J. chem. Soc.* **1956**, 4768
- ⁷ ROBERTS, J. D. *J. Amer. chem. Soc.* 1956, **78**, 611
- ⁸ BUNNETT, J. F. *Chem. Rev.* 1951, **49**, 293
- ⁹ MIZUNO, Y. and SIMAMURA, O. *J. chem. Soc.* **1958**, 3875
- ¹⁰ DE LA MARE, P. B. D. and RIDD, J. H. *Aromatic Substitution*, p 161. Butterworths: London, 1959
- ¹¹ BREWSTER, R. Q. and SLOCOMBE, R. *J. Amer. chem. Soc.* 1945, **67**, 562
- ¹² BOSSHARD, H. H., MORY, R., SCHMID, M. and ZOLLINGER, H. *Helv. chim. Acta*, 1959, **42**, 1653
- ¹³ SUTER, C. M. *The Organic Chemistry of Sulphur*, p 485. Wiley: New York, 1944
- ¹⁴ OTTO, R. and TROGER, J. *Ber. deutsch. chem. Ges.* 1893, **26**, 993

Fractionation of Low Molecular Weight Polymers by Liquid Chromatography

P. I. BREWER

A liquid chromatographic method is described for the fractionation of polymers which contain a negligible amount of material with a molecular weight greater than about 10 000. The sample is dissolved in cyclohexane and passed down a column packed with small pieces of crosslinked butyl rubber swollen with the same solvent. Partition takes place between the free cyclohexane and the cyclohexane imbibed in the rubber. The distribution coefficient varies with the molecular weight of the sample, tending to zero for high molecular weight polymers and to unity for substances with molecular weights of the same order as that of cyclohexane. It is shown that the distribution coefficient of a solute can be related to its molecular weight by the Flory-Rehner theory. Values of distribution coefficients so calculated are smaller than those obtained experimentally.

If a solution of a substance is passed through a column packed with small particles of a gel swollen with the solvent it is found that the volume of solvent necessary to elute the substance depends upon the molecular weight of the substance. If the molecular weight is sufficiently high, the substance passes through the column without penetrating into the gel and is eluted with a volume of solvent equal to the void volume of the column. As the molecular weight of the substance decreases, the elution volume gradually increases until it becomes equal to the total volume of the solvent in the column. The molecular weight range over which this takes place depends upon the porosity of the gel.

If V is the total volume of the column

$$V = V_0 + V_r + V_i \quad (1)$$

where V_0 is the void volume of the column, V_r is the volume of the gel before swelling and V_i is the volume of the solvent in the swollen gel. The corrected retention volume of the solute, V_c , is the elution volume of the substance less the void volume of the column. It can be shown that the distribution coefficient, K , of the substance between the solvent imbibed by the gel and the free solvent is given by

$$V_c = KV_i \quad (2)$$

The technique has been described as gel filtration¹ and gel permeation chromatography²; it has been recently reviewed by Determann³.

It has been shown that columns packed with natural rubber can be used to separate low molecular weight substances⁴. In this paper the use of columns packed with butyl rubber to fractionate low molecular weight polymers is described and an attempt is made to explain the mechanism of the separation.

EXPERIMENTAL

The packing was prepared from chlorobutyl rubber (Enjay grade HT-10-66, 1.1 to 1.3 per cent chlorine) containing 4.8 per cent zinc oxide crosslinked by heating at 153°C for 30 minutes. The rubber was cut into small pieces and covered with cyclohexane. The swollen rubber was disintegrated in a Waring Blendor in the presence of cyclohexane. The particles of rubber were then sieved in the same solvent and the fraction between 60 and 100 mesh collected. Soluble material was then extracted from the rubber by boiling several times with cyclohexane.

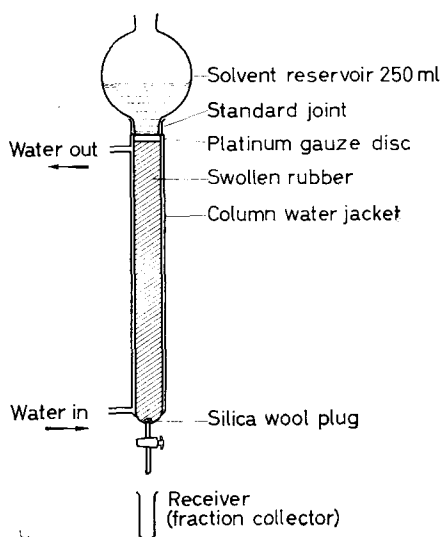


Figure 1—Apparatus for liquid chromatography

The column, 100 cm long and 1.5 cm diameter (*Figure 1*) was packed by first filling it with cyclohexane and then placing a suspension of rubber in cyclohexane in the solvent reservoir. The tap at the bottom of the column was opened so that the particles passed down the column under gravity and the flow of the liquid. When no further movement of the packing took place, the excess was removed and the top covered with a piece of fine mesh wire gauze. When it became necessary to repack the column, the packing was transferred to the solvent reservoir by inverting the column and shaking, it was then allowed to settle as before.

A sample was placed on the column by removing the solvent above the packing and adding 2 to 5 ml of a 1 to 2 per cent solution of the sample in cyclohexane. The tap at the bottom of the column was then opened and the sample solution passed into the packing. The top of the column was rinsed with 2 ml of cyclohexane and when this had passed into the packing the rinsing was repeated once more. The solvent reservoir was then placed in position and filled with cyclohexane. Fractions of 4 ml were collected by means of an automatic fraction collector. The flow rate was adjusted to about 10 ml per hour so that the elution of the sample was completed in about 18 hours. Water at 30°C was circulated through the

FRACTIONATION OF LOW MOLECULAR WEIGHT POLYMERS

water jacket. The fractions were transferred to porcelain crucibles and evaporated to dryness on a water bath. Weighings were carried out on a semimicro balance. It was necessary to make blank corrections which usually amounted to about 0.05 mg of non-volatile residue for each fraction. Usually > 95 per cent by weight of the sample taken was recovered.

Number average molecular weights were determined with a Mechrolab Vapour Pressure Osmometer (VPO); benzene was used as solvent at a temperature of 37°C. The instrument was calibrated with pure biphenyl. Apparent molecular weights were determined at several concentrations and molecular weights at infinite dilution were obtained by extrapolating the reciprocals of the apparent values to zero concentration.

Spectroscopic grade cyclohexane was used as the eluant. The materials used to calibrate the column were the purest commercially available. The pentaerythritol tetrastearate was recrystallized several times from benzene, and the resulting material had a molecular weight of 1200 by VPO (calculated 1200). The polypropylene glycols were acetylated by boiling with acetic anhydride. The excess anhydride was decomposed with hot water and after extracting several times with water the product was dried by heating gently under vacuum.

RESULTS

Sample size and column temperature

Neither the sample size nor the column temperature affected the column efficiencies markedly. Usually 50 mg of sample was taken and dissolved in 2 to 5 ml cyclohexane.

Calibration of column

The elution volume was assumed to be the volume corresponding to the maximum of the elution curve. The void volume was obtained by determining the elution volume of a polymer which did not permeate into the packing; usually a polyisobutene fraction $M_v = 5.4 \times 10^5$ was used. Increasing the viscosity of the solution of the sample caused a distortion of the elution curves (Figure 2).

Figure 2—Effect of viscosity on the elution curve of a polyisobutylene fraction ($M_v = 5.4 \times 10^5$)

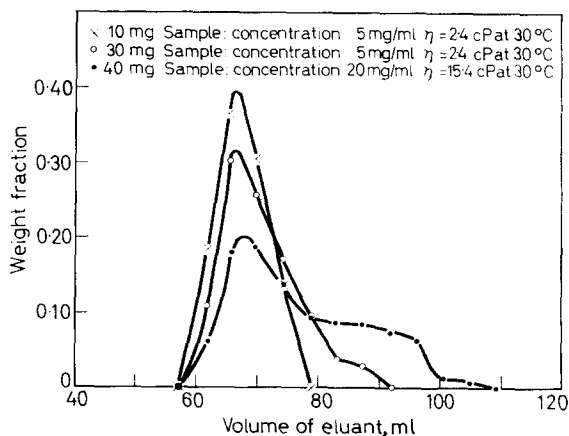


Figure 3 shows the elution curve of a mixture of polyisobutene and squalane. It will be seen that the elution volume of squalane is 146 ml, whereas that of the polyisobutene is 62 ml, hence the corrected retention volume of squalane is 84 ml.

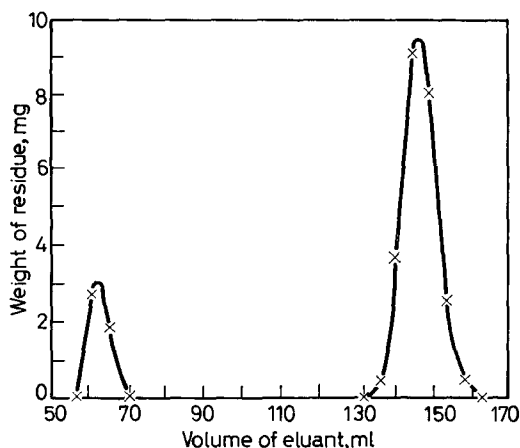


Figure 3—Elution curve of a mixture of 5 mg polyisobutene ($\bar{M}_v = 5.4 \times 10^5$) and 25 mg squalane (mol. wt 424)

Previous work⁴ with columns packed with natural rubber had shown that a linear relation existed between the logarithm of the corrected retention volume and molecular weight for a number of different types of compounds. A similar relation was found for columns packed with butyl rubber. Figure 4 shows a plot of \log (corrected retention volume) against molecular

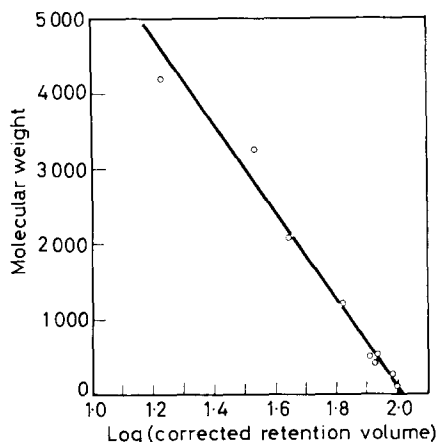


Figure 4—Variation of \log (corrected retention volume) with molecular weight

weight for the substances shown in Table I. The equation of the line is

$$\text{Molecular weight} = -5830 \log V_c + 11770 \quad (3)$$

Thus, the first 4 ml fraction eluted after the void volume should contain all material with a molecular weight greater than about 9400. Below this value the separation obtained increases as the molecular weight decreases.

FRACTIONATION OF LOW MOLECULAR WEIGHT POLYMERS

Table 1. Calibration curve data

Substance	Molecular weight	Method of determining molecular weight	Corrected retention volume, ml
Azulene	128	From formula	100
Stearyl alcohol	270	From formula	96
Squalane	424	From formula	84
β -Carotene	537	From formula	86
Pentaerythritol tetrastearate	1 200	From formula	66
Acetylated polypropylene glycol 425	509	Vapour pressure osmometer	81
Acetylated polypropylene glycol 2 000	2 090	Saponification	45
Acetylated polypropylene glycol 3 000	3 270	Saponification	35
Acetylated polypropylene glycol 4 000	4 200	Saponification	17

Polypropylene glycols were irreversibly absorbed on the packing but the acetylated glycols behaved normally. It is believed that this was due to the presence of zinc salts in the rubber; when they were removed the effect disappeared. The elution curve of a mixture of acetylated polypropylene glycols is shown in *Figure 5*.

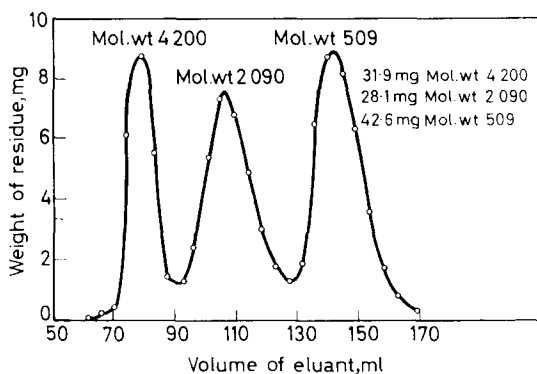


Figure 5—Elution curve of a mixture of acetylated polypropylene glycols

The efficiency of the column was found to be approximately the same as that found previously for natural rubber columns, i.e. the height of a theoretical plate was about 1.3 mm. The efficiency decreased with time probably due to channelling caused by movement of the packing. This had little effect on corrected retention volumes but increased the width of the elution curves. When the loss of efficiency became serious the column was repacked and the relation between corrected retention volume and molecular weight redetermined. The rubber also became more porous with age, i.e. the slope of the calibration line increased. This change was very slow and was probably due to the continued swelling of the rubber.

Applications

The elution curves for a commercial low molecular weight polyisobutene and a 30 per cent styrene-70 per cent butadiene copolymer are shown in *Figure 6*. The molecular weight scale at the top of the figure was calculated

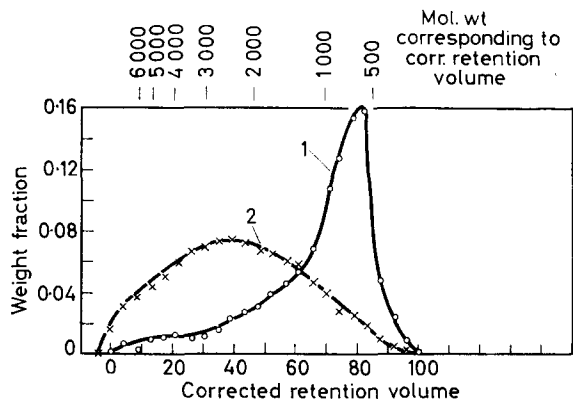


Figure 6—Elution curves of (1) a polyisobutene and (2) a styrene-butadiene copolymer

from equation 3. Plots of the logarithm of the molecular weight against the cumulative weight fraction on a normal probability scale are shown in *Figure 7*. The styrene-butadiene copolymer gave a straight line but the polyisobutene plot was curved, possibly due to the removal of low molecular weight material during manufacture. This would also account for the pronounced asymmetrical form of the elution curve. The number average molecular weights calculated from the distributions were: polyisobutene 930, (VPO 870); styrene-butadiene copolymer 2 050, (VPO 2 200).

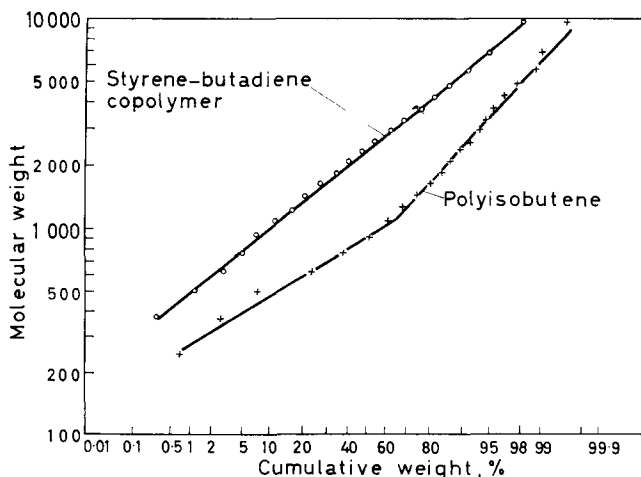


Figure 7—Log-probability plots of low molecular weight polymers

FRACTIONATION OF LOW MOLECULAR WEIGHT POLYMERS

A low molecular weight styrene-butadiene copolymer was fractionated by extracting with acetone; *Figure 8* shows the elution curve for the first

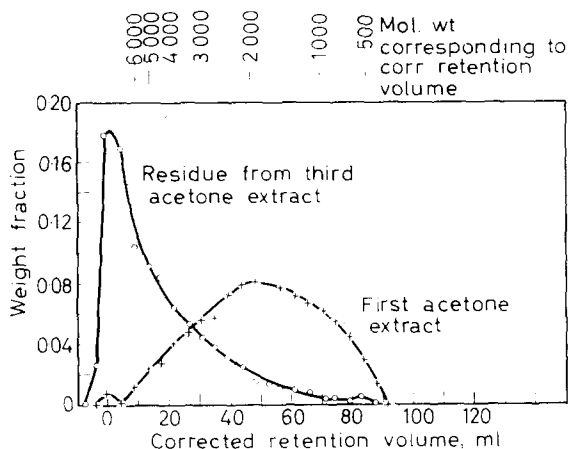


Figure 8—Elution curves of fractions from a styrene-butadiene copolymer

acetone extract and the residue after three acetone extracts. The residue contained a considerable amount of high molecular weight material which passed through the column with no fractionation and was eluted at the void volume. The number average molecular weight of the extract calculated from the distribution was 1 630, (VPO 1 340).

The elution curve of an experimental polymer is shown in *Figure 9*.

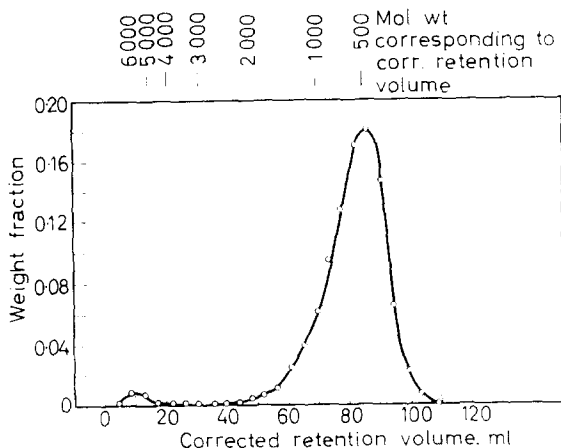


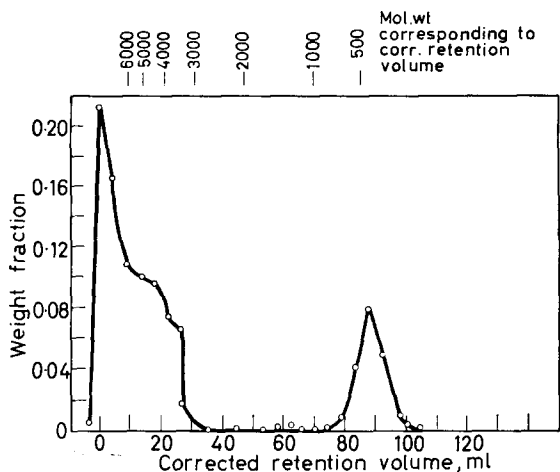
Figure 9—Elution curve of an experimental polymer

Most of the sample had a molecular weight of about 500 but a small quantity of material with a molecular weight of 6 000 was also present. Altering the conditions of polymerization showed that it was possible to increase the yield of the higher molecular weight component.

This technique can also be most useful for separating low molecular

weight polymeric plasticizers. Infra-red examination of the cyclohexane soluble part of a mastic had shown that uncrosslinked butyl rubber and an ester were present but it could not be determined if a low molecular weight polyisobutene was also present. The elution curve (Figure 10) showed that no low molecular weight polymer was present. The distortion of the peak due to the butyl rubber was caused by the high viscosity of the sample applied to the column.

Figure 10—Elution curve of the cyclohexane soluble material from a mastic



DISCUSSION

Martin and Synge⁵ have shown that the shape of the elution curve for a pure substance is approximately gaussian. It appears therefore that there is a considerable overlap in molecular weights between fractions taken in this work. No increase in the degree of separation was obtained on re-chromatographing certain fractions. These were eluted at the same corrected retention volumes as before. Increasing the length of the column increases the degree of separation but it also increases the time of a run and the number of fractions to be handled. Decreasing the size of the rubber particles increases the column efficiency but this material was more difficult to prepare. Although columns packed with butyl and natural rubber give separations over approximately the same molecular weight range, butyl rubber packing is preferred. It is more stable than natural rubber; in addition swollen butyl rubber is softer and more easily reduced to the required size.

The mechanism of gel chromatography

If the separations obtained depended upon the differential rate of diffusion into the gel it would be expected that altering the flow-rate would affect the retention volume. However, it was found that when the flow-rate was increased from 10 to about 40 ml/h, the retention volumes remained unchanged although the column efficiency decreased. Other investigators have also found^{1,2} that flow rate has little effect on retention volume.

Porath⁶ and Laurent and Killander⁷ have explained the separations obtained with Sephadex packed columns in terms of steric exclusion of the solutes from the gel particles; the larger the particles the less they penetrate into the swollen Sephadex. In both these theories the gel is supposed to consist of a rigid matrix. This cannot be so for rubber packing. The solvent in the rubber must be under pressure since at equilibrium the elastic reaction of the network must balance the osmotic pressure. Thus, there must be partition of the solute between the free solvent and the solvent under pressure. In the theory given below it will be shown that this difference in pressure can partly explain the decrease in solubility of substances in the swollen rubber and also the fact that the distribution coefficient decreases as the molecular weight of the substance increases.

The distribution of the solute molecules between the free solvent and the solvent in the rubber will be in accordance with the Boltzmann distribution, i.e.

$$\ln n/n_0 = \ln K = -W/RT \quad (4)$$

where n_0 is the number of solute molecules per unit volume of free solvent, n is the number of solute molecules per unit volume of solvent in the rubber, W is the work done when one molecular volume of solute passes from the free solvent to the solvent in the rubber, R is the gas constant and T the absolute temperature.

$$\text{Now} \quad W = \pi V_s \quad (5)$$

where π is the osmotic pressure and V_s is the molar volume of the solute. If the effect of the solute on the osmotic pressure is ignored the osmotic pressure can be obtained from the Flory-Rehner theory.

$$\pi = (-RT/V_0) \{ \ln(1 - \varphi_p) + \varphi_p + \chi \varphi_p^2 \} \quad (6)$$

where V_0 is the molar volume of the solvent, φ_p is the volume fraction of rubber in the swollen rubber and χ is the rubber solvent interaction parameter. Hence

$$\ln K = (V_s/V_0) \{ \ln(1 - \varphi_p) + \varphi_p + \chi \varphi_p^2 \} \quad (7)$$

It will be seen that $\log K$ should be proportional to the ratio of the molar volumes of solute and solvent rather than to the molecular weight of the solute. Plotting this ratio against \log (corrected retention volume) had little effect on the general scatter of the data in *Figure 4*. This may be due to ignoring the effect of the solute on the osmotic pressure but the fact that a linear relation is obtained suggests that this effect may be small.

Values of K calculated from equation 7 and the experimental values obtained from the corrected retention volumes are shown in *Table 2*. Le Bas's data were used to calculate the molecular volumes. The experimental values of φ_p were found to be 0.227 for natural rubber and 0.135 for butyl rubber. The values of χ were taken as 0.36 for natural rubber, toluene; and 0.44 for butyl rubber, cyclohexane. It will be seen that the experimental values of K are considerably lower than the values calculated from equation 7. There is some uncertainty about the values of χ but even if these are taken as zero the calculated values of K are still higher than the experimental values.

Table 2. Calculated and experimental values of K

Substance	Molecular weight	Natural rubber			Butyl rubber		
		K calc. from eq. 7 $\phi_p=0.227$	K calc. from eq. 7 $\phi_p=0.351$	K calc. from corr. retention volume	K calc. from eq. 7 $\phi_p=0.1355$	K calc. from eq. 7 $\phi_p=0.385$	K calc. from corr. retention volume
Azulene	128	0.98	0.95	0.98	1.00	0.96	0.99
Stearyl alcohol	270	0.96	0.88	0.89	0.99	0.89	0.95
Squalane	424	0.93	0.81	0.81	0.99	0.83	0.83
Tristearin	891	0.87	0.66	0.67	—	—	—
Pentaerythritol tetrastearate	1 200	0.84	0.58	0.59	0.97	0.63	0.65
Acetylated polypropylene glycols	509	—	—	—	0.99	0.84	0.80
	2 090	0.77	0.43	0.38	0.96	0.49	0.45
	3 270	—	—	—	0.94	0.33	0.35
	4 200	—	—	—	0.92	0.24	0.17

Thus, the difference in pressure due to the osmotic pressure calculated by means of equation 7 is insufficient to account for the difference in solubility and some other factor must be involved. If the experimental values of K for squalane are substituted in equation 7 it is found that $\varphi_p = 0.351$ for natural rubber and 0.385 for butyl rubber. If these values of φ_p are used to calculate values of K for other compounds, much better agreement with the experimental values is obtained (*Table 2*). Thus, the other factors involved are equivalent to an increase in pressure above that generated osmotically according to equation 7. It may be due to a sieving action such as that proposed by Porath and by Laurent and Killander and is possibly related to chain stiffness and size and number of pendant groups.

Esso Research Ltd,
Abingdon,
Berkshire

(Received June 1965)

REFERENCES

- ¹ FLODIN, P. *Dextran Gels and Their Application in Gel Filtration*. AB Pharmacia : Uppsala, 1962
- ² MOORE, J. C. J. *Polym. Sci. A*, 1964, **2**, 835
- ³ DETERMANN, H. *Angew. Chem. (Internat. ed.)*, 1964, **3**, 608
- ⁴ BREWER, P. I. *J. Inst. Petrol.* 1962, **48**, 277
- ⁵ MARTIN, A. J. P. and SYNGE, R. L. M. *Biochem. J.* 1941, **35**, 1358
- ⁶ PORATH, J. *Pure appl. Chem.* 1963, **6**, 233
- ⁷ LAURENT, T. C. and KILLANDER, J. *J. Chromatogr.* 1964, **14**, 317

Yield Stress Behaviour of Poly(ethyl methacrylate) in the Glass Transition Region

J. A. ROETLING

The tensile yield stress of poly(ethyl methacrylate) was measured over a wide range of strain rates at temperatures both above and below the glass transition temperature. The observed yield stress behaviour is readily described by the Ree-Eyring modification of the Eyring viscosity theory. Two rate processes are involved, and these are continuous through the glass transition temperature. The appearance of a transition depends, to a large extent, upon the type of data presentation employed.

IN A previous paper¹ it was shown that the tensile yield stress behaviour of poly(methyl methacrylate) (PMMA) could be described over a wide range of strain rates and temperatures by the Eyring² viscosity theory if the assumption was made that two rate processes were involved in the deformation. The stresses due to these processes were treated as being additive as in the Ree-Eyring³ modification of the theory. Even from a cursory examination of the stress-rate of strain-temperature data it was evident that the behaviour could not be described by a single process. However, it was not too surprising that two processes should be involved since other types of measurement also show two processes in this temperature range. Further, the activation energies obtained from this analysis were in agreement with those obtained from other measurements. These processes are believed to be due to different modes of motion (or degrees of freedom) of the molecular segments rather than being due to different species of flow units. The present paper reports the results of similar measurements made on poly(ethyl methacrylate) (PEMA), but whereas the measurements made on PMMA were all made in the glass state, the measurements reported here were extended through the glass transition temperature in an attempt to determine whether or not the observed deformation processes are continuous in the transition region.

EXPERIMENTAL

Some physical characteristics of the PEMA sample used in this investigation are given in *Table 1*. The sample contained no stabilizer, lubricants or other additives, and no comonomer was used in its preparation. Test specimens were injection moulded bars of the type used in the previous investigation and were moulded under fairly hot conditions in order to minimize specimen shrinkage at test temperatures near the glass transition

Table 1. Sample characterization (PEMA)

$[\eta]$ Acetone	0.298
\overline{M}_v Acetone	1.04×10^5
\overline{M}_w	1.32×10^5
\overline{M}_n	0.46×10^5
$\overline{M}_w/\overline{M}_n$	2.87

temperature. Experimental procedure was the same as described previously. The results of the measurements on the PEMA sample are shown in Figure 1, where the ratio of yield stress to absolute temperature (σ/T) is

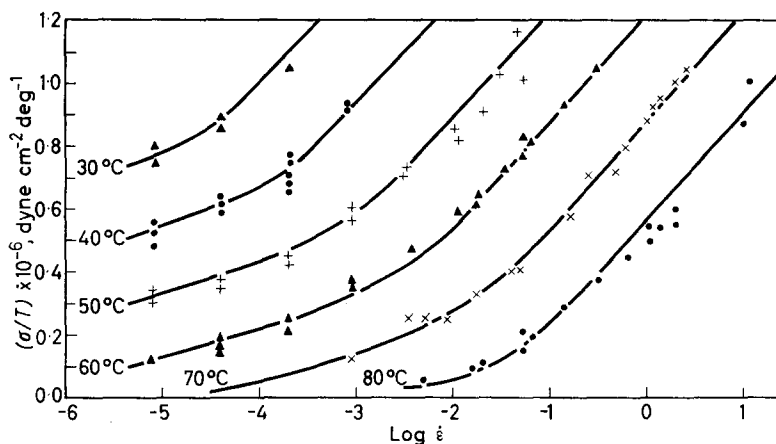


Figure 1—Measured ratio of yield stress to temperature as a function of rate of strain

plotted against the strain rate for each of several constant temperatures. The solid curves drawn through the data were calculated from the equation

$$(\sigma/T) = \sum_i (1/A_i) \sinh^{-1} \{ (C_i \dot{\epsilon}/T) \exp(\Delta H_i/RT) \} \quad (1)$$

where σ denotes yield stress (dynes cm^{-2}), $\dot{\epsilon}$ is strain rate (sec^{-1}), T is temperature ($^{\circ}\text{K}$), and the A_i , C_i and ΔH_i are material constants. The values of these constants are given in Table 2 and were chosen so as to result in

Table 2. PEMA constants

Process (<i>i</i>)	α	β
ΔH_i (kcal/mole)	98	32
A_i	23×10^{-6}	9.2×10^{-6}
$\ln C_i$	-127	-38

a reasonably good fit of equation (1) to the data. As with PMMA, the equation describes the data very well if it is assumed that two processes are involved but a good fit cannot be obtained if only a single process is assumed.

DISCUSSION

The glass transition temperature (T_g) of PEMA, determined dilatometrically⁴, is 65°C. Although the yield stress measurements extend through the glass temperature, no difficulty was experienced in fitting equation (1) to the data. It appears, therefore, that the rate processes involved are continuous through T_g . The data, as plotted in *Figure 1*, show no apparent indication of a transition in this range of rates and temperatures, other than a decrease of the yield stress to very low values at the higher temperatures and lower strain rates. This seeming lack of evidence of a transition is primarily due to the type of plot employed. In other types of measurements (e.g. stress relaxation modulus, creep compliance, and oscillatory measurements of modulus) it is common practice to plot the logarithm of the measured quantity as a function of temperature. *Figure 2* shows

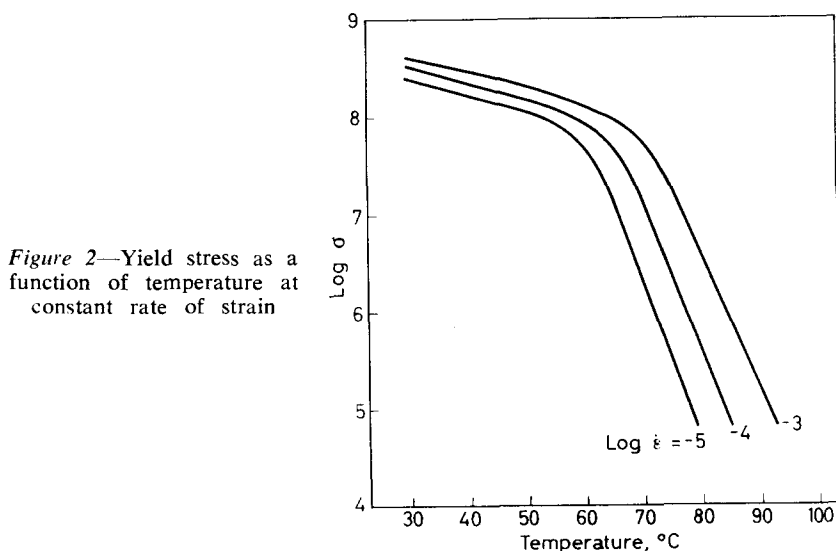


Figure 2—Yield stress as a function of temperature at constant rate of strain

plots of the logarithm of the yield stress as a function of temperature at constant strain rate, for three different strain rates. These curves were calculated from equation (1) using the constants given in *Table I*. In this type of plot the 'transition' is quite apparent and, as is usual, the transition temperature is dependent upon the rate of testing.

Before proceeding with the discussion, let us define an apparent viscosity, η , as the ratio of yield stress to strain rate (i.e. $\eta = \sigma / \dot{\epsilon}$). Then, under conditions that all processes involved are linear [i.e. $\sinh^{-1}(C\dot{\epsilon}/T) = C\dot{\epsilon}/T$], from equation (1) we obtain

$$\eta = \sum_i \eta_i = \sum_i (C_i / A_i) \exp(\Delta H_i / RT) \quad (2)$$

Making use of the constants given in *Table I*, it is found that this viscosity is due almost entirely to the α -process when in the glass state or at temperatures slightly above T_g . At temperatures well above T_g it is the

β -process which is dominant. Thus a plot of $\log \eta$ against $1/T$ is very similar to that obtained⁵ for inorganic glasses in the transition region. That is, the process with the higher activation energy is dominant at the lower temperatures and the process with the lower activation energy is dominant at the higher temperatures. It may also be seen that if equation (2) is used to calculate the temperature at which $\eta_\alpha = \eta_\beta$, this temperature is found to be equal to 94°C (i.e. $T_g + 29^\circ\text{C}$) for PEMA and 160°C ($T_g + 55^\circ\text{C}$) for PMMA. In the region where the viscosities for the two processes are comparable in magnitude, the apparent activation energy will be varying. This is also the region covered by the well known WLF equation⁶. The WLF equation predicts a variation in the apparent activation energy over a wider range of temperatures than does equation (2) but the use of equation (2) with the constants obtained from the yield stress measurements is a rather severe extrapolation of the data to higher temperatures and to much lower strain rates. Therefore some deviation from the behaviour predicted by the WLF equation might well be expected. Moreover, there are at least two other possible reasons for this deviation. (It is assumed here that the WLF equation correctly describes the variation of the apparent Newtonian viscosity with temperature but it is also possible that this assumption is not valid.) The Eyring model, while it does an excellent job of relating the linear and non-linear behaviour regions and seems to work well, particularly in the non-linear region, is inadequate in that it does not provide for a distribution of relaxation times in the linear region. This is probably the major reason why equation (2) predicts a variation in the apparent activation energy over only a narrow temperature range. It is also very probable that a third process, a non-recoverable flow*, occurs at temperatures well above T_g and contributes to the apparent variation in activation energy. The occurrence of such a process, while not apparent from the yield stress measurements, could be important at higher temperatures.

According to equation (2), that is, in the linear region, the viscosity of PEMA or of PMMA at T_g is due almost entirely to the α -process. If it is assumed that this viscosity is the same for these two materials, when each is at its glass temperature, then, using the constants given in Table 1 together with those previously reported for PMMA, and assuming the T_g of PMMA to be 105°C, the T_g of PEMA is calculated to be 66°C. This agrees well with the dilatometrically measured value and indicates some degree of consistency of the results obtained with PEMA with those previously obtained with PMMA.

As has been noted above, equation (1) describes the yield stress behaviour, and an apparent viscosity at yield may be obtained by dividing the yield stress by the strain rate. It is also possible that the equation thus obtained describes the viscosity at stresses below the yield stress (although the strain rate associated with the flow at stresses below yield would be less than the overall strain rate and would not be known). If this is so, then equation (2) will apply at very low stresses and it is possible to calculate the ratio

*Deformations due to the segmental motions involved in the α - and β -processes appear to be recoverable, as evidenced by apparently complete recovery of the tensile specimens upon heating above T_g .

of the Newtonian viscosity at room temperature, for example, to that at the glass temperature (65°C). This ratio, which is about 10^9 to 10^{10} (α -process), is about the same magnitude as the ratio of the Newtonian viscosity to the viscosity at yield (both measured at room temperature), although this latter ratio is dependent on the strain rate. That is, the stress at yield causes a speeding up of the α -process which is comparable to that caused by heating to the glass temperature. In the opinion of the author, this does occur. The result is that segmental motions of the type involved in the α -process always occur at yield although this same type of motion is essentially 'frozen out' at low stresses (linear region) if the temperature is less than T_g . This stress-induced decrease in viscosity, and hence in relaxation time, which the Eyring theory predicts, can thus account for the apparent 'stress-lowering of T_g ' which has been reported^{7,8}. In view of this stress-induced decrease in relaxation time and since it is the segments with the longer relaxation times which will be most affected, it is also reasonable to expect a narrowing of the distribution of relaxation times at high stresses. It may be for this reason that the Eyring model generally seems to be quite useful in the non-linear behaviour region although it is inadequate, as noted above, in the linear region. Once this model has been extended to include a distribution of relaxation times it should prove exceptionally useful, for even in its present form it provides some useful connections between the linear and non-linear behaviour regions.

The author is indebted to Mr W. W. Moore III for very capable assistance in the gathering and reduction of data, and to Mr L. R. DeFonso for computational assistance.

*Rohm and Haas Company,
Research Laboratories,
P.O. Box 219, Bristol, Pa*

(Received July 1965)

REFERENCES

- ¹ ROETLING, J. A. *Polymer, Lond.* 1965, **6**, 311
- ² GLASSTONE, S., LAIDLER, K. J. and EYRING, H. *The Theory of Rate Processes*, pp 480-483. McGraw-Hill: New York, 1941
- ³ REE, T. and EYRING, H. *J. appl. Phys.* 1955, **26**, 793
- ⁴ ROGERS, S. S. and MANDELKERN, L. *J. phys. Chem.* 1957, **61**, 985
- ⁵ CONDON, E. U. *Amer. J. Phys.* 1954, **22**, 132
- ⁶ FERRY, J. D. *Viscoelastic Properties of Polymers*, pp 212-232. Wiley: New York, 1961
- ⁷ BRYANT, G. M. *Text. Res. (J.)*, 1961, **31**, 399
- ⁸ VINCENT, P. I. *Polymer, Lond.* 1960, **1**, 7

The Equilibrium Polymerization of Monomers which are Solvents for Their Polymers: Case of Tetrahydrofuran

K. J. IVIN and J. LEONARD

Published data on the equilibrium polymerization of tetrahydrofuran have been reassessed making allowance for non-ideal mixing of the polymer and monomer. Taking the polymer-monomer interaction parameter as 0.3, we obtain $\Delta H_{ic} = -3.0$ kcal mole⁻¹ and $\Delta S_{ic} = -9.8$ cal deg⁻¹ mole⁻¹.

SEVERAL papers have recently appeared concerning the equilibrium polymerization of tetrahydrofuran, M, induced by cationic catalysts such as phosphorus pentafluoride¹, triphenylmethyl hexachloroantimonate² or trialkyloxonium salts³. The equilibrium concentrations $[M_c]$ at different temperatures have been used to derive the heat and entropy of polymerization using the simple formula⁴

$$\ln [M_c] = \Delta H / RT - \Delta S^0 / R \quad (1)$$

However, this formula is valid only if the mixture of monomer and polymer behaves ideally over the range of compositions covered by the experiments. In the present case the range covered is from two per cent conversion of monomer at 80°C to 95 per cent conversion at 0°C. It is therefore of interest to re-examine the data, making some allowance for non-ideal mixing by use of the Flory-Huggins expression⁵, in the absence of appropriate activity data.

Consider a homogeneous equilibrium mixture containing a volume fraction ϕ_1 of monomer and ϕ_2 of polymer of degree of polymerization n . The free energy of polymerization in an equilibrium mixture is zero and may be expressed as the sum of three terms: $-\Delta\bar{G}_1$, the free energy change for the removal of one mole of liquid monomer from the mixture; ΔG_{ic} , the free energy of polymerization of one mole of liquid monomer to one base-mole ($1/n$ moles) of amorphous (liquid or non-glassy solid) polymer; and $\Delta\bar{G}_2$, the free energy change for the addition of one base-mole of polymer to the mixture.

$$\therefore -\Delta\bar{G}_1 + \Delta G_{ic} + \Delta\bar{G}_2 = 0 \quad (2)$$

Inserting the appropriate expressions for $\Delta\bar{G}_1$ and $\Delta\bar{G}_2$ from the Flory-Huggins expression we obtain

$$\Delta G_{ic} = RT [\ln \phi_1 - (\ln \phi_2) / n + 1 - 1/n + \chi (\phi_2 - \phi_1)] \quad (3)$$

where χ is the polymer-monomer interaction parameter. If n is sufficiently

large and ϕ_2 is not too small this can be reduced to

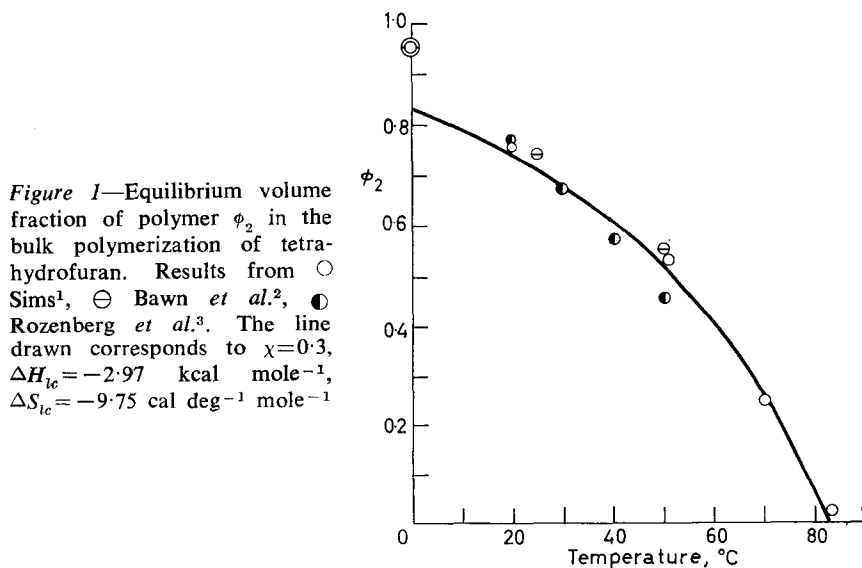
$$\Delta G_{ic} = RT [\ln \phi_1 + 1 + \chi (\phi_2 - \phi_1)] \quad (4)$$

If it is now assumed that χ has a constant value, independent of ϕ_1 and T , it is possible to calculate ΔG_{ic} at different temperatures from the values of ϕ_1 and $\phi_2 (= 1 - \phi_1)$ and to derive ΔH_{ic} and ΔS_{ic} . It is convenient to tabulate the function $[\ln \phi_1 + 1 + \chi (\phi_2 - \phi_1)]$ for given values of χ so that $\Delta G_{ic}/RT$ may be read off at a particular value of ϕ_1 . This is shown in *Table 1*. It may be seen that the function is not very sensitive to the value chosen for χ .

Table 1. $\Delta G_{ic}/RT$ as a function of ϕ_1

ϕ_1	$\Delta G_{ic}/RT$		
	$\chi=0.3$	$\chi=0.4$	$\chi=0.5$
0.01	-3.31	-3.21	-3.12
0.05	-1.73	-1.64	-1.55
0.1	-1.06	-0.98	-0.90
0.2	-0.43	-0.37	-0.31
0.3	-0.09	-0.05	-0.01
0.4	0.14	0.16	0.18
0.5	0.31	0.31	0.31
0.6	0.43	0.41	0.39
0.7	0.52	0.48	0.44
0.8	0.60	0.54	0.48
0.9	0.65	0.57	0.49
0.95	0.68	0.59	0.50
0.99	0.70	0.60	0.50

The equilibrium data of three groups of workers for the polymerization of tetrahydrofuran are summarized in *Figure 1*. There is good agreement



in the range 0° to 30°C but above this temperature there is some scatter. Bawn *et al.*⁶ now believe that their original values of ϕ_2 at 50° and above are too low because of destruction of chain centres before the establishment of equilibrium. Their revised value at 50° is shown in *Figure 1* and is in good agreement with that of Sims¹. Their values at higher temperatures have been omitted from the graph. The molecular weights of the polymer are quite high, probably greater than 10 000 in all cases, so that equation (4) is a valid approximation.

The data were treated as follows. A smoothed curve was drawn through the experimental points (this curve is not shown in *Figure 1*). The temperatures at which $\phi_2=0.95$, 0.90 etc. were read off the smoothed curve and the values of $\Delta G_{ic}/RT$ found by consulting *Table 1*. These were plotted against $1/T$. A straight line could not be obtained no matter what value of χ was chosen, nor is the situation improved by allowing χ to vary within reasonable limits with composition or temperature. The procedure adopted was therefore to draw a number of straight lines and from these to recalculate the variation of ϕ_2 with temperature to find which set of parameters gave the best fit. The result is shown in *Figure 1*. The curve drawn is that corresponding to $\chi=0.3$, $\Delta H_{ic}=-2.97$ kcal mole⁻¹, $\Delta S_{ic}=-9.75$ cal deg⁻¹ mole⁻¹. The uncertainty in these quantities is estimated to be ± 1 kcal mole⁻¹ for ΔH_{ic} and ± 2 cal deg⁻¹ mole⁻¹ for ΔS_{ic} . The divergence between theory and experiment is probably due mainly to experimental errors and neglect of the variation of ΔH_{ic} and ΔS_{ic} with temperature.

The value of ΔH_{ic} is in good agreement with the value of -3.5 kcal mole⁻¹ estimated⁴ from the data of Skuratov *et al.* It is interesting to note that the values which have been computed⁴ for the hypothetical polymerization of cyclopentane, $\Delta H_{ic}=-5.2$ kcal mole⁻¹, $\Delta S_{ic}=-10.2$ cal deg⁻¹ mole⁻¹ are comparable in magnitude with those for the polymerization of tetrahydrofuran, showing that the change from >CH_2 to >O causes little change in ring strain.

The ceiling temperature for the polymerization of pure tetrahydrofuran, giving soluble polymer, is $80^{\circ} \pm 3^{\circ}\text{C}$. It should be noted that this is *not* given by $\Delta H_{ic}/\Delta S_{ic}$ since this takes no account of the partial molar free energies of the monomer and polymer.

We thank Dr A. Ledwith for making his results available to us in advance of publication. J. L. thanks the National Research Council of Canada for a post-doctoral fellowship.

Department of Physical Chemistry,
University of Leeds

(Received September 1965)

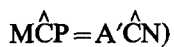
REFERENCES

- ¹ SIMS, D. J. *chem. Soc.* **1964**, 864
- ² BAWN, C. E. H., BELL, R. M. and LEDWITH, A. *Polymer, Lond.* **1965**, **6**, 95

- ³ ROZENBERG, B. A., CHEKHUTA, O. M., LUDWIG, E. B., GANTMAKHER, A. R. and MEDVEDEV, S. S. *Vysokomol. Soedineniya*, 1964, **6**, 2030
- ⁴ DAINTON, F. S. and IVIN, K. J. *Quart. Rev. chem. Soc., Lond.* 1958, **12**, 61
- ⁵ FLORY, P. J. *Principles of Polymer Chemistry*, Ch. 12. Cornell University Press: Ithaca, 1953
- ⁶ Personal communication from Dr A. Ledwith

CORRECTION

The last line of the caption to *Figure 5* on page 478 of this volume should read:



It is regretted that the manuscript contained an error at this point.

³ ROZENBERG, B. A., CHEKHUTA, O. M., LUDWIG, E. B., GANTMAKHER, A. R. and MEDVEDEV, S. S. *Vysokomol. Soedineniya*, 1964, **6**, 2030

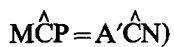
⁴ DAINTON, F. S. and IVIN, K. J. *Quart. Rev. chem. Soc., Lond.* 1958, **12**, 61

⁵ FLORY, P. J. *Principles of Polymer Chemistry*, Ch. 12. Cornell University Press: Ithaca, 1953

⁶ Personal communication from Dr A. Ledwith

CORRECTION

The last line of the caption to *Figure 5* on page 478 of this volume should read:



It is regretted that the manuscript contained an error at this point.

Abnormal Structures in Polyvinylchloride I—A Method of Estimating Labile Chloride Groups in Polyvinylchloride

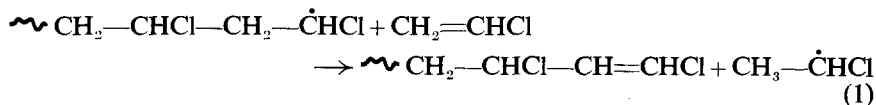
W. I. BENGOUGH and M. ONOZUKA*

An attempt has been made to estimate the amount of allylic chloride and tertiary chloride structures present in polyvinylchloride. Preliminary work using 2,4-dichloropentane, 4-chlorohexene-2, and 3-ethyl-3'-chloropentane as model compounds with secondary chloride, allylic chloride and tertiary chloride structures, has shown appreciable differences in the reactivity of these groups towards metal acetates in ester exchange reactions. The addition of a second component such as pyridine or epichlorhydrin was found to be necessary to produce a stable ester structure. Procedures have been devised for estimating allylic chlorides and tertiary chlorides present in polyvinylchloride based on results with model compounds. The extent of chloride replacement by acetate has been determined from the i.r. absorption at 1720 cm⁻¹. Support for the procedures adopted has been obtained from work with alkali-treated PVC and chlorinated alkali-treated PVC, and although the method is not yet quantitative, an indication of the relative proportions of allylic and tertiary chloride structures present in polyvinylchloride can be obtained. Results with fractionated commercial PVC indicate that the higher molecular weight fractions contain largely tertiary chloride structures whereas the lower molecular weight fractions contain more allylic chloride groups.

DEHYDROCHLORINATION, chain scission, and crosslinking reactions¹⁻⁵ all occur during the thermal degradation of polyvinylchloride (PVC), but dehydrochlorination affects the colour of the polymer which is most undesirable commercially. Consequently this reaction has been studied in greatest detail. It is now generally agreed that dehydrochlorination proceeds by the successive elimination of hydrogen chloride along the polymer molecule forming polymer chains containing 7 to 15 double bonds^{6,7}. The precise mechanism of the process is, however, still not fully understood.

Dehydrochlorination of PVC occurs at a measurable rate at temperatures of around 150°C, whereas higher temperatures are necessary to produce similar rates with chloroalkanes⁸ containing the repeating structural unit (—CH₂—CHCl—) of the polymer. This difference in thermal stability is believed to be due to the presence of abnormal structures^{2,9,10} (e.g. allylic chloride, and tertiary chloride structures) in the polymer molecules.

Allylic chloride groups could arise during polymerization by chain transfer reactions with monomer¹¹ as in reaction 1.



*Present address: Kureha Chemical Industry Company Ltd, Tokyo, Japan.

Tertiary chloride structures are also probably produced during polymerization by chain transfer reactions with polymer molecules¹¹ followed by normal propagation at the free radical site formed in such reactions. Such reactions are believed to occur more frequently at later stages of the polymerization reaction when polymer is present in excess. Other abnormalities in the polymer structure may arise through the incorporation of catalyst fragments at the ends of the polymer chains, or through termination by disproportionation, or combination.

The presence of labile chloride structures in PVC has been clearly demonstrated by Frye and Horst¹² who found that the labile chloride groups are replaced by carboxylate groups when PVC is heated with metal carboxylate stabilizers. No attempt, however, was made to differentiate between allylic and tertiary chloride structures in the polymer. In the present work by using model compounds we have been able to differentiate between allylic, secondary and tertiary chloride structures by the ease with which they exchange with metal carboxylates. It has proved necessary to carry out the reactions in the presence of pyridine or epichlorhydrin to avoid elimination of the carboxylic acid during the reaction. Based on results obtained with model compounds attempts have been made to distinguish between allylic chloride and tertiary chloride structures present in PVC. Some success has been achieved but a more detailed study will be necessary before the method can give quantitative results.

EXPERIMENTAL

Materials

Commercial polyvinylchloride (Geon 111) was precipitated from tetrahydrofuran solution with distilled water to remove residual peroxide catalysts and suspending agents used in the polymerization process.

2,4-dichloropentane, 4-chlorohexene-2, and 3-ethyl-3'-chloropentane were prepared as reported previously^{8,13}. *o*-Dichlorobenzene was purified by fractional distillation.

Tetrahydrofuran was distilled under nitrogen with potassium hydroxide to remove peroxides immediately before being used.

Pyridine and epichlorhydrin were used without further treatment.

Cadmium, barium and lead acetates were dried at 130°C before being used.

Alkali-treated PVC (chloride content 56.0 weight per cent) was prepared by treating a one per cent solution of commercial PVC (chlorine content 56.4 weight per cent) in tetrahydrofuran with one tenth its volume of 0.1 molar potassium hydroxide in methanol for one hour at room temperature. The polymer was finally precipitated and washed with water, then dried before use.

Chlorination of PVC or alkali-treated PVC was carried out by passing chlorine gas through a two per cent solution in tetrahydrofuran for 10 minutes at -78°C, and allowing reaction to proceed at about 0°C for 15 hours. The chlorine content of chlorinated PVC was 56.7 weight per cent.

Fractionated samples of PVC were prepared by the method of Freeman

and Manning¹⁴. The polymer was separated into four fractions only so that each would contain a sufficient quantity for subsequent experiments.

Procedure

Attempts at replacing chloride in the model compounds by acetate were made by mixing half-equimolar amounts of metal acetate with the model compound and maintaining at a constant temperature for a fixed time. In some experiments pyridine or epichlorhydrin was added, and in others, solvent was also added to simulate the treatments used with polymers.

The extent of reaction was determined by analysing the reacted mixture for unreacted chloroalkane and for alkene, acetic acid and acetic ester formed during the reaction, by means of gas chromatography, and i.r. spectrophotometry.

Two treatments based upon the results obtained with model compounds were used in attempts to esterify allylic and tertiary-chloride structures in the polymer. These are referred to as treatments A and B and are as follows.

Treatment A (for allylic chloride groups in PVC)

0.12g of cadmium acetate and 0.8ml of pyridine were added to a solution of 0.1g of PVC in 30ml of tetrahydrofuran and 2.5ml of water. The reaction mixture was heated for two hours (except where otherwise stated) at a temperature of 67°C. The polymer was then precipitated by adding excess methanol, filtered and washed with methanol and dried under vacuum at 64°C.

Treatment B (for tertiary chloride groups in PVC)

0.1g of polymer which had been subjected to treatment A was dissolved in 15 ml of *o*-dichlorobenzene. 0.23g of cadmium acetate and 0.8 ml of pyridine were added, and the mixture was heated for one hour at approximately 100°C. Afterwards the polymer was separated as in treatment A.

Preparation of polymer film

0.1 g of polymer was dissolved in 10 ml of *o*-dichlorobenzene and the solvent removed under reduced pressure at 70°C. The film remaining still contained some *o*-dichlorobenzene as plasticizer. It was folded and pressed between stainless steel metal plates at 140°C for three minutes. The *o*-dichlorobenzene was then extracted from the film with carbon tetrachloride using a Soxhlet extractor. The film was finally dried and its i.r. spectrum measured.

The i.r. spectra of polymer films were measured using the Perkin-Elmer Infracord Spectrometers Models 137 and 237. Measurements were made in the range 4 000 to 1 400 cm⁻¹.

Intrinsic viscosity measurements were carried out in nitrobenzene solution (0.4g polymer/100 ml solvent) at 30°C in an Ubbelohde suspended-level viscometer. Intrinsic viscosities were calculated from the equation

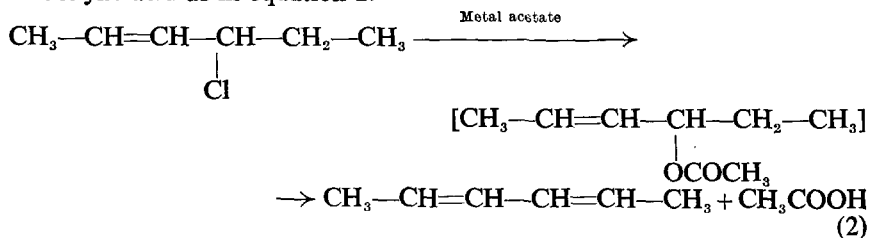
$$[\eta] = (2^{\frac{1}{2}}/c) (\eta_{sp} - \ln \eta_r)^{\frac{1}{2}}$$

where η_{sp} is the specific viscosity, η_r is the relative viscosity and c is the concentration in g/dl respectively.

RESULTS AND DISCUSSION

Model compounds

In ester interchange reactions between chloroalkanes and metal carboxylates side reactions frequently occur resulting in the liberation of the carboxylic acid as in equation 2.



Fortunately the extent of decarboxylation can be measured by i.r. spectroscopy, since the carbonyl and carbon-oxygen single bond stretching frequencies of the acetates formed from 4-chlorohexene-2, and 3-ethyl-3'-chloropentane occur at 1740 and 1240 to 1250 cm^{-1} respectively, compared with 1710 and 1285 cm^{-1} for the corresponding groups in acetic acid. The ratio of acetic acid to ester present after the reaction can thus be obtained from the ratio of the optical densities at the above frequencies. Calibration curves for acetic acid and 4-acetoxypentane, and acetic acid and 3-ethyl-3'-acetoxypentane are given in *Figures 1(a)* and *1(b)* respectively.

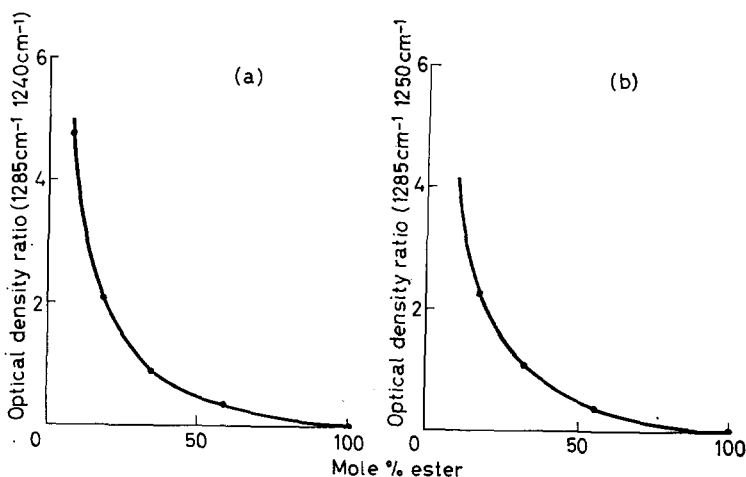


Figure 1—Calibration curve relating optical density ratio to mole percentage of ester present for binary systems involving acetic acid and (a) 4-acetoxypentane, and (b) 3-ethyl-3'-acetoxypentane

In preliminary experiments in which model compounds were treated with cadmium, barium and lead acetates for ten minutes at various temperatures, 2,4-dichloropentane was unaffected even at temperatures up to 180°C. 4-Chlorohexene-2 was partially decomposed (about 50 to 60 per cent) at

ABNORMAL STRUCTURES IN POLYVINYLCHLORIDE I

room temperature with cadmium acetate, but was unaffected by barium and lead acetates. At 80°C lead acetate produced some decomposition (about 30 per cent) but barium acetate had no effect on 4-chlorohexene-2. No reaction occurred between the metal acetates and 3-ethyl-3'-chloropentane at room temperature; at 80°C partial reaction occurred with cadmium acetate but there was no reaction with barium and lead acetates; at 180°C some reaction also occurred with the latter two acetates.

In the above reactions more than half the product was usually unsaturated hydrocarbon formed by acetic elimination during the ester exchange process (reaction 2). This side reaction was eliminated completely by carrying out the reaction in the presence of either pyridine or epichlorhydrin.

These preliminary results indicate that (1) secondary chlorides do not react with cadmium, barium or lead acetates under the above conditions, (2) allylic chloride groups react much more rapidly than tertiary chlorides, (3) cadmium acetate is much more reactive than either barium or lead acetate, and (4) pyridine or epichlorhydrin is necessary to prevent the liberation of acetic acid during the reaction. In further work cadmium acetate and pyridine have been used in most experiments and attempts have been made to differentiate between allylic chloride and tertiary chloride by adjusting the temperature of the reaction.

The above reaction conditions will clearly not be suitable for use with polymer because of the different physical properties of the polymer, and the low concentration of allylic and tertiary chloride structures in the polymer. Suitable conditions for carrying out the reactions with polymer were therefore obtained by trial and error. Treatment *A* is believed to allow reaction with allylic chloride groups but not with tertiary or secondary chloride groups, while treatment *B* should allow both allylic and tertiary chlorides to react but not secondary chlorides. Support for this view is given by the results in *Table 1* which refer to the treatment of model compounds at 67°

Table 1. Effect of reaction conditions on the esterification of model compounds in the presence of 1.2 g of cadmium acetate and 0.8 ml of pyridine

Experiment number	1	2	3	4	5
Tetrahydrofuran, ml	10	10	10	—	—
<i>o</i> -Dichlorobenzene, ml	—	—	—	10	10
2,4-Dichloropentane, g, I	1	1	1	1	1
4-Chlorohexene-2, g, II	—	0.083	—	—	—
3-Ethyl-3'-chloropentane, g, III	—	—	0.094	—	0.094
Temperature, °C	67	67	67	100	100
Time, h	2	2	2	2	2
% Conversion (based on compounds II or III when present)	0	86	0	0	78

and 100°C. 2,4-Dichloropentane does not react with cadmium acetate at either temperature; 3-ethyl-3'-chloropentane reacts to about 80 per cent conversion in two hours at 100°C but does not react at 67°C, while 4-chlorohexene-2 reacts to about 86 per cent at 67°C. The concentrations of tertiary and allylic chlorides used in the model compound experiments are much higher than those expected to be found in PVC. This was because

the model compounds had to be analysed in the presence of solvent, etc., whereas the polymer could be separated from the solvents by precipitation, and made into a film prior to i.r. analysis.

Polyvinylchloride

Because of lack of a suitable press it was not possible to produce polymer films of the same thickness each time. The optical density of the film at $2\,550\text{ cm}^{-1}$ was therefore used as a measure of the film thickness. This procedure is justified by the results in *Figure 2* in which the optical density

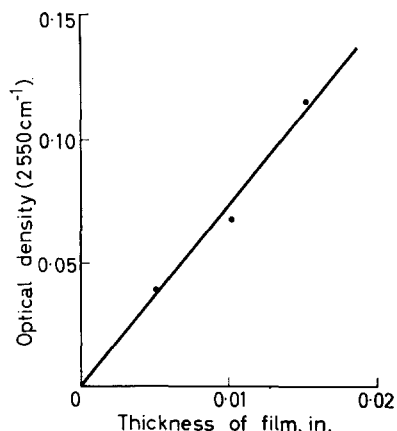


Figure 2—Relation between optical density at $2\,550\text{ cm}^{-1}$ and film thickness

at $2\,550\text{ cm}^{-1}$ is shown to be directly proportional to the film thickness. The ester absorptions have therefore been reported relative to the absorption at $2\,550\text{ cm}^{-1}$ to allow for variation in the thickness of the film used in the i.r. spectra measurements.

Reaction of the polymer samples with cadmium acetate and pyridine led to an increase in the relative absorption at $1\,720\text{ cm}^{-1}$. The effect of introducing allylic chloride structures in the polymer (by alkali treatment) can readily be seen by comparing spectra (a) and (b) in *Figure 3*. In both cases treatment *A* was used, but the absorption in (b) is clearly very much more marked than in (a) where untreated PVC has been used. Again the effect of pyridine which was observed for model compounds clearly applies to the polymer as well. This can be seen by comparing spectra (b) and (d) of *Figure 3*. In the absence of pyridine (spectrum d) the absorption at $1\,720\text{ cm}^{-1}$ is very small compared with that obtained for the reaction carried out in the presence of pyridine (spectrum b).

An appreciable removal of allylic chloride structures was effected by chlorinating the alkali-treated PVC. The spectrum of this chlorinated polymer after being subjected to treatment *A* is given in spectrum (c) of *Figure 3*. It will be noticed that the absorption at $1\,720\text{ cm}^{-1}$ is very small compared with that in spectrum (b).

A more quantitative measure of these effects is obtained from the ratio of the optical densities at $1\,720$ and $2\,550\text{ cm}^{-1}$ for the various treatments.

ABNORMAL STRUCTURES IN POLYVINYLCHLORIDE I

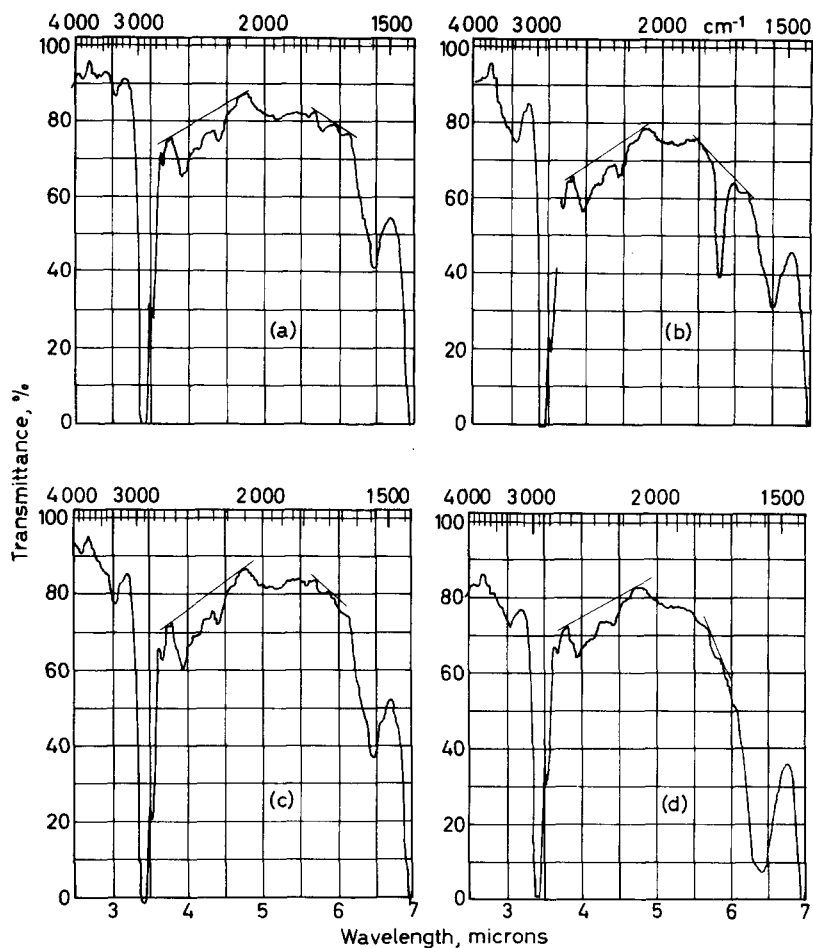


Figure 3—I.r. spectra of various samples of polymer after being subjected to treatment *A* with cadmium acetate and pyridine: (a) precipitated PVC; (b) alkali-treated PVC; (c) chlorinated alkali-treated PVC; (d) polymer as for B, but esterification carried out in the absence of pyridine

The results indicate a small carbonyl absorption (optical density ratio ~ 0.11) in the original precipitated polymer. This may be due to catalyst fragments in the polymer or to oxidative structures formed during its manufacture. Treatment *A* produces an increase in the optical density ratio (o.d.r.) to 0.27 indicating the presence of labile chloride structures (probably allylic) in the polymer. When this is followed by treatment *B* the o.d.r. increases to 0.31, indicating the presence of some less labile chloride structure, possibly tertiary chloride structures. Alkali-treated PVC when subjected to treatment *A* gave a value of 2.9 for the o.d.r. If, however, pyridine is omitted from the reactants and the procedure otherwise kept the same as

treatment *A*, the o.d.r. is only about 15 per cent of the value obtained in the presence of pyridine. Chlorinated alkali-treated PVC gave a very low value (0.14) for the o.d.r. after treatment *A*, but a much higher value (0.42) after treatment *B*. The low value is probably due to the removal of allylic chloride structures by chlorination, and was to be expected. The rather high value of the o.d.r. following treatment *B* is rather surprising. One possible explanation is that tertiary hydrogen may be removed and replaced by tertiary chlorine during the chlorination, thus increasing the proportion of tertiary chloride structures in the polymer.

As pyridine is basic in character the possibility that it might induce dehydrochlorination could not be ignored. A sample of PVC was therefore subjected to treatment *A* but without adding the cadmium acetate: after the two hour treatment cadmium acetate was added in appropriate amount and it was again heated for two hours. The final polymer gave the same o.d.r. as the sample which had not been pretreated with pyridine. Similar control runs on treatment *B* also indicated that pyridine under the conditions of our experiments did not aid the dehydrochlorination process.

Slight modifications of treatments *A* and *B* show that the value of the o.d.r. does not differ significantly if the time of heating is one or two hours, nor does it depend on the amount of pyridine present provided at least 0.4 ml is present in the mixture. There is perhaps a small indication that the o.d.r. may depend slightly on the time of reaction in treatment *B*, but this is by no means certain.

An attempt to determine whether there is any variation in the types and proportion of labile chloride structures in polymer of different molecular weight was made by fractionating the polymer, and subjecting the fractions obtained to treatments *A* and *B*. The results are given in *Table 2*.

Table 2. Optical density ratio of fractionated PVC esterified by treatments *A* and *B*

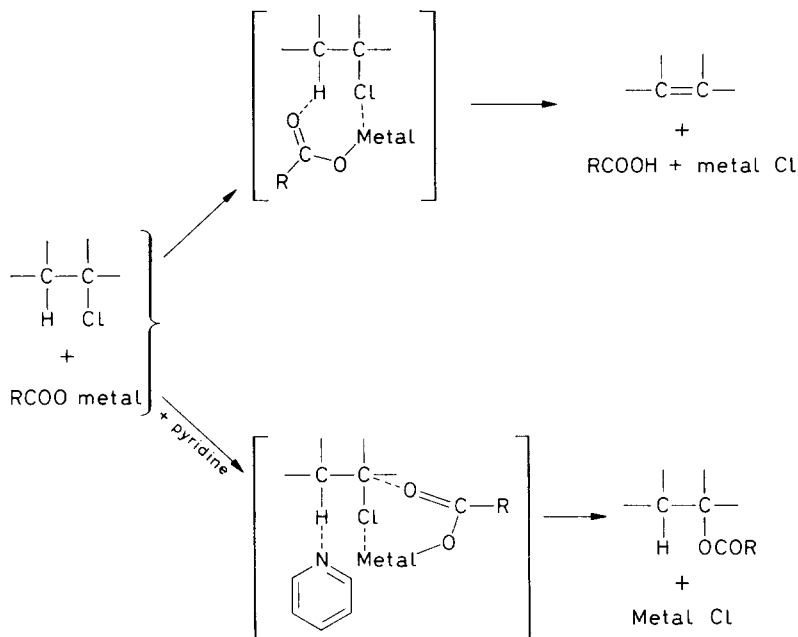
Fraction number	Degree of polymerization	Optical density ratio ($1720\text{ cm}^{-1}/2550\text{ cm}^{-1}$)	
		Treatment <i>A</i>	Treatment <i>B</i>
1	3170	0.17	0.34
2	1350	0.18	0.31
3	920	0.40	0.35
4	<920	0.45	0.42

Fractions 1 and 2 show an appreciable increase in the o.d.r. after treatment *B* whereas fractions 3 and 4 show no such increase. This presumably means that the chloride in the latter two fractions is appreciably more labile than that in the first two fractions, i.e. in the higher molecular weight material. This difference can be explained qualitatively if the higher molecular weight polymer is of a branched structure whereas the lower molecular weight polymer is linear. Branching might give rise to the tertiary chloride structures, which from the results with model compounds would be expected to react less readily with cadmium acetate than allylic chloride groups.

The effect of pyridine on the reaction between allylic chloride or tertiary

ABNORMAL STRUCTURES IN POLYVINYLCHLORIDE I

chloride structures and metal carboxylates is very marked, and applies to these structures whether they be present in simple molecules or in high polymers. One explanation which we tentatively put forward is that the pyridine shields the hydrogen of the CH_2 group from reaction with the oxygen of the carboxylate. Suggested transition states for the reaction with and without pyridine are given in the following scheme.



The action of epichlorhydrin can be explained in a similar way since its oxygen atom may act as an electron donor.

To conclude, it is clear from the work with model compounds that the rate of reaction of allylic chlorides with metal acetates is much faster than that of tertiary chloride structures. The results with alkali-treated polymer, and chlorinated alkali-treated polymer indicate that similar differences in rates of reaction also apply when the allylic chloride and tertiary chloride structures are incorporated in polymer molecules. The treatments *A* and *B* we believe give us a very approximate measure of the proportions of such structures present in the polymer. It must be pointed out that this is only an approximate estimate, as it is quite possible that a small percentage of tertiary chloride structures may react with treatment *A*, while it is probable that not all these structures react completely under treatment *B*. A much more thorough kinetic analysis of the two reactions would be necessary to obtain quantitative results, and this would necessitate the production of branched polymer molecules of known structure. In the meantime the present work offers some indication of the amounts of allylic and tertiary chloride structures in polyvinylchloride.

The authors wish to thank the Science Research Council (formerly Department of Scientific and Industrial Research) for an equipment grant, British Geon Ltd for the supply of monomer and polymer, and the Kureha Chemical Industry Company Ltd, Tokyo, Japan, for granting study leave to M.O.

*Thomas Graham Laboratories,
University of Strathclyde,
Glasgow, C.I.*

(Received May 1965)

REFERENCES

- ¹ OHTA, M. and IMOTO, M. *Kogyo Kagaku Zasshi*, 1951, **54**, 473
- ² DRUESDOW, D. and GIBBS, C. F. *Mod. Plast.* 1953, **30**, 123
- ³ DRUESDOW, D. and GIBBS, C. F. *Circ. U.S. Nat. Bur. Stand. No. 525* (1953) 72
- ⁴ IMOTO, M. and OHTSU, T. *Koka*, 1953, **56**, 802
- ⁵ BENGOUGH, W. I. and SHARPE, H. W. *Makromol. Chem.* 1963, **66**, 45
- ⁶ HIRAYAMA, K. *Nika*, 1954, **75**, 27, 667
- ⁷ BOHLMANN, F. and MANNHARDT, H. J. *Ber. dtsh. chem. Ges.* 1956, **89**, 1307
- ⁸ ASAHINA, M. and ONOZUKA, M. *J. Polym. Sci. A*, 1964, **2**, 3505
- ⁹ ARLMAN, E. J. *J. Polym. Sci.* 1954, **12**, 543
- ¹⁰ BAUM, B. and WARTMAN, L. H. *J. Polym. Sci.* 1958, **28**, 537
- ¹¹ BENGOUGH, W. I. and NORRISH, R. G. W. *Proc. Roy. Soc. A*, 1950, **200**, 301
- ¹² FRYE, A. H. and HORST, R. W. *J. Polym. Sci.* 1959, **40**, 419
- ¹³ ASAHINA, M. and ONOZUKA, M. *J. Polym. Sci. A*, 1964, **2**, 3515
- ¹⁴ FREEMAN, M. and MANNING, P. P. *J. Polym. Sci. A*, 1964, **2**, 2017

Monocyclopentadienyltitanoxanes

L. SAUNDERS and L. SPIRER*

By the hydrolysis of $C_5H_5TiCl_3$ in water and in aqueous sulphuric acid two types of monocyclopentadienyltitanoxane polymers were obtained. The first was a compound of formula $(C_5H_5TiClO)_n$ † which was characterized by chemical and by x-ray single crystal analysis, and by light scattering. The second compound was a higher polymer, which was examined by chemical analysis, by ionic decomposition in sulphuric acid and by electron micrography; it was considered to be built up of $(C_5H_5TiO)_n^+$ chains joined together by sulphate groups. The material was unusually transparent to electrons, suggesting that it consists of thin laminae curled to form tubular needles like those formed by silicates such as asbestos. Using an ion exchange resin the compound $(C_5H_5)_2Ti(COOCF_3)_2$ ‡ was prepared from $(C_5H_5)_2TiCl_2$. It was found to be a stable non-polymeric substance. Attempts made to obtain polymeric compounds of titanium having trifluoromethyl groups and hexachlorocyclopentadienyl groups attached to the titanium atom were unsuccessful.

THE aim of this work has been to explore the possibility of forming polymers with Ti—O—Ti— chains from organo-titanium compounds containing direct metal organic carbon bonds¹.

Hydrolysis of titanium alkoxides gives polymers of low molecular weight, about 1 700, which have good heat resistant properties. In these compounds, titanium exhibits the coordination number of six² and the organic groups are bonded to titanium through oxygen. In compounds in which titanium is directly bonded to organic carbon, its coordination number is four and hence such compounds might more readily form polymers of a linear structure and higher molecular weight.

An organo-titanium compound, phenyltitanium triisopropoxide³, containing a direct titanium carbon bond, was described by Herman and Nelson in 1953. Shortly afterwards Wilkinson and Birmingham⁴ reported the preparation of titanium compounds containing cyclopentadienyl groups. The latter type of compound is reasonably stable whereas the former type easily loses organic groups on hydrolysis.

In this research attempts have been made to replace the chloride ions of dicyclopentadienyltitanium dichloride, by hydroxyl, using an ion exchange resin, silver oxide, sodium hydroxide and ethoxide. The resulting compounds, however, all appeared to be completely inorganic, although it was possible to replace chloride ions by trifluoroacetic groups and obtain a compound in which dicyclopentadienyltitanium moiety is bonded to two oxygen atoms; the substance was not polymeric.

*Present address: Physical Chemistry Department, Imperial College of Science and Technology, London S.W.7.

†The preparation of $(C_5H_5TiClO)_n$ has been described by Gorsich⁵; the present paper gives further information about the structure of the compound in which $n=4$.

‡This compound was recently reported by Drozdow, Klebanski and Bartoszew¹¹ using different methods of preparation.

While studying the reaction of cyclopentadienylmagnesium bromide with titanium tetrabutoxide, insoluble substances were obtained which were isolated and examined. The analysis showed that they contained one cyclopentadienyl moiety per titanium atom and could be polymeric; further work was therefore carried out with the monocyclopentadienyl compounds. An attempt to isolate monocyclopentadienyltitanium dibutoxy bromide from the above reaction by a method described in a patent⁵ was not successful and attention was directed to the preparation of the compound $C_5H_5TiCl_3$, reported by various authors. Conflicting information has been given about the melting point of this substance. According to the patent⁵ it was prepared by the reaction between cyclopentadienyl lithium and titanium tetrachloride giving a liquid boiling at 35°C at 1 mm of mercury pressure. Gorsich⁶ used the reaction between dicyclopentadienyltitanium dichloride and titanium tetrachloride and found the melting point 185°C. Sloan and Barber⁷ used the reaction between dicyclopentadienylmagnesium and titanium tetrachloride and reported the melting point to be 145°C.

In this research it was prepared by the method used by Gorsich and the product obtained was sublimed under a vacuum. The melting point of the compound was found to be 210°C and this melting point has been subsequently confirmed in various communications⁸⁻¹⁰. The hydrolysis of this substance with water and with sulphuric acid gave products the preparation and the analysis of which form the subject of this communication.

EXPERIMENTAL

Throughout this work, the conventional vacuum and drybox technique was used for handling substances which were sensitive to moisture.

(A) Preparation of dicyclopentadienyltitanium ditrifluoroacetate, $(C_5H_5)_2Ti(CF_3CO_2)_2$ ¹¹

A saturated benzene solution of dicyclopentadienyltitanium dichloride $(C_5H_5)_2TiCl_2$, prepared according to the method of Wilkinson and Birmingham⁴, was run through a column packed with ion exchange resin in its trifluoroacetic form*. The filtrate obtained was evaporated and the residue crystallized from chloroform. The product, an orange substance of m.pt 175°C, was freely soluble in benzene, ethyl acetate, ethyl alcohol and moderately soluble in chloroform.

Analysis—Calculated for $C_{14}H_{10}TiO_4F_6$: Ti, 11.9. Found: Ti, 12.0.

The measurement of molecular weight by ebullioscopy showed that the compound was monomeric.

(B) Preparation of monocyclopentadienyltitanium trichloride, $C_5H_5TiCl_3$

Two grammes of $(C_5H_5)_2TiCl_2$ in (6 g) titanium tetrachloride was refluxed for six hours^{6,7}, the excess of $TiCl_4$ was removed by distillation *in vacuo* and the residue sublimed at 140° (0.05 mm of mercury). The product was recrystallized without decomposition from anhydrous benzene. M.pt 210°.

In the crystalline state the compound remains unchanged for several months.

*The ion exchange resin, Amberlite 400, was prepared by washing it successively with ten per cent solution of sodium hydroxide, water, ten per cent aqueous trifluoroacetic acid, water, alcohol, ether and benzene.

MONOCYCLOPENTADIENYL TITANOXANES

Analysis—Calculated for $C_5H_5TiCl_3$: C, 27.4; H, 2.3; Cl, 48.5; Ti, 21.8. Found: C, 27.9; H, 2.3; Cl, 49.4; Ti, 22.0.

*Crystal data*¹²—Crystals of $C_5H_5TiCl_3$ were found to be monoclinic and to belong to the space group either P2, Pm or P2/m, the last being most likely¹³. The unit cell dimensions were $a=6.65 \text{ \AA}$, $b=10.35 \text{ \AA}$, $c=6.52 \text{ \AA}$, $\beta=115.1^\circ$. The calculated density was 1.79 g cm^{-3} for two molecules to the unit cell which compares with observed density of 1.73 g cm^{-3} .

(C) *Preparation of cyclotetracyclopentadienylchlorotitanoxane, $(C_5H_5TiClO)_4$*

This substance was obtained when $C_5H_5TiCl_3$ in methanol solution was hydrolysed by water. The product was filtered and recrystallized from xylene. It was insoluble in water, petrol ether, ethyl ether, chloroform, slightly soluble in toluene (0.166 per cent wt/vol at 20 C) and in xylene, it formed small yellow plates of m.pt 260°C .

Analysis—Calculated for $(C_5H_5TiClO)_4$: C, 36.5; H, 3.1; Cl, 20.9; Ti, 29.1. Found: C, 36.1; H, 3.1; Cl, 20.9; Ti, 28.5.

The substance has a low solubility and a moderately high molecular weight. In such circumstances molecular weight determination from cryoscopic or ebullioscopic measurements is inaccurate and the light scattering method was therefore used.

Measurement of molecular weight by light scattering—The measurement was carried out with an initially saturated solution of $(C_5H_5TiClO)_n$ in toluene and the molecular weight was calculated from the plot of K_c/R_{90} against concentration. These values on extrapolation to zero concentration gave molecular weight of 630 (656 required for $n=4$). The data used were (i) refractive index increment $dn/dc=0.248$, (ii) refractive index of toluene 1.496, (iii) depolarization of polarized light due to solute $P=0.11$ and (iv) corrected $(K_c/R_{90})_{c \rightarrow 0}=1.58 \times 10^{-3}$ (see Figure 1). K_c is constant

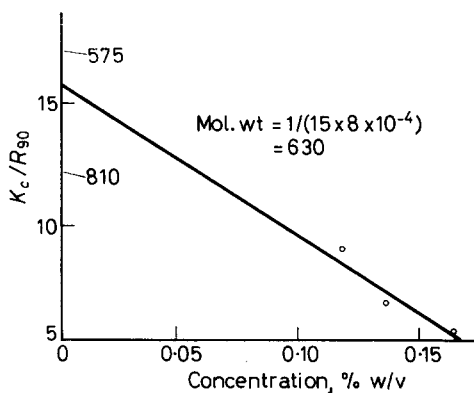


Figure 1—Estimation of molecular weight of $(C_5H_5TiClO)_4$ by light scattering method

found by calibration of the light scattering apparatus and R_{90} is the Rayleigh ratio for the light scattered at an angle of 90° to the incident beam.

X-Ray examination of $(C_5H_5TiClO)_4$ ¹³—Measurements were made on crystals which were of the shape of plates about 0.05 mm thick and 0.3 mm across, *Figure 2*¹².

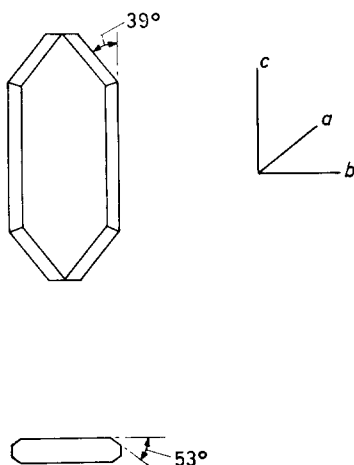


Figure 2— $(C_5H_5TiClO)_4$ crystals

The crystals of $(C_5H_5TiClO)_4$ were found to be orthorhombic and belonged to the space group $Cmcm (D_{2h}^{17})^{14}$; the unit cell dimensions were $a = 15.28 \text{ \AA}$, $b = 11.69 \text{ \AA}$, $c = 14.50 \text{ \AA}$, to an accuracy of about 0.1 per cent. The observed density was $1.66 (\pm 0.02) \text{ g cm}^{-3}$ and the density calculated from the unit cell dimensions for 16 of the structural units C_5H_5TiClO was 1.686 g cm^{-3} . The difference is probably due to cavities in the crystal and the values other than 16 for the number of structural units are ruled out.

A set of oscillation photographs covering 90° was taken about the b axis, the reflections found were:

hkl	$h + k = 2n$	$h00$	$(h = 2n)$
$0kl$	$(k = 2n)$	$0k0$	$(k = 2n)$
$h0l$	$l = 2n (h = 2n)$	$00l$	$(l = 2n)$
$hk0$	$(h + k = 2n)$		

Several elongated non-polar ring configurations can be envisaged which would accommodate the bond angles for Ti and O and possess the required symmetry.

The crystal has neither piezo-electric properties nor optical activity.

(D) Preparation of cyclopentadienyltitanium oxide sulphate

Diluted sulphuric acid added to a saturated solution of $C_5H_5TiCl_3$ in methanol caused the solution to gel. Under the optical microscope a hair-like precipitate was seen and was separated from the liquid by centrifuging. It appeared to be insoluble in organic solvents and in water but it dissolved in concentrated sulphuric acid.

MONOCYCLOPENTADIENYL TITANOXANES

Analysis—Calculated for $[C_5H_5TiO(SO_4)_4H_2O]_n$: C, 30; H, 3.6; Ti, 24.6; S, 8.2. Found: C, 24.1; H, 3.2; Ti, 21.38; S, 10.0.

Conductimetric and cryoscopic studies of ionic decomposition of $[C_5H_5TiO(SO_4)_4H_2O]_n$ in anhydrous sulphuric acid—Conductimetry: The sulphuric acid was prepared by adding oleum to the concentrated acid until the minimum conductivity $1.04 \times 10^{-2} \text{ ohm}^{-1} \text{ cm}^{-1}$ was obtained. Taking precautions to avoid the absorption of water from the atmosphere the molar conductance was calculated from the equation: $\Lambda = 10^3 \kappa / c$ where κ is specific conductance due to solute and c is concentration in moles of $C_5H_5TiO(SO_4)_4H_2O$ units.

Table 1. Molar conductivities at 25°C

c , mole l^{-1}	Λ , molar conductance $\text{ohm}^{-1} \text{ cm}^2$
0.03	643
0.04	600

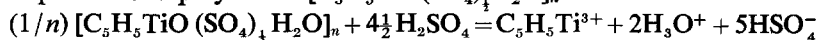
The conductance indicates the presence of more than four hydrogen sulphate ions per titanium atom, as the conductances are higher than those reported by Gillespie and Wasif¹⁵ for tetra(hydrogen sulphate).

Cryoscopy: The sulphuric acid was prepared by adding oleum to the acid until a freezing point of about 10.4°C was obtained (10.371°C)¹⁶. The substance was then added to the acid and the freezing point depression was measured by means of a Beckmann thermometer. The apparatus and all the operations were protected from atmospheric moisture. The number of particles formed due to the solute is calculated by the equation: $v = \theta / 6.12 \times m$, where θ is the freezing point depression, m the molality of $[C_5H_5TiO(SO_4)_4H_2O]$ and 6.12 is the cryoscopic constant of sulphuric acid. The results show that the number of particles formed per titanium atom is eight.

Table 2. Calculation of the number of particles from the freezing point depression

Molality, m	Freezing point depression, θ	Number of particles, v
0.00196	0.10	8.33
0.00818	0.41	8.18

The results of the conductimetric and the freezing point depression measurements indicate that the reaction with sulphuric acid is what would be expected for a polymer of $[C_5H_5TiO(SO_4)_4H_2O]_n$.



*Examination of $[C_5H_5TiO(SO_4)_4H_2O]_n$ by electron microscope and x-ray powder pattern*¹⁷—The substance in the form of a yellow powder was wet with methanol in which it was insoluble and was mounted for electron microscope examination on a thin carbon support film on a standard grid. At low magnifications (Figures 3, 4 and 5), the material consisted of micro-

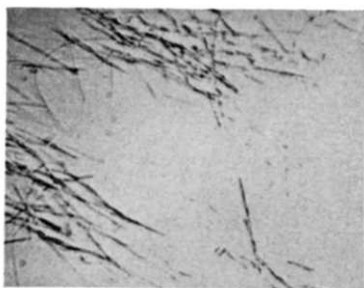


Figure 3—Optical micrograph $\times 1\ 000$

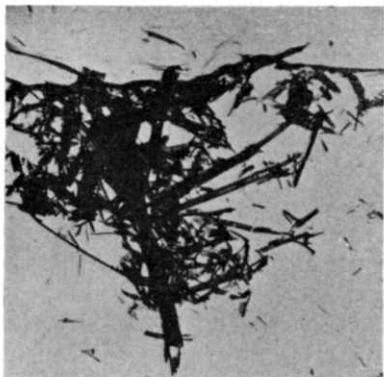


Figure 4—Electron micrograph $\times 4\ 000$

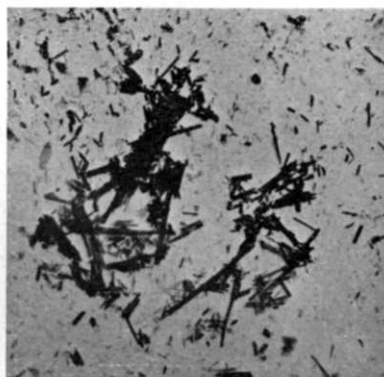


Figure 5—Electron micrograph $\times 4\ 000$

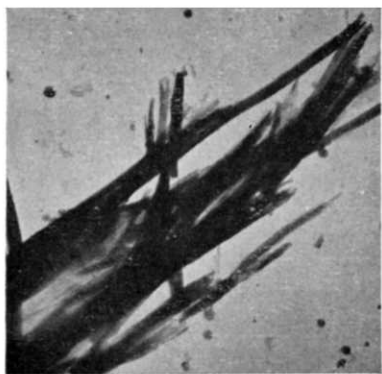


Figure 6—Electron micrograph $\times 20\ 000$

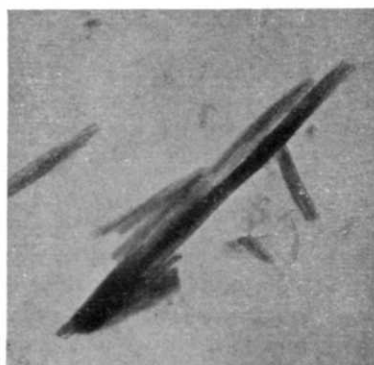


Figure 7—Electron micrograph $\times 30\ 000$

MONOCYCLOPENTADIENYL TITANOXANES

crystalline needles. At higher magnifications (*Figures 6, 7 and 8*), these crystals appeared unusually transparent to electrons, suggesting that they may be composed of thin laminae curled to form a tubelike structure as occurs in silicates, such as chrysotile asbestos.

A very weak x-ray powder pattern was obtained from this material. Six lines only were visible, as follows:

Spacing, Å	8.8	8.0	5.9	4.95	4.05	3.28
Intensity*	<i>m</i>	<i>vw</i>	<i>m</i>	<i>w</i>	<i>w</i>	<i>vw</i>



Figure 8—Electron micrograph $\times 30\,000$

(E) *Infra-red spectra*

A Perkin-Elmer double beam spectrometer with a potassium bromide prism was used. The samples were prepared in discs pressed from potassium bromide except $(C_5H_5TiClO)_4$ taken in paraffin mull and $C_5H_5Ti(OC_2H_5)Cl_2$ taken in carbon tetrachloride.

The assignment of bands was made after Lippincott and Nelson¹⁸ for ferrocene.

The bands at $3 \times 10^3\text{ cm}^{-1}$ were attributed to the i.r. active stretching frequencies. The strong band at 800 cm^{-1} occurs in all compounds containing a π -bonded cyclopentadienyl ring. In ferrocene it occurs at 810 cm^{-1} and is assigned to a perpendicular hydrogen wagging mode. A weaker band in ferrocene at 840 cm^{-1} which is not always present in other cyclopentadienyl-metal complexes is assigned to another perpendicular hydrogen wagging mode. This band could be seen in $(C_5H_5)_2Ti(OCOCF_3)_2$.

The next strong absorption occurred at $1\,020\text{ cm}^{-1}$ and was assigned to a parallel hydrogen wag. The remaining two strong bands to be seen at $1\,110\text{ cm}^{-1}$ and $1\,420\text{ cm}^{-1}$ occur quite generally in compounds containing π -bonded cyclopentadienyl rings, but a wide variation in intensity exists. The band at $1\,400\text{ cm}^{-1}$ has been assigned to a C—C stretching mode and the $1\,110\text{ cm}^{-1}$ band to a ring breathing mode.

**m*—medium, *vw*—very weak.

Table 3. The main i.r. absorption bands in cm^{-1} in the spectra of various cyclopentadienyltitanium complexes and ferrocene

Compound	C—H stretch	Addenda stretch	Bands characteristic of $\text{C}_5\text{H}_5\text{M}$ compounds	
$(\text{C}_5\text{H}_5)_2\text{Fe}$	3 085	1 758–1 620	1 411	1 108
$(\text{C}_2\text{H}_5)_2\text{TiBr}_2$	3 250	1 380	1 002	811
$(\text{C}_5\text{H}_5)_2\text{Ti}(\text{OCOCF}_3)_2$	3 250	1 750:1 620:1 380	1 410	1 020
$\text{C}_5\text{H}_5\text{TiCl}_3$	3 250		880	840
$\text{C}_5\text{H}_5\text{TiCl}_2(\text{OCH}_3)$	3 250	1 680	1 200	1 140
$\text{C}_5\text{H}_5\text{TiCl}_2(\text{OC}_2\text{H}_5)$	3 250	1 380	1 020	840
$\text{C}_5\text{H}_5\text{Ti}(\text{SO}_4)_2\text{O}\cdot\text{H}_2\text{O}_n$	3 500	1 620:1 200	830	800
$(\text{C}_5\text{H}_5\text{TiClO})_4$	3 250		1 410	1 108
			830	770
			1 410	1 100
			1 020	880
			880	
			1 410	1 110
			1 020	950
			1 410	1 140
			1 020	840
			1 410	1 020
			800	

DISCUSSION

The oxide of m.pt 260°C obtained by aqueous hydrolysis of $\text{C}_5\text{H}_5\text{TiCl}_3$, has been characterized by x-ray analysis, light scattering study and chemical analysis as a tetramer of formula $(\text{C}_5\text{H}_5\text{TiClO})_4$ and a configuration

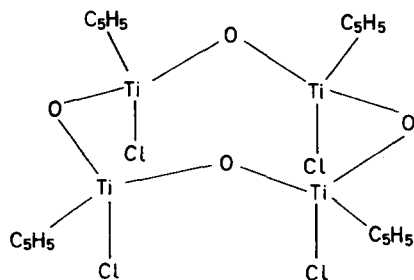


Figure 9—Cyclotetracyclopentadienyl-chlorotitanoxane (structural unit)

as in Figure 9 is envisaged, where the tetrahedral arrangement at the titanium atom is observed together with the symmetry required for the CmCm space group. It contains a ring of four titanium and four oxygen atoms.

The same oxide has been reported independently by Gorsich¹⁰, who considers it as $(\text{C}_5\text{H}_5\text{TiClO}_4)_n$ where $n=3$, but the results of this investigation as well as the study of another oxide, for which the molecular weight was determined, indicate that the tetrameric structure is more probable. Rohl *et al.*¹⁹ reported the preparation of various oxides by hydrolysis of

MONOCYCLOPENTADIENYL TITANOXANES

pentamethylcyclopentadienyltitanium trichloride which ranged from trimers to hexamers.

The precipitate $[C_5H_5TiO(SO_4)_2H_2O]_n$ obtained by acidifying $C_5H_5TiCl_3$ in methanol with aqueous sulphuric groups seems to be built from C_5H_5Ti units joined by oxygen and sulphate groups to each other to form a planar structure as shown in *Figure 10*. The electron microscope photographs

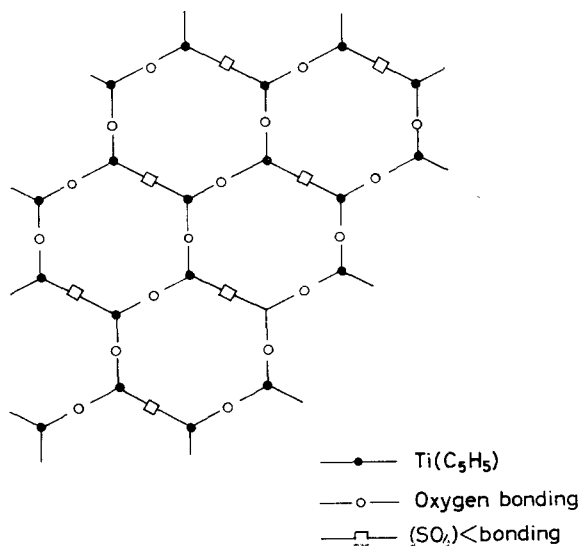


Figure 10—Cyclopentadienyltitanium oxide sulphate,
 $[C_5H_5Ti(SO_4)_2O]_n$ (segment of a structural layer)

show that it forms laminae resembling (chrysotile) asbestos and a similar type of structure has been suggested.

It might be an organic analogue of inorganic titanium oxide sulphate. The latter described by Lundgreen²⁰ is a long chain polymer built up of $(TiO)_n^{2n+}$ chains, which are joined to each other by sulphate groups. It contains water molecules, one per titanium atom and crystallizes in needle-like microcrystals.

$C_5H_5TiCl_3$ can be converted into monoalkoxyderivatives $C_5H_5TiCl_2OR$ by refluxing with the appropriate alcohol. It is thought that these could be useful starting materials for further polymerization studies.

These substances do not show any outstanding thermal stability but their preparation has revealed that the formation of various polymers with one cyclopentadienyl ring per titanium atom is possible.

Another approach that has been investigated in this research was the formation of titanium compounds with completely halogenated organic groups. It was expected that compounds of titanium with trifluoromethyl and pentachlorocyclopentadienyl groups might be stable and on hydrolysis form polymers in which the incombustible and bulky halogenated groups would protect titanium from further oxidation. These attempts failed but from recent information it appears that the use of halogenated aryls might

be successful. It might be that the preparation of compounds with partially halogenated hydrocarbons as $C_5H_5X_nTiCl_3$ might give polymers of better thermal stability than these obtained here.

The work is published by permission of the Ministry of Defence (Navy Department), whom we thank for a grant to one of us (L. Spirer).

The authors wish to thank Dr J. Godfrey (Admiralty Material Laboratory) for electron microscope photographs, x-ray powder pattern and comments on the cyclopentadienyltitanium oxide sulphate, Mr D. Bromley (AML) for x-ray analysis of various crystals reported here, and Dr R. Robinson for examination by light scattering.

*Physical Chemistry Department,
School of Pharmacy, University of London,
London, W.C.1*

(Received July 1965)

REFERENCES

- ¹ SPIRER, L. 'Studies of some organic compounds of titanium'. *Ph.D. Thesis*, University of London, July 1962
- ² BRADLEY, D. C., GAZE, R. and WARDLAW, W. *J. chem. Soc.* **1955**, 3977
- ³ HERMAN, D. F. and NELSON, W. K. *J. Amer. chem. Soc.* 1953, **75**, 3877
- ⁴ WILKINSON, G. and BIRMINGHAM, J. J. *Amer. chem. Soc.* 1954, **76**, 4281
- ⁵ *Brit. Pat. No. 793 354* (16 April 1958)
- ⁶ GORSICH, R. D. J. *Amer. chem. Soc.* 1958, **80**, 4744
- ⁷ SLOAN, C. L. and BARBER, W. A. J. *Amer. chem. Soc.* 1959, **81**, 1364
- ⁸ GIANNINI, U. and CESCA, S. *Tetrahedron Letters*, 1960, **14**, 19
- ⁹ NESMEYANOW, A. N., NOGINA, O. V. and BERLIN, A. M. *Izvest. Akad. Nauk S.S.S.R., Otdel. khim. Nauk*, **1961**, 804
- ¹⁰ GORSICH, D. R. J. *Amer. chem. Soc.* 1960, **82**, 4211
- ¹¹ DROZDOW, G. V., KLEBANSKI, A. L. and BARTOSHEW, V. A. *Zh. obsch. Khim., Mosk.* 1963, **33**, 2422
- ^{12, 13} BROMLEY, D. Private communications
- ¹⁴ *International Tables for the Determination of Crystal Structure*. Bell: London, 1935
- ¹⁵ GILLESPIE, R. J. and WASIF, S. *J. chem. Soc.* **1953**, 229
- ¹⁶ GILLESPIE, R. J. and ROBINSON, E. A. *Adv. inorg. Chem. Radiochem.* 1959, **1**, 412
- ¹⁷ GODFREY, D. J. Private communication
- ¹⁸ LIPPINCOTT, E. R. and NELSON, R. D. J. *Amer. chem. Soc.* 1955, **77**, 4990
- ¹⁹ ROHL, H., LANGE, E., GÖSSL, T. and RÖTH, G. *Angew. Chem.* 1962, **74**, 155
- ²⁰ LUNDGREEN, G. *Ark. Kemi*, 1957, **10**, 397

The Separation and Fractionation of Polystyrene at a Lower Critical Solution Point

C. D. MYRAT* and J. S. ROWLINSON

Solutions of polystyrene in methyl acetate separate into two liquid phases at lower critical solution temperatures which lie above 120°C. Phase boundaries were determined for one broad, one moderately sharp and five very sharp fractions of polystyrene. Pressures up to 45 atm displace the curves uniformly to higher temperatures.

The phase boundaries of the sharp fractions form a regular family of curves which is cut by the curves of the broader fractions. It is suggested that the determination of such a curve is a rapid way of characterizing a polymer.

The broadest sample was separated into seven fractions by successive precipitation in an apparatus that could be used up to 50 atm. The efficiency of the fractionation was good at high molecular weights but poor at low molecular weights.

POLYMER solutions generally separate into two phases on heating to temperatures above the normal boiling point of the solvent. It has been shown that the temperature of separation depends strongly on the mean molecular weight of the polymer¹⁻³. This dependence and the unusual shapes of some of the phase boundaries² suggest that there is considerable fractionation of the polymer between the two phases. The system polystyrene plus methyl acetate has been chosen to study this point and the results below confirm that fractionation does occur.

The choice of polymer was determined by the comparative ease with which both sharp and broad fractions can be obtained, and a solvent was chosen which gives phase boundaries that are at low temperatures and vapour pressures and whose positions depend strongly on the molecular weight of the polystyrene.

Materials

Seven samples of polymer were used. The first (PS 1) had a broad distribution of molecular weights. It was prepared by Distillers Co. Ltd, and supplied by the National Chemical Laboratory. Green and Vaughan⁴ have determined the molecular weight distribution.

The other samples were sharp fractions prepared by anionic polymerization. PS 2, 6 and 7 were supplied by Dr R. H. M. Simon of Monsanto Co., Springfield, Mass., and PS 3, 4 and 5 were supplied by Prof. G. Allen of Manchester University. (Samples PS 4 and 5 are the same as those of the same name in the paper of Allen and Baker³.) The number averages in

*Present address: Department of Chemistry, Demokritos Nuclear Centre, Athens, Greece.

Table 1 were determined by the supplier by osmometry. The weight averages in the last column were determined by us from the equation⁵

$$[\eta] = 1.03 \times 10^{-4} M^{0.74} \quad (\text{Benzene } 30^\circ\text{C})$$

Table 1

Sample	M_n (supplier)	M_w (supplier)	M_w (this work)
PS 1	30 000	390 000	—
PS 2	48 000	48 000	50 000
PS 3	59 000	59 000	—
PS 4	55 000	64 900	—
PS 5	95 000	99 100	—
PS 6	177 000	195 000	184 500
PS 7	246 000	270 000	266 000

Methyl acetate of 98 per cent quoted purity was treated twice with phosphorus pentoxide and distilled fractionally in a dry column. The middle fraction was treated again with phosphorus pentoxide, re-distilled and stored over silica gel. The pentoxide should not only dry the ester but should remove any free methanol. The normal boiling point was $57.1^\circ \pm 0.1^\circ\text{C}$ and the refractive index 1.3600 at 20°C and 5.893 \AA .

Phase equilibria

The temperature of the separation into two liquid phases in equilibrium with the vapour was obtained by heating slowly solutions in sealed glass tubes (8 mm \times 140 mm internal dimensions), as described previously². The upper limit of concentration that could be reached was fixed by the viscosity of the solutions. The temperatures were reproducible to about 0.5°C for the sharp fractions but those for PS 1 show greater scatter. The results are shown in *Figures 1 and 2*.

The effect of pressure on the phase boundaries was studied in the apparatus used for the experiments on fractionation, which is described below. Here the boundaries were observed by reducing the pressure at constant temperature rather than by changing the temperatures at constant pressure. The temperature was controlled to $\pm 0.2^\circ\text{C}$ and the pressure was reproducible to ± 0.5 atm. However, its absolute accuracy may be a little less because of friction in a piston that formed part of the apparatus. The results for PS 1 (two concentrations) and for PS 2, 6 and 7 (one concentration each) are shown in *Figure 3*. Six fractions of PS 1 were also studied but the results are not shown since they were all similar to those of *Figure 3*.

Fractionation

Two attempts were made to fractionate PS 1 by repeated separation into two phases. The first was a method of successive extraction. Each step consisted of the addition of more solvent, equilibration, and removal of the upper layer. This method has been used at a lower critical point of polyisobutylene solutions by Baker⁶. However, it was difficult to prevent the bulk of the polystyrene being lost in the first few extractions and the method was abandoned.

THE SEPARATION AND FRACTIONATION OF POLYSTYRENE

Figure 1—Phase boundaries of solution of the sharp fractions PS 2, 3, 4, 6 and 7. The temperature is shown as a function of weight fraction of solute. The dashed curves are the boundaries for PS 1 and 5—see Figure 2

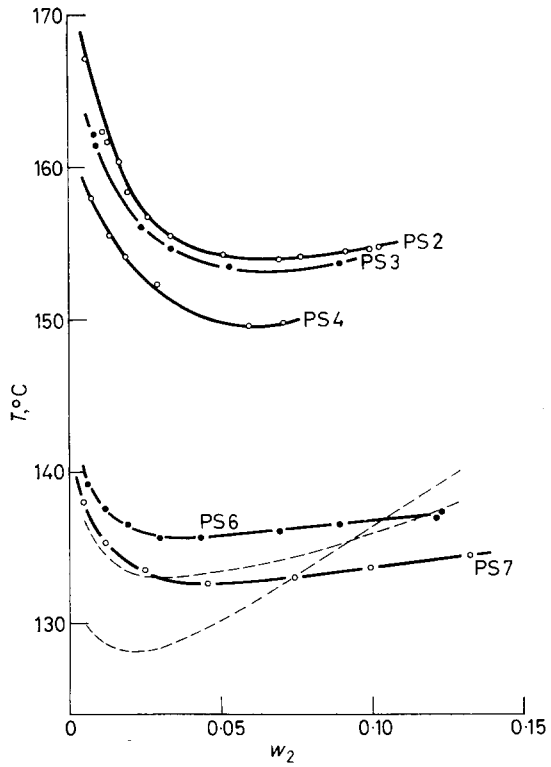
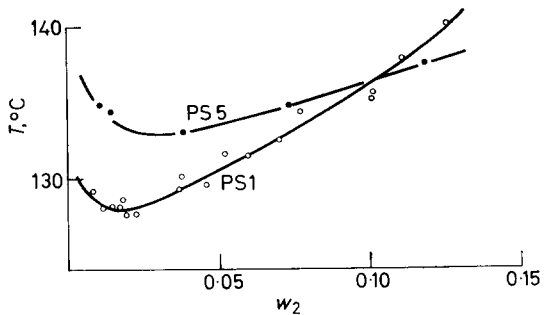


Figure 2—Phase boundaries for the moderately sharp fraction PS 5 and the broad fraction PS 1



The second and more successful fractionation was made by successive precipitation. Each step consisted of adjusting the concentration temperature and pressure to bring the system into the two-phase region and the removal of the lower phase. The actual phase change was always brought about by an isothermal change of pressure. The concentration at precipitation was kept at about two per cent so that the volume ratio of lower to upper phases was about 1:20.

The apparatus is shown in Figure 4. The solution was contained in the cell A which was a liquid height indicator (Type JA, made by Richard Klinger Ltd). It capacity was 60 cm³ and front and back walls were glass

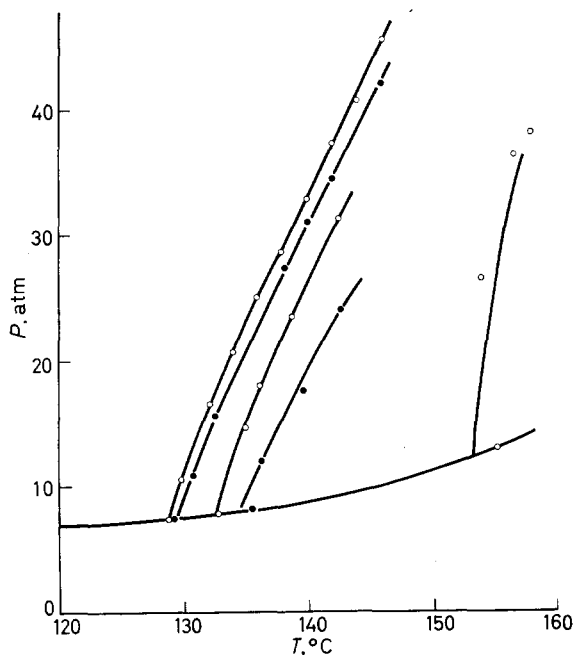


Figure 3—Effect of pressure on separation temperature. The curves are, from the left, PS 1 ($w_2=0.0214$), PS 1 ($w_2=0.0434$), PS 7 ($w_2=0.0260$), PS 6 ($w_2=0.0288$), PS 2 ($w_2=0.0282$)

windows 1.5 cm thick. The solution was confined over mercury which filled also a vessel *B* that was situated a little higher than *A*. The reserve of solvent was in the vessel *C*. Pressure was applied to the mercury by means of a cylinder (not shown) the lower part of which contained mercury and the upper part oil. The oil lines led to the pump, Bourdon gauge and dead-weight gauge. The mercury and oil were separated by a steel piston 5 cm in diameter which floated on the mercury and was sealed with O-rings. The friction of this piston introduced an uncertainty of about $\frac{1}{2}$ atm into the pressure of the mercury.

The separation was brought about by a reduction of pressure across a phase boundary, after which the system was brought to equilibrium by rocking the cell *A* to-and-fro, when mercury splashed up its sides. The lines leading from the upper parts of *A* were disconnected during stirring. The two layers were removed from *A* by re-connecting the lines and transferring them successively to *B* by displacement with mercury. They were then removed through the valve on *B* and the polymer precipitated.

The fractionation of PS 1 into seven fractions is shown in Figure 5. Two sharp samples PS 6 and PS 7 were studied in the same apparatus also at 2.6 per cent concentration. In each case there was a substantial fractionation in the first step but the operation could not be continued because of lack of material. PS 6 ($M_w=184\,500$) was separated into $M_w=164\,500$

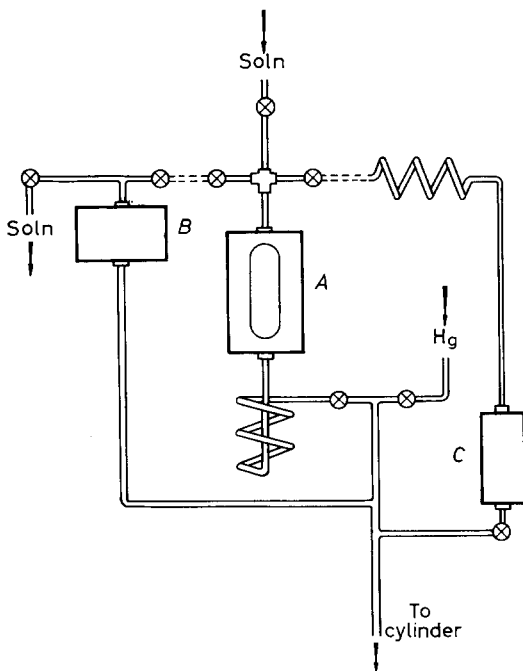


Figure 4—Sketch of apparatus used for fractionation

(64 per cent) and $M_w = 208\,500$ (17 per cent), and PS 7 ($M_w = 266\,000$) was separated into $M_w = 236\,000$ (68 per cent) and $M_w = 299\,000$ (14 per cent).

Volume of mixing

Substantial contractions on mixing near the LCST have been found for polyisobutylene in *n*-pentane², and for a pentane and a hexane in liquid methane⁷. They appear to be the rule near the LCST. The positive slopes of

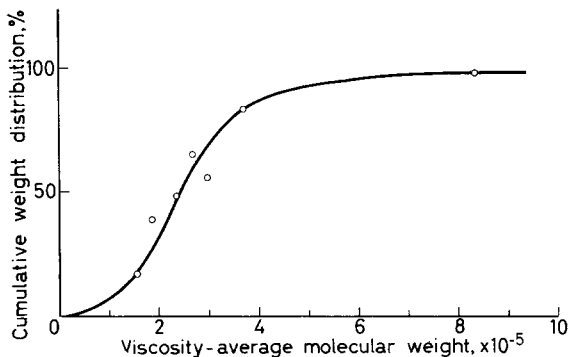


Figure 5—Fractionation of PS 1, a cumulative weight distribution as a function of the viscosity-average molecular weight

the lines in *Figure 3* imply that they are present here also^{3,8}. A direct check was made for PS 1 at 2.3 per cent by weight in the apparatus used for fractionation. The contraction ($-\Delta V/V$) was 5.6 per cent at 130° to 136°C and appeared to increase with temperature.

DISCUSSION

The phase diagrams of *Figures 1* and *2* are similar to those previously reported¹⁻³. However, the effect of the width of the distribution of molecular weights on the shapes of the phase boundaries for polystyrene is now brought out clearly. The sharp fractions PS 2, 3, 4, 6 and 7 form a regular family of curves which do not cross. Sample PS 5, which is moderately sharp, departs from this pattern and crosses the curves for PS 6 and PS 7. The broad sample PS 1 shows a much greater departure. Its position appears to be determined by its weight-average at low concentrations and by its number-average at high concentrations.

The minima of the curves for the sharp fractions move slowly to lower concentrations as the mean molecular weight increases. A Flory-Huggins plot of the concentrations at which the solutions separate into coexistent phases of equal volume, against the square root of the chain length, suggests a LCST for infinite molecular weight at 121°C. These concentrations are close to the minima of the phase boundaries. The broad fractions neither conform to the Flory-Huggins plot nor are the minima points of equal volume.

The change of the pattern of these curves with the mean molecular weight and with the width of the distribution about that mean suggests that such curves could be used for the rapid characterization of polymer fractions. Once a polymer-solvent system has been mapped out then the determination of a curve can be quickly made and gives not only an estimate of the

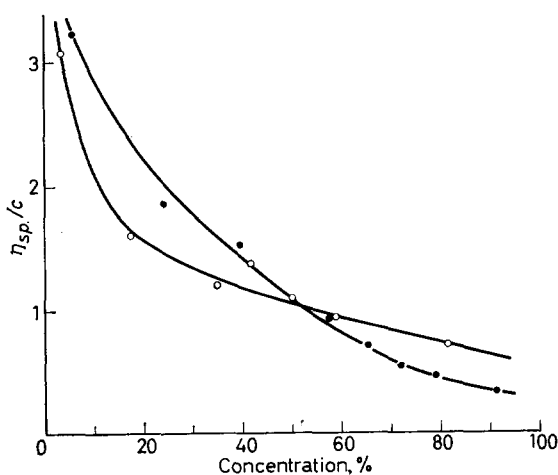


Figure 6—A comparison of the fractionation with that of Vaughan (closed circles). The ratio of specific viscosity to concentration at $c=4\text{ g l}^{-1}$ as a function of cumulative weight per cent

first moment (or mean) of M , but also of its second moment (or width of distribution).

The substantial effect of pressure on the LCST is shown in *Figure 3*. It is much greater than that commonly found at the UCST, as Allen and Baker have also shown³, because of the greater volume changes on mixing at these high reduced temperatures of the solvent.

The experiments on fractionation show that, although no great efficiency was achieved, it is possible to use a LCST for useful separations. *Figure 6* compares our results with those of Green and Vaughan⁴ who used the method of solvent evaporation. The curve obtained here shows poor fractionation at low molecular weights, but may be open to improvement. The method has several advantages. First, the sensitivity of the phase boundary to molecular weight makes it possible to split even sharp fractions. Secondly, the volume of the solution can be kept low (60 cm³ here) and moderate concentrations (two to three per cent) can be used. Thirdly, the slope of the p/T lines allows the separation to be made by a change of pressure rather than temperature^{3,6} which leads to a rapid and uniform precipitation and so should make it easier to reach equilibrium. The greatest disadvantage is the need to work above atmospheric pressure. The mechanical problem of containing the pressure is easily solved, but the manipulation of the solutions is less easy and we think that it is this difficulty that is responsible for the low efficiency of the process. Better handling technique might yield good fractionation since the method seems to be intrinsically sensitive.

We wish to thank Dr K. E. Bett for advice, Shell Research Ltd for the support of some of this work, and Prof. G. Allen, Drs R. H. M. Simon and M. F. Vaughan for the gifts of samples mentioned in the text. One of us (C.D.M.) thanks the Greek Atomic Energy Commission for a maintenance grant.

*Department of Chemical Engineering and Chemical Technology,
Imperial College,
London, S.W.7.*

(Received July 1965)

REFERENCES

- ¹ FREEMAN, P. I. and ROWLINSON, J. S. *Polymer, Lond.* 1960, **1**, 20
- ² BAKER, C. H., BROWN, W. B., GEE, G., ROWLINSON, J. S., STUBLEY, D. and YEADON, R. E. *Polymer, Lond.* 1962, **3**, 215
- ³ ALLEN, G. and BAKER, C. H. *Polymer, Lond.* 1965, **6**, 181
- ⁴ GREEN, J. H. S. and VAUGHAN, M. F. *Chem. & Ind.* 1958, 829
VAUGHAN, M. F. *Nature, Lond.* 1962, **195**, 801
- ⁵ SCHULTZ, A. R. and FLORY, P. J. *J. Amer. chem. Soc.* 1952, **74**, 4760
- ALLEN, V. R. and FOX, T. G. *J. chem. Phys.* 1964, **41**, 337
- ⁶ BAKER, C. H. *Thesis*, University of Manchester, 1962
- ⁷ DAVENPORT, A. J., ROWLINSON, J. S. and SAVILLE, G. *Trans. Faraday Soc.* In press
- ⁸ ROWLINSON, J. S. *Liquids and Liquid Mixtures*, p 165. Butterworths: London, 1959

Reactivity Ratios for the Copolymerization of Acrylates and Methacrylates by Nuclear Magnetic Resonance Spectroscopy

N. GRASSIE, B. J. D. TORRANCE, J. D. FORTUNE and J. D. GEMMELL

Nuclear magnetic resonance spectroscopy has been applied to the analysis of copolymers of methyl methacrylate with ethyl acrylate, propyl acrylate, butyl acrylate, ethyl methacrylate and methyl acrylate and the reactivity ratios calculated. In the first four of these systems accurate analyses were possible by comparing the $-\text{O}-\text{CH}_2-$ and $-\text{O}-\text{CH}_3$ absorption bands which are sufficiently resolved. A lower order of accuracy was achieved for the methyl methacrylate-methyl acrylate system as neither incorporates $-\text{O}-\text{CH}_2-$ structures, and recourse had to be made in this case to measurement of the total absorption for analytical purposes. Even this method cannot be used, however, when both monomer molecules contain the same number of protons, as for example ethyl methacrylate and propyl acrylate.

FEW values of reactivity ratios for pairs of acrylate and methacrylate monomers have been reported. This is principally due to the fact that the similarities of the structures of the components make analysis of the copolymers difficult. Elemental analysis cannot be made accurate enough for the purpose¹ and the application of i.r. or u.v. spectroscopic methods would require the two monomers to have absorbing structures which are significantly different.

The gas-liquid chromatographic analysis of pyrolysis products has been applied but may be of doubtful quantitative validity¹. Radiometric² and isotopic³ methods are the only ones to have been used successfully but, being time consuming and requiring elaborate experimental technique, have only been applied to a few isolated systems.

This paper shows how nuclear magnetic resonance spectroscopy can be successfully used for such monomer pairs, although this method also has its limitations. It has previously been used to determine the monomer content of vinyl acetate-ethylene copolymers^{4,5} but reactivity ratios were not calculated. The method is clearly widely applicable to copolymer analysis and is particularly valuable for its rapidity and simplicity.

EXPERIMENTAL

Monomer purification

Methyl methacrylate (MMA) (I.C.I. Ltd), methyl acrylate (MA) (B.D.H. Ltd), butyl acrylate (BuA) (Koch Laboratories), ethyl acrylate (EA) (Light and Co.), ethyl methacrylate (EMA) (I.C.I. Ltd) and propyl acrylate (PrA)

(prepared by alcoholysis of methyl acrylate⁶) were washed with caustic soda solution to remove inhibitor, subsequently with distilled water, and dried over calcium chloride. The monomers were vacuum distilled and stored at -18°C .

Polymerization

Copolymers of MMA with MA, EA, PrA, BuA and EMA were studied.

After degassing and distillation in vacuum, monomer mixtures of known composition were polymerized in bulk under vacuum to about five per cent conversion. The pair MMA-MA was polymerized at 65°C with 0.075 per cent w/v azoisobutyronitrile as catalyst. All other pairs were polymerized at 60°C with 0.18 per cent w/v catalyst.

The copolymers were precipitated three times from chloroform solution by methanol and dried in a vacuum oven for 24 hours at 50°C .

Copolymer analysis

N.m.r. spectra were obtained using a Perkin-Elmer R10 60 Mc/s spectrometer with integrator using 20 mg copolymer samples dissolved in 1 ml of CDCl_3 . Ten integrals were obtained for each sample and the average used for the calculation of copolymer composition.

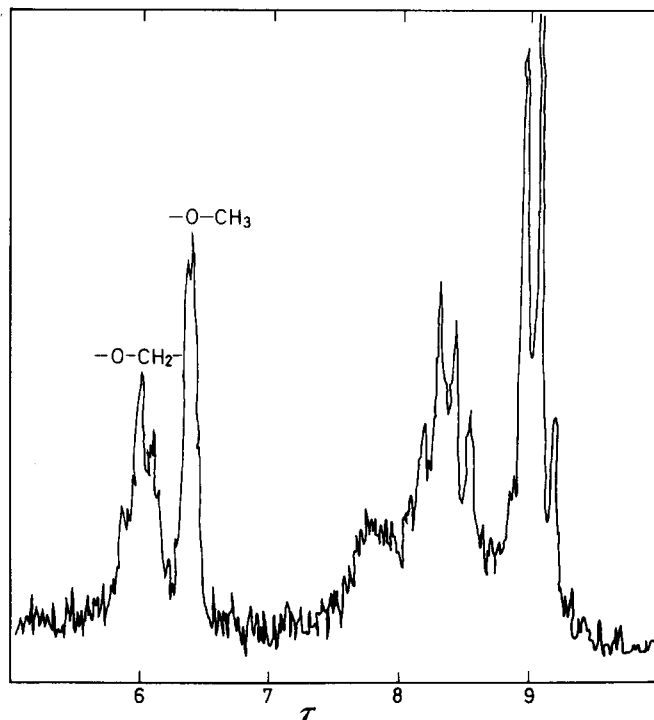


Figure 1—Nuclear magnetic resonance spectrum of 1-4, MMA-PrA copolymer

RESULTS AND DISCUSSION

In the n.m.r. spectra of the copolymers MMA-EA, MMA-PrA, MMA-BuA and MMA-EMA the peak due to the $-\text{O}-\text{CH}_3$ protons (in MMA) was resolved from those due to the $-\text{O}-\text{CH}_2-$ protons (in the second monomer) as shown for a representative example in *Figure 1*. The monomer compositions of the copolymers were calculated from the ratios of the areas under those peaks, as measured by the integral curves, the areas being proportional to the number of protons contributing to the peaks. Thus

$$I_{-\text{OCH}_2-} \propto 2 \text{ (number of second monomer units in chain)}$$

$$I_{-\text{OCH}_3} \propto 3 \text{ (number of MMA units in chain)}$$

in which $I_{-\text{OCH}_2-}$ and $I_{-\text{OCH}_3}$ are the integrals of the $-\text{OCH}_2-$ and $-\text{OCH}_3$ peaks respectively.

If X is molar ratio MMA/second monomer in copolymer, then

$$I_{-\text{OCH}_2-} / I_{-\text{OCH}_3} = 2/3X$$

No characteristic peaks could be distinguished for MMA-MA copolymers, MA and MMA both contain $-\text{O}-\text{CH}_3$ groups and the absorptions

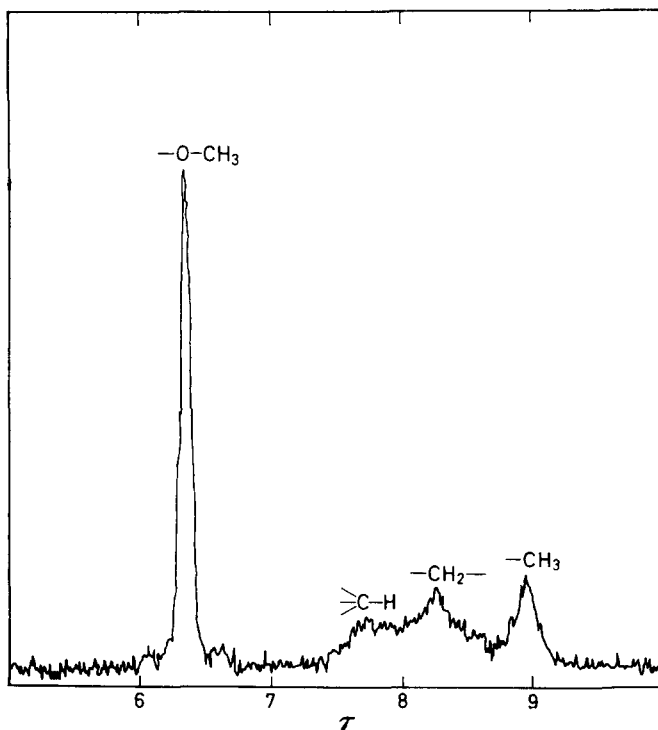


Figure 2—Nuclear magnetic resonance spectrum of 1-5, MMA-MA copolymer

due to the tertiary protons in MA and the methylene protons overlap as illustrated in *Figure 2*. Thus the total proton difference (8 from MMA, 6 from MA) between the two monomers had to be used here to calculate copolymer composition. Thus, if X = molar ratio MMA/MA in copolymer, then

$$I_{\text{total}}/I_{\text{O-CH}_3} = Y = (8X + 6)/(X + 1) \cdot 3$$

Therefore

$$X = (3Y - 6)/(8 - 3Y)$$

The ratios obtained by averaging ten determinations of the appropriate integrals when applied to the appropriate equations above gave the values for copolymer compositions shown in *Table 1(a)* and *(b)*.

Table 1. Nuclear magnetic resonance spectral analyses
(a)

Monomer pair M_1 M_2	Molar ratio in monomer mixture (M_1/M_2)	$\frac{I_{\text{-OCH}_2\text{-}}}{I_{\text{-OCH}_3}}$	Molar ratio in copolymer (X)
MMA EA	4.05	0.08	8.76
	2.02	0.15	4.45
	1.01	0.23	2.78
	0.52	0.47	1.39
	0.25	0.67	0.78
MMA PrA	4	0.09	7.41
	2	0.20	3.33
	1	0.32	2.0
	0.5	0.63	1.06
	0.25	0.97	0.69
MMA BuA	4	0.09	7.41
	2	0.17	3.92
	1.2	0.26	2.56
	1	0.34	1.96
	0.25	1.01	0.66
MMA EMA	0.125	2.86	0.23
	4	0.15	4.44
	2	0.29	2.39
	1	0.67	1.0
	0.5	1.27	0.53
	0.25	2.53	0.26

(b)

Monomer pair M_1 M_2	Molar ratio in monomer mixture (M_1/M_2)	$\frac{3I_{\text{total}}}{I_{\text{O-CH}_3}}$	Molar ratio in copolymer (X)
MMA MA	5.2	7.77	7.7
	1.0	7.32	1.94
	0.85	7.33	2.0
	0.38	6.86	0.76
	0.20	6.78	0.64

From the values of M_1/M_2 and X shown in *Tables 1(a)* and *(b)*, reactivity ratios were calculated by the method of Mayo and Lewis⁷, using the equation

$$r_2 = (M_1/M_2) \{ (1/X) [1 + (M_1/M_2) r_1] - 1 \}$$

THE COPOLYMERIZATION OF ACRYLATES AND METHACRYLATES

r_1 versus r_2 plots for the systems under investigation are illustrated in *Figure 3*. In estimating r_1 and r_2 values from the data the intersections of adjacent lines were discounted, and the reactivity ratios obtained are shown

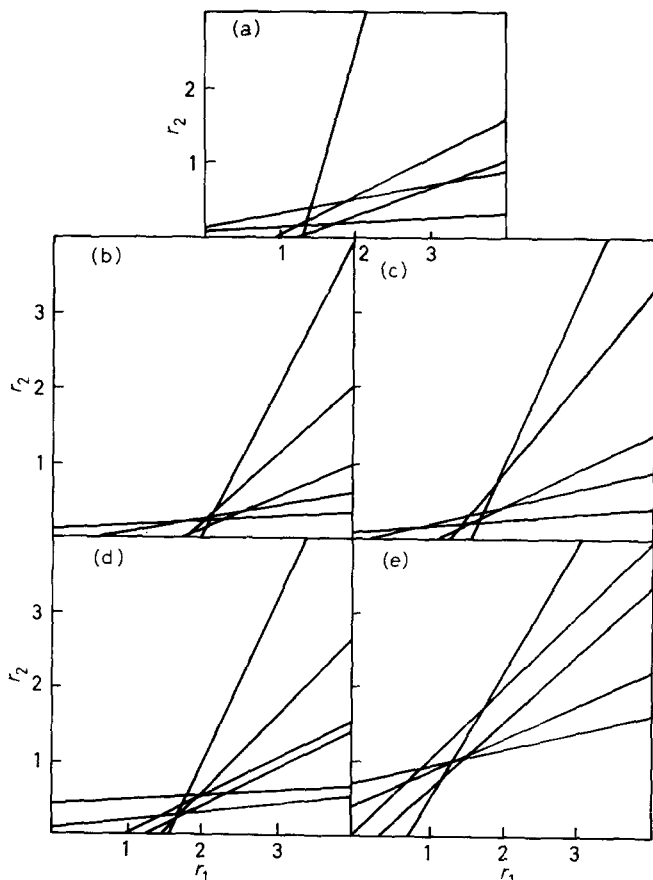


Figure 3— r_1 versus r_2 plots for (a) MMA-MA; (b) MMA-EA; (c) MMA-PrA; (d) MMA-BuA; (e) MMA-EMA

in *Table 2*. These values are seen to be in good agreement with those calculated from Q and e data for these monomers^{9,10} with the exception of the MMA-EA system.

The last column in *Table 2* shows the only other results obtained directly for the radical copolymerization of these systems. The values for MMA-MA were obtained by the use of deuterated monomer³ (polymerization temperature 130°C) while the MMA-EMA system was studied by the use of radioactive tracers², and both are in reasonable agreement with the present results.

Thus nuclear magnetic resonance spectroscopy offers a general method

Table 2. Reactivity ratios

Polymerization temperature, °C	Monomer pair		Experimental		Q-e values		Other experimental values	
	M ₁	M ₂	r ₁	r ₂	r ₁	r ₂	r ₂	
65	MMA	MA	1.8 ± 0.4	0.35 ± 0.1	1.9	0.5	2.3 ± 0.5	0.47 ± 0.1
60	MMA	EA	2.03 ± 0.12	0.24 ± 0.12	1.43	0.73	(at 130°C)	
60	MMA	PrA	1.61 ± 0.1	0.29 ± 0.1	—	—	—	—
60	MMA	BuA	1.8 ± 0.1	0.37 ± 0.1	1.86	0.37	—	—
60	MMA	EMA	1.09 ± 0.1	0.98 ± 0.1	1.08	0.96	0.92	1.08

of analysis of copolymers with an accuracy comparable with that achieved by other analytical methods. It has the additional advantages that it is rapid and can cope with monomer pairs whose similarity in structure makes other analytical methods inapplicable. It is clearly of maximum use among the acrylates and methacrylates where one of the monomers does not incorporate the —O—CH₂— structure. It is still useful, although less accurate when this is not so, provided the constituent monomers have different numbers of protons as in the MMA-MA system. It cannot be readily applied, however, when both monomers incorporate —O—CH₂— groups and the same number of protons, as for example, the system ethyl methacrylate-propyl acrylate.

Chemistry Department,
University of Glasgow,
Glasgow, W.2.

(Received July 1965)

REFERENCES

- HAM, G. E. *Copolymerization, High Polymers*, Vol. XVIII. Interscience: New York, 1964.
- BEVINGTON, J. C. and MALPASS, B. W. *European Polymer Journal*, 1965, **1**, 19
- SHIMA, M. and KOTERA, A. *Polymer Sci. A*, 1963, **1**, 1115
- PORTER, R. S., NISKSIC, S. W. and JOHNSON, J. F. *Analyt. Chem.* 1963, **35**, 1948
- CHEN, H. Y. and LEWIS, M. E. *Analyt. Chem.* 1964, **36**, 1394
- REHBERG, C. E. and FISHER, C. H. *J. Amer. chem. Soc.* 1944, **66**, 1203
- MAYO, F. R. and LEWIS, F. M. *J. Amer. chem. Soc.* 1944, **66**, 1594
- ALFREY, T. and PRICE, C. C. *J. Polym. Sci.* 1947, **2**, 101
- YOUNG, L. J. *J. Polym. Sci.* 1961, **54**, 411
- OTSU, T., ITO, T. and IMOTO, M. *J. Polym. Sci. B*. 1963, **3**, 113

Note and Communication

Surface Tension of Polyethylene Melt*

THE surface tension of liquid polymer plays important roles in the various stages of processing such as moulding, spinning, laminating, etc. Liquid polymers are highly viscous and susceptible to pyrolysis or oxidation. Customary methods of surface tension measurement are not suitable for melts. On the other hand, the melts are usually transparent, and bubbles formed in them can be observed clearly. The sessile-bubble method has been applied to the determination of melt surface tension of linear polyethylenes.

EXPERIMENTAL

Phillips type polyethylenes, Sholex 6015 and Sholex 6050, were used. The characterization data are as follows^{1,2}:

Sholex 6015; $[\eta] = 1.68$ (dl/g), $\overline{M}_v = 8.0 \times 10^4$

Sholex 6050; $[\eta] = 1.51$ (dl/g), $\overline{M}_v = 6.9 \times 10^4$

A cell was devised as a container of the melt and bubbles. It is shown schematically in *Figure 1*. Parallel glass sides with polytetrafluorethylene

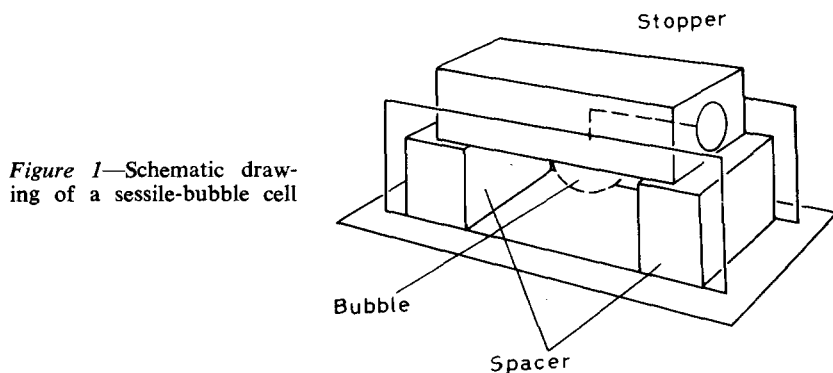


Figure 1—Schematic drawing of a sessile-bubble cell

spacers were held by pinch-clips to be set up on a baseplate of glass. A rectangular brass block, which had a capillary vent-hole and a silicone-rubber stopper, was fitted to cover the melt and bubbles in the cell. Polymer blocks of the exact volume on melting to fill the cell were moulded out of

*Preliminary results of this communication have been referred to in a review article; Sakai, T. *Setchaku* (Adhesion and Adhesives, Japan), 1964, 8, 911.

Sholex pellets, at temperatures around 150°C and load pressures 5 kg/cm², within about five minutes after melting, and allowed to cool to room temperature.

The cell containing a polymer block and covered with the brass block was placed in an electric oven which was fitted with parallel windows. After substitution of the inner atmosphere with nitrogen gas, the temperature in the oven was gradually raised. The temperature was controlled to within $\pm 0.5^\circ\text{C}$ by a sensitive bimetallic spiral regulator. Purified nitrogen gas was syringed through the stopper and the vent-hole to form a bubble in the molten polymer. Those bubbles were allowed to rest at a definite temperature for enough time to equilibrate. The diameter $2r$ and the height h of the bubbles in the steady state were measured to 0.01 mm using a travelling microscope, and a fluorescent lamp as the illuminating source. The diameters were 4 to 7 mm.

Staicopolus's empirical equations have been used for the calculation of surface tensions. They correlate the maximum radius r of a sessile bubble, distance h from the umbilicus to the plane of r , and liquid density ρ_L to the surface tension γ as follows³

$$\gamma = \rho_L g r^2 / BF^2 = \rho_L g h^2 / BG^2$$

where g denotes the acceleration due to gravity,

$$B = \exp P_B(z) - 1.7, \quad F = P_F(z), \quad G = P_G(z),$$

$$z = [(r/h) - 1.5922] / 0.5922$$

and each $P_i(z)$ is a fourth order polynomial of z . The coefficients and numerical tables have been given³.

In the liquid state, the specific volumes of polyethylene have been shown to be independent of the types^{4,5}. Linear equations to express the temperature change have been reported. They are consistent within one per cent. The changes in surface tension with such differences were negligible compared to other factors. The melt densities of materials were calculated from the following equation of Gubler and Kovacs⁴, $1/\rho_L = 1.1495 + 9 \times 10^{-4}t$, where t is the temperature in $^\circ\text{C}$.

RESULTS AND DISCUSSION

Recently, Schonhorn and Sharpe have investigated the surface tension of molten polyethylene by the ring method⁶. The material is a low-density type, and has a number average molecular weight of 10^4 . Over the temperature range from 125° to 193°C, their results can be expressed by the equation

$$\gamma = 57.1 - 0.076T$$

The present melt surface tensions of linear polyethylenes are shown in *Figure 2* as a function of temperature. Within the range of 146° to 200°C, the data points can be represented by the following equations:

$$\gamma = 58.0 - 0.072T$$

$$\gamma = 38.2 - 0.072t$$

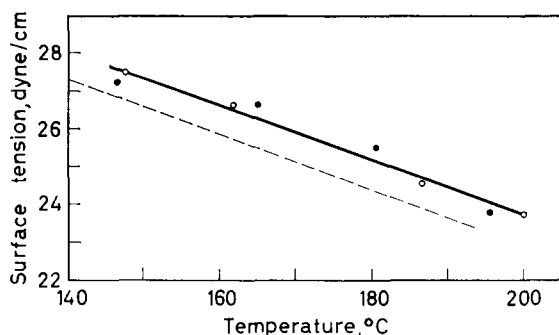


Figure 2—The melt surface tension as a function of temperature; filled circles are for Sholex 6015, open circles for Sholex 6050, and the solid line represents the least square equation, $\gamma = 38.2 - 0.072t$. The dashed line relates to results by Schonhorn and Sharpe⁶

where γ is the surface tension in dyne/cm at temperature $T^\circ\text{K}$ or $t^\circ\text{C}$. Taking into account the differences in the materials, we may regard our results as reasonable.

The temperature coefficient $-\text{d}\gamma/\text{d}T$, the surface entropy, varies with the number of carbon atoms in a molecule in the case of series, such as the normal paraffins, the triglycerides, etc.⁷. The values $-\text{d}\gamma/\text{d}T$ fall gradually to a nearly constant value as molecular chains are lengthened. The limiting value for the n -alkanes has been estimated⁸ to be about 0.06 dyne/cm deg. at 150°C . This value corresponds to that of idealized polyethylene. The discrepancy between this value and that of $-\text{d}\gamma/\text{d}T$ obtained seems to exceed experimental error. Some other factors, however, such as the rate effect in the ring method⁹ or molecular weight distribution of materials, might have been the cause of the deviation. Further studies are thought to be necessary to elucidate this and other problems concerning the surface tension.

T. SAKAI

Textile Research Institute of the Japanese Government,
4 Sawatari, Kanagawa,
Yokohama, Japan

(Received April 1965)

REFERENCES

- ¹ KATAOKA, T. and UEDA, S. *Bull. Textile Res. Inst., Japan*, 1962, No. 62, 9
- ² CHIANG, R. *J. Polym. Sci.* 1964, **B2**, 855
- ³ STAICOPOULOS, D. N. *J. Colloid Sci.* 1962, **17**, 439; 1963, **18**, 793
- ⁴ GUBLER, M. G. and KOVACS, A. J. *J. Polym. Sci.* 1959, **34**, 551
- ⁵ RICHARDSON, M. J., FLORY, P. J. and JACKSON, J. B. *Polymer, Lond.* 1963, **4**, 221
- ⁶ SCHONHORN, H. and SHARPE, L. H. *J. Polym. Sci.* 1965, **A3**, 569
- ⁷ ADAM, N. K. *The Physics and Chemistry of Surfaces*, pp 162–163. Oxford University Press: London, 1941
- ⁸ STARKWEATHER JR, H. W. *Polymer Engineering and Science*, 1965, **5**, 5
- ⁹ NEWMAN, S. B. and LEE, W. M. *Rev. sci. Instrum.* 1958, **29**, 785

Gegenion Effects in the Cationic Polymerization of Tetrahydrofuran

THE cationic polymerization of tetrahydrofuran (THF) to high molecular weight polytetramethylene oxide is now well established¹⁻³. Typical

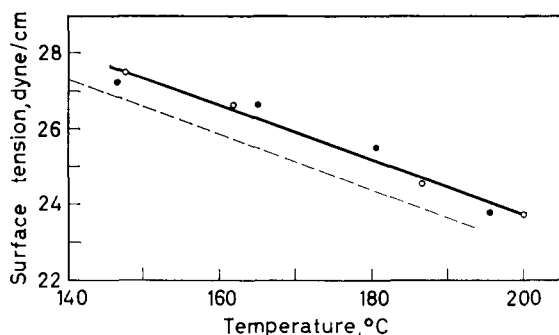


Figure 2—The melt surface tension as a function of temperature; filled circles are for Sholex 6015, open circles for Sholex 6050, and the solid line represents the least square equation, $\gamma = 38.2 - 0.072t$. The dashed line relates to results by Schonhorn and Sharpe⁶

where γ is the surface tension in dyne/cm at temperature $T^\circ\text{K}$ or $t^\circ\text{C}$. Taking into account the differences in the materials, we may regard our results as reasonable.

The temperature coefficient $-\text{d}\gamma/\text{d}T$, the surface entropy, varies with the number of carbon atoms in a molecule in the case of series, such as the normal paraffins, the triglycerides, etc.⁷. The values $-\text{d}\gamma/\text{d}T$ fall gradually to a nearly constant value as molecular chains are lengthened. The limiting value for the n -alkanes has been estimated⁸ to be about 0.06 dyne/cm deg. at 150°C . This value corresponds to that of idealized polyethylene. The discrepancy between this value and that of $-\text{d}\gamma/\text{d}T$ obtained seems to exceed experimental error. Some other factors, however, such as the rate effect in the ring method⁹ or molecular weight distribution of materials, might have been the cause of the deviation. Further studies are thought to be necessary to elucidate this and other problems concerning the surface tension.

T. SAKAI

Textile Research Institute of the Japanese Government,
4 Sawatari, Kanagawa,
Yokohama, Japan

(Received April 1965)

REFERENCES

- ¹ KATAOKA, T. and UEDA, S. *Bull. Textile Res. Inst., Japan*, 1962, No. 62, 9
- ² CHIANG, R. *J. Polym. Sci.* 1964, **B2**, 855
- ³ STAICOPOULOS, D. N. *J. Colloid Sci.* 1962, **17**, 439; 1963, **18**, 793
- ⁴ GUBLER, M. G. and KOVACS, A. J. *J. Polym. Sci.* 1959, **34**, 551
- ⁵ RICHARDSON, M. J., FLORY, P. J. and JACKSON, J. B. *Polymer, Lond.* 1963, **4**, 221
- ⁶ SCHONHORN, H. and SHARPE, L. H. *J. Polym. Sci.* 1965, **A3**, 569
- ⁷ ADAM, N. K. *The Physics and Chemistry of Surfaces*, pp 162–163. Oxford University Press: London, 1941
- ⁸ STARKWEATHER JR, H. W. *Polymer Engineering and Science*, 1965, **5**, 5
- ⁹ NEWMAN, S. B. and LEE, W. M. *Rev. sci. Instrum.* 1958, **29**, 785

Gegenion Effects in the Cationic Polymerization of Tetrahydrofuran

THE cationic polymerization of tetrahydrofuran (THF) to high molecular weight polytetramethylene oxide is now well established¹⁻³. Typical

NOTE AND COMMUNICATION

Friedel-Crafts halides are the normal catalysts for this type of polymerization¹ but previously it has been shown² that reproducible data are most conveniently obtained using stable carbonium ion salts as initiators. In particular triphenyl methyl and tropylium carbonium ions are the most effective for THF polymerization.

Using triphenyl methyl hexachloroantimonate initiation of THF polymerization was rapid and complete at 25°C or above and there was no significant chain destruction during the lifetime of the kinetic measurements. Chain termination became appreciable when the reaction mixtures were allowed to reach thermodynamic monomer-polymer equilibrium, especially at higher temperatures. On account of chain termination the maximum conversion attained at 50°C was 43 per cent monomer to polymer. This value is significantly less than that (56 per cent) obtained at the same temperature but using catalysts having PF₆⁻ as gegenion³.

With tropylium hexachloroantimonate as catalyst⁴, initiation was quite slow at 50°C and the polymerizations reached an equilibrium conversion of 54.5 per cent monomer to polymer. This value is very close to that

Table 1. Bulk polymerization of THF using triphenyl methyl carbonium ion salts* as initiators

Gegenion X ⁻	[Ph ₃ C ⁺ X ⁻] 10 ³ M	Temp. °C	[ⁿ Bu ₄ N ⁺ UF ₆ ⁻] 10 ² M	10 ⁴ R _p mole l ⁻¹ sec ⁻¹	$\frac{R_p(\text{PF}_6^-)}{R_p(\text{SbCl}_6^-)}$
PF ₆ ⁻	2.14	25	—	2.64	2.40
SbCl ₆ ⁻	2.14	25	—	1.11	
PF ₆ ⁻	3.82	25	—	4.47	2.35
SbCl ₆ ⁻	3.82	25	—	1.91	
PF ₆ ⁻	4.52	50	—	15.8	1.50
SbCl ₆ ⁻	4.52	50	—	10.6	
PF ₆ ⁻	6.65	50	—	24.8	1.61
SbCl ₆ ⁻	6.65	50	—	15.4	
SbCl ₆ ⁻	1.68	50	—	3.76	—
SbCl ₆ ⁻	1.68	50	1.25	5.01	1.33
SbCl ₆ ⁻	1.68	50	4.72	5.88	1.57

*Equilibrium conversions monomer to polymer:

Ph₃C⁺SbCl₆⁻; 73 per cent (25°C), 43 per cent (50°C)

Ph₃C⁺PF₆⁻; 76.5 per cent (25°C), 56 per cent (50°C)

obtained in the PF₆⁻-containing systems where initiation is also much slower than propagation.

In order to clarify these discrepancies the polymerization of THF has been studied using triphenyl methyl hexafluorophosphate (Ph₃C⁺PF₆⁻) as initiator. With this salt initiation was much more rapid than with C₇H₇⁺SB⁻Cl₆ but not quite so rapid as with Ph₃C⁺SbCl₆⁻. The relevant kinetic data are shown in Table 1, which also contains data obtained using mixtures of Ph₃C⁺SbCl₆⁻ and ⁿBu₄N⁺PF₆⁻ as initiator in order further to

NOTE AND COMMUNICATION

clarify the effect of gegenion. Table 2 shows relevant molecular weight data for the various catalysts.

Table 2. Bulk polymerization of THF

Catalyst	10 ³ [Catalyst]	Temp.	Mol. wt*	Measured DP†
	M	°C	at equil.	Calculated DP
Ph ₃ C+PF ₆ ⁻	5.41	25	339 800	2.6
Ph ₃ C+PF ₆ ⁻	3.94	25	476 600	2.6
Ph ₃ C+PF ₆ ⁻	2.34	50	365 900	3.4
Ph ₃ C+PF ₆ ⁻	3.27	50	374 600	3.5
Ph ₃ C+PF ₆ ⁻	3.58	50	280 600	3.2
Ph ₃ C+PF ₆ ⁻	5.02	50	267 600	3.7
Ph ₃ C+SbCl ₆ ⁻	1.37	25	144 500	0.31
Ph ₃ C+SbCl ₆ ⁻	3.53	25	72 510	0.38
Ph ₃ C+SbCl ₆ ⁻	4.93	25	59 400	0.45
Ph ₃ C+SbCl ₆ ⁻	1.0	50	71 170	0.17
Ph ₃ C+SbCl ₆ ⁻	2.0	50	51 550	0.24
Ph ₃ C+SbCl ₆ ⁻	4.0	50	50 160	0.47

*Estimated from the expression $[\eta]=2.98 \times 10^{-4} M^{0.75}$. Intrinsic viscosities measured in benzene at 25.0°C.
 †Calculated on the basis of one polymer chain per catalyst molecule.

It is clear from the results in Tables 1 and 2 that whereas rates of polymerization are not very different for the two gegenions SbCl₆⁻ and PF₆⁻, molecular weight of the products is very much greater for the latter. Furthermore there is apparently no termination using Ph₃C+PF₆⁻ since the equilibrium conversion at 50° was 56 per cent monomer to polymer.

Clearly then the principal effect of replacing SbCl₆⁻ by PF₆⁻ is to cut down chain transfer processes severely. There is a large probable error in the estimated degree of polymerization for these very high molecular weight samples, obtained with PF₆⁻ gegenion, and it may be that at room temperature or below, only one chain grows per catalyst molecule.

Transfer reactions in the bulk polymerization of THF must involve either hydride ion abstraction from the alpha methylene of THF or tetramethylene-oxy units in the polymer, or degradative oxonium ion formation with the ethereal oxygen atoms of polymer chains. The great difference in the rates of these reactions between propagating oxonium ions having SbCl₆⁻ or PF₆⁻ as gegenion is not well understood but probably results from different degrees of ion pair agglomeration in the two systems.

We thank Dr J. K. Boulton, Distillers Co. Ltd, for a gift of triphenyl methyl hexafluorophosphate.

C. E. H. BAWN
 R. M. BELL
 C. FITZSIMMONS
 A. LEDWITH

*Donnan Laboratories,
University of Liverpool*

(Received September 1965)

REFERENCES

- ¹ BAWN, C. E. H., BELL, R. M. and LEDWITH, A. *Polymer, Lond.* 1965, **6**, 95
- ² MEERWEIN, H., DELFS, D. and MORSCHER, H. *Angew. Chem.* 1960, **72**, 927
- ³ DREYFUS, M. P. and (Mrs) DREYFUS, P. *Polymer, Lond.* 1965, **6**, 93
SIMS, D. *J. chem. Soc.* 1964, 864
- ⁴ BAWN, C. E. H., FITZSIMMONS, C. and LEDWITH, A. Unpublished work

Classified Contents

- Abnormal structures in polyvinylchloride
I—A method of estimating labile chloride groups in polyvinylchloride, 625
- Acrylamide in water, effect of pH on the polymerization of, 451
- Acrylates and methacrylates, reactivity ratios for the copolymerization of, by n.m.r. spectroscopy, 653
- Acrylonitrile, gamma irradiation polymerization of, in the presence of solid additives, 515
- Aldehyde polymerization, entropy of stereoregularity in, 333
- Application of irreversible thermodynamics to the kinetics of polymer crystallization from seeded nuclei, 231
- Aromatic polypyromellitimide, thermal degradation of an, in air and vacuum II—Effect of impurities and nature of degradation products, 49
— III—Pyrolytic conversion into a semiconductor, 319
- Block copolymers of styrene, butadiene and isoprene, multiple glass transitions of, 141
- Bulk crystallization kinetics of polypropylene and polybutene, 213
- Bulk polymerization of styrene, *p*-methoxystyrene and *p*-chlorostyrene, 157
- Calculation of unperturbed polymer dimensions from perturbed ones, 361
- Cationic polymerization [of isobutylene], consequences of chlorine exchange between methyl chloride and aluminium chloride in, 237
- Cationic polymerization of 3-methylbutene-1 IV—Molecular weight/intrinsic viscosity relationship for poly-3-methylbutene-1, 175
- Cationic transannular polymerization of norbornadiene, 133
- Cocrystallization in copolymers of alpha olefins I—Copolymers of 4-methylpentene with linear alpha olefins, 249
- Cold-drawing and crystallization of polyethylene terephthalate, 107
- Collagen—saline system, solution- and bulk-thermal-transitions in, 90
- Comparison of linearity of high density polyethylene and polymethylene, 512
- Composition and temperature dependence of polymer—solvent interaction parameters, 455
- Consequences of chlorine exchange between methyl chloride and aluminium chloride in cationic polymerization, 237
- Copolymers of 4-methylpentene with linear alpha olefins, 249
- Correction of errors in polymer testing using diffracted ultrasonic waves, 399
- Cotton fibre, fine structure of, as revealed by swelling during methacrylate embedding, 427
- Crystalline Olefin Polymers*, Part II, review of, 88
- Crystallization of polyamides II—Nylon 6 and Nylon 66, 367
- Determination of number-average molecular weights of polyamides in 90 per cent formic acid by thermoelectric differential vapour pressure lowering, 447
- Determination of unperturbed dimensions of polymer molecules by viscometry of moderately concentrated solutions, 373
- Dictionary of Plastics*, review of, 85
- Dislocations*, review of, 84
- Dynamic mechanical properties of some iodine-substituted 1-olefin polymers, 535
- Effect of crystallization conditions and temperature on the polymorphic forms of polyethylene, 243
- Effect of impurities and nature of degradation products [of aromatic polypyromellitimide], 49
- Effect of oxidation on spherulite size in polyethylene films, 15
- Effect of pH on the polymerization of acrylamide in water, 451
- Effect of temperature and monomer concentration on the structure and molecular weight of poly-3-methylbutene-1, 287
- Elastic Liquids: An Introductory Vector Treatment of Finite-Strain Polymer Rheology*, review of, 87
- Elastomer, vapour pressure of a swollen crosslinked, 541
- Entropy of stereoregularity in aldehyde polymerization, 333

- Equilibrium polymerization of monomers which are solvents for their polymers: case of tetrahydrofuran, 621
- Ethylene oxide, polymerization of, by some organic compounds, 509
- Fibre Structure*, review of, 84
- Fine structure of cotton fibre as revealed by swelling during methacrylate embedding, 427
- Fractionation of low molecular weight polymers by liquid chromatography, 603
- Fractionation, separation and, of polystyrene at a lower critical solution point, 645
- Free radical and anionic polymerization of some *N*-substituted maleimides, 419
- Free radical [vinyl] polymerizations with rapidly decaying initiators, 63
- Fundamental studies on cationic polymerization IV—Homo- and co-polymerizations with various catalysts, 579
- Gamma irradiation polymerization of acrylonitrile in the presence of solid additives, 515
- Gegenion effects in the cationic polymerization of tetrahydrofuran, 661
- ω -Halo-olefin polymers, preparation of, 531
- Infra-red Spectroscopy of High Polymers*, review of, 172
- Infra-red spectrum of syndiotactic polypropylene, 223
- Internal pressure of crystalline polymers, 220
- Intramolecular hydride shift polymerization by cationic mechanism III—Structure analyses of deuterated and non-deuterated poly-4-methyl-1-pentene, 111
- V—The effect of temperature and monomer concentration on the structure and molecular weight of poly-3-methylbutene-1, 287
- Iodine-substituted 1-olefin polymers, dynamic mechanical properties of some, 535
- Isobutene, homopolymerization of, with various catalysts, 579
- Isobutene, kinetic measurements on the cobalt-60 gamma-initiated polymerization of, in the presence of zinc oxide, 1
- Isobutene-isoprene, copolymerization of, with various catalysts, 579
- [Isobutylene], consequences of chlorine exchange between methyl chloride and aluminium chloride in cationic polymerization of, 237
- Keratin—water system, solution- and bulk-thermal-transitions in, 90
- Kinetic measurements on the cobalt-60 gamma-initiated polymerization of isobutene in the presence of zinc oxide, 1
- Kinetics and mechanism of trioxan polymerization, 269
- Kinetics of the polymerization of styrene initiated by *n*-butyl lithium, 102
- Light scattering and ultra-violet absorption studies on dilute aqueous solutions of poly-4-vinylpyridinium chloride, 303
- Linearity of high density polyethylene and polymethylene, comparison of, 512
- 'Living' polymer after cationic initiation, 93
- Lower critical solution phenomena in polymer—solvent systems, 181
- Manufacture of Plastics*, Vol. I, review of, 173
- Method of estimating labile chloride groups in polyvinylchloride, 625
- 3-Methylbutene-1, cationic polymerization of, IV, 175
- Effect of temperature and monomer concentration on the structure and molecular weight of polymer of, 287
- 4-Methylpentene, copolymers of, with linear alpha olefins, 249
- Model polyethers I—Synthesis by the Williamson reaction, 403
- Molecular weight dependence of isothermal long period growth of polyethylene single crystals, 25
- Molecular weight/intrinsic viscosity relationship for poly-3-methylbutene-1, 175
- Monocyclopentadienyltitanoxanes, 635
- Monomer—polymer equilibrium and ceiling temperature for tetrahydrofuran polymerization, 95
- Monomer reactivity ratios of a ternary system, 98
- Multiple glass transitions of block polymers, 141
- Nature of degradation products [of aromatic polypyromellitimide], 49
- Newer Methods of Polymer Characterization*, review of, 86
- Norbornadiene, cationic transannular polymerization of, 133
- α -Olefin copolymers, pyrolysis—hydrogenation—GLC of, 561
- Piperazine polyamides, thermal degradation of, I, 483
- Polyacetone, 411
- Polyamides, crystallization of, II—Nylon 6 and Nylon 66, 367

- Polyamides, determination of number-average molecular weights of, in 90 per cent formic acid by thermoelectric differential vapour pressure lowering, 447
- Poly(arylene sulphones), synthesis of, by polycondensation of aryl-sulphonyl chlorides under Friedel-Crafts conditions, 589
- Polybutene, bulk crystallization kinetics of, 213
- Polybutene-1 oxides, proton spin-lattice relaxation in, 385
- Polycapromide (Nylon 6), structure of gamma form of, 465, 624
- Polyethylene, effect of crystallization conditions and temperature on the polymorphic forms of, 243
- Polyethylene, fractionated linear, application of irreversible thermodynamics to crystallization of, 231
- Polyethylene, polyoxymethylene and polytetramethylene oxide, internal pressure of, 220
- Polyethylene single crystals, molecular weight dependence of isothermal long period growth of, 25
- Polyethylene terephthalate, cold-drawing and crystallization of, 107
- Polyethylene, thermal conductivity of, 205
- Polyethylene melt, surface tension of, 659
- Poly(ethyl methacrylate), yield stress behaviour of, in the glass transition region, 615
- Polymerization of ethylene oxide by some organozinc compounds, 509
- Polymerization of isobutene, kinetic measurements on the cobalt-60 gamma-initiated, in the presence of zinc oxide, 1
- Polymerization of vinylcarbazole by electron acceptors, 549
- [homo- and co-] Polymerizations [of isobutene and isoprene] with various catalysts, 579
- Polymer-solvent interaction parameters, composition and temperature dependence of, 455
- Polymer-solvent systems, lower critical solution phenomena in, 181
- Polymer stereoregularity, $n \rightarrow \pi^*$ transition of carbonyl group and, 503
- Polymers of halogen-substituted 1-olefins, 531
- Polymethylmethacrylate, yield stress behaviour of, 311
- use of frictional coefficients to evaluate unperturbed dimensions in dilute solutions of, 197
- Poly-4-methyl-1-pentene, intramolecular hydride shift polymerization of, by cationic mechanism, 111
- Poly(olefin sulphones), some grafting reactions involving, 339
- Poly- α -olefins, pyrolysis-hydrogenation-GLC of, 343
- Polypropylene, bulk crystallization kinetics of, 213
- infra-red spectrum of syndiotactic, 223
- Polypropylene, thermal degradation of, promoted by organic halogen compounds, 193
- [Polystyrene and polymethylmethacrylate], use of frictional coefficients to evaluate unperturbed dimensions in dilute solutions of, 197
- Polystyrene, separation and fractionation of, at a lower critical solution point, 645
- Polystyrene transition in solution, proton magnetic resonance study of the, 100
- Polyvinylchloride, abnormal structures in, 625
- method of estimating labile chloride groups in, 625
- thermal conductivities of samples of, 77
- Poly-4-vinylpyridinium chloride, light scattering and ultra-violet absorption studies on dilute aqueous solutions of, 303
- Premix Molding*, review of, 88
- Proceedings of the Tihany Symposium on Radiation Chemistry*, review of, 172
- Propagation reactions in the copolymerization of styrene and *p*-chlorostyrene by perchloric acid, 497
- Proton magnetic resonance study of the polystyrene 'transition' in solution, 100
- Proton spin-lattice relaxation in polybutene-1 oxides. A comparison with related polymers, 385
- Pyrolysis-hydrogenation-GLC of poly- α -olefins, 343
- Pyrolysis-hydrogenation-GLC of α -olefin copolymers, 561
- Pyrolytic conversion of an aromatic poly-pyromellitimide into a semiconductor, 319
- Radiochemical studies of free radical vinyl polymerization III— Bulk polymerization of styrene, *p*-methoxystyrene and *p*-chlorostyrene, 157
- Reactivity ratios for the copolymerization of acrylates and methacrylates by n.m.r. spectroscopy, 653
- Rubbers, stress strain relation of swollen, 397
- Separation and fractionation of polystyrene at a lower critical solution point, 645

- Some grafting reactions involving poly-(olefin sulphones), 339
- Spherulite size in polyethylene films, effect of oxidation on, 15
- Stress strain relation of swollen rubbers, 397
- Styrene-whitening in high-impact polystyrenes, 437
- Structure analyses of deuterated and non-deuterated poly-4-methyl-1-pentene, 111
- Structure of gamma form of polycapromamide (Nylon 6), 465, 624
- Styrene and *p*-chlorostyrene, propagation reactions in the copolymerization of, by perchloric acid, 497
- Styrene, kinetics of the polymerization of, initiated by *n*-butyl lithium, 102
- Styrene, *p*-methoxystyrene and *p*-chlorostyrene, bulk polymerization of, 157
- Surface tension of polyethylene melt, 659
- Synthesis [of model polyalkylene ethers and trialkylene glycols] by the Williamson reaction, 403
- Synthesis of poly(arylene sulphones) by polycondensation of aryl-sulphonyl chlorides under Friedel-Crafts conditions, 589
- Tetrahydrofuran, equilibrium polymerization of, 621
- gegenion effects in the cationic polymerization of, 661
- 'living' polymer after cationic initiation of, using benzenediazonium hexafluorophosphate, 93
- Tetrahydrofuran polymerization, monomer-polymer equilibrium and ceiling temperature for, 95
- Thermal conductivities of polymers I—Polyvinyl chloride, 77
- II—Polyethylene, 205
- Thermal degradation of an aromatic poly-pyromellitimide in air and vacuum II—Effect of impurities and nature of degradation products, 49
- Thermal degradation of an aromatic poly-pyromellitimide in air and vacuum III—Pyrolytic conversion into a semiconductor, 319
- Thermal degradation of piperazine polyamides I—Poly(terephthaloyl *trans*-2,5-dimethylpiperazine) and poly(oxalyl *trans*-2,5-dimethylpiperazine), 483
- Thermal degradation of polypropylene promoted by organic halogen compounds, 193
- Thermal transitions of synthetic and biological polymers in bulk and in solution, 90
- $n \rightarrow \pi^*$ transition of carbonyl group and polymer stereoregularity, 503
- Trioxan polymerization, kinetics and mechanism of, 269
- Ultra-violet degradation of scissioning copolymers, 523
- Upturn effect in non-Newtonian viscosity of polymer solutions, 35
- Use of frictional coefficients to evaluate unperturbed dimensions in dilute polymer solutions, 197
- Vapour pressure of a swollen crosslinked elastomer, 541
- Vinyl acetate-ethyl acrylate copolymer system, ultra-violet degradation of, 523
- Vinylcarbazole, polymerization of, by electron acceptors, 549
- [Vinyl]polymerizations, on free radical, with rapidly decaying initiators, 63
- Viscosity, non-Newtonian, of polymer solutions, upturn effect in, 35
- Yield stress behaviour of poly(ethyl methacrylate) in the glass transition region, 615
- Yield stress behaviour of polymethylmethacrylate, 311

Author Index

- ALLEN, G. and BAKER, C. H.: Lower critical solution phenomena in polymer-solvent systems, 181
- ANGELO, R. J., IKEDA, R. M. and WALLACH, M. L.: Multiple glass transitions of block polymers, 141
- AYREY, G., LEVITT, F. G. and MAZZA, R. J.: Radiochemical studies of free radical vinyl polymerization III—Bulk polymerization of styrene, *p*-methoxystyrene and *p*-chlorostyrene, 157
- BAIR, H. E.: See BRUCK, S. D. and BAIR, H. E.

- BAKER, C. H.:** See ALLEN, G. and BAKER, C. H.
— See FATOU, J. G., BAKER, C. H. and MANDELKERN, L.
- BALDWIN, F. P.:** See KENNEDY, J. P. and BALDWIN, F. P.
- BAMFORD, C. H.:** On free radical polymerizations with rapidly decaying initiators, 63
- BAUMBER, M. W.:** See LEESE, L. and BAUMBER, M. W.
- BAWN, C. E. H., BELL, R. M. and LEDWITH, A.:** Monomer-polymer equilibrium and ceiling temperature for tetrahydrofuran polymerization, 95
— FITZSIMMONS, C. and LEDWITH, A.: Gegenion effects in the cationic polymerization of tetrahydrofuran, 661
- BELL, R. M.:** See BAWN, C. E. H., BELL, R. M. and LEDWITH, A.
— See BAWN, C. E. H., BELL, R. M., FITZSIMMONS, C. and LEDWITH, A.
- BENGOUGH, W. I. and ONOZUKA, M.:** Abnormal structures in polyvinyl chloride I—A method of estimating labile chloride groups in polyvinylchloride, 625
- BHATTACHARYYA, S. N.:** See PATTERSON, D. and BHATTACHARYYA, S. N.
- BILLICK, I. H. and KENNEDY, J. P.:** Cationic polymerization of 3-methylbutene-1 IV—Molecular weight/intrinsic viscosity relationship for poly-3-methylbutene-1, 175
- BLAKEY, P. R. and SHELDON, R. P.:** Cold-drawing and crystallization of polyethylene terephthalate, 107
- BLEARS, D. J.:** See CONNOR, T. M. and BLEARS, D. J.
- BRADBURY, E. M., BROWN, L., ELLIOTT, A. and PARRY, D. A. D.:** The structure of the gamma form of polycapromide (Nylon 6), 465, 624
- BRADFIELD, G.:** Correction of errors in polymer testing using diffracted ultrasonic waves, 399
- BRANDON, R.:** See PASIKA, W. M. and BRANDON, R.
- BREWER, P. I.:** Fractionation of low molecular weight polymers by liquid chromatography, 603
- BROWN, G. R. and PEPPER, D. C.:** Propagation reactions in the copolymerization of styrene and *p*-chlorostyrene by perchloric acid, 497
- BROWN, L.:** See BRADBURY, E. M., BROWN, L., ELLIOTT, A. and PARRY, D. A. D.
- BRUCE, J. MALCOLM and FARREN, D. W.:** The polymerization of ethylene oxide by some organozinc compounds, 509
- BRUCK, S. D.:** Thermal degradation of an aromatic polypyromellitimide in air and vacuum II—Effect of impurities and nature of degradation products, 49
— — III—Pyrolytic conversion into a semiconductor, 319
— Thermal degradation of piperazine polyamides I—Poly(terephthaloyl *trans*-2,5-dimethylpiperazine) and poly(oxalyl *trans*-2,5-dimethylpiperazine), 483
— and BAIR, H. E.: Determination of number-average molecular weights of polyamides in 90 per cent formic acid by thermoelectric differential vapour pressure lowering, 447
- BUCKNALL, C. B. and SMITH, R. R.:** Stress-whitening in high-impact polystyrenes, 437
- BURNOP, V. C. E.:** Polyacetone, 411
- BUROW, Mrs S. P., PETERLIN, A. and TURNER, D. T.:** Upturn effect in non-Newtonian viscosity of polymer solutions, 35
- BYWATER, S.:** See COWIE, J. M. G. and BYWATER, S.
- CAVERHILL, A. R. and TAYLOR, G. W.:** The thermal degradation of polypropylene promoted by organic halogen compounds, 193
- CLARK, K. J. and POWELL, T.:** Polymers of halogen-substituted 1-olefins, 531
- CONNOR, T. M. and BLEARS, D. J.:** Proton spin-lattice relaxation in polybutene-1 oxides. A comparison with related polymers, 385
- CORNET, C. F.:** The calculation of unperturbed polymer dimensions from perturbed ones, 361
— The determination of unperturbed dimensions of polymer molecules by viscometry of moderately concentrated solutions, 373
- COWIE, J. M. G. and BYWATER, S.:** The use of frictional coefficients to evaluate unperturbed dimensions in dilute polymer solutions, 197
- CUBBON, R. C. P.:** The free radical and anionic polymerization of some *N*-substituted maleimides, 419
— and MARGERISON, D.: The kinetics of the polymerization of styrene initiated by *n*-butyl lithium, 102
- CUDBY, M. E. A., FEASEY, R. G., JENNINGS, B. E., JONES, M. E. B. and ROSE, J. B.:** Synthesis of poly(arylene sulphones) by polycondensation of aryl-sulphonyl chlorides under Friedel-Crafts conditions, 589
- CURRIE, D. J., DAINTON, F. S. and WATT, W. S.:** Effect of pH on polymerization of acrylamide in water, 451

- DAINTON, F. S.: See CURRIE, D. J., DAINTON, F. S. and WATT, W. S.
- DALTON, F. L.: Kinetic measurements on the cobalt-60 gamma-initiated polymerization of isobutene in the presence of zinc oxide, 1
- DARSKUS, R. L.: See JORDAN, D. O., KURUCSEV, T. and DARSKUS, R. L.
- DLUGOSZ, J.: The fine structure of cotton fibre as revealed by swelling during methacrylate embedding, 427
- DREYFUSS, M. P. and DREYFUSS, P.: A 'living' polymer after cationic initiation, 93
- DREYFUSS, P.: See DREYFUSS, M. P. and DREYFUSS, P.
- EASTMOND, G. C.: review of *Dislocations*, 84
- EATON, E. C. and IVIN, K. J.: Some grafting reactions involving poly(olefin sulphones), 339
- ELLINGER, L. P.: The polymerization of vinylcarbazole by electron acceptors, 549
- ELLIOTT, A.: review of *Infrared Spectroscopy of High Polymers*, 172
— See BRADBURY, E. M., BROWN, L., ELLIOTT, A. and PARRY, D. A. D.
- ESTEVEZ, J. M. J.: review of *Dictionary of Plastics*, 85
- EVENHUIS, J. K.: See VAN SCHOOTEN, J. and EVENHUIS, J. K.
- FARREN, D. W.: See BRUCE, J. MALCOLM and FARREN, D. W.
- FATOU, J. G., BAKER, C. H. and MANDELKERN, L.: The effect of crystallization conditions and temperature on the polymorphic forms of polyethylene, 243
- FEASEY, R. G.: See CUDBY, M. E. A., FEASEY, R. G., JENNINGS, B. E., JONES, M. E. B. and ROSE, J. B.
- FITZSIMMONS, C.: See BAWN, C. E. H., BELL, R. M., FITZSIMMONS, C. and LEDWITH, A.
- FORTUNE, J. D.: See GRASSIE, N., TORRANCE, B. J. D., FORTUNE, J. D. and GEMMELL, J. D.
- GEE, G., HERBERT, J. B. M. and ROBERTS, R. C.: The vapour pressure of a swollen crosslinked elastomer, 541
- GEMMELL, J. D.: See GRASSIE, N., TORRANCE, B. J. D., FORTUNE, J. D. and GEMMELL, J. D.
- GORDON, M. and HILLIER, I. H.: The bulk crystallization kinetics of polypropylene and polybutene, 213
- GRANT, I. J. and WARD, I. M.: The infrared spectrum of syndiotactic polypropylene, 223
- GRASSIE, N., TORRANCE, B. J. D., FORTUNE, J. D. and GEMMELL, J. D.: Reactivity ratios for the copolymerization of acrylates and methacrylates by n.m.r. spectroscopy, 653
- HAWARD, R. N.: review of *Crystalline Olefin Polymers*, Part II, 88
- HERBERT, J. B. M.: See GEE, G., HERBERT, J. B. M. and ROBERTS, R. C.
- HILLIER, K. W.: review of *Fibre Structure*, 84
— See GORDON, M. and HILLIER, I. H.
- HINKAMP, P. E. and TUNG, L. H.: Comparison of the linearity of high density polyethylene and polymethylene, 512
- HINLICKY, J. A.: See KENNEDY, J. P. and HINLICKY, J. A.
- HOBIN, T. P.: Model polyethers I—Synthesis by the Williamson reaction, 403
- HOWELLS, E. R.: review of *Newer Methods of Polymer Characterization*, 86
— review of *Elastic Liquids: An Introductory Vector Treatment of Finite-Strain Polymer Rheology*, 87
- IKEDA, R. M.: See ANGELO, R. J., IKEDA, R. M. and WALLACH, M. L.
- IVIN, K. J.: See EATON, E. C. and IVIN, K. J.
— and LEONARD, J.: The equilibrium polymerization of monomers which are solvents for their polymers: case of tetrahydrofuran, 621
- JENNINGS, B. E.: See CUDBY, M. E. A., FEASEY, R. G., JENNINGS, B. E., JONES, M. E. B. and ROSE, J. B.
- JONES, M. E. B.: See CUDBY, M. E. A., FEASEY, R. G., JENNINGS, B. E., JONES, M. E. B. and ROSE, J. B.
- JORDAN, D. O., KURUCSEV, T. and DARSKUS, R. L.: Light scattering and ultra-violet absorption studies on dilute aqueous solutions of poly-4-vinylpyridinium chloride, 303
- KAIL, J. A. E.: The dynamic mechanical properties of some iodine-substituted 1-olefin polymers, 535
- KANG-JEN LIU and ULLMAN, R.: Proton magnetic resonance study of the polystyrene 'transition' in solution, 100
- KENNEDY, J. P.: See BILLYCK, I. H. and KENNEDY, J. P.
— See WANLESS, G. G. and KENNEDY, J. P.
— and BALDWIN, F. P.: Consequences of chlorine exchange between methyl chloride and aluminium chloride in cationic polymerization, 237

- KENNEDY, J. P. and HINLICKY, J. A.: Cationic trans-annular polymerization of norbornadiene, 133
- and SQUIRES, R. G.: Fundamental studies on cationic polymerization IV—Homo- and co-polymerizations with various catalysts, 579
- SCHULZ, W. W., SQUIRES, R. G. and THOMAS, R. M.: Intramolecular hydride shift polymerization by cationic mechanism V—The effect of temperature and monomer concentration on the structure and molecular weight of poly-3-methylbutene-1, 287
- KHAMIS, J. T.: Monomer reactivity ratios of a ternary system, 98
- KRIGBAUM, W. R.: See ROE, R.-J. and KRIGBAUM, W. R.
- KUIST, C. H. and MAXIM, L. D.: The ultraviolet degradation of scissioning copolymers, 523
- KURUCSEV, T.: See JORDAN, D. O., KURUCSEV, T. and DARSKUS, R. L.
- LANCELEY, H. A.: Effect of oxidation on spherulite size in polyethylene films, 15
- LANE, Sister K.: See SHELDON, R. P. and LANE, Sister K.
- LEDWITH, A.: See BAWN, C. E. H., BELL, R. M. and LEDWITH, A.
- See BAWN, C. E. H., BELL, R. M., FITZSIMMONS, C. and LEDWITH, A.
- LEESE, L. and BAUMBER, M. W.: Kinetics and mechanism of trioxan polymerization, 269
- LEONARD, J.: See IVIN, K. J. and LEONARD, J.
- LEVITT, F. G.: See AYREY, G., LEVITT, F. G. and MAZZA, R. J.
- MAGILL, J. H.: Crystallization of polyamides II—Nylon 6 and Nylon 66, 367
- MANDELKERN, L.: See FATOU, J. G., BAKER, C. H. and MANDELKERN, L.
- MARGERISON, D.: See CUBBON, R. C. P. and MARGERISON, D.
- MASON, P. and RIGBY, B. J.: Thermal transitions of synthetic and biological polymers in bulk and in solution, 90
- MAXIM, L. D.: See KUIST, C. H. and MAXIM, L. D.
- MAZZA, R. J.: See AYREY, G., LEVITT, F. G. and MAZZA, R. J.
- MYRAT, C. D. and ROWLINSON, J. S.: The separation and fractionation of polystyrene at a lower critical solution point, 645
- NORTH, A. M. and RICHARDSON, D.: Entropy of stereoregularity in aldehyde polymerization, 333
- ONOZUKA, M.: See BENGOUGH, W. I. and ONOZUKA, M.
- ONYON, P. F.: review of *Manufacture of Plastics*, Vol. I, 173
- review of *Premix Molding*, 88
- PARRY, D. A. D.: See BRADBURY, E. M., BROWN, L., ELLIOTT, A. and PARRY, D. A. D.
- PASIKA, W. M. and BRANDON, R.: The $\pi \rightarrow \pi^*$ transition of the carbonyl group and polymer stereoregularity, 503
- PATTERSON, D. and BHATTACHARYYA, S.N.: Composition and temperature dependence of polymer-solvent interaction parameters, 455
- PEPPER, D. C.: See BROWN, G. R. and PEPPER, D. C.
- PETERLIN, A.: Molecular weight dependence of isothermal long period growth of polyethylene single crystals, 25
- See BUROU, Mrs S. P., PETERLIN, A. and TURNER, D. T.
- POWELL, T.: See CLARK, K. J. and POWELL, T.
- PROVOOST, F.: Gamma irradiation polymerization of acrylonitrile in the presence of solid additives, 515
- RICHARDSON, D.: See NORTH A. M. and RICHARDSON, D.
- RIGBY, B. J.: See MASON, P. and RIGBY, B. J.
- ROBERTS, R. C.: See GEE, G., HERBERT, J. B. M. and ROBERTS, R. C.
- ROBINSON, V. J.: review of *The Proceedings of the Tihany Symposium on Radiation Chemistry*, 172
- ROE, R.-J. and KRIGBAUM, W. R.: Application of irreversible thermodynamics to the kinetics of polymer crystallization from seeded nuclei, 231
- ROETLING, J. A.: Yield stress behaviour of poly(ethyl methacrylate) in the glass transition region, 615
- Yield stress behaviour of polymethylmethacrylate, 311
- ROSE, J. B.: See CUDBY, M. E. A., FEASEY, R. G., JENNINGS, B. E., JONES, M. E. B. and ROSE, J. B.
- ROWLINSON, J. S.: See MYRAT, C. D. and ROWLINSON, J. S.
- SAKAI, T.: Surface tension of polyethylene melt, 659
- SAUNDERS, L. and SPIRER, L.: Monocyclopentadienyltitanoxanes, 635
- SCHULZ, W. W.: See KENNEDY, J. P., SCHULZ, W. W., SQUIRES, R. G. and THOMAS, R. M.

- SHELDON, R. P.: *See* BLAKEY, P. R. and SHELDON, R. P.
- and LANE, Sister K.: Thermal conductivities of polymers I—Polyvinyl chloride, 77
- — Thermal conductivities of polymers II—Polyethylene, 205
- SIMS, D.: Internal pressure of crystalline polymers, 220
- SMITH, R. R.: *See* BUCKNALL, C. B. and SMITH, R. R.
- SPIRER, L.: *See* SAUNDERS, L. and SPIRER, L.
- SQUIRES, R. G.: *See* KENNEDY, J. P. and SQUIRES, R. G.
- *See* KENNEDY, J. P., SCHULZ, W. W., SQUIRES, R. G. and THOMAS, R. M.
- TAYLOR, G. W.: *See* CAVERHILL, A. R. and TAYLOR, G. W.
- THOMAS, R. M.: *See* KENNEDY, J. P., SCHULZ, W. W., SQUIRES, R. G. and THOMAS, R. M.
- TORRANCE, B. J. D.: *See* GRASSIE, N., TORRANCE, B. J. D., FORTUNE, J. D. and GEMMELL, J. D.
- TURNER, D. T.: *See* BUROW, Mrs S. P., PETERLIN, A. and TURNER, D. T.
- TURNER JONES, A.: Cocrystallization in copolymers of alpha olefins I—Copolymers of 4-methylpentene with linear alpha olefin, 249
- TUNG, L. H.: *See* HINKAMP, P. E. and TUNG, L. H.
- ULLMAN, R.: *See* KANG-JEN LIU and ULLMAN, R.
- VAN DER HOFF, B. M. E.: The stress strain relation of swollen rubbers, 397
- VAN SCHOOTEN, J. and EVENHUIS, J. K.: Pyrolysis-hydrogenation-GLC of poly- α -olefin, 343
- — — Pyrolysis-hydrogenation-GLC of α -olefins copolymers, 561
- WALLACH, M. L.: *See* ANGELO, R. J. IKEDA, R. M. and WALLACH, M. L.
- WANLESS, G. G. and KENNEDY, J. P.: Intramolecular hydride shift polymerization by cationic mechanism III—Structure analyses of deuterated and non-deuterated poly-4-methyl-1-pentene, 111
- WARD, I. M.: *See* GRANT, I. J. and WARD, I. M.
- WATT, W. S.: *See* CURRIE, D. J., DAINTON, F. S. and WATT, W. S.